

SPRINGER
REFERENCE

Franz J. Dahlkamp

Uranium Deposits of the World

USA and Latin America

**Uranium Deposits of the World
USA and Latin America**

Franz J. Dahlkamp

Uranium Deposits of the World

USA and Latin America

Franz J. Dahlkamp
Oelbergstr. 10
53343 Wachtberg b. Bonn
Germany

A C.I.P. Catalog record for this book is available from the Library of Congress

ISBN: 978-3-540-78555-2

The entire set of four volumes is available under the following:

Print ISBN 978-3-540-78559-0

Electronic ISBN 978-3-540-78560-6

Print and electronic bundle ISBN 978-3-540-78556-9

This work is subject to copyright. All rights are reserved, whether the whole or part of the material is concerned, specifically the rights of translation, reprinting, reuse of illustrations, recitation, broadcasting, reproduction on microfilms or in other ways, and storage in data banks. Duplication of this publication or parts thereof is only permitted under the provisions of the German Copyright Law of September 9, 1965, in its current version, and permission for use must always be obtained from Springer-Verlag. Violations are liable for prosecution under the German Copyright Law.

© Springer-Verlag Berlin Heidelberg 2010

The use of registered names, trademarks, etc. in this publication does not imply, even in the absence of a specific statement, that such names are exempt from the relevant protective laws and regulations and therefore free for general use.

Springer is part of Springer Science+Business Media

springer.com

Printed on acid-free paper

SPIN: 12236176 2109 — 5 4 3 2 1 0

Acknowledgments

The author wishes to acknowledge the contributions of his many associates in the uranium industry, national and international institutions, and universities whose ideas, observations, and data through the years have directly or indirectly become a part of this report. Many of them are included in the list of selected references, but there are additional many more who contributed during discussions, field trips, and mine visits. As cited in the text, many colleagues provided information by personal communication. Without their generous support it would not have been possible to compile a presentation as comprehensive as given in this volume.

More specifically, the author is deeply indebted to those who gave freely of their time in reading and correcting in an early stage specific chapters of the original manuscript, particularly E.N. Harshman (Wyoming Basins), R.B. Smith (Texas Coastal Plain), J.D. Rasmussen (Arizona Strip Area), A.E. Saucier (Grants Uranium Region), and J.K. Thamm (Salt Wash districts).

The author also is highly appreciative to the following individuals who spent their time over many years for critical discussions, providing information, reviewing, and updating descriptions of individual deposits or districts: S.S. Adams, F. Barthel, P. Bruneton, G. Catchpole, W.L. Chenoweth, J.F. Davis, W. Finch, B. Free, G. Ruhrmann, J. McMurray, J. Otton, T.C. Pool, J.D. Rasmussen, N.N. Reynolds, A.R. Wallace, and C.W. Voss.

My whole-hearted gratitude goes to Thomas C. Pool. He undertook the laborious and irksome endeavor to read, revise, and improve the entire text, which included the wearisome search for many missing or replacements of outdated data.

The contributions and comments of all these colleagues substantially improved the report, but may not necessarily endorse its contents.

M. Stasch and S. Kirchofer skillfully prepared most figures of the manuscript.



Preface

An important prerequisite to the long-term use of nuclear energy is information on uranium ore deposits from which uranium can be economically exploited. Hence the basic purpose of this book is to present an overview of uranium geology and data characteristic for uranium districts and deposits in the United States of America and Latin American countries. With respect to the classification terminology of uranium deposits used in this volume, the reader is referred to the typological classification system of uranium deposits presented in Part I *Typology of Uranium Deposits* in the first volume of the series *Uranium Deposits of the World - Asia* (Dahlkamp 2009).

An additional goal is to provide access for the interested reader to the voluminous literature on uranium geology. Therefore a register of bibliography as global as possible, extending beyond the immediate need for this book, is provided.

The original concept of this work, which was to provide an encyclopedia of uranium deposits of the world in a single publication, was soon doomed. The material grew out of all feasible proportions for a book of acceptable size and price as a wealth of data on uranium geology and related geosciences too vast for one volume became available during the past decades. So the original idea had to be abandoned in favor of a four- or five-volume publication covering the five continents. Each volume contains presentations of individual uranium districts, deposits, and noteworthy occurrences organized by countries. For the sake of comprehensiveness, not all the information could be distributed without some repetition.

These volumes were not originally designed as a product for its own sake. They evolved as a by-product during decades of active uranium exploration and were compiled thanks to a request by the Springer Publishing Company. Numerous publications as well as routine research work on identifying characteristic features and recognition criteria of uranium deposits, combined with associated modelling of types of deposits for reapplication in exploration, provided the data bank.

Finally it was not so much the author's intention to present data and his own views on uranium geology and metallogenesis, but theories and models of other geoscientists who worked on any given deposit, in order to stimulate and encourage further research to achieve continuous progress in the understanding of uranium deposits and their metallogenesis.

Franz J. Dahlkamp

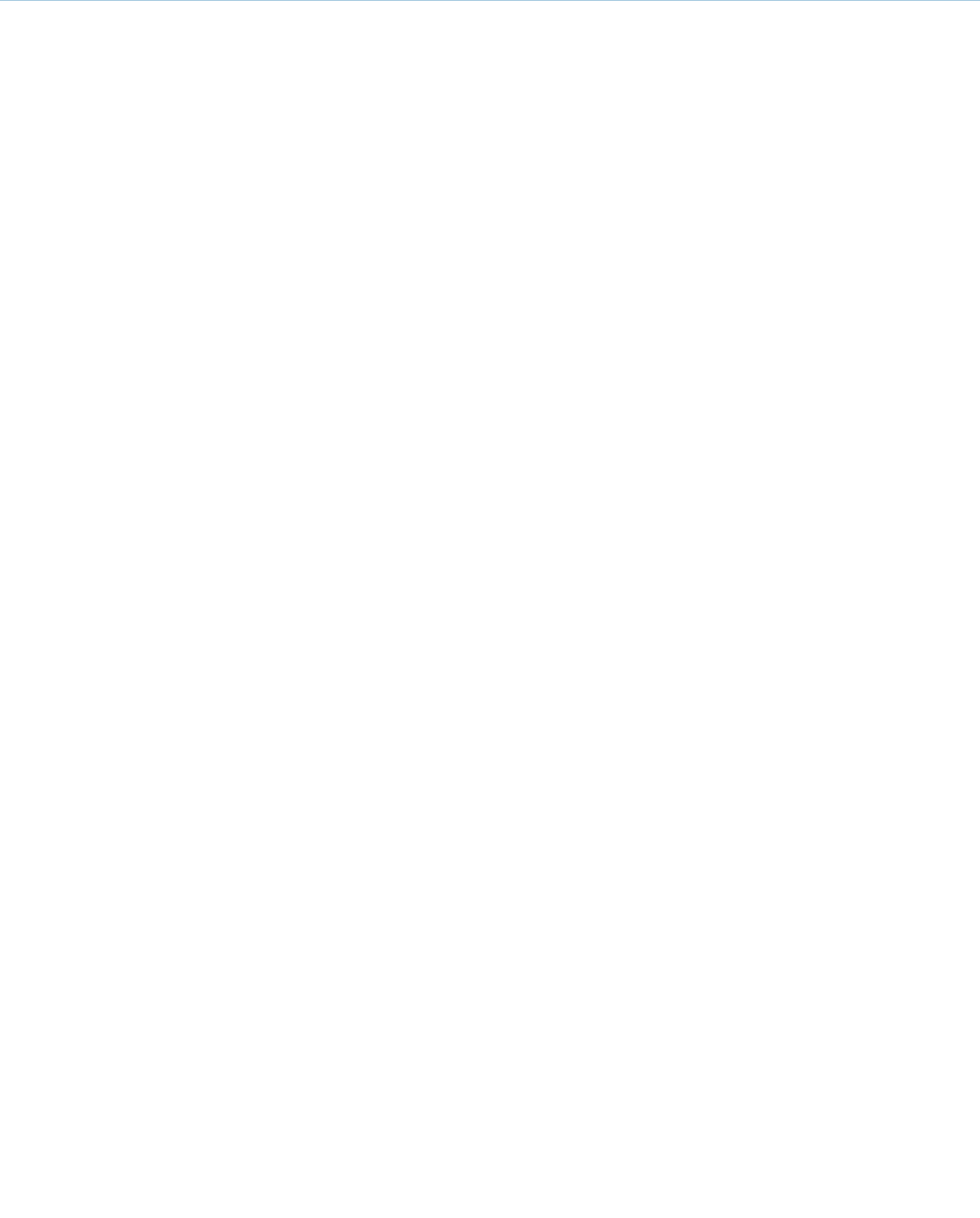


Table of Contents

Acknowledgments	v
Preface	vii
Remarks, Definitions, Units	xiii
Part I United States of America	1
Chapter 1 Colorado Plateau	9
1.1 Grants Uranium Region, Southeastern Colorado Plateau	12
1.2 Salt Wash Uranium Districts, Northern-Central Colorado Plateau	64
1.3 Chinle Uranium Districts, Western-Central Colorado Plateau	94
1.4 Arizona Strip Area, Southwestern Colorado Plateau	119
Chapter 2 Wyoming Basins	149
2.1 Gas Hills, Wind River Basin	173
2.2 Shirley Basin	176
2.3 Great Divide Basin	181
2.4 Bison Basin	192
2.5 Powder River Basin	193
2.6 Sand Wash and Poison/Washakie Basins, Colorado–Wyoming	206
Chapter 3 Black Hills	209
3.1 Southwestern Black Hills, Edgemont Area, South Dakota	212
3.2 Northern Black Hills, Wyoming-South Dakota	214
Chapter 4 Northern Great Plains	219
4.1 Dakota Plains – Uraniferous Lignite Areas	219
4.2 Nebraska Plains, Crawford Area	221
4.3 Denver–Julesburg Basin Colorado-Wyoming-Nebraska	226
Chapter 5 Northern Rocky Mountains	233
5.1 Spokane Mountain Area, Washington State	234
5.2 Mount Spokane Area, Washington State	241
5.3 Flodelle Creek Area, Washington State	242
5.4 Coeur d’Alene District, Idaho	242
5.5 Pryor Mountains – Little Mountains District/Wyoming–Montana	244
5.6 Copper Mountain District, Wyoming	245
5.7 Pedro Mountains, Little Man Mine, Central-Eastern Wyoming	249
5.8 Southern Granite Mountains, Sheep Creek, Central Wyoming	250
5.9 Granite Mountains, Central Wyoming	250
Chapter 6 Colorado and Southern Rocky Mountains	253
6.1 Front Range, Colorado	253
6.2 Tallahassee Creek District-Thirtynine Mile Volcanic Field, Colorado	270
6.3 Marshall Pass District, Colorado	275
6.4 Cochetopa District, Colorado	279
Chapter 7 Basin and Range Domain	281
7.1 McDermitt Caldera District, Nevada–Oregon	282
7.2 Lakeview District, Oregon	290
7.3 Austin District, Nevada	291
7.4 Beatty Volcanic Center, Nevada	291

7.5 Spor Mountain/Thomas Caldera, Utah	291
7.6 Marysvale Volcanic Complex, Utah	292
7.7 Date Creek Basin, Arizona	300
7.8 Sierra Ancha/Apache Proterozoic Basin, Arizona	304
7.9 Hillside Area, Arizona	305
7.10 Black Hawk District, Burro Mountains, New Mexico	306
7.11 Bingham, Utah	309
Chapter 8 Texas Coastal Plain Uranium Region	311
8.1 Deposits in the Upper Eocene Jackson Group	335
8.2 Deposits in the Late Oligocene Catahoula Formation	339
8.3 Deposits in the Early Miocene Oakville Formation, Fleming Group	345
8.4 Deposits in the Late Miocene-Early Pliocene Goliad Formation, Citronella Group	350
Chapter 9 Appalachian Highland and Piedmont Region	357
9.1 Piedmont Province, Virginia	357
Chapter 10 Alaska	367
10.1 Bokan Mountain, Prince of Wales Island, Southeastern Alaska	367
Chapter 11 Pacific Coast Region	373
Chapter 12 Uraniferous Phosphorite Regions	375
12.1 Land Pebble District, Central Florida	375
12.2 Phosphoria Formation, Idaho-Montana-Utah-Wyoming	376
Chapter 13 Chattanooga Black Shale Region	379
Bibliography	381
Part II Central and South America	413
Chapter 1 Mexico	417
1.1 Sierra de Peña Blanca, Chihuahua State	417
1.2 Burgos Basin, La Sierrita Area, Nuevo León State	425
1.3 Other Uranium Occurrences in Mexico	425
Chapter 2 Argentina	427
2.1 Northern Sub-Andean Region (Norte Subandino)	429
2.2 Transition Mountain Region (Sierras de Transición)/Tinogasta District	429
2.3 Precordillera Region	430
2.4 Pampas Mountain Region	431
2.5 Sierra Pintada Region	433
2.6 Andean Geosyncline Region (Geosinclinal Andino)	439
2.7 San Jorge Gulf Basin/Chubut Region (Cuenca del Golfo San Jorge)	440
Chapter 3 Bolivia	447
3.1 Sevaruyo District	447
Chapter 4 Brazil	451
4.1 Caetité Massif Region, Lagoa Real District	452
4.2 Central Ceará Region, Itaitaia/Santa Quitéria Deposit	457
4.3 Poços de Caldas Region	462
4.4 Seridó Region	468
4.5 Paraná Basin	470
4.6 Quadrilátero Ferrífero Region	474
4.7 Rio Preto-Campos Belos Region	477

4.8 Serra de Jacobina Region	477
4.9 Serra dos Carajás Region	479
4.10 Other Uranium Resources in Brazil.	480
Chapter 5 Peru.481
5.1 Macusani District.	481
Bibliography487
Subject Index493
Geographical Index.505
Uranium Minerals Index.517



Remarks, Definitions, Units

Organization of the Volume

The focus of this volume is on the characterization of uranium deposits in the USA and Latin American countries with noteworthy uranium deposits.

It contains synoptic descriptions of uranium districts and deposits including metallogenetic concepts. The latter are based on data and views of geoscientists who have actually worked on these deposits, their metallogenetic models are not necessarily congruent, however, with interpretations and definitions of the Typology Scheme presented in the volume *Uranium Deposits of the World: Asia* (Dahlkamp 2009).

Graphic presentations and tables had to be limited to the extent considered necessary to illustrate the principles of geological setting and configuration of deposits. However, quantity and quality of illustrations are variable depending on the availability and reliability of data in the source material.

Confidence of Data

Not all deposits are well researched and, on some, research data were not available. Some data are vague, if not biased or wrong. Other data are presented ambiguously, being easily misinterpreted. Interpretation of certain criteria may likewise be conflicting. Descriptions of the same district or deposit or specific features thereof by different authors are not necessarily unanimous and sometimes confusing. This is in particular the case for resource and grade figures. The uncertainties associated with resource estimation are considerable, and generally accepted procedures and baseline parameters (e.g. cutoff grade and/or ore thickness) for preparing such estimates have not always been available.

Concerning uranium metallogenesis, its principles are at present sufficiently well understood only for some types of deposits, whereas other types are understood to a lesser extent and in varying degrees and therefore permit space for speculation or geofantasy.

The attempt was made to reconcile conflicting data and deviating hypotheses as far as possible in order to give at least an idea of the overall geological situation and size of a district or deposit. It has to be admitted, however, that this demanding task was not always satisfactorily achieved. In any event, the various views are presented and in case the reader requires more precise information, the original literature should be reviewed or the original author(s) should be contacted for additional data.

Citing of Authors

The chapters on all the countries include a reference list of authors whose data have been used directly or indirectly or who have contributed work to the country, district, or deposit described in that particular chapter. This scheme was selected to

- (a) serve as a reference index on literature pertaining to the respective country, district, or deposit. The list is restricted to respective principal uranium papers and to contributions to general geology with relevant or possible implications on uranium geology. Special publications not directly related to uranium geology, e.g., age dating of rocks, are cited in the text (titles of the papers can be found listed according to the author's name in the Bibliography);
- (b) credit authors who have worked on the given district or deposit;
- (c) reduce the immense repetition of authors' names to a bearable minimum within the text. In this kind of synoptically presentation, often using numerous papers on a single district or deposit, a complete citation of all authors would in many instances have required a list of names after a couple of sentences or a short section. Alternatively, numbers referring to authors and their papers could have been used. My preference is, however, to see the name of an author and not a colorless number, which, in addition, requires searching in the bibliography for the numbered individual. Although the selected system may not satisfy all authors who wish to see their names precisely repeated, they may forgive me for the sake of easier reading.

Bibliography

This section is organized in alphabetical order of authors' names and provides complete coverage of the papers cited in the text and reference lists. Papers published since the final revision of the manuscript have been added in the bibliography but, for technical reasons, could be incorporated into the standing manuscript only in exceptional cases.

The attempt was made to provide a bibliography as complete as possible, but some papers are still missing. This deficiency does not reflect my disregard to the respective contribution, but should rather be excused as an imperfection on my side. Proceedings of workshops, symposia, etc., were in many instances not published until several years later. Meanwhile, some authors had published the workshop data elsewhere, or the data had been disseminated otherwise, and hence the material may have had influenced and may have found access to publications of others prior to the printing of the original presentation. Consequently, publication years of reference data do not necessarily reflect the first presentation of results.

Geological, Mineralogical, Mining, and Related Terms

Connotation and spelling of geological and mineralogical terms are, in principle, understood as and based on those given by: Thrush and the Staff of the Bureau of Mines (eds.), 1968, in “A Dictionary of Mining, Mineral, and Related Terms”, US Dept. of the Interior Washington, DC. Exceptions or additions to this are:

Clarke value (= background value): Mean content of a chemical element in the Earth’s crust as a whole or in its particular segments and specific rocks (e.g. for granite).

Costs, expenditures: In US \$ unless otherwise stated.

Deposit: This term is not restricted to economic U deposits but used in a broader sense to signify all U concentrations with U tenors distinctly elevated above common background U values of a corresponding (host) rock type.

Granite/granitoid, pegmatite/pegmatoid, etc.: The terms are used synonymously and not in their strict genetic sense. Various authors apply both words differently and the connotation is not always clear.

Mineralization, alteration, etc.: These terms are used in both connotations, to denote the process implied and the product of the process.

Monometallic mineralization/mineralogy (simple mineralization/mineralogy): Denotes ore containing U only as a recoverable element, although many other metals may be present but in trace or subeconomic quantities.

Ore: Synonymous with (potentially) minable mineralization.

Polymetallic mineralization/mineralogy (corresponds to complex mineralization/mineralogy of some authors): Denotes ore containing at least two different metals including U in economic or potentially economic amounts.

Property/deposit: Due to the legal landholding situation in the USA, the size of exploration and/or mining concessions do not necessarily cover the full size of a deposit but only parts thereof. In consequence, the amount of properties given in publications is often in excess of that of actual deposits. On the other hand, some properties, for example large ranches, may contain two or more individual deposits.

Regolith: Refers to saprolite/paleosol. It is not used in the sense often applied in Canada, where weathered rocks are also called regolith. Herein, the term regolithic rock is preferred.

Resource/reserve, production, and grade figures: Calculated in metric tons (t or tonnes) U and percent (%) U (respectively, in ppm U for low-grade values). Used figures represent published data or best estimates based on published data and personal communication (for more details, see further below paragraph Confidence of Resource Data).

Secondary uranium minerals: This term, commonly referring to colored U minerals, was abandoned in favor of *hexavalent U (U⁶⁺) minerals*, to avoid confusion. “Secondary U minerals” are of primary origin in several deposits, e.g., in surficial deposits. Both terms, primary and secondary, have been restricted in this volume to their strict genetic sense denoting primary or secondary origin of a given mineral.

Types of uranium deposits: The nomenclature used in this volume is based on the typology scheme presented as Part I in the volume *Uranium Deposits of the World: Asia* (Dahlkamp 2009).

Uraninite/pitchblende: In this volume, *uraninite* is used for the macrocrystalline, more or less euhedral variety of UO_{2+x} , which typically occurs in rocks of higher P-T metamorphic grades (amphibolite grade and higher, contact metamorphic), igneous rocks such as granite and pegmatite but also in vein- and veinlike-type deposits. *Pitchblende* is used for UO_{2+x} varieties of micro- or crypto-crystalline, colloform (collomorphous, botryoidal, and spherulitic) habit, which typically occur in low-grade metamorphic and nonmetamorphic rocks such as greenschist facies metasediments and more or less arenaceous sediments, and in most vein- and veinlike-type uranium deposits. It is understood that both varieties crystallize in the same crystallographic system, the cubic system, but have certain discriminating physicochemical properties (for details, see Fritsche et al. 1988, 2001 and Ramdohr 1980).

The term pitchblende was the first name used for black uranium oxide minerals back in 1565 and is widely used, particularly in Europe. Uraninite is a term commonly used for all kinds of uranium oxides in American literature. Worldwide, both terms are applied by a number of authors variably and in an overlapping way. The criteria used by various geoscientists to differentiate between uraninite and pitchblende are sometimes conflicting and can lead to confusion.

Terminology of U Resources

OECD-NEA/IAEA replaced several of the category terms of resources in the 2005 Red Book, which they had used in their biannual Red Books through 2003. In this volume, the former terms were maintained in order to avoid a complete revision of the manuscript. For comparison, [Table I.1](#) provides a listing of the former and new resources terminology of OECD-NEA/IAEA, combined with more or less equivalent categories used in other countries.

Resource/reserve definitions with respect to confidence classes and cost categories of an ore deposit cannot be achieved from purely geological parameters. Economic considerations have to be included. Demand for the commodity and related price/cost factors dictate whether a localized metal concentration is a deposit that can be profitably exploited presently or in the future, or whether it is a mineral occurrence of only scientific or academic interest. OECD-NEA/IAEA have accordingly established a cost category system that subdivides the various confidence resource classes into resources recoverable at <US \$ 130/kg U, <US \$ 80/kg U, and <US \$ 40/kg U, which was used as far as data were available.

National Resource Data

In this volume, the national resource data were taken from the biannual OECD-NEA/IAEA publications Uranium: Resources, Production and Demand, informally termed Red Books. It should be noted, however, that the national resource figures published in the Red Books are provided by government agencies. Some of these national authorities occasionally underestimate the real

■ **Table I.1.**

Approximate correlation of terms used in resources classification systems of OECD-NEA/IAEA until 2003 and since 2005, and selected countries.

	Identified resources (Known conventional resources)			Undiscovered resources (Undiscovered conventional resources)		
	Demonstrated	Inferred	Undiscovered			
Australia	Measured	Indicated	Inferred	Undiscovered		
Canada (NRCan)	Measured	Indicated	Inferred	Prognosticated	Speculative	
CIS	A+B	CI	C2	P1	P2	P3
OECD-NEA/IAEA 2005 (OECD-NEA/IAEA <2003)	Reasonably assured (RAR)		Inferred (EAR-I)	Prognosticated (EAR-II)	Speculative (Speculative)	
United States (DOE)	Reasonably assured		Estimated additional		Speculative	
UNFC	G1	G1 + G2	G3	G4		

Note: The terms listed are not strictly comparable as the criteria used in the various systems are not identical. "Grey zones" in correlation are therefore unavoidable, particularly as the resources become less assured. Nonetheless, the chart presents a reasonable approximation of the comparability of terms. CIS Russian Federation, Kazakhstan, Ukraine, Uzbekistan, etc.; UNFC United Nations International Framework Classification for Reserves/Resources-Solid Fuels and Mineral Commodities

recovery costs. Therefore, some of the national resource figures appear in, and consequently inflate to a certain extent, lower cost resource categories of the Red Book tables. On the other hand, changes in the market price of uranium may increase or decrease the figure of established economic resource quantities.

Confidence of Resource Data for Individual Deposits

Available resource figures for individual deposits or districts do not necessarily correspond to the OECD-NEA/IAEA nomenclature and categories, since mining companies have not necessarily applied the terminology suggested by OECD-NEA/IAEA, or their published figures are not attributed to one or the other category. Hence, in many cases it remains unclear whether in situ (geological) or recoverable (mining) reserves/resources are given, i.e., whether or not mining dilution and milling losses are included, whether the numbers refer to RAR to EAR categories or to any other equivalent category of reserves/resources (e.g., proven, probable, inferred, or possible reserves). Mining dilution can reduce recoverable reserves to less than 75% of the in situ tonnage and can downgrade the ore mined to 85% or less of the in situ grade. In addition, the cutoff factors (grade and minimum dimensions/thickness of ore layers or veins) for reserve/resource calculations are not always given. Depending on the cutoff factors used, reserve/resource figures can augment or decrease.

For this reason reserve, resource, and grade figures given for individual deposits or districts are, except for verifiable figures, the best estimates of, but not always, in situ tonnages and grades based on various, not necessarily published, information. Also, the terms reserves and resources are not used in this volume in their strict sense but more synonymously. This means that, independent of their status of confidence, no great distinction is made between the terms “resources” (except for being used in rather undefined or not clearly defined cases) and “reserves” [more restricted to clearly defined (potentially) economic resources].

Abbreviations

a.o.	among others and/or others
a.s.l.	above sea level
EAR	estimated additional resources
Ga (b.y.)	billion years = 1000 Ma
ISL	In situ leaching method (also referred to as ISR/in situ recovery method)
lb	pound (7000 grains = 16 ounces = 451 grams)
Ma (m.y.)	million years
RAR	reasonably assured resources
redox	reduction–oxidation (boundary)
REE	rare earth elements
sh.t.	short ton
t	metric ton(s) (tonnes)
U_{eq} or % eq. U	equivalent uranium measured by geophysical methods
U_{met}	metallic uranium or natural uranium

Conversion Factors

1 t	=	1	metric ton
1 t	=	1.1023	sh.t. = 2200 lbs
1 t U	=	1.18	t U ₃ O ₈
1 t U	=	1.30	sh.t. U ₃ O ₈ = 2600 lbs U ₃ O ₈
1 t U ₃ O ₈	=	0.848	t U
1 t U ₃ O ₈	=	1.1	sh.t. U ₃ O ₈ = 2200 lbs U ₃ O ₈
1 sh.t. U ₃ O ₈	=	0.769	t U
1 sh.t. U ₃ O ₈	=	2000	lbs U ₃ O ₈
\$1/lb U ₃ O ₈	=	\$2.6	/kg U
\$1/kg U	=	\$0.3824	/lb U ₃ O ₈



United States of America

Prior to the early 1980s, the USA rated in terms of both resources and production as one of the leading uranium countries of the western world. Remaining uranium resources combined with production result in a total endowment of 704,000 t U.

Present-day (status year-end 2003) uranium resources, adjusted for mining dilution and processing losses, are estimated at 342,000 t U RAR in the less than US \$ 130/kg U cost category including 102,000 t U in the less than US \$ 80/kg U cost category (OECD-NEA/IAEA 2007).

With respect to uranium recovery, the USA was the dominant producer of the western world prior to 1981/1982. Slumping of the uranium market in the early 1980s forced the successive closure of all conventional U mines except for some sandstone-type deposits that were amenable to ISL technology. In total, the USA produced ca. 362,000 t U from the Second World War through 2007. Peak annual production was 16,804 t U in 1980; by 2003 it had dropped to 769 t U (OECD-NEA/IAEA 1983, 2005), but had again increased to 1,748 t U in 2007 (US-DOE/EIA May 13, 2008).

Historical U production came from between 2,500 and 3,000 individual mines, many of which were small operations, particularly on the Colorado Plateau. Most mines produced ore from sandstone U deposits. In 2007, production came from one mill (White Mesa mill, Blanding, Utah) fed by four small underground mines (*Pandora*, *Sunday/St. Jude*, *Topaz*, *West Sunday* in the Uravan Mineral Belt, Colorado Plateau), and five ISL operations (*Crow Butte* in Nebraska, *Alta Mesa*, *Kingsville Dome*, and *Vasquez* in Texas, and *Smith Ranch/Highland* in Wyoming). Several more mines and ISL facilities are scheduled for production in 2008 and subsequent years in Colorado, New Mexico, Texas, Utah, and Wyoming. Most future production is expected to come from ISL operations.

Resources are known from several uranium provinces, whereby those in the western states contained the majority of uranium deposits (▶Fig. I.1). The overwhelming part of resources, more than 90%, was and still is contained in sandstone-type deposits, the rest in vein, collapse breccia pipe, bituminous or karstic limestone, lignite, and volcanic-type deposits. In addition to these standard types of uranium deposits, there are various other types of uranium resources including black shale, phosphorite, copper, and beryllium deposits from which uranium may be recovered as by-product to other commodities. These by-product resources can be very large but grades are low to very low, on the order of several tenths to some hundredths of a percent.

All established *sandstone-type* U deposits and major occurrences are located in the western part of the North American subcontinent, where they occur from the southern part of the province of British-Columbia in SW Canada southward to the state of New Mexico and Texas in the USA. Most of these sandstone U deposits are contained in continental

sediments of Mesozoic and Tertiary age within intermontane basins on the Colorado Plateau, and in the Cordillera (Rocky Mountains) that formed during the Laramide Orogeny. Characteristically, most U ore-hosting basins are within or adjacent to Precambrian terrane (◀Fig. I.2). An exception is U deposits in south Texas and in adjacent northeastern Mexico, and probably in the Great Plains; they occur in Tertiary and Cretaceous, respectively, marginal marine environments.

Three prominent uranium provinces with *sandstone-type* U deposits exist in the USA: Colorado Plateau, Wyoming Basins, and Texas Gulf Coastal Plain. A few sandstone deposits are known in the Great Plains (Nebraska), the Black Hills, the Basin and Range domain, northern Rocky Mountains (Spokane area, Washington state), and Colorado Rocky Mountains (Tallahassee Creek). Some of the sandstone-type ore bodies are large but many are of small-to-moderate size and of low-to-moderate grade.

Vein-type U deposits are of small-to-medium size and of medium-to-high grade. Most vein U deposits are situated in the Front Range, Colorado Rocky Mountains. Others occur in the Rocky Mountains of central Colorado, in the Spokane region of the northern Rocky Mountains in northeastern Washington state, in the Basin and Range province, in the Colorado Plateau province of Utah, Arizona, New Mexico, and in the Piedmont province of Virginia. A stockwork *metasomatic-type* U deposit was mined at Bokan Mountain in the panhandle of Alaska. A peculiar kind of U deposits, the *collapse breccia type*, is found in the Arizona Strip area. *Volcanic-type* U occurrences are known from the western and northern Basin and Range physiographic province in Utah, Nevada, and Oregon (◀Fig. I.1).

Uraniferous *phosphorite-type* deposits occur in the southeastern and northwestern states and uranium *copper porphyry-type* deposits in the western states. Uranium could be recovered as a by-product from both types. Other huge but very low-grade uranium resources are contained in *black shale*, in particular in the Chattanooga Shale in Tennessee and adjacent states.

▶Table I.2 provides a synopsis of principal uranium provinces (in *italic*) and major districts, where uranium was produced or could be potentially produced in the USA.

Historical Review of Uranium in the United States of America

U discoveries in the 19th century

The earliest records of uranium discoveries in the USA date back to 1816, when Cleaveland reported two sites with “earthy green oxide of uranium” near *Brunswick, Cumberland County in Maine*, and near *Baltimore in Maryland*. The next record is from 1835 by Shephard who noted green uranium mica found in pegmatites near *Middletown, Connecticut*, and near *Chesterfield, Hampshire County in Massachusetts*.

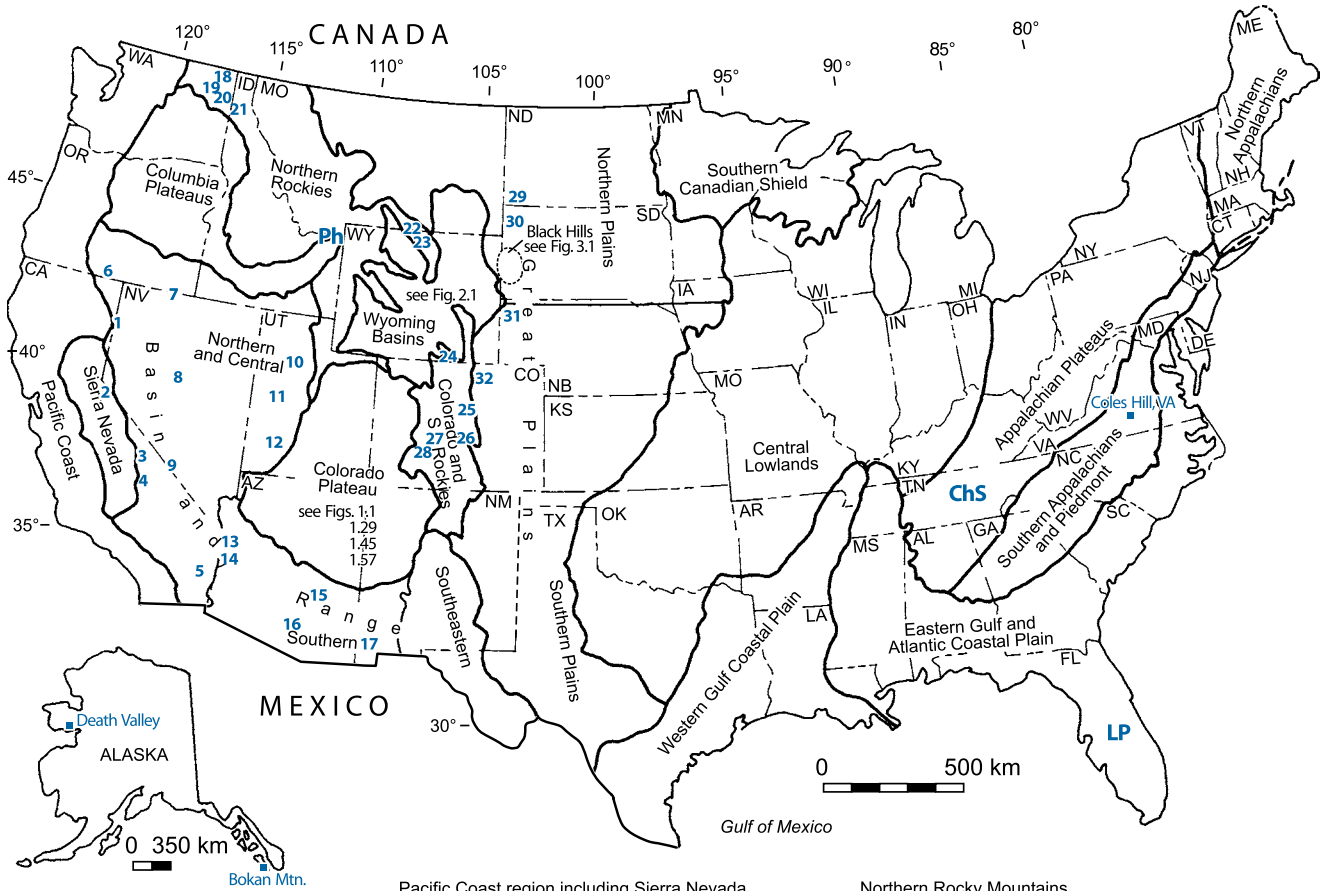
Reported early uranium discoveries in the 19th century in western states of the USA include:

California: 1868 Stanislaus mine in Calaveras County, U minerals in gold-telluride ore (Genth 1868).

Colorado: 1872 Wood mine, near Central City, Gilpin County, pitchblende in Au-bearing veins (Peirce 1872); 1875

Fig. I.1.

USA, uranium provinces and regions (number in blue refer to uranium districts and isolated deposits) (Uranium provinces after US DOE 1980).



Ph Phosphoria Fm region, ID-MO-WY-UT

ChS Chattanooga Shale region, KY-TE-AL

LP Land Pebble phosphat district, FL

Pacific Coast region including Sierra Nevada

- 1 Petersen Mtn./Antelope Range, CA-NV
- 2 Sonora Pass, CA
- 3 Coso Range, CA
- 4 Kern River Canyon area, CA
- 5 McCoy Mts., Mohave Desert, CA

Basin and Range Domain

- 6 Lakeview, OR
- 7 McDermitt, NV
- 8 Austin/Early Day, NV
- 9 Beatty area/Black Bonanza-Red Dog, Daisy, NV
- 10 Bingham, UT
- 11 Spor Mtn./Yellow Chief, UT
- 12 Marysvale, UT
- 13 Hillside Mine, AZ
- 14 Date Creek Basin/Anderson Mine, AZ
- 15 Sierra Ancha, Apache Basin, AZ
- 16 Suahuarita/Twin Buttes, AZ
- 17 Burrow Mts./Black Hawk, NM

Northern Rocky Mountains

- 18 Flodelle Creek, WA
- 19 Spokane Mtn. district/Midnite, Sherwood, WA
- 20 Mt. Spokane/Daybreak Mine, WA
- 21 Coeur d'Alene, ID
- 22 Pryor Mts. district, MO
- 23 Little Mts. district, WY
- 24 Medicine Bow Mts., WY

Colorado and Southern Rocky Mountains

- 25 Front Range, CO
- 26 Tallahassee Creek district, CO
- 27 Marshall Pass district, CO
- 28 Cochetopa district, CO

Northern Great Plains

- 29 Dakota Plains/Belfield, ND
- 30 Dakota Plains/Cave Hills, Slim Buttes, SD
- 31 Nebraska Plains/Crow Butte, Big Red, NB
- 32 Denver-Julesburg (Cheyenne) Basin, Weld County, CO

Leyden Coal mine, Jefferson County, green U ochre and aggregates of orange crystals (carnotite) in sandstone of Cretaceous Laramie Formation adjacent to coal seams (Berthoud 1875); 1881 Paradox Valley region; 1895 Roc Creek, a tributary to Dolores River, Montrose County (Uranium Mineral Belt), carnotite in sandstone (Min. Indust. 6, 1898, and 7, 1899; Proc. Colorado Sci Soc, 6, 1901).

South Dakota: 1885 Bald Mountain, Lawrence County, pitchblende and autunite(?) in quartz veins in gneiss (Stillwell 1885).

Texas: 1887 SW of Bluffton, Llano County, uraninite, nivenite, and gummite in pegmatite (Hidden and McIntosh 1889).

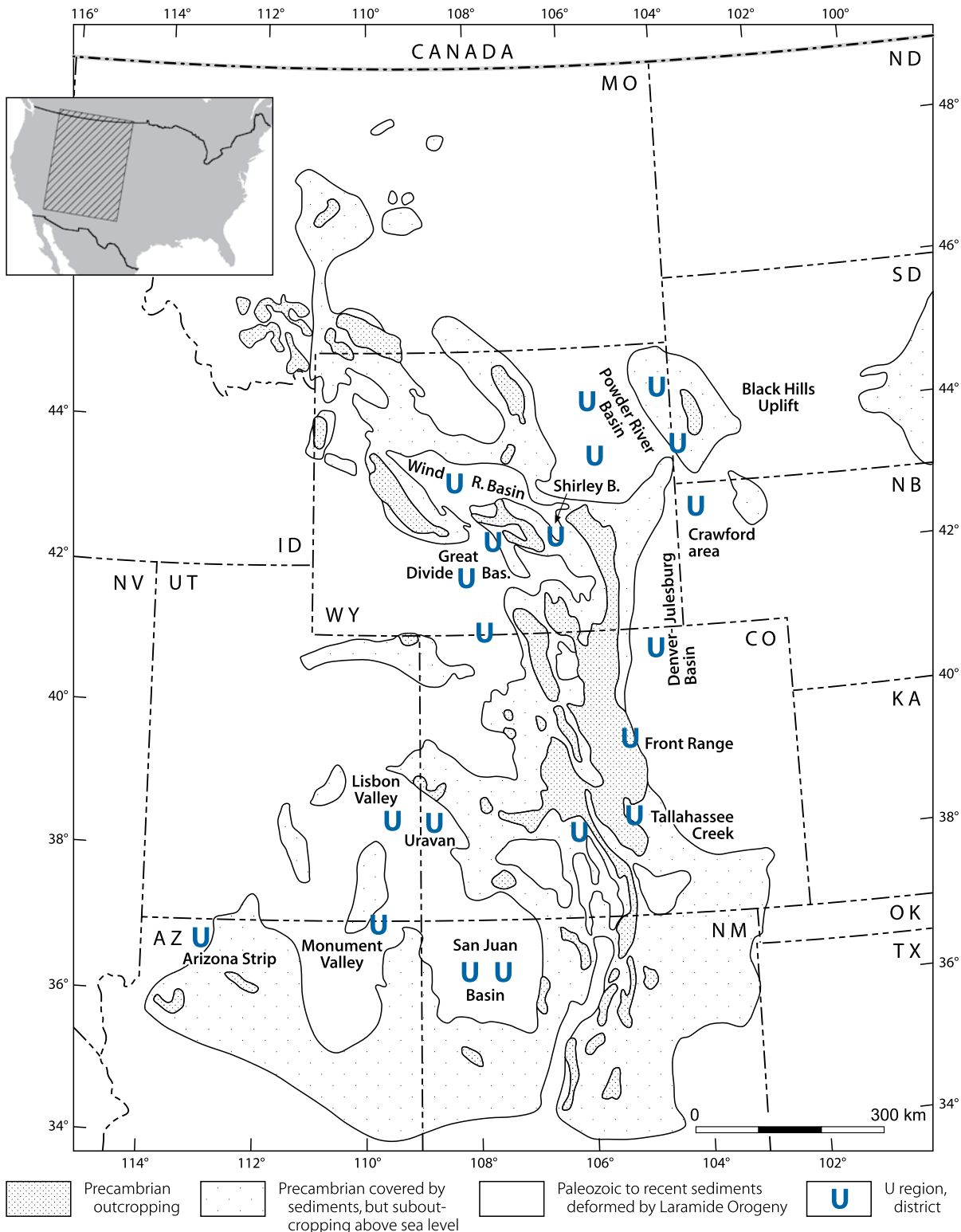
Utah: 1881 Silver Reef district near Harrisburg, Washington County, carnotite associated with carbonaceous matter in sandstone of Triassic Chinle Formation (Rolker 1881); 1890 Marysvale, uranium in volcanics.

Significant uranium discoveries in the 20th century

Intensified uranium exploration took place from the 1940s to the 1950s organized by the US-AEC due to the demand for uranium for nuclear weapons, and again from the late 1960s to the early 1980s for the peaceful use of nuclear energy (details see below).

In spite of intensified exploration efforts during the second uranium boom period, only few uranium districts or significant deposits were discovered in new areas. They include the Coles

Fig. I.2. Western USA, spatial relationship of prominent uranium regions/districts to Precambrian crystalline basement terrane. (after Mallory 1972)



■ Table I.1.

Principal uranium provinces and selected districts with uranium production or potential production in the USA.

Province – major Districts	Type of Deposits	Province – major Districts	Type of Deposits
<i>Colorado Plateau</i>		<i>Colorado+Southern Rocky Mtns, WY-CO-NM</i>	
– Grants U region, NM	ss (+bit ls)	– Front Range, CO	Ve
– UraVan Mineral Belt, CO-UT	ss	– Gunnison-Marshall Pass, Co	ve
– Lisbon Valley/Big Indian Wash, UT	ss	– Tallahassee Creek, CO	ss
– Monument Valley-White Canyon, AZ-UT	ss	<i>Basin & Range</i>	
– Arizona Strip area, AZ	bxp	– Lakeview, OR	volc
<i>Wyoming Basins</i>		– McDermitt, NV	volc
– Wind River Basin/Gas Hills, WY	ss	– Spor Mtn, UT	volc
– Shirley Basin, WY	ss	– Marysvale, UT	volc
– Great Divide Basin/Green Mts, Red Desert, WY	ss	– Date Creek Basin; AZ	lacust
– Powder River Basin, WY	ss	– Apache Basin/Sierra Ancha, AZ	ve-stwk
– Poison/Washakie Basin, WY-CO	ss	– Burro Mts/Black Hawk, NM	ve
<i>Black Hills</i>		<i>Texas Coastal Plains</i>	
– Southern Black Hills/Edgemont, S.D.	ss	– Karnes County, TX	ss
– Northern Black Hills/Hulett, Carlisle, WY-S.D.	ss	– Live Oak County, TX	ss
<i>Great Plains</i>		– Duval-Webb-Brooks Counties, TX	ss
– Northern or Dakota Plains, N.D.-S.D.	lig, ss	<i>Alaska Panhandle</i>	
– Nebraska Plains/Crawford Area,	ss	– Bokan Mountain	metasom/ve
– Southern Plains/Denver-Julesburg Basin, CO-WY	ss	<i>Piedmont, PA-VA-NC</i>	
<i>Northern Rocky Mtns, WA-ID-MO-WY</i>		– Danville area, VA	ve
– Spokane Area, WA	ve, ss	<i>Florida</i>	
– Stevens County, WA	ss	– Land Pebble district	phosph
– Pryor Mts-Little Mts, MO-WY	surf/karst	<i>NW USA</i>	
– Copper Mtn, WY	surf?ve ?	– Phosphoria Fm areas	phosph

Type of Deposits: *bit ls* bituminous limestone; *bxp* breccia pipe; *lacust* lacustrine, stratiform; *metasom* metasomatic; *phosph* phosphorite; *ss* sandstone; *stwk* stockwork; *surf* surficial; *ve* vein, *volc* volcanic

Hill deposit near Danville in Virginia discovered in 1978 and Crow Butte in Nebraska discovered in 1980. Most other discoveries were in established districts, which were already known for their uranium potential.

Exploration revived again in 2003/2004 due to drastically increased uranium prices. Some milestones of exploration success are reflected in the following discoveries.

Sources of Information. Chenoweth 1975, 1980a–c, 1985a, b, 1991; Crawley 1983; OECD-NEA and IAEA bi-annual reports 1970–2007; Shawe et al. 1991; Chenoweth, personal communication.

Colorado Plateau

Sandstone-type deposits

[GUR Grants Uranium Region/San Juan Basin, New Mexico. Sandstone-type deposits, host formations (in brackets): *SWMbr*

Salt Wash Member, Jurassic Morrison Formation, *WCMbr* Westwater Canyon Member, Jurassic Morrison Formation, *ChFm* Chinle Formation]

1899/1900 La Sal Creek and Moab, Utah (*SWMbr*)

1904 Temple Mountain, San Rafael Swell, Utah (*ChFm*)

1905 Green River and Thompson, Utah (*SWMbr*)

1907 White Canyon, Utah (*ChFm*)

1913 Lisbon Valley-Big Indian Wash, Utah (*ChFm*), and

Henry Mountains, Utah (*SWMbr*)

1918 Monument Valley, Utah (*ChFm*)

1920s Todilto Trend/Grants area, GUR (Todilto Limestone)

1939 La Sal, Utah (*SWMbr*)

1949 Inter River, Utah (*ChFm*)

1950 Cameron, Arizona (*ChFm*)

1951 Laguna/Jackpile, GUR (Jackpile Ss/Brushy Basin Member, Morrison Formation)

1952 Church Rock, GUR (*WCMbr*)

1955/56 Ambrosia Lake, GUR (WCMbr)
 1969 Marquez/Rio Puerco and Borrego Pass, GUR (WCMbr)
 1970 Mount Taylor, GUR (WCMbr)
 1972 Crown Point, GUR (WCMbr)
 1975 Nose Rock, GUR (WCMbr)

Breccia pipe deposits, Arizona

Late 1940s Hack Canyon 1
 1951 Orphan Lode
 1979 Hack Canyon 2
 1981 Kanab North
 1984 Rose
 2008 A1 pipe (discovered by Quatterra Resources, April 8, 2008)

Wyoming Tertiary Basins

Sandstone-type deposits

(GDB Great Divide Basin, PRD Powder River Basin, WRB Wind River Basin, WB Washakie Basin. Host formations: EBSFm Eocene Battle Springs Formation, EWFm Eocene Wasatch Formation, EWRFm Eocene Wind River Formation, MBPFm Miocene Browns Park Formation)

1936 Lost Creek, GDB (EBSFm)
 1951 Pumpkin Buttes, PRD (EWFm)
 1952 Monument Hill, PRD (EWFm)
 1953 Gas Hills/Lucky Mc, WRB (EWRFm)
 1953 Baggs, WB (MBPFm)
 1954 Crooks Gap, GDB (MBPFm)
 1955 Shirley Basin (EWRFm)
 1968 Highland, PRD (EWFm)
 1979 Jackpot/Green Mountain, GDB (EBSFm)

Black Hills

1951 Edgemont, South Dakota (sandstone type, Cretaceous Inyan Kara Group)
 1952 Carlisle, Wyoming (sandstone type, Cretaceous Inyan Kara Group)

Great Plains

1948 Belfield, N Dakota (lignite type, Paleocene Fort Union Fm)
 1980 Crow Butte, Nebraska (sandstone type, Oligocene White River Group)
 1978 Centennial, Denver-Julesburg Basin, Colorado-Wyoming (sandstone type, Cretaceous Fox Hills Sandstone and Laramie Fm)

Rocky Mountains

1918 Silver Cliff Mine, Hartville Uplift, Wyoming (Ag vein with U, Cu, Au)
 1949 Schwartzwalder, Colorado (veins in Paleoproterozoic metamorphics)
 1954 Midnite, Washington (vein-stockwork in Mesoproterozoic Togo Fm.)
 1954 Tallahassee Creek, Colorado (sandstone type in Tertiary strata)
 1955 Sherwood, Washington (sandstone type in Late Cretaceous-Paleocene conglomerate)
 1955 Pryor Mtns, Montana (surficial type in Mississippian

Madison Limestone)
 1983 Flodelle Creek, Washington (surficial type in peat-bog)

Basin and Range

1949 Marysvale/Central Ming District, Utah (volcanic vein)
 1951 Date Creek Basin, Arizona (lacustrine stratiform type, Tertiary Chapin Wash Fm.)
 1950 Sierra Ancha/Apache Basin (vein-stockwork in Mesoproterozoic Dripping Spring Quartzite)

South Texas Coastal Plain

1954 Western Karnes County (sandstone type, Tertiary sediments)
 1955 Duval and Starr Counties (sandstone type, Tertiary sediments)

Alaska Coast Range

1955 Bokan Mountain (metasomatite/vein in Bokan Mountain Granite)

Piedmont

1978 Coles Hill, Virginia (vein in Precambrian-Paleozoic Fork Mountain Fm)

Production

The documented first uranium production in the USA came 1872 from the *Wood mine* in Central City area, Gilpin County, Colorado. Together with a few other mines, it produced intermittently some 50 t U from 1872 to 1898. Another early uranium recovery was from the REE- and U-bearing pegmatite deposit *Barringer Hill* in Texas that was found in 1887.

U production on the *Colorado Plateau* began 1898, where carnotite ore (named after the U-V mineral carnotite) in sandstone had been found prior to 1880. The first shipment came from the *Copper Prince mine* at Roc Creek, Montrose County, Colorado where ten tons of ore at a grade in excess of 20% U and 15% V were produced in 1898.

Noteworthy uranium mining commenced in 1910, in a region of southwestern Colorado and southeastern Utah, which later became one of the largest uranium districts on the Colorado Plateau known as *Uravan Mineral Belt*. This uranium served initially as dye-stuff for staining glass and porcelain, and later on, until 1923, for the extraction of radium. After an interim period of relative inactivity, carnotite ore was recovered from 1933 to 1940 for the production of vanadium.

With the onset of development of nuclear weapons during the Second World War, demand for uranium increased dramatically. From 1943 onward, uranium was extracted for the Manhattan Project initially by the retreatment of dump material from the vanadium era in the Uravan Mineral Belt. Based on the "Atomic Energy Act" from 1946, the "Atomic Energy Commission" (AEC) was founded, which began in 1947, an intensified exploration program. Numerous uranium deposits were discovered not only in known regions, such as the Colorado Plateau, but also in new areas in almost all western states of the USA as well as in Texas and Pennsylvania. All significant uranium districts with sandstone-type U deposits were found by the mid 1950s. Numerous mines on the Colorado Plateau, in the Wyoming Basins, Black Hills, Rocky Mountains, South Texas

Coastal Plains, and isolated deposits in other regions went into operation in the 1950s. Most operations were active until the end of the year 1970, when the government-financed uranium procurement program for military purposes ended.

This uranium epoch reached its zenith about 1960. Between 1960 and 1962, 27 processing plants were in operation that achieved a peak production of 13,600 t U in 1960. Subsequently, production dropped to a low of 7,600 t U in 1966. In total, 165,000 t U were produced between 1948 and 1971.

The wide-scale construction of nuclear power plants in response to the OPEC oil embargo in 1973 provided a new incentive for uranium exploration and mining. From the mid 1970s, production increased steadily to a peak of 16,800 t U in 1980 (world production 54,000 t U) making the USA the leading uranium producing country in the western world. In this year, *conventional mining* delivered 14,280 t U (7,390 t U at an average ore grade of 0.08% U from some 50 open pit and 6,890 t U at 0.12% U from about 300 underground mines) feeding 23 conventional mills. *Unconventional operations* produced 2,520 t U (or 15% of the total) from 11 ISL operations and, as by-product, from six wet-process phosphoric acid plants, two copper leach operations, and one beryllium-uranium project. Approximately 10% of the 1980 US production was derived from multiproduct ores. In 1981 and 1982, two additional conventional mills and two wet-process phosphoric acid plants were established.

Uranium from *phosphorite* was recovered from 1952 to 1961, when three producers in Florida recovered approximately 400 t U from wet-process phosphoric acid. Then, uranium recovery from phosphoric acid ended due to high costs. With the introduction of the DEPA-TOPO recovery technology and rising U prices in the late 1970s, renewed interest in extracting uranium from phosphorite emerged and nine uranium extraction plants went on stream between 1978 and 1981, eight in Florida and Louisiana based on phosphorite from Florida, and one plant in Alberta, Canada, which treated phosphorite

imported from Idaho. An output of 720 t U was reached in 1980 and, until 1991, annual production fluctuated around 1,300 t U with a peak of 1,360 t U in 1988. Since then uranium production from phosphorite dropped to about 380 t U in 1997 derived from two remaining facilities in the USA. The last facility, Uncle Sam in Louisiana, closed in 1999. In total, uranium production from phosphorite amounted to some 19,000 t U.

In the period 1981–2003, annual uranium production dropped steadily. All conventional mills closed successively, the last three, Panna Maria, Texas, and Pathfinder in Shirley River Basin, Wyoming, in 1992, and the White Mesa mill, Utah, in 1996. In 1991, the last underground uranium mine in the USA located on the Colorado Plateau abandoned operation. In the same year, the Rhode Ranch open pit operation in Texas, and in 1992 the last open pit in the USA located in the Gas Hills district, Wyoming, ceased mining. Remaining production came only from Crow Butte, Nebraska, where ISL uranium extraction had commenced in 1991 and, until 1999 as a by-product of phosphate.

The recession in the US uranium industry is reflected in the following production figures. Production amounted to 5,700 t U in 1984 with eight mills operating. It dropped in 1991 to 3,500 t U, 7% of which derived from conventional mining with two mills in Texas and Wyoming, and 93% from unconventional exploitation, mainly by ISL methods and phosphoric acid plants, and to a minor extent from mine waters. By 1993, production had declined further to some 1,300 t U that came from four ISL plants in Nebraska, Texas, and Wyoming, two phosphoric acid plants in Louisiana, and a mine water extraction plant in the Grants Uranium Region, New Mexico. The down trend continued until 2003, when annual production was 769 t U by two in situ leach production facilities, Crow Butte, Nebraska, and Kingsville Dome, Texas. Increasing uranium prices from 2003 to 2007 have stimulated exploration as well as development of both formerly known and new deposits. As a consequence, US production has increased as already outlined earlier.

Chapter 1

Colorado Plateau

The Colorado Plateau is one of the prominent uranium (-vanadium) provinces of the world. It encompasses almost 350,000 km² in western Colorado, southern Utah, northern Arizona, and northwestern New Mexico. A great number of peneconcordant, tabular sandstone-type uranium deposits in Jurassic and Triassic formations have been discovered therein. Most deposits are clustered in districts of variable size. In addition, Permian sediments host ore bodies in collapse breccia pipes in the Arizona Strip area, Arizona (► Figs. 1.1 and ► 1.1).

Sandstone-type uranium was mined from over 2,200 properties located in some 35 former mining districts. The largest classical mining districts include the *Grants Mineral Belt/Ambrosia Lake*, New Mexico (Westwater Canyon Member/Morrison Formation, Jurassic), *Uruan Mineral Belt*, Colorado–Utah (Salt Wash Member/Morrison Formation, Jurassic), *Lisbon Valley-Big Indian Wash*, Utah (Chinle Formation, Triassic), and *Monument Valley-White Canyon*, Arizona–Utah (Chinle Formation, Triassic) (see further down ► Figs. 1.29, ► 1.45, and ► 1.57 for minor uranium districts in Morrison and Chinle sediments.). Some U deposits occur in Permian, Cretaceous, and Tertiary sediments. Uranium production from deposits hosted in the Morrison Formation has been considerably greater than that from the Chinle Formation.

Sources of information. See References at Colorado Plateau districts sections.

Regional Geology of the Colorado Plateau

Based on Thamm et al. (1981), the regional geology of the Colorado Plateau may be summarized as follows (for a concise review of the geology of the Colorado Plateau uranium province, the reader is referred to Granger and Finch 1988, among others, and for specific parts thereof to authors listed at district descriptions).

The dominant feature of the Colorado Plateau has been its comparative structural stability since the close of the Precambrian time. During most of the Paleozoic and Mesozoic time, the plateau was a stable shelf without major geosynclinal areas of deposition, except during the Pennsylvanian.

At the beginning of the *Paleozoic Era*, the Precambrian basement had been eroded to a nearly flat plain upon which the Cambrian clastic sediments were laid down. After a hiatus marking the Ordovician and Silurian time, the Devonian and Mississippian limestones were deposited.

During the Pennsylvanian time, approximately 2,100 m of marine black shales and evaporites accumulated in the NW-trending Paradox Basin in southwestern Colorado and southeastern Utah. Folding within the basin along preexisting zones of weakness was accompanied by flowage of salt toward the anticlinal axes. The Uncompahgre Uplift continued to rise along

the NE edge of the basin, supplying arkosic debris, which formed continental sediments of Permian age. In the Arizona Strip region in the southwestern Colorado Plateau, mainly pelitic sediments but also fluvial arenitic facies were laid down during the Upper Pennsylvanian, while Permian sedimentation led to silty and fine sandy deposits with impure carbonatic, partly evaporitic strata of marine to littoral origin on top.

The plateau continued to be a stable area throughout the *Mesozoic Era*. A thousand meters and more of sediments of Triassic, Jurassic, and Early Cretaceous ages, largely of continental fluvial origin, were deposited from source areas to the east, and from the south and west. The submergence of the region as a block preceded widespread deposition of thick, black marine shales of the Upper Cretaceous Mancos Formation. The region was then uplifted, and the deposition of marginal marine and continental sandstones of the Mesaverde Formation marked the end of the Mesozoic Era.

The *Laramide Orogeny* of Late Cretaceous and Early Tertiary ages affected the plateau only slightly, compared to bordering areas, but produced the major structural features of the plateau. Nearly horizontal strata were gently flexed producing uplifts and basins. Spectacular monoclines of the region, actually the steeper limbs of asymmetric anticlines, displace strata vertically as much as 2,400 m, and some exceed 150 km in length. Monoclinical folds are interpreted to overlie basement faults; flexible sediments responded by bending, rather than breaking, across faults.

During the *Tertiary*, sediments of fluvial and lacustrine origin were deposited in early Eocene time in deeper parts of local basins, notably in the Uinta and San Juan basins.

Intrusions of diorite and monzonite porphyry laccoliths penetrated sediments at several points during the Middle Tertiary to form mountains of the central plateau. Dikes and sills of similar composition were intruded along the eastern edge of the plateau, probably in Miocene time. Near the southern and western margins of the plateau, probably beginning in mid-Tertiary time, volcanoes of the Mt. Taylor, Datil, and San Francisco fields, and volcanic fields of high plateaus were formed.

Faulting along the south and west sides of the plateau in mid-Tertiary time was followed by epeirogenic uplift and northeastward tilting of the plateau; continuing erosion since that time has shaped present landforms.

Stratigraphic Distribution of Uranium in the Colorado Plateau

Uranium is found in 14 different stratigraphic formations but the bulk of *sandstone-type* ore is hosted in seven stratigraphic units of two formations of Mesozoic age (► Fig. 1.2), i.e. the Westwater Canyon, Brushy Basin, and Salt Wash members of the *Late Jurassic Morrison Formation*, and the Moss Back, Monitor Butte, Petrified Forest, and Shinarump members of the *Late Triassic Chinle Formation*. Some U deposits occur in Permian, Cretaceous, and Tertiary sediments.

The *Morrison Formation* is a continental sequence of Late Jurassic age that occupies an area of approximately 1.5 million square kilometers extending far beyond the north and east

Fig. 1.1. Colorado Plateau, simplified geological map with the location of principal uranium regions and districts. (After Adams and Saucier 1981, Jobin 1962). *AZ* Arizona Strip, *GUR* Grants Uranium Region, *HM* Henry Mountains, *LV* Lisbon Valley-Big Indian, *MV* Monument Valley-White Canyon, *UB* Uravan Mineral Belt

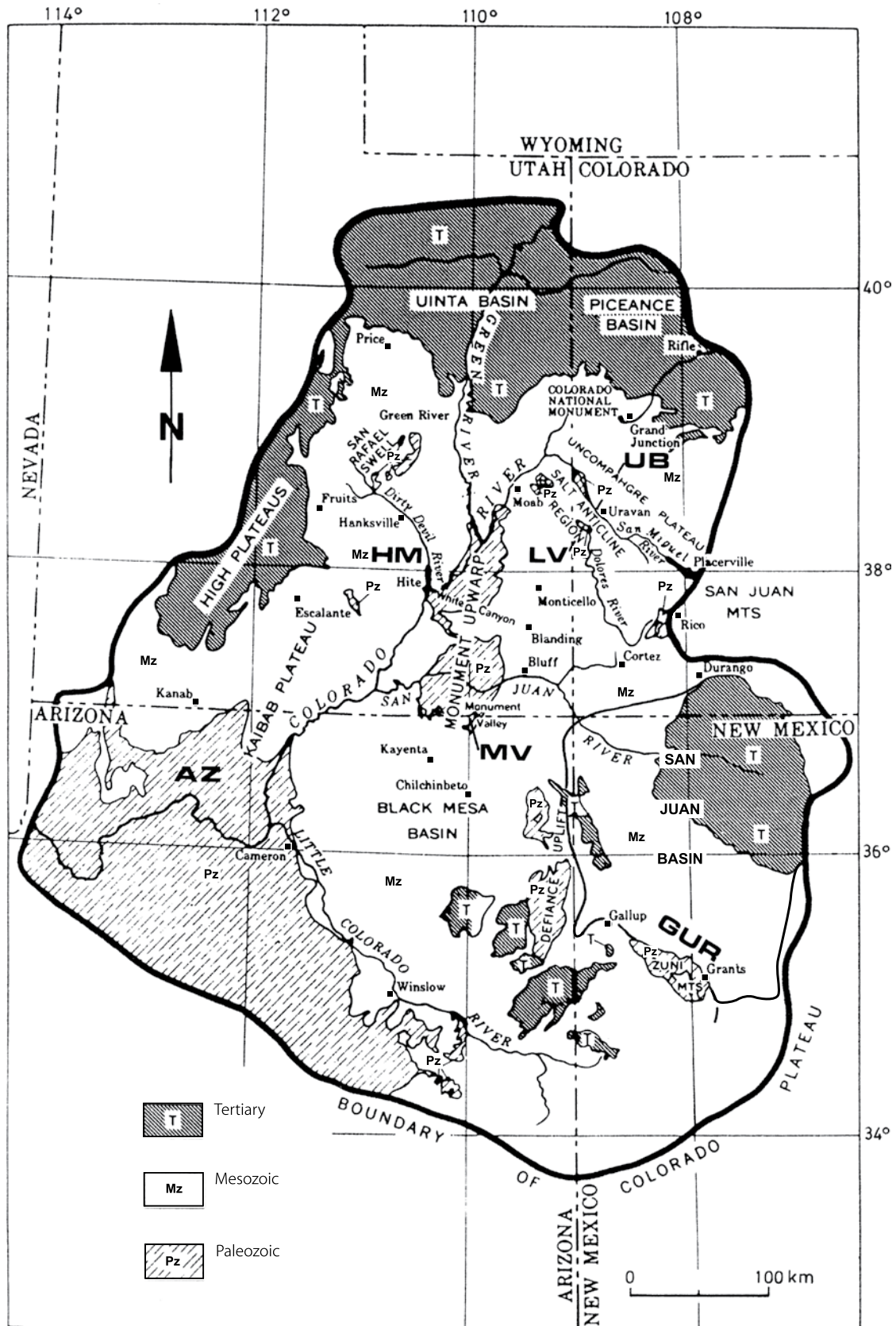
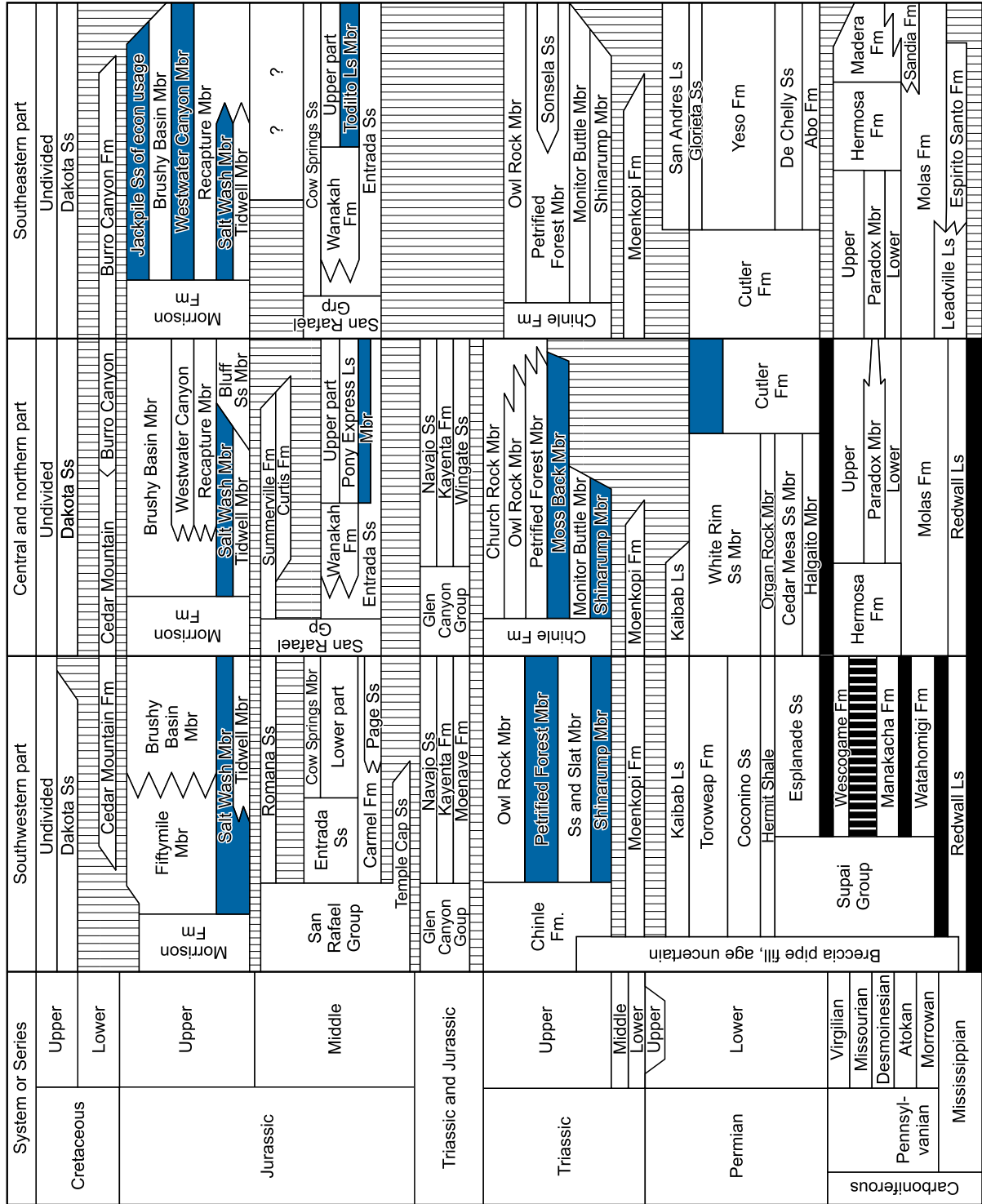


Fig. 1.2. Colorado Plateau, chart of the Paleozoic to Mesozoic stratigraphic units with indication of major uranium-mineralized formations (shown in blue). (After Peterson F. in Granger et al. 1988)



boundary of the Colorado Plateau into the Rocky Mountains and the Great Plains provinces.

In the Colorado Plateau, the Morrison Formation includes up to five members, each of continental origin (► Fig. 1.2), from top to bottom: the Brushy Basin, the Westwater Canyon, the Recapture, the Salt Wash, and the Tidwell members.

The Morrison Formation exhibits both conformable and disconformable relationships to underlying formations of Late Jurassic age within the Colorado Plateau. Formations of Early Cretaceous age conformably overlie the Morrison except in the southwestern portion of the plateau, where the Brushy Basin Member has been removed by pre-Dakota erosion; in this area, the Morrison is unconformably overlain by Late Cretaceous Dakota Sandstone.

In west-central New Mexico, in the southern San Juan Basin, fluvial sandstones of the *Brushy Basin* and the *Westwater Canyon members*, which overlie the Cow Springs Sandstone, constitute the major uranium-hosting units. The Brushy Basin Member is interbedded with, and generally overlies the Westwater Canyon sandstone. Both the Recapture and the Westwater Canyon members extend only into the southernmost portions of Colorado and Utah, and along with the Brushy Basin and Salt Wash members they intertongue and merge southward into the Cow Springs Sandstone.

In areas of major U production from the *Salt Wash Member* in Colorado and Utah, the Morrison Formation consists of only the Salt Wash and the conformably overlying Brushy Basin Member. In northeastern Arizona and northwestern New Mexico, an area of relatively minor Salt Wash U production, the Salt Wash intertongues with and is partially overlain by the Recapture Member.

The *Chinle Formation* is a continental sediment system of Upper Triassic age that originally covered almost the entire Colorado Plateau. It has been subdivided into two parts (Stewart et al. 1972), an upper redbed sequence with the Owl Rock and Church Rock members, and a lower bentonitic sequence that includes in descending order the Petrified Forest, the Moss Back, the Monitor Butte, the Shinarump, and the Temple Mountain members.

Fluvial sediments of the basal Chinle Formation rest unconformably upon the Lower Triassic Moenkopi Formation in the northwestern, central, and southern Colorado Plateau, and on the Permian Cutler Formation in the central northeastern plateau. Other formations of Upper Triassic age, e.g. the Wingate Sandstone conformably overlie the Chinle Formation.

Uranium deposits have been found in the lower portions of the Chinle Formation, in particular, in the Shinarump and in the Moss Back members, and to a lesser extent in the Petrified Forest and Monitor Butte members. The Shinarump Member occurs mainly in southeastern Utah and northwestern Arizona. The Moss Back Member extends from Lisbon Valley near the Utah–Colorado border, north and northwestward into the northern San Rafael Swell. The main uranium areas of the Monitor Butte Member are west of the Colorado River, extending approximately from the Orange Cliffs to the southern San Rafael Swell.

Collapse breccia-type deposits in the Arizona Strip area occur in terrain of flat-lying sediments ranging from Mississippian Redwall Limestone through Pennsylvanian and Permian

strata to the Kaibab Formation and, locally, into the Triassic Moenkopi Formation.

Principal Characteristics of Colorado Plateau Uranium Mineralization

The U mineralization of the Colorado Plateau is chiefly present in two settings, in fluvial arenitic sediments and in collapse breccia pipes.

Original *sandstone-type* U mineralization of the Colorado Plateau generally is of tabular shape peneconcordant to the enclosing fluvial arkosic sandstone. Fischer (1968) and Adler (1974), divided the Colorado Plateau sandstone-type U deposits into two types according to the type of organic matter contained within them. The primary mineralization of the Grants Uranium Region in the southeastern plateau contains abundant epigenetic, unstructured interstitial organic matter within host rocks of the Westwater Canyon and Brushy Basin members of the Morrison Formation that is coextensive with uranium. In contrast, deposits within the Salt Wash Member of the Morrison Formation and within the Chinle Formation contain dominantly detrital plant debris. Uranium in the Salt Wash and Chinle deposits occurs most commonly as coffinite and pitchblende, and often in or in close proximity to anomalous concentrations of detrital plant debris. An additional, important difference between the Salt Wash and Chinle deposits, and the Westwater Canyon–Brushy Basin deposits is their vanadium content.

Uranium–vanadium weight ratios for the Salt Wash-hosted mineralization range from 1:1 to 1:20 and for Chinle deposits from less than 1:1 to 1:5, hence these deposits are more often vanadium deposits with uranium as an accessory component. Deposits in the Westwater Canyon and Brushy Basin members generally have uranium to vanadium ratios less than 1:1 and ratios exceeding 1:2 have not been reported.

Apparently restricted to the Arizona Strip area, known *collapse breccia-type* deposits consist of polymetallic mineralization but with variable dominance of uranium, base or precious metals. Ore is confined to permeable pipe fill, mostly sandy intervals, and faults peripheral to the pipe.

1.1 Grants Uranium Region, Southeastern Colorado Plateau

Located in northwestern New Mexico, the Grants Uranium Region (GUR) is one of the largest uranium regions in the world. Most of its uranium deposits are hosted in Westwater Canyon–Brushy Basin sandstones of the Upper Jurassic Morrison Formation. In addition, small uranium deposits occur in the Cretaceous Dakota Sandstone and in the Middle Jurassic Todilto Limestone.

The Westwater Canyon–Brushy Basin deposits consist of tabular ore concentrations, the first ore generation of which is intimately associated with humate, these deposits are therefore classified as continental fluvial, uranium–humate type.

These deposits are clustered in several districts within the classical Grants Mineral Belt in sensu stricto and adjacent trends

■ Fig. 1.3.

Southeastern Colorado Plateau, San Juan Basin, the figure shows major structural elements, extent of the basin, and the situation of the Grants Uranium Region (GUR) between the Zuni Uplift of Proterozoic crystalline rocks and the Chaco Slope. Individual districts of the uranium region are outlined. (After Santos and Turner-Peterson 1986 based on Kelley 1951) (*Principal U districts*: A.L. Ambrosia Lake incl. Mt. Taylor, Cpt. Crownpoint incl. Nose Rock and Borrego Pass, C.R. Church Rock, La Laguna incl. Rio Puerco-Bernabe Montano, S.L. Smith Lake-Mariano Lake)

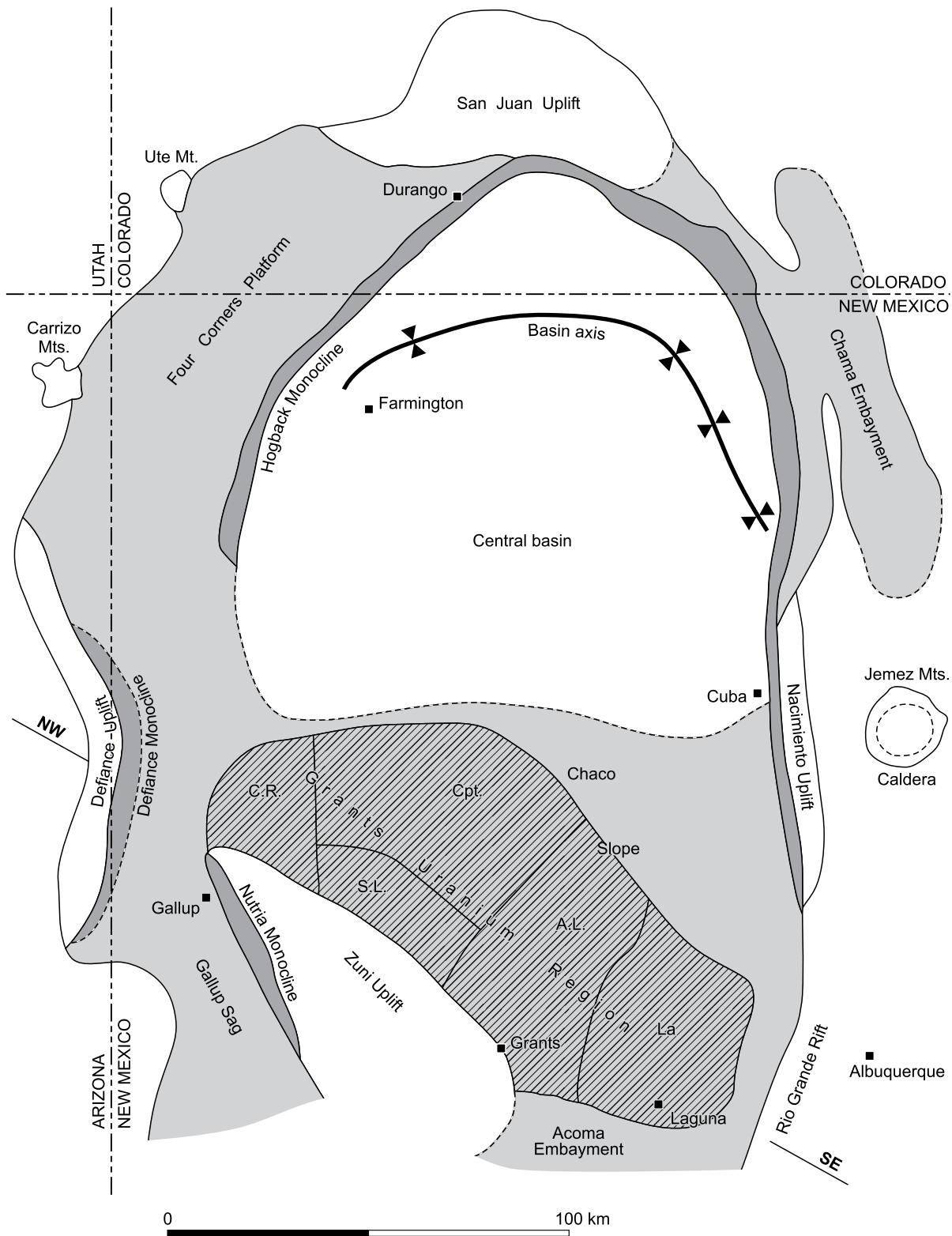
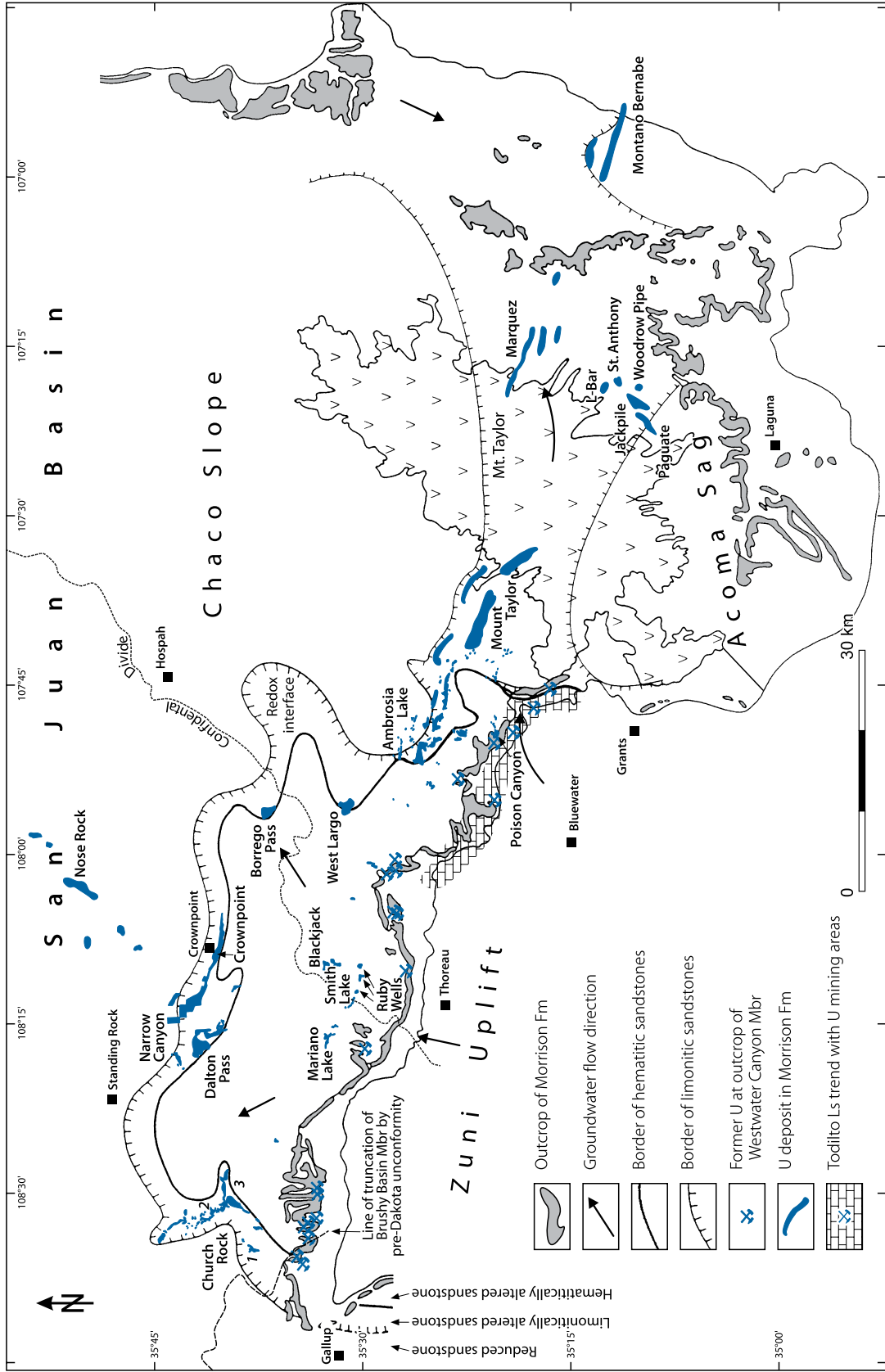


Fig. 1.4.

Southeastern San Juan Basin, Grants Uranium Region, generalized map with location of uranium districts/deposits and distribution of Tertiary-Quaternary oxidation fronts in the sandstone of the Westwater Canyon Member, Morrison Formation. The map also shows the location of the U mineralized Todilto Limestone trend to the south of Ambrosia Lake. (After Kirk and Condon 1986, McCammon et al. 1986, McLaughlin 1963, Saucier 1980)



to the north and east. The classical Grants Mineral Belt is 10–30 km wide and extends for about 130 km ESE–WNW from Laguna in the east to Gallup in the west. Mining districts within this belt are, from east to west: *Laguna*, *Mt. Taylor* or *Marquez*, *Ambrosia Lake – Poison Canyon*, *Smith Lake – Black Jack*, and *Church Rock – Gallup*. Subsequent discoveries have made the boundaries of this mineral belt rather indefinite and have added other districts north, down the structural dip, and east along the trend. They include: *Crownpoint* and *Nose Rock*, north of Smith Lake, and *Rio Puerco* including *Bernabe-Montano*, the easternmost known U deposit (▶ Figs. 1.3 and ▶ 1.4). The deposits in all these districts are very similar in principle, but occur at variable depths ranging from outcrop at the southern boundary to more than 1,200 m downdip to the north.

The Grants Uranium Region had original resources estimated of at least 240,000 t U in the \$80/kg U cost category at a grade averaging between 0.1 and 0.2% U [McCammon et al. (1986) calculated a total of discovered resources of 358,090 t U and 745,710 t U based on a cutoff grade of 0.085 and 0.0085% U, respectively] More detailed figures of resources, grades, and production are included in subsequent chapters covering individual mining districts.

After the discovery in 1950, about 170 mines produced 127,000 t U from fluvial sandstone of the Upper Jurassic Morrison Formation from 1951 to 1989, when mining ceased. In addition, 3,700 t U were recovered from mine water from 1963 to 2001. The Ambrosia Lake district, formerly the single largest uranium producing area in the USA, delivered more than half of the amount.

The Grants Uranium Region delivered in addition 2,570 t U from 1950 to 1985 from the Middle Jurassic Todilto Limestone, ca. 500 t U from Entrada Sandstone, and ca. 185 t U from Dakota Sandstone (Chenoweth and Holen 1980; McLemore and Chenoweth 2003).

Sources of Information. Abundant information on the Grants Uranium Region has been published by many authors including those listed in Section References and Further Reading at the end of this chapter. This includes three memoirs, edited by Kelley (1963a), Rautman (1980), and Turner-Peterson et al. (1986) that contain extensive background information by many authors. McLemore (1983, 2002), McLemore and Chenoweth (1989, 1991, 2003), and McLemore et al. (2002) have published comprehensive data on the uranium deposits, mines, and resources in New Mexico, which provide extensive information including that of the Grants Uranium Region.

Adams and Saucier (1981) have compiled a geological model study on “uraniferous humate deposits,” as they call the uranium mineralization in the Grants region. Adams and Saucier’s (1981) documentation describes the known geology of the Grants region adequately and presents a comprehensive synopsis of the regional setting and local characteristics of the uranium deposits, their recognition criteria and the fundamental principles of ore formation. The subsequent description has drawn extensively from Adams and Saucier’s (1981) report, and in many cases specific text has been quoted but with some modifications (therefore not set in quotation marks). Updates were taken from more recent publications, in particular, from Granger and Santos

(1982), Holen (1982), and Crawley et al. (1984). The memoir edited by Turner-Peterson et al. (1986) provides extensive multidisciplinary research data and the reader is referred to this excellent publication for more information.

Adams and Chenoweth (personal communication) provided valuable data, and Saucier kindly reviewed this section of the Grants region and amended and improved the content and text.

Regional Geological Setting of Mineralization

The Grants Uranium Region lies in the southeastern part of the Colorado Plateau. It extends inside and along the southern border of the San Juan Basin; along the Zuni Uplift to the south and the Chaco Slope to the north. The Rio Grande Trough forms the boundary to the east and the Defiance Uplift to the west (▶ Fig. 1.3).

The present-day San Juan Basin is the southeastern extension of the Late Jurassic San Juan depositional trough. The old trough was flanked by two NW–SE-trending highlands, the Uncompahgre to the NE and the Mogollon to the SW. During Late Jurassic time, three broad alluvial fans were deposited in the trough. They constitute the major part of the Morrison Formation and correspond, from oldest to youngest, to the Salt Wash Member in the north, the Recapture, and the Westwater Canyon–Brushy Basin members in the south.

Although the depositional paleoslope was generally NE, down the Mogollon flank, the sandstones also follow, along the southern basin margin, a pronounced paleocurrent system trending to the SE and parallel to the axis of the trough.

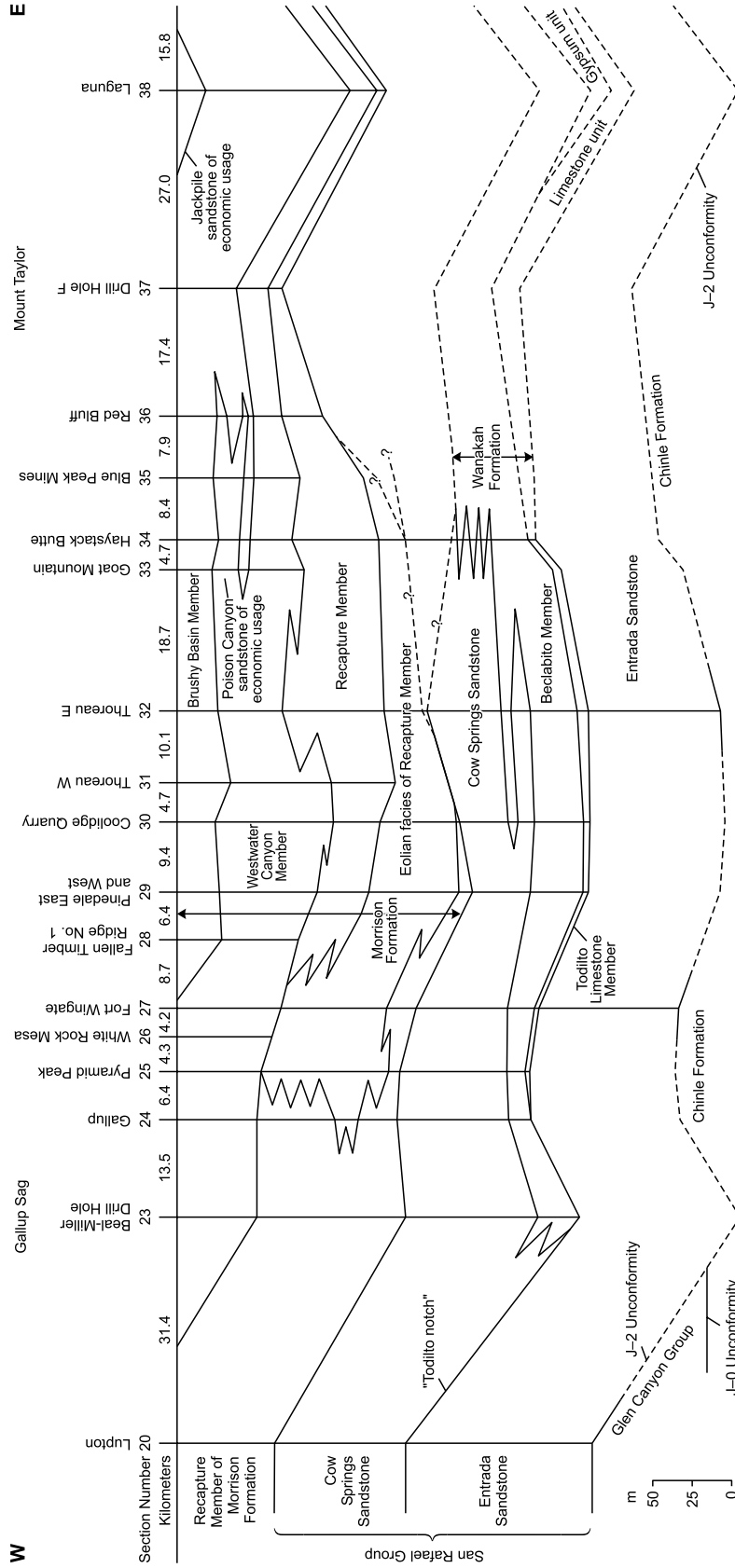
The Morrison strata were deposited on the Cow Springs Sandstone, which is underlain in sequence by the Beclabito and Todilto Limestone members of the Wanakah Formation, and the Entrada Sandstone of Middle Jurassic age (▶ Figs. 1.5–1.7). In Upper Cretaceous time, southern outcrops of the Morrison Formation were partly eroded before they were unconformably transgressed by the Dakota Sandstone and the Mancos Shale. Tertiary volcanics of Mt. Taylor cover the Mesozoic sediments between the Laguna and the Ambrosia Lake.

Younger tectonic movements of presumably Laramide age (Cretaceous/Tertiary) resulted in the formation of the present Zuni Mountains in the southern part of the San Juan Basin and caused a slight tilt of the Morrison strata to a shallow (less than 5°) dip to the N and NE. Faulting at the same time caused displacements of generally minor magnitude.

Most uranium deposits of the Grants region are in sandstones of the Westwater Canyon and Brushy Basin members of the upper part of the Morrison Formation. The Morrison Formation is up to 180 m thick and comprises from top to bottom the

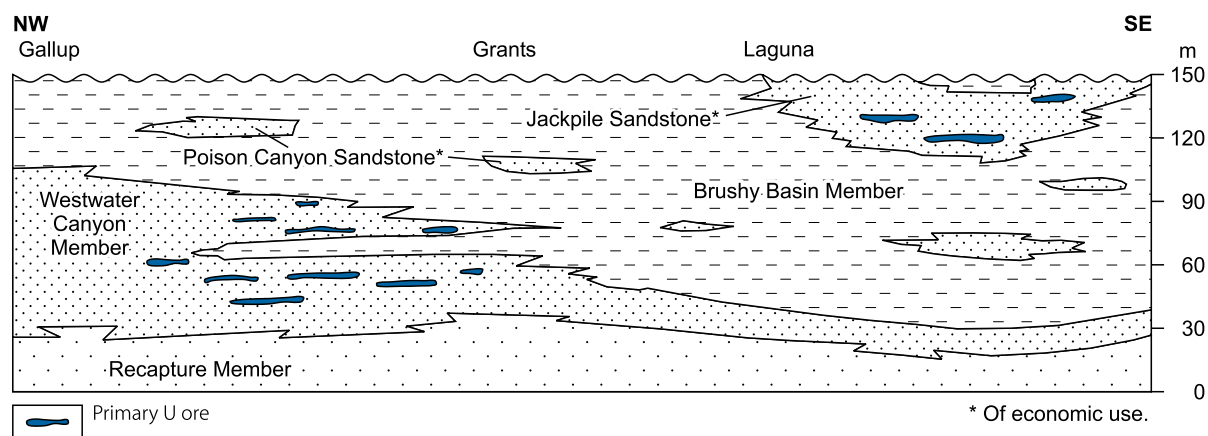
- **Brushy Basin Member**, 6–90 m thick, thickening to north and east. It consists mainly of lacustrine, greenish-grey mudstone with widespread, in part rather thick, intercalations of crossbedded feldspathic sandstone. The predominant clay mineral is montmorillonite derived by devitrification of volcanic ash (for other clay minerals see Chap. Principal Host Rock Alteration). Turner-Peterson (1985) separates the Brushy Basin Member laterally into four depositional facies

Fig. 1.5. Grants Uranium Region, schematic stratigraphic W-E profile from Gallup in the west to Laguna in the east (Condon and Peterson 1986) (AAPG 1986, reprinted by permission of the AAPG whose permission is required for further use)



■ Fig. 1.6.

Grants Uranium Region, schematic NW–SE stratigraphic section of the Morrison Formation along the southern part of the mineral belt illustrating the distribution of uranium mineralization and the interrelationship of host sandstone units (location see Fig. 1.1.0-1A). (After Turner-Peterson and Fishman 1986 based on Hilpert 1963)



- between the margin and the center of the former Brushy Basin lake: alluvial plain, mudflat, playa margin, and central playa facies (Figs. 1.8 and 1.9).
- Two uranium mineralized sandstone units are assigned to the Brushy Basin Member:
 - Jackpile Sandstone, up to 70 m thick, located in the eastern and topmost section of the Brushy Basin Member. It hosts U deposits in the Laguna district
 - Poison Canyon Sandstone, up to 25 m thick, hosting deposits in the Mount Taylor and some in the Ambrosia Lake districts.
- Westwater Canyon Member** is the host for ore bodies in most of the districts of the Grants region. The Westwater Canyon Member is 15 m thick in the Laguna district and thickens to 80 m in the Ambrosia Lake district. Locally it can be as much as 100 m thick. It is composed of buff to grey, poorly sorted, crossbedded, fine- to very coarse-grained arkose to feldspathic sandstone with local intercalations of grey, often montmorillonitic mudstone. It contains variable amounts of humate and organic plant material. Minor amounts of heavy minerals are common (Cadigan 1967; Adams et al. 1974). The Westwater Canyon Member interfingers with the Brushy Basin sediments and is locally intercalated with a thin pelitic horizon, designated as “K-Shale.”
- Recapture Member**, 10–60 m thick, consists of alternating beds of grey sandstone and grey to maroon silt- and mudstones, which interfinger with Westwater Canyon sandstones.

Sandstone interbeds of the Morrison Formation are generally cross-bedded, coalesced, thick tabular units with scoured basal surfaces. Sedimentological features and associated facies and their relationships indicate that the clastic sediments were deposited in fluvial, overbank, and lacustrine environments.

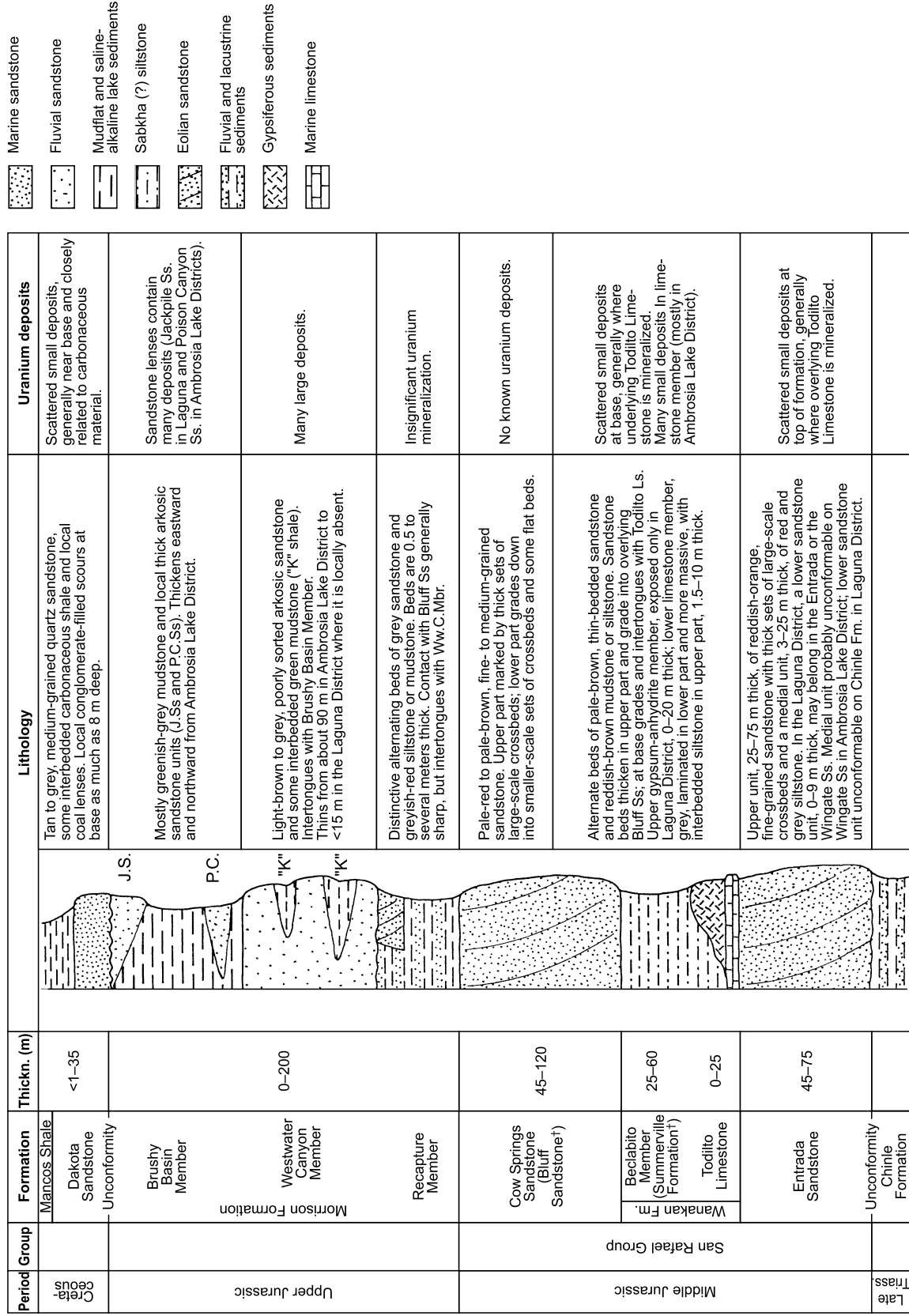
Adams and Saucier (1981) report the lithologic composition of ore-hosting sandstones of both the Westwater Canyon and Brushy Basin members as ranging from 30 to 99% quartz, 2 to 24% feldspar, 9 to 16% clay-minerals, 1 to 35% rock fragments,

and trace to 0.5% heavy minerals. The sandstones contain widespread but irregularly distributed plant remains in the form of silicified and/or carbonized logs, branches, leaves, and grass. Humate impregnates the sandstones in large, blanket-like masses and averages about 0.1–0.25% in weight. The sandstones have variable amounts, up to 5% of pyrite when reduced, and hematite and/or limonite when oxidized (Knox and Gruner 1957). The Westwater Canyon sandstone contains 5–15 ppm uranium when reduced and 1–2 ppm uranium when oxidized (Brookins 1979).

Galloway (1980) interprets the Westwater Canyon depositional environment as a wet alluvial fan derived by rivers flowing between NE and SE from a source in the SW (Fig. 1.10). This is indicated by the occurrence of coarsest sandstone and the thickest part of the fan near the SW margin of the San Juan Basin. Their source was probably either the ancient Zuni or Mogollon highlands, which provided the igneous and metamorphic material for the Westwater Canyon alluvial fan, complemented by widespread volcanic ash-fall material. The more proximal part of the fan has been truncated by late Jurassic to late (?) Cretaceous pre-Dakota erosion. The proximal to mid-section of the fan consists of braided bed-load channel facies, which grades down-fan into straight bed-load, sinuous mixed-load, and finally distributary mixed-load channel facies at the distal front system. All major uranium deposits occur in the mid-fan facies.

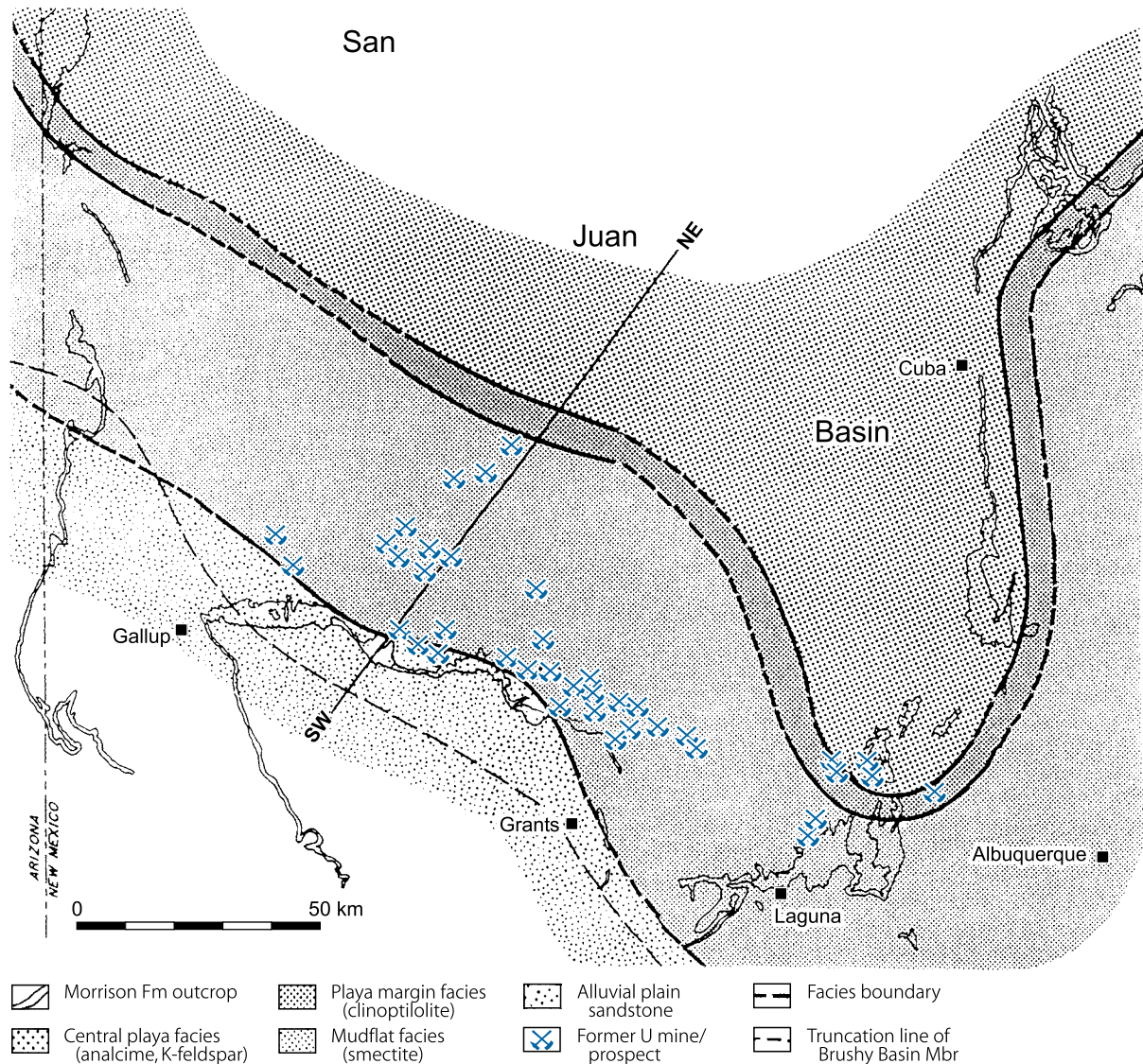
Chimney-like breccia pipes constitute interesting, structural phenomena, hundreds of which have been found between Laguna and Gallup. The pipes are most numerous in the Cow Springs Sandstone and the Beclabito Member/Wanakah Formation but are also common in the Morrison Formation where they may carry uranium mineralization in several places. In the Laguna area, the pipes are mainly concentrated in linear belts, which follow the flanks of pre-Dakota folds in the Todilto Limestone. As many as 65 pipes have been found here in trends up to 5 km long. In the Grants area, the greatest concentration of pipes is found around Haystack Butte where there is no clear relationship to folds or faults.

Fig. 1.7. Grants Uranium Region, columnar section showing the stratigraphic position of U deposits and lithologies of the Middle and Upper Jurassic rocks. (* indicates former names). (After Adams and Saucier 1981, Turner-Peterson and Fishman 1986, description after Hilpert 1963)



■ Fig. 1.8.

Grants Uranium Region, generalized map of facies distribution for the Brushy Basin Member of the Jurassic Morrison Formation and the location of major U deposits. The facies pattern indicates the development of an alkaline-saline lake in a closed basin during Brushy Basin Formation time. (After Turner-Peterson and Fishman 1986 based on Turner-Peterson 1985; AAPG 1985, reprinted by permission of the AAPG whose permission is required for further use)



Principal Host Rock Alteration

Alteration phenomena include reduction, oxidation, montmorillonitization, kaolinitization, chloritization, sulfidization, Na metasomatism, and destruction of detrital feldspar, magnetite, and ilmenite.

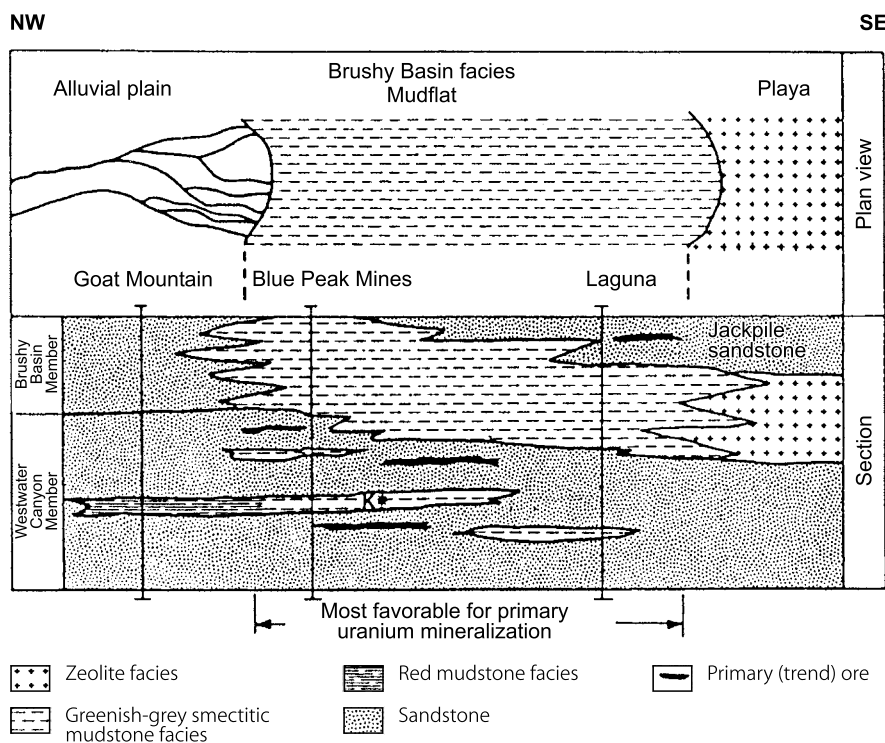
The bulk of the Westwater Canyon sandstone and the Brushy Basin sandstone lenses are reduced due to diagenesis under reducing conditions. Geological evidence suggests that these sandstones, at least some of them, experienced oxidation and re-reduction in pre-Dakota time. Reduction or re-reduction presumably occurred in conjunction with humate formation from originally water-soluble organic substances, probably of plant origin.

Early alteration of pyroclastic material produced montmorillonite, smectite, illite, and mixed layer clays. The process overlapped in part with the reduction of portions of ore hosts, in particular of the upper part of the Westwater Canyon sandstones and of the entire Jackpile Sandstone. Reduction destroyed the detrital magnetite and ilmenite with local replacements by pyrite (Figs. 1.11 and 1.12).

In a *subsequent stage*, but partly overlapping the destruction of ilmenite and magnetite, humic material together with uranium precipitated in the Westwater Canyon sands, where they are overlain by the Brushy Basin mudflat facies mentioned earlier. Typically, reduced sands contain humate often in large quantities as well as detrital organic matter and pyrite.

Fig. 1.9.

Grants Uranium Region, diagrammatic section extending from the southern part of the Ambrosia Lake district in the NW to the Laguna district in the SE, illustrating the relationship of U-mineralized sandstone in the Westwater Canyon Member and the Jackpile sandstone to sedimentary facies in the Brushy Basin Member and "K" shales. The zone overlain by greenish-grey mudstone/mudflat facies is supposedly the most favorable for U mineralization in the Morrison Formation sandstone. Similarly, facies changes in the "K" shale appear to be also a significant factor as suggested by the position of mineralization in the Goat Mountain-Blue Peak mines area. (Turner-Peterson 1985; AAPG 1985, reprinted by permission of the AAPG whose permission is required for further use)



The alteration and replacement of feldspars, including albitization and probably the replacement of sodium by potassium in an outer shell of sanidine grains (Austin 1980), developed locally within the Jackpile Sandstone, and in a wider range within the Westwater Canyon sandstones. Clay coatings of various compositions formed within sandstones in proximity to uraniumiferous carbonaceous material. Subsequent to the formation of ore lenses, baryte and calcite precipitated and kaolinite crystallized as nests within the sands. Figure 1.13 shows the paragenetic sequence of the various alteration events.

In a later, *post-Laramide alteration stage*, Morrison sandstones were affected by a regional oxidation front, which advanced from the southern outcrop zone of the Morrison Formation into the San Juan Basin. The oxidation zone extends from the outcrop for a few to 25 km downdip as indicated by the red hematitization of the sandstone. At its distal front, it grades into a zone of brown limonitic sandstones, less than 1 km to several kilometers wide, which borders downdip reduced grey sandstones.

The spatial distribution of oxidation varies greatly due to local changes in and to the discriminative gross permeability of sandstone bodies. Sandstone lenses embedded in impermeable mudstone, such as found in the Brushy Basin Member, may still be unoxidized at the outcrop. In contrast, the underlying more continuous sandstone horizons of the Westwater Canyon Member may be oxidized many kilometers downdip from the

outcrop, but also enclose remnant islands of unoxidized sandstones where local conditions prohibited oxidation.

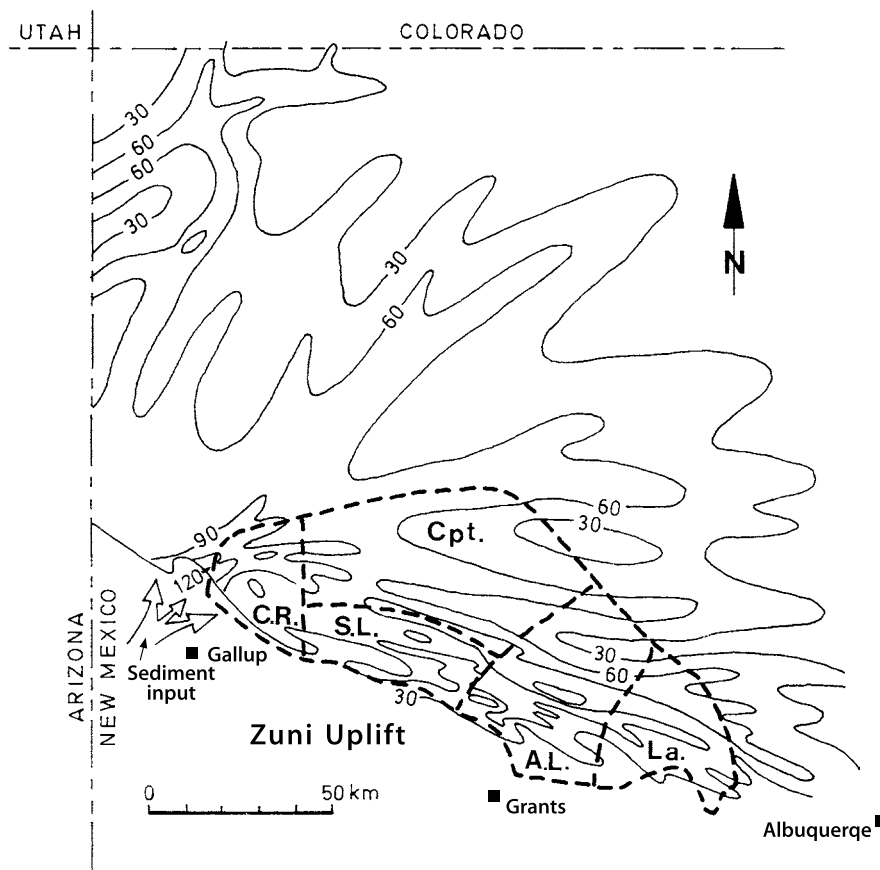
In more detail, the following alteration characteristics are noted. Albite replacement rims surround detrital feldspar grains. Authigenic clay coats detrital clasts within and immediately adjacent to uraniumiferous humate lenses. These clays are dominantly illite-montmorillonite in the Jackpile Sandstone, and dominantly chlorite or a mixed-layer chlorite phase in the Westwater Canyon sandstone at the Ambrosia Lake. Montmorillonite rims and clasts are altered to Mg chlorite. The montmorillonite is supposedly derived from an alteration of volcanic ash.

Hansley (1986a, b) and Reynolds et al. (1986) document alteration patterns of feldspars and Fe-Ti oxides in the Westwater Canyon sandstones. The strongest alteration of these minerals is proximal to the Brushy Basin pelites and limited to those of the mudflat facies (Figs. 1.11 and 1.12). With increasing vertical distance to the Brushy Basin contact, the intensity of alteration decreases. Turner-Peterson (1986) remarks that in the Jackpile Sandstone, similar alteration patterns occur extending from the intervening Brushy Basin mudstone into the overlying and underlying sand units with decreasing alteration intensity at greater distance from the Brushy Basin mudstone facies.

Riese et al. (1980) analyzed authigenic minerals in the Westwater Canyon Member. They conclude from their findings that compositional variations exist within and adjacent to

■ Fig. 1.10.

Grants Uranium Region, interpretive isolith map of the Westwater Canyon Member of the Jurassic Morrison Formation and location of the main uranium districts. The arrows to the southwest indicate the direction of sediment input (isopachs in meter, contour interval is 30 m). (After Galloway 1980)



uranium mineralization: Montmorillonite is the dominant clay mineral formed downdip of an ore body, chlorite is enriched in the ore zone, and kaolinite and altered montmorillonite are enriched on the updip side.

Whitney (1986) reports preliminary results on the distribution pattern of clay minerals in the Morrison Formation based on samples from the Crownpoint area: (a) Pure smectite coats grains in the Westwater Canyon Member in the shallowest sections; the smectite exhibits a similar texture as mixed-layer illite-smectite in deeper sections. (b) Expandability of the illite-smectite decreases laterally toward the basin center and is, in a vertical section, greater proximal to the upper and lower sandstone-mudstone contacts than at the center of a sandstone bed. (c) Fe chlorite formed texturally on top of the smectite and illite-smectite reflecting a post smectite origin. (d) Smectite in the Brushy Basin and Recapture members remain 100% expandable. (e) Kaolinite developed as the latest clay species; kaolinite abundance is highest in the middle section and decreases in the shallower and deeper sections.

Bell (1986) established a lateral zoning of facies-related clay mineral patterns in the Brushy Basin Member, which formed in response to the early diagenetic hydro-geochemical alteration of volcanic ash and saline-alkaline lake sediments. (a) Greenish-grey mudstone of the mudflat facies contains smectite formed by

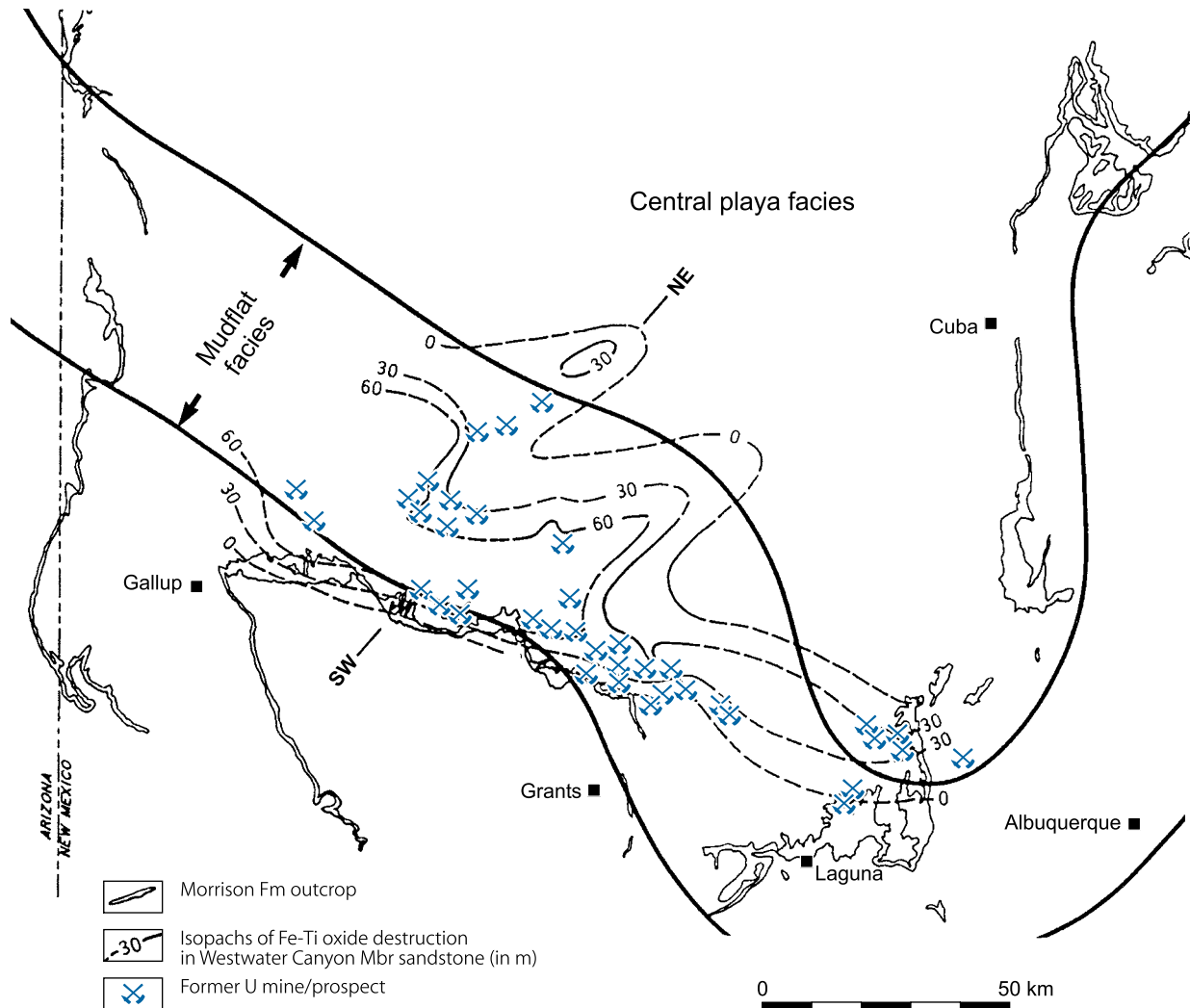
the alteration of volcanic ash in marginal zones of the former lake where a recharge of fresh water created an environment of pH 7–8.5. (b) More basinward from the mudflat facies where fresh groundwater was less available and the environment was dominated by increasing alkalinity and salinity, clinoptile formed. (c) At or near the center of the basin, analcime was derived from the alteration of tuffaceous material. Also in the central facies of the Brushy Basin Member, but apparently restricted to the western part of the San Juan Basin, authigenic K feldspar formation has been noted by Turner-Peterson and Fishman (1986).

Principal Characteristics of Westwater Canyon-Brushy Basin Uranium-Humate Mineralization

The bulk of the uranium ore in the Grants Region is in unoxidized deposits. Some minor deposits contain oxidized ore. Reduced deposits are differentiated into primary and redistributed mineralization. In principle, all ore of pre-Dakota age, which is offset by Laramide faults and associated uniformly with humate has been attributed to primary mineralization (also termed pre-fault, blanket, trend, black band, and uraniumiferous humate mineralization). All ore of post-Laramide age, which is

Fig. 1.11.

Grants Uranium Region, compository map of isopachs of Fe-Ti oxide destruction in sandstone beds of the Westwater Canyon Member and main facies of the Brushy Basin Member. Most of the U ore bodies are positioned in the zone of greatest Fe-Ti oxide destruction, which largely extends below the mudflat facies. (After Turner-Peterson and Fishman 1986; AAPG 1986, reprinted by permission of the AAPG whose permission is required for further use)



randomly associated with humate, is termed redistributed mineralization (also named post-fault and stack ore) (explanations see later). Figure 1.14 provides a summary of characteristics of the various types of ore and their litho-stratigraphic distribution, and Fig. 1.15 the structure and the alteration-related position of ore.

The following characteristics of mineralization are summarized from Adams and Saucier (1981) with updates mainly from Granger and Santos (1982, 1986), Holen (1982), and Crawley et al. (1984) as well as other authors as cited.

Reduced mineralization: Principal uranium minerals are coffinite, pitchblende, sooty pitchblende, and black amorphous urano-organic complexes/uraniferous humate. Ore phases are distributed interstitially in the host sandstone and coat sand grains.

- **Primary ore:** Much of the uranium is present in urano-organic compounds/uraniferous humate. Associated minerals include

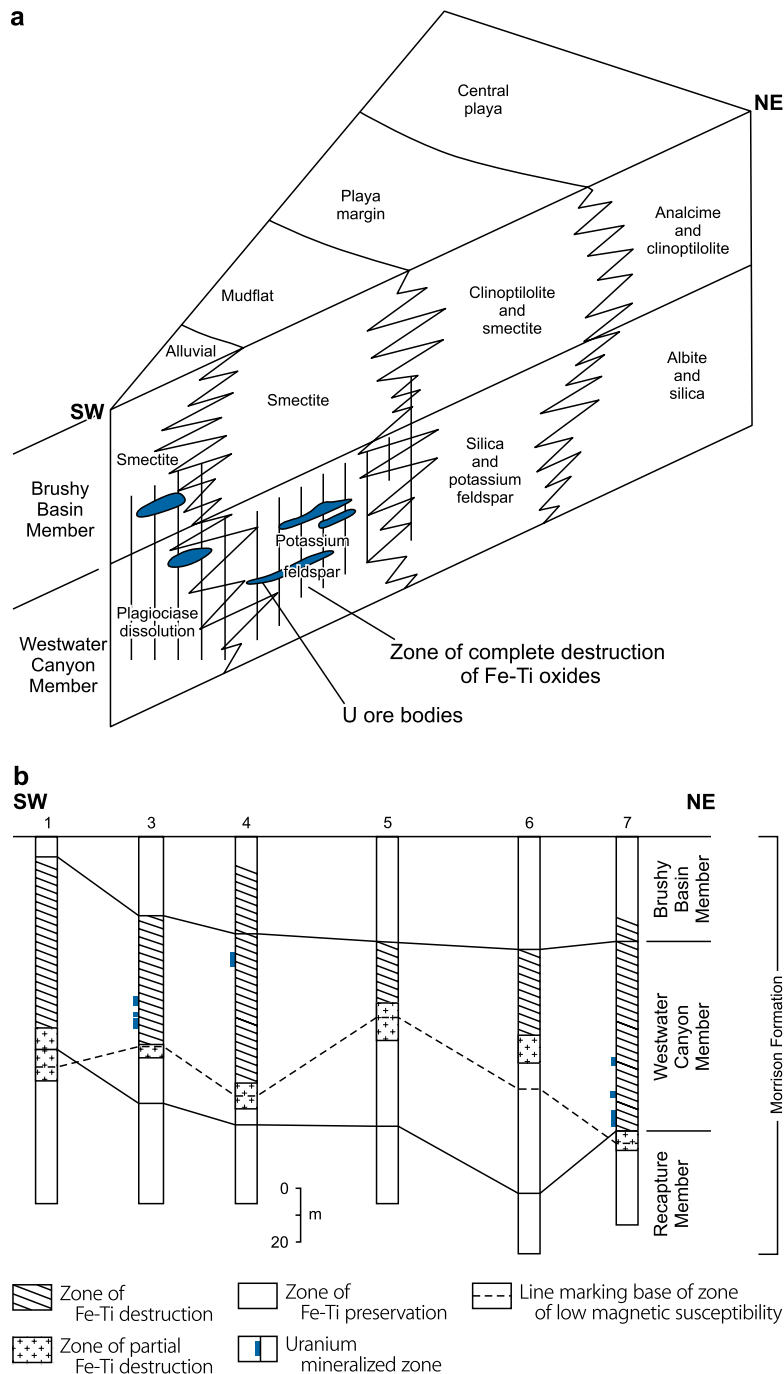
pyrite, marcasite, jordisite, ferroselite, chalcopyrite, galena, wurtzite, calcite, baryte, and kaolinite. Spirakis and Pierson (1986) report elemental enrichments of As, Cu, Fe, Mn, Mo, S, Se, V, Y, and organic carbon along with U. As and V rarely occur in the form of ore minerals in primary mineralization. They appear to be dominantly fixed by humate. Mo and commonly Se form haloes around primary ore zones. V prevails in the western section of the mineral belt

- **Redistributed ore:** Coffinite is the dominant U mineral. Pitchblende is very rare. Associated minerals include monroseite, paramonroseite, haggite, ferroselite, native selenium, pyrite, marcasite, and calcite (Granger and Santos 1986). Mo is practically missing.

Humate is an essential constituent of the primary ore, in which it is coextensive with uranium at a ratio of approximately 1:1 by weight (Granger et al. 1961), whereas in redistributed,

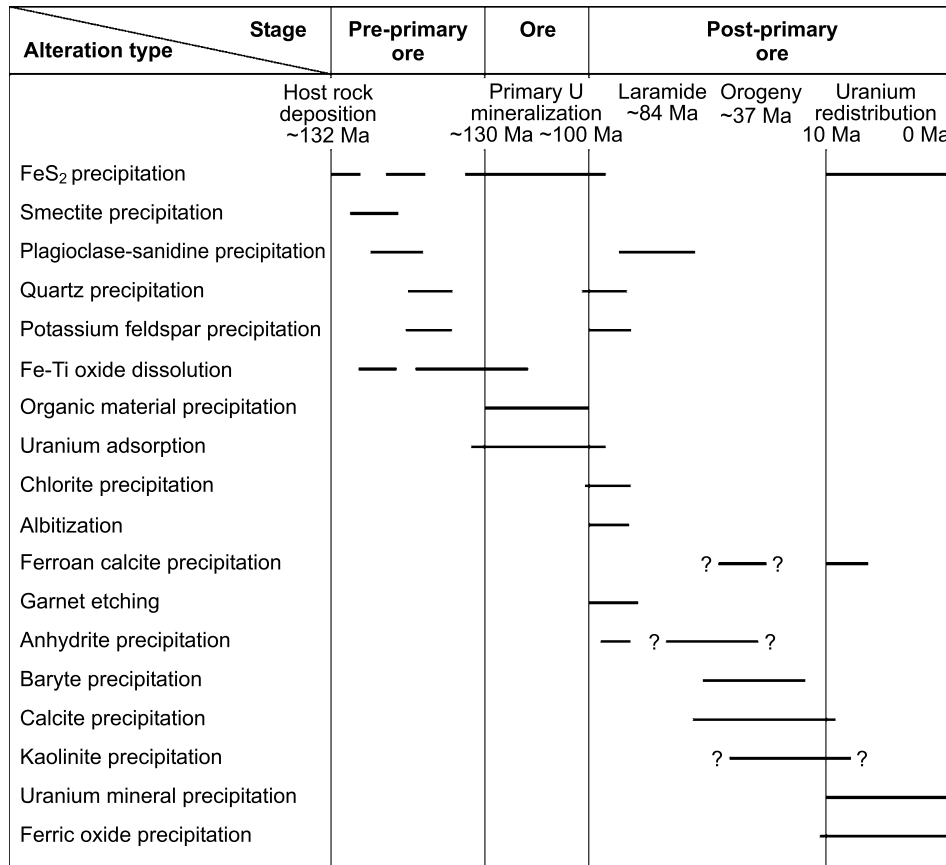
■ Fig. 1.12.

Grants Uranium Region, (a) block diagram illustrating the distribution and relationship of diagenetic alteration minerals/patterns in sandstone of the Westwater Canyon Member, and depositional facies and alteration minerals in the overlying Brushy Basin Member; (b) stratigraphic section showing intervals of destruction of Fe-Ti oxide minerals in the Westwater Canyon and Brushy Basin members. The dashed line marks the base of the zone of low magnetic susceptibility, which corresponds to the boundary between the zone of almost complete destruction of Fe-Ti oxides in the uppermost Westwater Canyon Member and an underlying zone of preservation of these minerals. (After (a) Hansley 1986b, (a and b) Turner-Peterson and Fishman 1986; AAPG 1986, reprinted by permission of the AAPG whose permission is required for further use)



■ Fig. 1.13.

Grants Uranium Region, paragenetic sequence of diagenetic alteration and mineralization events in sandstones of the Morrison Formation. (Turner-Peterson and Fishman 1986; AAPG 1986, reprinted by permission of the AAPG whose permission is required for further use)



unoxidized mineralization the ratio is highly variable, probably due to the discriminative separation of the uranium from humate. Some redistributed ore is virtually barren of organic complexes.

The dominant coffinite is dispersed in an organic phase, which may contain an undetermined amount of uranium in other forms, principally organic compounds. Some primary tabular ore bodies in Ambrosia Lake have scattered patches of jordisite surrounding uraniferous humate. The richest disseminations of jordisite appear to occur below or along edges of ore bodies. Selenium is dispersed in both the uranium ore and the surrounding jordisite ore, but it tends to be more often concentrated along the upper surface of ore layers in unoxidized deposits (Granger et al. 1961).

Redistributed mineralization may be distinguished from primary mineralization by these features: no recognizable vanadium minerals are found in primary ore, whereas montroseite and paramontroseite are common in redistributed ore. Molybdenum is never redistributed, and calcite cement is rare in redistributed ore. Redistributed ore may contain baryte, marcasite, and pitchblende in minor amounts. These minerals are not generally associated with primary ore but are good indicators for nearby oxidation. Selenium is usually in a more distinct zone associated with the oxidation front in redistributed ore.

Spirakis and Pierson (1986) provide geochemical data of ore samples from some districts as given in [Table 1.1](#).

Spirakis and Pierson (1986) note that the comparison of redistributed mineralization of the Church Rock district with primary mineralization from other districts of the Grants region indicates a chemical separation of Ca, Cu, Fe, Mn, Mo, Pb, Se, Sr, Y, and V from U during the redistribution process. Trace amounts of elements such as As, Co, Sb, Ta, Th, and REE are enriched near ore zones. REE is particularly concentrated in ore zone chlorite (Brookins et al. 1977).

Brookins (1980a) reports that trace elements, particularly REE, which occur with uranium mineralization, locally display zoning. REE are depleted in oxidized ground, whereas vanadium, originally precipitated as V³⁺ in chlorites, remains at the original site after oxidation to V⁵⁺. In general, trend ore bodies are characterized by a high content of chlorite and illite, or illite and illite-montmorillonite at variable fractions of these minerals. In contrast, ore near a redox front contains primarily kaolinite.

Oxidized mineralization: Principal ore minerals are uranyl vanadates, -phosphates, -sulfates, -carbonates, subordinately uranyl silicates, and hydrous urano-oxides. Most uranyl carbonates and -sulfates are probably post-mining species. Other associated minerals and elements include pascoite, native selenium, thenardite, thermonatrite, gypsum, Mn oxides, and limonite (Granger 1963; Hounslow 1967; Kittel et al. 1967).

Litho-stratigraphic distribution of uranium mineralization: Unoxidized fluvial sandstones of the upper Morrison Formation are the dominant uranium hosts. They contain almost 98% of all

Fig. 1.14.

Ambrosia Lake area, idealized cross section presenting a summary of features associated with uranium mineralization. (Crawley et al. 1985 based on Holen 1982)

Primary ore

(Also called pre-fault ore, trend ore, black band ore)

- thin – generally < 2.5 m
- higher grade – generally averages >0.20% U
- offset by Laramide-Tertiary faults
- sharp ore to waste boundary
- coextensive with humate and/or carbonized vegetal material
- color – dark grey to black
- age – Pre-Dakota; field relationships indicate that at least some primary ore is immediate post-depositional in age

Redistributed ore

(Also called post-fault ore, stack ore, secondary ore)

- thick – generally > 3 m up to 46 m
- lower grade – generally <0.20% U
- sometimes localized by Laramide-Tertiary faults and fractures
- diffuse ore to waste boundary
- may or may not be associated with humate or carbonized vegetal material
- color varies from dark brownish grey to light grey, probably depending on amount of humic material present
- age – oxidation that resulted in the redistribution of primary ore started after regional uplift and erosion in late Miocene or early Pliocene time and continues to the present

Types of primary ore

A variety of ore body characteristics has resulted in different interpretations of ore habit and genesis. At least three types of primary ore are described in the literature.

1. Blanket ore: undulating blanket with pronounced, ESE-trending thickenings or "rolls"; coextensive with humate; very little vegetal material
2. Channel ore: stronger facies control than blanket type; sometimes follows individual channels from tens of meters to as much as 2 km; associated with more carbonized and silicified vegetal material (plus humate) than blanket ore
3. Wyoming roll-type ore: geometry in plan and cross-section is pre-Dakota age; geometry in plan and cross-section is similar to Wyoming rolls, but upper and lower limbs are generally wider; oxidized interior has been rereduced. Note: Not to be confused with redistributed ore which is also thought to be genetically similar to Wyoming roll ore

- A "Ghost ore bodies"; oxidized environment
- B Remnant primary ore bodies; oxidized environment
- C Redistributed ore bodies at advancing Tertiary-Quaternary oxidation front
- D Primary ore bodies; reduced environment

- E Primary ore bodies in Brushy Basin sand bodies; reduced environment except near outcrop
- F Ore bodies in Todilto Limestone
- G Small ore bodies in fluvial sandstone, or associated with lignitic material, at the base of the Dakota Ss

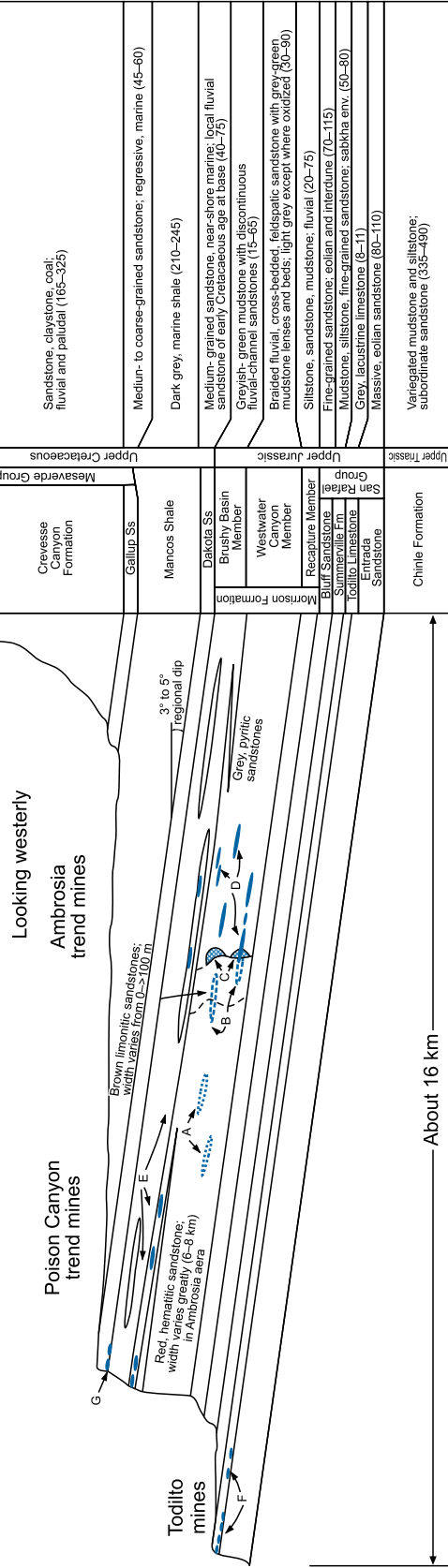
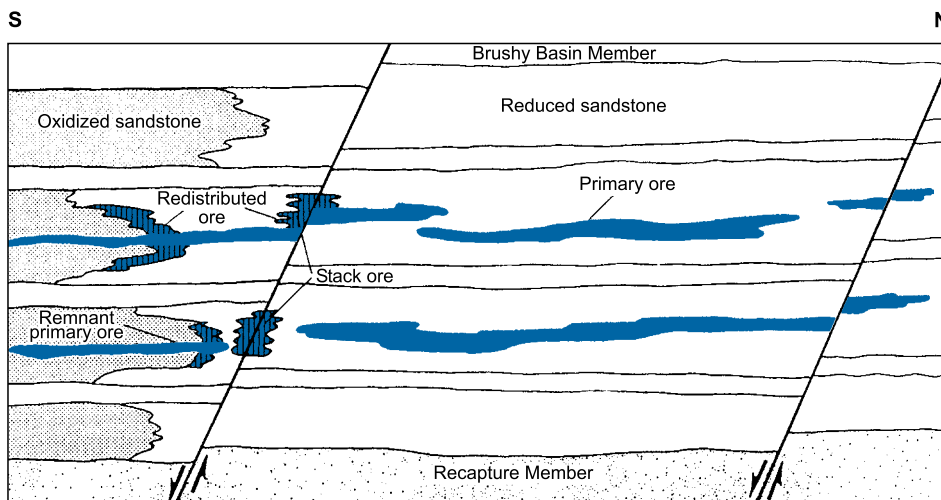


Fig. 1.15.

Grants Uranium Region, diagrammatic S–N section illustrating the structural position and configuration of primary and redistributed U mineralization in the Morrison Formation sandstones. Primary mineralization forms elongate tabular ore lenses suspended within reduced sandstone while redistributed mineralization has accumulated along faults and at the contact between oxidized and reduced sandstones. Remnant primary mineralization occurs as islands within oxidized sandstone. (After Turner-Peterson and Fishman 1986; AAPG 1986, reprinted by permission of the AAPG whose permission is required for further use)



uranium resources in the Grants Uranium Region. Most of the ore occurs within the thickest (up to 100 m) part of sandstone bodies within the *Westwater Canyon Member*. Significant deposits exist in the *Poison Canyon Sandstone*, a sandstone tongue, up to 25 m thick, extending laterally from the upper Westwater Canyon into Brushy Basin sediments in the southern Ambrosia Lake district. The *Brushy Basin Member* contains major ore bodies in the *Jackpile Sandstone* (up to 70 m thick), in the Laguna district, and in other sandstone lenses in the Ambrosia Lake and Smith Lake districts. Other formations including the Late Cretaceous *Dakota Sandstone*, which directly overlies the Morrison Formation, and the Jurassic *Todilto Limestone* and the Jurassic *Entrada Sandstone*, which underlie the Morrison Formation, contain only small deposits. These other formations account for some 2% of the total resources.

Many, but not all, of the Grants region deposits are found in the vicinity of the redox boundaries between red to brown hematitic and limonitic sandstone updip and grey pyritic sandstone downdip. Crawley et al. (1984) note that perhaps 80% of the known ore bodies, both primary and redistributed, are within a kilometer or two of an oxidation front, but significant primary deposits also occur many kilometers downdip from the redox front.

Primary and redistributed mineralization in reduced Westwater Canyon–Brushy Basin sandstones can also be distinguished by geometric habit and distributional preferences (see Fig. 1.20a–d for geochemical patterns of the ore types). These characteristics permit a further differentiation into subtypes as described by Holen (1982).

Primary mineralization may be subdivided into three categories: peneconcordant ore, including blanket and channel ore, roll-type ore, and perhaps breccia pipe ore.

(a) **Peneconcordant** ore bodies (Figs. 1.15–1.18, 1.19a, b) are undulating, relatively thin, tabular, or sheet-like lenses suspended subparallel to the sandstone stratification (blanket ore). The contact of the ore with the barren rock is sharp and is usually marked by an abrupt color change from dark grey to light grey or yellowish-white country rock. Mineralized blankets thicken locally to ore pods, also called “rolls” (not to be mixed up with Wyoming-type rolls). Axes of “rolls” trend generally ESE–WNW, subparallel to the direction of sediment transport. They may be isolated or connected by a thin filament of mineralization. Ore pods often appear to be simply crenulations in the blanket. These “rolls” occur where the mineralized blanket cuts sharply across sandstone bedding to a different elevation. In cross section, the step up resembles a flattened S, where mineralization in sandstone is not only thicker but is often higher in grade.

In many cases, mineralization is elongated parallel to WNW–ESE-trending axes of sandstone lenses, i.e. it parallels the orientation of the sedimentary transport direction, as expressed by channel scours, cross-bedding, log orientations, etc., in the host rock (channel ore).

(b) **Roll-type** ore bodies (Fig. 1.19c) are well-developed in the Smith Lake and the Crownpoint districts. They are C-shaped similar to rollfront deposits in the Wyoming Basins but with wider upper and lower limits. Ore occurs entirely in re-reduced sediments. C-roll mineralization is interpreted to have been formed by pre-Dakota oxidation fronts (Holen 1982), which mobilized uranium and reconcentrated it within the primary ore bed. The C-shape geometry in cross section is due to groundwater drag along the upper and lower contacts of the sandstone unit. Roll-type mineralization exists only where preexisting primary ore was available for

Table 1.1.

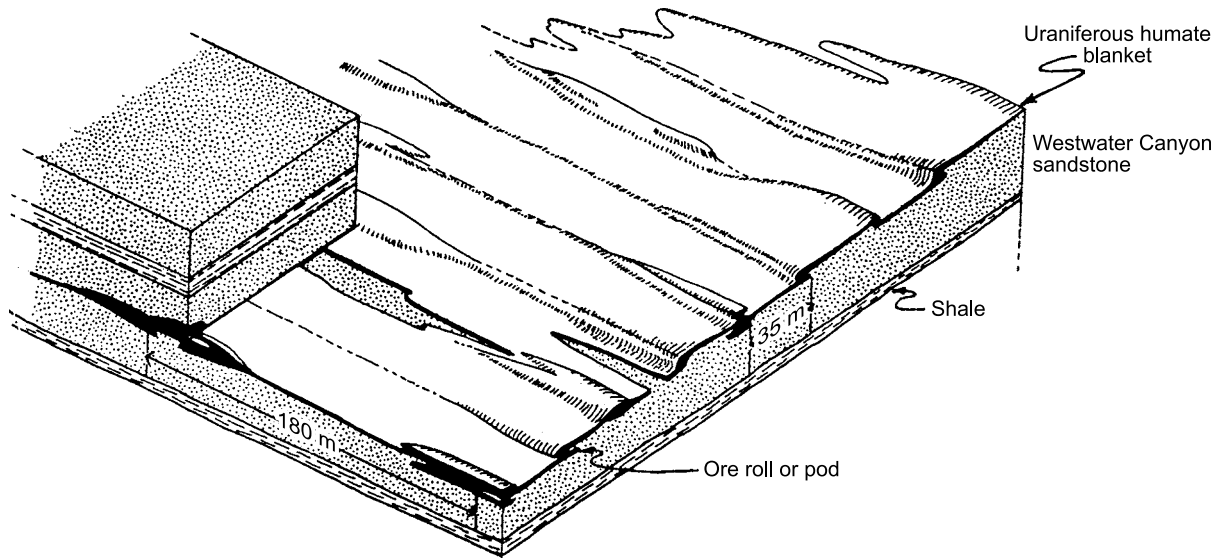
Grants Uranium Region, geochemical composition of uranium mineralized samples from the principal mining districts

Element	Church Rock ¹	Smith Lake District		Ambrosia Lake District ⁴			Laguna District
		Mariano Lake ²	Ruby ³	Primary	Secondary	Mudstones	Jackpile ⁵
Values in percent							
Fe	0.74 (0.89)	1.67 (0.85)	1.19 (0.55)	0.96 (0.77)	0.82 (0.77)	1.87 (2.65)	0.22 (0.14)
Mg	0.16 (0.23)	0.14 (0.12)	0.18 (0.13)	0.21 (0.17)	0.16 (0.17)	1.05 (1.40)	0.08 (0.04)
Ca	0.18 (0.36)	0.21 (0.15)	0.96 (0.31)	1.19 (0.40)	1.93 (0.40)	0.68 (0.79)	0.12 (0.05)
Ti	0.09 (0.11)	0.13 (0.12)	0.10 (0.12)	0.10 (0.10)	0.09 (0.10)	0.24 (0.23)	0.08 (0.07)
Al	4.55 (4.43)	5.55 (5.31)	5.27 (4.85)	3.55 (3.60)	4.20 (3.60)	5.11 (6.38)	1.5 ^b (-)
Na	0.96 (0.67)	0.81 (0.74)	1.22 (1.32)	1.15 (0.63)	1.19 (0.63)	0.76 (0.64)	0.3 ^b (-)
K	2.52 (2.33)	2.74 (2.47)	3.09 (3.14)	2.41 (2.41)	2.44 (2.41)	2.71 (2.80)	1.5 ^b (-)
Total C	- (-)	- (-)	0.65 (0.06)	0.60 (0.14)	0.36 (0.14)	0.27 (0.09)	- (-)
Org C	- (-)	0.30 (0.02)	0.43 (0.05)	0.32 (0.065)	0.048 ^a (0.065)	0.33 (0.048)	- (-)
Min c	- (-)	- (-)	- (-)	0.17 (0.035 ^a)	0.40 (0.035 ^a)	0.060 (0.086)	- (-)
Fe	- (-)	0.83 (0.41)	0.57 (0.65)	2.80 (0.62)	- (-)	- (-)	- (-)
FeO	- (-)	0.67 (0.47)	0.53 (0.10)	- (-)	- (-)	- (-)	- (-)
Total S	0.045 (0.011)	0.49 (0.07)	0.27 (0.01 ^a)	0.55 (1)	- (-)	- (-)	- (-)
Element	Values in parts per million						
Mn	81.4 (154.3)	82 (43)	355 (249)	264 (174)	226 (174)	356 (109)	55.3 (12.7)
Ba	811 (664)	820 (782)	907 (1,052)	669 (560)	826 (560)	394 (386)	617 (300)
Be	1.19 a (89a)	1.27a (-)	188 (175)	1.08a (0.65a)	0.54a (65a)	3.78 (1.69)	1.5b (-)
Co	0.72a (0.42a)	1.50a (-)	3.38a (1.29a)	- (-)	- (-)	- (-)	7.0a (-)
Cr	- (-)	4.58 (5.92)	- (-)	5.21 (7.77)	4.95 (7.77)	14.6 (21.5)	3.0b (-)
Cu	4.39 (5.53)	6.21 (5.08)	5.12 (4.22)	8.46 (4.10)	7.6 (4.10)	20.8 (19.8)	6.19 (3.58)
Mo	- (-)	27 (5.5a)	1.67a (-)	21.8a (5.10)	3.6a (5.10)	570 (7.2)	3.0b (-)
Ni	2.45a (4.39a)	1.48a (-)	4.40 (3.58)	- (-)	- (-)	- (-)	- (-)
Pb	21.4 (~20)	38 (12.9)	21a (5.9a)	45 (13.4)	12a (13.4)	77.2 (12.4)	32.8 (-)
Sr	108 (130)	98 (78)	178 (124)	177 (94)	196 (94)	229 (361)	29.3 (9.5)
V	117 (37)	808 (106)	642 (185)	634 (52)	1,517 (52)	1,166 (98.7)	482 (49)
Y	7.16 (9.61)	18 (-)	18 (10.8a)	16.3 (13)	11.5a (13)	14.4 (33.2)	7.0
Zr	- (-)	120 (99)	113 (28a)	93 (112)	83(112)	107 (161)	108 (100)
Ga	5.85a (4.90a)	9.6 (7.83)	10 (3.9a)	4.42 (9.9)	3.76a (9.9)	18.49 (9.46)	- (-)
Yb	- (-)	1.88 (1.14)	0.89a	- (-)	- (-)	- (-)	- (-)
Se	- (-)	20.4 (9.49)	11.57 (1.89)	59.65 (7.65)	15.4 (7.65)	79.9 (6.7)	1b (-)
U	1,487 (32)	1,280 (42)	1,068 (28)	1,817 (18)	1,273 (18)	606.6 (17.1)	1,500 (29)
As	- (-)	23.1 (3.67)	5.36 (1.40)	38 (-)	- (-)	- (-)	20b (-)
eqU	974 (292)	- (-)	1,505 (89)	1,828 (19)	1,103 (19)	1,414 (47.3)	- (-)

Geometric means for sample suits containing >100 ppm U; values in parentheses next to each sample are the amounts of that element in the background sets (Spirakis & Pierson 1986 based on ¹Spirakis et al. 1983, ^{2,3}Pierson et al. 1983, ⁴Spirakis et al. 1981, ⁵computed from data for 50 samples from Moench & Schlee 1967, ^a data may be in error, ^b indicates mean from mill pulp data from Moench & Schlee 1967, - no data or inconclusive data)

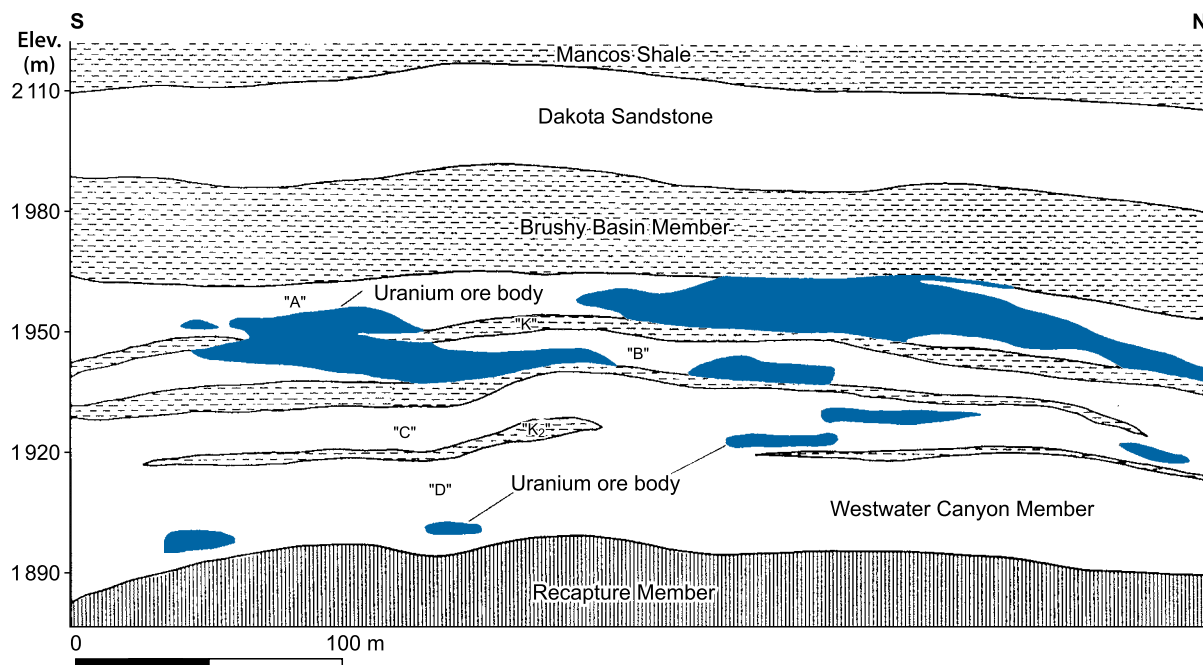
■ Fig. 1.16.

Ambrosia Lake district, south trend, diagrammatic block diagram of a primary, pre-fault ore blanket illustrating the various shapes of this type of mineralization. (After Adams and Saucier 1981 based on Roeber 1972)



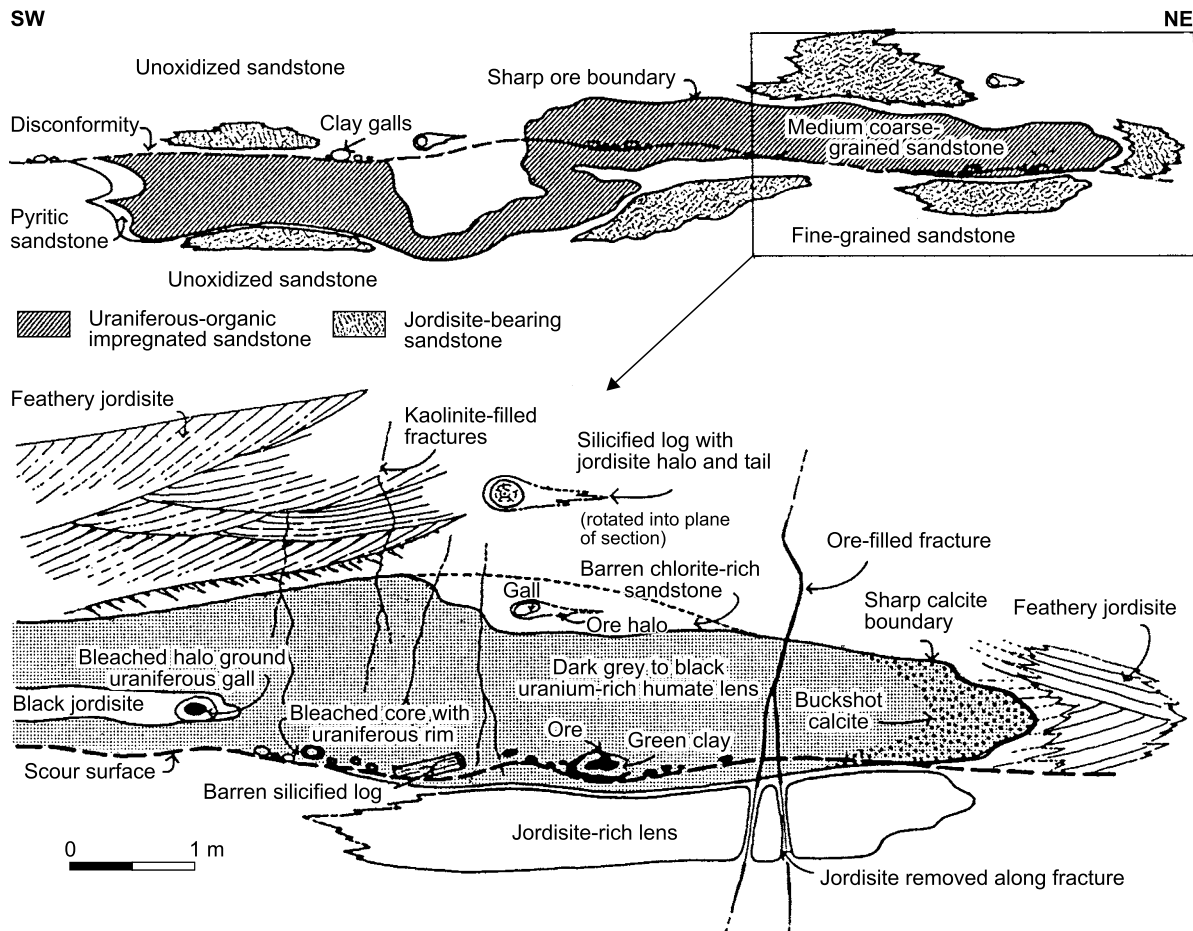
■ Fig. 1.17.

Ambrosia Lake district, Section 30 mine, S–N cross section showing the distribution of U ore lenses in the Westwater Canyon Member sandstone and their relationship to interbedded and over- and underlying less permeable sediments. (After Clary et al. 1963)



■ Fig. 1.18.

Ambrosia Lake district, Ann Lee and Section 27 mines, composite diagram of features associated with mineralization. (After Adams and Saucier 1981 based on Squires 1970, Kendall 1971)



remobilization. The reprecipitation of uranium usually occurred within 300 m or less, and probably not farther away than about 1,000 m from its origin

Holen (1982) attributes roll-type ore to primary mineralization, probably for its supposed pre-Dakota formation and its close association with humate. Adams and Saucier (1981), like other investigators, include roll-deposits in the redistributed category. They argue that both mineralogy and chemistry are the same as stack ore. The difference is that C-roll mineralization is stratigraphically rather than structurally controlled

- (c) **Breccia pipe**-hosted mineralization is restricted to those pipes that cut primary ore. Only three of such ore-bearing pipes have been found, the *Cliffside mine*, Ambrosia Lake district, the *Doris mine*, Poison Canyon trend, and the *Woodrow mine*, Laguna district (see Fig. 1.22 in Sect. 1.1.2). The pipes are chimney-like collapse structures, which cut the Westwater Canyon and the Brushy Basin sediments. The pipes are bounded by ring faults and tend to flare outward toward their top, which is below the Dakota unconformity. The center part is composed of down-faulted material. The core may be a massive sandstone lacking any visible texture, or it may be brecciated siltstone in a clayey matrix. Some

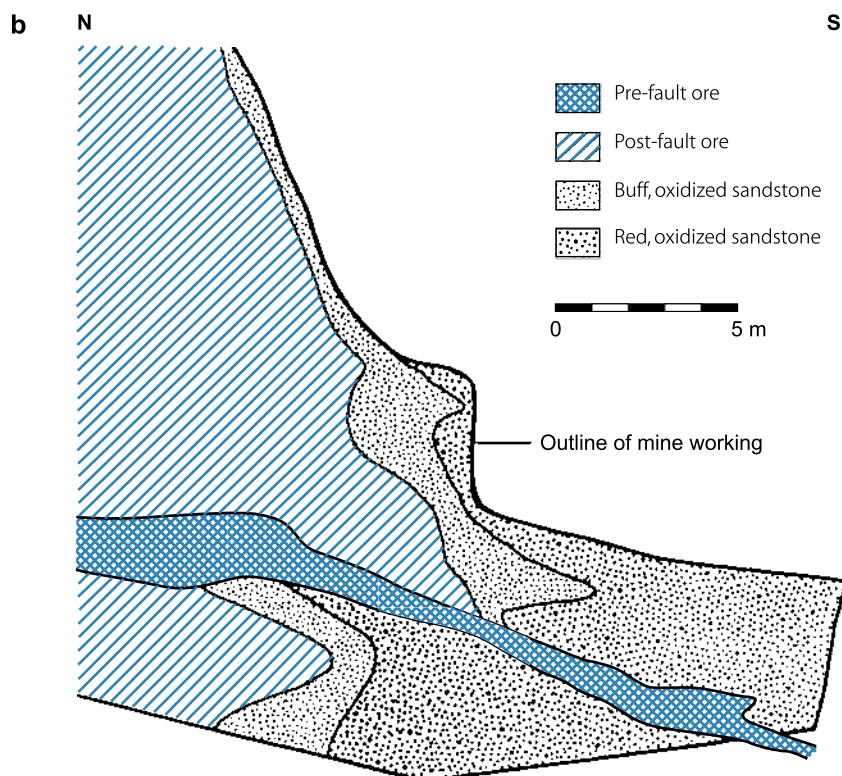
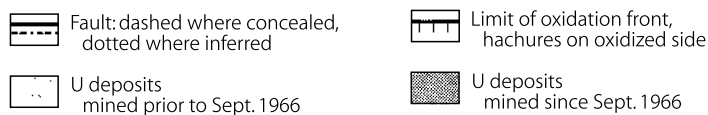
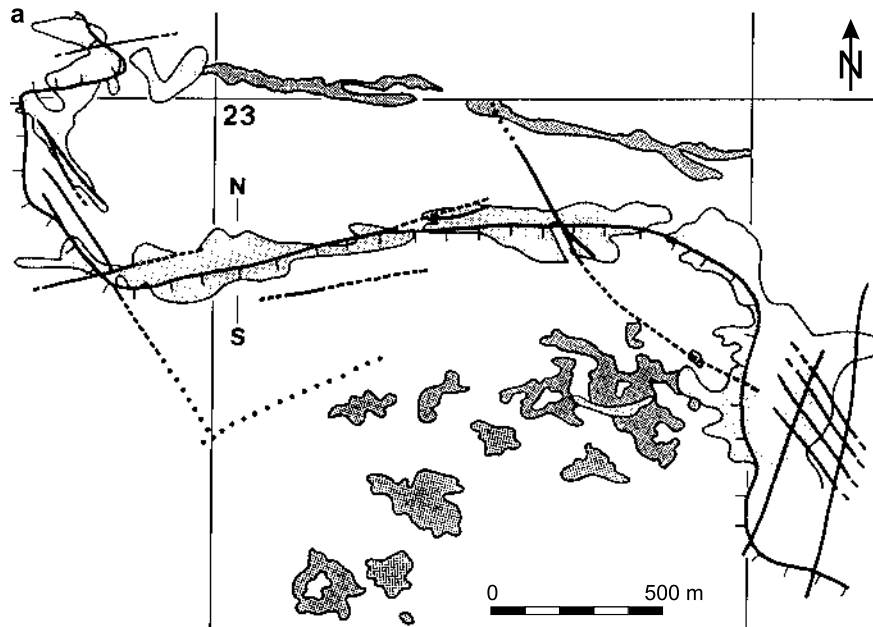
pipe material is better cemented than the surrounding host rock, but most materials show little or no difference in cementation.

Mineralization with grades locally in excess of 1% U is predominantly concentrated in the upper portion of the pipes. It consists of down-faulted blocks of strata-controlled primary ore or redistributed ore as in the *Woodrow pipe*. Remobilized uranium impregnates the breccia matrix. At the *Cliffside mine*, the pipe contains matrix- and structure-controlled ore, whereby ore within the pipe is controlled by NE-SW-striking joints and is thick and of higher grade than correlative ore outside the pipe. This ore seems to have been remobilized and emplaced in conjunction with late Jurassic displacements by the nearby San Mateo fault.

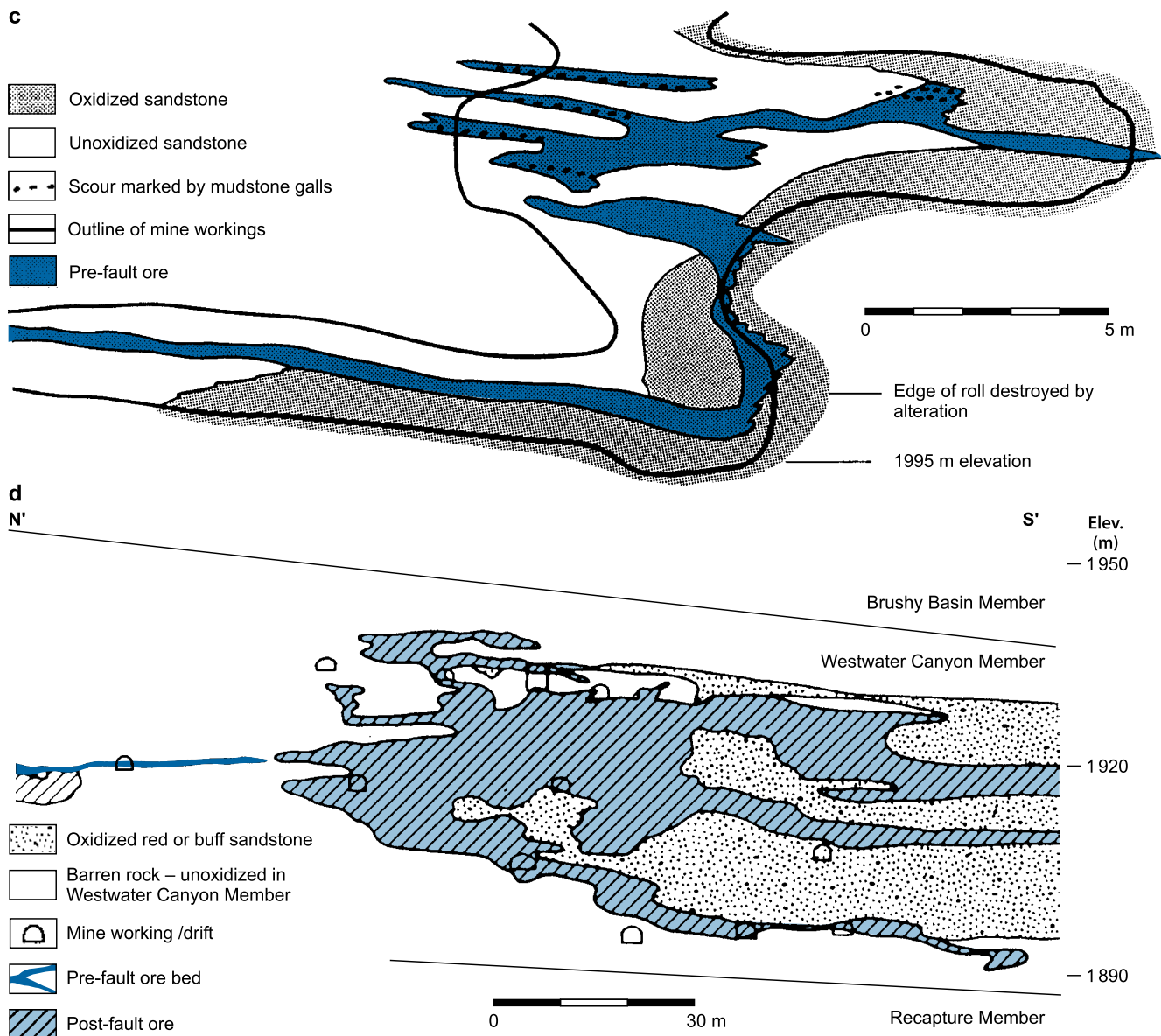
- Redistributed mineralization** (stack and post-fault ore) (Fig. 1.15) is tectonically and lithologically controlled, but, in some cases, it may also be of roll-type configuration (Fig. 1.19b and d). This type of ore is considered to have been formed by the redistribution of primary mineralization, but apparently only in the Westwater Canyon sandstones since no redistributed stack ore has been noticed in the Jackpile or other sandstones.

■ Fig. 1.19.

Ambrosia Lake district, Section 23 mine. (a) Map of distribution and geometry of U ore bodies in Westwater Canyon sandstone. The ESE–WNW-trending ore zone at the northern edge of the mine consists of pre-fault primary mineralization. Mineralization along the redox boundary (line with hachures) is of post-fault, roll-type nature but encloses pre-fault mineralization. Ore bodies within oxidized sandstone are remnants of pre-fault mineralization. (b) Generalized cross section through a variably oxidized sandstone zone illustrating the relationship of post-fault roll- or stack-type mineralization and remnant pre-fault trend mineralization. (c) Cross section of pre-fault, highly irregular S-roll mineralization originally emplaced entirely in reduced sandstone. The undulating oxidation front advanced in post-ore time. (d) N–S cross section showing post-fault, roll-type U mineralization associated with the contact zone of oxidized sandstone. (After Granger and Santos 1986; AAPG 1986, reprinted by permission of the AAPG whose permission is required for further use)



■ Fig. 1.19. (Continued)



Stack ore bodies usually cross-cut sandstone strata concentrating in or along steeply dipping faults of Tertiary age or younger, primarily where oxidized sandstones are in contact with unoxidized (Figs. 1.15 and 1.19a, b, and d). The redistributed ore usually has a relatively sharp updip contact against thick oxidized sandstone. It engulfs the primary blanket ore in reduced strata by impregnating the sandstone above and below the primary blankets. The redistributed ore is darker and richer close to the oxidation front and gradually fades into reduced ground across the fracture zone. Where several ore blankets with primary uranium existed, the redistributed ore can mineralize intervening barren ground creating thick sections of fairly continuous ore.

Stack ore is surrounded by a zone of limonitic and locally bleached rock, which evidently is transitional into red, hematitic sandstone. The width of the limonite zone varies from a few

meters (e.g. at Ambrosia Lake) to many tens of meters (e.g. at Church Rock).

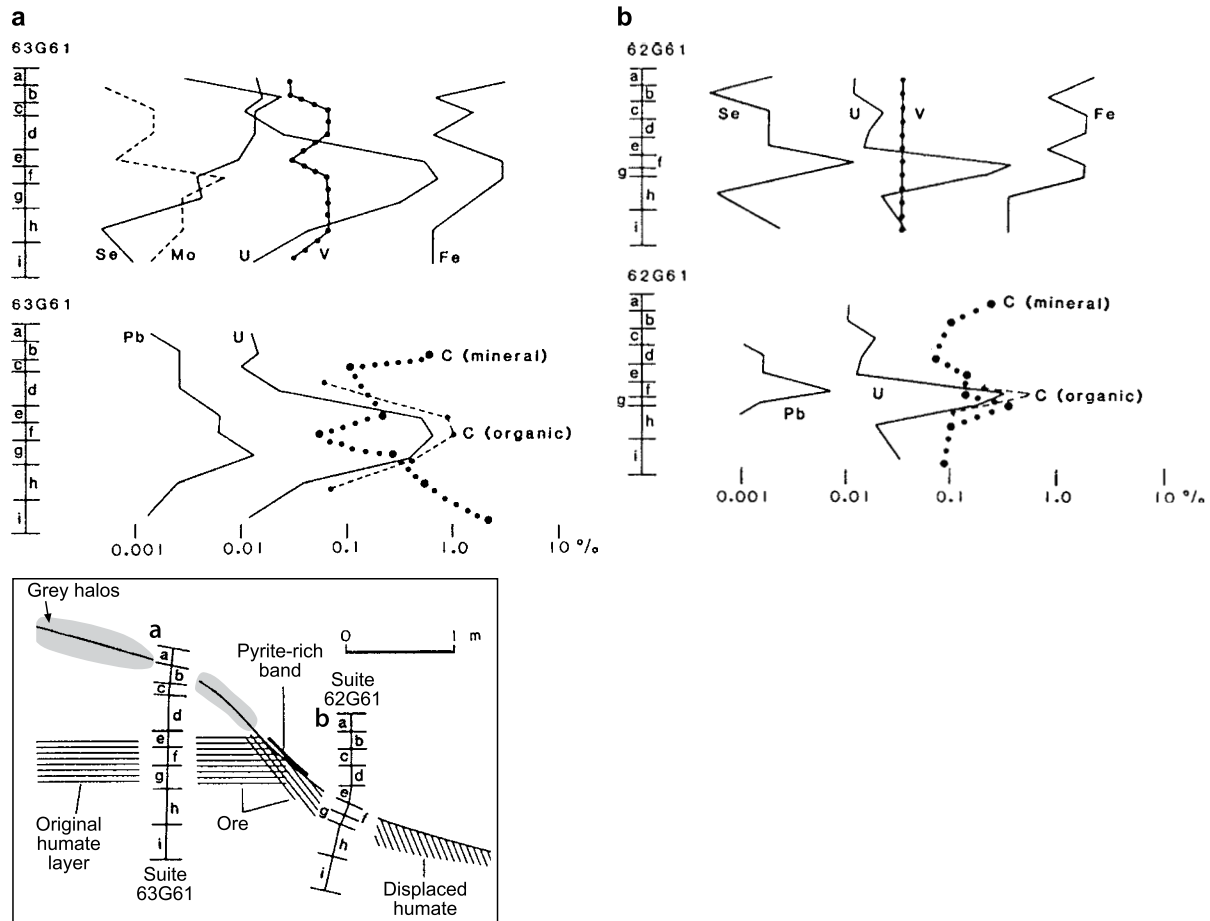
Finally it needs to be mentioned that ore habits are noticed similar to those found in the Salt Wash Member of the Uravan Mineral Belt or in the Chinle Formation where the generally nonoxidized Brushy Basin pelites, which are in depositional continuity with the two principal host sand units, the underlying Westwater Canyon and the overlying Jackpile sandstones pelites, are oxidized.

General Shape and Dimensions of Deposits

Primary mineralization: Blanket and channel ores generally form relatively thin peneconcordant lenses with sharp boundaries between the ore and the barren ground. *Blanket ore* exhibits

Fig. 1.20.

Ambrosia Lake district, Section 23 mine. Quantitative distribution of selected elements across (a) a pre-fault horizontal ore layer, (b) redistributed pre-fault ore layer, (c) oxidized layer, a few meters within the oxidized zone showing the chemical changes caused by oxidation; samples *a* to *g* reflect moderate oxidation while samples *i* to *o* demonstrate much stronger oxidation associated with leaching, as evidenced by the lower ratio of uranium to organic carbon, (d) reduced sandstone layer hosting a pre-fault S-shaped ore roll paralleled by a grey mineralized halo. (After Granger and Santos 1986; AAPG 1986, reprinted by permission of the AAPG whose permission is required for further use)



a more undulating sheet-like shape with WNW-ESE-trending “roll-like” thickenings, whereas *channel ore* is more tabular and elongated, sometimes following individual fluvial sand channels for as much as 2,000 m. Individual ore lenses range from several tens of meters up to about 2,000 m in length, from several meters up to some hundreds of meters in width, and from a few centimeters to over 5 m but usually less than 2.5 m in thickness.

Roll-type ore bodies exhibit C-shapes in cross section. Their upper and lower limits are generally wide and the host rock on the convex updip side has been reduced again.

McCammon et al. (1986) calculated statistical averages for the various configuration modes of primary deposits. At a cutoff grade of 0.084% U, trend-type deposits average a grade of 0.19% U and a resource of 6,150 t U. Corresponding figures for roll-type and remnant-type deposits are 0.14% U and 7,970 t U, and 0.17% U, and 1,145 t U, respectively.

Three *breccia pipes* containing uranium ore bodies have been discovered. The pipes range from a few decimeters to more than 25 m in diameter. Their vertical extension can be up

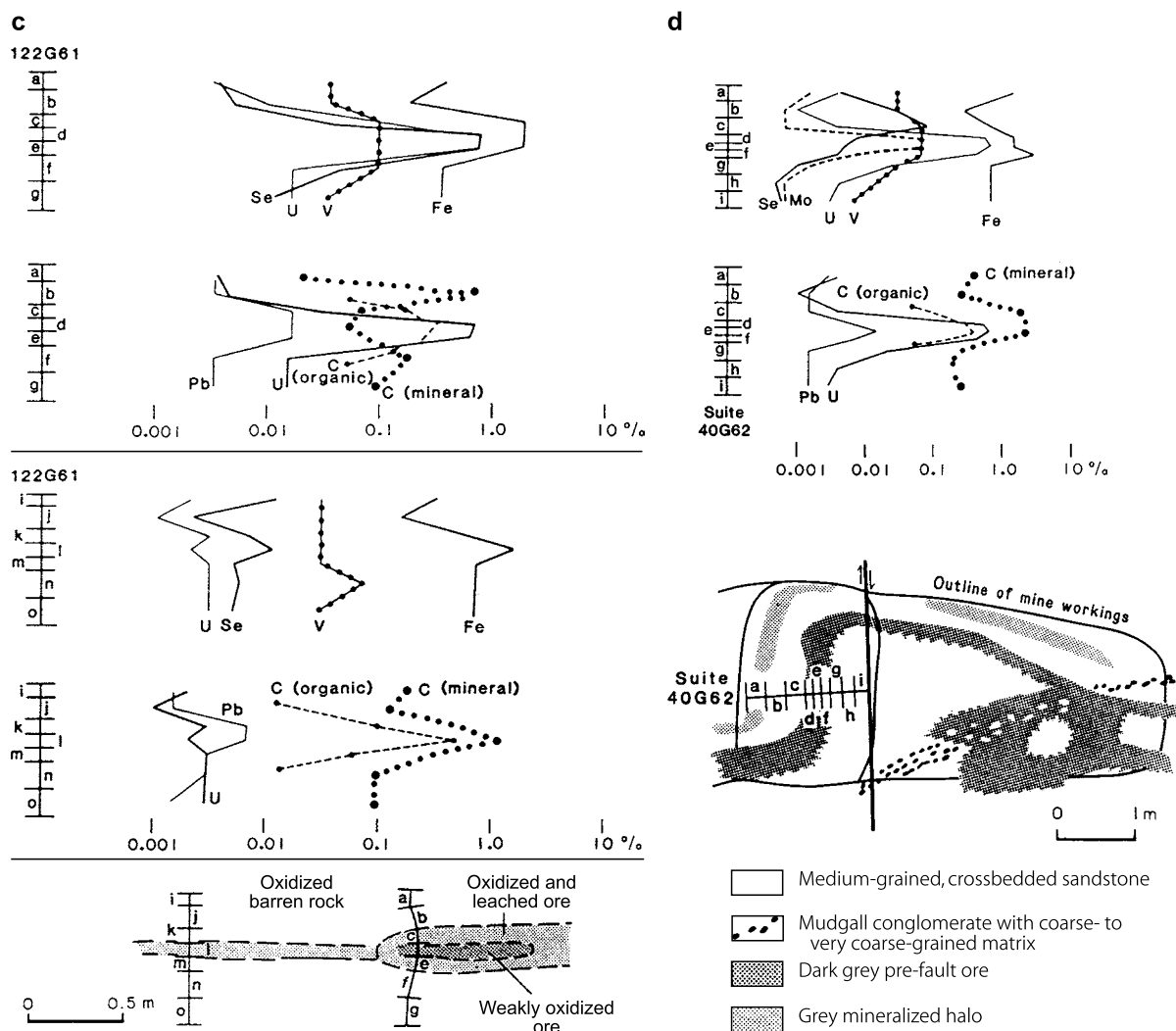
to 70 m (Woodrow pipe, Laguna district). The grade is generally higher than in peneconcordant ore and may be greater than 1% U.

Redistributed mineralization: Stack deposits are variable in shape as a result of ore emplacement along often steep-dipping structures from which uranium penetrated adjacent permeable beds. In some cases, this configuration may resemble a tree in cross section. Individual ore bodies range in length to 100 m or more, and in width and thickness from a few meters to more than 40 m. The average width is approximately 3 m. Grades are generally lower than in the primary ore, averaging between 0.1 and 0.2% U.

Geochronology

Brookins (1980a, b) reports Rb–Sr age datings from three districts using montmorillonite and chlorite-rich materials from ore

■ Fig. 1.20. (Continued)



■ Table 1.2.

Grants Uranium Region, Rb–Sr age datings from ore zones in the Westwater Canyon and Brushy Basin members (Brookins 1980b)

Locality Analyzed material	Jackpile-Paguata	Ambrosia Lake	Smith Lake
Barren-rock montmorillonite	142 ± 14 Ma	131 ± 26 Ma	–
Chlorite-rich ore zone material (from trend ore)	–	139 ± 10 Ma	139 ± 13 Ma
Ore zone material (chlorite-rich)	115 ± 9 Ma	–	–
Ore zone material	110 ± 10 Ma	–	–

zones in the Westwater Canyon and the Brushy Basin members as given in ▶ Table 1.2. Rb–Sr minimum ages for the Late Cretaceous Dakota Sandstone and the Mancos Shale are 93 ± 8 Ma and 83 ± 11 Ma, respectively (Obradovich and Coban 1975).

U–Pb isotope ages of ores from the Ambrosia Lake and Smith Lake districts have been analyzed by Ludwig et al. (1984). Four samples of *redistributed ore* from Ambrosia Lake give almost concordant ages of 3.4–12.5 Ma, which support the

hypothesis that most redistributed ore formed during and after the late Tertiary probably in several periods peaking perhaps at 13–10 Ma ago. In accordance with Saucier's (1980) suggestion, that there were at least two main events of oxygenetic destruction of primary ore, Ludwig et al. (1984) cite information by HC Granger that the 10–13 Ma old samples are from redistributed ore associated with hematitic alteration, whereas the 3.4 Ma old sample is from a limonitic zone.

Rosenberg and Hooper (1982) applied fission-track methods to date Ambrosia Lake ore and interpret their results as indicative for late Tertiary formation ages. *Primary ores* that were not clearly affected by alteration yield apparent minimum ages of about 130 Ma. Primary ores that evidently experienced some degree of alteration show losses in Pb and radioactive daughter products and occasionally uranium gains as well.

Ludwig et al. (1984) interpret their isotopic data from Smith Lake district ores as reflecting ages older than 100 Ma with a possibility that Smith Lake ores are only 10–20 Ma younger than analyzed ores of the Ambrosia Lake district.

Relatively young U–Pb isotope ages have been established by Ludwig et al. (1982) for ore from the Church Rock district. Most of the samples were taken from the UNC mine (nose and limb ore of rollfront), KMc mine, and Phillips mine (Dakota Sandstone or channel in uppermost Brushy Basin and Westwater Canyon members). These samples yield Pleistocene ages of 1 Ma and less with groupings around 0.9 and 0.5 Ma. One sample of a mineralized bone fragment (UNC–Church Rock mine) has much older apparent ages of 68.7 ± 0.5 Ma ($^{206}\text{Pb}/^{238}\text{U}$) and 95 ± 1 Ma ($^{207}\text{Pb}/^{235}\text{U}$), which are, although very discordant, within the range of discordant apparent ages of primary uranium ore from the Smith Lake district. The material of this sample is interpreted to be a relict of incompletely remobilized, primary ore of Jurassic or Cretaceous age. Another sample (KMc mine) has respective discordant ages of 7.84 ± 0.04 Ma and 9.56 ± 0.06 Ma, which seem to reflect late Tertiary mineralization. Ludwig et al. (1982) note that these ages are similar to those of redistributed, post-fault, organic-poor ores from the Ambrosia Lake district.

Pleistocene (less than 150,000 years old) apparent U–Pb isotope ages are also published by Ludwig et al. (1977) from the Hogback No. 4 mine. This ore is hosted by Dakota Sandstone at the westernmost end of the Grants Uranium Region near Gallup, New Mexico.

Principal Ore Controls and Recognition Criteria

As listed by Adams and Saucier (1981) and others, significant ore-controlling or recognition criteria of carbon–uranium deposits in the Upper Jurassic Morrison Formation of the Grants Uranium Region are as follows. For complementation, also see the schematic cross section of Fig. 1.14, in which Crawley et al. (1985) document in graphic-textural form the principal criteria of primary and redistributed ores in the Ambrosia Lake area. Note that these authors include all ore types of pre-Dakota age in “primary ore” and attribute all post-Dakota (Tertiary and younger) ore to “redistributed ore.”

Host Environment

- The host sedimentary sequence of the Upper Jurassic Morrison Formation is a fluvial arenite–pelite alternation of a midfan facies of a wet alluvial fan (Craig et al. 1955; Galloway 1980)
- Tuff-derived bentonitic clays are abundant in the sediments, particularly in the interbedded mudstones

- The ore-hosting sands represent a bed-load-dominated facies deposited in straight to sinuous stream systems of the mid- to distal section of the alluvial fans of the Morrison Formation (Galloway 1980)
- Favorable host units have a high sandstone to mudstone ratio of 4:1 to 1:1, a gross thickness of the host sandstones above average, and a good continuity of the sandstone beds
- Thicknesses of Westwater Canyon sandstone units of up to 100 m are especially favorable, as are Jackpile sandstone thicknesses of as much as 70 m
- Accumulation of thickened sandstone in linear trends (Figs. 1.6, 1.15), which appear to be controlled by paleomorphological sedimentary conditions
- Sandstones with poor sorting and a wide range in grain size appear to make better hosts than sandstones of moderate to good sorting and finer-grained constituents
- The Brushy Basin shale, which is in depositional continuity with the two principal host sands, the Westwater Canyon and Jackpile sandstones is generally not oxidized
- Tuff-derived bentonitic clays are abundant in sediments, particularly in the interbedded mudstones.

Alteration

Alteration phenomena of host rocks along mineralized trends (Fig. 1.13) include

- Reduction as indicated by destruction of detrital magnetite, ilmenite, and local formation of authigenic pyrite
- Corrosion of quartz and redeposition of silica
- Partial dissolution of detrital feldspar
- Partial coating of detrital feldspar by an albite replacement rim
- Removal of ferric iron from mudstones
- K feldspar crystallization and argillization of tuffaceous material in the eastern central part of the San Juan Basin
- Authigenic clay rims on detrital clasts within and immediately adjacent to uraniferous humate lenses consist
 - predominantly of illite–montmorillonite in Jackpile sandstone
 - predominantly of chlorite or a mixed-layer phase in Westwater Canyon sandstone at Ambrosia Lake
 - Mg chlorite replaces montmorillonite clay rims and clasts
- Compositional variations of clay mineral within and adjacent to uranium mineralization show
 - montmorillonite is dominant downdip of an ore body
 - chlorite is enriched in the ore zone, and
 - kaolinite and altered montmorillonite are enriched updip of the ore (Riese et al. 1980)
- Characteristically the most intense decomposition of Fe–Ti oxides and feldspars in Westwater Canyon and Jackpile sandstones is restricted to the proximity of the mudflat facies of intervening Brushy Basin pelites where the bulk of mineralization also occurs (Turner-Peterson et al. 1986) (Figs. 1.11, 1.12a).

Mineralization

Primary peneconcordant ore in blankets, pods, and channels is controlled by lithology–stratigraphy and mineral-geochemistry as indicated by

- Coextensive distribution of uranium with humate in most deposits
- Association of uranium with enrichments of As, Cu, Fe, Mn, Mo, S, Se, V, and Y
- Location of ore bodies in reduced, pyrite, plant debris, and humate-bearing sandstones
- Position of tabular ore generally at several stratigraphic levels along linear trends of thickened sandstone (► Figs. 1.6, 1.15, 1.26)
- Blanket ore is more sheet-like, is coextensive with humate, and contains very little detrital vegetal material
- Channel ore has a stronger facies control than blanket ore, sometimes following individual channels (► Fig. 1.23)
- Channel ore contains humate but also more carbonized or coalified and silicified detrital vegetal matter than blanket ore.

Early roll-type mineralization associated with peneconcordant ore horizons is similar in character to the Wyoming rolls except that oxidized sandstone on the convex, updip side has been re-reduced.

Breccia pipe mineralization is characterized by

- Pipes down-dropped in sandstones adjacent to fractures
- Restriction to Morrison sandstones
- Matrix- and structure-hosted mineralization
- High ore grades but small resources.

Redistributed post-fault ore as typically found in stack deposits (► Fig. 1.15) is controlled by structure, lithology, and redox boundaries as reflected by

- Presence of faults and fractures (of Laramide-Tertiary age) cutting primary mineralized rock
- Presence of reduced and oxidized sandstones along an oxidation front at or near the structures.
- Humate and detrital plant material may or may not be associated with uranium
- Probable chemical separation of Ca, Cu, Fe, Mn, Mo, Pb, Se, Sr, V, and Y from uranium.

Redistributed, late rollfront mineralization is similar to that in Wyoming. Typical features are

- Localization of ore at nose and limb zones of vertically stacked rolls, marking the contact between oxidized and reduced sandstones
- Oxidized sandstone generally seems to be limonitic near the redox front but becomes hematitic within tens to hundreds of meters updip, as described by Ludwig et al. (1982) from the UNC Church Rock mine.

Metallogenetic Concepts

The following synopsis addresses salient ingredients and processes that are thought to may have had an impact on the

metallogenetic evolution of the various ore generations and types in the Grants Uranium Region.

Uranium Ore Generations

At least three generations of uranium mobilization and deposition tend to have generated uranium deposits of the Grants Uranium Region as we know them today:

1. In late Jurassic time, during and soon after sedimentation of the Morrison host sandstones;
2. In late Jurassic to middle-late Cretaceous time during the erosional interval prior to deposition of the Dakota Sandstone; and
3. In Miocene to recent time posterior to the Laramide Orogeny, i.e. during the present erosional period.

The original and principal U mineralization can be classified as tabular, peneconcordant sandstone type and within this category as uraniumiferous humate subtype according to Adams and Saucier (1981). All other types of mineralization, ranging from pre-Dakota roll type to Tertiary and Recent redistributed ore, appear to have been probably formed from the tabular ore during several periods when oxygenated meteoric waters could have entered the Morrison aquifers.

1. **Primary tabular ore:** The genesis of this humate-associated trend and channel uranium ore is still controversial but most obviously, it represents the first accumulation of ore-grade uranium that originated at least 140 to 130 Ma ago in intimate association with humate. This humate association suggests a critical influence of humic acids on both the formation and the site of deposition of primary trend ore. Therefore, the identification of the source of humic acids and the processes involved in their formation, mobilization, and finally precipitation as humate are critical for any metallogenetic modeling as discussed later.

Adams and Saucier's (1981) postulate a formation by diagenesis-related processes of primary peneconcordant and pod-like ore early after the sedimentation of the Morrison Formation in late Jurassic time, and forward the following geologic relationships in support of their assumption:

- Faults of Laramide age offset ore blankets hence the ore must be older than the Laramide Orogeny
- An ore pod or roll in the Jackpile Sandstone in the Paguate mine, Laguna district, was truncated by the pre-Dakota erosion surface, hence the ore must be pre-Late Cretaceous in age
- Tabular ore layers of primary ore have been found down-dropped in a few breccia pipes. The pipe structures do not penetrate the Dakota Sandstone and appear to have formed sometime in late Jurassic Brushy Basin/Morrison time
- Age dating on authigenic chlorite (Brookins 1980b; Lee and Brookins 1978) in Westwater Canyon trend ore of the Ambrosia and Smith Lake districts yield Rb–Sr ages of about 139 Ma and about 110 and 115 Ma for supposedly remobilized ore in the Jackpile mine. The latter would be compatible with post-trend roll-type ore at Smith Lake. It is not known, however, whether chlorite formed contemporaneously with

ore, or whether it formed by the progressive alteration of montmorillonite subsequent to uranium mineralization

- Age dating on authigenic montmorillonite in barren rock yields about 131 Ma in Ambrosia Lake deposits and about 142 Ma in the Jackpile-Paguete deposit, Laguna district.

The age dates are very probably minimum ages of primary mineralization and host rocks. The younger age of the Jackpile ore-stage chlorites may also represent a redistribution event in early Cretaceous time.

2. **Pre-Dakota roll-type and breccia pipe ore:** This generation includes early roll-type mineralization and also some breccia pipe ores that probably evolved in late Jurassic to mid-Cretaceous times by remobilization of primary ore.

Early roll-type mineralization located within peneconcordant ore horizons is similar in character to Wyoming rolls except that it is entirely in reduced sandstone. Roll ore was apparently generated by oxidation processes with redistribution of primary peneconcordant uranium into C-shaped bodies. Later alteration processes re-reduced oxidized sandstone on the convex, updip side of the roll.

Breccia pipe mineralization occurs in pipes down-dropped in the Morrison sandstones that contain peneconcordant primary mineralization. These pipes originated during deposition of the uppermost sandstone unit within the Morrison Formation member in which they occur. They have never been found to penetrate either the overlying Dakota Sandstone or the underlying Todilto Limestone. High-angle normal and reverse faults cut in many places, but not everywhere, the strata adjacent to the pipes and these pipes may be genetically related to these faults. In this case, penecontemporaneous deformation in the area may have aided in a compaction or dewatering process of fine-grained sediments resulting in spring vents, and then the pipes probably formed by gravitational foundering of sand into underlying water-saturated siltstones.

3. **Post-Laramide stack and rollfront ore:** This mineralization is tied to a broad tongue of hematitic oxidation believed to be Miocene or younger, which migrated down the north slope of the Zuni Uplift. Age dates on redistributed ores in the Ambrosia Lake and Church Rock districts give apparent ages around 8–10 Ma. Samples from a rollfront in the Northeast Church Rock mine and from other mines in the Church Rock district are 1 Ma and younger. Ludwig et al. (1982) interpret ages up to 1 Ma as being related to a rollfront-type distribution of earlier formed ore by Pleistocene groundwater, perhaps to those that created the present-day limonitic zone within Westwater Canyon sandstones. They interpret the 10 Ma age to represent an earlier phase of redistributed ore formation, perhaps related to the Tertiary oxidation front that formed the hematitic zone in Westwater Canyon sandstones.

Influence of Pre- to Syn-Morrison Tectonism

In the Grants Uranium Region, pre- to syn-Morrison tectonic movements probably influenced, at least indirectly, the setting of the primary mineralization (Moench and Schlee 1967; Saucier 1967a, b). The long, parallel, thick host rock trends and the

mineral trends themselves may be considered to be the result of subtle folds. Subsidence and folding are suspected to have developed in response to displacements in the basement, perhaps along ancient, reactivated deep-rooted structures, contemporaneously with sedimentation and parallel to the north flank of the Zuni Uplift (Wentworth et al. 1980). N–S-trending asymmetric cross folds, which evolved in late Westwater Canyon time, further influenced the depositional pattern.

These structures produced a series of trends, the most productive of which are located parallel to the NW–SE-trending Zuni Mountains and include the Church Rock, Smith Lake, Ambrosia Lake, Mt. Taylor, Marquez, and Bernabe-Montano districts. A similar trend is reflected by the NE–SW-trending Jackpile Sandstone with its major deposits in the Laguna district. The Marquez and Bernabe-Montano deposits are emplaced in unusually thick sections of Westwater Canyon strata accumulated at intervals in NW–SE trends adjacent to steep eastern flanks of N–S-oriented arches (Kozusko and Saucier 1980).

Adams and Saucier (1981) stress in particular the following features (as quoted with slight modifications):

- ▶ Well-developed channel systems broadened and lost definition in crossing some of the northerly trending anticlines. Domal areas, which probably existed in Morrison time, such as the Ambrosia and San Mateo domes are practically unmineralized because the streams avoided these positive areas. The combination of unfavorable facies and higher structural position makes it likely that subsequent groundwaters also avoided these structures. Structural lows of Jurassic age are the sites of the largest primary uranium deposits and it probably is not wrong to assume that without the structural influence on the trends the primary uranium mineralization in the Grants region would probably be a much broader scattering of smaller ore bodies along shorter, ill-defined trends.
- ▶ The structural situation changed at last in middle Tertiary time when oxidizing waters entered from the outcrop. Mineralized areas that became structurally high in Tertiary time escaped oxidation to some extent. The Ambrosia Lake area is presently a horst bounded on the east by the San Mateo fault and on the west by the Ambrosia fault zone. Late Tertiary oxidation borders it on three sides and may actually surround the horst entirely.
- ▶ The unusually intense faulting between Gallup and Laguna may also have contributed to the protection of the Ambrosia Lake area from more extensive oxidation (Santos 1970). Contrary to popular belief, the structurally deformed areas appear to hinder or retard groundwater circulation and, therefore, prevent the oxidation and destruction of earlier formed ores. Outstanding examples are the Poison Canyon mine, the Black Jack No. 1, Section 28 (Smith and Peterson 1980), and on a larger scale, the Northeast Church Rock mines and Bernabe-Montano Grant, which is preserved within the Rio Puerco fault zone. A lesser known but outstanding example is Kerr-McGee's Section 22 mine where primary blanket ore is preserved in a graben, and stack ore occurs around the outside of the bounding faults (Corbett 1964).

Alteration Processes

Morrison sediments were affected by several stages of alteration (Fig. 1.13). Adams and Saucier (1981) note that almost immediately after their deposition, volcanic material in sandstones was altered to clay, but the volume of such clay was insufficient to restrict permeability, except in very thin lenticular sandstones, which were silicified or consisted of argillized finer-grained sandstones.

Lee (1976) presented a simple general paragenetic sequence for postdepositional alteration in ore-bearing sandstones, which is compatible with results of most other studies on the Westwater Canyon sands and those of Adams et al. (1978) on the Jackpile Sandstone. In sequential order:

1. Smectite (montmorillonite) formation
2. Bleaching of host sandstone and alteration of detrital heavy minerals to pyrite and Ti-oxides
3. Formation of clay-organo-complexes and enrichment of uranium
4. Chlorite formation concomitant with humate coagulation and coffinite precipitation
5. Oxidation of pyrite, development of roll-type and other redistributed ores, and formation of nest kaolinite.

During an early reducing stage, magnetite and ilmenite were destroyed and locally replaced by pyrite. Turner-Peterson et al. (1986) established that destruction of the Fe-Ti oxides as well as detrital feldspars was most intense proximal to intervening Brushy Basin pelites and was regionally restricted to the mudflat facies of the Brushy Basin Member (Figs. 1.11 and 1.12).

Turner-Peterson and Fishman (1986) note a lateral distribution pattern of clay minerals derived by an alteration of tuffaceous material in the Brushy Basin Member. Alteration and zoning resulted from “chemical zonation of pore waters in the saline-alkaline lake sediments during an early diagenesis and reflects a lateral basinward increase in alkalinity and salinity.” Mineralization occurred in the Westwater Canyon sands where they are overlain by the Brushy Basin mudflat facies. The mudflat facies characteristically contains smectite formed in response to alteration in an environment of pH 7–8.5 (Bell 1986).

During this period of diagenesis, elements of the various mineral constituents contained in pyroclastics were liberated and carried by groundwater through the sandstones until chemical conditions were encountered forcing their precipitation.

Preliminary chemical analyses (Della Valle 1980, personal communication in Adams and Saucier 1981) point to an increase in the concentration of rare earth elements (REE) from the Recapture and lower Westwater Canyon sediments into the upper Westwater Canyon sandstone and then a decrease in the Brushy Basin Member. This may suggest a leaching of REE in the Brushy Basin and in the lower Westwater Canyon sediments relative to the upper Westwater Canyon sandstone. REE leaching from the lower Westwater Canyon is also indicated by lower concentrations of REE in its minus 2 mesh fraction. Adams and Saucier (1981) attribute the REE leaching to the long history of the mild oxidation of the affected part of the lower Westwater Canyon sandstone as evidenced by the general preservation of ilmenite-magnetite and the presence of hematite. Sodium, on

the other hand, increases slightly in the upper part of the Westwater Canyon Member, which is compatible with evidence for widespread albitization.

Later, after the diagenetic processes mentioned earlier, the introduction of oxidizing solutions followed and resulted in extensive oxidation reflected by hematitization and limonitization, and a partial redistribution of primary ore. Oxidation processes began as early as Middle Tertiary and may still be active at present [Saucier (1980) considers hematitic oxidation to have taken place in late Oligocene or early Miocene time and limonitic oxidation in Pliocene or Holocene time]. Hematitic sandstones have been found up to 25 km downdip from the Morrison Formation outcrops and as deep as 720 m in the Crownpoint area. Weak oxidation may extend much further north of Crownpoint as reflected by the redistribution of uranium mineralization along oxidation fronts in the Nose Rock area (Clark 1980). Adams and Saucier (1981) state that in the southern half of the San Juan Basin, particularly in the lower part of the Westwater Canyon Member, two episodes of oxidation occurred, a widespread early mild oxidation and a common but more limited late oxidation that affected the matrix of sandstones. They also note that the abundance of detrital magnetite in the Westwater Canyon Member in the northern part of the Grants Uranium Region is suggestive that this region was never strongly reduced by solutions influenced by either indigenous or introduced organic substances.

The dominant oxidation in the Westwater Canyon Member on the Chaco Slope at least, is late Cenozoic in age. Oxygenated solutions have probably removed a large amount of uranium on their path through the Grants Uranium Region except locally where the oxidation front encountered, in its basinward advance, organic-rich primary trend deposits. Between such ore deposits, oxidation has advanced farther north. There are generally no uranium accumulations along these interfaces as found, for instance, on similar oxidation fronts in the Wyoming Basins. It is not established whether this is due (a) to an oxidation process, which totally destroyed primary mineralization or (b) to the fact that these fluids merely traversed areas in which no significant uranium deposits existed, and because of a lack of sufficient uranium contained in invading oxygenated waters, no deposits could form. The latter assumption is favored for the Chaco Slope. Well-developed redox fronts exist here and uranium, if available in the solutions, should have precipitated. An exception is the Church Rock district where younger rollfront ore bodies are described by Ludwig et al. (1982).

Another noteworthy criterion may be the generally non-oxidized nature of the Brushy Basin pelites, which are in depositional continuity with the two principal host sand units, the underlying Westwater Canyon and the overlying Jackpile sandstones. Where such pelites are oxidized, ore habits are similar to those found in the Salt Wash Member of the Uravan Mineral Belt or in the Chinle Formation.

Potential Sources of Uranium

The source of uranium is still in dispute. Intraformational felsic pyroclastics either within host sands themselves or in adjacent Brushy Basin mudstones may be envisioned as a potential source of uranium. This postulation, however, is derived mainly from

circumstantial evidence provided by the frequent association of uranium deposits with tuffaceous sedimentary sequences.

Much of the uranium and associated elements such as Mo and Se may also have derived from altered igneous material within sandstones at some distance up the hydrologic gradient from where the deposits are presently located. Especially the coarse facies proximal to the sedimentary source that was later removed by erosion is thought a favorable source for ore-forming elements. It may also be assumed that some kind of combination of all sources mentioned contributed, to various degrees, uranium to the deposits.

With respect to the amount of volcanic material needed for considering the Morrison inherent volcanics as a viable uranium source by quantity, Adams and Saucier (1981) note that volcanics constitute 20% or more of the original Westwater Canyon and Jackpile sandstones and a substantially larger percentage of the intervening Brushy Basin mud- and siltstones. As such, the Morrison strata probably contained sufficient volcanic components.

Squyres (1970) and other later workers suggest that the diagenetic alteration of the volcanic tuff in the Brushy Basin Member may have released uranium and other metals to groundwater and adjacent sandstones. It is not known, however, whether and to what extent the clay constituents originated by diagenetic alteration or sedimentation.

Brookins (1979) and Della Valle (1980, personal communication in Adams and Saucier 1981) report a Th:U ratio for the Brushy Basin Member of about 1.5 and interpret this as one point of evidence that uranium has not been released from this member. Another point may be given by Della Vella's findings that REE have been apparently depleted in the Brushy Basin pelites as mentioned earlier. Such a process requires a reducing, probably organic-bearing groundwater capable of complexing or chelating the REE (Della Valle in Adams and Saucier 1981; McLennan and Taylor 1979) while depressing the solubility of uranium. On the other hand, higher Th:U ratio values in the Westwater Canyon strata, particularly in the lower part of the member as compared to those in the Brushy Basin sediments, as reported by Brookins (1979), suggest that the Westwater Canyon sediments have most likely provided uranium for ore formation. This is compatible with the generally reduced state of the Brushy Basin sediments implying low uranium solubility, whereas pervasive mild oxidation prevailed in the lower Westwater Canyon sandstone as reflected by the state of ilmenite and magnetite, which are not destroyed by reduction and carry hematite rims.

In conclusion, Adams and Saucier (1981) suggest that (a) alteration of felsic pyroclastics during their transport and very soon after their deposition, released uranium and other metallic ions to the fluid system, which may already have accumulated some uranium by alteration of tuffaceous material in the area of provenance, and (b) that the Westwater Canyon sediments have provided uranium while the Brushy Basin strata have contributed little or no uranium.

Paleo-Groundwater

It may be deduced that due to the hydrolysis of volcanic detritus in the Morrison sediments, surface and shallow groundwaters in Late Jurassic time were alkaline (pH of about 8), oxidizing,

and had a concentration of dissolved substances in the range of 1,000 ppm or less with sodium in excess over calcium (Squires 1969). Furthermore, it seems probable that if uranium and associated elements were derived mainly from felsic volcanic tuff, either or both in the area of provenance or from volcanics deposited within the sediment, then uranium and its associated elements should also have been present in Late Jurassic groundwaters. Uranium probably was on the order of 50–300 ppb, transported perhaps in the form of uranyl carbonate complexes, as suggested by Gruner (1956) and/or by fulvic acid complexes as postulated by Schmidt-Collerus (1979). Granger et al. (1961) assume that organic matter from decaying plant debris in the Westwater Canyon Member was dissolved in the stream and underflow waters during the Westwater Canyon deposition. Precipitation along the interface between the underflow and deeper, slower moving groundwaters resulted in an elongated distribution of organic material parallel to deposition trends, and in the formation of multiple layers of organic material during continuing sedimentation. The correlation of humic matter and paleo-water table or chemical interfaces parallel to, but below the water table, would more easily explain the extensive tabular ore bodies such as found in the Jackpile–Paguete deposit. But peculiar features, such as the ore pods described by Moench (1963) in the Jackpile deposit also suggest early destruction or shifting of humate lenses soon after their formation.

Uraniferous Humate

Humate is a term introduced by Granger et al. (1961) to describe the particular carbonaceous substance associated with the primary U mineralization of the Grants region. Humate constitutes 0.05–0.5% by weight of the host sandstone. Its dominant characteristic is its ubiquitous and coextensive association with uranium in primary tabular trend and channel ores. Although unmineralized humic material has reportedly been found, no completely uranium barren humate has been confirmed in the Westwater Canyon sandstone.

Adams and Saucier (1981) stress the influence and involvement of humic material in uranium geochemistry as follows:

1. Humic substances such as fulvic acids are thought to be capable of transporting uranium over long distances in natural waters
2. No other naturally occurring chemical substances are known that have a greater ability to extract uranium and other cations from extremely dilute solutions than humic substances. Metal concentrations can build up very rapidly under adequate chemical conditions. The only salient parameters for metal accumulation are the quantity of humic material present and the amount of metal transporting waters that come into contact with it
3. Once precipitated, the humic substance protects its accumulated uranium by becoming more refractory with age and by maintaining strong reducing conditions in its environment.

Crawley et al. (1984) have reviewed pertinent publications on the origin and formation of humate and state that proposed sources for humate include plants growing on the surface of the

active alluvial fan, plant debris incorporated into the host sandstone, plant material deposited with clay and mud of associated lacustrine deposits, and, the Dakota and pre-Dakota swamps developed on the Morrison sandstone suboutcrops (Granger 1968). Most hypotheses suggest the decay and mobilization of the organic substance in groundwater and the precipitation of humate where organic-rich water encountered other groundwater of different chemical composition (see also Turner et al. 1993 for more detailed information on the nature and role of organic matter in sandstone uranium deposits).

The initial humate precipitation may have been in the form of flocculated gel that continued to concentrate uranium through the process of chelation and complexing (Squires 1974; Schmidt-Collerus 1979). Some uranium, however, which may have been transported by organic acid complexes, may have co-deposited with humate. Eventually, humate gel matured and hardened through bacterial action, oxidation, and radiation. Some formerly complexed uranium was probably released to form, in the case of presence of silica, coffinite.

Origin of humate: Two principal hypotheses are forwarded on the provenance of humate in the Grants Uranium Region, an intrinsic source and an extrinsic source in relation to uranium mineralized sandstone units. Both models envisage a Morrison-internal source. The intrinsic model derives humate from plant debris in the Westwater Canyon sandstones, and the extrinsic model from that in the Brushy Basin pelites, and probably from a particular facies of the latter, namely the mudflat facies as proposed by Turner-Peterson et al. (1986). A third concept envisaging an external, non-Morrison source in the form of surface vegetation or swamps, has been discussed by Granger et al. (1961) and, in modified form, by Turner-Peterson and Fishman (1986). The two internal source models comply best with the established geochemical and geological parameters of the region as discussed later.

Adams and Saucier (1981) in their "Working Model I" and Turner-Peterson et al. (1986) in their "Lacustrine-Humate Model" propose that humate originated from claystone and mudstone of the Brushy Basin Member. Criteria of this model are: Detrital plant fragments and abundant volcanic ash were incorporated into lacustrine sediments of the Morrison Formation. Early diagenesis of these more pelitic sediments produced reducing, alkaline solutions able to solubilize humic material. These solutions or pore waters, which may have constituted as much as 70% of the volume of the lake sediments, was expelled under compaction into adjacent fluvial sand horizons of the Westwater Canyon Member. Another groundwater system moving through these sandstone aquifers was less alkaline and probably less reducing. The interaction of the two solutions resulted in a geochemical interface, which forced mobile humic substances to deposit as insoluble humate. The "lacustrine-humate model" of Turner-Peterson et al. (1980, 1986), which is also used to explain tabular uranium deposits elsewhere, involves reactions with Fe and Al hydroxides and the formation of organo-clay complexes in precipitation of the humate.

In contrast to an extrinsic origin of humate, several authors propose an autochthonous, sandstone-internal source of humate.

Jacobson (1980), for example, rejects the concept of an extrinsic origin for structureless humic material in the L-Bar deposits of the Laguna district. His observations indicate that syngenetically deposited, finely divided vegetal detritus in the host sandstone is an adequate source. Uranium could have been extracted and fixed by partially degraded carbonaceous material from both surface and groundwater during the remaining deposition of the Morrison Formation.

Falkowski (1980) also derives humate from buried vegetal matter within the Westwater fluvial system, and many papers in Memoir 15 (Kelley 1963a) indicate a close association of uranium with buried vegetal material and its derivatives.

In Adams and Saucier's (1981) Model II, humic acids originated from buried organic material in sandstones, and the presumption is made that "all the humic matter, and most of the uranium, was derived from the Westwater Canyon sandstones rather than from the Brushy Basin mudstones." This hypothesis corresponds more or less to the "internal source model" of Turner-Peterson and Frishman (1986).

Humate accumulation: A principal problem for any metallogenic modeling of primary peneconcordant humate-uranium mineralization, including the models mentioned earlier is to find a reasonable explanation for the accumulation of such large quantities of humate as found in the Ambrosia Lake and adjacent districts. Adams and Saucier (1981) argue if the chemical parameters, as believed, remain qualitatively the same for the accumulation of only a few kilograms, or a million tonnes then the extreme size of the humate masses must mainly be controlled by distinct lithologic-geologic factors. These factors include the size of the fluvial sediments itself, the amount of buried vegetal material, and the porosity and permeability, which in turn are dependent upon the depositional environment and the climate. Assuming the climate remained constant during the mineralizing processes, the other geologic variables were mostly a function of some structural preparation. The highest concentration of transported organic debris tends to be located adjacent to the Zuni Uplift area in sedimentary trends that possibly are downwarps controlled by pre- to syn-Morrison basement displacements, as already described earlier, and which channeled and caused the superposition of high-energy fluvial systems. These shallow, elongated depressions also subsequently funneled groundwaters, which transported dissolved humic substances and uranium along the same trends. As a result, very subtle structural influences controlled the accumulation of unusually large quantities of uraniumiferous humate and its deposition in relatively thin, sheet-like lenses elongated in the downstream direction along axes of downwarps. As such, this unique characteristic of uraniumiferous humate-type of uranium deposits was produced.

Assuming that humate precipitated as tabular bodies along a shallow, horizontal chemical interface below the water table, it can be hypothesized that the earlier described distribution of uranium, selenium, and molybdenum may suggest that the humate body developed at a redox interface, which separated surface-derived oxidizing water from deeper, perhaps H_2S -rich, reducing groundwater (Saucier 1980). The hydrochemical system may have been, in principle, similar to that, which

generated redox fronts in Tertiary Wyoming Basins. The marked difference is in the time of introduction of oxygenated solutions. Oxygenated water migrated in the Wyoming Basins long after sediment deposition and progressed as large tongues down dip in slightly tilted sandstone horizons (see Chap. 2: Wyoming Basins). In contrast, as suggested by Adams and Saucier (1981), redox fronts in the Morrison Formation were active more or less synsedimentary migrating as a horizontal interface vertically down into fresh sediments from the depositional surface.

Metallogenetic Models

The majority of models proposed for the formation of primary tabular ore imply that the deposition of ore was governed by a groundwater interface between two solutions of different chemical composition and/or oxidation-reduction states. Fischer and Shawe (1956) have already proposed such a model as early as 1947. Later prepared models, such as Model I and II by Adams and Saucier (1981) and the lacustrine-humate and internal source models by Turner-Peterson and Fishman (1986), or the brine-interface model by Fishman and Turner-Peterson (1986), have refined or incorporated portions of these early concepts.

Since humate was, by all indications, instrumental in the fixation of uranium to form first generation uranium, humate is a critical factor in deciphering the genesis of large humate-uranium deposits in the Morrison sandstones. As mentioned earlier, it remains open to discussion, however, whether humate derived from pelites of the Brushy Basin Member or from sandstone units of the Morrison Formation. To match both options, Adams and Saucier (1981) have prepared two alternative genetic models for primary uranium ore, which are presented later in a slightly modified form.

The essential criterium for the *first model* is the regional, early alteration pattern, particularly ilmenite-magnetite reduction and destruction, and feldspar alteration, both of which are the result of organic-rich reducing solutions derived from the Brushy Basin Member. The proposed ore-forming process then relies on the juxtaposition of the Brushy Basin Member and the underlying and overlying sandstones of the Westwater Canyon and Jackpile units. The *second model*, instead, presumes that all humic material, and most of the uranium, was derived from Westwater Canyon and Jackpile sandstones rather than from Brushy Basin mudstones.

Model I of Adams and Saucier (1981)

Sedimentation: Thick sands of the Westwater Canyon Member below and the Jackpile Sandstone above were laid down as a continuous sedimentary sequence with the intervening Brushy Basin Member under an arid or semiarid climate. The thickness of sands (50–100 m) and muds (60–120 m) permitted the development of a major hydrologic system with high transmissivity and an integrated hydrochemical system that was active from the moment of sedimentation and early diagenesis. This sedimentary sequence provided an extraordinary chemical potential

due to the juxtaposition of two inherently unstable components, organic material in the form of plant debris and volcanic glass within pyroclastic intercalations. The diagenesis and alteration of these constituents are capable of independently producing widespread alteration assemblages; but due to their interaction, this potential was enhanced by hydrologic conditions in the Morrison strata, which promoted the development of an efficient metallogenetic system.

Both the sands and presumably the muds received substantial amounts of organic debris during their deposition. Silicified logs and occasional carbonized logs, or trash pockets, attest to organic debris deposited with sands, whereas fine carbonaceous matter is essentially absent in sands, presumably due to its destruction. No organic debris is still found in the muds but circumstantial evidence indicates its former presence.

In conclusion, argillaceous and arenaceous sediments of the Brushy Basin and Westwater Canyon members contained all components necessary for the formation of uranium-humate mineralization. The principal chemical factors are that uranium occurred in volcanic glasses, and organic material occurred in the form of detrital plant debris. Mudstones and sandstones would provide the hydrologic conditions necessary for post-depositional diagenesis, compaction, and dewatering of pelites, and for development of chemical interfaces in groundwater for the formation of ore deposits.

Hydrologic systems and diagenesis: With the accumulation of pelites of the Brushy Basin Member over the Westwater Canyon sandstone, a regime of two juxtaposed groundwaters of different chemistries evolved. Waters in the Westwater Canyon sandstone, particularly in deeper portions, were locally oxidizing and locally reducing depending upon the influence of indigenous organic debris. In general, however, groundwater flowing through the Westwater Canyon aquifers apparently never had a strongly reducing effect as attested by the widespread occurrence of unaltered ilmenite and magnetite in deeper portions of the sand and by hematite rims almost ubiquitously coating these grains. It rather appears that the Westwater Canyon sands were affected by percolating oxygenated water coming from recharged areas. This oxidizing water decomposed most fine organic debris, which was presumably present in considerable quantity in the sands leaving only silicified and carbonized larger fragments. It is further postulated that the groundwater was not strongly oxidizing because ilmenite and magnetite have only thin hematite coatings. This concept assumes a continuous flow of groundwater within the Westwater Canyon sands beginning with the time of their deposition.

With the sedimentation of the overlying Brushy Basin Member, groundwater within the Westwater Canyon Member was confronted with solutions of a markedly different composition. The Brushy Basin sedimentation presumably advanced progressively over the Westwater Canyon sediments from more distal portions of the fluvial fan back toward the fan head by depositing finer-grained sediments consisting of 40–60% solids by weight, the remainder being pore waters. With increasing thickness of the Brushy Basin sediments, contained water commenced to be expelled. Due to the strong influence by volcanic material, the chemistry of these mobilized solutions became

alkaline and hence capable of dissolving fine organic debris dispersed within the Brushy Basin facies. These fluids imposed the typical greyish-green to green reduction colors upon the Brushy Basin pelites before waters were expelled into underlying or overlying aquifers. Organic-enriched alkaline and reducing solutions released from the Brushy Basin sediments down into the Westwater Canyon sandstone altered detrital ilmenite, magnetite, and feldspar. Alteration was strongest at the top of the Westwater Canyon strata, which is compatible with such an interpretation. Since reducing Brushy Basin fluids were in distinct chemical contrast to oxidizing or very mildly reducing groundwater flowing in the Westwater Canyon sands, a chemical interface must have developed. It is postulated that along this interface, primary uranium–humate mineralization most probably precipitated.

The configuration and position of the fronts between the two groundwater regimes was probably controlled by the rate of flow of the Westwater Canyon groundwater and the volume and lateral changes in flow rates across the Brushy Basin–Westwater Canyon interface. In the vicinity of present-day ore districts of the Grants region, the Westwater Canyon Member thickens unusually at the expense of the overlying Brushy Basin Member, and upper sands of the Westwater Canyon Member laterally interfinger with the Brushy Basin sediments. This lithologic interrelationship provides a unique geometry for the discharge and concentration of greater volumes of reducing solution from the Brushy Basin Member laterally into the overthickened Westwater Canyons sands.

Ore formation: The hypothetical mixing of the two solutions outlined earlier provides a fairly simple mechanism for the formation of peneconcordant uraniferous humate deposits. Where the Brushy Basin solutions mixed with the Westwater Canyon groundwater, a decrease in pH occurred, leading to the precipitation of organic material, which is notably less soluble in more acid solutions. Depending upon hydrodynamics, the interface between the two water regimes supposedly has fluctuated vertically leading to the deposition of vertically stacked organic-rich lenses and to numerous local complexities in alteration, ore distribution, and mineral paragenesis. The fixation of humate in tabular lenses that locally transform into S-shaped rolls may have been the simplest minerochemical response to the redox interface between the two water regimes. Once precipitated, humic matter may have allowed the initiation of other alteration processes. Silica, alumina, and alkali and alkali-earth cations originally complexed on organic material were released. The liberation of these ions partly resulted in the formation of authigenic clay rims on detrital clasts through changes in the chemical environment around organic material and partly through its degradation. Since these clay phases are best developed proximal to ore, and since the chemical components, particularly alumina, do not commonly travel and concentrate in such a mode, circumstantial evidence suggests that the dissolved organic substance was the medium for dissolution, transport, and ultimate release of these elements. Furthermore, feldspars were altered and replaced within reduced zones and, consequently, considerable amounts of alumina and silica must have been released.

It may also be postulated that once humic material had been precipitated as gel-like masses in the form of tabular zones in sandstone, the continued percolation of groundwater and the hydrodynamic setting would have modified the organic distribution into those shapes that have been identified in deposits of the Ambrosia Lake district (Squyres 1970) and in other districts. Furthermore, solutions migrating through and past humic zones are thought to have introduced small amounts of uranium in solution, particularly as the solutions were mildly oxidizing. With time, the expulsion of the Brushy Basin waters into the Westwater Canyon sands probably diminished and ultimately ceased. This permitted the deeper, more oxidizing water system to increasingly encroach upon the shallower reduced groundwater regime. Such a groundwater flow could continuously contribute small amounts of uranium to the deposits, ultimately producing relatively high grades for sandstone-type U deposits. The solutions, however, are required to have not been sufficiently oxidizing to completely destroy the mineralization. Once the groundwater regime became more stagnant at the end of the Jurassic depositional period, it changed to mildly reducing due to the influence of residual detrital and epigenetic carbonaceous material. This final process created the widespread characteristic drab color of the sandstones now seen in the subsurface. A similar metallogenetic evolution may be envisioned to have operated between the Brushy Basin pelites and the Jackpile Sandstone following their deposition.

Model II of Adams and Saucier (1981)

Prerequisites to this hypothesis are

1. The source of all humic material and most of the uranium was the Westwater Canyon sandstones and not the Brushy Basin mudstones
2. Sufficient organic debris was buried with the sediments creating an anaerobic environment below the static water table (Love 1964, Jensen 1958)
3. Bacterogenic H_2S and CO_2 , methane, and hydrogen gas from the fermentation of vegetal material cause a drop in pH as proposed by Rackley (1976)
4. Iron in groundwater and in iron-bearing detrital grains may react with H_2S to form monosulfides, and eventually, stable pyrite.

This organic–chemical reduction of sands can develop very early and at shallow depths.

Hydrologic systems and diagenesis: The surface and shallow groundwater in late Jurassic time are assumed to have been oxidizing due to the arid or semiarid climate, and alkaline with a probable pH of about 7.5–8 due to hydrolysis of volcanic ash in the sediments. Humic acids leached from plant debris by alkaline solutions in the upper oxidizing portions of channel sediments could have migrated down to the static water table. At this position, they encountered a pH environment sufficiently low so that the flocculation of humic substances occurred. The flocculation of humic material will definitely occur at a pH of 5, but may begin at a higher pH value if the humic acids contain metallic ions. The precipitation of uranyl humate complexes at a pH of 6.5 are reported by Schmidt-Collerus (1969).

Humate will be distributed in the form of broad, tabular, semi-horizontal masses in channel sands, perhaps as shallow as 5 m below the streambed. As soon as the channel deposit is buried, the humate lens is protected by the development of an acidic reducing environment, and by the continued adsorption of cations. Once adequate younger sediments cover the channel deposit, the sequence can be repeated over again at a higher stratigraphic level as in the Jackpile Sandstone, if organic material is contained in overlying sediments.

Ore formation: The surface and shallow groundwaters may have contained between 50 and 300 ppb U probably in the form of both uranyl carbonate complexes, as suggested by Gruner (1958) and organic acid complexes, as proposed by Schmidt-Collerus (1979). The precipitation of uranyl humate complexes could have occurred directly as a result of the drop in pH across the subhorizontal redox interface, whereas the uranyl carbonate complexes were probably broken up by deeper acid solutions and liberated uranium became available for the enrichment of uraniumiferous humate. Hydrogen sulfide generated in humate gel by bacteria is assumed by Adams and Saucier (1981) to be the cause for the precipitation of Fe, Mo, Se, and As as sulfides. Molybdenum apparently precipitated in a negative colloidal sulfide, which was repelled by negative humic colloids. This is considered the reason why jordisite mineralization is almost never in direct contact with humate.

With ongoing time, the tabular humate impregnation matured and hardened into a brittle material that coated grains and filled interstices in sandstone. During maturation, which was accompanied by oxidation, microbial attack, aging, and radiation, organic molecules broke down and much of the complexed uranium and vanadium was released. Uranium associated with silica to form coffinite, and vanadium entered the lattice of authigenic chlorite.

The diagenetic process outlined earlier is postulated to have taken place as an efficient early stage shortly after the sands were deposited. During this episode, the ability of humate to collect and accumulate uranium diminished rapidly. The labile nature of both the volcanic source material and the organic acids also attests to the assumption of a very early age for the ore-forming process.

The grade and magnitude of any ore body that formed according to Adams and Saucier's (1981) Model II processes require as salient ingredients: (a) an initial concentration of humic substances, (b) a uranium-bearing water, and (c) a permeability of the host sands, which steered the rate of exposure of uranium to organic particles. All of these parameters had a maximum coincidence immediately after the deposition of the host sandstones.

The **lacustrine-humate and internal source models** proposed by Fishman and Turner-Peterson (1986), Turner-Peterson (1985), and Turner-Peterson and Fishman's (1986) correspond in principle with Model I and, to some extent, with Model II, respectively, of Adams and Saucier (1981).

In the *lacustrine-humate model*, groundwater was expelled by compaction from pelites of a large playa lake into underlying fluvial sands, but based on their studies, particularly on the

distribution of altered Fe-Ti oxides, feldspars, and authigenic clay minerals, these authors constrain the origin of both, the solubilizing fluids and the humic acids to the mudflat facies of the Brushy Basin Member. The expelled humate or secondary organic material precipitated in the sands as a result of flocculation into tabular bodies. Uranium was then precipitated from groundwater during or after the formation of the humate bodies.

In the *internal source model* of Turner-Peterson and her coworkers, the solubilizing fluids also originated from pore waters of the mudflat facies and migrated into adjacent sandstones, but it was here where they dissolved organic debris to form humate and uraniumiferous humate mineralization, respectively.

Granger and Santos (1986) forward a *brine-interface model*, in which uranium and humate were deposited during diagenesis by reduction at the interface of meteoric fresh water and groundwater brines.

Sanford (1992, 1994) presents another version of the brine-interface model based on the paleohydrologic analysis of groundwater flow during late Jurassic and early Cretaceous times. He postulates (a) two types of groundwater, a local, relatively dilute, shallow meteoric and an underlying regional saline groundwater; (b) groundwater migrated down dip driven by gravity, not compaction (as proposed in some of the earlier discussed models); (c) a gravitationally interface was formed by these two waters in areas of regional and local groundwater discharge; (d) uranium precipitated in areas where mixed regional and local groundwater discharged shortly after the sedimentation of the host rocks; and (e) that the tabular shape of ore bodies resulted from an early, stable density-stratified interface between a local dilute groundwater and a regional saline water, and (f) where this interface intersected humate lenses.

Fluvial continental sediments resting upon evaporitic marine sediments as present in the Grants Uranium Region (and also in the UraVan Mineral Belt/Paradox Basin, and Henry Mtns. district/Henry Basin with U-V deposits in the Salt Wash Member) provide an optimal environment for the conditions listed earlier, since they are capable of contributing the fresh water and the brine necessary to form the postulated interface.

In his "four-layer-finite-difference model," Sanford (1994) proposes that the direction of groundwater flow as well as recharge and discharge sites were controlled by paleotopography, shoreline situation, and density contrasts in the lake and pore waters.

Saline waters originated as fresh water in highlands west and south of the basin, and interacted along its pathway with evaporitic marine sediments (e.g. gypsum-anhydrite in Todilto Limestone) at depth below the Morrison Formation; this "saline groundwater was not the alkaline-saline pore water from the Brushy Basin lake" (Sanford 1994).

Favorable paleotopographic and geological-sedimentological parameters and environments for the development of tabular uranium deposits existed in the San Juan Basin (a) where the alluvial plain merges into a mud flat since this is the area of

mixing of chemically different groundwater types; (b) in syn-depositional synclines reflected by reduced lacustrine mudstones or channel sandstones, because the concave slope morphology causes upward flow and mixing of groundwater at an interface and also promotes the accumulation of organic matter; and (c) where major aquifers thin or pinch out and, consequently, force deep regional groundwater flow upward to interact with shallow dilute groundwater.

Crawley et al. (1984) comment on the understanding of the metallogenesis of the Grants Uranium Region that the diversity of local ore body characteristics, which are often the cause for controversial genetic interpretations, require more than one phase or process of mineralization to account for the accumulation of both humate and uranium in primary ores. According to Jacobsen's (1980) model for the L-Bar deposits, Laguna district, the present shape of the ore bodies essentially coincide with the original distribution of plant debris that was concentrated by normal sedimentary processes. Such a model may in general be valid for primary mineralization emplaced in channel sands rich in carbonized vegetal material. It is less likely to be applicable to primary blanket or roll-shaped mineralization, which apparently formed in a facies containing little vegetal debris and which displays shapes difficult to attribute to sedimentary processes. Primary roll-shaped ore poses an additional problem since its formation is difficult to explain by the same process, which formed penecondordant ore. It is worth noting, however, that the channel ore as well as the blanket ore occasionally occur in the same mine in the Ambrosia Lake district.

Description of Individual Districts of the Grants Uranium Region

For location of districts/deposits see [Figs. 1.3](#) and [1.4](#).

1.1.1 Marquez/Rio Puerco District and Bernabe-Montano Area

The main part of the Marquez or Rio Puerco district is located N of the Laguna district approximately 30 km NNE of the town of Laguna. It stretches over a NNW–SSE distance of about 20 km. Known deposits include from NW to SE: *Marquez*, *Marquez Canyon*, *Juan Tafoya*, *San Antonio Valley*, and *Rio Puerco*. About 15–20 km to the ESE of Rio Puerco is the *Bernabe-Montano deposit*. It is attributed to this district because it occurs at the Rio Puerco paleostream, which runs across the Bernabe deposit.

1.1.1.1 Marquez/Rio Puerco

Discovered in 1969 in the eastern foothills of Mt. Taylor, mineralization occurs generally at significant depths down to 600 m. Original resources of the district (status 1983) were 8,400 t U at grades averaging 0.09% U. About 10 t U were recovered in 1979–1980 (McLemore and Chenoweth 2003).

Sources of information. Bowman and Livingston 1980; Moore and Lavery 1980 unless otherwise cited.

Geological Setting of Mineralization

Uranium ore of the Rio Puerco district appears to be exclusively restricted to lower sandstones of the Westwater Canyon Member, Morrison Formation. The *Westwater Canyon Member* ranges from 70 to 100 m in thickness and consists of sandstone with interbedded mudstone. Sandstones constitute approximately 70% of the thickness. Two prominent sandstone units exist separated by the “K”-shale horizon.

The lower U-hosting unit is thicker and is composed of elongated, WNW–ESE developed channel sands. Typically, these sands are fine- to coarse-grained, poorly to well-sorted, and moderately cemented calcareous feldspathic quartz sandstones. Calcite with kaolinite and montmorillonite are major matrix components with subordinate cryptocrystalline silica and iron oxides. Calcite constitutes as much as 30 vol% of the rock and frequently replaces quartz and feldspar. Detrital heavy minerals are remarkably rare in the Rio Puerco district. Small coalified wood fragments are identified by Bowman and Livingston (1980). The color of lower sands is commonly light grey except where limited ferruginous staining causes a reddish hue or where carbonaceous matter turns the color into brown or black.

Baum (in Bowman and Livingston 1980) envisages two sources of the allogenic constituents of the Westwater Canyon host sandstones: Well-rounded, equigranular grains of quartz, microcline, and untwinned perthitic orthoclase hint at a pre-existing sedimentary rock source. Fragments of volcanic debris and glass, irregularly shaped corroded quartz, and zoned plagioclase indicate a rhyolitic progenitor.

The lower sandstone unit encloses a rather pervasive greenish mudstone bed, the “K 1” shale, of 3 m thickness in Marquez Canyon and increasing to 8 m farther east. The sand above the “K 1” shale has a consistent thickness of 30–35 m, whereas the basal sand below the mudstone ranges from less than 1 m to as much as 25 m in thickness in a sedimentary lens having an elongate NW–SE axis.

The upper sandstone unit contains abundant mudstone in the western part of the Marquez area but becomes more arenaceous to the east and southeast. Upper unit sands are mixed fine- to coarse-grained, but are generally finer grained than sands of the lower unit and are moderately to poorly sorted, feldspathic to arkosic in composition, and grey in color. They are reduced and contain pyrite as well as other iron sulfides together with carbonaceous debris.

Approximately 40 m thick sediments of the Brushy Basin Member rest upon the Westwater Canyon Member. These sediments are greenish mudstones interbedded with two fine-grained and well-cemented kaolinitic sandstone horizons. The sands are considered an equivalent of the Jackpile Sandstone. Locally, basal mudstone is intercalated with thin limestone laminae. Cretaceous sediments, almost 500 m thick, cover the Jurassic Morrison Formation. Some northerly trending normal faults dissect the area. They caused displacements of several meters to tens of meters.

The alteration of the Westwater Canyon host rocks is evidenced by the presence of authigenic kaolinite nests, corrosion of quartz grains, sericitization of feldspars, and replacement of quartz and feldspar by calcite.

Mineralization and Dimensions

The *Marquez deposit* includes the *Marquez Canyon* and the *Southeast* ore bodies, which are 1,500 m apart in ESE direction. Resources (status 1983) amount to ca. 7,000 t U at a grade of 0.09% U (McLemore and Chenoweth 2003).

According to Bowman and Livingston (1980), coffinite and pitchblende are the principal U minerals. Hexavalent U minerals are very rare. Large quantities of pyrite of probably several generations are present in the Southeast ore body. At Marquez, pyrite is found within and outside of ore boundaries. Although limited in quantity, ferric iron minerals (hematite) exist in both ore bodies suggesting some relationship to ore formation. Uranium minerals occur in two modes, at least in well-mineralized samples: (a) As fine-grained disseminations and as discrete larger particles (less than 1 mm) in the sandstone matrix, and (b) in coatings around quartz grains. Coatings are composed of uranium minerals, carbonaceous matter, very fine-grained pyrite, iron oxides, and carbonates. Extrinsic trace elements coextensive with mineralization but genetically not necessarily related to it include As, Ca, Co, Cr, Fe, Mn, Mo, Ni, Pb, V, Y, and Zr.

Ore is contained almost exclusively (99%) in the lower Westwater Canyon sand unit where it occurs in three horizons as peneconcordant, elongated zones of reasonable continuity along the WNW–ESE trend direction. The *upper ore horizon*, positioned in a 15 m thick interval between the “K”-shale and the “K-1” shale beds, is generally of low U grade, and the ore is in radiometric equilibrium. The *median ore horizon*, as much as 3 m thick, lies immediately above the “K-1” shale bed and contains better grades than the two other horizons. Ore in this horizon is in some radiometric disequilibrium. In Marquez Canyon, uranium appears to be chemically enriched, whereas in the Southeast ore body, where almost all ore is in the median zone, uranium shows a slight chemical deficiency. The *lower horizon* occupies an interval below the “K-1” shale. It is often conterminous with the boundary of the subjacent Recapture Member. This sand horizon splits locally into two levels. It contains a higher tonnage but at a lower grade than the median ore horizon. At Marquez Canyon, chemical uranium assays are higher than radiometric values.

Ore body configuration in the Rio Puerco district is commonly controlled by the morphology of a braided paleofluvial system except in two areas, Marquez Canyon and another in the southeast, where mineralization is governed by the morphology of a meandering paleostream. At *Marquez Canyon*, where uranium spans a vertical interval of almost 50 m, the median ore zone resembles, in plan view, a meander bend convex to the south. West of the bend, ore follows the regional NW–SE trend, and to the east it continues for at least 600 m from the bend. An analogous configuration of the same ore horizon exists in the

Southeast ore body. Here, the WNW–ENE stream direction was apparently deflected or overprinted by a meander resulting in a southward deviation of ore for about 100 m, which then turns eastward again and continues along the normal trend. In both areas, ore accumulated preferentially within point bar accumulations. The lateral ore boundary along the northern edge of ore zones is often more abrupt, in contrast to the southern margin where it is gradational.

The *San Antonio Valley* hosts two uranium deposits approximately 4 km apart in N–S direction (Chenoweth and Holen 1980). The deposits lie at a depth of 270–390 m and contain 1,350 t U at a grade of 0.085% U (Pool, personal communication).

The *Antonio Valley deposit* as described by Moore and Lavery (1980) is of trend type. It consists of three NW–SE-elongated, flat-lying, tabular uranium zones in reduced Westwater Canyon sandstone. The zones are approximately 1.6 km long, 3 km wide, and 2–4 m thick. Coffinite in a fine-grained organic matrix is the dominant U mineral. There is some radiometric disequilibrium in the ore body. The NE edge has 14% excessive chemical uranium, whereas the SW margin is depleted in uranium. The authors reason that groundwater flowing from NE to SW through the ore body may have caused a mobilization of uranium daughter isotopes, which have been redeposited in the central and southwestern parts of the deposit.

Ore Control and Metallogenic Aspects

Bowman and Livingston (1980) note the following characteristics governing ore control and ore-forming processes:

- Ore emplacement is peneconcordant and primarily of pre-fault trend type with only one local exception on the eastern upthrown margin of the Marquez Canyon fault
- Uranium precipitation and ore zone configuration was influenced by the presence of humate and possibly subordinate hydrogen and iron sulfides in permeable sand beds and along mudstone horizons
- Uranium precipitated preferentially in generally WNW–ESE-oriented paleochannels, which had developed some degree of sinuosity due to stream meandering (point bar mineralization).

1.1.1.2 Bernabe-Montano Grant

Bernabe-Montano is the easternmost known deposit of the Rio Puerco district and, as such, also of the Grants Uranium Region. It is situated approximately 15–20 km ESE of Rio Puerco, just off the SE edge of the Colorado Plateau. Resources (status 1971) were estimated on the order of 5,800 t U at a grade of 0.085% U (McLemore and Chenoweth 2003).

Sources of information. Kozusko and Saucier 1980; McLemore 1983; McLemore and Chenoweth 1989, 2003; McLemore et al. 2002; Porter 1981 unless otherwise cited.

Geological Setting of Mineralization

Uranium is hosted in a thick sandstone lobe interpreted by Galloway (1978) to be a distal fan facies of the southeastern edge of the Westwater Canyon alluvial fan. U mineralization is structurally located where the SE flank of the San Juan Basin is disrupted by numerous faults of the Rio Puerco fault zone. These faults are of late Tertiary to Quaternary age. They strike about NNE–SSW, are 400–800 m apart within the Bernabe-Montano Grant, and form a series of narrow horsts and grabens with displacements of several tens to hundred meters. As a result of faulting, the regional inclination of strata is reversed, thus the ore-hosting Morrison sediments dip at about 3° SE in the Bernabe-Montano area.

The mineralized **Westwater Canyon Member** is 30–100 m thick and commonly consists of light grey to light reddish-brown, cross-bedded, medium-grained, poorly sorted, and moderately well cemented pyrite-bearing feldspathic sandstone layers interbedded with subordinate, discontinuous lenses of grey-green and locally light reddish mudstones of variable, generally small thickness. Organic material is present as humate and, but rarely, as detrital relics. The Westwater Canyon rests upon mudstone and sandstone of the Recapture Member and on the eolian Bluff Sandstone. It is overlain by Brushy Basin mudstone (30–75 m thick) and Jackpile Sandstone (0–90 m thick) of the upper Morrison Formation, and is successively overlain by Late Cretaceous Dakota Sandstone, Mancos Shale, and Gallup Sandstone.

Oxidation probably due to young southeasterly migrating oxygenated groundwater affected the Westwater Canyon sandstone. As a result, sandstone in the northern section of the Bernabe-Montano area is altered to a yellowish grey color where the pyrite content was decreased and some uranium was remobilized.

Mineralization and Dimensions

Mineralization consists of multiple stacked uraniferous humate blankets in reduced sandstones. Coffinite and some pitchblende appear to be the principal U minerals. They are intimately associated with organic matter in blackish sooty material that fills voids and coats sand grains. Vanadium and selenium show some zonal arrangement. Pyrite is a common constituent of mineralized zones.

Ore bodies occur within two mineralized trends, characterized by minor diastems or scours and multilayered sedimentation. The northern trend is about 4.5 km long and the southern about 10 km long. Both trends are up to 600 m wide, and are within a 3,200 m wide, WNW–ESE-trending zone, which is thought to be an eastern extension of the Rio Puerco paleofluvial system. These trends contain multiple stacked horizons of uraniferous humate, which appear to have accumulated in thicker and laterally more continuous Westwater Canyon sandstone.

Mineralized sandstone beds are several centimeters to more than 3 m thick, 450–600 m wide, and several hundred meters to

a few kilometers long. In stacked sections, the thickness may accumulate to 25 m. Ore is distributed in a discontinuous and poddy mode. Individual ore zones consist of tabular, narrow, elongated, and sinuous lenses, 60 m or less in width, within each mineralized sheet. They are located more or less in the central portion of the mineralized trend. In these belts, uranium grade decreases from a core zone toward the edge of the blanket. Although ore lenses generally seem to be distributed without a distinct pattern throughout the Westwater Canyon Member in the Bernabe-Montano deposit, there is a selected part of it, in which they are usually confined to either the upper, middle, or lower part of the member. The weak oxidation front, which progressed southward to the margin of the northern, organic-rich mineralized trend, has dispersed uranium in thicker but lower grade mineralization along the northern edge of the trend. Late Tertiary faults with displacements of as much as 100 m or more offset the ore zones.

Delineated resources are positioned at depths from 450 to 600 m. Grades vary considerably from traces to more than 1% U, averaging 0.085% U.

Ore Controls and Metallogenic Aspects

The Bernabe-Montano deposit is in most respects similar to those in other districts of the Grants Uranium Region but it has some geologic differences. Kozusko and Saucier (1980) and Porter (1981) list the following features:

- Mineralization is emplaced in the distal facies of the Westwater Canyon alluvial fan, which is composed of often discontinuous sandstone lenses. These lenses are interpreted to be part of meander channels, which cross and cut off each other
- Uranium appears to be localized in a fairly straight mineral trend, where sandstones are slightly thicker and laterally more continuous and are interpreted as straight to sinuous channel deposits of the meandering river system
- Unusually large halos of lower grade mineralization surround ore zones
- Ore horizons are displaced by faulting that created horsts and grabens
- Faulting reversed the dip of sediments to the SE
- Faulting is of late Tertiary to Quaternary age, i.e. it is younger than that in other parts of the Grants region
- An oxidation interface approaches the mineralized area from the north. It is destructive to mineralization but has caused only a minor redistribution of original U mineralization at the northern margin of the northern ore trend
- Oxidation advancement seems to have been stopped or slowed when approaching the uraniferous humate masses or blankets
- Better mineralization apparently occurs in structurally low areas along the trend.

The discontinuity of significant mineralization and variations of ore grade and quantity are explained by Kozusko and Saucier (1980) to be a result of lateral variation in geochemical and

sedimentological conditions along any given sand sheet and by a tortuous network of favorable sandstone facies within the sandy layers.

Uranium source and ore-forming processes are considered identical to those of other deposits in the Grants Uranium Region as described earlier.

1.1.2 Laguna District

The Laguna district, discovered in 1951, is located about 50 km E of Grants, north of the small town of Laguna, and includes the *Jackpile-Paguete* (open pit and underground mines), *St. Anthony/M6* (open pit, underground), *L-Bar Ranch* (underground), and *Woodrow* (underground) deposits in the Late Jurassic Jackpile Sandstone. A few small deposits have been found south of Laguna including the *Crackpot* and *Sandy* mines, where ore is hosted by crinkly and platy zones of outcropping Todilto Limestone. Original resources including the production of the Laguna district were on the order of 70,000 t U. Production from 1951 to 1983 amounted to ca. 39,000 t U at a mining grade of 0.09% U. The uranium–vanadium ratio varied between 3:1 and 1:2.

Sources of Information. Adams et al. 1978; Baird et al. 1980; Beck et al. 1980; Brookins 1975a, b; Crawley 1983; Jacobsen 1980; Jensen 1963; Kelley et al. 1968; Kittel 1963; Kittel et al. 1967; Lee and Brookins 1978; McLemore 1983; McLemore and Chenoweth 1989, 2003; McLemore et al. 2002; Megrue and Kerr 1965, 1968; Moench 1963; Moench and Schlee 1959, 1967; Nash 1967, 1968; Nash and Kerr 1966; Schlee 1957, 1959, 1963; Schlee and Moench 1961; Wylie 1983. A comprehensive description of the area, particularly on the Jackpile-Paguete deposit, is given by Moench and Schlee (1967), which is used for the following description with amendments from the other authors listed and Adams SS, Jacobsen L, and Saucier AE (personal communication).

Geological Setting of Mineralization

Uranium mineralization occurs in the Jackpile Sandstone (a local term for an intercalated arenite stratum) in the uppermost part of the Brushy Basin Member/Morrison Formation. The *Jackpile Sandstone*, locally as much as 60 m thick, is spread over an area up to 20 km wide and more than 50 km long. It was presumably deposited in a NE-trending structural depression, which splits into two branches, about 30 km N of Laguna (Schlee and Moench 1961). The Jackpile Sandstone is unconformably overlain by Dakota Sandstone, which is locally silicified at its base. Mancos Shale rests on the Dakota Sandstone. The sediments dip with about 2° NNW into the San Juan Basin.

The Jackpile Sandstone is a fluvial, intensely cross-bedded, poorly sorted, ENE-trending channel filling. It consists of a yellowish to light-grey, friable carbonaceous sub-arkose, cemented mainly by clay minerals and lesser calcite adjacent to mineralization. Bentonitic clay galls are numerous throughout the sandstone. The grain size is highly variable ranging from silt

to pebble. Near the Dakota Sandstone unconformity, sandstone interstices are filled with greenish to white kaolinite. Sandstone is interbedded with discontinuous lenses of bentonitic mudstones, generally less than 3 m thick. In the vicinity of ore, greenish montmorillonite is often developed.

The Jackpile Sandstone hosts only peneconcordant trend ore. Mineralized lenses are horizontal and generally have a flat or planar upper surface that cannot be related to either lithologic composition or sedimentary structures. No stack-type mineralization has been found, but there are mineralized breccia pipes such as the Woodrow pipe.

Mineralization and Dimensions

Mineralization occurs in several deposits extending over a SW–NE distance of about 6 km from the Paguate open pit in the SW to the L-Bar underground mine in the NE. Individual deposits have the following characteristics.

1.1.2.1 Jackpile-Paguete

This deposit consisted of two large ore bodies, Jackpile and Paguate. Both were mined by open pit operations from 1951 to 1983 and are depleted after producing some 35,000 t U at a mining grade of 0.08–0.11% U (0.035% U cutoff grade).

All significant mineralization mined was restricted to epigenetic carbonaceous matter within sandstone and consisted mainly of coffinite mixed with uraniferous carbonaceous material, which impregnates sandstone by replacing clay minerals and quartz but not feldspar (Nash 1968). The ratio of carbonaceous matter to uranium was about 1:1 by weight (Adams et al. 1978). The ore occurred in lenses ranging in size from thin, discontinuous, and pod-like accumulations to ore trends, 3–10 m thick and as much as 35 m long (Fig. 1.21). Lenses were elongated subparallel to the NE-trending Jackpile channel and were grouped in the thicker, 30–70 m thick, portion of the channel. Although uranium is dispersed throughout the whole thickness, it is concentrated in three principal horizons, the deepest of which is 120 m under surface. The Jackpile ore body was about 1,500 m long, averaged about 800 m in width, and was as much as 120 m thick. The Paguate ore body had a length of more than 3,000 m and a width averaging about 60 m. Both ore bodies and some ores on their extensions may have been part of a continuously mineralized Jackpile trend that was transected by erosion.

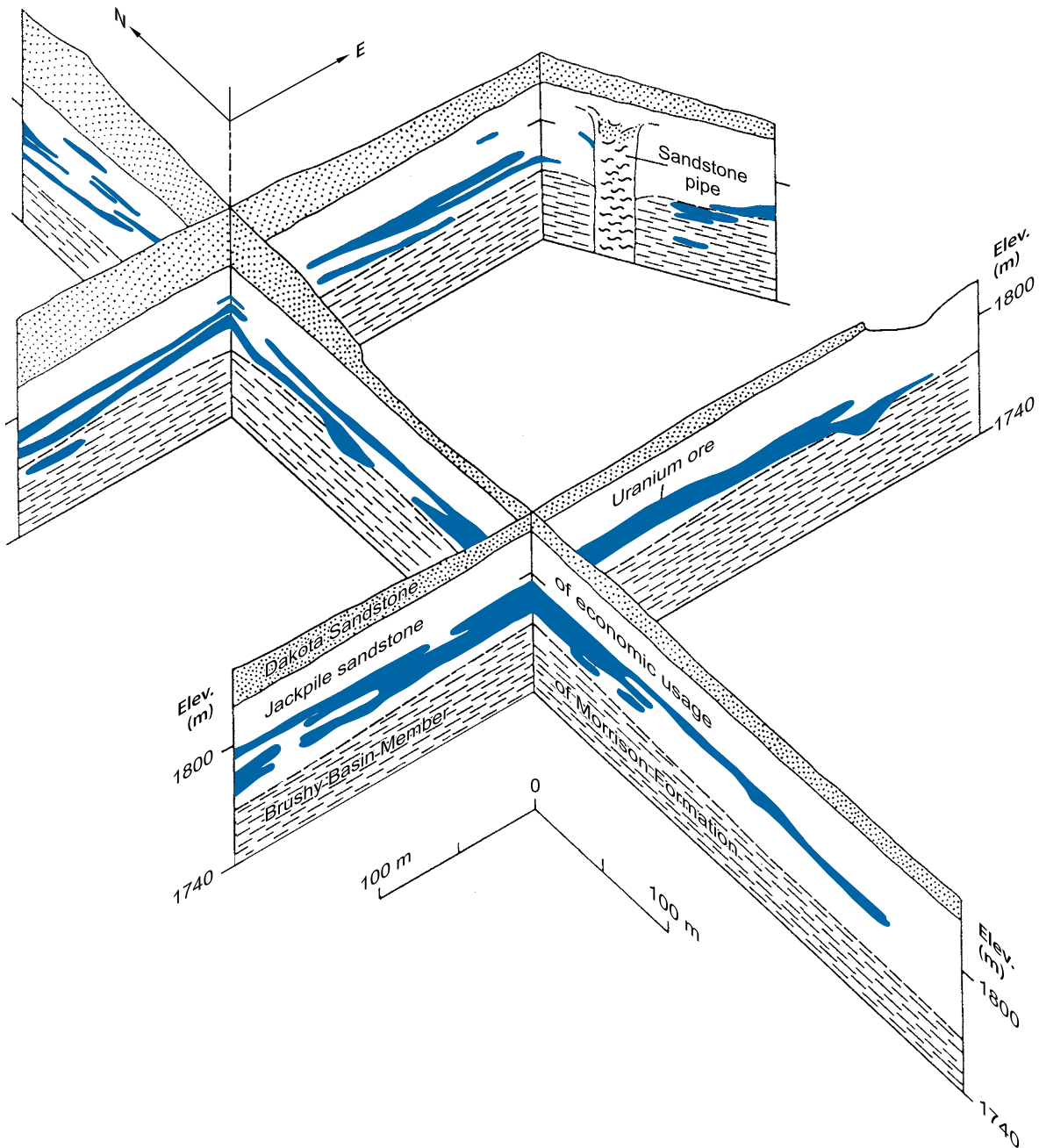
1.1.2.2 Woodrow Breccia Pipe

The Woodrow pipe is located about 2 km E of the Jackpile deposit (Fig. 1.4). It yielded a total of only 52 t U, but with 1.07% U (McLemore 1983) it had the highest average grade in the district.

The Woodrow pipe (Fig. 1.22) was an almost vertical, slightly to the east deviated, circular structure filled with breccia and bounded by marked ring fractures. The pipe cropped out

■ Fig. 1.21.

Laguna district, Jackpile deposit, generalized fence diagram of the southeastern part of the deposit showing the tabular nature and marked continuity of uranium mineralization. (After Moench 1963)



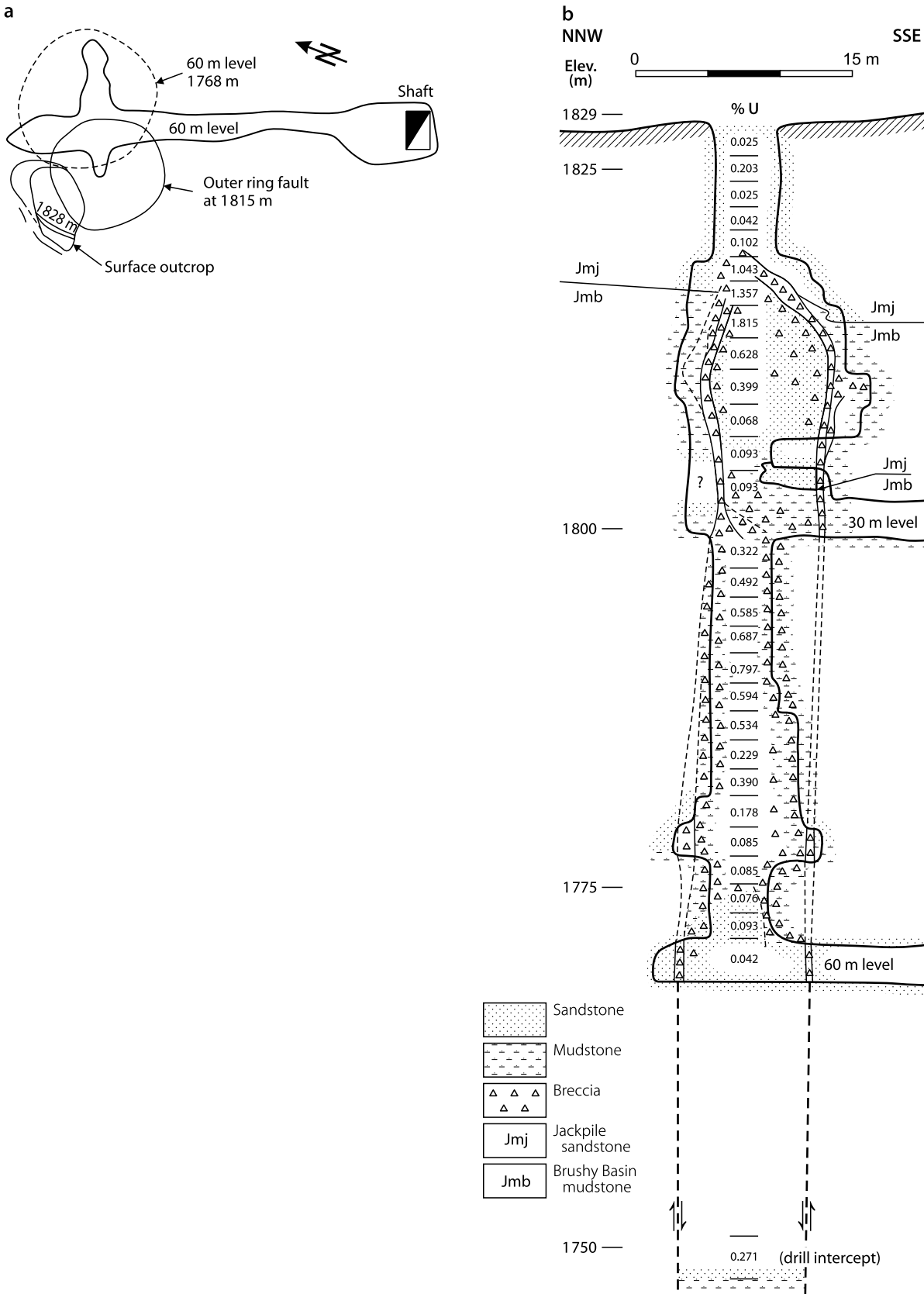
at surface in the basal part of the Jackpile Sandstone and penetrated downward with a variable diameter from 7 to 12 m for at least 90 m into Brushy Basin mudstone and sandstone. Jackpile Sandstone blocks had been dropped for about 12 m from the outer sandstone–mudstone contact downward.

The best mineralization occurred in the upper 30 m of the pipe where the grade averaged 1.3% U, 0.05% V_2O_5 , and 1.4% $CaCO_3$. The grade declined rapidly downward, from more than 0.5% at the 30 m level to less than 0.1% U at the 60 m level. It averaged 0.27% U and 0.03% V_2O_5 in this interval.

In the upper 30 m of the pipe, mineralization was particularly well developed at the level of the exterior stratigraphic sandstone–mudstone contact, where the pipe changes strike and dip, and where the pipe is filled with sandstone fragments. In this distinct interval, mineralization occupied circular ring faults and that part of the interior of the pipe that was heavily brecciated, as well as radiating fractures and permeable sandstone layers outside the pipe where the ore extended locally for up to 3 m away from the pipe contact. In the lower part, the pipe was filled with brecciated grey–green mudstone

Fig. 1.22.

Laguna district, Woodrow pipe, plan and section showing configuration, infill, and uranium grades in the pipe. (After Woodrow 1963)



and mineralization was confined to the interior of the pipe where it occurred as disseminations and coatings on brecciated mudstone fragments throughout the core of the pipe. Coffinite was the principal U mineral and lesser pitchblende. Associated minerals are abundant pyrite and less marcasite (Wylie 1963).

The *Jackpile pipe* is another pipe similar to the Woodrow pipe but by far less mineralized.

1.1.2.3 St. Anthony/M-6

Located about 3 km NE of the Jackpile mine, the St. Anthony/M-6 deposit is hosted in [Jackpile Sandstone](#) and contained essentially the same mineralization as that of the Jackpile-Paguete deposit. An early underground mine exploited an ore body about 300 m long, 15–90 m wide, up to 10 m thick, and situated at a depth of about 75 m. The grade was 0.12–0.2% U. In a later stage, two open pits, located about 800 and 2,000 m, respectively, to the ESE of the old mine, and an underground mine (Willie P ore body) exploited other ore bodies at a depth of about 100 m. The ore-hosting Jackpile Sandstone in this area is 25–35 m thick and contains original resources (status 1982) of 3,200 t U at a grade of 0.08% U (Pool, personal communication).

1.1.2.4 L-Bar Ranch/J.J. No. 1 Mine

This deposit is situated ca. 6 km to the NNE of the Jackpile mine and about 3 km in northwesterly direction of the St. Anthony deposit. It is the furthest northerly and downdip of known significant U deposits in Jackpile Sandstone. Original resources of the L-Bar Ranch deposit including production were reportedly 8,500 U at a grade of about 0.1% U. Remaining resources (status 1981) amount to 5,350 t U at a grade of 0.14% U (McLemore and Chenoweth 2003).

Mineralization is made up of numerous, fairly discontinuous thin lenses of uranium distributed throughout the entire section of the [Jackpile Sandstone](#). Jacobsen (1980) describes the mineralization as scores and possibly hundreds of tabular concordant lenses considered segments of channel fills and bars deposited by a large braided NE-trending stream. Richer parts of the deposit are clusters of partially coalescing mineralized depositional stretches. The Jackpile Sandstone is 25–30 m thick at the L-Bar Ranch, has a median grain size of 0.2–0.3 mm, and consists of 60–90% quartz, the remaining being feldspar and clay minerals. Shale or mudstone interbeds are rare.

Ore occurs in the form of elongated tabular lenses suspended in a larger envelope of low-grade mineralization over a stratigraphic interval of 6–20 m. “Barren” sandstone still contains 20–80 ppm U. Lenses may be as much as several tens to a hundred meters wide, up to 300 m long, and as much as 3 m in thickness. Top and bottom boundaries are abrupt and almost planar, whereas lateral limits are commonly gradational. Uranium is distinctly associated with carbonaceous matter, which is preferably concentrated in finer-grained sandstone, in greenish argillaceous beds, and in mudstone pebble conglomerates.

Organic material is present in two forms, (a) as syngenic detrital coaly particles of more or less the same size as the sand grains and as concentrations, normally to 2 mm thick, along bedding planes; both are interpreted to be products of normal sedimentary processes. And (b) as epigenetic humate coating and staining grains over intervals from a few centimeters to several tens of meters often in lenticular accumulations that dissect sedimentary structures. Jacobsen (1980) considers and has good proof that the grain-coating humate derived from humic acids, which formed from in situ decay of Jackpile internal detrital vegetal matter.

1.1.3 Mount Taylor District

This uranium district was discovered in 1970 near San Mateo about 15 km to the SE of and in continuation of the Ambrosia Lake district.

Original resources (status 1982) were estimated at about 47,000 t U at a grade averaging 0.2% U. This endowment includes some 19,000 t U at mining grades of ca. 0.4% U or more. The main deposit is *Mt. Taylor*. It was developed by a shaft, about 1,000 m deep, in the eastern section of a 10 km long mineralized trend. Limited exploitation produced some 1,800 t U at an average grade of about 0.4% U. Mining conditions were difficult with large amounts of water inflow (average about 15,000 L/min) and temperatures of about 55°C.

Sources of Information. Alief 1988; Alief and Kern 1989; Burgess et al. 1987; McLemore 1983; McLemore and Chenoweth 1989, 2003; McLemore et al. 2002; Riese 1977, 1979; Riese and Brookins 1977, 1980, 1984; Riese et al. 1980; Alief and Kern (personal communication). Riese’s various papers provided the base for the following description, updated by data of Alief and his coworkers or otherwise stated.

Geological Setting of Mineralization

Uranium occurs at depths from 900 to 1,200 m in arkosic sandstone beds of the *Westwater Canyon Member* of the Jurassic Morrison Formation. The Morrison Formation rests on the Jurassic Cow Springs Sandstone and is overlain by 700–900 m of psammitic and pelitic sediments of the Cretaceous Dakota to Menefee formations, which in turn are capped by 200–300 m of Tertiary volcanics (basalt etc.) of the 3,400 m high Mt. Taylor volcano.

Three members represent the Morrison Formation, from top to bottom, the Brushy Basin, Westwater Canyon, and Recapture members. The *Brushy Basin Member*, 15–45 m thick, is composed of variegated greenish and pink clay-mudstone and channel sandstone. It contains in its basal part the *Poison Canyon Sandstone*, which is mineralized locally. The *Recapture Member*, 15–50 m thick, consists of greenish and pink variegated mudstone, siltstone, sandstone, and minor limestone.

The *Westwater Canyon Member*, 40–70 m thick, is thought to be a southeasterly extension of the same channel system that

hosts the Ambrosia Lake district. According to Burgess et al. (1987), this member consists of alternating channel sands and shales. Six sand units, each 3–18 m thick (av. 6–9 m), are identified (Fig. 1.23) and denominated A to F. The A, B, and C sands are in the upper Westwater Canyon Member (30–45 m thick) and the D, E, and F sands are in the lower Westwater Canyon Member (10–25 m thick). Intervening shales, 0–12 m thick, separate the sand units. Because shale beds are commonly discontinuous, except the “K” shale, sand horizons coalesce with each other. The “K” shale averages 3.5 m in thickness and separates the upper from the lower Westwater Canyon Member. To the NW of the mine, strata have a shallow dip in an easterly direction and turn northerly within the mine area where the inclination is 0–5° N. At the SE end of the district, the dip increases to 20° N. Changes in strike and dip are attributed to the volcanic activity of Mt. Taylor. Minor faults are exposed in the mine. A major fault, the San Rafael Fault, runs near the mine to the east. Its SE block is down-dropped for 150–180 m. Most faults strike NNE–SSW.

Westwater Canyon sediments were deposited from northeasterly and easterly flowing rivers and from a southeasterly oriented stream system that intersected the first two channel trends.

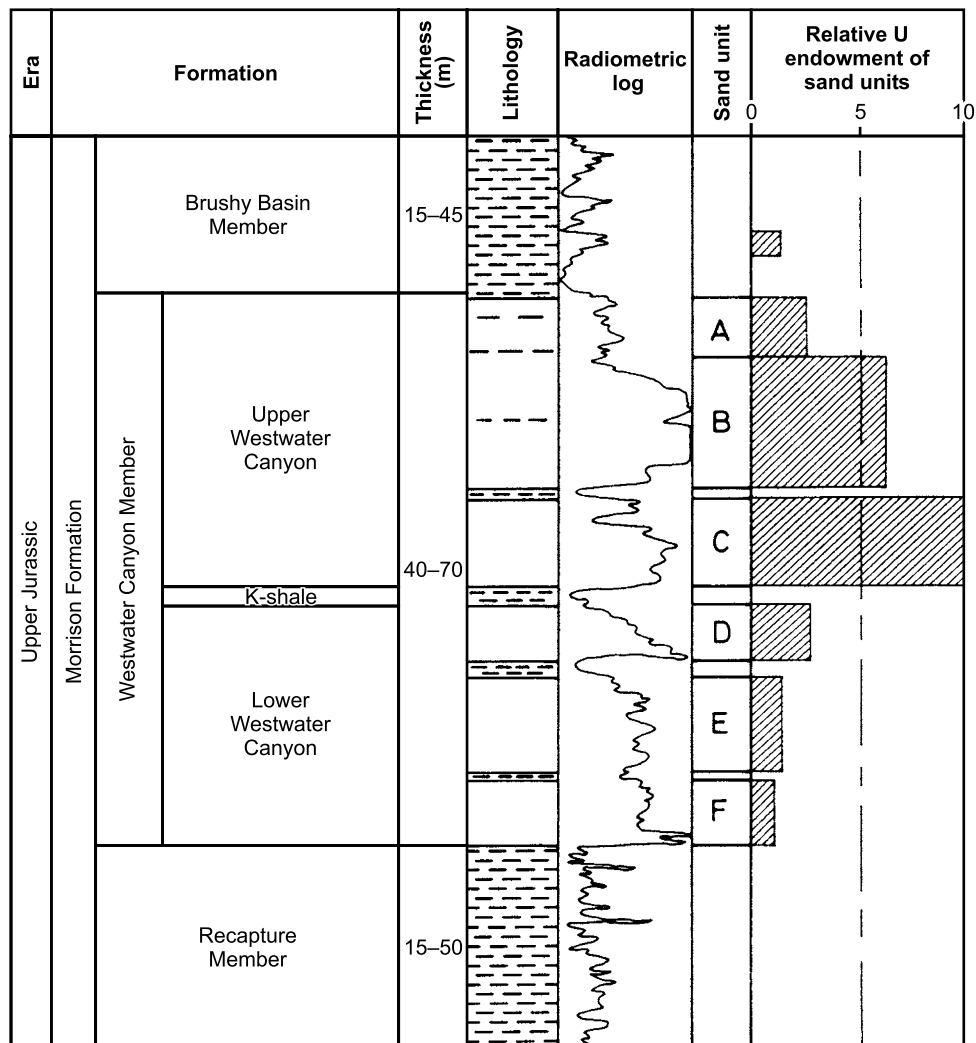
Mineralization and Dimensions

Only primary-type uranium ore has been identified so far at Mt. Taylor. Mineralized sands contain 10–15% opaque material imprinting a dark to black color on the rock. Carbonaceous substances and uranium mineralization accompanied by some pyrite constitute the opaque material. Ore essentially consists of coffinite and uraniferous organic complexes while pitchblende tends to be absent. Organic material is apparently present in two generations. Ore substances fill interstices, coat sand grains, and cement sand in ore zones, whereas sand is almost unconsolidated outside of ore zones.

Riese (1979) points out that limited amounts of pyrite occur both updip and downdip from mineralization. Calcite, as a

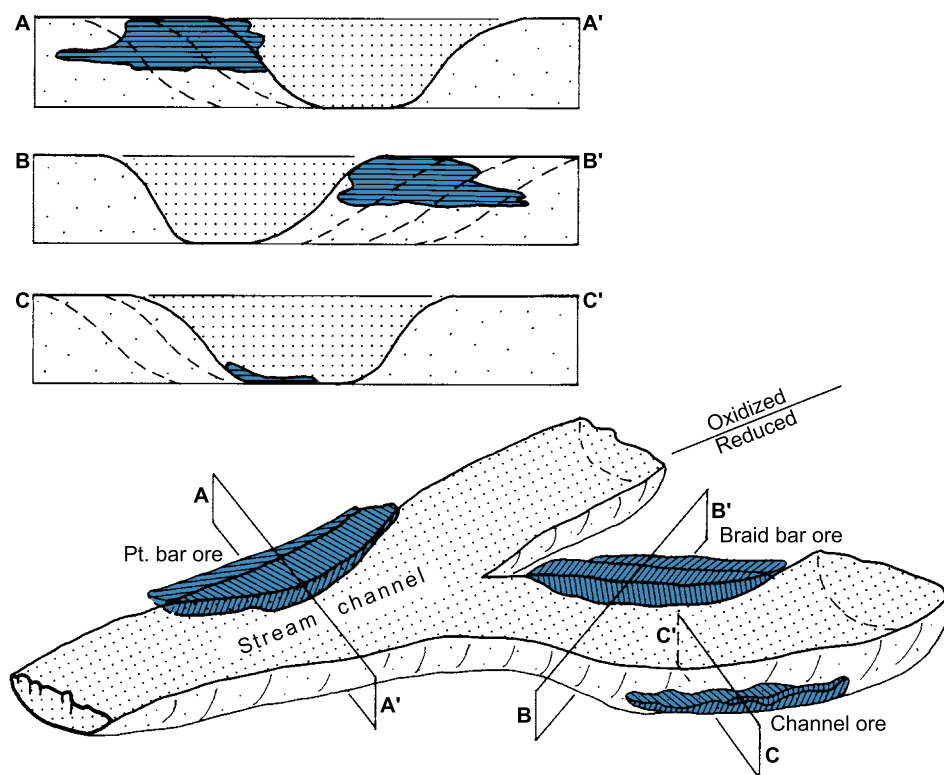
Fig. 1.23.

Mount Taylor mine, stratigraphic column with the distribution of uranium (radiometric log) and relative endowment of uranium in the recognized sand units (A to F) of the Westwater Canyon Member. (After Burgess et al. 1987)



■ Fig. 1.24.

Mount Taylor district, block diagram and cross sections illustrating the spatial relationship between ore bodies and sedimentary facies of the Westwater Canyon Member. Length of the channel is ca. 3.2 km, and the width ca. 0.8 km. (After Riese and Brookins 1984). (This figure was published in *Uranium*, v 1, p 193, by Riese and Brookins, *The Mount Taylor uranium deposit, San Mateo, New Mexico, USA*, Copyright Elsevier 1984)



matrix constituent, concentrates along down-dip and bottom edges of ore lenses. As, Se, Mo, and some other trace elements are zoned across the deposit in the direction of the dip. Montmorillonite, chlorite, and kaolinite seem to reflect a vague zoning from unaltered down-dip sediments, through the mineralized zone and into up-dip altered sediments.

All six sandstone horizons are mineralized to various degrees (● Fig. 1.23). Burgess et al. (1987) note that the “C” sand is the most prolific exhibiting the most continuous and highest grade ore. It immediately overlies the “K” shale. The next best horizon is the “B” sand, which is positioned with an intervening clay break above the “C” unit. It contains significant uranium resources immediately SE of the Mt. Taylor mine. The other four sandstone units contain scattered and low-grade uranium mineralization. Ore-hosting sandstones are arkosic in composition. Sand grains are medium to coarse in size, mostly of subangular to subrounded shape, and are medium to well sorted.

Ore is spatially related to meanders and is preferentially located at point bar deposits. Ore also occurs at braid bars and in channel fills (● Fig. 1.24). Riese and Brookins (1984) state that the localization of ore is controlled by an interplay of structure and stratigraphy as indicated by a discontinuous arcuate form and strict adherence of ore to particular stratigraphic environments. Ore is locally quite thick, appears to transect across-stratigraphic layers and displays tentacle-like developments

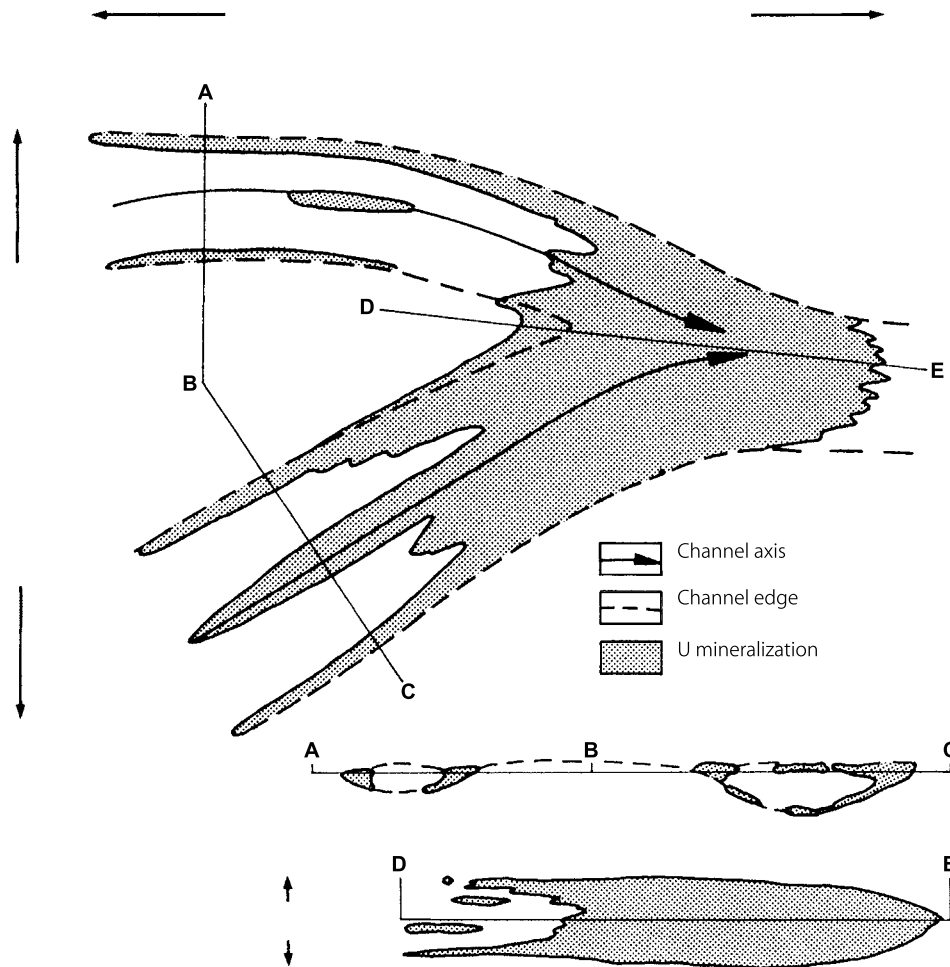
down dip. The authors note that Mt. Taylor ore differs from most deposits in the Ambrosia Lake district for it does not occur at an iron redox interface nor is it very pyritiferous.

Alief (1988) specifies the configuration of mineralization at the Mt. Taylor mine. Trend ore commences at the west end of an ore zone as “long skinny rollfront-type deposits”, 3–4.5 m wide, 3–6 m thick, and in excess of 800 m long. Mineralization begins to accumulate proximal to edges, tops, and bottoms of individual sand channels presumably in zones of relatively limited permeability. Going east, these trend ores, which locally exhibit a “C” shape, become more continuous and wider. Trends finally coalesce near and behind the convergence of channels (“interchannel island areas”) to form massive ore bodies. In plan view and cross section, this configuration resembles an octopus, the thin appendices constitute the tentacles and the coalesced massive ore lobe the body (● Fig. 1.25).

The established ore trend of the Mt. Taylor district is about 10 km long in NW–SE direction and about 0.5–2 km wide. It includes a number of high-grade ore zones interspersed with low-grade mineralization. High-grade ore occurs in at least three sites at the Mt. Taylor mine. At the northwestern most site, ore is emplaced in the “C” sands, has a NW–SE length of ca. 250 m and a width of 120–150 m. Combined with an easterly adjacent ore zone, it accounts, for ca. 4,000 t U, at an in situ grade of about 0.47% U. The high-grade zone is developed where

■ Fig. 1.25.

Mount Taylor mine, planview and sections of mineralization in the “C” sandstone unit documenting the marked increase of ore at the confluence of two channels. (After Alief, personal communication 1987)



WNW–ESE-trending channels merge with channels oriented NE–SW. Ore contains ca. 1% organic carbon in carbonaceous complexes and 0.4–3.5% inorganic carbon, present mainly as CaCO_3 . The carbonate content averages 1% CaCO_3 , but locally augments to several percent with highest carbonate contents of ca. 4% associated with highest ore grades. Mo is present from traces to 0.1%. Pyrite content is about 2.5%. Another high-grade ore body is on trend to the SE of the foregoing ore zone. It contains approximately 14,000 t U at an in situ grade of 0.6% U (Alief, personal communication).

Alief (1988) postulates the following parameters as critical prerequisites for high-grade ore at the Mt. Taylor mine: (a) Quantity of organic material, (b) permeability of sands, (c) convergent zones of two channel systems, (d) position of ore-hosting sand on top of the “K” shale interbed, and (e) thickness of “K” shale ca. 5–7.5 m.

With respect to ore formation, Riese and Brookins (1984) point to the relationship of uranium to organic material that indicates two episodes of organic enrichment and implies that organic processes were as essential as inorganic mechanisms in

ore formation. Riese and Brookins’s (1984) *model for ore genesis* includes

- Devitrification and leaching of pyroclastic fractions incorporated in the Morrison sediments by organic acids
- Release of uranium to groundwater and its transport as dicarbonate–tricarboxylate compounds and possibly as organic ligands
- Downdip migration of solution causing an alteration of montmorillonite, which has derived from volcanic ash, to chlorite
- Reduction of dissolved uranium by organic material in point bars of paleostream systems and
- Adsorption of organically complexed uranium onto the ore-stage chlorite.

Ongoing diagenesis closed, at one stage, pathways for solutions by restricting their downdip migration in paleochannels. This caused some leaching of trace elements, particularly iron, by oxygenated groundwater and formed uranium concentrations along paleochannels.

1.1.4 Ambrosia Lake District

The earlier given general description of the Grants Uranium Region is largely based on data from the longtime established Ambrosia Lake district. For this reason, the reader is referred to the general chapter on the Grants region in order to obtain basic information on the Ambrosia Lake district, and for detailed data he may consult the papers of the listed authors. The following text presents the principal individual characteristics of the Ambrosia Lake district.

Discovered in 1955, the Ambrosia Lake district is located approximately 30 km N of Grants. This district contained the bulk of resources in Westwater Canyon sandstone in the ESE-oriented *Ambrosia Lake trend* and in Poison Canyon sandstone in the parallel *Poison Canyon trend*, about 10 km to the south (▶ Fig. 1.26). A further 3 km to the south, uranium occurs in Todilto Limestone along the *Todilto Bench* (▶ Figs. 1.4 and 1.14) (see Section 1.1.11 Uranium in Todilto Limestone). The *West Ranch area*, supposedly an annex of the district, lies in a northwesterly direction from the Ambrosia Lake trend.

Four ore types are distinguished: Primary trend ore, redistributed roll and stack ore, and relict ore bodies. The grade of redistributed ore is generally lower than that of primary ore. The uranium–vanadium ratio for primary trend ore is 2:1 to 10:1 and about 1:1 for redistributed stack ore.

Original resources of the Ambrosia Lake district, including production, were on the order of 130,000 t U at a grade averaging between 0.1 and 0.35% U.

Almost 30 underground mines were active in the Ambrosia Lake trend, most were named after the section in which they occur, about eight underground mines and two open pits were worked on the Poison Canyon trend, and some 40 small mines, mostly open pits, produced uranium from Todilto Limestone ore bodies.

Conventional mining lasted from 1957 to 1990 and produced 73,000 t U at ore grades between 0.1 and 0.4% U (McLemore and Chenoweth 2003). Peak annual production with 7,208 t U was attained in 1978. In addition, over 2,500 t U was recovered from 1964 to 2000 from waters from underground mines, which contained from a few to as much as 20 ppm U.

Sources of Information. Berglof and Wampler 1965; Birdseye 1957; Brookins 1975a, b; Clark and Havenstrite 1963; Clary et al. 1963; Corbett 1964; Crawley 1983; Cronk 1963; Dooley et al. 1966; Falkowski 1980; Fitch 2006; Foster and Quintanar 1980; Gabelman et al. 1956; Gould et al. 1963; Granger 1960, 1962, 1963; Granger and Inqram 1966; Granger and Santos 1982, 1986; Granger et al. 1961; Harmon and Taylor 1963; Hazlett and Kreek 1963; Jensen 1963; Kelley 1963a; Kelley et al. 1968; Kendall 1971; Kittel et al. 1967; Knox and Gruner 1957; Lee and Brookins 1978; Ludwig et al. 1984; Mathewson 1953a, b; McLaughlin 1963; McLemore 1983, 2002; McLemore and Chenoweth 1989, 1991, 2003; McLemore et al. 2002; Myers 2006; Pierson and Green 1980; Rapaport 1963; Rautman 1980; Roeber 1972; Santos 1968, 1970, 1975; Smith and Peterson 1980; Spirakis et al. 1981; Squires 1963, 1970, 1974, 1980; Tessoroff 1980; Thaden and Santos 1956; Turner and Gunderson 1980; Turner-Peterson et al.

1980, 1986; Young and Ealy 1956; Zitting et al. 1957, Wertz (personal communication).

Geological Setting of Mineralization

The shallow north-dipping *Westwater Canyon Member* of the Morrison Formation is the major uranium host. The *Morrison Formation* is about 150 m thick in most of the district but thickens toward the N and W to some 240 m. At outcrop, the *Westwater Canyon Member* has a thickness of 15 m. It thickens to 35–80 m in the central section of the Ambrosia Lake district, where it lies 200–300 m under surface. The Westwater Canyon strata conformably overlay the Recapture Member and are overlain by the Brushy Basin Member with which it intertongues (▶ Figs. 1.6 and 1.14).

The Westwater Canyon rocks consist chiefly of light yellow to grey, fine- to coarse-grained, poorly sorted, cross-bedded subarkosic sandstone interbedded with laterally discontinuous bentonitic mudstone layers ranging from a few decimeters to 12 m in thickness. Sandstone–mudstone ratios range from about 2:1 to 10:1. They decrease in the upper part of the Westwater Canyon Member. Sandstone–mudstone distribution appears to be the result of numerous overlapping fluvial channels.

At its top and above a 5–8 m thick mudstone layer, the Westwater Canyon Member contains the Poison Canyon Sandstone, a clastic unit lithologically similar to the Westwater Canyon sandstone. Along outcrop, the Poison Canyon Sandstone is about 15 m thick (e.g. at the Poison Canyon mine), and varies elsewhere between 10 and 25 m in thickness. It extends for several kilometers to the east and north where it grades into the Brushy Basin Member.

The Westwater and Poison Canyon sandstones are in gradational contact to the overlying 20–60 m thick Brushy Basin Member, which dominantly consists of greenish-grey, often bentonitic mudstone with thin interstratified sandstone lenses. The Cretaceous Dakota Sandstone lies on top of this sequence.

The Ambrosia Lake district is dissected by mainly NNE–SSW-trending faults such as the Ambrosia fault zone in the west and the San Mateo fault zone in the east of the district.

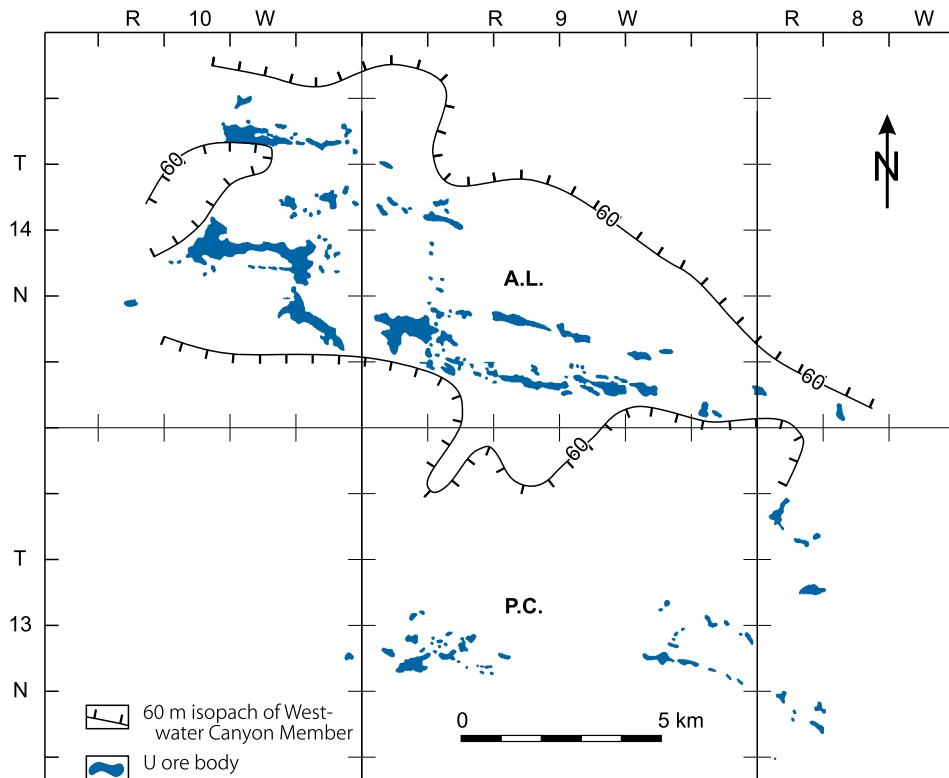
Mineralization and Dimensions

The primary trend ore consists predominantly of uraniferous humate, coffinite, and occasionally pitchblende. Ore impregnates host sands and forms crenulated blanket-like bodies, which are roughly tabular and have irregular lateral boundaries.

Ore bodies are aligned in two parallel trends, the Ambrosia Lake trend and the Poison Canyon trend (▶ Fig. 1.26). The *Ambrosia Lake trend* extends for about 15 km in ESE–WNW direction, from about the Lee Ranch (ore depth 800 m) and the Johnny M deposits in the east to the West Largo deposit (depth 660 m) in the west where the trend apparently terminates against the Ambrosia Lake fault zone. It probably continues eastward under the Mt. Taylor volcanic field where it may be linked with

Fig. 1.26.

Ambrosia Lake district, map of distribution of uranium ore bodies. Two ore zones occur in the Westwater Canyon Member sandstones in the Ambrosia Lake trend (A.L.) to the north and a third zone in the Poison Canyon Sandstone/Brushy Basin Member in the Poison Canyon trend (P.C.) to the south. (After Santos 1963)



the Mt. Taylor ore bodies. The belt is 2 km wide in the E and 4 km in the W and occupies the thicker portion of the Westwater Canyon sandstone, i.e. where the sand is more than 60 m thick. The Ambrosia Lake belt encloses several subparallel ESE–WNW-oriented ore zones. Individual ore zones are 150–1,000 m wide and up to 2 km or more long. They are composed of multiple peneconcordant sand horizons, 3–20 m thick, which are interbedded by discontinuous mudstone layers. Uranium commonly occurs in sand beds as tabular accumulations that range in thickness from several centimeters to more than 5 m averaging about 2 m and extend in length from a few meters to several hundred meters. Redistributed ore often forms stack deposits along faults, which may be as much as 40 m or more thick.

Oxidation altered the Westwater Canyon sandstone to the south of the Ambrosia Lake trend, and apparently destroyed most of the former ore, leaving behind only islands of reduced sandstone with remnant deposits such as the Section 28 deposit to the SW of the main Ambrosia Lake trend, or more or less oxidized, or “ghost” deposits, such as perhaps the Sandstone mine. (For more details of characteristics of mode and distribution of U mineralization, see ▶ Figs. 1.14–1.20 in the earlier given general chapter of the Grants Uranium Region.)

The *Poison Canyon trend* parallels the Ambrosia Lake trend a few kilometers to the south but was only partially affected by oxidation. The Poison Canyon trend spans some 15 km from the

western Section 8 and 18 deposits and the Blue Peak mine, where ore was found at the surface, in a southeasterly direction to the San Mateo mine where ore lies at a depth of almost 420 m. Most Poison Canyon ore is concentrated near the base of the sandstone where it exceeds 12 m in thickness. Poison Canyon mineralization has a rather sharp boundary along its southern margin, which roughly parallels the long axis of the sandstone tongue, whereas the northern limit is gradational and irregular. Kelley et al. (1968) interpret this irregular boundary as the result of uranium distribution down dip along NE–SW-striking fracture systems, which may extend for about 3 km as inferred from Section 7 and 8 ore bodies.

1.1.5 Smith Lake District

Discovered in 1950, the Smith Lake district is located about 50 km NW of Grants and 30 km WNW of Ambrosia Lake. Principal deposits include *Black Jack No. 1* and 2, *Mac No. 1* and 2, *Ruby No. 1* to No. 4, and *Mariano Lake*. Eight underground mines, 60–140 m deep, produced greater than 5,000 t U in total at an ore grade of 0.17% U from 1951 to 1985. McLemore and Chenoweth (2003) report remaining resources (status 1983) of ca. 13,500 t U at a grade of 0.2% U contained in the Mariano Lake ore bodies.

Sources of Information. Brookins 1975a, b; Fishman 1981; Fishman and Reynolds 1986; Green and Jackson 1975a, b; Hoskins 1963; Hanshaw and Dahl 1956; Jenkins and Cunningham 1980; Kelley et al. 1968; Lee and Brookins 1978; Ludwig et al. 1984; MacRae 1963; McLemore 1983; McLemore and Chenoweth 1989, 2003; McLemore et al. 2002; Place et al. 1980; Ristorcelli 1980; Sachdev 1980; Santos 1963.

Geological Setting of Mineralization

Uranium occurs in Brushy Basin and Westwater Canyon sandstones of the Morrison Formation. The regional dip of the sediments is 3–5° to the NNE. The *Brushy Basin Member* is a fairly consistent unit, 25–65 m thick, which contains sandy intervals 5–25 m thick separated by mudstones. Sandstones are considered an extension or equivalent of the Poison Canyon Sandstone. According to Ristorcelli (1980), the U-hosting *Brushy Basin Member* consists of three green–grey to red feldspathic sandstone layers interbedded with green–grey (on top) and maroon (bottom) colored mudstones. Sandstones are poorly sorted, poorly consolidated, and contain a relative high amount of clay and up to 5% pyrite, when unoxidized.

The *Westwater Canyon Member* is some 60 m thick in the Smith Lake area and thickens to 85 m about 15 km N of Smith Lake. A laterally continuous, brownish mudstone horizon, 4–10 m thick, separates the Westwater Canyon Member into an upper and lower unit. Sediments are slightly folded along N to NW-trending axis. Most prominent is the Mariano Lake anticline. Mainly N–S and NE–SW-oriented faults with local displacements of up to a few meters dissect the deposits. An oxidation front affected the area and imposed a red hematitic and brown limonitic overprint on the sandstones.

Ristorcelli (1980) identified two distinctly different kinds and periods of alteration at the eastern end of the Smith Lake district (Ruby mines). The first is characterized by abundant kaolinite and ferrous iron minerals and is found with and around the poddy trend ore, the second is reflected by altered illite–montmorillonite and ferric iron minerals associated with and updip from roll-type ore.

Mineralization and Dimensions

Mineralization is found in an SE–NW-trending zone extending from the Ruby mines in the east to the Mariano deposit in the west, a distance of some 10 km. Most uranium is in sandstone of the Brushy Basin Member except for the Blackjack No. 1 mine, which is in upper Westwater Canyon sandstone. Although some primary E–W-striking trend ore is present, most uranium is in roll- and stack-type mineralization at or near the edge of a northerly advancing redox front that separates pyritic from hematitic–limonitic sandstones. Host rock immediately adjacent to ore is often strongly bleached.

The Ruby deposit, located at the eastern end of the Smith Lake district, contained four ore bodies, No.1 to No.4 with original resources totaling some 2,500 t U at a grade between

0.13 and 0.17% U. Uranium ore was mined at depths from 60 to 135 m and was restricted to the lower two sandstone horizons of the Brushy Basin Member mentioned earlier.

The *middle sandstone* horizon averages 15 m in thickness and contains both trend- and roll-type ores. Trend ore occurs as discontinuous blanket-like pods in unoxidized, pyritic, calcite-cemented sands 300–600 m downdip from the oxidation front. The redox interface is almost horizontal, and consequently unoxidized, pyritic sandstone directly overlies oxidized hematitic sands. As a result, ore bodies have a more wedge-shaped geometry, are generally less than 1.5 m thick, and always occur within the upper 3 m of the interface. Trend ore characteristically is associated with kaolinite filling interstices in the sands. In contrast, roll-type ore is accompanied by illite–montmorillonite, which coats sand grains, is overprinted by younger kaolinite, and is associated with hematitic alteration.

The *lower sandstone* horizon is generally less than 6 m thick and contains only roll-type mineralization. Ore is mostly emplaced at a laterally extensive redox front but occasionally occurs as much as 450 m updip behind the interface. Sands updip from the redox zone are hematitic. A limonitic alteration front zone often has advanced for 30–450 m further down dip. Ore is generally but not always concentrated in classical C-shape configuration at the limonite–pyrite interface.

The Black-Jack No. 1 deposit (MacRae 1963) is located in the center of the Smith Lake district, at the east end of the Mariano Lake anticline. Original resources were reportedly on the order of 1,000–2,000 t U. U mineralization is hosted in sands of the middle and upper Westwater Canyon Members. At least three distinct N–S-striking strike-slip faults intersect the deposit. Seven ore zones are identified, the lower three of which intertongue in the northern part of the deposit forming an E–W-trending primary blanket-type ore body of about 1,000 m in length, 150 m in average width, and between several centimeters and 10 m thick. The southern part of the deposit contains shorter, NE–SW-trending ore lenses. Characteristically, sharp contacts between ore and barren rock form the northern edges of these ore lenses. The upper four zones are composed of generally redistributed, low-grade ore emplaced in N–S-oriented fault zones where the ore can be stacked as much as 30 m. Host rocks are extremely bleached.

The Black-Jack No. 2 deposit (Hoskins 1963), located at the SW end of the Mariano Lake anticline, contained reportedly several hundred tonnes of U in a sandy channel correlated with the Poison Canyon Sandstone. The sand ranges in thickness from 5 to 15 m and contains three trend-type ore zones; the lowermost near the base of the sandstone was the most productive.

Mariano Lake: This deposit is located at the western end of the Smith Lake district. Mineralization occurs at a depth of approximately 100 m in the lowest sandstone unit of the 25–40 m thick Brushy Basin Member. The ore-hosting sand is a fluvial arkosic facies, 7.5 m in average thickness, that is interbedded between two fairly continuous, commonly less than 3 m thick, grey bentonitic mudstone horizons (Jenkins and Cunningham 1990). Normal, around N–S-striking faults with displacements of commonly less than 15 m cut the Mariano Lake deposit.

The Mariano Lake ore displays a C-shaped configuration with its tails commonly sitting at sandstone–mudstone contacts and pointing southward, which may imply that ore formed in response to a northerly advancing oxidation front. Mineralization essentially consists of a mixed U–V–humate assemblage. No primary uranium minerals have been identified. The ore zone is high in vanadium and generally, except locally, low in molybdenum and contains, in addition, higher concentrations of As, Ba, Ce, Pb, Se, Zn, and organic carbon. Selenium is concentrated in the near-oxidized zone. Calcite is practically absent. Elements show a zoning across the ore body similar to classical rollfront deposits in Wyoming. The coexistence of baryte and selenite with pyrite indicates Eh conditions overlapping the pyrite–hematite boundary (Place et al. 1980).

Authigenic clay minerals include presumably pre-ore stage montmorillonite, concentrated in the oxidized zone, chlorite concentrated in the ore zone and formed at the expense of montmorillonite during ore deposition, and kaolinite as the last formed clay mineral, which is concentrated in the non-oxidized zone. Some mixed-layer montmorillonite–illite replaces kaolinite. Detrital Fe–Ti minerals are altered to anatase, rutile, and hematite in oxidized, and pyrite in non-oxidized sands (Sachdev 1980).

Metallogenetic Aspects

Most Smith Lake ore appears to be similar to primary tabular mineralization coextensive with humate masses in the Ambrosia Lake district and therefore several authors conclude a similar genesis. For example, Fishman (1981) considers the Mariano Lake deposit as principally containing primary ore without significant redistribution and explains the irregular boundaries and the occasional C- and S-shape geometry as a result of destructive oxidation by groundwater in relative recent geologic time. In contrast, Place et al. (1980), Ristorcelli (1980), and Sachdev (1980) describe a typical rollfront configuration for several deposits with ore accumulation along the contact between oxidized and reduced sandstones. Jenkins and Cunningham (1980) conclude that the Smith Lake ore is clearly of rollfront type but also includes distinct criteria of a peneconcordant diagenetic ore type.

1.1.6 Church Rock District

Located approximately 25 km NE of Gallup, the Church Rock district is the westernmost extension of the Grants Uranium Region. McLemore and Chenoweth (2003) report resources of 28,000 t U contained in deposits of Church Rock Section 8 and 17, NE Church Rock, NE Church Rock No. 1, 2, and 3, and Mancos. Grades range from 0.17 to 0.21% U.

Uranium was discovered in 1952 and mining began in the same year and lasted until 1986. Nine mines produced 6,200 t U at ore grades from 0.13 to 0.17% U (Chenoweth, personal communication). Former mines include *Old Church Rock*, *Church Rock No. 1* and 2, *Northeast Church Rock*, and *Phillips*, as

well as the *Hogback No. 4*, and *Diamond No. 2* mines, situated 10–15 km S of the actual Church Rock district. The Church Rock No. 1 and 2 and Northeast Church Rock underground mines operated in depth of 450–520 m.

Sources of Information. Brookins 1975a, b; Chico 1963; Fitch 2005; Gabelman 1956; Kelley et al. 1968; Ludwig et al. 1977, 1982; McCarn 2001; McLemore 1983; McLemore and Chenoweth 1989, 2003; McLemore et al. 2002; Pelizza and McCarn 2004; Peterson 1980a, b; Pierson and Green 1980; Reimer 1969; Saucier 1967a, b; Sharp 1955 unless otherwise cited.

Geological Setting of Mineralization

Uranium mineralization has been found in sandstone throughout the Westwater Canyon Member of the Morrison Formation, and in some ore pods in the basal part of the Dakota Sandstone.

Morrison sediments dip slightly to the north. They are underlain by the Middle Jurassic Cow Springs Sandstone, which consists of clean, well-sorted, fine- to medium-grained quartzose sandstone of supposedly eolian provenance. The Morrison Formation is transgressed with a gentle angular unconformity by Cretaceous Dakota Sandstone, which fills paleochannels scoured into Brushy Basin mudstones. Immediately south of the Church Rock area, Dakota Sandstone rests directly upon the Westwater Canyon Member due to pre-Dakota erosion of the entire Brushy Basin Member in this area. Other Cretaceous sequences of both marine and continental origin overlie the Dakota Sandstone. A number of faults dissect the district including the prominent NE–SW-trending Pipeline fault.

The Westwater Canyon Member is up to 75 m thick in the Church Rock district and thins to the south. It comprises as much as eight sandstone horizons separated by green and reddish mudstone lenses of commonly limited lateral continuity. Sands are fine- to very coarse-grained, subarkosic to arkosic sediments.

The Brushy Basin Member is preserved in the district only as a feather-edge, thin, erosional remnant layer. This layer consists of greenish-grey, silty, and sandy mudstones, which are partly derived from pyroclastic material.

Mineralization and Dimensions

The Church Rock district contains some primary but mainly redistributed uranium in Westwater Canyon sandstone, and minor mineralization in Dakota Sandstone.

Westwater Canyon Member: Mineralization occurs in the proximal facies close to the main input area of the Westwater Canyon alluvial fan postulated by Galloway (1980). Uranium concentrations occur widely scattered throughout seven of eight sandstone horizons within this member. Prominent deposits are situated in a NE–SW-trending zone, 1–1.5 km wide and almost 10 km long. Seemingly, much of the mineralization is to some extent controlled by fracture zones along the NE–SW-striking Pipeline fault. Redistributed uranium forms ore bodies up to 6 m

or more thick that are often aligned in a NW–SE direction, normal to the Pipeline fault.

Ludwig et al. (1982) report that in the *Northeast Church Rock mine*, uranium accumulated at the nose and limbs of many vertically stacked redox interfaces. Immediately adjacent to the reduced sandstone contact, oxidation has produced limonite, which changes into hematite within tens to hundreds of meters further up dip from the redox front. In some contrast, the relation of uranium mineralization to redox interfaces is less obvious in the *Church Rock No. 1 and No. 2 mines*.

Peterson (1980a, b) describes *Church Rock Section 13* mineralization as forming elongate tabular, redistributed uranium ore bodies that parallel iron-redox interfaces peripherally along zones of highest permeability and local presence of organic material within the lowest four sandstone horizons of the NE–SW-trending Westwater Canyon fluvial system. The Westwater Canyon sandstone is bleached where directly overlain by Dakota Sandstone. Bleaching is spotty, ranges in thickness from less than a meter to 10 m or more, and tends to be superimposed on older oxidation phenomena. The Brushy Basin Member is up to 10 m thick and thins to zero just south of the Section 13 occurrence. Sporadic primary mineralization is still preserved in the uppermost part (C-zone) of the Westwater Canyon Member.

Pelizza and McCarn (2004) report an ore zone extending from *Church Rock Section 8* southward into *Section 17* for 1,600 m long and up to 300 m wide. U mineralization occurs stacked in several sand horizons. Individual ore lenses average 3 m in thickness and are stacked to a cumulative thickness of 24 m. In situ resources amount to 5,730 t U.

Dakota Sandstone: Mineralization is principally of small magnitude and may occur in Dakota paleochannels cut into the uppermost Brushy Basin Member (*Old Church Rock mine/Phillips mine*). The Old Church Rock mine is near the Pipeline fault zone. The *Hogback No. 4 mine*, located near Gallup south of the Church Rock district has uranium in the form of pitchblende and associated pyrite in well-cemented, very fine-grained, nearly white quartzose sandstone (Ludwig et al. 1977) and in a uraniferous bed 0.3–1 m thick of black fissile shale containing abundant coaly fragments. The shale experienced some strong weathering as indicated by U^{6+} minerals, iron oxides, and jarosite (Gabelman 1956) (see also Section Uranium Deposits in Cretaceous Dakota Sandstone).

Ore Control and Metallogenetic Aspects

Based on field evidence, Peterson (1980a, b) postulates the pre-Dakota geochemical cell processes in Section 13 to have formed at least part of the redistributed tabular U mineralization in the Westwater Canyon sandstone. Primary mineralization in the uppermost C-zone of the Westwater Canyon was not affected by this cell probably due to its position above the pre-Dakota water table during the time of redistribution. The position and shape of this redistributed mineralization indicate a control by essentially stationary humate masses, exerting strong reducing conditions in channel-margin facies of the Westwater Canyon fluvial system.

The bleaching of the Westwater Canyon strata, where in direct contact with the Dakota Sandstone, has been interpreted by Granger (1968) and Squires (1972) as a result of infiltration by acid waters derived from Dakota swamps. Peterson (1980a, b) objects to this conclusion and argues that this bleaching is superimposed on preexisting oxidized Westwater Canyon rocks hence hematite-forming oxidation processes, which are considered instrumental for uranium redistribution, must be of pre-Dakota age. The pre-Dakota influx of oxygenated groundwater that apparently penetrated only the middle and lower horizons of the Westwater Canyon Member took place in consequence of tectonic movements resulting in the northward tilting of all pre-Dakota strata, erosion of their outcrop, and exposure of strata-heads of the Morrison Formation to meteoric waters.

Assuming that Peterson (1980a, b) is correct in his interpretation, then there must have been an additional period of redistribution of uranium in Tertiary to Quaternary time as documented by Ludwig et al. (1977, 1982). Except for two samples, their U–Pb isotope investigations of samples from four mines resulted in apparent ages, which are all younger than 1 Ma and which suggest the possibility of two main Pleistocene age groupings around 0.9 and 0.5 Ma. Samples from Dakota Sandstone ore in the *Hogback No. 4 mine* yielded apparent ages of less than 0.15 Ma. Of the two samples with older ages, a mineralized bone fragment has an apparent age of about 68 Ma.

1.1.7 Crownpoint District

The Crownpoint district is situated in the NW part of the Grants Uranium Region, some 70 km NW of Grants and 20 km N of the Smith Lake district. Uranium was discovered in 1972 and subsequently the following deposits were delineated (from W to E): *Narrow Canyon*, *Dalton Pass*, *North Trend*, *South Trend*, *Canyon*, *Crownpoint*, and *Monument* distributed over a WNW–ESE stretch of some 20 km from the Dalton Pass to the town of Crownpoint and beyond. All deposits occur at depths from 600 to 750 m.

Total resources of the district are in excess of 35,000 t U at grades ranging from less than 0.1% U (*Narrow Canyon*) to 0.2% U (*South Trend*).

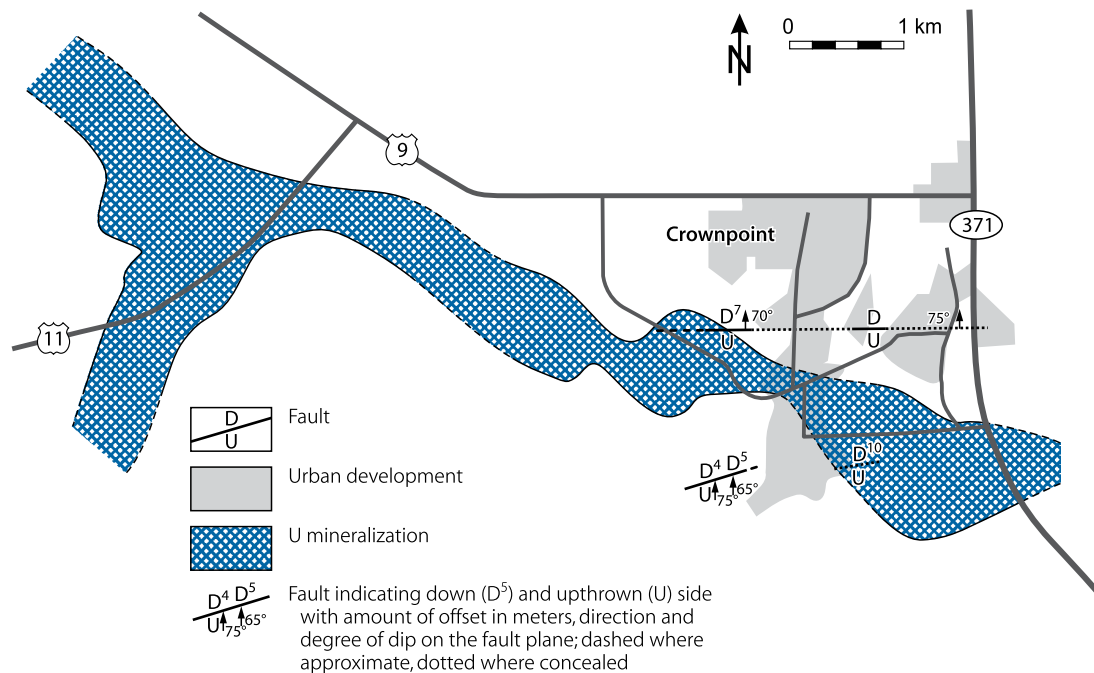
Pelizza and McCarn (2004) report in situ resources of 15,000 t U for a portion of the Crownpoint deposit and 10,400 t U for Crownpoint Unit 1. The latter is a western extension of the former but separated by another concession, about 800 m wide. Both are part of the larger Crownpoint deposit (Fig. 1.27a).

Sources of Information. Chenoweth and Holen 1980; McLemore 1983; McCarn 2001; McLemore and Chenoweth 1989, 2003; McLemore et al. 2002; Myers 2006a, b; Pelizza and McCarn 2004; Wentworth et al. 1980.

The following is a description of mineralization in Section 29, which hosts the eastern portion of the Crownpoint deposit, summarized from Wentworth et al. (1980) unless otherwise noted. Resources of this section are estimated at up to 4,000 t U at a grade of about 0.12% U.

Fig. 1.27a.

Crownpoint deposit, generalized map with outline of the deposit. (After McCarn 2001)



Geological Setting of Mineralization

Deposits of the Crownpoint district are located on the Chaco Slope in the San Juan Basin (Figs. 1.3 and 1.4). The Crownpoint deposit proper, located at the town of Crownpoint, is emplaced in the *Westwater Canyon Member* of the Morrison Formation. The *Westwater Canyon Member* consists of sandstone and mudstone of fluvial provenance deposited in an ESE–WNW-trending channel system.

The *Westwater Canyon Member* rests upon grey and red-brown mud- and siltstones of the *Recapture Member*. Bentonitic mudstone with lenses of silt- and sandstones of the *Brushy Basin Member* (25–40 m thick) conformably overlie the *Westwater Canyon* strata. They are transgressed along a regional unconformity with considerable relief by *Dakota Sandstone* and younger Cretaceous sediments totaling 550 m in thickness.

In *Section 29*, the *Westwater Canyon Member* is largely ca. 110 m thick, but thins to approximately 75 m at the southern edge and also to the north of *Section 29*. Maximum composite sandstone thickness is about 105 m along the ESE–WNW main channel axis due to an increase in number and thickness of individual sandstone beds in the upper part of the *Westwater Canyon Member*. Five distinct sandstone horizons are present, denominated A, B, C, D, E (from top to bottom), each 10–30 m thick. Interstratified pale-green mudstone layers with sparse red mottling are several centimeters to 10 m thick.

Sandstones are feldspathic, fine- to medium-grained, poorly sorted, moderately cemented, and grey in color. They contain pyrite except where oxidized. Grain size tends to decrease toward the north in the lower C and D sands.

The alteration of a northward moving oxidation front, probably belonging to the regional oxidation front postulated by Saucier (1980), has approached the southern part of *Section 29*. It transformed grey, pyritic *Westwater Canyon* sandstones into a reddish hematitic facies. The alteration pattern is complex reflecting a differential oxidation of various sandstone horizons. Lower sandstone beds were apparently affected more strongly than the upper A and B horizons.

Sediments dip 1–2° NNE. No faults are recorded in *Section 29*, although NE–SW-trending faults with limited displacements have been identified elsewhere in the Crownpoint district.

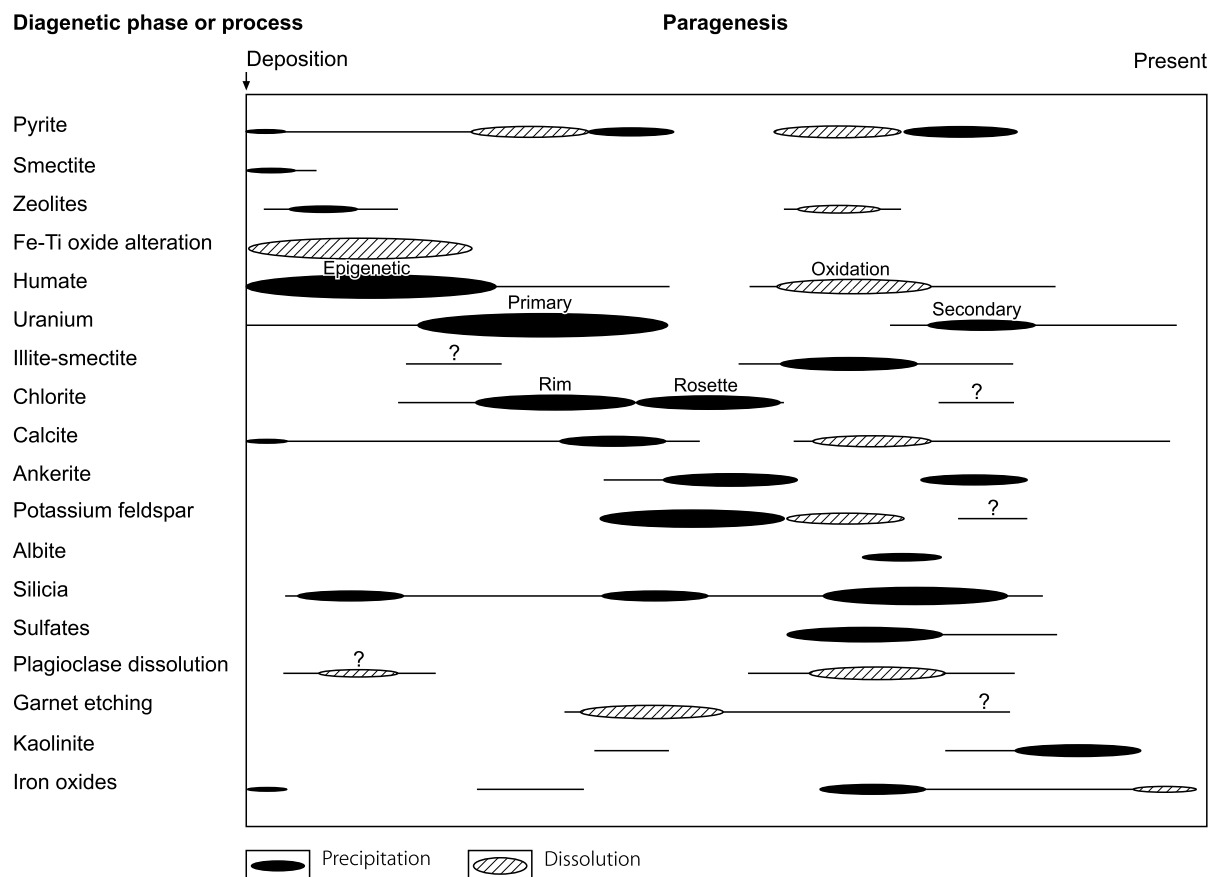
Mineralization and Dimensions

Wentworth et al. (1980) describe Crownpoint *Section 29* mineralization as similar in host rock, ore geometry, and U minerals to some other major deposits in the Grants U Region. Coffinite is the principal U mineral with sparse to minor amounts of amorphous urano-organic clay complexes, and some U^{6+} minerals. A paragenetic sequence of ore and alteration minerals is shown in Fig. 1.27b.

Mineralization in *Section 29* occurs in four of the five sandstone horizons mentioned earlier, in descending order, in the A, B, C, and D horizons in the upper and middle *Westwater Canyon Member*. The lowest sandstone bed E is not mineralized. Uranium in each sandstone horizon concentrates in a series of pods, which individually are irregular in shape but which are principally elongated parallel to the regional WNW–ESE sedimentary trend. Pods and lenses may overlap, coalesce, or are arranged en echelon. Individual ore lenses are from about 1 to

■ Fig. 1.27b.

Crownpoint area, paragenetic sequence of alteration and mineralization in the Morrison Formation. (Hansley 1986b; AAPG 1986, reprinted by permission of the AAPG whose permission is required for further use)



60 m wide and from a few centimeters to 6 m thick. Collectively, the lenses spread over a width of approximately 600 m and an WNW–ESE length of at least 1,600 m bounded only by property limits.

Pelizza and McCarn (2004) note a length in excess of 8 km in WNW–ESE direction and a width varying between 290 and 760 m for the ore trend in the *Crownpoint* and *Unit 1* property. Ore beds average 4 m in thickness and are stacked to a cumulative thickness of 37 m.

Uranium pods are distributed from south to north in successively lower sand units, i.e. ore bodies in the D sand are farther north than those in the C, B, and A horizons. Wentworth et al. (1980) explain this setting, particularly that of the main ore shoots in the D and C sands, as a rejuvenated northward, downdip transport of the uranium from its original depositional site. Further advance was apparently impeded by a decrease in grain size and hence permeability in the D and C sands on the northern side of the Crownpoint channel. Some remnants of the former D and C ore remained in the south part of Section 29.

Wentworth et al. (1980) state that Rb–Sr age dating on ore-stage clay minerals (139 Ma) supports a Late Jurassic age of U mineralization for the Crownpoint Section 29 ore and refer to

Lee and Brookins (1978) who report a similar age for U mineralization at Smith Lake.

1.1.8 Nose Rock District

The Nose Rock district, located approximately 20 km NE of Crownpoint and about 50 km NNW of Ambrosia Lake, is the northernmost known U district in the Grants U Region. Uranium was discovered in 1975 and subsequently several deposits were delineated in a depth of some 950 m. McLemore and Chenoweth (2003) report resources (status 1983) of 3,730 t U at 0.14% U, and 4,770 t U at 0.14% U for two deposits in the northern part of the district, and 9,615 t U at 0.085% for the *Nose Rock No. 1*, and 13,925 t U at 0.085% for the *Nose Rock* deposit.

Sources of Information. Clark 1980; McLemore 1983; McLemore and Chenoweth 1989, 2003; McLemore et al. 2002; Rhett 1980. The subsequent text is largely based on Clark (1980) and Rhett (1980). Clark (1980) restricts his description to the NW portion of the deposit in Section 31, which he considers typical for the district. Rhett (1980) elaborates in detail on the significance of heavy minerals in relation to uranium

mineralization of the Nose Rock district with a probable impact on the entire Grants U Region.

Geological Setting of Mineralization

Uranium is emplaced in sandstones of the Westwater Canyon Member/Morrison Formation. The [Westwater Canyon Member](#) is approximately 50 m thick at Nose Rock but thickens markedly northward. It consists of grey, almost entirely reduced, weakly cemented, feldspathic sandstones of fluvial provenance interstratified with thin, discontinuous lenses of montmorillonitic mudstone. A persistent mudstone marker bed separates the Westwater Canyon Member into an upper and lower unit. All ore is in the lower unit. Sandstones contain organic matter and ubiquitous diagenetic pyrite. Locally, pyrite replaces, either partially or completely, the organic substance resulting in a pyrite matrix that cements detrital rock constituents. Detrital heavy minerals include apatite, garnet, ilmenite, magnetite, rutile, tourmaline, and zircon.

Greenish-grey bentonitic mudstone, lenticular arkosic sandstone, and thin freshwater limestone of the Brushy Basin Member, about 45 m thick, overlie the Westwater Canyon strata. In contrast to other districts, the Brushy Basin sediments are highly siliceous and much harder than elsewhere. Approximately 900 m of Cretaceous sediments cover the Morrison Formation. These sediments dip at a low angle to the north. Faults are rare.

Host Rock Alteration

Several alteration events in pre-Dakota time affected the host rocks, whereas the more recent oxidation front of Tertiary to Quaternary age has not reached the district and is found about 20 km updip to the south. Two kinds of alteration processes are noted by Rhett (1980) and Clark (1980), an early oxidation and a late diagenetic re-reduction event, the latter overprinted the previous. Early oxidation, attributed to a roll-type geochemical cell by the two authors, is indicated by subtle remnants of hematitic staining, some reddish, oxidized clay galls now overgrown by a rim of green clay minerals, and decay of feldspars to kaolinite or a mixture of kaolinite and montmorillonite. During the re-reduction phase, matrix chlorite formed and ferric iron oxides were reduced to ferrous minerals.

Mineralization and Dimensions

In the selected area of Section 31 described by Clark (1980), three superimposed uranium rolls occur in sandstone beds separated by thin, lenticular mudstones in the lower part of the Westwater Canyon Member. Where two or all three rolls are stacked, the cumulative ore thickness may be 15 m or more. The thickness of individual rolls ranges from less than a meter to more than 7 m. Grades vary between 0.01 and 0.25% U. Limbs, which contain significant amounts of uranium, extend for

considerable distance in a NW direction from the roll-head. In some cases, they can be traced as low-grade mineralization for almost 1 km. Rolls extend along strike for at least 1,000 m in a sinuous line in NE–SW direction.

Coffinite is the principal U mineral. It is intimately intergrown with carbonaceous matter. Ferroselite has accumulated near the redox interface and is particularly abundant adjacent to interior sides of mineralized limbs. Jordisite is distributed in an irregular halo in front of uranium rolls. Subtle relics of hematite staining occur in the near interior portion of rolls. Ore is in radiometric equilibrium.

Rhett (1980) identified the following authigenic heavy minerals in addition to detrital heavy minerals in ore-hosting sandstones at Nose Rock: Anatase, baryte, ferroselite, galena, greenockite, goethite–hematite, pyrite, and siderite. The mineral association and spatial position of these minerals in relation to the rollfront is as follows: Siderite is commonly intergrown with clays, mainly montmorillonite, and typically occurs in exterior and seepage zones. Baryte is present in three varieties: Clear to white baryte is ubiquitous in both interior and exterior barren ground; yellow baryte is typically associated with intense mineralization, it contains inclusions of pyrite and organic matter; pink and red baryte occurs spatially close to mineralization and correlates with anatase and bleached magnetite–ilmenite in near interior zones, the red color apparently results from minute inclusions of hematite. Galena and, less commonly, greenockite are most abundant in seepage zones but also occur in ore zones. Pyrite of diagenetic origin is common in exterior ground, whereas matrix pyrite is restricted to sandstone rich in organic matter, in which it replaces the organic substance to various degrees. Locally, organic matter is completely pyritized so that sand grains are embedded in pyrite cement. Goethite–hematite coat sand grains and occasionally form ferruginous cement. These two Fe minerals are interpreted as relics of an early oxidation regime and correlate well with indicator minerals of the barren interior zone such as anatase and bleached Fe–Ti oxides.

Anatase has a positive quantitative correlation with bleached Fe–Ti oxides and is obviously characteristic for barren interior ground. As documented by Adams et al. (1974), anatase probably derives when magnetite–ilmenite are reduced by reaction with organic matter thereby losing much of their iron, and some titanium to form anatase. Surviving remains are white to tan bleached Fe–Ti oxide grains, which often still reveal the original magnetite–ilmenite intergrowth texture. Unaltered magnetite–ilmenite is typical for sands free of organic matter. In contrast, altered bleached Fe–Ti oxides are typical for (former) organic-rich terrane; and they are in particular diagnostic in combination with some surviving unaltered magnetite–ilmenite for barren interior ground. Carbonized iron–titanium oxides occur, less commonly, in the seepage zone immediately down gradient from the nose of a roll.

Rhett (1980) subdivides the environment of the Nose Rock rollfront system into four zones:

- **An exterior zone** downdip in front of the ore roll is barren of uranium and essentially unmodified by ore-forming processes. Recognition criteria include presence of unaltered magnetite–ilmenite, clear white baryte, siderite, composite

grains of siderite–montmorillonite, and diagenetic pyrite, but absence of matrix pyrite, minimal alteration of feldspar, dominance of montmorillonite among clay minerals and as a relatively common matrix constituent.

- **A seepage zone** located immediately in front of the roll interface. Its characteristics include incipient ore-related or -indicative authigenic minerals such as matrix pyrite, organic cement, carbonized Fe–Ti oxides, anatase, galena, and occasionally greenockite and earthy jordisite. Clear white baryte is locally prevalent.
- **An ore zone** that occupies the space between the (iron) redox interface and the seepage zone and contains uranium ore, often in the form of uranium- and sulfide-mineralized organic substance. Typical minerals include matrix pyrite, altered and carbonized Fe–Ti oxides, anatase, yellow and red baryte often choked with pyrite and hematite inclusions. Organic cement and coatings of sand grains are common, ferruginous cement is locally prominent, iron-rich chlorite and kaolinite are the dominant phyllosilicates.
- **An interior zone** practically barren of uranium. Diagnostic minerals are altered iron–titanium oxides, anatase, relics of yellow and red baryte, and locally organic coatings and corroded matrix pyrite. Feldspars are heavily altered. Chlorite and kaolinite are the prevailing phyllosilicates.

Metallogenetic Aspects

Clark (1980) and Rhett (1980) suggest that the Nose Rock uranium ore formed early in the Late Jurassic–Early Cretaceous erosional interval by rollfront/geochemical-cell processes probably contemporaneous with primary ore emplacement at Ambrosia Lake. A southeast migrating front oxidized interior sediments, which originally were deposited under reducing conditions in a fluvial depositional system. Oxygenated fluids transported uranium to, and deposited it at redox interfaces within the Westwater Canyon sandstones.

Subsequent invasion of reducing solutions during the latter part of the Late Jurassic–Early Cretaceous erosional period caused re-reduction of red-colored oxidized interior ground. Perhaps vegetated swamps of the lowermost Dakota deposition furnished a source of required reductants. Reducing fluids that invaded the Westwater Canyon sands impeded any rollfront advance and commonly obliterated macroscopic evidence of the former oxidation event. Some authigenic minerals genetically related to rollfront mineralization were not affected by reducing agents, however, and were used by Rhett (1980) to identify geologic events resulting in the formation of the Nose Rock uranium deposits.

1.1.9 Borrego Pass

This district is located about halfway between Ambrosia Lake and Crownpoint. Two deposits are known: *Borrego Pass* and, about 10 km to the south thereof, *West Largo*. Uranium is hosted in sandstone horizons of the *Westwater Canyon Member* at

depths from 600 to 660 m. Resources are some 5,000 t U at a grade of 0.13% U (cutoff grade 0.043% U/1.8 m) at *Borrego Pass*, and about 5,000 t U at a grade of 0.17% U (cutoff grade 0.085% U/1.8 m) at *West Largo* (Continental Oil Company 1978, DOE-GJBX-2/83).

1.1.10 Uranium Deposits in Cretaceous Dakota Sandstone

The Dakota Sandstone contained small uranium deposits in the southern part of the San Juan Basin, which delivered in excess of 190 t U. Ore mined had grades ranging from 0.10 to 0.25% U and averaged 0.178% U (Chenoweth 1989). The Dakota Sandstone-hosted U deposits are similar to redistributed uranium mineralization in the Morrison Formation and occur near primary and redistributed ore in the Morrison Formation. Deposits in Dakota Sandstone are typically tabular masses, which range in size from thin ore shoots a few decimeters in length and width to masses up 750 m long and 300 m wide. Larger deposits are only a few decimeters thick, but a few are as much as 7.5 m thick (Hilpert 1969).

Uranium occurs associated with carbonaceous plant material in the basal part of channel sandstones or in carbonaceous shale and lignite. The distribution of mineralization tends to be controlled by faults, fractures, or joints, and by underlying permeable sandstone of the Brushy Basin or Westwater Canyon members.

The largest deposit was at the Old Church Rock mine in the Church Rock district, which delivered more than 70 t U from Dakota Sandstone ore. In this deposit, uranium is associated with a major NE–SW-oriented fault (Chenoweth 1989, McLemore and Chenoweth 2003).

1.1.11 Uranium Deposits in Middle Jurassic Todilto Limestone

Fractured, organic-rich limestone of the Middle Jurassic Todilto Formation in the San Juan Basin contains in excess of 100 uranium deposits and occurrences. Most of these are at the southern margin of the Grants Uranium Region, in the southern Ambrosia Lake and Laguna uranium districts (Figs. 1.5 and 1.14). Minor occurrences are known in the Chama Basin (Abiquiu), Nacimiento Mountains, and Sanostee district in the Chuska Mountains.

Uranium mineralization is hosted in fractured limestone rich in organics and therefore it may be classified as uraniumiferous bituminous-cataclastic limestone type. Finch (personal communication) proposes the term “intra-folded/fractured organic-rich limestone uranium deposits” as a Todilto specific definition. (Similar deposits are known in Kyrgyzstan and China, see Dahlkamp 2009, Vol. Uranium Deposits of the World: Asia.)

Uranium was discovered in Todilto limestone in the early 1920s. Mining lasted from 1950 to 1981 and delivered 2,570 t U. Documented uranium production came from 42 mines located

north and west of the town of Grants and south of Laguna. Some minor production came from elsewhere in the San Juan Basin. The largest cluster of uranium deposits is the Faith, where 12 mines produced 1,143 t U at an ore grade of 0.2% U.

Sources of Information. Berglof 1992; Chenoweth 1985a; Finch and McLemore 1989; Gabelman 1956; Gabelman and Boyer 1988; Green 1982; Hilpert and Moench 1960; McLaughlin 1963; McLemore 1983; McLemore and Chenoweth 1989, 1991, 2003; McLemore et al. 2002; Rawson 1980; Lucas and Anderson 1996; Truesdell and Weeks 1960; Chenoweth and Finch, personal communication unless otherwise noted.

Geology and Mineralization

The Jurassic Todilto Formation (also known as Todilto Limestone) consists predominantly of carbonates and evaporates, which originated in a paralic salina or sabkha environment within a Jurassic basin that occupied much of the present San Juan Basin in northeastern New Mexico and southwestern Colorado. The Entrada Sandstone underlies and coastal plain and tidal flat sediments of the Wanakah (or Summerville) Formation rest upon the Todilto Formation.

The Todilto Formation includes two members (Lucas and Anderson 1996). The basal *Luciano Mesa Member*, from 2 to 13 m in thickness, is chiefly a kerogen-rich, straticulate limestone subdivided into three horizons: a basal platy or laminated horizon 2–5 m thick, a crinkly or crenulated horizon 1–3 m thick, and an upper massive horizon, from near zero to 5 m thick. The overlying *Tonque Arroyo Member* consists largely of gypsum and anhydrite. It varies greatly in thickness, up to a maximum of 61 m, but is absent west of Grants where most of the known Todilto uranium deposits are located.

Heterogeneous folds and fold-like structures, and folding-related fractures deform Todilto beds. The folds show great variability in fold trends, and a wide range in size and geometry. Ore-hosting folds are anticlinal in nature, commonly less than one meter in amplitude, and limited to certain laminae generally near the middle of the Todilto Formation (Fig. 1.28).

Pitchblende is the predominant U mineral in *unoxidized ore*, along with lesser coffinite, blue–black vanadium minerals such as paramontroseite and haggite, pyrite, fluorite, baryte, and hematite. *Oxidized ore*, which is typical near the surface, comprises a large variety of hexavalent U minerals. Tyuyamunite, metatyuyamunite, and uranophane are most abundant. From an economic point of view, pitchblende was apparently most important followed by tyuyamunite and uranophane.

Pitchblende occurs mainly as impregnation and replacement along fractures and bedding planes. Locally, pitchblende forms rims around pyrite and mineral grains within the limestone (Lavery and Gross 1956). Coffinite occurs as massive, brown to black replacements of limestone. According to Truesdell and Weeks (1960), coffinite is not associated with fluorite-bearing uranium ore.

Paramontroseite and also haggite are found in fractures with abundant coarse calcite and minor baryte. At the *Flat Top mine*,

paramontroseite occurs in thin veins up to 2 cm thick and approximately 30–60 cm long along the east limb of a N–S-trending fold in the massive limestone member.

Tyuyamunite and metatyuyamunite are present as massive to small scales, laths, radial aggregates, occasionally as powdery masses in fractures, and as thin coatings on fracture and bedding surfaces in the limestone.

Uranophane typically coats fractures and locally bedding planes in the form of radiating clusters of acicular crystals, and occasionally as thicker felted masses or acicular crystals in voids. It is most abundant in oxidized Todilto deposits that are low in vanadium (Weeks and Thompson 1954).

Gangue minerals include baryte, fluorite, and calcite. The first two are more or less coextensive with U minerals. Black, coarse-crystalline calcite and younger white calcite fill fractures and voids. Purple to purple–black and clear fluorite occur as tiny crystals (<3 mm) and fine-grained, irregular replacements. Locally fluorite and pitchblende are intergrown, calcite cuts fluorite, and late fluorite is zoned (Lavery and Gross 1956). Baryte forms clear to brown blades.

Pyrite and hematite are common constituents in Todilto ore with subordinate cryptomelane and psilomelane. Pyrite occurs as an individual mineral and occasionally coats calcite crystals. Hematite is present as disseminations or as pseudomorphs (0.3–1 mm) after pyrite cubes (Rapaport 1952).

High-grade pitchblende ore contains microscopic galena crystals and often fine-grained hematite. The latter may impose a reddish color on both the ore and the host rock.

Geochronological analyses give an age of 155–150 Ma for unoxidized uranium ore in the Todilto Formation, i.e. the ore is close in age to that of the Todilto host sediments and older than the 130 Ma old trend ore in the Morrison Formation (Berglof 1992; Berglof and McLemore 1996; Finch 1991). Uranophane yields U–Pb ages of 7–3 Ma (Brookins 1981b), which confirm Tertiary redistribution of uranium as likewise established for sandstone ore elsewhere in the Grants Uranium Region.

Mineable unoxidized ore is restricted to organic (kerogen)-rich limestone beds of the basal Luciano Mesa Member, in which it is controlled by (a) intraformational fold structures and associated fractures within the folds, and (b) organic (kerogen) matter that occupies these structures and laminae in the limestone (Fig. 1.28).

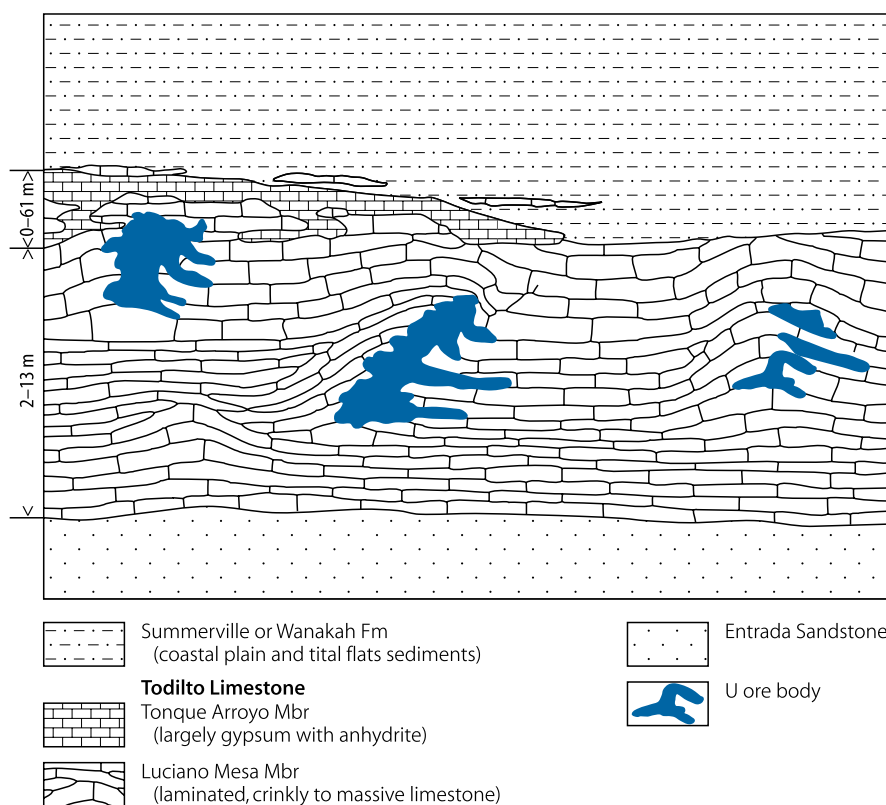
Metallogenetic Aspects

Metallogenesis of uranium deposits in the calcareous Todilto Formation is not yet comprehensively researched. A number of theories are forwarded but still they require verification.

Hilpert (1969) reports that uranium ore in the Todilto limestone is confined to areas where the overlying gypsum-anhydrite Tonque Arroyo Member is absent. Apparently, due to this fact, uranium could have penetrated locally into overlying sands of the Wanakah (Summerville) Formation where it formed minor mineralization. In a few locations, pitchblende mineralization also extends into the Entrada Sandstone, immediately below deposits in Todilto limestone.

■ Fig. 1.28.

Todilto U deposits, schematic section illustrating the affinity of uranium ore to intraformational folds and fractures in the organic-rich basal Luciano Mesa Member of the Middle Jurassic Todilto Formation. [After Finch and McLemore 1989, Berglof and McLemore 2003 (reproduced by permission of New Mexico Geological Society)]



McLemore and Chenoweth (2003) suggest that, after deposition of the Todilto limestone in Middle Jurassic time in a paralic salina or sabkha environment on top of the permeable Entrada Sandstone, eolian sediments of the transgressing Wanakah (Summerville) Formation have produced intraformational folds locally in the soft muddy, limey, organic-rich Todilto beds before they were indurated and fractured. Uraniferous waters, recharged in a highland to the southwest, percolated through the Entrada Sandstone and migrated into the Todilto limestone by evapotranspiration or evaporative pumping. Uranium precipitated within intraformational folds and associated fractures in the limestone, where it encountered organic material (Finch and McLemore 1989; Rawson 1981).

Berglof and McLemore (2003) summarize the sequence of actual ore-forming events as follows. After folding and fracturing had generated permeability in the limestone, recrystallization, renewed fracturing, and dissolution affected the host limestone. During an early hydrogenic stage, which probably caused additional dissolution, chlorite, dolomite, and illite were deposited in the fractures. The subsequent original mineralization stage began with deposition of early fluorite and pyrite, followed by precipitation of pitchblende and coffinite associated with pyrite, baryte, and fluorite. Pyrite, baryte, and fluorite are locally intergrown with U minerals but also precipitated along fractures and bedding planes in barren limestone within about a

meter or so of uranium ore. In a following stage calcite, baryte, vanadium clay minerals, and pyrite formed, and furthermore Fe- and Mn-oxides. Supergene alteration occurred repeatedly.

It may be noted that Berglof and McLemore (2003) believe that the Todilto is the source rock for petroleum that is produced from the Entrada Sandstone in the San Juan Basin.

Selected References and Further Reading for Chapter 1.1 Grants Uranium Region

Adams and Saucier 1981; Adams et al. 1974, 1978; Adler 1974; Alief and Kern 1989; Alief 1988; Austin 1963, 1980; Baird et al. 1980, 1986; Beck et al. 1980; Bell 1986; Berglof 1992; Berglof and McLemore 2003; Berglof and Wampler 1965; Birdseye 1957; Bowman and Livingston 1980; Brookins 1975a, b, 1976, 1979, 1980a, b, 1981b; Brookins et al. 1977; Burgess et al. 1987; Cadigan 1967; Chapman et al. 1979; Chenoweth 1953, 1977, 1985a, 1989a; Chenoweth and Holen 1980; Chenoweth and Stehle 1957; Chico 1963; Clark and Havenstrite 1963; Clark 1980; Clary et al. 1963; Coffin 1921; Condon and Peterson 1986; Continental Oil Company 1978; Corbett 1964; Craig et al. 1955; Crawley 1983; Crawley et al. 1984, 1985; Cronk 1963; Dooley et al. 1966; Ethridge et al. 1980; Falkowski 1980; Finch 1967, 1991; Finch and McLemore 1989; Fischer 1947; Fishman and Reynolds 1986; Fishman 1981; Fishman et al. 1984; Fishman and Turner-Peterson 1986; Fitch 1980; Fitch 2005, 2006; Forhan 1977; Foster and Quintanar 1980; Gabelman 1956; Gabelman and Boyer 1988; Gabelman et al. 1956; Galloway 1978, 1980; Gould et al. 1963; Granger 1960, 1962, 1963, 1968; Granger and Finch 1988; Granger and Inqram 1966; Granger and Santos 1982, 1986; Granger et al.

1961; Green and Jackson 1975a, b; Green 1980, 1982; Hafen et al. 1976; Haji-Vassiliou and Kerr 1973; Hanshaw and Dahl 1956; Hansley and Spirakis 1992; Hansley 1984, 1986a, b; Harmon and Taylor 1963; Hatcher et al. 1986; Hazlett and Kreek 1963; Hicks et al. 1980; Hilpert and Moench 1960; Hilpert 1963, 1969; Holen and Hatchell 1986, 1988; Holen 1982; Hoskins 1963; Hounslow 1967; Huffman and Lupe 1977; Jacobsen 1980; Jenkins and Cunningham 1980; Jensen 1963; Jobin 1962; John 1962; Kelley 1951, 1955, 1963a, b; Kelley et al. 1968, 1969; Kendall 1971; Kirk and Condon 1986; Kirk et al. 1986; Kittel 1963; Kittel et al. 1967; Knox and Gruner 1957; Kozusko and Saucier 1980; Laverty and Gross 1956; Lease 1980; Lee and Brookins 1978, 1980; Lee 1976; Leventhal and Threlkeld 1978; Leventhal 1980; Lucas and Anderson 1996; Ludwig 1980; Ludwig et al. 1977, 1982b, 1984; MacRae 1963; Martinez 1979; Mathewson 1953a, b; McCammon et al. 1986; McCarn 2001; McLaughlin 1963; McLemore 1983, 2002; McLemore and Chenoweth 1989, 1991, 2003; McLemore et al. 2002; McLennan and Taylor 1979; Megrue and Kerr 1965, 1968; Melvin 1976; Meunier 1989; Miller and Kulp 1963; Moench 1962, 1963; Moench and Schlee 1959, 1967; Moore and Lavery 1980; Myers 2006a, b, c; Nash and Kerr 1966; Nash 1967, 1968; Obradovich and Coban 1975; Pelizza and McCarn 2004; Peterson 1980a, b; Peterson 1980; Peterson and Turner-Peterson 1980, 1987; Pierson and Green 1980; Pierson et al. 1983; Place et al. 1980; Porter 1981; Rackley 1976; Rapaport 1952, 1963; Rautman 1980; Rawson 1980; Reimer 1969; Rhett 1980; Ridgley 1980; Ridgley et al. 1978; Riese and Brookins 1977, 1980, 1984; Riese 1977, 1979; Riese et al. 1980; Ristorcelli 1980; Roeber 1972; Rosenberg and Hooper 1982; Sachdev 1980; Sanford 1992, 1994; Santos and Turner-Peterson 1986; Santos 1963, 1968, 1970, 1975; Saucier 1967a, b, 1974, 1976, 1980; Sayala and Ward 1983; Schlee and Moench 1961; Schlee 1957, 1959, 1963; Schmidt-Collerus 1969, 1979; Sears et al. 1974; Sharp 1955; Shawe 1956a, b; Smith and Peterson 1980; Spirakis and Pierson 1986; Spirakis et al. 1981, 1983; Squyres 1963, 1970, 1974, 1980; Steele 1984; Stewart et al. 1972; Tessoroff 1980; Thaden and Santos 1956; Thaden and Zech 1986; Truesdell and Weeks 1960; Turner et al. 1993; Turner and Gunderson 1980; Turner-Peterson and Fishman 1986; Turner-Peterson 1981, 1985, 1986; Turner-Peterson et al. 1980, 1986; US-AEC 1959; US-DOE 1980, 1983; US-EIA 1989; Webster 1983; Weege 1963; Weeks and Thompson 1954; Wentworth et al. 1980; Whitney and Northrop 1984; Whitney 1986; Wylie 1963; Young and Delicate 1965; Young and Ealy 1956; Young 1960; Zitting et al. 1957; Adams et al., personal communication.

1.2 Salt Wash Uranium Districts, Northern-Central Colorado Plateau

(Uranium–Vanadium Deposits in the Jurassic Salt Wash Member, Morrison Formation)

The principal areas of uranium mineralization and mining in the Jurassic Salt Wash Member, Morrison Formation, are located in the northern-central part of the Colorado Plateau (► Fig. 1.29). V–U ore is the characteristic commodity of the Salt Wash deposits with vanadium generally more abundant than uranium, i.e. the ore is by quantity more a vanadium ore than a uranium ore. Nevertheless, in most cases, vanadium and uranium are coproducts and both constituents are necessary for production.

Total production from all the Salt Wash districts is 38,730 t U prior to 1988 (only minimal production from the Salt Wash occurred between 1988 and 2007), 27,400 t U of which and about five times as much vanadium were produced in the Uravan Mineral Belt (Chenoweth, personal communication). Three other mining districts have each produced at least a 1,000 tonnes of uranium; the remaining amount came from seven minor districts. Significant resources are known to remain in the Uravan Mineral Belt, and in the districts of La Sal–La Sal Creek,

Green River, and Henry Mountains. Other areas or districts probably contain smaller resources.

Sources of Information. Abundant information on the Salt Wash uranium deposits has been published by many authors including those listed in Section References and Further Reading at the end of this chapter.

Thamm et al. (1981) compiled all relevant data of the Salt Wash-type sandstone-hosted uranium deposits. They describe the known geology of the Salt Wash deposits adequately and present a comprehensive synopsis of the regional setting and local characteristics of the deposits, as well as the recognition criteria and a hypothesis on ore formation. The following description has drawn extensively from Thamm et al.'s (1981) report and in many cases their text has been used in the form of quotations, abbreviated and modified, and therefore not set in quotation marks. More recent concepts of the origin of the V–U Salt Wash deposits are given by Northrop (1982), Northrop and Goldhaber (1990), and Goldhaber et al. (1991) based on comprehensive metallogenetic studies of mineralization in the Henry Mountains area, Utah. J.K. Thamm kindly reviewed this section dealing with the Salt Wash deposits, amended and improved the content and text.

Regional Geological Setting of Mineralization

The uranium-hosting *Salt Wash Member* of the Late Jurassic Morrison Formation occurs in the northern part of the Colorado Plateau. It is overlain by the Brushy Basin Member of the upper Morrison Formation and is underlain by the Tidwell Member of the lower Morrison Formation (► Fig. 1.2). The Salt Wash Member is approximately time equivalent with the Recapture Member, which is distributed mainly in the southern Colorado Plateau but which contains little uranium. Both members constitute the lower portion of the Morrison Formation. They were deposited almost synchronously as separate alluvial systems, but merge and intertongue in the Four Corners area of the Colorado Plateau. The southwestern boundary of the Salt Wash sediments along the Arizona–Utah border resulted from erosion.

The *Salt Wash Member* consists of continental fluvial sediments, very similar in composition to host rocks of other major sandstone uranium districts in the western USA. The dominant source area of Salt Wash sediments was west and southwest of its present distribution. The Salt Wash alluvial plain gradually advanced across the depositional area as a series of coalescing fluvial fans. Major depositional trends extended northward and eastward into the Green River area, northeastward or eastward into the Uravan area, and southeastward into the Lukachukai–Carrizo area. A structural high at the Four Corners, which diverted major paleodrainage systems around it to the north and south, separates the Uravan lobe from the Lukachukai–Carrizo lobe. Other existing or growing structures, such as the salt anticlines of the Paradox Basin in the Uravan area, the Monument Upwarp, small domes and monoclines in northeast Arizona and northwestern New Mexico, and transverse structures in the Henry Mountains area probably diverted or impeded

Fig. 1.29.

Colorado Plateau, distribution and facies of the Salt Wash Member of the Jurassic Morrison Formation and location of uranium districts/deposits hosted in this member. (After Craig et al. 1955, Mullens and Freeman 1957, Fischer 1968, Thamm et al. 1981)

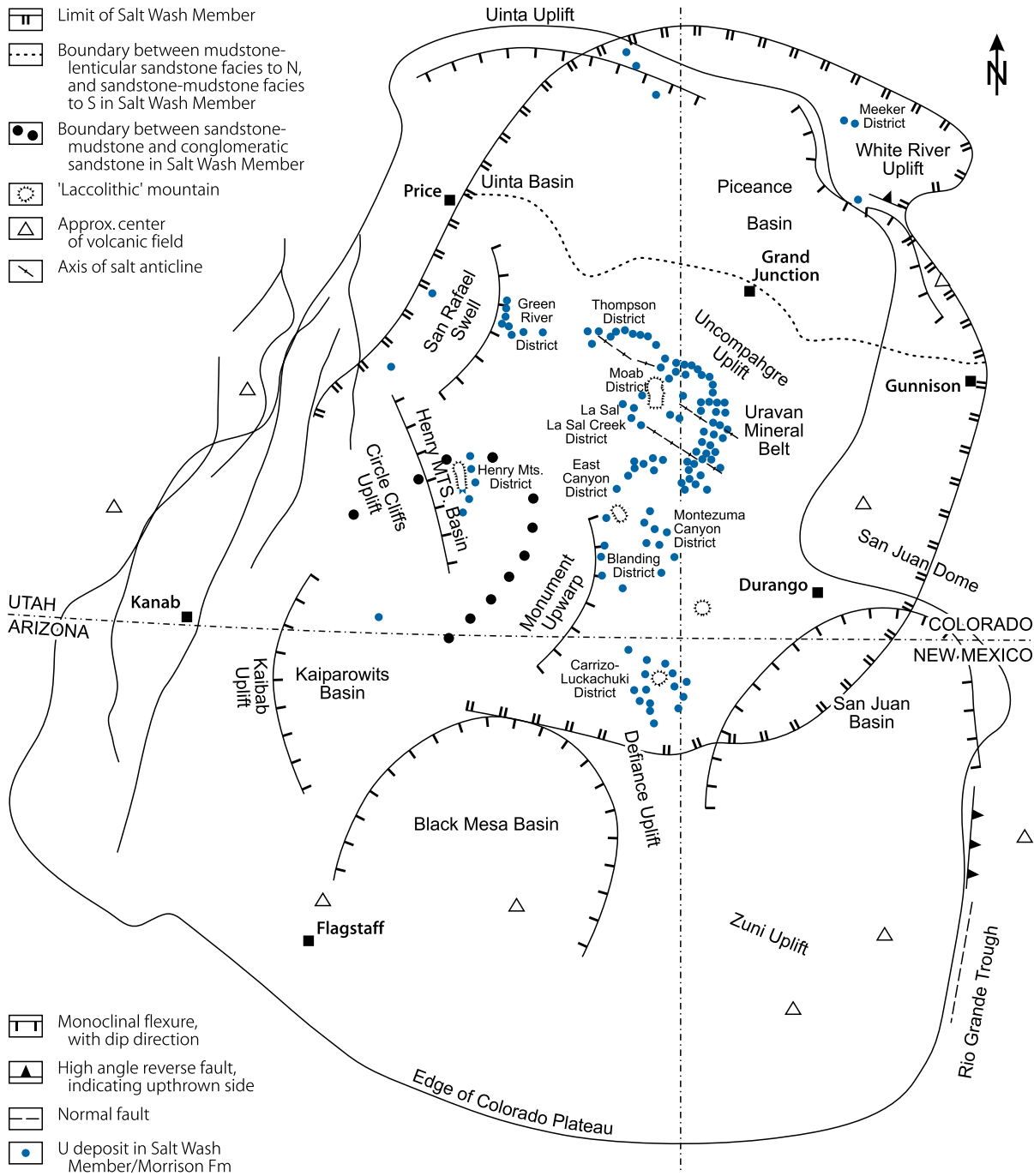
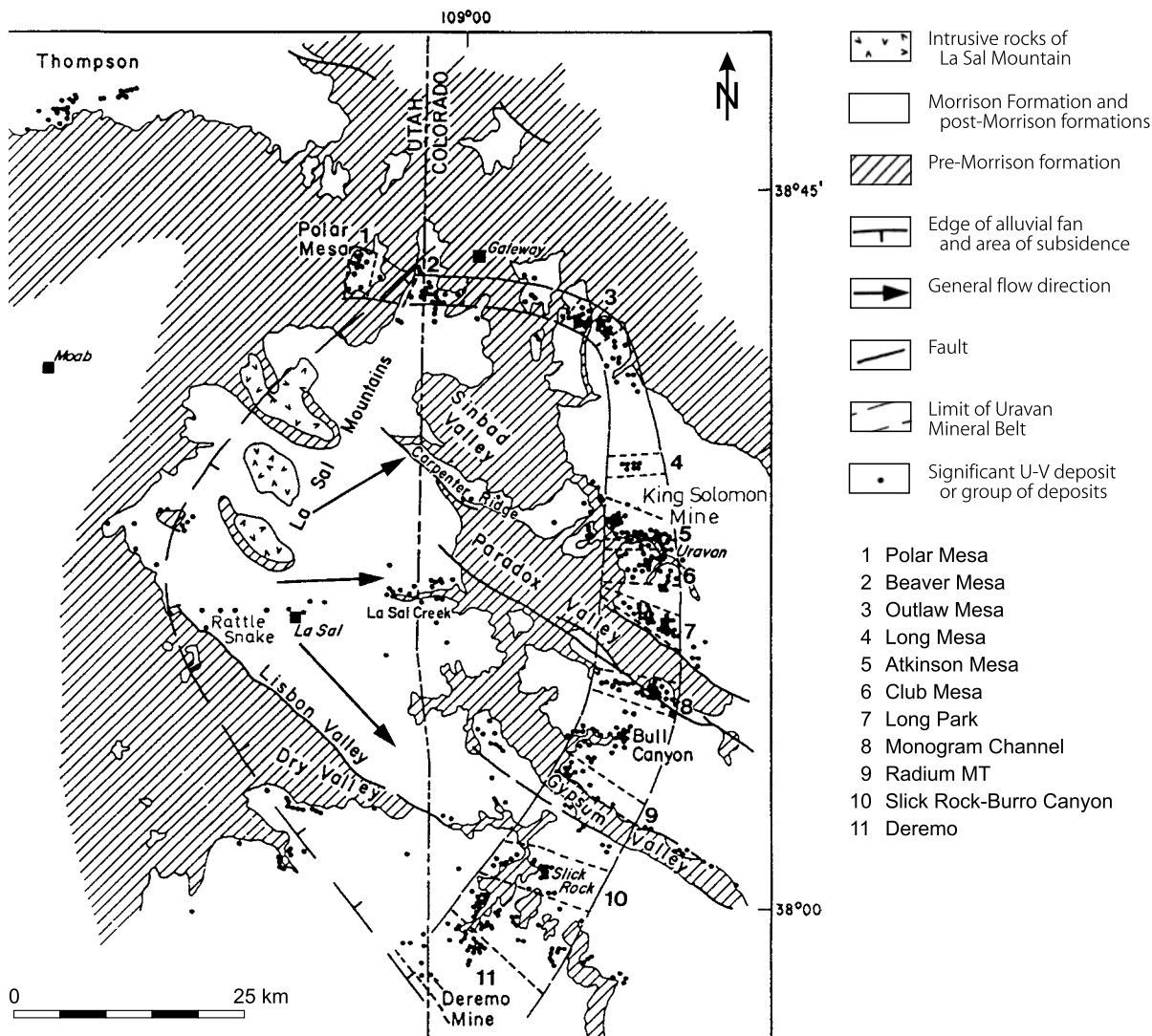


Fig. 1.30.

Uravan Mineral Belt, generalized geological map indicating the outline of the belt with position of significant U-V deposits or groups of deposits at the toe of an alluvial fan of the Salt Wash Member of the Morrison Formation. Deposits often cluster in “cross trends” (numbered 1 to 11). (After Butler and Fisher 1978, Motica 1968)



sedimentation. As a result, a restricted but marked increase in the thickness of the Salt Wash sediments developed in the Uravan district, perhaps in response to a local downwarp within the Paradox Basin. A similar thick sequence of Salt Wash sediments accumulated in the Henry Basin due to local tectonic subsidence.

Thamm et al. (1981) classify the Salt Wash sandstones as orthoquartzites to feldspathic orthoquartzites, which were deposited during a semiarid climate as braided and meandering stream and floodplain deposits, apparently on a broad plain where vegetation was abundant along the watercourses.

Clay lenses rich in volcanic debris were deposited locally as basal mud in shallow ponds or lakes. Peterson (1980) considers grey mudstones above, below, or lateral to reduced bodies of sandstone, to have been significant sources of humic and fluvic acid fluids that were expelled during the compaction of the sediments.

Proximal facies of the alluvial system are characterized by high sandstone to mudstone ratios and braided stream deposits. These facies consist of thick, massive sandstone units that contain only a few thin interbeds of clay. They were deposited under high-energy conditions. In the more distal facies, e.g. farther to the east, in the Uravan area (Fig. 1.30), a much lower sandstone to mudstone ratio prevails in those meandering stream deposits. A great part of channel sediments of this alluvial fan section subsided below the water table early on and preserved accumulations of detrital plant debris, which subsequently contributed to the formation of carbon-facies sandstones. Adjacent overbank muds were oxidized above the water table and are now represented by the hematitic sediments that bound many ore zones.

Distal facies of the alluvial fan systems were deposited under conditions of low energy flow as discrete channel sandstones and floodplain clays. Still farther to the east, sedimentology

changes to lacustrine environments where, in standing water, horizontally laminated sandstones and mudstones with little carbonaceous material were laid down. Most of the carbonaceous debris was obviously accumulated within the fluvial channel and floodplain sequence as streams gradually slowed and lost their transport capacity eastward.

The Brushy Basin Member of the upper Morrison Formation rests upon the Salt Wash Member without a marked gap since sedimentation continued throughout the Salt Wash period and into the Brushy Basin time without interruption. The Brushy Basin Member consists of dominantly oxidized fluvial sediments presumably deposited in a floodplain environment. Large volumes of acid volcanic ash from contemporaneous eruptions to the south and west are incorporated in these sediments. Brushy Basin deposition was followed by a cycle of erosion, then by the deposition of the Burro Canyon and Dakota sandstones and the thick black shales of the Mancos Shale.

Principal Host Rock Alteration

Ore-hosting sediments of the **Salt Wash Member** contain both reduced and oxidized facies. Shawe (1956a, b) describes both facies in detail from the Slick Rock area in the southern Uravan Mineral Belt (► Fig. 1.30). Sedimentological and alteration features comparable to those of the Slick Rock district are postulated to be present in other Salt Wash districts as well but are not yet satisfactorily researched.

Shawe (1976a) distinguishes three facies of Salt Wash sediments in the Slick Rock area: (a) an oxidized redbed facies, (b) a reduced carbon facies, and (c) a reduced altered facies. Mineralogically and chemically, the rocks of these three facies are very similar except that the redbed facies is altered by oxidation.

Rocks of the carbon facies and altered facies are megascopically indistinguishable. Significant differences exist, however, in the relative abundance of heavy minerals, the black opaque fraction thereof, and pyrite between these two facies, and the redbed facies as well. The amount of black opaque minerals in the carbon facies is about two-thirds of that in redbed facies rocks, and almost zero in the altered facies due to their almost complete destruction. Pyrite is absent in the redbed facies, sparse in the carbon facies, and moderately abundant in altered facies rocks. Small, but perhaps significant, differences in the amount of trace elements in the three facies have been noticed (see later).

The redbed facies is composed of oxidized, reddish-brown rocks, which contain hematite derived from the in situ decay of iron-bearing detrital minerals. Clay minerals in the redbed facies are mainly illite and mixed layer illitic clays. Minor amounts of silica cement and baryte occur in widespread but irregular distribution. The normal calcite content of redbed facies sandstones averages about 10%, but when mineralized the redbed facies sandstone contains only about 2.5% calcite. The heavy mineral content of the redbed facies sandstone is 0.31% in weight, 59% of which are black opaque minerals. The redbed facies contains the highest amount of heavy and opaque minerals of all three facies.

Reduced carbon facies rocks include sandstones, siltstones, and mudstones with carbonaceous debris. The carbon-facies sediments are generally light grey below the zone of oxidation and tan to light brown in outcrop and near-surface exposures. Clay minerals and calcite content are similar to those in redbed sediments. Silica cement is common and makes up about 10% of the sandstones. Much of the silica is present as overgrowths on detrital quartz grains. Baryte and anatase are widely distributed in small amounts. Pyrite is sparse and erratically distributed.

The heavy mineral content in carbon facies rocks is 0.16% in weight, 42% of which are black opaque minerals. The heavy mineral content of carbon facies sandstone is approximately half that of redbed facies sandstone, but is slightly more abundant than in sandstone of the altered facies. Black opaque oxides, mainly magnetite and ilmenite, are less abundant in carbon facies sandstone than in sandstone of the redbed facies, but are much more abundant in carbon facies sandstone than in altered facies sandstone.

Reduced altered facies rocks are host to V–U deposits in the Slick Rock area. The sediments are light grey below the water table and tan or light brown in the zone of oxidation. Clay minerals in this facies are similar to those in redbed and carbon facies. Silica cement is widely distributed, amounting to 5–15% in sandstones. Some detrital quartz grains and some authigenic silica overgrowths have been partly dissolved. Shawe (1976a) interprets this as indicative of at least two stages of postdepositional silica dissolution and precipitation. Calcite is a common constituent of altered facies rocks. In some areas, calcite replaces detrital grains of quartz, chert, and feldspar. Baryte is common and occurs in similar amounts as in redbed and carbon facies rocks.

The heavy mineral content of altered facies sandstone is 0.11% in weight. Black opaque minerals are very sparse, amounting to only 2% thereof, but pyrite is relatively abundant. Shawe's (1976a) data indicate that altered facies sandstone of the Salt Wash Member contains approximately 4 ppm U, i.e. four times more than found in the redbed facies or carbon facies sandstones.

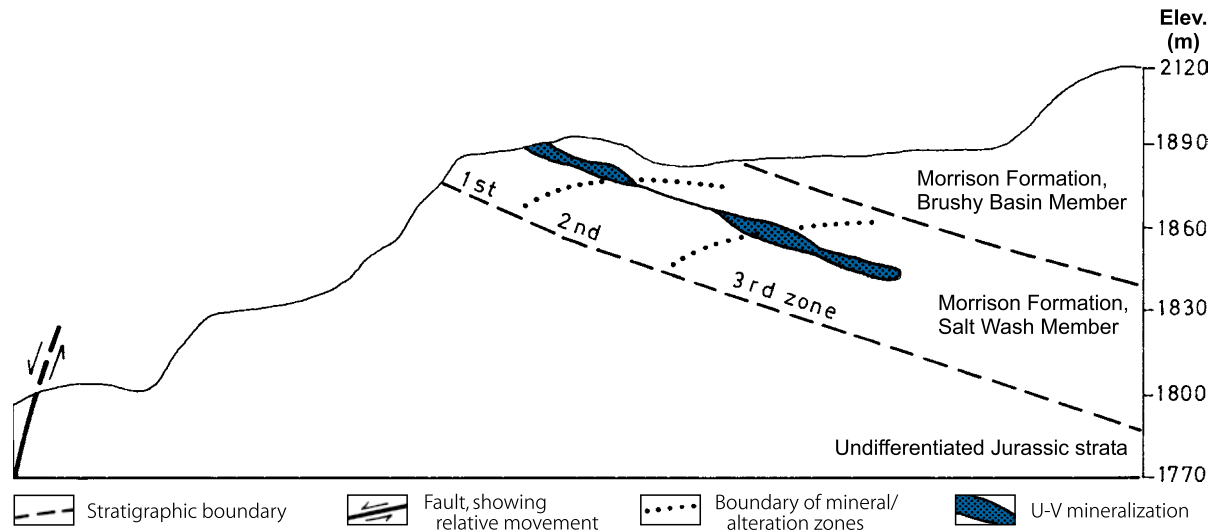
Although Shawe's (1976a) differentiation of alteration in the Slick Rock area has not been satisfactorily established in all Salt Wash ore districts, it may reflect processes, which can be applied, with reservation, to the other Salt Wash districts.

Thamm et al. (1981) address this subject and present the following interpretation. The dominantly red color of floodplain sediments presumably results from the oxidation of magnetite and ilmenite to hematite under alternating wet and dry conditions of deposition. This oxidation also destroyed any carbonaceous debris, which had accumulated in the floodplain environment. These redbed facies sandstones and mudstones do not contain uranium deposits and rarely contain uranium occurrences.

Grey sandstones and mudstones, which fill channels, were deposited under conditions permitting the formation of a reducing environment as reflected by the presence of pyrite and carbonaceous material. Otherwise, these two components would have been destroyed. When individual small channels within major channel systems were abandoned, trapped pore water in

Fig. 1.31.

Uravan Mineral Belt, Bitter Creek mine, generalized cross section demonstrating the progressive oxidation of primary mineralization in the Salt Wash Member deposits. The near-surface ore zone (1st zone) is completely oxidized and typically contains carnotite ore. The deeper, 2nd zone is partially oxidized by downward percolating oxygenated meteoric waters and consists of "blue-black" ore of mixed and intermediate oxidation states. The deepest, 3rd zone is relatively unaffected by meteoric water and contains primary mineralization. (After Heyl 1957)



the sands became stagnant and reducing from the decay of buried vegetal material. Reduced zones could have been small to large, depending on the size of the abandoned channels and the amount of organic debris within them.

Larger channels with abundant carbonaceous debris underwent more intense reduction. More intensely reduced channel segment sands tend to occur particularly near the base of thicker sandstone units along one margin of a major channel system. This stronger reduction liberated iron from magnetite and ilmenite. This type of alteration, represented by the altered facies of Shawe (1976a), corresponds to alteration associated with deposits of the Grants U Region (Adams and Saucier 1981). Completely destroyed ilmenite and magnetite may indicate groundwater flow within altered facies rocks as deduced from relict grains present elsewhere in strongly reduced sands that are hydrologically isolated (Adams et al. 1974). It should be noted, however, that the organic-rich carbon facies of the Salt Wash Member also contain incompletely altered ilmenite and magnetite.

The Salt Wash Member was finally covered by the Brushy Basin Member, which is dominantly composed of oxidized tuffaceous siltstones and shales with discontinuous conglomerate lenses at their base. As these overlying fine-grained sediments and oxidized floodplain deposits marginal to the channel systems began to compact, oxidizing pore waters were probably squeezed out from these pelites and expelled into the channel-sandstone aquifers. These solutions supposedly contained significant amounts of uranium derived from alteration of tuffaceous material.

The fluids would have tended to move into deeper reduced ground oxidizing outer margins of reduced sands as they advanced. However, reduced channel sandstones surrounded by

redbed sequences locally contain islands of red shale, and less commonly, red sandstone with no visible connection to bounding red sediments. This suggests that the channel sequence originally contained redbeds, which have been affected by diagenetic reducing processes active along channel axes. It may be assumed, in fact, that the redox boundary oscillated for some period of time in response to the rate of groundwater flow within reduced channels and fluid introduction from compacting oxidized sediments.

Breit and Goldhaber (1983) established alteration products as authigenic dolomite, calcite, baryte, kaolinite, chlorite, pyrite, and albite in the Salt Wash Member in the area of the Dolores anticline, the Gypsum Valley anticline, and the intervening Disappointment Valley syncline within the Uravan Mineral Belt. Kaolinite and dolomite are the principal authigenic phases across the Dolores anticline, whereas chlorite and calcite are the dominant authigenic phases within the syncline. The sharp boundary between the two mineralogical zones coincides with the Dolores zone of faults. A zone of copper enrichment also occurs and is centered on this series of the Dolores faults.

Principal Characteristics of Salt Wash Mineralization

According to Thamm's et al. (1981) description of ore mineralogy and characteristics of V-U mineralization in the Salt Wash sandstones, mineralization occurs in various degrees of oxidation, depending largely upon their proximity to the surface and their position with respect to the water table (Fig. 1.31). Three types of mineralization are distinguished, all three are ubiquitous in all areas of the Uravan Mineral Belt:

- Unoxidized mineralization referred to as primary or black ore,
- Partially oxidized mineralization or blue-black ore, and
- Oxidized mineralization or yellow carnotite ore.

Unoxidized mineralization: The main ore minerals are pitchblende and coffinite, montroseite, and vanadium aluminosilicates. Minor to trace amounts of Ag, As, Cu, Co, Cr, Fe, Mo, Ni, Pb, Se, and Zn typically have accumulated in mineralized zones compared with unmineralized Salt Wash sandstones.

Pitchblende and coffinite are very fine grained. Both are commonly intimately associated with carbonaceous debris or coalified wood. Pitchblende occurs as hard lustrous grains and as soft waxy material occasionally as sooty pitchblende. Pitchblende may replace plant material, in particular cell walls of fossil wood. It also replaces iron sulfides and detrital quartz grains in sandstone near vegetal debris. Coffinite is largely associated with carbonaceous material, in which it commonly fills cell cavities.

In unoxidized ores, vanadium of low-valency state occurs in the form of vanadium oxide minerals and in a suite of vanadium alumina-silicates including vanadium-bearing chlorites and vanadium hydromicas. Vanadium oxides predominate over vanadium aluminosilicates in ore bodies with vanadium-uranium ratios of less than 15:1. Montroseite is the most common vanadium oxide mineral. It forms steel-black, prismatic, lath-shaped crystals, or brittle crystalline black masses. Montroseite tends to form rosettes in sinuous bands in sandstone and fossil wood. It fills the cell structure of the latter, but obscures the wood structure by its elongate bladed crystal habit. Montroseite oxidizes easily to paramontroseite. Vanadium oxides and silicates occupy pore spaces of sandstone. Both also replace detrital quartz grains and fossil wood.

Pyrite and marcasite are dominant associated minerals of unoxidized mineralization. Pyrite of diagenetic, pre-ore origin occurs as discrete nodules or impregnates or forms pseudomorphs after wood (Weeks et al. 1959). In Shawe's (1976a) carbon facies, pyrite constitutes about 1% of the heavy minerals fraction. This low content would indicate an environment of formation with a very low iron and/or sulfur content.

A younger generation of pyrite, characterized by euhedral and massive habits and contents of cobalt and nickel, is associated with the mineralization. Shawe (1976a) determined for the *Slick Rock* area a pyrite content of 7% in the heavy mineral fraction in altered ore-bearing facies of third rim sandstone. The increase from 1% in barren reduced sandstone to 7% near ore bodies indicates an addition of sulfur and possibly iron. Shoemaker et al. (1959) suggest that iron is strongly enriched in ore zones. This is qualitatively compatible with roll-type deposits except that the Salt Wash mineralization contains distinctly less pyrite than most rollfront deposits.

Other accessory minerals include jordisite, galena, and sphalerite, as well as copper and silver minerals. Jordisite is the most abundant. Jordisite occurs in layers, 0.3–0.5 m thick, which are always underneath V–U mineralization. Jordisite has never been found intermixed or cross-cutting V–U ore.

Calcite, dolomite, and baryte are present within and close to mineralization as cement in sandstone. The total carbonate contained in most Salt Wash ore is less than 6%.

Oxidized mineralization: In zones of oxidation, two varieties of ore are distinguished: Partially oxidized “blue black ore” and completely oxidized “yellow carnotite ore.” Partially oxidized blue–black ore contains the uranyl vanadate rauhite as the principal uranium mineral, and doloresite and hewettite as predominant V⁴⁺ and V⁵⁺ minerals.

Completely oxidized yellow ore contains uranyl vanadates, primarily tyuyamunite and carnotite, and a series of vanadates including hewettite, pascoite, hummerite, and rarely, navajoite. Ore can be brown, red, orange, and yellow in color.

Partial oxidation has altered the primary U and V oxides, pitchblende, coffinite, and montroseite, first, for example, to rauhite and subsequently by complete oxidation to carnotite. Vanadium fixes all available hexavalent uranium in the form of uranyl vanadates. Excess vanadium crystallizes to the vanadates mentioned earlier. In contrast, vanadium aluminosilicates in unoxidized ore remain relatively stable during oxidation processes. Apparently, there is virtually no change in the V–U ratios of the ore during the oxidation processes, only a change of mineralogy.

Unoxidized ore constitutes the majority of deposits. The preservation of this dark grey to black mineralization is due to its position below the water table. Ore consists of black ore minerals impregnating the sandstone matrix and replacing some detrital quartz and feldspar grains. Ore minerals tend to be homogeneously distributed, except for heterogeneities of the sandstone itself. V–U minerals and associated gangue minerals are fine grained and intimately mixed, making megascopic mineral identifications practically impossible.

Intermediate between unoxidized black ore and fully oxidized yellow carnotite ore is *blue–black ore*. This ore shows a strong affiliation with accumulations of carbonaceous matter, as does carnotite ore, presumably reflecting areas of greatest resistance to intense oxidation and destruction.

Oxidized ore consists predominantly of finely dispersed uranyl vanadates and vanadates that impregnate the host sandstone matrix. Virtually all uranium released from primary V–U minerals during oxidation is protected against removal by its incorporation into vanadate minerals. Ore bodies, therefore, underwent essentially no loss of uranium or other metals. In contrast, ore with low vanadium contents experienced more significant uranium movement.

Zoning of ore and ore-related elements similar to that of Wyoming rollfronts, Mo, Se, U, and V in particular, is evident across roll and tabular ore in Salt Wash Member deposits (► Figs. 1.32–1.34; ► Tables 1.3 and ► 1.4). However, the orientation and sequence of Se–V–U–Mo zoning differs between ore shapes and between deposits. Rolls or C-shaped configurations usually display zones with selenium on the concave side of the uranium–vanadium zone, whereas calcite has commonly crystallized at the convex side.

Tabular deposits tend to show more variation with selenium concentrated at the top, bottom, or top and bottom of ore lenses, although in general, selenium was most commonly precipitated

Fig. 1.32.

Uravan Mineral Belt, Deremo mine, diagrammatic cross section of a redox boundary entirely within a Salt Wash sandstone horizon and distribution of U–V mineralization and associated elements. (Numbers refer to samples given in Table 1.3) (Thamm et al. 1981, based on Union Carbide Corp.)

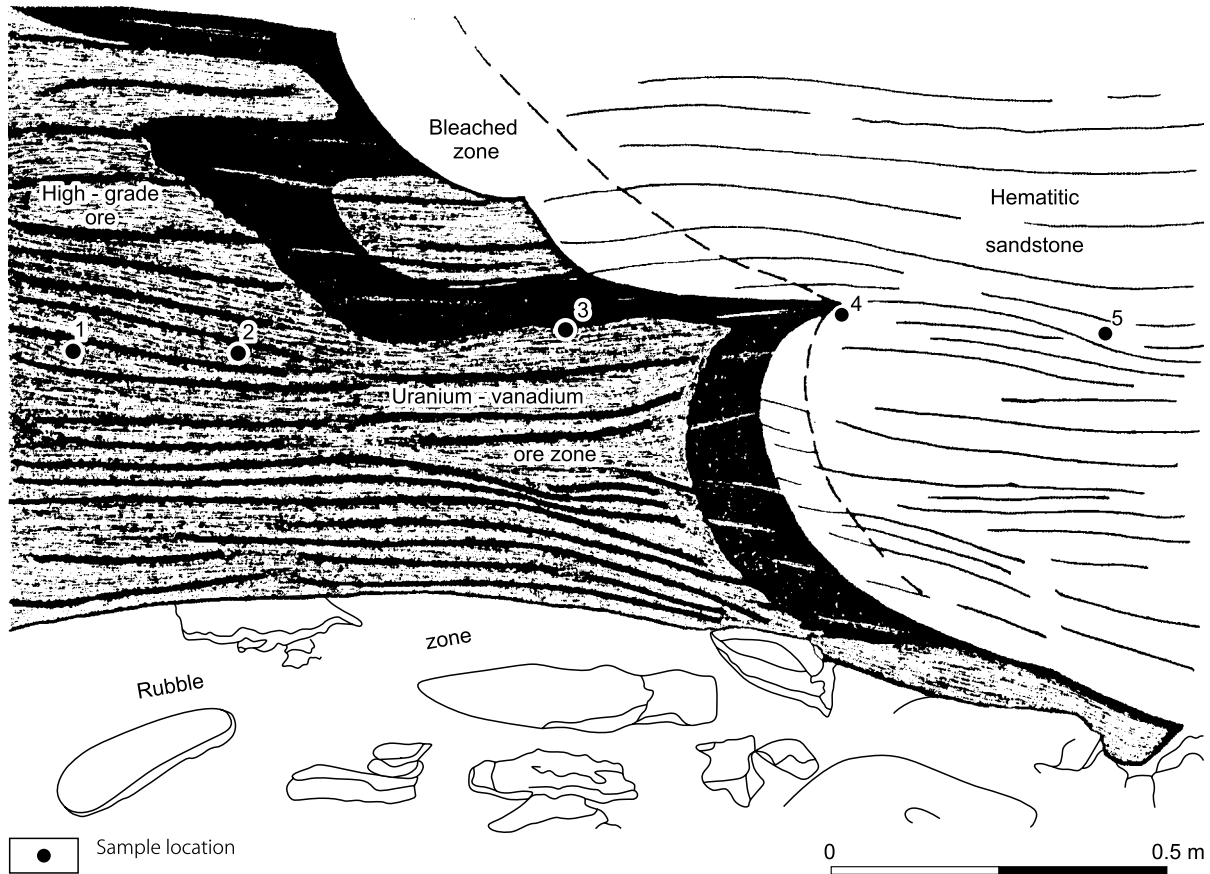


Table 1.3.

Element (concentration in ppm)	Sample Number				
	1	2	3	4	5
U	803	878	1,013	113	371
V	17,807	38,037	52,939	280	250
Se	365	520	470	255	115
Mo	20	25	5	<5	<5
Cu	78	170	502	302	40
Pb	<5	<5	15	190	10
Zn	19	38	62	13	9
As	63	38	68	20	25
S	635	1,012	736	220	230
Cr	8	14	13	5	5
Fe ³⁺ /Fe ²⁺	2.5	1.9	2.8	4.1	9.8

at the top of a tabular ore zone. In contrast to this scheme, Brooks and Campbell (1976) describe from the *La Sal Mine*, Utah, a systematic zoning of Se–V–U–Mo from the bottom to the top of ore lenses. An inverted ore-forming system or irregularities in ore horizons are thought to be the reason for inverted element zoning.

The similarity of elemental zoning patterns to those established by Harshman (1974) for rollfronts in the Wyoming Basins is suggestive (a) of an oxidation–reduction gradient involved in the formation of Salt Wash ore and (b) of an oxidation potential that generally decreased upward through the ore zone. In contrast to Wyoming rollfronts, however, there is no (major?) oxidized sandstone tongue in the Salt Wash host rocks.

Uranium mineralization forms two *geometric configurations of ore bodies*, which can be physically transitional into each other: (a) Tabular ore bodies concordant to bedding and often lenticular elongated parallel to the sedimentary trend, and (b) roll-shaped ore bodies that discordantly transect the bedding.

Roll-shaped ore bodies are sinuous and elongated parallel to local sedimentary textures, major channels, or axes of good permeability. The upper and lower surfaces of rolls are commonly bounded against clay-rich beds or lenses. In roll-shaped ore

Fig. 1.33.

Central Uravan Mineral Belt, Virgin No. 3 mine, cross sections of U-V rolls and content of U, V, As, and Se in the various parts of the rolls. (Numbers refer to samples given in Table 1.4) (Thamm et al. 1981, based on Shawe 1966)

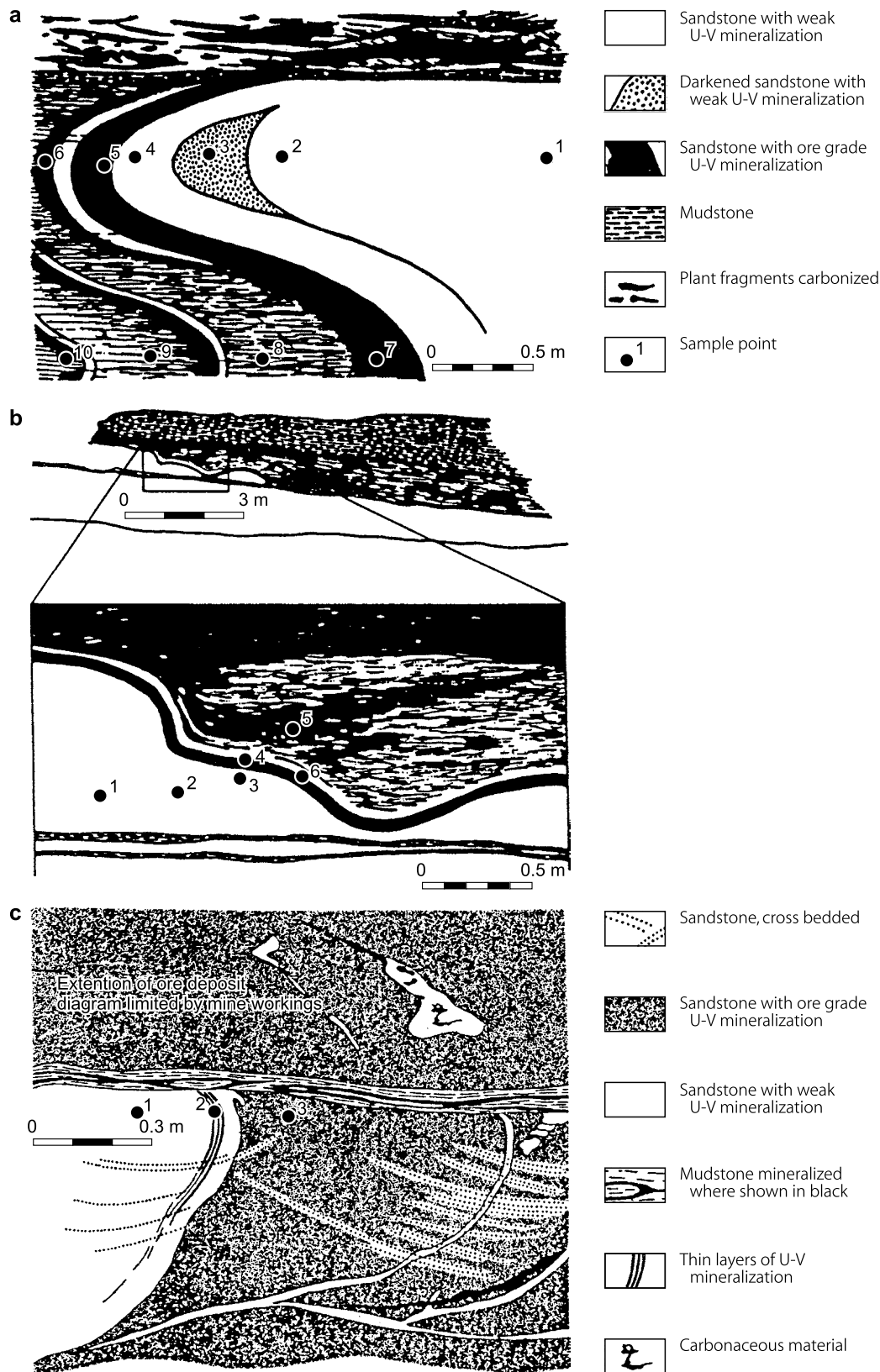


Table 1.4.

Element Sample no.	eqU (%)	U (%)	V (%)	As (ppm)	Se (ppm)
Figure a 1	0.004	–	0.3	20	10
2	0.005	0.006	0.2	50	20
3	0.003	–	0.3	40	20
4	0.003	–	0.2	10	200
5	0.065	0.068	1.5	40	70
6	0.11	0.12	2.5	40	15
7	0.073	0.12	2.5	60	7
8	0.016	0.021	2.5	20	10
9	0.041	0.051	2.5	40	10
10	0.13	0.15	2.5	90	15
Figure b 1	0.009	0.011	0.09	40	20
2	0.008	0.009	0.09	10	10
3	0.03	0.027	0.2	20	50
4	0.22	0.34	1.2	100	150
5	0.66	0.4	1.5	150	20
6	0.39	0.61	1.2	150	1,500
Figure c 1	0.008	0.012	0.09	10	40
2	0.1	0.15	0.2	20	1,500
3	0.17	0.17	6.0+	40	30

bodies, an influence of sedimentological properties and textures, and fluid flow direction toward the convex side of rolls is apparent. The concave boundary of rolls is generally sharper and more darkly colored. An abrupt contact between barren and mineralized rocks is very common. In contrast, the convex side of the rolls shows a gradual transition into unmineralized rock. The coloration of the host sandstone by V–U mineralization strongly accentuates the difference between the concave and convex side of the rolls.

The distribution and relative abundance of tabular and roll-shaped mineralization is locally and regionally variable. For example, tabular ore bodies prevail in the *Uravan Mineral Belt*, whereas roll mineralization is reportedly dominant in the *La Sal trend*. Shawe et al. (1959) established that roll-shaped mineralization is more abundant in host sandstones containing numerous shale horizons. The shale interbeds appear to break the mineral horizon into a series of rolls within intervening sands. Massive sandstones, by contrast, typically contain more tabular mineralization. This seems to reflect the tortuous hydrology of interbedded sand-shale sequences, which tend to produce rolls, whereas simple hydrologic interfaces may develop and produce tabular mineralization in a more homogeneous aquifer.

As pointed out earlier, the distribution of Salt Wash V–U mineralization is strongly influenced by sedimentological

properties on both a regional and local scale. On a regional scale, clusters or trends of deposits are emplaced within major sedimentary channels in which they tend to be aligned along margins. Most ore trends are oriented parallel to paleocurrent directions, which suggests an affinity to a broader hydrologic system.

Characteristic *local scale parameters* controlling ore position include a relatively thick reduced sandstone, abundant carbonaceous material, and interbedded grey mudstones or mudstone conglomerates. Highly cross-bedded channel sandstone containing organic matter is the predominant host rock. In contrast to the general ore trend, long axes of individual ore bodies may strike at oblique angles to major trend axes. Individual deposits or lenses of mineralization commonly terminate against shale horizons, channel margins, and any other sedimentological feature that creates changes in permeability.

Within ore lenses, the distribution of uranium and vanadium is strongly controlled by sedimentological peculiarities. Ore minerals are concentrated along cross-bedding planes, adjacent to scour surfaces, and in clay gall zones.

In the *Lukachukai Mountains*, Arizona, most major ore bodies and clusters of closely spaced smaller ore bodies appear to be spatially related to boundaries of reduced host sandstone with adjacent oxidized sediments (Nestler and Chenoweth

1958). This phenomenon also appears to a certain extent in other districts such as those of *La Sal*, *Slick Rock*, and many others.

Two different varieties of lithologically controlled *reduction-oxidation boundaries* can be distinguished. The first variety is entirely within sandstone, whereas the second is between dominantly sandstone and dominantly mudstone sections.

The redox boundary that is entirely within sandstone seems to occur typically within major channel systems. In this setting, oxidized sands are generally located in the upstream direction, i.e. from where sediments were derived. This relation is compatible with the regional distribution of oxidized and reduced sediments as reflected by their coloration. Proximal to the source area, rocks are red in color; they change to grey and grey-green toward the distal part of the depositional system. Minor redistribution and enrichment of mineralization appear to have taken place at this type of redox boundary.

Ore bodies related to the second mode of redox boundary are confined to reduced channel sands, adjacent to oxidized overbank deposits. They are commonly larger and more numerous near the redox interface than in reduced sands more distant from such contacts (Fig. 1.35).

In general, the highest-grade ore in any deposit occurs proximal to the redox boundary. Where narrow zones of grey, reduced sandstone extend into red, oxidized sands, both ore grade and continuity substantially increase. These zones, bounded above and below by red sediments, do not make major ore bodies in themselves, but constitute high-grade pods within larger deposits.

Within various Salt Wash districts, V-U mineralization appears to show some kind of a stratigraphic preference to different Salt Wash units. The upper third of the Salt Wash Member is the most productive unit in the *Uravan Mineral Belt*.

Fig. 1.34.

La Sal mine, contents and distribution of a U, V, Fe, and b Mo and Se across a tabular U-V zone. (After Thamm et al. 1981, based on Brooks and Campbell 1976)

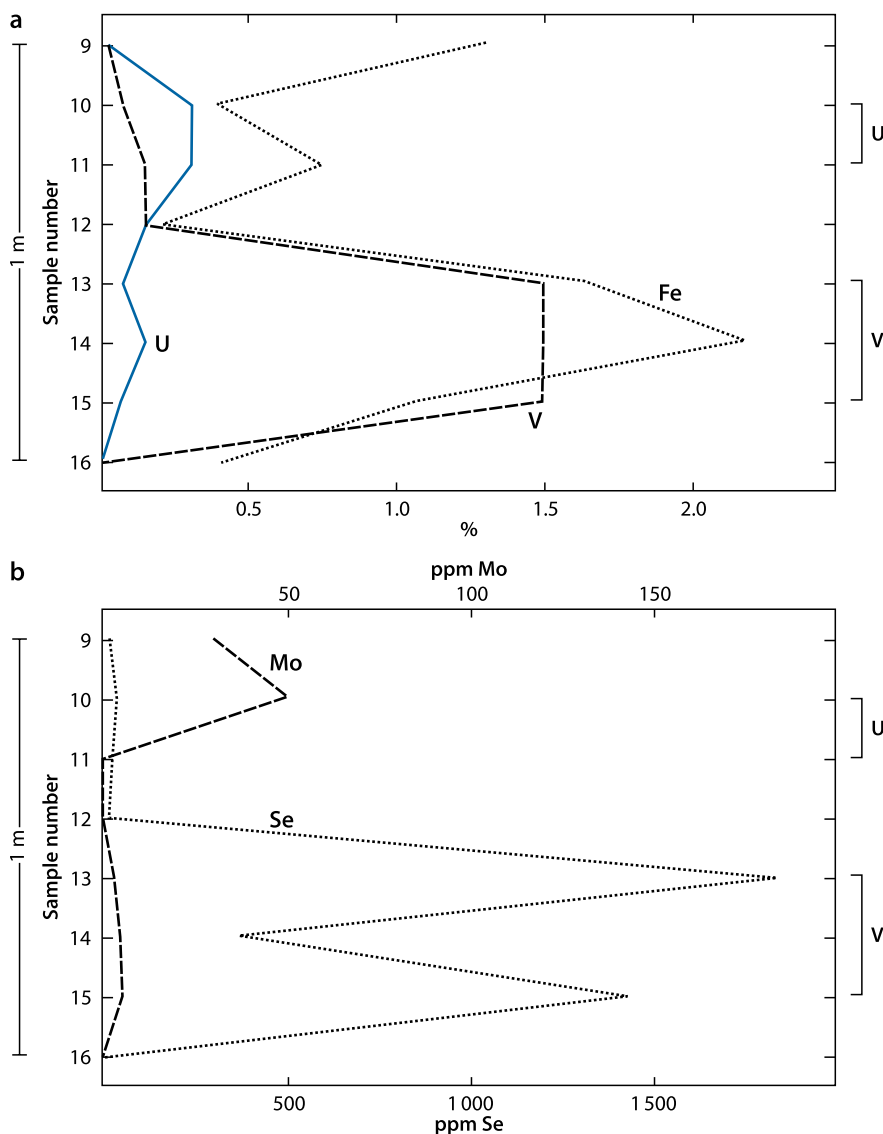
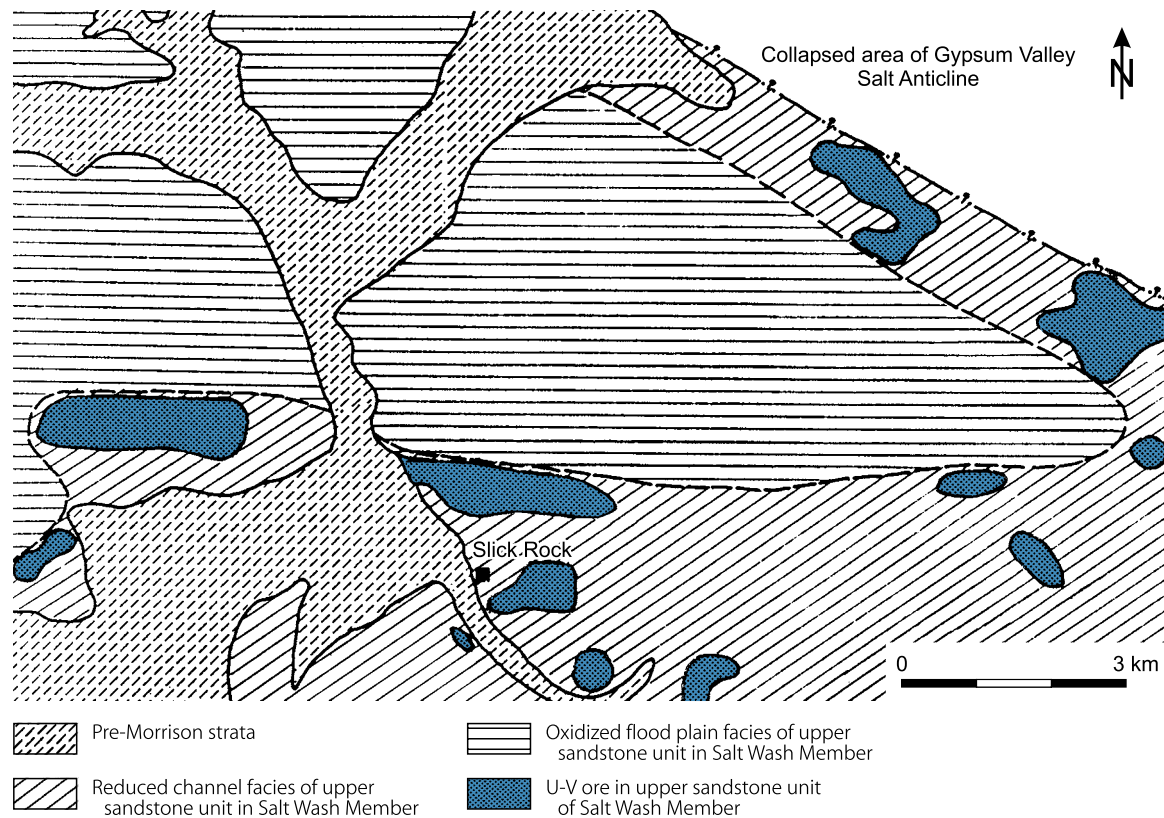


Fig. 1.35.

Uravan Mineral Belt, Slick Rock area, generalized geological map of the distribution of reduced facies and oxidized flood-plain sediments of the upper sandstone unit of the Salt Wash Member and the spatial relationship of ore bodies to these facies. (After Thamm et al. 1981, based on Union Carbide Corp.)



The so-called third rim or upper sandstone in that area refers to a single, semicontinuous sandstone unit at the top of the Salt Wash Member. In other districts, the upper sandstone is not necessarily the most important ore host, even though it may be present in the stratigraphic section. In both the *Meeker* and *Thompson districts*, most ore is in the lower sandstones. Large deposits in the *Little Rockies district* of the Henry Mountains are likewise within the lower sandstone of the Salt Wash Member.

Some major Salt Wash ore bodies in the upper sandstone unit are locally overlain by sporadically mineralized Brushy Basin sandstone as, for example, in the *La Sal district*. In one area in the La Sal district, mineralization greater than 1.5 m at 0.16% U occurs in the Brushy Basin sandstone, which rests on ore-grade mineralization in the Salt Wash Member.

Phoenix (1958) noted the proximity of basal conglomeratic horizons in the Brushy Basin Member to deposits in the underlying Salt Wash Member of the *Uravan Mineral Belt*. These observations suggest that permeable beds in the basal Brushy Basin may have been instrumental in the formation of at least some Salt Wash deposits. The beds possibly acted as channelways for the dewatering of Brushy Basin shales and directed uraniferous solutions into the Salt Wash where hydrologic continuity existed.

General Shape and Dimensions of Salt Wash Deposits

Ore bodies are commonly of relatively small size and occur in erratic distribution as illustrated in Fig. 1.36. As mentioned before, two geometric configurations of ore bodies exist as described by Thamm et al. (1981): tabular and roll-shaped ore bodies; both may grade into each other (Fig. 1.37).

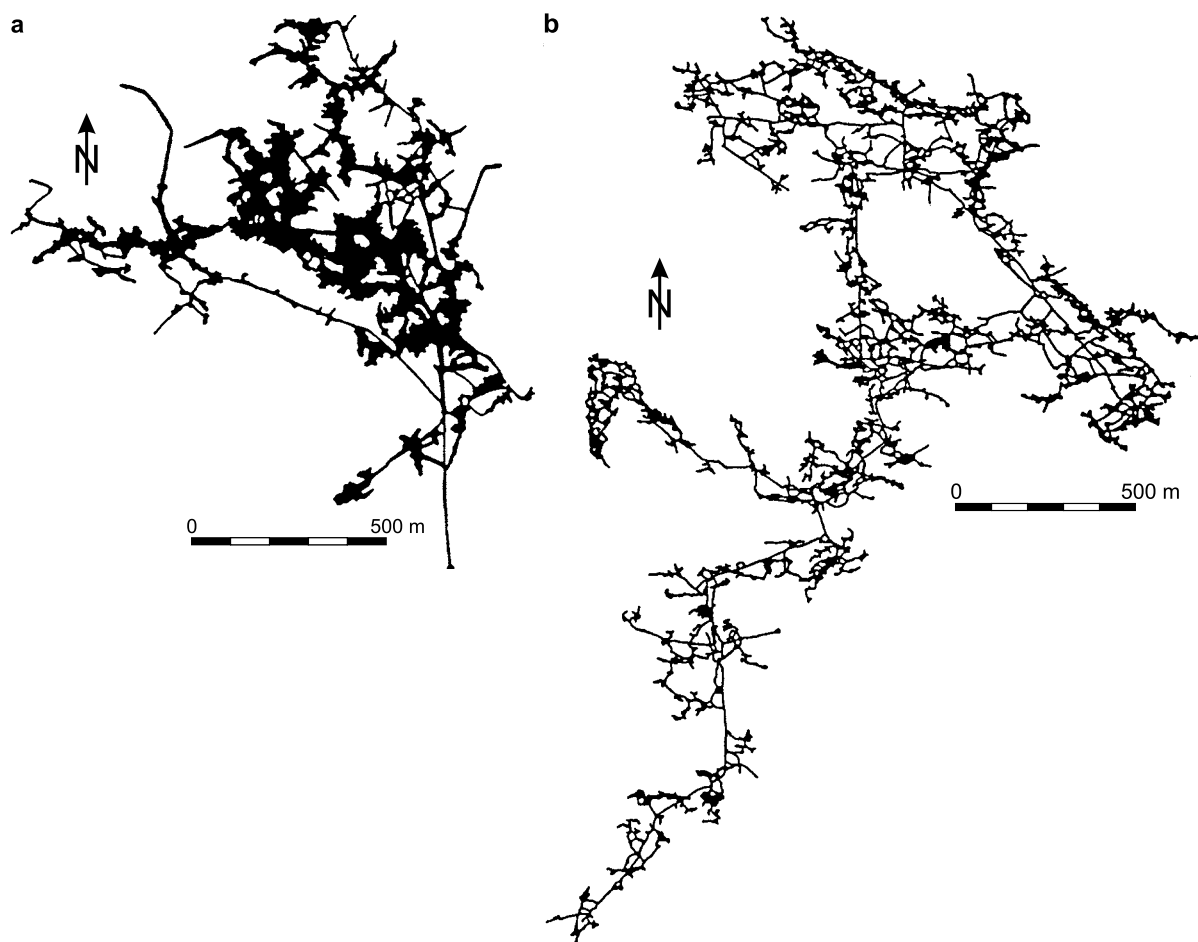
Tabular ore bodies are typically elongated parallel to sedimentary trends and concordant to bedding (Fig. 1.38). Their horizontal extensions generally are small, on the order of some few to tens of meters. Ore averages about 1–1.5 m in thickness but in a few places ore thickness approaches 10 m. Although individual ore bodies may locally be connected by weak mineralization, ore more commonly terminates abruptly against barren rock.

Roll-shaped ore bodies, in plan view, are generally narrow, not more than a few decimeters to about one meter wide. They are sinuous and elongated parallel to local sedimentological features. Most rolls are O- or S-shaped in cross section, but various other shapes also occur (Fig. 1.39). Concave roll boundaries are commonly sharp, whereas convex sides are diffuse.

In general, the distribution of V–U mineralization in the Salt Wash deposits is rather erratic and unpredictable as compared

■ Fig. 1.36.

Southern Uravan Mineral Belt, (a) Deremo mine, (b) King Solomon mine, planview demonstrating the small size and irregular distribution of ore pods, and complexity of the mine workings in the Salt Wash Member sandstone. (Thamm et al. 1981, based on Union Carbide Corp.)



with other types of sandstone uranium deposits particularly with the more continuous rollfronts of the Wyoming Basins and tabular humate uranium ore bodies of the Grants U Region.

Although mineralization is widespread, it is generally thin. Only locally does it become sufficiently thick and high grade to be economic. Even within deposits, shapes, orientations, and dimensions of ore pods are often highly erratic. This is particularly the case in the *Uravan Mineral Belt*, whereas deposits in the *Henry Mountains* appear to be more tabular and continuous.

Another characteristic phenomenon of Salt Wash-type V-U mineralization is that the majority of significant Salt Wash ore deposits are concentrated within a small number of areas. Within the *Uravan Mineral Belt*, some 15 small areas present in cross-trends have produced the bulk of the ore from that district, which has accounted for almost 80% of the production of all Salt Wash districts. Most other Salt Wash production has been mined from approximately ten small, widely separated districts within the Colorado Plateau (► Fig. 1.29). In conclusion, only a small number of districts, each of restricted size, contained a large percentage of the Salt Wash V-U ore mined. The many small

mines outside of these districts have contributed only a small fraction of produced ore.

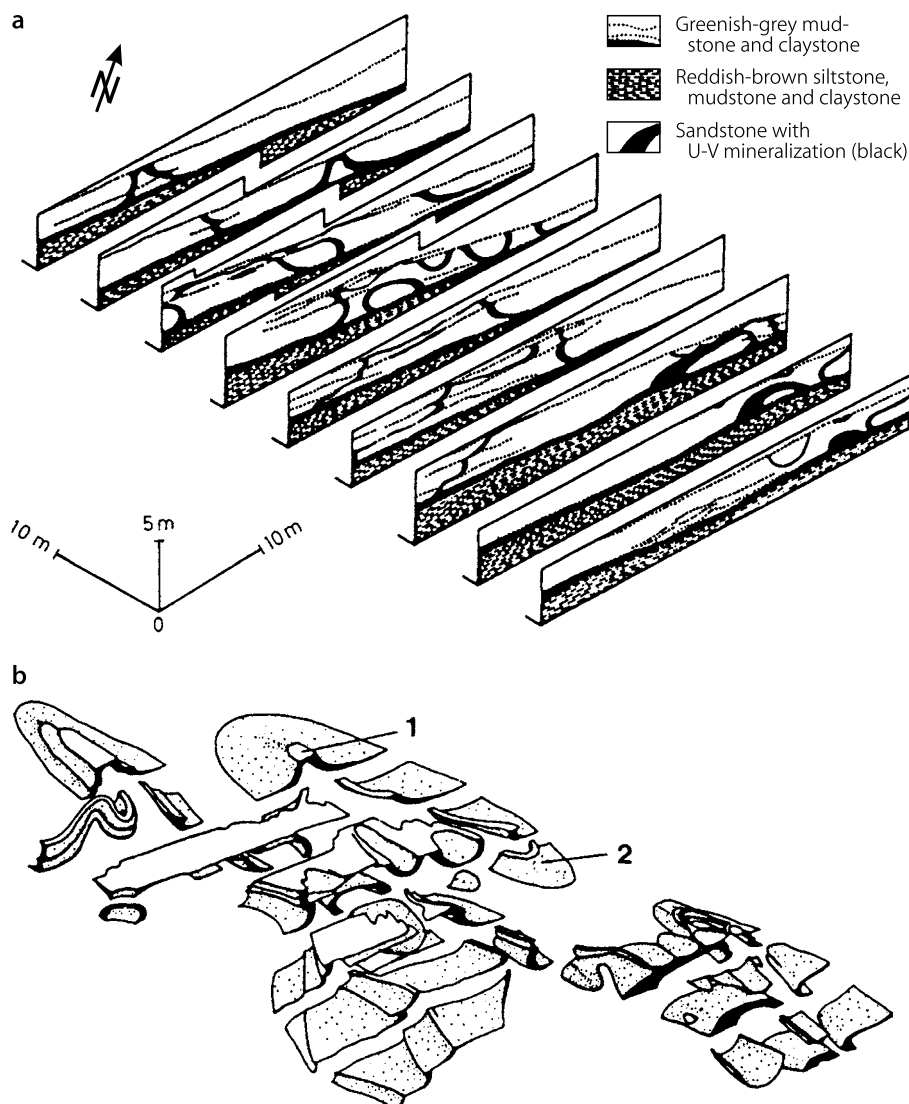
The average grade of ore mined prior to 1980 was approximately 0.2% U. In the early 1980s when the uranium price was up to about \$100/kg U, lower grade ore was recovered at an average grade close to 0.13% U.

In most of the producing districts, the ore contains from 3 to 15 times more vanadium than uranium. The mined ore has averaged approximately 1.25–1.50% V_2O_5 . Important exceptions are the *Green River district*, Utah, where the V-U ratio is less than 3–1, and the larger ore bodies in the *Henry Mountains* area, where the ratio is approximately 1–1. Discounting the few local exceptions, the ores, both reduced and oxidized, are in radioactive equilibrium.

Ore bodies tend to be clustered within elongated favorable zones a few kilometers long by several hundred to thousand meters wide. Average production from these elongated areas has ranged from a few hundred thousand tonnes to a few million tonnes of crude ore. Individual ore bodies range in size from a few tonnes to more than one million tonnes of crude ore.

Fig. 1.37.

Uravan Mineral Belt, Slick Rock trend, Cougar mine, (a) cross sections and (b) cutaway block diagram of the west-central edge of the ore zone showing the tabular to roll-type configuration of the U-V mineralization hosted in Salt Wash Member sandstone. Note that at point 1, the ore surface is against mudstone and at point 2, against sandstone. (After Shawe, Daniel R., Archbold, Norbert L., Simmons, George C., 1959, Society of Economic Geologists, Inc., *Economic Geology*, Fig.7, p. 410)



Potential Sources of Uranium and Vanadium

The **uranium source** is still open to debate. The Salt Wash deposits and other uranium deposits of the Colorado Plateau, as for example, those in the Chinle sediments occur within a province of uraniferous Precambrian basement. Thamm et al. (1981) suggest that the uranium-enriched Precambrian rocks or younger uraniferous igneous or volcanic rocks constitute possible sources for much of the uranium now found in sandstone deposits of the Colorado Plateau. As may be deduced from other regions where sandstone-type uranium deposits are associated with uraniferous pyroclastics, these relations in the Salt Wash region provide a reasonable circumstantial argument that tuffaceous constituents incorporated within the Salt Wash host sandstones and the overlying Brushy Basin pelites were the source of uranium;

this idea is based, however, more on the presence of tuffaceous material in various Salt Wash districts than on geochemical documentation.

The **vanadium source** in Salt Wash deposits, which are essentially vanadium deposits, is likewise unknown. Favorite hypotheses suggest that vanadium was derived by either (a) decomposition of detrital magnetite and ilmenite within the host sediments, (b) diagenetic introduction from the overlying Cretaceous sediments, and/or (c) leaching and erosion of Paleozoic sediments located west of the Colorado Plateau.

All of these hypotheses are, to some extent, plausible, but remain speculations. For example, Fischer and Stewart (1961) point out that the vanadium-rich sandstone deposits of the Colorado Plateau are confined to second-cycle sandstones, one of which is the Salt Wash Member. Vanadium may have been

Fig. 1.38.

La Sal district, (a) generalized map of distribution of reduced channel sand facies and oxidized flood plain sediments of the upper sandstone unit of the Salt Wash Member. All ore is in the reduced channel facies where it occurs at several levels as shown in the cross sections of (b) the western part of the La Sal district, and (c) the La Sal mine. [After (a) Thamm et al. 1981, and (b, c) Kovschak and Nylund 1981 (reproduced by permission of NM Geological Society)]

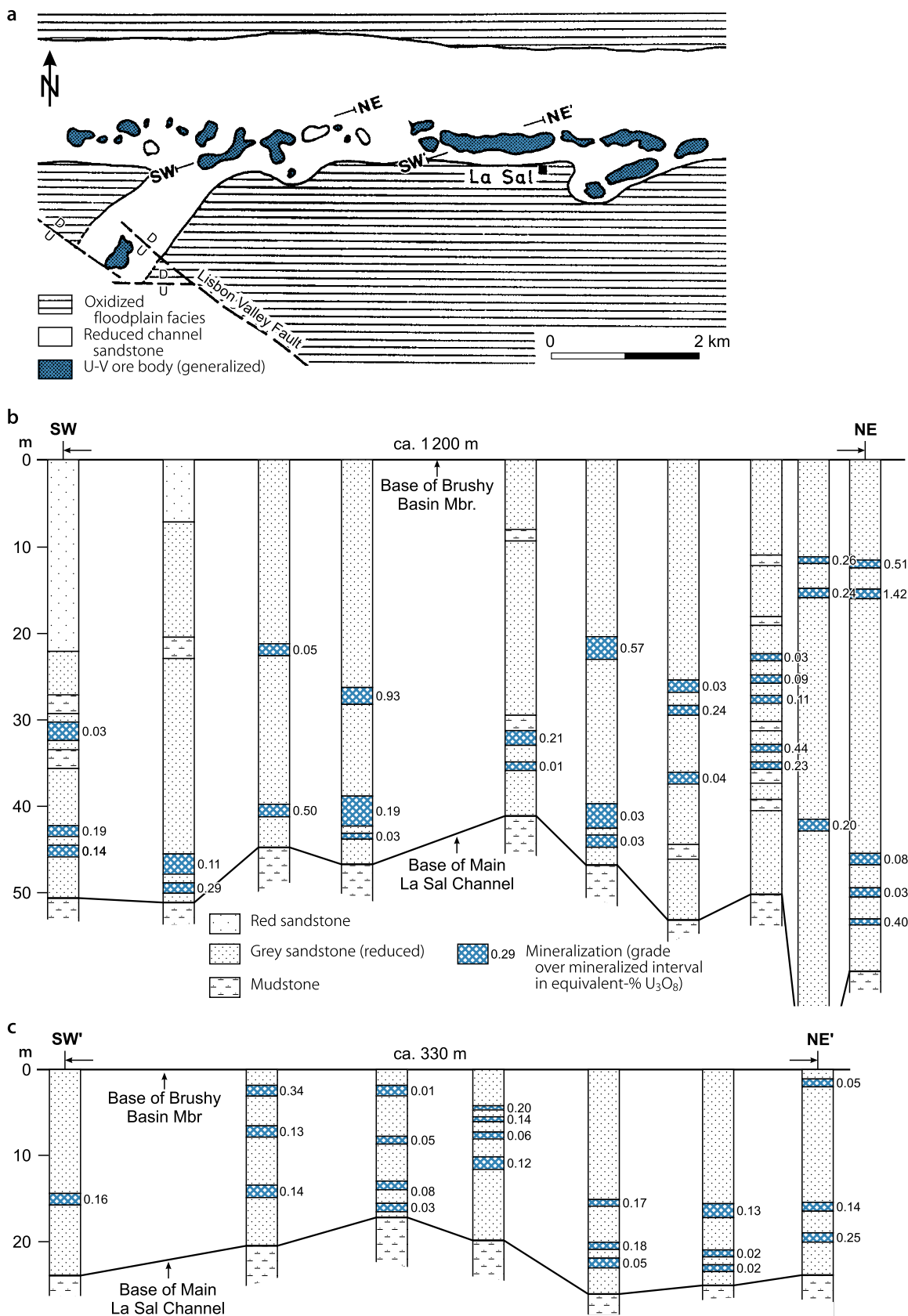
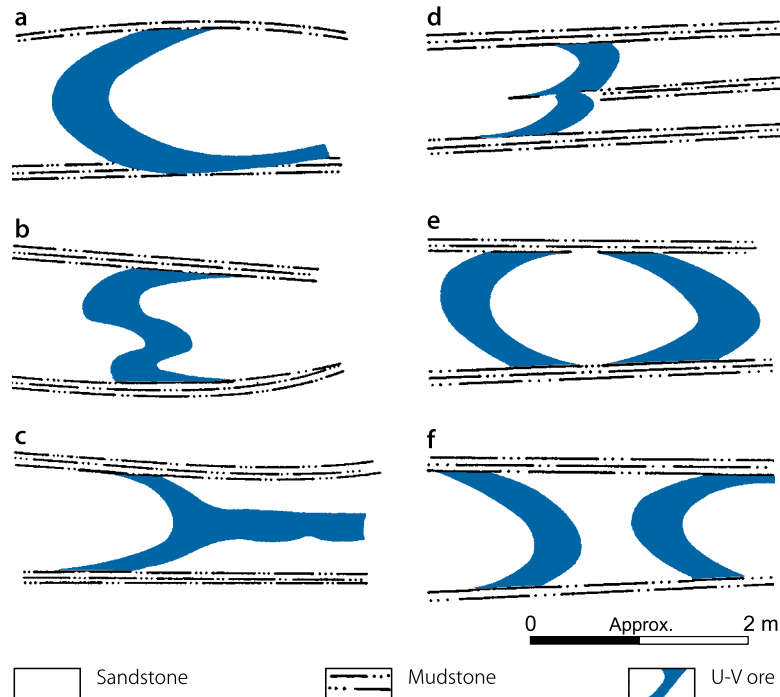


Fig. 1.39.

Uravan Mineral Belt, schematic cross sections displaying various configurations of roll-shaped U–V concentrations in the Salt Wash Member. (Roll types: (a) C roll; (b) S roll; (c) socket roll; (d) two rolls separated by a thin layer layer of mudstone; (e) mirror image C rolls, convex loop; (f) mirror image C rolls, concave loop) (Shawe 1956a)



preserved in ilmenite and magnetite, which might be expected to be more concentrated in second-cycle sandstone than, for example, in arkosic sandstone. If most of the vanadium originated in the course of alteration from magnetite and ilmenite, the question arises as to why deposits of the Grants U Region contain so little vanadium, although magnetite–ilmenite destruction on a large scale has been undoubtedly documented there by Adams et al. (1974, 1978) as discussed in Chap. 1.1 Grants U Region.

Principal Ore Controls and Recognition Criteria

Most Salt Wash deposits are primarily not uranium deposits but vanadium deposits. As such, they represent a special subtype among peneconcordant sandstone-type U deposits. In summary, Thamm et al. (1981) list the following principal ore control and recognition criteria of deposits in the Salt Wash Member of the Jurassic Morrison Formation:

Host environment and alteration

- Host rocks are continental clastic sediments of Jurassic age associated or interbedded with tuffaceous sediments
- The dominant host rock for all significant uranium ore bodies is an altered-facies sandstone of fluvial provenance characterized by
 - megascopically buff to grey sands
 - relative high permeability

- some combination of detrital plant debris, minor redistributed humate and iron sulfides, and
- largely or completely altered detrital ilmenite and magnetite.
- The redbed facies sandstones and mudstones, which accumulated as oxidized sediments under floodplain and overbank depositional conditions, do not contain uranium deposits and rarely contain uranium occurrences
- The Brushy Basin Member of the Morrison Formation, which overlies the Salt Wash Member, is largely, if not dominantly, oxidized in the general region of the Salt Wash deposits. This is consistent with the oxidized nature of mudstone sequences marginal to major Salt Wash channels. It is in contrast, however, to the dominantly reduced state of the Brushy Basin Member in other parts of the Colorado Plateau. Whatever solutions of compaction, the Brushy Basin Member contributed to the ore-hosting Salt Wash sediments, therefore, were likely oxidizing rather than reducing
- The color of the Salt Wash sediments, which indicates the state of oxidation or reduction, reflects a kind of regional zoning. Oxidized sediments are more common proximal to the sediment source areas, whereas reduced sediments prevail toward the distal depositional areas. The *Uravan Mineral Belt* occurs within the zone of transition and inter-fingering between the dominantly oxidized and dominantly reduced sediments

- In all the Salt Wash districts, zones of reduced grey sandstone with carbonaceous material and interbedded grey clays appear to be directly associated with ore deposits
- Although all the major Salt Wash V–U deposits occur in some proximity to oxidized sediments (redbed overbank deposits or oxidized sandstone), the mineralization itself is generally confined entirely to reduced sandstone, without adjacent tongues of oxidized sandstone. This suggests that the ore did not originate by the mechanism that forms roll-type deposits of the Wyoming Basins type. Mineralization is, in this respect, more like that of deposits of the Grants U Region, which similarly occur within reduced sandstones. The Salt Wash deposits contrast to the Grants deposits, however, by their association with plant debris, whereas redistributed humic material is not a significant ore component in the Salt Wash Mineralization.

Mineralization

- Small, low-grade occurrences of U mineralization are widespread within the reduced sediments of the Salt Wash Member
 - Larger deposits are restricted to major sandstone channels, e.g. in the *Uravan Mineral Belt*, or thicker alluvial sand accumulations, e.g. in the *Henry Mountains*, thus indicating as in other sandstone uranium districts, that major deposits are associated with major transmissive sandstones
 - Mineralization is dominantly tabular, elongate, and lenticular, mostly peneconcordant with host rock bedding. Occasionally mineralization crosses the bedding at a sharp angle in the form of a roll. No apparent genetic difference, however, appears to have caused the tabular and roll-shaped configurations. They differ only in their shape
 - Zonal distribution of uranium, vanadium, and selenium is similar across both tabular and roll ore bodies as established in the *Slick Rock area*, *Uravan Mineral Belt* by Shawe (1966, 1976a), i.e. both types were probably formed by the same mineralizing processes. The different shape is presumably due to local changes in hydrology in response to sedimentological peculiarities, which perhaps separated waters of different oxidation potential and composition. Consequently, the Salt Wash rolls are not true redox fronts and hence differ fundamentally from the Wyoming roll-type deposits in their genesis
 - The more typical tabular mineralized lenses, which vary in thickness from a few centimeters to a few meters, generally have a sharp upper boundary and a more diffuse lower boundary
 - Salt Wash V–U ore bodies are generally of small size but of reasonably high grade
 - Ore bodies consist of V–U accumulations within broader zones or trends in the form of commonly thin, discontinuous and rather erratic mineralization. This geological setting and behavior probably reflects a specific ore-forming mechanism controlled by host sediments of variable transmissivity. A typical example is the *Uravan Mineral Belt* while deposits in the *Henry Mountains* district are an exception. The latter are more tabular and continuous due to a supposedly more uniform hydrology of the ore-hosting sandstones
 - The suspended position of ore lenses within a particular level in the host sandstone indicates a unique mechanism of ore emplacement. Ore lenses rarely touch either the upper or the lower contact of the host sandstone bed, although, locally, mineralization has been so intense as to almost totally replace the detrital fabric of the host lithology. No property of the host beds has been established as a control for this stratigraphically precise yet territorially very broad-scale tendency of ore localization within the host bed.
- Peculiarities of the sedimentological evolution of the Salt Wash sediments appear to have influenced, on a regional as well as local scale, localization of uranium districts and ore bodies.
- **On a regional scale**, existing or growing structures active at the time of Salt Wash deposition obviously controlled patterns and types of Salt Wash sedimentation, which in turn influenced the localization of ore districts. Many ore trends in the *Uravan Mineral Belt*, for example, are adjacent and parallel to the NW–SE-trending salt anticlines of the underlying Paradox Basin of Pennsylvanian age. This suggests that halokinetic movements of Paradox Basin evaporites, active at the time of Salt Wash sedimentation, diverted major stream flows into channels paralleling those axes. Similarly, in the *Henry Mountains* growing structures influenced depositional trends and patterns of the lower Salt Wash Member in that area as established by Peterson (1980). Stokes (1954a, b) and Huffman and Lupe (1977) concluded that active structures in northeastern Arizona and northwestern New Mexico exerted a pronounced control on the depositional pattern of the Morrison sedimentation in the *Lukachukai-Carrizo district*. Stokes (1954d) also reported similar structural phenomena from *Cottonwood Wash* in southeastern Utah.
 - **On a large scale**, V–U districts are localized along thick depositional axes of sedimentation. The *Henry Mountains* and *Green River* districts coincide with a thick, N–S-trending depositional axis. The *Lukachukai-Carrizo* deposits occur within a NW–SE trend of thicker sandstones. Deposits of the *Uravan Mineral Belt* are situated within an area of generally thicker sedimentation, but, in addition, are positioned within a transitional zone of large-scale facies changes. Immediately west of the *Uravan Mineral Belt*, the Salt Wash Member is composed dominantly of floodplain sediments cut by relatively few but large distributary sand-filled channels. Within the mineral belt itself, smaller but more numerous distributary channels occur interspersed with areas of floodplain deposits. East of the *Uravan Mineral Belt*, the Salt Wash Member is composed of nearly continuous layers of horizontally bedded, generally fine-grained sandstone typical of low energy waters. A W–E section across the *Uravan Belt* shows a Salt Wash transition from a meander belt of coarse-grained arenites to a meander belt of fine-grained arenites, and finally to prograding delta sands. Shawe (1962) suggests that the thicker Salt Wash sediments

in the UraVan Mineral Belt were deposited in a small shallow basin.

- **On a local scale**, as pointed out by Tyler and Ethridge (1981), the highest-grade mineralization in the *UraVan Belt* is dominantly associated with point bar deposits within the meandering stream channels. The two authors specify the composition of the point bars as a kind of transitional facies between meandering and braided stream deposited sandstones. Northrop (1982) reports, that this relationship between sandstones of certain channel-facies and the V–U grade in an ore body also characterizes deposits in the *Henry Mountains*. This peculiar position of high-grade ore concentrations in distinct channel facies requires some control on the intensity of mineralizing processes either by the paleo-hydrological regime or by some V–U fixing lithological components deposited preferentially at particular sites within the channels.

Metallogenetic Concepts

Metallogenetic models forwarded for the Salt Wash V–U deposits vary widely from synsedimentary to hydrothermal ore-forming processes. All salient features, however, are more suggestive for a formation from groundwater at low temperatures than for an either hypogene hydrothermal or synsedimentary or syngenetic origin.

Nash et al. (1981) and Northrop (1982) (details see later) consider epigenetic ore formation along a solution interface existing within the host sandstone between a saline fluid and meteoric water, a concept already proposed as early as 1947 by Fischer.

Thamm et al. (1981) visualize the ore-forming process as follows (see also paragraph Host Rock Alteration). After the channel-sandstone systems of the Jurassic Salt Wash Member were covered by the dominantly oxidized, tuff-interbedded pelites of Brushy Basin Member, diagenesis caused the expulsion of oxidizing pore waters from Brushy Basin sediments into Salt Wash channel aquifers. These solutions are considered to have contained significant amounts of uranium leached from the tuffaceous material. The site of vanadium–uranium precipitation was at the boundary between reducing groundwater and a more oxidizing, but not necessarily hematite-producing groundwater system.

Chemical conditions for the ore-forming process as suggested by Thamm et al. (1981) include a partial decomposition of plant trash in deeper channel sands, which contributed humic acids to groundwater. In result, a reducing environment developed a forcing decomposition of ilmenite and magnetite with subsequent leaching therefrom of iron and vanadium. The hydrolysis of pyroclastic material liberated silica and alumina and produced a rise in pH, which further promoted the decomposition of plant material. Zones of contact between these reducing solutions and the more oxygenated, U^{6+} -bearing solutions expelled from adjacent Salt Wash redbeds overlying the Brushy Basin sediments and recharge areas up the hydrologic gradient were the sites of ore formation.

The dominant groundwater movement followed the same direction as sediment transportation. Oxidizing groundwater,

which was under hydrologic head from compacting pelites above and marginal to the channel axes migrated tangential to and into reduced sands. In more uraniferous, thicker sand units as found, for example, in the Henry Mountains region, the redox contact assumed a simple tabular configuration and produced more consistent, tabular ore bodies of the Tony M/Shooting Canyon and adjacent deposits. Where sediments consisted of complexly interbedded sand-shale sequences, the solution interface became contorted between shale interbeds, which led to mineralization of a mixed tabular-roll pattern.

The precipitation of ore elements at the interface between an overlying oxidizing and an underlying reducing groundwater system produced an element zoning that proceeded from selenium and vanadium at the top, through uranium to molybdenum at the bottom of the mineralized section. This is the element pattern most commonly observed in Salt Wash deposits. But, as stated earlier, ore rolls also produce inverted element arrangement on their overturned limbs.

V–U mineralization most commonly occurs within altered-facies sandstone commonly adjacent to carbon-facies sandstone, both of which contain carbonaceous material. There is, however, no evidence of the mode of oxidized sandstone tongues that are typically associated with rollfront U deposits as known from the Wyoming Basins. It appears, therefore, that uraniferous solutions were sufficiently oxygenated to carry uranium in the hexavalent state but were sufficiently low in oxidation capacity to leave the majority of the carbonaceous debris unaltered. The absence of redistributed humate within V–U mineralization suggests that the pH of the two mixing solutions was sufficiently similar to prevent the precipitation of humate from an alkaline-reducing groundwater.

Once deposited, V–U mineralization remained essentially at the site of its precipitation. There is no evidence that changes in groundwater patterns resulting from regional tectonic movements or local intrusions caused significant migration of ore elements, especially in ore of high vanadium content. The majority of the original Salt Wash ore minerals that became oxidized remained in situ due to fixation of uranium in insoluble secondary V–U minerals.

Granger and Warren (1981) suggest that the precipitation of insoluble U^{4+} and V^{4+} minerals resulted by reduction of U^{6+} by V^{3+} , but they point out that such a redox regime requires a groundwater composition other than that derived from the Morrison sediments. They propose that the solution possibly originated from underlying evaporite-containing strata, and that this solution carried uranium and sufficient magnesium to displace complexed vanadium and aluminum contained in soluble humate. The coupled precipitation of uranium, vanadium, and aluminum as hydroxide gels co-precipitated Mg^{2+} and K^+ , which subsequently aged to form the clay-bearing assemblages characteristic of the mineralization.

Breit and Goldhaber (1983) studied authigenic minerals in the Salt Wash Member in the Dolores anticline, the Gypsum Valley anticline, and the intervening Disappointment Valley syncline. Their results indicate a multistage geochemical history with implications for the genesis of both vanadium–uranium and copper deposits of the region. Authigenic minerals include albite, baryte, calcite, chlorite, dolomite, kaolinite, and pyrite.

Some of them, in particular dolomite and chlorite, imply the presence of saline fluids. These postulated saline fluids are believed by the authors to have influenced the formation of vanadium–uranium deposits. Potential sources for these brines include evaporites in the Pennsylvanian Paradox Formation, which occupy cores of the anticlines, and paleoformation waters in the Morrison Formation.

Northrop (1982) researched the origin of the Salt Wash mineralization in the Henry structural basin, which encompasses the *Henry Mountains district*. Since the Henry Mountain deposits are in many aspects typical of the tabular-type Salt Wash mineralization that occur throughout the Colorado Plateau, Northrop's findings may have a principal bearing on the regional metallogenesis of the Salt Wash V–U deposits. Northrop (1982) based his metallogenetic evidence on chemical and isotopic compositions and stratigraphic distribution of authigenic/diagenetic mineral phases, in particular on those phases, which are more or less cogenetic with V–U mineralization. His documentation of ore related tabular-planar layers of authigenic dolomite cement, the ^{18}O and ^{13}C of these dolomites, and the ^{34}S values of disulfide phases, suggest a high Mg to Ca ratio of greater than 1:1, enrichment in dissolved sulfate and carbonate, and probably also an abundance of Na for brines derived from the Tidwell Unit, which underlies the Salt Wash Member. Brines or other fluids did not deplete any ore and ore-related elements (Co, Cr, Mo, Ni, Se) of the Tidwell Unit and the author concludes that these brines, unlike the ore fluids, were confined within the Henry Basin. In contrast, uranium and vanadium have been mobilized from the two higher Salt Wash and Brushy Basin members and were transported by meteoric fluids to sites of ore formation in the Henry Basin.

Northrop (1982) identified four stratigraphic positions of a stable brine-meteoric water interface in the Henry Basin. Dolomite maxima superjacent to each interface position indicate the general position of an interface, whereas the mineralogy and composition of clay minerals define the exact position of an interface. Chlorite and/or chlorite–smectite, enriched in vanadium and magnesium, only occur at the brine-meteoric water interface position, which in turn also controls the localization of V–U ore.

Mineralization is restricted to intrabasinal synclines, in which it is confined to those sites where the brine-meteoric water interface intersects sandstone horizons containing anomalous concentrations of organic matter. Where sandstone does not contain detrital organic debris, Mg- and V-enriched chlorites still occur. These lateral extensions of ore related gangue(?) minerals also contain anomalous uranium above the normal background values of the Salt Wash sandstone.

The authigenic clay mineral in the upper part of the mineralized interval in the Tony M ore body is a V-bearing chlorite. It apparently derived from a precursor smectite and detrital illite–smectite. Clays in mineralized zones and in their unmineralized lateral extensions show an asymmetric distribution of Mg and V into the interlayer octahedral sheets in ore-clays, with Mg generally more abundant than Fe in chlorites.

The destruction of pre-mineralization clay minerals as well as quartz generated a siliceous-rich environment, which probably caused the silicification as observed in zones of quartz over-

growths positioned both above and below vanadium–uranium ore horizons. The prevalence of coffinite may likewise be the result of abundant availability of silica. The provision of silica is further indicated by the close spatial relationship between coffinite and vanadiferous chlorite (Goldhaber, unpublished data in Northrop 1982).

Northrop (1982) concludes from his data that the formation of the V–U mineralization in the Henry structural basin/Henry Mountains is the result of distinct geological features associated with integrated processes:

1. The appropriate setting and kind of sedimentation within the Henry Basin provided (a) an evaporite horizon in the Tidwell Member of the Morrison Formation, (b) sandstones containing abundant, preserved detrital organic matter, and (c) an available source of uranium and vanadium in the overlying Salt Wash and Brushy Basin members
2. Diagenesis generated a saline fluid from the Tidwell Member evaporites but unlike vanadium–uranium transporting fluids, the brines remained confined within the Henry Basin
3. Oxygenated meteoric waters moving downward into the basin leached uranium and vanadium from the overlying Salt Wash and Brushy Basin members
4. Deposition of ore elements occurred at a stable interface between reducing saline and oxidizing meteoric fluids.

Description of Individual Salt Wash Uranium-Vanadium Districts

For location of districts see [Fig. 1.29](#)

1.2.1 Uravan Mineral Belt, Colorado

The original Uravan Mineral Belt in southwestern Colorado is an arcuate, elongate belt some 110 km long and 3–10 km wide. It extends from Egnar in the south, through Uravan in the center, to Gateway in the north. By geologic inference, the original belt can be extended northwestward to the Thompson–Yellow Cat area and southwestward to the Blanding–Cottonwood area in Utah, then covering an area 220 km in length ([Figs. 1.29](#) and [1.30](#)).

First reports on uranium in the Uravan Belt date back to 1881. In the early years and for a long period, the ore mined consisted only of yellow uranium vanadates derived from near-surface oxidized deposits. Since the 1970s, however, most of the mining produced pitchblende, coffinite, and montroseite from deeper, unoxidized levels.

Original resources of the Uravan Mineral Belt were estimated on the order of 40,000 t U contained in more than 1,000 properties. Production until 1988 amounted to 32,000 t U and about five times as much vanadium, which largely derived from almost 1,000 small underground mines and a few open pit operations (Chenoweth, personal communication). [Crawley (1983) reports a production through 1987 of some 35,000 t U from 16.7 mio t of ore that averaged 0.2% U and 1.65% V_2O_5 .] Remaining potential resources are estimated at about 36,000 t U in the \$30/lb U_3O_8 forward-cost category.

Sources of Information. Bowers and Shawe 1961; Breit and Goldhaber 1983, 1985; Carter and Gualtieri 1965; Chenoweth 1981; Crawley 1983; Doelling 1969; Fischer and Hilpert 1952; Heyl 1957; Motica 1968; Shawe 1962, 1966, 1976a, b; Shawe et al. 1959; Thamm et al. 1981; Tyler 1981; Tyler and Ethridge 1981; US-AEC 1959; Adams et al., personal communication.

Geological Setting of Mineralization

The Uravan Belt lies within the Paradox Basin. V–U mineralization occurs in terrestrial sediments of the Salt Wash Member of the Late Jurassic Morrison Formation. The Salt Wash Member is overlain by greater than 100 m of mudstones containing volcanic ash of the Brushy Basin Member, and rests concordantly upon marine shales and thin-bedded sandstones of the Middle Jurassic Summerville Formation. Within the belt, Jurassic beds are gently folded but normally dip with less than 6° to ENE, except where they have been tilted by post-ore block faulting associated with salt anticline collapse.

The Salt Wash sediments were deposited as a flood plain or broad alluvial fan by a distributary stream system. A stratigraphic inference is that the Uravan Belt represents a zone along the leading edge of that fan, which grades to the east of Uravan into thinner and more regular bedded fine-grained sandstones, whereas to the west of the belt, conglomeratic sandstones with only sparse coalified plants prevail. It is speculated that the source of the Salt Wash stream system was in Utah, about 50–60 km to the west of Uravan, and that perhaps structural deformation during the deposition of the Salt Wash induced differences in sedimentation that account for the favorable lithology.

Within the Uravan Belt, the Salt Wash Member consists of interbedded sandstone and mudstone 90–120 m thick. The sandstones form as many as seven distinct units, called rims, which often coalesce into three thick channel fills.

The uranium host rock is cross-bedded, fine to medium-grained arkosic quartz sandstone. It contains up to 6% carbonate and large amounts of coalified substance partly in the form of fossil trunks of trees, and pebbles or galls of clay. The sandstone normally is red, tan, or grey colored but where mineralized, the color is pale brownish in oxidized environment and light grey in unoxidized environment. At some distance away from mineralization, the sandstones are predominantly red. Interbedded mudstones are red and grey in color and bluish to grey-green where carbonaceous matter is present.

The salient feature of the Uravan Belt is the presence of distinctive 1–3 km wide cross trends where over 75% of the ore occurs. These trends are distributed at fairly regular intervals of about 3–5 km along the length of the belt and are aligned approximately normal to the axis (Fig. 1.30). Some of these cross trends are parallel to and some cross the NW–SE-trending salt anticline folds. These cross trends, such as the Deremo, Burro Canyon (Slick Rock), Monogram Mesa, Club Mesa (Uravan) consist of thicker sandstone lenses in up to several suprajacent layers.

In the vicinity of Uravan, a thick and extensive layer of sandstone, referred to as the “third rim sandstone,” makes up the upper part of the Salt Wash Member. The largest ore bodies are in the bottom third of this unit. The deeper lying “second” and “first rim sandstones” are less mineralized.

Host Rock Alteration

Host rock alteration in the Uravan Belt is well exemplified by Shawe’s (1976a) description of the host rock alteration in the Slick Rock district.

Redbed facies, carbon facies, and reduced altered facies Salt Wash rocks are altered derivatives of a single-parent sediment assemblage of uniform composition. The *redbed facies* received its red color by hematitization resulting from diagenetic processes, which caused at least the partial oxidation of Fe-bearing detrital minerals to form hematite. Light grey *carbon facies* rocks formed diagenetically in reducing environments associated with carbonaceous material. Some of the original black opaque minerals were destroyed by reduction in connate solutions and released iron was precipitated as pyrite. *Reduced altered facies* rocks appear to have formed by the action of later-to-post-diagenetic solutions, which reacted with sediments of both redbed and carbon facies rocks and virtually destroyed almost all of the contained magnetite and ilmenite.

Mineralization

Main uranium and vanadium ore minerals, respectively, are pitchblende and coffinite, and montroseite and vanadium alumino-silicates in the *unoxidized zone*; and carnotite, rautite, tyuyamunite, metatyuyamunite, and other uranyl vanadates, and corvusite, pascoite, and other vanadates in the *oxidized zone*. Associated minerals and elements include pyrite, marcasite (in the unoxidized zone) and minor amounts of selenium, molybdenum, and copper. With a few local exceptions, both oxidized and unoxidized ores are in radioactive equilibrium.

V–U ore is predominantly found in the “third rim sandstone” in the upper part of the Salt Wash Member that has an average thickness of approximately 10 m but which can be up to several tens of meters thick. Over 90% of ore mined came from this unit, the rest from second and third rim sandstones.

Shape and Dimensions of Deposits

More than 1,300 small-to-medium-size ore lenses and pockets have been found to date, mainly clustered in the *Slick Rock, Gypsum Valley, Bull Canyon, Uravan, Gateway, Polar, and Beaver Mesa* areas (from S to N, Fig. 1.30). Most ore occurs from near surface down to 250 m. Deposits do not reveal any apparent geometric

relationship to each other. Their shape is usually tabular concordantly to bedding and aligned parallel to the sedimentary trend of the host sandstone. Boundaries are rather irregular (Fig. 1.32) and are mostly expressed by a sharp drop in grade. Average thickness is 1.20 m, but can reach 10 m. Occasionally, roll-type mineralization (Figs. 1.33 and 1.39) has formed, particularly in thicker sandstone sections, cutting discordantly through the bedding in C and S-like shapes. Such ore bodies are often much thicker, up to several meters, and of higher grade than blanket deposits.

The V–U ore bodies of the Uravan Mineral Belt generally have closer spacing, larger size, and as a whole are of higher grade than those in adjacent areas and other districts in the northern Colorado Plateau. Grade is rather inconsistent, ranging between weakly mineralized sandstones and several percent of uranium and vanadium. Mined ore averaged 0.16–0.3% U with a V–U ratio of about 5:1 but the ratio ranges widely from 3:1 to 10:1. Within the Uravan Belt, vanadium content increases southward from *Gateway* (3:1) to *Slick Rock* (8:1). These ratios include both oxidized and unoxidized ores.

Resources of individual ore bodies vary considerably, from single mineralized tree trunks with a few tonnes of ore to ore shoots with, although rarely, up to almost a million tonnes of ore. Most of the ore bodies contain less than 3,000 t of ore, which means that the quantity of uranium in individual ore shoots normally ranges from less than 1 t U to several tens of tonnes, rarely to a thousand tonnes of U or more.

One of the larger ore bodies developed by an open pit is the C-JD-7 deposit in the *Monogram Mesa, Bull Canyon area*. Its estimated size is 1 mio t of ore at 0.2% U and 1.25% V₂O₅ containing 2,000 t U and 12,500 t V₂O₅. The depth of ore ranges from 15 to 110 m due to faulting. One of the largest underground operations is the *Deremo-Snyder Mine* in the southern *Slick Rock area*. It consists of numerous ore lenses that line up in an irregular pattern for almost 2,800 m in NE–SW direction, with a maximum width of more than 1,800 m at its NE end, whereas the SW end is only a narrow zone less than 100 m wide. Ore occurs at depths from 195 to 210 m. Individual lenses are up to 5 m thick and up to 100 m or more in length.

Ore Controls and Metallogenetic Aspects

Salt Wash mineralization of the Uravan Belt is sedimentologically–lithologically controlled. Arkosic sandstones with a high grade of coalified vegetal constituents and of great thickness, host the largest and highest-grade ore bodies. In contrast to other Salt Wash uranium districts, where ore occurs mainly in narrow scours or channels, Uravan mineralization is concentrated in wider streambeds.

Ore deposits formed only in epigenetically altered carbon-facies rock but their discriminative distribution or selection of location within this facies remains enigmatic. Likewise, the relative proportions of sandstone facies and their distribution, and the metallogenetic significance of altered facies is not understood. Since the abundance of carbonaceous material is similar in carbon-facies and altered-facies sands, it seems most

likely that the difference is due to the transmissivity of altered-facies sands and the more thorough leaching of ilmenite and magnetite by reducing groundwater.

Although the origin of uranium remains dubious, volcanic ash in mudstone interbeds is considered the most likely U source. It is further assumed that carbonaceous matter acted as a reducing agent to precipitate and localize ore minerals.

1.2.2 La Sal-La Sal Creek District, Utah

Discovered in 1939, this district is located approximately 50 km SE of Moab (Fig. 1.30). Deposits occur in an E–W trending belt up to 1.6 km wide and about 30 km in length, extending from the La Sal Creek area at the Colorado–Utah border westward to the La Sal Junction–Rattlesnake area. Major deposits/mines in the area are *Beaver Shaft*, *Snowball*, *Hecla*, *La Sal*, *Mike*, and *Pandora* with estimated resources on the order of 3,000–4,000 t U at a grade of about 0.2% U.

Production until 1979 from about 20 properties totaled almost 2,500 t U at an ore grade of 0.27% U and 1.46% V₂O₅. With this amount of production, the La Sal–La Sal Creek district is the largest producer of Salt Wash uranium after the Uravan Mineral Belt.

Sources of Information. Kovschak and Nylund 1981; Carter and Gualtieri 1965.

Geological Setting of Mineralization

The La Sal–La Sal Creek district is located in the western part of Paradox Valley (Fig. 1.30). It is underlain by Paleozoic to Mesozoic sediments, which were intruded by Late Cretaceous to Early Miocene dioritic, monzonitic, and syenitic porphyries in the La Sal Mountains. Halokinesis resulted in four major NW–SE-trending structural features, from east to west: La Sal Creek syncline, Pine Ridge anticline, East Coyote–Browns Hole syncline, and Lisbon Valley anticline.

The Pine Ridge anticline area was affected by a large, post-mineralization collapse structure resulting in the Pine Ridge collapse with a vertical displacement of some 90 m. It divides the district into the easterly located La Sal Creek area (approximately 10 km long) and the westerly located La Sal area, with the main La Sal channel about 20 km long terminated at La Sal Junction by an erosional rim. The Lisbon Valley anticline seems to have been a salient feature to some extent during early Salt Wash deposition, since on the western end of the La Sal mineralized trend lower Salt Wash sandstone development is lacking, whereas on the eastern end a normal Salt Wash sequence exists.

The main La Sal Salt Wash channel (Fig. 1.38a) is an unusually straight channel filled with medium- to coarse-grained, diagenetically reduced, grey sandstone that exhibits minor variations in color, grain size, carbonaceous debris, and internal sedimentary structures. Mudstones underlying the

channel are greenish-grey, which reflects diagenetic alteration of red mudstones as commonly found away from mineralized channels.

Near the town of La Sal, the main La Sal channel has an extreme thickness of more than 32 m and a width in excess of 1,600 m. In contrast, sandstones on the eastern and western extremities of the La Sal trend average only 12–15 m in thickness. Coalescing channels are found on the western end, whereas the main channel bifurcates on the eastern end. The thick accumulation of sandstones along portions of the main channel near La Sal can be interpreted as a result of the coalescing and superimposition of two channels, one trending northeasterly, which comprises the mineralization around the Rattlesnake Pit, and a weakly mineralized channel trending due east from the La Sal Junction. Another conclusion could be that the main La Sal channel is the product of a major trunk or distributary stream, which was closer to the source area and acted as the feeder to many of the channels of the southern Uravan Belt located to the east.

Mineralization

In *unoxidized zones*, pitchblende, coffinite, montroseite, and vanadium aluminosilicates are the principal ore minerals. In *oxidized zones* (above the water table), carnotite, tyuyamunite, and corvusite are dominant ore minerals. Unoxidized ore is typical only for the central La Sal channel (Fig. 1.38a–c), whereas in the La Sal Creek zone oxidized ore is more common. The remobilization of uranium in oxidized zones tends to be of only limited quantity, however, due to fixation by abundant vanadium.

Ore occurs entirely within reduced grey sandstones, generally intimately associated with carbonaceous debris. Ore minerals are homogeneously distributed, except for heterogeneities within the sandstone; they impregnate the matrix of the host sandstone and replace some detrital quartz and feldspar grains. No or only limited variance in grain size is noticed between ore-hosting and unmineralized sandstones, as is also the case between red and grey sandstones. This implies that grain size had only limited, if any, influence on the localization of mineralization.

Mineralization mainly occurs on the southern downdip channel margin where grey channel sandstone begins to interfinger with pinkish sandstone and red overbank mudstone. Significant mineralization appears proximal to reddish bordering sediments.

Shape and Dimensions of Deposits

Deposits in the main *La Sal channel* (Fig. 1.38) are more elongated and include more roll-shaped ore bodies than the typical Salt Wash deposits in other districts as can be seen, e.g. in the *La Sal mine*. Ore bodies in this mine are markedly narrower and more elongated parallel to the channel direction than comparable deposits in the Uravan Belt. They occupy an area approximately 1,600 m in length and 50–100 m in width, in which they

are hosted in multiple horizons, between 1 and 2 m thick each, through the sandstone profile with barren zones between ore horizons. Ore bodies in the *La Sal Creek* sector are more tabular but are modified by rolls and are smaller in size; they average about 1 m in thickness, reach up to 200 m in length, and up to 100 m in width.

In general, the La Sal U–V deposits comprise on the order of tens of thousands of tonnes ore at grades locally as high as 1.2% U.

Ore Controls and Recognition Criteria

As concluded from Kovschak and Nylund (1981), the V–U mineralization in the *main La Sal channel* exhibits the following diagnostic features:

- Relative straight configuration of the ore-hosting channel
- Unusual thickness of channel fill composed of a homogeneous sandstone, void of intercalated well-defined mudstone beds
- Coarser grain size of channel sandstone than in other Salt Wash districts
- High amount of roll-shaped ore bodies (in spite of the fact that the La Sal channel appears as a homogeneous sandstone, void of well-defined mudstone beds, which are considered elsewhere as important for the roll formation)
- Concentration of mineralization on the southern downdip margin of the channel and where grey sandstones begin to interfinger with red and pink sandstones and red overbank mudstones
- Location of mineralization entirely within reduced grey sandstone
- Intimate association of mineralization with carbonaceous debris
- Tuffaceous sediments resting upon the arenaceous Salt Wash unit.

The first four parameters are somewhat different to the nearby Uravan Belt deposits, whereas the other four criteria are typical for Salt Wash mineralization.

Deposits in the *La Sal Creek* section are more representative of typical deposits of the Uravan Mineral Belt. They are tabular and roll shaped only to a lesser degree, associated with carbonaceous trash, and occur in depressions and along scour surfaces within and along the channel margin.

1.2.3 Lukachukai–Carrizo Mountains District, Arizona–New Mexico

Located mainly in northeastern Arizona and to a minor extent in northwestern New Mexico (Fig. 1.29), this district includes several areas with numerous small U deposits in an irregular belt that extends from northwest of the Carrizo Mountains southeastward into New Mexico and southward into the Lukachukai Mountains in northeastern Arizona.

Total production of the Lukachukai–Carrizo Mountains district from almost 170 properties amounted to 1,520 t U and

8,740 t V_2O_5 . Ore grades averaged 0.2% U and 1.15% V_2O_5 . Remaining resources are less than 18,000 t averaging 0.17% U and 1% V_2O_5 (status 1990).

Sources of Information. Chenoweth 1967; Chenoweth and Malan 1973; Huffman et al. 1980; Masters 1955; Nestler and Chenoweth 1958; Peirce et al. 1970; Scarborough 1981; Stokes 1953a; Chenoweth, personal communication.

Regional Geological Setting and Mineralization

The Morrison Formation is 250 m thick in this district. The Salt Wash Member is lithologically extremely variable both vertically and laterally. Sand lenses are rarely thicker than 3 m and rarely extend laterally for more than a few hundred meters. In the NW part of the district (*northwest-Carrizo area*), the Salt Wash Member is approximately 60 m thick and consists of grey to greenish, fine-grained, well-sorted, cross-bedded quartzose sandstone lenses with minor interfingering claystone and siltstone layers. Fossil carbonized plant material and logs are relatively abundant. The rock matrix is mainly calcite.

In the *southeastern Carrizo Mountains*, the Salt Wash Member is about 70 m thick and includes a 10–15 m thick lower part and a 55–60 m thick upper part. Huffman et al. (1980) using Galloway's (1978) sedimentological interpretation of the Salt Wash wet alluvial fan system, attribute the lower unit of predominantly mudstone and siltstone to a distal fan facies and the upper unit to a mid fan facies. The latter has a much greater fraction of braided-stream sandstones and contains essentially all of the ore in the *Eastside mines*.

In the southern part of the district, in the *southern Lukachukai Mountains*, the Salt Wash sandstone thins due to erosion. Here it contains mud galls and abundant calcium carbonate cement.

Numerous V–U occurrences and a number of carnotite ore bodies have been found in the basal 10–25 m of the Salt Wash Member in the northwest Carrizo and Lukachukai Mountains, and in the upper Salt Wash Member in the southeast Carrizo Mountains.

The predominant mineralization in the NW Carrizo Mountains area is a vanadiferous micaceous to clay-like material and locally uranyl vanadates (tyuyamunite, carnotite, etc.), whereas in the Lukachukai Mountains tyuyamunite prevails with some pitchblende in carbonized logs. The minerals occur as coating on sand grains, as replacement of carbonized plant remains, and as interstitial cement. Most of the mineralization has accumulated in irregularly shaped, elongated, tabular lenses that contain abundant carbonaceous matter. Mineralized zones are generally small and thin (0.1–2.5 m) but can be made up of clusters of small rich pods separated and surrounded by weak mineralization. The best mineralization is often found along bends in paleochannels, and where channels are scoured into abandoned channel-fill deposits. Some remobilized ore is controlled by joints and fractures.

In comparison, ore bodies in the Lukachukai mining area tend to be larger, suspended slightly higher in the Salt Wash Member, and have lower V grades as reflected by V–U ratios near 4:1 versus 9:1 than ore bodies in the Carrizo area.

1.2.3.1 Carrizo Mountains Area

The Carrizo Mountains extend from northeastern Apache County, Arizona, easterly into San Juan County, New Mexico. A great number of small V–U deposits straddle the state line, in the area between Bitlabito and Red Rock, Arizona, to King Tutt Mesa in New Mexico.

Uranium was discovered in the Tsitah Wash area in 1918, and, in 1921, in the east Carrizo Mountains south of Bitlabito. Some mining for vanadium took place during the 1920s and again from 1942 to 1944. Exploitation of uranium began in 1948 and lasted until 1968. During this period, some 120 mines produced about 200 t U and 2,100 t V_2O_5 from some 110,000 t of ore with grades of 0.19% U and 2.25% V_2O_5 . *Cove Mesa*, *King Tutt Mesa*, and the *Rattlesnake Group* in the *Tsitah Wash-Black Rock Point areas* contained the best deposits. *Cove Mesa*, 2 km² in size, was the most productive mining area. It delivered 66 t U and 564 t V_2O_5 at ore grades averaging 0.19% U and 1.61% V_2O_5 . Ore was treated in the Durango mill in Colorado until 1953 and subsequently in the Ship Rock mill, New Mexico.

Source of information. Landmark/Weston (1988).

Geology and Mineralization

The Carrizo Mountains are on the northeast flank of the Black Mesa Basin. They consist of the Carrizo laccolith and sills of diorite porphyry that have been intruded into a Mesozoic sedimentary suite including the Jurassic Morrison Formation posterior to the deposition of V–U ores. No obvious large-scale redistribution of uranium could be observed as a result of this thermodynamic event.

Hosted in quartzose sandstone lenses within the lower 15 m of the Salt Wash Member of the Jurassic Morrison Formation, V–U ore bodies are geologically similar to those in the Lukachukai Mountains except that they are richer in vanadium and smaller. Host sands are well sorted, cross stratified, contain carbonaceous debris, and are interbedded with claystone and mudstone. Their color is grey to greenish except adjacent to ore bodies where they can be limonite stained. Greenish-grey mudstone commonly rests upon and/or underlies mineralized sandstone intervals.

Ore bodies tend to cluster in paleochannels cut into sandstone, particularly along bends where carbonaceous matter has been accumulated. Ore bodies are irregular and elongated parallel to paleochannels, and have lateral dimensions of ca. 25–50 m, a thickness of about 0.6 m, and high grades. High-grade ore pods with grades of 2–5% U locally are ca. 3–6 m in size. Some redistributed mineralization occurs along fractures in fault zones.

The ore is greyish in color, micaceous, and contains clay-like material. Tyuyamunite and metatyuyamunite are the principal U-bearing minerals. Vanadium minerals include pascoite, volborthite, montroseite, and oxidation products thereof. Ore averages a vanadium/uranium ratio of 9:1. Associated minerals include pyrite, iron oxides, and pinkish calcite. The latter often

occurs as cement. The ore minerals coat sand grains and replace carbonized vegetal matter.

Ore Controls, Recognition Criteria, and Metallogenetic Aspects

Huffman et al. (1980) present the following parameters typical for uranium accumulations in the Salt Wash sandstones of the Carrizo Mountains:

Favorable host environment for V–U ore bodies is provided by

- Lower midfan facies whereas distal and upper midfan facies contain only minor mineralization
- Presence of partially to completely abandoned channel-fill deposits, and
- A sedimentologic composition characterized by
 - 25–75% cross-bedded, transmissive sandstone in channel-fill deposits
 - 10–40% parallel-bedded sandstone of limited lateral extent of both high-energy channel-fill deposits and lower energy, partially abandoned fill and overbank sediments
 - sandstone–mudstone ratios of 1.5–6
 - average sandstone unit thickness of about 1–6.5 m
 - alternations of 0.3–3.0 from sandstone to mudstone per 3 m thickness.

The presence of partially to completely abandoned channel-fill deposits is considered by Huffman et al. (1980) a key factor instrumental in the localization and concentration of uranium because these lithologies provide (a) organic matter with chemical reduction capacity, (b) clay and mud for decreasing transmissivity, and (c) permeable, porous sand lenses of limited lateral extent.

Subsequent scouring of these fossil channel sediments by younger streams incorporates mud and organic debris into clay-clast conglomerates as basal-lag deposits of overlying channel sandstones, which, in turn, creates a conduit from which uraniumiferous fluids can enter organic-rich sands of partially abandoned channels where it may precipitate to form ore.

1.2.3.2 Lukachukai Mountains Area

This mining area is situated in northeastern Apache County, Arizona, in the southeastern Lukachukai Mountains. The latter form the northwest spur of the Chuska Mountains.

Uranium was discovered in 1949, at first on Mesa-I. Production began in 1950 and reached a peak during 1955. Ore was processed at the Ship Rock mill in New Mexico until its closure in 1968. During the 19 years of operation, 49 properties produced 1,340 t U and 6,695 t V_2O_5 largely by underground mining. Ore averaged 0.2% U and 1.02% V_2O_5 . Most production came from a small area (17 km²) in the southeastern Lukachukai Mountains, from mines on *Mesa I*, *Mesa II*, *Mesa IV-1/4*, *Flag* and *Three Point* mesas.

Source of information. Landmark/Weston 1988.

Geology and Mineralization

Located on the northern tip of the Defiance Uplift, the Lukachukai Mountains V–U area is capped by the Early Tertiary Chuska Sandstone, which unconformably rests upon a wedge of the Morrison Formation. The Salt Wash Member occupies an area of 32.5 km² and outcrops continuously around the mountains; it has been removed by pre-Chuska erosion east of Mesa I and south of Two Prong Mesa.

All major deposits are located on the shallow-dipping SW limb of the Chuska syncline where they are grouped in a well-defined belt that trends nearly N–S across the southeast end of the Lukachukai Mountains. Ore bodies consist of clusters of numerous small pods, separated by weak mineralization that are hosted in paleochannels in three stratigraphic horizons some 10–25 m above the base of the Salt Wash Member. Ore bodies are up to 300 m in length, 100 m in width, from less than 1 to 6 m in thickness, and occur at an average depth of about 120 m. Highest-grade mineralization is found in trough-type cross-stratified sandstone.

Oxidized V–U mineralization prevails. Tyuyamunite is the principal ore mineral, with minor carnotite, and a variety of vanadium minerals. Some pitchblende occurs as a replacement of carbonaceous matter. Calcite, pyrite, and Fe-oxides are abundant. Ore minerals replace carbonaceous debris, fill interstices, and coat sand grains in the host rock.

1.2.4 Chilchinbito District, Arizona

Discovered in 1950, this area contains U mineralization in the Salt Wash Member at the foot of Black Mesa between Chilchinbito and Rough Rock, Arizona. From 1951 to 1958, two properties produced 0.7 t U and 0.034 t V_2O_5 . The ore contained 0.63% U, 0.03% V_2O_5 , and 31% $CaCO_3$. The ore-hosting Salt Wash Member consists of approximately 40 m of interbedded greyish-brown, fine- to very fine-grained sandstone and grey, green, and reddish-brown siltstone and mudstone. Hexavalent U minerals and calcite are associated with fossil logs and other plant debris in sandstone lenses 3–12 m above the base of the Salt Wash Member. Mineralized fossil logs are at least 35 cm in diameter and over 3 m long (Landmark/Weston 1988).

1.2.5 Green River District, Utah

The Green River district, also known as Tidwell Mineral Belt, includes the area south of the town of Price, on both the east and west side of the Green River (► Fig. 1.29). Production from 94 properties totaled some 1,460 t U and 1,100 t V_2O_5 . Ore averaged 0.17% U and 0.19% V_2O_5 with a carbonate content between 6 and 10%.

Sources of information. Chenoweth 1975; Johnson 1959; Trimble and Doelling 1978; US-AEC 1959; Chenoweth, personal communication unless otherwise noted.

Geological Setting and Mineralization

The district lies in a broad shallow synclinorium, which plunges gently northward. It is filled with a 1,200 m thick sequence of sediments ranging in age from Pennsylvanian to Cretaceous. The sediments are gently folded into secondary anticlines, synclines, and flexures whose axes trend northeastward. Northwesterly trending faults displace the sediments for less than 15 m in general, but a few for up to 60 m, particularly across the west flank of the trough.

Uranium occurs predominantly in the Salt Wash Member, but minor mineralization has also been found in the Brushy Basin Member, and in the Monitor Butte Member of the Chinle Formation. The most important of the generally small ore bodies are clustered in NE–SW-trending fluvial channels of the Salt Wash Member in a narrow belt on the western side of the synclinorium adjacent to the northeastern flank of the San Rafael Swell.

Ore is hosted by a conglomeratic to fine-grained fluvial sandstone unit, 12–21 m thick, in the upper third of the approximately 60–70 m thick Salt Wash Member. This sandstone is white, grey, buff, or light brown, poorly sorted, and chiefly composed of quartz grains with varicolored chert cemented by calcite or dolomite (6–10%), and locally by clay. The sand contains asphalt-like carbonaceous matter of plant and probably also of petroliferous origin particularly in point bar, levee, crevasse-splay, and channel-bottom environments. This carbonaceous material appears to have played a key role in fixing the ore.

Coffinite and, less commonly, pitchblende, montroseite, and paramontroseite are the principal uranium and vanadium ore minerals. Oxidized minerals include tyuyamunite, uranopilite, schroëckingerite, liebigite, and corvusite. The uranium–vanadium ratio is 1:1 to 1:2. Pyrite and marcasite are abundant. Some sphalerite, chalcopyrite, and clausthalite are also reported. Ore minerals are closely associated with asphalt-like carbonaceous material. They occur as thin coatings on and as dissemination among quartz grains, and as a replacement of cement and carbonaceous matter.

Individual ore bodies are generally small, ranging up to 5,000 t of ore. Several bodies occur in clusters that aggregate 10,000–25,000 t of ore. Most of the ore bodies are tabular and generally concordant with bedding and are aligned parallel to N to NE-trending lenses of sandstone that fill scours.

Larger mines, including the UP Shaft, are located in the *Buckmaster Draw* on the western side of the district. They exploited ore lenses contained in a sandstone unit 12–24 m thick and 75–180 m below the surface. These ore lenses parallel the N to NNE direction of the paleostream and occur concordant to bedding in several horizons between 9 and 24 m below the top of the Salt Wash Member.

UP Shaft was the most productive of these mines. It exploited 0.3–1.5 m thick ore lenses with up to 35 t U at a grade of about 0.25% U that consisted of high-grade shoots intermittently with weak mineralization over a NNE–SSW length of approximately 200 m and a width of up to 40 m, and in some parallel trends.

1.2.6 East Canyon–Dry Valley District, Utah

This district is centered at East Canyon, half way between the Lisbon Valley to the north and Monticello to the south (Fig. 1.29). 440,000 t of ore grading an average of 0.14% U and 1.3% V_2O_5 and yielding 590 t U and 5,730 t V_2O_5 have been produced from over 70 properties but only nine of which have yielded over 5,000 t and two of these over 50,000 t of ore. One of the larger producers was the *Columbus-Rim mine*.

Sources of Information. Chenoweth 1975; Doelling 1969; Chenoweth, personal communication.

Geology and Mineralization

The Salt Wash Member, 10–150 m thick, hosts V–U ore in thick sandstone lenses in its upper part. The host rock is light-brown, cross-bedded sandstone interbedded with lenses of siltstone and mudstones, containing plant remains and fossil logs. Ore is composed of greyish-black, partly argillaceous vanadium mineralization with uranyl vanadates (carnotite, tyuyamunite a.o.) that forms both tabular and roll-shaped bodies with dimensions of up to 60 m in length, 10 m in width, and 0.9–1.2 m in thickness. Some smaller and lower grade ore lenses occur in conglomeratic sandstone with bentonitic mudstone interlayers in the eastern part of the district.

1.2.7 Cottonwood Wash District, Utah

The Cottonwood Wash (or Blanding) district is located 10–15 km SW of Blanding, centered at the junction of the Brushy Basin and Cottonwood Washes (Fig. 1.29). After the discovery of uranium in 1930, some 50 properties have been mined. They produced 400 t U and 2,110 t V_2O_5 at an average ore grade of 0.12% U and 0.96% V_2O_5 . The largest producers were the *Big Hole* and *Cottonwood mines*. Some small deposits in the Westwater Canyon and Brushy Basin members have been mined south and north of Cottonwood Wash.

Sources of Information. Chenoweth 1975; Doelling 1969; Meunier 1984; Meunier et al. 1987; Pitman 1958; Chenoweth, personal communication.

Geology and Mineralization

Most deposits are clustered on the flank of the Comb monocline where the beds change dip from 6° to nearly horizontal. A fluvial sandstone unit 35–50 m above the base of the Salt Wash Member provides the host rock. Mineralization is concentrated in sandstones with interbedded mudstone lenses and enrichments of carbonaceous matter. Calcite cements the host sandstone. Fossil logs are abundant and contain some high-grade ores. The long axis of ore bodies parallels the sedimentary trend of the Salt Wash sandstones.

In reduced zones, pitchblende together with montroseite and pyrite occurs disseminated in the host rock. In oxidized zones, tyuyamunite with corvusite, pascoite, roscoelite and vanadiferous clay minerals, and iron oxides prevail. Ore minerals replace plant remains, fossilized wood, and matrix material, and fill interstices between sand grains.

Ore bodies are elongated tabular lenses with dimensions of up to 100 m in length, 50 m in width, and 0.3–1.5 m in thickness. Clusters of ore bodies can occur in an area of more than 300 m by 200 m. Although some individual properties contained up to 50,000 t of ore, only 15 properties produced more than 5,000 t of ore each.

1.2.8 Thompsons District, Utah

Located between Thompsons in the north and the Arches National Monument to the south (► Fig. 1.29), this district was discovered in 1905 and has produced 235 t U and 1,390 t V_2O_5 from ca. 90 properties. The ore averaged 0.18% U and 1.16% V_2O_5 .

Sources of Information. Chenoweth 1975; Stokes 1952; Stokes and Mobley 1954; Chenoweth, personal communication.

Geology and Mineralization

Mineralization is found through an interval of 60 m in all levels of the Salt Wash Member, but most ore bodies occur in the lower 35–40 m of the member. The chief producing area was in a northeasterly trending fluvial sandstone belt of a complex system of superimposed paleochannels.

Carnotite, tyuyamunite, and vanadium oxides are the principal ore minerals with minor coffinite and pitchblende. Gypsum is abundant. Ore minerals form coatings, disseminations, or fill pore spaces in the host sandstone. In most cases, ore has been concentrated around fossil vegetal trash. Small high-grade ore pods with grades up to 5% U and 15% V_2O_5 are associated with carbonized and silicified logs.

Ore bodies have tabular and roll-type shapes. Tabular ore lenses are up to 60 m long, 15 m wide, and average almost 1 m in thickness. At the *Flat Top No. 1 mine*, a single ore roll was minable over a length of 300 m.

1.2.9 Henry Mountains District

The Henry Mountains district is located in central-south Utah, between the towns of Hanksville to the north and Bullfrog to the south (► Fig. 1.29). It extends over a N–S distance of approximately 55 km and includes from N to S the mining areas of *North Wash*, *Trachyte*, and *Little Rockies* (with *Del Monte*, *Shooting Canyon*, and *Lost Spring*) (► Fig. 1.40).

Uranium was discovered in 1913. Former production until 1979 from some 120 properties has been about 250 t U and 770 t V_2O_5 . The ore averaged 0.25% U and 1.35% V_2O_5 . Revived

exploration found in 1977 new deposits (Tony M etc.) in the *Shooting Canyon* area with resources estimated at between 6,000 and 13,000 t U.

Sources of Information. Carpenter 1980; Chenoweth 1980; Northrop 1982; Northrop et al. 1982; Northrop and Goldhaber 1990; Peterson 1977, 1978, 1980a; Peterson and Turner-Peterson 1980; Plateau Resources 1983; Pool 2007a, b, c; Thamm et al. 1981; Wanty 1986; Wanty et al. 1987a, 1990; Whitney and Northrop 1986; Thamm, personal communication.

Geological Setting of Mineralization

The Henry Mountains mineral belt lies on the southeast flank of the Henry structural basin, which subsided from middle Jurassic time onward as indicated by the thickening of the *Summerville Formation*, a mudstone unit with marine evaporitic facies. The Jurassic *Morrison Formation*, the host of V–U deposits, is up to 230 m thick and overlies unconformably the Summerville Formation. In the Henry Basin, the Morrison Formation includes three members, from top to bottom, the Brushy Basin Member, the Salt Wash Member, and the Tidwell Member.

The *Brushy Basin Member* is predominantly a red and grey mudstone. The *Tidwell Member* consists mainly of marginal marine and continental red and grey mudstone with minor grey sandstone, and partly bedded and evaporitic limestone. The V–U hosting *Salt Wash Member* together with the Tidwell Member is 50–150 m thick.

The *Salt Wash Member* consists of fluvial and lacustrine sediments of slightly feldspathic, quartzose sandstone with minor amounts of interbedded lenses of red, green, and grey mudstone and siltstone, and of lenses of poorly sorted quartz, chert, and mudstone pebble conglomerate. Sandstone beds are thin, bedded to massive, with a dominance of medium to thick beds. Sandstone grain size varies between fine and very coarse-grained, sorting between well to poor, and color between white to light grey to buff. Calcite is the common cement with lesser silica. Carbonized plant fragments and amorphous carbonaceous substance occur in the sediments.

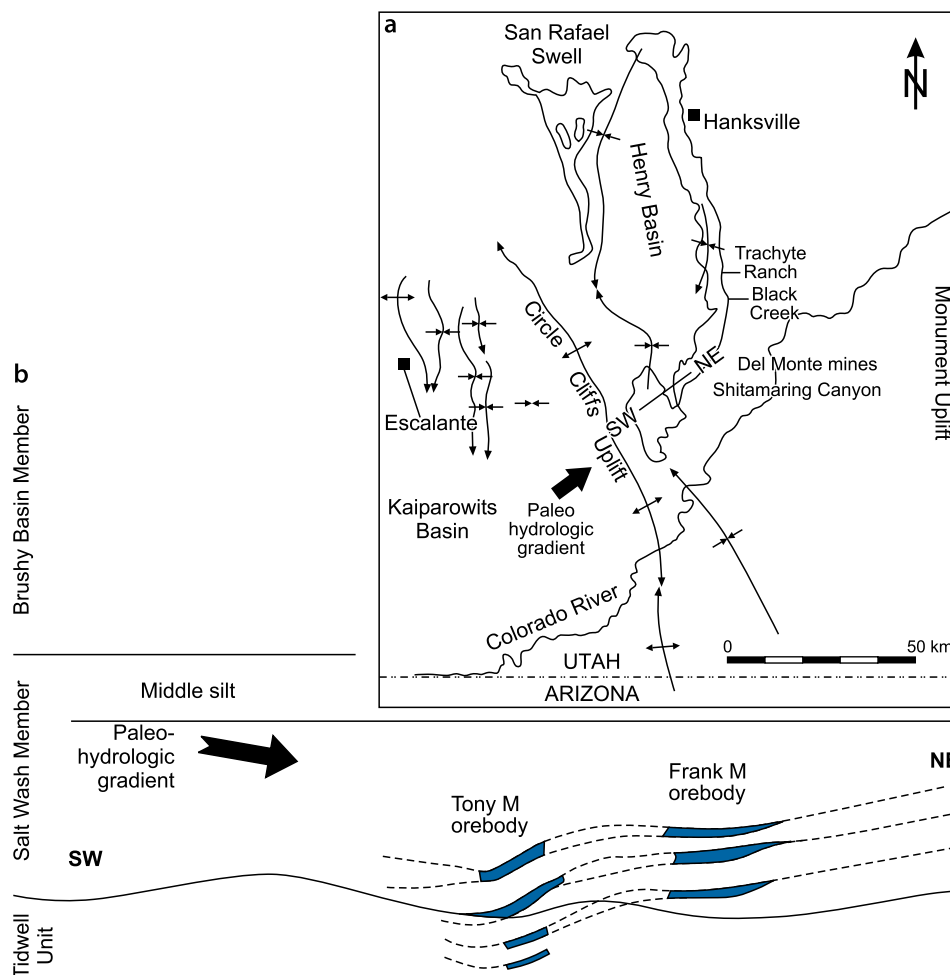
Peterson (1980a) subdivides the Salt Wash Member into a lower, middle, and upper sequence based primarily on differences in stratification ratios and cross-bedded dip vector resultants (► Fig. 1.41).

Mineralization

Most of the early mined deposits contained oxidized mineralization consisting mainly of tyuyamunite followed by carnotite and autunite. Vanadium minerals include metaheawettite and corvusite. Pyrite, limonite, jarosite, and gypsum are common ore constituents. The U:V ratio of oxidized ore is on the order of 1:4. Later discoveries (*Tony M*, *Frank M*, and *Edward R. Farley* deposits in the *Shooting Canyon-Del Monte area*) (► Fig. 1.42) established ore in reduced sandstone with coffinite, pitchblende,

■ Fig. 1.40.

Henry Mountains district, (a) structural map with location of U mineralized areas, and (b) schematic stratigraphic SW–NE section illustrating the tabular shape and position of ore bodies in the Salt Wash Member and the underlying Tidwell Member, and proposed correlation between mineralized zones and their unmineralized extensions. The paleo-hydrologic gradient was from SW to NE during the Morrison Formation time. (After Northrop 1982)



and montroseite as principal ore minerals. Ore minerals coat sand grains and fill porous spaces in sandstone and also fill pores or cells in carbonized plant fragments.

Almost 98% of the ore occurs in the afore mentioned lower sequence and in the basal part of the middle sequence of the Salt Wash Member (Fig. 1.41). These strata were apparently deposited in intrabasinal depressions. Most of this ore forms tabular lenses suspended in sandstone beds. Ore lenses only rarely touch the upper or lower contacts of host beds. Uranium generally concentrates in those sandstone facies that are enriched in detrital carbonaceous matter and that occur in the vicinity of a distinct grey, lacustrine mudstone layer. In general, richer ore bodies are in sandstones overlain by this mudstone facies, whereas mineralization underlain by this mudstone is relatively low in grade and thinner or more discontinuous. In a few cases, ore was found in a short lateral distance of about 30–150 m away from the grey mudstone bed.

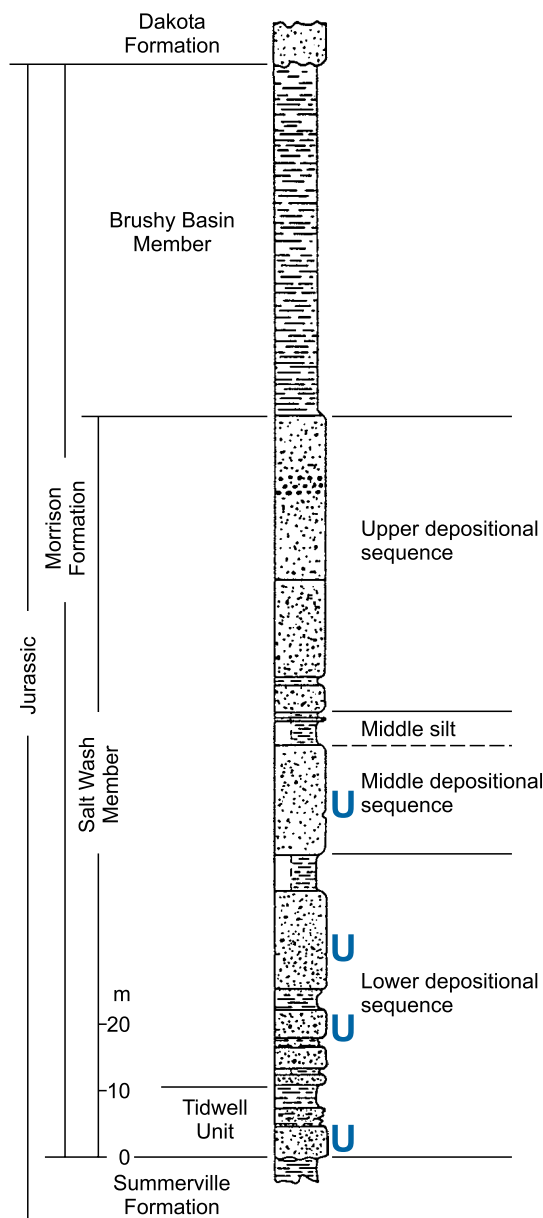
Dimensions of Individual Ore Zones and Deposits

Chenoweth (1980) subdivides the Henry Mountains mineral belt from north to south into three mining zones: North Wash, Trachyte, and Little Rockies. These zones contributed approximately 20, 37, and 40%, respectively, of the former Henry Mountains production. The deposits mined have been small and oxidized; they ranged in size from a few tonnes to several hundred tonnes of ore (average 70 t), yielding from fractions of one tonne to about 25 t U. Grade was variable, ranging from 0.13 to several percent uranium.

In the *North Wash zone*, the principal ore bodies occur in a light grey, limonite-stained, medium- to coarse-grained to conglomeratic sandstone, which is cross-bedded and friable in part and lies 45–55 m above the base of the Salt Wash Member. Ore consists of uranium–vanadium minerals (U:V ratio 1:5), which are associated with carbonized logs, and which also

■ Fig. 1.41.

Southern Henry Mountains, Shooting Canyon area, litho-stratigraphic section documenting the position of uranium mineralization in the various depositional units of the Salt Wash and Tidwell members of the Morrison Formation. (After Peterson 1980a) (reproduced by permission of Utah Geology Ass.)



impregnate argillaceous, carbonaceous sandstone lenses. Carbonaceous trash and grey- to reddish-brown mudstone lenses, galls, and blebs are common constituents of mineralized intervals. Ore bodies are small and discontinuous.

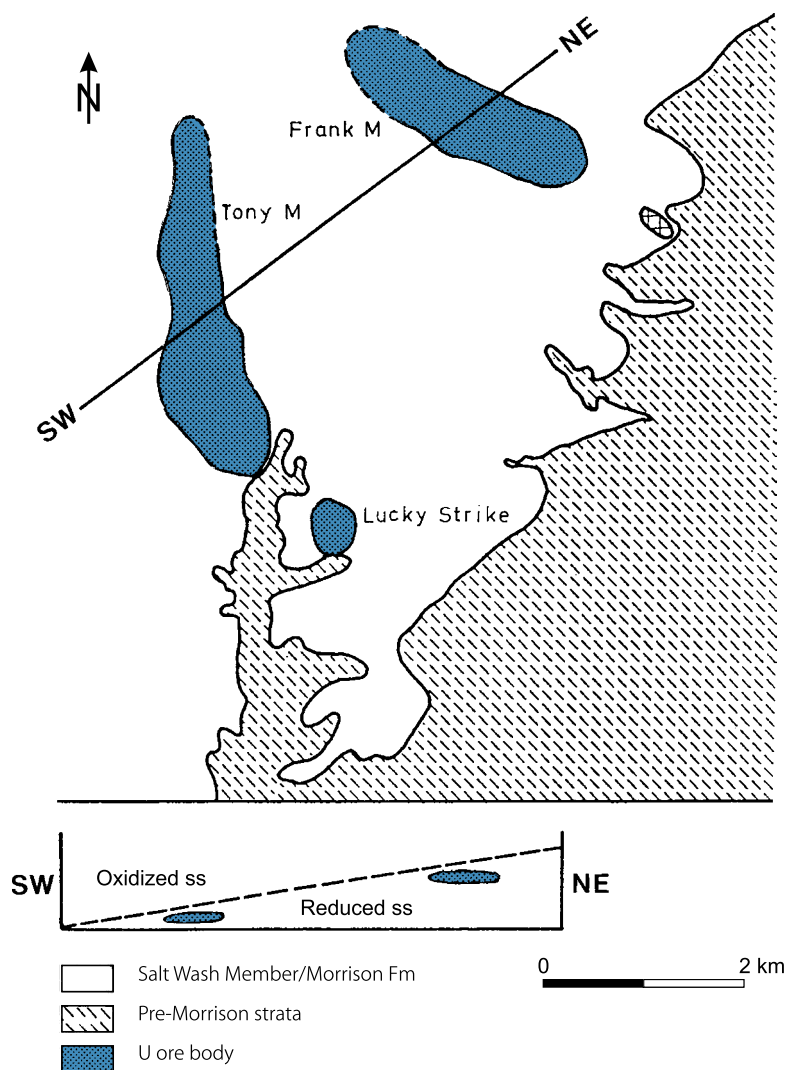
The *Trachyte zone* hosts ore bodies 36–40 m above the base of the Morrison Formation in the same type of Salt Wash host rock and environment as in the North Wash zone. Ore bodies, however, are larger and more continuous than those in North Wash. Their dimensions average 15 m in length, 6 m in width, and 0.6 m in thickness. Clusters of ore shoots may form a trend up to 120 m in length. Ore has a U:V ratio of 1:8 and contains generally in excess of 10% CaCO_3 .

The *Little Rockies zone* includes the areas of Del Monte, Shooting Canyon, and Lost Spring (from N to S). At *Del Monte*, ore shoots occur in a zone 15–30 m above the base of the Morrison Formation; in *Shooting Canyon* they are 6–15 m, and at *Lost Spring* they are 3–15 m above the contact. With the exception of the later discoveries (Tony M, Frank M, Edward R. Farley) the former known deposits in the Little Rockies are small, discontinuous, and often oxidized. They are, however, exceptionally high grade with some ore bodies averaging 4% U. The U:V ratio averages 1:3, and the CaCO_3 content is generally less than 6%.

Individual deposits of the Little Rockies zone consist of vertically and horizontally close-spaced, small, thin lenses of

■ Fig. 1.42.

Southern Henry Mountains district, Shooting Canyon, generalized geological map of outline of major ore bodies, which are emplaced in reduced sand facies of the lower sequence of the Salt Wash Member as shown in the cross section. (After Thamm et al. 1981, based on Plateau Resources Ltd.)



argillaceous and carbonaceous sandstone rich in carbon trash and grey to red clay galls that are impregnated with tyuyamunite. Lenses are irregular in planview and in cross section. They range from centimeters to 1 m in thickness, and thicken and thin irregularly. Ore bodies average about 1 m by 1.5 m in lateral extent, and are generally elongated parallel to the dominant sedimentary trends, which range in direction from northwest to northeast. The lower surface is nearly flat to gently irregular, and in places it is a scour surface. Many ore bodies are underlain by a grey mudstone bed or tightly cemented sandstone containing up to 30% CaCO_3 . The overlying ore commonly is relatively friable.

Grey mudstone beds commonly rest directly upon ore bodies or occur within 3 m above them. These beds thicken conspicuously over many ore bodies and either thin to a featheredge over barren areas, or continue for several tens of meters as a parting between sandstone beds.

Uranium ore bodies commonly have abrupt lateral and vertical cutoff limits, but grey vanadiferous clay intercalated with sandstone may persist between adjacent uranium ore bodies. Halos of limonite, presumably derived from oxidation of pyrite in ore, may extend 3–5 m laterally and vertically from ore bodies.

As one of the late discoveries, the *Shooting Canyon-Del Monte area* near the settlement of Ticaboo contains three adjacent deposits, *Tony M* (discovered 1977), *Frank M*, and *Edward R. Farley* (Fig. 1.42). These deposits are at greater depth and of larger size than the formerly mined deposits. They occur below the water table and consist largely of reduced ore in mixed fluvial-lacustrine sediments of a channel system, 120–150 m thick, of the Salt Wash Member.

These three deposits are estimated to contain 6,000–13,000 t U depending on the applied cutoff grade. *Tony M* and *Frank M* deposits account for almost half of these resources. Grades are strongly variable as typical for Salt Wash ore. Although U

contents in pockets reach up to 1% or more, in situ grades of potentially minable sections average 0.17–0.25% U, but due to dilution by the irregular grade distribution, mining grades average approximately 0.1–0.15% U, at a cutoff grade of 0.085% U and a thickness of 0.9 m. Resources of the *Edward R. Farley* deposit are on the order of 3,500–5,000 t U, at a grade of 0.1–0.17% U, including about 1,700–3,400 t U at a grade of 0.27–0.32% U. Additional probable resources are estimated at almost 8,500 t U and possible resources at about 6,000 t U in the \$130/kg U cost category (Chenoweth 1980). The high-cost category indicates that the potential resources are only of low grade.

At the *Frank M deposit*, the Salt Wash strata strike about NE–SW and dip 5° NW and include four mineralized horizons. The two better-mineralized horizons are sandwiched in the middle at depths of 120–150 m below surface and some 10–30 m above the base of the Salt Wash Member. They average about 0.05 to greater than 0.1% U but contain high-grade pockets. Located 2.5 km to the SW of the Frank M deposit, the *Tony M deposit* is likewise confined to the two middle levels, up to 20 m above the base of the Salt Wash Member. The *Edward R. Farley* and associated ore bodies, situated about 1 km to the SSE of the Tony M deposit, are in a similar stratigraphic position as those of the Tony M deposit.

Carpenter (in Thamm et al. 1981) attributes the *Frank M* and *Tony M* deposits to two superjacent ore zones with the following characteristics (► Fig. 1.43). Coffinite and montroseite are the dominant ore minerals but, as reflected by a U:V ratio of 1:1, the vanadium content is by far less than in other Salt Wash deposits. Selenium and molybdenum are generally present. These two elements are zoned in both ore zones, with selenium concentrated at the top of the zones. Carpenter recognized a barren zone between the two ore horizons, which contains (a) uranium concentrations generally only slightly above the background, (b) considerable vanadium in chlorite rather than in montroseite, (c) abundant quartz overgrowths, and (d) lower concentrations of virtually all elements, including aluminum, sodium, potas-

sium, and calcium. He interprets the latter as evidence of clay and feldspar dissolution. Alternatively, it may reflect the dilution of these elements by the introduction of considerable quantities of silica into the sandstone matrix. Carbonaceous plant debris is disseminated throughout the ore zones, the barren zone, and the adjacent unmineralized sandstone. Minor amounts of structureless organic matter have been noted, but humate lenses have not been described.

Typically, better grade pods within the Shooting Canyon ore bodies contain several tenths of one percent to more than 1% U and are dominantly restricted to highly heterogeneous Salt Wash sands. These facies are characterized by a mixture of coarse- to fine-grained sands containing clay galls, clay partings, argillaceous intercalations, organic debris, and intense cross-bedding. The extension of these heterogeneous segments is highly variable and unpredictable. In contrast, uniform sand beds commonly contain only low-grade mineralization.

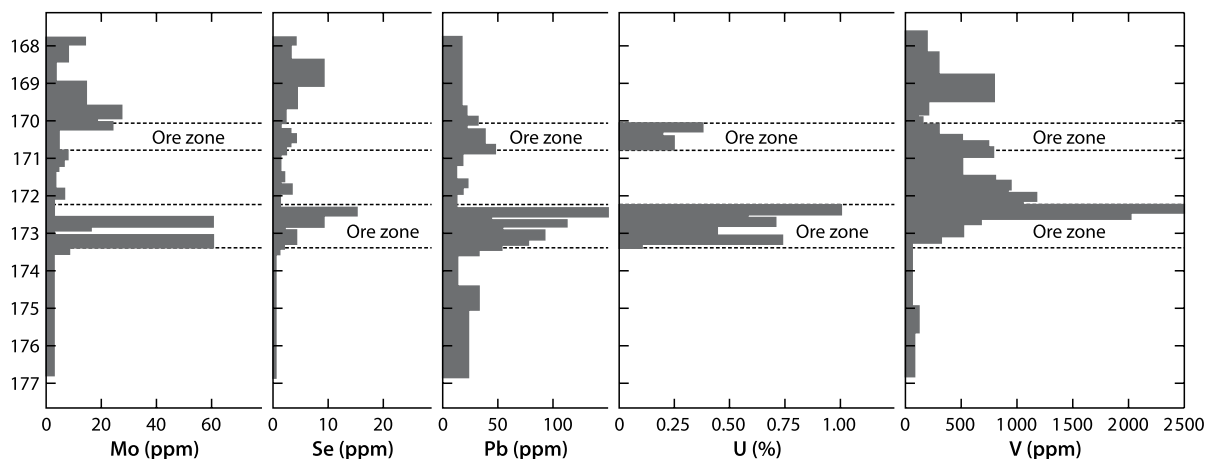
Metallogenetic Aspects

A model for the formation of uranium deposits in the Henry Mountains is presented by Peterson (1980a) based on his studies of the depositional environment of the Salt Wash Member. The basic premise of the model is that compaction squeezed pore fluids with elevated salinity from the evaporitic Tidwell facies. Anoxic fluids were expelled from the muddy sediments, rich in organic matter, into the nearby Salt Wash sandstone beds. Here, Tidwell brines interacted with detrital organic debris, becoming more reduced, and humic acids were fixed as tabular humate deposits. This process generated a strongly reduced environment with a distinct redox boundary between saline brines and overlying oxygenated meteoric water where ore formation took place.

Northrop (1982) expanded and refined the concept mentioned earlier based on work in the Shooting Canyon

■ Fig. 1.43.

Southern Henry Mountains district, Shooting Canyon, Tony M mine, contents and distribution of U, V, Mo, Se, and Pb from a core hole through the ore horizon (depth interval in feet). (After Thamm et al. 1981, based on Carpenter 1980)



deposits. He derived his metallogenetic evidences from chemical and isotopic composition data and litho-stratigraphic distribution of authigenic-diagenetic mineral phases related to U–V mineralization. As illustrated in Fig. 1.44, Northrop documents, in essence, the existence of two fluid systems in the Henry Basin, a lower saline fluid with reducing potential generated by diagenesis from evaporites in the Tidwell Member and an upper oxygenated meteoric solution, which leached indigenous U and V(?) from the Salt Wash and Brushy Basin members. Ore deposition took place at the stable interface of the two fluid systems.

1.2.10 Moab District, Utah

This district covers an area to the southeast of Moab on the southwest flank of the La Sal Mountains (Fig. 1.29), including the *Yellow Circle deposits*. Mining for radium, vanadium, and uranium, or a combination of these elements has been intermittent since 1911. Production came from more than 100 properties and totaled 83,000 t of ore prior to 1983. Ore averaged 0.22% U and 1.41% V_2O_5 and contained 180 t U and 1,170 t V_2O_5 .

Sources of Information. Butler and Fisher 1978; Chenoweth 1975, 1983; Doelling 1969; Johnson and Thordarson 1966; Wardwell 1946; William 1964.

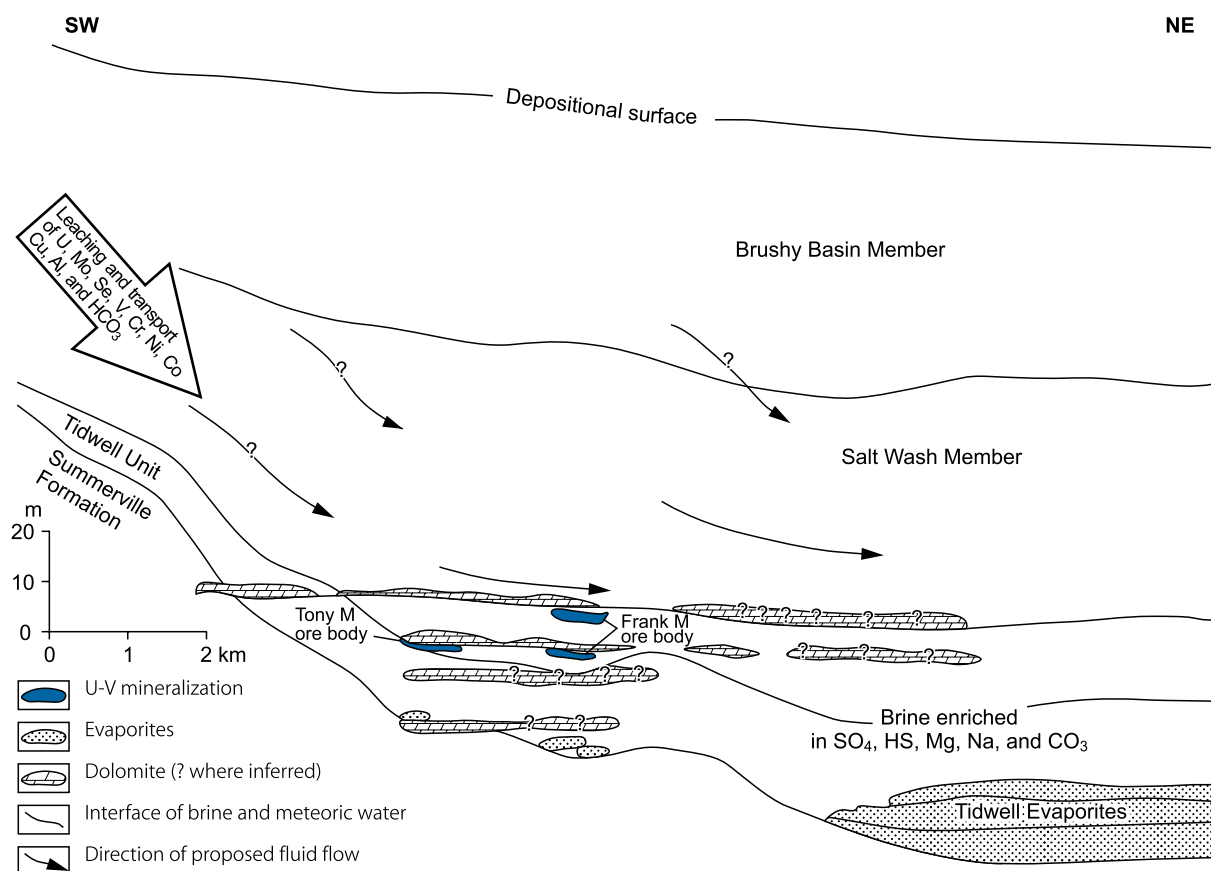
Geology and Mineralization

In the Moab district, the Salt Wash Member is 75–100 m thick. The most productive zones are in the upper part of the member, about 55–63 m above the base of the member. Other ore zones are 69–72 m and 81–90 m above the base. The host rock is greyish-white, cross-bedded fluvial sandstone containing clay galls, mudstone partings, and abundant carbonized plant remains. It encloses interbeds of greenish mudstone lenses. Many faults cut and displace the ore horizons.

The Moab deposits comprise mostly oxidized mineralization. Main ore minerals are tyuyamunite, metatyuyamunite, and less carnotite, associated with vanadium oxides and -clays. The “clay” minerals are largely chlorite and/or hydromica. Pitchblende has been found on deeper levels. The amount of vanadium generally exceeds that of the uranium at a ratio of 5:1, but the ratio can vary from place to place. Ore is commonly

Fig. 1.44.

Southern Henry Mountains district, Shooting Canyon, restored diagrammatic section with the presentation of mineralizing processes during the period of formation of the upper uranium horizon in the *Frank M* ore body. The ore zones were originally horizontal but are now tilted at ca. 2° SW. (After Northrop 1982)



associated with carbonaceous matter and iron oxides, mainly limonite.

Ore bodies are small, commonly lenticular in shape, up to 60 m long, 10 m wide, and up to 1.5 m thick. Some have been coalesced or have merged into larger lenses. Locally, some rolls have formed in sections with greenish and brownish clay galls, carbonaceous beds, and log fragments.

From the 100 properties mined, only 13 have produced more than 500 t of ore each. One property, the *Yellow Circle Group* in the upper *Cane Canyon* produced 60% of the district from two sandstone lenses. The lower and most productive lens was about 13 m thick and the upper lens from 1.5 to 9 m thick. The lenses are separated by 7.5 m of greenish-grey mudstone.

1.2.11 Montezuma Canyon District, Utah

This district centers along Montezuma Canyon, approximately 20–25 km SSE of Monticello (Fig. 1.29). Production totaled 130 t U and 370 t V_2O_5 at ore grades of about 0.21% U and 0.7% V_2O_5 . Some 60 properties have been mined but only nine have produced more than 1,000 t of ore. Two of these have produced more than 25,000 t of ore.

Sources of Information. Chenoweth 1975; Doelling 1969; Huff and Lesure 1965.

Geology and Mineralization

Ore bodies occur in thick sandstone lenses suspended in the middle part of the Salt Wash Member. The largest ore shoots are in a sinuous, asymmetric lens of sandstone in the central Montezuma Canyon where, in the *Strawberry mine*, the lowest ore body is about 8 m and the highest about 20 m above the base of the Salt Wash Member. The host sandstone is whitish, brown-stained, cross-bedded, and medium grained. It contains vegetal remains, large fossil logs and claystone pellets, and is cemented by calcite and often by roscoelite. Ore forms roll-like curved surfaces that transect bedding.

Carnotite and tyuyamunite are the principal ore minerals associated with dark grey vanadates. Pitchblende, coffinite, montroseite, and pyrite are present below the groundwater table. Ore minerals coat cavities and joint surfaces and impregnate the host rock. The richest ore is concentrated near carbonized logs and carbonaceous trash pockets. Some mineralization in the Montezuma Canyon shows zoning: uranium–vanadium minerals impregnated in a greyish-greenish sandstone often form a core zone, which grades into a brownish, iron-stained, porous sandstone with carbonized plant remains, which again is enveloped in a greyish cemented sandstone speckled with dots of limonite.

The deposits mined were all small. Ore bodies averaged up to 30 m in length, 15 m in width, and from a few centimeters to 2 m in thickness. Elliptical-shaped ore shoots were 6–12 m long, 3–6 m wide, and 1.2–3 m thick. In the *Cottonwood mine*, the largest producer, an ore lens in olive-grey sandstone was 0.3–1.2 m thick. The ore was localized around clay seams and

carbonaceous trash. Ore layers in the *Strawberry mine* are from 0.03 m to more than 0.3 m thick, forming roll-like curved surfaces that transect the bedding.

1.2.12 Meeker District, Colorado

This district is located in northwestern Colorado on the north-east margin of the Colorado Plateau (Fig. 1.29). The deposits, although smaller, are similar to those in the Urvan Mineral Belt. Underground mines on 26 properties have produced from medium-grained Salt Wash sandstones 90 t U and 385 t V_2O_5 at an ore grade of 0.25% U and 1.13% V_2O_5 (Boyer 1956; Chenoweth 1980).

Selected References and Further Reading for Chapter 1.2 Salt Wash Districts

Botinelly and Weeks 1957; Boutwell 1905; Boyer 1956; Bowers and Shawe 1961; Breit 1986; Breit and Goldhaber 1983, 1989; Brooks and Campbell 1976; Brooks et al. 1978; Burwell 1920; Butler and Fischer 1978; Butler et al. 1920; Carpenter 1980; Carter and Gualtieri 1965; Chenoweth 1975, 1978, 1980, 1981, 1983; Chenoweth and Malan 1969, 1973; Coffin 1921; Crawley 1983; Doelling 1969; Ethridge et al. 1980; FGM 2007; Finch 1967; Fischer 1947, 1950, 1957, 1959, 1960, 1968, 1970, 1974; Fischer and Hilpert 1952; Fischer and Stewart 1960, 1961; Fleck and Haldane 1907; Galloway 1978; Garrels 1955, 1957; Garrels and Larsen 1959; Goldhaber et al. 1983; Granger and Finch 1988; Granger et al. 1988; Gruner 1954a, b; Hansley and Spirakis 1992; Hess 1914; Heyl 1957; Hillebrand and Ransome 1900, 1905; Hintze 1967; Huff and Lesure 1962, 1965; Huffman and Lupe 1977; Huffman et al. 1980; Isachsen 1955; Jobin 1962; Johnson 1959; Johnson and Thordarson 1966; Keller 1959; Kerr 1958; Koeberlin 1938; Kovschak and Nylund 1981; LaPoint and Markos 1977; McLemore 1983, 2002; McLemore and Chenoweth 1989, 1997, 2003; McLemore et al. 2002; Meunier 1984, 1989; Meunier and Breit 1987; Meunier et al. 1987; Miesch 1962, 1963; Miller and Kulp 1963; Motica 1968; Nestler and Chenoweth 1958; Newman 1962; Newman and Elston 1959; Nash et al. 1981; Noble 1960; Northrop 1982; Northrop and Goldhaber 1990; Northrop et al. 1982; Peirce et al. 1970; Peterson 1977, 1978, 1980a, b; Peterson and Turner-Peterson 1980; Phoenix 1958; Pitman 1958; Plateau Resources Ltd. 1983; Pool 2007b; Rackley 1976, 1980; Ridgley et al. 1978; Scarborough 1981; Scott 1961; Shawe 1956a, b, 1962, 1966, 1976a, b; Shawe et al. 1959; Silver et al. 1980; Spirakis 1977, 1991; Spirakis et al. 1984; Stokes 1953a, b, c, 1954a, b, c, d, 1967a, b; Stokes and Mobley 1954; Thamm et al. 1981; Trimble and Doelling 1978; Tyler 1981; Tyler and Ethridge 1983; US-AEC 1959; Wanty 1986; Wanty et al. 1987a, b, 1990; Weeks 1951; Weeks et al. 1957, 1959; Whitney and Northrop 1986; Wright 1955; Young 1978; Young et al. 1957; Adams SS, Chenoweth WL, and Thamm JK, personal communication.

1.3 Chinle Uranium Districts, Western-Central Colorado Plateau

(Uranium Deposits in the Triassic Chinle Formation)

Second only to the Jurassic Morrison Formation, the Triassic Chinle Formation contains a substantial number of uranium deposits of the Colorado Plateau, particularly in its central-northern and western sections. Most deposits consist of more or less lenticular ore pods located within distinct channels and generally in the lower part thereof. They are therefore classified as basal-channel sandstone-type U deposits.

Eight principal mining districts have produced in excess of 42,000 t U from the Chinle Formation. The Lisbon Valley district has delivered almost 75% of this amount. Most remaining Chinle production came from a large number of generally small mines clustered in small areas scattered throughout southeastern Utah and northeastern Arizona (► Fig. 1.45, ► Table 1.5). The Moss Back Member was the most prolific unit of the Chinle Formation, followed by the Shinarump Member. The Monitor Butte Member carried ore only locally.

Mined ore grades averaged 0.22–0.30% U and 0.15–0.3% V₂O₅. An exception was the Monument Valley district with a vanadium content of almost 1% V₂O₅. As can be seen, in contrast to the Salt Wash hosted V–U deposits, most Chinle ore bodies normally contain less vanadium than uranium.

The Monument Valley and White Canyon districts host the most typical basal-channel deposits, whereas the largest district, the Lisbon Valley district, also referred to as Big Indian Wash district, is in many respects different from other deposits in Triassic Chinle sandstones. It has larger ore bodies and a unique geology since the ore-hosting Moss Back Member of the Chinle Formation was deposited in an area of halokinetic anticlines, a feature not common elsewhere. This situation would justify the separation of the Lisbon Valley deposits from other Chinle districts. It is included here, nevertheless, since both stratigraphic position and time of ore formation correspond to that in other Chinle districts.

Sources of Information. Malan 1968, Wood 1968, Stewart et al. 1972, Chenoweth 1975 and Huber 1980 published comprehensive studies of various districts with Chinle mineralization that were used as the main base, partly in the form of abbreviated and modified quotations, for the following descriptions amended by the data of other authors mentioned in the description of individual districts.

Regional Geological Setting of Mineralization

The Chinle Formation of the Late Triassic age is subdivided into seven members (► Table 1.6) that extend over large parts of the Colorado Plateau. The Chinle Formation is about 600 m thick in southwestern Utah. From there, it thins gradually to approximately 50–100 m in the eastern and northern parts of the plateau. Chinle sediments formed during a continental semiarid to arid climate. Gravel, sand, silt, and mud were deposited by braided and meandering streams on a wide-ranging alluvial plain in channels, lakes, and extensive mud flats. Highlands to the south of the depositional terrane such as the Mogollon Highland are considered to be the main source area of these sediments, although the ancestral Uncompahgre Mountains may have contributed material to the Chinle Formation in the northeastern and eastern part of the Colorado Plateau. The principal sediments are red or varicolored mudstones and siltstones, and generally light-colored sandstones and conglomeratic sandstones. The latter occur particularly at the base of the Chinle Formation. Carbonaceous debris, including carbonized or silicified fossil logs, is locally abundant.

The evolution of the Chinle Formation was initiated by the pre- or early Chinle erosion that affected the Lower to Middle Triassic Moenkopi Formation, which consists of continental, locally gypsiferous, sandy, and silty redbeds interfingering with minor amounts of marine calcareous sediments. This erosion generated broad valleys and low divides and locally deeper channels cut into Moenkopi strata as in Monument Valley, and in other places into pre-Moenkopi strata such as the Cutler Formation in the Lisbon Valley. Various Chinle members were deposited on this unconformity in the following sequence.

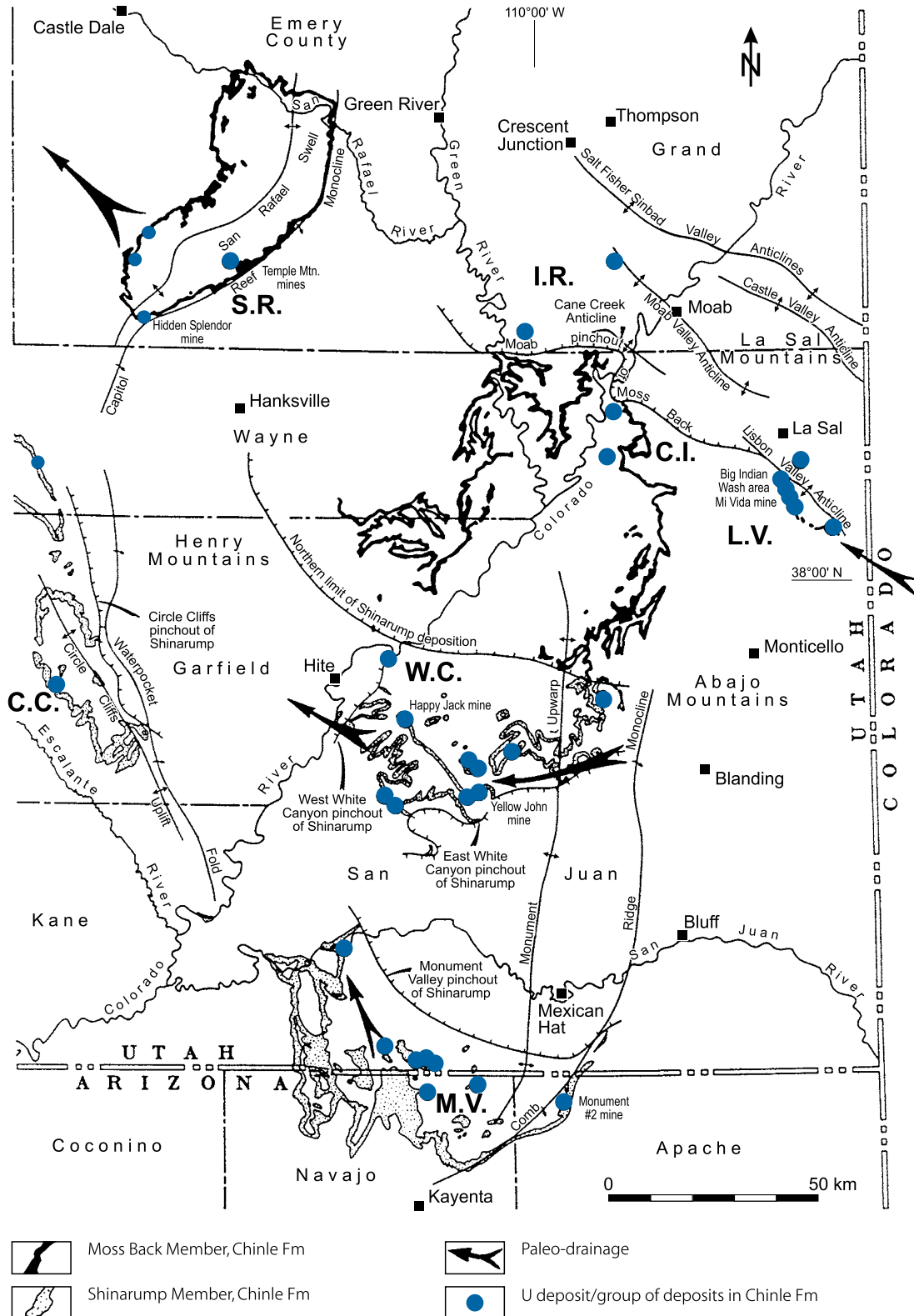
- (a) The **Shinarump Member** forms the basal Chinle unit. It consists of light-grey sandstones and conglomerates with rare lenses of mudstone and some volcanic material. Clastic sediments are cemented variably by calcite and silica and contain locally abundant carbonized and silicified plant fragments and logs. Moenkopi rocks below the generally very distinct unconformity often show a quarter of a meter or more of bleaching, particularly under mineralized scour and fill of paleochannels.

The Shinarump Member forms a fairly extensive and uniform blanket with distinct channel developments of reworked coarse psammites and psephites with thicknesses and distribution mainly controlled by paleosurface relief. Thickness ranges on average between 15 and 30 m, but locally attains 100 m and more. Stream flow was from the south and southeast in northern Arizona and southern Utah, and from the east in western Colorado and eastern Utah. Shinarump sediments grade upward and intertongue laterally with younger members of the Chinle Formation. Local subsidence caused the abandonment of segments of Shinarump rivers and subsequently their preservation as valley-fill or blanket-type deposits. Reducing conditions prevailed in certain areas where groundwater tables were probably high.

- (b) The **Monitor Butte Member** is the next younger Chinle unit. It consists predominantly of fine-grained sediments with abundant plant remains and some volcanic constituents. This member developed as the area continued to subside and stream gradients decreased.
- (c) The **Moss Back Member** as the next Chinle unit was deposited in channel systems and associated overbank deposits after a period when the general subsidence was interrupted and erosion prevailed. The Moss Back Member consists of fluvial siltstones, sandstones, and conglomerates with siltstone and limestone pebbles, particularly in the central Colorado Plateau (Lisbon Valley area). Volcanic debris and abundant carbonaceous materials are common constituents in the fluvial sediments. The lithology of pebbles indicates that the source of the Moss Back Member was not only external highlands, but also Chinle material itself, which may testify to a period of rapid growth of salt anticlines of the Paradox Basin during early Moss Back time.
- (d) The **next higher Petrified Forest Member** comprises mainly montmorillonitic/bentonitic mudstones, claystones, and siltstones that were apparently laid down by quiet-water sedimentation in sluggish streams, large lakes, and floodplains

Fig. 1.45.

Colorado Plateau, distribution of the Triassic Chinle Formation and location of uranium districts and typical deposits (Note: not shown are Cameron and Holbrook areas in central northern Arizona where U was also produced from Chinle sediments). (After Bailey and Childer 1977) (**U districts:** C.C. Circle Cliffs, UT; C.I. Cane Creek-Indian Creek, UT; I.R. Inter River-Seven Mile Canyon-Mineral Canyon, UT; L.V. Lisbon Valley-Big Indian Wash, UT; M.V. Monument Valley, AZ-UT; S.R. San Rafael Swell (Central Temple Mountain Belt, Northern Belt, Southern Belt), UT; W.C. White Canyon area, UT (Deer Flats, Elk Ridge, Red Canyon, Upper Cottonwood Creek, Upper Indian Creek, White Canyon)



■ Table 1.5.

Central-northern Colorado Plateau, principal mining districts with uranium hosted in the Chinle Formation and their production through 1984 (Chenoweth WC and Pilmore DM pers. commun)

Area/district	Production		Grade	
	Ore (metric t)	U (metric t)	U (%)	V2O5 (%)
Lisbon Valley, (Big Indian Wash), UT	>13 mio	>34,000	0.26	0.15–0.30
White Canyon area, UT-AZ (White Canyon, Red Canyon, Deer Flats, Elk Ridge, Upper Cottonwood, Upper Indian Creek)	ca. 1.7 mio	ca. 3,800	0.22	0.02–1.2 (av. 0.23)
Monument Valley, UT-AZ	ca. 1.2 mio	ca. 3,360	0.27	0.94
San Rafael Swell, UT (Northern Belt, Central Temple Mountain Belt, Southern Belt)	500,000	>1,100	0.22	
Cameron area, AZ (include Holbrook and Lee's Ferry areas, AZ)	265,000	470	0.18	0.03
Inter River-Seven Mile Canyon, Mineral Canyon, UT	185,000	460	0.25	
Circle Cliffs, UT	50,000	ca.100	0.21	
Cane Creek-Indian Creek UT	34,000	75	0.22	
Total	>16 mio	>42,000	0.22–0.3	0.15–0.3

during a time of minor subsidence, intense volcanism, and flourishing vegetation.

After deposition of the Petrified Forest Member, environmental conditions apparently changed. Vegetation must have decreased, since the Petrified Forest Member is the uppermost Chinle unit with abundant plant remains.

- (e) Highly oxidized redbeds of the *Owl Rock and Church Rock members* of the upper Chinle Formation indicate a more arid climate. Characteristic sediments include basal, alternating light blue–grey claystone and limestone, followed by orange–pink–reddish siltstones and sandstones, typical deposits of flood basins and lacustrine environments with several large fluvial systems and numerous smaller river systems.

Pronounced structures in the domain of Chinle sedimentation include, in the region around the Lisbon Valley in southeastern Utah and southwestern Colorado, domes and anticlines uplifted by halokinesis of evaporitic sediments of Pennsylvanian age within the Paradox Salt Basin. The largest structure further to the south and not related to salt anticlines is the Monument Upwarp, which may have influenced the sedimentation of Chinle deposits. In areas with salt anticlines, almost all major structural elements trend NW–SE. Another set of faults, often with strike-slip displacements, strikes NE–SW. Ten major NE–SW-trending lineaments, possibly related to basement faulting have been identified, with apparent displacements of 5–9 km.

Principal Host Rock Alteration

Bleaching is the most prominent macroscopical alteration feature found around uranium mineralization. It can extend into underlying formations. Oxidation and reduction affected various ore-hosting Chinle units partly in repeated phases (for more see description of districts).

Principal Characteristics of Mineralization

The ore mineralogy of Chinle uranium deposits varies according to its unoxidized or oxidized state. The respective mineral assemblages are the following:

Unoxidized zone: Pitchblende and coffinite are the main U minerals, and montroseite, locally doloresite, vanadium-bearing mica, -chlorite and -clay the prevailing vanadium phases. Associated minerals include sulfides of Cu, Fe, Mo, Pb, Zn, and trace minerals containing Se, Cr, Ni, Co, Ag, and Cd.

Oxidized zone: Hexavalent U minerals mainly consist of uranyl compounds, in the presence of vanadium of uranyl vanadates. Other species include higher-valent vanadium oxides and hydromicas, copper carbonates, native copper, etc.

Most Chinle uranium deposits have been found in north-eastern Arizona and southeastern Utah. They occur in whichever member locally forms the base of the Chinle Formation, e.g. the

■ Table 1.6.

Central-northern Colorado Plateau, stratigraphic units of the Triassic Chinle Formation. [After (a) Stewart et al. 1972, (b) O'Sullivan & Maclachlan 1975]

Epoch	Formation	Subdivision	Member	
			(a)	(b)
Late Triassic	Chinle	Upper red bed part	Church Rock	Mite Bed
			Owl Rock	Siltstone Mbr Limy Mbr
		Lower bentonitic part	Petrified Forest	Claystone Mbr
			Moss Back	Moss Back
			Monitor Butte	Mudstone Mbr
			Shinarump	Shinarump
			Temple Mtn	Temple Mtn

Moss Back Member in the Lisbon Valley-Big Indian Wash or the Shinarump Member in the White Canyon and Monument Valley districts (► Fig. 1.46). Uranium ore typically occurs in thicker parts of conglomeratic sandstone lenses, which, with the exception of that in the Lisbon Valley district, occupy paleochannels or scours cut into underlying formations. Carbonized fossil wood fragments and logs are common in these lenses, and ore appears to be concentrated where this material occurs.

By comparison with other Chinle districts with typical basal-channel U deposits, Huber (1980) notes for Lisbon Valley mineralization the following features of contrast:

- Lisbon Valley ore bodies group to two or three large, semicontinuous deposits with relatively high resources. Other districts, in contrast, contain isolated linear mineralized pods of small tonnage that are not connected
- Lisbon Valley ore averages almost 0.26% U, whereas the average grade of other districts within Chinle sandstone is around 0.21% U, except in Monument Valley where the grade averages 0.28% U
- The geological position of the Lisbon Valley ore bodies does not appear to be related to deep channel scours as is the case for other districts
- The geochemical composition of the Lisbon Valley ore is, to a certain extent, different from that of other Chinle districts. The White Canyon district is rich in Cu and Ag, low in V, while Deer Flats and Elk Ridge contain both Cu-U and U-V type ore. The San Rafael Swell district generally contains more V and less Cu than other districts.

General Shape and Dimensions of Deposits

The distribution of uranium mineralization in sandstones of the Triassic Chinle Formation is rather erratic and unpredictable, similar to that in the Jurassic Salt Wash Member of the Morrison

Formation. Deposits are widespread, but are generally small and thin. Mineralization only locally becomes sufficiently thick and high grade to be economic.

Ore bodies are usually composed of closely spaced lenses peneconcordant to bedding. Boundaries of ore bodies are often irregular amoeba-like and expressed by a sharp drop in uranium grade. Ore lenses range from less than 1 m to more than 300 m in length, from a few decimeters to over 100 m in width, and average about 0.5–2 m in thickness except for a few places where the ore thickness approaches 13 m. Individual ore bodies range in size from a few tonnes to more than one million tonnes of ore containing from a fraction of a tonne to several hundreds of tonnes rarely a thousand tonnes or more of uranium.

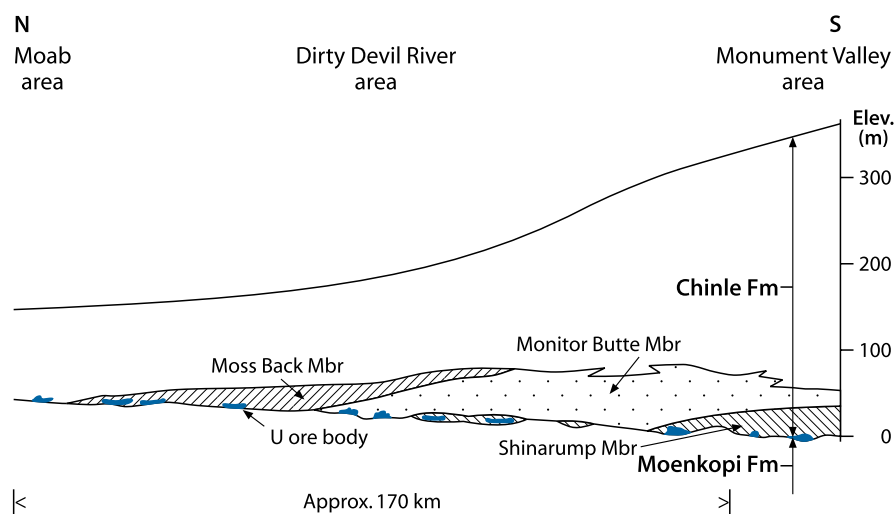
Ore bodies tend to be clustered within elongated favorable areas characterized by paleochannels a few kilometers long and up to several hundred meters wide. Average production from these areas has ranged from several thousand tonnes of ore to 1.5 million tonnes, and in the Big Indian-Lisbon Valley district to more than 13 million tonnes of ore.

Principal Ore Controls and Recognition Criteria

Uranium mineralization of the Lower Triassic Chinle Formation is classified as a peneconcordant type of sandstone deposit and most deposits can be attributed to the basal-channel class. The basal-channel association is particularly characteristic for ore bodies within the Shinarump Member. Otherwise, the Triassic Chinle deposits exhibit similarities to mineralization in the Jurassic Salt Wash Member, Morrison Formation, except for the quantity of vanadium. Excluding the Lisbon Valley deposits, where special ore-related conditions exist as discussed later in chapter Lisbon Valley District, major ore-controlling parameters or recognition criteria of basal-channel Chinle deposits include:

■ Fig. 1.46.

North-central Colorado Plateau, diagrammatic N–S section from Moab to the north and Monument Valley to the south showing the regional distribution of the basal members of the Chinle Formation and associated position of uranium deposits. (After Johnson and Thordarson 1966 based on Stewart et al. 1959)



Host Environment

- Host rocks are reduced, buff to grey feldspathic sandstone and conglomerate of continental fluvial origin filling channel systems scoured into pelitic–psammitic sediments
- Arenites are interbedded and/or covered by pelitic overbank facies partly containing tuffaceous material
- Carbonaceous debris is abundant in channel systems
- Arenaceous sediments have a relatively high permeability.

Alteration

- Significant alteration features are related to redox processes as reflected by color changes of both host and country rocks. Most prominent is bleaching around uranium mineralization
- Calcitization and silicification cemented host rocks to some extent.

Mineralization

- Pitchblende and coffinite are the principal uranium minerals
- Associated minerals include vanadium minerals, and sulfides of a number of other metals, most of them in trace amounts
- Uranium mineralization commonly occurs associated with or near accumulations of detrital plant debris, redistributed humate, and iron sulfides
- Uranium mineralization occurs disseminated in reduced arenites but also replaces quartz grains, clay particles, and particularly plant fragments. Locally, it extends as fissure filling into underlying mud/siltstones
- Uranium occurs in a wide distribution of small, low-grade occurrences within reduced sediments while larger, economic deposits are restricted to distinct sandstone channels of the locally present lowest Chinle member

- Deposits consist of a number of closely spaced small ore pods of medium grade commonly located in the lower part of a channel
- Preferential sites of ore bodies are fluvial paleochannels, where these channels converge, and where permeable channel sands gradually change into impervious carbonaceous mudstone
- Ore bodies are mostly lenticular in shape, more or less concordant with bedding, but locally also show roll shapes
- The location of ore bodies in the Shinarump and Monitor Butte members is lithologically–topographically controlled by relatively narrow channels and local accumulations of reductants, particularly carbonaceous trash therein
- The location of ore bodies in the Moss Back Member in the Lisbon Valley district is in broader channels in which ore is restricted to a zone above the unconformable suboutcrop of the Cutler Formation
- Ore bodies bound in narrow Shinarump and Monitor Butte channels are small whereas those in the Moss Back Member in the Lisbon Valley district are relatively large.

Metallogenetic Concepts

Huber (1980) presents a model for the geologic evolution and related formation of uranium deposits in the Lisbon Valley district that may be applicable in principle, although with restrictions, for other Chinle uranium districts in the northern Colorado Plateau. In his model, one important criterion in the evolution and formation of Chinle deposits tends to be tectonic events, which influenced both sedimentation and subsequent geochemical processes.

1. Regionally, the Lisbon Valley district is located within the Paleozoic Paradox Basin. Clastic debris was transported from

the Uncompahgre Highland of the Ancestral Rocky Mountains into the Paradox Basin in Pennsylvanian time. Detritus was deposited together with evaporites of great thickness. The compaction of salts initiated halokinesis resulting in NW–SE-trending anticlines, which are related to fault zones in the Precambrian basement. Anticlines probably deflected rivers that deposited lower Chinle sandstones in Triassic time. Where river systems were of a degrading nature similar to those in Shinarump time, they may have scoured into rising bedrock. But where these streams were of an aggrading nature similar to those in Moss Back time, they probably flowed in structurally lower areas, and, as a result, Triassic inter-anticlinal areas accumulated the greatest thickness of sandstone

2. Physicochemical conditions prevailing in these fluvial sediments were suited to permit uranium ore-forming processes and the accumulation of uranium to deposit sizes. The climate was humid enough to support ample vegetation as reflected by the abundance of carbonaceous debris in lower Chinle sediments. The character of fluvial sedimentation varied from braided channels to meandering channels. Reasons for such variations are probably multifold: (a) the establishment of topographic nick points in response to rising salt domes produced different stream gradients; (b) abundant vegetation stabilized bank deposits which, in turn, confined channel systems; (c) the amount and composition of detritus delivered from the source area, coupled with variable discharge rates, produced different types of sedimentary sequences
3. Uranium mineralizing processes were probably initiated soon after the deposition of fluvial sequences. Huber (1980) suspects that uranium was transported in near-surface groundwater that migrated down the hydrologic gradient along river valleys. Wherever these solutions with dissolved uranium encountered organic matter/humate along the course of the riverbed, uranium was extracted from the water and fixed as a colloid or adsorbed on organic debris forming protore or small ore shoots
4. The source of uranium could have been uraniferous volcanic ash preserved in the form of bentonitic clays in lower Chinle sediments or uranium-enriched granites, which supplied clastic material, or possibly both. Such granite has been identified in one of the source terranes. Metzger (1978, personal communication to Huber 1980) reports 12 ppm U contained in surface samples of the Trimble Granite in the San Juan Mountains
5. After the deposition of lower Chinle sandstones, the climate apparently became more arid and a change in the groundwater table possibly occurred during this episode. This is indicated by the oxidized nature and general lack of plant debris in upper Chinle sediments
6. In consequence of the criteria mentioned earlier, conditions during the sedimentation of upper Chinle sequences would have permitted the introduction of oxidizing waters into permeable older Chinle lithologies where they could dissolve any protore uranium and transport it to redox interfaces. The nature and degree of these processes, which are considered

by Huber (1980) to have acted in the form of a geochemical cell, are believed by the author to have been highly variable throughout the central Colorado Plateau. In the salt anticline region of the Paradox Basin, these cells were probably of a stronger and better-defined nature than those in areas to the west. The reason for this contention is based on the assumption that salt anticlines were positive features allowing large quantities of oxygenated waters to enter into host rocks in valleys, and to mobilize larger amounts of uranium

7. The salt anticline area east of the Lisbon Valley may have initially contained numerous small uranium ore bodies similar to those of the districts of Elk Ridge, White Canyon, and various belts of the San Rafael Swell. These “first generation” ore bodies are believed to have formed as a result of leaching uranium from overlying volcanic ash and its subsequent precipitation by carbonaceous matter and/or humate concentrations contained in lower Chinle sandstones. In these districts, small ore bodies survived
8. In contrast, continued inflow of oxygenated waters into the salt anticline region around Lisbon Valley is thought to have destroyed smaller deposits and the mobilized uranium has become the source for the “second generation” of larger and richer uranium deposits of the Lisbon Valley district. Where oxygenated waters were prevented from invading sandstone units that contained “first generation” ore bodies because of differential groundwater flow, or any other obstacle, the uranium ore body would remain behind as an island surrounded by the geochemical cell.

In summary, a generalized model for basal Chinle-type uranium deposits and their formation as suggested by Huber (1980) based on his investigation of the Lisbon Valley district requires the following ingredients and processes:

- (a) Fluvial deposition of clastic sediments into channel systems within a basin adjacent to a granitic highland. Exposed granitic rock provided detritus as well as a possible source of uranium
- (b) Potential host sandstones containing a high percentage of overbank facies that tended to constrict later groundwater flow
- (c) Abundant carbonaceous debris preserved in the channel system by rapid deposition. Organic matter is considered a prerequisite for the establishment and preservation of a reducing environment
- (d) Preservation of fluvial sediments by a cover of more pelitic, in part tuffaceous strata
- (e) Volcanic debris in and above sandstones constituting a second potential source of uranium
- (f) Uplift of a portion of the sedimentary basin permitting introduction of oxygenated, uraniferous(?) groundwater into sediments. This initiated a geochemical redox cell and local formation of smaller uranium ore bodies as found in Shinarump channels of the Monument Valley district
- (g) Continued supply of oxygenated water to the geochemical cell remobilized protore uranium and also dissolved uranium from preexisting small ore bodies. Uranium was transported to the edge of the tectonically active area where

it formed relative large deposits at the redox boundary as in the Lisbon Valley district.

Although Huber's (1980) model, at least points a to f, appears valid, in principle, since it covers essential prerequisites and processes for the metallogenesis of basal-channel-bound uranium deposits as found in the Shinarump and Monitor Butte members of the Chinle Formation. His interpretation, however, of the formation of larger Lisbon Valley ore bodies by an expanding geochemical redox cell (point g) does not satisfactorily explain the restricted position of ore bodies above the unconformable sub-outcrop of the Cutler Formation as discussed in chapter Lisbon Valley District.

Description of Individual Chinle Uranium Districts

For location of districts see [Fig. 1.45](#).

1.3.1 Lisbon Valley-Big Indian Wash District, Utah

The Lisbon Valley district, also referred to as Big Indian (Wash) district, is located in southeastern Utah ([Fig. 1.45](#)). First reports on uranium date back to 1913. Uranium deposits are aligned in a NW to NNW-trending, slightly arcuate belt 25 km long and almost 1 km wide, approximately 8 km of which have been eroded in the central section ([Fig. 1.47a, b](#)).

Deposits in this district are in many respects different from those in other Chinle districts. On the one side, it has larger ore bodies and a unique geology since the ore-hosting Moss Back Member was deposited in an area of halokinetic anticlines, a feature not common elsewhere. On the other side, the stratigraphic position of ore bodies and the time of the ore formation correspond to that in other Chinle districts.

Original resources of the Lisbon Valley district amounted to about 38,000 t U of which some 30,000 t U have been produced by some 30 underground mines through 1987. Mined ore averaged a grade of 0.262% U and 0.15–0.30% V₂O₅. Molybdenum in some mines reached grades of 0.03–0.07%, with a maximum of 0.25% Mo. Large portions of ore have a high average carbonate content, frequently more than 15% CaCO₃.

More than 96% of uranium production has come from the Moss Back Member of the Late Triassic Chinle Formation and about 4% from the Permian Cutler Formation and the Jurassic Salt Wash Member/Morrison Formation. Ore bodies in Cutler sediments are generally small, between a few tonnes to some tens of tonnes contained uranium with a few exceptions where ore bodies contained up to 400 t U.

Although remaining proven reserves are only a few thousand tonnes of uranium, probable potential resources are estimated to be in excess of 20,000 t U in the \$80/kg U cost category, most of which occur at greater depths (300–900 m) at the NW and SE ends of the mineral belt.

Sources of Information. Abrams et al. 1984a, b; Beahm and Hutson 2007; Bohn 1977; Butler and Fisher 1978; Campbell and

Steele-Mallory 1979; Crawley 1983; Dix 1953; Doelling 1969; Finch 1959; Fleshman 2005; Gruner et al. 1954a, b; Huber 1980; Isachsen 1954; Landmark/Weston 1988; Lekas and Dahl 1956; Loring 1958; Purvance 1980; Stokes 1967a, b; US-AEC 1959; Weir and Puffet 1960; Wood 1968; Chenoweth, personal communication. Huber's (1980) comprehensive description of the stratigraphy and sedimentology of the ore-hosting Moss Back Member of the Triassic Chinle Formation and its uranium occurrences has served, partly in modified quotations, for the principal description amended by the information of other authors as listed.

Geological Setting of Mineralization

On a regional tectonic basis, the Lisbon Valley ore zone is on the southwest flank of the Lisbon Valley anticline within the Paradox Basin. This basin is an extensive sedimentary trough, which developed since the Pennsylvanian time and is filled with a sedimentary sequence as shown in ([Fig. 1.48](#)).

The U-hosting Moss Back Member, lowest unit of the Chinle Formation in the Lisbon Valley district, transgressed with a slight unconformity (2–3° in the northwest and southeast zones, 6° in the central zone) over the truncated Cutler Formation ([Fig. 1.47c](#)). The latter consists of tan to reddish terrestrial sediments with only rare coaly substances. The paleosurface of Cutler sediments is partly almost smooth, but at other places it is incised by channels with a difference in relief of 10 m or more.

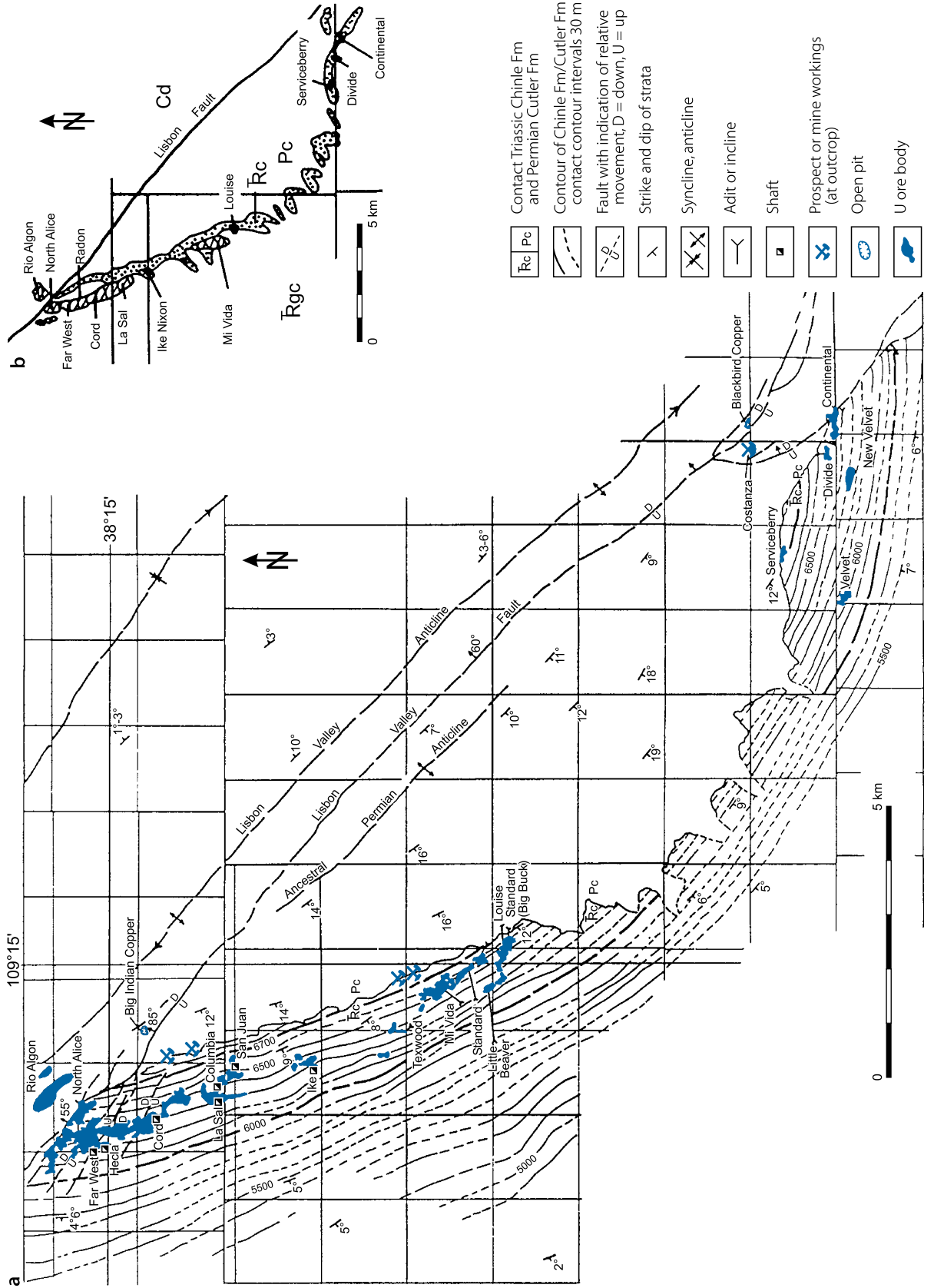
The Moss Back Member is overlain by red upper Chinle sediments, some 400 m thick, of lacustrine and fluvial silt- and mudstones with bentonitic clays. The bentonite is regarded as derived from volcanic ashes and tuffs. Thick, carbonaceous, locally uraniferous sandstones with mudstone interbeds and brownish-grey conglomerates with lenses of coarse-grained sandstone of the Salt Wash Member of the Jurassic Morrison Formation rest upon this sequence.

The *Moss Back Member*, 4–24 m thick, comprises light grey, grey-green, and dark brown sediments presumably of granitic and volcanic provenance that were deposited on flood plains by strongly meandering streams. Uranium is preferentially concentrated in the lowermost section, up to 6 m thick, which is composed of fluvial, cross-bedded, fine- to coarse-grained to conglomeratic, poorly sorted, arkosic sandstones with a carbonatic (up to 30% CaCO₃) matrix. These arenites are interbedded with mudstones and calcareous sandy conglomerates. Variable amounts of coalified organic matter occur in sandy lenses and pockets within and above the basal portion of mineralized sandstone, and in coal-rich mudstone layers overlying ore beds.

Huber's (1980) facies analyses of fluvial sandstones of the Moss Back Member in the Lisbon Valley-Big Indian area suggest that these sands were deposited in a type of point bar meander belt, or perhaps the Donjek-type braided stream (Miall 1977) environment. Two separate fluvial depositional systems are identified and possibly a third, and accordingly Huber (1980) subdivides Moss Back sandstones, from bottom to top, into three units: A, B, and C, based on lateral relationships of facies, cross-bedding directions, and sequence of primary sedimentary structures. Along the outcrop in the central part of the district

Fig. 1.47.

Lisbon Valley district, (a) generalized map showing major structures, contours of the Triassic Chinle – Jurassic Cutler formations contact, and outline of uranium deposits hosted in the Moss Back Member at the base of the Chinle Formation, (b) outcrop map of the Chinle Formation and location of uranium deposits, (c) SW–NE cross section across the district demonstrating the restriction of uranium deposits hosted in the Moss Back Member sandstone to at and above the angular suboutcrop of the Cutler Formation. [After (a) Chenoweth 1975, and Wood 1968 (reproduced by permission of AIME), (b) Huber 1980 based on Doelling 1969, (c) Lekas and Dahl 1956 (reproduced by permission of Utah Geology Ass.)]



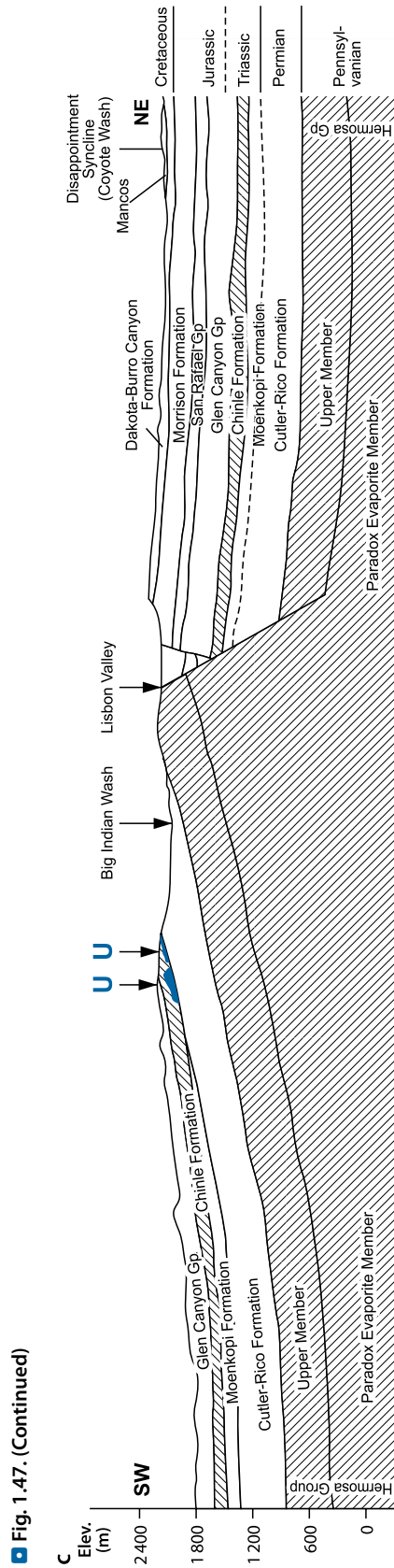
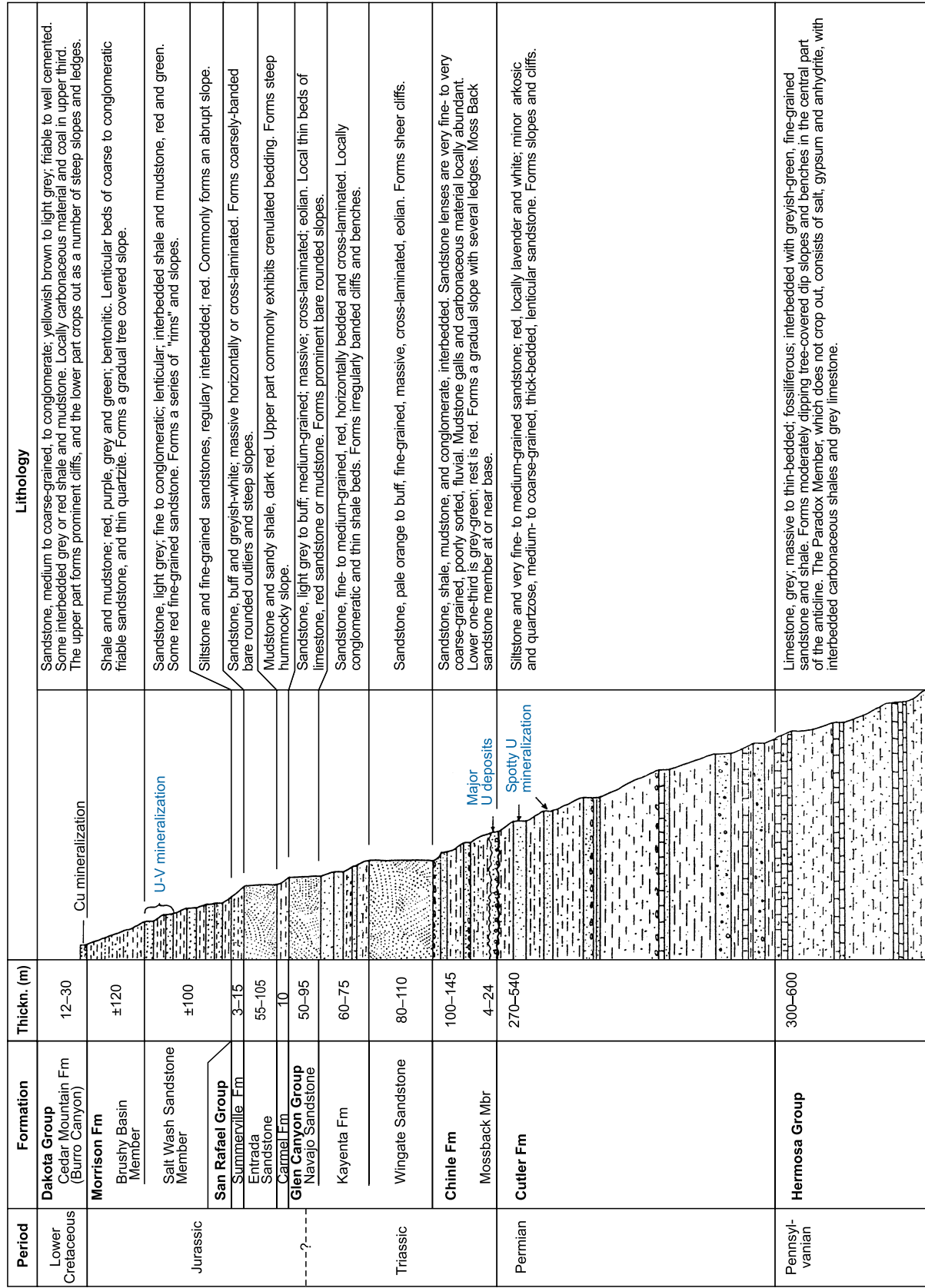


Fig. 1.47. (Continued)

Fig. 1.48. Lisbon Valley district, generalized litho-stratigraphic column. [After Wood 1968 (reproduced by permission of AIME), US-AEC 1959]



near Spiller Canyon, a thick sandstone body (unit A) is present. The stream that deposited this sandstone may have been the first one to have discontinued. Overbank sedimentation covered this abandoned area. Throughout the rest of the Moss Back deposition, the main fluvial channel distribution was generally restricted to the northern part of the Lisbon Valley district.

The basal-channel system represented by unit B in the northern area apparently had a more southwesterly transport direction, whereas current directions of the upper system (unit C) indicate a different area of origin for this stream system.

Huber (1980) further points out that primary sedimentary structures suggest at least two separate stream systems (units B and C) are present along the outcrop. Both sequences exhibit, in their basal section, sedimentary patterns reflecting channel floor facies. These basal units are in turn overlain by usually cross-bedded channel facies. In the case of the lower system (unit B), the channel floor facies frequently has an upward transition to fine-grained overbank facies with the in-channel facies absent, or if it is present, thickness is greatly reduced. Both systems are topped by overbank facies. (For more on these fluvial systems see Section Metallogenetic Aspects.)

The Lisbon Valley anticline evolved by post-Chinle halokinesis. It is cut by the post-ore Lisbon Valley fault of Laramide age (Fig. 1.47a and c). This fault trends NW–SE along the long axis of the Lisbon Valley anticline and dips 50 to 85° NE. It bifurcates near the northwest and southeast ends into several branches creating a number of horst and graben structures. As a result, ore beds are displaced at both the northern and southern end of the Big Indian belt. The northeastern block is downdropped by almost 1,200 m in the central part and by about 600 m at its northwest and southeast ends, where it cuts off mineralized Moss Back/Chinle sediments. Crosscutting NW–SE faults with minor displacements occur locally.

Chinle sediments dip between 10 and 15° SW and Cutler beds up to 20° SW in the southwestern block of the Lisbon Valley fault. Outcropping Jurassic and Cretaceous sediments of the northeastern block dip with 5° or less toward northeast. The inclination of all strata flattens to the edge of the anticline.

Host Rock Alteration

Bleaching is widespread and pronounced throughout the Moss Back and Cutler sediments at the unconformity where uranium mineralization occurs.

Mineralization

Pitchblende with some coffinite, montroseite, and doloresite are the principal U and V ore minerals in Moss Back sandstone. These ore minerals commonly occur as interstitial, disseminated grains, which have remained unoxidized in near-surface ore bodies due to protection by calcite cement in the sandstone. Associated minerals and elements, present in minor quantity, comprise galena, jordisite, pyrite, some copper, zinc, cadmium, and strontium minerals. Metatuyuyamunite, pascoite, corvusite,

a.o. occur in rare oxidized intervals. The sequence of mineral formation is presented in a paragenetic scheme for the Mi Vida deposit in Fig. 1.49.

In contrast to the Moss Back-hosted ore, mineralization in Cutler and Morrison sediments consists predominantly of carnotite, becquerelite, vanadiferous hydromica, copper carbonate, etc., documenting an oxidized environment. Morrison sediments also contain higher V/U ratios, averaging 2–3 to 1 that locally rise to 15 to 1.

The distribution of ore-forming elements in Moss Back-hosted ore shows a vertical sequence, from the top downward, from molybdenum to calcium, uranium, vanadium, and to copper. This sequence resembles the upper limb of a rollfront-type deposit as known from the Wyoming Basins.

A distinct vanadium zoning is present as reflected by a V/U ratio of less than 1 in the northern part of the district that increases southward to 2.5 to 1. Strontium behaves the opposite way with grades dropping toward south. Molybdenum forms halos around southern ore bodies. In the north, Mo was found adjacent to secondary faults.

Ore bodies are confined to basal sandstone and conglomerate of the Moss Back Member of the Chinle Formation, and concentrate, in particular, where the Moss Back Member consists of thicker, feldspathic, conglomeratic sandstone units and where these sandstones unconformably overlie thicker, more porous, truncated Cutler sandstone beds. They also appear to be located at a uniform elevation interval.

Almost 95% of all mineralization was found in small- to medium-sized ore bodies on the southwestern side of the Lisbon Valley fault. Only few ore bodies were discovered – perhaps due to limited exploration – across the Lisbon fault in the northeastern downthrown block, at the Lisbon Mine at a depth of 770 m at the northwest end of this block, and at the Constanza Mine to a depth of up to 300 m at its southeast end.

In the northern part of the district, large linear ore bodies are believed to be generally confined to the basal-channel system (unit B). The long axes of these ore lenses are approximately perpendicular to the NW-trending channel system.

In the southwestern block, mineralization occurs in a slightly arcuate belt, which, in principle, coincides with the NW to NNW-trending suboutcrop of the truncated Cutler Formation.

The mineralization of the *Rio Algom deposit/Lisbon Mine* (Purvance 1980) on the northeastern flank of the faulted Lisbon Valley anticline occurs in Moss Back beds at or within a few meters of the erosional unconformity with the underlying Cutler Formation. Host rocks consist of interbedded mudstone, sandstone, and conglomerate. Mudstones directly overlying the Cutler Formation vary in thickness and texture depending on the depositional facies. Arenites are medium-grained channel facies and range from locally conglomeratic units to cross-bedded bars or lenses. Their type and thickness depend on the size of the channel system. Conglomerates are made up of granular to pebble-size mudstone clasts embedded in clay or mud matrices that are well cemented by CaCO₃. Carbonaceous matter occurs above or within ore as coalified logs, twigs, and flake-size debris. These accumulations are broken up, compressed, and commonly contain iron and, exceptionally,

Fig. 1.49.

Lisbon Valley district, Mi Vida deposit, paragenetic scheme of mineralization in the Moss Back Member. (After Huber 1980, Gross 1956, Schmitt 1968)

Mineral	Stage	Early	Late
Cement			
Quartz		—————	
Baryte		—————	
Clay		—————	
Calcite		—————	
Sulfides			
Pyrite and marcasite		—————	
Chalcopyrite		—————	
Galena			—————
Greenockite			—————
Ore minerals			
Vanadium clay		—————	
Pitchblende		—————	
Coffinite		—————	
V ⁴⁺ oxide		—————	
Montroseite		—————	
Corvusite		—————	
Metatyuyamunite			—————
Pascoite			—————

copper sulfides. These rock series can be attributed to three different depositional systems throughout the Lisbon Mine area. Thick, green mudstone and black shale sequences reflect floodplain and back swamp-type environments; whereas sandstone-conglomerate units represent thick, massive channel deposits or thin, interbedded, braided stream sediments that were probably deposited in a northward-trending, braided channel, and floodplain fluvial system.

In addition to sedimentary control, the Lisbon Mine mineralization also reflects an impact by structural criteria. Faulting and structurally higher terrane tend to change the pattern of ore localization. Faults, which trend across an ore body, both inhibit and enhance uranium concentration. Also, faults and several episodes of reactivation events have redistributed ore constituents. Stratigraphically lower, interbedded units seem to have trapped ore while structural high areas were left unmineralized.

Shape and Dimensions of Deposits

As mentioned earlier, U deposits occur in two blocks separated by the Lisbon Valley fault. The ore-bearing zone of the *southwestern block* is almost 1 km wide and was originally about 25 km long, about 8 km of which have been eroded in the southern-central section (Fig. 1.47a). Accordingly, two main ore sectors exist, an approximately 10 km long northern and a 7 km long

southern sector. Ore bodies of the SW block are covered by up to several hundred meters of younger sediments but are locally exposed by deep erosion cuts.

Ore bodies in the Moss Back sediments have a peneconcordant lens-like shape with an irregular, amoeba-like boundary with a sharp drop of U grade. Ore lenses on the west side of the Lisbon fault commonly have a NW-SE-oriented length axis that follows the suboutcrop of the Cutler Formation. Lenses dip 6–8° SW. Their dimensions are on the order of few centimeters to 13 m in thickness (average 2 m), up to 100 m in width, and up to 300 m or more in length. Thickness and grade varies within lenses (Fig. 1.50). Resources of individual ore bodies range from a few tonnes to several hundred tonnes of uranium in the southern part of Lisbon Valley and up to 4,000 t U and perhaps more, in the northern area.

The *southwestern block* contained a total of more than 9,000 t U in its *northern area*. The main deposits of its northerly section were *North Alice* (ca. 1,500 t U, 0.233% U), *Far West*, *Hecla*, *Cord*, *Radon*, *Columbia*, *La Sal*, and *San Juan*. A little further south, three middle-sized ore bodies (*Ike*, *Nixon*, *Texwood*) existed with up to 1,300 t U each. The *La Sal No. 2 mine*, discovered in 1975 near the Columbia Homestake ore body, occurs in Cutler host rocks and probably contains 1,000–1,500 t U at an estimated ore grade of 0.2% U. Ore occurs within an up to 9 m thick arkosic unit of which the upper 1.5–3 m and the lower 3 m are mineralized. Deposits in the *southern part* of

the northern sector include *Mi Vida* (ca. 7,600 t U, 0.3% U), *Standard*, *Little Beaver*, *Louise*, and *Big Buck*.

The *southern area* is about 7 km in length. The original eight ore bodies including *Serviceberry*, *Velvet*, *Divide*, and *Continental* were small in size with reserves between a few tonnes and several hundreds of tonnes of uranium each. Some new ore bodies have been discovered with higher grades and larger resources than the old ones including the *New Velvet deposit* with estimated resources of about 2,000 t U at a grade of 0.5–1% U, and another approximately 400 t U at a grade of less than 0.13% U. The New Velvet deposit extends eastward into the new Section 2 ore body with resources of about 600 t U at a grade of 0.32% U and 0.6% V_2O_5 .

The *northeastern block* hosts deposits at depths from 600 to 900 m. One of the deeper deposits (Rio Algom deposit) was exploited by the *Lisbon Mine*. It had original reserves of about 6,500 t U at a grade of ca. 0.19% U contained in an ore body from 0.3 to 3 m in thickness and 600 m in width.

Ore Controls and Recognition Criteria

Mineralization in the Lisbon Valley-Big Indian district belongs to the lithologically controlled peneconcordant sandstone-type of uranium deposits. Ore controlling parameters of deposits on the southwest flank of the Lisbon Valley anticline include

- Uranium is preferentially concentrated in the basal sandstone horizon of the Moss Back Member of the Chinle Formation, which rests directly on truncated Cutler strata
- High concentrations of vegetal-organic matter occur in lenses or pods within and above the basal uraniumiferous sandstone unit, and occur disseminated in mudstones above uraniumiferous sandstones
- Host sandstones of the Chinle and Cutler formations are bleached within and adjacent to mineralization
- Ore bodies occur predominantly in zones where the thickness of the lower Moss Back sandstone exceeds 12 m and where this horizon overlays the suboutcrop of porous, friable, pale-grey bleached, fine-grained sandstone of the Cutler Formation
- Ore bodies are laterally spread over a larger area at the northwest and southeast end of the Lisbon anticline where beds have a shallower dip and the angle of unconformity between the Chinle and Cutler sediments is narrower as in the central section where dips and angles are steeper
- There is no apparent local correlation of paleochannels and ore
- Chinle ore is generally not oxidized, although it occurs 100 m or more above the present groundwater table
- Small pitchblende occurrences are found in the Cutler Formation but only where the overlying Chinle also contains ore. In contrast, carnotite mineralization does not exhibit this spatial relationship
- In the stratigraphically younger Dakota Sandstone, copper mineralization exists near major faults but only very little uranium has been found
- No uranium has been discovered in the Lisbon Valley fault itself except where the fault cuts ore in the Moss Back Member.

Metallogenetic Aspects

A general model for geological evolution and related uranium metallogenesis in Chinle sediments has been presented earlier in Section Metallogenetic Concepts. In the following, more specific parameters for the understanding of the development of the uranium-hosting depositional fluvial system and metallogenesis of uranium deposits in the Lisbon Valley-Big Indian district are presented.

Huber (1980) and other workers as well assume that the position of the ore belt is related to an ancient pre-Chinle anticline, which began to form in Permian time and continued to grow but with intermittent movement into Triassic time. Erosion that followed the early uplift of the anticline removed that portion of the Lower Triassic Moenkopi Formation, which covered the structure and some of the upper Cutler Formation prior to the deposition of basal Chinle sediments across the old anticline.

In the Lisbon Valley area two separate fluvial paleochannel systems, and possibly a third, are present within lower Chinle strata. Ore-hosting paleochannels tend to have formed by a more west to southwest oriented river system than the overlying system.

Further to the west of Lisbon Valley, a separate fluvial system flowed northwestward and joined the Lisbon Valley fluvial system southwest of La Sal Junction. The Hatch Rock syncline and a small anticline near the confluence of these two stream systems apparently influenced the direction and sedimentation of Chinle rivers. These two structures are probably the result of contemporaneous salt anticline growth, which affected sedimentation by deflecting streams away from active salt domes into structural and topographically low areas.

The Lisbon Valley U belt is located near a regional color change within the lower Chinle strata as reflected by the transition between red sediments to the east and greenish-grey sediments to the west. Huber (1980) interprets this alteration feature and associated formation of uranium deposits as indicating a possible district-wide geochemical zoning that resulted from the reaction of oxygenated water with humate. This would explain the alignment of uranium mineralized areas perpendicular to the channel system.

Huber (1980) postulates that oxidizing groundwater involved in the *metallogenesis* of the Lisbon Valley U deposits, was introduced along flanks of active salt anticlines. These solutions migrated down the hydrologic gradient and mobilized metals in host sandstones, which were earlier concentrated by organic substances in the form of protore or small ore shoots. With the continued recharge of oxygenated water, geochemical cells achieved sufficient capability to expand into border areas of the salt anticline region. To permit these processes, the following geologic conditions appear to have played a salient role:

- Fluvial sandstones that were deposited in a basin that formed adjacent to large-scale uplifts
- Initially, streams incised valleys into underlying formations. But, with a change in the stream gradient due to erosion in the provenance area, streams began to aggrade and fill the depression with clastic sediments whereby local structures

obviously constricted stream systems into areas between positive anticlinal highs

- Abundant vegetation flourished in the flood basin and associated fluvial environments. Decaying vegetation in swamps produced humic acids that entered shallow subsurface water. Rapid burial preserved accumulated plant material in the channel and channel margin areas
- A period of sedimentation dominated by volcanism followed the deposition of Chinle sandstones as documented by clays derived from volcanic ash. Streams transported and deposited volcanic material in the floodplain and lacustrine environments. These sediments blanketed the area and covered the sandstones. Tectonic uplift and climatic changes that accompanied this period of extensive volcanism allowed the introduction of large quantities of oxygenated water into shallow channel sandstones. The final ore-forming geochemical cell may have been initiated at this time
- Groundwater flow generally followed paleochannels. The geochemical cell probably continued to grow and migrate as long as ample oxygenated water was recharged. This migration proceeded as far as the border area of the tectonically disturbed region. Here, humate and bacterial-generated reducing conditions created a favorable environment to form major ore bodies.

Consequently, Huber's (1980) model envisions three main parameters, in addition to the normal physicochemical conditions, to be critical for the formation of Chinle uranium deposits in the Lisbon Valley district: tectonics, here resulting from halokinesis, related sedimentation patterns, and related subsequent geochemical cycles. In summary:

- Uplift initially created a gradient from a highland to a basin to which the streams flowed. The tectonic movement of small salt anticlines appears to have influenced regional as well as local sedimentology
- An adequate uranium source is present in the area (tuff, granite), which released sufficient uranium to form initially small ore shoots or protore in carbonaceous zones of fluvial sediments
- Continued growth of salt anticlines, coupled with a possible change in climatic conditions, established geochemical cells. These cells were active as long as tectonic and sedimentologic conditions allowed for recharge by oxygenated water
- Protore uranium within stream sediments was dissolved in the cell, transported down the hydrologic gradient, and precipitated at the cell edge. The distribution of these cells was generally restricted to the basal portion of the channel system
- Although the shape of cells is believed to have been tube-like, the shape of deposits became tabular due to modification by humic material.

Although Huber's (1980) model may be valid in principle, his interpretation, however, of the formation of larger Lisbon Valley ore bodies by an expanding geochemical redox cell does not satisfactorily explain the restricted position of ore bodies to the

suboutcrop of truncated Cutler Formation sandstones. In this particular case, it appears more likely that uranium was precipitated from migrating fertile solutions by reductants such as methane or hydrogen sulfide, which emanated at the Cutler-Chinle unconformity into the Moss Back sandstone as suggested by Chenoweth and other workers. Support for this hypothesis is provided by the migration of hydrocarbons through the Cutler Formation. Potential sources for these reducing gases exist in oil and gas fields in sub-Cutler formations, which are known near the Lisbon Valley district. Reducing agents released from these fields could have traveled upward into and along the Cutler strata to its suboutcrop. Where these reducing agents entered the overlying Moss Back Member, they could have generated a reducing zone in which mobile uranium in solution was reduced and precipitated and as such controlled the localization and shape of many ore bodies as suggested by most other authors. In summary, the Lisbon Valley deposits represent a special type of basal-channel uranium deposits independent of different metallogenetic concepts favored by workers of the district.

1.3.2 White Canyon District, Utah

The White Canyon district, also referred to as *Natural Bridges district*, is located in the southeast corner of Utah (Fig. 1.45). Uranium deposits are found in a crescent-shaped belt, some 60 km long and up to 30 km wide, which extends from the Colorado River in the southwest to the Dugout Ranch in the northeast. It includes deposits in the *White Canyon, Red Canyon, Deer Flats, Elk Ridge, Upper Cottonwood, and Upper Indian Creek* areas (Figs. 1.51 and 1.52).

Uranium was discovered in 1907 and subsequently some 120 properties (110 underground, 10 open pit mines) produced cumulatively 4,560 t U. Deposits ranged in size from a few tonnes to more than 550,000 tonnes of ore, but only five properties were larger than 45,000 t. The latter accounted for more than 60% of production from the White Canyon district. Most productive mines were *Happy Jack* and *Radium King*, which together produced almost 1,500 t U.

About half of the deposits had resources of less than 1,000 tonnes of ore. The grade of deposits mined was variable; it averaged 0.22% U, from 0.02 to 1.2% V_2O_5 (av. 0.23%), and from 0.12 to 1.3% Cu (av. 0.69%).

Sources of Information. Chenoweth 1975; Doelling 1969; Dubiel 1983; Finch 1959; Johnson and Thordarson 1966; Lewis and Campbell 1965; Malan 1968; Miller 1955; Thaden et al. 1964; Pitman 1958; US-AEC 1959; Chenoweth, personal communication.

Geological Setting and Mineralization

On a regional basis, the White Canyon district is located along the western flank and crest of the Monument Upwarp. The area is underlain by a sequence of Permian to Jurassic sediments as presented in Fig. 1.53. Nearly all ore bodies in the White Canyon district occur in channels of the *Shinarump Member* of

Fig. 1.51.

Monument Valley–White Canyon area, (a) geological map with distribution of uranium districts and major deposits. Uranium is hosted in the Shinarump Member, the basal unit of the Triassic Chinle Formation in this region as shown in sections (b) and (c.) The Chinle sediments are eroded in the central part of the area (shown in white). [After Malan 1968 (reproduced by permission of AIME)]

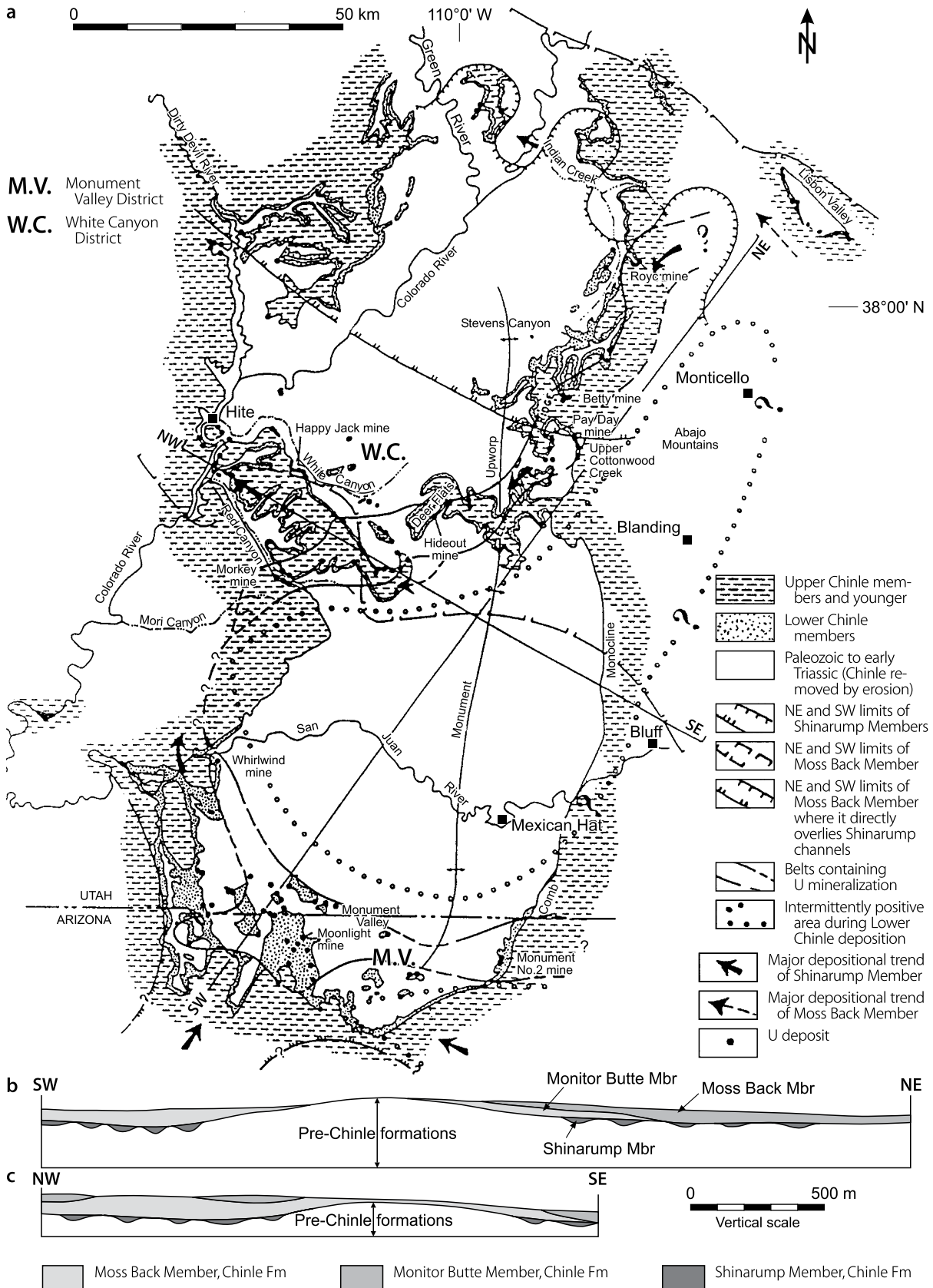
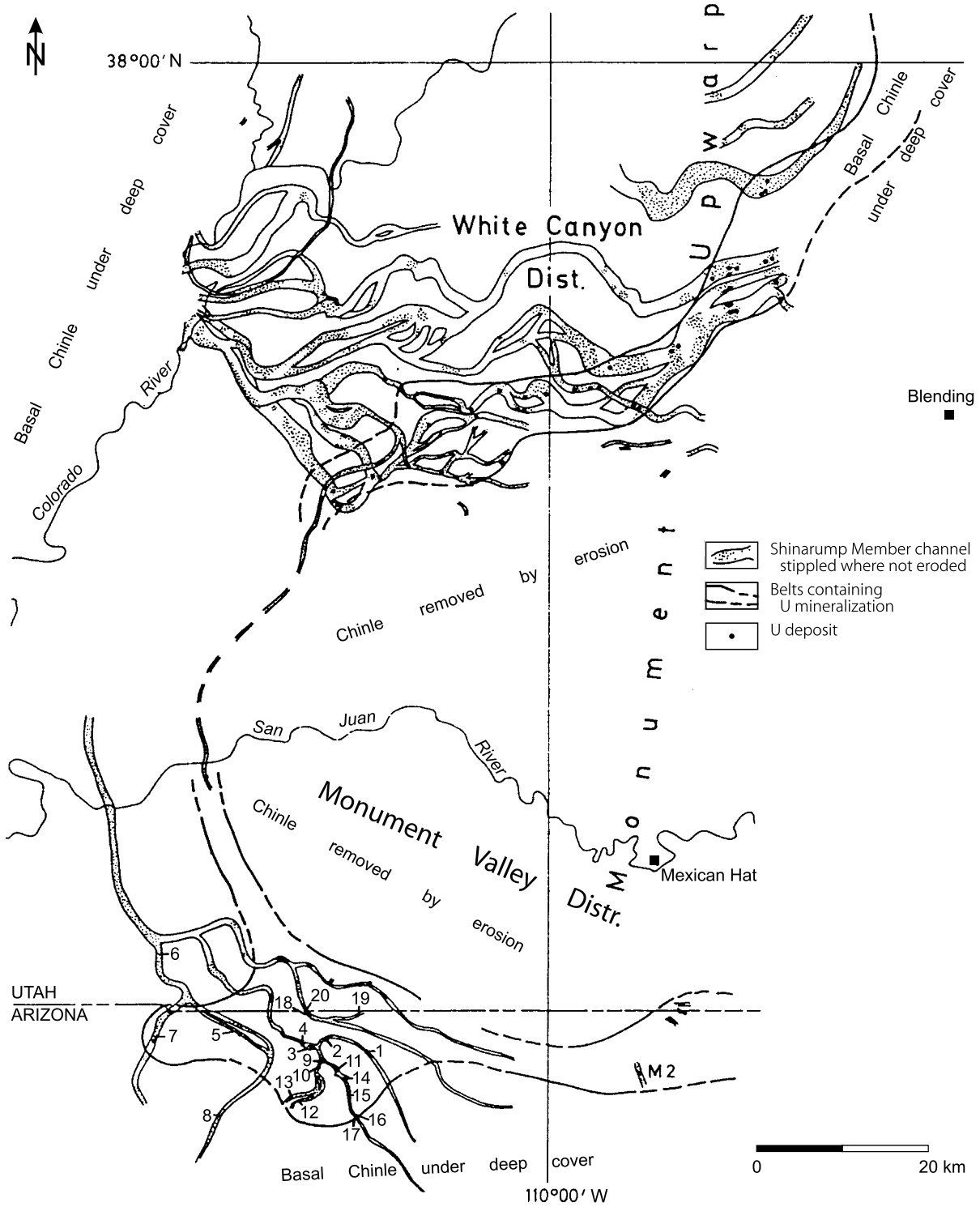


Fig. 1.52.

Monument Valley and White Canyon districts, map of the Shinarump channel systems and location of uranium deposits. [After Malan 1968 (reproduced by permission of AIME)] (Former mines: 1 Monument-Mitten 2; 2 Moonlight; 3 Daylight; 4 Starlight; 5 Tract 11; 6 Tract 14; 7 Tract 17; 8 Tract 2a; 9 Sunlight; 10 Bif Four; 11 Big Chief; 12 Boot Jack; 13 Joe Rock; 14 Naschoy; 15 Alma-Segin; 16 Black Rock; 17 Sally; 18 Fern; 19 Harvey Black; 20 Radium Hill; M2 Monument 2)



■ Fig. 1.53.

Monument Valley–White Canyon area, generalized litho-stratigraphic column of the Permian–Triassic–Jurassic profile with stratigraphic position of U deposits in Shinarump Member channels. [After Malan 1968 (reproduced by permission of AIME)]

Period	Formation Member	Thickness (m)		Lithology
Jurassic	Glen Canyon Group	Navajo Ss	90–200	Grey to buff, massive, crossbedded sandstone
?		Kayenta Fm	40–80	Interbedded, red sandstone and reddish-brown siltstone and mudstone
		Wingate Ss	75–105	Massive orange to reddish-brown, fine-grained, eolian sandstone
Triassic	Chinle Fm	Upper Members	145–275	Reddish-brown, thinbedded, calcareous mudstone, siltstones and sandstones overlying grey to green bentonitic clays and purple to chocolate brown mudstones with numerous sandstone lenses
		Moss Back Mbr	0–45	Grey, congl. sandstone
		Monitor Butte Mbr	0–75	Variogated benton. mudstone with Ss lenses
		Shinarump Mbr	0–75	U deposits Congl. Ss, carb. shale
	Moenkopi Fm	0–135	Interbed. chocolate brown siltst. and light brown fine-grained Ss	
	Permian	Cutter Fm	White Rim Mbr	0–15
Hoskinnini Tongue			3–45	Reddish-brown silty sandstone
De Chelly Sandstone Mbr			0–135	Massive, tan, fine-grained eolian sandstone
Organ Rock Tongue		50–225	Reddish-brown siltstone and fine-grained sandstone	
Cedar Mesa Sandstone Mbr		135–360	Massive, buff-white, eolian sandstone with thin red siltstone partings near top	
Halgaito Tongue		0–140	Reddish-brown siltstone and fine-grained sandstone	

the Triassic Chinle Formation. These paleochannels are incised into the Lower Triassic Moenkopi Formation and are largely filled with sandstone and conglomerate with abundant carbonaceous matter.

Uranium ore bodies are primarily restricted to favorable carbonaceous sandstone and conglomerate scour fills in the lower part of the Shinarump Member (Fig. 1.54a), but in a few mines ore extends downward for few meters into siltstone of the underlying Moenkopi Formation. Some channels enclose up to three separate subparallel ore-bearing scours. Not all scours in paleochannels, however, are mineralized with uranium. Meander loops of the channels provide the most favorable sites for ore accumulation.

In unoxidized ore bodies, pitchblende is the principal U mineral. It is commonly associated with copper sulfides (bornite,

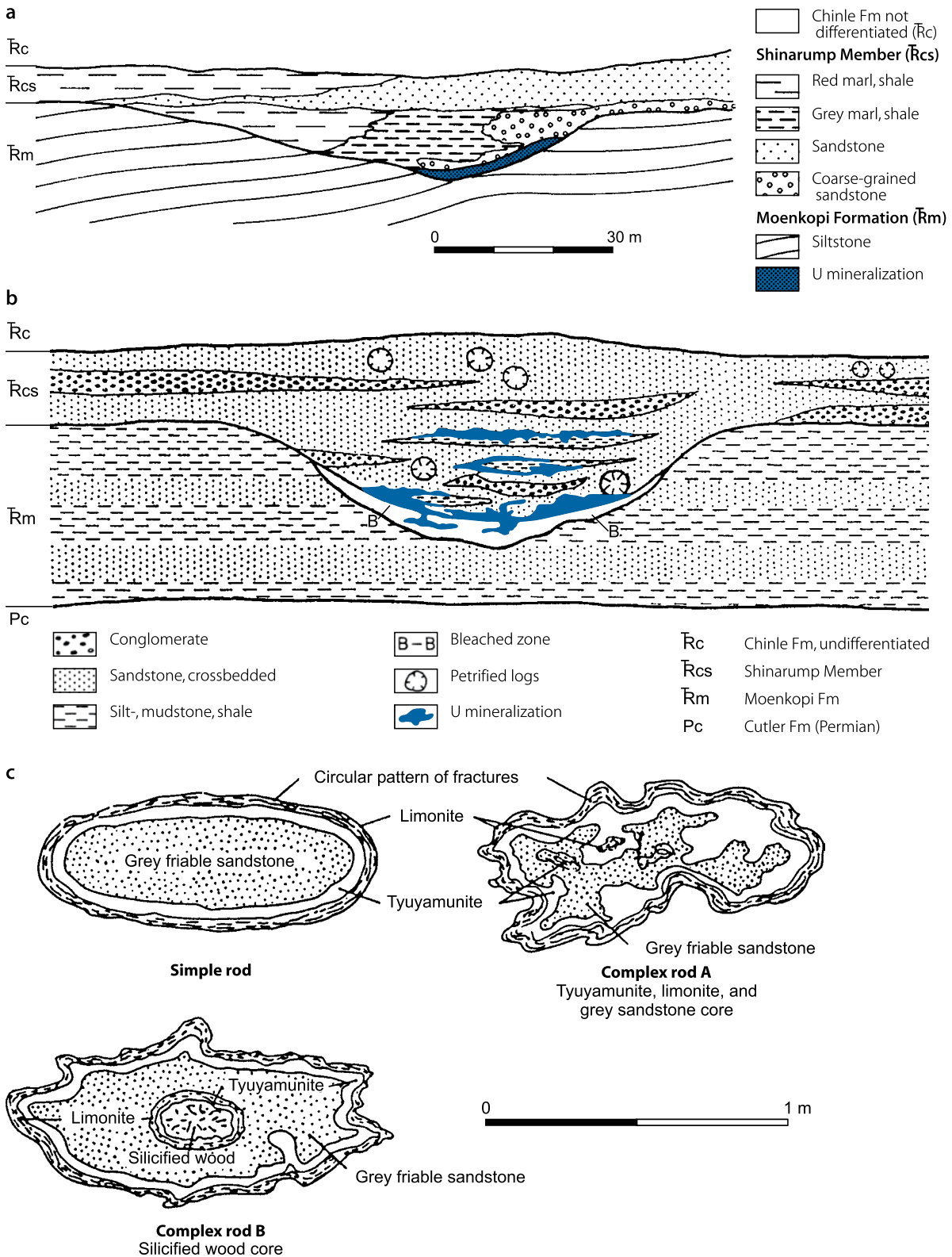
chalcopyrite, chalcocite, and covellite) and often with montroseite. Oxidized deposits contain uranyl minerals and secondary vanadium and copper minerals. Calcium carbonate is commonly present as a cementing matrix of the sandstone host rock. The copper content in the White Canyon area increases from east to west, whereas no pattern of distribution is evident for vanadium.

Shape and Dimensions of Deposits

Most deposits are linear in plain view with some deposits having a curvilinear to nonlinear shape. Deposits are usually composed of closely spaced, lenticular mineralized pods, or lenses oriented subparallel to bedding. Ore pods/lenses range commonly from 0.3 to 3.6 m in thickness, from about 1 to 100 m in length, and

Fig. 1.54.

White Canyon (a) and Monument Valley (b), diagrammatic sections illustrating the position and lithologic environment of uranium ore bodies in basal channels of the Shinarump Member, Chinle Formation. (c) Details of rod ore bodies in the Monument No. 2 mine. (After (a) Miller, Leo J. 1955, Society of Economic Geologists, Inc., *Economic Geology*, Fig. 3, p. 159; (b) Mitcham, Thomas W., Evensen, Charles G., 1955, Society of Economic Geologists, Inc., *Economic Geology*, Fig. 2, p. 172; c Witkind 1956)



occur at depths from 50 to 150 m. The average width is about one tenths to one fifths of the length. One mine had minable ore over a length of 2,100 m.

One of the largest deposits, exploited by the *Happy Jack* underground mine, White Canyon area, had an average thickness of 1 m, a width of 6–150 m, and a curvilinear length of almost 300 m. The average mining grade was 0.17% U, 0.23% V_2O_5 , and 0.69% Cu. Most of the ore was in the Shinarump Member but some mineralization also extended as much as 5 m into siltstone of the underlying Moenkopi Formation.

1.3.3 Monument Valley District, Utah

Monument Valley is located south of the White Canyon district, along the Arizona–Utah border (Fig. 1.45). Uranium was known in this region as early as 1918, but the first commercial discovery was made in 1942 at the site of the Monument No. 2 Mine.

Established original resources of the Monument Valley district exceeded 1.4 mio t of ore with a content of about 3,900 t U. Some ore was mined for its vanadium content from 1942 to 1944. Mining for uranium began in 1948 and lasted until 1969. During this period, 50 mines (42 underground, eight open pits) produced, cumulatively, 3,360 t U and 11,300 t V_2O_5 . Mined ore averaged 0.28% U and 0.94% V_2O_5 . Vanadium was recovered from 97% of the production. Production reached its peak during 1955, when 14 mines were operating.

Shallow deposits at or near the outcrop were mined by adit or open pit methods. Deeper deposits at depths of up to 180 m were accessed by shafts or inclines. The *Monument No. 2* mine was by far the most prolific producer. It delivered far more than half of the district's production. Other larger producers include the *Moonlight*, *Sunlight*, and *Boot Jack* mines.

A small upgrading plant was installed at the Monument No. 2 Mine. From 1957 to 1965, ore was processed at the Mexican Hat mill, Utah, and thereafter at Moab, Utah.

Sources of Information. Chenoweth and Malan 1973; Doelling 1969; Drouillard and Jones 1955; Dubiel 1983; Elevatorski 1978a, b; Finch 1959; Isachsen and Evensen 1956; Johnson and Thordarson 1966; Landmark/Weston 1988; Lewis and Trimble 1959; Malan 1968; Scarborough 1981; Stokes 1967a, b; US-AEC 1959; Witkind and Thaden 1963; Chenoweth, personal communication.

Geological Setting and Mineralization

The Monument Valley district is situated in the southern part of the Monument Upwarp where erosion has dissected a high table-land to a level where the Shinarump Member outcrops around the perimeter of the uplift and also caps mesas in Monument Valley.

Uranium deposits are hosted in paleochannels of the *Shinarump Member*, from 3 to 75 m thick, which are incised into red siltstone of the Moenkopi Formation (Fig. 1.54b). Channels tend to be U-shaped, relatively narrow, and are filled with mainly sandstone and conglomerate. Deposits consist of

closely spaced lenticular ore pods, which are generally concordant with bedding. Ore pods/lenses are primarily restricted to scours in or near the bottom of channels. Host rocks are cross-bedded, fluvial arkosic sandstones with locally abundant carbonaceous matter in which best mineralization is located where discontinuous cutting and filling took place. In a few mines, ore extended downward as much as 5 m from the Shinarump channel into underlying beds. Commonly there is only one ore-bearing scour, but not all scours in paleochannels contain uranium mineralization.

The largest deposit, *Monument No. 2*, contained both oxidized ore and unoxidized ore. Prevailing ore minerals in the *oxidized zone* include tyuyamunite, carnotite, hewettite, navajite, etc.; other mines also contained torbernite, uranophane, uranopilite, etc. *Unoxidized ore* comprises pitchblende, coffinite, montroseite, corvusite, vanadium hydromica, and sulfides of Fe, Cu, and Pb. Some elemental zoning is noticed: higher vanadium grades occur below and down dip of uranium ore zones, and the vanadium content decreases from east to west, whereas copper increases in the same direction.

Ore minerals impregnate sandstone voids, replace quartz grains, clay particles, and fossil plant debris, and fill vertical fractures, which extend beneath the scour base. Calcium carbonate, ranging from 1.4 to 10.3%, more or less cements the ore and the host lithologies. It is generally inversely proportional to vanadium content but it does not correlate with copper.

Shape and Dimensions of Deposits

Most deposits mined were small to medium in size and at shallow depths from 10 to 20 m. They consisted of closely spaced mineralized lenticular pods and rods (Fig. 1.54b and c) oriented concordant with the bedding. Single ore pods ranged from a few meters to almost 100 m in length and from less than 0.5 to 3.6 m in thickness. The ratio of length to width was commonly 5 to 1 but could be up to 50 to 1. Deposits ranged in tonnage from a few to approximately 700,000 t of ore. About half of the deposits contained less than 1,000 t. Ores mined contained an average of 0.28% U, 0.94% V_2O_5 , 0.3–2.5% Cu, and 4.6% carbonate.

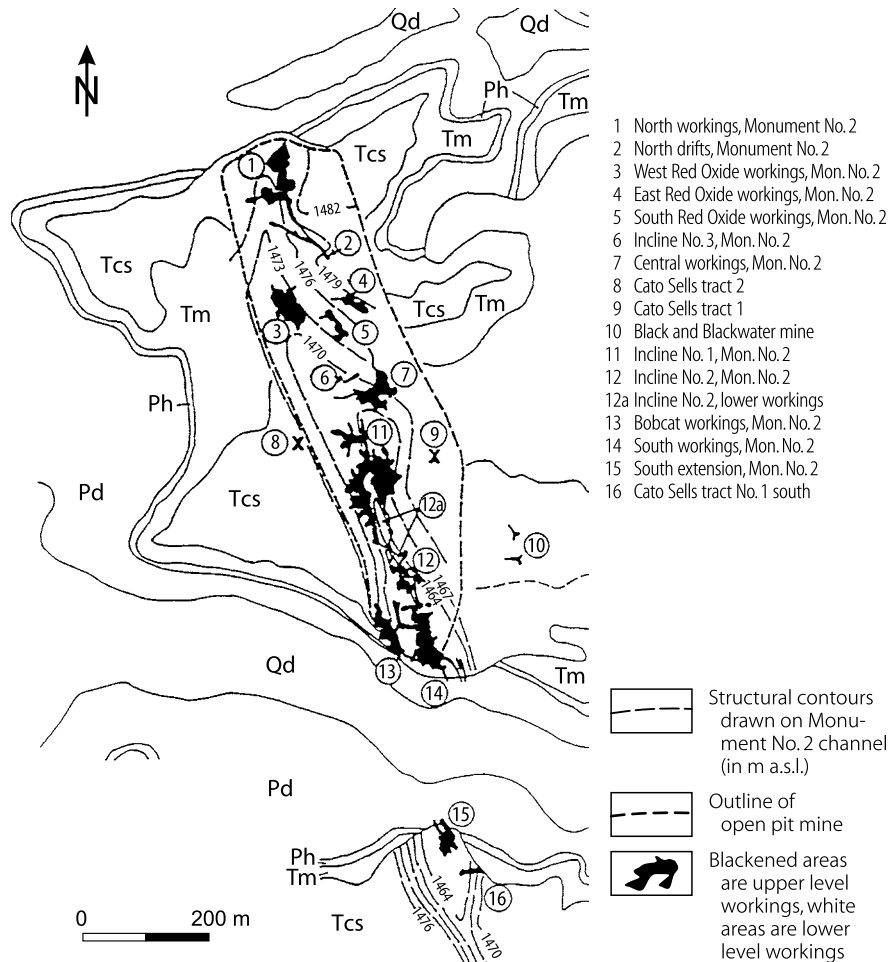
The largest deposit, *Monument No. 2*, credited for 690,000 t of ore, averaging 0.29% U and 1.42% V_2O_5 , and 2,030 t U and 9,800 t V_2O_5 , was emplaced in a Shinarump paleochannel scour extending for at least 3 km in a N–S direction within a wider depression or scour about 15 m deep cut into underlying Moenkopi and DeChelly strata. A narrow, inner scour is another 10 m deep and 200 m wide. The ore-bearing scour is eroded to the north and south. The best ore occurred in typical cigar- or rod-shaped concentrations as much as 2.5 m in diameter and 30 m long (Fig. 1.55).

1.3.4 Inter River District, Utah

The Inter River district covers a triangular-shaped area between the Green and Colorado rivers. It includes the *Seven Mile Canyon* and *Mineral Canyon* areas (Fig. 1.45). Uranium was

Fig. 1.55.

Monument Valley district, Monument No. 2 deposit, geological map with outline of uranium ore bodies and location of former mines (indicated by numbers) in a Shinarump channel segment. (After Witkind and Thaden 1963, US-AEC 1959) (Litho-stratigraphy: C Cutler Fm; Pd DeChelly Sandstone; Ph Hoskinnini tongue of Cutler Fm; Qd dune sand; Tcs Shinarump Mbr, Chinle Fm; Tm Moenkopi Fm)



discovered in 1949. In total, 56 mines including 48 underground operations produced 830 t U. Mined ore averaged a grade of 0.25% U. The production of only five mines exceeded 4,500 t of ore, one of them accounted for more than 45,000 t of ore. The vanadium content was generally very low except in deposits in the Church Rock Member where the U to V ratio was 1:7.

Sources of Information. Chenoweth 1975; Doelling 1969; Drouillard and Jones 1955; McRae and Grubaugh 1957; Chenoweth, personal communication.

Geological Setting and Mineralization

The majority of deposits occur at depths from 50 to 150 m in paleochannels of the flat-lying *Moss Back Member* of the Chinle Formation, which are incised down to 15 m into the Moenkopi Formation. The host rock is fine- to coarse-grained sandstone with interbedded siltstone, mudstone, and clay galls

and limestone- pebble conglomerate. The ore and host rock are cemented by calcite resulting in a high-carbonate content (av. 27%). Carbonaceous material is abundant.

Host rocks of the *Seven Mile Canyon* area are somewhat different from other Chinle districts since they are generally finer grained (and as such similar to lower Chinle sediments of the Rio Algom deposit/Lisbon Mine in the Lisbon Valley district). Chenoweth (1975) describes Seven Mile Canyon host rocks as being lenticular and containing argillaceous mudstone, limestone- and mudstone-pebble conglomerate, and carbonaceous mudstone and sandstone of the basal part of the Chinle Formation at or near the underlying unconformity.

Six deposits have been found in the *Church Rock Member* (Black Ledge) of the Chinle Formation. They are hosted in carbonaceous sandstones containing mudstone and siltstone galls, which change color from reddish purple to greenish-grey near uranium mineralization. Some subeconomic uranium mineralization occurs in Cutler and Moenkopi sediments.

All deposits are largely oxidized with remnants of pitchblende in larger ore bodies. Ore minerals are mainly hexavalent U minerals associated with copper carbonates and sulfides, and minor vanadium-, silver-, and cobalt-bearing minerals.

The *C-Group deposit* was one of the larger deposits mined. Ore occurred in a Shinarump paleochannel cut 15 m deep into the Moenkopi Formation. Ore bodies averaged 60 m in length, 6 m in width, and 0.6 m in thickness. Large amounts of carbonaceous debris and calcite cement were in the host rocks. Mined ore had grades from 0.25 to over 1% U and 24% CaCO₃.

1.3.5 Cane Creek-Indian Creek District, Utah

Discovered in 1949, this district extends from Cane Springs Canyon in the north to Indian Creek in the south, on the east side of the Colorado River (▶ Fig. 1.45). Eighteen mines produced a total of 110 t U at an ore grade of 0.22% U from deposits at a depth of 20 m. Most ore mined was extracted from lenticular ore bodies in the Triassic Moss Back Member, but some uranium was also recovered from fracture fillings in this member, and in the Permian Cutler and Rico formations.

Sources of Information. Chenoweth 1975; Corey 1959; Dix 1953; Chenoweth, personal communication.

Geological Setting and Mineralization

Most ore from the *Cane Creek* area was mined from lenticular ore bodies in the *Moss Back Member* of the Chinle Formation. Mineralization occurred in shallow channels incised into the Moenkopi Formation. Channels are filled with medium- to fine-grained, locally carbonaceous, grey sandstone, calcareous siltstone, greenish mudstone, and limestone-pebble conglomerate. Ore bodies are associated with carbonaceous pods within channels and host rocks are cemented by calcite. Pitchblende is the main U mineral at depth while hexavalent U minerals prevail near the surface. Vanadium and copper minerals are widespread but not abundant.

On the northeast flank of the Cane Creek anticline, structure-controlled mineralization was found in at least six NW-SE-trending faults in the Cutler Formation. The structures are 30–150 m apart. Each of them is up to 6 m wide. Vertical displacements are as much as 12 m. Material in fault zones consists of calcite- and clay-cemented sandstone, minor siltstone and shale, and along one fault zone of biotite-quartz mylonite derived from Cutler arkose. Uranium minerals fill small fractures, impregnate fault gouge, and are disseminated in arkosic sandstone adjacent to the faults and fractures. A uraniferous organic substance, described as pyrobitumen, is locally present in the structures.

The *Indian Creek* area contains small sedimentary deposits of uranium–vanadium with small amounts of copper in coarse-grained arkosic sandstones and at the contact of arkose and underlying red mudstone.

1.3.6 San Rafael Swell District, Utah

This district is the northwestern-most exposure of U-bearing Chinle Formation on the Colorado Plateau (▶ Fig. 1.45). It contains three mineralized belts: a northern belt, a central or Temple Mountain belt, and a southern belt. Uranium has been known in this district since 1904. Production from 122 mines, 115 of which were underground operations, totaled 1,440 t U at a grade of about 0.22% U.

Sources of Information. Clark and Million 1956; Hawley et al. 1968; Johnson 1957; Lupe 1976; Trimble and Doelling 1978; US-AEC 1959; Young et al. 1957; Chenoweth, personal communication.

Geological Setting and Mineralization

Uranium deposits of the San Rafael Swell consist of small, tabular ore bodies positioned at depths of about 30 m in small scours in the *Moniture Butte and Moss Back members* of the Chinle Formation. In the central Temple Mountain belt, pipe-like collapse structures are also mineralized.

Mineralization consists of a great variety of minerals as documented in ▶ Fig. 1.56. Uranium occurs generally as pitchblende associated with minor amounts of chalcopyrite, chalcocite(?), galena, molybdenite(?), montroseite, and sphalerite. Hawley et al. (1968) have classified the mineralization into four categories: V–U, Zn–Pb–U, Cu–U, and Cu–REE–U assemblages. The Pb and REE minerals are considered to be distinctive and the others are dominant elements of the deposits.

1.3.7 Circle Cliffs District, Utah

The Circle Cliffs area is located on the west side of the Colorado River, to the west of Hite, south of the Henry Mountains (▶ Fig. 1.45). Uranium was reported as early as 1915. Production amounted to 28 t U and derived from 30 mines, six of which were open pits. The ore mined averaged 0.21% U.

Sources of Information. Davidson 1967; Chenoweth, personal communication.

Geological Setting and Mineralization

Mineralization occurs at depths of some 50 m in scours and channels of the *Shinarump Member* of the Chinle Formation, and where these erosional structures are cut into the Moenkopi Formation. Ore lodes are largely bound to a 0.5–1 m thick horizon above the Shinarump-Moenkopi contact. Uranium deposits are small and discontinuous. They form high-grade ore pods that are a few decimeters in cross section and up to a 100 m or more in length. Uranium is present as pitchblende together with pyrite, marcasite, galena, and sphalerite. Additional elements in minor or accessory amounts include Ag, Co, Mo, Ni, Y, and Yb.

Fig. 1.56.

San Rafael district, paragenetic scheme of mineralization in the Monitor Butte and Moss Back members. (After US-AEC 1959 compiled by G.W. Chase)

Mineral	Stage	Syngenetic		Diagenetic	Epigenetic			Super-genetic
		Detrital	Anaerobic (sulfur cycle) environment		Cementation	Oxidation Reduction	Oxidation	
Quartz pebbles		—						
Chalcedonic chert pebbles		—						
Limestone pebbles		—						
"Asphaltite" pebbles		—						
Humic material		—						
Lignite		—	—	—	—			
"Asphaltite" (from humic acid)			—	—	—			
Marcasite			—	—	—			
Pyrite			—	—	—	—		
Native arsenic			—	—	—	—		
Concretion of humic material			—	—	—			
Silica			—	—	—			
Pitchblende				—			—	
Montroseite				—			—	
Sphalerite				—			—	
Galena				—			—	
Tennantite				—			—	
Bornite				—			—	
Chalcocite				—			—	
Covellite				—			—	
Ferroselite				—			—	
Calcite				—	—		—	
Cobaltomenite				—	—		—	
Dolomite					—		—	
Siderite					—		—	
Goethite					—		—	
Corvusite					—		—	
Realgar						—	—	
Mariposite						—	—	
Rauvite						—	—	
Metazeunerite						—	—	
Abernathyite						—	—	
Bieberite						—	—	
Malachite						—	—	
Azurite						—	—	
Gypsum						—	—	
Strontianite						—	—	
Baryte						—	—	
Celestite						—	—	
Chalcedony						—	—	
Asphalt						—	—	
Uranium carbonates							—	—
Uranium phosphates							—	—
Uranium silicates							—	—
Uranium sulfates							—	—
Vanadates							—	—
Vanadites							—	—
Basic hydrous sulfates							—	—

1.3.8 Cameron District and other Mining Areas in Northeastern Arizona

The Cameron district forms a curved belt nearly parallel to the Little Colorado River and extends for some 40 km from the north to the southeast of the village of Cameron. The main mining area is approximately 3–8 km wide but several mines occur outside of this area.

The first reported discovery of uranium (in the Kayenta Formation) dates back to 1950 and the first discovery of commercial significance was made in 1952, in the Petrified Forest Member of the Chinle Formation.

From 1952 to 1963, 475 t U at a mining grade of 0.18% U were produced in 98 mines, 93 of which were open pits.

This figure includes some 450 t U produced from the *Petrified Forest Member* in 67 mines, about 24 t U were recovered from the *Sandstone and Siltstone Member* in 27 operations, and 0.21 t U by three mines in the *Kayenta Formation*. Production in the Cameron district reached a peak in 1957 with the most productive area located 3–5 km east of Cameron where ten properties, within 2.5 km², produced 102 t U. Mining was by open pit methods (93 mines) to depths of about 50 m, and eight underground mines opened from pit walls and by vertical shafts.

About 3 t U at an ore grade of 0.17% were recovered from Shinarump and lower Petrified Forest sand and mud channel fills near the village of *Lee's Ferry*, on the Colorado River, ca. 110 km N of Cameron.

About 4 t U at an ore grade of 0.13% U and 0.14% V_2O_5 were mined in 13 mines from thin sandstone beds in the Chinle Formation north of the town of *Holbrook* in northeastern Arizona, ca. 160 km SE of Cameron.

Sources of Information. Akers et al. 1962; Austin 1964; Chenoweth and Magleby 1971; Chenoweth and Malan 1973; Landmark/Weston 1988; Peirce et al. 1970; Scarborough 1981; Spirakis 1980; US-AEC 1959; Chenoweth, personal communication.

Geological Setting and Mineralization

The ore-hosting Chinle Formation crops out in a broad belt nearly parallel to the Little Colorado River, on the southwest flank of the Black Mesa Basin. This formation is divided, around Cameron, into (in ascending order) the Shinarump, Sandstone and Siltstone, Petrified Forest, and Owl Rock members. U ore bodies are largely confined to the lower part of the Petrified Forest Member and, to a minor extent, the Sandstone and Siltstone Member.

The *Petrified Forest Member* hosts U ore bodies within NW to NNW-trending fluvial channels cut into bentonitic claystone and mudstone. Channels are filled with poorly consolidated, cross-stratified, fine- to medium-grained sandstone that contains reworked clay pellets, varying amounts of carbonaceous matter, and silicified-carbonized fossil logs. The logs occasionally reach lengths of 15 m or more. Sandstone lenses average 6 m but can be up to 10 m in thickness. Its continuity is generally poor but some sand lenses could be traced for more than 1.5 km.

Mineralization consists chiefly of oxidized U and U-V minerals filling pore spaces in sandstones and in fossil logs; but in spite of pervasive oxidation, ores are in radioactive equilibrium but for a few local exceptions. According to Austin (1964), fossil logs locally contain mineralization in the reduced state but where fossil logs are exposed to oxidation, pitchblende and coffinite are altered to uranophane, zippelite, boltwoodite, schroëckerite, and uranocircite while pyrite and marcasite are transformed to hematite, limonite, and iron sulfates. Sulfates, especially gypsum and baryte replace primary pyrite and calcite in shrinkage cracks in carbonaceous material. Some deposits contain oxidized logs surrounded by double alteration halos. Austin (1964) attributes this feature to complex oxidation processes involving groundwater and hydrologic changes by the downcutting history of the Little Colorado River.

The main chemical elements related to U ore zones include Ca, Cd, Co, Cu, Mn, Mo, Ni, Pb, and V, whereas Zn is notably absent. Ore bodies in the *Huskon No. 10* and *11* mines contain notable trace amounts of Mo and Co-bearing minerals. The best mineralogical guides to U ore are fracture films of blue Mo oxide, calcite-gypsum-baryte gangue minerals, and bleaching of country rocks from grey to a yellow or buff color probably due to oxidation of sulfides in protore halos.

Privileged intervals for ore concentration in channels tend to occur in abrupt depressions of the channel bottom or at changes

in a channel's direction such as meander bends, and show an affinity to more carbonaceous layers. Most ore bodies are encased in an alteration halo of bleached sandstone and mudstone. Ore bodies and halos terminate abruptly downward against impermeous mudstone.

The most productive unit in the Cameron district, the *Petrified Forest Member* contained ore from the surface to a depth of 40 m with as many as three ore zones within 30 m of a section. Ore bodies are commonly elongated parallel to the trend of channels, except for some ore bodies with nearly perpendicular orientation to the fluvial trend. Ore bodies mined ranged in size from a single mineralized fossil log to the *Jack Daniels* deposit with 68 t U in a nearly continuous ore body, 135 m by 90 m in lateral extension. The second largest deposit, *Charles Huskon 4-Paul Huskie-3*, produced 52 t U from a cluster of ore pods grouped in an area 300 m by 165 m.

The upper 10 m of the *Sandstone and Siltstone Member* contains ore in thin-bedded, cross-stratified, fine- to medium-grained sandstone with abundant carbonaceous trash and mineralized fossil logs. Deposits in this member yielded a total of about 24 t U from 27 operations. The largest ore body contained 2.5 t U.

Some mineralization was also found in fine-grained sandstone lenses in the middle part of the *Kayenta Formation* of Upper Triassic-Jurassic age.

Numerous collapse structures have been identified around Cameron including the *Riverview Mine*, which is described in Chap. 1.4 Arizona Strip Area. Some silicified "plugs" intruding the Moenkopi Formation northwest of Cameron have bleached halos in Moenkopi beds and peripheral radioactive pyrite-copper anomalies, as well as argillic (kaolinite to illite) alteration.

Selected References and Further Reading for Chapter 1.3 Chinle Uranium Districts

Abrams et al. 1984a, b; Akers et al. 1962; Austin 1964; Beahm and Hutson 2007; Bohn 1977; Butler and Fisher 1978; Campbell and Steele-Mallory 1979; Chenoweth and Magleby 1971; Chenoweth and Malan 1969, 1973; Chenoweth 1975; Clark and Million 1956; Corey 1959; Crawley 1983; Davidson 1967; Dix 1953; Doelling 1969; Drouillard and Jones 1955; Dubiel 1983; Elevatorski 1978a, b; Finch 1959; Finnell et al. 1963; Fischer 1968; Fleshman 2005; Gross 1956; Gruner et al. 1954a, b; Hawley et al. 1968; Hintze et al. 1967; Huber 1980; Isachsen and Evensen 1956; Isachsen 1954; Jennings 1976; Johnson and Thordarson 1966; Johnson 1957; Koch et al. 1964; Landmark/Weston 1988; Lekas and Dahl 1956; Lewis and Campbell 1965; Lewis and Trimble 1959; Loring 1958; Lupe 1976; Malan 1968; McRae and Grubaugh 1957; Miesch 1963; Miller and Kulp 1963; Miller 1955; Peirce et al. 1970; Pitman 1958; Purvance 1980; Rackley 1976; Scarborough 1981; Schmitt 1968; Spirakis 1980; Stewart et al. 1972; Stokes 1967a, b; Thaden et al. 1964; Thomson 1967; Trimble and Doelling 1978; US-AEC 1959; Weir and Puffet 1960; Weir 1960; Witkind and Thaden 1963; Wood 1968; Young 1964, 1978; Young et al. 1957; Chenoweth and Pilmore, personal communication.

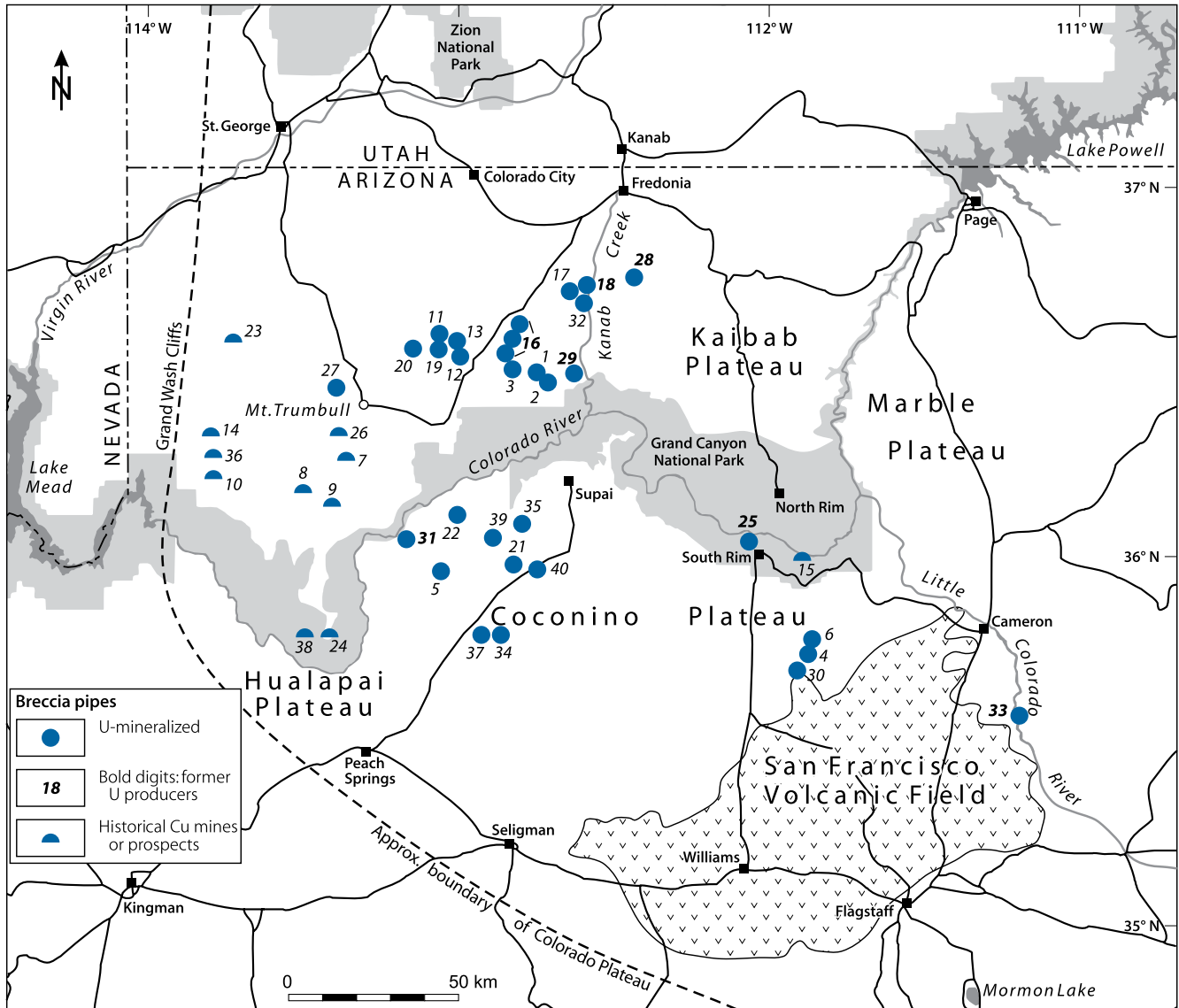
1.4 Arizona Strip Area, Southwestern Colorado Plateau

The "Arizona Strip" uranium district in northern Arizona extends beyond the geographic limits of the Arizona Strip proper. The term "Arizona Strip area" is thus more appropriate.

Fig. 1.57.

AZ Strip area, northern Arizona, location of mineralized breccia pipes. (Based on published data and personal communication by McMurray, Pool, Spiering, and Wenrich)

[**Explanation:** *bold letters* indicate breccia pipes with U production; *italic letters* indicate U prospects with \pm U mineralization; normal letters indicate mainly Cu-bearing pipes/historical Cu mines or prospects. Breccia pipes: (1) *A-1*, (2) *A-20*, (3) *Arizona 1*, (4) *Black Box*, (5) *Blue Mtn*, (6) *Canyon*, (7) *Chapel*, (8) *Copper House*, (9) *Copper Mountain*, (10) *Cunningham*, (11) *DB-1*, (12) *EZ-1*, (13) *EZ-2*, (14) *Grand Gulch*, (15) *Grandview*, (16) *Hack 1*, *Hack 2*, *Hack 3*, (17) *Hermit*, (18) *Kanab North*, (19) *Lisa*, (20) *Lizard*, (21) *Lynx*, (22) *Mohawk Canyon*, (23) *Near Miss*, (24) *Old Bonnie*, (25) *Orphan*, (26) *Parashant*, (27) *Pat*, (28) *Pigeon*, (29) *Pinenut*, (30) *Red Horse Wash*, (31) *Ridenour*, (32) *Rim*, (33) *Riverview*, (34) *Rose*, (35) *Sage*, (36) *Savannic*, (37) *SBF*, (38) *Snyder*, (39) *Wate*, (40) *4½*]



This district is located in the NW corner of Arizona, bounded to the N and to the W by the Utah and Nevada state lines, and extends south and southeast of the Grand Canyon on the Coconino Plateau.

A substantial number of mineralized collapse-breccia pipes have been identified in the Arizona Strip area since the late 1800s. These pipes were initially prospected for Au, Ag, and Cu but may also contain anomalous amounts of U and other metals.

Figure 1.57 shows the principal old mines and prospects,

which were primarily mined for copper with grades as high as 15% Cu.

The actual exploration and mining of breccia pipe uranium deposits started in 1951 when uranium ore was found on the dump of an old copper prospect, the *Orphan Lode*, on the South Rim of the Grand Canyon. By the time mining ended in the early 1960s, the *Orphan Lode* had produced almost 1,700t U as main product as well as copper and silver as by-products. The *Riverview* and *Ridenour* pipes were the only

other mines at that time with recorded U production: less than 2 t U combined.

This type of breccia pipe became the target for an extensive exploration campaign again during the 1970s and 1980s, and resulted in the discovery of a number of uranium deposits as shown in [Fig. 1.57](#). Most of the U-rich pipes occur within a 40–60 km wide and 120–150 km long SE–NW-trending belt, extending from about Cameron to the SE through the Red Butte–Grand Canyon area and Hack Canyon–Pigeon area to about 30 km S of the Arizona–Utah state line, between Fredonia and Colorado City to the NW. The SW boundary of the belt is approximately along Mohawk Canyon on the eastern Hualapai Indian Reservation.

Minable breccia pipes contain resources in the range from a few hundreds to about 2,000 t U. Total resources discovered so far are on the order of 12,000–15,000 t U contained in about 20 pipes. Production grades are generally high, averaging from 0.3 to 0.7% U or even more. Silver, copper, and vanadium are recoverable from some uranium breccia pipes.

Breccia pipes mined from 1981 to 1991 are located in the general area of Kanab Creek, a tributary of the Colorado River on the north side of the Grand Canyon and include the *Hack Canyon No 1, 2, and 3*, *Hermit*, *Kanab North*, *Pigeon*, and *Pinenut* pipes. Total production was approximately 7,350 t U at an average grade of just over 0.4% U.

Except for ore-bearing breccia pipes, the Arizona Strip area shows very little mineralization. A few Pb–Zn and some Cu, Ag, and V showings are recorded from the paleo-karst of the Mississippian Redwall Limestone. Small sandstone-type deposits have been mined from Chinle sediments in the Cameron district at the southeastern extremity of the area. A small sandstone-type U occurrence hosted in Chinle sediments was explored near Colorado City, Arizona, on the northwestern boundary of the district.

Sources of Information. See authors listed in Section References and Further Reading... at the end of Chapter Arizona Strip.

Regional Geological Setting of Mineralization

The regional geological setting is the classical one of the Grand Canyon region with its well-known stratigraphy and history (Billingsley 1978a, b; Breed and Roat 1976; Four Corners Geol. Soc. 1969; Karlstrom et al. 1974). The rock sequence, as depicted in [Fig. 1.59](#), ranges in age from Precambrian to Permian and locally Triassic. These rocks were intruded and capped in places by Miocene to late Pleistocene volcanics. The oldest rocks include the Lower to Middle Proterozoic Vishnu Group metasediments (>2,000 Ma) and metavolcanics (1,820–1,750 Ma), and the Zoroaster Igneous Complex (1,770–1,725 Ma, all ages from Nations and Stump 1981), which is granitic in part. Rocks are metamorphosed in greenschist to upper amphibolite grade facies, the higher grade predominating. Regional metamorphism occurred ca. 1,700 Ma ago. Moderately deformed Upper Proterozoic limestones, sandstones, and shales of the Unkar and Chuar Group rest unconformably on the older rocks.

The Precambrian units are separated from overlying Paleozoic–Mesozoic sediments by an angular unconformity. Marine to marginal continental limestones, mudstones and silty to sandy formations of Cambrian to Permian age are almost horizontally bedded. Locally, Triassic rocks of the marginal continental Moenkopi and continental Chinle formations rest as remnants unconformably upon older strata.

Breccia pipe-hosting Mississippian to lower Triassic lithostratigraphic units show the following characteristics (McKee 1978). An approximate outline of the distribution of the various units is given in [Fig. 1.58](#).

Mississippian Redwall Limestone, 150–200 m thick: Generally a very pure carbonate rock containing less than 1% quartz and clay-size particles. At several localities, most notably at Supai Village, copper, lead, zinc, silver, and vanadium mineralization have been noticed in this rock.

The Redwall Limestone is divided into four members, in ascending order, the Whitmore Wash, Thunder Springs, Mooney Falls, and Horseshoe Mesa members. The *Whitmore Wash Member* is a fine-grained dolomite in the eastern Grand Canyon, grading into an even, fine-grained limestone in the west. The *Thunder Springs Member* contains thin layers and elongated white chert lenses that alternate with limestone or dolomite beds. Individual layers are up to 20 m thick. The chert presumably derived from the replacement of carbonate mud on the sea floor. The *Mooney Falls Member* consists of massive limestone beds 1–10 m thick. The *Horseshoe Mesa Member* is thin-bedded aphanitic limestone, locally containing oolitic limestone and thin chert as lenses.

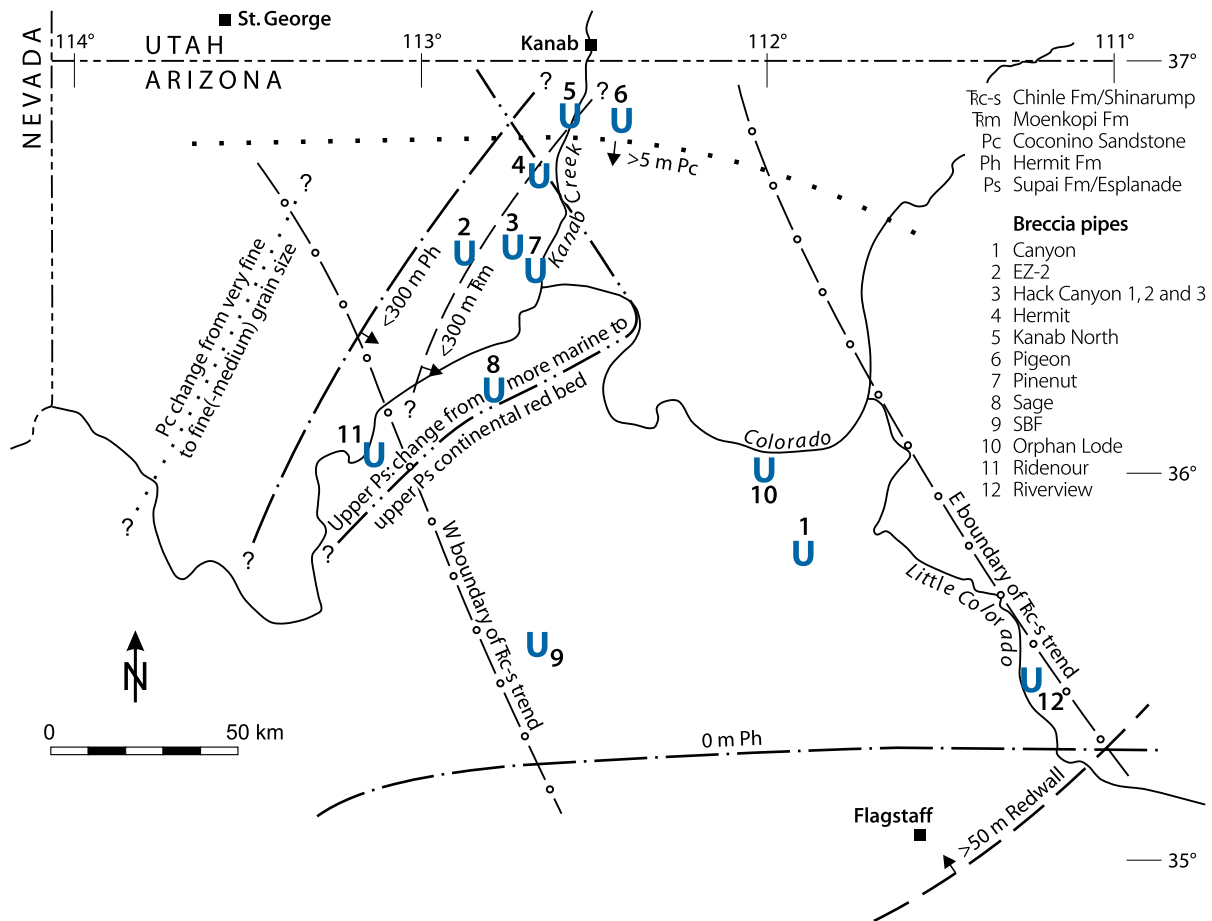
Billingsley et al. (1986) document that the paleosurface of the Redwall Limestone was eroded and incised by streams as much as 120 m deep. Karst development proceeded simultaneously with fluvial erosion creating underground caverns and sinkholes in the limestone. Sinkholes and caves proximal to stream channels were subsequently filled with terrestrial and marine sediments of the Surprise Canyon Formation. Some collapse terminated in early Pennsylvanian time, whereas at other sites collapse continued as evidenced by thickening and sagging of certain strata above individual collapse areas.

Pennsylvanian to Early Permian Supai Group: Composed of a red series of sandstone, mudstone, siltstone, and carbonate, this group is present throughout the Grand Canyon area. McKee (1982) has subdivided the group into four formations, the Watahomigi, Manakacha, Wescogame, and Esplanade. The *Watahomigi Formation* consists of carbonates and mudstones with little or no sandstone. The unit is some 100 m thick in the western Grand Canyon region and thins to about 30 m in the eastern part. In the western Grand Canyon region, there are numerous basal Supai channels exposed, which cut into the underlying Redwall Limestone. The channels average 300 m wide, and are 80–120 m deep. They are filled with conglomerate, sandstone, siltstone, and limestone in the upper part. The sandstone contains logs with weak uranium mineralization. The *Manakacha Formation*, some 100 m thick, is predominantly sandy with siltstone, mudstone, and carbonate. The *Wescogame Formation* comprises chiefly sandstone with minor carbonate and mudstone. In the western Grand Canyon region, the Wescogame changes into predominantly carbonate. The for-

Fig. 1.58.

Arizona Strip area, inferred distribution and thickness of Mississippian Redwall to Permian Coconino and Triassic Moenkopi and Chinle/Shinarump formations, and location of selected U ore-bearing breccia pipes. (After Karlstrom et al. 1974, McGee and Gutschick 1969, Mallory et al. 1972, and other unpublished sources)

(Stratigraphy: Rc-s; Chinle Fm/Shinarump Mbr; Rm Moenkopi Fm; Pc Coconino Sandstone; Ph Hermit Fm; Ps Supai Fm/Esplanade) (U ore-bearing pipes: 1 Canyon; 2 EZ-2; 3 Hack Canyon 1, 2, and 3; 4 Hermit; 5 Kanab North; 6 Pigeon; 7 Pinenut; 8 Sage; 9 SBF; 10 Orphan Lode, 11 Ridenour, 12 Riverview)



mation is 30–50 m thick and fills channels as much as 25 m deep incised into the underlying formation. The *Esplanade Sandstone* is dominantly a cross-stratified, fluvial to estuarine sandstone, with minor siltstone and mudstone in the central and eastern Arizona Strip area. The sands are high-energy deposits laid down along a strandline on the relatively flat surface of the Wescogame Formation. This surface is dissected by numerous small channels as much as 10 m deep. In the north-central and northwestern parts of the Arizona Strip area, bedded gypsum probably of lagoonal origin, is intercalated in the sandstone. The sand is thought to have originated from a source to the N to NW. It is 60–120 m thick, thickening to the NW and N to NE. In the western Arizona Strip area, the Esplanade Sandstone interfingers with the *Pakoon Limestone*.

Fossils and clay mineralogy indicate that the Watahomigi and Manakacha formations are marine in origin. The Wescogame and Esplanade formations are continental in the eastern Arizona

Strip area, whereas in the west they grade into marginal marine and marine facies.

Permian Hermit Formation (formerly Hermit Shale): Red and varicolored thin-bedded siltstone and silty sandstone containing 3–10% hematite. Sediments are fine- to very fine-grained, calcareous, micaceous, and commonly moderately to well sorted. The thickness of this formation varies considerably; it pinches out near Flagstaff, but achieves a thickness of up to 400 m in the western Arizona Strip area.

Permian Coconino Sandstone: Generally a fine-grained, light-colored, eolian sand composed almost entirely of well-rounded, mostly clear quartz grains with less than 5% feldspar and rock fragments, and less than 15% clay or carbonate matrix. Portions of this horizon are commonly yellowish to pale orange colored, whereas others are whitish to light yellowish or tan. Limonite specks and staining are common in outcrops. Cross-bedding, long parallel ripple marks, and occasional fossil

tracks are distinctive features of this unit. The Coconino Sandstone thins progressively from a maximum of 150 m along the Mogollon Rim in central Arizona to a thin tongue that eventually pinches out near the Arizona–Utah border. Toward the NW, it apparently changes into a more marginal marine, finer-grained facies.

Permian Toroweap Formation, 80–250 m thick: Composed of marine to littoral sediments, the Toroweap Formation is divided in ascending order into the Seligman, Brady Canyon, and Woods Ranch members. The *Seligman Member* comprises medium-bedded sandstone, siltstone, gypsum, and carbonate. Hydrocarbon impregnation is ubiquitous throughout the member. The *Brady Canyon Member* is composed of limestone, dolomite, and sandstone. Chert nodules and fossils are widespread constituents. Landais et al. (1989) suggests that this member is the source of hydrocarbons (oil, kerogen) found in the breccia pipes. The mostly marine kerogen has matured sufficiently enough to produce oil components. The *Woods Ranch Member* consists of a gypsiferous bed, limestone, and dolomite with some sandstone, partly deposited in intraformational channels. Where gypsum is depleted, the sandstone fraction increases.

Permian Kaibab Formation, 80–250 m thick in the Arizona Strip area and thickening to the W and NW: Representing the most widespread carbonate sequence of the Permian System in northern Arizona and adjacent Utah and Nevada, the Kaibab Formation includes two members. The *Fossil Mountain Member* consists of dominantly limestone, sandy limestone, and calcareous sandstone. Chert nodules, up to 25 cm in diameter, and fossils are common. The overlying *Harrisburg Member* is composed of gypsiferous layers, pinkish silt-sandstone, buff sandstone, chert, and some limestone beds. The sandy facies partly fills intraformational channels. Locally, gypsum and redbed facies are missing, as near Hack Canyon.

Lower Triassic Moenkopi Formation: Subdivided into many members of distinct lithologic character (Stewart et al. 1972), this mixed continental and marine sequence occurs widespread throughout most of the western Colorado Plateau. Its original thickness (now largely eroded) in the Arizona Strip area ranged from more than 500 m in the western-most part to about 100 m at the eastern boundary. In the eastern Arizona Strip area, it consists almost entirely of horizontally stratified siltstone, claystone, limestone, dolomite, and gypsum, which are attributed to six members, in ascending order, the *Timpoweap Member*, a red siltstone, grey limestone, and chert pebble conglomerate; the *Red Lower Member*, dominantly red siltstone; the *Virgin Limestone Member* composed of limestone and siltstone; the *Middle Red Member*, dominantly red siltstone; the *Shnabkaib Member* consisting of siltstone, gypsum, and limestone grading eastward into red siltstone; and the *Upper Red Member*, dominantly red siltstone.

Upper Triassic Chinle Formation: At the eastern and northern margin of the Arizona Strip area, outcrops of the continental fluvial *Shinarump Member* (av. 10 m, in channels >30 m thick), the lowest unit of the Chinle Formation, are found. The unit was formerly distributed in NW-oriented channel systems extending from the E and SE edge of the area to the NW. Most is now eroded. Shinarump channels at the eastern edge of

the area contain minable uranium deposits as in the Cameron district.

Late Miocene to Late Pliocene volcanics: Lava flows of mainly basaltic composition and subrecent cinder cones, such as Sunset Crater in the outskirts of Flagstaff erupted locally around 1064–1065 AD. A number of lava-capped buttes rise above the general landscape, and lava flows cover large areas of the southern part of the area. Diatremes and plugs formed during the Pliocene in the Hopi Buttes. No Phanerozoic plutonic rocks are known so far, and it is generally assumed that none exist.

Major *tectonic features* of the Arizona Strip area include blockfaulting (e.g. the Kaibab Uplift) and lineaments. The latter include the Grand Wash, Hurricane, and Toroweap faults, all trending generally N to NNE with the upthrown side to the east. Other less prominent fault systems strike NNW and NE.

Collapse Breccia Pipes

Collapse structures, called “collapse breccia pipes” or simply “breccia pipes,” occur in formations younger than Mississippian. Wenrich and Sutphin (1989) report that “thousands of solution-collapse breccia pipes crop out in the canyons and on the plateaus of northwestern Arizona.” Breccia pipes resulted from the roof collapse of caverns (paleokarst) in carbonate strata of the Mississippian Redwall Limestone. They should not be confused with diatreme pipes, which resulted from volcanic gaseous explosions. The generally circular collapse transgresses chimney-like upward into the overlying, essentially flat bedded sediments, from the Redwall Limestone as much as 1,200 m into the Permian Kaibab Limestone, and, locally, into the overlying Lower Triassic Moenkopi Formation or the Upper Triassic Chinle Formation. A pipe may outcrop at surface or may be blind (▶ Fig. 1.59).

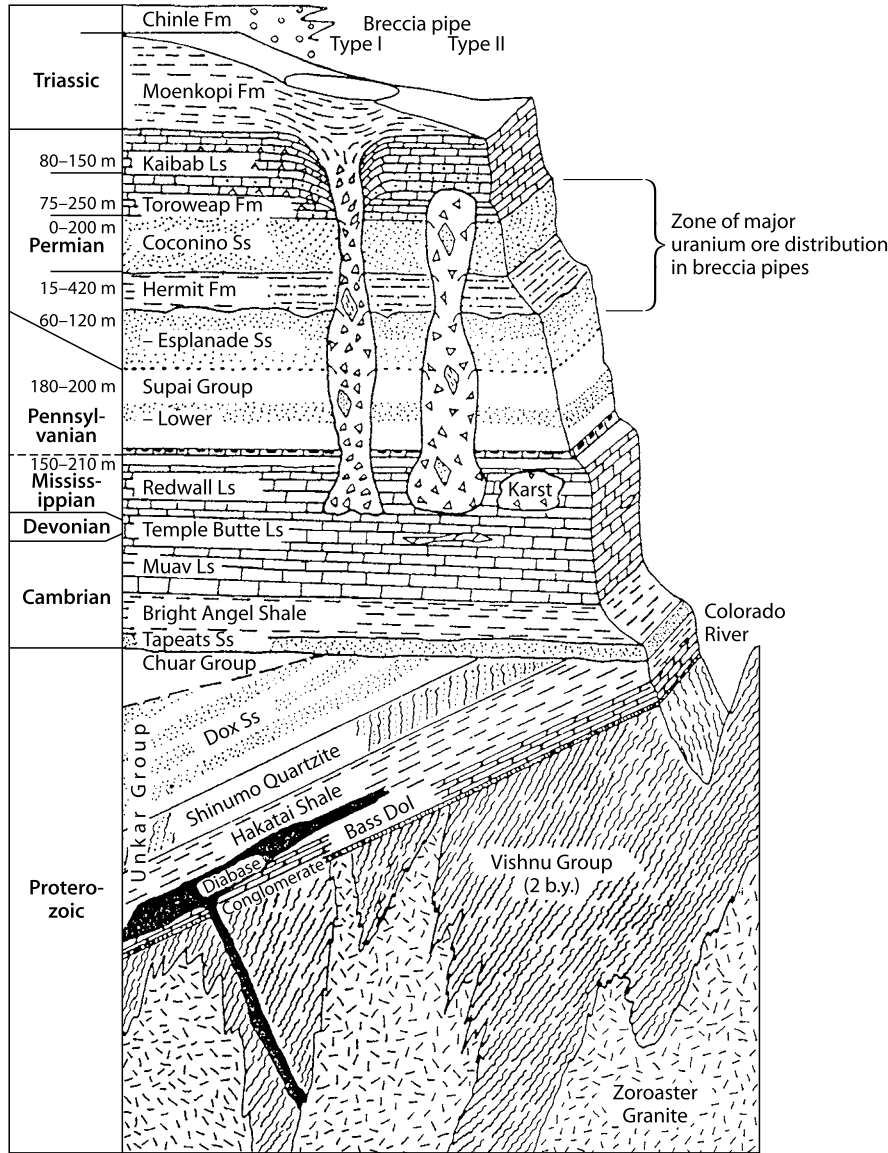
A breccia pipe consists of a throat from base to near surface, ranging in diameter from about 15 to 100 m or more, which widens to a collapse cone when the pipe stopped upward to the Kaibab or Moenkopi surface. In surface expression, these cones reach diameters of up to 750 m (EZ-2 pipe). The cone results from the dissolution of gypsum and other leachable material of the Kaibab and Toroweap formations causing a gradual thinning of affected strata toward the pipe throat as discussed in Chap. Principal Host Rock Alteration.

In contrast, a pipe, which does not outcrop but ends in the Fossil Mountain Member/Kaibab Formation, such as the Hack 2 pipe, has no associated solution cone. Holland (personal communication) points out, however, that the Hack 2 and the adjacent Hack 3 pipes are in a restricted sedimentological environment characterized by a lack of gypsum and redbed deposition in the Harrisburg Member as compared to other areas. At the EZ-2 pipe, for example, approximately 100 m of limestones and evaporites of the Kaibab and Toroweap formations have been removed by dissolution. Moenkopi sediments then downdropped and filled the cone up to 110 m thick at its center (Krewedl and Carisey 1986).

Breccia pipes are filled with a breccia, the fragments and matrix of which consist of downward displaced material made

Fig. 1.59.

Arizona Strip area, diagrammatic stratigraphic section and position of collapse breccia pipes. Type-I: outcropping, Type-II: blind. (After Holland, personal communication, stratigraphy after Breed and Roat 1976)



up of sediments from stoped formations. The amount of vertical displacement is variable in each pipe. It may be as much as 200 m as in the Kanab North pipe (Rasmussen, personal communication). A description of the breccia will be presented in more detail further in the following text.

No regional system of distribution or an affinity to surface exposed lithologic or structural features could be established to date to explain satisfactorily the location of breccia pipes at the sites where they are. There is circumstantial evidence, however, that pipes are structurally controlled, mainly by NW–SE and NE–SW fault systems or their intersection. This hypothesis would also explain why so many breccia pipes occur in or adjacent to canyons; the latter obviously follow major structures. An alignment of breccia pipes along NW and NE trends was noticed by Wenrich and Sutphin (1989); they document that fracture sets of these directions were imposed on the Redwall

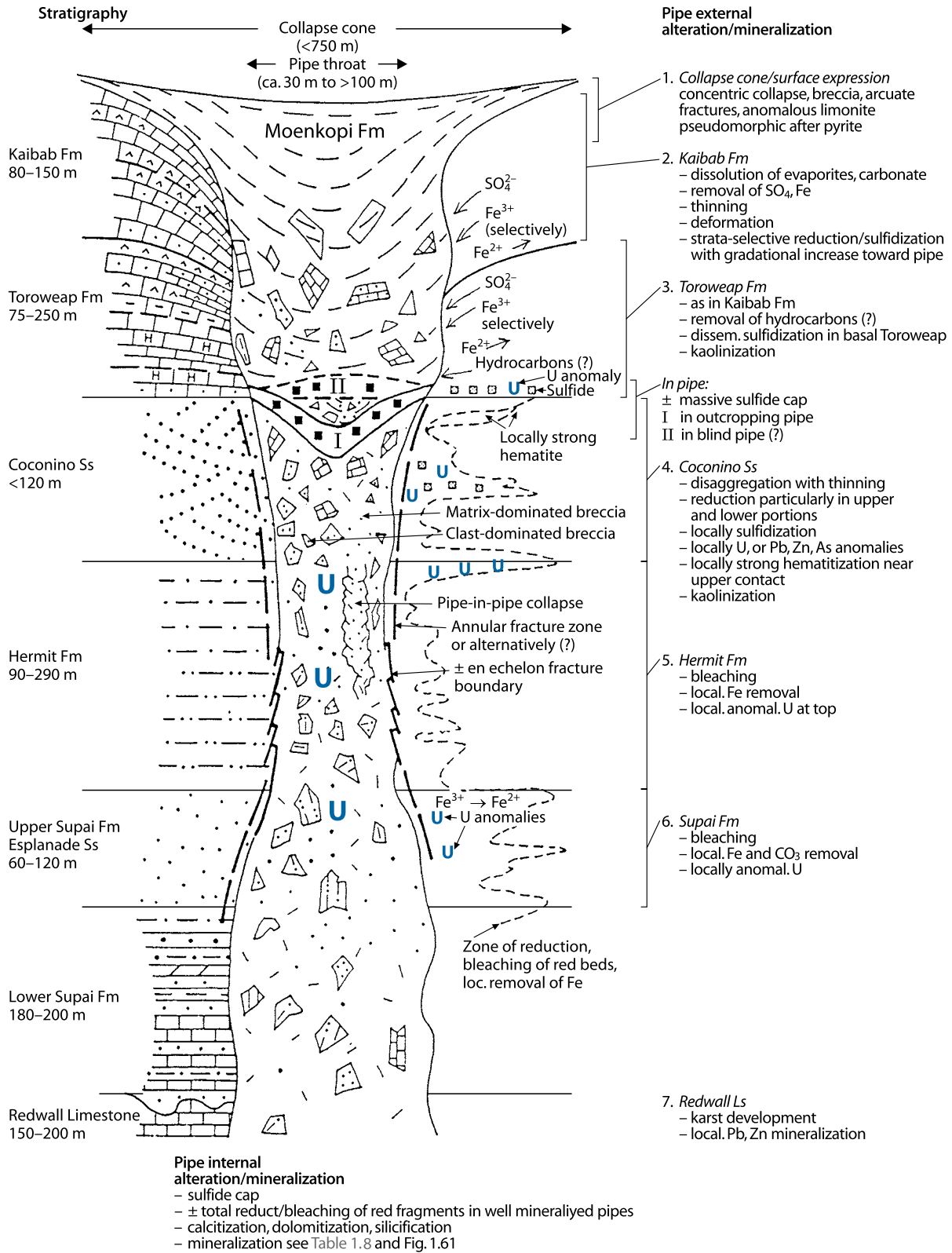
Limestone prior to the deposition of younger sediments. Ring fractures, encasing a breccia pipe, apparently also developed prior to jointing of Pennsylvanian and younger strata. The authors conclude that pre-Pennsylvanian NE and NW fracture systems apparently controlled groundwater migration during the Mississippian and exerted a significant impact on localization and development of karst in the Redwall Limestone and consequently on the site of breccia pipe stopping.

Principal Host Rock Alteration

A variety of alteration phenomena including metasomatism affected, either both or separately, pipe infill as well as strata peripheral to a pipe (Fig. 1.60). Most alteration processes tend to have been very mild although some produced striking color changes. Furthermore, it is not established which alteration pro-

Fig. 1.60.

Arizona Strip area, diagrammatic section of an outcropping breccia pipe with modes of alteration and mineralization, which may or may not be present.



cesses were related to mineralization and which developed during pipe formation itself.

Pipe infill alteration, which may be present to various degrees in different pipes, includes reduction, metasomatism, authigenic mineral formation, and late oxidation.

(a) **Reduction** of clasts and matrix is most visibly reflected by

- Bleaching of normally tan Coconino sandstone to a light grey
- Bleaching of red Hermit and red Esplanade/Supai material to grey or greenish-grey; including red, light grey, whitish-grey, and dark grey solution banding, forming subparallel, slightly arcuate, centimeters-wide bands grading into aligned nodules locally, and
- Sulfidization (mainly pyrite), forming massive sulfide caps in many pipes near the Toroweap-Coconino contact, and disseminating downward decreasing with depth.

Infiltrated hydrocarbons as well as other reducing agents may have reduced parts or all of pipe infill down to the Redwall Limestone. Hydrocarbons have accumulated particularly at the lowermost Toroweap Formation-upper Coconino Sandstone interval in the form of black buttons, commonly associated with the sulfide cap. Reduction preferentially affected both the matrix material and small-size clasts. Large, compact fragments, particularly of fine-grained material such as Hermit siltstone, may be reduced only in an outer shell, the interior remaining oxidized. Yet, in rich mineralized pipes such as Hack 2, large fragments can completely be reduced.

(b) **Metasomatism, desintegration, and authigenic mineral formation** include

- Ca-, Mg-, Fe-carbonatization; dolomitization is widespread except in ore zones, where calcitization prevails and Mg is depleted or was never introduced. Sideritization is a minor phenomenon. Carbonatization can produce a rock containing 30–50% carbonate instead of the original 90% quartz
- Desilicification by quartz grain destruction
- Silicification in the form of quartz overgrowth
- Gypsum and baryte formation and possibly the replacement of gypsum by baryte and/or anhydrite
- Kaolinitization (mainly in sandstone) and illitization (in shale and siltstone)
- Late and apparently mild oxidation reflected by limited destruction of pyrite with minor hematitization or limonitization.

These processes, or at least part thereof, resulted in the cementation of both rock fragments and pipe infill matrix.

Strata alteration peripheral to pipes are reflected in various stratigraphic units by the following phenomena:

Kaibab and Toroweap formations

- Dark grey coloration associated with sulfidization (mainly pyrite, up to a few percent) proximal to and within ca. 30 m of the pipe contact decreasing progressively outward. Pyrite

forms cubes up to about 1 cm, which weather to limonite or are dissolved leaving characteristic vugs or box works behind

- Some dolomitization of limestone (additional to diagenetic dolomitization)
- Locally in Toroweap Formation, the kaolinitization of montmorillonite–smectite
- Dissolution of gypsum, anhydrite, and carbonate, most notably in the evaporite-rich Harrisburg and Woods Ranch members. This process provokes a conical thinning of as much as 50% of the strata. Remaining rocks essentially consist of a vuggy, siliceous, and cherty solution breccia often with limonite and box work textures after pyrite near the pipe, grading outward into their progenitors. Dissolution progresses toward the pipe with strongest intensity near the pipe. As a result, affected strata dip inward toward the pipe with greatest dips near the center and a gradual decrease outward. Inclination also decreases with depth down to the Coconino level. Strata below the Coconino Sandstone are flat bedded. The magnitude of a solution cone is variable. Krewedl and Carisey (1986) note for the EZ-2 area a diameter of solution influence of ca. 750 m or ten times that of the pipe diameter. The maximum removal of ca. 100 m strata thickness extends over an area about 300 m in diameter.

Coconino Sandstone

- Light to dark grey coloration for several hundreds of meters away from the pipe contact; near the pipe contact (within ca. 10 m) associated with disseminated sulfide development and often radioactivity
- Locally, in the upper section of the unit, hematitization reflected by red–brown Fe oxides in minifractures and as dissemination in porous sandstone extending for several meters, rarely for a few tens of meters away from the pipe boundary
- Selective desilicification by quartz disintegration and removal for up to 10 m away from a pipe
- Silicification by quartz overgrowth
- Kaolinitization of matrix-bound montmorillonite–smectite
- Locally dolomitization forming a matrix of the sand.

Hermit Formation

- Bleaching of the normally brick-red strata to light grey colors along abrupt boundaries in response to hematite reduction for distances up to some 10 m away from a pipe
- Solution banding often gradational into bleached zones; bands are in the centimeter range, arranged almost parallel and consist of pyrite, hematite, or goethite/limonite
- Local removal of iron (up to 40% of assumed original amount)
- Local dolomitization or calcitization
- Some near-pipe concentration of U, Mo, and Cu.

Esplanade/Supai Formation

- Bleaching and grey coloration associated with sulfidization (disseminated pyrite).

Principal Characteristics of Mineralization

Heterogeneous ore mineralogy is typical for collapse-breccia pipes as documented by various authors and compiled in a state-of-the-art list by Wenrich et al. (1989). Pitchblende is the most frequent uranium mineral, locally coffinite. Minor amounts of U⁶⁺ minerals occur in \pm oxidized intervals. A series of associated minerals, but not necessarily paragenetic ones, are present in variable amounts including sulfides, arsenides, sulfoarsenides, locally oxides, carbonates, and sulfates of Cu, Co, Fe, Mo, Ni, Pb, and Zn. Traces of Ag, Au, Ba, Cd, Cr, Cs, Hg, Sb, Se, Sr, and V are also present (Table 1.7). The bulk of Pb in galena is non-radiogenic. Both, galena and sphalerite have characteristics comparable to Mississippi Valley-type mineralization (Rasmussen et al. 1986). Gangue minerals associated with mineralization are ankerite, baryte, calcite, collophane, chalcedony, dolomite, fluorite, quartz, siderite, and always as latest, anhydrite and gypsum, but mineral assemblages vary from pipe to pipe. The Orphan Lode and Hack pipes, for example, contain a large variety of ore minerals, whereas the Pigeon pipe has a more simple mineralogy (Rasmussen and Gautier, personal communication) (Table 1.8).

Wenrich and Sutphin (1989) distinguish three *paragenetic stages* of mineralization succeeded by a fourth, supergene stage (Fig. 1.61).

Stage 1 is characterized by the introduction of carbonate and sulfate and leaching of silica. Principal minerals are coarsely crystallized calcite, dolomite, and baryte, minor amounts of siderite, coarse, euhedral plates of kaolinite, and some anhydrite.

Stage 2 consists of Ni, Co, and Fe arsenides, sulfoarsenides, and sulfides including siegenite, bravoite, millerite, gersdorffite, niccolite, rammelsbergite, pararammelsbergite, arsenopyrite, and dominantly pyrite and marcasite. The minerals are small (<0.2 mm), often euhedral and commonly display zoning within individual crystals. The prevailing zonal assemblage starts with siegenite followed by bravoite and pyrite. A second less common zoned mineral phase consists of niccolite, pararammelsbergite, and rammelsbergite. The zoned minerals are embedded in carbonates and sulfates of stage 1.

Stage 3 represents the uranium/pitchblende phase with formation of Pb, Zn, Cu, Fe sulfides, and quartz and a second phase of calcite. Metallic minerals include bornite, chalcopyrite, chalcocite, djurleite, digenite, covellite, tennantite, enargite, galena, sphalerite, and late hematite. Some minerals occur in two or three generations. Pitchblende is present in at least two generations. Botryoidal pitchblende was precipitated in the coarse crystalline calcite matrix, in vugs, and as coatings on detrital quartz grains. This pitchblende generation is overgrown by sulfides, which also fill shrinkage cracks in pitchblende spheres. The second pitchblende generation partly encloses sulfides such as chalcopyrite and galena.

Stage 4 is characterized by supergene minerals formed by oxidation and remobilization. Locally, as in a breccia pipe exposed in the Mooney Falls Member of the Redwall Limestone west of Peach Springs Canyon, rare secondary minerals such as powellite, tyuyamunite, conicalcalcite, talmessite, and hoernesite

associated with hematite, dolomite, and ankerite have been identified by Wenrich and Sutphin (1989).

Rasmussen et al. (1986) note for the Hack Canyon pipes an approximate paragenetic sequence of quartz + carbonates, followed by baryte, sulfides + sulfoarsenides, pitchblende, sulfides, carbonates, and quartz. These authors also report from the Hack Canyon pipes additional jordisite and state that, in contrast to the Orphan Lode, sphalerite crystallized early in the paragenetic sequence. In these pipes, pitchblende occurs as veinlets and stringers in fractures, both within the pipe and in an annular ring closely surrounding the pipe, as pseudo-stratiform mineralization in permeable sandstone blocks, and predominantly disseminated in irregular masses in mainly sandy matrix within the reduced, highly brecciated interior of the pipes. Ore-hosting lithologies have derived from strata ranging from the Seligman Member/Toroweap Formation to the Esplanade/Supai Group.

When present, uranium is distributed through large portions of the pipes with values above background, whereas ore-grade material is generally concentrated in sections filled with permeable sands. These particular sections are located, within the pipe, just below the Coconino-Hermit contact from the stratigraphic pile forming the “wall rock,” or just below the Hermit-Supai boundary.

Sulfides occur disseminated in variable amounts within the whole pipe, from the Kaibab Formation level at the top, down to the lower Esplanade Sandstone level/Supai Formation. Pyrite content ranges from less than 1% to a few percent outside uranium-bearing zones. In ore zones it increases up to 15%.

A particular concentration of sulfides is presented by a *sulfide cap* that is composed of up to 80% pyrite and marcasite, and located above the uranium ore, at a level corresponding to the stratigraphic Toroweap–Coconino contact. The sulfide cap is found in many ore-bearing pipes (e.g. in Hack 1, 2, and 3), yet it is missing in others. The thickness of the sulfide cap ranges from 3 to 15 m within a pipe, thinning to less than one meter just outside the pipe (for more details of mineralization, see description of selected pipes).

Strata-bound (pipe-unrelated) sulfides are ubiquitous in the Kaibab and Toroweap formations, in which they account for less than 0.5% of the rock mass, and never more than 1%, except in the occurrence earlier mentioned proximal to a pipe.

A characteristic constituent of at least the ore-bearing breccia pipes, although present in variable amounts, is altered organic matter described by Landais (1986) as kerogen, fluid oil, oil impregnation, solid black bitumen, and hydrocarbons in fluid inclusions. Both, oil and bitumen are highly altered by water washing and biodegradation. Highly insoluble bitumen, associated with pyrite, is derived by oxidizing and sulfate-reducing bacteria and the influence of both brine and meteoric waters (established in fluid inclusions). Pratt (in Wenrich and Sutphin 1989) analyzed in black, glassy, hydrogen–sulfur-rich pyrobitumen 85.6% C, 3.74% S, and 50 ppm Ba, 3 ppm Cr, 50 ppm Ni, 50 ppm Pb, 100 ppm V, 15 ppm Zr, and 70 ppm Si. The pyrobitumen never experienced temperatures in excess of 150°C but has been intensely altered.

Table 1.7.

Arizona Strip area, chemical analyses of breccia pipe samples. (After Wenrich and Sutphin 1989)

Element	Ore-grade breccia pipes			Orphan Lode	Ridenour mine	Chicken mine	Copper Mountain mine	Apex mine	Mohawk Canyon pipe
Al ₂ O ₃ %	1.27	5.18	1.68	1.27	–	0.416	2.84	0.37	5.06
C inorg %	0.17	0.01	11.2	1.29	0.01	3.07	7.01	0.21	0.02
C org %	0.02	2.76	0.10	3.70	<0.01	0.19	0.88	0.10	0.13
C total %	0.19	2.77	11.3	4.99	<0.01	5.39	7.89	0.31	0.15
CaO %	1.30	0.53	30.4	16.8	–	13.2	19.6	0.35	0.02
K ₂ O %	0.64	1.23	0.28	0.53	–	0.11	0.92	0.04	0.90
MgO %	0.22	0.40	15.5	5.48	–	0.22	11.5	0.16	0.20
Na ₂ O %	0.36	0.46	<0.15	0.04	–	0.01	0.72	0.25	<0.15
P ₂ O ₅ %	0.05	0.33	0.09	0.01	–	0.01	0.08	<0.10	<0.05
SiO ₂ %	81.4	54.0	7.26	–	–	–	28.7	3.71	83.2
LOI	4.05	14.6	41.1	–	–	–	30.4	15.0	5.02
Ag ppm	40	49	<1	9	20	13	36	<2	<2
As %	0.44	0.35	0.0017	0.12	0.21	0.019	0.046	1.4	0.14
Au ppm	<8	<8	0.1	<8	<0.05	10	34	0.1	<8
Ba ppm	360	16	455	140	904	9	94	260	180
Be ppm	<1	7	<1	<1	14	<1	<1	<1	<1
Cd ppm	40	23	<2	<2	<4	950	420	49	<2
Ce ppm	325	58	11.5	12	106	<4	19	9	12.6
Co ppm	8.94	310	14.5	99	202	69	333	9000	19.5
Cr ppm	10	170	8.02	14	18.3	11	23.8	18	28.1
Cs ppm	69.9	–	<1	–	8	–	1.53	–	1.57
Cu %	1.2	0.26	0.016	2	0.55	0.032	0.22	4.6	0.0036
Eu ppm	1.29	40	0.29	<2	13.4	<2	0.91	<2	0.2
F %	0.01	0.09	0.04	0.02	0.02	0.02	0.03	–	0.02
Fe ₂ O ₃ %	3.74	14.5	2.17	4.0	–	1.19	1.63	67.7	5.22
Ga ppm	<40	27	5	14	<8	<4	5	240	5
Hf ppm	21.8	–	1.03	–	0.31	–	3.42	–	5.35
Hg ppm	0.5	1.1	0.03	–	0.16	0.58	15	–	0.06
La ppm	312	25	5.1	6	4.42	<2	10.8	3	8.35
Li ppm	10	33	35	11	40	<2	7	3	11
Lu ppm	–	–	0.06	–	1	–	0.18	1	0.13
MnO %	21	0.02	0.22	0.0221	–	–	0.08	0.13	<0.02
Mo ppm	80	820	6	26	260	4	35	460	29
Nb ppm	5	–	<4	–	26	–	5	–	–
Nd ppm	140	56	6.34	11	100	<4	13.8	<4	5.79

Table 1.7. (Continued)

Element	Ore-grade breccia pipes			Orphan Lode	Ridenour mine	Chicken mine	Copper Mountain mine	Apex mine	Mohawk Canyon pipe
Ni ppm	60	1300	12	150	520	22	560	3500	90
Pb %	0.33	0.17	0.044	0.029	0.42	0.58	0.12	0.16	0.011
Rb ppm	–	–	8.21	–	128	–	21.2	–	24.5
S total %	4.13	12.8	<0.01	2.47	0.01	0.02	0.03	0.06	3.7
Sb ppm	15.8	–	0.55	–	2.89	–	1.84	–	1.48
Sc ppm	1.53	25	1.39	<2	6.83	<2	2.15	<2.0	1.93
Se ppm	29	9.8	<0.1	–	6.8	1.2	78	–	3
Sm ppm	–	–	1.34	–	39.4	–	3.75	–	1.12
Sr ppm	110	460	200	46	290	150	140	150	90
Ta ppm	<0.71	<40	0.13	<40	<0.45	<40	0.24	<40	0.3
Tb ppm	0.99	–	<20	–	5.7	–	0.48	–	0.15
Th ppm	1.16	<4	1.42	<4	4.84	<4	2.09	<4	1.93
TiO ₂ %	0.09	0.28	0.36	0.67	–	0.01	0.16	0.04	0.2
U %	1.21	0.95	0.34	1.0	0.31	0.01	0.0027	0.0029	0.0024
V ppm	20	3900	48	7	4000	15	67	21	21
Y ppm	30	110	12	12	72	3	13	5	3
Yb ppm	2.04	13	2	–	8.1	<1	1.08	<1	0.82
Zn %	0.7	0.56	0.0029	0.011	0.015	10	2.87	2.7	0.0018
Zr ppm	–	–	37	–	720	–	–	–	110

General Shape and Dimensions of Deposits

Although 40–50 U-mineralized pipes have been found to date, only about 15 pipes contained minable ore (>0.3% U, >500 t U). Resources in minable breccia pipes range from several hundred to about 2,000 t U at grades averaging 0.3–0.7% U or even more. Silver, copper, and vanadium are recoverable from some of the uranium breccia pipes.

Collapse-breccia pipes are nearly circular, vertical to steeply inclined or, rarely, curved, and chimney- to hourglass-like in shape. The diameter of the pipes is often constricted through the Hermit Shale interval, and wider in the Toroweap, Kaibab, and Supai intervals, which possibly reflects a different behavior of these units to the collapse process. The peripheral boundary of a pipe is mostly, though not everywhere, sharp. In some places, it is defined by a set of concentric fractures (the annular ring), which surround a zone of sheared and brecciated host rocks that grades into the pipe-filling breccia.

Pipe diameter average from 15 to 100 m or more (minimum ca. 30 m for a minable pipe) varying according to the dissected rock facies and perhaps the magnitude of the original cavern in the Redwall Limestone. The vertical extension can be as much as

1,200 m depending on the local thickness of strata between Mississippian and Triassic formations. U ore bodies are generally found below the elevation of the Coconino Sandstone, i.e. at depths from 200 to 600 m, unless they are exposed in a canyon wall as a result of erosion.

Regional Geochronology

The age dating of pitchblende from the Orphan Lode mine yields a minimum age of 141 Ma, i.e. a late Jurassic age (Miller and Kulp 1963). Krewedl and Carisey (1986) report U–Pb ages of 184 and 165 Ma for ore from the EZ-2 pipe.

U–Pb isotope dating of uranium ore by Ludwig et al. (1986) and subsequently by Ludwig and Simmons (1992) indicates two major periods of uranium mineralization: (a) 200 ± 20 Ma for the *Hack 2* and *3*, *Kanab North*, and *EZ 1* and *2* ore, which is roughly time equivalent with ages inferred for strata-bound U deposits hosted in late Triassic strata in southern Utah and northern Arizona; and (b) at about 260 Ma as indicated for the *Canyon* and *Pinenut* pipes. Age determinations of ore from the *Pigeon*, *Orphan*, and *Arizona-1* deposits yield results suggesting

Table 1.8.

Arizona Strip area, ore minerals of selected breccia pipes

Mineral/Breccia pipe	Hack	Pigeon	Orphan	Canyon
Arsenopyrite	x		?	
Bornite		x	x	x
Bravoite	x	x	x	x
Chalcocite	x		x	x
Chalcopyrite	x	x	x	
Cinnabar			x	
Clausthalite	x		x	
Cobaltite			x	
Coffinite			x	
Covellite	x	x	x	
Digenite			x	x
Enargite (Luzonite)	x	x		
Galena	x	x	x	x
Gersdorffite	x	x	x	
Hematite	x		x	
Ilsemanite	x			
Jordisite	x			
Marcasite	x	x	x	
Millerite	x			
Pitchblende	x	x	x	x
Proustite			x	
Pyrite	x	x	x	x
Rammelsbergite			x	
Siegenite	x		x	
Skutterudite			x	
Sphalerite	x	x	x	
Stibnite			x	
Violarite		x		
Tennantite-tetrahedrite	x	x	x	

Orphan Lode: Gornitz & Kerr 1970, Koford 1969; Hack, Pigeon, Canyon: Rasmussen JD and Gautier AM, pers. inform.)

that these deposits were apparently mineralized before 220, 186, and 169 Ma, respectively, but no useful upper age limits can be inferred.

Ludwig et al. (1986) address the problem involved in establishing reliable ages for ore in breccia pipes. They note that determinations by the U–Pb isotope method is hampered by (a) the pervasive and continuous open-system situation affecting both Pb and radioactive isotopes of uranium, and (b) the presence of large quantities of common Pb, isotopic ratios of which are significantly variable.

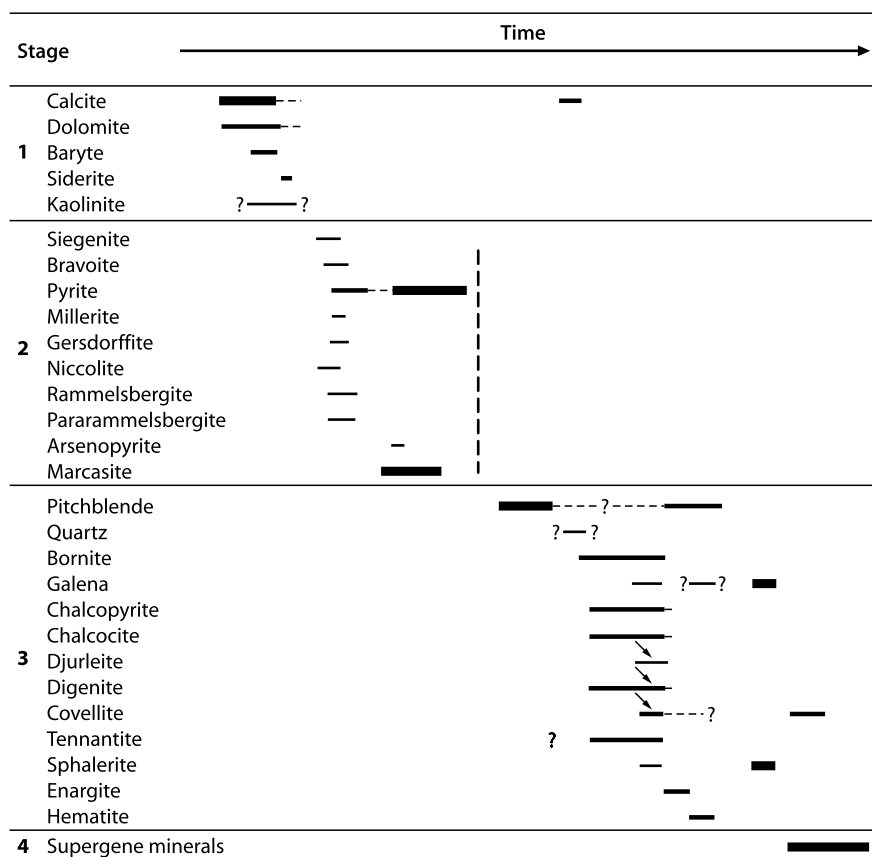
Fluid Inclusions and Stable Isotopes

Homogenization temperatures and salinities of fluid inclusions from selected pipes yield the following values:

- Gypsum, anhydrite, calcite, sphalerite: 54° to 125°C (average 90°C) (Landais in Krewedl and Carisey 1986)
- Calcite, dolomite, sphalerite: 80° to 173°C (salinity >9 wt% eq. NaCl with most common values >18 wt% eq. NaCl), primary inclusions in sphalerite indicate filling temperatures

■ Fig. 1.61.

Arizona Strip area, paragenetic sequence for minerals in breccia pipes (*hatched vertical line indicates fracturing of pyrite*). (After Wenrich and Sutphin 1989, Rasmussen and Gautier, personal communication)



of 80° to 100°C and secondary inclusions 103–173°C (Wenrich and Sutphin 1989)

- Sphalerite from *Hack 1* and 2: 93° to 115°C (salinity 9.9–18.4 wt% eq. NaCl) (Rasmussen et al. 1986)
- Calcite in vugs in Harrisburg Member distant of any known pipe: 53° to 60°C (Wenrich and Sutphin 1989)
- Quartz in vugs in silicified breccia (*Blue Mountain* pipe, no ore): 91° to 107°C and 256° to 317°C (high T probably due to young volcanism <1 Ma); late stage quartz unrelated to mineralizing event: 81° to 90°C (salinity 1.4–5.5 wt% eq. NaCl) (Wenrich and Sutphin 1989).

Based on fluid inclusion studies on samples from the *Orphan*, *Hack 2*, *Kanab North*, and *Cunningham* pipes, Behr HJ (in Adamek et al. 1990) identified the following fluid systems:

System (a) represents the earliest fluid system in breccia pipes and occurs in healed microfractures that had formed posterior to the emplacement of detrital grains, and in quartz overgrowths. This fluid system is of higher temperature (homogenization temperature T_h : 250 to >350°C), hypersaline (melting temperature T_m : -28 to -35°C) with a complex composition of NaCl + KCl + CaCl₂, and contains CO₂. Some fluid inclusions attest to critical homogenization and boiling conditions, which caused a complete separation of CO₂ from solution.

System (b) is apparently the most significant volumetrically and persistent fluid system in breccia pipes. It consists of primary inclusions in dolomite and sphalerite, and secondary inclusions in quartz and microfractures. Fluids have a simple composition characterized by NaCl, a medium salinity (T_m : -10 to -23°C) with T_h between 120 and 160°C.

System (c) is a late, low-saline fluid system (T_m : 0–3°C) with T_h between 50 and 120°C.

System (d) is a pure CO₂ system released by H₂O–CO₂ fluids.

Mixed systems composed of fluids (b) and (c) and CO₂ are found at the intersection of microfractures and at the margin of grains.

Lead isotopes

Galena with non-radiogenic lead has Pb₂₀₆/Pb₂₀₄ ratios greater than 19, and Pb₂₀₈/Pb₂₀₄ ratios greater than 38 comparable to Mississippi Valley-type mineralization. Approximately 1,800 Ma old basement rocks are the assumed source of lead (Ludwig, personal communication).

Sulfur isotopes

δ³⁴S values in breccia pipes are -3 to -20, and in non-mineralized Kaibab and Toroweap sediments +12 to +14 (Adamek, personal communication).

Potential Sources of Uranium

No viable uranium source is established as yet, but it is thought that potential uranium sources may have existed in (a) crystalline Proterozoic basement underlying the Arizona Strip area, (b) crystalline Proterozoic rocks already outcropping in Triassic time in the Mogollon Highland at the southern margin of the Colorado Plateau, (c) fluvial channel sediments of the lower Chinle Formation of Triassic age, which covered as a NW–SE belt part of the Arizona Strip area, (d) fluvial sediments of the Jurassic Morrison Formation distributed to the E and NE of the Arizona Strip, and/or (e) altered volcanics forming the bentonitic component in the Petrified Forest Member of the Chinle Formation.

Principal Ore Controls and Recognition Criteria

Breccia pipe-hosted uranium ore bodies may be best defined, although with restrictions, as a special case of tectonic-lithologically controlled U deposits. Uranium occurs (a) in a fracture-controlled mode both within the pipe breccia, and in an annular ring closely surrounding the pipe and (b) as pseudo-stratiform mineralization in permeable sandstone blocks or as dissemination in the sandy matrix of the pipe infill.

The principal recognition criteria of uranium ore-bearing breccia pipes, which may or may not be ore-controlling parameters are as follows (for references see previous text).

Mineralization

- Principal U minerals are pitchblende with minor coffinite
- Associated metallic minerals include sulfides, arsenides, sulfoarsenides, locally oxides and sulfates of Co, Cu, Fe, Mo, Ni, Pb, and locally, mostly in traces, Ag, Au, Sb, and V
- Principal gangue minerals include Ca–Mg–Fe carbonates, Ba and Ca sulfates and phosphates, and Si-oxides
- Mineralization is present in three main stages
- Galena in U-bearing pipes generally has a distinct Pb isotope composition as compared to that in barren pipes and non-pipe sulfides in the region
- Galena (non-radiogenic Pb) and sphalerite show features comparable to Mississippi Valley-type Pb–Zn mineralization
- Irregular aggregates of degraded, vitreous organic substances are abundant in some pipes, notably Pigeon
- Ore minerals/elements occur in highly variable quantity and distribution from pipe to pipe
- Ore-bearing pipes commonly have a massive sulfide (pyrite) cap located at and/or below the Toroweap–Coconino stratigraphic contact.

Alteration

- Bleaching (common at all pipes)
- Pyritization (common)
- Dolomitization (common but variable intensity)
- Calcitization (variable)
- Gypsum/anhydrite formation (variable, locally none)

- Silicification (minor)
- Desilicification (common)
- Mg-depletion (dedolomitization) (locally in ore zones).

Stratigraphic interval of breccia pipe setting

- From Mississippian Redwall Limestone upward through Pennsylvanian–Permian Supai Group, Permian Hermit, Coconino, Toroweap and Kaibab formations, locally into the Lower Triassic Moenkopi and rarely into the Upper Triassic Chinle formations
- Not all pipes dissect the full stratigraphic interval but may end blind in the Toroweap or the Kaibab Formation.

Breccia pipe configuration

- Vertical to steeply inclined, sometimes slightly curved structure of pipe to hourglass shape, circular to oval in planview, as much as 1,200 m deep
- Constriction of pipe through the Hermit Formation (ferruginous siltstone) to as much as half the diameter (ca. 20–60 m) within overlying (arenaceous and carbonatic) and underlying (arenaceous, pelitic, and carbonatic) strata
- Gradual increase of pipe diameter upward through Coconino, Toroweap, Kaibab interval, flaring up to 150 m at upper termination or outcrop, and downward through the Supai Formation to as much as 120 m
- Surface expression of pipes, persistent up into the Moenkopi Formation, is a circular conical depression up to 750 m in diameter, and as much as 100 m deep filled by downdropped Moenkopi sediments
- Strata above the Coconino Sandstone dip pipe-ward due to concentric, centripetal removal of evaporitic and calcareous constituents of the Toroweap and Kaibab formations
- Pipes are bordered by concentric fractures (annular ring fractures) (e.g. *Orphan*) or by steeply outward inclined sets of fractures interconnected by flat inward dipping fractures (e.g. *Pigeon*).

Lithologies of pipe infill

- Intrapipe breccia consists of angular to rounded rock fragments ranging in size from a few millimeters to several meters, embedded in a matrix derived both from the peripheral host strata and overlying formations
- Any given section can be clast dominant (versus matrix) or matrix dominant although large fragments are most frequent near the pipe boundary
- Clasts in mineralized sections of most pipes consist of more or less silicified or carbonate-cemented and reduced Coconino, Hermit, minor Toroweap, and Esplanade/Supai material (e.g. *Hack 1, 2, 3, EZ-2, Orphan, Canyon*). Clasts in pipes in the northern part of the Arizona Strip, where the Coconino Sandstone pinches out, are chiefly derived from the Hermit, Toroweap, and Fossil Mountain/Kaibab formations with very minor Coconino Sandstone (*Pigeon, Kanab North*)
- Mineralized matrix ranges from (a) reduced Coconino- or Esplanade-derived sand and Hermit-derived silt/sand,

loosely to strongly cemented by clay, sericite, calcite, gypsum, and/or anhydrite (*Hack, Orphan*) to (b) Hermit- and Toroweap-derived silt/sand cemented by clay, sericite, dolomite, and/or calcite (*Pigeon, Kanab North*). The first variety is of good porosity and permeability, whereas the latter is of lower permeability

- Ubiquitous altered hydrocarbons (pyrobitumen etc.) occur in all ore-bearing pipes although in highly variable quantities. The highest concentrations commonly occur at the lower Toroweap to upper Hermit stratigraphic intervals.
- In mineralized levels, clasts are pale tan or light grey to whitish due to bleaching and reduction, and matrix material is pale tan to light grey and dark grey. At depth, only the outer shell of clasts may be bleached, whereas the interior retains the original color, e.g. tan to red for Hermit and Esplanade fragments. Locally, a transition zone of grey and red solution banding is found
- Pipe infill may be a structurally simple though heterogeneous assemblage of downfaulted material from stoped strata or it may show a more complex structural zoning of material repeatedly displaced by selective internal subsidence forming “pipe in pipes”
- Vertical displacement of pipe fill ranges from near zero at the pipe boundary to more than 200 m in “pipe in pipe” sections.

Mineralized pipe intervals/ore-hosting lithologies

- Uranium ore persists intermittently in irregular ore bodies over a vertical interval of as much as 270 m (at *Canyon* at depth from 270 to 540 m) from the Coconino Sandstone stratigraphic level downward into the middle Supai Formation level
- Ore grade mineralization occurs in lithologic zones of favorable permeability that are a function of pipe-fill material and structure. Favorable hosts are the following:
 - loosely packed matrix material of dominantly sandy composition
 - porous sandy or vuggy, silty-sandy, rarely calcareous clasts
 - fractures, joints, or fissures within the pipe breccia or along the annular ring. Near these structures, uranium may impregnate tongue-like into permeable wall rocks
- Most favorable host for disseminated mineralization is partially or uncemented, medium- to fine-grained sand derived from the Coconino Sandstone, the Esplanade Sandstone, and, to minor degree, sand-siltstone from the Hermit, and lower Toroweap formations. In the latter case, however, mineralization is more fracture-hosted than in purer sands
- Most frequent stratigraphic intervals peripheral to U ore zones within the pipe are
 - at and below the Coconino-Hermit contact (e.g. *Hack, Kanab North, EZ-2* and *Canyon*)
 - within the Hermit interval (*Pigeon, Kanab North, Pinenut, Hack, EZ-2, Orphan*)
 - at and below the Hermit-Esplanade/Supai contact (*Orphan, Pigeon, Kanab North*).

- Uranium ore distribution in selected breccia pipes includes the following traits:

- *Orphan Lode*: (a) in fissures and fractures of the annular ring around the pipe border in siltstone from the middle Hermit to the middle Supai interval, (b) as irregular masses within the pipe at the lower Hermit to middle Supai interval, particularly as dissemination in the relatively porous, more or less (post ore?) carbonate-cemented neo-sandstones of the Coconino-derived matrix, but locally also in fractures and faults, (c) highest grades (>1% U) are in the upper part of the pipe at the top of the Supai interval, the center of the pipe, and a heavily brecciated zone at the northern pipe boundary (siltstone and claystone breccia clasts are not mineralized) (see later [Fig. 1.62a](#))
- *Hack 1*: disseminated and fracture filling in Coconino-derived sands beginning at the periphery of the pipe adjacent to the Hermit and dipping toward the pipe center. Hermit-derived breccia material (siltstone) on the same elevation as the ore is unmineralized, its fragments are largely still red in their interior and only their rims are bleached
- *Hack 2*: disseminated and minor fracture-controlled ore occurs in mostly Coconino Sandstone-derived matrix sands in the pipe center, through the upper and lower Hermit Shale interval
- *Pigeon*: ore is in fractured and jointed Hermit-, Toroweap-, and Kaibab-derived silt-sand matrix located in the “pipe in pipe” structure and in fractures at the pipe contact within the middle and lower Hermit and upper Supai interval
- *Kanab North*: ore is in similar material as in Pigeon but distributed between the lowermost Toroweap and upper Supai intervals.

Metallogenetic Concepts

Metallogenetic considerations have to take into account (a) litho-stratigraphic and hydrodynamic conditions required to generate breccia pipes, (b) sources for ore-forming components, (c) conduits for mineralizing solutions, and (d) processes to activate the required mobilization, migration, and interaction of ingredients involved in pipe and ore formation. Required conditions include

- A sequence of flat-lying sediments including permeable and impermeable lithologies
- Presence of a basal limestone layer affected by paleo-hydrologic regimes to develop karst structures with large cavities
- Adequate structural systems, e.g. sets of joints or shears, to permit karst development and collapse of cavities associated with stoping of chimney-like breccia pipes in flat-lying sediments
- Psammitic strata providing porous and transmissive pipe-fill material in a volume and consistency to host ore bodies. The

best candidates are continental or littoral arenaceous facies of sufficient thickness

- Transmissive systems/conduits to permit the migration of mineralizing fluids and other hydrochemical agents required for ore formation, and to pass fluids to the optimum site of ore emplacement
- A thick sequence of relatively impermeable sediments completely enclosing the breccia column, such as siltstones and mudstones, in order to contain the mineralizing fluids in the pipes, and prevent their loss or dilution in the surrounding sediments
- A source of uranium capable to supply the U amounts needed for forming economic ore grades and resources
- A source of reducing agents and other ore associated components such as S, SO₂ (perhaps originating from decomposition of gypsum), Fe²⁺, hydrocarbons a.o. supplying the essential elements to create a reducing environment within any pipe
- Adequate permeability as the principal factor controlling the emplacement of ore-forming minerals in breccia columns
- Sufficient porosity and space for accumulating viable ore bodies
- Distinct epeirogenic, geohydrologic, and climate-dependant conditions to generate the necessary processes for leaching, transport, and concentration of elements involved in ore formation.

Regional litho-stratigraphic constraints on the formation and distribution of uranium ore-bearing breccia pipes.

Individual stratigraphic units of the Arizona Strip area may have contributed in a positive or negative way to the above requirements. Their parameters permit tentative delineation of a potential area of U ore formation based on information by authors listed earlier as follows (► Fig. 1.58):

Redwall Limestone

- Sufficient thickness of the carbonatic unit is required for formation of karst caverns large enough to initiate stoping of pipes of adequate size. Assumed minimum thickness of the karst unit in the Redwall Limestone is ca. 25 m, which is present throughout the Arizona Strip area
- Zones affected by strong karst development (controlled by fracture sets oriented NW–SE and NE–SW according to Wenrich and Sutphin 1989)
- Redwall sediments may have provided a source of Pb, Zn, and other metals for the pipe mineralization.

Upper Supai Formation/Esplanade Sandstone

- Arenaceous redbed strata with minor siltstone–mudstone beds may provide both permeable pipe infilling and rocks for annular ring ore
- Red beds constitute a potential source of Fe for Fe–sulfide formation in the pipe
- Distribution of favorable lithology: to the E of a line trending about NNW–SSE on the N side of Grand Canyon and

running somewhere between the Kanab Creek and the Hurricane Fault; south of Grand Canyon the line turns SW near Peach Springs Canyon. Westward of this line, the Esplanade grades into the marine Pakoon Limestone.

Hermit Formation

- Dominantly ferruginous siltstones are commonly unfavorable hosts for disseminated mineralization unless they become more sandy, as appears to be the case in some northern segments of the Arizona Strip area, or where they are jointed and fractured. The annular ring and other pipe-bounding faults within the Hermit interval are good ore hosts
- Where too thick and too fine-grained, silts may more or less seal the interior of breccia pipes, particularly those pipes with small diameters, hence hampering the circulation of mineralizing fluids
- The unit represents a potential source of Fe
- Distribution: the Hermit thickens from a 0 isopach near Flagstaff to the N and W with a thickness of 120 m at the south rim of Grand Canyon, ca. 200 m at Pigeon and EZ-2, and ca. 300 m at Andrus Canyon.

Coconino Sandstone

- This fine- and locally medium-grained quartzose sandstone provides the most important host material for disseminated mineralization in many pipes
- The minimum thickness for providing sufficient host material for ore-bearing pipe fill is estimated to be 5–10 m
- Zones of limited consolidation at the time of pipe formation would have permitted the flow of larger amounts of sands into the pipe (sometimes indicated by concentric thinning around pipes)
- Non-cemented zones could have served as conduit for mineralizing fluids
- Distribution: the northern limit of the Coconino Sandstone is along a more or less E–W-trending 0 isopach running about 10–30 km S of the Arizona–Utah state line, turning SE on the Paria Plateau. The Coconino thickens southward to about 25 m in the Hack Canyon area, 75 m at the Orphan Lode, and 120–150 m in the Red Butte area. The grain size apparently decreases in the western part of the Arizona Strip along a transition zone, which is more indicative of a marginal marine than a continental environment of deposition.

Toroweap and Kaibab formations

- Much of the soluble material of the two formations has been leached concentrically around breccia pipes and parts thereof certainly entered the pipe
- Interbedded arenaceous facies, which become more abundant from about Kanab Creek eastward, may have been the source of ore-hosting sand and silt pipe infill (e.g. in Pigeon and Kanab North)
- Evaporitic gypsiferous beds are a potential source of sulfur (all sulfide caps in pipes are at the lower Toroweap interval)

- Hydrocarbons are abundant in the two lower Toroweap members and are considered to be candidates for reducing agents in breccia pipes; in addition, two oilfields in SW Utah produce from the Kaibab Formation
- Distribution: both formations occur throughout the Arizona Strip area, with typical marine sediments to the W and some littoral influence to the E.

Moenkopi Formation

- Pelitic to semipsammitic, partly calcareous sediments of this formation probably formed a rather impermeable cover over most of the Permian and older rocks of the Arizona Strip, particularly in its western section, hampering downward migration of solutions
- Distribution: originally (now largely eroded) throughout the Arizona Strip area, thickening from about 120 m near Marble Canyon in the E and Red Butte in the SE to 300–350 m in the Kanab area to the N and in excess of 500 m near Grand Wash Cliffs to the W.

Chinle Formation

- Channel-filling fluvial arenites of the Shinarump Member are host to minable U deposits (e.g. near Cameron at the eastern edge of the Arizona Strip area). Uranium has formed coeval with the 220–200 Ma old uranium generation in breccia pipes. This opens the aspect that uranium of both hosts derived from the same source and/or uranium has been transported from Chinle channels through structural pathways into pipes, perhaps via a permeable intermediary conduit like the Coconino or Supai sandstones.
- Distribution: originally (now largely eroded) in a NW–SE oriented belt, 80–130 km wide, spread from the Petrified Forest National Park area in the far SE through Cameron to Kanab–Colorado City in the NW and further beyond. The flow direction was from SE to NW.

Breccia pipe- and ore-forming processes

A solution breccia pipe containing economic U ore bodies is a unique feature requiring the coincidence of multiple geologic, structural, paleohydrologic, and metallotectonic factors, as documented earlier.

The actual formation of breccia pipes in the Arizona Strip area is a result of a karst phenomenon that began in late Mississippian time in Mississippian Redwall Limestone (Billingsley et al. 1986) and continued intermittently into late Triassic Chinle time. Karst development in the course of a discriminative dissolution of the limestone was controlled by a pre-Pennsylvanian joint pattern (Wenrich and Sutphin 1989). Where roofs of caverns within the karst system did collapse, the collapse process stopped progressively upward into overlying flat-bedded strata, probably along the intersection of fracture or shear systems, and produced as final result the breccia pipe.

The consistency of pipe-filling material suggests, that the Coconino Sandstone, the most significant although not the only lithologic facies hosting disseminated ore within the pipe, was poorly cemented at the time of subsidence either because it was

not yet lithified or because it disaggregated during brecciation. Similar aspects are probably also valid for arenaceous facies of other formations such as the Esplanade. A slurry of loose sand and finely divided breccia may have entered the pipe and poured downward. These masses filled interstices between larger blocks of siltstone, mudstone, and other lithologies or, where more abundant, constituted the massive sandstone pipe fill as found in the Orphan, Hack 2 and 3, and EZ-2 pipes. Repeated pipe internal subsidence occurred after arenaceous infilling, locally forming secondary structures such as “pipe in pipes” prior to a final and complete cementation of sands.

Initial ore introduction must have taken place sometime before the final cementation of ore-hosting sands. Several pulses of mineralization occurred as indicated by the paragenetic interrelationship of ore and gangue minerals. In a first stage, dominantly carbonates and sulfates (baryte) were introduced succeeded in stage 2 by Fe, Ni, Co sulfides and arsenides. Stage 3 is the principal uranium phase. Pitchblende was deposited in two phases in association with Cu, Fe, Pb, and Zn sulfides, as well as quartz and calcite. The presence of calcite may suggest that uranium was transported as a uranyl carbonate complex.

When the mineralizing fluids entered the more open spaces (breccia zones, porous sands, fissures, annular ring fractures, etc.), pressure release in mineralizing solutions probably took place, which caused the break up of uranyl compounds. And where adequate reducing conditions existed, pitchblende, and other minerals as well, were deposited. Hydrocarbons or dissolution of early sulfides/pyrite presumably furnished the reducing capacity to reduce U^{6+} to form pitchblende. The local coexistence of hematite after pyrite supports such an interaction of oxygenated fluids with reduced matter.

Hydrocarbons in the lower Toroweap and the Kaibab formations may have entered the pipe during its stoping period and (concurrent?) dissolution of leachable Toroweap rocks in the pipe-associated cone. Prior to uranium precipitation, hydrocarbons may also have created the reducing environment to precipitate early sulfides, particularly Fe sulfides of the sulfide cap. Redbeds in the Permian sediments provide a potential source for iron. This early reducing event may have been simultaneously responsible for the reduction and bleaching of oxidized sediments surrounding any sulfide-mineralized pipe. As such, these reduction halos would not indicate uranium ore bodies in a pipe. Instead, they would only document that reducing processes had been active which, however, is a prerequisite for the formation of uranium ore.

Ore-forming solutions, at least those that deposited calcite, dolomite, and sphalerite but not necessarily pitchblende, had temperatures ranging from about 80 to 170°C and had moderate salinities always between 9 and 19 wt% eq. NaCl. In comparison, strata-hosted calcite in vugs of the Harrisburg Member/Kaibab Formation yields filling temperatures of 53 to 60°C and a salinity of 4.8 to 21 wt% eq. NaCl (Wenrich and Sutphin 1989), which most likely represent the temperature of the geothermal gradient at the time of calcite formation.

Adamek et al. (1990) interpret the results of their fluid inclusion studies to mean that the complex salinity composition of the earliest fluid system identified in the pipes indicates a

derivation of the high salt component of mineralizing fluids from deep basinal brines that were seated immediately above the basement or in fractures within the basement. These brines were probably activated by and intermixed with a deeper, CO₂-rich fluid system of higher temperature and lower salinity. Rising fluids may have carried both gold and base metals but, due to high salinity, their pH was relatively low regardless of CO₂ content, and consequently, gold solubility was low as well. The authors take this as a reason for the absence of or only very minor (as in the Orphan Lode) gold values in most collapse-breccia pipes in the Grand Canyon region except for the Copper Mountain pipe. High Au values in this pipe are attributed to ore-forming solutions of somewhat different nature better suited for gold transfer and concentration.

Sulfur isotopes give $\delta^{34}\text{S}$ values ranging over a spread similar to that of common sandstone-type U deposits on the Colorado Plateau but which is in contrast to the narrow range of isotopic ratios from magmatic hydrothermal deposits, i.e. the ore-forming fluids were not of hypogene, but, more likely, of some sort of supergene or diagenetic-hydrothermal origin.

Lead isotope systematics of galena containing non-radiogenic lead is comparable to Mississippi Valley-type mineralization, which is consistent with the formational environment earlier mentioned. Ludwig (personal communication) also notes that the likely Pb source is an approximately 1,800 Ma old basement rock thus precluding a derivation from overlying strata for lead but not necessarily for uranium.

Time constraints on the episode of mineralization are provided by the stratigraphic sequence involved in the collapse and by radiometric pitchblende ages from the pipes analyzed (see Chap. Regional Geochronology). U–Pb isotopic time brackets are given by a minimum of 141 Ma (Orphan Lode) and 260 Ma (Canyon), provided the data are valid. The period of pipe formation is comprised within the late Permian and the Triassic and that of ore by the oldest host rock, viz. the Esplanade Sandstone. Consequently, the first uranium introduction is not older than the Esplanade Sandstone, which appears to be consistent with the 260 Ma U–Pb pitchblende age, and almost certainly not younger than Triassic. These time constraints prohibit any relationship between primary uranium ore emplacement and Miocene or younger magmatic or tectonic events, such as volcanic phases or changes in geohydrology of the Colorado Plateau, due to its uplift.

An open question remains, however, namely the significance of the four age groupings at ca. 260, 220–200, 184–165, and 141 Ma. They may suggest, after an initial uranium introduction at 260 Ma, a renewed influx of uranium or recrystallization episodes or both.

Ludwig and Simmons (1992) see no evidence in U–Pb isotope data for uranium metallogenesis related to Laramide tectonism, mid-Tertiary volcanism, or late Tertiary uplift. They consider clustering of ages in a number of uranium deposits at about (or slightly younger than) the age of the lower part of the Chinle Formation (late Triassic) to indicate that uranium in these deposits may have been leached from volcanic ash in the Chinle sediments by groundwater that was mobilized from changing hydrologic gradients caused by regional uplift to the southwest.

Since Pb isotope ratios of galena in U-mineralized pipes are more radiogenic than those of sulfides in uranium-poor pipes or in occurrences away from pipes, Ludwig and Simmons (1992) interpret this isotopic contrast to suggest that fluids, which passed through the pipes interacted with the Proterozoic basement, possibly through fracture systems, which are thought to have controlled the location and evolution of the pipes themselves.

Once ore had been emplaced, presumably after, or less likely simultaneously with visible wall rock alteration (see above), some remobilization of mineralization occurred. This assumption is deduced from the presence of at least two pitchblende generations reported by Wenrich and Sutphin (1989). Such remobilization would explain the younger ages.

The *source of the uranium* is still enigmatic. Considering the different age determinations, it can be speculated that U sources could have been uraniferous sandstones of Permian, Triassic, or perhaps Jurassic age, which are now eroded to a large extent in the Arizona Strip area, but also Proterozoic basement rocks (as postulated for Pb), either in the late Paleozoic–Mesozoic Mogollon Highland located to the S to SE or immediately underlying the Arizona Strip area. All sandstones, including the Shinarump and Petrified Forest members of the Triassic Chinle Formation nowadays preserved from erosion only at the boundaries of the area, e.g. in the Cameron district and along the Arizona–Utah state line, may be the likely direct or indirect uranium source, at least for the 220–200 Ma old U generation. This formation does contain uranium deposits, and, to some extent, the same suite of ore-forming elements as found in the breccia pipes locally. The 220–200 Ma period of breccia pipe mineralization corresponds to that in Chinle sediments, e.g. 206 ± 1 Ma in the Mi Vida mine, Lisbon Valley, and in the Supai Formation, in which the Promontory Butte prospect yields a primary age of 220–200 Ma (Ludwig et al. 1986). In contrast to the 200 Ma age group, no convincing correlation with any uranium ore-forming process elsewhere on the southern Colorado Plateau could be established for the 260 Ma old pitchblende.

It seems that the area susceptible to being favorable for the formation of uranium ore bodies within existing breccia pipes tends to be primarily restricted to a relative small stretch extending south and southeastward from Fredonia and Colorado City through and beyond the Grand Canyon village area. This assumption is based on the distribution of the Chinle and other critical strata such as the Coconino or Esplanade formations, as well as formations providing chemical elements needed for a favorable geochemical environment for ore precipitation as discussed earlier.

Wenrich and Sutphin (1989) forward, in summary, the following litho-tectonic, hydrodynamic, and geochemical parameters and sequence of events involved in pipe and ore formation in the Arizona Strip area, during the period after karstification and deposition of (Permian) sediments and cementation of interbedded sandstones by carbonate:

- A stable cratonic domain maintaining a very low hydrologic gradient such that connate waters were retained in their host

sediments and became increasingly enriched in saline and metallic elements

- A later episode of an extensive dissolution of carbonates
- Subsidence of a basin with steepening of the hydrologic gradient and associated migration of saline and metal-rich connate water into highly transmissive conduits provided by breccia pipes
- Deposition of Co, Cu, Fe, Pb, and Zn-rich ores with dominant pyrite within the pipe. Sulfides are suggested as an excellent reductant and trap for later U-rich solutions
- A crystalline highland with highly uraniferous magmatic source rocks that was connected by an aquifer with sulfide-hosting breccia pipes, permitting a downdip migration of uranium pregnant waters to the pipes
- A subsequent period of cratonic stability lasting until present times to prevent the destruction and oxidation of ore bodies by meteoric water.

With respect to *regional conduits* for the lateral migration of ore-forming solutions, any metallogenetic model involving a lithologically fairly uniform horizon such as the eolean Coconino Sandstone as a conduit for these solutions faces certain problems. Particularly, the discriminative selection of pipes for ore formation that occur adjacent to barren pipes in the same area and in the same sequence of strata instead of a mutual ore emplacement in all pipes requires explanation. A more discriminative pathway for the solutions could more easily explain this phenomenon, for example, more localized conduits such as structures through which fluids could migrate from uranium mineralized Chinle channels into the Coconino horizon and then downdip along the unit, or directly, into a breccia pipe. Another option would be more channel-hosted arenaceous strata, such as in the Esplanade Sandstone, which are developed predominantly in the central to eastern part of the Arizona Strip area, or perhaps silty-sandy channels in the Toroweap Formation.

Description of Selected Breccia Pipe-hosted Uranium Deposits

See [Fig. 1.57](#) for location of breccia pipes described.

1.4.0.1 Orphan Lode

The Orphan Lode is located 3 km west of Grand Canyon Village, on the south rim of the Grand Canyon of the Colorado River. The lode was intermittently in production from 1956 to 1969 and yielded 456,000 t of ore containing 1,664 t U, 3,006 t Cu, 3,425 kg Ag, and small amounts of vanadium. The mining grade averaged 0.365% U; the grade was highest in the upper section of the pipe, averaging almost 1% U on the 30 m level, and lower in the deeper part, averaging 0.085% on the 120 m level. Early production was about 1,000 t/month at a grade of almost 1% U.

Sources of Information. Chenoweth 1986a; Chenoweth and Malan 1969; Gornitz 1969; Gornitz and Kerr 1970; Gornitz et al.

1988; Kofford 1969; Magleby 1961; and Scarborough 1981 unless otherwise cited.

Geological Setting of Mineralization

The Orphan Lode is a nearly circular, chimney-like, vertical breccia pipe (for configuration and dimensions see Chap. Shape and Dimensions of Deposits), which crops out in the lower part of the Coconino Sandstone in the southern slope of and about 300 m below the rim of the Grand Canyon ([Fig. 1.62a](#)). The root of the pipe is probably in the middle of the Mississippian Redwall Limestone as suggested by a deep drill hole, which intersected from thereon only undisturbed rocks down to the Cambrian Tapeats Sandstone. Upward, the pipe has penetrated at least through the Pennsylvanian Supai Group and Permian Hermit Formation to the present Coconino Sandstone outcrop position.

A comparison of endo- and exocontact pipe structures shows that one shear pattern within the pipe apparently has the same NNE to NE trend as the strike of the Bright Angel fault, and another has a NW trend roughly parallel to the NW-striking faults of Laramide age.

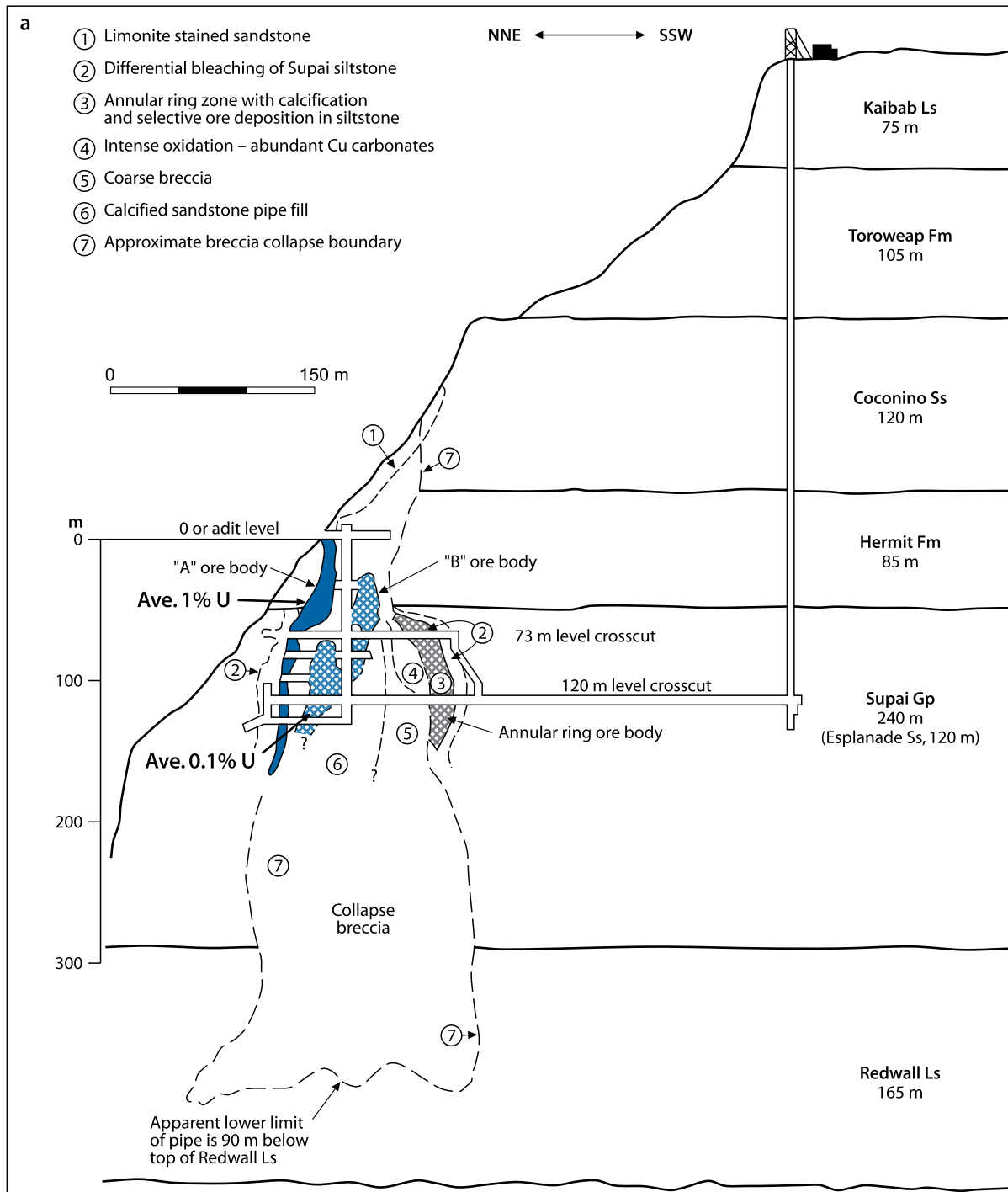
The Orphan pipe is filled with breccia and is bounded by a peripheral, sheared, and brecciated zone of wall rocks, which grade into a set of concentric, circular fractures termed annular ring. The brecciation and subsidence of wall rock clasts within the pipe increases downward caused by multiple pipe internal collapse events. Pipe fill consists of downward displaced breccia, which ranges from clast-dominated to matrix-dominated material. Clasts include massive Coconino Sandstone and angular siltstone, shale, and limestone fragments of the Hermit and Supai formations. Down-dragged Coconino Sandstone fragments are found as much as 80 m below the base of the Coconino horizon and blocks of Hermit rocks have down-dropped over 100 m to the 150 m mine level. Down-faulted clasts range in size from a few millimeters to several meters in diameter and their edges are angular to well rounded. The upper level of the pipe is mostly filled with loosely consolidated sandstone. The center of the pipe contains massive sandstone blocks. Siltstone and shale breccia fragments prevail near the margins of the pipe. Calcareous sandstone envelopes pipe fill at the contact of the pipe, and usually forms the matrix, together locally with pyrite.

The annular ring is a peripheral zone of faulting, fracturing, slumping, and in situ brecciation around the pipe. Within the various flat-lying wall rock formations, the ring has developed differently. The ring within the Toroweap Formation is essentially expressed by only minor reverse faults; within the Coconino Sandstone it is characterized by both normal and reverse faults with small displacements and by fracturing, grading outward into undisturbed sediments. In the Hermit interval, the ring is a distinct zone, from 2 to 6 m in thickness, of disturbed and altered shale with well-defined boundaries.

The Supai section is characterized by marked variations in width due to differential competency of individual beds. In more competent sandy beds, the annular ring zone is as much as 22 m wide and fractures tend to occur in a parallel arrangement. In

Fig. 1.62.

Arizona Strip area, Orphan Lode, (a) cross section showing the stratigraphic setting, lithology, alteration, and position of ore bodies in the breccia pipe. (b) plan view of 73 m (245 ft.) and 120 m (400 ft.) levels. (After (a) Scarborough 1981 based on Kofford 1969, Gornitz and Kerr 1970; (b) Scarborough 1981 based on Gornitz and Kerr 1970)

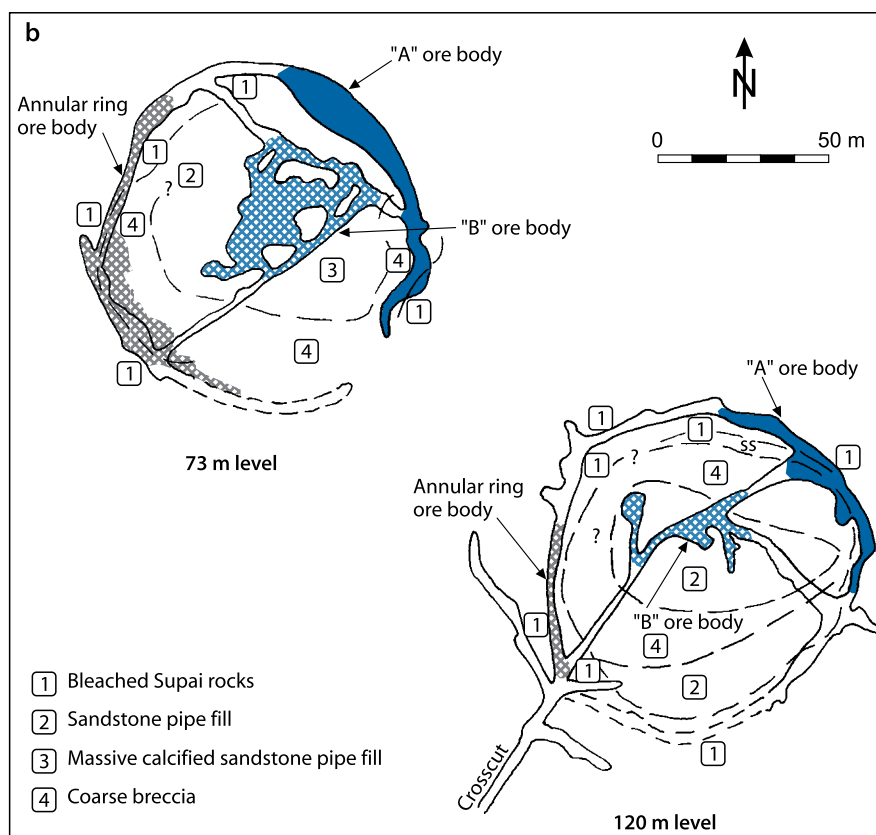


the lower Supai strata, the ring becomes ill-defined near the contact with the Redwall Limestone.

Other features of the Orphan pipe reported by various authors include the following:

- Faulting in the pipe and annular ring was recurrent and may be pre- to post-mineralization in age. Both normal and reverse faults occur
- Secondary pipe structures occur as distinct pipe-like features within the pipe and exhibit in situ brecciation and displacements of up to tens of meters
- Both structural and solution folding are common. Tight structural folds reflect a semi-consolidated plastic state
- Pseudo-bedding of pipe material ranges from laminated to thick bedded; is from plane to rolling, with very irregular contact; it also exhibits pronounced cross-bedding

■ Fig. 1.62. (Continued)



- In the upper part of the pipe, between the adit and 7.5 m level, some units contain thin laminae of pyrite-rich, black, carbonaceous mud that alternates with sandy material
- Injection of breccia fragments or sandstone between bedding planes in shale have produced sill-like textures.

Host Rock Alteration

Rocks within and adjacent to the Orphan Lode were affected by various alteration processes as reflected by

- Bleaching of normally red sediments within the pipe and near its contact, with tongues extending up to 30 m into surrounding permeable beds. In particular, Hermit siltstones and Supai sandstones, which normally contain 3–10% hematite, are bleached to a grey color
- Ca, Mg, Fe carbonatization occurred in two stages. The early stage resulted in cementation of sandstone pipe fill with partial replacement of quartz grains by coarse-grained calcite and dolomite, particularly at pipe margins. A later, apparently ore-related, stage produced calcite veinlets in bleached Supai rocks, vugs of calcite crystals with chalcopyrite and hematite inclusions, and calcite crystals in siltstone. Siderite appears in minor amounts; it overgrows dolomite. Carbonate can accumulate to 30–50% of rock volume, which originally contained about 90% quartz. Calcite and dolomite first appear in significant quantities at about the 30 m level, i.e. just above the Hermit–Supai contact

- Pyritization resulted in a local addition of pyrite to the carbonate matrix
- Silicification led to quartz overgrowth on detrital quartz in the pipe but also in the Coconino Sandstone horizon; and it generated authigenic quartz that partially replaced matrix material and sand grains. The overgrowth has been succeeded by carbonate cementation and corrosion of quartz
- Argillization is reflected by significant amounts of kaolinite and illite inside and outside the pipe but its relation to ore genesis is still dubious. Kaolinite tends to predominate in quartz sandstone or calcareous sandstone of pipe fill, whereas illite is abundant in shale and siltstone breccia. There is no difference in clay content between mineralized and barren rocks.

Mineralization

According to papers by Gornitz and coworkers, and Kofford (1969), pitchblende is the main U mineral (lattice constant $a_0 = 5.418\text{--}5.422 \text{ \AA}$) followed by coffinite. Associated ore minerals are dominated by sulfides and oxides of iron and copper. Sulfides, arsenides, and oxides of Co, Mo, Ni, Pb, and Zn occur in minor to accessory amounts (see ▶ Table 1.8 for ore minerals found in Orphan ore). In addition, Ag in galena and native Au may be present. Gangue minerals include calcite, dolomite, siderite, and baryte. Supergene processes have produced a number of secondary minerals including U^{6+} minerals and sooty pitchblende, and have upgraded portions of ore zones, such as in the "B" ore zone.

Pitchblende mostly occurs as thin films around detrital quartz grains, but may also occur in banded veins. Within high-grade ore, shrinkage cracks in spherules or botryoidal pitchblende are filled with calcite and bornite. Pyritization resulted in a local addition of pyrite to the carbonate matrix.

High-grade uranium ore from the annular ring is invariably intergrown with red, earthy hematite, and sulfides, e.g. a core of disseminated pyrite or chalcopyrite is surrounded in sequence by concentric rings of pitchblende, a thin band of bleached rock, and a diffuse halo of hematite. Some samples from the annular ring show pitchblende intergrown with niccolite, rammelsbergite, chalcopyrite, and hematite, indicating a rapid and simultaneous precipitation.

Pyrite is by far the most abundant sulfide. Tennantite-tetrahedrite and chalcocite are next in abundance. Arsenopyrite is locally prevalent, particularly in the upper part of the pipe. The remaining sulfide minerals are relatively sparse, except in local sections. Most minerals are extremely fine grained. Some organic carbon (0.35–0.45%) is present in the form of very fine-grained amorphous material.

Metallic minerals show a certain lateral and vertical zoning. Pitchblende and pyrite prevail in the center of the pipe, but grade outward to an assemblage of chalcocite, tennantite, minor galena, and nickel-cobalt arsenides with pitchblende at the pipe margins. Galena is composed of common lead. The amount of pitchblende and associated galena decreases downward with the bulk of the uranium occurring above the 110 m level. Copper concentrations extend below the uranium. Pyrite and marcasite are ubiquitous throughout the vertical extent of the pipe. Oxidation products are also found throughout the pipe, primarily in permeable zones.

Adamek et al. (1990) report analyses of 18 ore samples collected from dumps. Ten unoxidized samples had identifiable Au (>5 ppb), four of which with the highest gold tenors contained 10–45 ppb Au, 3–44 ppm Ag, 0.55–1.615% U, 0.67–8.55% Cu + Pb + Zn, and 0.10–1.35% As. No correlation between Au and other elements could be established and no special relationship between Au and certain lithologies. All gold-bearing samples show a variable degree of silicification, which is also a common feature in non-auriferous pipes. Quartz overgrowths on detrital quartz grains belong to the oldest mineral phases in breccia pipes.

Shape and Dimensions of Deposit

The *Orphan pipe* is a nearly circular collapse structure extending vertically from 90 m below the top of the Redwall Limestone upward to the Coconino Sandstone, a vertical extent of at least 500 m (Chenoweth 1986a, b). It is not known, however, whether the pipe formerly extended higher in the section since the Kaibab, Toroweap, and part of the Coconino and Hermit formations are eroded (Fig. 1.62a and b). The pipe is funnel shaped. The neck of the funnel extends from the 30 m level to the surface, i.e. where the pipe cuts the Hermit Formation, and there flares outward. The neck is geometrically regular and the pipe wall is fairly smooth. At the 0 m mining level, the pipe is roughly

circular with a diameter of 45 m. At the 30 m level, the pipe is somewhat ovate, and has axes of 50 m in length and 30 m in width. The pipe begins to widen below the Hermit-Supai (Esplanade Sandstone) contact to form an irregular bell shape, with a maximum diameter of 115 m at the 110 m level, and, if the mineralized annular ring is included, the diameter widens to about 150 m. Pipe diameter greatly increases in the Redwall Limestone, until it terminates in the middle of this formation.

The pipe is bounded by concentric, circular tension fractures forming the earlier described annular ring. The width of the ring is 2–6 m in the Hermit Formation interval. It varies markedly in the Supai Group, where the ring is up to 22 m wide in more competent sandy beds, which host fractures filled with high-grade ore.

Mineralization in the Orphan Lode shows an irregular distribution by grade and quantity. Ore occurs in (a) fissures and fractures of the annular ring (“A” ore body) and (b) as irregular masses in the highly fractured and brecciated central interior of the pipe (“B” ore body) (Fig. 1.62a and b). The latter are partly embedded in lower grade mineralization or separated by barren pipe fill breccia.

Annular ring ore (“A” ore body) is generally concentrated near the perimeter of the pipe, in particular just below the level where the pipe constricts in the upward direction. It has been found downward to near the 165 m level and appears to bottom out on top of a shale bed in the Wascogame Formation/Supai Group.

“B” ore extends from near the pipe outcrop to about the 135 m level and occurs preferentially in relatively porous, carbonate-cemented sandstones of the breccia matrix, but is also locally controlled by fractures and faults. Siltstone and claystone breccia fragments are generally unmineralized. Kofford (1969) believes the “B” ore body lies within an interior “pipe-within-pipe,” which was displaced downward with respect to the “A” ore body.

Most of the uranium was located above the 110 m level, for a vertical distance of approximately 110 m. The highest grades occurred between the 67 m level and the adit level (0 m). Grades on the 30 m level were over 1% U decreasing downward to 0.1% U on the 120 m level. High-grade U ore was also mined from the center of the pipe, as well as from a heavily brecciated zone at the northern pipe boundary. Copper mineralization was mainly distributed between the 67 and 120 m levels.

Geochronology, Fluid inclusions

Uranium-lead dating by Miller and Kulp (1963) of pitchblende produced discordant patterns for the time of mineralization ranging from 402 to 87 Ma with a best estimate for a minimum age of 141 Ma (late Jurassic). Fluid inclusions from euhedral calcite, which contain solid inclusions of chalcopyrite and hematite parallel to growth directions, yield homogenization temperatures between 60° and 110°C (Gornitz and Kerr 1970) that fall within the range of values also established at other pipes.

Ore Controls and Metallogenic Aspects

The prime control for uranium ore is its emplacement in a cylindrical vertical collapse structure. The pipe is apparently located at the junction of two shear zones trending NNE to NE and NW. This setting may indicate that the position of the pipe is controlled by one or both of these structures. If both control the pipe location, then the NW-trending fault, which parallels structures of Laramide age, must have originally been older than Laramide, but may have been reactivated during Laramide time.

Ore location is controlled

- Within the pipe, by
 - sections dominated by sandstone fragments or sandy matrix, which originated from the Coconino Sandstone and from sandier beds of the Esplanade Sandstone/Supai Group, and
 - stratigraphic intervals where the pipe cuts the Hermit Formation and the upper part of the Supai Group
- Peripheral to the pipe, by
 - fractures of the annular ring marking the pipe boundary, particularly above the Hermit-Supai contact
 - breccias just inside this fracture zone, and
 - disturbed and undisturbed sandy to silty beds in a 2–15 m wide ring just outside the pipe in the Supai sediments.

In general, ore grade and quantity in the annular ring zone is directly related to the intensity of fracturing and shearing, i.e. more ore occurs in areas having a greater intensity of structural deformation.

1.4.0.2 Hack Canyon Breccia Pipes

The Hack Canyon No. 1, 2, and 3 breccia pipes are located on the north side of the Grand Canyon, some 70 km SSW of the town of Kanab, Utah, in the general vicinity of Kanab Creek Canyon. Abundant copper carbonate minerals and associated iron oxide mineralization most notably located adjacent to the Hack No. 1 pipe and located over the Hack No. 3 pipe were discovered in the early 1940s, and, in the late 1940s, anomalous surface radioactivity and pitchblende mineralization was found in outcrop.

The three Hack Canyon deposits were mined by underground methods and are exhausted. Over a mine life of nearly 8 years (1980–1988), they produced a total of 3,669 t U at an average ore grade of 0.545% U. (Hack 1: 546 t U, 0.449% U; Hack 2: 2,692 t U, 0.597% U; Hack 3: 431 t U, 0.427% U) (Pool and Ross 2007). Ore was treated in the White Mesa mill near Blanding, Utah.

Source of information. Casebolt LL, written commun. (1988).

Geological Setting of Mineralization

The Hack Canyon uranium deposits occur within three individual, vertically oriented, collapse breccia pipes, which

intersect over 300 m of Permian sedimentary strata, from the Coconino Sandstone through the Hermit Formation into the Supai Group, and further down into the Mississippian Redwall Limestone. Nearly 100% of the economic U mineralization contained in these breccia pipes is restricted, stratigraphically, to the upper 190 m of the Hermit Formation.

The erosion of strata enclosing these breccia pipes has exposed pipe structures to varying degrees. In the case of *Hack No. 1*, the erosion process had removed most of the sedimentary rocks and pipe material down to the top of the Hermit Formation. The pipe structure itself, however, was covered with over 10 m of talus, which masked the presence of this pipe. The *Hack No. 2* breccia pipe was a blind deposit. No surface expression of a breccia pipe was apparent and the complete local stratigraphic column remained intact. The *Hack No. 3* breccia pipe outcrops on the side of Hack Point in the mouth of Robinson Canyon. The pipe is exposed stratigraphically in the Toroweap Formation. Portions of the pipe/country rock contact are associated with abundant copper carbonate minerals.

Host Rock Alteration

The most obvious alteration feature is bleaching of normally red-brown Hermit beds to a characteristic grey-green color adjacent to a mineralized breccia pipe as well as the bleaching of the collapse breccia itself. The normal red-brown color of Hermit sediments is imparted to the rock by hematite staining the dolomite matrix surrounding individual quartz grains. Alteration to a grey-green color is the result of a reduction or sulfidization of ferric iron to marcasite and pyrite and also a removal of up to 40% of the original iron and, to a lesser extent, of calcium carbonate, manganese, vanadium, and nickel. The removal of these elements and minerals is attributed to leaching by an acidic to neutral and reducing solution (Energy Fuels memorandum, Honea 1982). In addition to the removal of certain elements, an increase in uranium, arsenic, and copper levels is noted in altered Hermit Shale. The increase of these elements is related to the later mineralizing phase and did not necessarily correlate to the alteration process.

Spacially, the upper part of the Hermit Formation, which encases the breccia column, is bleached along the Coconino Sandstone/Hermit Formation contact. The depth of bleaching increases concentrically with proximity to the pipe. The lateral extension of this bleaching from the breccia column contact into the country rock is a function of permeability. Individual beds of the Hermit Formation with higher permeability are bleached up to 100 m or more out from the pipe contact.

Mineralization

Pitchblende is the dominant U mineral in the Hack Canyon pipes. It is often associated with pyrite and tennantite. Pitchblende accounts for approximately 99% of the U-bearing material identified in thin and polished sections. The remaining 1% is distributed among brannerite, cheralite, and meta-autunite.

Authigenic metallic minerals include arsenopyrite, bornite, bravoite, chalcopyrite, clausenthalite, covellite, enargite, galena, gersdorffite, hematite, ilsemannite, jordisite, marcasite, pyrite, siegenite, sphalerite, and tennantite. Authigenic nonmetallic minerals include anhydrite, baryte, calcite, collophane, gypsum, kaolinite, and quartz. A paragenetic sequence of mineral formations is given in [Fig. 1.61](#) in context with that of other pipes.

Pillmore DU (written commun. 1988) notes that four paragenetic elemental/mineral zones have been identified within the Hack 2 breccia pipe: pyrite, Ni-Co, Mo-Zn-Ba, and Pb zones (for details see Chap. 1.4.0.3 Pigeon pipe).

Fluid inclusions in sphalerite crystals indicate a sphalerite deposition from saline solution (9.9–16.4 wt% NaCl eq.) at relatively low temperatures between 93.4° and 106.0°C (Cunningham, personal communication).

Age determinations of pitchblende from the 1,250 m level of the Hack No. 2 mine yield U/Pb ages of 200 ± 10 Ma, which coincide with the Triassic/Jurassic boundary (Ludwig et al. 1986).

Ore and associated minerals fill interfragmental open spaces where they occur both as an added cement or matrix, which surrounds the clastic fraction of the breccia and also as an interstitial filling of the Coconino Sandstone and Toroweap Formation clasts. The less permeable Hermit-derived clasts are only mineralized at their outer margins. Some replacement textures, most notably pitchblende replacing chalcopyrite, are present.

Mined ore-grade segments of Hack breccia pipes typically contained a major portion of sand-size material as opposed to silt-size or smaller material. The major portion of quartz sand was derived from Coconino Sandstone, which, in the Hack Canyon area, attains a thickness of approximately 30 m. Additional sandy material originated from the Toroweap Formation.

Higher U grade portions of ore bodies were in breccias composed of both sandstone clasts and matrix. In this mode of ore, pitchblende filled nearly all available pore space between sand grains. The next major type of ore consisted of breccias composed of siltstone and mudstone clasts of Hermit origin suspended in a Coconino sand matrix. In this ore type, essentially only the matrix was mineralized. This ore variety forms lower ore shoots, which extend downward from main ore bodies and occurred where available Coconino sand diminished with depth.

Ore-bearing segments of the Hack Canyon deposits all occur, stratigraphically, in the upper 200 m of the Hermit Formation. Apparently, the relatively impermeable character of this thick sequence of siltstones and mudstones, which completely encloses the breccia column, contained the mineralizing fluids and prevented their migration or dilution in surrounding sediments.

Shape and Dimensions of Deposits

The [Hack No. 1](#) breccia pipe is elliptical in horizontal view. The major axis trends NE-SW and is approximately 100 m long

while the shorter is 73 m long. The pipe contained ore over a vertical extent of 78 m in a nearly circular body in plan view with a wine glass-shaped vertical section. Upper ore lodes, situated near the Coconino/Hermit formations interface, were narrow, arcuate pods, which occurred adjacent to, and inside of the pipe/country rock contact. These arcuate pods were isolated by a circular central core of protore. Ore distribution moved toward the central portion of the pipe with depth and coalesced into a near circular body, 43 m in diameter, at the 1,261 m elevation above mean sea level. Ore stopped abruptly at the 1,234 m elevation.

The [Hack No. 2](#) breccia pipe is a nearly circular and vertical structure with a diameter of 73 m. Ore formed a continuous carrot-shaped body, which occupied the east central portion of the collapse structure. Ore persisted over a vertical interval of 189 m, from the Coconino/Hermit contact at an elevation of 1,341 m down to the 1,152 m level. The ore body attained a maximum diameter of 61 m at the 1,286 m elevation, which gradually diminished to approximately 12 m in diameter at the 1,152 m level where an assay wall of 0.25% U was reached.

The [Hack No. 3](#) breccia pipe is a nearly circular and vertical structure with a diameter of 73 m and a depth extension of 136 m, extending from slightly above the Coconino/Hermit contact at an elevation of 1,343 m down to the 1,207 m level. The ore body was of arcuate shape within, and adjacent to the southwestern pipe contact. With increasing depth, it gradually moved to the central portion of the pipe and attained a maximum diameter of 43 m at the 1,283 m elevation. The ore shoot gradually decreased in diameter to 9 m at an elevation of 1,207 m, where it ended abruptly.

1.4.0.3 Pigeon Breccia Pipe

This breccia pipe is located some 40 km S of Kanab. The Pigeon deposit was exploited from 1983 to 1990 by an underground mine and is depleted after producing 2,192 t U at an ore grade of 0.55% U (Pool and Ross 2007).

Sources of Information. Pillmore DU, written commun. (1988) including data from Energy Fuels Exploration R&D (1982, 1985).

Geological Setting of Mineralization

The Pigeon breccia pipe surface anomaly is exposed in upper units of the Harrisburg Member of the Permian Kaibab Formation as reflected by a red coloration of the normally tan to grey beds of the Harrisburg Member. The mineralized section of the pipe intersects, downward, the Permian Coconino Sandstone, a 1.5 m thick, fine grained, eolian cross-bedded sandstone, the Permian Hermit Formation, 236 m thick, composed of red, thinly-bedded siltstone and mudstone, and the top 24 m of the Esplanade Sandstone of the Supai Formation, which is a cross-stratified fluvial to estuarine sandstone of Pennsylvanian to Early Permian age.

The Pigeon breccia pipe has a well-defined surface indication, expressed as a topographic depression. This depression has the form of a cone with inward dipping beds that are tilted for over 610 m from the center of the cone. Dip increases toward the center of the depression to over 20°. Faults and fractures with a displacement of up to 4.6 m dissect the area. Some faulting does show a relationship to the collapse, displaying a ring fracture pattern.

Host Rock Alteration

The alteration of the pipe enclosing formations and the pipe infill includes reduction and late oxidation phenomena, as well as related authigenic mineral formation. The Esplanade Formation exhibits bleaching and grey coloration associated with sulfidization (disseminated pyrite). Normally dark brick-red strata of the Hermit Formation are bleached to a light grey along bedding planes within horizontal sandy zones for 100 m and more from the pipe. Bleaching is a result of iron removal, with no noticeable difference, other than color, in thin sections between unbleached and bleached samples. Liesegang banding, often seen along the margin of bleached and unbleached Hermit rocks, are also common. These bands are parallel and consist of pyrite and hematite. Dolomitization and calcitization are also present in the Hermit Formation as well as in pipe infill. The Coconino Sandstone is reduced from a tan to a light to dark grey color. In the Kaibab and Toroweap formations, alteration has caused dark grey coloration associated with sulfidization (predominantly pyrite), forming a massive sulfide cap in the Toroweap Formation. Pyrite disseminates downward into the upper portion of the Pigeon ore body, and is seen most often as pseudomorphs after marcasite.

Mineralization

Pitchblende is the predominant U mineral; coffinite is rare. Pitchblende fills interstices between gangue minerals and coats quartz grains. U mineralization also rims Hermit shale fragments and penetrates slightly into their relatively impermeable center. Yellow uranium precipitates are occasionally seen in drifts or open stopes. U mineralization is very frequently found together with other metals in a close association with clay, calcite, and gypsum/anhydrite in breccia matrix/cement. The sulfide content in ore amounts to 3–4%.

Metallic and gangue minerals occur in relatively high concentrations within the Pigeon pipe. The metallic mineral assemblage includes bornite, bravoite, chalcopyrite, cobaltite, covellite, enargite (luzonite), jordisite, galena, gersdorffite, hematite, ilsemanite, marcasite, millerite, pyrite, siegenite, sphalerite, violarite, and tennantite–tetrahedrite. Anhydrite, baryte, calcite, colophane, gypsum, kaolinite, and quartz are the most abundant gangue minerals. They occur as clasts and as interstitial filling in and about breccia fragments.

Iron oxides are abundant along fault zones and as a coating around chert nodules in the Fossil Mountain Member of the

Kaibab Limestone. Manganese oxides also coat some chert nodules. Hematite pseudomorphs after pyrite and marcasite are noted throughout the area, particularly in the Harrisburg Member of the Kaibab Formation. Copper carbonates and bitumens also occur in the Harrisburg Member. Irregular aggregates of degraded, vitreous organic material are frequent in the pipe.

Four paragenetic elemental/mineral zones have been identified within the Pigeon pipe similar to those in the Hack 2 breccia pipe: pyrite, Ni–Co, Mo–Zn–Ba, and Pb zones. The *pyrite zone* occurs, stratigraphically, from the Coconino/Hermit contact to 60 m below the contact. It consists of wide bands of a heavy concentration of pyrite-after-marcasite pseudomorphs. Also found laced with the pseudomorphs, is a late stage, black glassy hydrogen–sulfur-rich bitumen that tends to have formed at a fairly low temperature, at less than 100°C. Landais (1986) established a formation age of about 160–100 Ma for the bitumen. The *Ni–Co zone* lies below the pyrite zone and persists downward to about the 1,274 m elevation. It is characterized by millerite, siegenite, and bravoite. Pyrite is also prominent throughout this zone. The *Mo–Zn–Ba zone* is positioned below the 1,274 m elevation and extends to the 1,250 m level. Jordisite, sphalerite, and baryte as well as pyrite are typical minerals in this zone. The *Pb zone* lies below the 1,250 m elevation and continues to the 1,167 m elevation. The dominant sulfide mineral is galena, but pyrite, chalcopyrite, marcasite, sphalerite, and tennantite also occur.

The distribution of the U mineralization is almost entirely controlled by transmissivity within the pipe. The most permeable zones are provided by small clast, sandy matrix-dominated breccias, as well as open fractures along the margin of the pipe.

The litho-stratigraphic section enclosing the Pigeon pipe combined with the material of the Hermit Formation, which collapsed into the pipe, form an almost non-permeable shell around and a lower boundary within the pipe, respectively, for ore-forming solutions and as such a unique litho-stratigraphic trap for the massive, high-grade uranium concentration.

Shape and Dimensions of Deposits

In planview, the Pigeon pipe is roughly circular in shape, and appears to be vertical with a minimum vertical extension of approximately 855 m. Pipe diameter is ca. 107 m between outside edges of fracture-controlled ore.

U mineralization occurs over a 260 m vertical interval (from ca. 200 to 460 m below the surface); it includes an ore-grade mineralized portion that approaches 60 m in diameter within the pipe and has a continuous vertical extent of over 200 m with no barren intervals.

Stratigraphically, the ore body is confined to the Hermit Formation interval extending from the Coconino/Hermit contact on the top to 18 m below the Hermit/Esplanade contact on the bottom. The bottom of the ore body below the Hermit/Esplanade contact is approximately centered within the breccia column. Its lower limit is made up of large blocks of the Hermit

Formation, which collapsed into the pipe, and intervened between the ore and the Esplanade derived breccia below. This brecciated Hermit material forms a non-permeable zone 24 m below the Hermit/Esplanade contact, which apparently acted as a seal. No U mineralization was found below this level (elevation 1,167 m).

Fracture-controlled ore around the margin of the Pigeon pipe is different from ore in the annular rings seen at the Orphan Lode. Fracture-controlled ore at the Pigeon is located in circular stress fractures around the outside edge of the pipe. Large, displaced Hermit blocks surround the central, small clast-matrix dominant ore chute, and fractures are found along the contact between in-place Hermit and these large blocks. These fractures average 30 cm in width, and occur within a zone from 60 cm up to 15 m wide. Fractures are separated by 10–30 cm of waste. Pitchblende ore in the fractures is high grade, ranging from 1% U to 20% U.

Metallogenetic Aspects

Mineral relationships indicate a change of the hydrochemical system involved in the metallogenetic process from early acidic pH conditions to basic conditions as reflected by pyrite pseudomorphs after marcasite, which requires a change from a lower pH to a higher pH. This conclusion is also suggested by the removal of dolomite from altered Hermit rocks. The occurrence of quartz and calcite indicates a higher or basic pH as late minerals in the paragenetic sequence are deposited, and that the pH of the system increases with time.

Acidic conditions that occurred in the breccia pipe were able to mobilize the phosphate in the system and as such could have dissolved detrital collophane in mineralizing solutions. As pH increases, collophane would be re-precipitated. Since some pitchblende is enclosed within authigenic collophane, it is concluded that pitchblende was deposited as the pH of the system rose. This relationship does not exclude the possibility, however, that pitchblende was precipitated before and/or after the rise in pH.

Eh conditions of the system can be deduced from relationships of pitchblende replacing sulfides. This suggests that pitchblende was forming as sulfides were oxidized. The antipathy of uranium for hematite in spotted ore specimens strengthens this suggestion. Since this ore is still very high in sulfide content (3–4%) it can be assumed that not all of the reducing capacity was used.

In summary, mineralization is controlled by intervals of high permeability within the pipe and evolved by a hydrochemical system that changed from a relatively lower pH or acid environment to a high pH environment through time. Late alkaline conditions prevailed when calcite and quartz were precipitated combined with the oxidation of sulfide when the pH was rising (Pillmore DU, written commun. 1988).

1.4.0.4 Kanab North Breccia Pipe

Discovered in 1981, this breccia pipe is located 230 m off the east edge of the Kanab Creek canyon, 45 km SSW of Kanab. The

deposit was mined by underground methods to a depth of 462 m from 1987 to 1991. Original resources including production amounted to 1,065 t U at a grade of 0.53% U (Pool and Ross 2007).

Source of information. Norris J, written commun. (1988).

Geological Setting of Mineralization

The breccia column penetrates down through sedimentary units of the Permian Kaibab, Toroweap, Coconino, and Hermit formations, and presumably extends, as do all other breccia pipes in the region, through the Permo-Pennsylvanian Supai Group into solution cavities in the Mississippian Redwall Limestone. The surface depression of the pipe is in part filled by sediments derived from the Triassic Moenkopi Formation. Clasts of the Fossil Mountain Member/Kaibab Formation were found 150 m below the surface, which indicates a stratigraphic vertical displacement of almost 300 m.

The actual breccia pipe consists of a slightly elliptical collapse column with axes of 55 m in NNW and 46 m in NE direction. The breccia column appears to rake, from the top of the exposed portion to the bottom, at 15° from vertical almost due east. The upper portion of the pipe is similar to other deposits mined for uranium on the Arizona Strip. It comprises a core of small-clast breccia derived mostly from the Fossil Mountain and Brady Canyon members contained in a matrix of Brady Canyon material. The core is surrounded by a large-clast breccia with clasts of the Brady Canyon Member and Hermit Formation in a Hermit-derived matrix, enclosed by a very large clast breccia sometimes even a mosaic texture of Hermit in Hermit rocks. This, however, is where the similarity to the rest of the deposits on the Arizona Strip ends.

The pipe from the 1,186 m sublevel to the bottom of the section exposed by mining is unique. It changes from roughly vertical to the earlier mentioned rake. In this interval, mineralization is contained in three distinct types of lithology. From the 1,186 m sublevel down to about 1,128 m, the breccia consists of about 30% of large to very large clasts of mostly Brady Canyon Member and Hermit Formation origin contained in a predominantly light grey, clayey matrix of Hermit material. The clasts are generally angular and consist of mostly siltstone, claystone, and dolostone. Most uranium mineralization is trapped in very small bowls of shale formed by the down dropping of clasts into unlithified sediments of Hermit origin. The mineralization appears as thin, elongated lamina of shale with pitchblende, less than 30 cm in vertical dimension but in excess of 3 m in horizontal dimension. In some segments, these thin bands are close enough together to make ore; however, in most of this section they are not.

From the 1,128 m to the 1,062 m (bottom sublevel), U mineralization is hosted in a small-clast breccia on the west side of the pipe. Clasts occupy from 30 to 60% of the volume. Fragments consist of limestone, dolostone, and siltstone with many jasperized silicious nodules of Toroweap and Hermit origin. Most clasts vary from subround to angular and range in

size from coarse-grained sand size to 1.2 m in diameter. The matrix consists of light to dark grey silt- to clay-size material derived from Hermit siltstone and silty carbonate. Disseminated humate is probably a constituent of the darker matrix. The matrix also appears to contain the overwhelming majority of mineralization.

The most unique ore-bearing lithology in the Kanab North mine is located on the east side of the pipe on the same level as above. In this segment, there is a small-clast breccia, very similar to the one described earlier, adjacent to a shear zone. This shear zone roughly delineates the boundary of the pipe. The breccia contains only low- to marginal-grade ore while sandy beds that are cut by concentric fractures forming the peripheral part of the pipe host the major portion of the ore peneconcordant to the bedding. These beds range in thickness from 0.3 to 1.5 m, usually with an equivalent bed of shale above and below. Ore grade in these beds is high, grading and thinning away from the fractures.

Mineralization

Pitchblende, at times sooty in character, is the prevailing U mineral. Pitchblende occurs as irregularly shaped to microbotryoidal aggregates filling open spaces. Coffinite occurs together with pitchblende interstitial to sand grains in sands of the lower portion of the deposit.

The sulfide assemblage is made up mostly of pyrite and marcasite, both of which fill open spaces between fragments and replace matrix components. Some pyrite is zoned and contains well-defined cores of thin bands of bravoite. Marcasite is usually associated with larger pyrite aggregates, and is concentrated near margins of such aggregates. These Fe sulfides are particularly abundant in the upper 30 m of the exposed pipe, which would indicate a sulfide cap or hood lying above the U mineralization. Gersdorffite is present in lower portions of the deposit as a matrix constituent in some lower Hermit sands. Copper minerals include relatively abundant chalcopyrite and smaller amounts of chalcocite, enargite, and tennantite. All of these minerals appear to be later than pyrite and show a general sequence indicating early enargite followed by tennantite, chalcopyrite, and chalcocite. Chalcocite replaces both chalcopyrite and tennantite. Sphalerite appears to be deposited coeval with chalcopyrite. Locally, it forms relatively coarse-grained and abundant aggregates. In peripheral fractures, sphalerite occurs as fillings and sometimes as euhedral tetrahedrons on calcite crystals. Galena is locally abundant in the matrix and as tiny inclusions in pitchblende. Jordisite has been observed only in upper portions of the pipe forming a halo around high-grade pitchblende ore.

As indicated earlier, most ore in the Kanab North deposit is concentrated in the breccia matrix rather than within clasts. The matrix consists predominantly of calcite, dolomite, chert, chalcadony, quartz, kaolinite, illite, with minor anhydrite, baryte, and black opaque humates (biobituminens?). Allogenic components, which probably originated from clastic sediments hosting the breccia pipe, include small quantities of microcline, plagioclase,

muscovite, biotite, glauconite, and collophane as well as accessory amounts of zircon, monazite, apatite, tourmaline, garnet, rutile, leucosene, ilmenite, magnetite, and hematite.

1.4.0.5 Pinenut Breccia Pipe

The Pinenut pipe is located ca. 60 km S of Kanab and 11 km SE of the Hack Canyon deposits. The deposit was partially mined in 1987–1988 and is not depleted. Original resources including production were 556 t U an average grade of 0.445% U (Pool and Ross 2007).

Source of Information. Rasmussen TL, written commun. (1986, 1989).

Geological Setting of Mineralization and Alteration

The surface expression of the Pinenut breccia pipe is a cone-shaped trough roughly 915 m in diameter and 60 m deep. For the most part, geologic exposures in the cone are the uppermost strata of the Harrisburg Member of the Permian Kaibab Formation. The central core of the pipe is situated under an alluvium-covered valley at the center of the conical depression. Beneath the alluvium, siltstones from the Triassic Moenkopi Formation fill the upper 60–90 m of the collapse.

A marked reduction of pipe infill starts in the lower 15–30 m of the Moenkopi-derived plug at the top of the breccia pipe. Brecciated siltstones from the Hermit Formation located adjacent to ore are pervasively bleached. Parallel Liesegang bands often occur at the contact between bleached and unaltered siltstones. Secondary oxidation of reduced material within the pipe is noticed in small, isolated places.

Mineralization

The ore mineralogy is, for the most part, similar to the Hack Canyon deposits. Pitchblende, the predominant U mineral, occurs in small spaces between gangue minerals, coats quartz grains, and rims breccia clasts of siltstone derived from the Hermit Formation. Pyrite occurs in concentrations between 30 and 80% of the total rock immediately above and within the uppermost segment of ore-grade mineralization. This corresponds to sulfide caps reported at most other ore-hosting breccia pipes. Cu-bearing sulfide minerals are locally abundant. Covellite appears to be the dominant mineral species and occurs as a cementing agent of Coconino-derived sands. Other metallic minerals include bornite, chalcocite, chalcopyrite, galena, hematite, ilsemanite, siegenite, and sphalerite.

Fractures throughout the breccia pipe are filled with gypsum, the most common nonmetallic mineral in the Pinenut pipe. In addition, quartz, calcite, collophane, and Ra-bearing baryte have been observed. Preliminary observations indicate a possible association of nickel-bearing sulfides and baryte with clasts

derived from the Brady Canyon Member of the Permian Toroweap Formation (personal communication by Gautier 1985, Honea 1982, and Rasmussen TL 1986).

Ore-bearing sandy breccias occur adjacent to barren or weakly mineralized, brecciated siltstones along the planar truncation and at the base of most ore intervals. This strongly indicates permeability-controlled ore deposition along these boundaries. Ore-grade mineralization elsewhere is defined by irregular and gradational changes in uranium content. Mineralization in the lower third of the ore body is continuous and averages over 0.7% eq. U. The upper two-thirds of the ore body are of lower grade and irregular.

Shape and Dimensions of Deposits

Uranium mineralization in the Pinenut ore body extends from 268 to 479 m below the surface. It includes ore-grade mineralization in an elipsoidal column roughly 150 m tall, stratigraphically positioned within the Hermit Formation. The top end of this column is 12 m below the base of the Coconino Sandstone and the bottom end is 49 m above the Hermit/Esplanade formational contact.

Horizontal dimensions of the column average 60 m in N–S and 27 m in E–W direction. The column is plunging approximately at 80° to S10° E. The ore body is abruptly truncated along its western edge by a mostly planar feature striking N10° W and dipping between 70 and 80° W. All the other edges of the main ore body are irregular with several small, isolated pods of ore nearby.

1.4.0.6 Arizona 1 Breccia Pipe

This breccia pipe is situated 10 km S of the Hack Canyon deposits. The Arizona 1 pipe is exposed at the surface where the throat diameter is on the order of 60–90 m. Vertical displacement in the throat averages some 50 m. Uranium mineralization is distributed irregularly over a depth interval of approximately 200 m mainly at the stratigraphic level of the Hermit Formation to a maximum depth of some 420 m from surface (Pool and Ross 2007). This pipe has been partially developed for mining, but development was suspended in 1991 prior to production.

1.4.0.7 Copper Mountain Breccia Pipe

The Copper Mountain breccia pipe is situated in lower Andrus Canyon on the Shivwits Plateau. It produced mainly copper with little uranium (>30 kg U, 0.11–12% eq. U). Workings were in the Supai Formation above an unconformable contact with Redwall Limestone (Scarborough 1981).

Sources of Information. Adamek et al. (1990) amended by data from Wenrich and Silberman (1984) and Wenrich (1985).

Geology and Mineralization

The collapse-breccia pipe is deeply eroded; it is exposed at an elevation from 1,040 to 970 m at the stratigraphic level of the lower part of the Esplanade Sandstone and lower section of the Supai Group. The pipe structure plunges about 45° SE, has a diameter of about 210 m, and consists of a polymictic breccia core, some 100 m in diameter, surrounded by a zone of severely broken wall rock. Hematite-filled ring fractures form the outer limit of the pipe structure. Dolomitization of core material is pervasive. Bleached and dolomitized sandstones with anomalous Ag, As, Ba, Co, Cu, Ni, Zn, and U contents form an alteration halo, up to 250 m in width, around the pipe. Cu and U reach peak concentrations in fractured rocks at the southeastern periphery of the pipe core. U was preferentially concentrated at the water table. The central portion of the core is metal poor.

Intense supergene oxidation, reflected by almost complete replacement of sulfides by limonite and secondary minerals of Ag, Cd, Cu, and Zn affected the pipe down to an elevation of about 960–920 m. Anomalous Au concentrations occur exclusively within the limonitic zone and, similar to other metals, along the SE margin of the breccia core in an arcuate body up to 50 m wide (based on an arbitrarily defined isopleth of 0.14 ppm Au). Within this partly eroded body, a zone between elevations of 998 and 988 m is particularly enriched and contains an average of 4.37 ppm Au and 19.25 ppm Ag; with maximum values of as much as 150 ppm Au. Above and below this zone, the average grade is approximately 0.9 ppm Au and 8.7 ppm Ag. An amount of approximately 300 kg Au was estimated to be contained within the enriched zone.

In a data set of 52 samples collected from drill cores from the pipe core, Au shows positive correlation at the greater than 95% significance level with Ag, Pb, and Zn. Likewise, Ag is clearly correlated with Pb and Zn. The ore mineral assemblage consists of very fine-grained particles of disseminated gold associated with acanthite and smithsonite in a matrix dominated by goethite and lepidocrocite. Additional minerals in this assemblage include Cu carbonates, covellite, greenockite, and hemimorphite, and relics of bornite, chalcopyrite, marcasite, and pyrite.

The gold concentration at Copper Mountain is clearly the result of supergene processes. Assuming that the gold derived from the original pipe, Adamek et al. (1990) postulate a higher initial gold endowment in the Copper Mountain pipe than that in the Orphan Lode and other pipes in order to arrive at the given gold enrichment at Copper Mountain.

1.4.0.8 Canyon Breccia Pipe

The Canyon pipe is an explored, but undeveloped, breccia pipe located about 40 km SSE of the Grand Canyon on the Coconino Plateau.

Source of Information. Pool and Ross 2007.

Geology and Mineralization

The pipe is expressed on the surface by a broad shallow depression in the Permian Kaibab Formation. It is essentially vertical for at least 700 m from the Toroweap Formation to the upper Redwall Limestone. The ultimate depth of the pipe is unknown. The pipe has an average diameter of less than 60 m, but it is considerably narrower through the Coconino and Hermit strata (ca. 25 m). An annular ring surrounds the pipe.

Mineralization extends vertically both inside and outside the pipe over some 540 m, but ore grade mineralization has been found mainly in the Coconino, Hermit, and Esplanade stratigraphic intervals and at the margins of the pipe in fracture zones, i.e. at depths ranging from about 270 to 540 m. Sulfide zones occur scattered throughout the pipe but are markedly concentrated in the form of a sulfide cap near the Toroweap–Coconino stratigraphic contact. The cap averages 6 m thick and consists of pyrite and bravoite. The ore assemblage includes uranium–pyrite–hematite with massive copper sulfide mineralization common in and near the U ore zone. Mineralization appears to be strongest in an annular fracture zone in the lower Hermit–upper Esplanade strata.

1.4.0.9 Rose Breccia Pipe

The Rose pipe is located within the Coconino Plateau to the south of the Grand Canyon, about 70 km NW of Williams, Arizona. It was discovered in 1984 and, in 1990, intermittent anomalous uranium values were drill intersected.

Source of Information. Pool (2007c) unless otherwise noted.

Geology and Mineralization

The Coconino Plateau is underlain by sedimentary and volcanic rocks ranging in age from the upper Paleozoic to the Quaternary. Flat-lying strata of the Lower Permian Kaibab Formation lies at or near the surface in the vicinity of the Rose pipe (Billingsley et al. 1986). The Kaibab Formation consists of the Harrisburg and Fossil Mountain members. The Harrisburg Member averages 37 m thick and consists of shale, sandstone, and gypsiferous siltstone interbedded with fossiliferous limestone, dolomitic sandstone, and silicified chert beds. The underlying Fossil Mountain Member averages 75 m in thickness and comprises cherty limestone and sandy limestone.

Drill cores from the 81 to 87 m interval show breccia with some pyrite, hematite, and limonite, as well as silicification; and from the 200 to 207 m interval, brecciated, vuggy, fractured (open and rehealed) rock with strong limonitization, but also containing pyrite and marcasite. The rock is described as both light blue grey to grey shale and blue green varved shale, and strongly oxidized, fine-grained limey Coconino sandstone.

Limited drilling intersected intermittent uranium mineralization at depths from 345 to 552 m at the western margin of the Rose breccia pipe. Uranium mineralization starts about 38 m below the stratigraphic contact between the Coconino Sandstone and the Hermit Formation and extends into the Supai Group. Mineralization is hosted in breccias and sand flows in the pipe interior as well as in the ring fracture zone immediately outside of the pipe. Sulfide mineralization occurs in many parts within the Rose pipe and adjacent wall rocks. Alteration is pervasive, however variable in intensity and is particularly marked in some zones by the oxidation of iron sulfides to brightly colored limonite and hematite.

Mineralization shows considerable variability as to grade and thickness. Based on a cutoff grade of 0.042% eq. U, intersected ore intervals range from less than 0.15 to 15 m and average 0.055 to 0.12% eq. U. In addition to uranium, chemical analyses from the 420 to 435 m interval and from the 527 to 530 m interval have unusually high concentrations of various metals as reflected by some core intervals assaying as much as 4.1% As, 0.95% Ba, 0.49% Co, 0.62% Mo, and 2.77% Ni. These contents are 2–25 times higher than published maximum values from other breccia pipes in the region (Table 1.7).

1.4.0.10 Other U-bearing Breccia Pipes on the Coconino Plateau

There are several breccia pipes with known uranium mineralization located within about 25 km of the Rose pipe including the SBF, Blue Mountain, and Lynx pipes.

The **SBF pipe** is located about 1.5 km west of the Rose pipe. This pipe was drilled in the 1980s. Uranium mineralization was encountered in the pipe.

The **Blue Mountain pipe** is located about 25 km WSW of the Rose Pipe. The highest-grade intersection was 3 m of 0.072% eU (Van Gosen et al. 1989).

The **Lynx pipe** is situated some 15 km north of the Rose pipe (16 km SSW of the Sage pipe). The Lynx pipe has two throats (or two separate pipes) that converge near the surface, sharing the same surface collapse cone of depression. There is a block of undisturbed ground between the two throats that correlates very well with stratigraphy outside the pipes. Mineralization extends presumably to a depth of about 560 m. The best intercept was encountered in the annular ring system between undisturbed country rock and the breccia column (5.3 m–1.93% U at a depth of 538 m) (McMurray, personal communication).

1.4.0.11 Selected Former Breccia Pipe Mines and Prospects in the Arizona Strip Area

Scarborough (1981) provides the following information on some former Cu–U-bearing breccia pipes that have been mined or prospected prior to the 1970s (location see Fig. 1.57).

Copper House breccia pipes No. 1 and 2 (0.14% U, 3.99% Cu; 0.01% V_2O_5); *No. 1 pipe*: The limestone of the Toroweap Formation has collapsed 90 m through the Coconino Sandstone into the Hermit Formation stratigraphic interval. The Coconino Sandstone is altered to yellow and purple. Underlying Supai rocks are bleached. A circular fracture zone exhibits bleaching. *No. 2 pipe*: Radioactivity occurs along fractures trending N50° W in bleached Supai Formation. Basalt(?) dikes and a fault zone occur in the immediate area of mineralization.

Copper House, Coalition No. 2 breccia pipe (0.04% U, 0.02% V_2O_5 , 4.57% Cu): U and Cu minerals occur in a curving brecciated zone in bleached and fractured coarse-grained rocks of the Supai Formation.

Cunningham mine: Radioactivity is associated with Cu and Fe fracture fillings in well-bedded silty facies of the Redwall Limestone, 45 m below its top. The main tunnel intersected Fe and Cu mineralization in a 2.5–3.0 cm wide vein dipping 30° S.

Grandview mine (Last Chance mine): 1.6% U. This deposit lies along the WNW-trending Cremation fault. Uranium minerals are associated with limonite, copper carbonates, silicates, and sulfate minerals. These minerals along with minor pyrite and other sulfides were found along brecciated, bleached, and marbleized Redwall Limestone in a pipe-like body cutting the basal Supai Formation and upper Redwall Limestone. Metazeunerite/zeunerite was identified in a limonitic gossan-type. The presence of kaolinite and fully hydrated zeunerite suggests a temperature of formation below 70°C.

Old Hack Canyon mine (located near Hack Canyon No. 1 mine described earlier): In situ grades ranged from 0.07 to 1.52% U. Production amounted to 1,200 t ore at 0.15% U plus 50 t ore at 0.007% U yielding 1.87 t U. This deposit of breccia pipe origin exhibits slump structures possibly involving Toroweap and Coconino sandstones and Hermit shale. Rocks are bleached and silicified. Pitchblende mixed with chalcocite occurred in the breccia zone and in some of the coarser grained sandstones. Fractures were coated with brochantite, bieberite, chalcantite, erythrite, malachite, metatorbernite, torbernite, and zippeite.

Ridenour mine: In situ grades were as high as 1.79% U, 10.38% V_2O_5 , and 14.15% Cu, with traces of cobalt. Cu production amounted to 900 t. U was recovered from 13 t ore at 0.127% U and 2.38% V_2O_5 giving 17 kg U and 310 kg V_2O_5 . Carnotite-type mineralization associated with copper carbonates, silicates, and sulfides along with pyrite and iron oxides was hosted in an inferred pipe-like body of fractured and bleached rocks of collapsed Supai Formation sediments. Mineralization was both disseminated and in vein-like structures, and strongest

along the pipe periphery. The vanadium to uranium ratio was greater than 10:1. Carnotite was associated with carbon. Thin coatings of metatuyamunite formed on stope faces at ground water seeps. Volborthite was abundant.

Riverview Group No. 1–9: This group of pipe-like deposits is located near Cameron, Arizona; two of which were mined in the past. The *Riverview mine* has a recorded production of 1.5 t U. Ore averaged 0.32% U, 0.03% V_2O_5 , and high-grade Cu. In situ U grades ranged up to 2.1%. Metatorbernite with considerable malachite occurred in a 36 m diameter pipe-like structure that crops out in the Moenkopi Formation. Blocks of lower Chinle (Shinarump?) sandstone have dropped into the Moenkopi Formation and fill the top of the column. Ore occurs in the upper 16 m of the pipe in these sandstone blocks as well as in a siltstone and mudstone breccia derived from the Moenkopi Formation, but mostly in a peripheral fracture zone. The structural situation resembles that of the Orphan Lode. Also, the ore (high U, high Cu, very low V) more closely resembles that of the Orphan Lode than that of other U deposits in the Cameron area (intermediate U, intermediate V, some Mo, and Cd). The *Savannic mine* (or Bronze L mine) produced Cu by underground methods from fractures/shears along bedding planes in the Redwall Limestone. The main mineralized shear is 0.3–0.9 m wide and dips 60° E. It contained Cu, Fe, and Mg minerals and dolomite, which were cemented by calcite. No U mineralization is recorded.

Selected References and Further Reading for Chapter 1.4 Arizona Strip Area

- Adamek et al. 1990; Baillieul and Zollinger 1982; Barrington and Kerr 1963; Billingsley et al. 1986; Bowles 1965, 1977; Boyden 1978; Breed and Roat 1976, 1978; Brown et al. 1990; Chenoweth and Malan 1969; Chenoweth 1986a; Finch 1967; Four Corners Geol. Soc. 1969; Gornitz 1969; Gornitz and Kerr 1970; Gornitz et al. 1988; Granger and Raup 1962; Hoffman 1977; Jensen et al. 1960; Karlstrom et al. 1974; Kofford 1969; Krewedl and Carisey 1986; Landais et al. 1987, 1989; Ludwig and Simmons 1988, 1992; Ludwig et al. 1986; Magleby 1961; Mathews 1978b; McKee 1978; Miller and Kulp 1963; Miller 1954a, b; Nations and Stump 1981; O'Neill et al. 1981; Peirce et al. 1970; Pool and Ross 2007; Pool 2007c; Rasmussen et al. 1986; Scarborough 1981; Stewart et al. 1972; Sutphin 1986; Van Gosen et al. 1989; Watkins 1976; Wenrich 1985a, b, 1986a, b, 1989, 2007; Wenrich and Huntoon 1989; Wenrich and Palacas 1990; Wenrich and Silberman 1984; Wenrich and Sutphin 1989; Wenrich et al. 1986, 1989; Wenrich-Verbeek and Verbeek 1982; Wenrich-Verbeek et al. 1982; and pers. commun. by Adamek P, Casadevall WC, Casebolt LL, Cunningham CG, Energy Fuels Exploration R&D staff, Gautier A, Hillard P, Holland R, Honea RM, Ludwig KR, Mathisen IW, McMurray J, Norris J, Pillmore DM, Pool TC, Rasmussen JD, Rasmussen TL, Spiering ED, and Wenrich KJ.

Chapter 2

Wyoming Basins

The Wyoming Basins constitute a prominent uranium province, second in magnitude in the USA only to the Colorado Plateau. There are nine designated basins in Wyoming, all of which contain uranium occurrences. Significant uranium production has come from the *Wind River*, *Great Divide*, *Shirley*, and *Powder River* basins. Minor uranium production was in the *Washakie* and *Sand Wash basins* in southern Wyoming-northwestern Colorado (►Fig. 1.1 and ►2.1).

The Wyoming Basins are host to rollfront (or roll-type) uranium mineralization, a distinctive subtype of sandstone-type uranium deposits. Although roll-type uranium ore bodies occur in other regions, e.g., in southern Texas, and although a number of geologists consider all uranium ore bodies in sandstone in the western USA to be of a more or less similar genesis, Wyoming rollfront deposits reveal certain physical and chemical characteristics that suggest a distinctive metallogenesis, to some extent at least different from other types of sandstone uranium deposits.

Remaining resources (<\$130/kg U category, status end 2002) in Wyoming are estimated at about 141,000t U at an average grade of 0.065% U (US EIA 2003).

Uranium mining began in 1952, and produced through 2006 about 84,000t U. More than 100 mines had been active during this period. Most were conventional underground and open pit operations, and only a few extracted uranium by in situ recovery or ISR (also referred to as in situ leaching or ISL) technology.

Sources of Information. Authors listed in section References and Further Reading, at the end of Chapter 2 Wyoming Basins, and personal communication by Andrus (1984), Catchpole G (2008), Harshman EN (1984), Pool TC (2008), Schäffer (1984), and Voss WC (1984) provided the base for the following text, in particular, however, Harshman and Adams (1981) who have elaborated in great detail on the principal characteristics of uranium deposits in the Wyoming Basins. Harshman EN kindly reviewed the original manuscript of the chapter Wyoming and has amended and improved both the content and text.

Regional Geological Features of the Wyoming Basins

The major rollfront uranium deposits of Wyoming occur in intermontane Tertiary basins (►Fig. 2.1), which range in size from a few hundred square kilometers (Shirley Basin) to several thousand square kilometers (Powder River Basin). These basins were downwarped during the Laramide Orogeny, and most were developing by Late Cretaceous or Early Paleocene time. Subsidence, uplift, and displacement along faults at the margins of some basins continued through most of the Tertiary, but in

most cases later tectonism did not greatly affect the basin fill and its uranium deposits.

Tertiary sediments of the Wyoming Basins are dominantly of continental provenance and range in age from Paleocene to Quaternary as shown in ►Table 2.1. These sediments reflect high relief and rapid erosion of source areas in response to Laramide block faulting and mountain uplift, which was accompanied, during deposition of younger formations, by explosive felsic volcanism.

The *Paleocene Fort Union Formation* is the oldest of the Tertiary sequence. It is present in all Wyoming Basins, but in the Shirley Basin it was largely removed by erosion prior to deposition of younger rocks. The Fort Union Formation not only consists largely of fine-grained, quartzose sandstone with admixed silt, clay, and coal of fluvial or lacustrine origin but also contains beds of coarse stream debris, particularly near the mountain fronts that flank the basins. The coarse facies is composed of quartzose sandstone, limestone, chert, and sandstone pebbles that are derived from Paleozoic and Mesozoic rocks in the uplifts. Arkosic facies are rare. Formation thickness ranges from less than 30 m in the Shirley Basin up to 900 m in the Powder River Basin. Fort Union strata rest upon an erosion surface with several tens of meters of relief cut into Paleozoic and Mesozoic rocks. It is unconformably overlain by Early Eocene sediments.

The *Early Eocene Wasatch, Wind River, and Battle Spring* formations occur in all four major basins in Wyoming and provide the host for the principal uranium deposits. Each of the three formations ranges in total thickness from about 150 m in the Shirley Basin to more than 900 m in the Great Divide Basin. The three formations are approximate time equivalent, and have many lithologic, textural, and compositional similarities. They comprise a sequence of arkosic sandstone, conglomerate, siltstone, claystone, carbonaceous shale, and coal of fluvial and lacustrine origin. In contrast with the underlying Paleocene rocks, the Wasatch Formation and stratigraphic equivalents contain much granitic debris.

On a regional basis, Early Eocene sediments can be divided into a mountainward lithologic facies comprising coarse-clastic rocks with boulders as much as 7.5 m in diameter and a basinward facies composed of fine-grained clastic sediments with some interbedded pebble, cobble, and boulder beds. The two facies interfinger and intertongue. Correlation of gross lithologic units can be made over many kilometers, but individual coarse-grained beds have limited continuity. Sandstone units range from a few to 60 m in thickness. They are separated by siltstones and claystones of similar thickness.

The *Upper Eocene Wagon Bed Formation*, up to 100-m thick, overlies conformably the Lower Eocene strata and occurs in the Wind River and the Shirley basins, but erosion has removed large quantities of the sequence mainly at the change from Eocene to Oligocene. The Wagon Bed Formation is considered the most impervious formation of the Tertiary sequence. It is largely of fluvial origin with volcanic interbeds. Lithologies include silicious bentonite, siltstone, mudstone, sandstone, and yellowish or greenish-grey tuff. In some areas, the tuff has been altered to clinoptilolite; in other areas, it is relatively unaltered. Considerable amounts of poorly sorted

■ Table 2.1.

Wyoming and adjacent western South Dakota, principal stratigraphic units in uranium districts. (After Harshmann and Adams 1981 based on Harshman 1968; and Boberg 1981)

Era	Period	Epoch	Group/formation		
			Central + SE Wyoming	Black Hills	
Cenozoic	Quaternary	Recent-Pliocene	Stream alluvium and terrace gravels		
		Tertiary	Pliocene	Ogallala Fm	Ogallala Fm
	Miocene (?)		Browns Park Fm (U)	(Absent)	
	Miocene		Arikaree Fm	Arikaree Fm	
	Oligocene		White River Fm	White River Fm	
	Eocene		Wagon Bed Fm (U) Wind River Fm (U) Wasatch Fm (U) (Puddle Springs Fm ^a) (U) (Battle Spring Fm ^b)(U)	(Absent)	
	Paleocene	Fort Union Fm (U)	Fort Union Fm (U)		
Mesozoic	Cretaceous	Upper	Lance Fm	Hell Creek Fm Fox Hills Fm or Ss	
			Lewis Sh	Pierre Sh	
			Mesa Verde Fm (U)		
			Steele and Gody Shs	Niobrara Fm	
			Frontier Fm	Carlile Sh, Greenhorn Fm, Belle Fourche Sh	
		Lower	Mowry Sh	Mowry Sh	
			Thermopolis Sh	Newcastle Ss, Skull Creek Sh	
			Cloverly Fm	Inyan Kara Gp (U) Fall River Fm (U) Lakota Fm (U)	
		Jurassic	Morrison Fm	Morrison Fm	
			Sundance Fm	Sundance Fm	
	Gypsum Spring Fm		Gypsum Spring Fm		
	Nugget Ss		(Absent)		
	Triassic	Chugwater Fm	Jelm Fm Chugwater Fm	Spearfish Fm	
		Dinwoody Fm	Goose Egg Fm		
	Paleozoic	Permian	Phosphoria Fm	Minnekahta Ls	
			Park City Fm	Opeche Fm	
		Pennsylvanian	Tensleep Ss	Casper Fm	Minnelusa Fm
Amsden Fm					
Mississippian		Madison Ls	Pahasapa Ls		
Devonian		(Absent)	Englewood Fm		

Table 2.1. (Continued)

Era	Period	Epoch	Group/formation	
			Central + SE Wyoming	Black Hills
	Ordovician		Bighorn Dol	Whitewood Ls
				Winnipeg Fm
	Cambrian		Gallatin Ls	Deadwood Fm
			Gros Ventre Fm	
			Flathead Ss	(Absent)
	Precambrian			Granitic and metamorphic rocks

(U) Units with significant uranium production
^{a, b} The mountainward facies of the Wasatch Formation is designated.
^aBattle Spring Formation in the Great Divide Basin
^bPuddle Springs Formation in the Gas Hills area

Formation contain significant rollfront-type U deposits in the Wyoming Basins. The most favorable host rocks are friable, fine- to coarse-grained or pebbly, arkosic sandstones, which have been compacted by the weight of thousands of meters or more of sediments that once rested upon them. These favorable sandstones contain considerable amounts of pyrite and carbonaceous matter, and occasional iron-stained mudstone clasts and tabular mudstone splits. Their detrital heavy minerals fraction varies between 1 and 5%. Sand- or silt-filled channels with crossbedding are universally present.

Calcite cement or concretions are sparse and commonly account, in favorable sandstones unaffected by mineralization processes, for less than 1%. Calcite accumulations, however, occur in association with ore bodies.

Carbonaceous material is dispersed through host sandstones with somewhat greater concentration on cross-stratification beds. This organic debris consists predominantly of leaf and twig fragments, but occasionally also of humic material. The latter coats sand grains. A few large pieces of tree trunks and branches, some silicified and others carbonized, are found in the Shirley Basin host rocks. The organic carbon content of host rocks ranges widely from place to place but probably averages 0.5% or less.

Pyrite of diagenetic origin occurs disseminated in all reduced uranium host rocks, but locally also as cement in coarse-grained sandstone or replacement of carbonaceous material. Pyrite content of sandstone in an ore-bearing horizon that was unaffected by ore-related alteration ranges from less than 1 to about 3%.

Below the water table, and where not oxidized or altered by ore-forming solutions, host sandstones are generally light grey or greenish-grey depending on the amount of pyrite, organic material, and mineralogical rock composition.

Sandstone horizons are interbedded with fine-grained facies ranging from mudstone or claystone to compact but somewhat friable siltstone. These facies are brown to tan, greenish-grey, dark grey, and almost black when high in organic material.

Lithological suites favorable for ore deposition are found principally in the central part of fluvial systems in the basins, in

large fans that range in length from a few kilometers or tens of kilometers as in the Wind River and the Shirley basins to as much as 60 km in the Great Divide Basin.

Individual sandstone beds within fans have only a limited lateral continuity. Thicknesses range from a few to several tens of meters. Although widespread, favorable sandstone units contribute only a limited fraction of the total volume of sediments in the basins.

According to Galloway (1979b), sediments were deposited under coarse bed-load conditions or on distal parts of wet alluvial fans in two major Paleocene-Early Eocene drainage systems (Fig. 2.2a and b). During the time of sedimentation, a tropical or semi-tropical climate prevailed with dry periods probably alternating with wet periods. The warm climate began in the Cretaceous and lasted through the Early Tertiary, probably becoming temperate by Middle Oligocene.

Principal Host Rock Alteration

The most prominent alteration phenomenon in uranium-hosting sandstones of the Wyoming Basins is an oxidation tongue with related mineral alterations that ends downdip in a redox front with differential authigenic mineral distribution. Although host rocks in various basins exhibit certain differences in character and extension of these alteration features, there are some distinct similarities caused by this oxidation of sandstones in the major districts.

Harshman and Adams (1981) list the common cognition features for altered sandstones, as compared to normally grey unaltered sand(stone) (a) a distinctive change in color, (b) a considerably higher selenium content, (c) a generally higher eq.U/U ratio, (d) much lower calcium carbonate, organic carbon, and sulfate contents, and (e) partial or complete destruction of some or most heavy minerals, particularly pyrite and magnetite.

Figure 2.3a shows the terms used in the description of roll-type U ore bodies. Figure 2.3b illustrates in simplified cross sections the principal types of alteration in some uranium

mining districts (for more details see next paragraph); and [Fig. 2.4](#) illustrates the different alteration and mineralization zones, related authigenic minerals, and chemical reactions involved.

Two generations of pyrite exist in reduced ore-bearing sandstone horizons, downdip from the redox front. As mentioned earlier, a diagenetic pyrite, which is thought to have resulted from reaction of biogenic hydrogen sulfide with iron-bearing minerals; and a second pyrite variety that is restricted to zones of mineralization and related to uranium ore-forming processes.

Oxidative alteration penetrates host formations in a tongue-like fashion. Tongues may range considerably in size and shape. They can have lateral extensions of several hundreds of square kilometers and thicknesses of as much as a few tens of meters. In most districts, there are several altered tongues and associated mineralization within a generally favorable sequence of aquifers, each separated from the other by an intercalated aquiclude

horizon. In some instances, superimposed tongues of oxidized sandstone are connected by altered sand filling a depositional breach in bounding impermeable sediments. Although altered tongues frequently overlap, their edges are rarely superimposed. Tongues of oxidized sandstone may or may not completely occupy the sandy interval in which they are confined. Incompletely, oxidized intervals occur most frequently at ends of oxidation tongues.

Principal Characteristics of Mineralization

Pitchblende and coffinite are the principal U minerals that commonly accumulate in a rollfront at the head of an altered tongue, the characteristic features of which are shown in [Fig. 2.5a–d](#). U minerals coat sand grains fill voids in sandstone and possibly replace organic matter. Uranium is accompanied by a number of

Fig. 2.2.

(a) Wyoming, regional setting of present and inferred Paleocene–Eocene drainage systems, alteration tongues, and principal uranium districts. (b) Wyoming, central and southern Powder River Basin, regional paleoflow patterns and facies distribution of the upper Fort Union-lower Wasatch(?) fluvial systems and position of uranium deposits. (After Galloway 1979c; Harshman and Adams 1981)

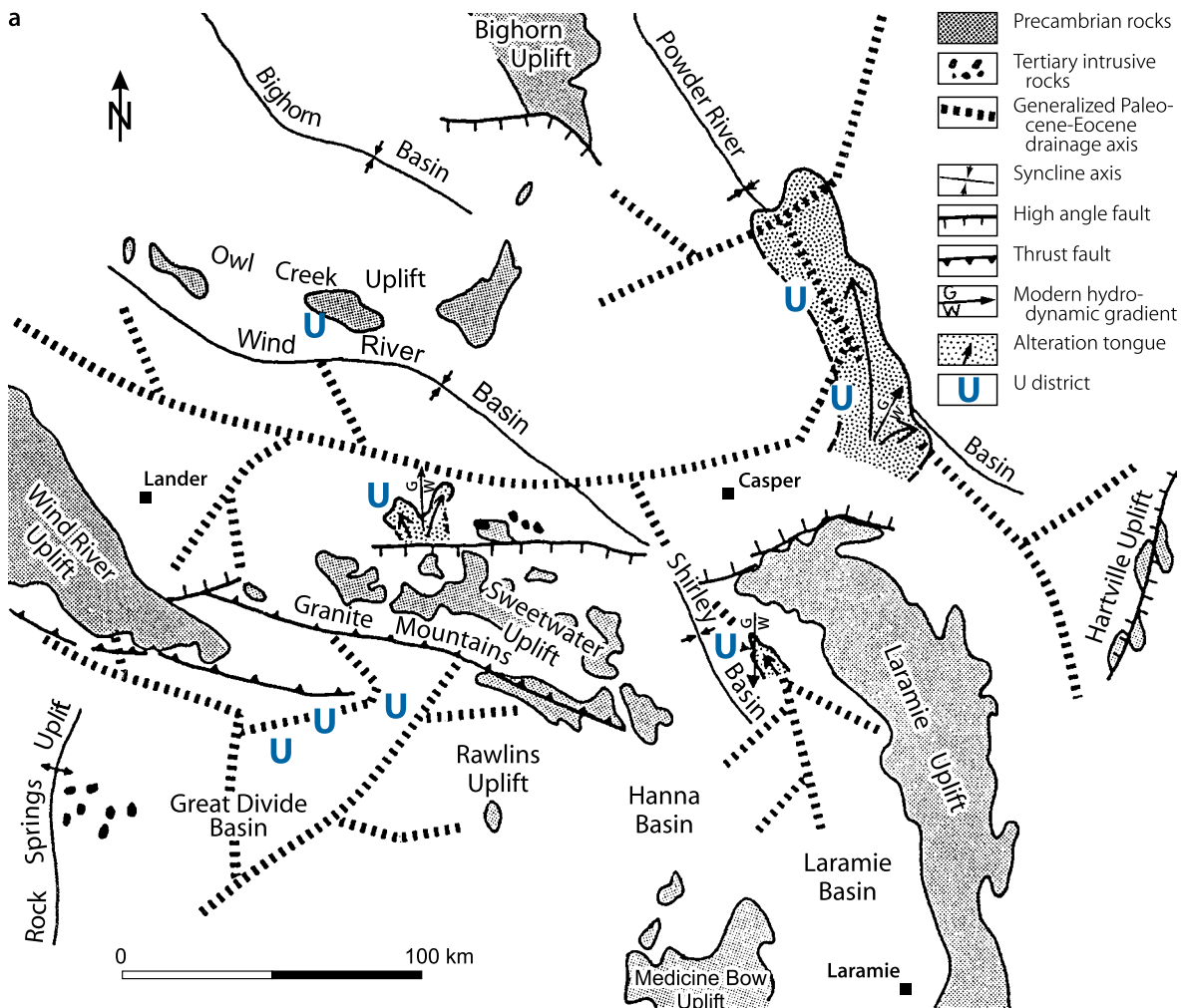
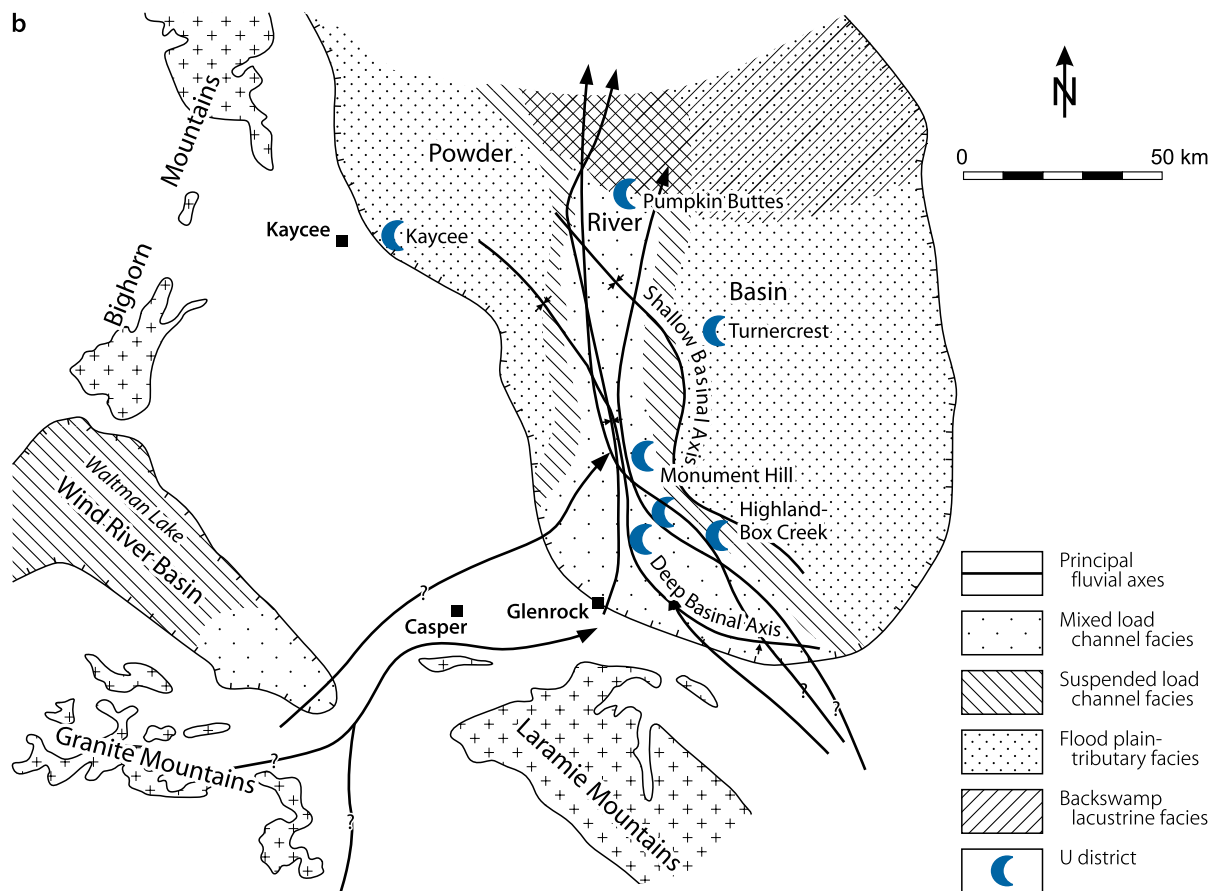


Fig. 2.2. (Continued)



elements, which have been deposited in or adjacent to the roll-front at the head of an altered tongue (Fig. 2.6a and b). Selenium occurs as native selenium and ferroselite on the concave side of the rollfront, and as native Se in reduced mineralized rocks. Molybdenum (jordisite, MoS_2) and calcite are present on the convex side. Other elements include arsenic, phosphorus, and copper.

Pitchblende and coffinite commonly occur as intimate intergrowths. Uraniferous material with variable reflectance, intermediate between that of pure coffinite and pitchblende, is commonly present (sooty pitchblende?). Semiquantitative microprobe analyses always show the presence of major quantities of Ca and Si in both pitchblende and coffinite, but no other major metals besides U (Harshman and Adams 1981).

Ludwig (1978) for his geochronologic studies subdivided uranium ore in the Shirley Basin into three types: (a) disseminated pitchblende ore, (b) calcite-cemented ore, and (c) massive pitchblende ore, a division that can be, somewhat generalized, applied to most deposits in the Wyoming Basins.

Disseminated pitchblende ore. Samples derived from water-saturated, essentially unconsolidated, texturally and mineralogically immature, coarse-grained arkose. One of the samples with 7.6% U contained abundant charcoal-like organic material. Such carbonaceous trash is moderately common in unaltered arkose, in many cases with well-preserved log- or limb-like forms.

Pitchblende and pyrite were moderately abundant (0.5–2% by volume of each) in the samples. Grain coatings of pitchblende and organic material give ore a grey-black cast. Pitchblende, pyrite–marcasite, and rare baryte were the only nondetrital minerals identified in ore.

Pitchblende samples appeared quite pure with pyrite as the only visible contaminant. Pitchblende grains were deep black, with a pitch-like luster on unbroken surfaces. Near-equant, 0.1–0.3-mm microbotryoidal forms were common. Pyrite samples (with ca. 70% pyrite) from ore contained several types of impurities including pitchblende, a rust-brown amorphous material (goethite?), fragments of detrital grains, and aggregates of an amorphous white material (clay?). Marcasite and ferroselite may also have been present, but were not recognized.

Three main types of pyrite forms were observed: (1) Euhedral and subhedral grains, ca. 100 μm in diameter, with cubic and cubo-octahedral habits; (2) roughly equant aggregates (100–500 μm in diameter) of small crystals (1–10 μm); and (3) irregular and rod-shaped grains, many of these were aggregates of smaller crystals, but some had a smooth surface. Forms (2) and (3) include typical framboidal habits, which perhaps were formed during early diagenesis of the sediment.

Many “charcoal” lumps had a checkerboard-patterned surface similar to burnt wood, while surfaces of others were conchoidal and had a pitch-like luster. Sparse accumulations looking like white salts were enclosed in several lumps.

■ Fig. 2.3.

(a) Wyoming, correlation of terms describing various features of sandstone hosted roll-type uranium ore bodies. (b) simplified sections across the edges of altered sandstone tongues documenting the most common types of alteration features present in major uranium districts. (After Harshmann and Adams 1981)

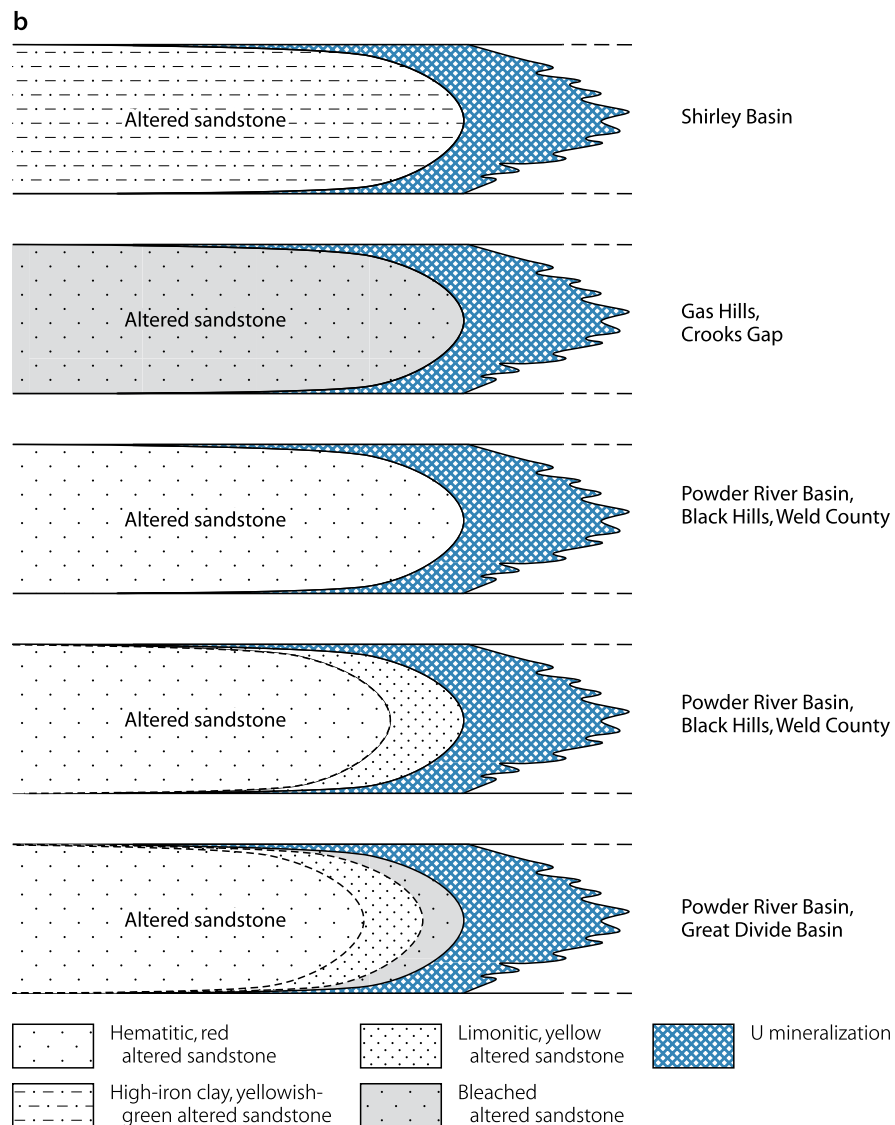
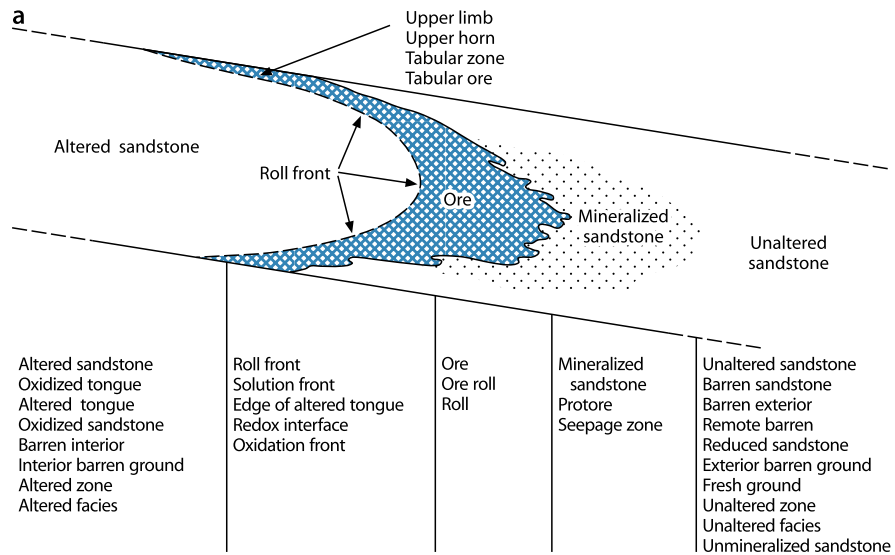
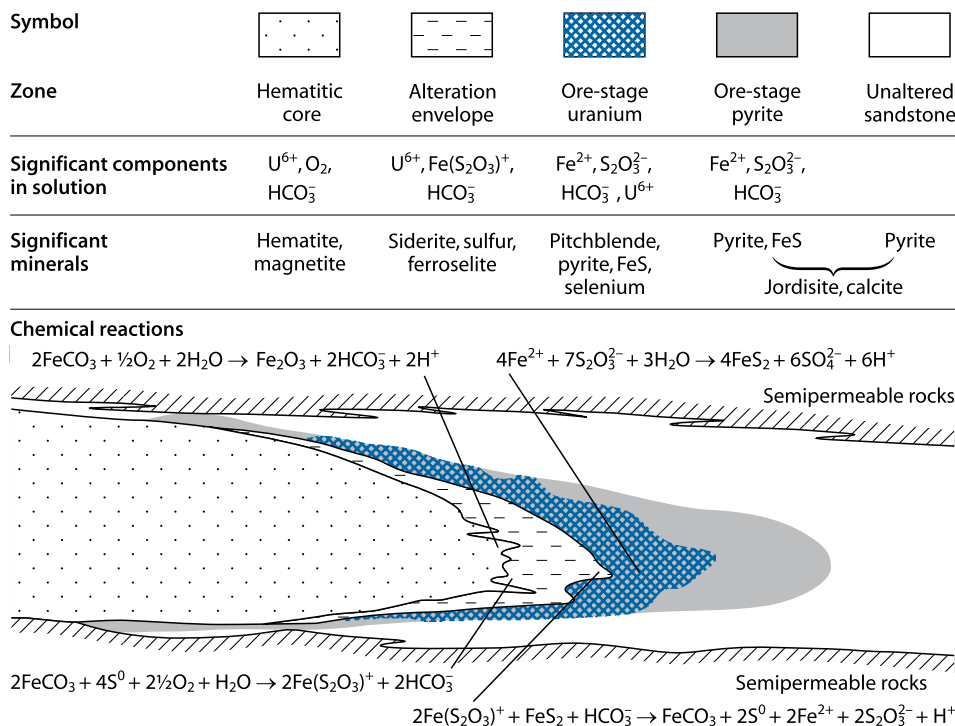


Fig. 2.4.

Wyoming Basins, idealized scheme of a rollfront system with alteration zones, related mineral components, solution components, and summary reactions in the Fe–S–O–CO₂ aqueous system during formation of a rollfront deposit. (After Granger and Warren 1974)



Calcite-cemented ore. This ore is unusual in its high grade (10.4% U) and its texture. Calcite forms a pervasive matrix for detrital grains of mostly quartz and feldspar, with a few heavy minerals, and also corrodes feldspar. Pyrite–marcasite (ratio 20–50/1) and pitchblende are intimately associated. These minerals occur both as incomplete replacements of and as rims around detrital grains. Neither pitchblende nor pyrite–marcasite show crystal faces. Ore is dense, tough, and low in permeability.

Massive pitchblende. The investigated sample (55–61% U) was very small. It consisted almost entirely of pitchblende, with very minor quartz and pyrite. Pitchblende showed no oxidation effects.

Redox front-related distribution of ore and associated elements and minerals. Harshman (1974) investigated in much detail the geochemistry in ore bodies within and adjacent to redox fronts in various Wyoming Basins. One of his striking results is the great similarity of the distribution of elements in most deposits. Essential elements and minerals are arranged, in summary, in the following patterns.

Uranium has been added to reduced sandstone in zones close to or in contact with edges of altered sandstone tongues. The redox interface for uranium coincides with that for iron in some deposits; in others the uranium interface is separated from the iron interface by as much as 5 m of pyrite-bearing reduced sandstone. The uranium content of altered sandstone is slightly

greater (6 ppm) than that of unmineralized reduced sandstone (2–4 ppm), at least within 300 m of the rollfront.

Iron occurs predominantly as ferric iron in altered sandstone and as ferrous iron in unaltered reduced sandstone. Iron, principally as pyrite and to a lesser extent as marcasite constituent, has been added to reduced sandstone at and for some distance away from the edges of altered tongues. In some deposits, the amounts added were small and there is little difference in total Fe content in unaltered and in mineralized sandstone. In other deposits, the Fe content of mineralized sandstone may be an order of magnitude greater than in unmineralized, reduced sandstone.

Pyrite is most abundant in reduced, mineralized sandstone at the edge of altered sandstone tongues, and gradually decreases in quantity toward unaltered sandstone. In most deposits, pyrite extends beyond the uranium mineralization. Pyrite has been destroyed generally, but not always completely, in most altered oxidized tongues. Marcasite associates with pyrite and is most abundant in mineralized reduced sandstone at and adjacent to edges of altered tongues (Fig. 2.7a and b). Pyrite and marcasite in altered sandstone may result from either incomplete oxidation of ore-stage pyrite–marcasite or from post-ore sulfidization and reduction of hematite and limonite/goethite.

Selenium is known in all deposits. It occurs in narrow zones at the edge of altered tongues, astride the edge, or in reduced mineralized sandstone close to the edge. Selenium in altered sandstone may be present as ferroselite (FeSe₂) or native Se, but in reduced sandstones it is generally present as native Se. Trace

■ Fig. 2.5.

Wyoming, cross-sections with characteristics of roll-type uranium deposits. (a) typical strata-controlled position and shape, (b) Shirley Basin, (c) Gas Hills, (d) Powder River Basin (Highland mine). (After (a) Harshman 1974; (b) Bailey 1965; (c) King and Austin 1966 (reproduced by permission of AIME); (d) Langen and Kidwell 1974)

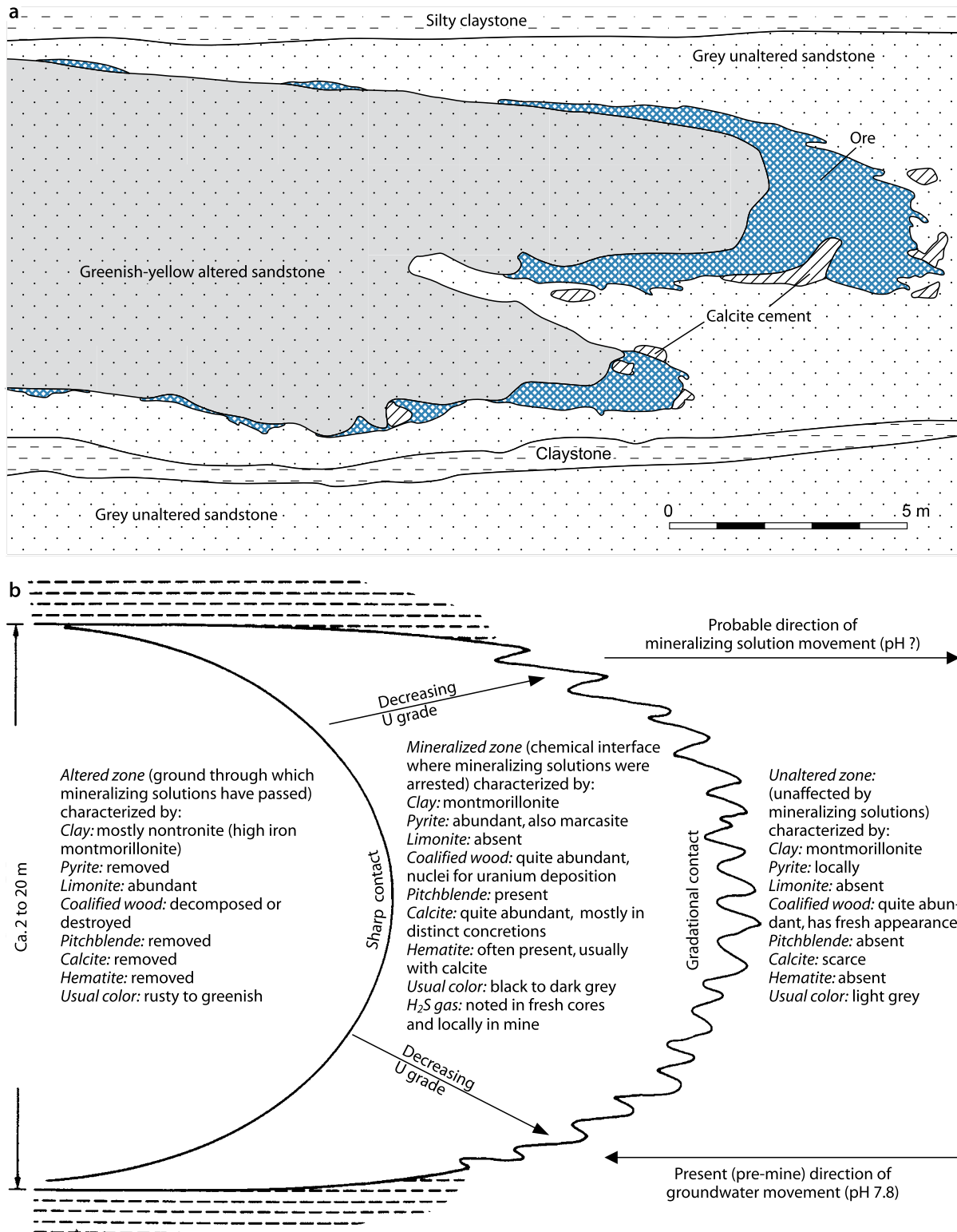
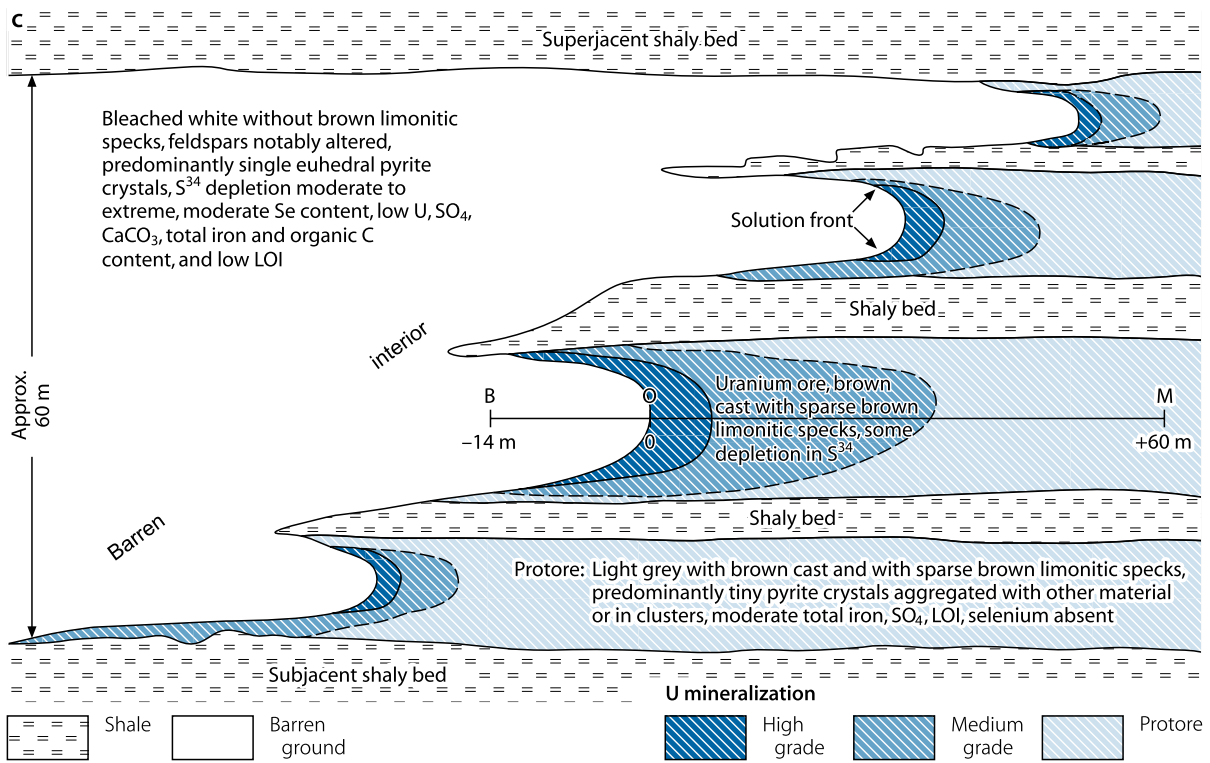
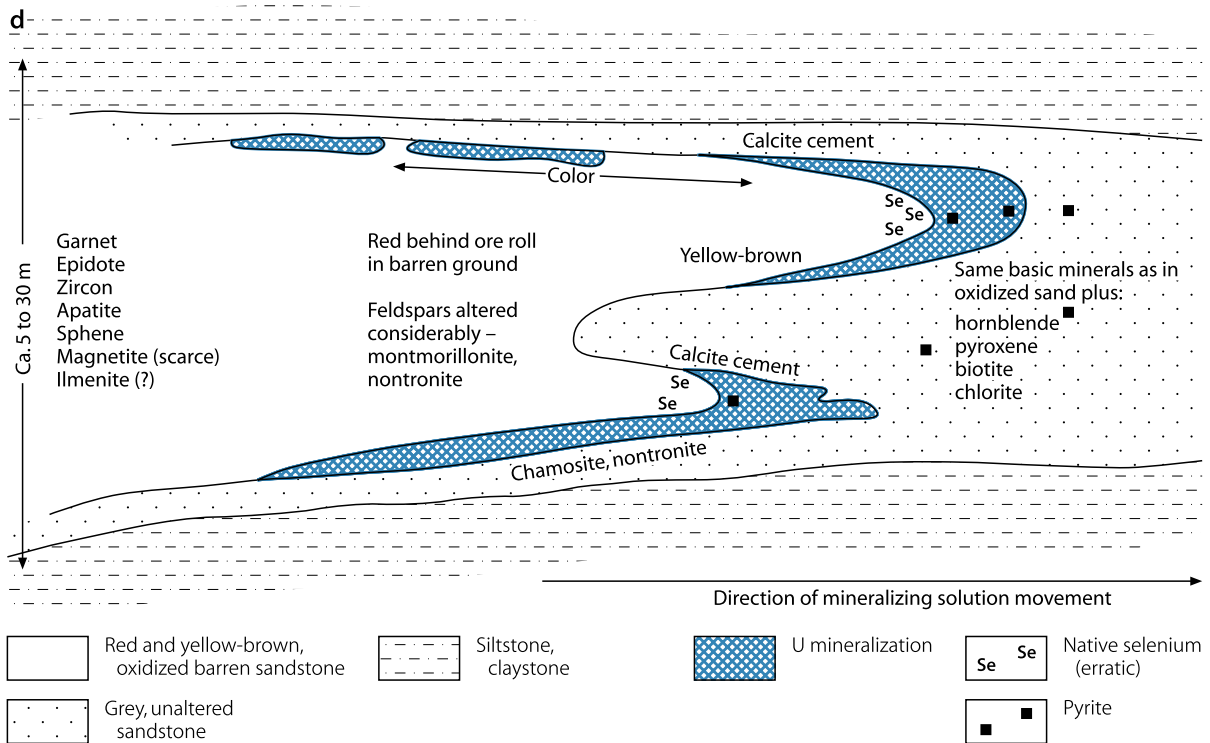


Fig. 2.5. (Continued)



Line B-O-M indicates position of principal traverse from barren (B), through solution front (O) into mineralized zone (M)



■ Fig. 2.6.

(a) Wyoming and South Texas, geochemical profiles illustrating the distribution of U, Se, V, Mo, and pyrite across mineralized redox fronts. (b) Shirley Basin, graphic summary of epigenetic mineral deposition. Lengths of arrows indicate relative positions and widths of zones through which minerals were deposited; dashed lines show intervals of possible deviations from normal conditions. ((a) Harshman 1974, (b) Harshman 1972; Harshman and Adams 1981)

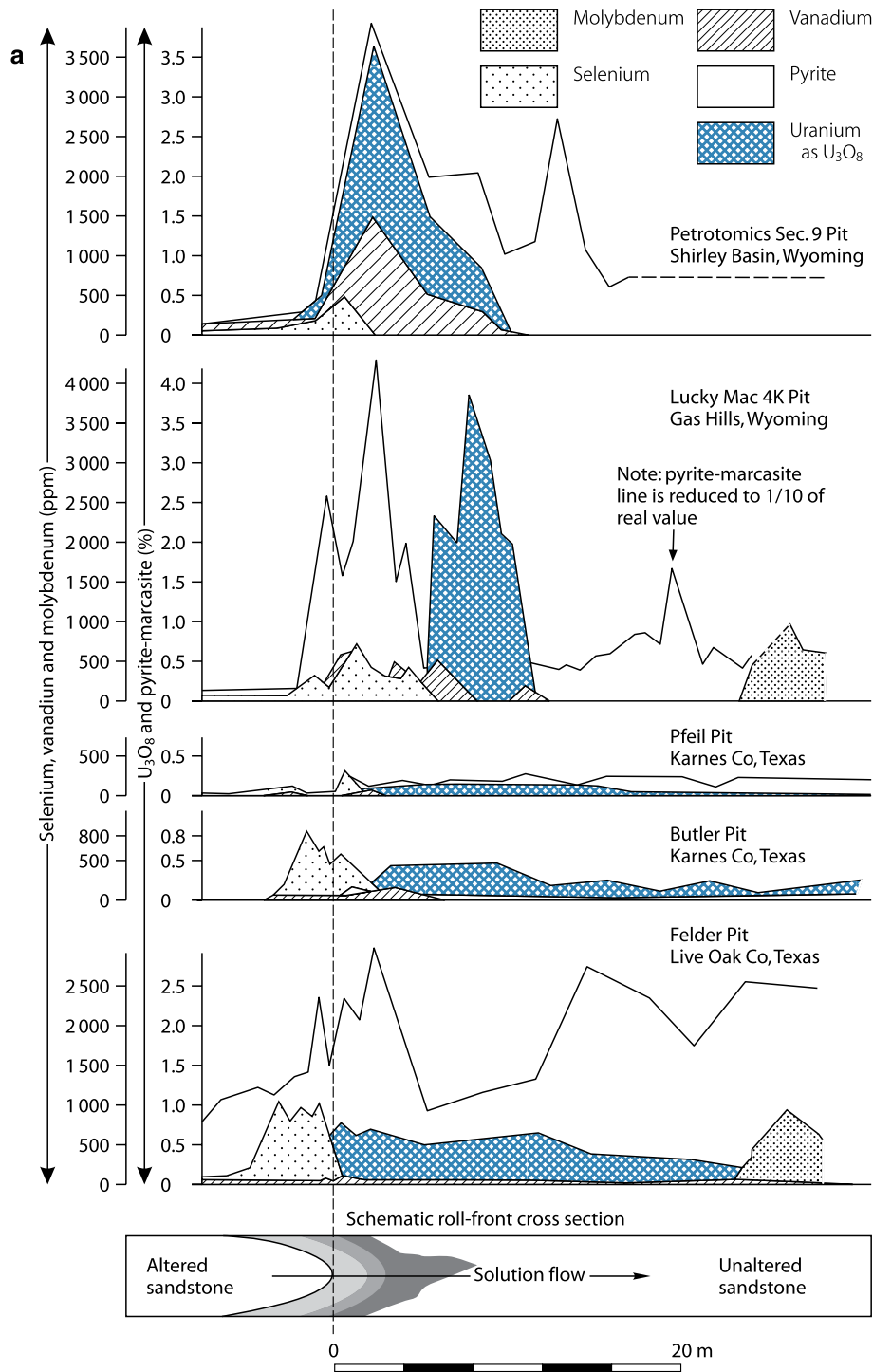


Fig. 2.6. (Continued)

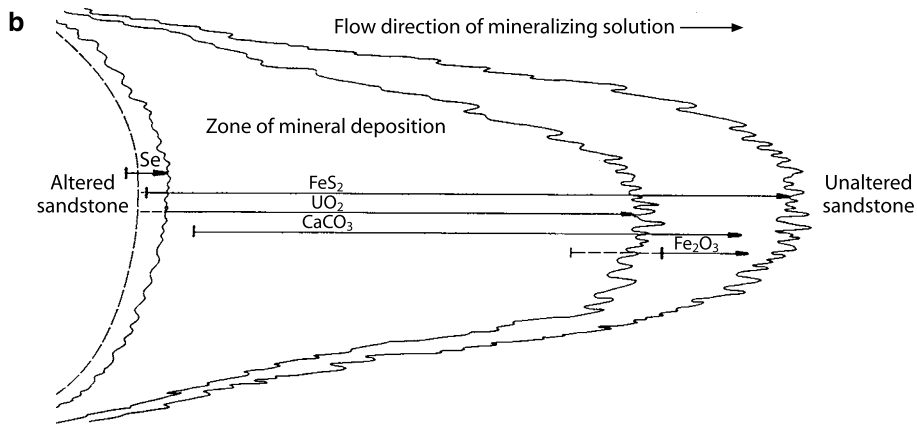
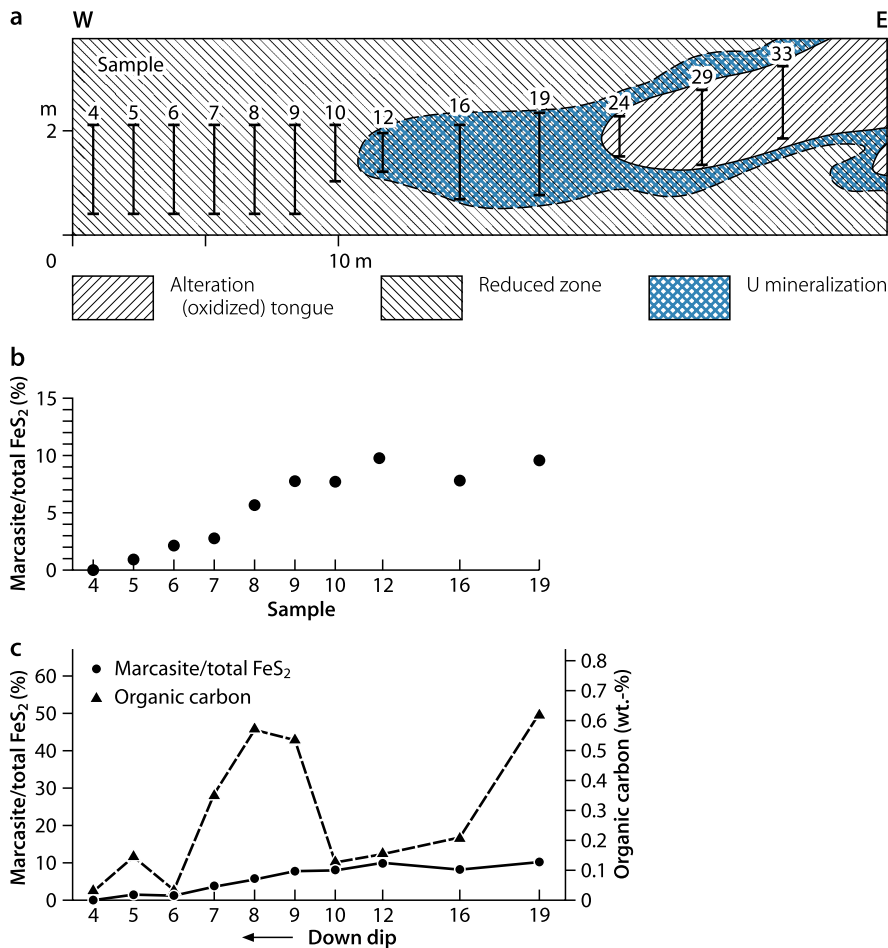


Fig. 2.7

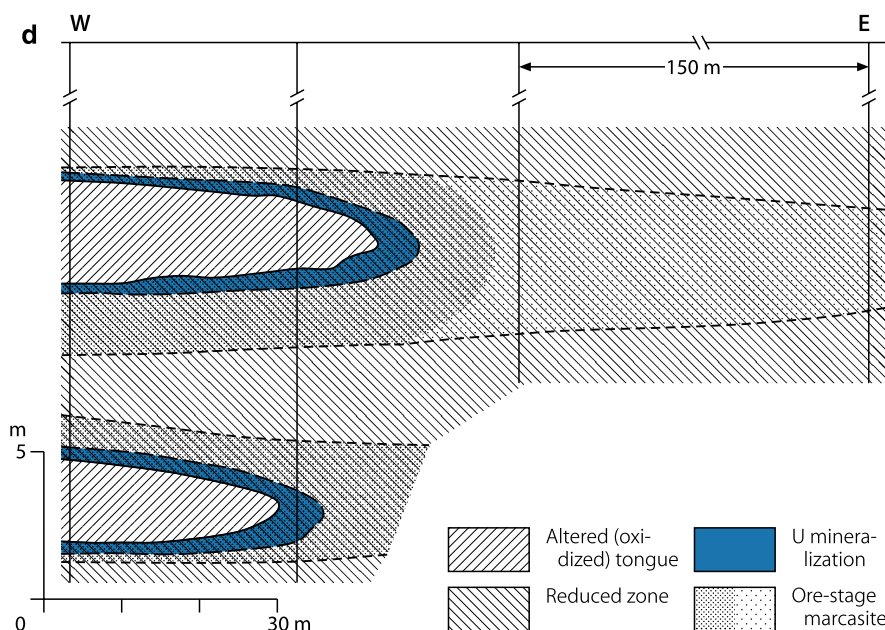
(a-c) Shirley Basin, Petrotomics Section 9 pit, W-E cross-section showing (a) the distribution of geochemical zones, (b) related abundance of marcasite expressed as ratio of marcasite/total FeS_2 , and (c) abundance of organic carbon. (After Reynolds, Richard L., Goldhaber, Martin B., 1983, Society of Economic Geologists, Inc., *Economic Geology*, Fig. 9, p. 114; Fig. 12, p. 118; (a) and (b) based on Harshman 1972). (d) Powder River Basin, Irigary deposit, eastern part, W-E cross-section illustrating prominent geochemical zones and ore stage marcasite. (After Reynolds, Richard L., Goldhaber, Martin B., 1983, Society of Economic Geologists, Inc., *Economic Geology*, Fig. 8, p. 113)



amounts of Se may be present in pyrite and marcasite near the convex side of the rollfront. The Se amount in altered sandstone tongues is always greater than in unaltered sandstone, sometimes by one order of magnitude.

Molybdenum, predominantly as jordisite (MoS_2), is present in many deposits often in significant quantity. It is concentrated in reduced sandstone at the distal edge of mineralized zones. Amounts range from a few tens of ppm to several percent Mo.

■ Fig. 2.7 (Continued)



Molybdenum values are relatively high in the Gas Hills and the Crooks Gap deposits, whereas the Shirley Basin deposits contain less than 3 ppm, and deposits in the Powder River Basin apparently lack Mo. Altered sandstone has slightly lower Mo contents than unaltered, reduced sandstone.

Vanadium amounts to only a few hundred parts per million in most rollfront ore bodies. It is positioned in mineralized, reduced sandstone in a zone close to the rollfront where it overlaps zones in which ferroselite, pyrite, and uranium are concentrated. Altered sandstone contains more vanadium than does unmineralized, reduced sandstone.

Arsenic occurs in amounts of up to ca. 1% in the Gas Hills where it correlates well with pyrite. In the Shirley Basin, amounts are generally less than 50 ppm, and the correlation with pyrite is only fair.

Beryllium values range from 1.5 to 5.5 ppm in the Gas Hills and the Shirley Basin. It is associated with uranium in the ore and is below 1.5 ppm in altered and unaltered sandstone.

Copper amounts range from 10 to 20 ppm. It does not correlate with other ore elements or minerals. Some copper tends to have been removed from altered sandstone, but if so, it was apparently transported beyond the mineralized area.

Carbon ranges widely in amount and distribution in organic substances and in minerals (principally calcite) as well. Organic carbon content has generally a rather erratic distribution ranging in unaltered sands from less than 0.05% in some deposits to as high as 2% in others. Mineral carbon shows similar ranges. In most deposits, both organic and mineral carbon contents are higher in reduced sandstone than in oxidized sandstone. No consistent direct correlation could be established between organic carbon and uranium contents in mineralized sandstone. There is, however, an indication of some migration of organic carbon, probably from altered sandstone, into mineralized sandstone and its deposition along with uranium and associated elements.

Sulfate sulfur has been removed from altered sandstone where it was originally present in gypsum. It amounts to 1% or more in mineralized sandstone in the Gas Hills and the Shirley Basin, where gypsum has also been identified in the ore.

Phosphate occurs in many deposits, but no uranium phosphate mineral has been identified except for carbonate-fluor-apatite that cements sandstone in the Gas Hills. Uranium/phosphate ratios range from 0.02 to about 30, so the phosphate-uranium relationship is not a direct one with the exception of a relationship between high U contents and high P_2O_5 contents. While U ore commonly contains less than 0.5% P_2O_5 , phosphate contents rise as high as 1% P_2O_5 in samples containing 2 or 3% U in both the Gas Hills and the Shirley Basin ores.

General Shape and Dimensions of Deposits

U mineralization forms roll-shaped ore bodies discontinuously emplaced in lateral direction along and in or immediately adjacent to a redox front at the margin of oxidized sandstone tongues. In its simple form, the configuration of an ore body resembles in plan view an irregularly laid pipe or roll that follows the edge of an altered sandstone tongue, and in cross-section a crescent with variably long tails. Simple crescent-shaped ore bodies are rare, however. Most ore bodies are complex and consist of several rolls interconnected by their zones of mineralization.

Ore boundaries generally transect stratification of host sandstones at sharp angles although the tails of the crescent or roll may be peneconcordant with bedding. The inner contacts of ore and altered sandstones, i.e., the concave side or trailing edge of a roll, are generally sharp, whereas the outer contacts of ore and unaltered sandstone, i.e., the convex side or leading edge of a roll, are gradational. Here, the uranium content gradually decreases until it merges with unmineralized sandstone.

Dimensions of U deposits vary according to the permeability of ore-hosting sandstones and the extent and geometry of the redox front in addition to geochemical factors, e.g., in the Shirley Basin and the Gas Hills, U deposits are mainly narrow and of high grade, whereas in the Great Divide Basin they are wide and of relatively low grade, suggesting an inverse relation of grade to width.

The general form of roll-type ore bodies shows a typical thickness of a few tens of centimeters to 10 m thick but up to 15 m thick in the apex zone, widths perpendicular to the redox front from a few centimeters to several hundred meters, and strike lengths of up to several kilometers. Small ore bodies are found on the top and bottom surfaces of altered tongues and associated with small bodies of residual unaltered sandstone enveloped by altered tongues (see illustrations in description of individual districts for typical settings and configurations of deposits and types of ore bodies and their dimensions). The average grade of ore mined ranged from 0.05 to 0.2% U, although in restricted places, the content was as high as 50% U.

Regional Geochronology

Mineralizing (or uranium redistribution) processes in the Tertiary Wyoming Basins continued over a large time span from the early Oligocene or earlier probably to the present. In this course of history, significant migration of both ^{234}U and total U occurred within the ore bodies within the last 100,000 years as can be inferred from studies by Dooley et al. (1964) and Rosholt et al. (1964, 1965a, b). This migration of decay isotopes of uranium has profoundly affected the U/Pb ages in the ore minerals hampering a precise age dating.

Ludwig (1978) points out some of the problems involved in the age dating. His results of isotope analyses (see further below) from ore of the *Shirley Basin*, which are compatible with similar data from ore of the *Gas Hills*, the *Crooks Gap*, and the *Highland Mine/Powder River Basin*, show a complex picture of uranium-daughter migration for both permeable and nearly impermeable ores, both within and beyond the boundaries of total ore samples. All of the analyzed pitchblende samples have experienced both lead and long-term ^{238}U radioactive-daughter loss, so that the purest pitchblende yielded the lowest and most discordant apparent ages. Calculations indicate that time-integrated leakages of uranium daughters are as much as 55% for lead and 66% of $^{238}\text{U}_{\text{r.d.}}$. Analyses of total ore samples suggest that disseminated pitchblende ores have also had significant $^{238}\text{U}_{\text{r.d.}}$ leakages (ca. 20%), but that an impermeable, very high-grade ore has a time-averaged $^{238}\text{U}_{\text{r.d.}}$ leakage of less than $2.4 \pm 1\%$. A similar result of significant $^{238}\text{U}_{\text{r.d.}}$ migration was reported by Rosholt et al. (1965a) from ore of the Powder River Basin.

Not all uranium daughter isotopes lost by pitchblende are lost by the total ore. Pyrite in the ore was found to have gained 130–620 ppm of radiogenic lead, with $^{207}\text{Pb}/^{206}\text{Pb}$ values suggesting pitchblende as the source. Also, a separate specimen of coalified wood in a disseminated pitchblende ore contained 800 ppm of unsupported ^{206}Pb and ^{210}Pb without unsupported ^{207}Pb , a condition almost certainly due to long-term incorporation

of $^{238}\text{U}_{\text{r.d.}}$. The Pb-isotopes value in the wood would be equivalent to an unrealistic $^{207}\text{Pb}/^{206}\text{Pb}$ age of $-5,850$ Ma.

In summary, present U–Pb isotope ratios are the result of migrating Pb from the total ore that became incorporated in pyrite and of migrating radioactive daughter isotopes from the total ore that was trapped by substances such as coalified wood. As a result of this migration and reconcentration of uranium daughters from pitchblende into various other sites, the significance of U–Pb apparent ages of one or two samples from such an ore is extremely difficult to interpret as the “ages” can be affected more by the particular mix of radiogenic lead-bearing phases than by the actual age of the ore. Ludwig (1978) concludes, nevertheless, that geochronometry of such open systems is possible as long as the isotopic composition of lead lost from the total ore is similar to that of lead gained by pyrite.

Dooley et al. (1974) determined uranium–lead ages on two samples of massive pitchblende from the *Gas Hills* and the *Shirley Basin*, as well as on three samples of high-grade ore from the two districts. The massive pitchblende samples gave an age of 22 ± 3 Ma for both districts. The high-grade ore samples yielded ages from 29 to 22 Ma (middle Oligocene to early Miocene). The authors conclude that the 22 ± 3 Ma (earliest Miocene) age is the most reliable.

Ludwig (1978) age dated samples from three mines and three types of ores in the Shirley Basin as given in [Table 2.2](#) (see also chapter Principal Characteristics of Mineralization for mineralogical sample descriptions). Ludwig’s (1978) investigations yielded low U/Pb ages of pitchblende grains, high U/Pb discordant ages of pyrite separates, and U/Pb discordant ages intermediate between pitchblende and pyrite of total ore samples. The author infers from his data that the time of pitchblende formation in the Shirley Basin for the youngest ore sample analyzed was apparently 24 ± 3 Ma, whereas the oldest sample was formed before 35 Ma. The discrepancy between these two ages implies that conditions favorable to the movement and concentration of uranium in the Shirley Basin may have existed for more than a single, short interval, and that sources for uranium in the Shirley Basin ore bodies must have existed from at least early Oligocene time.

U–Pb isotope analyses by Ludwig (1979) on samples from the *Gas Hills* and the *Crooks Gap* districts suggest that mineralization in both districts is at least 26 Ma old, with at least some pitchblende–coffinite formation before 35 Ma. Pb/U apparent ages from the highest quality samples scatter in a range of 35–26 Ma, and by inclusion of all samples the interval increases from 41 to 12 Ma.

Age dating on ore from the *Highland Mine* in the *southern Powder River Basin* by Santos and Ludwig (1983) yielded, with the exception of one sample, U–Pb apparent minimum ages of less than 3 Ma and showed significant normal discordance, probably due to continuous preferential loss of ^{238}U daughter products. The exceptional sample yields apparent ages of 11 and 4.3 Ma, but it remains unclear whether this sample has lost uranium or if it represents a truly older time of mineralization.

Sharp and Gibbons (1964) analyzed samples from a near-surface deposit near Pumpkin Butte, and from a small open pit

Table 2.2.

Shirley Basin, characteristics of analyzed ore samples and apparent ages (Ludwig 1978)

	Calcite-cemented ore	Disseminated pitchblende ore	Massive pitchblende ore
Uranium content	12%-unusually high grade	1–2%, only moderately higher than avg. ore	65–72%, extremely high grade
Permeability & coherence	Low permeability, very competent	Highly permeable, unconsolidated	Low permeability, competent
Occurrence	Isolated blocks or zones in some mines	Common ore type near rollfronts	Rare
Other remarks	Calcite–pitchblende–pyrite as matrix to and replacement of detrital grains of original arkose	0.1–2.0 mm grains and coatings of pitchblende and pyrite disseminated in arkose host; ±carbonaceous lumps	
Age limits (Ma)	21 26±2 24+	28 23 25	35
Main assumptions ^a	a b,c,e b,d,e	a a a	a
Sample/mine	Petrotomics, Sec. 9 Pit	A2 A5 A7, Utah Int. Pit	MU-2 Walker Pit, KMG

*Main assumptions:

^a Sample has not lost U^b Sample has neither gained nor lost U^c Sample has not lost ²³⁸U radioactive daughters^d Recent radioactive-daughter leakage is similar to past leakage^e Pyrite radiogenic lead is similar to lead lost by ore

about 15 km NNW of the Highland Mine and got ages ranging from 13 to 7 Ma.

Potential Sources of Uranium

The two most probable uranium sources include (a) uraniferous granitic rocks of Paleoproterozoic to Archean age that crop out in the peripheral ranges of the basins and (b) uraniferous pyroclastic layers of Eocene and younger age that rest upon or once overlaid older basin fill. The relative significance of these two potential sources can be inferred, but not conclusively proven. However, some strong evidence is given by the geochemistry of these two lithologic units, and by the hydrochemistry of groundwater flowing within and departing from them, and carrying uranium and other elements typical for rollfront mineralization.

Granitic rocks. Rocks from the Laramie and the Shirley mountains, considered to be the sources of the arkose in the Shirley Basin, and partly in the Powder River Basin contained 0.5–7 ppm of leachable uranium (Harshman 1972). Springwater samples from these granitic ranges contained 1–8 ppb uranium (pH 6.2–7.0).

Granites of the Sweetwater Uplift that furnished much of the arkosic host sediment in the Shirley Basin, the Gas Hills, and the Crooks Gap–Great Divide Basin contain up to 30 ppm U or more (Fig. 2.8). These granites apparently experienced a substantial depletion of uranium as can be deduced from existing radiogenic lead amounts. Rosholt et al. (1973) and Stuckless and Nkomo (1978), based on U/Pb isotope analyses, estimated a 70–75% loss of uranium in these granites over the last 40 Ma. They propose

this mobilized uranium to be the progenitor of Wyoming deposits for several reasons:

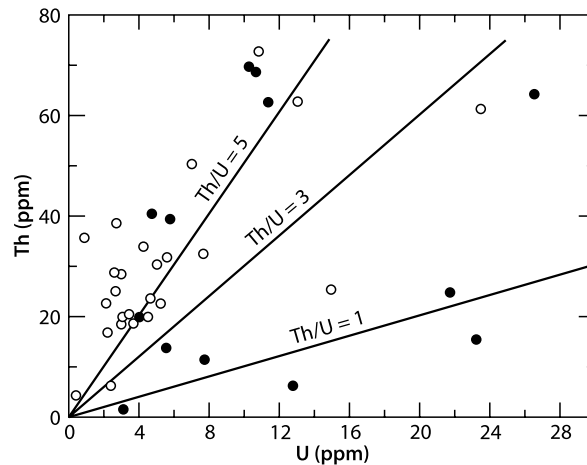
- Uranium districts are on the flanks of the Granite Mountain.
- Granites have lost large amounts of uranium.
- Arkosic host rocks do not appear to be a reasonable source of uranium.
- The timing of the uranium loss from the granite agrees with the radiometric age dates of the ores.

Tuffaceous sediments. Zielinski (1980) reports 250 ppm U in chalcidony collected from and directly beneath accumulations of rhyolite ash in the White River Formation in the Shirley Basin. He postulates that uranium and silica were leached from the ash by downward percolating groundwater and were precipitated as an uraniferous silica gel directly above the relatively impervious claystone underlying the silicified material. A minimum age of 20 Ma was obtained for uraniferous silica and 32.4 ± 2.6 Ma for the overlying rhyolite tuff. These investigations show that uranium has been leached from the ash and carried by groundwater at the time the Shirley Basin deposits are thought to have formed between 35 and 20 Ma ago.

Samples of groundwater issuing from springs near the base of the upper unit of the tuffaceous White River Formation in the Shirley Basin contained from 8 to 10 ppb U. Water from springs at the base of the White River Formation, in a more tuffaceous section, contained 19–52 ppb U (Harshman 1972). This is two to ten times more uranium than was found in waters from the Wind River Formation in an unmineralized area west of the Shirley Basin. In addition, these water samples contained from a few to a few tens of parts per billion Mn, Ni, Pb, and Se.

■ Fig. 2.8.

Wyoming, Granite Mountains, graph of Th vs. U concentrations showing the range of contents of these two elements in Precambrian granite, which is considered a source of uranium. Two samples (not shown) from a depth below 30 m contained more than 30 ppm U and had a Th/U ratio of less than 1. (After Stuckless 1979)



Criteria in favor of the tuffaceous sediments as U source rocks include, according to Harshman and Adams (1981):

- Tuffaceous rocks of Middle and Upper Eocene age and of Early Oligocene age (45–32 Ma) are spatially more closely associated with uranium deposits than are granites.
- Tuffaceous rocks are now supplying uranium to the groundwater and may have supplied even more shortly after their deposition and during the compaction of their ashy constituents.
- The ages determined by Ludwig (1978, 1979) of 35–25 Ma for the Shirley Basin, the Crooks Gap, and the Gas Hills deposits are younger than the 45.4–32 Ma ages, respectively, for the Wagon Bed and the White River tuffaceous rocks in the Granite Mountains area (Love 1970) and the Shirley Basin (Zielinski 1980).
- The timing of acidic volcanic activity and deposition of tuffaceous sediments in central Wyoming is in concordance with radiometric ages of uranium ores.

Other uranium sources. Among other considered source rocks, ore-hosting arkoses are proposed as a potential uranium source, several criteria, however, contradict this assumption:

- Readily soluble uranium in granitic rocks, from which arkoses in the Wyoming Basins were derived, would have been leached during the long period of oxidation, weathering, and disintegration in the uplands and subsequent transfer of these arkoses into the basins.
- Quartzose host rocks in the Black Hills should have contained even less of the elements needed to form the deposits since they are second-cycle sediments whose mineral components have been through two cycles of weathering, disintegration, transportation, and deposition.
- Altered and unaltered sandstones from the various Wyoming Basins and from the Black Hills, taken from a few to

several hundred meters or more from ore, contain from two to five times more selenium in altered than in unaltered sandstone.

- Altered sandstones in the Shirley and the Powder River basins contain from 1.5 to 10 times as much uranium as unaltered sandstones.

It has to be concluded from these data that uranium and selenium have been introduced into sandstone from an external source since a material balance documents an increase in the amount of uranium and selenium in the system after alteration and mineralization and thus, ore-hosting sandstones have to be excluded as a U source.

Ludwig (1979), using radiometric data, concludes that the inferred limits on the time of mineralization in two districts (Crooks Gap and Gas Hills) do not resolve the question of the major source material for uranium except to require a source to have existed from at least Oligocene time. The major uranium source could have been either old granites or Eocene or Oligocene tuffaceous rocks, perhaps both.

Principal Ore Controls and Recognition Criteria

According to Harshman and Adams (1981), significant ore-controlling or recognition criteria of rollfront uranium deposits in the Tertiary basins of Wyoming are as follows:

Host environment

- Intracratonic/intermontane basins downwarped into and surrounded by highlands of granitic and metamorphic complexes of Archean to Paleoproterozoic age and filled with Cretaceous to Tertiary sediments
- Most favorable host sediments are:
 - Medium- to coarse-grained, carbonaceous, pyrite-bearing (<1–3%), arkosic sandstones of fluvial provenance

- Largely of granitic origin
- Rich in detrital organic debris
- Favorable sedimentological settings are:
 - Along late Paleocene-early Miocene drainage systems
 - Principally in the central part of fluvial systems, where stream gradients are moderate
 - Permeable carbonaceous channel sands of considerable longitudinal continuity
 - Interbedding of permeable arenite beds in impermeable pelitic horizons as found in shallow, but wide stream channels strata dipping with only slight angles, generally less than 5°
- Cover of early Eocene host rocks by fine-grained clastic sediments admixed with volcanic debris of middle Eocene (White River Formation) to Pliocene age providing
 - Potential sources of uranium and
 - Protection of older arkosic host rocks and most of their uranium deposits from Pleistocene and recent erosion and oxidation.

Alteration

- Host rocks show effects of reduction and epigenetic oxidation
- Reducing conditions are reflected by diagenetic pyrite and grey color
- Epigenetic oxidation phenomena of altered sandstones include (► Figs. 2.3 and 2.4)
 - Distinctive change in color from the normal grey of unaltered sand to pink or yellow
 - Partial or complete destruction of some or most of the heavy minerals, particularly pyrite and magnetite
 - Much lower calcium carbonate, organic carbon, and sulfate contents than in unaltered sand
- Oxidative alteration penetrates host strata in tongue-like fashion from outcrop down the hydrologic gradient
 - In most districts as several altered tongues, each separated from the other by an intercalated impervious horizon
 - Edges of these altered tongues are rarely superimposed
- Superimposed oxidized sandstone tongues can be connected by altered sand filling a depositional breach in bounding impermeable sediments
- Oxidized sandstone tongues may or may not completely occupy the sandy interval in which they are confined
- Unoxidized sandstones are separated from oxidized sandstones by redox fronts that constitute the furthest downdip or outer penetration front of oxidizing groundwater
- Incompletely oxidized intervals prevail at redox fronts at ends of oxidation tongues.

Mineralization

- Mineralization consists essentially of pitchblende, sooty pitchblende, and coffinite
- Associated elements and minerals include Mo, Se, As, and P minerals, pyrite and marcasite in reduced, and hematite and goethite in oxidized sandstone
- U, Fe, Mo, Se, V, and As are distributed in a characteristic elemental zoning across the redox interface (► Fig. 2.6)

- Mineralization is preferentially hosted in arkosic sandstone horizons, which are interbedded with continuous impermeable beds, and which dip gently, generally <5°
- Mineralization occurs in or immediately adjacent to redox fronts in the marginal zone of oxidized sandstone tongues
- Ore bodies typically exhibit a roll- or crescent-shaped configuration with trailing tails on the hanging and footwall side of the ore-hosting arenite horizon
- Ore boundaries generally transect stratification of host sandstones at sharp angles while tails of the crescent or roll may be peneconcordant with bedding
- Ore bodies are dispersed at irregular intervals along redox fronts
- Mineralization is not uniformly distributed everywhere along the edge of oxidized tongues
- Uranium concentration is apparently highest
 - At the convex side of the redox interface at the outer edge of an altered tongue
 - Where zones of mineralization narrow down
 - Where local concentrations of carbonaceous debris and/or pyrite are present in the rollfront zone
 - At changes of permeability partly caused by gradation of coarse arkosic sandstone into finer grained beds
- Best ore bodies seem to be at changes in strike of the rollfront and where the direction of flow of solutions was nearly perpendicular to the edge of the rollfront
- Deposits range from narrow and high grade (Shirley Basin, Gas Hills) to wide and relatively low grade (Great Divide Basin, Powder River Basin) indicating a tendency to an inverse relation of grade to width
- Lower grade, wider deposits frequently occur in sandstones with small amounts of carbonaceous plant remains and/or small amounts of pyrite in unaltered host rock
- Higher grade, relatively narrow deposits are associated with larger amounts of carbonaceous debris and/or pyrite.

Metallogenetic Concepts

A variety of models have been put forward to explain the formation of rollfront-related uranium deposits in the Wyoming Basins. Harshman and Adams (1981) have comprehensively analyzed all information on the formation of this type of uranium deposits in Wyoming and elsewhere. The following is an excerpt largely based on their findings and conclusions, unless otherwise cited.

Sandstone-type uranium deposits in the Wyoming Basins are related to *roll* or *redox fronts* that are frontal edges of an altered sandstone tongue in permeable arkosic sandstone interbedded with \pm less impermeable strata. A rollfront is a dynamic feature migrating down a hydrologic gradient, generally basinward, by mineral oxidation and dissolution on its updip side and deposition on its downdip, reduced side.

In *sensu stricto*, the redox front is an oxidation–reduction interface for iron. This interface may, but mostly does not, coincide with redox interfaces of other elements. Nevertheless, there is a striking similarity in the distribution of elements and

minerals along redox fronts in all roll-type uranium deposits in the Wyoming Basins and in other regions as well, e.g., the Black Hills or the Texas Coastal Plains in USA and basins in Kazakhstan, Uzbekistan, and elsewhere in the world. Neither the size of the deposits nor the geologic environment in which they occur seem to have had much effect on this distribution, a fact that suggests similar genetic processes were responsible for all rollfront uranium deposits.

Depositional environment of host rocks

Most favorable host sediments are permeable medium- to coarse-grained carbonaceous, arkosic sandstones of fluvial provenance interbedded with impermeable pelitic sediments of late Paleocene to early Eocene age. These favorable lithologic settings for ore emplacement are found along two Paleocene-Early Miocene drainage systems in Wyoming, and principally in the central part of the fluvial systems (Fig. 2.2a and b). Rock constituents derived from granitic highlands, such as the Granite Mountains or the Laramie Range that surrounded the downwarping basins. Favorable sediments belong to an erosional cycle of late Paleocene to early Eocene age. During this period, braided streams deposited wet alluvial fans on basin flanks, and bed-load streams deposited coarse arkosic sediments in the lower reaches of basins. The climate was tropical to semitropical with pronounced long and short term fluctuations in precipitation. Vegetation was abundant and relics thereof were incorporated in sediments. Water tables in the lower parts of basins were high, and thus reducing conditions were maintained in sediments as reflected by formation of diagenetic pyrite.

Very coarse debris in the proximal parts of an alluvial fan probably experienced intense oxidation during dry periods when stream flow was low and groundwater tables dropped. The reducing environment necessary for the ore-forming process was thereby destroyed soon after deposition of any organic debris, if in fact reducing conditions ever existed in these marginal zones of basins. In addition, the rate of groundwater flow through this coarse material was probably much greater than that believed to be optimum for forming the redox interface necessary for U deposition. In contrast, flood plain and lake bed sediments in the lower part of a basin remained in a reduced state long after deposition due to their pelitic nature, which greatly inhibited water migration through them.

Between these two extremes existed a terrane of moderate stream gradients where permeable carbonaceous channel sands with considerable longitudinal continuity and interbedded fine-grained sediments were deposited in shallow but wide stream channels. These provided favorable sedimentary environments that host most uranium deposits in the Wyoming Basins.

Early Eocene host rock arkoses and associated sediments were buried by fine-grained clastic sediments admixed with volcanic debris from Middle Eocene through the Pliocene, but interrupted by periods of erosion. This burial by younger formations subsequently served to protect Early Eocene arkosic rocks and most of their uranium ore bodies from Pleistocene and Recent erosion and oxidation.

Uranium sources and mobilization

As mentioned earlier, Precambrian granites of basin-peripheral mountain ranges and intraformational tuffaceous sediments, in particular of the White River Formation, are thought to be the most likely sources of uranium. During an early stage, in early Eocene time, weathering and erosion of granites may have released uranium to vadose waters. Some uranium may have been carried by groundwater and deposited in lignitic material and in carbonaceous siltstones, in reduced basin fill, but no ore formation or any preconcentration of uranium in the later host sediments, i.e., protore formation, took place. Actual ore-forming uranium was liberated from these source rocks during a later stage, apparently between middle Eocene and middle Oligocene, and transported by oxygenated groundwater down permeable horizons to redox fronts where it precipitated as will be discussed later.

Potential factors influencing uranium precipitation and accumulation

Uranium availability and transport media, hydrodynamic factors, and reduction potential in aquifers were in the first instance instrumental in the quantity and quality of uranium fixation, whereas local lithology of the host rocks probably exercised only a limited control on ore localization as indicated by the principle discordance of ore boundaries with stratification of the host sandstones.

As mentioned earlier, there appears to be an inverse relation of grade to width in the Wyoming rollfront U deposits, and a frequent direct relation of lower grade, wider deposits to sandstones with small amounts of carbonaceous plant remains and/or small amounts of pyrite in unaltered host rock, which contrasts with larger amounts of carbonaceous debris and/or pyrite associated with higher-grade, relatively narrow deposits. This fact suggests that the gradient in the zone of deposition may have been

- (a) Steep in the case of narrow high-grade deposits, which promoted rapid dumping of transported elements or
- (b) Relatively flat for wide, low-grade deposits where precipitation of transported elements would have been slow and would have extended over a considerable distance.

Other factors that might affect the Eh gradient are

- (a) The rate of flow of the mineralizing solution through reduced sandstone, which could compress or extend the zone through which deposition takes place and
- (b) The kind and availability of reductants for reaction with mineralizing solutions.

Oxidizing and reducing processes and environments

Although there is a wide agreement on the concept of a migrating redox front responsible for ore formation, there remains some disagreement on the oxidizing and reducing processes

involved. Two *alternative geochemical systems* are paramount: biogenic–biochemical processes and chemical processes. Perhaps a combination of both might have achieved the geochemical environments necessary for ore formation as summarized from Harshman and Adams (1981) in the following.

Biochemical system. Rackley (1976) states that an all-biogenic system involves two species of bacteria functioning in two very restricted environments of different Eh and pH zones, distinctly separated from another by the redox interface. On the reduced, downdip side of the front (Fig. 2.9), anaerobic bacteria of the genus *Desulfovibrio* predominate. They are sulfate reducers, derive their energy from organic matter in the sandstone or in solution, and produce H_2S . Other bacteria may assist by breaking down cellulose into products usable by *Desulfovibrio* in its life process. These bacteria are strict anaerobic and generate an environment of pH 7.8–8.4 and an Eh of -200 mV or less.

On the oxidized or altered, updip side of the redox front, *Thiobacillus ferro-oxidans* and related bacteria prevail. They are strictly aerobic, derive their carbon from CO_2 , their energy from nitrogen and sulfur compounds, hydrogen, and iron, and they are capable of producing pH conditions as low as 1.8, although the optimum pH for maximum activity is from 2 to 4. In addition to producing a low pH, they are capable of producing Eh values as high as $+760$ mV, although such high values are unlikely in a natural environment. *Thiobacillus* is thought to act as an intermediate agent in the conversion of pyrite to iron hydroxide

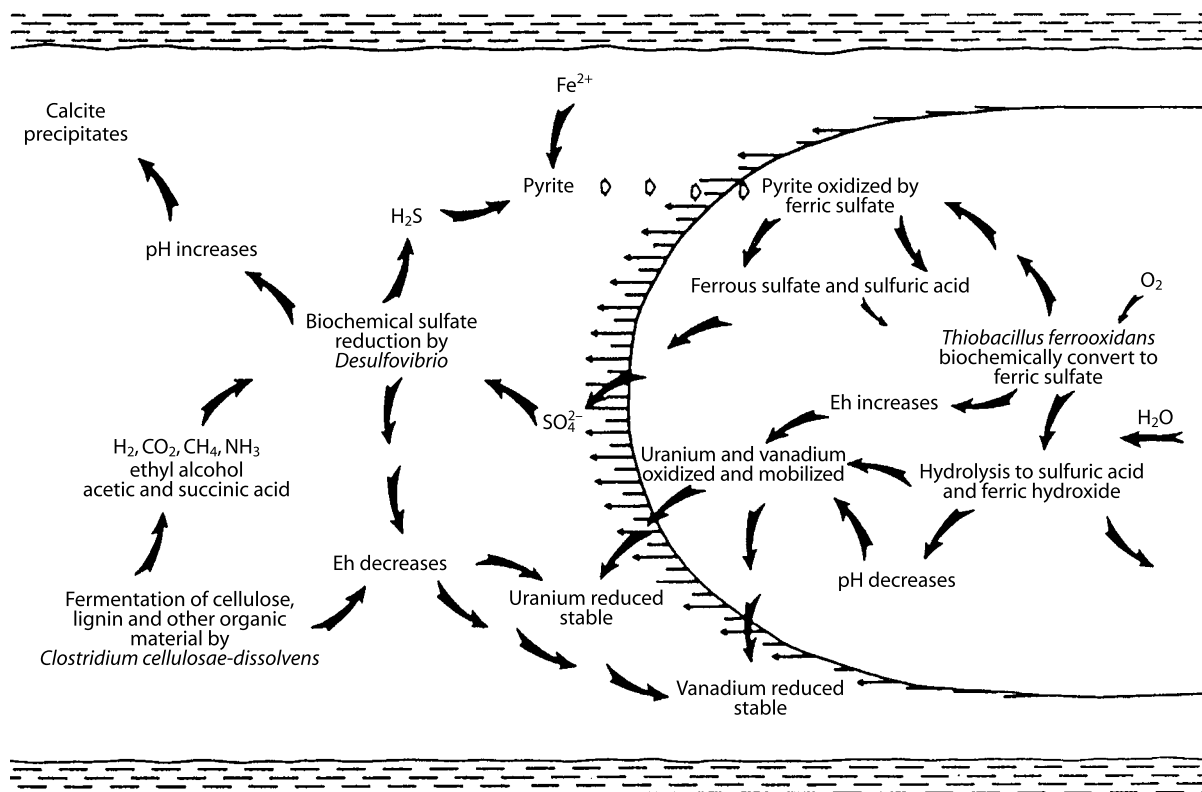
and eventually to goethite, hematite, or high-iron montmorillonite. The first step is the reaction of pyrite, ferric sulfate, and water to produce ferrous sulfate and sulfuric acid; the second step is the biochemical oxidation (by *Thiobacillus*) of ferrous sulfate and sulfuric acid to ferric sulfate and water; and finally the hydrolysis of ferric sulfate to ferric hydroxide and sulfuric acid. Excess sulfate in the system is carried across the front into the reducing environment of *Desulfovibrio*, where it is reduced to H_2S .

This biogenic system is almost self-perpetuating and it needs only oxygen, pyrite, CO_2 , and organic matter to complete the oxidation, migration, and reduction cycle required by a dynamic system of deposition. Ingredients of the system can be furnished by constituents of the host sandstones (pyrite, organic matter, CO_2) and the mineralizing solution (oxygen and CO_2).

With respect to the need for pyrite, Austin (Written Communication in Harshman and Adams 1981) points out that there is no need for sulfide to initiate the process as long as there is a supply of sulfate in the groundwater. It can be assumed, however, that once the process is started, at least part of the sulfate will be provided by oxidation of pyrite or other sulfides, and if the sulfide is pyrite, the oxidizing bacteria can, and most likely will, accelerate the process and provide the continuous system described. If the sulfide is a less stable phase, such as marcasite or other metal sulfides, the process has much less need of oxidizing bacteria. The biogenic system requires no sulfur more reduced than sulfate for initiation, whereas the inorganic system relies on more reduced phases such as sulfide.

■ Fig. 2.9.

Wyoming Basins, possible chemical reactions in a host sand bed (white) involved in the formation of and across a rollfront due to bacteria activity. (After Rackley 1972; AAPG 1972, reprinted by permission of the AAPG whose permission is required for further use)




Studies by Thode et al. (1951) on the role played by sulfate-reducing bacteria reveal that bacteria selectively reduce the lighter ^{32}S . Cheney and Jensen (1966) report that sulfur isotope analyses from the Gas Hills, from both diagenetic pyrite in unaltered sandstone and pyrite in the ore, have the wide isotopic spread in the $^{32}\text{S}/^{34}\text{S}$ ratios and the relative enrichment in ^{32}S that is typical of H_2S of biogenic origin.

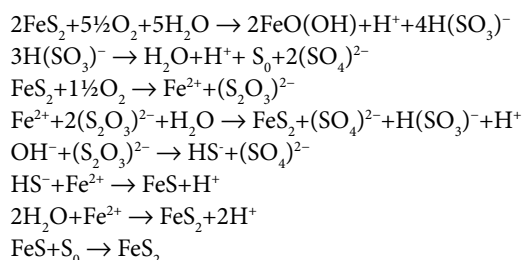
Reynolds and Goldhaber (1983) arrive at a similar conclusion based on their sulfur isotopes studies for pre-ore stage pyrite in Wyoming and South Texas rollfront U deposits (see chapter 8 Texas Coastal Plain).

Support to the biogenic system is given by Shchetochkin and Kislyakov (1993) for U deposits in the Chu-Sarysu Basin, Kazakhstan (see Dahlkamp 2009, Uranium Deposits of the World: Asia), and earlier by Lisitsyn and Kuznetsova (1967). The latter sampled waters from wells and mine openings in and near roll-type deposits in an artesian basin at an undisclosed location in the former U.S.S.R. From the limited geological data given, one can conclude that the deposit (or deposits) is similar in all major aspects to those in the Wyoming Basins, and that it was forming at the time of their investigation. The host rocks are permeable Cretaceous sandstones, and waters flowing in the mineralized zone have a pH of about 7.5, and an Eh of about -200 mV . The authors conclude that (a) the negative Eh results from anaerobic activity of microflora that produce H_2S and H_2 and (b) the character and distribution of elements within the deposit depend on the relative amounts of the various products of microbiological activity. Lisitsyn and Kuznetsova's (1967) data tend to confirm the presence of H_2 - and H_2S -forming bacteria in water on the reduced and mineralized side of the redox interface, but the presence of *Thio-bacteria* in oxidized sandstone near the interface is open to question.

Chemical-biochemical system. This model postulates that mineralizing solutions are alkaline and oxygenated when they approach the redox interface. Without the aid of bacteria, solutions oxidize pyrite to sulfuric acid and ferrous sulfate. The oxidation process will be slow if pyrite is the only sulfide, but much faster if marcasite or other sulfur-deficient species are present. These products are transported downdip into the reduced mineralized zone where sulfate-reducing bacteria transform sulfate to H_2S and sulfuric acid is converted to gypsum by the alkaline environment of slightly calcareous arkose.

Chemical system. Granger and Warren (1969, 1974,  Fig. 2.4) have demonstrated that solution, migration, and redeposition of elements along a rollfront can be accomplished by inorganic chemical reactions and without intervention of bacteria. They recognize the probability that widely disseminated pyrite in unaltered ground and that pyrite destroyed in the altered tongue is of biogenic origin and formed shortly after deposition of the host sediments. Their thesis is that oxidation of pyrite at the rollfront is accomplished by the mineralizing solution, but that the amount of oxygen in that solution is limited. This results in the formation of soluble, metastable, partly oxidized sulfur species, which are carried downdip by the mineralizing solution until

they spontaneously undergo disproportionation; that is, they disintegrate into equivalent amounts of more reduced species such as H_2S , and more oxidized species such as sulfate $(\text{SO}_4)^{2-}$. Sulfate is kinetically inert to further reduction or oxidation reactions and this leaves the more reactive reduced metastable sulfur species and H_2S to control the environment. Chemical theory and laboratory experiments support the above considerations and show that isotopic fractionation of sulfur, similar to that caused by biochemical reactions, can result from inorganic chemical reactions. It appears therefore, that a pyrite-bearing sandstone is completely capable of establishing and maintaining a rollfront, once oxygenated water is introduced, without the participation of any organic components. Granger and Warren (1969) propose for this process the following reactions:



Two other reductants have been proposed because of their spatial relation to the deposits, vegetal material, and H_2S .

Coalified woody-material. Coalified woody-material or humates derived from such material are present in all host rocks of Wyoming deposits. For this reason, as well as for the fact that some ore contains as much as 0.5–1% organic carbon, some investigators suggest that organic carbon is the direct reductant of uranium and associated elements. It is noticed, however, that some samples containing 0.5% or more uranium have 0.5–1% organic carbon while other samples with similar amounts of uranium contain only a trace or a few hundredths percent organic carbon, or vice versa, i.e., high carbon and none or low uranium. These observations suggest that the correlation between uranium and organic carbon within the roll-type system is neither simple nor consistent, hence the precipitation of uranium by organic material may not be the only important mechanism. Studies by Schmidt-Collerus (1969, 1979), Kochenov et al. (1965), and others, suggest that organic matter may initially complex uranium from solution for subsequent reduction by the oxidation reaction of carbon and sulfide, and perhaps other elements.

Hydrogen sulfide (H_2S). The close spatial relation between uranium deposits in Wyoming Basins and oil and gas-producing Cretaceous formations may hint to a possible genetic relation between uranium deposition and H_2S from sour gas. Grutt (1957) postulates that H_2S derived from sour gas was the precipitant for ore minerals in the Gas Hills district. He points out that producing oil and gas wells are adjacent to the area, that gas from the wells contains as much as 2% H_2S , that there are gas seeps in the area, and that exploration drilling encountered H_2S in the Wind River Formation. He proposes that sour gas ascended along faults that border the district on the south,

entered the unconformity at the base of the Wind River Formation, and intruded the host sandstone where it rests upon the unconformity.

On the basis of investigations on the isotopic composition of crude oil, sulfate water, and H_2S associated with the oil, Vredenburg and Cheney (1971) conclude that if the original petroleum-derived H_2S was depleted in ^{34}S compared to the petroleum from which it was generated, it might have had a composition, which would support, at least to a certain extent, Grutt's hypothesis. On the other hand, they state that pyrite enriched in ^{32}S and calcite enriched in ^{12}C occur around woody material as well as in asphalt in the Gas Hills district, a fact, which suggests that bacterially generated H_2S was also important.

The earlier presented documentations make it difficult to decide what kind of chemical processes were ultimately responsible for the ore-forming chemical environment in and adjacent to rollfronts. Experimental work by Goldhaber and Reynold (1979) and Reynold and Goldhaber (1983) may shed some light on this problem, however. Their studies on marcasite of Texas and Wyoming uranium deposits, and on geochemical environments analogous to those governing the formation of rollfront deposits, indicate that relatively low pH and the presence of elemental sulfur favor marcasite, whereas higher pH and the presence of polysulfide ions favor pyrite, i.e., a salient factor in the formation of marcasite or pyrite as ore-stage minerals is the complex interrelationship of pH and sulfur species that are the precursors of iron-disulfide minerals.

Conditions that favor marcasite as the dominant ore-stage iron disulfide are most likely to arise in noncarbonaceous rocks. In rocks with considerable organic matter, the presence of polysulfide ions and pH buffering by anaerobic bacterial metabolic processes apparently led to the formation of ore-stage pyrite. Since in the Wyoming Basins most ore-stage iron sulfide is in pyrite, this can be regarded as a clear implication that biochemical activity was responsible for reduction along the redox front.

Austin (1970) reached a similar conclusion based on his sulfur isotope studies of Wyoming rollfront deposits noting the well-defined redox interface for iron, the lack of identification of intermediate sulfur species resulting from nonbiochemical processes, and the ubiquitous nature of sulfate-reducing bacteria.

Ludwig and Grauch (1980), based on their studies of coexisting pitchblende and coffinite in deposits in the Gas Hills, the Powder River Basin, and the Crooks Gap, present a mineral-chemical relationship as a possible indicator for the ore-forming environment. Both uranium minerals contain significant amounts of calcium and without any marked fractionation of the calcium between pitchblende and coffinite. But there is a distinct difference in the calcium content in the samples from the three basins; the two uranium phases have each, respectively, less calcium. This possible systematic difference in calcium content may reflect differences in the conditions of ore formation in deposits of the three basins.

[For more recent research on biogenic and abiogenic formation of uranium oxides see, for example, Bargar et al.

(2008), Finch and Murakami (1999), O'Loughlin et al. (2003), Suzuki et al. (2005), Wall and Krumholz (2000)]

Character of mineralizing fluids

Oxygenated groundwater was the salient factor for alteration of host rocks and formation of U mineralization in the Wyoming Basins when it percolated down permeable horizons on flanks of basins. Originating in granitic, metamorphic, and sedimentary rocks of mountains updip from host rock outcrops, such groundwater commenced to invade exposed or truncated edges of early Eocene sediments after deposition of the White River and younger formations, i.e., at about Oligocene time.

All elements in the deposits and the nature of alteration associated with them can be related to the geochemistry of groundwater under the environmental conditions which existed in the Wyoming Basins at the time the deposits were thought to have formed. A major physico-chemical factor for dissolution, migration, and precipitation of the various elements in rollfront-type deposits is based on the change capability of the oxidation potential (Eh) and of the acidity grade (pH) of mineralizing fluids.

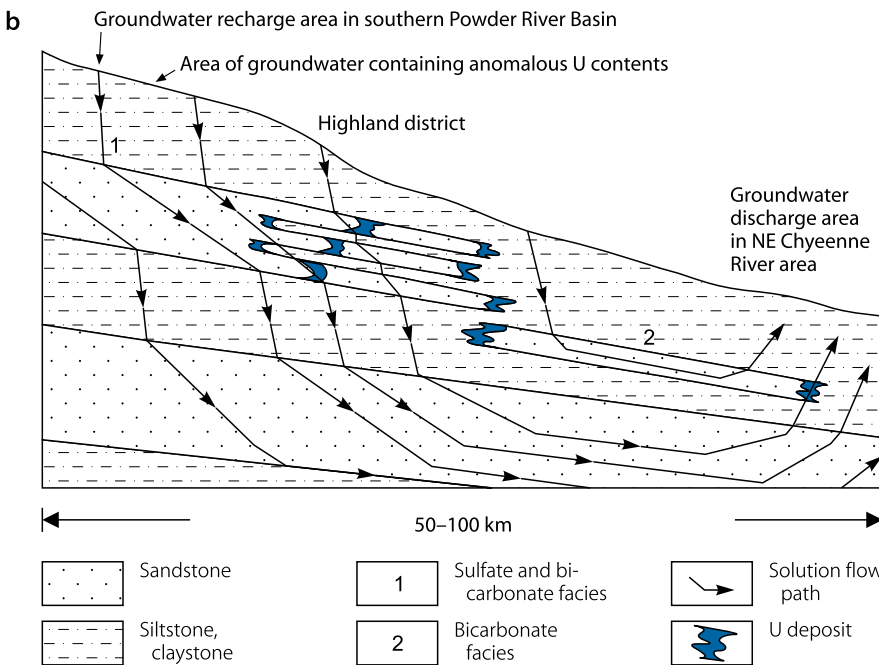
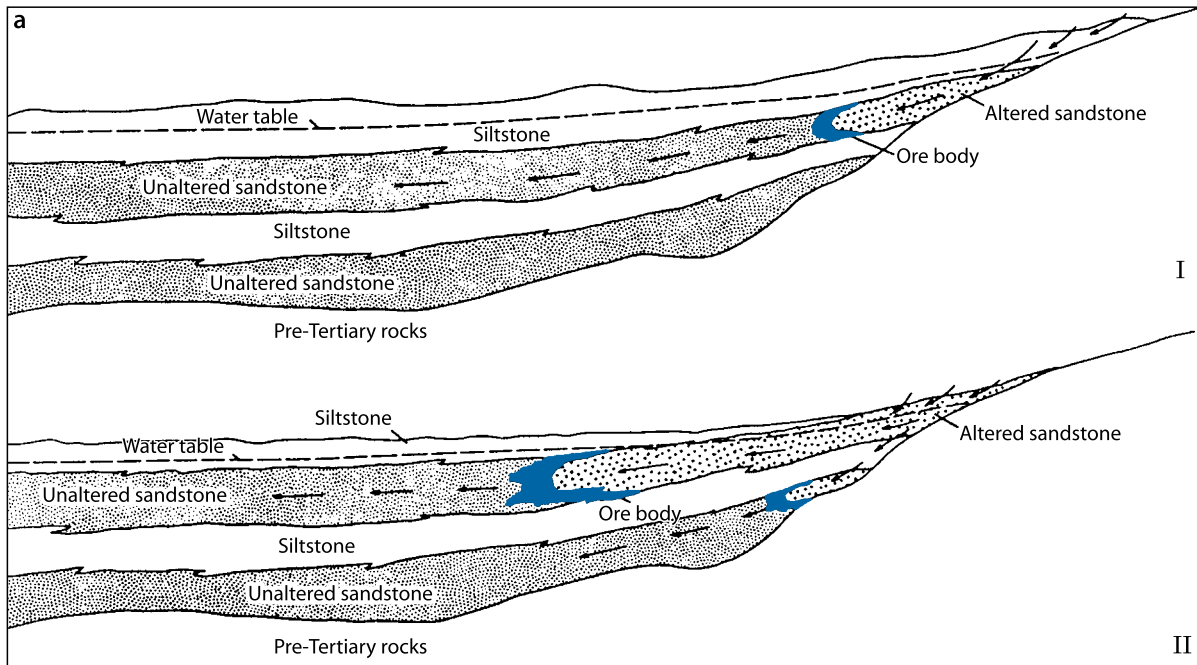
Figure 2.10a–d shows postulated paths of alteration and mineralizing solutions, and Figure 2.11 shows the presumed path of a solution unit within an Eh–pH diagram, as the solution moves from an oxidizing environment in altered sandstone through the rollfront and into unaltered sandstone. The postulated decrease in Eh downdip from the redox front for iron would cause elements requiring the lowest Eh for this reduction to be deposited the furthest advanced from the edge of the iron redox interface. Figure 2.12 is a composite Eh–pH diagram documenting equilibrium boundaries between the relatively soluble and insoluble forms of Se, V, U, and Mo, and between pyrite and two ferric iron compounds, expressed for conditions of temperature, pressure, and solution composition and concentration, which approximate, in simplified form, likely conditions in mineralizing solutions. If one assumes a starting solution with an initial pH of 7.5, then decreases its Eh from +300 to –300 mV near the rollfront, at constant pH, the diagram predicts the path of solution Eh will intersect element boundaries in the same order that they are actually found in roll-type deposits (Figure 2.6a and b). The diagram also shows that a one or two unit decrease in pH concurrent with decreasing Eh will not change the sequence of deposition.

It is worth mentioning that almost identical Eh and pH conditions with those of the Wyoming Basins have been established along traverses extending from altered sandstone through ore and into unaltered sandstone in sedimentary basins in Kazakhstan and Uzbekistan (for details see Dahlkamp 2009, Uranium Deposits of the World, Asia).

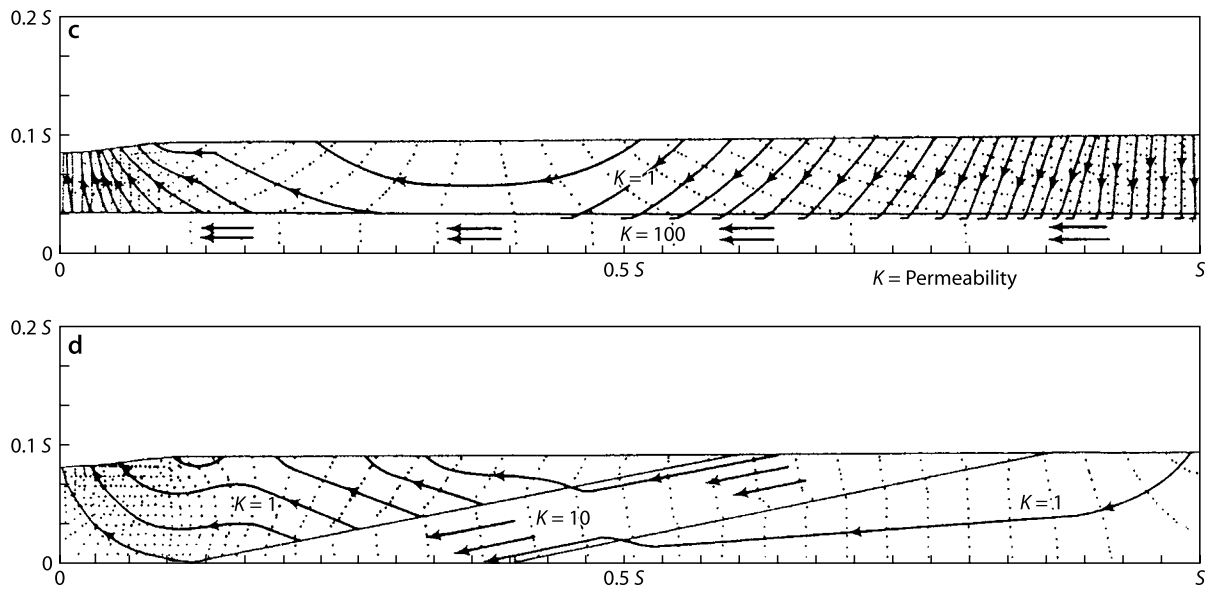
The pH of present groundwater varies between 7.0 and about 8.5 in practically all uranium-bearing Wyoming Basins. This does not necessarily prove that the same conditions prevailed during ore-forming times. The lithochemistry of basin fillings permits, however, this assumption since (a) ore-hosting arkoses contain considerable amounts of orthoclase and microcline as

Fig. 2.10

Wyoming Basins, hypothetical flow paths of mineralizing fluids, (a) general scheme; (b) in southern Powder River Basin, the figure also demonstrates the presumed deviation of flow directions by different litho-facies; (c) in a gently dipping, high-permeable unit overlain by a low-permeable unit, in which some flow occurs from overlying less permeable strata into the more permeable beds, which may enhance the propagation of a rollfront; (d) in a steeply dipping, high-permeable unit interbedded between two low-permeable units, in which the waters tend to move from the aquifer into and across the overlying aquitard. With increasing dip of the host sandstone, loss of groundwater into the overlying sediments retards and ultimately arrests the propagation of the rollfront. (After (a) Harshman 1972; (b) Dahl and Hagmaier 1974; Hagmaier 1971; (c) and (d) Harshman and Adams 1981, based on Kreitler 1979)

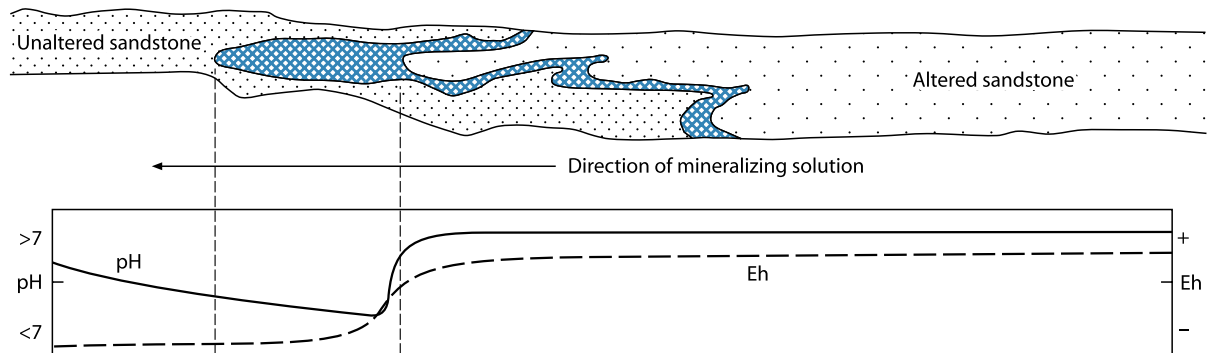


■ Fig. 2.10 (Continued)



■ Fig. 2.11.

Wyoming Basins, postulated Eh and pH conditions for groundwater during transportation and deposition of uranium and other elements (Harshman 1970)



well as some calcium carbonate, (b) the overlying White River and Arikaree formations are to some extent similar in composition to ore-bearing horizons except that they contain in addition a considerable fraction of tuffaceous material.

Since hydrolysis of silicate minerals such as feldspar increases the alkalinity of water and alteration of silica glass releases silica and alkali ions to groundwater resulting in pH values of 8.0 or more, it is reasonable to extrapolate that the constituents of arkoses and tuffs would have also generated in its early history an alkaline environment with the capability to buffer any through-passing solutions.

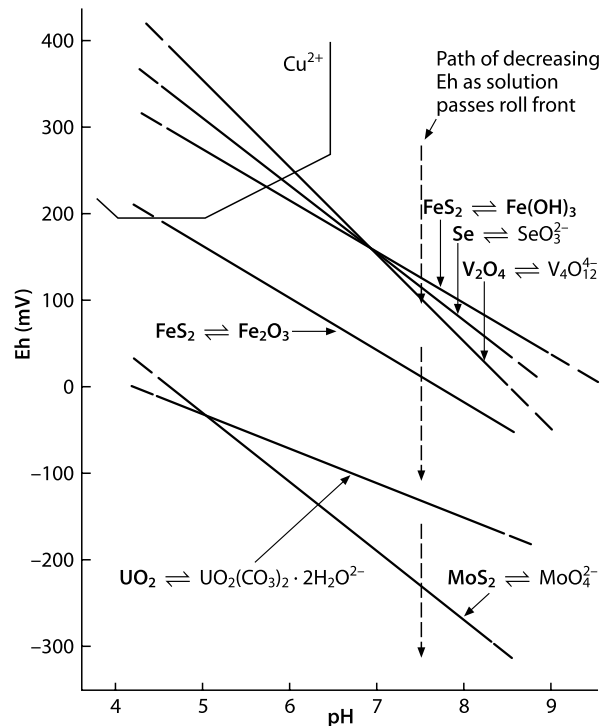
Groundwater in the ore-bearing Inyan Kara Formation near the outcrop in the Black Hills has positive Eh values of as much as +162 mV and up to -200 mV basinward from the deposits. It should be kept in mind, however, that these values may be somewhat in error due to loss of H_2S and CO_2 , or addition of O_2 in near-surface water.

Indirect evidence for the alkaline and oxidizing nature of ore-forming solutions can be found in the alteration phenomena they imposed on host rocks, and in the geochemical behavior of elements transported by these fluids. Alteration effects include (a) large-scale destruction of diagenetic pyrite and marcasite with simultaneous formation of goethite, hematite, and/or high-iron montmorillonite, (b) intense decomposition of plant debris, in part by oxidation to CO_2 , and (c) changes in ferrous/ferric iron ratios from 1:1 or less in altered sandstone to at least 2:1 in unaltered sandstone.

There is no direct proof of the exact chemical state in which extrinsic elements have been transported. Most of them can be carried in one mode or another at normal temperatures and pressures in fluids with a composition similar to present-day groundwater in the Wyoming Basins. Selenium may provide a clue for high pH and positive Eh values in paleo-groundwater, however, by the distinct conditions under which it is mobile in

■ Fig. 2.12.

Wyoming Basins, composite Eh and pH diagram for the mobility and stability of principal elements in rollfront U deposits, and for copper. Solid phases are in bold type. (After Harshman and Adams 1981 based on Harshman 1974; with data from Garrels 1960; Garrels and Christ 1965; Hansuld 1966; Hostetler and Garrels 1962; Lakin 1961; Lisitsin 1969)



natural water. Selenium can be dissolved and transported only in alkaline and oxygenated water in a natural environment.

In solutions of pH 7 or higher, and in the presence of SO_4^{2-} and CO_3^{2-} ions, selenium is easily oxidized to a mobile selenite ion which probably travels as a complex with sulfur. This complex is, however, unstable in acid-reducing environments in case the oxidation potential is too low and if iron is available, which is abundant in the host rocks. Under these conditions, the selenite ion forms an insoluble precipitate of basic ferric selenite, and, as a result, would behave and precipitate differently as it actually did in Wyoming rollfront deposits.

Uranium was probably transported as a uranyl ion. Somewhat generalized, it can be stated with respect to alkalinity that, in the presence of phosphorous, uranyl ions form predominantly (over 50%) complexes with phosphate between pH 4.5 and 7.5. Without phosphate, uranyl carbonate complexes prevail at pH higher than 4.5, but in the presence of $\text{UO}_2(\text{HPO}_4)_2$ they predominate only above pH 7.5.

Mo, Se, V, and As form oxygenated anionic complexes, which can be transported by solutions of pH near 8 and Eh above -200 mV conditions. These conditions are extant in groundwaters of the Wyoming Basins. Other ore-related elements are presumably carried in solution as simple cations.

It should be kept in mind that humic material complexes all elements found in roll-type deposits, but there is no proof that the dissolution, transport, and reprecipitation of such organic matter is an integral part of rollfront development (Harshman and Adams 1981).

Ore emplacement

In summary, Harshman and Adams (1981) view the actual ore-forming processes as follows: Oxygenated groundwater that carried uranium and associated elements probably was derived in part from the basin flanking Precambrian granitic massifs and in part from the tuffaceous White River Formation. Where these fertile solutions encountered a reducing environment and reached equilibrium with reduced host rocks by oxidation of host rock components, particularly pyrite and carbonaceous material, an interface, the redox/rollfront, was established between oxidizing conditions in the updip part of the host and reducing conditions in the downdip part. The interface actually consisted of several chemical fronts for each individual element (► Fig. 2.6a and b). Across this interface, deposition of U, Fe, Se, Mo, V, and other elements carried in solution has been most pronounced at the respective redox boundary for each element, and decreased rapidly as the solution moved beyond that interface into the reduced zone (see also chapter 2.2 Shirley Basin).

Any mineralized zone established at any time in the cycle would migrate generally in the downdip direction of groundwater flow by oxidation and solution on the updip side of the mineralized zone and reduction and redeposition on the downdip side. A continuous extrinsic supply of uranium and associated elements in the mineralizing solution passing through the zone of deposition would cause the mineralized zone to increase in both grade and magnitude and to eventually reach, particularly in gently dipping beds, the size of the present-day deposits.

The processes described earlier continue downdip in host horizons for distances of 8–20 km and to depths of several tens to several hundreds of meters below ground surface. As long as oxygen and slightly mineral-fertile water is supplied to the redox interface, mineralization will accumulate at a rate governed by the supply of oxygen, amount of pyrite and/or carbonaceous material, biological or abioblogical reduction of sulfur, rate of flow of the mineralizing solution, and possibly length of the altered tongue. The process is arrested when either the hydrologic system changes, the reduced zone is destroyed by oxidation, or oxygenated water invading the host sandstone at or near the outcrop or paleo-outcrop becomes diluted by reducing water entering the host aquifer from overlying sediments.

With respect to the time of ore emplacement, it appears that mineral deposition may have begun in middle Eocene time and not later than middle Oligocene time, and it may have continued over a period of several hundred thousand to several million years.

The apparent middle Eocene to middle Oligocene age of uranium ore in the Shirley Basin, the Gas Hills, and the Crooks Gap districts suggests that mineral deposition occurred at relatively shallow depths, for by middle Oligocene time the accumulation of tuffaceous rocks overlying the late Paleocene or early Eocene host sandstones was not more than 150–300-m thick, and may even have been considerably thinner. The early Tertiary age suggests also that deposits formed during or shortly after periods of volcanic activity that contributed large volumes of ash to the overlying Wagon Bed and the White River formations. It is believed to be more than coincidence that deposits were formed shortly after the first deposition of tuffaceous material in the Tertiary sequence, at a time when volcanic debris should be most susceptible to leaching by percolating groundwater, and at a time of little change in the hydrologic conditions extant when host rocks were deposited.

Some of the deposits, particularly those associated with limonite-bearing altered tongues (i.e., in the Powder River Basin) may have undergone redistribution of uranium and other elements in the original deposits until recent times.

According to Ludwig's (1978, 1979) age determinations, the periods during which uranium ore deposits in each district could have formed are probably intervals during which oxygenated groundwater could most readily have entered host horizons. This was the case (a) during deposition of host rocks, (b) during a post-Eocene period of erosion when parts of the host rock units were removed, and (c) during a post-Miocene to recent period of erosion when parts of the host rock units and most younger strata were eroded.

Although it is reasonable to expect that the host rocks were less accessible to an influx of oxygenated water during the time they were buried by younger tuffaceous strata, some minimum ages established for mineralization in the Shirley Basin (24 ± 3 Ma) indicate that such water penetrated parts of the host rock during this period.

The inferred limits on the time of mineralization in the Gas Hills and the Crooks Gap do not resolve the question of the major source material for uranium and other elements except to require a source to have existed from at least Oligocene time.

In terms of mechanism of mineralization, those appealing to initiation of roll-forming processes in the latest Eocene-early Oligocene erosion interval are perhaps the most readily reconciled with U–Pb isotope age data. Suggestions of true ages of mineralization as young as 30–28 Ma for the Crooks Gap and the Gas Hills districts and 24 ± 3 Ma for the Shirley Basin (Ludwig 1978), however, may require a longer period of uranium mobilization-remobilization than Childers (1974) or Rackley (1976) envisioned.

The range in ages of ore at the Highland Mine in the Powder River Basin indicates that this present-day U deposit formed in response to the latest post-Miocene influx of oxygenated water. Although post-Miocene erosion has permitted an influx of oxygen-bearing groundwater to the host rocks of other Wyoming districts, the distinctly older ages of dated deposits in each indicate that they were bypassed by this late influx. Groundwater flow patterns in these districts may have been changed by tectonic movement after deposits were formed, but before host rocks were exposed again in post-Miocene time. In the case of a post-ore reversal of groundwater flow, e.g., by tilting of the area, as noticed by Harshman (1972) for the Shirley Basin, previous deposits could even be turned into a stage of destruction.

Last but not least, it should be kept in mind that in the Shirley Basin, the Crooks Gap, and the Gas Hills districts some undated deposits may exist whose ages may be comparable to those of the Highland deposit. Also, it is possible that in the Powder River Basin undated deposits exist whose ages may be coeval with those in other basins (Harshman and Adams 1981).

For comparison and additional information of rollfront-type U deposits in other regions, the reader is referred to the South Texas Coastal Plains, USA (in this volume); and to the Chusarysu and Syr-Darya basins in Kazakhstan (Petrov et al. 1995), the Kyzylkum basins in Uzbekistan (Karimov et al. 1996), and the Ily and other sedimentary basins in China, described in Dahlkamp (2009) *Uranium Deposits of World, Asia*.

Description of Individual Districts in Wyoming Basins

(see [Figs. 2.1](#) and [2.2a](#) for location of basins and districts)

2.1 Gas Hills, Wind River Basin

The Wind River Basin, located in the center of Wyoming, is bounded by the Granite Mountains to the south, the Wind River Mountains to the west, and the Owl Creek-Copper Mountains to the north. All are granitic and metamorphic complexes of Archean to Lower Proterozoic age. The eastern boundary is the N-S-trending Casper Arch, which separates the Wind River from the Powder River Basin ([Fig. 2.1](#)).

The Wind River Basin hosts a major uranium-bearing area, the *Gas Hills* district. Discovered in 1953, this district had original resources (in situ and mined) of at least 55,000 t U at grades ranging from <0.06 to 0.35% U or more. [Cameco (2007 Annual Information Form, pp 46–47) reports for its Peach

property remaining proven and probable reserves of 7,577 t U at a grade of 0.11% U, and additional measured and indicated resources of 2,154 t U at a grade of 0.068% U (status December 31, 2007)]. Mining lasted intermittently from 1954 to 1988 and totaled some 25,000 t U (INI 2000). Mining grades averaged 0.10–0.16% U.

Since the start of production in 1954, approximately 65 mines had been active in three belts or trends within the Gas Hills district. Better known mines in the *Central Gas Hills* include the Frazier, John, Lamac, Lucky Mc, and Peach; in the *East Gas Hills* the Pay Aljob, Rim Group, and Star; and in the *West Gas Hills* the Dick, Ola, Sagebrush, and Sunset mines. Additional deposits include Day Loma, Clyde, Bret, Loco, Whiskey Peak, and others. Larger deposits were mined by open-pit methods (e.g., Lucky Mc) and the deeper and smaller ones by underground methods (e.g., Peach Shaft). Open pits had an ore to overburden ratio between 1:30 (Union Carbide Mine) and 1:26 (Lucky Mc).

Sources of Information. Anderson 1969; Armstrong 1970; Dooley et al. 1974; Harshman 1968; Harshman and Adams 1981; King and Austin 1966; Krewedl 1979; Rackley 1972; Snow 2007a, b; Soister 1968; US AEC 1959.

Geological Setting of Mineralization

The Wind River Basin hosts the prominent Gas Hills uranium district (Fig. 2.13). This district lies on the south flank of the basin, between the Granite Mountains of the Sweetwater Uplift to the south and a series of northwesterly trending, folded Cretaceous and older rocks that separate the district from the axis of the Wind River Basin some 80 km to the north.

The Wind River Basin is filled with Paleocene to Miocene predominantly clastic sediments with intercalated tuffs that rest upon Cretaceous to Cambrian sandstones, limestones, dolomites, and clay-mudstones (Fig. 2.14). Total sediment thickness is as much as 4,200 m of which the Tertiary sequence accounts for 600 m.

Gas Hills uranium ore bodies are hosted by the early Eocene *Wind River Formation*. This formation is – from top to bottom – subdivided into:

- An upper transition zone, up to 35 m thick in the extreme western part of the area, but thin in the main mining district
- The Puddle Springs Arkose Member, 120–240 m thick, which is the main host of uranium ore bodies, and
- A lower fine-grained member, 0–40 m thick, composed of pale yellow-grey to pale olive, sandy bentonitic claystones.

The lower fine-grained member was deposited on the north flank of the Sweetwater Uplift by meandering streams flowing northward into the Wind River Basin. After renewed uplift of the Granite Mountains, these mountains supplied the material for the ore-bearing Puddle Springs Arkose Member.

The *Puddle Springs Arkose Member* consists of two large coalescing alluvial fans that derived by multiple, laterally migrating, shallow, straight-channel, and braided bed-load streams. Fan position was governed by the principal streams

flowing northward from the Granite Mountains into the Wind River Basin, and by topographic features, which protruded above the floor on the south flank of the basin (Fig. 2.13). The lithology of the Puddle Springs Member comprises intermediate and distal alluvial fan conglomerates and moderately sorted medium- to coarse-grained arkose-sandstones grading northerly, downslope, into bed-load dominated fluvial channel-fill sands. A noticeable fining of material in the fans is observed toward the east and west and in areas where sediments lap on paleotopographically high areas. A few sandy boulder-to-pebble conglomerate horizons of braided-channel and sheetwash origin of individual fan lobes occur over wide areas.

Clastic sediments consist predominantly of quartz and feldspar with some muscovite, biotite, and fragments of granite, gneiss, slate, quartzite, and rarely limestone and mafic dike rocks. These sediments are poorly consolidated and cemented by a carbonatic and/or limonitic (in oxidized areas) matrix. Sandstones contain vegetal organic debris and disseminated epigenetic pyrite in nonoxidized facies.

Ore-hosting Eocene sediments dip now 1–3° to the south, i.e., toward their source area. The reversal of inclination from the originally shallow northerly dip occurred after ore deposition as a result of downfaulting of the Granite Mountains, probably in late Miocene time.

Host Rock Alteration

Oxidation and related transformation of rock constituents of the Puddle Springs arenites dominate alteration phenomena associated with U mineralization. They form an alteration tongue from 100- to 120-m thick in the central Gas Hills. This tongue envelops many mudstone lenses that separate permeable sandstone layers and terminates in redox fronts.

As compared to altered tongues in the Shirley Basin (see chapter 2.2), the Gas Hills altered sandstone tongue is larger, thicker, and considerably more complex, due to the more complex sedimentary character of the Gas Hills alluvial fans than that of the distal alluvial fan and bed-load fluvial environment of the Shirley Basin.

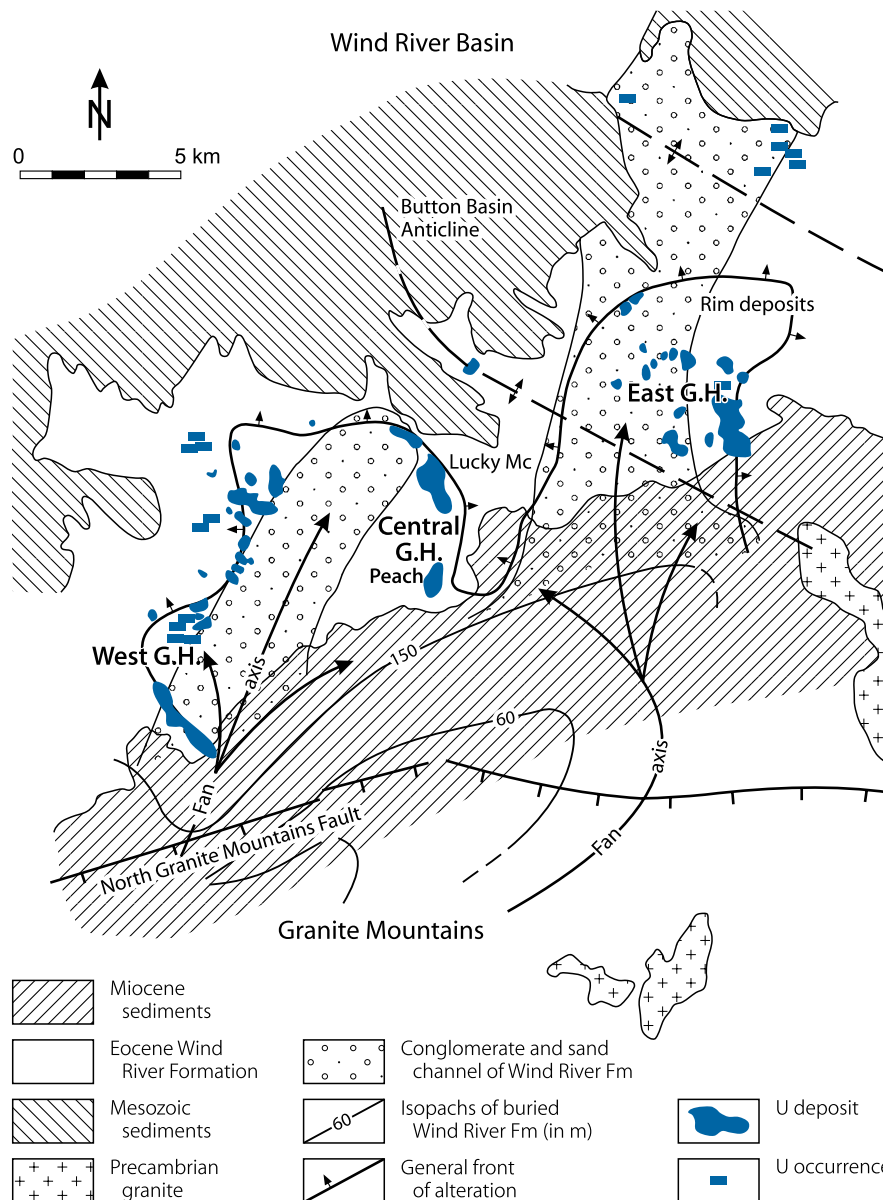
The mode of alteration created by these redox fronts is partly unique to the Wind River Basin, partly it is similar to other Wyoming Basins. Particularly, the pervasive color of altered sandstone is in marked contrast to most other basins. Nonoxidized sandstones are grey to greenish-grey, whereas altered (“bleached”) sands are from creamy to grey-white. Altered sands are practically barren of pyrite, but contain instead some hematite and limonite, and reduced amounts of carbonaceous substance (for redistribution of elements, see next paragraph and the Shirley Basin description).

Mineralization

Pitchblende, sooty pitchblende, and coffinite are the main U minerals. Pitchblende is the dominant U phase, but pitchblende to coffinite ratios can be as high as 40:60. These minerals coat

■ Fig. 2.13.

Wind River Basin, Gas Hills, sedimentary patterns and distribution of alteration front in the Wind River Formation moving northward from the Precambrian Granite Mountains. Uranium deposits are dominantly localized along the solution front. (After Galloway 1979a; Harshman and Adams 1981)



quartz grains and fill voids. Uranium is also present in organic matter, associated with the clay fraction of ore-bearing sandstone, in carbonate fluor-apatite, and, in a few outcrops, as uranyl minerals (autunite, etc.).

Associated elements and minerals include Mo, Se, As, and P, which form minerals related to the redox environment. Jordisite was the last mineral to have formed. Pyrite and marcasite occur in reduced sandstone, hematite and goethite occur in oxidized sandstone.

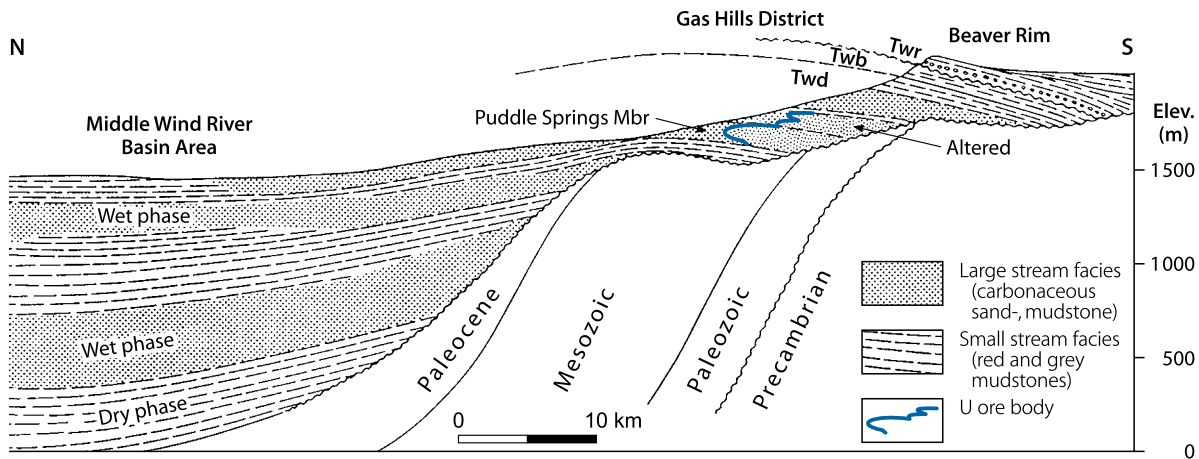
The paragenesis of ore minerals in the Gas Hills is similar to those in most other Wyoming Basins. In contrast to the Shirley Basin, however, where no molybdenum is present, the Gas Hills ore bodies contain abundant molybdenum.

The distribution of ore and ore-related elements in and near ore bodies can be summarized from Harshman and Adams' (1981) description as follows. By taking unaltered sandstone as a reference, the altered sandstone shows an increase of ferric iron, selenium, vanadium, and perhaps uranium, and a depletion in organic carbon, calcium carbonate, sulfate, pyrite, ilmenite, magnetite, total iron, arsenic, and perhaps copper and molybdenum.

Ferrous/ferric iron ratios are considerably lower in altered than in unaltered sandstone, but the amounts of iron in both altered and unaltered sandstone are considerably greater than, for example, in the Shirley Basin. Disequilibrium in favor of eq.U in low-grade samples is greater in altered than in unaltered sandstone, but the difference is not as great as in the Shirley Basin.

Fig. 2.14.

Wind River Basin, Gas Hills area, generalized N–S cross-section showing the pre-Wind River Formation morphology, distribution of Wind River Formation facies, and position of uranium rolls. (After Bailey and Childers 1977)



Shape and Dimensions of Deposits

Uranium mineralization occurs in an area 8 by 35 km in size in which ore deposits are grouped in three, between NE- and NW-oriented trends or belts within the large multiple lobate tongue of Puddle Springs Arkose (Fig. 2.13). These zones are 1–3.5-km wide, as much as 8-km long and separated by 1.5–6.5-km wide belts of none or only weakly mineralized sandstones.

Ore bodies are located principally along redox fronts at the margins of this large irregular tongue although some ore also occurs on the top and bottom surface. Redox fronts persist laterally as a sinuous, many kilometers long band through the Puddle Springs arenite. Ore bodies occur intermittently along this front at a depth from 30 to 150 m and locally deeper. Lateral extensions of the best ore bodies are as much as 1,000 m or more with little or no interruption. Thinner ore bodies, in contrast, are of far less lateral extent.

Ore bodies have a crescent shape in cross-section with long tails, or they may consist of several superjacent crescents separated by less permeable horizons (Fig. 2.15). Ore bodies range in thickness from several centimeters to almost 10 m, averaging about 3–5 m.

Deposits consist of a series of en echelon stacked ore bodies of variable sizes that in total occupy the edge of the altered tongue. As a result, a number of ore bodies occur through the total interval of 100–120 m of the redox front even though only one altered tongue is present. In most places, rolls are stacked so that successively higher rolls are displaced farther forward. In plan view, the rollfronts may be parallel to one another or they may cross, for each rollfront has its own sinuosity.

The trailing ends of crescent-shaped ore rolls have lengths of a few to over 100 m, averaging several meters to tens of meters. The lower limb generally extends farther back beneath the altered tongue than the upper limb, and this ore is generally thicker than the upper-limb ore. Lower-limb ore is almost always underlain by mudstone, whereas upper-limb ore may or may not be overlain by mudstone; and if not, the upper limb and the

upper surface of the altered tongue are separated from the next overlying mudstone by unaltered, unmineralized sandstone.

In addition to the principal ore bodies along the rollfront, there exist some near-surface oxidized ore bodies as well as deposits of reduced ore that are generally lenticular and represent uranium redistributed from older roll-type ore. Primary ore, however, contributes over 90% of the ore in the Gas Hills district. In the lower part of the Puddle Springs Member, uneconomic calcite-cemented uranium and pyrite-bearing sandstones occur, which are not associated with the altered facies and hence may have formed prior to the rollfront deposits.

Ore Controls and Recognition Criteria

The position and lobate nature of the oxidized tongue and consequently the location of ore bodies is broadly controlled by

- The position of two principal paleostream systems that form the Puddle Spring Arkose in the Wind River Basin
- The gross lithology and permeability of the host rock (arkosic sandstones are the best host rocks)
- Presence of vegetal carbonaceous matter, and locally, of structureless, amorphous organic substances
- Presence of sulfides.

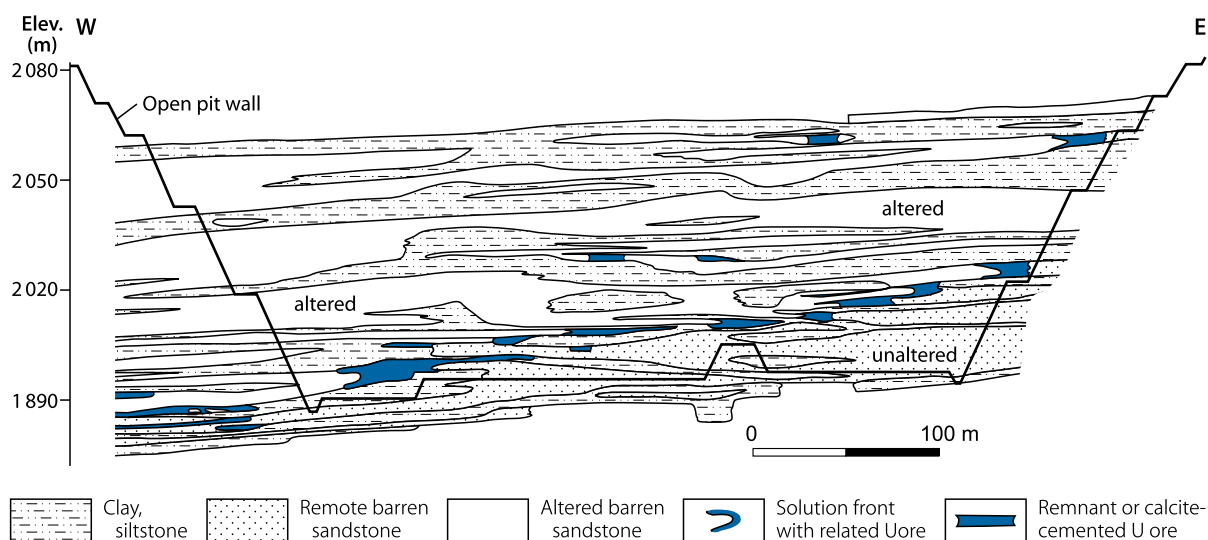
The more universal parameters and metallogenic aspects are similar to deposits in the other Wyoming Basins as discussed in earlier sections.

2.2 Shirley Basin

The Shirley Basin lies in southeast Wyoming between the southwestern part of the Shirley Mountains/Sweetwater Uplift to the west and the Laramie Mountains to the east (Fig. 2.1). Uranium deposits occur in the central part of the basin. They contained original resources of more than 47,000 t U at grades ranging from <0.07 to 0.5% U.

■ Fig. 2.15.

Gas Hills, Lucky Mc 4-J open pit, W–E cross-section, illustrating the complex distribution of ore bodies in the upper Wind River Formation. The U mineralized solution front at the top right extends for many kilometers along strike, whereas the ore body at the top right center is small in its lateral extension. It represents remnant ore that formed when mineralizing fluids passed through the sand aquifer, which locally contained abundant carbonaceous matter. The lower uraniumiferous front on the right side is also continuous for many kilometers, as are the fronts below and to the left. U mineralization below the solution front ore bodies is hosted in calcite-cemented, pyritiferous sandstone. It is not related to the solution front ores and presumably formed prior to the solution fronts. This mineralization does not constitute significant ore reserves. (After Anderson 1969)



Uranium was found in 1955, and exploitation lasted intermittently from 1960 to 1992. Around ten mines were in operation, including *Petrotomics/Dave, Section-9, Section-15, Pathfinder mine, Utah mine/F Group-Section-28, Homestake Nall Lease, and Kerr McGee mine*. Exploitation began by underground mining methods that later had to be abandoned due to water problems. Consequently, most mining was by open pits that had an ore to overburden ratio of up to 1:65 (*Pathfinder mine*). Production totaled 18,500 t U. Mining grades averaged 0.15–0.16% U.

Sources of Information. Bailey 1965; Harshman 1968, 1972; Harshman and Adams 1981; Melin 1964, 1969; Pool 2007a; Rackley 1972.

Geological Setting of Mineralization

The host to uranium ore, the early Eocene Wind River Formation, is approximately 150-m thick. It rests upon rocks of Precambrian to Cretaceous age and it is overlain by tuffaceous silt and mudstones of the Oligocene White River Formation.

The *Wind River Formation* is an arkose-bearing unit that largely derived from the Archean-Lower Proterozoic Shirley and Sweetwater mountains to the west. Individual arkose-sandstone horizons average less than 30-m thick. These beds were deposited within a braided fan and channel fluvial system, incised into Cretaceous and older rocks, by northerly flowing streams. In the western part of the basin, fluvial sediments were laid down on a

broad alluvial fan; in the central part of the basin in the main channel and adjacent overbank areas of the trunk stream; and in the eastern part of the basin in tributary channels and flood plains of streams that originated in the Laramie Mountains on the east flank of the basin.

Major uranium deposits occur in a well-defined belt of arkose-sandstone that lies west of a 30–120-m high buried ridge on the pre-Wind River erosion surface. This ridge has supposedly influenced the position of the host sandstone belt by controlling the area in which easterly flowing, high-gradient tributary streams joined the northwesterly flowing, low-gradient trunk stream. This produced a sequence of arkoses interbedded with silt and mudstones, greenish in color, and intercalated with lignitic beds.

Ore-bearing arkose-sandstones are medium to coarse grained and have a variable matrix of clay, silt, and fine sands with disseminated pyrite and abundant carbonaceous matter. Sands are only slightly cemented, partly by disseminated calcite. Locally, calcite-cemented lenses up to several meters long occur. Pyrite is widely distributed in unaltered sandstone as well as in altered sandstone close to ore. Unaltered sandstone contains about 1% pyrite, commonly as euhedral to subhedral crystals. Pyrite occurs as tiny grains attached to sand grains, replaces carbonaceous material and clay minerals, surrounds clay galls, locally cements gravelly cross beds, and forms occasionally grain aggregates. This widely distributed pyrite is thought to be of pre-ore diagenetic origin.

Post-ore tectonics tilted the Eocene sediments 1–5° to the north. Faults that offset ore bodies are rare.

Host Rock Alteration

Oxidation is the most prominent alteration phenomenon. Its most visible result is a striking color difference in the same lithologic horizon on both sides of redox fronts, i.e., between altered and unaltered sandstone. Nonoxidized sandstone is generally medium to light grey, whereas altered sandstone is almost everywhere greenish-yellow, but locally it can be orange, red- or reddish-brown as in the Nall Lease.

These diagnostic colors are caused by the differential content of ferrous and ferric iron. $\text{Fe}^{2+}/\text{Fe}^{3+}$ ratios changed considerably during alteration of the host sands although the total iron content remained almost the same. Unaltered sandstone has a $\text{Fe}^{2+}/\text{Fe}^{3+}$ ratio between 2:1 and 4.5:1, while the ratio in altered sandstone ranges from 1.5:1 to less than 0.4:1. Most of the iron is contained within the clay- and silt-sized fractions of the sandstone. In altered sandstone, these fractions can contain 30–40% of the total iron although these fractions constitute only a few percent of the sandstone. High iron-montmorillonite is a typical clay mineral in these fractions. It originated, partially at least, by alteration of amphibole minerals. In contrast, the pelitic fraction of unaltered sandstone contains only 10–15% of the total iron and has a low iron-montmorillonite as matrix constituent.

Kaolinite is present in considerable amounts in both sandstones, but did not experience any alteration. Feldspars likewise show only very limited alteration effects. Otherwise, pyrite, calcium carbonate, and largely also carbonaceous matter have been destroyed; biotite turned to a light greenish to bronze color, and hematite and limonite have been formed by alteration activity.

The selenium content differs markedly. Unaltered rocks contain from about 1–4 ppm Se with higher amounts generally in fine-grained carbonaceous strata, while altered rocks show an increase to between 10 and 40 ppm Se.

Copper, arsenic, and sulfate sulfur were removed by alteration processes, whereas vanadium, present in limited amounts only, was accumulated in altered sandstone. Uranium and its decay products occur in higher amounts in altered than in unaltered sandstone distant from ore. Unaltered and unmineralized sandstone in the ore-bearing horizon and barren sandstone above the ore-bearing interval contain 4–5 ppm uranium. Altered sandstone several hundred to a thousand meters behind the redox front contains 6–15 ppm uranium. Harshman and Adams (1981) point to the fact that in weakly mineralized samples (less than 0.1% U) the U to eq.U ratios show a distinct disequilibrium in favor of eq.U; and that disequilibrium is greater in altered than in unaltered sandstone.

There tends to be no obvious effect by alteration on physical properties of ore-bearing sands and hence, physical properties cannot have had an influence, on a local scale, on the location of the rollfronts and altered sandstone tongues, respectively.

Two superjacent altered tongues exist in the Wind River Formation in the Shirley Basin (► Fig. 2.16a). They are generally separated by 15–25 m of siltstone, but in some places the two sandy horizons are interconnected. The lower tongue is 20–30-m thick. It occurs in a single sandy horizon that rests unconformably upon the Cretaceous paleo-surface.

The upper altered tongue occurs in two sandy horizons that in some places are separated by 9–12 m of sandy siltstone, whereas in other places they rest one upon the other. The upper altered sandstone tongue ranges in thickness from 1 m or less near its western edge to about 20-m thick, a 100 m or so from the edge. It is commonly concordant with the shallow dip of the Wind River strata, but locally, the altered–unaltered sandstone interface transects sharply across sedimentary structures. The upper altered tongue lies at a depth of about 135 m at its northern end. It climbs at a dip of about 1° toward the south and loses its identity when it passes into the surface weathering zone and eventually crops out.

Mineralization

Pitchblende/sooty pitchblende, coffinite, and a uranium-organic complex or chelate(?) are the principal U phases. Associated minerals and elements include pyrite, marcasite, hematite, calcite, as well as native selenium, ferroselite, vanadium, and arsenic. Figure 2.6a shows the distribution of these elements, and ► Fig. 2.7a,b, and c the abundance of marcasite across a redox front in the Petrotoomics Sec.9 pit. In contrast to other Wyoming Basins, no molybdenum is present.

Pitchblende fills pores of the host sandstone, coats and fills fractures in sand grains, and replaces parts of grains, particularly feldspar. Pitchblende forms the inner rim on some sand grains, but in most cases it forms an outer rim on an inner pyrite and/or marcasite rim. If three rims are present, pitchblende lies between an inner and outer pyrite–marcasite rim. Shrinkage cracks in pitchblende are sometimes filled with pyrite–marcasite. The lateral extent of pitchblende distribution is only slightly less than that of pyrite.

Selenium is present in a sharply defined narrow zone astride the contact between altered sandstone and ore. In ore, selenium is present as small acicular crystals of native selenium, whereas in altered sandstone it occurs as ferroselite. In addition, pyrite contains selenium, particularly in the unoxidized ore-bearing part of the selenium-bearing zone.

Pyrite is present in at least two generations, a diagenetic and an ore-related generation. Ore-related pyrite is abundant, locally more abundant than uranium. It occurs in ore as small euhedral to subhedral crystals, as small aggregates, as coating on sand grains, and as botryoidal masses filling voids in host rock. Most euhedral pyrite is untarnished or only slightly tarnished, while pyrite coating sand grains are tarnished iridescent or bluish-black. Pyrite replaces feldspar along cleavages and forms single and multiple rims on sand grains. Multiple pyrite rims are commonly separated by a rim of pitchblende.

Mineralized sandstone with the highest pyrite content is mostly in contact with altered sandstone, but locally it is separated from altered sandstone by about a meter of material with a low pyrite content. On the outer extremity of ore bodies, pyrite extends farther from the altered sandstone tongue than does any other ore mineral except possibly calcite.

Marcasite is present in minor amounts. It is most abundant in ore near the contact with altered sandstone (► Fig. 2.7a, b, and c)

where it occurs intergrown with pyrite or in small isolated grains dispersed through calcite.

Calcite occurs in the ore matrix and in a halo surrounding ore (▶ Fig. 2.16b and c). Its distribution is less uniform than that of other epigenetic minerals, and it tends to form concretionary masses ranging from a few centimeters to a few meters in diameter. In many places, calcite is localized around accumulations of carbonized plant remains, and this calcite commonly contains hematite. The presence of hematite in this reduced environment has not been explained adequately, but it has also been observed at the Peach mine in the Gas Hills. In high-grade, calcite-cemented ore, feldspar grains surrounded by pitchblende are replaced by calcite obviously younger than pitchblende. In other places, pitchblende coats clearly older calcite concretions that are barren in their interior. Small corroded calcite concretions occur in a zone a few decimeters wide that borders altered sandstone tongues.

Shape and Dimensions of Deposits

Ore bodies group in an area some 15 km in length and up to 5 km in width in the central part of the Shirley Basin. Major ore bodies lie at depths between 50 and 100 m at the edges of the earlier mentioned two oxidized sandstone tongues (▶ Fig. 2.16a). Small ore pods are also found on the top and bottom surfaces of oxidized sandstone tongues some distance from their frontal margins. Other pods are associated with small irregular zones of unaltered sandstone that extend into altered tongues or may have survived as islands within tongues.

Some ore bodies have the simple crescent form in cross-section and, in planview, they are elongated parallel to the edge of the alteration tongue. Many ore bodies are of complex configuration, however, and consist of several rolls connected by thin zones of mineralization (▶ Fig. 2.16b–e).

The Shirley Basin ore bodies are not extensive in lateral dimension and in tonnage. Individual mined ore bodies had resources between a few hundred and several thousand tonnes of uranium, persisted in length along the redox front for rarely more than 750 m, and in width for several tens of meters with maxima of about 100 m. Thicknesses vertical to the rolls were commonly a few meters, occasionally up to 10 m. Trailing ends ranged from a few centimeters to some decimeters in thickness.

In situ ore grades ranged from a few hundredths to 20% U. The highest grade ore may or may not have been immediately adjacent to the altered sandstone contact. Asymmetric ore bodies (in cross-section) could have the highest grade and largest ore concentration in the lower limb of the crescent, but not necessarily. Ore along the top and bottom surfaces of tongues was commonly equally distributed.

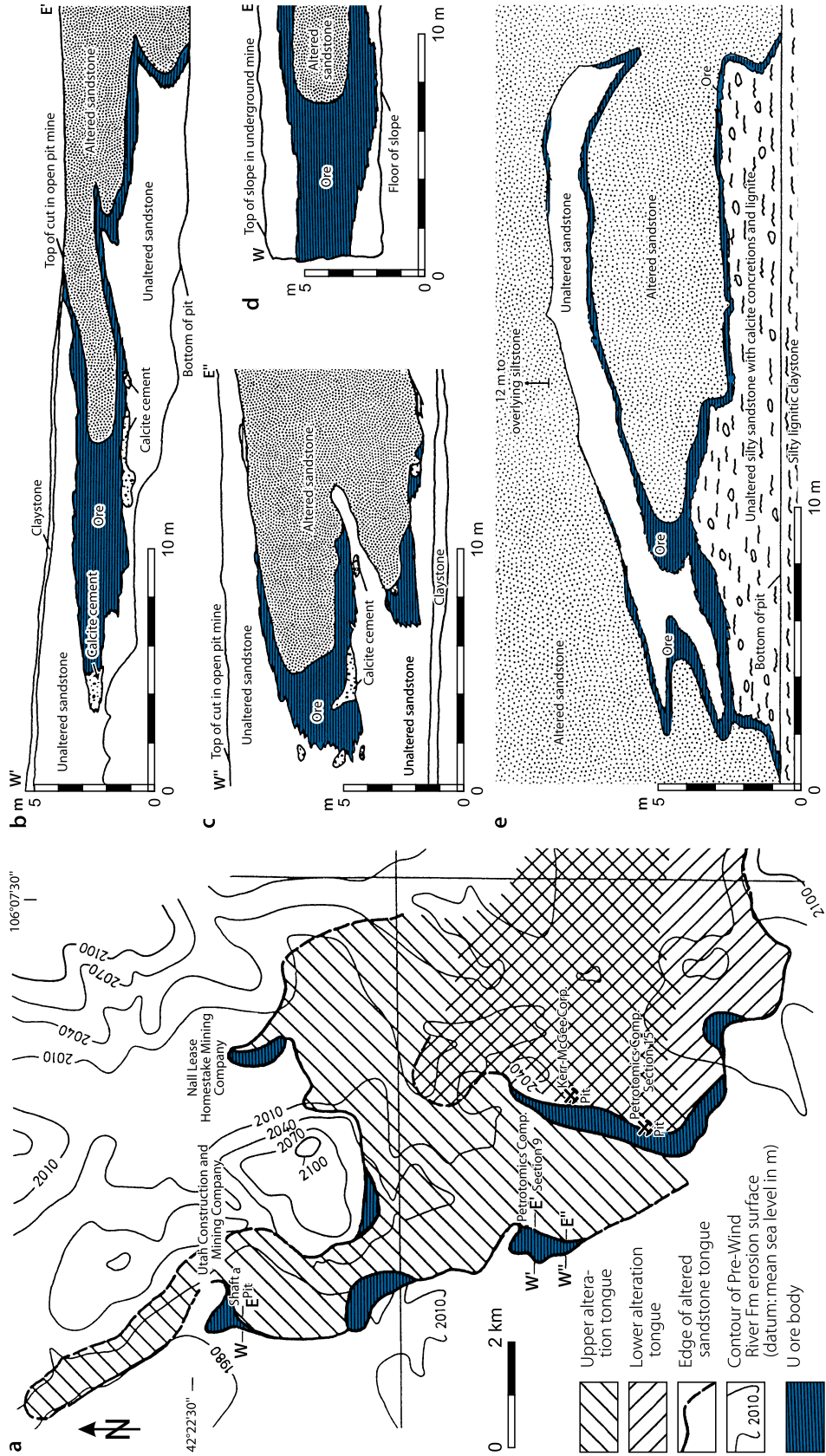
Ore Controls and Recognition Criteria

Harshman and Adams (1981) list the following ore-controlling or recognition criteria for the Shirley Basin U deposits in addition to features common for all the Wyoming Basins as discussed earlier:

- Favorable host environment is provided by
 - Two fluvial arkosic sandstone horizons of the Eocene Wind River Formation
 - Mainly granitic origin of host sands
 - Deposition of host sands along the axis of an old trunk stream
 - Separation of host horizons by a more or less impermeable horizon
 - Superjacent oxidation tongues within the two arkosic sandstone units.
- Permeability conditions controlling the position and limitation of alteration tongues include
 - A noticeable fining of host sands in both the upper and lower tongues toward the east and in the lower tongue toward the north
 - A pinchout by onlap of sandstone on a high area of the pre-Tertiary erosion surface to the north that governs the position of the northern extension of the upper tongue
 - A pinchout toward the west of sandstones hosting the upper tongue while those of the lower tongue continue for several kilometers but rise with the increase in elevation of the pre-Wind River erosion surface.
- Altered and unaltered ore-hosting sands do not exhibit any obvious differences in their physical properties, i.e.,
 - Alteration has not noticeably affected the physical properties of sands
 - Physical properties have not determined on a local scale the location of altered sandstone tongues, although on a regional scale these properties must have had a major influence on their locations.
- The deposition of ore and ore-related elements/minerals took place in a paragenetic sequence as follows:
 - Selenium was the first element to be deposited from a solution flowing from the altered tongue through the zone of mineral deposition
 - Pyrite-marcasite, pitchblende, and calcite followed, in that order, but with considerable overlap in time and place of deposition
 - Calcite in and surrounding ore bodies was deposited prior and posterior to pitchblende
 - Hematite was probably deposited last, but its paragenetic sequence is not well understood.

With respect to *metallogenetic considerations*, Harshman and Adams (1981) note that the sequence and spatial distribution of mineral deposition at any given point in the mineralized zone will not be the same as the sequence of deposition from a unit of solution flowing through the mineralized zone. Because the zone of deposition is of dynamic nature, migrating down the hydrologic gradient, the first mineral to be deposited at a given point will be that mineral whose band of deposition extends farthest in the direction of the flow, and the last mineral to be deposited will be the one whose band of deposition extends the least distance in the flow direction. The sequence of initial deposition at a point in the mineralized zone will be selenium, pyrite, hematite, calcite, pitchblende, and selenium. Arrowheads in ▶ Fig. 2.6b show the downstream limits of deposition bands.

Fig. 2.16. **(a)** distribution of an upper and lower altered sandstone tongue in the Wind River Formation and position of mineralization; **(b), (c), and (d)** sections across the western edge of the upper altered sandstone tongue; **(e)** cross-section of small ore pods along the bottom of the altered sandstone tongue ca. 360 m backwards from the edge of the tongue in Petrotomics Sect. 9 pit. (After **(a)** Harshman and Adams 1981; **(b, c, d, and e)** Harshman 1972)



2.3 Great Divide Basin

The Great Divide Basin is located between separate branches of the Continental Divide in southwestern Wyoming. It is bounded by the Granite Mountains to the north, the Wind River Mountains to the northwest, the Rock Springs Uplift to the west, the Wamsutter Arch to the south, and the Rawlins Uplift to the east (Fig. 2.1).

Four varieties of uranium mineralization are known in the Great Divide Basin: (a) rollfront sandstone-type deposits, (b) stratiform uranium concentrations (termed limb type by Klingmuller 1989), (c) surficial, caliche-type occurrences of schroëckerite, and (d) uraniferous lignite or subbituminous coal (ca. 30 ppm U). Only the first two modes are of economic interest for uranium.

Two main areas with uranium production and resources have been established. They are located in the *Green Mountains* at the northern edge and in the *Sweetwater/Red Desert* area in the central part of the basin (Fig. 2.17). In addition, several U deposits occur isolated in the Great Divide Basin.

Original resources (in situ and mined) of these two areas total an estimated 50,000 t U including about 8,200 t U of production. Mining grades varied between 0.039% U (Sweetwater) and up to 0.25% (Crooks Gap).

Sources of Information. Bailey 1969; Beahm 2006a, d; Boberg 1981, 2007; Childers 1974; Harshman and Adams 1981; Love 1970; Pipingos and Denson 1970; Sherborne et al. 1980; Stephens 1964; Wallis 2006a, b; Wallis and Rennie 2006; and Pool TC, Personal Communicaton.

Regional Geological Features of the Great Divide Basin

The Great Divide Basin is a topographic basin with interior drainage except for the Green Mountains range on its northern rim. It hosts uranium in sandstones of the Battle Spring Formation, a stratigraphic equivalent to the Puddle Springs Arkose of the Gas Hills on the north flank of the Granite Mountains, and the Wasatch and Wind River formations, all of early Eocene age. Spread along the northern margin of the Great Divide Basin, the Battle Spring Formation is a mountainward facies of the Wasatch Formation. The latter occupies the central part of the basin. The Wasatch and the Battle Spring formations interfinger and intertongue in a belt 25–30 km wide, trending about NW-SE, and located 30–50 km SW of the northern edge of the Great Divide Basin.

The Battle Spring Formation is a fluvial–alluvial unit as much as 1,750-m thick that was laid down on slightly folded, fine-grained rocks of the Paleocene Fort Union Formation and on folded pre-Tertiary rocks. It is, or was, overlain by tuffaceous rocks of late Eocene to Pliocene age.

The Battle Spring Formation comprises mainly arkosic sediments, primarily a mixture of interbedded conglomerates, sandstones, and siltstones. These strata are a poorly sorted assemblage of large boulders mixed with finer grained constituents

mainly feldspar and quartz. They were deposited in a composite wet alluvial fan by at least three coalescing major streams flowing southward from the Granite Mountains into the Great Divide Basin. In the northern part of the Great Divide Basin, conglomerates and conglomeratic sandstones prevail in the upper section and therefore some authors define the upper conglomerate sequence as a separate stratigraphic unit, Crooks Gap Conglomerate. Concurrent with deposition of coarse debris in the alluvial fans close to the Granite Mountains, fluvial, lacustrine, and paludal sediments of the Wasatch Formation were deposited in the center of the basin.

2.3.1 Green Mountains

The Green Mountains are an uplifted range on the northern margin of the Great Divide Basin. Uranium deposits occur in a stretch, 25 km in length and 4 km in width, from Crooks Gap in the west to Muddy Gap in the east. Deposits are mainly grouped in the *Crooks Gap* and the easterly adjacent *Green Mountain districts*, which combined account for estimated original resources (including production) at over 40,000 t U.

2.3.1.1 Crooks Gap Mining District

The Crooks Gap district lies in the western Green Mountains in southern Fremont County (Figs. 2.17, and 2.18). Deposits mainly consist of rollfront-type U mineralization, but there are also a few of structurally controlled mineralization. The latter are confined to the northern margin of the district and include the *Sheep Creek* deposit (see chapter 5 Northern Rocky Mountains).

Discovered in 1954, mining of uranium began in the same year and lasted until 1989. Original resources (in situ and mined) were reportedly on the order of 10,000 t U, some 8,000 t U of which were produced by 17 underground mines and open-pit operations. Mining grades ranged from 0.12–0.25% U. Largest mines included *Big Eagle Pit* (1976–1982), *McIntosh Pit*, *Golden Goose*, and *Sheep Mountain*.

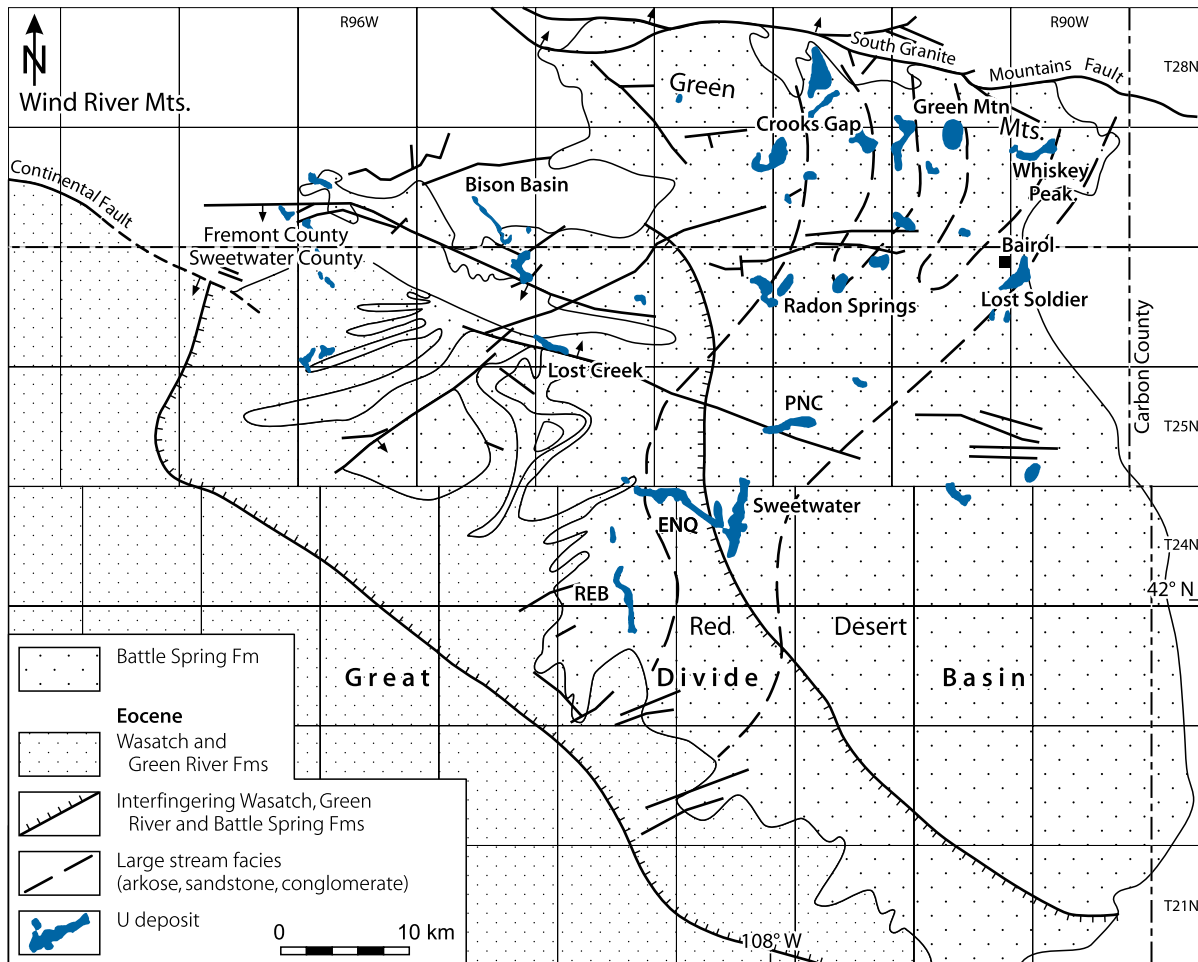
Sources of Information. Bailey 1969; Childers 1974; Harshman and Adams 1981; Love 1970; Pipingos and Denson 1970; Sherborne et al. 1980; Stephens 1964; Wallis and Rennie 2006.

Geological Setting of Mineralization

The Crooks Gap district lies on the northern margin of the Great Divide Basin immediately south of the Archean–Paleoproterozoic granitic complex of the Granite Mountains. Lithologies range from large boulder conglomerate through coarse-grained arkose-sandstone and siltstone to mudstone of the *Battle Spring Formation*. The coarse facies contain, in general, minor amounts of carbonaceous matter. Most sediments are poorly sorted with abrupt changes in nature and permeability of arkosic debris as typical for a proximal or medial wet fan

Fig. 2.17.

Northeastern Great Divide Basin, generalized geological map showing distribution of the Battle Spring, Wasatch, and Green River formations and location of uranium districts and selected deposits. (After Boberg 2005; Harshman and Adams 1981; Pipingos and Denson 1970)



depositional environment. In some areas, however, the Battle Spring sequence contains fluvial sediments that show moderate sorting as well as moderate to good lithologic continuity, and contain considerable amounts of carbonaceous trash. These sediments indicate a deposition in an aggrading fluvial system by southward flowing bed-loaded rivers, which originated in the Granite Mountains.

The strata are folded and faulted, and dip from a few to 20° SE or up to 65° SW. The steep dips and structures are thought to have resulted from post-ore faulting along the Emigrant Trail Thrust and South Granite Mountain fault system on the southern flank of the Granite Mountains.

Host Rock Alteration

Tabular alteration tongues occur in the lower 450 m of the Battle Spring Formation, a thickness considerably greater than in other Wyoming basins. These tongues of altered conglomerate and sandstone extend from the northern edge of the basin southward toward its center and have been traced over a length of at least 7 km and a width of some 4 km in the Crooks Gap area.

Altered sandstone tongues are complex and sinuous in plan as well as in section, and terminate in a series of small, irregular, sinuous rollfronts, probably caused by rapid changes in permeability of the host facies.

Altered zones of ore-bearing sandstone are depleted in organic carbon, calcite, gypsum, pyrite, Ca, total Fe, MgO, TiO₂, S, and SO₄. The contents of selenium, marcasite, and perhaps uranium are greater in altered than in unaltered sandstone.

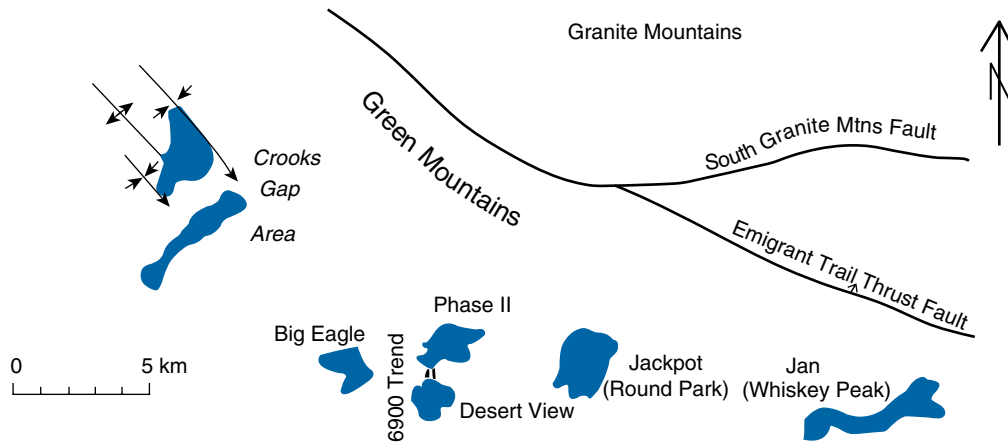
Where unaffected by surface oxidation, unaltered and unmineralized Battle Spring sandstone has a light grey, and altered sandstone has a bleached whitish color. In surface exposures, the altered Battle Spring sandstone is pink to pinkish-brown, whereas unaltered sandstone is drab white and tan.

Mineralization/Shape and Dimensions of Deposits

Pitchblende/sooty pitchblende and coffinite are the principal U minerals in unoxidized ground while uranyl phosphates, -silicates, -sulfates, and -vanadates are found near surface. Associated elements and minerals include pyrite, marcasite, selenium, molybdenum (jordisite), and calcite.

■ Fig. 2.18.

Green Mountains, Crooks Gap-Green Mountain-Whiskey Peak area, location of principal uranium deposits, (Courtesy of International Nuclear Inc. 2008, modified)



Coarse-grained sandstone is the preferred host rock. Ore minerals fill open spaces in sandstone, coat sand grains, and partly replace feldspar. Some ore occurs in coarse conglomerate in which it coats pebbles and boulders, as well as in siltstone and mudstone associated with carbonaceous matter, which it partly replaces.

Most ore bodies are more or less of roll shape and concentrate in narrow zones along margins of altered arenite tongues, similar to those in other Wyoming Basins; the Crooks Gap ore bodies differ from those, however, by their irregularity and lack of continuity. As a consequence, it is almost impossible to project a rollfront and related ore concentrations for more than 10 m from their known positions.

Ore bodies occur at depths from 30 to some 200 m (*Golden Goose* underground workings were at depths between 30 and 120 m). Ore bodies are of modest size. They extend outward from altered tongues for distances of less than 1 m to 10 m, rarely more. Grades range from a few hundreds to as much as 10% U. The highest grade ore may or may not be at the rollfront. In a more regional aspect, mineralization trends roughly parallel to bedding, i.e., it dips at about 10–20° SE. Synclinal structures preferentially appear to be mineralized.

Ore Controls and Recognition Criteria

The position and configuration of the altered sandstone tongue and related ore bodies appears to be controlled more or less by

- Permeable sediments that were deposited along with considerable carbonaceous debris in the channel of one of the major streams flowing from the Granite Mountains southward into the Great Divide Basin and
- The great variety of lithologies, and perhaps post-ore tectonism, which resulted in the extreme irregularity of the interface between altered and mineralized sandstone as well as the poor continuity of ore.

2.3.1.2 Green Mountain District, Wyoming

The Green Mountain uranium district is located in the eastern Green Mountains in Fremont County, central Wyoming. The location is on the northeastern margin of the Great Divide Basin immediately south of the Archean-Paleoproterozoic Granite Mountains (►Figs. 2.1 and 2.18).

Several deposits are identified. The large *Jackpot* deposit also known as *Round Park* or *Green Mountain* deposit was discovered in 1979 about 7 km east of Big Eagle. Between this deposit and Jackpot are the *Phase II* and *Desert View* deposits (both combined are also known as *Pathfinder's 6,900 Trend*). On the eastern extension, in a distance of ca. 7 km is the *Jan* (or *Whiskey Peak*) deposit near Whiskey Peak.

Klingmuller (1989) stresses the difference in morphology of deposits in the Green Mountain district (including Big Eagle) as compared to classical roll-type deposits in other Wyoming Basins. He points to the stratiform nature of uranium mineralization and defines the deposits as limb type.

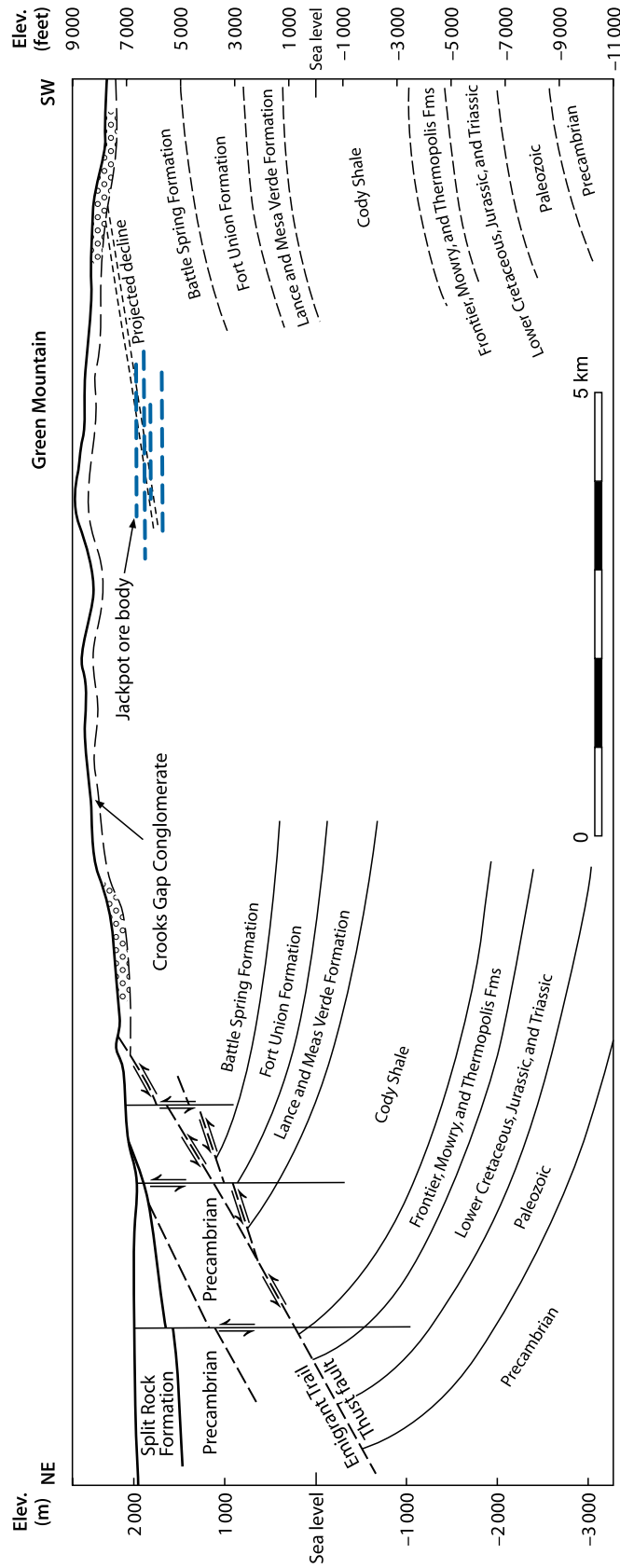
Resources of this district are estimated at over 30,000 t U. Some 16,000 t U of which at an ore grade of about 0.2% U (based on a cutoff grade of 0.085% U and a minimum thickness of 0.6 m) are attributed to the closely drilled *Jackpot* deposit.

Source of Information. Klingmuller 1989, unless otherwise noted.

Geology and Alteration

The Green Mountain uranium district is bordered to the north by the interjunction zone of the Emigrant Trail Thrust and South Granite Mountain fault system (►Figs. 2.1 and ►2.19). The ore-hosting *Battle Spring Formation* is in excess of 1,500 m thick. Regional dip of the strata is 1–3° NE, i.e., their dip is reversed from the original depositional inclination. Intermixed, impure conglomerates and conglomeratic arkosic sandstones prevail in the upper section, whereas arkosic sandstones and siltstones increase in abundance in the lower section. Conglomerates and

Fig. 2.19. Green Mountain, NE-SW section showing the stratigraphic and structural setting on the northeastern margin of the Great Divide Basin and position of the Jackpot deposit. (After GMMV Jackpot Mine, Draft, EIS, US Dpt Interior, BLM, Wyoming State Office, Rawlins, June 1995)



sandstones constitute in excess of 90% of the sedimentary sequence. Sandstone or siltstone intercalations are common in conglomerate. Most boulders consist of light colored to pinkish biotite granite. The sandstone fraction is composed of ca. 50% quartz, 35% feldspar, and 15% granitic rock fragments with minor sericite, chlorite, glauconite, and traces of zircon and tourmaline. Grains are angular to subrounded and commonly coarse to very coarse in size. Most sandstones are friable and lack cementation except near ore due to authigenic calcite, pyrite, or Fe oxides formation. Siltstones have essentially the same composition as the arenite fraction, but they may contain abundant vegetal organic matter and minor volcanic glass fragments.

Unaltered carbonaceous siltstones and related lithologies are grey and contain very fine-grained pyrite and/or marcasite. Locally, as in the Big Eagle area, fist-size pyrite-cemented concretions with a core of relic organic fragments are present in very coarse arkosic sands.

Alteration products and colors resemble those in other sandstone/rollfront-type U deposits that contain Fe sulfides in unoxidized facies. Oxidation affected Battle Spring sediments over a stratigraphic interval of more than 1,200 m, imposing a reddish to pinkish or orange hue on originally grey sediments. The position of redox boundaries in superjacent horizons may be overlapping or sloping. Interfingering of oxidized and reduced facies is a typical phenomenon.

Mineralization

Coffinite and pitchblende are the principal U minerals. They occur as grey to black amorphous interstitial fillings and impregnations (Ludwig and Grauch 1980).

Better grade U mineralization is preferentially associated with organic-rich siltstone lenses, in particular with those that immediately over- and underlie altered arkosic sandstones and conglomerates (Fig. 2.20a). Arkosic sandstones and conglomerates may also contain some mineralization but mostly at lower grades than those in siltstones.

Mineralized lenses are discontinuous and commonly less than 0.6 m thick, but can have relatively high grades as documented by Klingmuller (1989). He provides a number of drill intercepts as examples of “limb-type” mineralization in the Green Mountain district. Maximum and minimum values are given in Table 2.3. As can be seen, mineralized thicknesses range from 0.24 to 0.87 m and grades from 0.032 to 2.577% eq.U, while barren intervals between two mineralized intercepts vary between 0.24 and 7.59 m.

By applying a cutoff grade of 0.042% eq.U, Klingmuller (1989) states that 85% of ore intercepts in a part of *Pathfinder's* 6,900 Trend (or *Phase II*) are 0.6 m or less in thickness, and that 25% of these intercepts contain 1% eq.U or more.

At *Jackpot*, four major more or less overlapping ore trends have been identified at depths below 850 m (Fig. 2.20b). They are separated by about 90, 45, and 150 m barren intervals, i.e., they are distributed over a stratigraphic interval of 290 m. While a substantial part of these trends are stacked at *Jackpot*, in other areas ore trends are arranged en echelon or in a sloping pattern.

Additional uranium mineralization is drill indicated along an ESE–WNW trend some 6 km in length west of the *Jackpot* deposit and also to the east of *Jackpot* where mineralization of less than 0.1% U occurs at depths from 180 to 360 m.

In essence, mineralization of the Green Mountain district is characterized by thin ore lenses that lack continuity. Thick ore

Fig. 2.20.

Green Mountain, *Jackpot* deposit, (a) block diagram illustrating schematically the stratiform distribution of U mineralization in arenites of the Battle Spring Formation. Most U ore is <0.6-m thick and hosted in siltstone lenses dissected by fluvial channels. (b) Plan of U mineralization at various levels between 1,725 and 2,010 m above sea level. (After Klingmuller 1989)

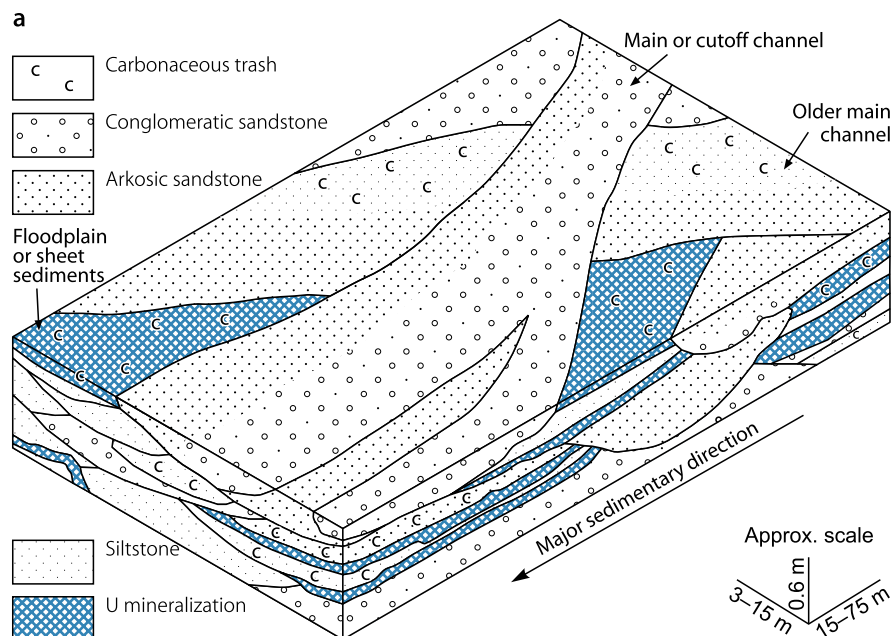


Fig. 2.20. (Continued)

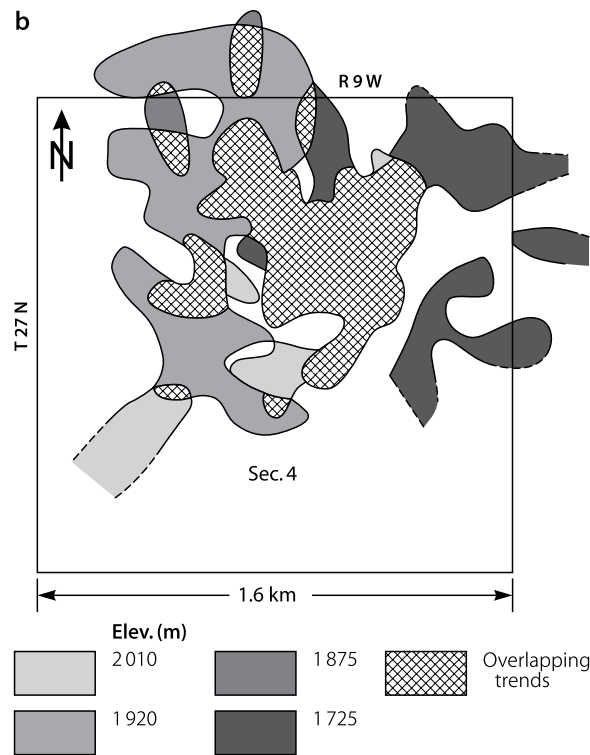


Table 2.3. Green Mountain district, ranges of thicknesses and grades of uranium mineralized lenses (Klingmuller 1989)

Mineralized thickness (cm)	39	36	87	51	24
Grade (% U)	0.032	0.033	0.085	0.170	2.577
Barren interval to top of next lower mineralized intercept (cm)	228	24	150	759	312
Mineralized + barren interval combined (cm)	267	60	237	810	336

lenses are almost absent. Movable ore bodies are practically confined to sites where a number of superjacent ore lenses occur and intervening barren intervals are thin.

Metallogenetic Aspects

Due to the position at a rapidly subsiding basin margin adjacent to a rising source terrane, the depositional energy gradient was too high to deposit larger quantities of pelitic material. As a consequence, continuous layers of aquicludes as well as favorable host horizons, such as those found in the other Wyoming Basins containing classical rollfront-type U deposits, are missing in the Green Mountain district. The host environment is a large body of lithologically heterogeneous aquifers without confining mudstone beds or even continuous semi-confining siltstone horizons.

Klingmuller (1989) postulates that uranium was introduced by surface waters into temporary depressions that had accumulated

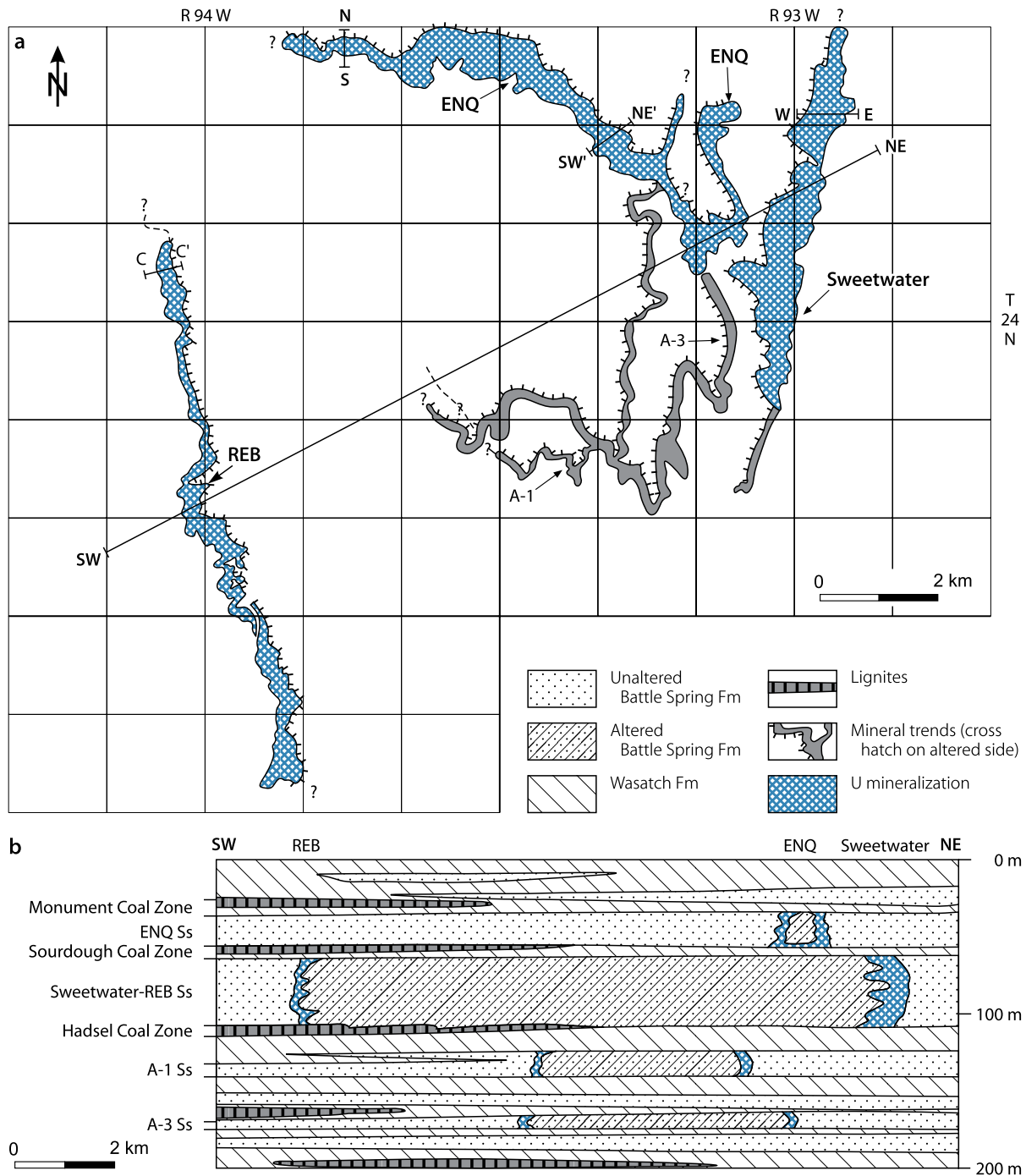
abundant carbonaceous debris in silts and grit-size sediments. These waters entered organic-rich depressions during or shortly after sedimentation. Uranium was precipitated in this reducing environment, but only in protore concentration. In a later stage, during Oligocene time, oxygenated waters invaded Battle Spring strata and generated a regional oxidation tongue or cell with complex redox interfaces over a stratigraphic thickness in excess of 1,200 m. Uranium was dissolved from the Battle Spring rocks by these oxygenated waters and was redeposited along the least permeable, discontinuous reducing facies, represented by carbonaceous siltstone lenses, forming “limb-type” ore.

2.3.2 Sweetwater District, Central Red Desert

The Sweetwater district is located in the central part of the Great Divide Basin. Deposits include *Sweetwater*, *ENQ*, and *REB* (Fig. 2.21a). Original resources (in situ and mined) of these three properties were on the order of 10,000 t U at grades

■ Fig. 2.21.

Central Red Desert, Sweetwater Mine area, generalized (a) map and (b) SW–NE cross-section with mineralized trends and relative position of altered sandstone tongues and associated uranium deposits. [After Sherborne et al. 1980 (reproduced by permission of AIME)]



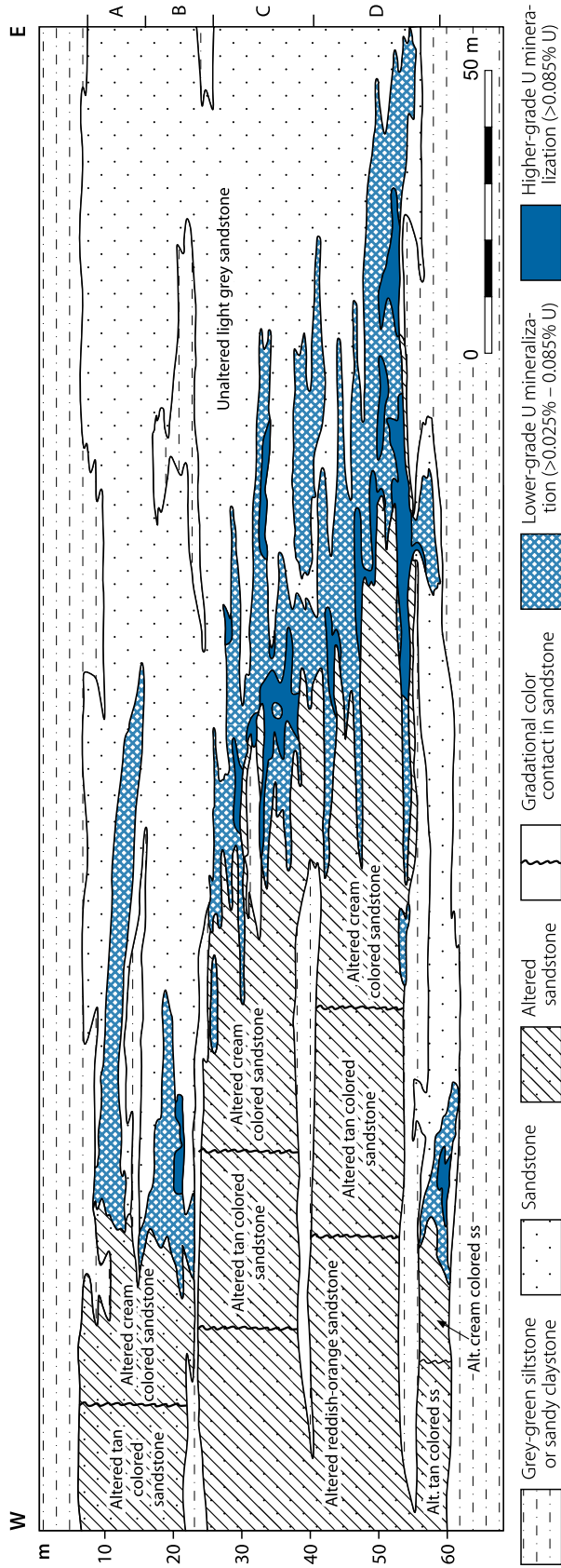
between 0.025 and 0.06% U. Only the Sweetwater deposit was partly mined.

Sources of Information. Boberg 1981, 2007; Harshman and Adams 1981; Sherborne et al. 1980, and Pool TC, personal communication.

Geological Setting of Mineralization

Sweetwater deposits occur in the transition zone where the more psammitic Battle Spring sediments interfinger with the psammitic to pelitic Wasatch sediments. The sediments of the **Wasatch Formation** are of fluvial, paludal, and lacustrine provenance and

Fig. 2.22. Central Red Desert, Sweetwater deposit, W–E cross-section depicting the highly heterogeneous geometry of uranium mineralized intervals in arenitic stratigraphic units A–D of the Wasatch Formation. [After Sherborne et al. 1980 (reproduced by permission of AIME)]



were apparently deposited in a distal fan and bed-load stream environment as reflected by their better sorting and better lateral continuity of individual beds than those in the Crooks Gap district.

Uranium occurs in a 180 m thick stratigraphic interval that contains four arenite units, termed, from top to bottom, ENQ, Sweetwater-REB, A-1, and A-3 sandstones (►Fig. 2.21b). The two upper ones are 20–45 m thick and the two lower horizons are thin. Thin mudstone beds separate these horizons. The mudstones grade southward toward the center of the basin into uraniumiferous lignite. Northward, toward the margin of the basin, they pinch out and the four sandstone horizons probably merge into one thick unit.

The two upper arenite units contain all major ore bodies, ENQ at the redox front in the ENQ sandstone, and Sweetwater and REB at the redox front in the underlying Sweetwater-REB sandstone. These two units consist of complexly intercalated sandstone lenses that range from less than 1 m to more than 22 m in thickness. Individual lenses in channel scours are characterized by crude fining-upward lithologies. They commonly commence with coarse pebbly sandstone near the base and grade upward to discontinuous sandy lags, planar foreset beds, and ripple drift cross-laminations. Larger channels contain festoon and planar cross-stratification, slump structures, and rare rip-up clasts. Vegetal carbonaceous debris is present in all sediments.

Host Rock Alteration

Oxidation of arenite in the four units has altered pyrite to goethite and hematite, and ilmenite to anatase, and has destroyed carbonaceous matter, hornblende, magnetite, and zircon, which are normally present in small amounts in host rocks.

The light grey hue of unaltered sandstone has changed in altered sandstone in the ENQ and Sweetwater-REB tongues to a predominant reddish to orange color. Near the margins of both tongues, there are changes in character of the alteration that tend to be related to the width and grade of mineralized sandstone.

The redox front in the Sweetwater-REB sandstone extends southward toward the center of the basin. It has an established length of some 10 km, a width of 8–11 km, and a thickness of 45–50 m. On the eastern edge of the tongue, near the Sweetwater deposit, a few thin lenses of grey-green siltstone or sandy claystone are interbedded in the predominantly reddish sandstone host. On the western edge, near the REB deposit, the tongue contains a number of laterally continuous carbonaceous mudstone and poorly sorted siltstone beds, which divide the tongue into five separate sandstone horizons all of which are altered.

The ENQ sandstone, which rests upon the Sweetwater-REB unit, encloses a large tongue of altered sandstone that projects southeasterly into the Great Divide Basin for a known length of about 8 km and a width of at least 1.5 km. The tongue lies above the eastern part of the Sweetwater-REB altered tongue, but it does not persist basinward as far south as the Sweetwater-REB tongue.

Coloration caused by iron oxides in the ENQ tongue is similar to that in the western part of the Sweetwater-REB tongue. Near the southeast limit of the tongue, altered sandstone is

yellow-grey-green, whereas unaltered sandstone is grey to grey-green. To the northwest, along the margin of the tongue, a zone of very subtle alteration, as much as 300 m wide, with coloration indistinguishable from unaltered sandstone, separates the normal yellowish alteration hue from mineralization at the front of the tongue. Where this zone of subtle alteration is present, mineralized sandstone adjacent to the rollfront contains yellow and pink, iron-stained quartz and feldspar grains. Highest grade mineralization seems to be situated where the zone of subtle alteration is widest.

Metallogenetic Aspects

Sherborne et al. (1980) have related the positions and margins of altered sandstone tongues and genetically related uranium deposits to basinward pinchout of permeable beds and isolation of groundwater flow within a few aquifers in the Battle Spring Formation. In the Sweetwater Mine area, a few thick tabular sandstone units, such as the Sweetwater-REB and ENQ, served as major laterally continuous aquifers in a thick section of inter-tonguing sediments of the Battle Spring, the Wasatch, and the Green River Formations. Mineralizing solutions, which only a few kilometers north had been dispersed throughout a thick section of highly permeable Battle Spring Formation sandstones, were funnelled into these tabular units, where tabular, low-grade, large-tonnage deposits, as well as higher grade, typical C-shaped, moderate tonnage deposits were formed at the edges of altered sandstone tongues.

2.3.2.1 Sweetwater Deposit

Original in situ resources of the Sweetwater deposit were approximately 7,300 t U. About 500 t U of which were recovered from 1981 to 1983 by open-pit mining. The average mining grade was 0.039% U (Pool TC, personal communication).

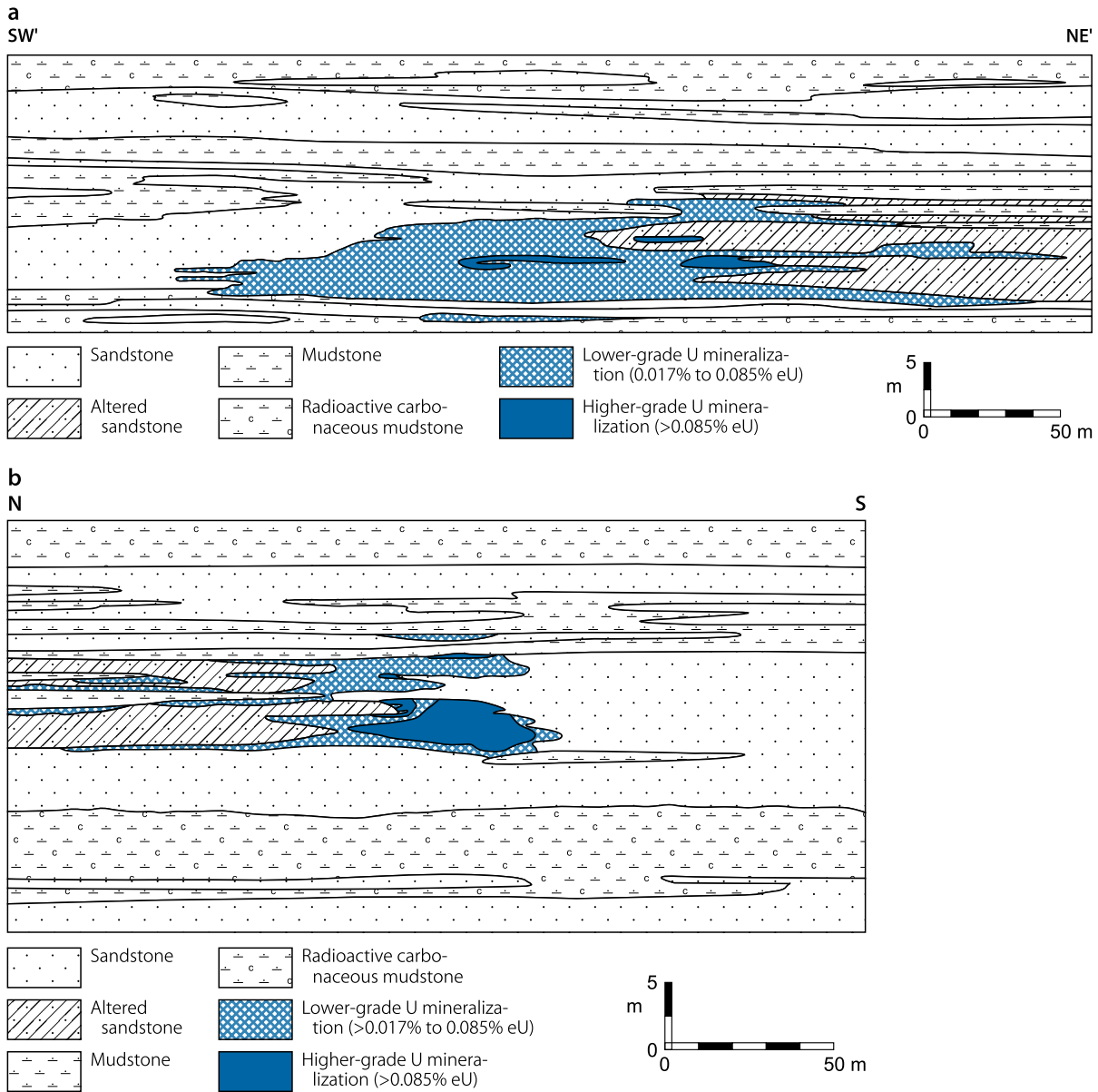
Geology and Mineralization

The Sweetwater deposit is situated along the eastern edge of an altered tongue in the Sweetwater-REB sandstone (►Fig. 2.21a). In this area, the normal reddish-orange hue of altered sandstone gradually changes to tan and then to cream-colored sandstone (►Fig. 2.22) in response to a decrease in the amount of hematite, goethite, and smectite, which coat grains of altered sandstone. This interval of color change can be from several 100–1,000 m in width, in which case ore bodies adjacent to the tongue are wide and low grade. Where the zone of color change extends over distances of only several meters, ore bodies tend to be narrower and of higher grade.

In the Sweetwater Mine area, the host sandstone can be subdivided into four sandy horizons separated by thin lenticular mudstones (►Fig. 2.22). Most ores are associated with the two lower sandstone horizons, which are thickest and laterally most persistent. Mineralization persists for almost 6.5 km along the

Fig. 2.23.

Central Red Desert, ENQ deposit, (a) SW–NE and (b) N–S cross-sections across the eastern and western part of the deposit, respectively, illustrating the grade distribution at the redox front in Wasatch sandstone. [After Sherborne et al. 1980 (reproduced by permission of AIME)]



edge of the redox front and extends outward from it into unaltered sandstone for 300 to as much as 750 m. Thickness of mineralization commonly ranges from 2 to 5 m, but may reach as much as 20 m where several sandy intervals merge to form stacked deposits. Most mineralized sandstone intervals have grades of about 0.04% U or less, with some sections containing 0.1% U or more.

Sweetwater ore is in marked disequilibrium, but with wide ranges in disequilibrium degree. Mineralization above the present groundwater table and when composed of hexavalent U minerals, uranium may be less or greater in amount than

indicated by gamma-ray readings. Ore below the groundwater table, which constitutes the bulk of the uranium endowment, shows a slight enrichment in chemical uranium contents compared to radiometric values.

2.3.2.2 ENQ Deposit

The ENQ deposit lies adjacent to the NW of the Sweetwater deposit. It is hosted in a 20 m thick, coarse-grained, tabular sandstone of the ENQ unit that is over- and underlain by

laterally continuous mudstones (► Figs. 2.21a and b; 2.23). Mineralization is mainly concentrated in the lower part of the sandstone unit where only few mudstone lenses exist. It is higher in grade but narrower in the NW part of the deposit than in the SE part or in the adjacent but deeper positioned Sweetwater deposit. In addition to well-developed roll-type mineralization, there is well-developed mineralization on both the upper and lower limbs of the roll. Widths of mineralized sandstone, including that on the limbs, ranges from about 30 to 480 m. Thicknesses are as much as 9–12 m. A halo of low-grade mineralization, as much as 300-m wide in the southeastern and 6 m in the northwestern part of the deposit, extends outward from higher grade roll-type ore.

2.3.2.3 REB Deposit

This deposit is located about 10 km WSW of the Sweetwater deposit (► Fig. 2.21a and b). Resources are reportedly almost 1,500 t U at a grade averaging about 0.06% U.

Geology and Mineralization

The REB deposit is at the western edge of the altered tongue within the Sweetwater-REB sandstone unit. Mineralization extends for 9 km in N-S length and from less than 15 m up to 300 m outward from the altered sandstone tongue into unaltered sandstone.

The sandstone unit is about 50-m thick and includes five tabular or lenticular sandstone horizons separated by laterally continuous carbonaceous mudstones and poorly sorted siltstones. Sandstone beds are thinner, and mudstones are more carbonaceous and more extensive than similar facies on the eastern margin of the altered tongue near the Sweetwater deposit.

The edge of the altered tongue shows a pattern of zoned iron oxide staining and orange feldspar coloration. The intensity of iron oxides is greatest at several 10–100 m from the tongue's edge and gradually decreases toward the edge. A second alteration zone is closer to the edge. It is characterized by light grey sandstones, almost indistinguishable from unaltered sandstone, and by oxidized, mottled, interbedded siltstone. A third alteration zone, characterized by orange-colored feldspars, is generally less than 100 m from the edge of the tongue. This orange color increases as the edge of the tongue is approached and is most intense near highest grade mineralization.

Most mineralization is in coarse-grained, thick, laterally continuous sandstone beds of units C and D. Mineralized sections in these two units commonly range from 1 to 4.5 m, with maxima of up to 10 m in thickness. Mineralization in the D unit is nearly continuous along the 9 km REB trend, whereas in other units it is less persistent. Mineralized bodies are C-shaped. Their average grade is almost 0.08% U, i.e., twice as much as that in the Sweetwater deposit. A very narrow transition zone intervenes between well-mineralized and barren sandstone.

2.3.3 Northern Red Desert

Several deposits have been identified in the northern portion of the Red Desert, including Lost Soldier to the SE and Lost Creek to the SW of Crooks Gap (► Fig. 2.17).

Source of Information. Wallis 2006 a, b.

Regional Geological Setting of Mineralization

Uranium is hosted in the Early Eocene Battle Spring/Wasatch Formation. This formation is comprised in the northeastern Great Divide Basin by stream and flood plain sediments represented by very coarse-grained, fan-like deposits as well as coarse- to medium-grained, arkosic sandstones interbedded with siltstone, mudstone, and rare thin conglomeratic layers. The strata dip westerly from 1° in the western part to 10° near the erosional edge of the Battle Spring Formation to the east, adjacent to the Lost Soldier anticline.

Metallogenetic Aspects

The original ore-forming processes are thought to have been, in principle, similar to those in other Wyoming Basins. Uranium was leached from the granite provenance area and intraformational arkosic sands by oxidizing solutions that percolated downdip through more permeable portions of paleodrainage conduits until reductants, perhaps associated with slowing of solution movement due to thinning sands and diminishing grain size, caused uranium to be precipitated as probable rollfront-type mineralization on the margin of the paleodrainage system. Subsequent post-depositional uplift and related erosion of much of the Eocene strata has apparently renewed downward percolation of oxygenated groundwater. As a result, uranium was partially leached and redistributed from upper portions of formerly formed mineralization.

Faults, which exist in the Lost Soldier and Lost Creek deposits, are thought to have influenced the redistribution process. These structural elements would have disrupted groundwater flow patterns and acted as conduits for migration of pregnant solutions. Where they encountered adjacent permeable strata with reducing capacity they entered these horizons and uranium was deposited as stacked, tabular-shaped mineralization, which often masks that of original rolls. This mineralization can have good continuity, but is not entirely stratiform for it dissects bed boundaries.

2.3.3.1 Lost Soldier

The Lost Soldier deposit is located near the settlement of Bairoil in the northeast corner of Sweetwater County, some 70 km NW of Rawlins and 12 km SE of the Jackpot deposit. It was discovered in 1969, and consists of rollfront and tabular ore bodies. Cameco published in its "Annual Report 1995" a resource

number of 10,230 t for the Lost Soldier project. A central core area contains reportedly over 8,800 t U.

Geology and Mineralization

According to Wallis (2006b), the stratigraphic [Battle Spring/Wasatch sequence](#) at Lost Soldier comprises thick, coarse- to medium-grained, arkosic sandstones, which constitute $\pm 60\%$ of the section, with interbedded thinner siltstone, mudstone, and rare thin conglomeratic layers. The strata dip westerly from 1° in the western part to 10° in the east, adjacent to the Lost Soldier anticline.

An E-W-trending normal fault (Lost Soldier fault) with a displacement of some 20–25 m, downdropped to the south, cuts the southern part of the deposit. At least two transverse faults with minor displacements branch off from the Lost Soldier fault to the northeast.

Ore bodies are not only of rollfront but also of tabular geometry, and occur sometimes in vertically-stacked position in more than one sand unit.

The Lost Soldier deposit includes a 3.25 km² core area with several mineralised horizons. Using a cutoff grade of 0.025% U, this core area includes an ore zone at depths of less than 150 m, with an area of approximately 0.53 km², has a total mineralized thickness of 3.8 m, averages 0.075% U, and contains ca. 3,100 t U. Additional inferred resources of lower grades occur in close vertical proximity to this ore zone. Further mineralization is drill indicated at greater depth. At least ten additional mineralized trends with ore-grade drill intercepts exit in the core area indicating additional resources. In addition, substantial resources occur at shallow depth along and within 15 m below the groundwater table.

2.3.3.2 Lost Creek

The Lost Creek deposit is located in northern Sweetwater County. The discovery of schroëckingerite along the Lost Creek in 1936 was the earliest discovery of uranium in sandstones in Wyoming. This near-surface ore was mined from 1954 intermittently until 1966. Later exploration found additional ore zones at greater depths as described below. Resources for the *Lost Creek deposit* and adjacent *Conoco "A"* project total as much as 7,000 t U.

Geology and Mineralization

As described by Wallis (2006a), [Wasatch sediments](#) at the Lost Creek include sandstones units as much as 15 m thick. Dip is gently to the west. These sandstones contain plant remains, minor dark accessory minerals, and occasional pyrite. Where altered, the sandstone color is changed from typically grey to buff, tan, or greenish-grey, and carbon trash and accessory minerals are more or less decomposed.

Post-depositional uplift and erosion of the area has eroded much of the Eocene sequence. Both pre- and post-mineral faults

with displacements ranging from minor to ca. 15 m with down-dropping of the southern segment exist in the Lost Creek area. These faults are orientated generally sub-parallel to the east–west mineral trend.

The Lost Creek mineral system is at least 6.5 km long, varies in width between 90 and 360 m, and includes three main mineralized zones. Orientation of these zones is generally east–west with altered ground to the north. Supergene leaching has resulted in some depletion of uranium in the upper zone of the deposit, whereas the middle and lower zones remained in radiometric equilibrium.

Although of low average grade ore thicknesses are relative high, in particular, where superimposed zones of redistributed uranium exist. Resources of an ore zone at Lost Creek located at a depth of about 150 m amount to some 3,000 t U (based on a cutoff grade of 0.02% U). Mineralization in this zone is at least 3 m in thickness and averages ca. 0.04% U. A similar amount of additional resources is drill indicated.

Using a cutoff grade of 0.025% U, combined resources of the Lost Creek deposit and adjacent Conoco "A" project reportedly total as much as 7,000 t U. Average depth is 150–200 m, thickness is 2.70 m, and grade is 0.044% U.

2.4 Bison Basin

This small basin is located in southern Fremont County, between the Wind River Range to the northwest, Crooks Mountain to the northeast, and Great Divide Basin to the south ([Fig. 2.17](#)). Deposits are of rollfront sandstone type. Uranium was produced in the 1960s and 1970s by conventional mining, and in the early 1980s by ISL methods. Remaining in situ resources total about 1,600 t U. Grades average from 0.04 to 0.06% U at a cutoff grade of 0.017% U.

Source of Information. Pool TC, personal communication.

Geology and Mineralization

Bison Basin is a small depression at the southeast end of the Wind River Range. It is separated from the Great Divide Basin by a basement high that extends eastward from the Wind River Range into central Wyoming. Precambrian crystalline rocks form the basement. It is overlain by a thick sequence of sediments ranging in age from Carboniferous, Cretaceous to Tertiary. Two major structural elements, the Wind River thrust, a steeply dipping regional fault, and the Bison Basin fault, a smaller thrust fault, occur at the south and north sides, respectively, of the basin.

Uranium is hosted in Eocene arkosic sediments, primarily sandstones of the [Wasatch Formation](#). Deposits are located along the flanks and bottom of the Cyclone Rim syncline, and are controlled by boundary faults at the margins of the syncline. Mineralized zones occur at depths from 45 to 195 m, primarily at 105–120 m below surface. A 6.5 km long mineralized trend, as much as 60 m in width, with grades in excess of 0.017% U

(cutoff grade) was delineated by drilling. In addition, several mineralized horizons were discovered.

2.5 Powder River Basin

The Powder River Basin in northeastern Wyoming is a NNW–SSE-elongated basin open to the north and bounded by the Laramie Mountains on the south, the Hartville Uplift on the southeast, the Black Hills on the east, and the Bighorn Mountains and Casper Arch on the west (▶ Fig. 2.1). The Powder River Basin contains uranium mineralization particularly in its central and southern portions as shown on ▶ Fig. 2.24.

Original resources (in situ and mined) of the Powder River Basin are estimated to be in excess of 100,000 t U. Conventional production is estimated to have been on the order of 15,000 t U while ISL production has been about 12,000 t U.

In total, approximately 130 mostly small operations have recorded production from the Powder River Basin since mining began in 1953. Most of the early mines were small working near-surface ore bodies with reserves each between a few tonnes and 1,000 t, rarely 10,000 t of ore, and grades between 0.15 and 0.4% U.

Conventional uranium mining was pursued in the early days in the *Pumpkin Buttes* and *Turnercrest districts*, and later in the *Highland Flats* and *Box Creek districts* (Highland, Bill Smith, Box Creek, etc., mines), and the *Monument Hill district* (Bear Creek mine).

In situ leach (or in situ recovery/ISR) operations or test projects were pursued at Brown Ranch, Charlie, Christensen Ranch, Collins Draw, Greasewood, Irigaray, North Butte, Reno Creek, Rolling Pin, Ruby Ranch, and Ruth in the *Central Powder River Basin* (Pumpkin Buttes and adjacent areas). ISL operations in the *southern Powder River Basin* were conducted in the Highland Flats district and on Smith Ranch. Highland was mined by open pit from 1972 to 1984; ISL commenced in 1988. The only active well fields in 2008 were on Smith Ranch.

Sources of Information. Childers 1970, 1974; Curry 1976; Dahl and Hagmaier 1976; Davis 1969; Grutt 1972; Harshman and Adams 1981; Langen and Kidwell 1974; Mrak 1968; Noyes 1978; Rubin 1970; Santos 1981; Sharp and Gibbons 1964; Sharp et al. 1964; Stout and Stover 1997; and Harshman EN, personal communication.

Regional Geological Setting of Mineralization

The Powder River Basin is an asymmetrical depression with its axis closely paralleling the western basin margin. The asymmetrical shape is the result of a westward shift of the structural axis, i.e., the line of greatest sediment accumulation, during sedimentary deposition. Tertiary strata dip gently to the west at 0.5 to 3° on the eastern flank of the basin, and on the western flank more steeply, 0.5 to 20° to the east with the dip increasing toward the western basin margin.

Tertiary sedimentation began with downwarping of the Powder River Basin associated with uplift of the peripheral

highlands in Laramide time, which initiated transgression of the early Paleocene *Fort Union Formation* over the Cretaceous marine Lance Formation. The lower Fort Union Formation consists mainly of second cycle, fine-grained clays, silts, and muds that derived mostly from Cretaceous rocks and were deposited by sluggish meandering streams flowing northward through the basin. In late Paleocene or early Eocene time, arkosic debris from the ancient Laramie and Granite mountains began to enter the basin by streams flowing toward the topographic axis of the basin then northward through its open end. The axially trending bed-load to mixed-load fluvial system deposited parts of the *upper Fort Union* and the *Wasatch formations* as well (◉ Fig. 2.2b). This bed/mixed load facies grades laterally and downslope into fine-grained, mixed-load, and suspended-load channel sediments. In addition to channel facies, there are flood plain silts containing small tributary channel sands and silts as well as mud and lignite of swampy lacustrine origin. Vegetal organic matter is often plentiful.

The Wasatch Formation is overlain locally by the tuffaceous Oligocene *White River Formation*, which is from 60 to 75 m thick. Large portions of the White River Formation, however, and all younger sediments of Miocene and Pliocene time are almost totally eroded.

Arenites of the upper Fort Union and the Wasatch Formations are *principal host rocks* for uranium mineralization. *Upper Fort Union arenites* crop out at the margins of the basin and reach a maximum thickness of about 900 m in the southern Powder River Basin. These arenites consist of fluvial, poorly sorted, coarse-grained, arkosic sandstones that form lenticular and wedge-shaped bodies, which interfinger laterally and are embedded with fine-grained facies. It is extremely difficult to correlate individual sandstone units with each other laterally because of their swiftly changing character in a range of 10–100 m.

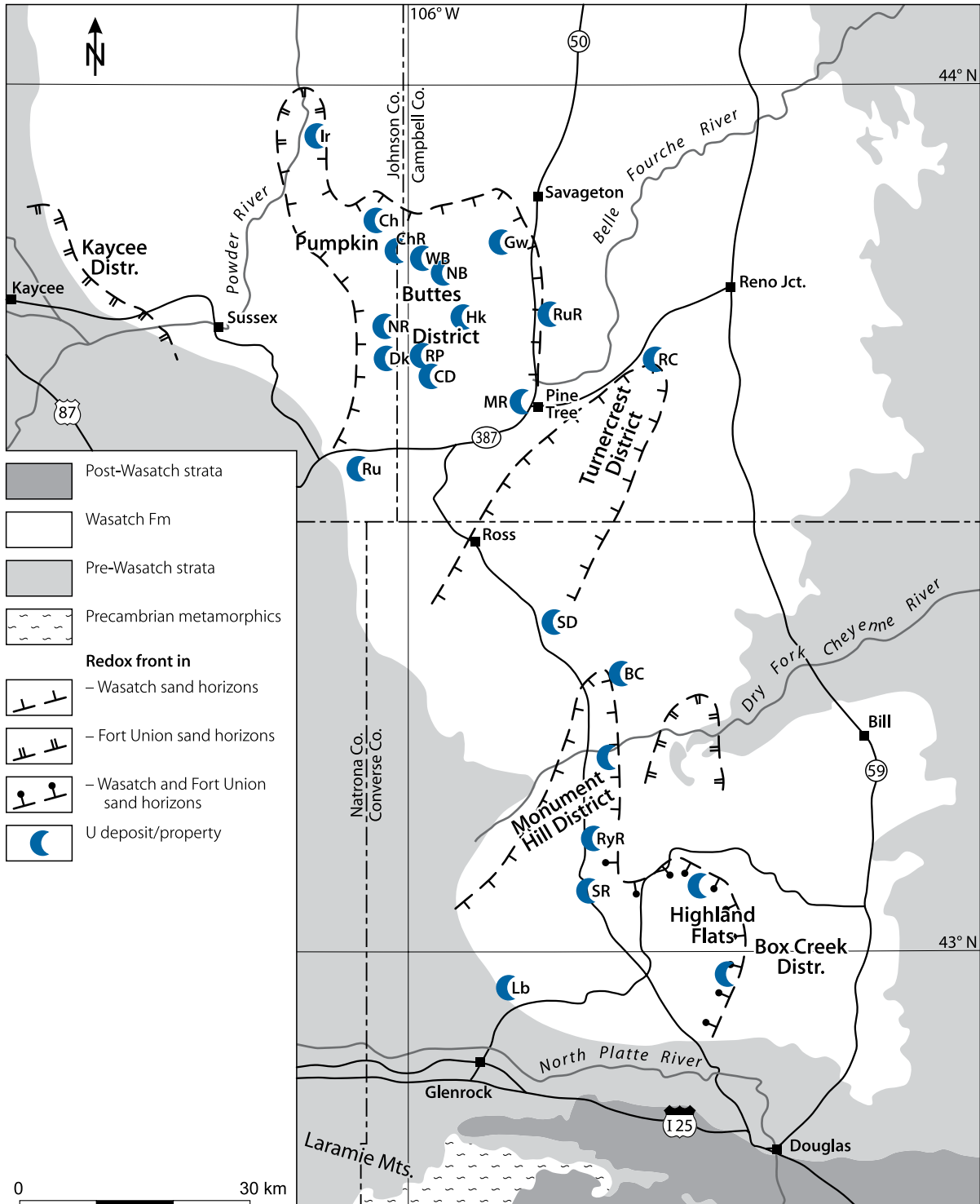
The *Wasatch Formation* ranges in thickness from 300 to 500 m thickening from south to north. It comprises thick lenses of coarse- to fine-grained arkose-sandstone interbedded with siltstone, coaly shale, lignite and, locally, thin conglomeratic beds. Siltstones and shales are semi-consolidated, whereas sandstones are brittle and friable. Coarse-grained facies are rather consistent in their areal extent. Individual sandstone units of the Wasatch Formation range from a few meters to 60 m in thickness and can be traced over distances from 1 km to almost 50 km and over widths from less than 100 m to several kilometers. Sandstone horizons are separated by claystones or siltstones, 30–60-m thick, although most principal sand units are interconnected.

Principal Host Rock Alteration

Alteration along redox fronts in the Fort Union and the Wasatch formations within the Powder River Basin differs from that of the Shirley Basin and the Gas Hills both in color and complexity. Altered tongues in the Powder River Basin are characterized by three distinctive colors that contrast sharply with the light grey of unmineralized sandstone. The main body of an altered tongue

Fig. 2.24.

Powder River Basin, generalized trends of redox fronts in Eocene Wasatch and Paleocene Fort Union formations, and location of uranium districts and selected deposits/properties (historical mine sites not shown; see Fig. 2.2b for regional paleoflow patterns and facies distribution of the upper Fort Union-lower Wasatch(?) fluvial systems). (Geology after Grutt 1972, redox fronts after Bailey and Childers 1977; and Boberg 1981) (*Uranium deposits/properties*: BC Bear Creek, CD Collins Draw, Ch Charlie, ChR Christensen Ranch, Dk Doughstick, Gw Greasewood, Hk Hank, Ir Irigaray, Lb Leuenberger, MR Moore Ranch, NB North Butte (Brown Ranch), NR Nichols Ranch, RC Reno Creek, RP Rolling Pin, Ru Ruth, RuR Ruby Ranch, RyR Reynolds Ranch, SD Sand Draw, SR Smith Ranch, WB West North Butte)



is red, due to hematite staining on sand grains. A zone of yellow, goethite-bearing sandstone lies between the red altered sandstone and ore. In some places, a zone of white-bleached sandstone is present between the goethite-bearing zone and ore (Fig. 2.3b).

The alteration process has increased the content of uranium, selenium, ferric iron, and perhaps chromium in sandstone, and decreased the content of carbonate, organic carbon, manganese, and sulfide sulfur. The total iron content of sandstone, however, has apparently not been substantially changed by alteration. Some detrital minerals such as pyroxene, hornblende, and biotite have been destroyed by the alteration process.

Altered sandstone tongues occur in an area about 130 km long and 8–30 km wide. The exceptional length of some of the altered sandstone tongues is due to the continuity of permeable sands in which an individual horizon can be traced along the basin axis for many kilometers.

Principal Characteristics of Mineralization

Pitchblende/sooty pitchblende and coffinite are the principal U minerals in unoxidized zones while uranyl vanadates (tyuyamunite, carnotite, a.o.) dominate near-surface oxidized zones. Associated elements and minerals include pyrite-marcasite, native selenium, calcite, occasionally some hematite, and some chromium in protore. Ore minerals fill open spaces in sandstone, coat sand grains, and fill cracks in, but also replace parts of sand grains.

High pyrite contents normally correlate well with high-uranium grades. In contrast, there appears to be no quantitative relation between organic matter and uranium. Carbonate correlates with uranium (1% CO_3^{2+} and more in front of, less than 0.1% CO_3^{2+} behind the front). The uranium–vanadium ratio ranges in an ore roll between 3 and 10 to 1, and is 1:1 in oxidized mineralization. U/eq.U ratios are generally slightly more than 1 for samples containing more than 0.1% U and generally slightly less than 1% for samples with less than 0.1% U.

More than 90% of U resources occur in the Tertiary Fort Union and Wasatch formations and therein principally in sandstone units with thicknesses between 30 and 40 m, rarely in thicker or thinner beds. Some minor U occurrences exist in the Cretaceous Lance Formation.

All Tertiary uranium deposits occur in fluvial, medium- to coarse-grained arkosic sandstones extending vertically over a stratigraphic thickness of 350–420 m. They are hosted in the

- *Box Creek-Highland Flats* district, in the southern Powder River Basin, in the uppermost Fort Union Formation or lowest Wasatch Formation
- *Monument Hill* district, adjacent to the north of Highland Flats, in the lower Wasatch Formation
- *Turnercreek* district, approximately 250 m stratigraphically higher than mineralization at Monument Hill
- *Pumpkin Buttes* district: mainly in the lower Wasatch Formation

- *Irigaray* area, to the west of Pumpkin Buttes, in the Fort Union Formation.

It may be worthwhile to mention that all lignites, although a predestined uranium collector, are practically barren of uranium. This suggests apparently that no uranium was available during the time of sedimentation of lignite precursor matter.

General Shape and Dimension of Deposits

Deposits in the Powder River Basin belong to the rollfront sandstone-type of uranium deposits, and as such they are similar in most aspects to those in other Wyoming Basins. Ore bodies are positioned at the edges and to a lesser extent on the top and bottom surfaces of two or more composite tongues of altered sandstone several times larger than those in other basins. They are roughly crescentic in cross section, but with many irregularities due to the complex lithology, resulting in multiple small rolls often in step-like order, one above the other (Fig. 2.25).

The concave side of a roll, i.e., the rear contact with altered sandstone, is generally sharp while the leading edge of the roll progressively contains less and less uranium and finally fades into unaltered unmineralized sandstone. Some Powder River deposits differ from those in other basins in that they have a relatively wide zone of low-grade mineralized sandstone (0.01–0.1% U) between higher grade ore and unmineralized unaltered sandstone (e.g. see later Fig. 2.32). This transition zone, which is generally less than 10 m in other districts, can be up to 100 m and more wide and 3–12 m thick in the Powder River Basin. The width of this zone appears to be inversely related to the width and grade of the higher grade ore it adjoins.

The edge of an altered sandstone tongue is commonly mineralized, but is not necessarily ore bearing. Ore bodies may persist laterally for several 100–1,000 m along the edge of an altered tongue and may be between 0.1 and 6 m thick but in general, they tend toward the smaller size. Trailing ends of a roll extend up to 100 m and more behind the leading edge. Locally, small tabular ore lenses can occur behind the rollfront in altered sandstone. They are always associated with vegetal-coaly material.

Principal Ore Controls and Metallogenetic Aspects

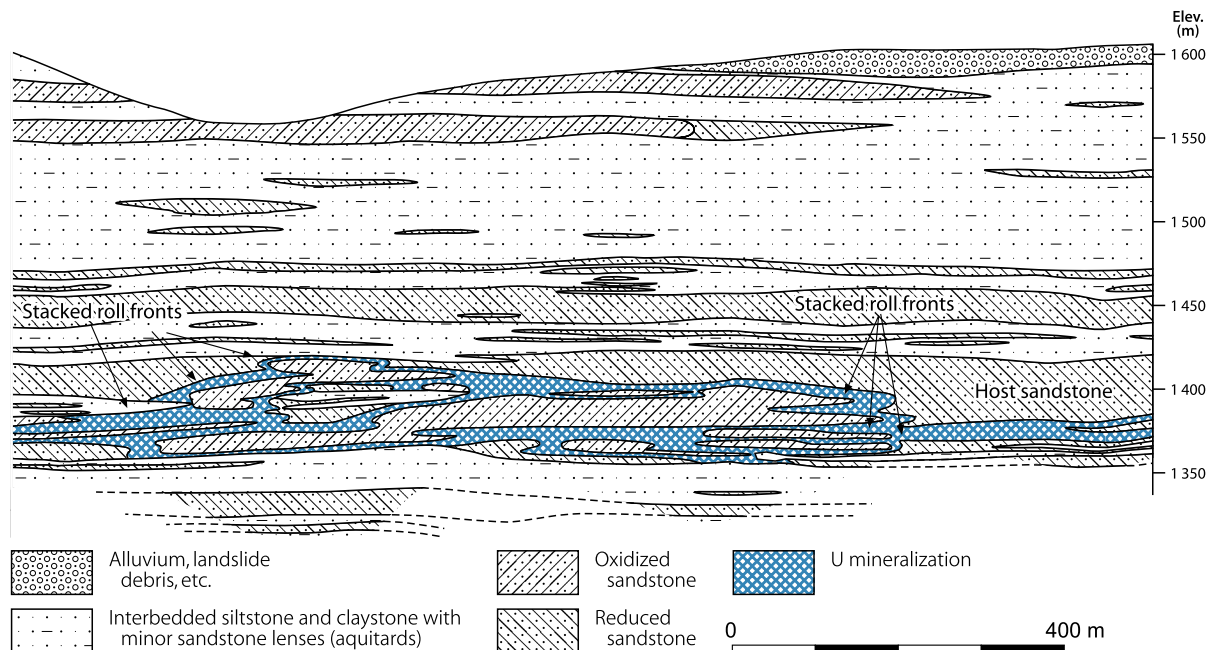
Although uranium deposits in the Powder River Basin show, in principle, the same ore controls and/or recognition criteria as deposits in other Wyoming Basins, there are some differences. The variable basement topography, which in part controls the position of redox fronts and as such the location of the ore bodies in the Shirley Basin and the Gas Hills districts, is absent in the Powder River Basin.

The position of the Powder River altered tongues is governed by

- (a) highly transmissive channel sands deposited by the principal streams flowing into the basin from the south and west and then northward along the axis of the basin;

Fig. 2.25.

Central Powder River Basin, Pumpkin Buttes district, diagrammatic section perpendicular to the migration direction of mineralizing solutions illustrating the complex nature of stacked rollfronts. (After Uranerz Energy Corporation 2008)



(b) decrease in permeability of stream channel sediments toward overbank, flood plain, and suspended-load facies; and

(c) predominance of lacustrine, fine-grained, suspended-load meander belt, and paludal sediments toward the north of the basin, which restricted deposits to the central and southern Powder River Basin.

In general, the position of redox fronts appears to be controlled by the 340–420 μm size fraction of sediments, at least at the Bear Creek Mine (Davis 1969).

In the Powder River Basin, rocks at rollfronts are generally limonite-bearing and age datings on ore of the Highland Mine yielded a range of ages of less than 3 Ma (Santos and Ludwig 1983). Both features can be interpreted as indicating either that the deposits formed in response to the latest post-Miocene influx of oxygenated water, or that former deposits have experienced post-Miocene to Recent remobilization within original older ore.

2.5.1 Selected Deposits/Properties in the Central Powder River Basin

Deposits are clustered in the *Pumpkin Buttes district* and adjacent areas. After the discovery of uranium in the Pumpkin Buttes in 1951, intermittent exploitation from 1952 to 1967 by some 55 open-pit mines produced some 80 t U from shallow, oxidized ore (Breckenridge et al. 1974). Since the late 1970s, exploitation applying ISL techniques has focused on deeper, reduced ore in the Eocene Wasatch Formation as at Christensen Ranch, Irigaray, Ruth, and other sites.

2.5.1.1 Christensen Ranch, Pumpkin Buttes District

The Christensen Ranch area is located at the boundary line between Johnson and Campbell counties at the northwestern margin of the Pumpkin Buttes district, approximately 170 km NE of the town of Casper. Original in situ resources (remaining and mined) amounted to over 5,500 t U at an average grade of 0.08% U. A total of 1,730 t U was produced by ISL techniques on a test scale from 1977 to 1981, and on a commercial scale from 1989 to 2001 when production ceased for economic reasons.

Source of Information: Rowson 2002.

Geology and Mineralization

Ore bodies are mainly hosted in the K horizon, up to 90 m in thickness, within the lower portion of the Eocene *Wasatch Formation* (Fig. 2.26b). Mudstone beds with interbedded lignite seams overlie and underlie the K horizon. Dip of strata is 1–2° NW.

Host rocks are fine- to coarse-grained, locally carbonaceous and pyritic, fluvial arkosic sands, with intercalated mudstone and siltstone stringers. Host sands are pink colored on the altered updip side of rollfronts and grey on the unaltered, downdip side. The entire K horizon is a hydrologically interconnected, water-saturated, confined aquifer with artesian conditions.

Ore bodies are of roll-shape and related to, in general, NW–SE-oriented redox fronts along which they occur where these fronts make a series of abrupt changes in strike. Depth to ore ranges from 90 to 180 m. The depth difference is essentially due to surface topography.

2.5.1.2 Nichols Ranch and Hank, Pumpkin Buttes District

The *Nichols Ranch* deposit straddles the Johnson and Campbell County line in the western Pumpkin Buttes district, some 10 km south of the Christensen Ranch ISL plant. In situ resources total 1,135 t U at 0.097% eq U. The *Hank* deposit, located about 10 km ENE of the Nichols Ranch deposit, contains in situ resources of 955 t U at ca. 0.1% eq U.

Sources of Information. Graves and Woody 2008; Brown K and Catchpole G 2008, 2009, personal communication.

Geology and Mineralization

The mineralized stratigraphic section of the Nichols Ranch and Hank deposits is characterized by the following features. The uranium-bearing Eocene *Wasatch Formation* is approximately 470 m thick in the western Pumpkin Buttes area. Sandstone-type uranium mineralization is hosted in the lower section of this formation. Up to seven sand horizons dipping from flat to 3° NE are identified in this section. They range in thickness from a few meters to some 50 m, but may also pinch out. Sandy mudstone/siltstone intercalations split sands locally into two or more sub-horizons (Fig. 2.26c).

Four prominent sand horizons (besides less pronounced sand layers), denoted – from bottom to top – as 1 (one), A, B, and F, are identified in the Nichols Ranch area, and six distinct sand units, A, B, C, F, G, and H, in the Hank area. Intervening non- or less-permeable horizons range in thickness from few meters to 45 m in the Nichols Ranch area, and up to 33 m in the Hank area. These aquicludes or aquitards are composed of mudstone or shale, silty shale, and shaly (poor) lignite horizons.

Arkosic sands of the A horizon are the principal uranium ore-bearing hosts in the Nichols Ranch area, and of the F horizon in the Hank area. Both sand horizons are bounded above and below by aquitards. The A and F sands are weakly to moderately cemented and friable. Grain sizes range from very fine- to coarse-grained and pebble. Sand constituents include quartz, feldspar, accessory biotite and muscovite, and trace amounts of carbonaceous debris. Pyrite and calcite occur in grey, reduced facies. Hematite or limonite staining is typical in oxidized facies as well as montmorillonite and kaolinite as alteration products of feldspars.

At Nichols Ranch the *A sand horizon* is 15–33 m thick and occurs at depths from 60 to 215 m. Mudstone and siltstone lenses, up to 4.5 m in thickness, 60–100 m N–S length, and 15–30 m in width, occasionally split the A sand horizon. An

aquitard consisting of grey mudstones and thin discontinuous light grey siltstones rests upon the A sand. This horizon is from 7 to 27 m thick, thickening to the northwest and thinning to the southeast. In the Hank area, this unit is composed mainly of mudstones, at least 25 m thick, and located at a depth of some 220 m.

The overlying, widespread *B sand horizon* ranges in thickness from 25 to 50 m. Elsewhere in the Pumpkin Buttes area it contains some large ore bodies including those at Christensen Ranch and North Butte.

The *C sand*, nil to 6 m thick, with underlying and overlying aquitards, 9–45 m thick, separates the B sand from the higher F sand horizon. The latter in the Pumpkin Buttes area is host to numerous uranium occurrences including ore bodies at Hank.

At Hank, the *F sand horizon* is from <20 to 25 m thick and composed of fine- to coarse-grained sand. U mineralization occurs in two stacked rollfronts, which may overlap or be separated laterally by 100 m or more. On Nichols Ranch, the F sand horizon is from zero to 6 m thick and contains discontinuous ore. The F sand is overlain by grey mudstones, 6–23 m thick, and rests upon an aquitard, 9–33 m thick, composed of grey mudstones, siltstones, dark grey carbonaceous shales, and poorly developed coal.

In both deposits, Nichols Ranch and Hank, uranium is present as amorphous uranium oxide, sooty pitchblende, and coffinite that coat sand grains and impregnate authigenic clay in voids. These U minerals form typical roll ore bodies controlled by redox fronts. At *Nichols Ranch*, uranium ore forms two wings or fronts, an eastern and western that join at a point to the north, termed the nose. Sandstone in between the wings and nose is oxidized and the exterior is reduced. At *Hank*, reduced sandstone facies lie to the east and oxidized facies to the west.

Due to the complex nature of fluvial sand deposition in the Wasatch Formation, uranium ore-bearing sandstone horizons at both, Nichols Ranch and Hank, contain at least two vertically stacked subsidiary rollfronts (Fig. 2.25), designated upper and lower fronts. Stacked rollfronts tend to result from small differences in sandstone permeability or the occasional vertical contact between sand members. The lateral distance between stacked rolls ranges from nil to over 60 m and may result in complex overlapping patterns. More specifically, approximate dimensions (rounded) of uranium mineralization are:

Nichols Ranch

Mineralized intervals range in grade from 0.017 eq.% U (cutoff grade) to 0.633 eq.% U, from 0.3 to 5.5 m in thickness, and from 15 to over 120 m, average 35 m, in width of rolls. Additional ore parameters of the three mineralized fronts are:

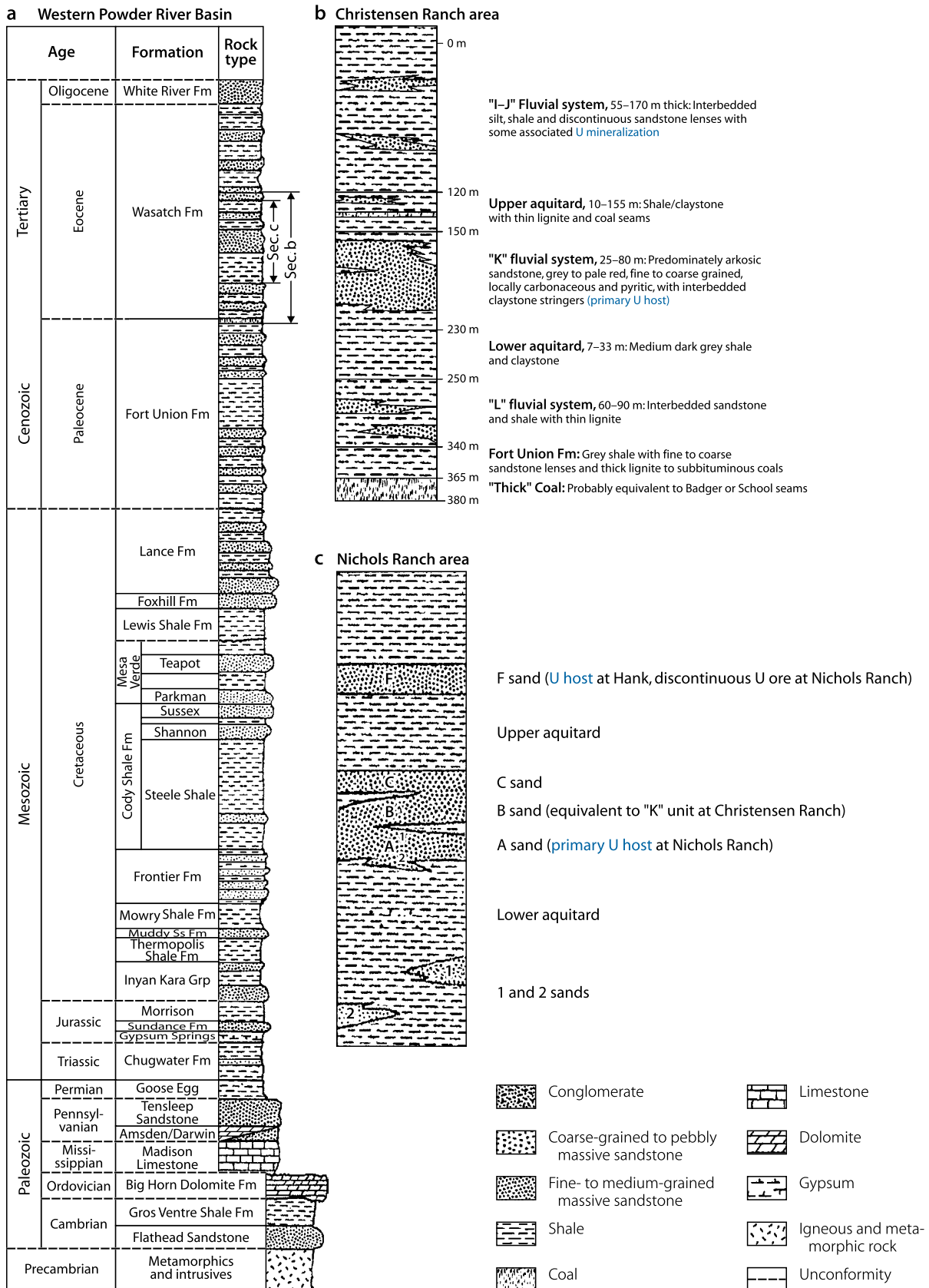
A sand lower front (or A1): Thickness <4.5 m, depth 125–215 m, av. 165 m, length 4,300 m

A sand upper front (or A2): Thickness <2.7 m, depth 130–200 m, av. 160 m, length 2,380 m

F sand horizon: Thickness nil to 6 m; depth <90 m, av. 75 m, discontinuous ore along a redox front >930 m in length

Fig. 2.26.

Central Powder River Basin, litho-stratigraphic column (a) of the western portion of the basin and (b) enlarged intervals of the U mineralized lower Wasatch Formation in the Christensen Ranch, and (c) Nichols Ranch areas. (After (a) Sharp et al. 1964; Uranerz Energy Corporation 2008; (b) Rowson 2002; (c) Uranerz Energy Corporation 2008)



On the basis of a grade times thickness ($G \times T$) cutoff factor of 0.20 (% U_3O_8 times feet), indicated in situ resources contained in the A1 and A2 sands total 860 t U at 0.092 eq.% U. Approximately two thirds of this quantity occur in the lower front (A1). Inferred in situ resources of 110 t U at 0.093 eq.% U are estimated for the F sand horizon (Beahm and Anderson 2007).

Hank F sand horizon

The F sand horizon at the Hank property includes the upper, middle, and lower sub-rollfronts. Mineralized intervals range in grade from 0.0025 to 0.321 eq.% U. Using a 0.2 GT cutoff (% U_3O_8 times feet), the trend width ranges from about 21 to 90 m, with an average frontal width of about 25 m. Mineralized thicknesses vary between 1 and 5.5 m, with an average thickness based on a cutoff grade of 0.017 eq.% U of 2.3 m. Mineralization occurs at a depth of 90–135 m, and persists along a length of 2,550 m. Measured and indicated in situ resources are estimated at 860 t U at 0.104 eq.% U, and inferred resources at 95 t U at 0.077% U (Graves and Woody 2008).

2.5.1.3 Additional Deposits/Properties in the Central Powder River Basin

Collins Draw, Pumpkin Buttes: ISL test 1980–1982 producing ca. 6 t U. In situ resources, measured plus indicated 220 t U at 0.075% U, inferred 320 t U at 0.076% U (Beahm and Anderson 2007).

Doughstick, Pumpkin Buttes: In situ resources measured and indicated 45 t U, at 0.057% U, inferred 400 t U at 0.057% U (Beahm and Anderson 2007).

North Rolling Pin, Pumpkin Buttes: ISL test in 1975; in situ resources, measured plus indicated 250 t U at 0.045% U, inferred 120 t U at 0.043% U (Beahm and Anderson 2007).

West North Butte, Pumpkin Buttes: In situ resources indicated 880 t U at 0.126% U, inferred 1,160 t U at 0.126% U (Beahm and Anderson 2007).

Irigaray, located NNW of Pumpkin Buttes: Partially exploited by ISL 1988–1990 producing 120 t U; reserves amount reportedly to 2,600 t U, 0.11% U.

Reno Creek, located SE of Pumpkin Buttes: ISL tested in early 1980s; in situ resources 4,700 t U at 0.047% U, hosted in Wasatch Fm. at depths of 30–120 m (Rocky Mountain Energy staff 1978 Personal Information)

Cameco (2007 Annual Information Form, pp 46–47) reports the following remaining reserves and resources for its properties in the central Powder River Basin (status December 31, 2007):

Brown Ranch/North Butte, Pumpkin Buttes district: proven and probable reserves: 3,269 t U, 0.085% U; additional measured and indicated resources: 3,154 t U, 0.059% U

Ruby Ranch, located E of Pumpkin Buttes district: proven and probable reserves: 2,115 t U, 0.076% U; additional measured and indicated resources: 269 t U, 0.10% U;

Ruth, located W of Pumpkin Buttes district: proven and probable reserves: 654 t U, 0.076% U; additional measured and indicated resources: 154 t U, 0.059% U (Note: Ruth produced 123 t U from 1982 through 1984 by an ISL pilot plant).

2.5.2 Selected Deposits/Properties in the Southern Powder River Basin

Deposits occur in the *Monument Hill* and *Highland Flats-Box Creek districts* and adjacent areas, and are hosted in the Eocene Wasatch and Fort Union formations (▶ Figs. 2.24 and 2.27). Deposits are of rollfront type and are characterized by uranium distribution and alteration features as illustrated in ▶ Fig. 2.28.

After the discovery of uranium in the *Monument Hills* in 1952, intermittent exploitation from mid-1950s to early 1980s was mainly by open-pit mines. Commercial exploitation by ISL techniques began in 1988 at Highland and, in 1997, on Smith Ranch.

2.5.2.1 Highland Mine, Highland Flats District

The Highland mine area lies some 25 km NE of the town of Glenrock and approximately 100 km ENE of Casper near the south end of the Powder River Basin (▶ Fig. 2.24). Original resources (in situ and mined) contained in a number of ore bodies (▶ Fig. 2.29) were on the order of 15,000–16,000 t U at grades between 0.07 and 0.13% U. Cameco (2007 Annual Information Form, pp 46–47) reports for its Highland property remaining proven and probable reserves of 961 t U at a grade of 0.10% U, and additional measured and indicated resources of 692 t U at a grade of 0.085% U (status December 31, 2007).

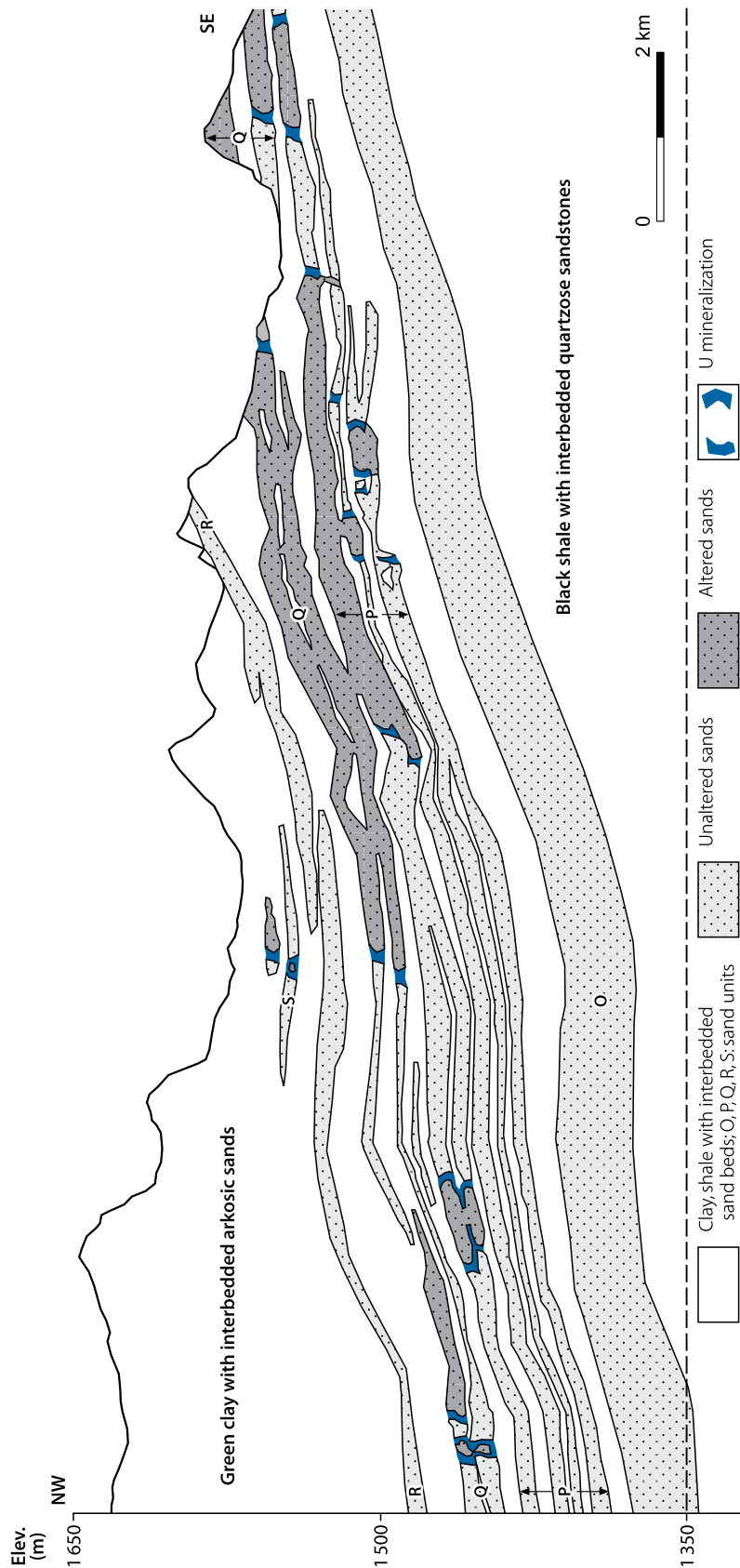
Former production came from several open pits, 60–180 m deep with an ore to overburden ratio of 1:75, producing from 1972 through 1984 some 9,000 t U. Minor production (ca. 700 t U) came from the Buffalo underground mine 195 m deep. ISL operations began 1988 and terminated in 2002 producing about 5,300 t U (Stover D and Pool TC, personal communication).

Sources of Information. Dahl and Hagmaier 1974; Langen and Kidwell 1974; and Stover D, personal communication.

Geology and Mineralization

Uranium is hosted in crossbedded, immature, poorly sorted, friable arkosic sandstones of the upper **Fort Union Formation**. Host rocks contain considerable amounts of coaly material and have good permeability. Rock constituents derived in part from

Fig. 2.27. Southern Powder River Basin, NW-SE section with distribution of altered sands and associated mineralized fronts in the Eocene Wasatch and Paleocene Fort Union formations. (After Rubin 1970)



a granitic terrane to the southwest of the basin, probably from the Laramie Range, and in part from the Hartville Uplift. The deposit is located almost directly on the basin axis where strata dip less than 1° NNW.

Roll-type ore bodies occur in three superjacent sandstone units, each 5–10 m thick, separated by 3–7 m thick beds of siltstone, mudstone, and lignite (Fig. 2.30). This sequence is 33 m thick in the south and thickens to 54 m in the north portion of the deposit. Its upper rim lies 60–180 m under a hilly surface. Ore bodies range from 20 to 200 m in width within each of the sandstone units.

Mineralization can be traced along the redox front for several kilometers but does not achieve ore-grade quality continuously (Fig. 2.29). Ore bodies are positioned

(a) At the eastern edge of two tongue-like easterly embayments considered to be meander bends

(b) At outer margins of host sandstones within bends where these transgress laterally into more pelitic sediments, coaly mudstones, and lignites and

(c) Aligned subparallel to the wedge-out boundary of each of the three sandstone horizons

Host sandstones are colored red by hematite on the concave side of rolls, turn yellowish-brown by limonite within the ore zone, and are grey and pyrite-bearing in front of the convex side of rolls. Coffinite is the principal U mineral; pitchblende/sooty pitchblende is present in lesser amounts. These minerals coat sand grains in thin, sooty, or earthy layers or form minute spherulitic or botryoidal concretions with diameters of less than 10 µm. Some ore is cemented by calcite.

2.5.2.2 Smith Ranch, Southern Monument Hill District

Discovered in the 1960s, the Smith Ranch deposit is located about 20 km NE of the town of Glenrock and ca. 15 km W of the Highland mine (Fig. 2.24). Original reserves amounted to 16,700 t U at grades averaging 0.084% U. Additional resources are estimated at 9,500 t U at an average grade of 0.09% U (Stout and Stover 1997).

Cameco (2007 Annual Information Form, pp 46–47) reports for its Smith Ranch property remaining proven and probable reserves of 3,654 t U at a grade of 0.10% U, and additional measured and indicated resources of 1,961 t U at a grade of 0.076% U (status December 31, 2007).

Exploitation of this deposit was originally attempted by an underground mine, 260 m deep, in 1977–1978 (known as *Bill Smith Mine* or *Shaft*). But due to bad ground, this technique was abandoned. ISL methods were tested in the period 1981–1991 in the Q sand (152 m deep in average) and subsequently in the O sand (229 m deep) producing a total of 132 t U (Stout and Stover 1997). Commercial operations by ISL techniques began in 1997 and produced through 2002 ca. 2,100 t U (Stover D, personal communication). Production has continued from 2002 through present, but production figures have since then been combined with output from Highland. Combined output 2003–2007 has been 3,200 t U.

Sources of Information. Stout and Stover 1997; Stover D, personal communication.

Geology and Mineralization

The Eocene *Wasatch Formation* is the uppermost Tertiary unit in the Smith Ranch area. It is from 60 to 90 m thick in the northern and southern portions, and as much as 150 m in the central area, and contains uranium mineralization in the basal E sandstone bed. A lignite seam (School Coal Seam) occurs at its base.

The underlying Paleocene *Fort Union Formation*, over 300 m in thickness, hosts uranium mineralization in arkosic sandstone horizons in the upper 215 m, which is the stratigraphic equivalent of the upper Fort Union sequence of the Highland deposit. Seven major sandstone horizons separated by mudstone/shale beds are identified in this section, arbitrarily named – from top to bottom – W, U, S, Q, O, M, and K. Uranium resources are primarily contained in the lower O, M, and K horizons. These horizons range from 3 to 60 m in thickness with the O horizon the thickest and most persistent.

Uranium ore bodies are typically crescent-shaped with the downdip side facing north. Depending upon the thickness, intercalated mudstone, and high-lime intervals, between one and 20 mineralized fronts may be present.

2.5.2.3 Bear Creek Mine, NE of Monument Hill District

Discovered in 1967, the Bear Creek mine is situated 110 km NE of Casper (Fig. 2.24) and was exploited by open pits 44–114 m deep. The ore to overburden ratio range was 25:1. Original resources (in-situ and mined) contained in seven ore bodies within a triangular area with side length of 6–8 km amounted to some 5,000 t U at a grade of about 0.12% U.

Sources of Information. Davis 1969; Hansink 1976; and Davis JF, personal communication.

Geology and Mineralization

Ore bodies occur in three stratigraphically superjacent sandstone horizons 200–240 m above the base of and within the 300 m thick *Wasatch Formation*. The stratigraphic thickness of the ore-bearing unit is 20–40 m (Fig. 2.31). The three sandstone horizons are in most places separated by siltstone and mudstone layers, but unify locally to become one sandstone unit up to 20 m in thickness.

The ore-bearing sequence is overlain by mud-, silt-, and sandstones, which interchange quickly by interfingering. Clay constitutes 60–90% of this sequence. The thickness of cover rocks increases from north to south from 30 to 90 m due to topographic relief.

Rollfront-type mineralization is bound to a redox front that follows the change from coarse- to fine-grained sandstone.

Fig. 2.28.

Southern Powder River Basin, distribution and radiometric values of U mineralization, color variations, and alteration features across a roll-type deposit. (After Rubin 1970)

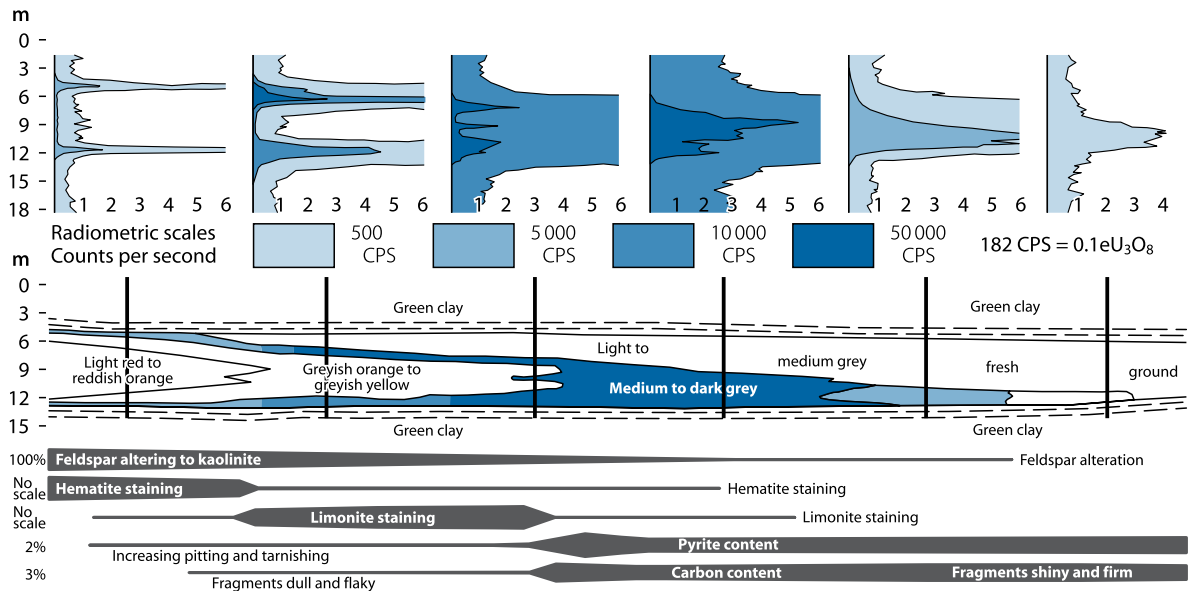
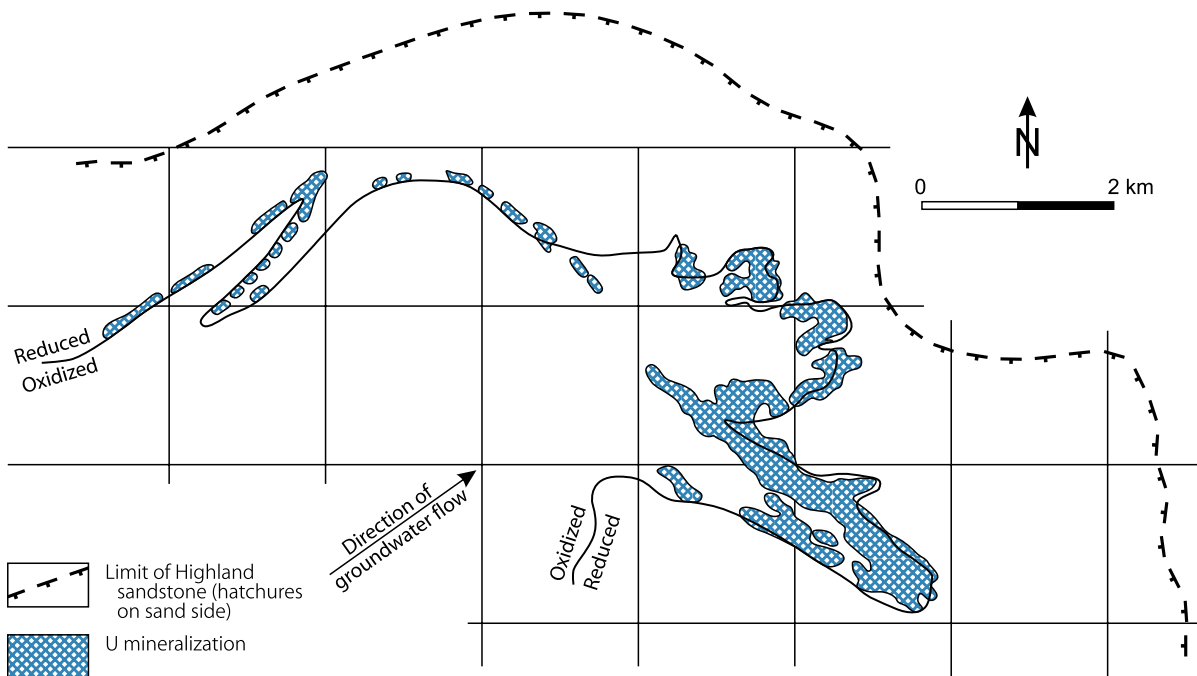


Fig. 2.29.

Southern Powder River Basin, Highland Flats-Box Creek district, Highland mine area, generalized map of distribution and relationship of the Highland sandstone unit of the Fort Union Formation, redox front, groundwater flow direction, and position of uranium mineralization. (After Dahl and Hagmaier 1974)



Altered sandstone is colored red by hematite. Along the redox boundary, hematite grades into limonite. Chemical changes associated with the redox front are shown in Fig. 2.32.

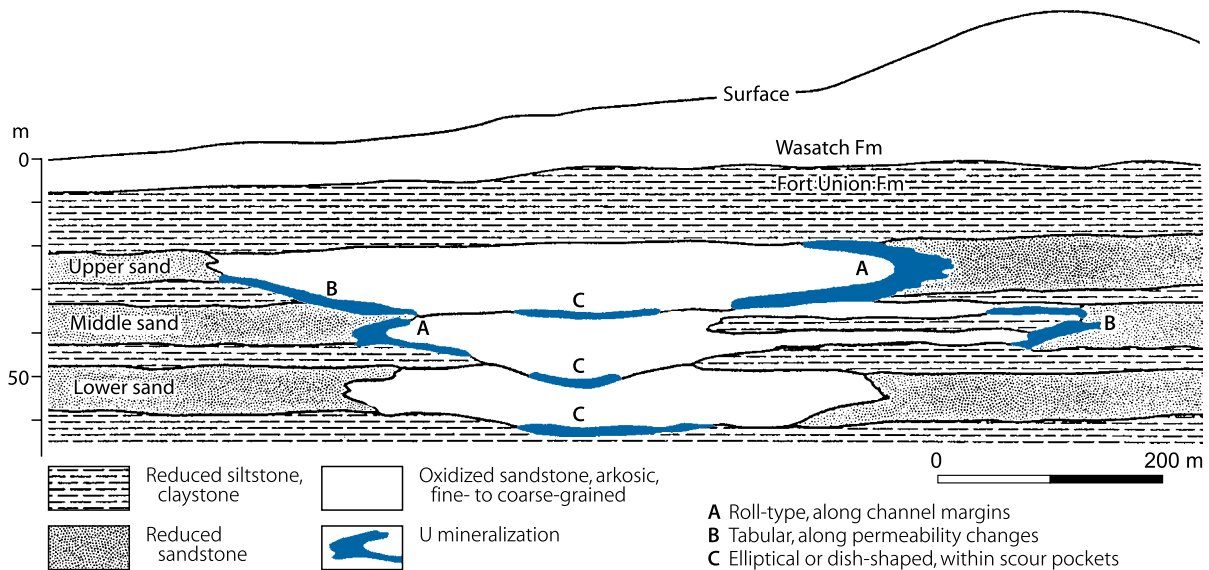
Pitchblende/sooty pitchblende, and coffinite are the principal U minerals; they are intricately associated with pyrite. Best mineralization occurs

- (a) On the western flank of a wide paleochannel
- (b) Where a wide zone of change in facies predominates and
- (c) Where the thickness of the host sandstones is 10 m or more.

The width of the seven ore bodies ranges between 90 and 210 m, and the thickness is up to 20 m.

■ Fig. 2.30.

Southern Powder River Basin, Highland mine, generalized cross-section normal to the altered sand channel, Fort Union Formation. Three principal types and settings of ore bodies are identified employed in three interconnected channel sections, cumulative 33-m thick in the south and 54 m in the north. (After Langen and Kidwell 1974)



2.5.2.4 Additional Deposits/Properties in the Southern Powder River Basin

Reynolds Ranch, located SW of Monument Hills district: measured and indicated resources: 4,423 t U, 0.051% U (Cameco 2007 Annual Information Form, pp 46–47).

Sand Draw (Allemand Ross Project), located about 10 km NW of Bear Creek: indicated resource 373 t U, 0.27% U; inferred resource 1,458 t U, 0.16% U (NRC August 30, 2006, Summary of August 22, 2006 meeting).

Mrak No. 2: This represents an example of a shallow ore body in the Monument Hill district. Ore occurred at a depth of 20–25 m and was mined by a pit prior to 1966. Production amounted to almost 40 t U. Grades ranged from <0.1 to 1.5% U over 0.6 m thick sample intervals as shown in Fig. 2.33 (Mrak 1968).

2.5.3 Kaycee District, Western Powder River Basin

This district is located about 115 km north of Casper in the western Powder River Basin (Fig. 2.24). A number of mostly small

■ Fig. 2.31.

Southern Powder River Basin, Monument Hill district, Bear Creek mine, schematic cross-section of the deposit illustrating the three varieties of uranium occurrences in two frontal systems within the Wasatch Formation. (After Hansink 1976)

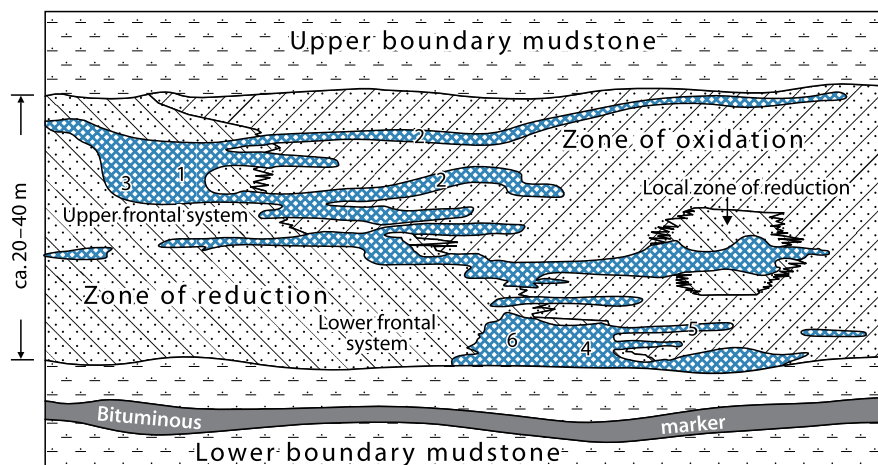


Fig. 2.32.

Southern Powder River Basin, Monument Hill district, Bear Creek mine, schematic section across the frontal zone of the deposit with distribution and contents of selected elements. (After Davis 1969)

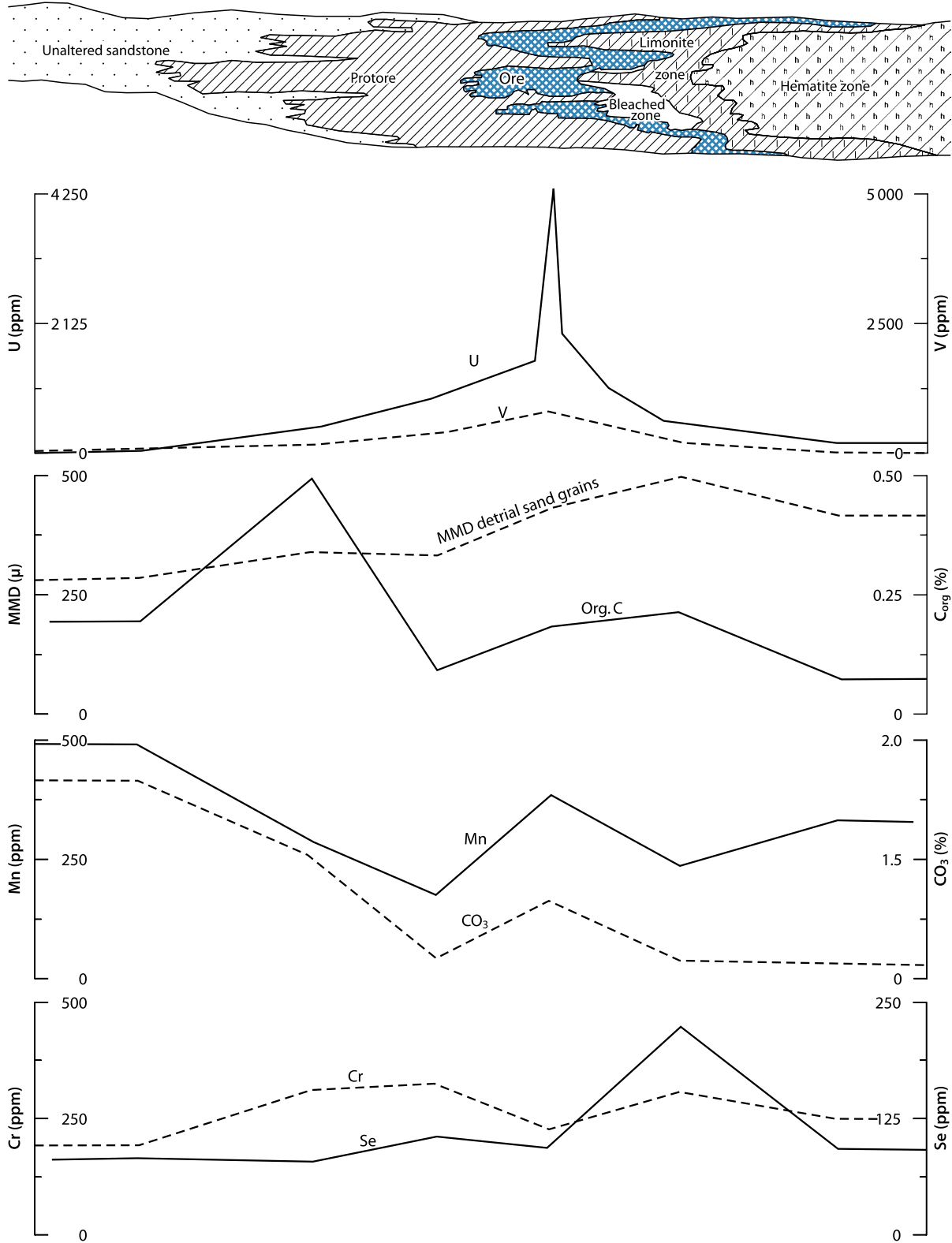
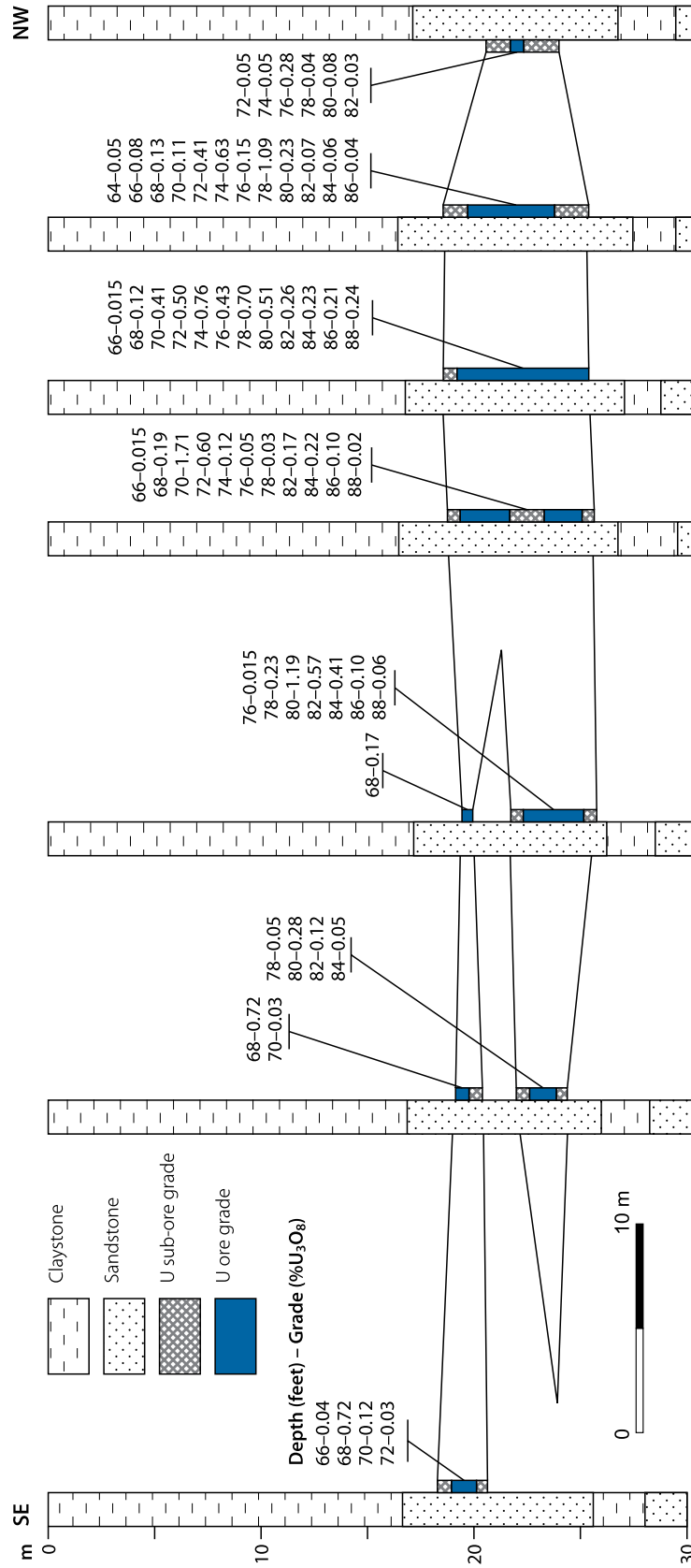


Fig. 2.33. Southern Powder River Basin, Monument Hill district, Mrak No.2 pit, SE-NW section showing the position of a shallow ore body and associated thickness and grade of mineralization in percent U_3O_8 per 2 ft. (0.6 m) intervals. (After Mrak 1968 (reproduced by permission of AIME))



ore bodies, with grades averaging 0.10–0.13% U have been found along a redox front almost 25 km long.

Sources of Information. Childers 1970, 1974.

Geology and Mineralization

The Kaycee area lies in a large broad syncline on the west flank of the Powder River Basin. The syncline plunges to the northeast and the Tertiary strata dip 10–25° E. It is believed that the beds were folded before the uranium deposits were formed (Childers 1970).

The Paleocene *Fort Union Formation* is the host for U deposits in the Kaycee district. It rests with slight angular discordance upon fluvial and lacustrine sandstones and shales of the late Cretaceous Lance Formation and is unconformably overlain by the fluvial early Eocene Wasatch Formation. The Fort Union Formation in the Kaycee area may be divided into three units: (a) an upper sand and shale unit about 300 m thick, (b) a middle grey shale and bentonitic unit 150–300 m thick, and (c) a basal sandy unit about 300 m thick. The sandstones are crossbedded, contain clay galls, and conglomerate lenses. The upper sandy unit has an extensive 75 m thick conglomeratic sandstone at the base, but other sandstones in the unit are lenticular and of limited lateral persistence. The upper unit contains considerable silt, shale, mudstone, and carbonaceous trash. Since the principal river draining the Wind River Basin may have flowed northeasterly through the Kaycee area and into the Powder River Basin in early Paleocene time, it can be assumed that at least part of the lower Fort Union Formation is a product of this stream.

Sandstones in the overlying *Wasatch Formation* are similar to those in the upper part of the Fort Union. They are interbedded with many mudstones, some of which are red and green and contrast with the grey Fort Union mudstones.

Ore bodies occur along the edges of large lobate tongues of oxidized Fort Union sandstone, which can be traced for almost 25 km. Altered arenites are stained red by hematite coatings on sand grains and contain iron-rich calcite concretions, but little or no carbonaceous material or pyrite. This contrasts with the grey, pyritic, carbonaceous unaltered sandstones, which locally contain coarse aggregates of pyrite, which are heavily stained with humate.

Ore bodies are of rollfront type and consist of pitchblende/sooty pitchblende and coffinite associated with pyrite and montroseite(?). The vanadium content is high, up to several times that of uranium, revealing some similarity to the Black Hills deposits, but being in contrast to ore in the southern Powder River and other Wyoming Basins.

Ore bodies are generally small. Thicknesses range from 1.5 to 10 m, and the width laterally from the redox interface is between 15 and 25 m. Grades average about 0.13% U but can be up to 1% U.

Outcrops of altered sandstone locally contain some hexavalent U minerals at sites where the sandstone is enriched in organic material. These small occurrences are probably residual

remains that have survived in otherwise oxidized sandstone by local high-organic concentrations in the sandstone.

2.5.4 Casper Arch, Nine Mile Lake

Located in the western vicinity of the Powder River Basin, 15 km N of Casper, the *Nine Mile Lake deposit* lies in the Casper Arch, which separates the Powder River Basin from the Wind River Basin. Resources amount to ca. 3,500 t U at a grade averaging 0.047% U. ISL testing took place in the late 1970s.

Uranium occurs in rollfront ore bodies similar to those in the Powder River Basin. The ore bodies are hosted in sandstone of the Cretaceous Mesa Verde Formation, which were deposited in a marginal marine environment. Mineralization occurs over a NNW–SSE length of 12 km at depths ranging from 30 to 45 m. Maximum width is some 30 m.

2.6 Sand Wash and Poison/Washakie Basins, Colorado–Wyoming

These two adjacent basins (Fig. 2.1) contain sandstone-type uranium deposits. Uranium was discovered in 1953 near Baggs and mined from 1954 through 1981 from some 20 operations.

The *Washakie Basin*, south Wyoming, hosts deposits in the *Baggs area* and in the *Poison Basin*, a subbasin of the Washakie Basin. Production came from eight properties and amounted to about 350 t U at grades averaging 0.17% U.

Deposits in the southerly adjacent *Sand Wash Basin*, northwestern Colorado, are grouped in the *Cedar Hills/Juniper Ridge area* and in the *Maybell area*. Recorded production from 11 properties was approximately 1,400 t U at a grade of 0.11% U. Most mining was by open pits, but some was by underground workings.

Exploration in the late 1970s delineated the *Juniper Ridge* deposit in the Poison Basin containing some 3,000 t U.

Sources of Information. Albrethsen Jr and McGinley 1982; Bergin 1959; Carlson 1957; Chenoweth 1986b; Goodknight 1983; Grutt 1972; Lewis 1977; Nelson-Moore et al. 1978; Ormond 1957; Schneider 1981; US AEC 1959.

Regional Geological Setting of Mineralization

Uranium deposits occur in two adjacent Tertiary basins. Those of the *Maybell area* are on the south flank of the Sand Wash Basin, and the *Baggs* deposits are on the east flank of the Poison Basin, a substructure of the Washakie Basin. Host to deposits in both basins is the *Miocene Browns Park Formation*. It has a maximum thickness of 350 m at Maybell and in excess of 150 m at Baggs. The Browns Park Formation is composed of fine- to medium-grained, well-bedded and partly cross-bedded, locally tuffaceous, calcareous arkosic sandstone of fluvial provenance. A 20–25 m thick basal conglomerate underlies the sandstone horizon. The strata have a gentle basinward inclination.

Unoxidized sandstone is medium to dark grey and may contain appreciable amounts of pyrite. Carbonaceous vegetal material is not, but asphaltite and “dead oil” are reported. Weathering/oxidation visible by a marked color change to chalky white, light grey, or buff affected the upper part of the formation to depths ranging from a few meters to almost 50 m under surface. The Browns Park Formation is essentially undisturbed except for gently plunging sedimentary synclines and some local normal faults. It was deposited on an Oligocene erosion surface and older, folded, and faulted rocks.

Mineralization, Shape and Dimensions, Metallogenetic Aspects

Pitchblende and coffinite associated with pyrite are typical in unoxidized sediments; hexavalent U minerals occur in oxidized, limonite-stained sands. Selenium and molybdenum minerals are reported from the Baggs area. Vanadium ranges from 0.05 to 0.16%. Asphaltite and “dead oil” occur locally in some deposits.

Uranium mineralization forms roughly tabular bodies conformable to bedding and restricted to a limited stratigraphic interval mostly in the upper Browns Park Formation. Movable uranium concentrations (>0.1% U) occur in groups of lenticular, discontinuous ore bodies, from 0.3 to almost 10 m in thickness, which tend to be localized along deeper parts of depositional synclines and along certain normal faults. The size of ore lenses ranges from less than one to more than 200 t U. Grades are highly variable both horizontally and vertically, ranging from 0.004 to 2.5% U. Movable ore is commonly surrounded by low-grade mineralization (<0.1% U), which is locally as much as 15-m thick. Ore bodies occur from the surface down to about 100 m.

It has been postulated for the origin and mode of emplacement of uranium that uranium may have been leached from intrinsic tuffaceous material in the Browns Park Formation, or from higher beds, transported by groundwater, and deposited in a reducing environment which may have been produced by hydrogen sulfide from natural gas.

Selected deposits of the Maybell and Baggs districts are characterized by the following features (US-AEC 1959).

In the *Maybell district*, the *Trace Elements Corporation mines* are located in an area where Browns Park sediments form an E-W-trending depositional syncline. Ore bodies are aligned along the axis of the syncline and invariably occur at or adjacent to normal faults with small displacements. Deposits consist of many smaller, thin to moderately thick, lenticular ore accumulations in gently dipping sediments distributed within a thicker stratigraphic interval. Ore grades are highly variable both horizontally and vertically within ore bodies. Movable ore is principally associated with large volumes of low-grade mineralization (0.03–0.08% U). Ore mined exclusive of this low-grade material, averaged 0.17% U and occurred in 1–8 m thick lenses. The largest known ore concentration is 460 m long, 150-m wide, and contains about 340 t U.

In the *Baggs district*, the *Poison Basin deposit* is hosted in unoxidized and oxidized Brown Park sandstone that forms a depositional syncline and is dissected by normal faults. The deposit extends to a depth of some 20 m below surface and consists of smaller, better grade (averaging 0.17% U for ore mined) ore bodies surrounded by abundant low-grade mineralization (<0.1% U) through the upper 20 m of the up to 150-m thick Browns Park Formation. Ore bodies are of lenticular or blanket-like configuration, generally concordant with very gently dipping sediments. Ore thickness is 1–3 m. Resources amount to almost 100 t U. On the south side of the deposit, drill holes encountered natural gas in the Brown Park Formation.

The *Teton No. 3 deposit*, located about 3 km to the W of the Poison Basin deposit, comprises narrow, discontinuous flat-lying ore lenses, less than 1.5 m thick, in an area 210 m long, 60 m wide, and 25–30 m deep. Average ore grade is 0.17% U with some pods exceeding 1% U.

Schneider (1981) provides some information on the *Juniper Ridge deposit* in the Poison Basin. Uranium mineralization is hosted in cross-bedded dune sands of the Brown Park Formation. Resources recoverable by open-pit mining amount to some 3,000 t U at an average grade of 0.05% U (cutoff grade of 0.017% U). They are contained in three minable ore bodies at depth of less than 80 m. About one third of these resources is above the water table and consists of oxidized ore, mainly autunite with minor brannerite. U/Ti ratios in brannerite range over a wide span. Quartz partly coats ore minerals. Additional ore components include 5.3% Ca carbonate, 250 ppm Mo, and minor Fe, Mg, Se, and V.

Selected References and Further Reading for Chapter 2 Wyoming Basins

Adler and Sharp 1967; Adler 1974; Albrethsen Jr and McGinley 1982; Anderson 1969; Armstrong 1970, 1979; Austin 1970; Baily 1965, 1969, 1980; Bargar et al. 2008; Beahm 2006a, b, c, d; Beahm and Anderson 2007; Bergin 1959; Boberg 1979, 1981, 2005, 2007; Breckenridge et al. 1974; Buswell 1980; Carlson 1957; Cheney and Jensen 1966; Cheney and Trammell 1973; Chenoweth 1980, 1986b; Childers 1970, 1974; Crawley 1983; Crew 1981; Curry 1976; Dahl and Hagmaier 1976; Davis 1969; Denson and Chisholm 1971; Dooly et al. 1964, 1974; Elevatorski 1976; Files 1970; Finch and Murakami 1999; Fischer 1970; Gabelman and Krusiewski 1964; Gabelman 1970; Galloway 1979 a, b; Goldhaber and Reynolds 1979; Goodknight 1983; Granger and Warren 1969, 1978, 1979; Graves and Woody 2008; Gruner 1956; Grutt 1957, 1972; Hansink 1976; Harris 1984; Harshman and Adams 1981; Harshman 1962, 1966, 1968, 1970, 1972, 1974; Houston 1969; Jensen 1958; Kashirtseva 1964; Keefer 1970; King and Austin 1966; Klingmüller 1989; Krewedl 1979; Langen and Kidwell 1974; Lattanzi and Pressacco 2005; Lease et al. 1974; Lewis 1977; Love 1970; Ludwig and Grauch 1980; Ludwig 1978, 1979; Masursky 1962; Melin 1964, 1969; Mrak 1968; Nelson-Moore et al. 1978; Noyes 1978; O’Loughlin et al. 2003; Ormond 1957; Pipiringos and Denson 1970; Pool 2007a; Rackley 1972, 1976; Reade 1976; Rowson 2002; Rozelle 2006; Rubin 1970; Santos and Ludwig 1983; Santos 1981; Schneider 1981; Seeland 1976; Sharp and Gibbons 1964; Sharp et al. 1964; Sherborne et al. 1980; Sheridan et al. 1961; Snow 2007a, b; Soister 1968; Stout and Stover 1997; Stephens 1964; Suzuki et al. 2005; US-AEC 1959; Van Houten 1964; Vickers 1957; Vine and Tourtelot 1970a, b; Wall and Krumholz 2000; Wallis 2006a, b; Wallis and Rennie 2006; Warren 1971, 1972; Zeller 1957; and Catchpole G, Davis J, Harshman EN, Hartman G, Pool TC, and Stover D, personal communication.



Chapter 3

Black Hills

The Black Hills extend from southwestern South Dakota into northeastern Wyoming (Fig. 1.1b). Uranium was known in the Black Hills as early as 1935, but it was not until 1951 that the first substantial ore accumulation was found near the town of *Edgemont* in the southwestern Black Hills, South Dakota. Subsequent exploration discovered numerous small rollfront-type and a few stratiform U-V occurrences in a 3–25 km wide belt that stretches for about 200 km along the western and northern flank of the Black Hills uplift (Fig. 3.1).

Exploitation lasted from 1952 through 1973. Deposits mined had grades from a few hundreds to several tenths of a percent, and resources of generally some tens to a few hundreds tonnes of uranium. The ore also contained vanadium at a V:U ratio of 1:1 to 2:1. Total production amounted to approximately 2,300 t U and 2,000 t V₂O₅ at mining grades averaging about 0.18% U and 0.3% V₂O₅. The bulk of this production (1,980 t U) came from the *Edgemont* area, South Dakota, in the southwestern Black Hills, and the *Carlile* and *Hulett Creek* areas in the northwestern Black Hills, Wyoming. In addition, several isolated small mines have contributed to the Black Hills production. Vanadium was recovered as the byproduct.

Sources of Information. Harshman and Adams (1981) and Chenoweth (1988) give synoptical descriptions of the geology of the Black Hills and its uranium deposits, which were largely used for the following summary, amended by data from Chenoweth WL (Personal Information) and authors listed at the end of Chap. 3 Black Hills in Sect. Selected References and Further Reading.

Regional Geological Setting of Mineralization

The Black Hills are a broad dome about 240 km long in NNW–SSE direction and 80 km wide (Fig. 3.1). The dome was uplifted during the Laramide Orogeny and consists of a Precambrian granitic and metamorphic core surrounded by outwardly dipping Paleozoic and Mesozoic rocks. The metamorphic suite includes, in the *Nemo district* on the northeastern flank of the Black Hills, South Dakota, the Lower Proterozoic *Estes Conglomerate*. The conglomerate rests directly upon late Archean granitic basement and contains relatively high background uranium, thorium, and gold (highly oxidized outcrop samples of quartzite-pebble and quartz-pebble conglomerate with matrices of micaceous quartzite contain, locally, 10–100 ppm U, 20–800 ppm Th, up to 1.4 ppm Au, and 5–25% pyrite) (Hills 1977, 1979).

Uranium mineralization is hosted in the Lower Cretaceous *Inyan Kara Group*, which crops out in an inward-facing hogback

of sandstones that is the outermost geomorphic expression of the Black Hills structure. *Inyan Kara* sediments rest conformably upon continental siltstones and claystones of the Jurassic *Morrison Formation* and are conformably covered by the Lower Cretaceous marine *Skull Creek Shale*.

The *Inyan Kara Group*, from 100 to 200 m in thickness, was apparently deposited during a period of transition from continental to marine conditions. The group is divided into the lower *Lakota Formation* and upper *Fall River Formation*.

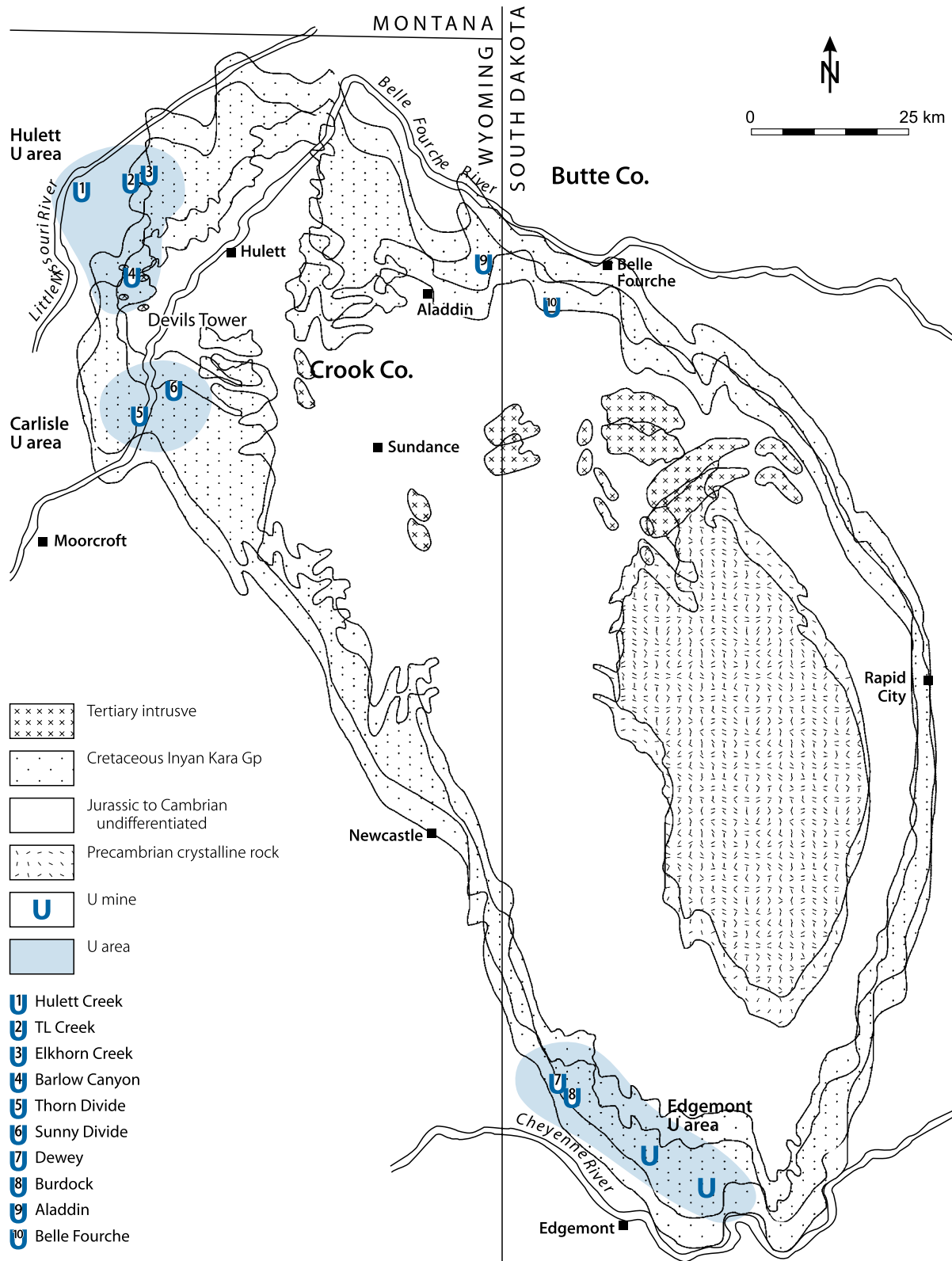
The *Lakota Formation*, from 60 to 150 m thick, is a nonmarine sequence with a poorly defined contact with underlying *Morrison* sediments. The formation is, in general, highly siliceous and consists of many intertonguing lenses of cross-stratified, fine- to coarse-grained, buff to white, fluvial sandstones, which are intercalated with varicolored siltstone and claystone of flood plain and lake deposits, and few lignite seams. Many of the sandstones form large interconnected lenses, but some occur as small and isolated lenses. A thin layer of discontinuous, dark grey to black sandstone and claystone containing humates and thin seams of low-grade coal form the basal part of the sequence. These beds grade upward into, and in some places are cut out by intertonguing dark-grey sandstones, composed of chert, quartzite, and quartz grains. These sandstones contain substantial amounts of organic matter and interstitial pyrite. Some are well cemented, others contain little cement and are friable. Claystones range from hard and silty to semi-plastic; many are bentonitic. Some sandstone lenses are broad and sheet-like, others are long and narrow. Sandstones thin from southeast to northwest.

The nature of *Lakota* sediments indicates that they have been deposited by streams of moderate gradient flowing northwesterly, somewhat parallel to the axis of the present Black Hills uplift. Streams moved laterally within their rather broad channels. Changes in the vigor of the streams caused considerable cutting and filling. This depositional environment would correspond to coastal plain-piedmont environment or a stable shelf environment of a continental platform with the shelf laying to the east of the inland sea that invaded the area at the close of *Inyan Kara* time.

The *Fall River Formation*, 25–45 m thick, overlies the *Lakota* with marked disconformity. It consists of thin bedded, tabular or tabular cross-laminated sandstone interbedded with a few thin grey to black siltstones and claystones. Sandstones are fine- to medium-grained, siliceous and carbonaceous, and predominantly of grey, buff, or brown color. They contrast markedly with the massive character of the nonmarine *Lakota Formation* and were apparently deposited in a coastal plain-delta environment and as such appear transitional between fluvial sediments of the *Lakota Formation* and marine shales of the overlying *Skull Creek Shale*.

The structure of the west flank of the Black Hills, where uranium deposits occur, is dominated by two monoclines separated by a structural terrace. Rocks to the east of the terrace dip 2–10° W, while to the west of the terrace dips steepen to 10–25° W. Most ore bodies are in the terrace structure where dips generally range from 1 to 3° W, but in some areas dips reverse to 1° E or

Fig. 3.1. Black Hills region, simplified geological map with location of selected former uranium mines. (After Bailey and Childers 1977; Chenoweth 1988a; Renfro 1969)



more. Other major and minor folds of diverse orientation are superimposed on these gentle structures.

Faults are less prominent and generally have displacements of less than 30 m. Northwesterly trending structures with steep dips are most common. The major structural elements are of pre-ore origin related to Laramide tectonism that caused the Black Hills uplift. Dissolution of underlying anhydrite beds is probably responsible for rare post-ore structural movements.

According to Harshman and Adams (1981) uranium-hosting Inyan Kara sediments were derived from source rocks and deposited under hydrologic conditions that differed distinctly from the source rocks and hydrologic conditions in the Wyoming Basins. The climate was at that time hot and humid, as indicated by fossil tropical to subtropical plants and spores. Source areas were apparently composed of Jurassic and older sediments as there is an almost complete lack of minerals of igneous or metamorphic origin in Inyan Kara sediments. Material in the lower part of the Inyan Kara group including some volcanic material had its source to the southwest, whereas that of middle and upper Inyan Kara clastic sediments derived from the southeast. At the end of the Inyan Kara time, the environment returned to marine conditions.

Uplift and erosion affected the Black Hills during the Paleocene and Eocene and resulted in the removal of a large amount of sediments overlying the Inyan Kara Group from flanks of the uplift. This debris was apparently transported out of the area by westerly and northerly flowing streams. Periods of gentle uplift, erosion, and deposition continued into middle and upper Eocene time when volcanic activity commenced.

Principal Host Rock Alteration

Similar to alteration features in the Wyoming Basins, U-hosting strata in the Black Hills enclose tongues of oxidized sandstone that extend downdip from the outcrop for about one to several kilometers. Tongue margins are much more irregular in the Black Hills, however, than in the Wyoming Basins due to the lithologic complexity of ore-hosting Inyan Kara sediments. The thickness of altered tongues is commonly 1.5–5 m, but may be as much as 10 m.

The tenor of U, V, Se, Fe³⁺, and As have been increased in altered tongues as compared with that in unaltered sandstone, and the amount of Fe²⁺ (principally pyrite), organic and mineral carbon, and perhaps Cu has been decreased. Pyrite, magnetite, and organic carbon are essentially completely destroyed in altered tongues. Pyrite has been oxidized to hematite and locally to goethite. Both iron oxides coat sand grains and occur pseudomorphic after pyrite. Hematite imparts a red or pinkish color and goethite a brownish-yellow color to altered sandstone. Where both, goethite and hematite occur in the altered tongue, goethite is in zones about a meter or so wide at the edge of the tongue. It thus intervenes between the red hematitic interior of the tongue and the rollfront, much the same as in Powder River Basin deposits.

Principal Characteristics of Mineralization

In contrast to the Wyoming Basins deposits, the Black Hills mineralization contains uranium and vanadium. The latter often equals or exceeds the uranium content as reflected by vanadium to uranium ratios commonly of about 1.5:1.

Pitchblende, coffinite, montroseite, pyrite, native selenium, jordisite, and calcite are the main minerals in unoxidized ore, i.e., downdip from the alteration interface. Para-montroseite, haggite, doloresite, and other vanadium minerals are typical for oxidized zones; they are all intimately intergrown with montroseite, which suggests that they are probably oxidation products of montroseite.

Pitchblende and coffinite are fine-grained, intermixed, and occur interstitially to sand grains. The two minerals are intergrown with bladed aggregates of montroseite and frequently replace pyrite. Pyrite is present in two generations, an early, probably diagenetic one, and a late, ore-related one. Early pyrite forms fine-grained cubic crystals emplaced in voids in sandstone. It is frequently associated with organic substances. Later pyrite is coarse-grained to nodular and closely associated with ore minerals. It is intergrown with marcasite near the rollfront, and often replaces quartz. Calcite completely fills the pore space in some ore bodies, and has corroded and replaced some quartz grains. Calcite concretions are common at the outer limits of ore. Needle-like crystals of native selenium occur adjacent to ore, in part, on the oxidized side of the rollfront.

Gott and Schnabel (1963) provide the following paragenetic scheme of ore minerals in the *Runge Mine*, Edgemont area: calcite, pyrite, pyrite-marcasite, first stage pitchblende, montroseite-haggite, second stage pitchblende. The place of jordisite in the paragenetic sequence is unclear, but spatially it lies toward the unaltered sandstone margin of ore, hence, was probably precipitated last from solution.

General Shape and Dimensions of Deposits

Ore bodies in the *northern Black Hills* are mainly of peneconcordant tabular type, and in the *southwestern Black Hills* mostly of rollfront type located at the distal edge and to a lesser extent along top and bottom surfaces of altered tongues in six sandstone horizons of the Lakota and Falls River Formations. The six sandstone horizons are informally denominated, from bottom to top, S-1 to S-6. The best ore bodies occur in units S-1, S-4, and S-5, which consist of fluvial coarse-grained channel sandstones, as much as 7.5 m thick, of considerable lateral extent and relatively good permeability.

In larger, more permeable channel sandstones, rollfronts persist laterally for several kilometers along the strike of sandstone beds; but the entire length of the rollfront may not be mineralized. In intervals where the sandy beds are discontinuous and interbedded with mudstone, the altered tongues are generally small, irregular, and poorly mineralized.

In contrast to deposits in the Wyoming Basins, however, host sandstones in the Black Hills are smaller, of lower permeability,

less arkosic, and over large areas probably much less transmissive. These factors obviously limit the size and grade of the Black Hills deposits.

The lithologic complexity of the Inyan Kara Group sediments has adversely affected the regularity of rollfronts, both laterally and vertically, and the shape, size, and mineral content of ore associated with them. Some ore bodies in channel sandstones with lateral extents of some kilometers and with somewhat isotropic permeability may approach the ideal C-shape. But, many deposits reflect the inhomogeneity of host sediments by their small tabular or complex sinuous bodies, which may or may not be interconnected.

Highest grades and most extensive mineralization are mostly confined to the nose of the roll, but mineralization of economic interest is also present in the upper and lower cusps of crescent-shaped ore rolls extending backward updip for several tens of meters. Such deposits range in size from a few hundred to a few tens of thousands of tonnes of mineralized sandstone containing from a few hundredths to over 1% uranium. Thicknesses of mineralized sandstone are commonly 3 m or less, but may be as much as 10 m.

Principal Ore Control and Metallogenetic Aspects

Ore controls are to a certain extent similar to those in the Wyoming Basins (for details see there). Harshman and Adams (1981) claim that deep burial of Inyan Kara host sediments was essential for later ore formation, since it preserved the required reducing environment until the early Tertiary period of uranium mineralization many millions of years later.

Uplift in Laramide time started the hydrologic cycle that stripped the thick sequence of impermeable rocks topping the Inyan Kara Group, exposed their truncated edges, and generated the gentle basinward dip essential for the flow of mineralizing waters. At about middle to upper Eocene time, oxygenated waters entered truncated edges of Inyan Kara strata. This water originated in granitic cores and flanking metamorphic and sedimentary rocks of mountain ranges updip from host rock outcrops, and transported uranium and other ore-forming elements downdip into host sandstones where reducing conditions for uranium precipitation existed.

Hart (1968) proposes that positions of altered tongues along which ore was deposited, were governed by movement of groundwater toward three principal streams, the Cheyenne, Belle Fourche, and Little Missouri rivers, that denuded the sedimentary succession and produced the present topography. Harshman and Adams (1981) argue that juxtaposition of these streams and the Edgemont, Carlile, and Hulett districts is the only evidence given as justification for this conclusion. The character of sandstones in the three areas and lateral changes in permeability may have had an equal or greater influence on selection of these districts.

Reliable isotopic ages on deposits are not available. It seems reasonable to assume, however, that they are about the same age as those in the Powder River Basin deposits, for the west flank of the Black Hills and the east flank of the Powder River Basin have

had about the same geologic, climatologic, and hydrologic histories since uplift of the Black Hills and downwarp of the basin in Laramide time.

3.1 Southwestern Black Hills, Edgemont Area, South Dakota

Uranium deposits are grouped in a 3–5 km wide belt, which extends for a length of some 35 km in a NW–SE direction to the N and E of the town of Edgemont in South Dakota (Fig. 3.1). After the discovery of uranium in 1951, slightly more than a hundred properties went into production exploiting ore bodies ranging in size from small pods with a few tonnes to 100 t U or more. Most of the early mining was by small open pit operations exploiting near-surface oxidized ore with mainly hexavalent U minerals.

Major producers include the *Gould*, *King*, and *Runge* mines. They produced in excess of 100 t U each, mainly from unoxidized ore at a depth of 100–150 m. Total former production (1952–1973) is estimated at about 1,000 t U. In situ ore grades ranged from <0.1 to 0.5% U and averaged around 0.12% U. The vanadium to uranium ratio averaged 2:1 in oxidized, and about 1–1.5:1 in unoxidized ore. Two explored deposits, *Dewey* and *Burdock*, and perhaps more are presently (2008) of economic interest.

Sources of Information. Bell and Bales 1954, 1955; Blake 1988; Gott and Schnabel 1963; Harshman 1968; Hart 1968; Smith 1991, 2005; and Smith RB, personal communication.

Geological Setting of Mineralization

In the *Edgemont area* at the southwestern margin of the Black Hills, uranium is hosted in the *Lakota and the Fall River Formations*. Host rocks are coarse- to fine-grained, permeable channel sandstones of considerable lateral continuity. They are bounded at top and bottom by impermeable mudstones. Sandstones are composed mostly of quartz and chert, and a few percent of microcline, albite, and kaolinite. Calcite may be locally abundant, but is generally rare.

Unaltered sandstone contains pyrite interstitially to sand grains or as small rod-like aggregates replacing carbonaceous matter. Carbonaceous vegetal material and humate is abundant in some sandstones. Associated fine-grained sediments are almost always carbonaceous. Heavy minerals, excluding pyrite, constitute about 1% or less of rock volume, i.e., their amount is considerably lower than in arkoses derived from granitic terrane. Magnetite is present in some, but not all, heavy mineral suites.

Mineralization, Shape and Dimensions of Deposits

Three quarters of the ore mined were emplaced in tabular, buff to brown, carbonaceous, fine- to medium-grained, fluvial sandstones in the basal part of the 30–45 m thick Fall River Formation

of the Lower Cretaceous Inyan Kara Group. The remainder production came from ore hosted in carbonaceous sandstones of the 75–150 m thick Lakota Formation.

Principal ore minerals in unoxidized ore include pitchblende, sooty pitchblende, coffinite, and vanadium minerals such as para-montroseite, haggite a.o. Associated minerals are pyrite, marcasite, calcite, and, locally, native selenium. Molybdenum is not common in ore of the Fall River Formation except in the Runge underground mines, where abundant jordisite and ilsemannite are associated with the uranium mineralization. Oxidized ore consists mainly of uranyl phosphates and -silicates, which are often accompanied by corvusite and rauvite.

Minerals of both oxidized and unoxidized ores fill sandstone interstices, coat sand grains, and impregnate carbonaceous plant remains. Pinkish to reddish hematite is found as a halo partly enveloping ore zones, which appear to occur downdip from the oxidized zone. The boundary between hematitic nonmineralized and mineralized zones is often fairly sharp.

Mineralization forms stratiform, mostly tabular to dish-shaped and roll-type ore bodies with thicknesses ranging from 1 to 6 m and averaging 0.17% U. Small pods and lenses of high-grade ore occur near-surface at the truncated outcrop of ore-hosting sands.

The *King Mine* ore body is somewhat tabular shaped at a facies change at the base of the Fall River Formation. Host rocks are interbedded, fine-grained, grey-brown sand-, silt-, and mudstones, which contain abundant carbonaceous plant remains, pyrite, and marcasite. Altered sandstone with pinkish hematite staining occurs adjacent to ore. The ore body had a length of 360 m, a thickness of about 1 m, a width of 3–12 m, and yielded ore averaging 0.3% U.

The *Gould Mine* was worked on roll-type and tabular ore bodies hosted in fluvial sandstone of the Lakota Formation. Ore varied in thickness between 3 and 5 m and averaged 0.2–0.25% U.

3.1.0.1 Dewey–Burdock Deposits

These two explored deposits are located NW of Edgemont, *Burdock* in northwestern Fall River County, ca. 25 km NW of this town, and *Dewey* in southwestern Custer County about 5 km NW from Burdock (► Fig. 3.2). In situ resources total almost 3,000 t U at an average grade of 0.18% U.

Source of Information. Smith 1991, 2005.

Geology and Mineralization

Uranium is hosted in several sand units of the [Lakota and the Fall River Formations](#). The Lakota sands were deposited by meandering streams across a channel system 6–8 km in width. The various uranium mineralized sand units are interconnected and form a near-continuous aquifer for groundwater migration. Similar channel patterns are noticed in the Fall River Formation, but channel sands are noticeably thinner.

Sands of the Lakota Formation are commonly upward fining with coarse- to medium-grained fractions at the base and fine-grained material at the top. Mineral constituents are predominantly rounded quartz with minor feldspar and heavy minerals. Carbonaceous matter is limited in the Lakota Formation and more abundant in the Fall River sediments. Sands are variably cemented by calcium carbonate. It appears that carbonate cementation, in most cases, preceded uranium mineralization and that little calcite was formed during the mineralization process.

Altered channel portions occur in several separate channel sands and show oxidation-related colors ranging from pink to dark red, or yellow to orange, and to brown on the reduced side as well as on the oxidized side near a rollfront. Rollfronts often exhibit shades of green in both clay and sand. Reduced sediments are always grey.

A major structure in the northern part of the Edgemont district, the ENE–WSW-oriented Dewey fault zone, trends to the north of the Dewey deposit.

Smith (1991, 2005) notes nine sand units (L1, L2A&B to L8 from oldest to youngest), on average about 6 m thick, in the Lakota Formation, and three sand horizons (F11–F13) in the basal Fall River Formation. Consistent clay beds commonly intervene between these sand horizons. Redox fronts in these sands can be traced for over 30 km on the Dewey–Burdock properties (► Fig. 3.2).

All sand units contain redox fronts with associated uranium mineralization, but in highly variable quantity. Rollfronts in individual sand units in each of the two formations commonly trend nearly parallel and indicate geochemical cell communication between individual sand units. If one sand unit pinches out, a different but associated rollfront is developed in another sand horizon in a different stratigraphic position. This situation suggests the presence of only two major geochemical cells, one in the Lakota and the other in the Fall River Formation.

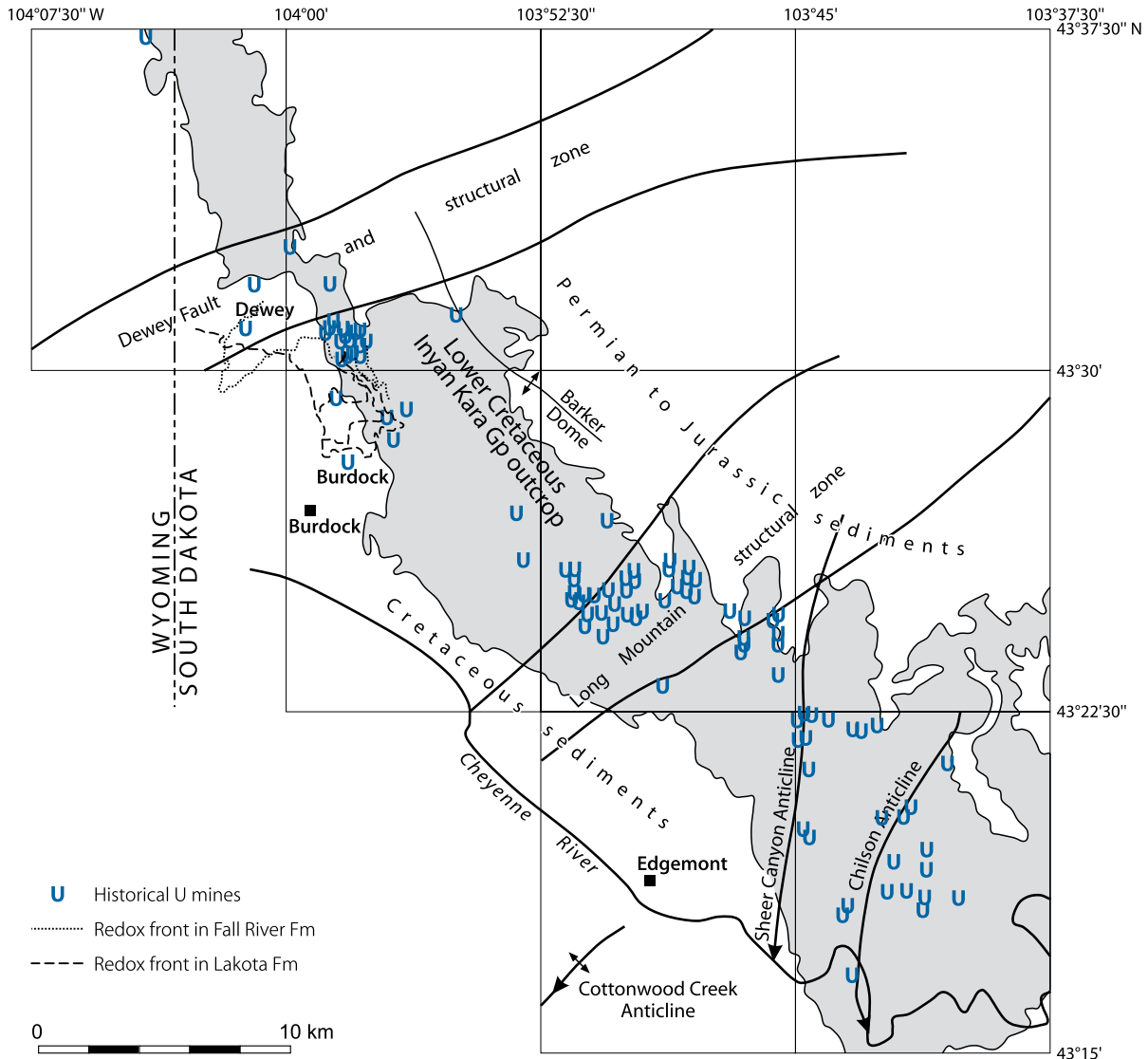
Ore bodies are of typical rollfront configuration. They occur discontinuously along redox boundaries, several kilometers in length, and are preferentially located along the flanks of sand channels. Often there is more than one mineralized unit within one of the above mentioned sand horizons.

Individual ore bodies range from few hundred to some thousand meters in length. Width of uranium concentrations ranges from seldom less than 15 to 30 m and more, and depends upon lithology and position within a channel. Ore body thickness is generally a function of the thickness of the sand host unit and ranges from 0.3 to 0.6 m in limbs to 2.7 m in rolls. Protore mineralization (<0.01–0.017% U) may be 5–7.5 m thick and almost ubiquitously impregnates the sand unit.

Uranium grades range from <0.01 to a few percent. The equilibrium factor is generally 1:1. Sand-grain size tends to have had little effect on uranium concentration. Coarse sands at the base of channel sand units may contain the same uranium concentration as fine-grained sands higher in the channel facies. Pyrite content is moderate to abundant within rollfronts with values up to 5%. In contrast to near-surface deposits, vanadium contents are low. At Burdock, the vanadium content tends to be only about one half of the uranium content.

Fig. 3.2.

SW Black Hills, Edgemont area, generalized structural map with location of uranium deposits and former mines, as well as course of redox fronts in Falls River and Lakota strata in the Burdock-Dewey area. (After Smith 2005 based on Gott et al. 1974)



At *Burdock*, established in situ resources feasible for extraction by ISL methods amount to almost 1,400 t U at an average grade of 0.17% U. These resources are confined to sands of the Lakota Formation with the majority of the resources being in the S2 sand unit. The depth of these resources varies between 90 m along the east side of the property and about 165 m in the southwest corner of the property. In contrast, all mineralization within the Fall River Formation is shallow and above the water table. Much of this shallow ore has already been exploited by historical open pit mining.

At *Dewey*, in situ resources amount to 1,535 t U, 1,270 t U of which at an average grade of 0.19% U are contained in the basal Fall River Formation and the remaining 265 t U at a grade of 0.14% U in the basal Lakota Formation. The F13 Fall River and the L2 Lakota horizons are the two most prolific uranium hosts. They contain over one-half of the total resources. Depth to the

Fall River ore is about 165 m and to Lakota ore ca. 225 m. The trend directions of these two ore zones are almost normal to each other and only locally overlap (Fig. 3.2).

3.2 Northern Black Hills, Wyoming-South Dakota

Uranium was discovered in 1952. Exploitation took place on 29 properties and lasted from 1953 through 1968. Mined deposits had resources generally from a few tonnes to a few hundred tonnes of uranium.

Production totalled ca. 1,200 t U and 2,000 t V₂O₅ and came mainly from the *Hauber* deposit in the *Hulett Creek* area (see below). Other producing properties include *TL Creek*, *Elkhorn Creek*, and *Barlow Canyon* in the wider *Hulett Creek* area, *Sunny*

Divide and *Thorn Divide* in the Carlisle area, and *Aladdin* and *Belle Fourche* in the northeastern Black Hills (Fig. 3.1). These other areas in total have produced only about 160 t U and 200 t V_2O_5 . Ore in the various mines averaged between 0.12 and 0.35% U and 0.02 and 0.38% V_2O_5 . The *Aladdin area*, South Dakota, delivered 2.7 t U and 2.7 t V_2O_5 at grades between 0.085 (*Helmer mine*) and 0.35% U (*A&H mine*) and 0.03 and 0.26% V_2O_5 (Chenoweth 1988).

Sources of Information. Bergendahl et al. (1961), Chenoweth (1988a), Chenoweth and Sharp (1970), Davis and Izett (1962), Hart (1968), MacPherson (1956), Pillmore and Mapel (1963), Robinson et al. (1964), Vickers (1957).

Geological Setting of Mineralization

Uranium occurrences are hosted in the Lakota and the Fall River Formations of the Lower Cretaceous Inyan Kara Group. According to Chenoweth (1988), uranium has been produced from the *Lakota Formation* at *Hulett Creek*, *Thorn Divide*, *Sunny Divide*, and near *Aladdin*. The *Hauber* deposit was the only one that produced ore from the Lakota Formation in the Hulett Creek area. This deposit is briefly described further below. At *Thorn Divide*, the *Homestake* and *Griffiths* deposits occur in a fine- to medium-grained carbonaceous sandstone near the middle of the Lakota Formation. The nearby *Laymon* and *Manke* deposits are in a carbonaceous, conglomeratic sandstone at the base of the Lakota Formation. Two deposits at *Sunny Divide* and three deposits northeast of *Aladdin* are hosted in carbonaceous sandstones in the basal Lakota Formation.

The *Fall River Formation*, 25–45 m thick, disconformably overlies coastal-plain sediments of the Lakota Formation and is overlain by marine deposits of the Skull Creek Shale. The Fall River Formation includes deltaic and marine facies. Deltaic facies constitute approximately 50% of the formation and consist of channel sandstone, interchannel sandstone and mudstone, and blanket sandstone that formed during erosion of abandoned deltas. Marine and marginal-marine rocks comprise offshore and lagoonal mudstone and shale, as well as bar and spit sandstone.

U–V deposits have been mined from the Fall River Formation at *Elkhorn Creek*, *Hulett Creek*, *Barlow Canyon*, *TL Creek*, and near *Belle Fourche* and *Aladdin*. The *Kay* and *Busfield* deposits at *Elkhorn Creek* occur in the upper part of the Fall River in and adjacent to an E-trending beach or barrier bar sequence. The *Ackerman* deposit, in the upper Fall River Formation, is in a northwest-trending deltaic fluvial channel. Host rocks are primarily organic rich, fine-grained sandstone interbedded with silty claystone. Six deposits on the *New Haven* claims and the two *Dennis* deposits in the *Hulett Creek area* were in the margins and basal portion of a NW-trending deltaic carbonaceous sandstone channel at the top of the Fall River Formation. The channel sandstone is about 600 m wide and 3–15 m thick, and can be traced for about 3 km (Gorman and MacPherson 1957). Deposits in *Barlow Canyon* and those southwest of *Belle Fourche* occur in a carbonaceous, fine-grained sandstone and siltstone in the

lower part of the Fall River Formation. The *Storm* deposit, at TL Creek, was hosted in carbonaceous sandstone in the top part of the Fall River Formation, and the *Helmer* deposit, near Aladdin, in carbonaceous sandstone in the lower Fall River Formation.

Mineralization, Shape and Dimensions of Deposits

In oxidized deposits, carnotite, tyuyamunite and meta-tyuyamunite are the principal ore minerals. In less oxidized ore, corvusite and rauvite are present. Pitchblende and coffinite are the main U minerals in unoxidized ores. Other uranium and vanadium minerals include autunite, uranophane, montrosite, and haggite (Hart 1968). Associated minerals are pyrite, marcasite, and calcite.

Uranium–vanadium ore bodies are tabular, lenticular masses within sandstone and conglomeratic sandstone beds, and are generally concordant with bedding. Detrital organic materials such as finely divided carbonaceous plant material, limbs, twigs, and branches are present in host rocks. Ore bodies are generally elongated parallel to the direction of sedimentation. They range in size from a single pod with a diameter of 3 m and a thickness of 0.3 m, to a body 300 m long, <225 m wide, and up to 3.5 m in thickness.

Within an ore body, the U–V minerals coat sand grains, fill interstices between grains, and are finely disseminated in organic matter. They also fill fractures and coat joints in deposits.

Tongues of hematite-stained pinkish-red sandstone are present at most deposits. This alteration is due to oxidation of pyrite in the sandstone by migrating groundwater, which remobilized some of primary, tabular ore deposits.

The *genesis of the deposits* is not yet fully understood, but two main theories have been proposed. Renfro (1969) proposed that uranium and other metals, indigenous to the Lakota and the Fall River sediments, were mobilized by oxygenated groundwater and transported downdip, where they were precipitated along a redox boundary. Hart (1968) proposed that uranium was leached by groundwater from tuffaceous beds of the Oligocene White River Group that were unconformably deposited across the eroded Black Hills uplift. Migrating groundwater carried uranium into permeable host rocks where it traveled down dip into reducing environments. Later groundwater movements remobilized and redeposited some ore elements.

3.2.1 Hulett Creek Area, Wyoming

Located at the northwestern edge of the Black Hills, about 25 km NW of the town of Hulett, the Hulett Creek area was the most productive uranium mining district of the Black Hills. Uranium was discovered in 1953, and four U–V deposits (*Hauber* and *New Haven* underground mines, *Sodak/Dennis 1 and 2* open pit operations) went into production. These deposits have produced 1,050 t U and 1,810 t V_2O_5 . The Hauber Mine alone accounted for 96% of the district's production. Ore mined at Hauber

averaged from 0.17% U and 0.18% V_2O_5 (Dennis 1) to 0.21% U and 1.38% V_2O_5 (New Haven) (Chenoweth 1988).

Geology and Mineralization

Deposits mined by open pit methods were in the Fall River Formation and were hosted by calcified and silicified sandstone lenses that contained abundant carbonaceous matter. Ore was concentrated at the margins and at the base of the sandstone and was generally oriented parallel to the lenses. Uranyl vanadates were the principal ore minerals above the water table, and pitchblende and coffinite associated with pyrite below the water table. Ore shoots ranged from about 3 to 10 m in thickness, 0.5 to 25 m in width, and 15 to 60 m in length.

3.2.1.1 Hauber Mine

The Hauber deposit, largest in the NW Black Hills, was exploited by underground workings accessed by a 116 m deep shaft. It has produced 1,010 t U and 1,570 t V_2O_5 from 1958 through 1967. Mining grades averaged 0.186% U and 0.32% V_2O_5 (Chenoweth 1988).

Sources of Information. Chenoweth 1988; and Hart 1968, unless otherwise noted.

Geology and Alteration

Ore bodies of the Hauber Mine were hosted in an ENE–WSW-oriented channel filled with fluvial sediments of the basal [Lakota Formation](#), which dip 2–5° NW and range in thickness from less than 3 m in the SW to 26 m in the NE. The channel facies comprise massive conglomeratic sandstone, sandstone, and siltstone lenses, locally interbedded with some minor shale and claystone beds. Sandstones are friable or poorly cemented with interstitial clay, pyrite, carbonate, and silica. Abundant calcite cements locally fine-grained sandstone and siltstone beds.

A NE–SW-trending tongue of pinkish-red stained sandstone occurs on the SE side of the ore trend except in the C area and the SE part of the B area, where red staining almost completely surrounds the ore pods (► [Fig. 3.3](#)). The staining is caused by hematite that coats sand grains and interstitial clay or clay balls.

The red sandstone tongue roughly coincides with thicker portions of the basal Lakota channel and probably represents the most permeable portion of the arenite horizon. It terminates some 350 m NE of the deposit, but is open to the southeast. The boundary line on ► [Fig. 3.3](#) represents the maximum extent of red staining in any one horizon, but this does not mean that the entire basal Lakota stratum is oxidized behind it. A small amount of limonitic sandstone, located near the ore trend, is included within the outline of the red sandstone.

Red staining may stop abruptly against ore or may terminate within several centimeters to about 1 m from ore. Near ore, an almost white-bleached zone and less commonly, a yellowish-brown zone of limonite staining occurs. This color change probably reflects the reducing nature within the ore body.

Mineralization

Pitchblende and coffinite, associated with vanadium minerals and pyrite, are the principal ore minerals. A corvusite group mineral coats as bluish-black substance quartz grains in various parts of the mine (Chenoweth and Sharp 1970).

The uranium to vanadium ratio of ore mined averaged 1:1.4, but ratios as great as 1:12 are known from various places throughout the mine. In situ ore grades averaged about 0.2% U, but some ore shoots had grades between 0.5 and 1% U.

Ore was hosted in carbonaceous dark grey to black sandstone of the Lakota Formation above the contact with the underlying Morrison Formation. Ore minerals were disseminated throughout the sandstone in irregular masses roughly concordant with bedding. They generally coincided with carbonaceous zones, but also impregnated more permeable rocks in scour and fill structures within arenite lenses. Although rather uncommon, small roll-shaped ore bodies were also present, particularly where small faults intersected the B and C segments of the deposit.

The deposit consisted of a series of roughly tabular ore bodies; most were situated adjacent to a fault zone. Faults also offset ore horizons. Ore bodies were enveloped in subeconomic mineralization, which is ubiquitous throughout the basal Lakota channel.

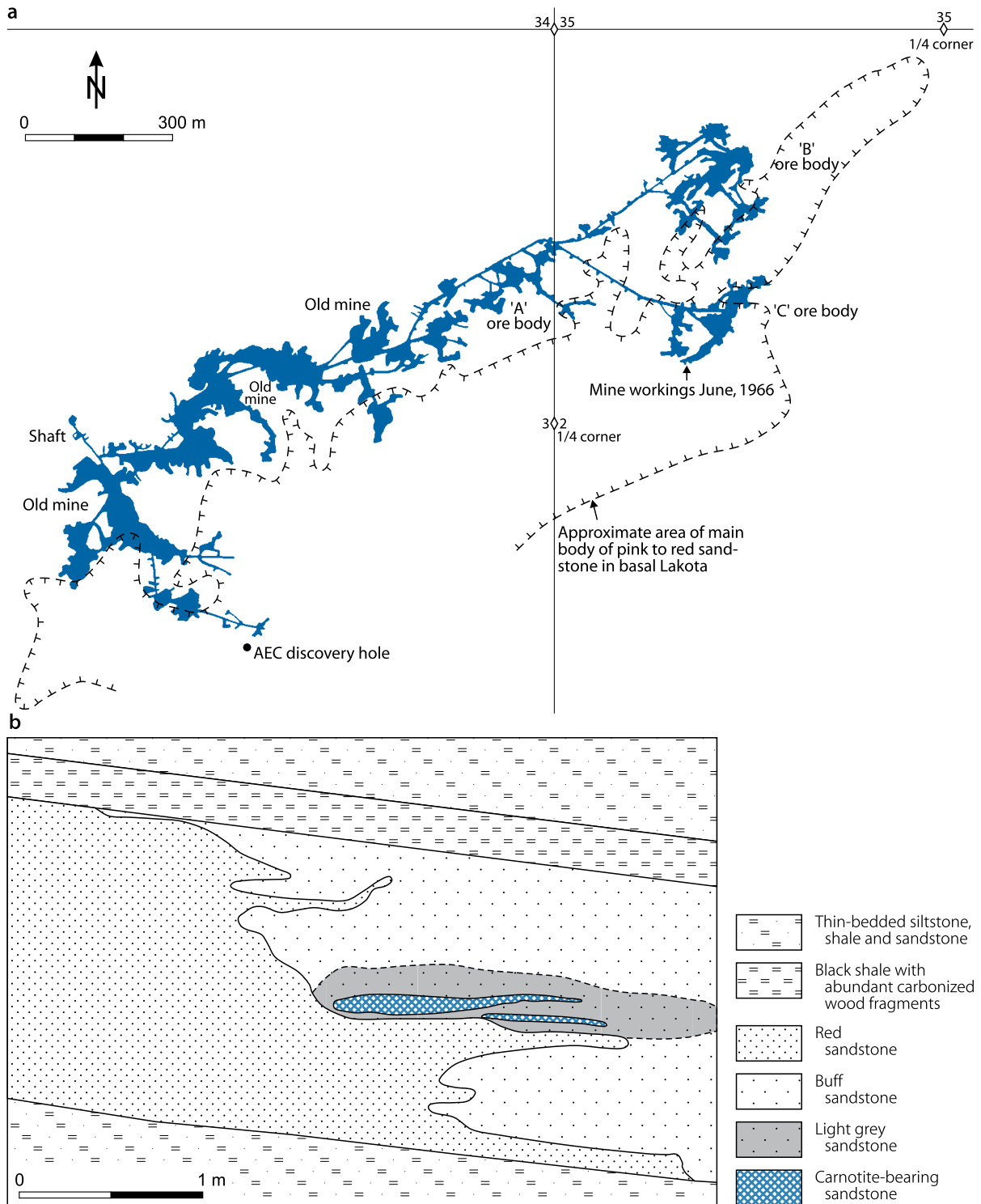
Ore bodies were located below the water table at depths between 90 and 120 m. They ranged from small pods about 3 m in diameter to a large irregular mass 300 m long and 150–225 m wide. Ore bodies averaged about 2 m in thickness with individual maxima up to 3.6 m and accumulated to combined minable thicknesses of up to 9 m.

Ore bodies were elongated in an ENE–WSW direction and, except for the C ore body, roughly paralleled the northwest flank of the distributary channel in the basal Lakota Formation. Ore pods of the C ore body were also elongated nearly parallel to the main trend, but occurred in the central part of the channel. Where the channel is less than 15 m thick, ore lodes were essentially confined to a single horizon. Their base was commonly within the basal 1.5 m of the Lakota Formation. In thicker sections of the channel, in particular in the B and C areas, ore occurred in multiple horizons with the uppermost ore located up to 25 m above the base of the formation.

Renfro (1969) suggests that the Hauber deposit was originally a rollfront type and that oxygenated groundwater redistributed uranium and vanadium to form the present tabular bodies. Chenoweth (1988) objects to this model and postulates that carbonaceous material in host rocks was the primary site of ore deposition (i.e., tabular ore was formed first), and, later, oxidizing groundwater redistributed some ore into small roll-shaped ore lodes. Compared with other sandstone-type U

■ Fig. 3.3.

NW Black Hills, (a) outline of mine workings and ore bodies of the Hauber Mine with boundary of oxidized, pink to red sandstone in the basal Lakota Formation; (b) cross-section illustrating the relationship of red and buff altered sandstone contact to carnotite mineralization in the basal Fall River Formation. (After (a) Chenoweth 1988a, (b) Vickers 1957) Society of Economic Geologists, Inc., *Economic Geology*, Fig. 4, p. 604



deposits in the western USA, the Hauber deposit resembles those of Salt Wash districts on the Colorado Plateau more than those of intermontane Wyoming Basins.

3.2.2 Carlile Area, Wyoming

This district is located about 45 km S of the Hulett Creek district. It includes four deposits in the *Thorn Divide* area, ca. 5 km E of Carlile, and two deposits in the *Sunny Divide* area further to the east (Fig. 3.1). The latter area has produced only about 1 t U and 0.3 t V_2O_5 at an ore grade of 0.18% U and 0.17% V_2O_5 . Mines in the *Thorn Divide* area have produced 112 t U and 177 t V_2O_5 at average ore grades from 0.15 to 0.23% U and 0.28 to 0.38% V_2O_5 (Chenoweth 1988). Ore was hosted in light grey to buff, friable, fine to medium grained, essentially flat-lying, locally cross-bedded and laminated Lakota sandstones. Mineralization forms

lenticular ore bodies parallel to bedding. Ore was found from near-surface to a depth of about 100 m. Near-surface mineralization consists of carnotite and tyuyamunite coating sand grains; deeper ore bodies contain pitchblende and coffinite associated with carbonaceous plant matter.

Selected References and Further Reading for Chapter 3 Black Hills

Albrethsen and McGinley 1982; Bailey and Childers 1977; Bell 1956; Bergendahl et al. 1961; Blake 1988; Chenoweth 1988; Chenoweth and Sharp 1970; Clement Jr and Bonner 2007; Davis and Izett 1962; Dodge Jr and Spencer 1977; Elevatorski 1976; Gorman and MacPherson 1957; Gott et al. 1974; Harshman 1968; Harshman and Adams 1981; Hart 1968; Hills 1977, 1979; MacPherson 1956; Page and Redden 1952; Pillmore and Mapel 1963; Renfro 1969; Robinson et al. 1964; Smith 1991, 2005; US AEC 1959; Vickers 1957; Waage 1959; and Chenoweth WL, Personal Information.

Chapter 4

Northern Great Plains

The Northern Great Plains host uraniumiferous lignite deposits in North and South Dakota and sandstone-type U deposits in Cretaceous–Tertiary basins in NW Nebraska, SE Wyoming, and NE Colorado (Fig. 1.1b).

4.1 Dakota Plains – Uraniferous Lignite Areas

The occurrence of Uraniferous lignite is widespread in the Dakota Plains north of the Black Hills extending into Canada. Lignite with better U grades, however, which has formerly been mined, is mainly confined to the *Slim Buttes* and the *Cave Hills* districts in the NW corner of South Dakota and the *North and South Belfield* areas in southwestern North Dakota. Some uraniumiferous lignite has also been recovered in the *Ollie-Carlyle* and the *Long Pine Hills* areas astride the North Dakota–Montana state border (Fig. 4.1). Total production from lignite of the Dakota Plains is about 550 t U. ERDA (1976) has estimated that the uraniumiferous lignite-hosting Fort Union Formation contains probable resources of 7,300 t U in the \$80/kg U cost category.

Sources of Information. Bailey and Childers 1977; Beroni and Bauer 1952; Chenoweth and Malan 1969; Denson and Gill 1956, 1965; Denson et al. 1959; Gill and Moore 1955; Gill et al. 1959; Harshman 1968; Karsmizki 1990; Moore et al. 1959; Murphy 2007; Noble 1973; Pipiringos et al. 1965; Towse 1957; US AEC 1959; KMG staff, personal communication.

Regional Geological Setting of Mineralization

The gently NE-dipping Paleocene *Fort Union Formation* on the southwestern flank of the *Williston Basin* is host to uraniumiferous lignites of the Dakota Plains. The Fort Union Formation consists of a thick, alternating sequence of lenticular and interfingering, dark grey to yellow sandstones, siltstones, mudstones, shales, and lignite beds of continental provenance. Three lignite-bearing members are contained in the Fort Union Formation: *Ludlow*, *Tongue River*, and *Sentinel Butte*, in ascending order. The Ludlow Member grades laterally into the marine, nonlignitic Cannonball Member. Carbonaceous shale, peaty clay, and brick-red clinker are commonly associated with lignite.

The Fort Union Formation rests upon the Cretaceous *Hell Creek Formation* (bentonitic claystone, sandstone, and lignite). It is unconformably overlain by remnants of the Eocene *Golden Valley Formation* (sandstone, mudstone, some thick lignite seams), the Oligocene *White River Group* (sandstone and bentonitic claystone of tuffaceous origin), and the Miocene *Arikaree Formation* (sandstone with a tuffaceous concretion zone near its base). The White River and the Arikaree strata probably formerly

covered most of the area. These two formations contain weakly radioactive material in tuffaceous beds.

Principal Characteristics of Mineralization, Shape and Dimensions of Deposits

Lignite beds, normally less than 1 m thick, contain uranium predominantly as a disseminated amorphous urano-organic complex, but some (sooty) pitchblende and various hexavalent U minerals have also been identified. Associated minerals and elements include molybdenum (0.04–1.3%) as jordisite or ilsemannite, arsenic (up to 3.2%), carbonate (calcite) (2–4%, rarely exceeding 6%), and some pyrite, jarosite, limonite, and gypsum. The ash content is commonly high (US AEC 1959).

Uranium-bearing lignites vary widely in texture and composition. They range from soft friable and spongy to a dense massive material with some hard woody fragments. Permeability is commonly high. Uranium content varies in a wide range, from <30 ppm to 0.5% U or more, and its distribution is irregular and spotty even within uniform lignite seams. “Minable” mineralization averages about 0.17% U in lignite beds 0.3–0.9 m thick (average 0.37 m). Higher grades averaging 0.25% U and 0.25% Mo are commonly confined to lignite less than 0.45 m thick, and about 75% of the uranium occurs in the top 5–10 cm of the mineralized bed.

Lignite containing ore-grade uranium concentrations is invariably overlain, or more rarely underlain, by porous sandstone aquifers. These sands show signs of thorough oxidation, which is thought to have resulted from through flow of oxygenated groundwater. The largest ore bodies occur below thick, massive, permeable sandstone, whereas higher clay contents in the overlying sediment generally mean lesser uranium contents in lignite.

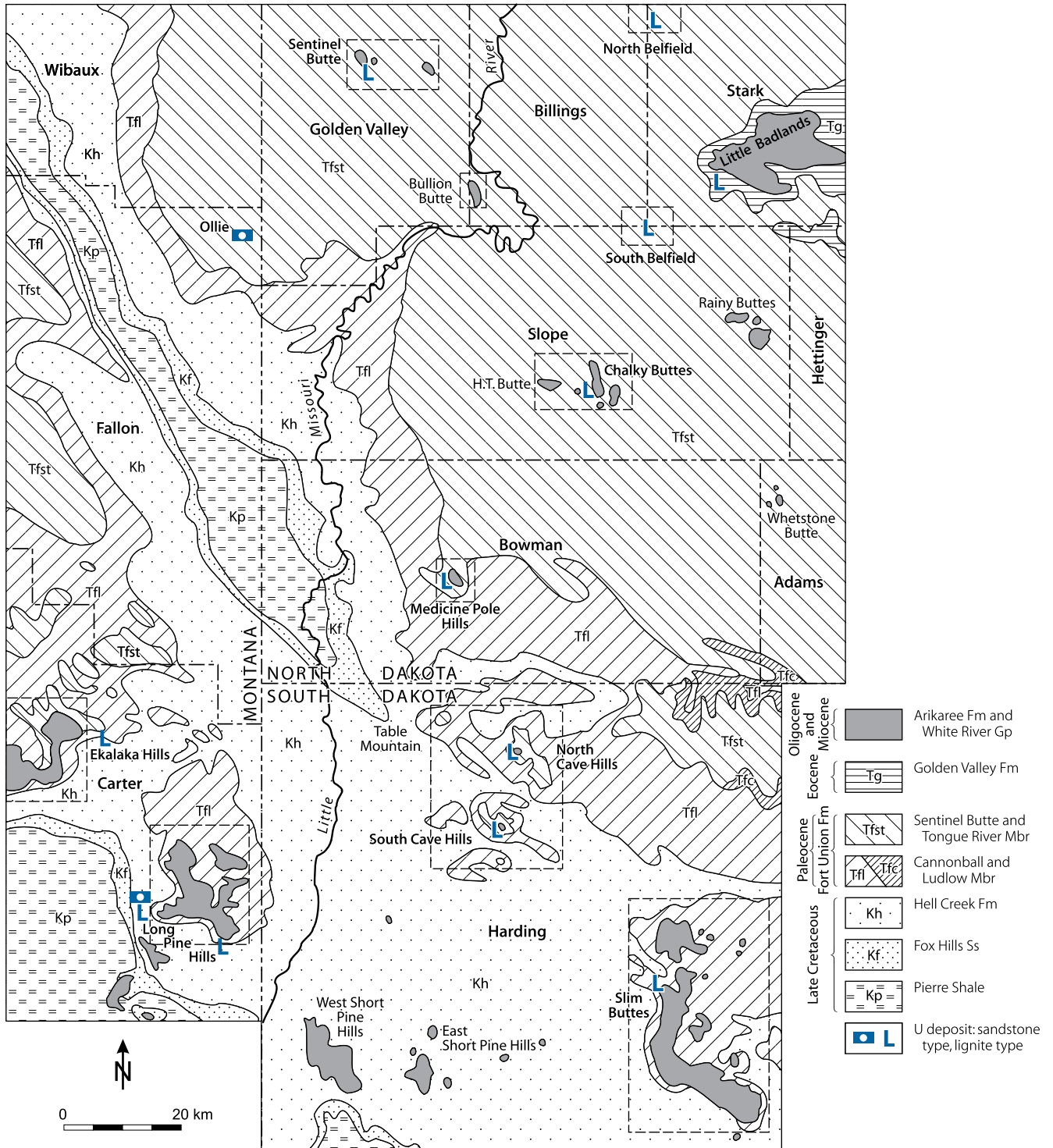
Principal Ore Controls and Metallogenetic Aspects

The position and concentration of ore-grade uranium in lignite of the Paleocene Fort Union Formation tends to be controlled by

- Weakly radioactive tuffaceous sediments unconformably overlying the lignite-bearing sequence
- Location of lignite seams or sections thereof proximal to the Eocene unconformity that marks the base of overlying sediments
- Presence of shallow, local, troughlike folds
- Adequate permeability of host lignites
- Composition of lignite (thin and more lenticular carbonaceous beds, less than 0.4 m thick, containing up to 50% ash were apparently more receptive to U concentration than thicker, more persistent, and ash-poor lignites)

Denson and Gill (1965) consider uranium of better grade deposits to be of epigenetic origin. Volcanic ash in the White River and the Arikaree Formations, which cover or once covered the area, was the source of uranium; downward percolating and laterally

Fig. 4.1. Northern Great Plains, simplified geological map showing former mining areas of uraniumiferous lignite in North and South Dakota and Montana. (After KMG map 1976, unpublished)



moving groundwater was the transporting medium, and uranium was fixed by the reducing action of carbonaceous matter in the lignite.

4.1.1 Principal Uraniferous Lignite Districts

North Dakota (Fig. 4.1): Four areas formerly produced about 250 t U from lignites in southwestern North Dakota. Largest production has come from the *South Belfield* area, followed by the *North Belfield* area. Minor amounts have been produced in the *Chalky Buttes* and the *Sentinel Butte* areas. Total uraniumiferous lignite resources in North Dakota are estimated at about 4–5 million tonnes.

Larger uraniumiferous lignite deposits are mainly in the *Sentinel Butte Member* of the Paleocene *Fort Union Formation*. Blanket-type mineralization generally has low uranium contents (<100–700 ppm U), but may have relatively uniform mineralization over large extensions. Compared to blanket-type mineralization, lenticular ore bodies are commonly irregular in shape and smaller in size, but are of higher grade ranging from <0.1 to 0.25% U.

In the *South Belfield* area, uranium only occurs in the upper 50–60 m of the *Sentinel Butte Member*. This section is about 120 m above the base of the member. U-mineralized lignite beds are 0.15–0.75 m thick. U grades vary markedly. Past production had grades from 0.08 to 0.2% U or more. Ore bodies are mostly lenticular and contain up to some 2,000 t of lignitic ore with between 1 and 5 t U.

In the *North Belfield* area, uranium is hosted by lignite and carbonaceous shale that overlies lignite. Otherwise, both geology and mineralization are similar to *South Belfield*. Mineralization in the *Chalky Buttes* area is commonly in lignite beds about 0.5 m thick, containing 30% ash and grading <0.01–0.02% U. The *Sentinel Butte* area hosts five U mineralized lignite horizons characterized by about 30% ash and 70 ppm uranium.

South Dakota: Uraniferous lignite deposits are located in the *Cave Hills* and *Slim Buttes* areas (Fig. 4.2). In the *Cave Hills* area, uraniumiferous lignite deposits are clustered in the *North* and *South Cave Hills* and in the *Table Mountain* areas. They are hosted in the *Fort Union Formation*; larger deposits in the *Tongue River Member* and smaller ones in the underlying *Ludlow Member*. The *Tongue River Member* is a sequence of massive, locally fine-bedded, sandstones interstratified with mudstone, siltstone, carbonaceous shale, and lignite. Uranium-bearing lignite beds, commonly 0.3–0.6 m thick, are within the basal part of the member and underlain by massive sandstone. In the *North Cave Hills*, grades of formerly mined lignite ranged from 0.1 to 0.34% U, but maximum values were reportedly up to 2.4% U at *South Riley Pass*. In the *South Cave Hills*, uranium occurs in a 0.5–0.6 m thick carbonaceous claystone layer, which contains abundant fluorapatite and which lies above a U-barren lignite seam, about 25–30 m below the top of the *Ludlow Member*. Some production averaged 0.3% U.

The *Slim Buttes* area contains uraniumiferous lignite in the *Ludlow Member*. Several mineralized beds 0.3–3 m thick are in

the upper section of the member in the northern part of the district, whereas in the southern part, uraniumiferous lignite occurs up to 1 m thick in the basal portion of the member. Better grade mineralization, in excess of 0.1% U, is restricted to lignite beds 0.3–1 m thick. The largest size and highest grade are found along the axis of a shallow trough where two or three beds, up to 0.6 m thick, contain between 0.04 and 0.28% U. Small tonnages of lignite mined averaged 0.28% U and 0.04% V_2O_5 . Some uranium mineralization occurs in sandstone of the *Ludlow Member*.

Southeastern Montana (Fig. 4.1): At *Ollie*, near the state border with North Dakota, the *Fort Union Formation* hosts uranium at the base of a micaceous sandstone that grades into lignitic shale. At *Long Pine Hills* in the SE corner of the state, lignitic beds, from 0.3- to 1.5 m thick, in the Paleocene *Fort Union Formation* and the Cretaceous *Hell Creek Formation* contain between 0.003 and 0.012% U. At *Ekalaka Hills*, NW of *Long Pine Hills*, lignite and carbonaceous shale beds, from 0.5- to 2.5 m thick, average 0.004% U.

4.2 Nebraska Plains, Crawford Area

The Crawford area is located in the northwest corner of Nebraska and includes two rollfront uranium deposits, *Crow Butte* and *Big Red*.

4.2.1 Crow Butte

The *Crow Butte* deposit is situated 6 km SE of the small town of *Crawford* (Fig. 4.3). Discovered in 1980, original in situ resources are estimated at over 12,000 t U at an overall grade of about 0.21% U (Collings et al. 1996). U recovery by ISL techniques began in 1991 with production to date (2008) of 4,700 t U.

Sources of Information. Catchpole and Kirchner 1993; Collings et al. 1996; Collings and Knode 1984; Gjelsteen and Collings 1988; Hansley and Dickinson 1990; Hansley et al. 1989; and Catchpole G and Kirchner G 2006, personal communication.

Geological Setting of Mineralization

Uranium ore bodies at *Crow Butte* are confined to the *Chadron Sandstone* unit of the Oligocene *White River Group* (Figs. 4.4 and 4.5). This group forms the basal unit of the Tertiary sequence at the northern margin of the *Cheyenne Basin* in NW Nebraska. According to Collings et al. (1996) the Tertiary sequence in the *Crow Butte* area comprises the following lithostratigraphic units – in descending order (in brackets local mining terms; stratigraphy after Swinehart et al. 1985).

Miocene Arikaree Group, 0–120 m thick: This group includes three fluvial sandstone units, which form the E–W-oriented *Pine Ridge escarpment* in northwest Nebraska, but are eroded in the deposit area.

Fig. 4.2.

Northern Great Plains, (a) block-diagram from Little Badlands to Slim Buttes in SW North Dakota and NW South Dakota (location see Fig. 4.1) illustrating schematically the stratigraphic distribution of uraniumiferous and barren lignite seams; (b) block-diagram of Slim Buttes documenting the restriction of U-enriched lignite to the pre-Oligocene unconformity; (c) bore hole log attesting to the typical preferential concentration of uranium in the top part of a lignite seam. (After Denson and Gill 1965)

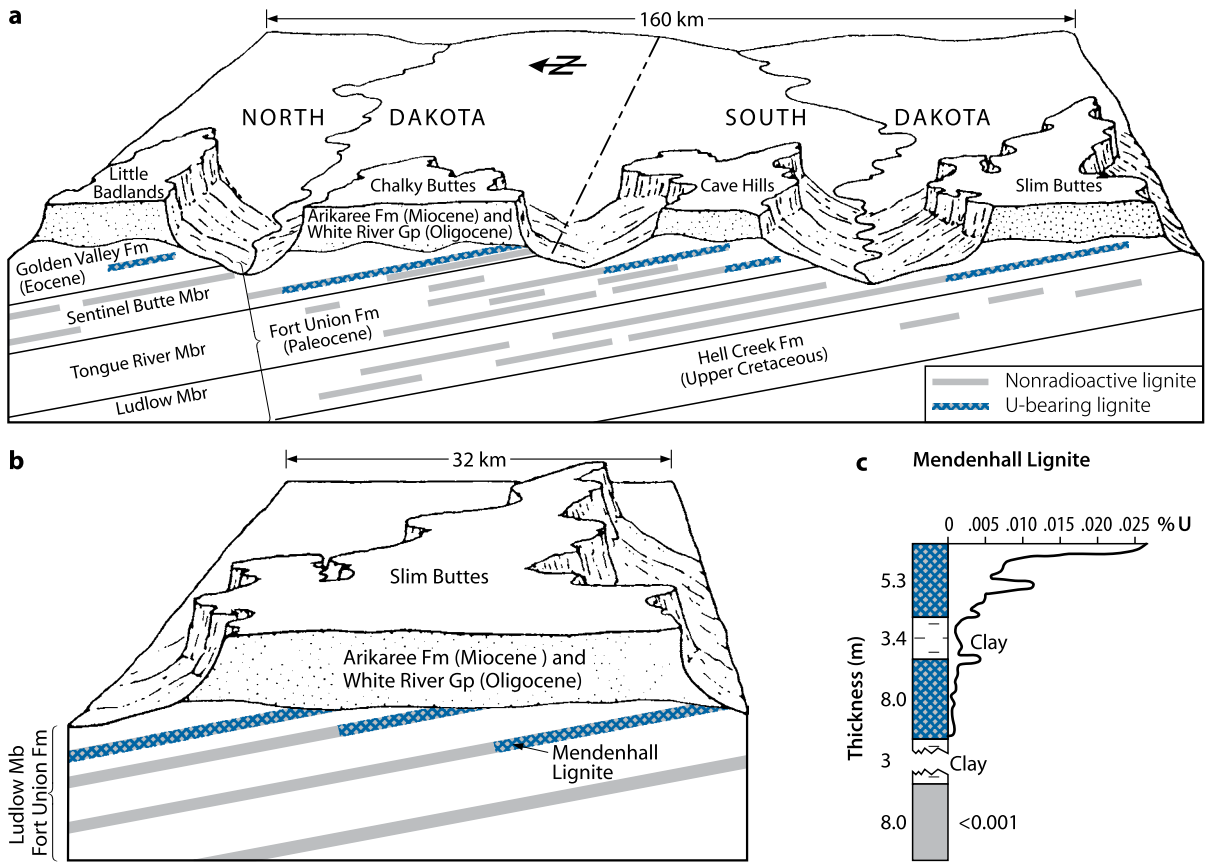
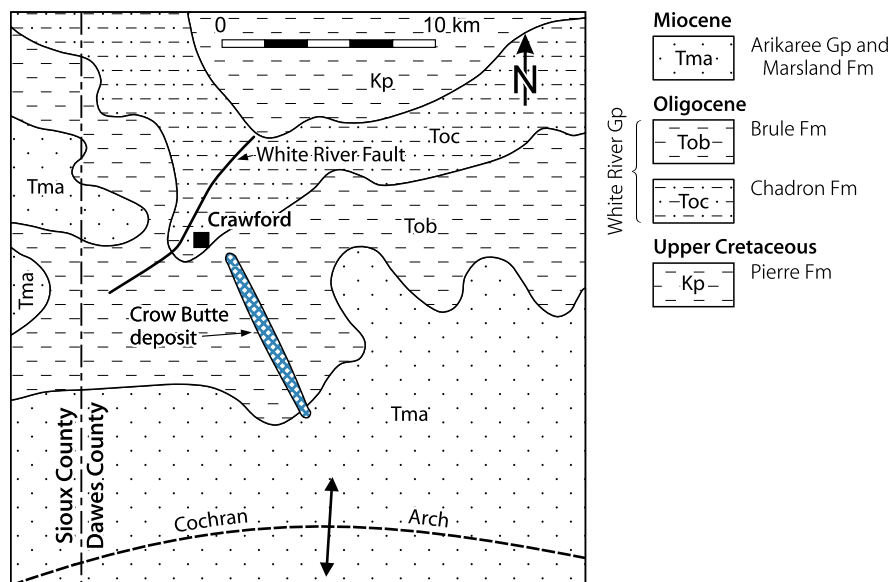


Fig. 4.3.

Crawford area, NW Nebraska, simplified geological location map of the Crow Butte U deposit. (After Collings et al. 1996)



■ Fig. 4.4.

Crow Butte deposit, litho-stratigraphic column. (After Collings et al. 1996 based on Swinehart et al. 1985)

Epoch	Gp	Formation	Member	Thickn. (m)	Profile	Lithology
Miocene	Arikaree	Monroe Creek – Harrison		120–180		Brown to buff, frequently thin, well cemented, hard sandstone stringers, pipy concretions interbedded with fine- to medium-grained loosely cemented sandstone
			Gering			
Oligocene	White River	Brule	Brown Siltstone	90–120		Buff siltstone, fairly massive, occasional ash layers, sandy near upper contact
			Whitney			
			Orella			
		Chadron	Upper	24–45	Green-grey siltstone and clay, massive, occasional limestone and gypsum	
			Middle	6–30	Light grey to light green bentonitic clay, frequently red clay at base	
			Basal (Chadron Ss)	0–30	Light grey to bright green arkosic sandstone, predominantly quartz with green and grey feldspar, trace chert and pyrite, local conglomerate with quartz pebbles and chalcedony, interbedded clay beds and galls	
Eocene?	Paleosol		0–3		Reddish-pink and yellow-brown mottled clay	
Cretaceous		Pierre Shale		360–450		Dark grey to black, non-calcareous shale

Oligocene White River Group, 60–300 m thick, separated into the Brule Formation, which is the outcropping formation throughout most of the area, and the Chadron Formation. Regionally and within the Crow Butte area, strata of these two formations dip gently at about 0.5–1° S.

Upper Brule Formation/Brown Siltstone Member and Whitney Member (Upper Monitoring Unit), 0–120 m thick: Primarily buff to brown siltstones with some small sandstone intercalations of limited lateral continuity.

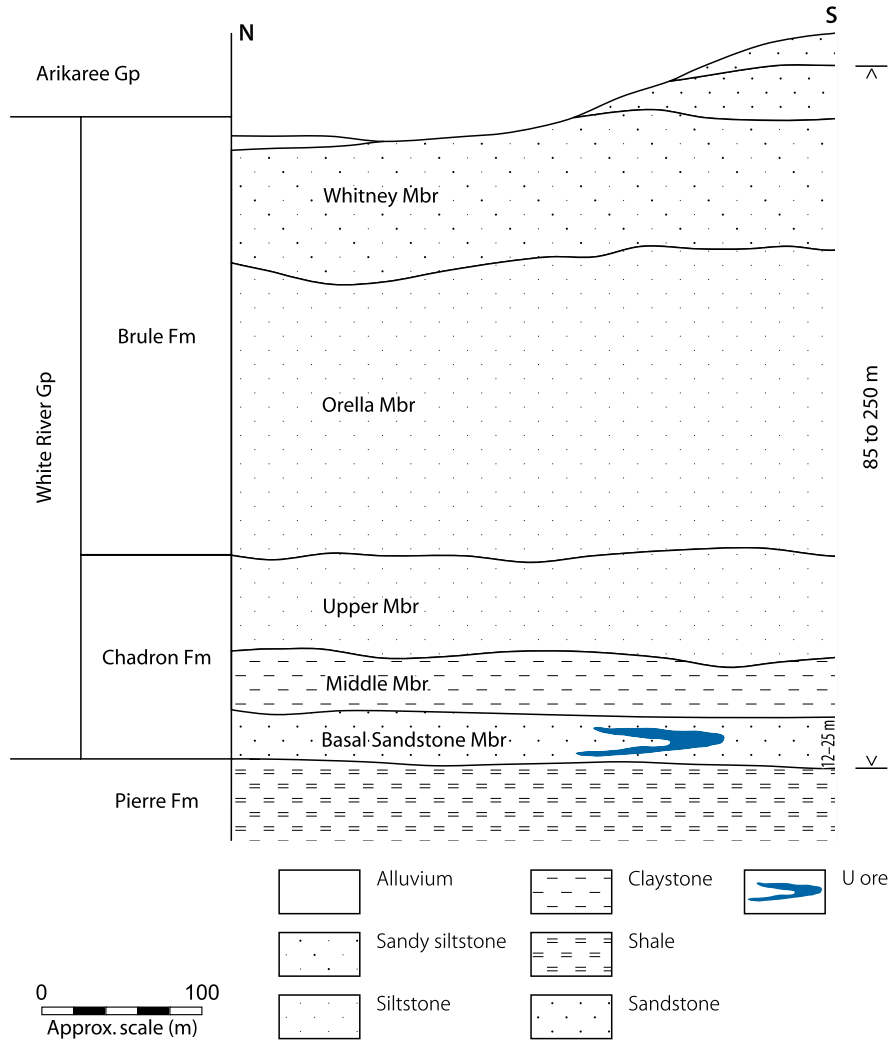
Lower Brule Formation/Orella Member – Upper Chadron Formation, 60–150 m thick (Upper Confinement Unit): The lower part of the Brule Formation and the upper part of the Chadron Formation are combined within the Crow Butte area for Brule sediments lie conformably on top of and grade transitionally into the Chadron facies. Together they form an

aquiclude that acts as the upper confinement of the mineralized Chadron Sandstone. The lower section of the Brule Formation consists mainly of siltstone and claystone with infrequent, fine- to medium-grained sandstone channels of limited lateral extent. The upper section of the Chadron Formation is a light green-grey bentonitic clay grading downward to green and frequently red clay. Red clay primarily comprises montmorillonite and calcite and contains grey-white bentonitic clay interbeds.

Chadron Formation with Chadron Sandstone at its base (Mining Unit): The Chadron Sandstone forms an extensive fluvial sandstone system at the base of the Tertiary sequence. It averages about 12–25 m in thickness within the Crow Butte area (Fig. 4.6), but reaches 30 m or more toward the west and pinches out to the northeast. Uranium-hosting sand is water saturated and forms a regionally extensive confined aquifer that

Fig. 4.5.

Crow Butte deposit, schematic N-S section across the deposit. Note that the U-hosting basal Chadron Sandstone Member may contain from one to five stacked ore rolls. (After NUEXCO 1983)



produces artesian (flowing) conditions where local topography is depressed.

The Chadron Sandstone is a coarse-grained arkosic sandstone with numerous clay galls up to 5 cm or more in diameter and frequent interbedded thin silt and clay lenses of varying thickness and continuity. Clay beds and lenses often separate the Chadron Sandstone into fairly distinct subunits. A persistent clay horizon typically brick red in color generally marks the upper limit of the Chadron Sandstone, but occasionally the Chadron Sandstone grades upward into fine-grained sandstone with varying amounts of interstitial clay material. Mineral constituents of the sandstone include 50% monocrystalline quartz, 30–40% plagioclase and K-feldspar; the remainder being polycrystalline quartz, chert, chalcedonic quartz, various heavy minerals, and pyrite. Clay minerals (kaolinite, montmorillonite, hydromica-illite, chlorite) amount to about 1% or less of rock volume (Collings et al. 1996).

Hansley et al. (1989) describe the ore-hosting sandstone as a coarse-grained, tuffaceous, arkosic litharenite composed of poorly

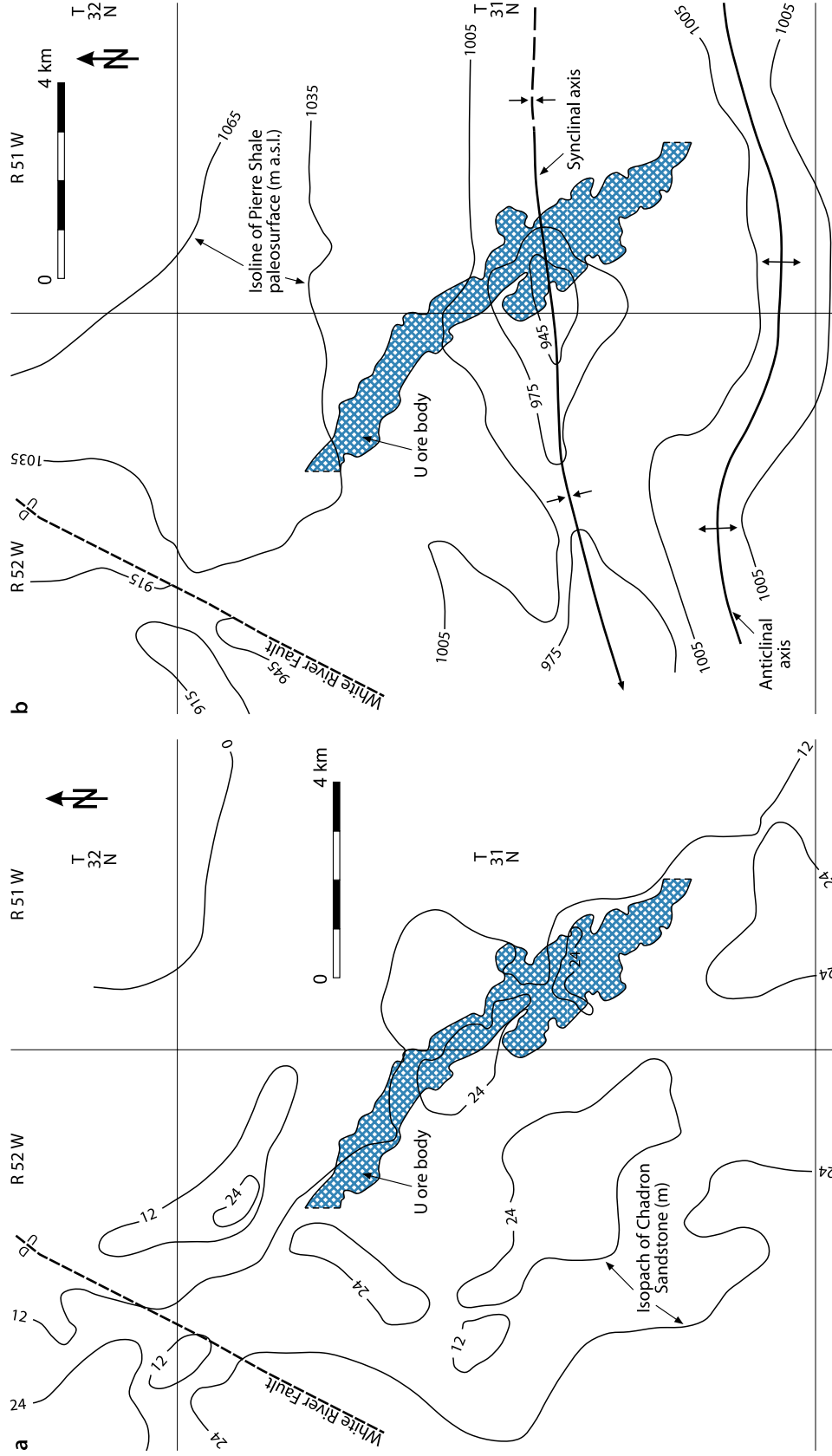
sorted, angular quartz, plagioclase, and K-feldspar grains, and igneous rock fragments that are loosely packed in a vitric matrix dominated by rhyolitic volcanic ash. Heavy minerals include garnet, ilmenite, magnetite, tourmaline, and zircon with minor amounts of apatite, biotite, epidote, and staurolite. Hansley and Dickinson (1990) note that fresh glass shards and feldspar grains along with minor authigenic smectite/illite (>90% expandable) attest to very limited diagenetic alteration.

Eocene Paleosol, <3 m thick: Veneer of reddish pink and yellow-brown mottled clay, locally present on the surface of the Pierre Shale.

Cretaceous Pierre Shale, 450 m thick (Lower Confinement Unit): Widespread, essentially impermeable, dark grey to black marine shale. Erosion had greatly reduced the thickness of this unit prior to Oligocene sedimentation and generated a major unconformity with considerable paleotopography.

Figure 4.6b illustrates the erosional paleotopographic surface of the Pierre Shale prior to deposition of the Chadron Formation and some current features of folding and faulting,

Fig. 4.6. Crow Butte deposit, (a) generalized isopach map of the Chadron Sandstone unit showing the differential thickening of this unit from NE to SW; (b) generalized isoline map of the paleosurface morphology of the Cretaceous Pierre Shale and major structural features with projected position of the deposit in the overlying Chadron Sandstone. (After Collings et al. 1996)



which evolved after deposition of the Chadron Formation. No significant faulting is present in the deposit. A major fault, the NNE–SSW-oriented White River fault, trends along the northwest margin of the area, about 2.5 km NW of the northern end of the wellfield. It has a vertical displacement of 60–120 m with the upthrown block on the south. The fault cuts both the Chadron and Brule formations suggesting a post-Oligocene age. A synclinal structure strikes E–W through the Crow Butte area and plunges west. An associated E–W-oriented anticline trends subparallel to the Cochran Arch through the southern part of the area (DeGraw 1969).

Mineralization

Coffinite (and pitchblende?) associated with Fe sulfides form the ore. They occur disseminated in the matrix of the host sandstone (Hansley et al. 1989). The organic content of the Chadron Sandstone is very low, ranging from 0.02 to 0.20% (Gjelsteen and Collings 1988). Hansley and Dickinson (1990) state that the highest U concentrations occur in the clay fraction of the sandstone matrix. Uranium is present as submicroscopic coffinite crystals, up to 2 μm in length, and in the amorphous matrix with Fe, P, Si, V, Ca, and Al. Authigenic pyrite and marcasite are abundant and are closely associated with coffinite. Tyuyamunite, metatyuyamunite, carnotite, and zippeite occur in localized oxidation zones.

Mineralization is of typical rollfront type controlled by a redox front system about 10 km long and up to 900 m wide hosted in the highly permeable Chadron Sandstone aquifer with distinct shale/clay confinement beds above and below (Figs. 4.4 and 4.5). Ore bodies, at any location, occur in one to five horizons. The ore thickness ranges from 1.5 to 4.5 m and the depth to ore bodies from the surface ranges from 85 to 250 m.

Metallogenesis of Crow Butte ore is thought to be similar to that of rollfront deposits in Wyoming Basins. Rhyolitic volcanic ash in the White River Group was probably the source of uranium. H_2S or Fe sulfides formed by sulfate-reducing bacteria are postulated to have provided reducing conditions for precipitation of uranium. Since oil and gas fields occur in the general area of Crow Butte, it would be of interest to see whether an influx of oil and/or gas like methane into Chadron sands may have played a role in forming favorable reducing conditions as, e.g., in South Texas U deposits.

4.3 Denver–Julesburg Basin Colorado–Wyoming–Nebraska

The Denver–Julesburg Basin extends from the Colorado Rocky Mountains northeastward through northeastern Colorado and southeastern Wyoming into western Nebraska. The southern portion of this basin is occupied by the Denver Basin and, separated by the Greeley Arch, the northern portion by the Julesburg basin. The latter is mainly in Wyoming and is also referred to as Cheyenne Basin. The Hartville Uplift to the north separates the Cheyenne Basin from the Powder River Basin (Fig. 4.7).

Except for *Centennial*, mostly small and low-grade roll-type U deposits such as *Grover*, *Keota*, and others containing a few tonnes to several hundreds of tonnes uranium are located in Weld County in northwestern Colorado and adjacent areas (Fig. 4.8). They are found as far north as Goshen Hole, Wyoming, which is a “geomorphic basin” within the Cheyenne Basin. Total resources of the Denver–Julesburg Basin are reportedly on the order of 5,000 t U.

Sources of Information. Bonner et al. 1982; Childers 1974; Ethridge et al. 1979; Reade 1976, 1978; Kirkham et al. 1980; Voss and Gorski 2007; Weimer 1973; and Bonner JA, Pool TC, and Voss WC, personal communication 2008.

Regional Geological Setting of Mineralization

The Weld County deposits are situated on the western and southern flank of the *Julesburg/Cheyenne Basin*, to the north of the Greeley Arch. The Julesburg Basin is bounded on the south by the Greeley Arch, on the west by the Colorado Front Range, on the northwest by the Hartville Uplift in Wyoming and on the east and northeast by the Chadron Arch in Nebraska (Fig. 4.7). The basin is filled with Cretaceous and Tertiary sediments, with Quaternary deposits on top. The Cretaceous formations include, from oldest to youngest, the *Pierre Shale*, the *Fox Hills Formation* (or *Fox Hills Sandstone*), and the *Laramie Formation* (equivalent to the Lance Formation in Wyoming) (Fig. 4.9).

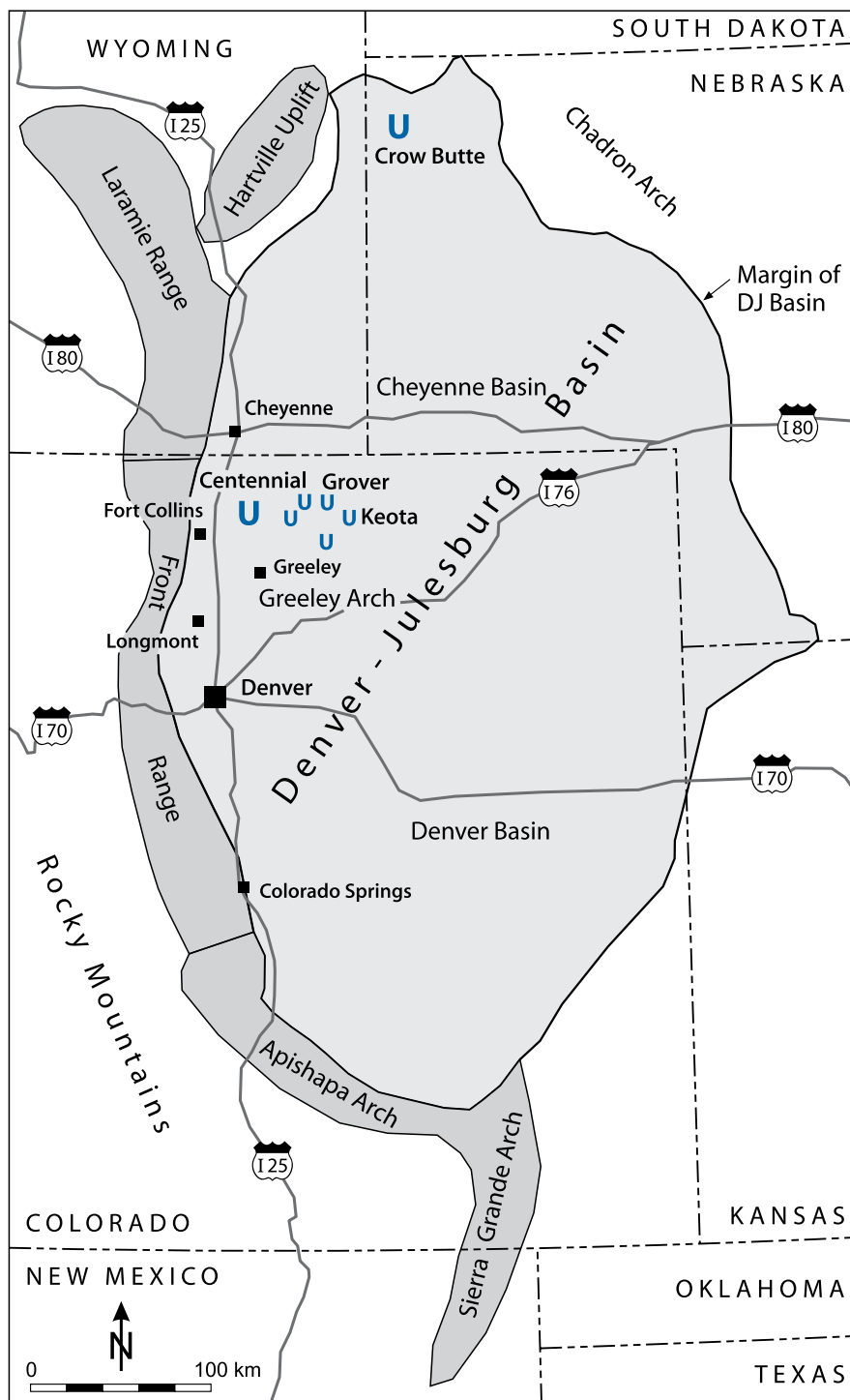
Along the western edge of the basin, the Cretaceous strata dip up to 5° E but flatten toward the east, with the basin axis trending generally north–south. Along the southern and eastern flanks of the basin, the formations are inclined 1° or less to the north and west, respectively.

Uranium deposits in Weld County occur in arenites of the Fox Hills and the Laramie Formations. The *Fox Hills Formation*, as much as 100 m thick, consists of several sandstone and local conglomerate horizons separated by carbonaceous shale. Sandstone horizons range from less than 1 to 10 m or more in thickness. Thin lenticular beds of lignite are locally intercalated. Host sandstones are grey to white, commonly medium to fine grained, moderately cemented, siliceous, quartzose to feldspathic, micaceous, and contain carbonaceous debris. Marine fossils occur in some sandstones. Fox Hills sediments were laid down in a littoral environment, transitional upward from marginal marine/delta front to barrier island conditions of sedimentation.

The *Laramie or Lance Formation*, up to 480 m thick, conformably overlies the Fox Hills Sandstone. It consists of shales, siltstones, and mudstones, and large channel arkosic sandstones. Lignite seams occur in the lower section of the formation. Sediments of the lower section were deposited in deltaic fluvial, lagoonal, and interdistributary environments, and those in the upper section in alluvial fluvial and overbank mudflat environments. Arenite horizons range in thickness from less than 1 to 30 m and consist of cross-bedded sands with slump features that were apparently deposited in major stream channels with moderate to low gradients. Sandstones are medium to fine grained, quartzose to feldspathic, micaceous, pyritic, and contain

■ Fig. 4.7.

Denver–Julesburg Basin and surrounding terrane, simplified map showing major geomorphological elements and apparent restriction of known U deposits in the Julesburg (or Cheyenne). Basin located to the north of the Greeley Arch in north-eastern Colorado. (After Voss and Gorski 2007, and Bonner J, personal communication 2008)

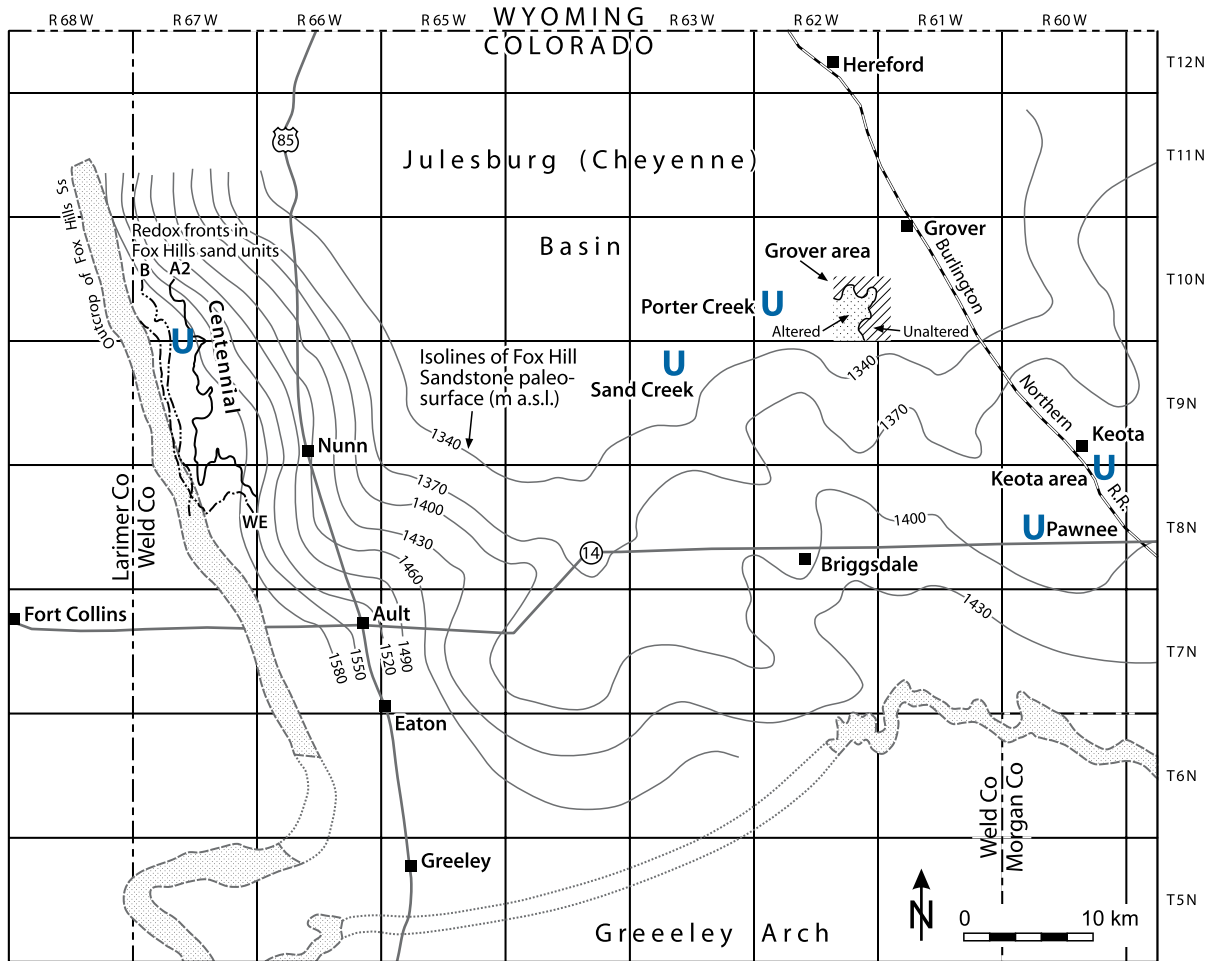


substantial amounts of fine-grained carbonaceous matter. These sediments derived from a source to the west and were deposited under continental or marginal marine conditions by eastward flowing streams. The environment of deposition, paleo-climate, and general character of host sandstones resemble to some extent those in the Black Hills.

The Oligocene *White River Group* unconformably overlies most Cretaceous rocks in the Weld County area, but a large part of it has been deeply eroded with only isolated remnants remaining. This group is divided into the *Chadron* and *Brule formations* in the Denver–Julesburg Basin. These two formations comprise coarse-grained to pebbly arkosic sandstones deposited

Fig. 4.8.

Denver–Julesburg Basin, Weld County. Most known U deposits occur in this area on the western slope of the Julesburg (or Cheyenne) Basin and northern slope of the Greeley Arch. (After Voss and Gorski 2007, and Bonner J, personal communication 2008)



in channels that locally cut into Cretaceous rocks. Siltstones and mudstones rest upon sandstone units. Tuffaceous material is abundant in all Oligocene rocks. Except for the basal part of the Chadron Formation, the *White River* rocks are of low permeability.

The early Miocene *Arikaree Formation* disconformably overlies, or at one time overlay, the *White River* sediments. It consists of fluvial sand, gravel, and clay with much tuffaceous material.

Quaternary arkosic gravel and sand deposits, which apparently derived from the *White River* and *Arikaree* groups as well as from granitic highlands to the west cover a large part of the present surface and fill large, wide, NW–SE-trending channels.

Host Rock Alteration

Oxidation is the most prominent alteration feature. It forms altered tongues in permeable sandstone beds extending down-dip from the outcrop or paleo-outcrop. Limonite-staining as a result of oxidative pyrite decomposition is the most visible

alteration product. Hematite occurs locally and generally several hundred to few thousand meters updip behind ore bodies. Plagioclase is altered by moderate to strong argillization. In outcrop, most of the sandstones of the *Fox Hills* Formation exhibit trace to pervasive limonite staining of various shades of yellow and orange. Red hematite staining is less common and occurs as scattered streaks in most outcrops. Generally, the more porous and thicker the sandstone, the more pronounced the alteration.

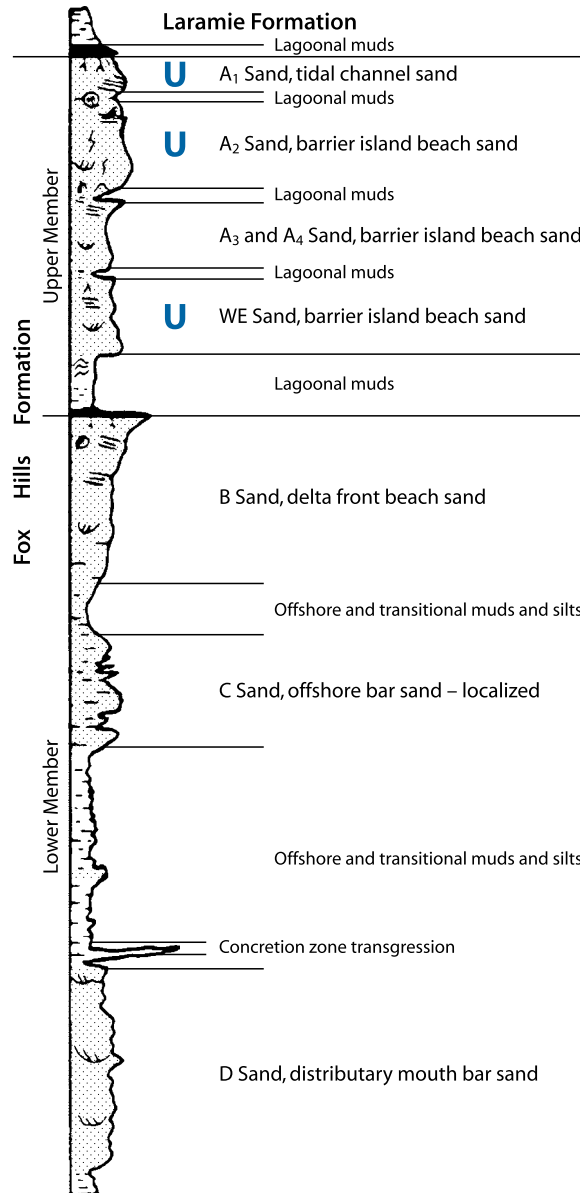
Mineralization

Pitchblende and coffinite are the principal U minerals. They are accompanied by pyrite and marcasite. Vanadium and molybdenum minerals occur in low amounts.

Deposits are of roll-type composed of single and simple to complex, or multiple and stacked rolls. Ore rolls occur adjacent to the edges of tongues of altered, iron oxide-stained sandstone. Ore-hosting sandstone is generally fine grained, moderately well sorted, of feldspathic to arkosic composition, with varying

■ Fig. 4.9.

Denver–Julesburg Basin, Weld County, generalized litho-stratigraphic column of the Fox Hills Formation on the western flank of Julesburg Basin. (After Voss and Gorski 2007 based on Rocky Mountain Energy Co. 1982)



amounts of volcanic, igneous, and sedimentary rock fragments. Chert is relatively abundant as small clasts. Pyrite occurs as small spherical aggregates in unoxidized sandstone. More specific features of selected uranium deposits are described further down.

Metallogenetic Aspects

Childers (1974) relates the mineralization to an extensive erosional unconformity between the Laramie (Lance) Formation and the overlying Brule and Chadron Formations of the White River Group. In the Goshen Hole area, which is north of, but geologically similar to Weld County geology, the Chadron Formation rests upon beveled edges of the Laramie Formation

and in places channels filled with conglomerate of the Chadron Formation are incised into the Laramie Formation. There is alteration but no mineralization in the lower Chadron channels, but mineral deposits occur where alteration solutions migrated from Chadron sediments downdip into the reducing environment of Laramie or Fox Hills sandstones.

Reducing agents were provided by numerous plants and shallow-sea animal remains within, and lignite in several layers overlying and underlying the uranium host sandstones (Voss and Gorski 2007).

The most likely source of uranium is seen in tuffaceous material in the Chadron and Brule Formations, which overlie or once overlie the area. The age of mineralization has not been determined, but it is reasonable to assume that mineralization was formed contemporaneously with that in the Wyoming

Basins, i.e., in late Eocene to middle to late Oligocene time. Some later modification of deposits and re-reduction of the oxidized sandstone may be related to the present hydrologic system.

4.3.1 Selected Uranium Deposits in the Cheyenne Basin

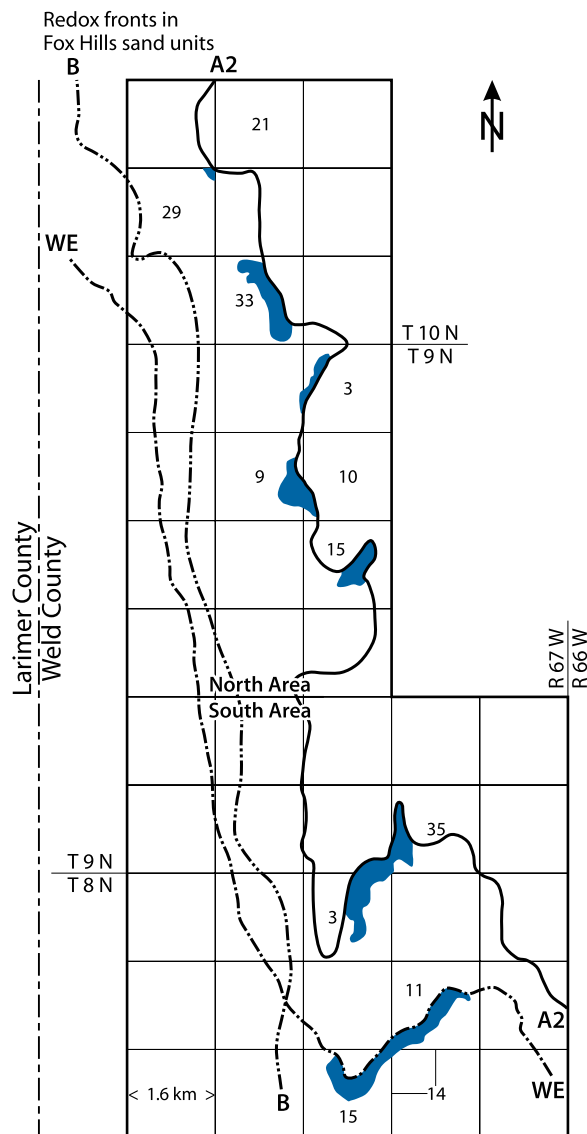
Centennial: As described by Voss and Gorski (2007), this deposit was discovered in 1974 in Weld County, approximately 20 km NE of Fort Collins, about 20 km south of the Colorado–Wyoming state line (Fig. 4.8). It is situated within the Cheyenne Basin and contains seven distinct roll-type uranium deposits with inferred in situ resources totaling almost 3,800 t U at an average grade of 0.08% U.

Uranium mineralization is hosted in sandstones of the *Late Cretaceous Fox Hills Formation*. On the western flank of the Cheyenne Basin, this formation can be separated into an upper and a lower member based on the depositional environment (Fig. 4.9). The upper member includes – from top to bottom – the A1, A2, A3, A4, and WE sand horizons and is thought to have been deposited in a barrier-island tidal-inlet terrane. The lower member includes the B, C, and D horizons.

Regional oxidation tongues exist in several separate sand units within the Fox Hills Formation. Redox interfaces along the downdip edge of these alteration tongues extend for at least 50 km in length in the Centennial area and are found throughout an area of more than 130 km². Uranium deposits occur discontinuously along redox boundaries of these systems and consist of ore bodies in juxtapositioned sand horizons (Figs. 4.10 and 4.11).

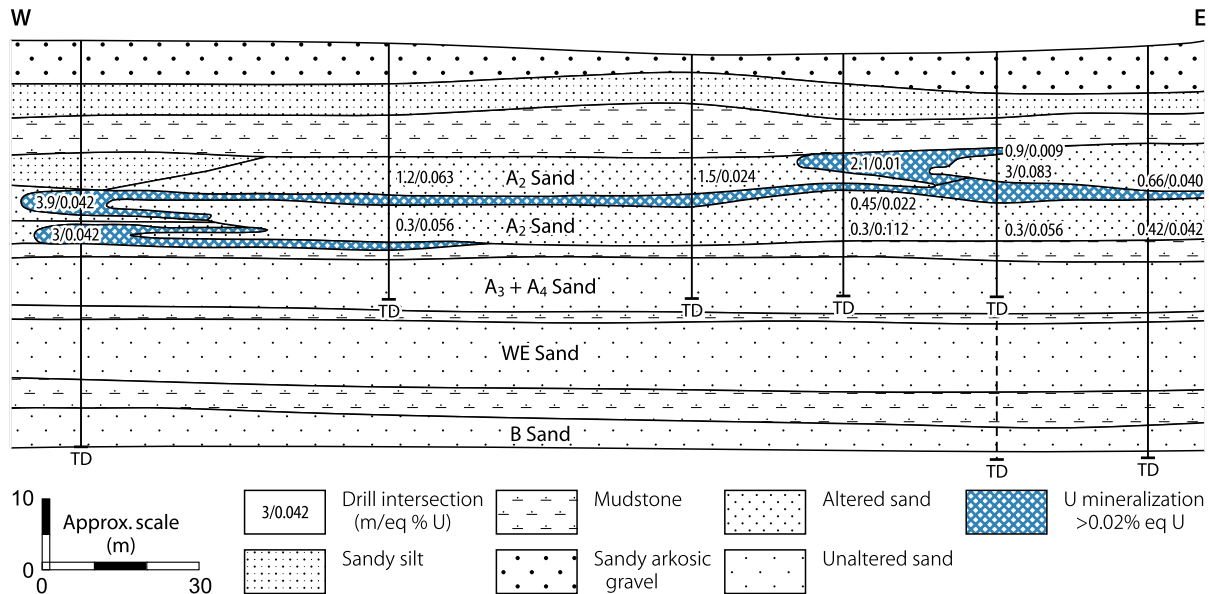
Fig. 4.10.

Centennial area, Weld County, location of uranium deposits in Upper Cretaceous Fox Hill Formation. (After Voss and Gorski 2007, and Bonner J, personal communication 2008)



■ Fig. 4.11.

Centennial area, Weld County, W–E cross-section showing shape, position, and grades of uranium ore bodies in the A2 sand horizon of the Upper Cretaceous Fox Hill Formation. (After Voss and Gorski 2007, based on Rocky Mountain Energy Co. files, and Voss WC, personal communication 2008)



At Centennial, only the A1, A2, and WE sands of the upper member host uranium ore while no economic uranium mineralization was found in the A3 and A4 sands or in the lower member. The same is true for the Laramie Formation, although redox fronts exist within this formation.

Seven distinct deposits are delineated at Centennial located in two areas (► Fig. 4.10). The *northern area* (also referred to as *Indian Springs*) hosts four deposits in the A2 sand at depths from 75 to 180 m, and the *southern area* contains three deposits at shallower depths from 25 to 38 m in the A1, A2, and WS sand horizons. Individual deposits range from some hundred meters to 2 km or more in length, and from about 15 to over 60 m in widths. The thickness of high uranium concentrations varies between 0.3 m in limbs and 3 m or more in rolls. Ore bodies in the northern area average 2.7 m and in the southern area 2.6 m in thickness. Tenor of uranium mineralization may range from minimal to a few percent at any point within an ore body and averages about 0.07–0.08% U.

At the shallow south end of Centennial, recent exposure to surface oxidation has affected previously formed uranium rollfronts and has partially remobilized mineralization resulting in radiometric disequilibrium and formation of tyuyaminite and metatyuyaminite.

Based on cutoff factors of 0.017% U and a GT factor of 0.2 (% U₃O₈ times feet), Voss and Gorski (2007) report resources totaling 1,480 t U at an average grade of 0.072% U for the four deposits in the northern area. Resources in the southern area

total 2,265 t U at an average grade of 0.084% U. They are contained in one deposit with 880 t U in the A1 + A2 sand horizons, and another deposit with 1,385 t U in the WE sand. A third deposit is located close to these two deposits.

Other reported deposits in Weld County include the following (possibly leachable resources from Pool TC, personal communication, geological data from Reade 1978 and Kirkham et al. 1980):

Keota, located 65 km east of Centennial, is hosted in the Fox Hills Formation. Possibly in situ leachable resources amount to ca. 690 t U. Grades range from 0.04 to 0.16% eq.U averaging 0.07% eq.U. Mineralization occurs at depths from about 80 to 100 m and ranges from 1.35 to 2.9 m in thickness.

Grover, discovered in 1970, lies approximately 55 km east of Centennial and about 5 km SW of the settlement of Grover. Possibly leachable resources are estimated at ca. 460 t eq.U at a grade of 0.05% eq.U contained at a depth of about 60–105 m in well-defined, N–S-trending channel sandstones of the Grover Sandstone/Laramie Formation, 7.5–37.5 m thick.

Buckingham also known as **Pawnee**, discovered in 1971, is located some 20 km SSE of the Grover deposit and about 5 km SW of the settlement of Keota. It is hosted in the upper part (Pawnee Sandstone) of the Fox Hills Sandstone in an E–W-oriented channel. Buckingham was/is subdivided into several properties that contained the following estimated resources: North Buckingham: about 285 t U at grades ranging from 0.055 to 0.1% eq.U, averaging 0.05 eq.U located at a depth of ca. 65 m

and ranging from 1.15 to 2.2 m in thickness. South Buckingham: about 390 t U at grades ranging from 0.039 to 0.53% eq.U, averaging 0.05 eq.U located at a depth of ca. 25 m and ranging from 2.4 to 3.5 m in thickness.

Porter Creek lies a few kilometers due W of Grover and contains possibly leachable resources of about 210 t U at grades ranging from 0.046 to 0.53% eq.U, averaging 0.07 eq.U. Mineralization is situated as much as 45 m deep.

Sand Creek, located ca. 15 km SSW of Grover, occurs in a well-defined, N–S-trending channel filled with Sand Creek Sandstone of the Laramie Formation, about 300 m above the top of the Fox Hills Sandstone. The rollfront is narrow, commonly less than 15 m wide, but ore grades are unusually high with drill intercepts of as much as 0.35% U and an average of 0.18% U. Resources are estimated at about 60 t U (Kirkham et al. 1980).

Selected References and Further Reading for Chapter 4 Northern Great Plains

For details of publications see Bibliography.

Bailey and Childers 1977; Beroni and Bauer 1952; Bonner et al. 1982; Brobst 1961; Catchpole and Kirchner 1993; Chenoweth 1988a; Chenoweth and Malan 1969; Chenoweth and Sharp 1970; Childers 1974; Collings and Knode 1984; Collings et al. 1996; Cuppels 1963; Davis and Izett 1962; DeGraw 1969; Denson and Chisholm 1971; Denson and Gill 1956, 1965; Denson et al. 1959; Elevatorski 1976, 1977; Ethridge et al. 1979; Gill and Moore 1955; Gill et al. 1959; Gjelsteen and Collings 1988; Gott and Schnabel 1963; Gott et al. 1974; Hansley and Dickinson 1990; Hansley et al. 1989; Harshman and Adams 1981; Harshman 1968; Hart 1968; Karsmizki 1990; Kirkham et al. 1980; Moore et al. 1959; Murphy E 2007; Noble 1973; NUEXCO 1983; Pipiringos et al. 1965; Reade 1976, 1978; Renfro 1969; Robinson et al. 1964; Ryan 1964; Smith 2005; Swinehart et al. 1985; Towse 1957; US AEC 1959; Vickers 1957; Voss and Gorski 2007; Waage 1959; Weimer 1973; and Bonner JA, Brown N, Catchpole G, Kirchner G, McMurry J, Pool TC, and Voss WC, personal communication.

Chapter 5

Northern Rocky Mountains

The regions with uranium occurrences in the Northern Rocky Mountains include the Northern and Middle Rocky Mountains covering an area from the Canadian border through north-eastern Washington State, northern Idaho, and northwestern Montana, southward to central and western Wyoming and northeastern Utah (Fig. 1.1b). Known uranium deposits are of various types and occur in diverse geological environments as listed below in the section entitled Types of Uranium Mineralization.

Sources of Information. Barrington and Kerr 1961; Becraft and Weis 1963; Elevatorski 1977; Graff and Houston 1977; Houston et al. 1977; Ludwig et al. 1981; Marjaniemi and Robins 1975a, b; Miller and Engels 1975; Milne 1979; Nash 1977, 1979; Nash and Lehrman 1975; Nash and Ward 1977; Norman 1957; Pearson and Obradovich 1977; Pernsteiner and Ikramuddin 1979; Robbins 1976, 1978; US AEC 1959; US Bureau of Mines 1977; Weiss et al. 1958; Weissenborn and Moen 1974, unless otherwise noted.

Regional Geology of the Northern Rocky Mountains

The region is geologically a complex terrane of mountain ranges and intermontane basins made up of rock units ranging in age from the Archean to Cenozoic. In Idaho and northeastern Washington, thick sequences of metasediments and sediments of Upper Proterozoic and Paleozoic age were intruded by large granitic plutons such as the Idaho and Loon Lake batholiths of Cretaceous to Tertiary age. In most of Wyoming, southwestern Montana, and northeastern Utah, the mountains are predominantly uplifted blocks with cores of Archean to Proterozoic granitic and metamorphic rocks. During the Tertiary time, volcanism produced large amounts of lava and pyroclastic material in northwestern Wyoming, central Idaho, and northeastern Washington.

Precambrian crystalline terrane of the Rocky Mountains comprises two major provinces of different ages of the orogenic-metamorphic evolution (Hedge et al. 1978). An ancient, Archean province prevails in the Northern Rocky Mountains, particularly in Wyoming and adjacent parts of Utah, Montana, and South Dakota. It is represented by mostly felsic granitic gneisses and associated metasediments, which were metamorphosed about 2,800 Ma ago, and later, between 2,760 and 2,500 Ma, intruded by tonalitic to granodioritic plutons.

The younger crystalline province is of Paleo- to Meso-proterozoic age. It is only sparsely exposed to the west and northwest of older terrane of the Northern Rocky Mountains, but occupies large areas in the Southern Rocky Mountains. It consists of a thick stack of sediments and volcanics deposited

between 2,000 and 1,800 Ma, which were regionally metamorphosed and intruded by numerous granodioritic plutons about 1,700 Ma ago. New intrusions of granitic plutons occurred 1,400 Ma ago and again, in central Colorado, 1,020 Ma ago.

The ancient platform was covered by Paleoproterozoic, 2,500–1,800-Ma old shelf-type sediments, including quartz-pebble conglomerates, preserved in a NE–SW-trending zone between southern Wyoming and the Black Hills. A younger, Meso- to Neoproterozoic, 1,500–900-Ma old sequence, the miogeosynclinal Belt Supergroup, was deposited over wide areas from western Montana into Idaho and northeastern Washington. Approximately equivalent series, isolated from the Belt Supergroup, include the Uinta Mountain Group in northeastern Utah and northwestern Colorado. A 1,700–1,500-Ma old sequence, the Uncompahgre Formation, is only preserved in southwestern Colorado.

Types of Uranium Mineralization

Known U deposits in the Northern Rocky Mountains belong to a variety of types of mineralization, including:

- **Vein-type** mineralization in Cretaceous granitic intrusives (*Mt. Spokane/Daybreak*, Washington State) and in older (meta-) sediments near the contact of a pluton (*Midnite*, Washington State) either as monometallic veins (*Daybreak*) or stockworks (*Midnite*), or as polymetallic lodes (*Coeur d'Alene* district, Idaho; *Little Man Mine*, Wyoming)
- **Vein- or veinlike-type** mineralization in Paleoproterozoic granitic rocks (*Copper Mountain*, Wyoming)
- **Peneconcordant sandstone-type** mineralization in Eocene sediments (*Sherwood*, Washington State; *Basin Creek area*, Idaho)
- **Karst-cavern fillings** in Paleozoic limestones (*Pryor and Little Mountains*, Montana-Wyoming)
- **Surficial peat-bog** mineralization of Holocene age (*Flodell Creek*, Washington State)
- **Oligomictic quartz-pebble conglomerate-type** mineralization of Lower Proterozoic age (*Medicine Bow Mountains*, Wyoming–Colorado).

Although a great number of uranium showings exist, only a few small to middle size deposits have been discovered, the most important being the *Midnite* and *Sherwood* mines in Washington State. Ore of the *Midnite* mine is of somewhat vein-stockwork character emplaced in Upper Proterozoic metasediments of the Togo Formation near the contact with a Cretaceous granitic pluton. In the *Sherwood* deposit, located 10 km S of the *Midnite* mine, peneconcordant sandstone-type uranium occurs in clastic sediments of the Sanpoil Volcanics of Eocene age.

In the *Basin Creek* area, central Idaho, similar sandstone-type U mineralization associated with sulfides and carbonaceous material occurs as a shallow zone in arkosic sandstone of Eocene age. Also in the *Basin Creek* area, small pitchblende-bearing veins are in Cretaceous quartz monzonite.

At *Mt. Spokane*, Washington, several small mines, including the *Daybreak* mine, exploited fractures filled with

dominantly hexavalent U minerals in alaskitic intrusive rocks of Cretaceous age.

The *Coeur d'Alene* Pb–Zn–Ag district in northern Idaho and northwestern Montana has some pitchblende in polymetallic Ag–Pb–Zn vein deposits.

In the *Pryor and Little Mountains* along the Montana–Wyoming border, ores composed of hexavalent U minerals have been mined from karst caverns in the Madison Limestone of Mississippian age and the Tensleep Formation of Pennsylvanian age.

At *Copper Mountain* in the Owl Creek Mountains, northwestern Wyoming, uranium occurs near-surface in highly fractured Precambrian granites and adjacent Tertiary sediments.

A belt of Paleoproterozoic quartz-pebble conglomerate extending from the Medicine Bow Mountains in southeastern Wyoming to the Black Hills in South Dakota contains radioactive mineralization in the Medicine Bow Mountains and the Sierra Madre along a supposedly intraformational unconformity in the Phantom Lake Group, the lowest unit of the Paleoproterozoic sequence (Graff and Houston 1977; Houston et al. 1977). Relatively high background uranium, thorium, and gold values are noted in the time-equivalent Estes Conglomerate in the Nemo district on the northeastern flank of the Black Hills, South Dakota (see chapter 3 Black Hills).

5.1 Spokane Mountain Area, Washington State

Three deposits are reported, *Midnite* and *Sherwood* on the south side, and the small *Spokane Mountain deposit* on the northern slope of Spokane Mountain (Fig. 5.1). Original resources of the three deposits were estimated to be on the order of some 15,000 t U, about 7,500 t of which have been mined as of 1988.

Sources of Information. Barrington and Kerr 1961; Becraft and Weis 1963; Ludwig et al. 1981; Milne 1979; Nash 1975, 1977, 1979; Nash and Lehrman 1975; Nash and Ward 1977; Norman 1957; Pearson and Obradovich 1977; Pernsteiner and Ikramuddin 1979; Robbins 1976, 1978; US AEC 1959; US Bureau of Mines 1977; Weiss et al. 1958; Weissenborn and Moen 1974.

Regional Geological Setting of Mineralization

The Togo Formation, from 900 to 6,000 m in thickness, is part of the Deer Trail Group (Belt Supergroup?) of Mesoproterozoic age, and is the oldest stratigraphic unit in the Spokane Mountain area. The Togo Formation consists of quartzite, phyllite, schist, marble, and calc-silicates, and intercalated amphibolized gabbro sills and dikes, which are regionally grouped in an upper quartzitic, a middle phyllitic, and a lower calcareous unit with intercalated gabbroic sills and dikes. Regional metamorphism of greenschist grade had formed and folded these rocks along NNE–SSW-oriented axes in, probably, Jurassic to early Cretaceous time.

During the Cretaceous, Togo metasediments were invaded by leucocratic plutons ranging in composition from hornblende granodiorite to porphyritic quartz monzonite and alaskite and associated leucocratic apophyses, pegmatite, and aplite. Contact metamorphism produced hornfels and skarn facies as much as 300 m distant from the intrusive contact.

In probably Eocene time, paleochannels were filled by coarse fluvial and pyroclastic sediments, and aphanitic flows of the Sanpoil Volcanics (formerly named Gerome Andesite or Gerome Formation). Hornblende dacite dikes are thought to represent probable feeder structures for pyroclastic volcanics.

Regional faults commonly strike around NW–SE, have a steep dip, and may have displacements of several tens of meters.

5.1.0.1 Midnite Mine, Washington State

This deposit was discovered in 1954, approximately 65 km NW of Spokane. It had original in situ resources of 8,700 t U at a grade of 0.12% U based on a cutoff grade of 0.042% U (Milne 1979). Some 6,800 t U have been produced from ten open pit operations during an early period from 1955 to 1963 and again from 1970 to about 1982.

Sources of Information. Ludwig et al. 1981; Milne 1979; Nash et al. 1975, 1977, 1979; Robbins 1978, and other authors cited.

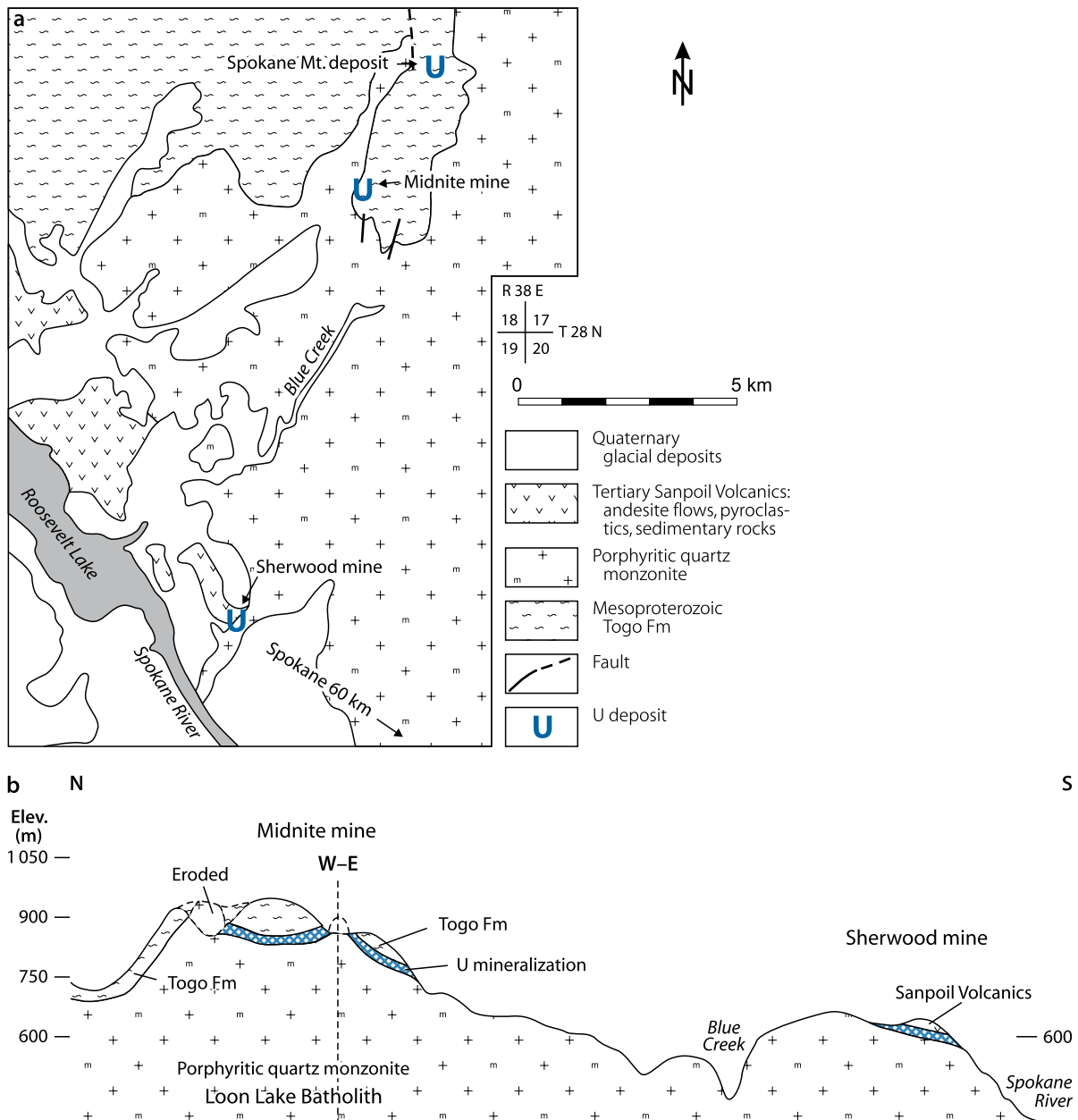
Geological Setting of Mineralization

The geological framework of the Midnite mine area consists of a porphyritic quartz monzonite batholith (Upper Cretaceous Loon Lake Batholith) and associated pegmatites and aplites intruded about 75 Ma ago into the Mesoproterozoic Togo Formation (Figs. 5.1; 5.2). Togo metasediments of \pm pelitic origin include quartz-, graphite-, sericite-rich phyllites, and quartz-muscovite schists containing coarse pyrite, often pseudomorphic after pyrrhotite; where contact metamorphosed, andalusite and biotite have developed within about 30 m of the intrusive contact. Calcareous metasediments of the contact aureole are fine-grained calc-silicate hornfels with ubiquitous quartz, calcite, diopside, and epidote, and medium- to coarse-grained skarn with garnet, tremolite, wollastonite, vesuvianite, and phlogopite. Some amphibolite sills up to 8 m wide, oriented NNE–SSW, and dipping ca. 80° E are intercalated in metasediments.

Porphyritic quartz monzonite is tan to pink, medium- to coarse-grained, and contains K-feldspar phenocrysts as much as 5 cm long. Biotite is common and often muscovite as well; the latter tends to be of secondary growth. This mineral composition is more typical for a two-mica granite (according to European nomenclature) than a quartz monzonite, which is also supported by chemical analyses. Analyses by Nash (1979) give an average content of 17 ppm U in fresh surface samples of granite. Uranium contents in zircons are likewise very high (3,100–4,500 ppm U). In contrast, fluorine contents reported by Pernsteiner and

■ Fig. 5.1.

Spokane Mountain area, geologic-lithological position of the Midnite and Sherwood deposits, (a) simplified geological map, (b) N-S section documenting the intimate spatial relationship of the two deposits to the Cretaceous porphyritic quartz monzonite of the Loon Lake Batholith. (After Milne 1979 based on Becraft and Weiss 1963; Dollinger U, personal information)



Ikramuddin (1979), average 480 ppm and as such are not high for this rock type. These authors report an average of 20 ppm U for granite.

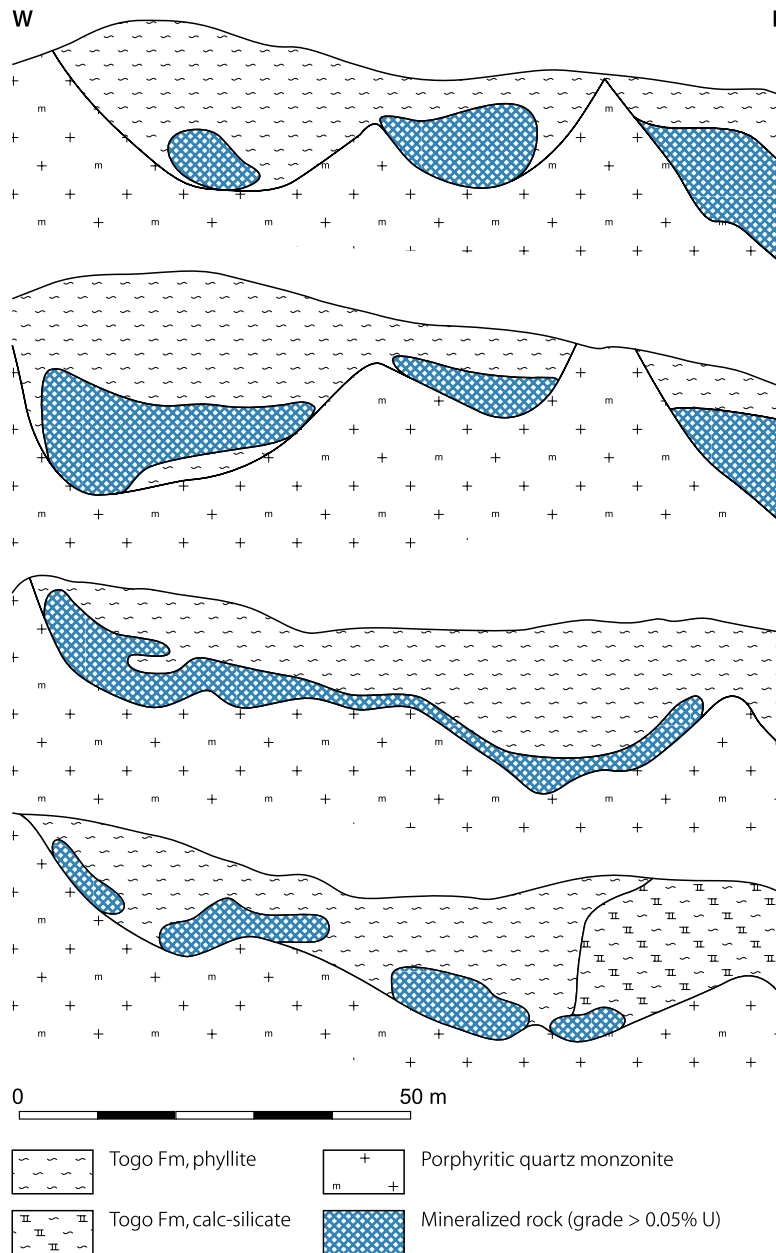
Older rocks are locally overlain by aphanatic flows of Early Tertiary Sanpoil Volcanics, dated at 51 Ma (Pearson and Obradovich 1977). N-S-trending dikes of very fine-grained hornblende dacite cut these flows. In the Midnite mine area, Eocene volcanics are now eroded, but are thought to have been positioned about 100 m above the present mineralization.

Togo metasediments are complexly folded. Fold axes trend NNE-SSW with limbs locally overturned. At the Midnite mine, which is positioned along the western edge of a roof pendant, 1.5 km wide in E-W direction and up to 200 m thick, strata strike NNE-SSW and dip 50-80° E and are considered to be the overturned western limb of an anticline.

Faults appear to be rare. They generally trend N-S, have a steep dip, and are not very persistent. A larger apparently pre-ore fault zone up to 20 m wide dissects the mining area and

Fig. 5.2.

Midnite deposit, cross-sections of several open pits showing the typical concentration of uranium mineralization in metasediments that fill depressions incised into Cretaceous porphyritic quartz monzonite. Ore bodies are up to 60-m thick. Depths to ore ranges from <5 to 30 m. (After courtesy of Dawn Mining Co.; Milne 1979 based on Nash and Lehrman 1975)



causes lateral displacements of 30–50 m. Faulting also sheared a dacite dike of Eocene age and displaces calc-silicate rock of the Togo Formation by at least 20 m, but does not offset a well-defined ore zone. Shearing and stockwork fracturing is common in zones of mineralization.

Host Rock Alteration

Alteration effects appear to be restricted to minor kaolinization and montmorillonitization. Montmorillonite-rich layers occur

in fractured calc-silicate rocks. Some alteration affected cataclastic dacite dikes. Hematitization is practically absent.

Mineralization

Pitchblende and coffinite are the principal U minerals. Associated minerals in reduced ore include pyrite, marcasite, chalcopyrite, bornite(?), sphalerite, and hisingerite. Hexavalent U minerals, mainly autunite, meta-autunite, and uranophane, are common above the water table.

Pitchblende and coffinite exhibit a colloform habit, have shrinkage cracks, and contain appreciable amounts of Ca and Si, and occasionally Fe. In pitchblende–coffinite veinlets, the pyrite–marcasite volume ratio is about 8:1, and essentially all marcasites are intimately associated with coffinite. In near-veinlet wall rocks, the ratio drops to less than 3:1. Hisingerite is closely intergrown with pitchblende and coffinite in ore, but forms almost pure veinlets in barren host rock. Nash and Lehrman (1975) report enrichments of As, Co, Mn, Mo, Nb, Ni, Pb, W, Y, and Zn in and around ore zones.

Ludwig et al. (1981) established the following paragenetic relationships of ore and related minerals: (a) pitchblende and pyrite crystallized first, (b) coffinite formed during or shortly after pitchblende, (c) brecciation occurred after formation of most pitchblende, but prior to that of most coffinite, which partially replaced pitchblende, (d) coffinite and marcasite filled remaining open fissures, (e) hisingerite formed late in this stage, locally with coffinite and marcasite, (f) some sphalerite crystallized early during coffinite formation, but most was formed very late.

Sericite–graphite phyllite and mica schist host most of the ore, although appreciable quantities of ore also occur in calc-silicate rocks. Hexavalent U minerals are locally present in amphibolitic sills, but only where sills are heavily brecciated. Adjacent calc-silicates may not be mineralized. There is almost no ore in quartz monzonite.

Ludwig et al. (1981) list the following distinctive features of mineral distribution and arrangement:

- Thicker ore zones coincide with troughs in the intrusive contact
- The upper boundary of mineralization is often subhorizontal, and locally persists at the same elevation on both sides of ribs of barren quartz monzonite
- Ponding updip or above planes that appear to have acted as hydrologic barriers, as at the intersection of the calc-silicate-phyllite contact with the batholith, and adjacent to some NW–SE-trending EM anomalies considered to represent altered fracture zones (Lehrman and Nash in Ludwig et al. 1981).

Shape and Dimensions of Deposits

Mineralization forms lenses of a tabular, pool-like configuration along subhorizontal or concave contacts of Togo metasediments with quartz monzonite, and as such they cut across lithologic boundaries of steeply dipping metasediments (Fig. 5.2). Ore minerals occur in these lenses (a) as disseminations along foliation in phyllite and schist generally adjacent to local shears, (b) as fillings of numerous mini-fractures commonly 1–3 mm, rarely 6 mm wide and arranged in a stockwork pattern in mica hornfels, and (c) along brecciated and intensely montmorillonitized layers, centimeter to meter thick, in calc-silicate hornfels.

Mineralization occurs in two main, roughly N–S-oriented depressions filled with Togo metasediments, 75–200 m thick, immediately above the intrusive contact. A rib of barren quartz

monzonite separates the eastern from the western depression. Discontinuous mineralization occurs in the *western depression* over 600 m in N–S length, 170 m in width, and over a vertical interval of up to 50 m, and encompasses an area of 380 by 170 m of prime mineralization. Mineralization in the *eastern depression* also extends for about 600 m in N–S length and averages 75 m in width, but widens to 210 m at its southern end. Mineralization spreads over a vertical interval of up to 60 m. Depth to ore ranges from less than 5 to 30 m.

Individual ore zones within the two depressions are as much as 200 m long and range from a few meters to 60 m in width, and from a few meters to 20 m and more (average ca. 15 m) in thickness. A low-grade protore zone, a few meters thick, with less than 100 ppm U separates minable ore from the intrusive contact.

Geochronology

Comprehensive isotope studies by Ludwig et al. (1981) on the geochronological frame of uranium ore and rocks of the Midnite mine yield, in summary, the apparent ages shown in Table 5.1.

In addition to age dates, isotope systematics reveal small-scale open systems of individual pitchblende–coffinite veinlets permitting diffusion of mobile ^{238}U daughter isotopes (probably ^{222}Rn) as indicated by anomalously high $^{207}\text{Pb}/^{206}\text{Pb}$ values in pyrite–marcasite within pitchblende–coffinite veinlets, whereas pyrite–marcasite in nearby wall rocks are enriched in ^{206}Pb .

Ore Controls and Recognition Criteria

Midnite mine mineralization may be attributed to vein- or veinlike-type uranium deposits. It is structurally controlled, discordant in metasedimentary host rocks, but not of simple vein

Table 5.1.

Midnite mine, age datings of country rocks and uranium mineralization. (After Ludwig et al. 1981, ^a Pearson and Obradovich 1977)

Rock type	Apparent age (Ma)
Porphyritic quartz monzonite	79 – 75
Zircon (Pb/U)	74 ± 4
Monazite (Pb/U)	69 ± 6
Apatite (fission track)	
Dacite dike	
Hornblende (K Ar)	51.8 ± 3.1
Zircon (fission track)	47.2 ± 1.9
Apatite (fission track)	47.5 ± 3.6
Sanpoil Volcanics ^a	±51
High-grade ore (>1% U) (Pb/U)	51 ± 0.5

type, rather it is of stockwork type, and it is spatially adjacent to a granitic intrusion. Recognition criteria and ore controls reflecting this situation include:

Host environment

- Upper Cretaceous quartz monzonite batholith containing roof pendants of the Mesoproterozoic Togo Formation
- Host rocks are metasediments and their contact-metamorphic equivalents present in troughs underlain and separated by ribs of quartz monzonite
- Host metasediments are intensely micro-fractured
- Quartz monzonite (two-mica granite) has high whole-rock U contents (17 ppm U in average), but probably had originally higher U contents as may be deduced from high U values in zircons (up to 4,500 ppm)
- Uraniferous quartz monzonite contains magnetite, indicating the presence of uranium phases in leachable form
- Crosscutting dacite dikes (related to Sanpoil Volcanics) emplaced \pm coeval with ore formation
- Only limited alteration represented by minor kaolinization and montmorillonitization.

Mineralization

- Two stages of U mineralization composed of early pitchblende-pyrite followed by coffinite-marcasite
- Other metals present in elevated amounts include As, Co, Mn, Mo, Nb, Ni, Pb, W, Y, and Zn
- Ore bodies
 - Are of tabular configuration transgressive through steeply dipping metasediments
 - Often have subhorizontal upper limits persisting in some places across ribs of barren quartz monzonite
 - Are ponding up dip or above planes as at intersections of lithologic boundaries, and adjacent to NW-SE-trending altered fracture zones
 - Have an internal structure of micro-fractures, shears, or stockworks, and
 - Show no oxidation effects and commonly little or no apparent alteration in primary ore zones.
- Ore bodies contain U and associated minerals
 - Disseminated along foliation in phyllite and schist generally adjacent to local shears
 - In mini-fractures arranged in a stockwork pattern in mica hornfels, and
 - In brecciated and intensely montmorillonitized layers in calc-silicate hornfels.
- Ore bodies occur primarily
 - In metasediments of reducing nature characterized by abundance of sulfides, mainly pyrite and less marcasite
 - Contained in troughs downwarped into quartz monzonite and
 - Immediately above the intrusive contact.
- Thicker ore zones coincide with thicker stacks of metasediments.

Metallogenetic Aspects

A variety of metallogenetic hypotheses for Midnite mineralization have been forwarded by various investigators of the deposit ranging from hypogene to supergene. Based on comprehensive research data, Ludwig et al. (1981) have presented a model of the critical ingredients of which are, in summary, as follows:

1. Age dating of pitchblende, dacite dikes, and Sanpoil Volcanics give almost identical Eocene ages of about 51 Ma, whereas porphyritic quartz monzonite was intruded about 75 Ma, which is significantly older than the age of U mineralization, i.e., present ore could not have derived directly from the intrusion
2. Faulting sheared a dacite dike of Eocene age and displaced markedly calc-silicate rock of the Togo Formation, but did not offset a well-defined ore zone, which supports a time of ore formation not older than Eocene
3. Fission track ages of apatite in quartz monzonite are, with about 60 ± 6 Ma, only slightly younger than zircon ages, which indicates that after this time no sustained high-temperature ($>100^\circ\text{C}$) hydrothermal event could have taken place much after intrusion time because otherwise fission tracks in apatite would have been significantly annealed
4. Textures of pitchblende-coffinite are similar to those in low-temperature, sandstone-hosted mineralization in Wyoming Basins
5. Porphyritic quartz monzonite provides a viable U source as may be deduced from its present-day high uranium background value, which presumably was originally higher as indicated by extremely high U contents of its zircons
6. A quantity of uranium equivalent to the endowment calculated by Ludwig et al. (1981) at 12,000 t U of combined total ore and subeconomic mineralization in the mine area appears unlikely to have been derived by supergene uranium liberation from quartz monzonite exclusively in early Eocene time, i.e., at about 51 Ma, the age of present ore. Constraints on the volume of quartz monzonite in a suitable tectonic-hydrologic position during pre- and early Eocene time have restricted the exposure of sufficient uranium to through-passing meteoric waters
7. Other theoretical uranium sources in the Midnite area such as the Togo metasediments or Sanpoil Volcanics (extrusive equivalent of hornblende granodiorite) contain only small amounts of uranium (1.6 ppm U, 3.3 ppm Th), which are insufficient for providing appropriate ore-forming U amounts, although the age of Sanpoil Volcanics and that of dacite dikes in the mine coincide with the age of U minerals crystallization.

In consequence of the above criteria, the authors propose a multistage metallogenetic evolution of Midnite ore that envisions:

(a) Initial introduction of uranium into Togo metasediments to form a disseminated, low-grade protore (ca. 100 ppm U?) during emplacement of porphyritic quartz monzonite, about 75 Ma ago. Relatively mild hydrothermal fluids are considered to have been the transporting media for uranium (and associated

elements?). Fluids caused metasomatism and addition of some Th (ca. 30 ppm) to Togo metasediments within a few meters of the pluton contact (Lehrman in Ludwig et al. 1981).

(b) Mildly heated waters of meteoric origin evoked pervasive redistribution and reconcentration of the pre-existing protore uranium in early Eocene time, possibly with some uranium contribution by surface leaching of quartz monzonite leading, at about 51 Ma, to the present-day ore concentration and distribution.

The actual final ore-grade concentration of uranium took place where ground was prepared by a combination of

- Fracturing and shearing of later host rocks in association with development of feeder structures and intrusion of feeder dikes to Sanpoil Volcanics
- Change of groundwater hydrology as a result of extrusion and coverage of protore metasediments by Sanpoil Volcanics, which possibly aided movement of uraniferous solutions into structural traps
- Mild heating of groundwater by volcanics, which possibly augmented chemical reactions during leaching and redeposition of uranium.

Possible reductants may have been metastable sulfur species of an intermediate oxidation state in a slightly acidic environment as may comparatively be deduced from the presence of late ore-stage marcasite. The ore-forming fluid probably only had a limited oxidation capacity for otherwise it would have altered and hematitized wall rocks more intensely than present in the Midnite deposit.

A cap of impermeable rocks of Sanpoil Volcanics preserved the neo-formed ore bodies and protected them from erosion and/or supergene leaching.

In essence, Midnite mineralization in its present form is thought to be a stockwork-fracture controlled vein- or veinlike-type uranium deposit of supergene-hydrogenic (hydrothermal) origin.

Note: Features, environment, and ore-forming processes, individually or combined, which in principal are similar to those of the Midnite deposit, except the commonly stronger wall rock alteration, are registered in other vein- or veinlike-type uranium deposits, for example, in some of the Hercynian deposits in central and western Europe, particularly in those of the Iberian Peninsula. Therefore, ore-forming processes suggested for Hercynian vein deposits in Europe may possibly also be considered for Midnite mineralization.

5.1.0.2 Sherwood Mine, Washington State

Discovered in 1955, the Sherwood mine located approximately 60 km NW of Spokane and 6 km SW of the Midnite mine (► Fig. 5.1a and b) had resources of about 5,500 t U at an average grade of 0.068% U based on a cutoff grade of 0.017% U (Robbins 1976). Some 730 t U of these resources have been mined by open pit operations (Chenoweth WL, personal information). Early mining lasted from 1958 to 1963 and produced 11 t U at a grade of 0.14% U. Mining was resumed in 1978, but was terminated in

1983. Stripping ratios ranged from 2.1 in the eastern ore body, to 4:1 in the western ore body with local ratios up to 20:1.

A small shallow deposit, the *Peters Lease*, containing about 400 t U occurs near the Sherwood deposit. The *Big Smoke* mine, a deposit similar to the Sherwood deposit, is located about 5 km S of the Sherwood mine.

Sources of Information. Marjaniemi and Robins 1975b; Milne 1979; Pearson and Obradovich 1977; Robbins 1976; US Bureau of Mines 1977; Weissenborn and Moen 1974.

Geological Setting of Mineralization

Sherwood mineralization is in a late Cretaceous to Paleocene fluvial conglomerate, from 20 to 60 m thick, which probably represents a basal unit of Eocene **Sanpoil Volcanics**. Conglomerate unconformably overlies porphyritic quartz monzonite of the Loon Lake pluton, supposedly the same as at the Midnite mine. Sanpoil Volcanics (15–100 m thick) were deposited on conglomeratic beds. They include often thin-bedded, uncemented to well-cemented (with carbonate) fluvial arkosic sandstone, conglomerate, carbonaceous shale, as well as pyroclastic sediments, semi-welded tuff, tuffaceous sandstone, and andesite lava flows. Formerly, Sanpoil rocks were considered to be part of the Oligocene Jerome Andesite. Miocene plateau basalt, 0–15 m thick, locally caps the Sanpoil Volcanics. Glacial deposits up to 3 m thick form the overburden (► Fig. 5.3).

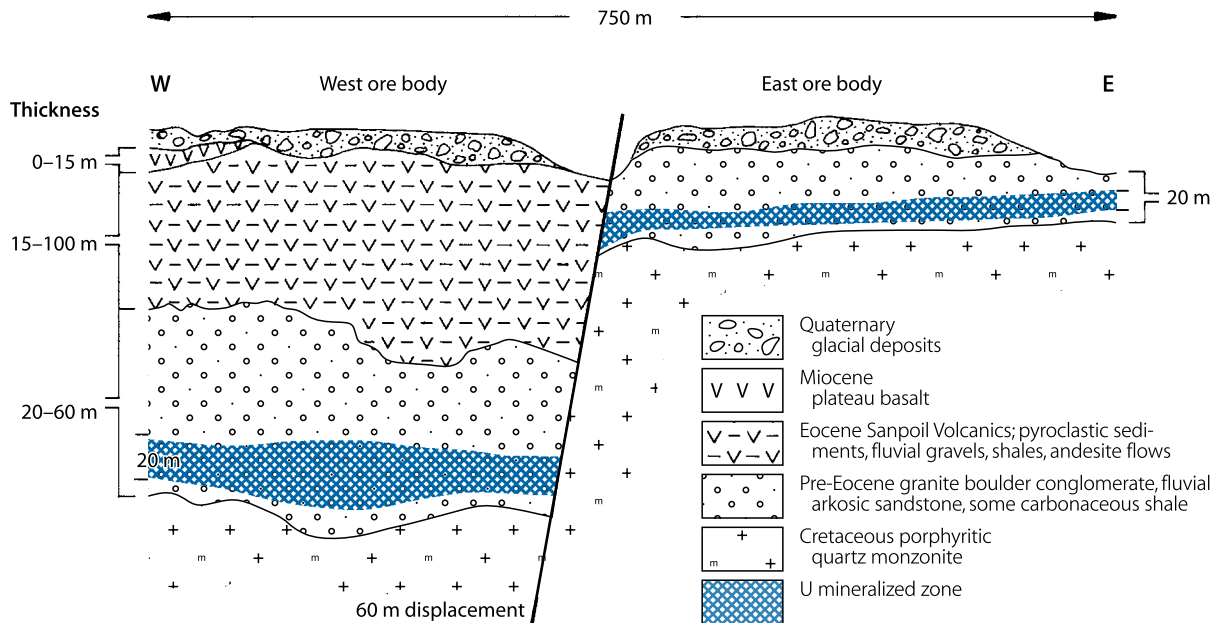
The ore-hosting unit is a poorly sorted, weakly cemented, porous and permeable conglomerate with some characteristics of a channel facies. It is composed of about 25% clasts and 75% fine-grained material (Veelik in Milne 1979). Clasts consist of cobbles and boulders, up to 1 m in diameter, of a variety of lithologies including partly decomposed granitic facies, carbonate, phyllite, and quartzite. Matrix material and interstratified layers consist of arkosic sand and clay/shale with disseminated carbonaceous material and lignitic or sub-bituminous coal stringers, pockets, and lenses. Carbonaceous material although scattered throughout the conglomerate appears to be more abundant in the lower two thirds of the unit, which has a carbon content of 10–12%. A major N–S-oriented and 5° W-dipping fault cuts through the deposit displacing the eastern segment about 60 m higher than the western segment. As a probable consequence, Sanpoil Volcanics and overlying rocks are eroded on the eastern side and uranium-bearing conglomerates almost crop out on surface covered only by glacial debris. Most of the upper sedimentary sequence of the uplifted eastern block is affected by strong oxidation down to a fluctuating water table.

Mineralization

Ore consists of fine-grained pitchblende and coffinite associated with pyrite in reduced ore below a fluctuating water table. Oxidized sediments contain hexavalent U minerals, predominantly meta-autunite and some metatorbernite. Marjaniemi and Robins (1975) report anomalous amounts of Ga (<10 ppm),

Fig. 5.3.

Sherwood deposit, generalized geological W–E cross-section illustrating the accumulation of stratiform U mineralization in basal pre-Eocene conglomerate-sandstone above Cretaceous porphyritic quartz monzonite. (After Milne 1979)



Li (<50 ppm), Mo (<80 ppm), Nb (<20 ppm), and Sn (<200 ppm) associated with Sherwood mineralization.

Uranium mineralization is intimately associated with carbonaceous matter within the conglomerate matrix and is best developed in basal layers of conglomerate close to the unconformity with porphyritic quartz monzonite. Pitchblende and coffinite coat sand grains, cobbles, and boulders, and fill fractures in clasts. Ore minerals are also present in partially decomposed granitic boulders, in yellowish-green bands in arkosic sand lenses, 15–150 cm thick, and in lignitic seams and pockets.

Mineralization in the uplifted eastern ore body, where protective cover rocks are eroded, consists almost entirely of oxidized ore and is in radioactive disequilibrium. The down-faulted western ore body, protected by as much as 100-m Sanpoil Volcanics, contains predominantly unoxidized ore.

Mineralization in the *Big Smoke* mine is in a granite-pebble conglomerate that contains seams of carbonaceous shale. The deposit is located along a fault contact between Sanpoil Volcanics (or Gerome Andesite?) and granitic rocks of the Loon Lake pluton.

Shape and Dimensions of Deposits

The Sherwood deposit extends over a NW–SE length of ca. 800 m and a width of about 450 m. As mentioned earlier, it is structurally separated into an upper eastern ore body and a lower western ore body (► Fig. 5.3). The western ore body, which is almost 20 m thick, is in the bottom part of a 20–60 m thick conglomerate unit lying at variable depths from 50 to 150 m under the surface. Ore of the eastern ore body occurs at a depth of 10–15 m and averages 5–6 m in thickness within a

conglomerate bed averaging 20 m in thickness. Mineralization is somewhat irregular in distribution and grades vary between 0.017% (cutoff grade) and 0.14 U averaging about 0.07% U.

Ore Controls and Recognition Criteria

Sherwood mineralization can be classified as a peneconcordant sandstone-type deposit. Principal ore controls or recognition criteria include:

- Emplacement in a coarse clastic fluvial sediment particularly in the bottom part of a conglomerate unit rich in carbonaceous matter
- Located adjacent to porphyritic quartz monzonite, which presumably contains anomalous uranium contents as deduced from similar (or the same) intrusives in the nearby Midnite deposit
- Irregular distribution of mineralization
- Reduced ore comprises pitchblende and coffinite associated with pyrite and anomalous amounts of rare metals
- Ore minerals occur within the conglomerate matrix and as fracture filling in its clasts
- Intimate association of uranium with carbonaceous matter that is preferentially concentrated in the basal portion of the conglomerate.

Metallogenetic Aspects

Milne (1979) offers two hypotheses for the source of uranium and ore formation. In both cases, the carbonaceous substance in the host conglomerate was the essential reductant.

(a) Erosion of granitic mountains in the Midnite area in early Tertiary time provided uraniferous granitic material, which was transported and deposited to the south in channels incised into the granitic surface. Uranium was mobilized from this debris by groundwater action and concentrated after or during extrusion of Sanpoil Volcanics.

(b) Thicker sequences of Sanpoil Volcanics may have possibly included uraniferous ash flows. Uranium was leached from these ash flows by groundwater and transported into channel conglomerate, where reaction with carbonaceous material may have created Sherwood mineralization.

In light of the more recent research results of Ludwig et al. (1981), the genetic model of these authors for the Midnite deposit may also have some impact in formulating a concept on formation of Sherwood ore, particularly since the Sherwood deposit lies on a structural trend with the Midnite mine. It may be envisaged that uranium was not only reconcentrated in rocks of the Togo Formation as in the Midnite area but also was leached from protore metasediments of the Togo Formation as well as from uraniferous quartz monzonites during or after extrusion of Sanpoil Volcanics. Mobilized uranium was transported along conglomerate filled paleochannels and redeposited at favorable locations provided by abundant organic debris.

5.1.3 Spokane Mountain Deposit, Washington State

This small deposit is located about 2 km NE of the Midnite mine, on the same structural trend as both the Midnite and Sherwood deposits. Uranium mineralization occurs in deeply weathered graphitic phyllite and chloritic schist of the Togo Formation. Metasediments are intensely sheared and fractured and displaced by several, around N–S-trending, high-angle faults. Principal ore minerals are meta-autunite and uranophane, and lesser pitchblende. Estimated resources are in the order of 400–1,300 t U at grades locally as high as 0.21% U. Ore is positioned at depths between 45 and 150 m (Dollinger U, personal information).

5.2 Mount Spokane Area, Washington State

Mount Spokane (not to be confused with Spokane Mountain) is located about 50 km NNE of Spokane. After discovery of uranium in 1954, approximately 30 small uranium occurrences have been found mainly on the western and southern slopes of Mount Spokane. Some ten properties have produced about 38 t U from open pits and adits (Chenoweth WL, personal information). The most famous deposit was Daybreak.

5.2.1 Daybreak Mine, Washington State

The Daybreak deposit is known not so much for its reserves or production, it produced about 20 t U at an ore grade of approximately 0.25% U, but for its spectacular meta-autunite crystals.

Sources of Information. Illsley 1957; Milne 1979; Norman 1957; US AEC 1959; Weiss et al. 1958.

Geology and Mineralization

Fracture-filling uranium mineralization is hosted in quartz monzonite, which varies considerably in rock facies, internal structure, and grain size. Pegmatite dikes up to half a meter thick are abundant. Many occur as nearly parallel bands, but cross-cutting dikes are also common. Plutonic rocks are jointed, dissected by many faults and shears, and altered to a depth of 15 m or more.

Most Daybreak ore mined was hosted by a major shear zone, in excess of 600 m long and locally 15 m wide, striking E–W and dipping 10–25° N. Quartz monzonite along the shear zone exhibits intense alteration and bleaching. Alteration phenomena include kaolinitization of feldspars and sericitization. Bleaching is apparently due to biotite replacement, removal of iron oxides, and decay of feldspars to clay minerals. The hanging wall of the shear zone is marked by a persistently bleached, greenish band of gouge and breccia, whereas the footwall is mostly indistinct and apparently gradational to the host rock. The main E–W shear zone is intersected by NW to N-striking, steeply SW-dipping minor faults and fractures.

Meta-autunite is the only known uranium mineral. No sulfides and gangue minerals are present. Meta-autunite occurs in spectacular crystals as much as 3 cm in size, green on the outer edges and greenish-black near the center when fresh. These crystals are commonly arranged in aggregates lining open fractures and vugs within the shear zone near the water table, forming pods, and vuggy masses as much as 10 cm thick and 1-m long. The degree of mineralization varies with the intensity of fracturing, but tends to be independent of alteration. Meta-autunite has been noted throughout a vertical interval of 30–40 m, but minable ore appears to extend only slightly below the water table. The richest and largest ore shoots have formed at the intersection of NW-trending, steeply dipping cross-fractures with the gently dipping E–W shear zone. Larger ore shoots consist of pods as much as 1.5 m long, more than 1 m wide, and 0.2–0.3 m thick. Meta-autunite also occurs locally in clayey veins within ore bodies. Elsewhere it is disseminated throughout an argillaceous gouge zone. Ore grades of the Daybreak mine range up to several percent U and average about 0.25% U.

Milne (1979) postulates supergene processes as the most likely mechanism for formation of the U mineralization. During a period of deep weathering in Tertiary time, circulating groundwater may have leached uranium from supposedly uraniferous quartz monzonite and redeposited it along a fluctuating water table as open-space filling. The actual cause for uranium precipitation in relatively large amounts and at given sites is not established.

Postulation of a hypogene hydrothermal origin, particularly in light of strong alteration, does not appear to be appealing for alteration is also noted in areas barren of mineralization, and, conversely, uranium is also present in unaltered rock. Lack of typomorphic minerals and elements commonly found in

hydrothermal deposits and the apparent lack of primary pitchblende or uraninite in deeper sections of the main shear zone below the water table also argue against a hydrothermal origin.

5.3 Flodelle Creek Area, Washington State

Located about 90 km N of Spokane, surficial-type U mineralization associated with peat-bog material was discovered in 1983(?) along the upper reaches of the north fork of Flodelle Creek in Stevens County, NE Washington State. Original resources were estimated at 450 t U at grades varying between 0.025 and 0.1% U. The *Meadow mine* produced 0.5 t U over a short period of mining beginning in the fall of 1983.

Sources of Information. Johnson et al. 1987, 1990; Otton and Zielinski 1986; Zielinski and Otton 1986; Zielinski et al. 1986, 1987, 1990.

Geology and Mineralization

Uranium concentrations are situated in a Holocene drainage basin (4.1 km²) controlled by glacial topography (Fig. 5.4a). Mineralization is hosted in a valley filled with organic-rich pond and stream sediments, as much as 4 m thick. Sediments range from peat (50–60% organic matter) to clay, silt, and sand all of which contain more than 0.5% organic matter. Intercalated Mazama volcanic ash yield ages of 7,000–6,700 years, and ¹⁴C dating of organic matter in peat give ages of about 5,100 years for upper and 6,650 years for lower host sediments. These sediments rest upon glacio-fluvial till and outwash approximately 15,000–12,000 years old. The basement consists of two-mica quartz monzogranite of Cretaceous Phillips Lake Granodiorite, which is locally fractured and faulted and is mostly covered by glacial drift.

No discrete U minerals occur. U is present as urano-organic complexes and/or adsorbed on organic material, but also on clay, marl, and grey to black silty sand particles. In variously decomposed twig fragments and dried peat, uranium shows a preferential association with fine-grained, structureless organic matter.

U distribution and tenors are highly variable; concentrations range from <100 to >1,000 ppm U with a maximum of 9,000 ppm U in organic-rich sediments of a little pond in the upper valley. Zinc (16–330 ppm) and molybdenum (<2–110 ppm) are slightly enriched in sediments. Total sulfur contents amount to 0.03–0.69%. Uranium values correlate highly with organic matter content ($r = 0.6–0.8$) and also with total sulfur contents. All uranium is in disequilibrium with uranium in large excess relative to daughter products, and lack of associated radioactivity.

Metallogenetic Aspects

According to the earlier mentioned authors, ore-grade uranium concentrations at Flodelle Creek have formed in glaciated

terrane in recent times as indicated by strong radioactive disequilibrium. Uranium precipitated and still precipitates where anomalously uraniferous feed waters from granitic country rocks intercept organic matter in the small drainage basin. Monzogranite containing from <1 to 80 ppm, and averaging ca. 16 ppm U provided the U source rock. Part of the uranium in this granite must be present in leachable form as indicated by shear-controlled near-surface mineralization grading as much as 500 ppm U.

The high variance of U distribution and tenors is explained by the mode of waters migrating through organic-rich sediments, direction of water flow, and transmissivity of peat and interbedded sediments. Waters involved are derived both from surface runoff from the small drainage basin and from springs that issue from till-covered slopes or valley-bottom sediments.

Pregnant waters carrying up to several hundred parts per billion U, appear to be neutral to slightly acidic and mildly oxygenated. Otton and Zielinski (1986) report Flodelle Creek head waters to have a pH range from 5.85 to 7.55, and contents of 17–318 ppb U, which is highly elevated as compared with a regional average of ± 2.4 ppb U in streams and springs. Most uranium is present in a dissolved state as indicated by its high covariation with Ca²⁺, Na⁺, Mg²⁺, and HCO₃⁻ ions, total dissolved solids, and conductivity. A small fraction of uranium tends to be bound by colloidal particles of clays, organic matter, and hydrous iron oxides. Mildly oxidizing conditions may be deduced from the high concentration of dissolved uranium, the absence of H₂S in the water and most sediments, as well as the presence of dissolved nitrate.

The fixation of uranium is less by reduction, but rather more by ion exchange and adsorption on organic material as reflected by the high-correlation coefficient of up to 0.8 for U to organic matter (Fig. 5.4b). The preferential association of uranium with fine-grained, structureless organic matter of variously decomposed twig fragments and peat suggests that surface area and degree of humification are significant factors on uranium fixation.

5.4 Coeur d'Alene District, Idaho

Located in northern Idaho, the Coeur d'Alene district is famous for silver and base metal vein deposits, but some veins also contain uranium, e.g., in the Bunker Hill and the Sunshine mines.

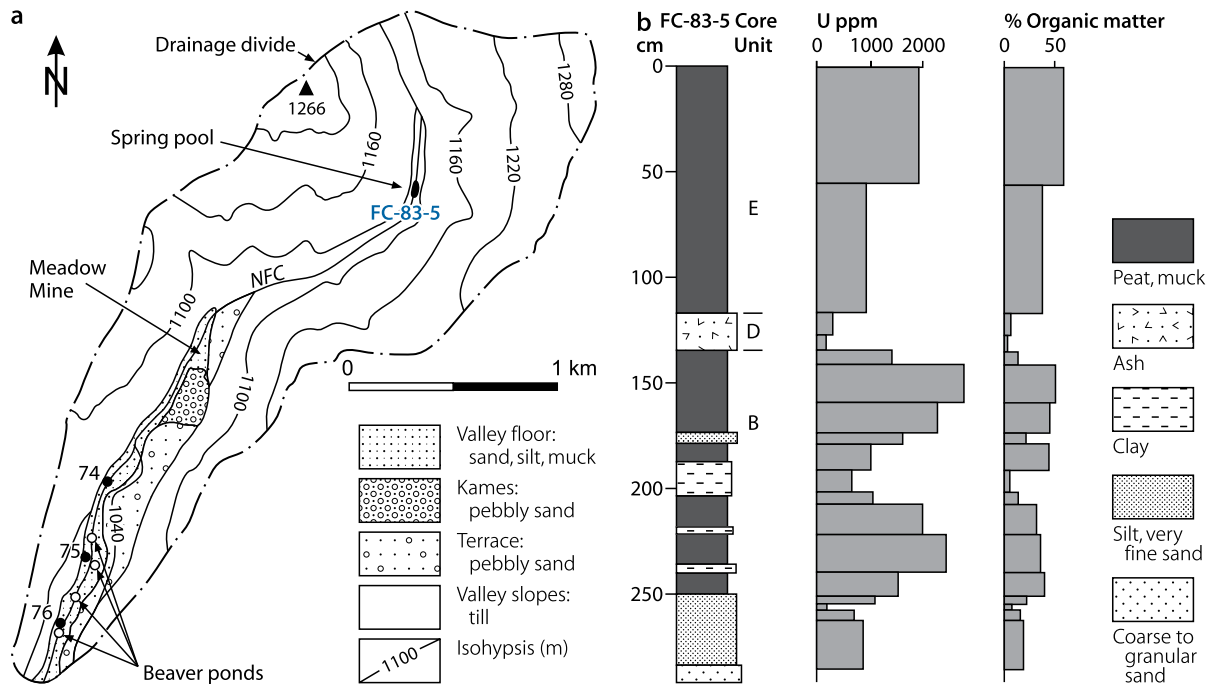
Sources of Information. Foehl 1999; Kerr and Kulp 1952; Leach et al. 1998; Thurlow and Wright 1950.

Geology and Mineralization

The Coeur d'Alene district is underlain by metasediments (quartzite, argillite, etc.) of the Mesoproterozoic Belt Supergroup intruded by the Mesozoic Idaho Batholith. Belt sediments are thought to have been deposited in a deltaic environment following Proterozoic mobile belt formation, 1,700–1,500 Ma ago. These sediments have undergone low-grade regional metamorphism to greenschist facies contemporaneously with igneous

■ Fig. 5.4.

Flodell Creek, (a) map of surficial deposits in the North Fork drainage basin (NFC), (b) lithological column with contents of U and organic matter from a core at the spring pool site documenting the high correlation of U and organic material. (After Johnson et al. 1987)



activity during which the granitic Idaho Batholith was emplaced. Structurally, the Coeur d'Alene district is located along the NW–SE-trending Lewis and Clark lineament. Hosted by the Proterozoic Belt Supergroup, Ag–Pb–Zn veins and U-bearing veins occur spatially associated in this district (including the Sunshine Mine) but with a mixed history of possibly Proterozoic and Cretaceous ages.

Mineralogically, uranium-bearing veins are of simple composition, being composed of uraninite (pitchblende?), red hematitic jasperoid, pyrite, and minor feldspars.

At the *Sunshine Mine*, U veins strike WNW–ESE and dip southward across a major regional fold, the Big Creek anticline, while Ag-bearing veins trend E–W. Brecciated textures are common in U veins. Much of this brecciation seems to be related to emplacement of cross-cutting silver veins. Wall rocks adjacent to U-bearing veins are silicified with jasperoid, the hematite-caused pink color of which resulted from oxidation of magnetite and sulfides in Belt Supergroup rocks. In addition, brannerite and uranium phosphate minerals occur, but are confined to near Ag-bearing veins.

According to Foehl (1999), U–Pb dating of U minerals produced a concordia age of 885 Ma and a discordia age of 82 Ma, whereas Leach et al. (1998) report U–Pb ages of 136 Ma for U-bearing veins of the Sunshine mine, which would suggest an association with emplacement of the granitic Idaho Batholith. In any event, both data indicate a formation of U-bearing veins pre-dating silver veins.

Silver-bearing veins contain argentiferous tetrahedrite with minor chalcopyrite in a gangue of siderite and quartz. Ag veins

tend to occur in second- or third-order tear fractures between major faults and most likely formed in Laramide time. Silver minerals are absent in uranium-bearing veins, but some uranium occurs in silver-bearing veins, which may have been introduced by argentiferous solutions that remobilized uranium from older U-stage mineralization.

Two discrete mineralizing events are postulated by Foehl (1999) based on structural relationships, ore textures, and nature of ore fluids necessary to form silver-base metal/sulfide-rich veins and uranium oxide veins. Veins appear to be related to similar tectonic stress fields, which would explain the coincident spatial distribution. Uranium mineralization may have been originally formed in the Belt Supergroup rocks at 885 Ma during the East Kootenay Orogeny prior to formation of silver- plus other metal-bearing veins. Formation of the latter is roughly coeval with intrusion of the Idaho Batholith and regional tectonism. As an alternative, uraniumiferous veins may have originated during the late Cretaceous and simply contain older lead. Both models may account for the spatial and possible geochemical relationship of the two differently mineralized veins in the Coeur d'Alene district.

In principal, Foehl's (1999) first hypothesis seems to be more likely when compared with somewhat similar vein deposits in the western Erzgebirge, like Jachymov in Czech Republic and Niederschlema-Alberode in Germany. Although of higher grade and larger U resources, vein deposits of U and Ag plus other metals in the Erzgebirge show a similar structural and mineralogical relationship in the distribution of U and Ag, etc., in time and space, the former pre-dates the

latter (details see Dahlkamp, Uranium Deposits of the World: Europe, in preparation).

5.5 Pryor Mountains – Little Mountains District/Wyoming–Montana

This district is located adjacent to the border between Wyoming and Montana (Fig. 2.1). It was discovered in 1955/1956 and includes two mineralized areas, the Pryor Mountains in central-south Montana and adjacent to the southeast the Little Mountains, about 50 km E of the town of Powell in central-north Wyoming. Mineralization is of the surficial karst cavern type. Original resources were estimated at a few hundred tonnes uranium. Production totalled 85 t U (Chenoweth WL, personal information). It came from 13 small underground mines, which exploited high-grade ore ranging from 0.4 to 0.7% U. Vanadium was a by-product.

Sources of Information. Bell 1963; Harshman 1968; Hart 1958; Hauptman 1956; McEldowney et al. 1977; US AEC 1959.

Geological Setting of Mineralization

The district lies on the northeastern margin of the Bighorn Basin, which originated during the Laramide Orogeny. Host rock for deposits is the upper part of the Madison Limestone of Early Mississippian age. In the Pryor-Little Mountains area, limestone generally is about 200 m thick and consists of a sequence of marine, light-grey, thin- to medium-bedded limestone, which rests upon Precambrian rocks. The Madison Limestone was slightly folded before it was transgressed by the Amsden Formation of Early Pennsylvanian age, and younger formations, up to late Cretaceous age, all of them of predominantly marine provenance. The Amsden Formation is 50–110 m thick and composed, from bottom to top, of red shale, thin-bedded limestone, quartzitic sandstone, and chert breccia. Red shales, from 5 to 20 m thick, invariably overlie the Madison Limestone.

During late Mississippian or early Pennsylvanian time, solution and karst development affected the Madison Limestone. Extensive solution networks along fractures, joints, and bedding planes generated an intricate and complex system of open spaces, specifically in a horizontal zone 3–20 m thick at depths from 40 to 60 m below the hanging wall of the Madison Limestone. A second period of solution perhaps modified the Paleozoic karst system in Tertiary time, after uplift during the Laramide Orogeny.

Collapse caverns and interconnecting channels are partly filled with solution breccia, which consist of downfallen blocks, chert fragments, and other insoluble residues of limestone, and with reddish-brown sand, silt, and clay washed in from the surface or from material of the overlying Amsden and younger formations. Fine-grained debris is well stratified in some caverns, but poorly bedded in others. In some areas, particularly at Big Pryor Mountain, crypto-crystalline silica replaces

carbonate of breccia fragments and cements sand, silt, and clay of the matrix. Other areas, e.g., the Little Mountains, experienced only very little silicification and fill material is only loosely consolidated.

Mineralization

Hart (1958) identified tyuyamunite and metatyuyamunite as the principal ore minerals. Associated minerals include calcite, hematite, gypsum, baryte, opal, and locally fluorite and celestite. Ore minerals occur as fine-powdery, bright yellow coatings on fractures and solution cavities, crusts on limestone blocks, calcite crystals and chert nodules, fissure and vug fillings, and disseminated in the matrix of fine-grained cavern fill.

The magnitude of ore bodies is highly variable conforming to the size and shape of the hollow space in which they occur. Individual ore bodies rarely contain more than 5,000 t of ore (>20 t U), but most have less than 500 t of ore. The grade commonly exceeds 0.4% U and 0.6% V₂O₅. Carbonate contents vary in response to silicification, but may be as high as 85%.

Although uranium is widespread in the area, there are two distinct cavity-controlled ore zones located along ancient to present major drainage routes cutting through the uplifted limestone unit: (a) a N–S-trending zone along the western flank of an anticline and on the west side of a thrust fault at Big Pryor Mountain and (b) a zone about 20 km to the SE, on the backslope of the Little Mountain monocline.

At *Big Pryor Mountain*, silicified breccia ore commonly occurs along or near the base of caverns. Mineralized material is underlain by up to about 1 m of clastic sediments. Ore minerals are found as coatings on chert fragments, which have been cemented by massive silica indicating a possible correlation of uranium and silica. The magnitude of individual ore bodies is highly variable ranging from trace amounts to 1,000 t of ore (4–8 t U) or more. The largest producer has been the Old Glory Mine, which yielded ore averaging 1.07% U.

At *Little Mountains*, ore bodies occur within an erratic network of solution channels and caves. Only very little silicification is noted in this area. Hart (1958) describes the East ore body of the *Feusner mine*, which is one of the largest deposits mined in the district. It has produced about 5,000 t of ore averaging about 0.7% U and 1% V₂O₅, yielding approximately 35 t U. The ore-hosting cavern is irregular in shape, 5–8 m high, 10–25-m wide, bound on the western side by a vertical N–S-trending joint. The length of the cave is almost 50 m paralleling the joint direction. The cavern floor is approximately 20 m beneath the mean surface of the Madison Limestone. Reddish-brown silt derived from the Amsden Formation and mixed with limestone clasts covers the central part in the form of a fan and the northern entrance part of the cave. Ore is disseminated in silt and breccia deposits of the fan at the entrance, and accumulated elsewhere in the cavern in two separate interstratified layers. The lower bed is 0.3–0.9 m thick and lies along the floor of the cave. The upper layer is 0.6–2.4 m thick. Both mineralized layers are coextensive throughout the cavern and extend into the fan deposit.

Metallogenic Aspects

Hart (1958) and Bell (1963) suggest two possible modes of uranium origin and emplacement. (a) Supergene concentration of uranium derived from tuffaceous sediments formerly overlying the Madison Limestone; and (b) introduction of uranium by hydrothermal solutions with subsequent oxidation of original ore minerals resulting in formation of uranyl vanadates as oxidized residues. From whence uranium and vanadium may have derived in this case remains unknown, however. Redistribution of mineralization continues to the present as indicated by radiometric disequilibrium in favor of chemical uranium.

5.6 Copper Mountain District, Wyoming

The Copper Mountain district is located on the southeastern edge of the Owl Creek Mountains in north-central Wyoming, some 60 km NE of the town of Riverton (Fig. 2.1). Uranium occurrences are found in Precambrian granitic rocks and in overlying Tertiary sediments (Fig. 5.5). Uranium was discovered in 1953, in the Eocene Teepee Trail sediments, and in the early 1970s in granite at the *North Canning* deposit, which is described further below. The district produced about 200 t U at ore grades averaging between 0.08 and 0.17% U between 1955 and 1970.

Sources of Information. Abrams et al. 1984b; Bramlett et al. 1980; Cramer et al. 1979; Ferris 1968; Gliozzi 1967; Hamil

1971; Nash 1980; Nkomo et al. 1978; Osterwald et al. 1959; Shrier and Parry 1982; Yellich et al. 1978, unless otherwise cited.

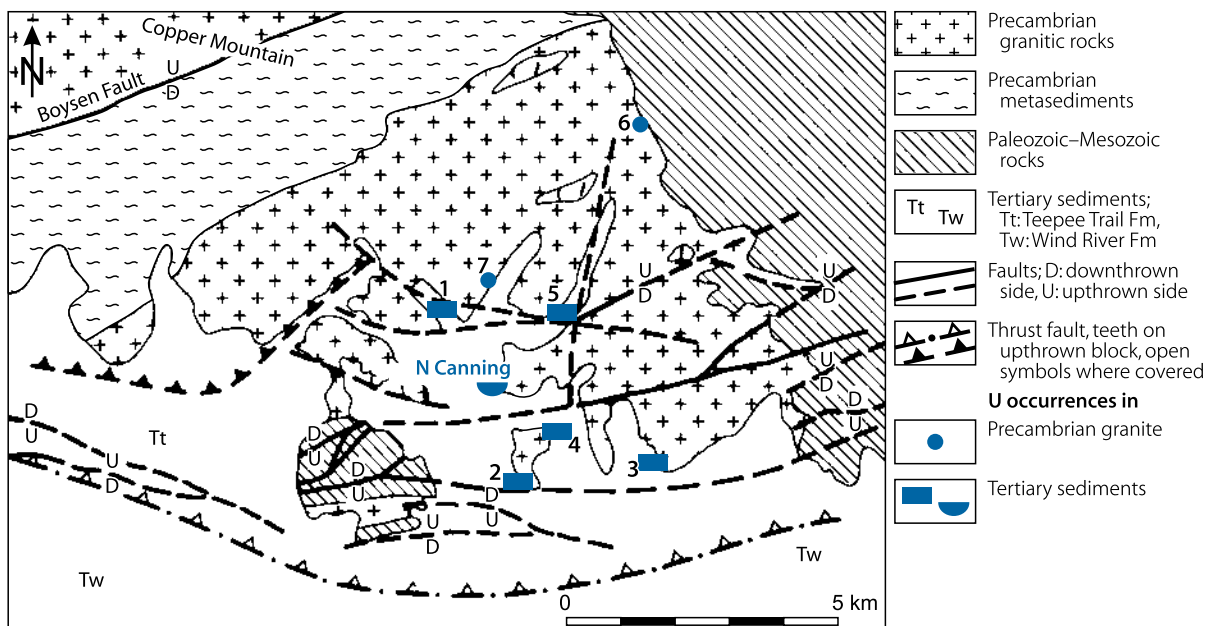
Regional Geological Setting of Mineralization

The Copper Mountain district is underlain by Archean metasediments and metavolcanics, which were intruded by a multiphase granitic complex with numerous granitic apophyses, and pegmatite and aplite dikes of varying composition. Metamorphics were regionally metamorphosed to amphibolite grade facies apparently 3,100 Ma while granitic intrusions yield an age of 2,645 Ma (Nkomo et al. 1978), and hence postdate regional metamorphism. Xenoliths of metasediments and granitic gneiss are common in granites. Archean rocks are cut by diabase dikes that have been dated at 2,100–1,900 Ma (Condie et al. 1969). Nonmarine and marine Paleozoic and Mesozoic sediments, up to about 4.5 km in thickness, rest unconformably upon the Precambrian rocks.

During the Laramide Orogeny, central Wyoming was affected by major physical tectonic deformation but not by metamorphism. The Owl Creek Mountains were uplifted, particularly in lower Eocene time, whereas in adjacent areas basins subsided estimated at more than 10,000 m in the adjoining Wind River Basin to the south. Compressional tectonics resulted in displacement and southward thrusting of the Owl Creek Mountains. Continued uplift with high-angle reverse faulting caused Precambrian units to override Paleozoic, Mesozoic, and Tertiary formations in the form of large thrust plates. Contemporaneously,

Fig. 5.5.

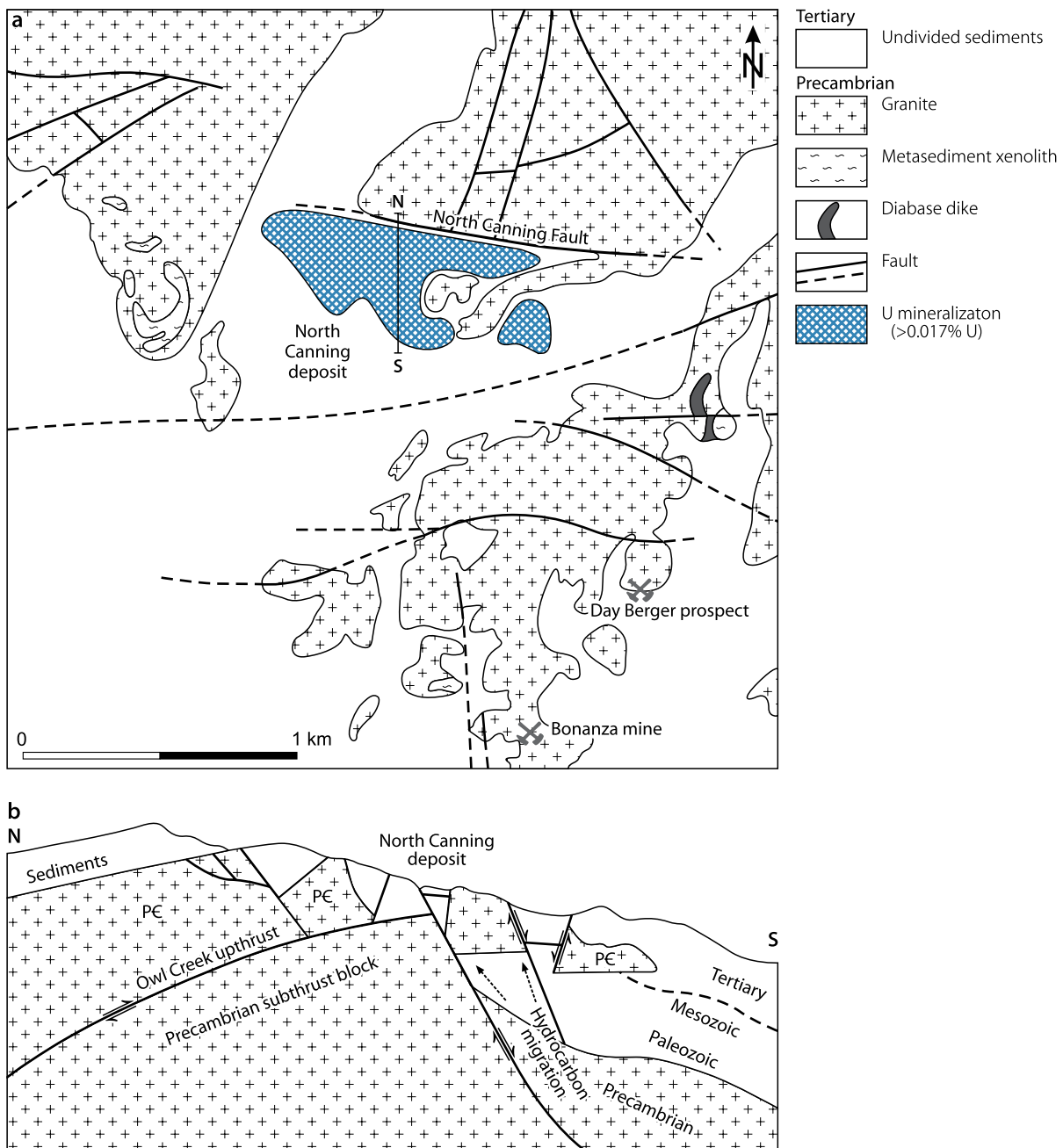
Copper Mountain area, central Wyoming, simplified geological map with location of uranium deposits/occurrences. (After Thaden 1976a, b; Cramer et al. 1979) (U occurrences: 1. Arrowhead mine, 2. Bonanza mine, 3. Schroeckingerite prospect, 4. Day-Berger prospect, 5. Hesitation prospect, 6. De Pass mine, 7. Last Hope prospect)



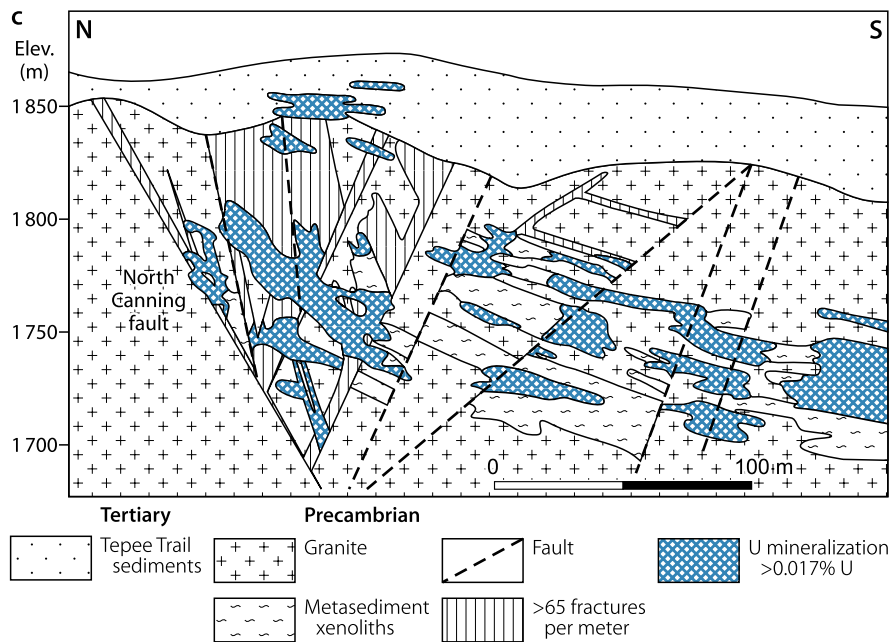
structural readjustment in the upper nappe created an intense and deep fault system in the frontal region along the southern edge of the Owl Creek Thrust. The major frontal thrust fault in this area is the South Owl Creek Mountain fault. It dips about 45° N. The Boysen fault, largest of the subsidiary normal faults dips about 60° S and marks the northern limit of this type of faulting above the main upthrust. Other normal and antithetic faults are numerous in the uplifted block; they generated grabens and horsts, and tilted basement blocks. Continued movement

along faults in the frontal zone created grabens that influenced deposition and erosion of the Lower Eocene Wind River Formation and the Middle to Upper Eocene Teepee Trail Formation. The Laramide thrust movement was essentially terminated by late Eocene as indicated by relatively undeformed sediments of the Teepee Trail Formation, which covers the main Owl Creek thrust fault zone. Tensional structural movements revived during Pleistocene time and resulted in local uplifts leading to erosion.

Fig. 5.6. Copper Mountain, North Canning deposit, (a) geological map, and (b) schematic section illustrating the structural position of the North Canning deposit at the toe of thrust collapse; (c) N-S cross-section with distribution of U mineralization and its relationship to intensely fractured zones and xenoliths in granite. (After (a) and (c) Shrier, Tracy, Parry, W.T., 1982, Society of Economic Geologists, Inc., *Economic Geology*, Fig. 2, p. 633, Fig. 3, p. 634; Thaden 1976a, b; Cramer et al. 1979; (b) Cramer et al. 1979)



■ Fig. 5.6. (Continued)



5.6.1 North Canning Deposit

This deposit has resources of approximately 2,500 t U at grades averaging 0.05% U (cutoff 0.017% U). Enclosed higher grade ore zones account for about 450 t U and average 0.08% U. More than 90% of these resources are in Precambrian rocks and the rest are in Tertiary clastic sediments.

Sources of Information. Cramer et al. 1979; Shrier and Parry 1982; Yellich et al. 1978; and Cramer RT, Davis JE, and Voss WC 1984, personal communication, unless otherwise cited.

Geological Setting of Mineralization

Uranium mineralization of the *North Canning* deposit and other sites at Copper Mountain occurs in brecciated Precambrian rocks of the frontal lobe of the upper Owl Creek Thrust Plate and in the overlying Teepee Trail Formation (▶ Fig. 5.6a, b). Precambrian rocks include various granites with enclosed xenoliths of amphibolite, biotite granite gneiss, biotite schist, and pegmatite. All granites are peraluminous, but have variable calc-alkali fractions, ranging from more potassium-rich microcline-albite to sodium facies, in part at least caused by alteration.

The dominant granitic facies is a medium- to coarse-grained, xeno- to hypidiomorphic granite composed of about 90% plagioclase, microcline, and quartz, the rest being biotite (traces to 10%), which is present as a brown and a green pleochroitic variety. Accessory minerals include apatite, magnetite, sphene, and zircon. The composition of rock-forming plagioclase is An 15 to An 25, and it may be zoned. Gliozzi (1967) mentions, in addition, small euhedral crystals of plagioclase (albite?) of a late

deuteric or metasomatic stage. A prominent variation of granite is a gneissic phase with contacts transitional over centimeters to meters; this gneiss is hypidiomorphic, coarse-grained or porphyritic, and comprises up to 30% biotite. Pegmatite and aplite dikes occur frequently, but randomly in the area. Their contacts with surrounding granite are sharp. Quartz and K-feldspar are dominant constituents. A large diabase dike occurs 1,500 m east of the North Canning deposit.

Sediments of the Teepee Trail Formation veneer Precambrian rocks. The Teepee Trail Formation is as much as 50 m thick and consists of (a) red- and orange-stained arkoses and conglomerates, and grey-green to dark red or brown siltstones, derived from Precambrian granites and metamorphics and (b) bentonitic clays and muds derived from volcanic detritus.

The North Canning area has been disturbed by enormous tectonism as reflected by abundant macroscopic faults, fractures, breccias, and pervasive microfracturing. Low-angle reverse and normal faulting, the most prominent being the North Canning fault, has disrupted continuity of lithologic units. Crushed and broken zones are typical for isotropic granites as opposed to more planar structural development particularly in mafic metasediments. Fracture density is greatest at the North Canning fault and in scattered places to the south of it (▶ Fig. 5.6c).

Host Rock Alteration

Shrier and Parry (1982) distinguish two stages of host rock alteration at the North Canning deposit. Stage I alteration has affected the Precambrian rocks throughout the Copper Mountain district as opposed to Stage II alteration, which is structurally controlled and restricted to uranium-mineralized zones.

Stage I alteration minerals in granites include chlorite, sericite, epidote, and hematite. Sericite replaces plagioclase, epidote replaces plagioclase and biotite, and chlorite sporadically replaces biotite. K-feldspar remained unaltered. Homogenization temperatures of fluid inclusions in quartz microveinlets associated with stage I alteration average 136° C.

Metasedimentary xenoliths are found both unaltered and intensely chloritized. Chlorite parallels schistosity in mafic metasediments, and is particularly prominent in brecciated hornblende and biotite gneisses and schists. It is not yet established, however, whether this chloritization is related to ore formation or not.

Stage II alteration is restricted to fractures and breccias and clearly post-dates stage I alteration. Stage II phenomena include neo-formation of Na-montmorillonite, minor kaolinite, rare chlorite, replacement of plagioclase by K-feldspar, and of magnetite by hematite/limonite, and bleaching. Na-montmorillonite fills small fissures 1–10 mm wide, and is a constituent of the matrix in breccias.

Montmorillonite is white to green, with reddish hematite staining in places. Plagioclase is largely absent; remnant grains are corroded and intensely transformed into K-feldspar. Neo-formed K-feldspar is locally a major constituent of the breccia matrix together with Na-montmorillonite and quartz. Magnetite, unaltered in unfractured to lightly fractured granite, is oxidized to hematite or hydrous iron oxides in zones of intense fracturing or brecciation, and in surface outcrops around the deposit. Iron staining decreases toward breccias. The latter are often bleached.

Brecciated granites experienced a depletion of CaO and Na₂O, and an enrichment of K₂O. Fracture zones show less chemical change, the effects are intermediate.

Mineralization

Pitchblende, sooty pitchblende, coffinite, and uranophane are the dominant U minerals. Uranium also appears to be adsorbed by clays or iron oxides. Pitchblende occurs as massive concretions, encrustations on rock fragments, and as coatings of pore spaces. Sooty pitchblende coats fracture walls in pockets within the rock matrix. Pyrite, present only in minor amounts, is intimately associated with pitchblende. It is found disseminated as 0.5 mm and smaller cubes with montmorillonite in fractures, but not where iron staining is prominent. In breccias, pyrite occurs as anhedral blebs with concretionary and intergranular pitchblende. Hematite staining commonly surrounds uranium mineralization.

Mineralization is hosted in breccia and fracture zones in intensely faulted Precambrian crystalline rocks and in overlying clastic sediments of the Teepee Trail Formation adjacent to the North Canning fault. Fractures with iron-stained clays or iron hydroxide fillings are most commonly mineralized. In contrast, mineralized breccias have no iron staining and are often bleached. Mineralization appears to concentrate in or adjacent to mafic metasedimentary xenoliths, which contain higher amounts of iron (pyrite) and calcite.

Shape and Dimensions of Deposits

The North Canning deposit has an irregular shape, and irregular distribution of uranium correlative to the intensity of faulting in the host granite and metasediments (Fig. 5.6a, c). On the north side, the deposit is terminated by the prominent North Canning fault from where it extends tongue-like southward. The southern, eastern, and western boundaries are transitional grading with decreasing uranium content into unmineralized rock.

The overall extension of mineralization, using an isogram of 0.017% U (cutoff grade) as limit, is approximately 1,200 m in E–W direction along the North Canning fault and between 200 and 400 m in N–S direction. Mineralization persists to a depth of about 150 m.

Ore Controls and Recognition Criteria

The North Canning deposit is both lithologically and structurally controlled. The prime parameters include

- Highly uraniferous Archean granite facies containing uranium in leachable form
- Xenoliths of mafic metasediments in granite
- A major fault (North Canning fault) of Laramide age cutting granite
- Intense faulting with zones of high density of fractures and breccia, associated with the North Canning fault
- Possible seepage of hydrocarbons, and/or H₂S, from underlying or adjacent sediments into ore-hosting Precambrian crystalline rocks as indicated by tar seeps and asphaltite in some underground workings.

Metallogenetic Aspects

While the source of the uranium is not questioned, the processes of mobilization, transport, and redeposition of the uranium in the North Canning deposit remain a subject of interpretation.

Highly uraniferous Archean granite facies tend to be a viable source of uranium. As reported by Nkomo et al. (1978) and Bramlett et al. (1980), surface rock chips from the southern granitic complex of Copper Mountain around and east of the North Canning deposit average 20 ppm U, at least 13 ppm U of which are in leachable form. Unaltered granite of this zone averages 35 ppm U (Shrier and Parry 1982).

Results of U/Pb systematics by Nkomo et al. (1978) are interpreted to document that granites have lost 20–75% of their uranium, probably during late Cretaceous or early Tertiary time for which significant uranium mobilization in the region is established. Assuming an average loss of 30% of uranium endowment, the original uranium tenor of uraniferous granite facies of southern Copper Mountain would have been up to 50 ppm U.

Mineralogic-chemical characteristics of ore and host rock alteration are consistent with some kind of low-temperature hydrothermal event though not of hypogene magmatic origin.

Fluid inclusions in quartz veinlets indicate an average formation temperature of 136° C. Likewise, the regional stage I alteration assemblage of quartz+K-feldspar+sericite+epidote±chlorite±hematite reflects an activity of a low-temperature fluid. This temperature is approximately consistent with that under a cover of 4.5 km thick sediments. The age of stage I alteration is not known.

The structure-confined stage II alteration assemblage of quartz+K-feldspar+Na-montmorillonite±hematite, which occurs associated with U minerals and pyrite, is indicative of a post-tectonic, low-temperature event, the exact age of which remains unknown. There is also no evidence directly linking the two alteration stages together. On the other hand, the position of uranium ore in structures of Laramide age and U/Pb isotope evidence suggest a connection between Laramide tectonism and a regional uranium mobilization.

Yellich et al. (1978) interpret the above data as indicative of complex supergene ore-forming processes. They consider a temperature increase during the Laramide uplift and thrusting, and contemporaneous upward migration of formation fluids containing dissolved sulfur(?) and chloride(?) ions, and hydrocarbons along structurally prepared pathways. Corrosive fluids attacked and altered the wall rocks. Descending meteoric water entering the structural system also became corrosive and altered structurally prepared granitic rocks at and near the surface. This solution leached and became pregnant with uranium. Uranium precipitated where these descending, uraniferous solutions commingled with upward migrating reducing solutions, hydrocarbons, sulfur-bearing waters, and/or possibly sodium (chloride) brines.

Shrier and Parry (1982) propose a low-temperature self-generating convective hydrothermal system for formation of the North Canning deposit in which heat was generated in uraniferous Copper Mountain granite by radioactive decay of uranium and thorium under 4,500 m of Paleozoic and Mesozoic sedimentary cover. Uplift and strong fracturing of heated granite during the Laramide Orogeny permitted the influx of meteoric or connate water containing dissolved oxygen. Convective circulation of heated solutions simultaneously altered granite (stage I alteration) and mobilized indigenous uranium at temperatures of 136°C (pressure corrected 181–226°C). Progressive chemical modification of solutions by water–rock interactions caused stage II alteration and precipitation of pitchblende probably by reaction of uranyl complexes with ferrous iron or sulfide solution species. Shrier and Parry (1982) discard involvement of organic carbon in reduction and precipitation of uranium.

5.6.2 Other Uranium Occurrences at Copper Mountain

Uranium occurrences in the Copper Mountain district are limited to either the Precambrian, mainly Archean, granites and metasediments, or Eocene Teepee Trail clastic sediments (Fig. 5.5). All occurrences are near surface. Identified uranium species include pitchblende/sooty pitchblende, coffinite, and hexavalent U minerals (chiefly uranyl phosphates and -silicates) (Finch 1957; Osterwald et al. 1959).

Bonanza mine: This small mine, located south of the North Canning area, produced uranium from rollfront mineralization in carbonaceous sands and silts of the Wind River Formation. Ore consisted of coffinite, pitchblende associated with pyrite, and hexavalent U minerals.

De Pass mine: A brecciated fault zone cutting biotite and hornblende schists, granite and diorite intrusions, and some diabase dikes is intermittently mineralized with Cu (as oxides and sulfides), gold, and silver. Uraninite occurs within brecciated quartz-carbonate rock. Uranium values are as high as 1%, but are confined to small pockets.

Little Mo-Arrowhead mine: Ore mined averaged 0.12% U and occurred in sediments of the Teepee Trail Formation and underlying granite. Uranium was associated with abundant carbonaceous trash and hematite alteration halos, and locally asphaltic matter.

Day-Berger prospect: Uranium occurs in bentonitic claystone and fresh water limestone.

Hesitation prospect: Tertiary debris accumulated within a N–S valley incised into Precambrian granites and contains U mineralization in the clay and sand matrix that surrounds granitic, mafic, and quartzitic boulders.

Last Hope prospect: Mineralization occurs in Teepee Trail Formation sediments and immediately subjacent in fractures in mafic dikes and granite of underlying Precambrian bedrock. Asphaltic residue is reported dripping in underground workings.

5.7 Pedro Mountains, Little Man Mine, Central-Eastern Wyoming

Located about 70 km SW of Casper in the Heaths Peak area of the Pedro Mountains, the Little Man mine was opened first for gold in the 1870s, but without success. It was reopened for uranium in 1954 and produced about 25 t U through 1956 at ore grades of 1–1.2% U from vein/stockwork ore. Renewed exploration during the late 1970s established several zones with low-grade uranium mineralization as well as copper-bearing zones.

Sources of Information. Harshman and Bell 1970; and Harshman 1985, personal communication; and Conoco staff 1988.

Geology and Mineralization

The Pedro Mountains are part of the eastern margin of the Sweetwater Batholith of Archean age (ca 2,600 Ma). The petrography of the intrusion ranges from quartz monzonite to granite. The prevailing facies in the Pedro Mountains is a biotite granite, which encloses xenoliths, as much as 2.5 km long or more, of metasediments and metavolcanics (chloritic, graphitic schists, amphibolite) that have been metamorphosed approximately 2,900 Ma ago. Diabase dikes were intruded 1,940 Ma ago. These dikes postdate mineralization.

Granite experienced two periods of alteration. An early one, about 2,450 Ma, resulted in the formation of epidote+albite+quartz along NNE-trending zones. The second took place about 2,350 Ma and is reflected by removal of Fe, Ca, and Mg from an aureole, 350 m wide, around xenoliths and produced white-bleached granite and pinkish, hematitic granite. Amphiboles were altered to a mixture of chlorite and biotite. A contact zone characterized by coarse-grained amphibole, feldspar, and quartz is developed along the margins of xenolith bodies.

Mineralization is polymetallic and is composed of Cu, Ga, Mo, Ni, Pb, Se, Th, U, and Zn, but U–Th do not appear to be paragenetically related to the other metals with the exception of perhaps Mo. Ore minerals include thorian uraninite, molybdenite, and sulfides of other metals. Uraninite often occurs as euhedral cubes (up to 0.2 mm large) enclosed in secondary quartz. Uraninite can have thin rims of pyrite and numerous radiating cracks that are partly filled by galena.

Mineralization occurs in the form of veinlets, stockworks, and impregnations in somewhat planar zones in and adjacent to metamorphic roof pendants along a NNW–SSE-trending zone about 8 km in length and up to 100 m or more in width. Gossan covers a large part of this zone under which sulfides usually show up at depths of 1.5–6 m below the surface.

Uranium mineralization is restricted to the aforementioned contact zone, whereas sulfides preferentially occur in somewhat irregular distribution in chlorite schist, biotite schist, graphite schist, and amphibolite of altered xenoliths, but also in the contact zone. Pyrite, pyrrhotite, and chalcopyrite associated with abundant, white to clear, coarse-crystalline quartz occur as veinlets, bands, and clots that are commonly aligned along foliation in the above mentioned schists and amphibolite. Pyrite also coats fractures in amphibolite.

Except for formerly mined high-grade ore and grab samples with up to 4% U, the grade at the Little Man mine is generally below 0.1% U. The U grade seems to increase with depth, at least to the drilled depth of 180 m. Uranium mineralized zones may be some 100 m-long and up to a few meters thick. A copper mineralized zone, from 3.5 to 6 m thick and at least 900 m long, has grades ranging from 0.2 to 1.65% Cu. Ni values range from 0.01 to 0.05%.

5.8 Southern Granite Mountains, Sheep Creek, Central Wyoming

The Sheep Creek U occurrence is located in the northern Green Mountains in central Wyoming, about 5 km south of Jeffrey City (►Fig. 2.1). It reportedly contains resources on the order of 1,000 t U or more, at mining grades below 0.1% U.

Sources of Information. Wertz L and other KMG staff 1979, personal communication.

Geology and Mineralization

Archean granite, dated 2,600-Ma old, occur overthrust upon Cambrian, Triassic, and Cretaceous sediments. Tertiary tuffaceous

sediments overlie the granite. The thrust-zone trends NW–SE and can be traced for more than 10 km; it forms fractured and brecciated intervals locally from 100 to 500 m wide. Faults were repeatedly reactivated. An uplift of granite supposedly took place in early Eocene time followed by a dropdown in late Eocene-early Oligocene time.

Sediments are overturned with the Cambrian Flathead (Cooder Sandstone, pinkish, with some glauconite) and Bucksprings (glauconitic sandstone, siltstone, shale) formations on top, followed by the Triassic Chug-Water Formation (redbed sandstones and siltstones), upon which, separated by the Hazel fault, the Cretaceous Cody Shale rests. Mississippian Madison Limestone containing fluid and dead oil occurs at the southwest end of the Sheep Creek U occurrence, and, to the south, arkosic sand and conglomerate of the Eocene Battlespring Formation that host the Golden Goose uranium mine.

The granite is strongly weathered from the unconformity down to a depth of several meters, followed downward for about 50 m by a zone of chloritization, which grades into a hematitic zone. The latter persists to depths of at least 500 m and includes locally reduced intervals at or near structures.

Uranium *mineralization* is structurally and minero-chemically controlled. It occurs in a complex structural setting along fractures and shears in granitic and sedimentary rocks, in particular in the upper 100 m below the granite surface, but persists along major faults to depths of several hundred meters. The depth extension of mineralization is controlled and limited by the thinning out of the fractured zone.

Ore is in radiometric disequilibrium in favor of uranium (about 10–15% higher). Better grade mineralization of about 0.09% U tends to be associated with structures in granitic rocks, whereas grades in sediments average about 0.07 % U. Favorable host sediments are characterized by the presence of pyrite and glauconite as in the Cambrian Bucksprings Formation, or by oil or asphaltic material as in the Mississippian Madison Limestone. Mineralized fractures in Madison Limestone contain 15–20% carbonate, and in sandstone, silt, and shale of the Bucksprings Formation 2–3% carbonate. Anomalous Hg contents of up to 70 ppb are found along the mineralized zone.

5.9 Granite Mountains, Central Wyoming

The Granite Mountains in central Wyoming (►Fig. 2.1) are considered a main source of uranium to the central Wyoming Basins (Stuckless et al. 1977; Stuckless and Nkomo 1978). The authors describe an alkali granite with various biotitic and leucocratic phases containing 8–9 ppm U. Isotope systematics show, however, that concentrations were above 30 ppm U before the post-Laramide event of major uranium mobilization.

Some mineralization with more than 0.1% U occurs in fractured rock affected by hydrothermal alteration. Alteration products in wall-rock granite include albite, epidote, and chlorite. Fractures are filled with hematite or hydrous iron oxides, pyrite, and uranium, but no uranium mineral could be identified. The authors exclude supergene processes as the cause for alteration or mineralization and propose a dilatency model

for mobilization of uranium. The described mineralization appears similar to the North Canning deposit at Copper Mountain, Wyoming.

Selected References and Further Reading for Chapter 5 Northern Rocky Mountains

For details of publications see Bibliography.

Abrams et al. 1984; Barrington and Kerr 1961; Becraft and Weis 1963; Bell 1963; Bramlett et al. 1980; Condie et al. 1969; Cramer et al. 1979; Elevatorski 1977; Ferris 1968; Finch 1967; Foehl 1999; Gliozzi 1967; Graff and Houston 1977;

Hamil 1971; Harshman and Bell 1970; Harshman 1968; Hart 1958; Hauptman 1956; Hedge et al. 1978; Houston et al. 1977; Illsley 1957; Johnson et al. 1987, 1990; Kerr and Kulp 1952; Leach et al. 1998; Ludwig et al. 1981; Marjaniemi and Robins 1975a, b; McAldoney et al. 1977; Miller and Engels 1975; Milne 1979; Nash and Lehrman 1975; Nash and Ward 1977; Nash 1975, 1977, 1979, 1980; Nkomo et al. 1978; Norman 1957; Osterwald et al. 1959; Otton and Reimer 1991; Otton and Zielinski 1986; Otton et al. 1989; Pearson and Obradovich 1977; Pernsteiner and Ikramuddin 1979; Robbins 1976, 1978; Shrier and Parry 1982; Stuckless and Nkomo 1978; Stuckless et al. 1977; Thaden 1976a, b; Thurlow and Wright 1950; US Bureau of Mines 1977; US AEC 1959; Van Gosen et al. 2007; Weiss et al. 1958; Weissenborn and Moen 1974; Yellich et al. 1978; Zielinski and Otton 1986; Zielinski et al. 1986, 1987, 1990; and Chenoweth WL, Conoco staff, Cramer RT, Davis JF, Dollinger U, Harshman, KMG staff, Voss WC, and Wertz L, personal communication.



Chapter 6

Colorado and Southern Rocky Mountains

The Colorado and Southern Rocky Mountains extend from south central Wyoming through Colorado into north-central New Mexico (Fig. 1.1b) and encompass a belt of N to NW-trending high mountain ranges and intermontane basins. Uranium is a widespread commodity in the Colorado and Southern Rocky Mountains, and occurs in a variety of environments as outlined further below.

Sources of Information. see individual districts and list at the end of this chapter.

Regional Geological Features of the Colorado and Southern Rocky Mountain Uranium Province

Proterozoic igneous and metamorphic rocks crop out in many of the mountain ranges and are bounded by distorted strata of the Paleozoic and Mesozoic age. Cambrian to Mississippian sequences are predominantly of shallow marine origin. During the upper Paleozoic and Mesozoic time, thick layers of both marine and continental sediments were deposited. The upper Cretaceous and Tertiary continental sediments, interbedded locally with pyroclastic rocks and volcanic flows, fill the intermontane basins. A NE–SW-trending zone rich in precious and base metals deposits, the Colorado Mineral Belt, extends from approximately Jamestown in north-central Colorado to the San Juan Mountains in southwestern Colorado. This zone was intruded by numerous plutonic and subvolcanic batholiths and stocks of late Cretaceous to early Tertiary age. The Southern Rocky Mountains were affected by deformation in the late Cretaceous-early Tertiary Laramide Orogeny, and again in the Oligocene and Miocene, producing the modern basement-cored uplifts.

Uranium deposit types found in the Colorado and Southern Rocky Mountains include various vein and sandstone types.

Vein-type U deposits are hosted by metamorphic and igneous rocks of Proterozoic age and by sediments of the late Paleozoic and Mesozoic age. Veins contributed the largest part of past production and contain most of the identified uranium resources of the region. Principal districts are *Ralston Buttes* in the Front Range west of Denver, *Marshall Pass* east of Sargents in the Sawatch Range, and *Cochetopa* south of Gunnison at the northern margin of the San Juan Mountains.

Tabular sandstone (-volcanic)-type U deposits occur in fluvial, lacustrine, and pyroclastic sediments of Tertiary age. The majority of these uranium resources are assigned to the *Thirtynine Mile Volcanic Field* where most of the resource is

contained in the principal Tallahassee Creek deposit, Hansen. Additional resources of this type are reported from *South Park*, which is adjacent to the north of Thirtynine Mile Volcanic Field.

Stratiform and roll-type U occurrences of minor importance are in sandstones of Permian, Jurassic, and Cretaceous age. Some production came from two mines in Cretaceous Dakota Sandstone in the *Morrison* area. Large vanadium deposits in the Jurassic Entrada Sandstone northeast of *Rifle*, near *Placerville*, and at *Barlow Creek-Graysill* north of Durango produced some 100 t of uranium. Ore from these deposits, referred to as *roscoelite-type* after the ubiquitous vanadium mica, grades about 0.06% U and has vanadium to uranium ratios of more than 20 to 1.

6.1 Front Range, Colorado

Located to the west of Denver, the N–S-trending Front Range hosts a great number of mostly small vein-type uranium deposits and occurrences in Proterozoic rocks as well as some sediment-hosted deposits (Fig. 6.1). More than 30 properties have produced uranium, mostly a few tonnes of high-grade ore.

The *Ralston Buttes district*, situated in the east-central Front Range, is the largest district, has had most production, and has the most assumed resources. It includes the Schwartzwalder Mine, the largest known vein-type uranium deposit in the United States. The *Central City district*, although economically not significant, hosts the Wood mine where pitchblende was first discovered in the USA in 1871. Additional districts and deposits are listed further below (Section 6.1.2).

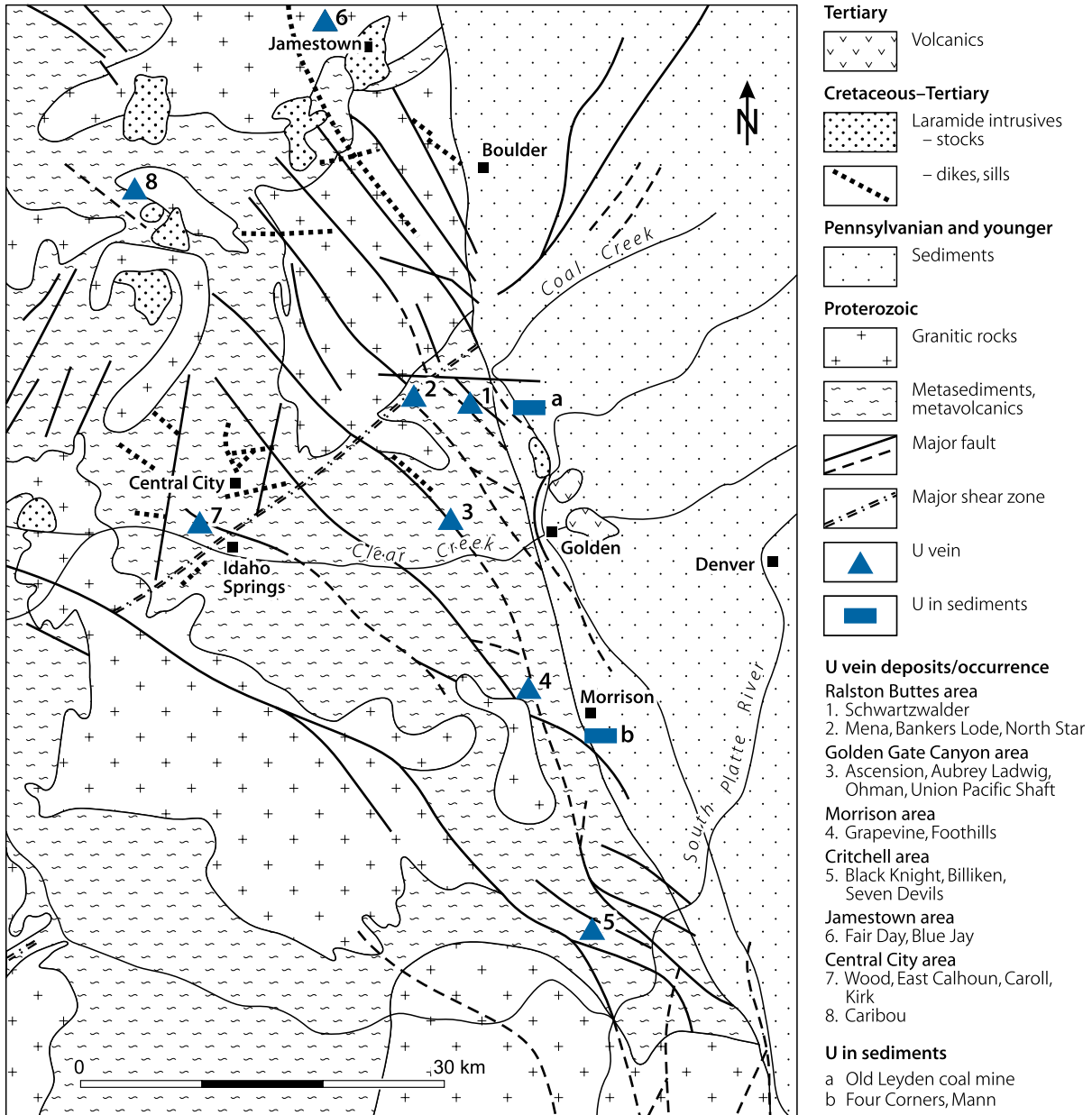
Sources of Information. Byrant et al. 1981; Carpenter et al. 1979; Chenoweth 1980; De Voto and Paschis 1980; Ferris and Bennett 1977; Fisher 1976; Ludwig and Young 1975; Ludwig et al. 1985; Nelson and Gallagher 1982; Nash et al. 1981; Nelson-Moore et al. 1978; Peterman and Hedge 1968; Peterman et al. 1969; Phair 1979; Phair and Jenkins 1975; Sheridan et al. 1967; Sims 1956, 1960, 1963; Sims and Sheridan 1964; Stark 1979; Tweto and Sims 1963; US AEC 1959; Walker et al. 1963; Wallace 1979, 1982, 1983a, b, 1986; Wallace and Karlson 1985; Wallace and Whelan 1986; Young and Hauff 1975; and Grauch R and Wallace AR, personal communication, unless otherwise stated.

Regional Geological Setting of Mineralization

The central Front Range is dominated by Lower Proterozoic metasedimentary and metavolcanic rocks of the Idaho Springs Formation, which exhibit intense isoclinal folding along E–W and NE–SW-trending axis. This assemblage was intruded by stocks and batholiths of granodiorite to granite composition during three major Proterozoic intrusive events. A thick sequence of Paleozoic and Mesozoic continental and marine sedimentary rocks, with redbeds of the Pennsylvanian Fountain Formation at its base, partially overlies and flanks the crystalline basement to the east. A 20–30 m thick regolith is developed in

Fig. 6.1.

Colorado Front Range, generalized geological map of the east-central part of the Front Range with location of uranium deposits and major uranium occurrences. (After Sims and Sheridan 1964; Tweto 1979; Wallace 1983a)



the Proterozoic metamorphic rocks beneath the Paleozoic unconformity.

Protoliths of the metamorphic rocks were shales, sandstones, and rhyolitic, dacitic, and andesitic volcanics, which were deposited prior to 1,750–1,700 Ma. At that time, assemblage was transformed to amphibolite facies rocks by regional metamorphism and was intruded syntectonically by granodiorite and quartz monzonite (e.g., Boulder Creek Granodiorite). At about 1,400 Ma, granites and quartz monzonites such as the Silver Plume Granite and associated pegmatites were emplaced, and some hydrothermal veins were formed at this time. The last

Proterozoic magmatic event was anorogenic and produced granitic to granodioritic intrusions of the Pikes Peak Batholith 1,040 Ma (Peterman and Hedge 1968).

During the Laramide Orogeny, 70–50 Ma, porphyritic intrusions of intermediate composition were emplaced to form the NE–SW-trending Colorado Mineral Belt, which intersects the Front Range about 20–30 km N and NW of the Ralston Buttes uranium district. Numerous mineral deposits are associated with these intrusions. Extensive volcanism of intermediate litho-chemistry was active chiefly in the western part of the Front Range in mid-Tertiary time, 40–25 Ma. Related

mineral deposits include gold–silver–base metal veins and molybdenum stockworks in porphyries (De Voto and Paschis 1980).

Several episodes of Proterozoic and Cenozoic tectonism affected and disrupted the Front Range region. Uplift and brittle deformation at about 1,200 Ma (Bryant and Naeser 1980) generated NE–SW-trending shear/fracture zones with intense wall rock cataclasis and mylonitization, as well as smaller, NW–SE-trending structures and cataclastic fault zones. Some fault zones were invaded by aplite, pegmatite, and diabase dikes during the late Proterozoic. Renewed movements associated with block faulting and mountain uplift in probably late Paleozoic (formation of Ancestral Rocky Mountains) and Laramide/late Cretaceous–Tertiary time (formation of present-day Rocky Mountains) very probably reactivated ancient structures as indicated by NE–SW-trending faults cutting Cenozoic sediments. These Laramide movements also created multiple NW to NNW-trending faults as well as numerous subsidiary fractures along these faults in the uplifted block west of the frontal reverse faults due to interaction between Laramide structures and frontal reverse faults. Rigid rotation of the basement is reflected by the steeply dipping Proterozoic–Phanerozoic unconformity along the eastern edge of the Front Range. As a result of episodic uplifts, Paleozoic and younger sediments were eroded from the basement and Proterozoic rocks were deeply dissected.

In the east-central Front Range, at least seven major faults or fault zones of NNW to NW direction can be traced for more than 60 km. They were reactivated repeatedly. Wallace (1982) reports up to five breccia generations. Faults cut both intrusive and metamorphic rocks, and contain characteristically different gangue minerals. Quartz and hematite predominantly cement fault-breccias in granitic rocks, whereas carbonates and adularia cement breccias in metamorphic terrane and also indurate quartz-hematite breccia where both gangue types overlap. Some fault segments contain abundant fluorite (Wallace 1982).

Principal Host Rock Alteration

Only limited alteration is spatially associated with most ore-bearing veins, commonly extending for only several centimeters to a few meters into wall rock. Two phases of alteration are noticed in major deposits of the *Ralston Buttes district*. Dominant alteration minerals of an early alteration phase are carbonates and sericite, which invade and bleach wall rocks, and replace mafic minerals. The degree of mafic minerals alteration and replacement may be an indicator of the relative intensity of this early type of alteration. A subsequent alteration phase, reflected by hematite-adularia growth, is superimposed upon the earlier assemblage in many places, but not everywhere, and gives a reddish hue to rocks immediately adjacent to veins (Wallace 1982, 1983a) (refer to chapter 6.1.01 Schwartzwalder Mine for more details).

Alteration of polymetallic veins of the *Central City district* (see next paragraph) consists of a wider halo of argillization, which encompasses a narrower halo of sericitization, silicification,

and pyritization that affected wall rocks to depths of only several decimeters.

Principal Characteristics of Mineralization and Related Uranium Districts

Two types of uranium mineralization are characteristic in the Front Range: (1) Uranium of Mesoproterozoic age associated with pegmatites (at and near *Ladwig*, *Ascension*, *Fair Day*, and other mines) and disseminated in migmatites adjacent to the Silver Plume Granite (*Wheeler Basin*, uraninite age ca. 1,450 Ma, Ludwig and Young 1975) and (2) uranium of Laramide/late Cretaceous to early Tertiary age emplaced in veins. Economic ore bodies are confined to the second type.

Veins in the east-central Front Range can be tentatively grouped into three categories based on different parageneses, varying geological setting, and at least spatial relation to the Colorado Mineral Belt. Pitchblende occurrences in the heart of the Colorado Mineral Belt are numerous, but are generally too small to be workable (groups (a) and (b), below). Veins of economic interest are strung out in a zone SE of the Mineral Belt (group c).

(a) Veins in the *Central City district* within the Colorado Mineral Belt have a *pitchblende-sulfide (pyrite)-quartz* mineralogy and occur in part in composite-type lodes with galena-sphalerite and locally with Au and Ag, all of which are unrelated and younger than the uranium stage (*Wood* and *East Calhoun* mines) (Sims 1956; Walker et al. 1963). These veins cut Proterozoic granite gneiss, schist, and calc-silicate rocks, which were intruded by Laramide (70–50 Ma) quartz monzonite and syenite stocks containing 10–40 ppm U and quartz bostonite dikes with 30–170 ppm U. Isotope ages of pitchblende are 70–52 Ma (Walker et al. 1983; Sims and Barton 1962; Phair and Jenkins 1975; Everhart 1956; Rice et al. 1982).

Uranium concentrations are irregular and principally of small size, rarely yielding more than a few tonnes of uranium. Similar Laramide mineralization is reported from the *Caribou* deposit, which is hosted in a composite monzonite stock in the NW margin of the Colorado Mineral Belt, about 30 km N of Central City.

(b) Veins at the northeastern end of the *Colorado Mineral Belt* are of two varieties, *pitchblende-pyrite-quartz* and *fluorite with minor uranium*. The latter contain an early stage of fluorite associated with some uranotorite and uraninite (pitchblende?), e.g., in the *Blue Jay* mine (Phair and Shimamoto 1952). Brecciation and neo-mineralization, perhaps by remobilization, formed several stages of fluorite mineralization in which pitchblende commonly occurs together with some chalcedony, quartz, ankerite, hematite, finely disseminated sulfides, and clays as a matrix constituent of brecciated fluorite. Veins are of Tertiary age. Uranium concentrations are spotty and principally of small magnitude and low grade. Pitchblende–pyrite–quartz veins are reported from the *Fair Day* mine. These veins follow a conjugate fault system of N- and NE-striking strike-slip faults in schists and gneisses of the Proterozoic Idaho Springs Formation and Boulder Creek Granodiorite. Ore is concentrated at

intersections of conjugate faults and in refractured portions of veins, which are located in graphitic–garnet–biotite gneisses, a transition zone between hornblende gneiss and mica schist. Granodiorite or granite is generally an unfavorable host, but is strongly argillized along fractures. Ore bodies are small, but locally of high grade. The largest known deposit, the *Fair Day* mine, produced almost 80 t U and had an ore grade of 0.48% U (Sims and Sheridan 1964).

(c) Veins in the *Ralston Buttes district* and adjacent areas (*Golden Gate Canyon district*) are located 20–40 km SE of the Colorado Mineral Belt. They include the only known deposits of economic significance in this part of the Colorado Rocky Mountains. Their principal ore mineralogy consists of an original paragenesis of pitchblende–ankerite–adularia overprinted by younger probably rejuvenated generations as outlined in chapter Schwartzwalder Mine. Anomalous amounts of base and precious metals are generally present. Dominant host rocks, which exerted an apparent litho-structural control, are graphitic garnet–biotite gneiss, calc-silicate gneiss, and quartzite. These rocks are interpreted as a transition zone lithology up to a few hundred meters wide between thick sequences of hornblende gneiss and mica schist of the Proterozoic Idaho Springs Formation. Garnet–biotite gneiss typically contains 5–10% disseminated pyrite plus pyrrhotite and anomalous amounts of Ag, B, F, Pb, Mo, U, and Zn (Young 1979a). Nelson and Gallagher (1982) interpret the transition zone lithologies as marginal marine sediments deposited under hypersaline conditions in an evaporitic environment. The authors consider elevated boron and fluorine contents as a proof for this interpretation. Wallace and Karlson (1985) conclude from their studies that these rocks formed in a back-arc basin with little or no evaporitic components.

Principal Ore Controls, Recognition Criteria, and Metallogenetic Aspects

Besides the dominant structural control, a lithological control appears obvious from the preferential affinity of uranium veins to distinct rock units and, in the particular case of the east-central Front Range, from the position of all vein uranium deposits, within or close to major hornblende gneiss units, except the *Bonzo* deposit, which is hosted by garnet and felsic gneisses. The factual role, however, played by these host lithologies in vein formation and ore concentration remains to be resolved. Three main implications may be envisaged independently or combined, namely that the metasedimentary/metavolcanic rocks provided (a) the source of the uranium, (b) a possible reducing environment for U reduction and precipitation, and/or (c) the proper brittleness to form fracture zones with balanced transmissivity for percolation of mineralizing fluids and porosity for ore accumulation.

Regional structural control is obvious by the localization of all mines with reported production in the Ralston Buttes and Golden Gate Canyon districts, as they all are clustered along three major NW–SE-trending fracture systems, namely the *Rogers fault* (*Schwartzwalder*, *Mena* mines), *Hurricane Hill fault*

(*Ascension*, *Ladwig*, *Ohman*), and *Junction Ranch fault* (*Foothills*, *Grapevine*). An additional regional structural control may perhaps be seen in the spatial position of vein deposits to the northerly trending lineament along the mountain front. All deposits occur within 10 km of that lineament. (For more details on the metallogenesis see the respective section in chapter Schwartzwalder Mine.)

6.1.0.1 Schwartzwalder Mine, Colorado

The Schwartzwalder vein deposit, known as Schwartzwalder Mine, is located in the east-central Front Range, approximately 20 km NW of Golden, Colorado (Fig. 6.1). From 1953 through 2000, the 750 m deep mine produced almost 7,500 t U at an ore grade of 0.408% U. Remaining resources are unknown, but thought to be at least on the order of 2,000–4,000 t U occurring in a drill-indicated depth down to 900 m or more. Ore was hauled to and treated in a mill at Canon City in southern Colorado.

Sources of Information. Adams and Stugard 1956; Bird 1958, 1979; De Voto and Paschis 1980; Downs and Bird 1965; Heyse 1972; Karlson and Krokosz 1983; Maslyn 1978; Nelson and Gallagher 1982; Paschis 1979; Rich and Barabas 1982; Sheridan et al. 1967; Walker et al. 1963; Wallace 1983a, b, 1986; Wallace and Karlson 1982, 1985; Wallace and Whelan 1986; Wallace et al. 1983; Wright 1980; Wright et al. 1981; Young 1977, 1979a, b, 1985; and Wallace AR, personal communication.

Wallace and his coworkers comprehensively and thoroughly researched both mineralization and alteration of the Schwartzwalder deposit. Their publications provided the prime source for the following description amended by data from the other listed investigators (in part as modified quotations), particularly by De Voto and Paschis (1980), Wright (1980), and Young (1979a). Wallace AR kindly reviewed this section and amended and improved both the content and text.

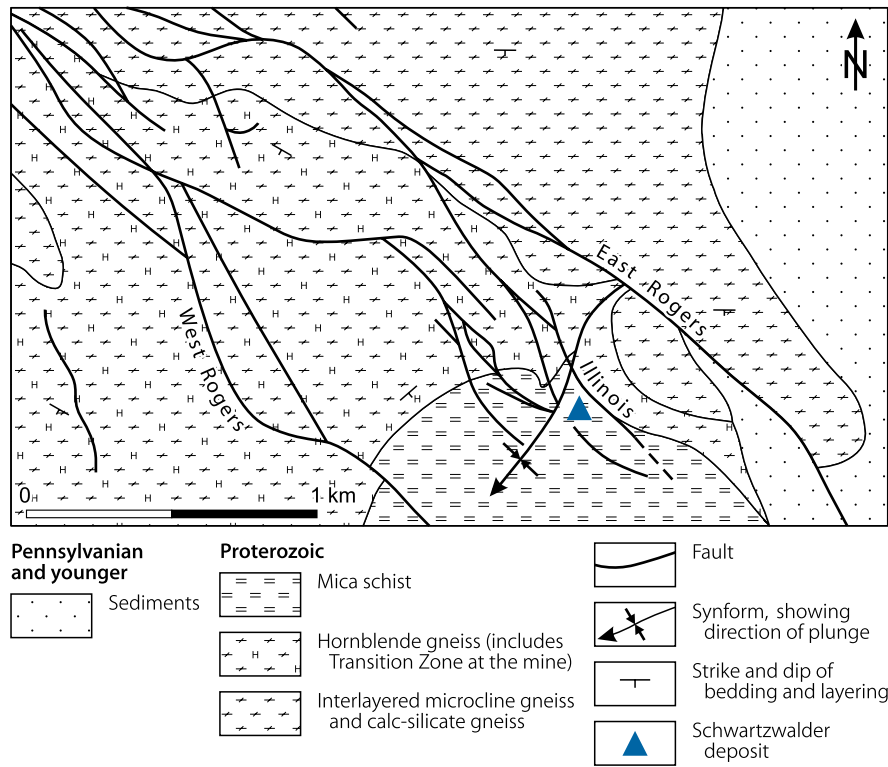
Geological Setting of Mineralization

The Schwartzwalder uranium deposit is located in an area with a complex array of structural dilation zones, fault branchings, deflections, or junctions between the E and W branches of the NW–SE-trending Rogers fault system (Fig. 6.2), and is hosted by Paleoproterozoic lithologies (formerly named Idaho Springs Formation) that were subjected to regional amphibolite-grade metamorphism about 1,750–1,700 Ma and to tight isoclinal folding. Retrograde metamorphism is very minor. Dikes of aplite and tourmaline–garnet-bearing pegmatite of Silver Plume age cut metamorphic rocks.

Phanerozoic sedimentary rocks occur east of the deposit. The nearest outcrop is about 500 m from the mine. Redbed facies of Pennsylvanian age form the basal sedimentary unit. Marine and continental sediments of Permian to Cretaceous age rest upon the redbeds. Regolithization of crystalline rocks extends from the Pennsylvanian unconformity for about 30 m downward.

■ Fig. 6.2.

Schwartzwalder Mine area, generalized geological-structural map of the area surrounding the mine. (After Wallace 1983a, based on Sheridan et al. 1967)



The *petrographic-stratigraphic sequence* at the Schwartzwalder deposit comprises of four major units of Paleoproterozoic age: mica schist, garnet–biotite gneiss, quartzite, and hornblende gneiss (Figs. 6.3 and 6.4) and minor quartz–feldspar rocks. Mineral assemblages of these metamorphic facies are given by Wallace (1983a) as follows:

Mica schist and garnet-biotite gneiss:

Quartz–biotite–almandine–muscovite–pyrite
 Biotite–quartz–almandine–muscovite
 Biotite–almandine–quartz
 Quartz–biotite–plagioclase–pyrite–muscovite
 Quartz–muscovite–microcline–biotite–magnetite
 Quartz–garnet–biotite–hornblende–plagioclase
 Quartz–biotite–muscovite–microcline–garnet

Quartzitic rocks:

Quartz–biotite
 Quartz–magnetite–pyrrhotite

Hornblende gneiss:

Hornblende–plagioclase–biotite–quartz
 Hornblende–plagioclase–actinolite–biotite–quartz–(calcite)
 Calcite–hornblende–biotite–clinopyroxene–scapolite–microcline

Quartz–feldspar rocks include plagioclase–quartz–biotite and quartz–plagioclase–microcline–biotite facies

According to Wallace (1983a), Schwartzwalder host rocks derived from submarine pyroclastics and from iron- and sulfide-rich pelitic sediments similar to other Precambrian iron formations. Sediments were probably deposited in a restricted shallow

basin in close proximity to submarine volcanic centers. Precursors of individual units would be:

- Mica schist: pelitic sediments
- Garnet–biotite gneiss: iron-rich pelites locally containing abundant sulfides and/or some carbonaceous matter, with intercalations of volcanics and local layers of hematitic or siderite-rich chert
- Quartzite: clastic sands or chemically precipitated chert with local laminations of sulfides, shales, and carbonates, grading laterally into pelitic sands (quartz–biotite schist)
- Hornblende schist: mixture of mafic pyroclastics and calcareous mud.

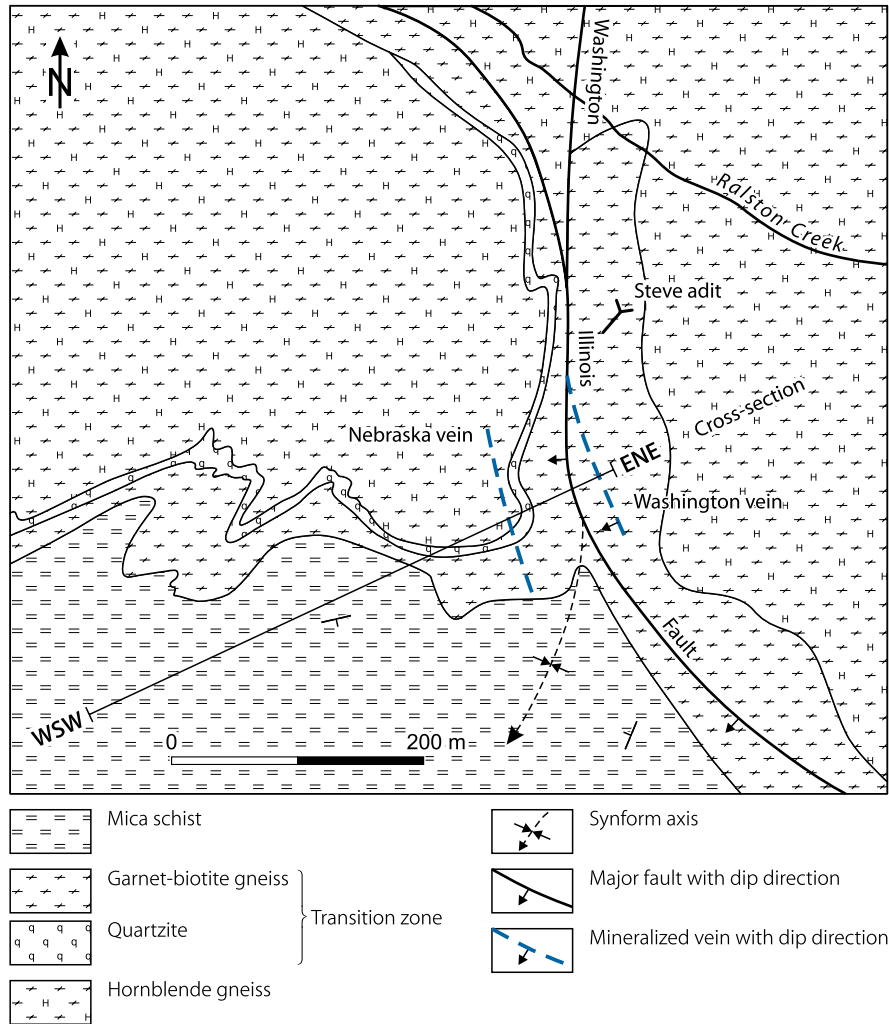
Hornblende gneiss and mica schist are thick and regionally extensive. Garnet–biotite gneiss and quartzite (termed “Schwartz” rocks by mine geologists) form a narrow transition zone between hornblende gneiss and mica schist. The original thickness of transition rocks is difficult to determine due to intense folding and faulting. Karlson and Krokosz (1983) report 15–30 m, whereas Wallace (1983a) estimates a thickness of 50–100 m.

The *structural position* of the Schwartzwalder deposit is dominated by two distinct elements of folding and faulting (Figs. 6.2 and 6.3):

(a) A tightly isoclinally folded *synform* with a nearly vertical NNE–SSW-striking axial plane and a steeply SSW-plunging fold axis. In the synform nose, the original thickness of ore-hosting

Fig. 6.3.

Schwartzwalder Mine area, generalized geological map of the mine area displaying the surface distribution of the four major lithologic units and the structural disposition. (After Wright 1980, in Wallace 1983a)



garnet-biotite gneiss and quartzite units of the transition zone is almost doubled to more than 100 m, whereas elsewhere mica schists occupy the fold core, bounded successively by garnet-biotite gneiss, quartzite, and hornblende gneiss.

(b) A set of two major, approximately parallel, NW-SE-striking faults (*E-* and *W-Rogers faults*) interconnected by diagonal cymoid faults trending NNW to WNW (Illinois fault) with a stacked series of tensional horsetail-type fractures off-branching into the hanging wall of the Illinois fault.

The *East* and *West Rogers faults* belong to a regional structure system consisting of a number of NW-SE-trending faults. The Rogers faults are approximately 1,000 m apart. Both dip 60–70° NE and exhibit intense shearing and brecciation over a width varying between a meter and some tens of meters. The East Rogers fault displaces the Proterozoic-Paleozoic unconformity for more than 100 m. The West Rogers fault cuts the synform.

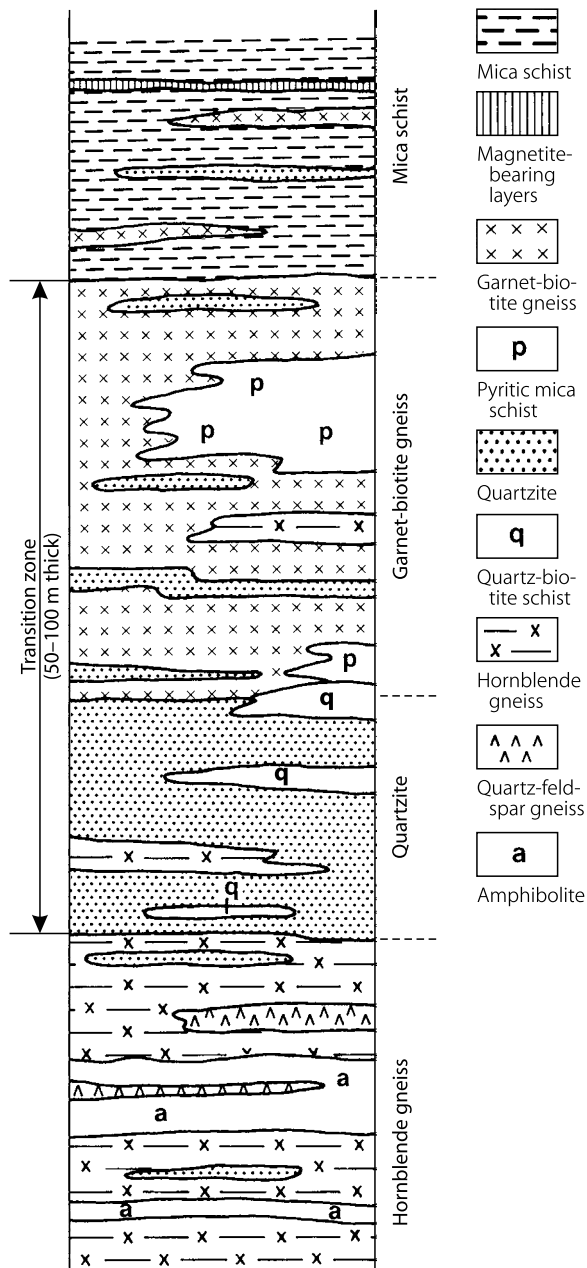
The *Illinois fault system*, which hosts the Schwartzwalder U veins, evolved through multiple tectonic activities. As a result, a

number of pre-ore and post-ore faults trending subparallel between WNW and NNW are developed (Figs. 6.3, 6.5, 6.6). Pre-ore faults dip 70–75° W and post-ore faults 60° W. Wright (1980) identified at least two successive periods of faulting in Proterozoic time: (a) an early, pre-Silver Plume period reflected by faults occupied by pegmatites of Silver Plume age, which parallel the Illinois fault in its footwall and also associated horsetail fractures and (b) a subsequent Proterozoic stage that apparently caused the drag of the synform.

Later stage faults must have been reactivated several times, namely in pre- to early Laramide time to permit entry of mineralizing fluids in Laramide time, and later on repeatedly during mineral deposition as documented by ore textures.

The post-ore Illinois fault formed along the pre-ore Illinois fault in late to post-Laramide time. On upper mine levels, the post-ore fault subparallels the pre-ore Illinois fault in the footwall, transects it between the tenth and 13th level (about 450–500 m below surface) accompanied by heavy brecciation, and then continues into the hanging wall where it splays into

■ Fig. 6.4. Schwartzwalder Mine, schematic lithologic profile of the major metasedimentary units and rock facies. (After Wallace 1983a, based on Sheridan et al. 1967)



two strands. Dip-slip movement caused displacements of more than 100 m. The post-ore Illinois fault is essentially an open structure locally filled by rubble or healed by calcite. In contrast, the pre-ore fault is characterized by matrix-filled breccia.

Horsetail fractures developed in a stacked fashion in competent rocks on the hanging wall side of, and apparently root in the pre-ore Illinois fault (► Fig. 6.5). Wright (1980) considers horsetail fractures to be of Laramide age. He describes two sets of horsetails. One strikes due N-S and the other NW-SE. Both dip easterly at changing attitudes varying between steep and

almost flat, and both are mineralized. No tensional horsetails exist in the incompetent footwall block. Displacement along the post-ore Illinois fault has truncated many horsetail veins below the 13th level.

Faults and fractures display a variety of characteristics and textures primarily in response to the competency of host rocks and the angle of intersection with foliation. Movements in relatively brittle, competent rocks such as quartzite and garnet-biotite gneiss of the transition zone produced fault zones commonly filled with angular breccia clasts, whereas diffuse, gauge-filled fault zones are typical for more ductile or incompetent rocks such as mica schist and, partly, hornblende gneiss. Horsetail veins exist as more integral, discrete fractures within rocks of the transition zone, but split up into numerous tight and smaller fractures when entering adjacent incompetent rocks. Fractures oriented parallel to foliation generally contain much more gauge than those oblique to foliation. Lateral and vertical changes in fracture orientation are accompanied by pinching and swelling of the structure.

Dikes of clastic material are a characteristic feature of the Schwartzwalder deposit. These dikes invaded many structures and veins except the post-ore Illinois fault. The latter is notably devoid of any clastic dikes. These dikes are a few centimeters to a meter wide and are composed of altered wall rocks and antecedent vein material cemented by a microcrystalline matrix of rock flour and authigenic, fine-grained carbonate and adularia. Dike contacts vary between well-defined and gradational. Gradational contacts are typical for sites, where adjacent wall rocks were disrupted by shearing and shattering.

Three generations of clastic dikes characterized by color varieties are noticed:

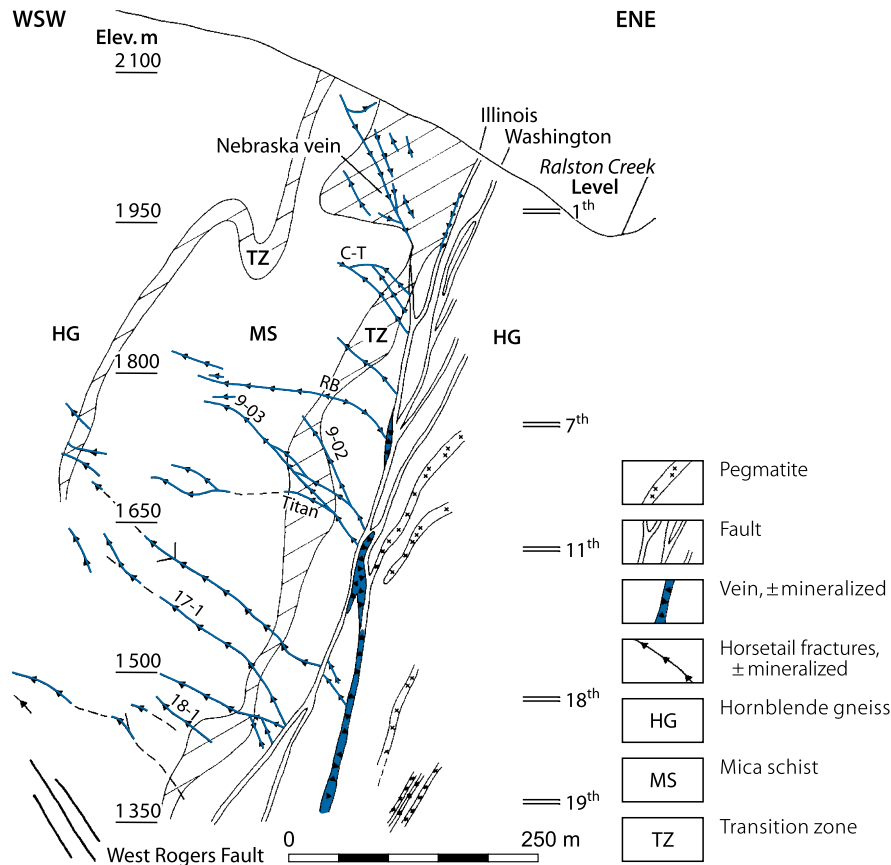
(a) An early, pre-ore generation of pink-colored dikes formed contemporaneously with and subsequent to hematite-adularia alteration in wall rocks. Pink dikes occur preferentially along the footwall of the Illinois and Rogers veins, but are less common along horsetail veins.

(b) A post-ore generation of dark grey dikes characterized by fragments and matrix particles of massive pitchblende, pyrite, and chalcopyrite additional to the before-mentioned constituents. Clastic dikes of this composition are emplaced along the Illinois vein below the 12th level and on horsetail veins as high as the sixth level. Grey dikes extend downward to about the 16th level, and as such they have an almost identical depth penetration as pitchblende veins.

(c) A later generation of pale green to cream-colored clastic dikes, which had formed subsequently to grey and pink dikes, is in lithological and textural composition almost identical to late dikes of the pre-ore episode except that ankerite becomes more Ca and Mg rich. Most lithic fragments were derived from altered rocks. Fragments of mineralization are markedly rare to absent even where dikes cut pitchblende veins. Cream-colored clastic dikes have a similar distribution as grey dikes but extend further into depth, i.e., below the 16th level where they may constitute the entire vein filling of the Illinois vein. A similar situation is noticed at depth along West Rogers' uraniumiferous veins.

Fig. 6.5.

Schwartzwalder Mine, geological WSW–ENE cross-section depicting principal veins, structures and horsetail fractures, and their lithologic position. (After De Voto and Paschis 1980; Paschis 1979; Wallace 1983a)



Host Rock Alteration

Altered wall rocks typically display bleached and overprinted reddish coloration along veins regardless of the presence or grade of mineralization. Alteration is mineralogically uniform throughout the 900 m vertical interval exposed by mine workings, but it nowhere affected extensively or invaded far into the wall rock. It may locally even be absent, even adjacent to pitchblende-bearing veins. Wallace (1983a) describes two successive assemblages of wall rock alteration (Fig. 6.7): (a) Early carbonatization and sericitization pseudomorphically replace all mafic minerals of host rocks within 2 m of veins indicating a large influx of CO_2 and concomitant loss of SiO_2 . (b) Subsequent hematitization and potassium feldspathization (adularia) replace pre-existing alteration minerals immediately adjacent to veins.

Assemblage (a) carbonate–sericite alteration products are of pale yellow-green color and extend for as much as 2 m from fractures into adjacent wall rocks, but without destroying primary rock textures. Sericite and Ca–Mg–Fe carbonates, mainly siderite, ankerite, and dolomite are the principal alteration products, with minor amounts of chlorite, paragonite, kaolinite, albite, and leucoxene. Siderite, marcasite, and pyrite substitute pyrrhotite and the first two replace pyrite of both metamorphic

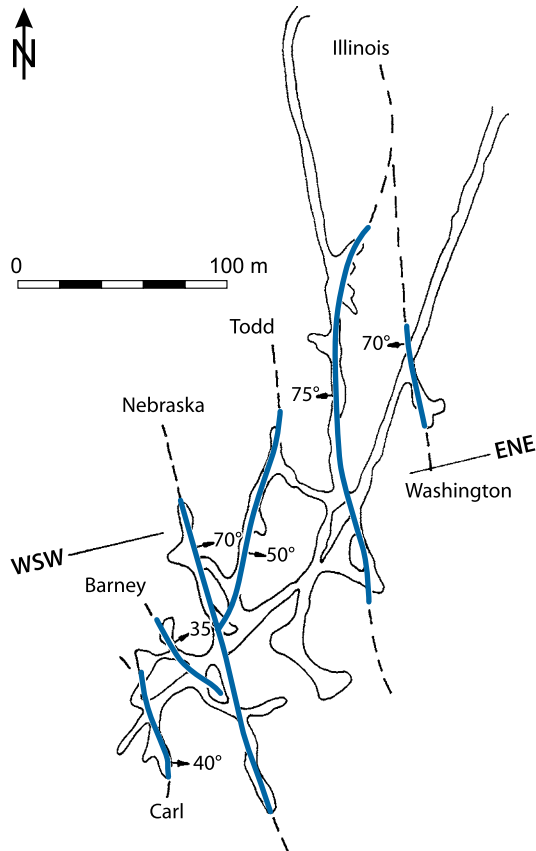
and alteration origin. Although carbonate and sericite pseudomorphically replace mafic rock constituents, they do not severely affect felsic minerals. A critical parameter for the relative intensity of this alteration type is the abundance of mafic minerals in any given wall rock.

Chemical behavior and changes associated with carbonate–sericite alteration are given by Wallace (1983a) as follows (Fig. 6.8):

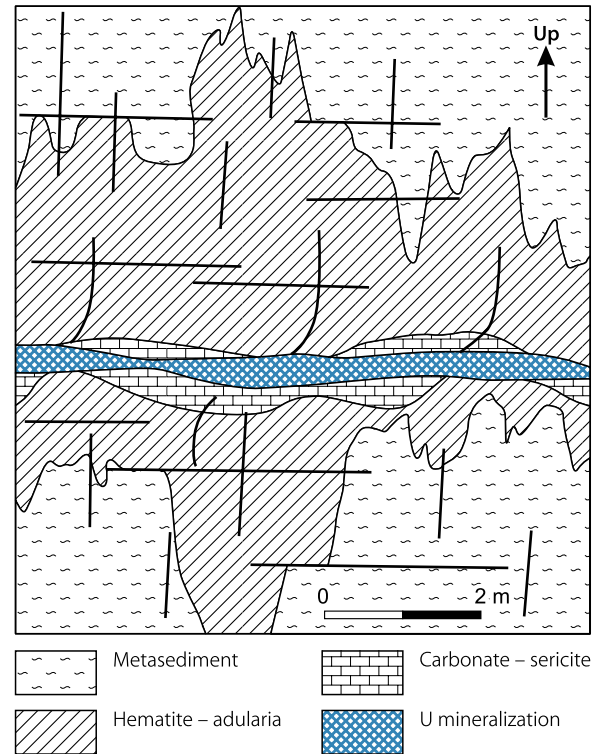
- Al_2O_3 and MgO remained relatively stable
- SiO_2 , FeO, Fe_2O_3 , and S decreased, whereas CO_2 increased in all rock types
- CaO and Na_2O increased in CaO-deficient garnet-biotite gneiss and were removed from CaO-rich hornblende gneiss
- K_2O remained stable in K_2O -rich garnet-biotite gneiss and increased in less potassic hornblende gneiss
- As, Be, Hg, Mo, Pb, Sb, and W contents increased in altered rocks but are also prevalent in veins as well. Ba is consistently depleted.

Assemblage (b) hematite–adularia alteration consists essentially of these two minerals, but adularia can be locally absent. Alteration extends as a reddish, asymmetric halo for rarely more than 20 cm into the wall of most fractures, but is missing on one or both sides along many vein segments. It is restricted to

■ Fig. 6.6. Schwartzwalder Mine, planview of the first level with distribution of major veins and mine workings. (After Paschis 1979)



■ Fig. 6.7. Schwartzwalder Mine, schematic illustration of the relative distribution of early carbonate-sericite and later hematite-adularia alteration zones along a vein. Vertical foliation is shown by vertical lines. Some of the foliation exhibits drag along the vein-hosting fault. (After Wallace 1983a)



rocks altered by type (a) alteration where it substitutes the earlier formed assemblage and relict feldspars as well. Hematitization also affected pre-ore breccia fragments. At sites of most intense impact of this alteration type along the Illinois and Rogers faults, most quartz and all primary textures are destroyed and a hard, microcrystalline intergrowth of hematitized adularia with irregular patches of carbonates was formed. Chemical investigations are too incomplete to be conclusive, but the data tend to indicate that the Fe^{2+}/Fe^{3+} ratio decreased only slightly, which is surprising for a hematite-forming alteration process.

Wallace (1983a) considers a range of 175–225°C as a reasonable estimate for the temperature during alteration processes, with somewhat higher temperatures in the second stage as compared to the earlier stage of alteration. He outlines as salient criteria for alteration:

- Introduction of large amounts of carbonate into wall rocks
- H_2CO_3 as the dominant aqueous carbon compound throughout alteration
- Stability of Fe-bearing minerals
- Sequential formation of, first, sericite, and rare albite replacing more basic plagioclase during the alteration phase affecting primary feldspars and mafic silicates but preserving muscovite; and, second, adularia

- Formation of an identical alteration mineralogy in both garnet-biotite and hornblende gneiss despite dissimilar metamorphic mineral assemblages
- Hematite-adularia crystallization by continued hydrothermal activity at the expense of many preexisting minerals; associated with an increase of K_2O as adularia formed, destruction of muscovite and albite with removal of Na_2O ; hematite dusting of primary feldspars and secondary adularia.

Mineralization

Schwartzwalder vein mineralization occurs predominantly in the Illinois, West Rogers, and associated horsetail structures. Ore consists essentially of pitchblende accompanied by a number of minerals as discussed below. Trace elements include those listed in Table 6.1 (As, Ba, Cu, Mo, Pb, Sb, Sr, Th, V, and Zn).

Multiple stages of mineral deposition and associated preceding and coeval stages of fracturing/brecciation are identified. Wallace (1983a) documents *three main successive paragenetic stages* and several sub-stages of hypogene uranium and base metal mineralization (Fig. 6.9):

Table 6.1.

Schwartzwalder Mine, summary of trace element concentrations in Illinois, Rogers, and horsetail veins (Wallace 1983a)

No. samples	Horsetail veins		Illinois vein		Rogers vein	
	13		9		9	
(ppm)	Mean	±	Mean	±	Mean	±
Ag	26.30	30.60	6.50 ^a	4.20	12.70 ^a	8.90
As	124	102	61.40	43	44.40	34.30
B	N	–	N	–	N	–
Ba	116	53	147	70	259	294
Be	1.80 ^a	1.40	1.94	1.16	2.94 ^a	2.88
Bi	1.50	2.60	3.22 ^a	3.36	0.29	0.13
Cd	2.54	2.20	1.82 ^a	0.93	2.64	4.73
Co	45.50	58.90	20.20	5.60	22.20	14.90
Cr	40.00	29.90	67.20	41.00	33.30	21.10
Cu	494	855	432	967	147	76
F	215	99	267	235	378	466
Ga	8.46 ^a	4.30	12.80	2.60	9.44 ^a	5.27
Hg	4.43	6.00	0.30	0.29	0.82	0.56
La	N	–	N	–	N	–
Mo	3,668	3,043	583	739	1,580	1,337
Nb	L	10.60 ^a	1.67	11.70 ^a	3.50	
Ni	64.60	53.60	42.60	17.20	42.30	29.30
Pb	4,285	5,383	629	971	1,974	1,666
Sb	166	166	78.40 ^a	93.80	69.40	75.60
Sc	7.77 ^a	3.68	15.20	4.50	8.56	2.24
Sr	149	79	149	71	223	177
Th	4,575 ^a	9,030	652 ^a	878	1,000 ^a	917
Tl	27.50	17.00	5.33 ^a	5.12	4.33 ^a	2.99
U	8,664	8,412	2,154	2,762	4,547	4,079
V	327	196	280	176	341	216
Y	23.50 ^a	15.70	19.40	4.64	18.90	10
Yb	1.65 ^a	0.85	2.00	0.66	N	–
Zn	239	543	237	226	367	620
Zr	83.80	72.60	72.20	47.40	80	37.70
W	N	–	N	–	N	
S%	1.14	1.03	0.42	0.36	NA	–
C% inorg.	4.17	2.41	5.08	0.77	NA	–
C% org.	0.66	0.70	0.47	0.21	NA	–

^a Maximum value only: samples with concentrations below detection limits were calculated on basis of value of detection limit

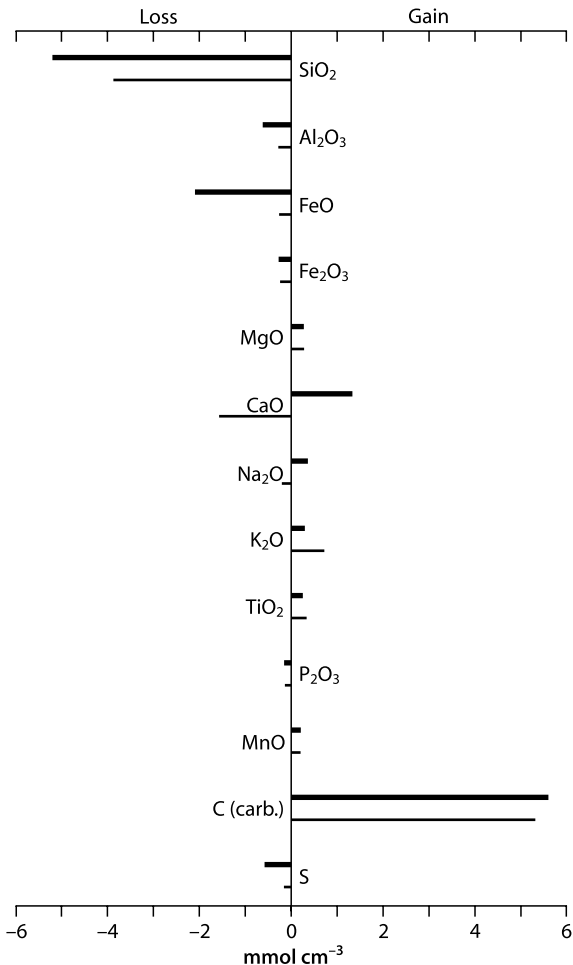
N: Not detected

L: Detected but at concentrations below accurate detection limit

NA: Not analyzed

■ Fig. 6.8.

Schwartzwalder Mine, graphic presentation of relative gains and losses of major oxides during early carbonate-sericite alteration of garnet-biotite gneiss (*thick upper bar*) and hornblende gneiss (*thin lower bar*) (in millimoles/cm³). Gains and losses are relative to the composition of the unaltered equivalent lithologies. (After Wallace 1983a)



I: Sulfide-carbonate-adularia

II: Pitchblende-coffinite-carbonate-adularia-sulfide

III: Calcite-sulfide.

Stage I mineralization is sparsely represented. It includes two mineral assemblages:

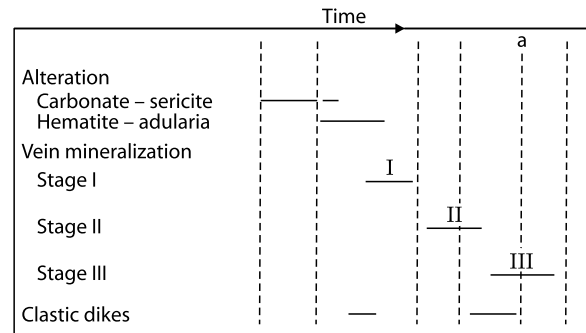
(Ia) Hematite-chalcedony-carbonate, which formed contemporaneously with the second stage of alteration

(Ib) Carbonates, mainly dolomite, non- to slightly hematitic adularia, and base metal sulfides including chalcocite, chalcopyrite, galena, pyrite, and zoned yellow sphalerite.

Stage II is the principal uranium phase and produced the bulk of vein fillings. Earlier workers (Heyse 1972; and others) describe only one major uranium generation. In contrast, Wallace (1983a) subdivides stage II into three substages, as presented in Fig. 6.10. Pitchblende and coffinite are the only uranium minerals. Pitchblende is paragenetically intergrown with an unnamed Fe-Mo-As-sulfide mineral with variable

■ Fig. 6.9.

Schwartzwalder Mine, paragenetic scheme of major episodes of alteration, mineralization, generation of breccia dikes, and major periods of faulting and related brecciation (*hatched vertical lines*). (*Mineral stage I: sulfide-carbonate-adularia; II: pitchblende-coffinite-carbonate-adularia-sulfide; III: calcite-sulfide*) *a* post-ore Illinois Fault. (After Wallace 1986)



Mo/As ratios. The mineral, formerly referred to as jordisite or molybdenite, is characteristic for horsetail ore, whereas it is markedly rare in fractured ore along the Illinois and West Rogers faults.

Substage IIa mineralization commenced with ankerite-dolomite and nonhematitic adularia followed by pitchblende, pyrite, chalcopyrite, galena, and the Fe-Mo-As-S mineral. Coffinite replaces pitchblende. All minerals commonly form a black, very fine-grained mixture filling voids in breccia zones and fractures. Pitchblende may occur as tiny spherules or colloform coatings of rock fragments. Some voids and small fractures are filled completely by massive pitchblende.

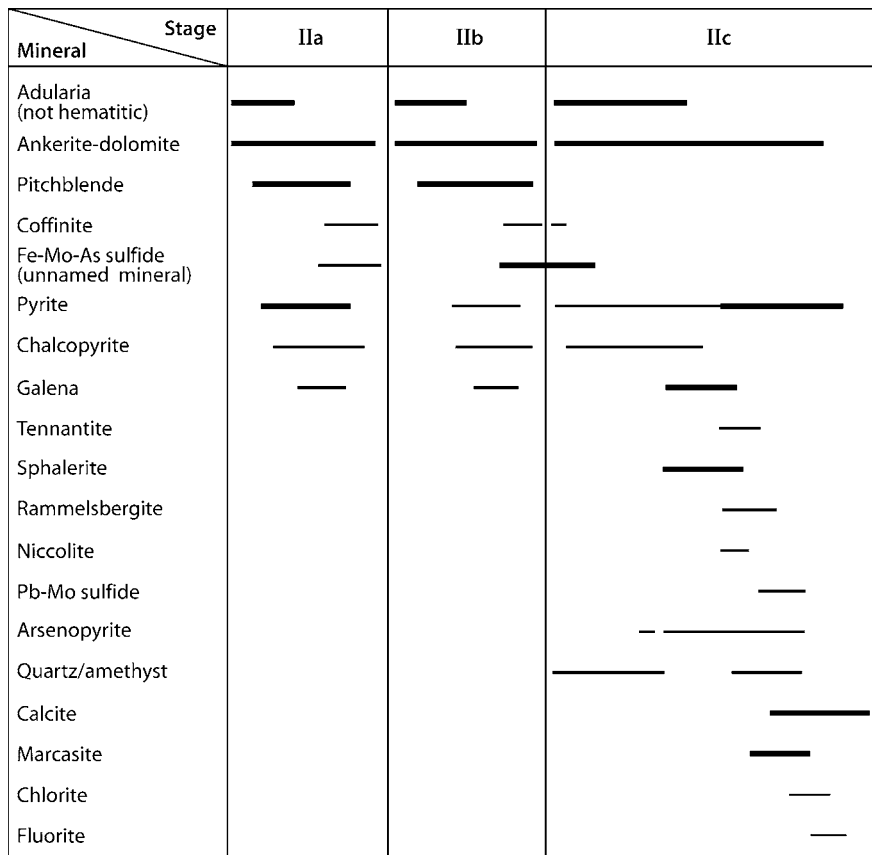
Substage IIb mineralization consists of principally colloform pitchblende intergrown throughout with minor amounts of disseminated sulfides including chalcopyrite, pyrite, galena, and Fe-Mo-As-sulfide. Gangue minerals are ankerite, dolomite, and nonhematitic euhedral adularia. Pitchblende and the other minerals fill interstices between breccia fragments of reopened veins.

Substage IIc mineralization is composed of a carbonate-sulfide assemblage with carbonate by far more abundant than sulfide. The assemblage fills voids and fissures, which remained open after pitchblende deposition. Principle sulfide and gangue minerals are the same as in substages IIa and IIb, but pitchblende is missing. Sulfide additions include yellow sphalerite, marcasite, and minor amounts of tennantite, niccolite, rammelsbergite, arsenopyrite, and a Pb-Mo sulfide containing Fe and minor Sb. Replacements are common. Added gangue minerals are quartz-amethyst, chlorite, fluorite, and calcite. Calcite was the last mineral to form. Carbonates show some zoning within a vein by a change from ankerite to dolomite and to calcite from the rim toward the center of the vein.

Stage III mineralization comprises a coarse-grained assemblage of calcite-sulfide, predominantly pyrite and marcasite with minor chalcopyrite. These minerals fill vugs and fissures in uranium veins and in post-ore structures such as the post-ore Illinois Fault.

■ Fig. 6.10.

Schwartzwalder Mine, paragenetic diagram of stage II mineralization. The *thickness of lines* indicates the relative abundance of minerals. (After Wallace 1983a)



Supergene mineralization is limited to the uppermost part of the deposit, above the first level. Complete transformation of pitchblende into hexavalent U minerals is virtually restricted to within 10 m of the surface.

Chemical investigations by Wallace (1983a) show distinct *trace element associations* for the horsetail vein system, and different and less distinct correlations for the Illinois and West Rogers veins. Mineralization of horsetail veins exhibits two associations of elements: (a) U, Mo, As, Hg, and Sb and (b) Ag, Co, and Ni. Uranium is also closely associated with Pb, S, and Zr. The marked U, Mo, and As correlation reflects the paragenetic relationship of pitchblende and the Fe–Mo–As sulfide mineral in horsetail veins, which survived fault movements. Mineralization in the Illinois and West Rogers veins, which has been subjected to recurrent disturbance, shows only weak correlation of these elements. The relationship between U and Mo and volatile elements As, Hg, and Sb is far less clear reflecting the far less common presence of the Fe–Mo–As sulfide in these reactivated structures.

Shape and Dimensions of Deposits

Uranium ore is distributed intermittently mainly in the steeply SW-dipping Illinois vein and in associated easterly dipping horsetail structures in its hanging wall. Some ore is in the

Washington vein, which parallels on the footwall side and joins in depth the Illinois vein (Figs. 6.4 and 6.5). The mineralized vein system extends laterally for approximately 150–200 m in NNW–SSE strike direction along the Illinois vein, and for 50–150 m in width perpendicular to and mainly on the western horsetail side of the Illinois vein.

Depth extension of the Illinois vein system as known from mining (to 20th level) and drill-intersection is more than 700 m under the present day surface. Wallace (1983a) attributes this deep penetration to down-faulting of some vein sections. Mineralization within the Illinois vein itself extends intermittently from the surface to the 15th–16th level. At this depth, the structure narrows from a width of about 5 m with relatively good ore grades to a width of about 1 m and is devoid of ore except for some brecciated ore at the footwall boundary. Unmineralized breccia and dikes of cream-colored clastic material fill the structure from the 16th–17th level downward. Carbonate–sericite alteration continues in a narrow, but persistent zone in wall rocks beyond the extent of uranium distribution to at least the 19th level. The distribution of grey clastic dikes, which become more prevalent below the 13th level, is restricted downward to primary ore segments, i.e., these dikes disappear below about the 16th level.

The 17-1 vein, one of the larger and lower-positioned horsetail structures, intersects the Illinois vein between the 16th and 17th level. Although mineralized with abundant primary ore on higher levels, uranium distribution in the 17-1 vein

becomes erratic and grades drop below the economic cutoff grade on lower levels. On the 16th level, just above the intersection with the Illinois, the 17-1 vein is less than 1 m wide and is replaced by a light colored clastic dike.

The West Rogers fault does not carry ore on the upper levels, but contains drill-indicated ore at a depth of about 900 m some 200–250 m to the west of the Illinois vein.

The width of mineralized veins varies from millimeters to several meters. Horsetail veins average about 0.5 m in width, and commonly contain high-grade ore. The Illinois vein has a width up to 15 m, but ore, although of large minable tonnage, is of relatively low grade. The length of ore shoots may be as much as 100 to 200 m as within cymoid loops of the Illinois vein. Horsetail veins, which root on cymoid bends, can have corresponding economic strike lengths and dip extensions of 150 m and more (Wright 1980).

Uranium grades are highly variable as reflected by values for annual ore production ranging from 0.46 to 1.32% U (average 0.67% U) during the period from 1953 through 1965 (cumulative production 830 t U), and from 0.178 to 0.76% U (average 0.39% U) from 1966 through 2000 (cumulative production 6,650 t U). Contents of trace elements can be greater than 100 ppm for As, Ba, Cu, Sb, Sr, V, and Zn, and several 1,000 ppm Mo, Pb, and Th (Wallace 1983a).

Stable Isotopes and Fluid Inclusions

For data of fluid inclusions and stable isotopes of oxygen, carbon, and sulfur in vein minerals and constituents of the metamorphic host rocks and alteration products, the reader is referred to the first part of the chapter Metallogenetic Aspects.

Geochronology

Ludwig et al. (1985) report well-defined U/Pb isotope ages of 69.3 ± 1.1 Ma for a suite of ore samples from the Titan vein, a structure in the horsetail section of the Schwartzwald deposit. The U/Pb isochron intercepts suggest that mineral components derived from a source 1,900 to 1,600-Ma old, which is equivalent to ages of metamorphic host rocks.

Other geochronological data of the Schwartzwald deposit and surrounding terrane include:

U/Pb (Heyse 1972): 68 ± 2 , 61, and 52 Ma. These ages were considered the most reasonable age dates of pitchblende from above the 6th level; they derived from a discordant age pattern of 76–18 Ma when using galena from the 4th level or common Pb corrections.

Fission track: 68.9–59.4 Ma, average 63.1 ± 2.2 Ma : apatites from fresh and altered wall rocks adjacent to 9×1 vein (Naeser 1978, Marvin and Dobson 1979)

63.9 Ma: apatite from a Proterozoic pegmatite 2 km SE of Schwartzwald (Naeser 1978)

109 Ma: apatite from Proterozoic gneiss in Golden Gate Canyon, 10 km SW of Schwartzwald (Naeser 1978)

(For additional regional geochronological data see the chapter Front Range, Colorado).

Potential Sources of Uranium

Uranium and the other metals are assumed to have derived from ore-hosting metamorphics. Whole rock U values in extensive hornblende gneiss, which is thought to have originated from submarine volcanic extrusions and pyroclastics, interbedded with clastic and chemical sediments, average 1–4 ppm U with maximum values of 52 ppm U. Garnet-biotite gneiss contains an average of 5–10 ppm U (max. 88 ppm U), quartzite 1.7–26.8 ppm U, and the mica schist unit 2.2–5.8 ppm U (Wallace 1983a). Wallace favors the extensive hornblende gneiss unit as the most likely source of uranium.

Indirect evidence such as isotope composition and no detected viable magmatic sources also support the assumption that vein-hosting metavolcanics and metasediments were the most likely source of uranium and other ore-related metals.

Ore Controls and Recognition Criteria

Schwartzwald uranium mineralization is attributed to vein-type uranium deposits. Mineralization exhibits primarily two salient controls: tensional large faults with associated horsetail fractures and affinity to distinct lithologies. In more detail, ore controls or recognition criteria sometimes in only a subtle or vague expression include:

Host environment

- Precambrian metasediments and metavolcanics formerly probably overlain by Pennsylvanian redbed sediments
- Presence of brittle rocks such as garnet-biotite gneiss and quartzite capable of reacting to tectonic stress by dilational fracturing and as such creating adequate transmissivity and space for minable ore shoots
- Increased thickness of favorable host rocks due to folding, particularly in the nose of the Schwartzwald synform, where the section of the transitional rock unit is approximately doubled in width
- Hornblende gneiss and mica schist are unfavorable hosts, but could have acted as barriers to the migration of mineralizing fluids due to more ductile reaction to faulting and related impermeable gouge formation
- Multiple stages of faulting, fracturing, and brecciation with repeated reactivation of major structures
- Laterally narrow but very deep (>1,000 m) system of continuous and interconnected permeable faults and breccias due to the structural combination of steeply dipping horizons of brittle transition zone rocks and their offset by the steeply dipping Illinois and Rogers fault system.

Alteration

- Wall rocks along veins exhibit two main stages of alteration:
 - Early carbonatization and sericitization in a wider halo and
 - Later K metasomatism and hematitization of limited extent overprinting the former.

Mineralization

- Multiple stages of mineral deposition are reflected in three main stages and several substages
- The principal U phase (stage II) is between two sulfide stages (I and III) that associate mainly with carbonates
- U minerals are pitchblende and coffinite paragenetically associated with a Fe–Mo–As mineral, and minor sulfides and arsenides
- Gangue minerals are Ca, Fe, Mg carbonates, and late chlorite and fluorite
- Ore veins show affinity to distinct lithologies, particularly to garnet-biotite gneiss, a former iron (and sulfur?) -rich pelitic sediment, and quartzite
- Ore-bearing veins are restricted to tensional structures such as the large Illinois and Rogers faults and associated horsetail fractures
- U ore is intermittently distributed in a few steeply dipping major veins and in a great number of tributary horsetail fractures
- Pronounced changes in the width of structures provided preferential sites for ore accumulation
- Pronounced changes in the width of veins are commonly related to branching of, and abrupt changes in strike and dip of major structures and horsetail fractures as well
- As indicated by trace element, disparities compared to horsetail veins, dilution of ore grades in major structures such as the Illinois vein are probably due to repeated reactivation of these structures.

Metallogenetic Aspects

Metallogenetic hypothesis have been put forward by a number of researchers, e.g., Fisher (1976), De Voto and Paschis (1980), Maslyn (1978), Nelson and Gallagher (1982), Rich and Barabas (1982). Models range from ore emplacement in Proterozoic/Silver Plume time to Mesozoic/Laramide time, and from ore-forming processes initiated by magmatic centers such as the Silver Plume or Laramide intrusives of the nearby Colorado Mineral Belt, to hypogene processes that generated convective cells leaching uranium and other metals from Proterozoic country rocks, and to supergene processes active along the Phanerozoic unconformity and deriving U from perhaps redbeds of the Pennsylvanian Fountain Formation or other sources.

Thorough research work by Wallace and coworkers narrowed the conceivable frame of ore formation to convective hypogene hydrotherms extracting ore elements from surrounding Proterozoic rocks and depositing them in distinct structurally prepared rock units during early Laramide time. Although partial aspects of the hypothesis need clarification and confirmation by further studies, the basic assumptions for the uranium source, nature of fluids, precipitants, P–T and hydrodynamic conditions are supported by many data. Wallace and his coworkers' criteria and conclusions may be summarized as follows.

Initial fluids involved in the alteration and early mineralization stage are postulated to have been evolved connate/

metamorphic water that possibly resided in deep storage reservoirs along major fault zones of Proterozoic ancestry, which possibly became reactivated during the Pennsylvanian uplift. These connate fluids contained abundant CO₂ and were in isotopic equilibrium with enclosing metamorphic rocks, but became mixed with some meteoric water from mineral stage IIc onward. Rich and Barabas (1982) suggest that mineralizing fluids were of organic or organo-aqueous character during stage I (early) adularia and stage II (late) ankerite formation and thus probably also during pitchblende deposition.

Many major pre-ore faults consisted of relative wide cataclastic zones composed of abundant anastomosing fractures, which provided large access and surface areas for element leaching in relation to rock volume within the zones. As a result of interaction with rocks, fluids could acquire proportionately large quantities of Ca, K, and other elements including uranium. Uranium very probably was mobilized as a soluble carbonate complex to reactions as may be deduced from the abundance of co-precipitated carbonates.

Wrucke and Sheridan (1968) note that in the Rocky Mountain Arsenal, 3 km NE of Denver, a drill hole intersected in a depth of about 3.6 km a 20–30 m thick regolithic profile in metamorphic rocks under the Pennsylvanian Fountain Formation. These regolithic rocks contained a large (50–150 km²) fracture-controlled reservoir of water with a high concentration of radium. A similar situation is assumed by Wallace (1983a) for hydro-tectonic conditions along the ancient Front Range zone, including the Schwartzwald area, prior to the Laramide Orogeny.

Fluids active during mineralization stages I and II had a calculated pH between 5 and 8, and contained abundant H₂CO₃ and HCO₃⁻. With an ongoing pressure and temperature decrease and associated mineral deposition, the pH value increased, whereas fugacities of O₂ and CO₂ decreased. Thermodynamic calculations indicate that sulfur species contained in fluids were initially dominated by sulfate, but probably transformed into sulfides with developing mineralization.

Wallace (1983a) presents analyses of carbon and oxygen (based on unpublished data by Whelan JF), and sulfur isotopes (based on Heyse 1972, and unpublished data by Whelan JF 1992). Wallace and Whelan (1986) interpret these data, as well as U/Pb and fluid inclusion data as follows:

Carbon: Dolomite in veins yield δ¹³C values between –2.4 and –7.3‰, which is close to those values analyzed in calcite from metamorphic country rocks, but is also within the range of magmatic carbon. Wallace (1983a) favors a derivation of carbon in hydrothermal vein carbonates from carbonate minerals in calc-silicate and hornblende gneiss units.

Oxygen: Silicates of metamorphic rocks yield δ¹⁸O values of 10–15‰. Minerals of early alteration and mineral stage I have δ¹⁸O values between 4.6 and 8.6‰, which are equivalent to those of magmatic fluids but may also reflect nonmagmatic solutions in equilibrium with their enclosing metamorphic rocks assuming a long residence time of fluids as discussed by Taylor (1979). Hence oxygen isotopes are inconclusive with respect to their source. Stage IIc fluids have δ¹⁸O values ranging largely from 0 to –5‰. This lighter composition may suggest an influx of

meteoric water mixing with either original fluids or less evolved connate water from overlying sediments. $\delta^{18}\text{O}$ values of stage III average -5.6‰ implying an entirely meteoric origin, which is compatible with the supposedly supergene provenance of paragenetically precipitated sulfides.

Sulfur: $\delta^{34}\text{S}$ data of stage IIc sulfides vary between $+1.6$ and -17.1‰ , but are scanty. These values compare with those of metamorphic sulfides, therefore Wallace and Whelan (1986) consider that vein sulfides derived from metamorphic progenitors. The calculated hydrothermal fluid composition also permits this assumption. On the other hand, they refuse a sulfur source in formerly overlying Phanerozoic sediments because sulfates have not been identified therein. Isotopically very light sulfides of stage III range from -18 to -41‰ $\delta^{34}\text{S}$. They are interpreted as possibly derived from late iron sulfides deposited from a sulfate-rich solution, but not from metamorphic or hypogene sulfides because such fluids would have had a $\delta^{34}\text{S}$ composition near 0‰ .

Uranium-lead: Wallace et al. (1983) report a $^{207}\text{Pb}/^{206}\text{Pb}$ ratio in hydrothermal galena indicating a 1,900–1,600-Ma old source, i.e., time equivalent to metamorphic country rocks. Analytical data also indicate very small concentrations of uranium in the source and a Th/U ratio of about 1.9. These data would exclude any magmatic source younger than the Boulder Creek Granodiorite, thereby refuting various models forwarded by authors using Silver Plume or younger age intrusions as sources for uranium.

P-T and hydrodynamic conditions: Estimated temperatures of mineral formation, as based on limited and not comprehensive data of alteration mineralogy, fluid inclusion micro-thermometry, and sulfur isotope fractionation, were approximately $175\text{--}225^\circ\text{C}$ during the alteration process, 225°C in mineral stage I, and decreasing to $100\text{--}125^\circ\text{C}$ in stage IIc (fluid inclusions in stage I sphalerite: 225°C , in stage IIc (?) amethyst and dolomite: $168\text{--}205^\circ\text{C}$; sulfur isotope fractionation of coexisting sphalerite and galena of stage IIc: 68° and 120°C).

Lithostatic pressures are estimated at 770–1,000 bars and hydrostatic pressures at 320–420 bars for the time of ore formation. These values are based on an emplacement depth of 3,200–4,200 m of ore as deduced from reconstruction of the tectonic position of the present Schwartzwalder ore zone in early Laramide time. A progressive change to a lower, more hydrostatic pressure during the later mineral stages may have been in response to development of the fault system and related uplift.

Uranium precipitation: The bulk of pitchblende formed between stages I and IIc together with certain sulfides (pyrite, chalcopyrite, Fe–Mo–As sulfide) and large quantities of carbonate (mainly ankerite) and adularia, whereas bornite, iron oxides, sericite, and graphite are notably absent. This assemblage is suggestive of a pH of 5–8, a dissolved CO_2 concentration of 4–10%, and a likely uranium transport as a uranyl carbonate or bicarbonate complex. Extraction of uranium from a fluid of this composition may be envisaged in two steps: first, destruction of the uranyl carbonate complexes; and second, reduction of hexavalent uranium of the uranyl compound into the tetravalent state to form pitchblende.

Wallace (1983a) suggests a break-up of uranyl complexes in response to a major tectonic episode and related drop of total pressure leading to effervescence of CO_2 , increase in pH and decrease of $f(\text{O}_2)$, and, consequently, to destabilization of uranyl carbonate complexes. Deposition of paragenetic adularia and ankerite can be triggered by the same mechanisms. A marked increase in the transmissivity of a conduit enhances conditions for adularia formation by both metastabilization of high K/Na ratios and elevation of pH in response to CO_2 evolution. A loss of CO_2 results in deposition of ankerite.

For reduction of hexavalent uranium, Wallace (1983a) proposes sulfur species coexisting with uranium in solution as eminent reducing agents. Original sulfur compounds, as outlined earlier, were dominantly sulfates, but may have also included significant amounts of intermediate sulfur. Through complex mechanisms and intermediate sulfate-thiosulfate and sulfate steps by sulfate reduction as outlined by Spirakis (1981), a progressively more reducing fluid can evolve with an associated temperature and pressure decrease caused by tectonic brecciation. This process may produce and allow H_2S or HS^- to reduce hexavalent U and precipitate it together with sulfides in a rapid process as documented by pitchblende–sulfide assemblages and textures in Schwartzwalder ore.

Wallace excludes any involvement of external reductants such as ferrous iron, methane, or organic matter as suggested by other authors (e.g., Adams and Stugard 1956; Rich and Barabas 1982). Wallace's arguments against these kinds of reductants are: (a) hematite is locally absent, (b) uranium also precipitated in fractures within iron-deficient quartzite, (c) hematite formed as an alteration product prior to pitchblende from which it was separated by unhematitized adularia, (d) iron sulfides and ankerite, not hematite, are the iron-bearing minerals paragenetically deposited with pitchblende, (e) carbonaceous material associated with pitchblende is not observed and chemical analyses indicate only small amounts (0.06–0.13% in weight) of organic carbon and no correlation of carbon with uranium.

Synopsis of metallogenetic processes

The Schwartzwalder and similar uranium vein deposits in the central eastern Front Range apparently evolved by complex multiphase processes in a terrane characterized by the coincidence of favorable metallogenetic parameters and its geologic history with the following postulated sequence of metallogenetic events (after Wallace 1983a):

Pre- to Early Laramide

- Reactivation of Proterozoic structures (perhaps related to uplift of western part of Front Range).

Early Laramide

- Mobilization and circulation of connate/metamorphic waters (perhaps by increasing heat-flow initiated by igneous intrusions of the Colorado Mineral Belt)
- Alteration stage I – sericite and carbonate (T: $175\text{--}225^\circ\text{C}$, P: 750–1,000 bars)

- Cataclasis/brecciation (perhaps related to uplift of central-eastern Front Range)
- Alteration stage II – hematite and adularia (T: 175–225°C, but higher in temperature than the earlier alteration, P: 750–1,000 bars)
- Mineral stage I: hypogene hydrothermal base metal sulfides, carbonate, adularia (T: ca. 225°C, P: 750–1,000 bars)
- Cataclasis
- Minerals stage II: hypogene hydrothermal pitchblende, sulfide, carbonate, in stage IIc mixed with supergene material (T: decreasing to 125°C in stage IIc, P: slightly lower than earlier)
- Cataclasis, active during stage II, injection of dikes of cataclastic material, initiation of stage III mineralization.

Late Laramide to Recent

- Cataclasis (post-ore Illinois fault system), continuation of stage III mineralization by supergene processes.

Although the processes directly responsible for emplacement of uranium ore have been largely deciphered by various researchers, the original source of uranium and possible initial preconcentrating processes, if any, in Proterozoic and/or Paleozoic time, i.e., prior to the principal and final vein formation in Laramide time, are still enigmatic. Indirect evidence such as isotope composition, restriction of mineralized veins to distinct lithologies, no detected magmatic source suggests that vein-hosting metamorphics were the source of uranium and other ore-related elements; this must be verified, however, by a regional geochemical-mineralogical study. It can be envisaged, however, that there existed synsedimentary uranium accumulations as indicated by some geochemical data from Front Range metamorphics (Wallace 1983a, b) and perhaps from Wheeler Basin on the western side of the Front Range (Young and Hauff 1975), where disseminated uraninite occurs in biotite-rich zones in migmatized gneiss adjacent to Silver Plume granite and pegmatite. Localized tenors are as high as 0.62% U. Age determinations by Ludwig and Young (1975) yield $1,446 \pm 20$ Ma for uraninite, which correlates with the intrusion of Silver Plume granite, hence these uranium accumulations are interpreted as remobilization and concentration of uranium and other elements during Silver Plume-related metamorphism. However, the important point for the Schwartzwalder area is that Ludwig's et al. (1985) work does not permit much, if any, preconcentration of uranium during metamorphism.

Actual ore emplacement in veins in early Laramide time is presently most convincingly explained by Wallace (1983a), who proposes the following metallogenetic evolution:

1. Intense *faulting* along the frontal zone of the developing eastern Front Range in early Laramide time by interaction of NW–SE-trending major faults and reverse faults along the eastern uplift boundary resulted in a dilation of the frontal zone
2. Sites for optimal and extensive ore emplacement in the Schwartzwalder area were prepared in pre- and early Laramide time by *tensional tectonism* in a segment of structural coincidence of steeply dipping layers of brittle garnet-biotite

gneiss and quartzite of the lithologic transition zone and its transection by a steeply dipping fault system. As a result, a laterally narrow, but deep stockwork of continuous and interconnected faults, fractures, and breccias was established (Illinois, Rogers faults, horsetail fractures). Repeated cataclasis was instrumental in the formation of various successive stages of alteration and mineralization by producing abrupt releases of confining pressure and related increases in permeability

3. Uranium mineralization began 69–70 Ma ago during incipient stages of Laramide uplift of the eastern Front Range and beneath a cover of Phanerozoic sediments approximately 3,000 m thick. Fission track investigations of apatite indicate a relatively high *heat flow* at this time. Heat was supplied through an increased regional thermogradient due to igneous activity in the Colorado Mineral Belt
4. Initial *hydrothermal solutions* originated from connate/metamorphic water that possibly resided in deep storage reservoirs along major fault zones of Proterozoic ancestry, which possibly became reactivated during the Pennsylvanian uplift. These connate fluids contained abundant CO₂ and were in isotopic equilibrium with enclosing metamorphic rocks, but became mixed with some meteoric water from mineral stage IIc onward. Rich and Barabas (1982) suggest that mineralizing fluids were of organic or organo-aqueous character during stage I (early) adularia and stage II (late) ankerite formation and thus also during pitchblende deposition. These fluids probably started a convective circulation in response to early Laramide tectonic movements. On their structurally prepared paths, they collected elements needed for ore formation from metamorphic country rocks. This was possible since many major pre-ore faults consisted of relatively wide cataclastic zones composed of abundant anastomosing fractures, which provided large access and surface areas for element leaching in relation to rock volume within those zones. As a result of interaction with rocks, fluids could acquire proportionally large quantities of CO₂, Ca, K, and other elements including uranium. Uranium was probably mobilized as a soluble carbonate complex. Pregnant solutions, which migrated into the most permeable sections of the fault zones and sites of later ore deposition, had a pH of 5–8 at the start of the alteration and ore formation phase
5. Two successive *wall rock alteration* assemblages were produced by hydrothermal fluids along virtually all existing faults and fractures except along late Laramide faults such as the post-ore Illinois fault, at a temperature of about 225°C and a pressure of 750–1,000 bars. Early alteration formed sericite and carbonate by CO₂ metasomatism and SiO₂ removal at relatively slow solution flow rates. Intermediate stages of brecciation increased the transmissivity and thereby the flow rate at contemporaneous CO₂ effervescence and pressure release. As a consequence, pH rose, oxygen fugacity dropped, and the second alteration assemblage of hematite and adularia replaced minerals of the early alteration stage
6. *Ore emplacement* occurred in three successive stages from hypogene hydrothermal fluids, except in stage III when supergene fluids entered the system. Early vein mineralization

formed at about 225°C and 750–1,000 bars similar to the P–T conditions of the alteration stage. During stage IIc, the temperature decreased to about 125°C and pressure dropped somewhat. Uranium was emplaced in virtually all accessible faults and horsetail fractures over a vertical interval of ca. 700 m below surface in the pre-ore Illinois fault system, and in the bottom part of the western strand of the Rogers fault where mineralization occurs at depths extending below 900 m under the present-day surface

Depth limitation of the mineralization may have been controlled by the threshold level of local pressure gradients, which extended deeper in larger and more open faults and at which ascending fluids started to effervesce CO₂ and consequently precipitated ore minerals. Uranium distribution and emplacement must have been rather uniform as indicated by the paragenesis and ore textures

7. *Mineralization events* began with stage I base metals, adularia, and carbonate. This event was only of minor magnitude. Stage II was the principal ore-forming period. It included three substages. The first two produced uranium ores together with volatile elements, which strongly correlate with uranium. Other minerals include base metal sulfides and sulfosalts, as well as ankerite and adularia. *Uranium transport* was in solution as uranyl carbonate or bicarbonate, and its *deposition* occurred when abrupt release of confining pressure due to revived tectonic movements caused effervescence of CO₂, increase of pH, and a corresponding break-up of the uranyl complex. Subsequent *reduction* of hexavalent to tetravalent uranium by aqueous sulfur species then precipitated pitchblende
8. During the later part of substage IIc and stage III, supergene fluids intermixed with hypogene solutions and precipitated dominantly carbonate, pyrite, and marcasite
9. Supergene overprinting of primary uranium minerals is restricted to within approximately 100 m below the present surface.

6.1.0.2 Other Uranium Deposits/Occurrences in the East-Central Front Range

A great number of uranium showings are known in the east-central Front Range. Most of them are associated with faults or breccia zones transecting the Proterozoic Idaho Springs Formation or equivalent metamorphic rocks. A few deposits are in sediments of Cretaceous age. In addition to the Schwartzwalder deposit, some ten other properties (► Fig. 6.1) have been subjected to mining, mainly by adits, shallow shafts, and open pits that are usually restricted to near-surface levels of mineralization.

Sources of Information. The following is a summary of deposits/occurrences recorded in literature, particularly in Carpenter et al. (1979), Nelson-Moore et al. (1978), Sheridan et al. (1967), and Sims and Sheridan (1964). For more details, the reader is referred to these publications.

Ralston Buttes area, located about 15 km NNW of Golden.

Mena mine (production ca. 2.5 t U, grade 0.22% U): Pitchblende, pyrite, galena, chalcocopyrite, and other Cu and Ni sulfides, as well as ankerite, calcite, quartz, and K feldspar occur in 0.3–2.5-m wide veins of the Rogers Fault system. Host rocks are amphibolite, hornblende gneiss, biotite gneiss, highly altered by mainly potassium alteration along breccia zones.

Golden Gate Canyon area, located about 5 km NW of Golden.

Ascension mine (production ca. 10 t U, grade 0.25% U): Fissures and veinlets with pitchblende and base metal sulfides, ankerite, calcite, and quartz are hosted within and adjacent to a major NW–SE-trending, steeply E-dipping breccia zone. Host rocks are garnet-biotite gneiss and calc-silicate gneiss, cut by pegmatite and other dikes. The wall rocks are altered along structures. Some ore is concentrated at the contact of pegmatite dikes.

Aubrey Ladwig mine (production almost 4 t U, grade 0.21% U): Pitchblende (and hexavalent U minerals in the near-surface zone), pyrite, some fluorite, almost no base metal sulfides occur in thin veins and ore pods along or near the contact of brecciated garnet-biotite gneiss and pegmatite.

Ohman mine (production 0.5 t U, grade 0.6% U): Pitchblende is distributed along a shear zone in hornblende gneiss.

Union Pacific shaft (no production, grades of samples range from <0.1% to several percent U): Thin veinlets (millimeters to 2 cm thick) contain pitchblende, pyrite, tetrahedrite, tennantite, chalcocopyrite, bornite, chalcocite, covellite, emplectite, galena, sphalerite, ankerite, calcite, and K feldspar. Host rocks are quartz-biotite-, biotite-hornblende-, and hornblende gneiss, cut by pegmatite and granitic segregations. Wall rocks in mineralized zones are altered by propylitization with chloritization, sericitization, hematitization, and K feldspathization. Ore-bearing veinlets occur along and adjacent to a brecciated fault zone (UP vein or fault) trending NNW–SSE and dipping 35° NE, and where this fault intersects hornblende gneiss.

Toledale area, located approximately 15 km W of Denver.

Foothill mine/Wright lease (production ca. 17 t U, grade 0.22% U): Pitchblende, finely disseminated and intimately intergrown with ankerite, is associated with pyrite, chalcocopyrite, galena, calcite, and K feldspar. These minerals form ore shoots in a NW–SE-trending 70° NE-dipping breccia vein, where this vein bends to the N and expands in width. The vein pinches out where it turns southward. Host rocks are schists, gneisses, and pegmatites. Ore is commonly concentrated in shoots adjacent to quartz-feldspar pegmatite.

Grapevine mine (production ca. 10 t U, grade 0.27% U): Pitchblende associated with pyrite, quartz, feldspar, hematite, limonite, and clay minerals fill fractures and fissures in hornblende gneiss.

Critchell area, located approximately 25 km SW of Denver.

Seven Devils/Stone Placer prospect (production ca. 4 t U, grade 0.37% U): Pitchblende and sulfides occur structurally controlled in gneisses and schists.

Morrison area, located approximately 10 km W of Denver. Uranium occurs in Dakota Sandstone of Cretaceous age adjacent to faults.

Four Corners/Morrison or Pallaora mine (production about 1 t U and some V_2O_5 , grade 0.17% U, 0.02% V_2O_5): Finely disseminated pitchblende and pyrite impregnate asphaltic material adjacent to a NW–SE-trending, 30–50° SW-dipping fault.

Man mine/Vanadium Queen (production ca. 6 t U, grade 0.23% U): Finely divided pitchblende and pyrite is contained in asphaltic material in a sandstone lens, adjacent to a NW–SE-trending 50° SW-dipping fault.

Old Leyden coal mine, a former coal producer, located approximately 10 km N of Golden (production ca. 2 t U, grade 0.3% U; estimated resources are 16,000 t of coal grading 0.17% U): Hosted in coal, carbonaceous claystone, and sandstone of the Cretaceous Laramide Formation, pitchblende, coffinite, hexavalent U minerals, pyrite, and marcasite contained in siliceous material fill fractures mainly in coal.

6.2 Tallahassee Creek District-Thirtynine Mile Volcanic Field, Colorado

The Tallahassee Creek uranium district (Fig. 6.11a), located approximately 35 km WNW of Canon City, contains strata-bound, mixed sandstone-volcanic-type U deposits. The district was the focus of uranium mining from small, shallow ore bodies during the 1950s, the first of which was discovered in 1954. About 15 operations produced a total of approximately 170 t U at an average ore grade of 0.21% U. Renewed exploration in the 1970s discovered larger ore bodies at depth including Hansen and Picnic Tree as discussed below.

6.2.0.1 Hansen and Picnic Tree Deposits

Discovered in 1977, the *Hansen* deposit has estimated resources of ca. 9,000 t U at an average grade of 0.068% U. Resources at *Picnic Tree* deposit, located about 700 m to the southeast of Hansen, are estimated at almost 1,000 t U at an average grade of 0.1% U.

Sources of Information. Ausburn (1981), Babcock (1980), Chapin (1965), Chapin et al. (1982), Epis and Chapin (1968, 1974), Epis et al. (1976, 1979), Hon (1984), McPherson (1959), Nelson-Moore et al. (1979), Shappirio (1963), and Bondurant KT and Pool TC (personal communication) unless otherwise stated.

Geological Setting of Mineralization

Uranium occurs at the southern margin of the Thirtynine Mile Volcanic Field and within a structural trough referred to as Echo Park Graben. The graben is filled with a sequence of Tertiary rocks of volcanic and sedimentary provenance ranging in age from early Oligocene (36 Ma) to early Miocene (19 Ma), the majority being emplaced between 36 and 27 Ma. The volcanics comprise andesite interspersed with rhyolitic to quartz latitic

ash-flow tuffs. Sediments consist of fluvial to lacustrine deposits. Major lineaments trend N to NNW. Faults strike around E–W and NE–SW.

The following composite litho-stratigraphic section presents the major Tertiary rock units of the area around the Tallahassee Creek uranium deposits (after Babcock 1980 based on data from Rampart Exploration Company, age dates from Obradovich in Epis and Chapin 1974) (Figs. 6.11b and c; 6.12).

Middle Oligocene

Gribbles Park, Thorn Ranch, East Gulch Tuffs, 60–240 m thick: pink to reddish-brown pyroclastics containing sanidine, plagioclase, quartz, and biotite (29 Ma).

Antero Formation, 0–60 m thick: whitish, massive, ash-fall tuff varying with lacustrine tuffaceous sediments, mainly siltstones (34 Ma).

Thirtynine Mile Andesite, 0–240 m thick: maroon to purple to dark grey, fresh to highly altered andesite flows, laharic breccia, some local intrusive breccia dike, and some flow breccias; commonly interbedded with tuffaceous waterlain sediments and unconsolidated agglomerates (34 Ma).

Early Oligocene

Tallahassee Creek Conglomerate

- Ash-Fall Member, <3 m thick (U host): green to grey-green to white-grey bentonitic claystone, probably derived from alteration of ash fall material
- Hansen Andesite/Latite Member, 0–15 m thick: grey to light purple-grey, dense porphyritic andesite or latite, vuggy in places where phenocrysts had been altered to clay; only very local distribution
- Conglomerate Member, 0–105 m thick: grey to green-grey to red-grey volcanic conglomerate with clayey to sandy matrix, with some intercalations of tuffaceous to arkosic sandstones to mudstones.

Wall Mountain Tuff, 0–50 m thick: buff to red-brown, moderately to densely welded ash-flow tuff of rhyolitic composition (35 Ma).

Eocene

Echo Park Formation (or Alluvium), 0–400 m thick (U host)

- Fluvial facies: interbedded grey to light grey, silty to clayey, arkosic to quartzose, fine- to coarse-grained, sometimes conglomeratic sandstone; grey to green siltstone and mudstone, some basal conglomerate; all may contain carbonaceous material
- Sheet Wash facies: red to red-brown conglomeratic mudstone (presumably derived from regolithic Precambrian basement by mudflows)
- Fanglomerate facies: red-grey to grey, pebble to boulder conglomerate with thin interbedded silty sandstone lenses

and occasional mudstones. Usually present in lower part of the Echo Park Formation or adjacent to steeply sloping Precambrian basement surfaces.

North of the Echo Park Graben, the Tertiary sequence rests upon Mesozoic sediments (Dakota Sandstone, Morrison Formation) and Paleozoic sediments (Minturn and Belden

formations, Fremont Dolomite, and Harding Sandstone). Within the graben including the mineralized areas, Tertiary rocks lie on Precambrian intrusives and metasediments including quartz monzonite of Silver Plume age and granodiorite and quartz diorite of Boulder Creek age.

As a result of Laramide uplift, most exposed Mesozoic, Paleozoic, and Precambrian rocks were eroded. In Eocene time,

■ Fig. 6.11.

Tallahassee Creek district, (a) generalized geological map with location of U deposits, (b) and (c) W–E sections showing basin geometry and facies distribution of the Eocene Echo Park Formation in the uranium district of the Echo Park Basin. Arrows at faults show relative vertical displacement directions but many faults have appreciable strike-slip components. (After (a) Epis et al. 1979; Hon 1984; courtesy of INI 2008; ((b) and (c) Chapin and Cather 1981; Ausburn 1981)

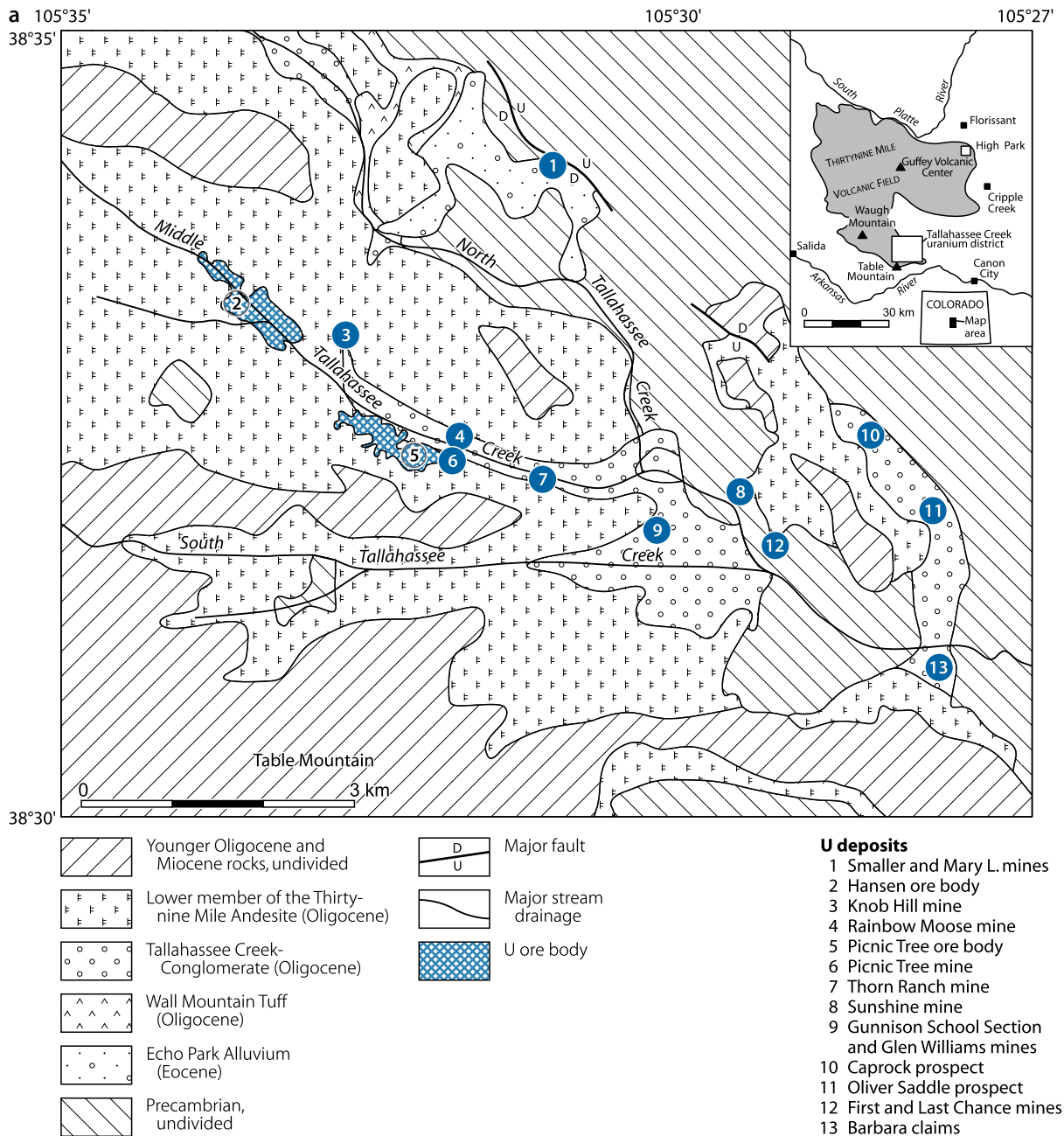
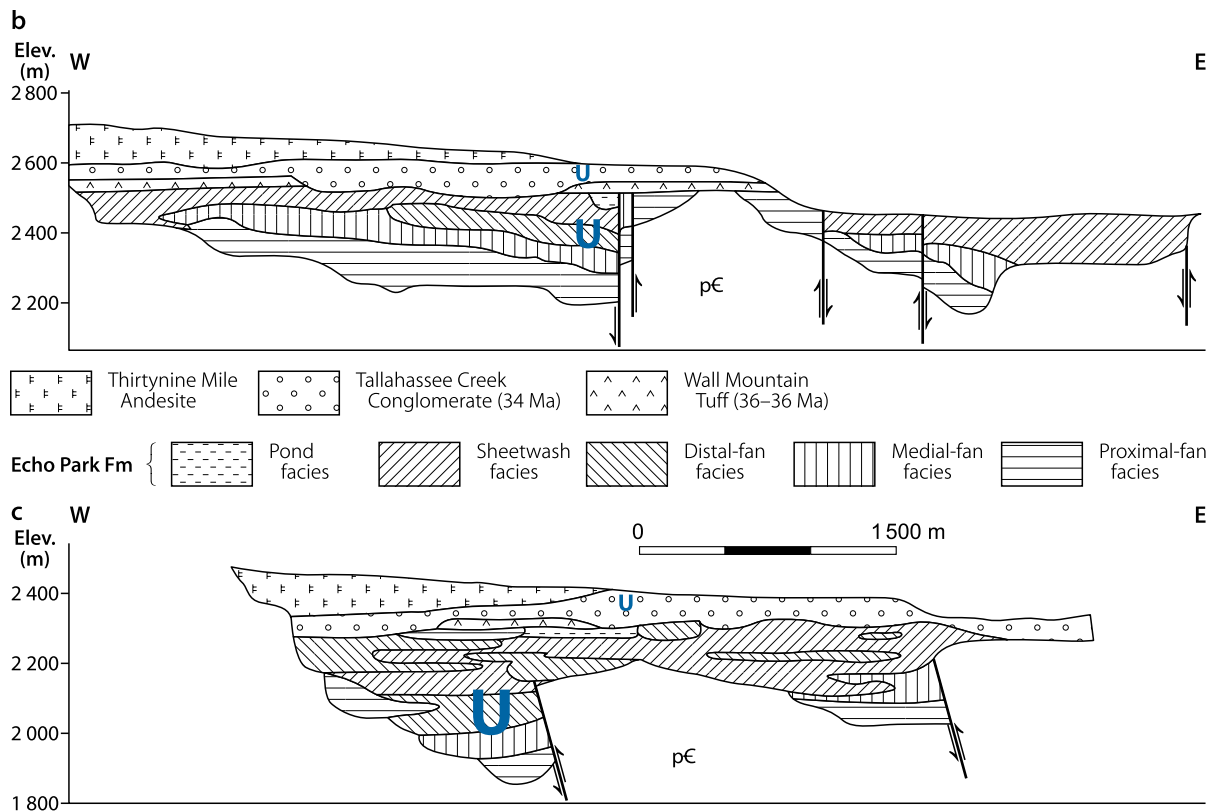


Fig. 6.11. (Continued)



erosional clastics were redeposited by drainage systems into the Echo Park and other grabens. Tectonic movements, mainly block faulting along the earlier mentioned structures, and volcanism disrupted drainage patterns during Oligocene and Miocene time.

The principal *uranium-hosting units* are the Ash Fall Member of the Tallahassee Creek Conglomerate (Picnic Tree ore body and earlier mined deposits) and the Echo Park Formation (Hansen ore body).

In the **central Tallahassee Creek** area, the *Tallahassee Creek Conglomerate* ranges in thickness from 0 to about 120 m. The *Ash Fall Member*, from 0.5- to 3 m thick, consists of grey-green kaolinitic and bentonitic claystone of fairly uniform thickness in the zone overlying the Hansen ore body. It is thicker and slightly sandy to conglomeratic due to reworking by fluvial action in the Picnic Tree area where it locally contains carbonaceous debris. The *Hansen Andesite/Latite Member* is found only on the eastern side of the Hansen ore body. The *Conglomerate Member* occupies the middle part of the Hansen ore body zone in a channel that scoured through the Wall Mountain Tuff and locally into the Echo Park Formation. Here, the Conglomerate Member comprises an upper volcanic cobble to boulder conglomerate with a clay-sand matrix, a middle conglomerate claystone layer, and a lower conglomerate of volcanic boulders with some sandy matrix. In the Picnic Tree area, the Conglomerate Member is mainly a volcanic conglomerate with a clay-sand matrix. The *Wall Mountain Tuff* has been largely eroded by extensive scouring leaving only four small isolated islands of welded tuff, up to 35 m thick, in the Hansen area.

In the **Hansen area**, the *Echo Park Formation* is chiefly a fluvial (sheetwash) sequence, up to 250 m and more thick where present. It is subdivided into three units:

(a) Interbedded sandy mudstones and clayey sandstones of low permeability represent the upper unit. These sediments contain carbonaceous debris, either disseminated or concentrated in thin silty lenses.

(b) The middle unit consists of sands and conglomerates of relatively good permeability. Considerable amounts of carbonaceous material are present as both disseminations in sand layers and accumulations in thin silty lenses.

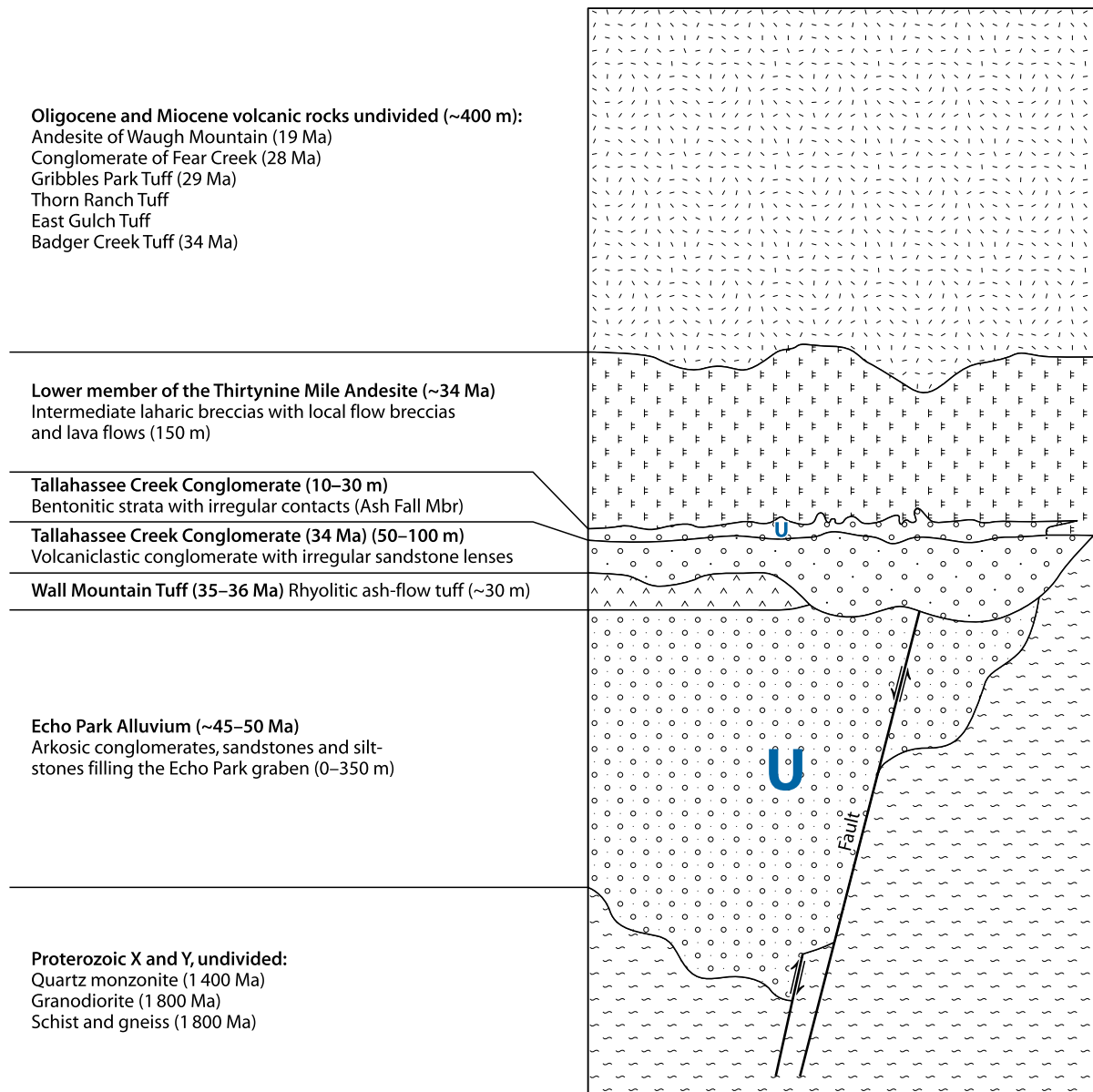
(c) The lower unit is a coarse conglomerate composed of cobbles to large boulders of Precambrian granite gneiss in a matrix (10–60% by volume) of pebbles, sand, and clay. Finer-grained layers in the upper section of the lower unit may contain abundant carbonaceous material. Transmissivity is fairly good in the upper horizons in contrast to the lower beds of the boulder conglomerate, which are well cemented.

Host Rock Alteration

Alteration features include argillization of feldspars in and around ore bodies, and oxidation in an outer halo. The middle unit of the Echo Park Formation exhibits the most intense feldspar alteration, whereas the upper unit shows moderate to intense alteration. All other formations were affected to variable degrees by feldspar decomposition.

■ Fig. 6.12.

Tallahassee Creek district, schematic litho-stratigraphic section showing basin fill facies prior to erosion, and U-mineralized stratigraphic intervals. (After Hon 1984)



Mineralization and Dimensions of Deposits

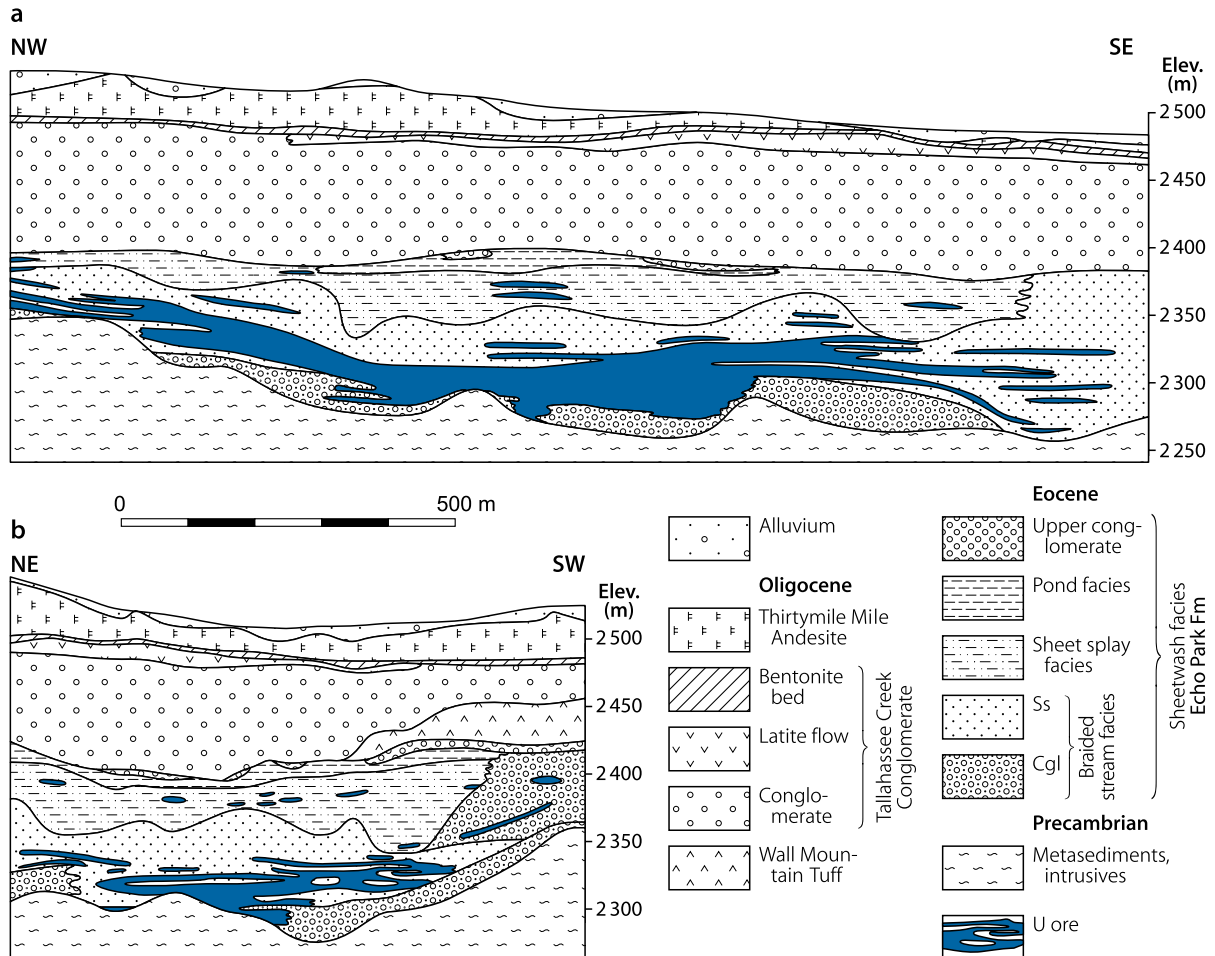
Two major ore bodies are delineated. *Hansen*, the largest ore body, is located about 700 m NW of *Picnic Tree* (► Fig. 6.11a). These deposits and almost all of the smaller ore bodies of the Tallahassee Creek district are of tabular, mixed sandstone-volcanic type emplaced in two Tertiary litho-stratigraphic formations, as mentioned earlier.

Hansen ore body (● Fig. 6.13): Very fine-grained sooty pitchblende and coffinite associated with pyrite occur within a matrix of montmorillonite, kaolinite, or mixed-layer montmorillonite, and minor illite, as an interstitial fraction or as partial grain

coatings mostly in impure or argillaceous arkosic sands. Ore minerals impregnate, in stratiform distribution, a fluvial facies of interbedded, more or less carbonaceous sandstone, mudstone, and pebble to boulder conglomerate in the upper part of the lower Echo Park Formation. Mineralization is interstratified with barren layers of siltstone, sandstone, and conglomerate. Sediments are contained in a paleovalley developed within a tectonic graben downfaulted into the Precambrian basement in late Laramide time. Mineralization is confined to a zone of reduction and argillization of feldspars. Reducing conditions are attributed to carbonaceous matter, which is abundant, in particular, in the finer-grained sediments. The reduced zone is surrounded by oxidized sediments, which may indicate a

Fig. 6.13.

Tallahassee Creek district, Hansen deposit, (a) NW–SE longitudinal section, (b) SW–NE cross-section. Uranium mineralization is hosted in basal braided stream sandstones, which contain abundant carbonaceous matter and are part of a major wet alluvial fan. The sheet-splay facies consists of alternating thin beds of argillaceous sandstone and sandy mudstone interpreted as overbank deposits of a stream with flashy discharge. They constitute an aquitard above the more permeable braided-stream sediments. Away from the wet-alluvial-fan, the Echo Park Formation comprises chiefly red, pebbly mudstones termed sheetwash facies. The bentonite bed at the top of the Tallahassee Creek Conglomerate is essentially barren of uranium above the Hansen ore body but hosts the Picnic Tree ore body about 0.5 km to the southeast. (After Chapin et al. 1982; Ausburn 1981)



geochemical cell system. Although mineralization is dominantly stratiform, at least some ore forms roll-like bodies that are positioned progressively lower in the ore-hosting formation from west to east.

The Hansen ore body is irregular in lateral extent, somewhat elongated in NW–SE direction with a length of approximately 2,500 m and a width of as much as 500 m. A wider halo of mineralization surrounds the ore body. The highest part of the ore body is at a depth of some 120 m, and the bottom is about 250 m deep. The average drill hole, using cutoff criteria of 0.6 m at 0.042% U, intersected a total of about 7 m of ore at an average grade of ca. 0.07% U.

Picnic Tree ore body: Very fine-grained sooty pitchblende and coffinite associated with pyrite occur disseminated in stratiform distribution, in locally carbonaceous kaolinitic–bentonitic claystone of the Ash Fall Member of the Tallahassee Creek Con-

glomerate. The sediments have been reworked and thickened by fluvial action and were deposited in an E–W-trending paleo-channel. Mineralization appears to be located on the south flank of this main Tallahassee Creek Conglomerate channel. The present tectonic position of the Picnic Tree ore body is on an upraised block that bounds the ESE edge of the Hansen area. As a consequence, the ore body lies at a relatively shallow depth of about 70 m. It is 0.5–10 m thick, approximately 1,000 m long in NW–SE direction, and up to 400 m wide. The clayey nature of the host rock poses a negative influence on the uranium recovery.

6.2.0.2 Other Deposits in the Tallahassee Creek District

At least 15 small mines have formerly worked on shallow ore bodies ranging in depth to 30 m below the surface in the Tal-

lahassee Creek area. They include the *old Picnic Tree* mine, from where, on trend, the new Picnic Tree ore body was discovered. Pitchblende and hexavalent U minerals, mainly autunite, are the principal U minerals in this near-surface mineralization. They are associated with pyrite, carbonaceous material, hematite, and limonite. Host rocks belong to the Ash Fall Member of the Tallahassee Creek Conglomerate. Irregularly distributed mineralization occurs in the upper 10 m of this member within altered, fine to coarse conglomerate consisting of boulders of Tertiary rhyolite and andesite and Precambrian granite, embedded in a matrix of fine-grained volcanic ash, tuff, and clay. Deeper ore bodies are tabular and commonly elongated along sedimentary trends. They are emplaced near the base of a tuffaceous sandstone unit, which unconformably overlies the Echo Park Formation and/or the Precambrian basement. A few ore bodies have been found in arkosic sediments of the Echo Park Formation (e.g., *Smaller or Mary L. mine*). The largest of these deposits contained about 40 t U and the smaller only a few tonnes uranium. Average ore grade was relatively high amounting to ca. 0.21% U.

6.3 Marshall Pass District, Colorado

The Marshall Pass district is located along the western flank of the southern Sawatch Range, a branch within the Rocky Mountains, approximately 60 km east of Gunnison, Colorado. Several vein-type uranium deposits and occurrences are known in the district. The *Pitch deposit* commonly referred to as Pitch Mine (formerly named *Pinnacle*) is the largest and highest grade deposit in the area. Additional uranium was mined from small deposits in the vicinity of the Pitch Mine. They are listed further below in the chapter Other Deposits.

Sources of Information. Chenoweth 1980; Dupree and Maslyn 1979; Goodknight 1981; Gross 1965; Malan 1959; Nash 1979, 1980, 1981; Nelson-Moore et al. 1978; Olson 1979, 1988; US AEC 1959; Ward 1978; and Mathisen M 1984, personal communication.

6.3.0.1 Pitch Mine

Original resources (including production) of the Pitch deposit amounted to 3,175 t U. Mining between 1959 and 1962 by underground methods produced 385 t U at an ore grade of 0.42% U. An additional 40 t U was recovered through underground leaching. Subsequent exploration (after 1973) outlined further resources of 2,750 t U at an average grade of 0.14% U. The major part of these reserves was mined from an open pit operation, which began in 1979 and ceased operating in 1984.

Sources of Information. Nash (1979, 1980, 1981) has described the geology and mineralization of the Pitch and adjacent uranium deposits and occurrences. The following description, unless otherwise stated, is an abbreviated excerpt from Nash (1981).

Geological Setting of Mineralization

The Marshall Pass district is underlain by intrusive, metamorphic, and sedimentary rocks ranging in age from Precambrian to Paleozoic. An erosional Paleozoic remnant is preserved in the Pitch Mine area, in particular to the west of the Chester fault (Fig. 6.14a and b). A few relicts of Tertiary volcanics occur near the Pitch Mine. The litho-stratigraphic section of these rocks in the Pitch area includes the following units (Nash 1981, Olson 1979).

Oligocene(?) <20 m thick: light colored quartz-latite flows (perhaps related to Tertiary andesitic volcanics of the San Juan Volcanic Field located further south)

>Unconformity<

Pennsylvanian Belden Formation (U ore host): rapidly alternating sequence of sandstone, shale, and limestone divided into three subunits: upper green and brown sandstone and grey shale (200 m or more thick), middle blue-grey limestone with red shale and fine sandstone (30–60 m thick), and lower white sandstone and black shale (40–90 m thick)

>Unconformity<

Mississippian Leadville Dolomite (U ore host), up to 130 m thick: dark grey dolomite and minor limestone with calcite and chalcedony veinlets and local black chert zones, and karst development and limonitization at the top of this unit

Devonian Dyer Dolomite, ca. 50 m thick: tan to light-grey dolomite

Devonian Parting Quartzite, ca. 5 m thick: varicolored shale and quartzite

>Unconformity<

Ordovician Fremont Dolomite, ca. 55 m thick: blue-grey limestone and dolomite

Ordovician Harding Quartzite, ca. 10 m thick: white quartzite, commonly with limonitic stain, and some black shale

>Unconformity<

Ordovician Manitou Dolomite, 75–90 m thick: light pinkish-grey dolomite

Cambrian Sawatch Quartzite, less than 1 m thick: vitreous quartzite

>Unconformity<

Precambrian: granitic and metamorphic rocks (mainly pegmatitic granite, hornblende-biotite schist, hornblende gneiss, and pegmatite), and metavolcanics, altered to a hematitic regolith on top.

Nash (1981) describes the U-hosting *Leadville Dolomite* at the Pitch deposit as a predominantly thin-laminated, medium- to massive-bedded dolomite, as much as 17 m thick, that occasionally contains thin intercalations of carbonaceous shale and sand. The color is blue-grey to black, often with a brownish tint. Black chert is common as veinlets, stringers, and concretionary nodules. The organic carbon content is commonly less than 0.5%. Pyrite ranges from about 0.2 to 16%. In contrast to this facies, the Leadville Dolomite found about 1 km west of the Pitch Mine is a fossil-rich, well-bedded, and cross-bedded limestone.

The *Belden Formation* is the second important uranium host. It consists of a sequence of generally thick-bedded to massive, medium grey to brownish-black limestone with rare dolomite,

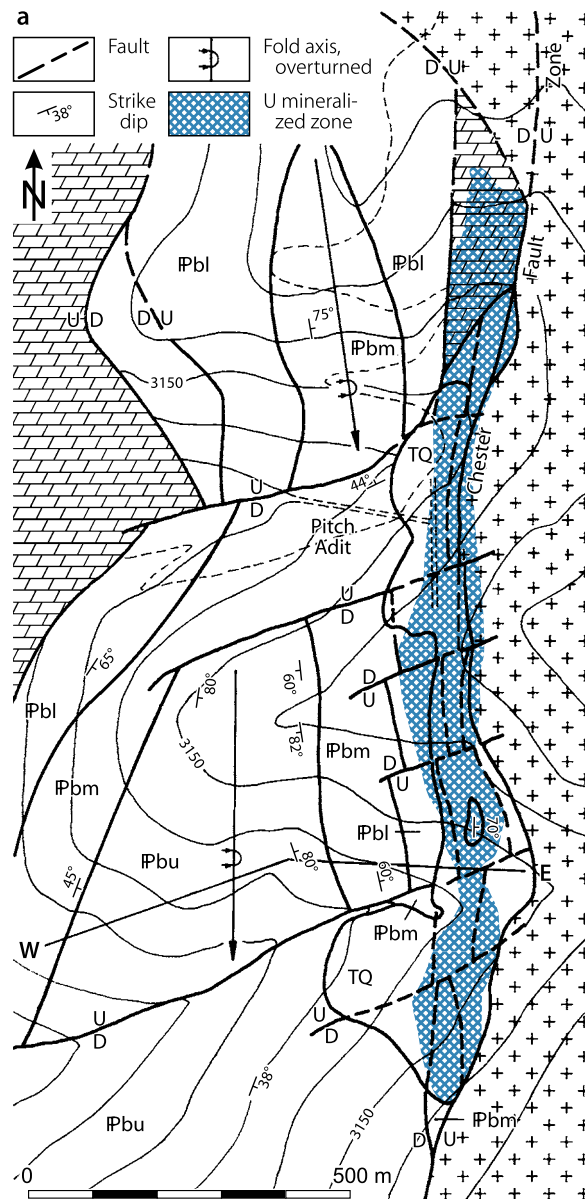
which locally contains green kaolinite; coarse-grained sandstone; black, clay-rich, fine-grained sandstone and red shales; kaolinitic coarse sandstone; green, clay-rich, fine-grained sandstone; and black and red shale cut by pink calcite veinlets.

The Pitch Mine area is transected by faults trending N-S, ENE-WSW, NNE-SSW, and NW-SE. Structurally, the Chester fault zone of supposedly Laramide age dominates the mine area. This zone consists of a complex set of multiple, predominantly reverse faults, oriented almost N-S, and dipping about 70° E. These faults displace Precambrian rocks thrust upon Paleozoic sediments on the east side of the Chester fault. The fault zone is 100-m wide in the mine area and shows net

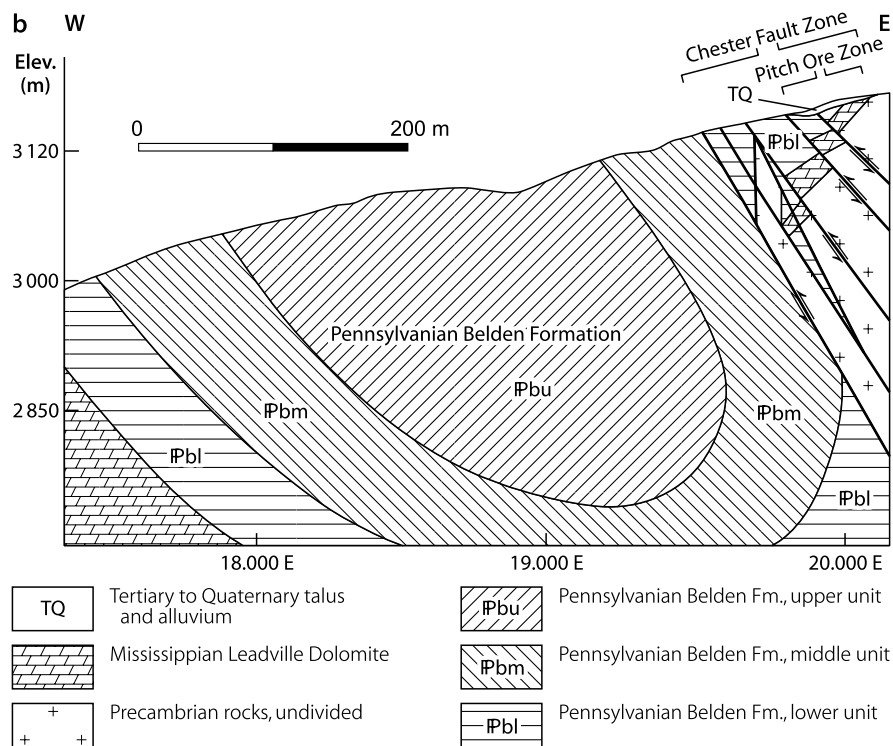
reverse displacement in excess of 600 m. ENE-WSW-trending faults cut the Chester fault zone. Within the fault zone, intense deformation and brecciation is widespread and resulted in complex inter-faulting and a breccia of mixed lithologies including Precambrian, Leadville, and Belden rocks. Pervasive cataclasis appears to be restricted, however, to dolomite within fault slices in the footwall of the Chester fault, whereas other rock facies reacted only by ductile deformation or remained unbroken. Maximum fracturing is observed where brittle dolomite beds are intersected by reverse fault planes at angles of about 70°. At lower angles of intersection, deformation is less intense.

■ Fig. 6.14.

Marshall Pass district, Pitch Mine area, (a) simplified geological map documenting the structural control of the Chester fault zone on the distribution of uranium mineralization; (b) schematic W-E cross-section illustrating the upthrust position of Precambrian rocks on the Pennsylvanian Belden Formation. (After (a) Nash 1981, based on Olson 1979, and Ward JM, Homestake Mining Co., unpublished data 1972-1977; (b) Nash 1981 (reproduced with permission of NM Geological Society))



■ Fig. 6.14. (Continued)



The Paleozoic sediments are folded along generally N-S-trending axes. Immediately west of the Chester fault, sediments form a relatively tight, south-plunging syncline with steeply dipping Leadville and Belden strata in its eastern limb (Fig. 6.14). Deformation is less developed to the west, where beds form gently warped broad folds.

Host Rock Alteration

Alteration phenomena include oxidation and leaching that affected, to various degrees, rocks along fractured and brecciated sections of the Chester fault zone to depths of more than 100 m. Other dolomite enriched in quartz and calcite is the common alteration product in which the original pyrite is oxidized to iron oxides, and thin films of iron oxides coat fissures and joints.

Some near-surface dolomite exhibits extreme leaching, oxidation, and a gossan composed of a porous and friable other rock of quartz and hematite/limonite and minor amounts of carbonate. Nash (1981) notes that other dolomites, independent of their grade of alteration, contain about 50–200 ppm uranium. Radioactive disequilibrium indicates that, in outcrop, these oxidized dolomites recently lost uranium.

Mineralization

Dominant U minerals are described as uraninite, pitchblende, and coffinite, but a major amount of uranium is present in minerals not yet identified. Uranophane and autunite are the most

common U phases in oxidized zones. Associated minerals include pyrite, marcasite, and minor amounts of chalcopyrite, chalcocite, covellite, galena, sphalerite, tetrahedrite, and hematite.

Pyrite is widespread in ore-hosting sediments where it occurs in various habits. According to Nash (1981), iron, molybdenum, lead, and sulfur are enriched in ore. Mo is enriched in both the Leadville and Belden sediments. It has a mean concentration of about 6.7 ppm in Leadville samples, and it ranges as high as 88 ppm in a high-grade ore sample. Total sulfur and iron, normative FeS_2 , and molybdenum contents correlate strongly with uranium, whereas organic carbon values in carbonates do not.

Pitchblende and coffinite generally occur together with pyrite and marcasite in pockets and small, millimeter- to rarely centimeter-wide veinlets within fractures and breccias of the Chester fault zone. Leadville Dolomite is the primary host rock. In particular, thoroughly brecciated, dark grey, chert-bearing dolomite with not well-cemented and recrystallized matrix is a favorable host. It contains zones of mineralization, which are thicker, more consistent, and of higher grade than those in other rock types. More than half of the resources are emplaced in this dark dolomite. Mineralized dolomite, in outcrop, forms a porous limonitic and silica-rich other gossan characterized by high radioactivity but low uranium values as mentioned earlier.

Sandstone, siltstone, and carbonaceous coaly shale of the Belden Formation are mineralized to a lesser extent. Some ore is emplaced in Precambrian granite, pegmatite, and schists in the hanging wall on the east side of the Chester fault. Reportedly, a drill hole also intersected U mineralization in a fluorite-bearing intrusive rock of unknown age (Laramide?).

Shape and Dimensions of Deposits

Minable ore of the Pitch deposit occurs in a structurally deformed zone approximately 1,500 m long, 100 m wide, and 120 m deep (► Fig. 6.14). Both the boundary of the ore body and the distribution of ore within it are somewhat irregular, chiefly due to structural control. Sections of high-grade ore with several percent U alternate with sections of sub-ore grades. The outer boundary follows, in principle, the N–S trend of the Chester fault zone except for a short extent along the ENE–WSW cross faults.

Ore mined between 1955 and 1962 came predominantly from high-grade ore in veins or shears cutting the Leadville Dolomite. Later found reserves (2,750 t U) consist of dispersed ore within brecciated dolomite of the Leadville Dolomite, complexly faulted between slices of psammitic and pelitic sediments of the Belden Formation.

Ore Controls and Recognition Criteria

Uranium mineralization of the Pitch deposit is both structurally and lithologically controlled in which the lithological control tends to be more exerted by geomechanical properties than by lithochemical components. In essence, established ore-controlling or recognition criteria may include:

Host environment

- Paleozoic calcareous sediments in tectonic contact with Precambrian crystalline rocks
- Remnants of Tertiary felsic volcanics locally resting upon older rocks
- Major reverse fault zone (Chester fault) trending N–S along which Precambrian crystalline rocks were thrust upon Paleozoic sediments
- Wide intervals of intense brittle deformation at interjunction of the N–S reverse fault zone with numerous ENE–WSW-trending cross-structures
- Most intense brittle deformation is in dolomite (Mississippian Leadville Dolomite) and, to a lesser extent, in sandstone, black shale, and coaly shale (Pennsylvanian Belden Formation)
- Maximum fracturing is at places where brittle dolomite beds are intersected by reverse fault planes at angles of about 70°; deformation is less intense at lower angles of intersection.

Alteration

- Variable oxidation and leaching along fractured and brecciated sections of the main fault zone to depths of >100 m
- Common alteration product is ocher dolomite characterized by quartz and calcite enrichment and replacement of original pyrite by Fe oxides, and thin films of Fe oxides in fissures and joints
- Replacement of dolomite near the surface by a gossan composed of a porous and friable ocher rock of quartz with hematite/limonite and minor carbonate

- Ocher dolomites contain about 50–200 ppm U independent of their grade of alteration
- At surface, outcropping ocher gossan that derived from mineralized dolomite has high radioactivity but low uranium contents.

Mineralization

- U minerals in reduced environment: uraninite, pitchblende, coffinite, and not identified minerals (containing a major amount of U)
- U minerals in oxidized environment: uranophane and autunite
- Associated minerals: pyrite, marcasite, and minor Cu, Pb, Zn sulfides, and hematite
- Concentration of ore in veins, pockets, and small veinlets in fractures, shears, and breccias in the footwall of a major reverse fault zone (Chester fault)
- Preference of ore to dolomite and, to a lesser extent, to sandstone, black shale, and coaly shale
- Best host rock with respect to grade and resources is dark grey (Leadville) dolomite in which sites of optimum ore emplacement are intervals of maximum brecciation and cataclasis governed by the interjunction of brittle dolomite beds, changes in dip of beds, and downward flexures of fault planes.

Metallogenetic Aspects

The metallogenesis of the Pitch deposit is still enigmatic. The source of uranium, the nature of ore-forming solutions, and uranium precipitating and concentrating processes still remain open for speculation. Only the rock mechanics leading to the favorable fracture-breccia system for ore emplacement are satisfactorily explained.

Nash (1981) attributes fracturing and brecciation of the Leadville Dolomite to karst development and tectonic faulting, and states that sites for optimum ore emplacement were provided by zones of maximum cataclasis, which in turn were governed by the interjunction of (a) brittle dolomite beds, (b) changes in dip of the beds, and (c) downward flexures of fault planes. Nash (1981) explains the pervasive cataclasis that appears to be restricted to dolomite to the fact that brittle dolomite was the most responding rock facies to tectonic stress. In contrast, other rock facies reacted only by ductile deformation or remained unbroken.

Dupree and Maslyn (1979) have proposed that uranium in the Pitch deposit largely occurs in black organic-rich matrix material of carbonate breccias that formed by sinkhole collapse and fill. Nash (1981) disagrees with this interpretation. He states that carbonate breccias are tectonic breccias and are clearly related to faulting along the Chester fault zone. Both the breccia and the uranium grade die out below and to the west of the faults.

Chemical controls on uranium emplacement are not well understood, but apparently involve co-precipitation of iron disulfide as pyrite and marcasite. The presence of a large

proportion of marcasite may have resulted from metastable sulfur compounds, which also may have acted as a reductant for uranium. Organic carbon can be excluded as reductant since the carbon content is uniformly low in ore-hosting dolomite and there is no correlation between carbon and uranium content.

With respect to the source of the uranium, a vague speculative hint may be given by the uranium-mineralized, fluorite-bearing intrusive rock reportedly intersected in depth by a drill hole. The age of the intrusive is unknown. But if it is of Laramide age, it may be considered a potential U source rock.

6.3.0.2 Other Deposits/Occurrences in the Marshall Pass District

In addition to the Pitch deposit, a number of small U deposits and occurrences have been detected in various lithologies in the Marshall Pass district. Some had minor production.

The *Little Indian No. 36* mine, located 2 km north of the Pitch Mine, is in Middle Ordovician Harding Quartzite where the quartzite is fractured at the north end of the Chester fault zone. Hexavalent U minerals fill fractures in the upper third of the quartzite horizon, where it contains a 1.5 m thick bed with carbonaceous trash, asphaltic pellets, and phosphatic fossil remnants. Production from the Little Indian No. 36 underground mine was about 25 t U at a grade of 0.41% U. Proven and probable reserves are approximately 1,000 t U at a grade of about 0.21% U distributed over a strike length of 300 m.

Other prospects in close proximity to the Pitch Mine include the *Little Indian Nr. 34*, located 2 km NNW of the Pitch pit, where mineralization occurs at the fault contact of Devonian Chaffee sandstone-dolomite and the Leadville limestone. At *Little Indian Nr. 6*, positioned 3 km SW of the Pitch, mineralization is also hosted in Chaffee sediments. The *Erie* prospect, situated 800 m north of the Pitch Mine, has mineralization in the Belden Formation.

Additional uranium occurrences have been found in brecciated rocks along the Chester fault between the north end of the Pitch and Little Indian mines. The resource potential is estimated at a minimum of 4,000 t U at a grade of 0.2% U.

In the *Harry Creek* area, located about 2 km southeast of the Pitch Mine, the *Lookout No. 22* and the *Marshall Pass No. 5* prospects produced some tonnes of uranium at ore grades of about 1% U. Most of the high-grade ore was in pockets in Eocene (?) carbonaceous regolithic alluvium developed in Precambrian granite gneiss, pegmatitic granite, and quartz monzonite, and in places overlain by Tertiary volcanic flows. Some vein-like ore was in fractures and small faults in Precambrian rocks. Mineralization includes concentrically banded masses of pitchblende rimmed by hexavalent U minerals. Fracture fillings in Precambrian rocks are associated with increased amounts of As, Cu, Nb, Pb, Zn, W, Y, and Zr. Nash (1980) proposes supergene processes for ore formation, uranium being derived from overlying volcanics. Other U occurrences include *Apache Nr. 4* and the *Big Indian Group*. Approximately 18 km east of the Pitch Mine, mineralization was found at the *Bonita mine* in a fault zone cutting Precambrian hornblende-gneiss.

6.4 Cochetopa District, Colorado

The Cochetopa (also named *Los Ochos*) mining district is centered approximately 30 km southeast of the city of Gunnison. The district extends north-south along Cochetopa Creek for some 15 km and is roughly 8 km in width. Production from three properties was in excess of 420 t U at a grade averaging 0.12% U. More than 75% of all production from the Cochetopa district came from the *Thornburg No. 1* and *No. 2* ore bodies. Exploration at the *East mine* on the Kathy Jo claims revealed one small ore body adjacent to the Los Ochos fault.

Sources of Information. Chenoweth 1980; Goodknight 1981; Goodknight and Ludlam 1981; Malan and Ranspot 1959; Nelson-Moore et al. 1978; Olson 1976, 1988; Ranspot and Spengler 1957; US AEC 1959; and Mathisen M 1984, personal communication.

Geology and Mineralization

The area of uranium occurrences is situated at the extreme northeastern limits of the San Juan Mountains volcanic field on the western flank of the Rocky Mountains. The district contains rocks ranging from Precambrian intrusives and metasediments to Jurassic and Cretaceous sediments. Oligocene volcanics and ash flows formerly covered the area.

Uranium mineralization occurs in fractures and breccias along major normal fault zones (Los Ochos and Cochetopa fault systems) that are believed to be of Laramide to mid-Tertiary age. The *Los Ochos ore bodies* are in fault breccia along the Los Ochos fault where it intersects the Jurassic Junction Creek and Morrison formations. The mineralogy is reported as both sooty to semi-hard, fine-grained uraninite and pitchblende, forming veinlets and finely disseminated grains along fractures. Uranium minerals are usually associated with marcasite and unidentified clay minerals. Hexavalent U minerals occur throughout the deposits. Gangue minerals consist primarily of chalcedony, baryte, various clay minerals, and quartz.

The width and magnitude of mineralization is commonly controlled by the degree of fracturing and brecciation imposed on wall-rocks. Alteration is well developed in mineralized terrane. Sandstones are silicified, bleached, and limonite stained along fractures; Precambrian crystalline rocks exhibit effects of kaolinitization, sericitization, and chloritization.

Although many characteristics are compatible with a hydrothermal genesis for uranium mineralization, an origin or secondary enrichment of mineralization by supergene processes associated with extrusion of formerly overlying Tertiary volcanics can also be envisaged.

Selected References and Further Reading for Chapter 6 Colorado and Southern Rocky Mountains

For details of publications see Bibliography.
Abbott 1982; Adams and Stugard 1956; Ausburn 1981; Babcock 1980; Bird 1958, 1979; Bryant and Naeser 1980; Byrant et al. 1981; Carpenter et al. 1979; Chapin 1965; Chapin et al. 1982; Chenoweth 1980; De Voto and

Paschis 1980; Downs and Bird 1965; Dupree and Maslyn 1979; Epis and Chapin 1968,1974; Epis et al. 1976, 1979; Everhart 1956; Ferris and Bennett 1977; Finiol 1987; Fisher 1976; Goodknight 1981; Goodknight and Ludlam 1981; Grauch et al. 1985; Gross 1965; Heyse 1972; Hon 1984; Karlson and Krokosz 1983; Ludwig et al. 1985; Ludwig and Young 1975; Malan 1959; Malan and Ranspot 1959; Marvin and Dobson 1979; Maslyn 1978; McPherson 1959; Naeser 1978; Nash 1979, 1980, 1981; Nash et al. 1981; Nelson and Gallagher 1982; Nelson-Moore et al. 1978, 1979; Olsen 1976, 1979; Paschis 1979; Peterman and Hedge 1968; Peterman et al. 1969; Phair 1979; Phair and Jenkins 1975; Phair and Shimamoto 1952; Ranspot and

Spengler 1957; Rice et al. 1982; Rich and Barabas 1982; Shappirio 1963; Sheridan et al. 1967; Sims 1956, 1960, 1963; Sims and Barton 1962; Sims and Sheridan 1964; Sims et al. 1955, 1963; Spirakis 1981; Stark 1979; Taylor 1979; Tweto 1975; Tweto and Sims 1963; US AEC 1959; Walker and Adams 1963; Walker et al. 1963, 1983; Wallace 1979, 1982, 1983a, b, 1986; Wallace et al. 1983; Wallace and Karlson 1982, 1985; Wallace and Whelan 1986; Ward 1978; Wright 1980; Wright et al. 1981; Wrucke and Sheridan 1968; Young 1977, 1979a, b, 1985; Young and Hauff 1975; and Bondurant KT, Grauch R, Mathisen M, Pool TC, and Wallace AR (personal communication).

Chapter 7

Basin and Range Domain

The Basin and Range geomorphic province extends in a curvilinear NW–SE direction from southern Oregon and Idaho through Nevada, parts of California and Utah, southern Arizona and New Mexico into the Big Bend region of Texas (Fig. I.1). It includes the Great Basin in Nevada and western Utah.

Except for a few noteworthy occurrences and numerous small uranium showings, no significant uranium deposit has been discovered, as yet, in the Basin and Range province, as reflected by a total production of only 1,050 t U up to 1980 (US DOE 1980). Production after 1980 amounted to a few hundred tonnes of uranium essentially as a by-product to copper from the two copper porphyry mines Bingham and Twin Buttes. Known deposits are either of good grade and low tonnage (e.g., Marysvale, Utah) or vice-versa (e.g., Anderson mine, Arizona).

Sources of Information. See section “References and Further Reading” at the end of the chapter Basin and Range Domain and descriptions of individual districts.

Regional Geological Features and Uranium Mineralization of the Basin and Range Domain

The Basin and Range geomorphic province evolved from Miocene to recent time by extensive high-angle block faulting that formed narrow N–S-trending mountain ranges of moderate to high relief separated by valleys and broad basins. Rocks of many types and ages occur.

Precambrian plutonic and metamorphic rocks crop out mainly along the northeastern margin (e.g., Wasatch Range) and in the southern part of the region. Thick sequences of marine sediments of Paleozoic age are typical for the Cordilleran geosyncline. Cenozoic rocks are chiefly of igneous and nonmarine sedimentary origin. They include thick lavas, fanglomerates, fresh water limestone, conglomerates, and large quantities of ash-flow tuffs, particularly in the Great Basin, of Tertiary age. In late Tertiary time, fluvial and lacustrine sediments mixed with tuffs and evaporites were deposited in numerous intermontane basins. Ephemeral saline lakes and playas are formed in response to the present interior drainage and arid climate.

The Basin and Range region was affected by the Nevadan (in the west) and Laramide (in the east) orogenies from middle Mesozoic through early Tertiary time. During this period, many igneous plutons were emplaced and numerous volcanic centers produced abundant volcanic material.

Most noticeable potential sources of uranium are provided by abundant uraniferous silicic–alkalic volcanics of Tertiary age as well as uraniferous granitic plutons of Precambrian and younger ages.

Uranium mineralization is most frequently related to Tertiary volcanics. Major occurrences are structurally controlled in volcanic rocks or in tuffaceous lacustrine sediments, often associated with calderas. Typical examples of this type include U deposits in the *McDermitt Caldera*, Nevada–Oregon, *Lakeview*, Oregon, *Spor Mountain* and *Marysvale*, Utah.

Although hosted by various lithologies of diverse ages, uranium-bearing veins are predominantly associated with Tertiary intrusions and formed predominantly during Tertiary time. Ag–Bi–Co–Ni–U veins associated with late Cretaceous–early Tertiary monzonite porphyry in the *Black Hawk* district, New Mexico are representatives of this type of deposits.

Most resources are confined to paludal–tuffaceous–lacustrine sediments such as at the *Anderson mine* in the Tertiary Date Creek Basin, Arizona. Mineralization in fracture, shear, and breccia zones are reported from a variety of environments ranging from the Precambrian Dripping Spring Quartzite, *Sierra Ancha*, Arizona, to deposits in the contact zone between Jurassic(?) granitic intrusions and Cambrian metamorphics as in the *Austin district*, Nevada, and last but not least in Eocene copper porphyries such as *Bingham*, Utah, and *Twin Buttes*, Arizona where uranium was extracted as a by-product of copper.

Bromfield in Offield (1979) reports that most Basin and Range uranium occurrences in southwestern Utah lie on or near an aeromagnetic high, which probably results from the combined influence of shallow Cenozoic calc-alkaline intrusives and later Cenozoic extrusions of a bimodal basalt–rhyolite suite. Alkalic rhyolites of these latter extrusives have been the apparent source of uranium in the occurrences in southwestern Utah.

Otton in Offield (1979) points out that uranium in Tertiary basins occurs principally in distal arkosic alluvial or lacustrine turbidite facies, which contain either enrichments of carbonaceous material due to moderately wet depositional environments or in highly altered silicified and/or zeolitized tuffaceous sediments developed under more arid conditions. Further concentration of uranium to higher grades (0.1% U or more) apparently required additional processes such as an active hydrothermal system as found associated with calderas.

Silver et al. (1980) investigated U–Th–Pb isotope systematics of three uraniferous granitic plutons (Lawler Peak, Ruin, and Dells) in southern Arizona. The granites are 1,450–1,400 Ma old and contain up to 40 ppm U (Dells Granite, Prescott–Chino Valley). The authors found evidence of significant uranium loss relative to thorium and lead in two of the three plutons: 25% in the Lawler Peak Granite, Bagdad mine area (calculated loss: ca. 100,000 t U) and up to 60% (or 6 ppm) in the Ruin Granite, Globe–Lake Roosevelt region, whereas the Dells Granite has lost very little of its uranium. Two periods of uranium loss could be established at about 230 Ma and within the last 75 Ma. These episodic losses can be related to Permo-Triassic and Laramide orogenies, and to volcanic events.

7.1 McDermitt Caldera District, Nevada–Oregon

The McDermitt caldera is located at the border between Nevada and Oregon, about 330 km NNE of Reno and 10 km W of the village of McDermitt (►Fig. 1.1b). Uranium was discovered in 1953. Mercury deposits were mined for some time. Lithium is present in subeconomic concentrations, but makes up a major resource. Mercury deposits with uranium concentrations between a few and 100 ppm U, and low-grade uranium occurrences averaging 0.02–0.04% U occur along and adjacent to the caldera complex (►Fig. 7.1) on the N and NE edge (*Aurora* (U), *Bretz* (Hg, U), *Cottonwood Creek* (U), *Opalite* (Hg, U), *McDermitt* (Hg), *Cordero* (Hg)), the W and SW edge (*Moonlight* (U), *Horse Creek* (U), *Granite Point* (U), *Old Man Springs* (U)) and in the southern part (*Fox/Thacker Pass* (U)). The largest uranium occurrence is *Aurora* with indicated resources of approximately 6,500 t U at a grade of 0.04% U. *Moonlight* was formerly mined and produced about 0.5 t U.

Sources of Information. Chemillac 2004; Dayvault et al. 1985; Files 1978; Glanzman and Rytuba 1979; Myers and Underhill 2005; Mc Kee 1976; Roper and Wallace 1981; Rytuba 1976, 1977, 1981; Rytuba et al. 1979; Rytuba and Conrad 1979, 1981; Rytuba and Glanzman 1978; Sharp 1955; Taylor and Powers 1955; Wallace and Roper 1981. The following description is paraphrased from papers by Rytuba and his co-authors and Roper and Wallace (1981) amended by data from Dayvault et al. (1985) and the other authors listed.

Regional Geological Setting of Mineralization

Precambrian and Paleozoic rocks constitute the basement of the McDermitt area. Tertiary volcanics have been intruded and to a large extent cover the basement. Precaldera volcanics dated 40–18 Ma are chiefly of calc-alkaline, mafic to intermediate composition.

The McDermitt caldera is a large Miocene collapse structure situated at the WNW–ESE-trending Nevada Rift close to its intersection with the NNW–SSE-oriented Oregon–Nevada Lineament. The elliptical caldera complex measures 45 km in N–S and 35 km in E–W diameters and consists of five overlapping and nested calderas. Resurgence produced an inner-caldera highland with domes of volcanic eruptions giving the caldera complex a doughnut-shaped morphology. The structural arrangements together with depositional systems permit a subdivision of the caldera complex into four principal structural and depositional environments. These divisions are in centrifugal direction, the resurgent center (10 by 30 km²), the moat-zone, the ring-fracture-zone, and the outflow zones.

Dayvault et al. (1985) note the following characteristics of the principal post-caldera volcanics and sediments with respect to their distribution in the four zones mentioned before.

Resurgent center: Predominantly silicic peralkaline rhyolite/comendite ash-flow tuffs with locally abundant lithic fragments (includes Jordan Meadow rhyolite).

Moat zone: Pyroclastic-lacustrine sediments comprised of varicolored white, brown to green, in part carbonaceous mudstone, shale, tuffaceous sandstone, air-fall tuff, and coarse-grained beds of lahars or landslide talus, which overlie flows of icelandite/Fe-rich andesite or dacite with peralkaline tendencies and peralkaline rhyolites (*Aurora* Series, details see *Aurora* deposit). Moat-fill sediments carry abnormal amounts of soluble extrinsic elements such as Cs, F, Li, Rb, Th, and U.

Ring fracture zone: One or more normal faults bound the moat. These faults dip steeply to moderately into the caldera. Breccias of sediments and talus, and lahars are found in the moat adjacent to the ring fracture zone.

Outflow zone: Several peralkaline rhyolite ash-flow sheets, 18–15 Ma in age, are typical for this zone. In the northern part of the caldera, they are intercalated with basaltic icelandite flows (*Bretz* Series, see *Aurora* deposit).

Rytuba and Conrad (1981) distinguish four episodes of rhyolitic volcanism, dated between 18.5 and 13.7 Ma, within and adjacent to the McDermitt caldera complex. During the first three episodes, large quantities of ash-flow tuffs were erupted and consequently the caldera collapsed. Each episode started with high-silicic peralkaline rhyolite (comendite) ash-flow tuffs (75% SiO₂, 11% Al₂O₃) and ended after a systematic change in chemistry with less siliceous ash flows (62–70% SiO₂, 13–15% Al₂O₃). Early comendite ash-flows contain higher concentrations of U (8–10 ppm), Th (ca. 20 ppm), Zr, F, and lower concentrations of Ba, Ca, Mg, P, Sr, and Ti when compared with end member tuffs of any episode. Hg stayed the same in the first three ash-flow sheets (20 ppb), but varied in the later eruption between 10 and 70 ppb. The progressive change in chemistry is believed by the authors to reflect venting from successively lower levels of a zoned magma chamber.

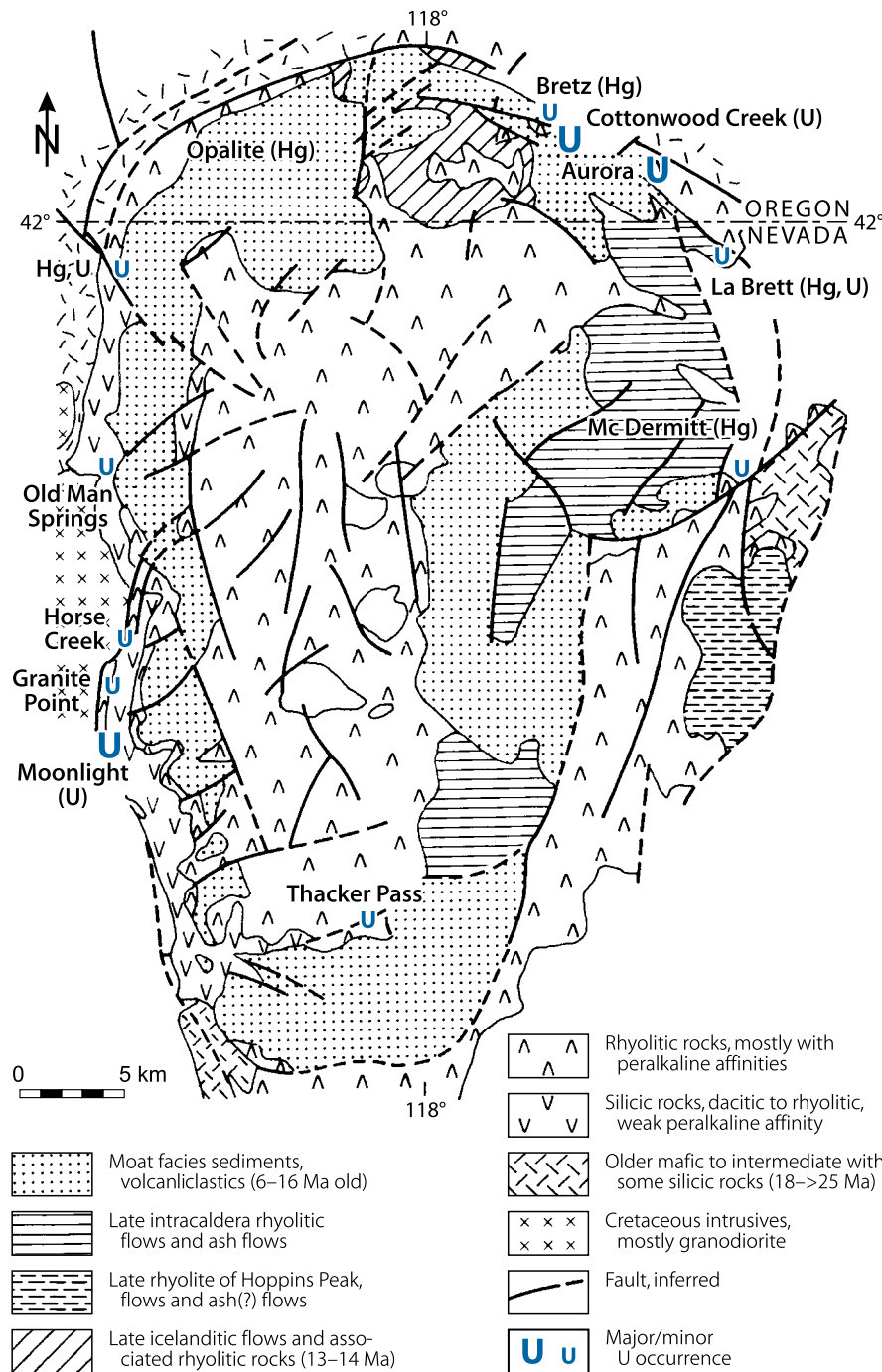
The fourth volcanic episode (14.9–13.7 Ma) is characterized by small intrusive bodies and domes with chemistry similar to early, high-silica rhyolites. These last rhyolites are considered to have tapped only an upper part of a similarly zoned magma chamber. Uranium deposits, according to Rytuba and Conrad (1981), are associated with emplacement of this last phase of comendite magma. An essential factor for this connection is the nonexplosive manner of emplacement, resulting in the formation of ore bodies by localizing magma and vapor in a small chamber rather than dispersing it in ash-flows as in older rhyolitic sheets.

Principal Host Rock Alteration

Several kinds of diagenetic and hydrothermal alteration affected the host rocks, and in particular the moat-fill sediments. They include argillization (Li-montmorillonite/hectorite, kaolinite, smectite, chlorite), zeolitization (analcime, clinoptilolite, erionite, mordenite), silicification (cristobalite, opalite, glass), carbonatization (calcite, dolomite), sulfidization (pyrite, marcasite), and potassium feldspathization. The first three are more typical in the vicinity of zones of U–Hg deposits, whereas K feldspathization is dominant within and near uranium ore zones. Rytuba et al. (1979) report seven large alteration systems

■ Fig. 7.1.

McDermitt Caldera, geological map illustrating the preferential location of uranium occurrences along the rim of the caldera. (After Dayvault et al. 1985 compiled from Castor et al. 1982; Berry et al. 1982; Dayvault RD 1983; Greene 1976; Rytuba and Glanzman 1978; Wallace et al. 1980, and industry personnel)



including five principal zones of K feldspathization within the McDermitt caldera complex. Three of the authigenic K feldspar zones located in the north and northeastern parts of the caldera enclose mercury deposits with appreciable amounts (50–200 ppm) of uranium. One other area encircles a uranium deposit (*Aurora*) associated with K feldspar and clinoptilolite alteration. These four K feldspar alteration zones on the north and

northeastern sides of the caldera are relatively small measuring 1–2 km in diameter. The fifth K feldspar zone is the largest. It extends along the southwestern side of the complex for almost 10 km where it is closely associated with intrusive bodies and flow domes, which host the *Moonlight* and *Horse Creek* U occurrences. Two additional alteration zones occur at *Crowley Creek* and *Rock Creek* where dominant zeolitization (clinoptilolite)

together with some local K feldspathization are associated with concentrations of U and Hg.

Rytuba et al. (1979) believe the K feldspar alteration areas define the central part of a fossil hydrothermal system (for description of zonation, see Aurora–Bretz). As a result of hydrothermal and/or diagenetic alteration processes, soluble elements such as Cs, F, Li, Rb, Th, and U, which are originally enriched constituents of rhyolitic rocks, were released and reconcentrated in moat-fill sediments, the first four elements to a large part in alteration products such as clay and zeolite minerals, and in potassium feldspar.

Principal Characteristics of Mineralization

The principal U minerals in unoxidized environments are very fine-grained pitchblende and coffinite associated with a suite of associated minerals and lithophile elements (▶ Table 7.1). Hexavalent U minerals occur in oxidized zones, in particular along fault zones.

Uranium mineralization within the McDermitt caldera complex is spatially confined to three environments:

- Ring-fracture zone (e.g., *Bretz*, *Moonlight-Horse Creek*)
- Outer zone of resurgent highlands (e.g., *Aurora*)
- Moat zone (e.g., *Cottonwood Creek*).

Mineralization in the ring-fracture and outer resurgent highland zones is epigenetic, that in the moat zone is syngenetic. Four principal types of uranium mineralization are identified, all of them occur in zones of strong alteration.

- a) **Epigenetic structure-bound/vein-type mineralization** commonly occur in steeply dipping fractures within rhyolitic intrusives and domes at the outer part of the resurgent highlands, in the ring-fracture zone (*Moonlight-Horse Creek*), and in mafic icelandite volcanics (*NE zone of Aurora*). This type includes two subtypes, one with uranium as the dominant element, the other with mercury. The U-dominant subtype commonly forms small occurrences (a few tonnes to some 10 t of uranium, except perhaps in the NE-Aurora zone, but no figures are published for that zone) with grades of as much as 0.12% U.
- b) **Epigenetic strata- and structure-bound mineralization** is emplaced peneconcordantly in permeable tuffaceous ash-flows and sediments of felsic to intermediate composition in part along unconformities, and in fractures along and adjacent to major structures, e.g., ring-fracture zone along the caldera rim (*Bretz*). Occurrences are small, a few tonnes to several tens of tonnes and grades are low, about 0.02% U.
- c) **Epigenetic strata-bound mineralization** occur peneconcordant in permeable layers within mafic to intermediate volcanics, for example in vesicular lava tops along intraformational unconformities and in breccia layers within icelandite units of the Aurora lava (e.g., *Aurora*). Some structural control on mineralization may be implied since mineralized areas are structurally affected (e.g., Aurora structure and

Boundary fault). Deposit sizes are small to medium (up to some thousand tonnes uranium), grades are generally low, less than 0.042% U

- d) **Syngenetic strata-bound mineralization** is hosted in tuffaceous-lacustrine moat-fill sediments (e.g., *Aurora-Cottonwood Creek*). Low-grade (less than 100 ppm U) disseminated uranium accumulation occurs in the basal sequence, and some better grades (about 0.02% U) in opaline marker beds within the sequence. Moat sediments also contain strata-bound mercury deposits, such as McDermitt, and opalite with minor to trace uranium. Hot springs are thought to have synsedimentary introduced the mercury.

The best uranium mineralization with respect to resources is in epigenetic strata-bound deposits (type c), specifically in highly altered porous vesicular and/or breccia layers of mafic lavas of basaltic–icelandic composition such as in the *Aurora* deposit. The best grades are found in epigenetic structure-bound deposits (type a) within host rocks of felsic and intermediate (*Moonlight*) or mafic (*NE zone of Aurora*) composition.

Principal Ore Controls and Recognition Criteria

Two regional features appear to exert control for geologic–tectonic localization of uranium occurrences: (a) Presence of highly uraniumiferous/metalliferous late-phase peralkaline rhyolitic magma forming domes and flows, which apparently constitute the dominant uranium source and (b) positioning of deposits at or near the ring-fracture zone inside the caldera rim. More specific ore controls and recognition criteria for various types of uranium mineralization found in the McDermitt complex are summarized in ▶ Table 7.1.

Metallogenetic Concepts

Nonexplosive rhyolites are regarded as the most likely source for all types of uranium and other metallic mineralization in the McDermitt caldera complex. Known data indicate multiphase processes involved in the variable release, transport, and depositional mechanisms of uranium as well as other metals, but the specific origin, nature, and significance of the fluids and the actual ore concentrating processes are not as well understood.

Open questions refer to the significance/dominance of (a) hypogene vs. supergene hydrothermal fluids in ore formation, (b) whether hydrothermal or diagenetic processes or both were critical in ore-related alteration (devitrification, zeolitization, K metasomatism), and (c) which kind of reductant and/or adsorbent (ferrous iron, clay minerals, carbonaceous matter, silica/opal) played a crucial role in uranium precipitation and concentration.

Rytuba and his co-workers propose a metallogenetic evolution for the various modes of uranium mineralization in the McDermitt caldera involving the following components and events:

Table 7.1.

McDermitt Caldera, ore controls and recognition criteria of modes and setting of uranium deposits (compiled from papers by Roper, Wallace, and Rytuba and his coworkers listed under Sources of information at begin of Chap. McDermitt caldera)

Type of deposit	Epigenetic structure-bound		Epigenetic strata-structure-bound	Epigenetic strata-bound	Syngenetic strata-bound
	Example	NE zone of Aurora			
Geologic setting	Commonly in steeply dipping fractures	Commonly in steeply dipping fractures	Peneconcordant along flat-lying unconformities and in fractures adjacent to major faults	Peneconcordant in permeable highly altered vesicular lava tops along intraformational unconformities and in breccia	Peneconcordant in basal-section and in marker horizons in moat-fill sediments
Tectonic location	Margins of resurgent highlands within caldera	Along ring fracture-zone at caldera rim	Along and adjacent to ring fracture zone at caldera rim	Resurgent highlands within caldera [near and at major structures (Aurora anticlinal structure, Boundary fault), but genetic relation to structures is obscure]	Intracaldera moat basins
Host rocks	Mafic to intermediate volcanics (Aurora: icelandite), minor felsic volcanics (rhyolite domes)	Felsic and intermediate volcanics [Moonlight: (peralkaline) rhyolitic domes + flows, dacite, and granodiorite]	Felsic, intermediate to mafic volcanics	Mafic to intermediate lavas of icelandite composition	Tuffaceous - lacustrine sediments
Host rock alteration	Argillization - early kaolinitization - late montmorillonitization	Argillization	Argillization (2 stages) - early kaolinitization - late montmorillonitization	Argillization - early kaolinitization - late montmorillonitization	Argillization
	Zeolitization	Zeolitization		Zeolitization	Zeolitization
	Silicification (opalite, quartz, less often cristobalite)	Silicification (opalite)	Silicification	Silicification (opalite, quartz, less often cristobalite)	Silicification (opalite)
	K feldspathization		K feldspathization	K feldspathization	K feldspathization
	Carbonatization	Carbonatization		Carbonatization	Carbonatization (calcite)
Principal mineralization	Dominant U (pitchblende-coffinite), subordinate Hg	Dominant U (pitchblende, coffinite) subordinate Hg	Dominant Hg, subordinate U and other metals (no distinct U mineral determined)	Dominant U (pitchblende-coffinite), subordinate Hg	Locally dominant Li, subordinate U

Table 7.1. (Continued)

Type of deposit	Epigenetic structure-bound		Epigenetic strata-structure-bound	Epigenetic strata-bound	Syngenetic strata-bound
	NE zone of Aurora	Moonlight – Horse Creek			
Example	NE zone of Aurora	Moonlight – Horse Creek	Bretz	Aurora	Cottonwood Creek
Associated minerals	Pyrite, leucoxene, fluorite, zeolites, silica, calcite, siderite	Pyrite, fluorite, quartz, zeolites, carbonate, apatite, jarosite, baryte	Pyrite, jarosite, silica, leucoxene, rutile, baryte, late montmorillonite, sulfides	Pyrite, fluorite, silica, zeolites, calcite, siderite, leucoxene	Pyrite, opalite, quartz, calcite, sporadic zeolites
Assoc. elements	As, F, Hg, Li, Mo, W, Zn	Ag, As, Ba, Cu, F, Hg, Mo, Sb, Sn, W, Zr	As, Cu, F, Hg, Mo, Pb, Sb, W, Zn, Zr	As, F, Hg, Li, Mo, W, Zn	As, Cs, F, Hg, Li, Mo, Rb, Th

- Volcanic activity extending over a long time period in a restricted area
- Eruption of rhyolite within the caldera complex with an initial magmatic enrichment of ore-relevant elements, which provided a source for later formation of U, Hg, and/or Li deposits
- Uranium mineralization in particular is associated with the last phase comendite magma of nonexplosive emplacement and not so much with the older high-silica rhyolite ash-flows, although both are chemically similar. (Non-explosive extrusion favors concentration of uranium by focusing magma and vapor in small near-surface intrusives and domes found along the margins of the complex rather than dispersing it in ash-flow sheets.)
- The Longridge caldera, the last formed of the five calderas that constitute the McDermitt complex, is the location of uranium mineralization in domes located along the ring fracture system and in volcanic rocks filling the caldera
- Near-surface hydrothermal systems developed contemporaneously with the comendite emplacement as a result of heat transfer to the crust. Seven large hydrothermal systems are identified in the McDermitt complex. They altered, perhaps together with diagenetic processes, large areas within the caldera-fill volcanics and sediments
- During hydrothermal and diagenetic alteration of fertile rhyolitic rocks, highly soluble elements such as U, Th, Cs, F, Li, and Rb were released and transported by fluids to the near-surface level where they were concentrated in moat-fill sediments within the closed basin created by the caldera collapse
- Extraction from solution and precipitation of the elements was caused by clay minerals, zeolites, potassic feldspar, and organic matter present in moat sediments as reflected by enrichment of Cs, Rb, Li, and F to a large part in these alteration minerals
- Five of the seven established areas of alteration became thus mineralized with uranium and/or lithium along and adjacent to the ring fracture system of the caldera
- An age of 13.3 ± 2 Ma is indicated for the hydrothermal event by resetting of K–Ar ages of ash-flow tuffs adjacent to ring fracture faults (Rytuba 1981). K–Ar dating of Hg ore of the

McDermitt deposit yields an age of 12.3 ± 7 Ma (McKee 1976), which is about 1.5 Ma younger than the collapse of the youngest caldera and close to the final emplacement of ring domes

- Formation temperatures of mineralization composed of uraninite associated with fluorite, quartz, and pyrite in the youngest rhyolites as indicated by fluid inclusions analyses are 210°C for fluorite and 310°C for quartz from a quartz-fluorite vein (salinity: 1.8% and 4.5% equivalent NaCl, respectively) (Rytuba and Conrad 1979).

Roper and Wallace (1981) propose a metallogenetic evolution for the Aurora–Bretz mineralization, which contrasts in several aspects to that suggested by Rytuba and his co-workers. Roper and Wallace note three principal types of mineralization and related ore-forming processes:

- (a) Higher grade, epigenetic, primary hypogene mineralization in steeply dipping fractures in mafic to intermediate lavas, e.g., in icelandite Aurora lava (*Aurora, Bretz*)
- (b) Dispersed, epigenetic, supergene mineralization in subhorizontal permeable layers in Aurora lavas (*Aurora*)
- (c) Synsedimentary mineralization in discrete moat lake beds originating from uraniferous syngenetic-hydrothermal solutions (*Cottonwood Creek*).

Basically these authors suggest a multiphase evolution by a combination of hydrothermal and supergene processes for ore formation.

- Hydrothermal fluids carrying uranium and associated elements are thought to be related to one of the peralkaline volcanic events and associated with a final period of hydrothermal (-tectonic) activity in the caldera, both of which may have been coincident with the formation of the Aurora anticlinal structure and the Boundary fault. These hypogene fluids apparently caused alteration and introduced U together with anomalous amounts of As, F, Hg, Li, Mo, Sb, and S into steeply dipping fractures to form primary mineralization in lavas
- At about the same time groundwater redistributed and dispersed uranium laterally along the more permeable layers (vesicular flow tops and breccia) within the Aurora lava sequence

- Favored facies for uranium concentration at Aurora and Bretz are intermediate to mafic lavas such as icelandite of the Aurora lava. This is apparently attributed to the fact that high Fe²⁺ contents provided reducing potential and montmorillonite alteration enhanced uranium deposition
- Final discrete pulses of uraniferous fluids, perhaps hot springs emanating from the lake floor or along the ring fracture zone, introduced uranium into the moat and formed synsedimentary uranium accumulations disseminated in basal lake beds and in marker horizons, often associated with silica but apparently not with organic material.

Cupp in Dayvault et al. (1985) relates uranium enrichments in moat-fill sediments to a fluctuating pH boundary caused by an alkaline groundwater system along the interface between fresh and old basinal groundwaters in sediments with precipitation of silica and uranium independent of carbonaceous matter.

Description of Selected Deposits in the McDermitt Caldera Complex

The subsequent description covers properties with uranium as the dominant commodity and a listing of mercury-dominated deposits, which carry some uranium (Fig. 7.1).

Sources of Information. Dayvault et al. (1985), Myers and Underhill (2005), Roper and Wallace (1981), Rytuba (1976), Rytuba and Glanzman (1978), Sharp (1955), Taylor and Powers (1955), Wallace and Roper (1981) unless otherwise cited.

7.1.0.1 Aurora–Bretz–Cottonwood Creek

Aurora is situated about 15 km NW of the village of McDermitt and about 1 km SSW of the *Bretz* Hg(-U) deposit at the NE rim of the McDermitt caldera (Fig. 7.2a). *Cottonwood Creek* mineralization stretches from *Bretz* to and beyond *Aurora*. *Aurora* hosts, in a near-surface position, the largest known resources (about 6,500 t U, 0.04% U) of any single volcanogenic uranium deposit in the Basin and Range domain.

Geological Setting of Mineralization

The *Aurora* and northeasterly adjacent *Bretz* properties (Fig. 7.2a and b) are underlain by intracaldera facies (*Aurora Series*) and outflow facies (*Bretz Series*) both of Miocene age, upon which tuffaceous lacustrine sediments rest (lithology after Wallace and Roper 1981).

Tuffaceous lacustrine cover sediments, up to 200 m in thickness, consist of well-bedded tuff, air-fall ash, laminated shale, siltstone, tuffaceous sandstone with fragments of devitrified glass, fine- to coarse-grained crystals, lithics, and organic debris. They enclose interstratified layers and discontinuous lenses of chalcedony, are locally strongly altered, and contain U in basal beds.

The *Bretz Series* forms the caldera wall and outflow along the rim of the caldera complex. The *Bretz Series* includes (a) rhyolite ash-flow tuff (four cooling units); (b) mafic to intermediate flows, basalt or icelandite; (c) rhyolite flows, domes, tuff; and (d) rhyolite ash-flow tuff and lava.

The *Aurora Series* constitutes intracaldera fill that laps onto *Bretz Series* rocks near the ring-fracture zone. The *Aurora Series* comprises

- *Aurora* icelandite lavas (<100 m thick) composed of lava flows, 5–15 m thick, of mainly icelandite composition, high in iron and alkalis, and medium amounts of silica. Individual flows have massive, unaltered central zones bordered by frequently altered vesicular to scoriaceous flow-tops and locally include breccia layers. This unit is the main U host. It contains U mineralization in altered flow-tops and breccia layers. Extrusive and intrusive rhyolite present in several generations of chiefly small, brecciated, aphyric domes and some flows. Some U occurs in upper sections of this unit
- Rhyolite lava of McDermitt Creek and
- Intracaldera ash-flow tuff.

Structural elements of the *Aurora–Bretz* area are inherited from the caldera formation and are subparallel to the nearby NW–SE-trending caldera rim. Four distinct structures are dominant:

- The outer rim fault is a zone of NW–SE-trending, steeply SW-dipping normal faults with less than 15 m displacement marking the contact between moat sediments and caldera rim volcanics. The *Bretz* Hg–U concentrations occur near or along this fault
- The inner rim structure parallels the outer rim fault and defines the northeastern margin of the *Aurora* icelandite lavas
- The Boundary fault is an arcuate zone of NW–SE-striking, steeply dipping and probably en echelon arranged normal faults with a total offset of 60–100 m. It forms the northeastern limit of the relatively shallow *Aurora* mineralization in the *Aurora* lavas and is obviously the southwestern boundary of a graben limited on the NE side by structures of the caldera rim
- The *Aurora* structure is a NW–SE-trending, gently SW-dipping, asymmetric arch-like feature bounded to the NE by the Boundary fault. The crest of the structure coincides with the axial zone of shallow mineralization in *Aurora* lavas, and their margins generally mark the boundaries of the *Aurora* ore zone.

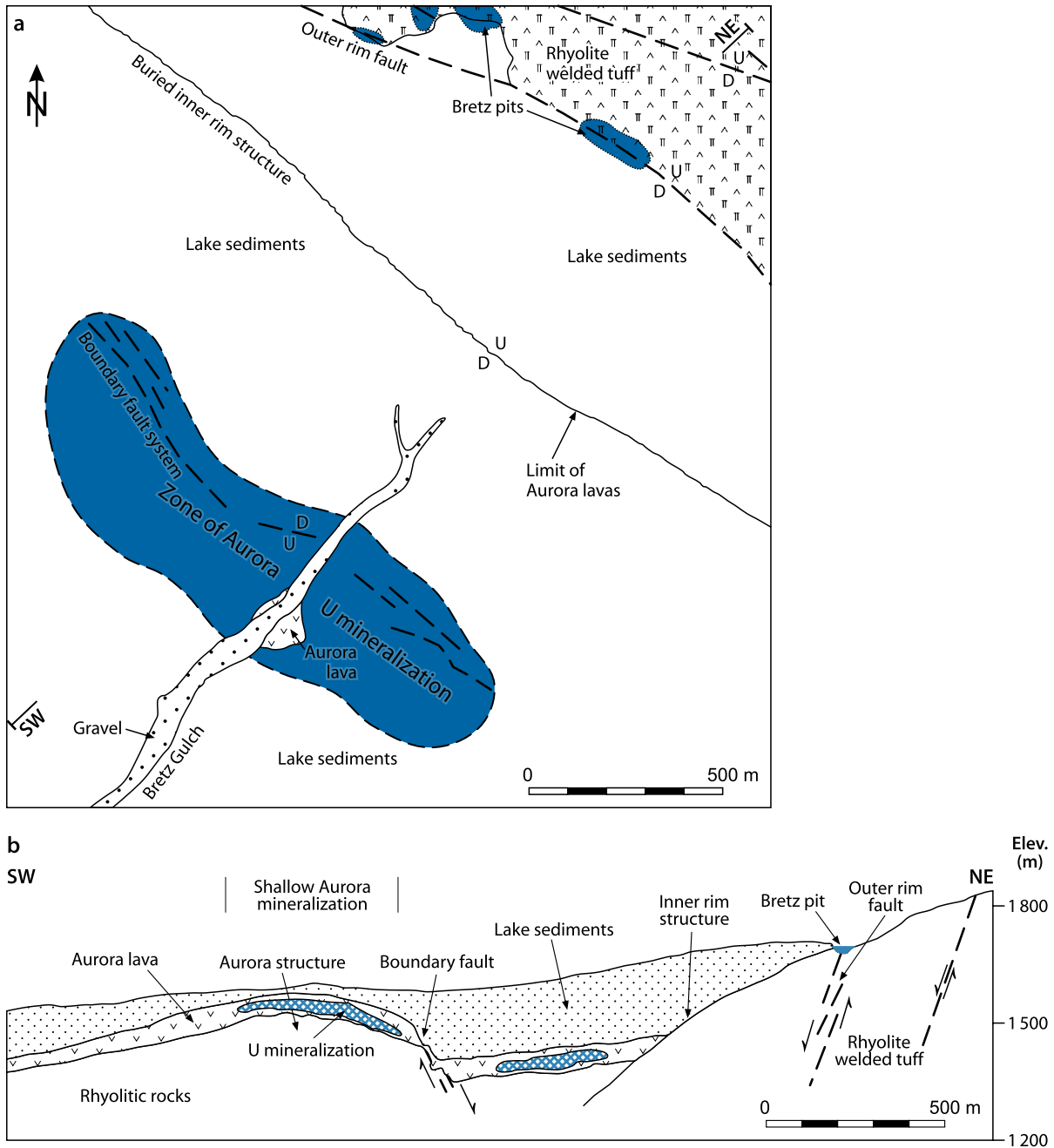
The *Bretz* area is structurally dominated by the ring-fracture system, a broad zone of multiple faults, usually having little offset but a few of which create block faulting.

Host Rock Alteration

Zones of intense alteration accompany uranium (*Aurora*) and/or mercury (*Bretz*) occurrences. Alteration and likewise

Fig. 7.2.

McDermitt Caldera, Aurora-Bretz, (a) simplified geological map and (b) SW-NE section showing the distribution of Aurora-type U mineralization in basal lake sediments and limitation of the shallow segment of this mineralization as well as the distribution of the Bretz Hg(-U) mineralization in rhyolite welded tuff along the outer rim fault of the caldera. (After Roper and Wallace 1981; AAPG 1981, reprinted by permission of the AAPG whose permission is required for further use)



mineralization within Aurora icelandite lavas at Aurora are confined to porous zones along flow tops, brecciated layers, and steeply dipping fracture zones. Mineralized rock is almost completely transformed into pyrite-bearing montmorillonite, chlorite, clinoptilolite, opal, and leucoxene. Other minerals in altered facies include iron oxides, marcasite, arsenopyrite, calcite, gypsum, and fluorite.

According to Dayvault et al. (1985), altered rocks have a groundmass of potassic feldspar, clay, quartz, and less often

crystalite; phenocrysts of plagioclase are altered to clay and vesicles are filled with jarosite, spherulitic siderite, and clay.

Rytuba et al. (1979) distinguish four zones of hydrothermal alteration within Aurora lavas surrounding the Aurora and Bretz deposits: (a) a central zone of K feldspar (Bretz) or K feldspar with clinoptilolite (Aurora); (b) a zone of clinoptilolite; (c) an outer zone of clinoptilolite with mordenite; and (d) at greater distance from the deposit, relict glass with varying amounts of clinoptilolite and erionite.

Alteration within the lacustrine sedimentary section is characterized by ubiquitous feldspar, smectite, calcite, and quartz, and sporadic zeolites (clinoptilolite, erionite).

Mineralization

Aurora: Very fine-grained pitchblende and coffinite are the principal U minerals. Some hexavalent U minerals occur locally, including umohoite (Roper and Wallace 1981). Pitchblende and coffinite occur as fine coatings around and between framboidal pyrite and as sparsely distributed minute grains in a leucoxene matrix.

Mineralization is emplaced in three principal lithological units: (a) dominantly in more mafic, icelandic layers of the Aurora lava unit; (b) in minor concentrations in the basal 20 m of overlying rhyolitic tuffaceous lacustrine sediments; and (c) locally in the upper part of underlying rhyolite domes. In more detail, these types of occurrence exhibit the following features.

Aurora icelandite lavas contain shallow uranium mineralization confined to the Aurora structure (▶ Fig. 7.2). This mineralization is primarily concentrated in subhorizontal, highly altered vesicular to scoriaceous layers along flow boundaries (flow tops) and in laharic or flow-breccia layers; and, less commonly, along deeply dipping fracture zones. The greenish-grey to black host rock is almost completely altered to clay-like material. In particular, late montmorillonite with abundant pyrite contains finely dispersed pitchblende and coffinite. Better grade mineralization is found along the northeastern side of the mineralized shallow lava zone in the form of sooty pitchblende-coffinite and associated pyrite coating steeply dipping fractures. Other elements associated in anomalous amounts with uranium mineralization include As, Hg, F, Li, Mo, Sb, W, and Zn. Dayvault et al. (1985) report uranium values in samples from altered Aurora lava of up to 0.25% U in the deposit, and up to 60 ppm U west of the deposit. Less altered rocks from massive central zones of the Aurora lava contain between 2 and 100 ppm U.

Aurora-Cottonwood Creek: Tuffaceous lacustrine sediments contain uranium enrichment in the basal 10 m of lake beds. In addition, two specific lithologic horizons (marker beds) about 2.5 m vertically apart and 0.5–2 m thick each, occur about 15–20 m above the Aurora lava, principally in the deeper part of the moat trough, i.e., on the NE flank of the “shallow mineralization” extending eastward almost to the Bretz mine. The two horizons are characterized by thinly bedded opal layers, pyrite layers 1–2 mm thick, varved opaline sediments, ash and diatoms, and minor amounts of carbonaceous matter. Some coarser grained tuff, particularly higher up in the sequence, contains more carbonaceous material. Where mineralized, sediments are altered to zeolites, montmorillonite, K feldspar, and other minerals. Uranium is concentrated up to 170 ppm. Associated trace elements are similar to those in Aurora lavas. Uranium pervades all the host rocks along the two marker horizons without an apparent preference to organic-enriched portions. According to Rytuba et al. (1979), beds higher in the sedimentary sequence

have U- and As-rich calcite layers; and U, Li, As, Hg are together or separately enriched in several organic-rich lacustrine clay-mudstones that alternate locally with black opaline-silica layers.

Rytuba (1981) lists the following maximum concentrations of elements in tuffaceous moat-fill sediments (in brackets main host mineral): <0.05% U (pitchblende); 0.02% Th (unknown mineral phase); 6.9% F (hectorite); 0.36% Li (hectorite), 0.64% Li (unidentified clay mineral); 0.06% Cs (analcime), 0.02% Cs (clinoptilite), 0.09% Cs (K feldspar); 0.1% Rb (K feldspar).

Within rhyolite domes, uranium is apparently confined to the upper contact of these domes where it occurs in steeply dipping fractures, which are believed to be downward extensions of mineralized structures in the overlying Aurora lava.

Bretz: This is primarily a mercury deposit with associated low-grade uranium. Dayvault et al. (1985) note that no discrete uranium minerals could be identified, and they assume that uranium occurs in extremely fine disseminations in silica, absorbed on limonite, or associated with sulfides and mercury. Other minerals in uraniumiferous rocks include limonite, jarosite, leucoxene, rutile, some baryte, abundant pyrite, and in trace quantities marcasite, chalcopyrite, galena, Hg-sulfide, and Sb-Fe-Cu sulfides. Trace amounts of primary zircon and xenotime occur in siliceous breccia. Additional trace elements include As, Fe, Mo, W, Zn, and Zr.

Preferential uranium-hosting facies are dominantly large siliceous masses, argillized tuffaceous sediments, and peralkaline ash-flow tuff located along the outer ring fracture zone. Uranium apparently occurs more along the flat-lying unconformities such as those at the base of intracaldera ash-flow tuffs and the top of rhyolite domes and flows rather than in steep fractures.

Alteration phenomena attributed to older mercury mineralization consists mainly of argillization and silicification while younger veinlets of montmorillonite and framboidal pyrite, which cut kaolinized and silicified rocks, are related to the uranium.

Shape and Dimensions of Deposits

Aurora: Mineralization extends in total over an area of 2,000 m by 1,000 m and consists of two zones. A shallow uranium zone in Aurora lava occurs at a depth between 20 and 120 m and is about 1,500 m long in NW-SE direction and 500 m wide. It covers an area almost identical with the NW-SE-trending anticlinal crest zone of the Aurora structure (▶ Fig. 7.2). Individual flows are 5–15 m thick within the up to 100-m thick Aurora lava. Uranium is concentrated along subhorizontal flow-tops and within breccia layers up to a few meters thick (grading about 0.04% U), and along steeply dipping fracture zones, which extend into underlying rhyolitic domes and flows and commonly carry better grades compared to the strata-bound mineralization.

Moat sediments host U mineralization west of the above mentioned shallow uranium zone. Low-grade mineralization occurs in the basal 10 m and in two distinct marker horizons at a depth of about 150–200 m within the moat trench. The two

main uranium layers (marker bed mineralization) are 0.5–2 m thick and carry about 0.02% U. These beds can be traced over an area of at least 3,600 by 1,000 m, but the full extent of uranium mineralization is not established. Uranium decreases in the marker beds southwestwards towards the Aurora lava mineralization, whereas to the northeast, near the Bretz mine, mineralized layers pinch out or are not mineralized.

Bretz deposit: Distribution of uranium mineralization roughly corresponds to that of mercury. It extends intermittently along the ring-fracture zone for about 3,800 m in NW–SE direction and ranges in width from 200 to 500 m. Mineralization locally crops out at surface. Grades are up to 0.02% U and occasionally more. Hg content may be up to 1.6% (Dayvault et al. 1985).

7.1.0.2 Moonlight

Moonlight, located at the southwestern edge of the McDermitt caldera, is the only deposit in the district with recorded uranium production (0.56 t U, 0.11% U).

Vein-type uranium mineralization is contained in a major fault trending N–S and dipping 50–60° E, which is part of the ring-fracture system. Host rocks on the hanging wall side are biotite–rhyolite breccia, and on the footwall side Miocene(?) rhyolite ash-flow tuff and dacite flows, and Mesozoic granodiorite. Near to and within mineralized intervals, wall rocks are altered to clay, adularia, opalite, and zeolite. Some carbonate, apatite, jarosite, baryte, and titanium oxides are present.

Pitchblende associated with pyrite and traces of other sulfides, fluorite, and quartz are typical minerals in unoxidized environments, while uranyl phosphates (meta-autunite, meta-torbernite) accompanied by limonite, fluorite, and smoky quartz prevail in oxidized zones. Dayvault et al. (1985) report a uraniferous clayey zirconium mineral occurring as patches in the breccia matrix and as late-stage veinlets. Anomalous amounts of Ag, As, Ba, Cu, F, Hg, Mo, Sb, Sn, W, and Zr are present. Fluid inclusions (with two phases) in quartz associated with the pitchblende homogenize at $340^{\circ}\text{C} \pm 7^{\circ}\text{C}$ (Rytuba 1976) indicating a relative high temperature of formation.

Mineralization occurs in a vein 1–5 m wide filled with breccia and siliceous cement. Depth extension is at least 50 m (Sharp 1955). Oxidized ore is exposed over a distance of more than 100 m and averages between 0.1 and 0.13% U. More mineralized outcrops are found along strike, a few hundred meters further north. A similar vein-type occurrence, *Granite Point*, is in a caldera ring-fracture approximately 2 km NNW of Moonlight.

7.1.0.3 Horse Creek

This occurrence is located at the west rim of the McDermitt caldera approximately 5 km N of Moonlight. It lies about 3 km NNE of and on the same ring-fracture as *Granite Point*. Resources are reportedly 2,500–4,000 t U at a grade of 0.02% U occurring at

depths down to 150 m. According to Dayvault et al. (1985), mineralogy and trace elements contents are very similar to *Moonlight* and *Granite Point*. Host rocks are peralkaline ash-flows and dacite flows. Some ore is in a NE–SW-striking shear zone, which dissects the N–S-trending ring-fracture.

7.2 Lakeview District, Oregon

Discovered in 1955, the Lakeview uranium district is located about 30 km NW of the town of Lakeview in south-central Oregon (Fig. 1.1b). The largest producer, the *White King* underground mine, produced approximately 135 t U at an ore grade of about 0.13% U from a depth of 20–100 m, and the *Lucky Lass* mine delivered almost 20 t U at a grade of 0.28% U.

Sources of Information. Castor and Berry (1981), Chenoweth and Malan (1969), Mahood (1983), Offield (1979), Waters (1955), and Patterson J personal communication.

Geology and Mineralization

Uranium mineralization is concentrated in the contact zone between late Tertiary rhyolite intrusive bodies and Miocene pyroclastic and lacustrine sediments. Walker (in Offield 1979) distinguishes regionally at least three principal events of peraluminous silicic intrusions 33–31, 15–14, and 8–7 Ma ago. Uranium accumulations appear to be associated with the two younger stages, and probably mostly with the youngest group of intrusives. Weissenberger in Mahood (1983) established K–Ar ages of 26 Ma for the ignimbrites and 8–7 Ma for the rhyolite domes of the Lakeview district.

The *White King* deposit is hosted in coarse pumiceous volcanic breccia, which locally has been completely silicified to a light colored lustrous mass of opalite grading laterally into moderately silicified and thoroughly argillized tuff-breccia. Host rocks at *Lucky Lass* comprise pumice lapilli-tuff, coarse lithophysae-bearing welded tuff, and rhyolite flows. Extensive argillization and less intense silicification generated a soft, pale-green rock composed chiefly of clay minerals, chlorite, and silica (Waters 1955).

Mineralization at the *White King* mine and other prospects consists of pitchblende, coffinite, and hexavalent U minerals accompanied by ilsemannite, realgar, orpiment, cinnabar, chalcidony, pyrite, and/or hematite, limonite. Ore is discontinuous and tends to be structurally controlled by shear and fracture zones. It forms veinlets, irregular masses, and disseminations in stockworks, which have been displaced by faulting and modified by groundwater redistribution.

Castor and Berry (1981) state that the Lakeview district does not contain peralkaline rocks and that ore has low fluorine contents. These parameters are somewhat atypical for North American volcanic uranium districts. In the opinion of these authors, geology and geochemistry indicate that uranium has originated from hydrothermal fluids related to intrusion of peraluminous rhyolite domes.

Weissenberger in Mahood (1983) arrives at a contrasting conclusion and proposes that ignimbrites may be the source of uranium with the proviso that at the White King mine, uranium was remobilized around a much younger rhyolitic dome. Weissenberger's arguments are: (a) the little rhyolite plug at the White King mine is too small to deliver all the uranium in that deposit, (b) occurrences of uranium mineralization in 26 Ma old ignimbrites, which are distant from any rhyolite domes, (c) lack of mineralization at most of the domes, and (d) presence of rather voluminous ignimbrites.

7.3 Austin District, Nevada

Discovered in 1953, this small uranium district is situated in central Nevada immediately south of the Reese River silver district (►Fig. 1.1b). Two mines have produced 42 t U. The larger operation, the *Early Day* (or *Apex*) mine, is located about 5 km SW of Austin. Mining was from open pits and adits and produced approximately 40 t U at an ore grade averaging 0.2% U.

Sources of Information. Chenoweth and Malan 1969; Sharp and Hetland 1954; Thurlow 1956; US AEC 1959.

Geology and Mineralization

Metasediments of the Cambrian Gold Hill Formation, principally quartzite and graphitic, pyritic shale were intruded by stocks of quartz monzonite of probable Jurassic age. The intrusive contact generally is almost conformable with bedding probably due to dragging of metasediments by the intrusion. Roof pendants are common in the quartz monzonite body. Numerous silicified fractures dissect the contact zone. Aplite dikes, often highly altered, cut the complex. A few major post-ore faults displace the rocks.

Mineralization is structurally controlled in a silicified intensely fractured zone, which dissects the intrusive contact and encloses an E–W-trending, 8–12 m wide, highly altered aplite dike. Although the mineralization is near the fault contact between metasediments and pluton, there is no direct proof that the igneous contact controls mineralization. The best ore is generally found in pyritic and graphitic shale near the intrusive contact, and along both the hanging wall and foot wall of the aplite dike. Primary ore consists of disseminations and fault and fracture fillings of pitchblende and coffinite with some chalcopyrite and bornite associated with quartz and fine-grained sericite. Apparently, redistributed mineralization as reflected by hexavalent U minerals, mainly autunite and less torbernite, occurs in cataclastic zones within quartz monzonite, quartzite, and shale.

Ore bodies are irregular to tabular in shape. The largest known ore body with grades in excess of 0.45% U is 38 m long, 6 m wide, and 3 m high, but uranium extends a further 6 m into each wall and at least another 15 m in length.

7.4 Beatty Volcanic Center, Nevada

Located in southern Nevada (►Fig. 1.1b), two U–Mo showings are reported from the Beatty volcanic center, Black Bonanza-Red Dog and Daisy.

Sources of Information. Ahern and Corn (1981), Garside (1973).

Geology and Mineralization

Repeated pulses of volcanism during the middle and late Tertiary generated the Beatty volcanic center and associated epithermal lithophile and precious metal mineralization similar to that in many other small, subeconomic, occurrences in the Basin and Range province.

At *Black Bonanza-Red Dog*, U–Mo mineralization is hosted in a silicified quartz-porphphyry dike and in adjacent silicified breccia; both host rocks are altered by widespread but incomplete argillization. At *Daisy*, U–Mo and precious metal mineralization accompanied by fluorite and calcite-clay gangue is linked to small plugs and dikes of quartz-feldspar porphyry.

7.5 Spor Mountain/Thomas Caldera, Utah

The Spor Mountain district lies about 140 km SW of Salt Lake City in central western Utah (►Fig. 1.1b). The district produced about 70,000 t of fluorspar prior to 1980 largely from pipes in Paleozoic dolomite, and contains beryllium deposits that rank among the largest of the world. Original uranium resources of the Spor Mountain area were estimated in the order of several hundred tonnes of U at a grade of about 0.06% U. Production prior to 1990 amounted to 165 t U (Chenoweth WC, personal communication).

Uranium is widespread at Spor Mountain, but uranium occurrences are commonly of subeconomic grade except in the *Yellow Chief* deposit. Discovered in 1954 and exploited by underground and open-pit methods, this volcanic-type deposit is in the Dell Valley separating Spor Mountain to the west from Topaz Mountain in the Thomas Range, to the east.

In addition, the Brush–Wellman Spor Mountain deposit, which is exploited primarily for its beryllium content (with estimated resources on the order of 25,000 t Be), also delivered uranium. The uranium was recovered as a by-product to beryllium from leach liquor at an annual rate of about 1–1.5 t U/year from 1982 to 1984 in the Delta mill of Brush–Wellmann.

Sources of Information. Bikun 1980; Bowyer 1963; Burt and Sheridan 1981, 1984; Finch 1967; Lindsey 1978, 1981; Ludwig et al. 1980; Sharp 1955; Shawe 1968, 1972; Staatz and Carr 1964; US AEC 1959.

Geology and Mineralization

Spor Mountain is underlain by Paleozoic carbonate sediments and some quartzite, which strike NE–SW and dip NW. This

sequence is cut by numerous faults and perpetrated by pipe-like breccia bodies containing uraniferous fluorite. Breccia bodies have developed associated with or adjacent to faults or intrusive breccia complexes. The *Thomas Mountain* consists of massive flows of light-grey rhyolite and associated volcanics of Tertiary age. *Dell Valley* between the two mountains is filled with Tertiary volcanic extrusives ranging from rhyodacite to rhyolite with interbedded sediments composed of detritus of volcanics and carbonatic sediments mixed with ash and tuff.

Volcanics erupted in four periods each separated by a hiatus and consist in ascending order of the following units and lithologies (Ludwig et al. 1980, Lindsey 1978, 1981, and Shawe 1972):

1. Drum Mountain Rhyodacite (42 Ma) and Mt. Laird Tuff (39 Ma): Lava and ash flows, breccia, and tuffs of rhyodacite to quartz latite composition; collapse of Thomas caldera; copper, gold, and manganese mineralization
2. Joy Tuff (38 Ma), Landside Breccia, and rhyolitic ash-flow of the Dell Tuff (32 Ma); collapse of Dugway Valley cauldron
3. Spor Mountain Formation (21 Ma): Beryllium Tuff Member overlain by flows and intruded by domes of the Porphyritic Rhyolite Member, all of alkaline character
4. Topaz Mountain Rhyolite (7–6 Ma): Flows and domes of alkali rhyolite, vitrophyre, and tuff.

Eruptions during the younger two episodes were associated with Basin- and Range-block faulting and accompanied by U, F, Be, and other lithophile metal mineralization (Cs, Li, Rb, Nb, Sn, Ta, W, etc.). Uranium and beryllium principally occur in the Beryllium Tuff Member of the Spor Mountain Formation, a topaz-bearing, high-silica, fluorine-rich, mildly alkaline rhyolitic rock.

Located in the Thomas caldera, the *Yellow Chief* mine exploited an ore body more than 100 m long, 30 m wide, about 3 m thick, and situated in a depth of about 25 m. Uranium in the form of hexavalent U minerals, such as autunite, beta-uranophane, carnotite, and uraniferous opal, was hosted in bentonitic and tuffaceous sandstone and conglomerate of probably lacustrine provenance within the Beryllium Tuff Member. U minerals occurred disseminated in loosely cemented sandstone, perhaps localized by clay, which coats quartz grains in permeable sand lenses interbedded between bentonitic and conglomeratic layers. Iron oxide staining is common. Constituents of the tuffaceous host sandstone include feldspar, smoky quartz, biotite, apatite, sphene, zircon, tourmaline, and montmorillonite.

Metallogenetic Aspects

Burt and Sheridan (1981) present a generalized hypothesis for U, Be, Li mineralization associated with fluorine-rich rhyolite and discuss the variety of processes and mechanisms leading to enrichments of lithophile elements including uranium during the magmatic evolution. For the ultimate ore formation such as found at the Yellow Chief deposit, Burt and Sheridan (1984) propose leaching by weathering and devitrification of uraniferous, fluorine-rich tuff related to topaz rhyolite to have been the

mechanism for economic uranium concentrations in underlying clastic sediments.

Ludwig et al. (1980) investigated U/Pb isotope systematics of uraniferous opals at Spor Mountain. Opals fill fractures commonly together with fluorite, calcite, quartz, and hexavalent U minerals. Veinlets are up to several centimeters wide and more than 20 m long and cut the Joy Tuff, the Spor Mountain Formation, and the Topaz Mountain Rhyolite. The authors established a geochronologic frame for formation of uranium and associated F and Be mineralizations. They interpret their data to represent that three discontinuous brief periods of opal growth are indicated at about 21, 16 to 13, and 9–8 Ma and present the following metallogenetic implications:

1. The oldest, 21 Ma old, uranium, beryllium, and fluorite generation is linked to volcanism and hydrothermal activity of the host Beryllium Tuff Member and the overlying porphyritic rhyolite member of the Spor Mountain Formation. The ore elements are considered as original constituents of rhyolite magma in which they were concentrated
2. The 13–16 Ma old opal group is confined to massive nodules and fracture fillings associated with beryllium deposits in the Beryllium Tuff Member. The dated time is thought to represent a minimum age of intense hydrothermal activity that has issued hydrotherms laterally into the porous and reactive tuff member. In response, rhyolitic tuff was altered to K feldspar and smectite (argillic and potassic alteration), and U, Be, and F minerals were deposited
3. The 9–8 Ma old opal generation is associated with weak mineralization. It occurs in young fracture fillings, which cut almost all volcanic units. It may reflect hot-spring activity after the last major rhyolite eruption or deposition by groundwater.

Lindsey (1981) interprets the U, Be, and F mineralization at Spor Mountain as originating from U-, Be-, and F-bearing fluids, which supposedly derived from the Beryllium Tuff Member magma. Where these fluids pervaded porous and transmissive dolomite-clast-rich tuff, which is interbedded with relatively impermeable layers, reaction with carbonate clasts caused incorporation of U in the lattice of fluorite and in opal nodules, and Be in bertrandite. The presence of hexavalent U minerals is believed to indicate interaction with groundwater that modified uranium distribution and deposited uranyl minerals.

7.6 Marysvale Volcanic Complex, Utah

The Marysvale uranium district is located some 260 km south of Salt Lake City and 6 km NNE of the town of Marysvale in west-central Utah (Fig. 1.1b). Deposits are of volcanic vein type and are preferentially concentrated in the *Central Mining Area* in the central part of the Marysvale volcanic field (Figs. 7.3 and 7.4a).

Uranium was discovered in 1949, and at least 14 veins have been mined since 1951. Production amounted to at least 540 t U by 1962 (Bromfield et al. 1982). Most of the uranium came from nine underground and open-pit mines (*Prospector*, *Freedom No. 1* and *No. 2*, *Bullion Monarch*, *Farmer John*, *Cloys*, *Potts*, *Wilhelm*,

and *Sunnyside*). The grade of ore was a few tenths of a percent uranium (Walker and Osterwald 1963).

More recent exploration in the Marysvale area has encountered significant thicknesses of low-grade mineralization (Havenstrite and Hardy 2006).

Sources of Information. Bromfield et al. 1982; Callaghan 1939, 1973; Callaghan and Parker 1961; Cunningham and Steven 1979a, b; Cunningham et al. 1982, 1994, 1998; Gilbert 1957; Gruner et al. 1951; Havenstrite and Hardy 2006; Kerr 1968; Kerr et al. 1957; Rasmussen et al. 1985; Rowley et al. 1988a, b, 1994; Shea 1982; Shea and Foland 1986; Steven and Morris 1987; Steven et al. 1978, 1979, 1981; Taylor et al. 1951; Walker et al. 1963; Walker and Osterwald 1956a, 1963a, b; Willard and Callaghan 1962.

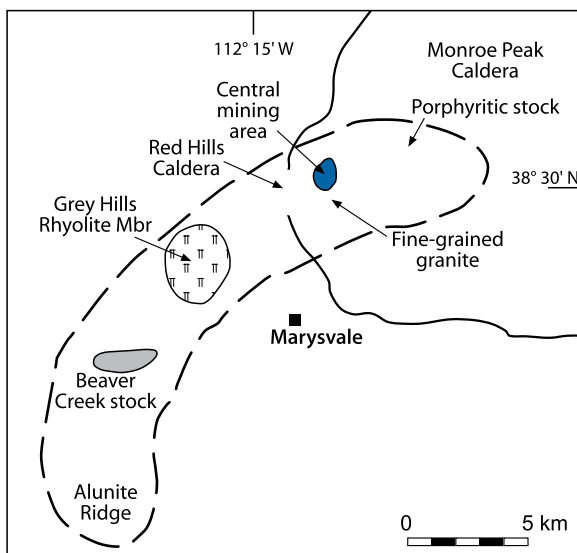
Cunningham et al. (1982, 1998) and Kerr (1968) published comprehensive studies of the Marysvale uranium district. The early publications by Walker and coworkers provide detailed descriptions of ore mineralogy and mineralization. These papers were used as the main base for the following description amended by data of the other authors mentioned above.

Geological Setting of Mineralization

The Marysvale volcanic field is located at the eastern margin of the Basin and Range province adjacent to the Colorado Plateau. The field consists of several calderas composed of Middle to Upper Tertiary volcanic rocks, which unconformably rest upon Mesozoic and Lower Tertiary sediments. The Central Mining Area lies at the western margin of the 23 Ma old Monroe Peak caldera, the largest caldera in the Marysvale volcanic field, and it overlaps with the small Red Hills caldera (► Fig. 7.3).

■ Fig. 7.3.

Marysvale, sketch map of the Marysvale volcanic field with location of the Central Mining Area. (After Cunningham et al. 1998)



According to Cunningham and his co-workers the Marysvale volcanic field includes the following lithologies (for distribution, see ► Figs. 7.3, 7.4a and b):

A 35–22 Ma old calc-alkaline sequence of intermediate-composition constitutes most volcanic rocks of the field. It includes as a late intrusion associated with the Monroe Peak caldera a quartz monzonite porphyry stock dated at 23 Ma (termed Central Intrusion or Central Intrusive). This intrusion underlies a large part of the Central Mining Area and contains anomalously high contents of uranium, thorium, and zirconium (Dunkhase 1980). Replacement alunite deposits underlain by pyrite-bearing, propylitized volcanics surround the stock.

Subsequently a suite of 22–14 Ma old alkali rhyolite and basalt lava flows and associated igneous rocks were extruded or intruded, respectively. Intrusions include 21 Ma old porphyritic stocks and volcanic domes as well as 20 Ma old hypabyssal, fine-grained granite. This granite was intruded into the Central Intrusion. It crops out north of the Central Mining Area and widens downward in deeper levels of the mining area.

Alkali rhyolite extrusions (Mount Belknap Volcanics) comprise a series of volcanic domes, lava flows, and ash-flow tuffs distributed in an elongate area ca. 25 km long and 5 km wide that extends from Alunite Ridge/Deer Trail Mountain northeastward into the Monroe Peak caldera. 19 Ma old volatile-rich, alkali rhyolite tuff (Red Hills Tuff Member of Mount Belknap Volcanics) was erupted in association with subsidence of the Red Hills caldera situated immediately west of the Central Mining Area. This tuff unit unconformably overlies the northeastern part of the Central Intrusion. Eighteen million years ago, volatile-rich alkali rhyolite lavas of the Gray Hills Rhyolite Member of the Mount Belknap Volcanics occur to the southwest of the Central Mining Area; and further to the southwest, the small Beaver Creek stock dated at 16 Ma.

Related to a hidden rhyolite stock below the Central Mining Area, brown, flow-banded, vitric rhyolite dikes dated at 18 Ma transect much of the aforementioned lithologies and associate with uranium veins. These glassy rhyolite dikes have the highest contents of Sr (675 ppm) and silica (76 wt.%) of any of the alkali rhyolites that were emplaced from 23 to 18 Ma. A vertical pipe of breccia composed of rounded to subangular fragments of the Central Intrusion in a matrix of comminuted rock and glassy rhyolite is exposed underground between the Sugar Daddy decline and the Prospector mine.

The Central Mining Area is dominated by Basin and Range tectonism reflected by post-ore NE-SW and NW-SE-trending regional faults; and Osterwald (1965) notes that the Central Mining Area is situated where these faults change direction. Prior to this structural event and also prior to mineralization, the entire Central Mining Area experienced uplift associated with block faulting and intense fracturing. Most major ore veins are located in or adjoin blocks that have been uplifted the most (► Fig. 7.4b).

Alteration

Two prominent types of alteration are noted by Kerr (1968). The first and earlier is reflected by numerous veins and white

Fig. 7.4.

Marysville, (a) geological map and (b) and (c) sections across the Central Mining Area. The N-S cross-section in (b) approximately follows a >500 m long cross-cut that connects the 300 level of the Prospector mine on the south with the 700 level of the Freedom mines to the north. (After Cunningham et al. 1998)

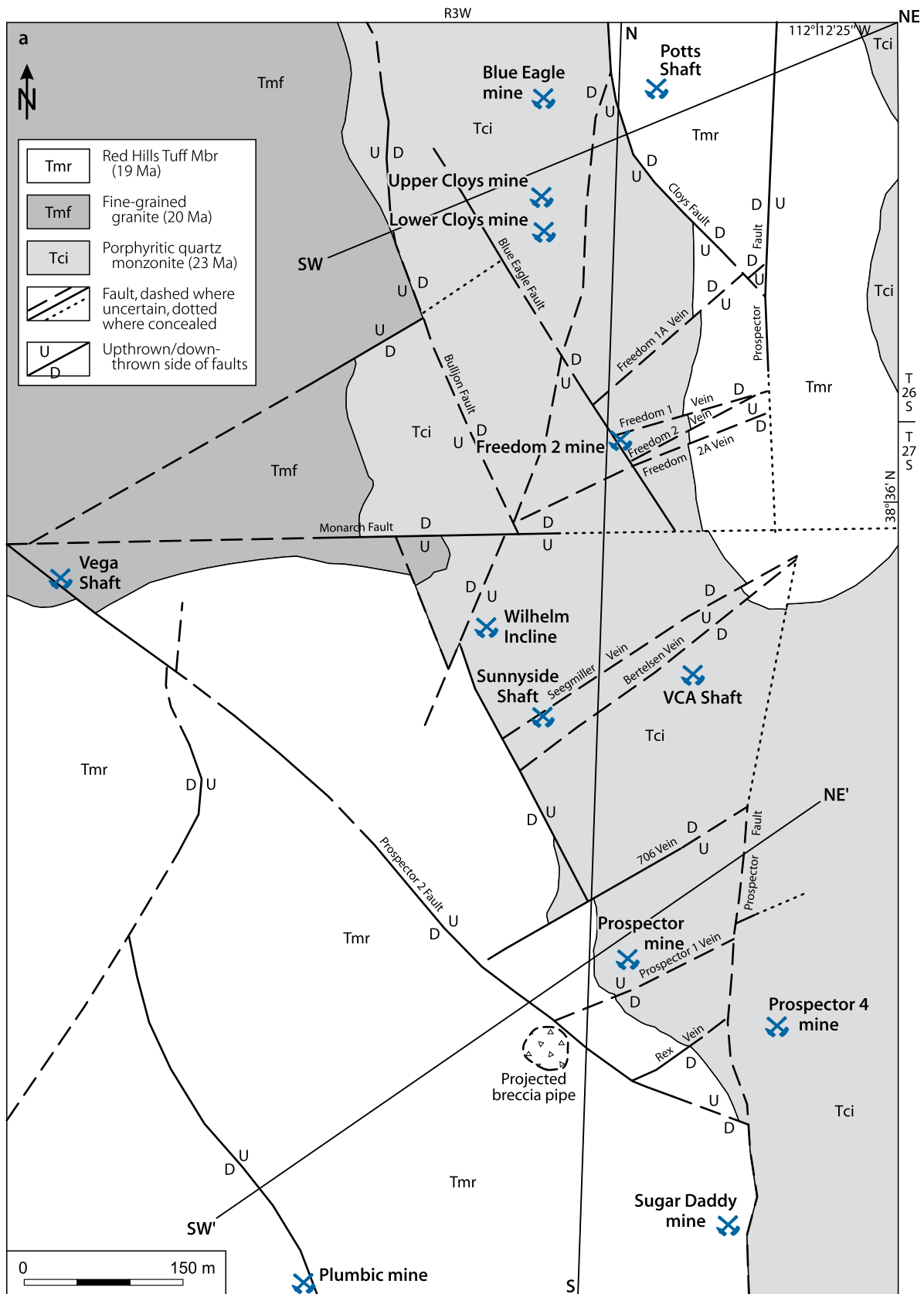
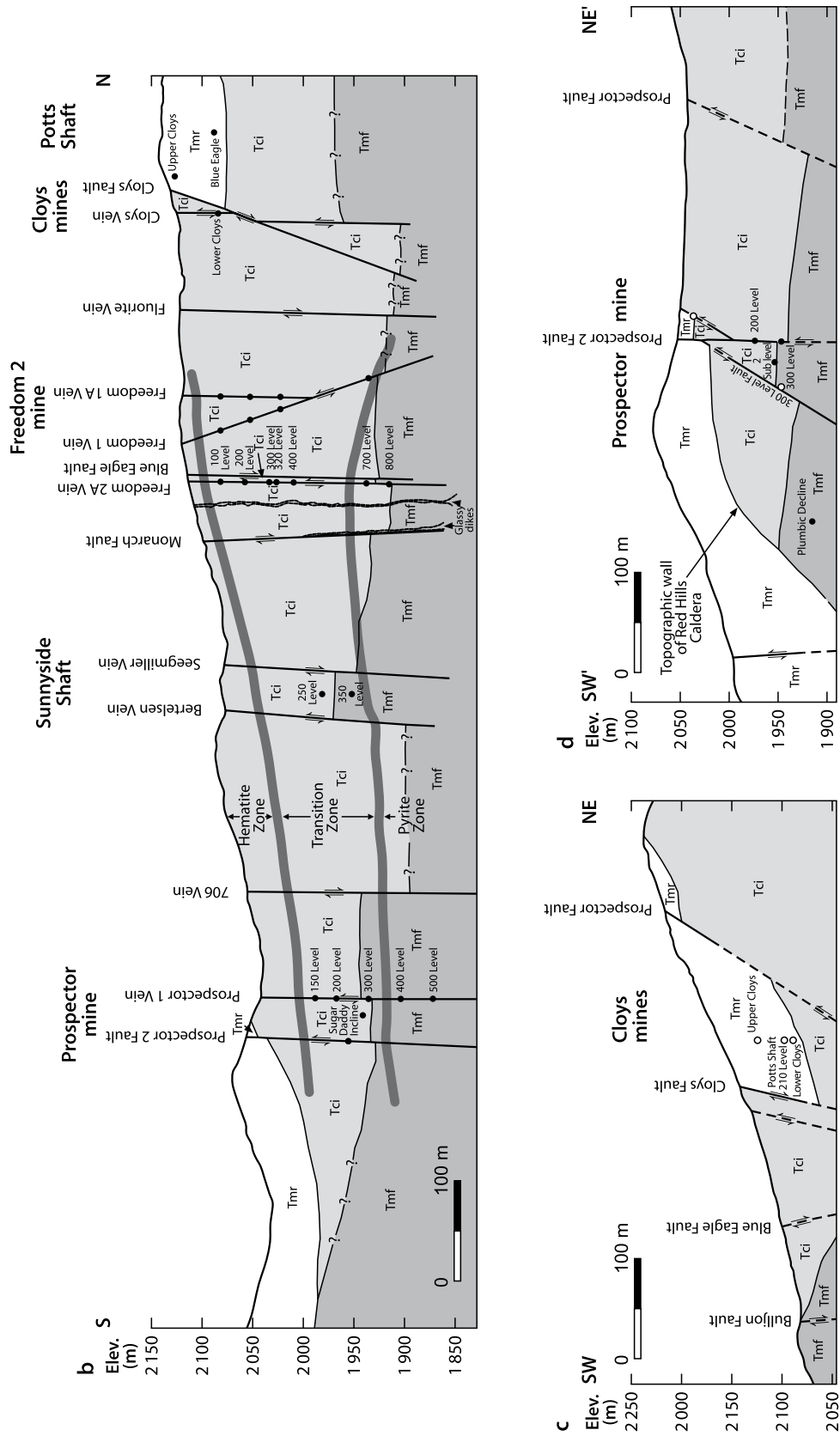


Fig. 7.4. (Continued)



replacement masses of alunite mainly in tuff units of the Bullion Canyon Volcanic Series. The later vein-associated generation is represented by vertically zoned wall rock alteration that apparently reflects lithology adjacent to veins. Sericitization and pyritization prevail at the deepest exposed mine levels, hematization is typical at higher levels, and kaolinitization near the surface. Later Cenozoic supergene processes resulted in hematite and gypsum formation.

Alteration halos adjacent to uranium veins range in width from several centimeters at depth to a few meters at the surface (El-Mahady 1966; Kerr 1968). For example, on the deepest accessible level of the Freedom 2A vein (Fig. 7.4b), feldspar of fine-grained granite is altered to sericite, and mafic minerals to pyrite in a layer about 5 cm wide on either side of the vein. In a transition zone at higher levels, the pyrite content decreases in vein walls, sericite is absent, and a few centimeter-wide envelope of hematitized, but much less altered, wall rock surrounds the veins. Near the present surface, above the hematite(-pyrite) transition zone, pyrite is virtually absent, wall rocks are altered to kaolinite, sooty pitchblende veins are associated with much more pervasively distributed hematite in wall rocks, and widths of alteration halos are on the order of 2 m. In geochemical profiles, hydration, SiO₂, and Al₂O₃ generally increase with approach to veins, and FeO, MgO, and CaO decrease in wall rocks (Cunningham et al. 1998).

Mineralization

Pitchblende is the principal U mineral below the groundwater table (ca. 30–40 m below surface) while sooty pitchblende and

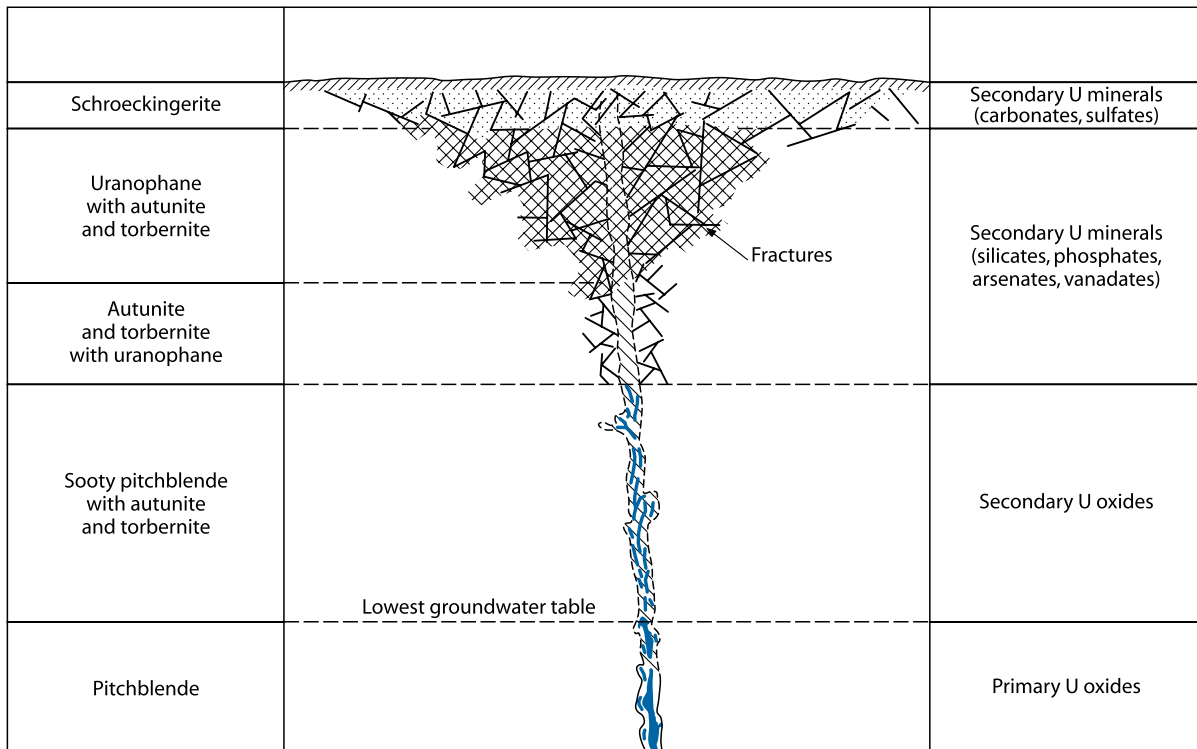
hexavalent U minerals prevail above the water table (Fig. 7.5). Some coffinite occurs at lower levels. U oxide phases include minute spherulites to aggregates of rounded pitchblende masses and finely crystalline uraninite. Unit cell dimensions of U oxide phases range from 5.38 to 5.45 Å (Kerr 1968).

Uranyl minerals include phosphates (autunite, meta-autunite, torbernite, metatorbernite, phosphuranylite), silicates (uranophane, β-uranophane), carbonates (schroekingierite), vanadates (rauvite, tyuyamunite), and sulfates (johannite, uranopilite, zippeite). They occur from the surface to depths of 30–40 m in broken ground above mineralized veins. Umohoite occurs just below the oxidized zone and may be supergene in origin. No U enrichment by supergene processes is apparent in the near-surface zone (Walker and Osterwald 1956; Kerr 1968).

Associated or spatially related minerals as given in a paragenetic scheme by Walker and Adams (1963) include quartz and chalcedony, pyrite, fluorite, and adularia in a first stage. After a period of brecciation, a second stage followed by continued deposition of these minerals along with marcasite, pitchblende, magnetite, hematite, jordisite, and carbonate. In a third stage, jordisite and carbonate continued to be formed. A late, supergene stage generated carbonate along with gypsum and iron and manganese oxides. Base-metal sulfide minerals are essentially absent.

Fluorite is abundant. Molybdenum is widely present in the deposits and is locally as abundant as uranium. Vein quartz tends to prevail on deeper levels. Fluorite occurs in clear, purple, and green colors. Clear fluorite has purple growth bands. Massive purple fluorite ranges from light to dark, almost black tones. Green fluorite tends to prevail on higher levels and is generally

Fig. 7.5. Marysvale, schematic section illustrating the zonal distribution of secondary and primary U minerals in an ore vein. (After Stugard jr. et al. 1952)



younger than purple fluorite, but not necessarily. Fluorite is locally intergrown with fine-grained quartz.

Most pitchblende/uraninite is intimately associated with pyrite, banded purple to black fluorite, jordisite, and coffinite at depth. Jordisite, fluorite, and pyrite increase with depth, whereas uranium decreases. Ore minerals occur together with quartz in veinlets, interstitial in vein breccia, and rare masses. Veinlets exhibit alternate bands of purple crystalline fluorite and purplish-black bands of mixtures of fine-grained fluorite, pyrite, and pitchblende. Some fluorite veins lack U or other ore minerals.

Pyrite is a typical ore constituent at depth, where it constitutes up to an estimated 15% of vein material on the deepest mine levels (El-Mahady 1966). Pyrite gradually diminishes upward and instead hematite develops first in vein selvages in the transition zone and then above in a more pervasive manner.

Semiquantitative chemical analyses of vein ore samples by Cunningham et al. (1998) show that ore contains as much as 3,000 ppm As, 50 ppm Co, 500 ppm Sb, 1,500 ppm Tl, traces of W, and highly variable Th. Tungsten is locally present as scheelite. According to analyses by Walker and Adams (1963), the ore may also contain Au, Ag, Cu, Pb, and Y.

U-bearing fluorite and quartz veins are spatially and genetically related to 19–18 Ma old vitric rhyolite dikes (Cunningham et al. 1982). These dikes together with ore veins are hosted in 23 Ma old quartz monzonite, 20 Ma old granite, and 19 old Ma rhyolite ash-flow tuff (Red Hills Tuff), and they are themselves transected by structures of the Basin and Range fault system.

Shape and Dimensions of Deposits

Mined uranium veins of the Central Mining Area are located in an oval area about 1 by 0.5 km in size in which the distribution of veins corresponds to the distribution of individual uplifted blocks. Uranium-bearing veins are exposed over a 300 m vertical range in the mines, but drill hole data document a vertical persistence of uranium mineralization although apparently of low grade to at least 600 m (Taylor et al. 1951).

The main uranium veins dip almost vertically and trend generally NE to ENE, but local variations are fairly common (Fig. 7.4a). They may consist of simple veins or a network of anastomosing veinlets. Ore-bearing portions of veins range from less than 30 m to over 450 m in length, and average 1.2–1.5 m in width and up to 6 m at vein intersections. Veinlets are as much as 0.5 m wide (*Freedom 2A vein*, 800 level). Ore shoots rise more or less vertically. In *Freedom 2 veins*, which cut quartz monzonite, ore was mined over a vertical interval of 225 m. Where veins are truncated by overlying rhyolite, both ore grade and width may be enlarged.

Brecciated vein intervals are frequent; they contain interstitial uranium impregnations. In rare instances, ore concentrates to masses 0.3 m across. Some of the richest ore was found in steeply plunging shoots at fault intersections and in intervals between a branch vein and an adjacent vein.

Uranium-bearing vein sections are mainly hosted in quartz monzonite and fine-grained granite. In general, uranium grades are somewhat higher in the former than in the latter. Some ore

bodies also occur entirely in rhyolite, but in the vicinity of quartz monzonite as in the *Cloys-Potts area*. Veins in this area contain ore bodies 3–15 m wide. (Kerr 1968; Kerr et al. 1957; Callaghan 1973).

A different mode of vein, which appears to be most abundant on upper levels, is represented by flat-lying, commonly concave downward fissure fillings (e.g., on *Prospector 200 level*). These veins tend to terminate against near-vertical faults (Cunningham et al. 1998).

Stable Isotopes and Fluid Inclusions

In general, fluid inclusions in vein quartz are hotter and more saline while fluid inclusions in fluorite are cooler and the least saline in Marysvale veins as documented by Cunningham et al. (1998). Fluid inclusions in quartz give homogenization temperatures of 190–260°C with a median temperature of 210–220°C. Fluid inclusions in green and purple fluorite yield median homogenization temperatures of 190–200°C, and in clear fluorite 170–180°C, i.e., they are slightly lower than in quartz. Fluid inclusion temperatures in minerals from deeper levels are hotter than those from near the present surface as indicated by samples from the *Freedom mine*, where, at the 800 level, most homogenization temperatures of inclusions in quartz and fluorite are in the 200–240°C range (ranges in quartz: 230–260°C, in fluorite: 190–220°C). Fluorite samples from the *Freedom 1* upper level yield temperatures generally in the range of 170–200°C. Near-surface samples also contain coexisting vapor and liquid-rich inclusions in fluorite, which indicates boiling at these uppermost levels. The median salinity is 0.0–0.5 wt.% NaCl equivalent for fluid inclusions in quartz and green and clear fluorite, and it is slightly higher, 0.5–1.0 wt.% NaCl equivalent, in purple fluorite.

Oxygen isotope studies by Cunningham et al. (1998) and Shea and Foland (1986) show a systematic tendency from depth to surface to heavier $\delta^{18}\text{O}$ values for wall rocks adjacent to veins. Whole rock $\delta^{18}\text{O}$ values change from 0.2‰ at depth to 4.7‰ at the surface and feldspar $\delta^{18}\text{O}$ values change from –3.7‰ at depth to 7.4‰ at the surface. For comparison, whole rock samples outside the mining area give $\delta^{18}\text{O}$ values from 0.2 to 4.0‰ and for feldspar phenocrysts from –3.7 to 6.0‰.

Hydrothermal solutions were dominantly of meteoric origin, but probably contained magmatic components. This is indicated by δD values of –140 to –130‰ for fluid inclusions in fluorite from uranium veins as compared to δD values of magmatic fluids, which averaged probably close to –70‰ in the Marysvale area (Beaty et al. 1986).

The $\delta^{34}\text{S}$ values in pyrite range over a large spread from –5.0 to 6.6 and suggest a variety of sulfur sources for the hydrothermal system.

Based on fluid inclusion data from samples of the *Freedom 1 vein*, Cunningham et al. (1998) calculated an estimated upper depth limit of vein formation within 115 m of the paleosurface. Arguments in support of this conclusion are as follows. A model based on a lithostatic gradient of 2.7 g/cm³ gives a depth of about 53 m for the *Freedom 1* upper level or about 23 m having been eroded. At these shallow depths, fluid pressures would be

expected to be generally hydrostatic and only increase toward lithostatic during episodes of deposition of quartz and fluorite in vein structures. About 195°C is the highest temperature at which most fluid inclusions in fluorite from the upper level homogenize to liquid. These inclusions contain about 0.8–1.4 wt.% eq. NaCl and are associated with sporadic vapor-rich inclusions, which suggests sporadic boiling of the solution near the surface. The depth below the water table at hydrostatic pressures and boiling conditions was some 145 m with a pressure of about 14 bar, which equates to about 115 m of rocks having been eroded from the original cover. Cunningham et al. (1998) consider this depth of 115 m as reasonable, for the deposit is adjacent to the Red Hills caldera that formed slightly before the deposit and the Red Hills Tuff on the caldera rim would have been thicker than it is at present.

Geochronology

Cunningham et al. (1982, 1998) report the following apparent ages for ore, gangue, and alteration minerals. Age data of country rocks were already given earlier in the chapter Geological Setting of Mineralization.

Uranium ore: 19–18 Ma

Whole-rock pitchblende+fluorite vein samples: 19.0 ± 3.7 Ma ($^{207}\text{Pb}/^{204}\text{Pb}$ - $^{235}\text{U}/^{204}\text{Pb}$ isochron age)

Vein quartz adjacent to pitchblende: 16.5 ± 4.3 Ma (fission track)

Sericite from wall rock adjacent to Freedom 2A vein/900 level: 20.5 ± 0.7 Ma (K–Ar).

Cunningham et al. (1998) also report ages of 14 Ma for gold, silver, base-metal mantos at Deer Trail Mountain (~15 km SW of the Central Mining Area) and alunite deposits at Alunite Ridge at the southwestern end of the Marysvale volcanic field.

Sources of Uranium

As shown in (▶ Table 7.2), the major lithologies in the Marysvale uranium field are apparently all anomalously enriched in uranium and may have constituted potential uranium sources in case the uranium is thought to have been liberated and collected by any kind of circulating fluids, meteoric and/or hypogene or a mixture of both, capable of leaching uranium.

Ore Controls and Recognition Criteria

Marysvale uranium-bearing fluorite and quartz veins represent volcanic-type uranium deposits. Apparent ore controls and/or recognition criteria include:

Host environment

- Tertiary volcanogenic complex composed of several calderas
- Extrusive rocks include alkali rhyolite tuffs and flows, and basalt lava flows
- Intrusive facies include granite, quartz monzonite porphyry, and rhyolite stocks as well as domes

- Vitric rhyolite dikes related to a rhyolite stock hidden below the Central Mining Area
- Anomalously high contents of U, Th, and Zr in quartz monzonite porphyry and other felsic facies
- Structural environment characterized by pre-ore and post-ore tectonism
- Pre-ore block faulting and intense fracturing related to uplift of the Central Mining Area
- Post-ore NE–SW- and NW–SE-trending regional faults related to Basin and Range tectonism.

Alteration

- Two prominent types of alteration exist:
 - Early widespread alunitization reflected by veins and replacement masses mainly in tuff
 - Later ore-related alteration in narrow aureoles adjacent to veins
- Ore-related wall rock alteration is vertically zoned reflected by
 - Sericitization and pyritization on deepest levels
 - Hematitization and kaolinitization at higher levels
- Near-surface supergene alteration overprinted the former by hematitization and gypsum formation.

Mineralization

- U minerals include pitchblende, uraninite, and coffinite below the water table
- Sooty pitchblende and hexavalent U minerals prevail above the water table
- Uraninite and coffinite as well as vein quartz tend to prevail on deeper levels
- Associated minerals may include jordisite, pyrite, marcasite, magnetite, hematite, quartz, chalcedony, fluorite, carbonate, and adularia
- Associated elements may include Ag, As, Au, Co, Cu, Pb, Sb, Th, Tl, W, and Y
- Fluorite is abundant and occurs on all levels in various colors
- Molybdenum is locally as abundant as uranium
- Veinlets exhibit banding of fluorite, pyrite, and pitchblende
- Some fluorite veins lack U or other ore minerals
- Ore occurs in simple veins or networks of anastomosing veinlets
- Veins trend generally NE to ENE and dip almost vertical
- Upper levels also contain flat-lying veins or veinlets
- Mined ore grades persist to depths of ca. 300 m and low-grade mineralization to at least 600 m
- Richest ore is in steeply plunging shoots at fault intersections and in intervals between a branch vein and adjacent vein
- U-bearing fluorite and quartz veins are located
 - In a relatively small area underlain by a hidden rhyolite stock that was intruded into a variety of igneous rocks
 - In structures within or adjoining blocks
 - Spatially close to vitric rhyolite dikes, which are descendants of the rhyolite stock

■ **Table 7.2.**

Marysvale district, contents of U, Th, F, and Sr in igneous rocks (in ppm). (After Cunningham et al. 1998)

Rock type (no. of samples)	U	Th	F	Sr
Quartz monzonite (Tci)				
• ±Fresh (1) ^a	15.1	69.7	0.15	
• ±Fresh w. hematite (1) ^b	194.0	47.0	0.17	
• Altered (6) ^c	15.3–85.2	19.0–63.5	0.12–0.21	
Fine-grained granite (Tmf)				
• Fresh (1) ^d	10.1	40.6	0.08	
• Altered (1) ^e	42.1	74.7	0.45	
• Altered (1) ^f	46.9	57.9	0.19	
Mount Belknap Volcanics	10.1–18.2		0.07–0.14	
Porphyritic alkali rhyolite dome (1)	15.2	37.2	0.07	288.00
Red Hills Tuff Mbr (Tmr) (1)	12.7	41.5	0.13	100.00
Vitric rhyolite dike (1) ^g	13.8	42.6	0.11	675.00

^a Relatively fresh rock cut by 1-cm wide U vein bordered by 1-cm wide hematite band

^b As before but within hematite band

^c 10–183 cm from Seegmiller vein

^d From northern end of Marysvale U district

^{e,f} Near Freedom 2a vein/900 level

^e 5 cm from vein, bleached and altered

^f 5–10 cm from vein fresher than ^e

^g Vertical dike cutting quartz monzonite between Freedom and Prospector mines;

Tci, Tmf, and Tmr are indices shown in [Fig. 7.4a](#) and [b](#)

- Preferentially in quartz monzonite and fine-grained granite
- Locally in rhyolite, but in proximity to quartz monzonite.

Metallogenic Aspects

Uranium veins in the Central Mining Area were emplaced by hydrothermal solutions in a distinct structural environment within a volcanogenic complex dominated by felsic intrusive and extrusive rocks. According to Cunningham et al. (1998), uranium-mineralized quartz and fluorite veins were generated about 18 Ma ago by a shallow hydrothermal system as part of a volcanic complex. Epithermal veins formed in a 1 km² area, above a cupola of a composite, recurrent, magma chamber at least 24 by 5 km in size that produced a sequence of 21–14 Ma old hypabyssal granitic and rhyolitic stocks, volcanic domes, rhyolite lava flows, and ash-flow tuffs.

Emplacement of uranium veins was related to intrusion of a rhyolite stock some 18 Ma ago into a cluster of older igneous stocks. The rhyolite stock caused differential uplift and generated roof blocks bounded by high-angle faults. Molybdenite-bearing, uranium-rich, vitric rhyolite dikes or apophyses related to this stock occupied these faults that offset the contact between the

Central Intrusion and 20 Ma old fine-grained granite. When the magmatic pressure was relieved by diatremes, the uplifted blocks began to settle back, and flat-lying, concave-downward, fractures formed locally by differential downward movement, particularly near high-angle faults.

In an early alteration stage, reflected by alunitization, low ¹⁸O meteoric water altered the rocks prior to mineralization and probably right after intrusion of the 20 Ma old granite. Subsequently, hydrothermal fluids activated by intrusion of the 18 Ma old rhyolite stock invaded the fractured edifice and formed uranium-bearing quartz and fluorite veins in high-angle and flat-lying faults. These veins are spatially and assumably genetically related to the above mentioned vitric rhyolite dikes. Fluid inclusion and stable isotope data indicate that the veins were deposited above the concealed rhyolite stock at shallow depth. The upper limit was at 23–115 m below the paleosurface, in a depth interval near the fluctuating interface between exchanged meteoric water and overlying steam-heated groundwater.

Ore-forming fluids consisted dominantly of meteoric water, but probably also had magmatic components. These hydrothermal solutions underwent physico-chemical changes on their upward way as attested by thermochemical data, vertical zoning of wall rock alteration, and mineral assemblages in the ore.

On the deepest mine levels, sericitization of wall rocks and the mineral assemblage in veins (uraninite/pitchblende, coffinite, jordisite, fluorite, molybdenite, quartz, and pyrite) combined with a lack of hematite suggest that H_2S was the dominant sulfur species, that oxygen fugacity was low, and that the pH value of the fluids was near neutral. Quartz and coffinite in these deep ores indicate a hydrothermal system saturated with silica. Uranium was probably present as a uranium–fluorine complex such as uranyl trifluoride as may be deduced from the general co-existence of fluorite and uraninite/pitchblende in the ore.

These data and thermochemical constraints indicate that the original deep fluids contained U, Mo, F, K, and H_2S and had an isotopic pattern of ca. $-1.5 \delta^{18}O_{H_2O}$, ca. $-130 \delta^{18}D_{H_2O}$, and a log fO_2 of about -47 to -50 . The pH value was about 6–7, the salinity at least 3%, and the temperature ranged from about $240 \pm 20^\circ C$ at depth to $190^\circ C$ over the 300 m vertical interval of mine workings.

Uranium minerals precipitated by reaction of these fluids with the wall rocks, perhaps on the deepest levels in association with sulfidation of mafic minerals. Liberated fluorine would be deposited as fluorite in response to calcium release by alteration of plagioclase.

On their ascension, fluids became progressively oxygenated and cooled due to boiling and degassing. As a result of changes in oxidation state and pH of these fluids in the upper vein system, pyrite plus sericite in the wall rocks gave way to hematite, which formed hematite selvages and kaolinization of wall rocks, and quartz, fluorite, minor siderite, and pitchblende were deposited in veins.

Near the surface, emanating volatiles probably condensed in overlying steam-heated groundwater and fluids became more acid and, in consequence, kaolinite strongly altered the wall rocks, pervasive hematite formed, and quartz, fluorite, and pitchblende precipitated in veins.

When the upper part of the mineralized system became exposed by erosion in a later phase, supergene alteration led to the formation of hexavalent U minerals, gypsum, and some of the shallow hematite alteration.

7.7 Date Creek Basin, Arizona

The northeastern Date Creek Basin contains U mineralization of tabular configuration hosted by carbonaceous lacustrine (\pm lutite) sediments with felsic pyroclastic components. Located approximately 70 km NW of Wickenburg in central-western Arizona, the Anderson deposit, commonly referred to as Anderson Mine, is a typical example (Fig. 1.1b). Otton J (2005, personal communication) defines this deposit as carbonaceous lacustrine uranium type.

Discovered in 1951, early mining by an open-pit and underground operation produced 12 t U at a grade of 0.12 U and 0.05% V_2O_5 . Resumed exploration during the 1970s found new resources of at least 12,000 t U at grades averaging 0.06% U. Additional resources, commonly of lower grade, are reported from other properties in the Date Creek Basin.

Sources of Information. Mueller and Halbach 1983; Otton 1977a, b; Priesemann 1977; Reyner et al. 1956; Sharp and Hetland 1954; Scarborough 1981; Sherborne et al. 1979; and Otton J 2005, personal communication. Otton (1977a, b) and Sherborne et al. (1979) described the Anderson deposit comprehensively while Mueller and Halbach (1983) investigated properties adjacent to the Anderson Mine area.

Geological Setting of Mineralization

The northeastern Date Creek Basin is underlain by a basement of dominantly Precambrian gneissic and granitic rocks upon which a 1,100 m thick sequence of Tertiary lacustrine sediments and volcanics rest unconformably. Pliocene to Holocene alluvium covers this sequence. Block faulting along steeply dipping NW–SE-trending faults in late Miocene to early Pliocene time caused moderate SW tilting of the Cenozoic strata (Fig. 7.6).

In the Anderson Mine area, Tertiary sediments thicken gradually south- and westward and thin north- and eastward where they onlap the Arrastra paleohigh. The Tertiary sequence is divided into (in descending order):

Pliocene to mid-Miocene basalts and coarse-clastic sediments, 0–30 m thick [10–9 Ma old basalt flows are undeformed; 13–12 Ma old Cobwebb(?) basalt is faulted].

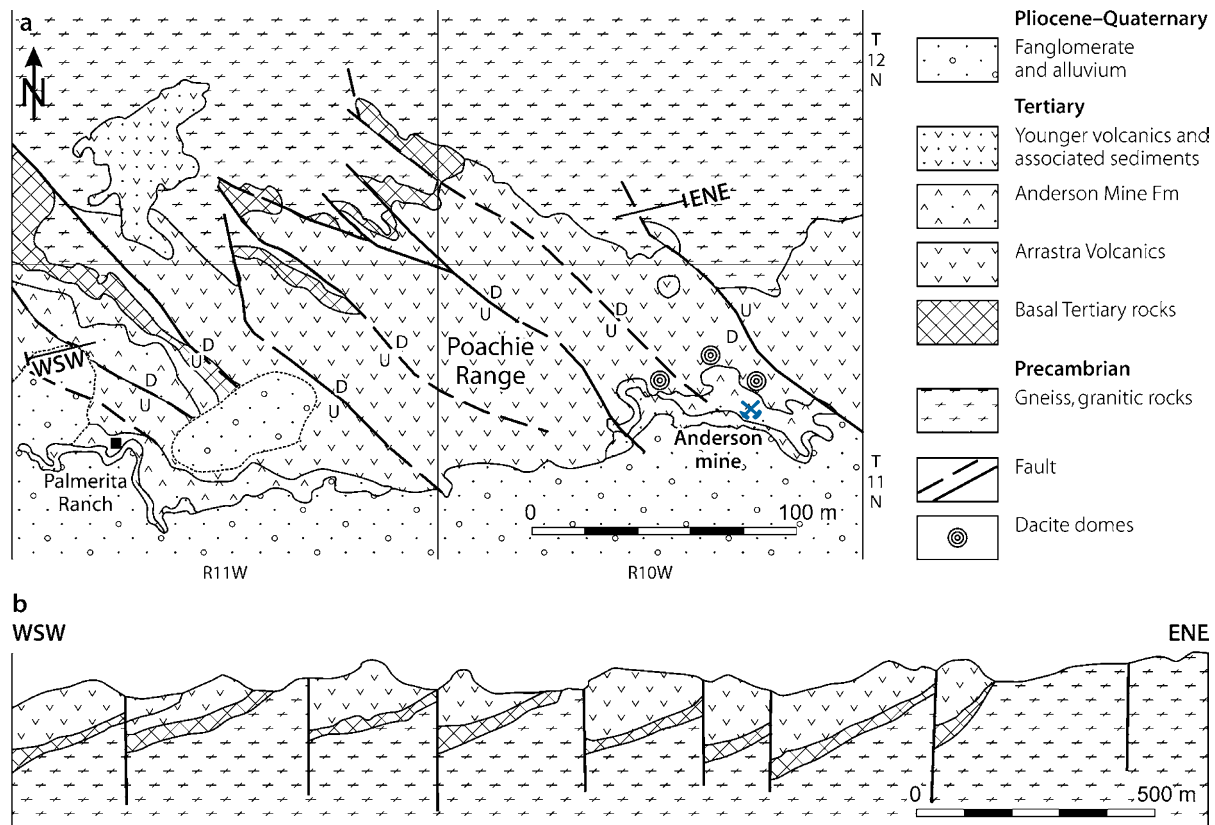
>Unconformity<

Early to Middle Miocene Chapin Wash Formation or stratigraphic equivalent, divided into Flat Top and Anderson Mine members:

- **Flat Top Member**, <170 m in thickness: Arkosic siltstone, sandstone, and conglomerate interbedded with minor bentonitic/tuffaceous siltstone.
>Unconformity<
- **Upper Anderson Mine Member**, 80–150 m thick in the mine, 300 m thick about 2.5 km further south: Predominantly tuffaceous, in part paludal, lacustrine sediments in the northern part of the Date Creek Basin (Anderson Mine area) grading into sandy deltaic sediments about 2.5 km south of the mine. The Anderson Mine Member includes:
 - Upper tuff and carbonate unit, <80 m thick: Greenish-grey, thick-bedded tuffaceous mudstone, reworked vitric tuff, fossiliferous marlstone, and limestone. Tuffaceous mudstone beds constitute much of this unit. Marlstone and limestone prevail in the eastern and southern mine area
 - Upper carbonaceous unit, about 20 m thick in the mine, 35 m further south: Greenish-grey bentonitic/tuffaceous mud- and siltstones interbedded with subordinate carbonaceous mudstone, tan marlstone, dolomitic limestone, tuff, lignite seams, and locally at the base up to 6 m thick limestone. Tan tuffaceous, gastropod-rich marlstone constitutes about one third of this carbonaceous unit (and of the lower carbonaceous unit as well)
 - Intermediate clastic unit, about 12 m thick: Tuffaceous siltstone and arkosic sandstone, greenish-grey to tan, southward of the mine interstratified with yellow-grey to

■ Fig. 7.6.

Northeastern Date Creek Basin, (a) generalized geological map with location of the Anderson mine; (b) WSW–ESE section indicating the marked block-faulting in this part of the basin. (After Sherborne et al. 1979; AAPG 1979, reprinted by permission of the AAPG whose permission is required for further use)



brown conglomeratic sandstone and green mudstone (interpreted as distal facies of a large alluvial fan-braided river system located west of the Anderson Mine and intertonguing with lacustrine sediments)

- Lower carbonaceous unit, about 25 m thick in the mine, 35 m further south: Lithologically very similar to the upper carbonaceous unit
- **Lower Anderson Mine Member** (or clastic unit), 0–120 m thick: Reddish to yellowish grey, coarse, poorly sorted arkosic and volcanic sandstone-conglomerate, reworked andesite lapilli with brick-red clay matrix, bentonitic siltstone (distal part of a south- and westward thickening subaerial fanglomerate, pinching out north of the Anderson Mine).

>Unconformity (>120 m relief)<

Oligocene(?) to Eocene(?) Arrastra Volcanics, more than 450 m thick: Basalt, andesite, andesitic tuff, interstratified conglomerate.

Eocene(?) Artillery Formation or stratigraphic equivalent, up to 100 m thick: Reddish clastic sediments with ignimbrite and andesitic agglomerate.

Host Rock Alteration

Alteration phenomena related to diagenesis and ore-related processes include argillization, carbonatization, silicification,

zeolitization, and pyritization, all of which affected, in varying intensity, the entire uranium-hosting Anderson Mine Member. Some alteration processes occurred in multiple phases.

Argillization and zeolitization of rhyolitic ash created light greenish-grey bentonitic clays, particularly smectite, illite, hectorite, and other mixed-layer clay minerals throughout the upper part of the Anderson Mine Member. Some clays are significantly enriched in lithium (up to 0.4%). Zeolites include heulandite–clinoptilolite. Argillization and zeolitization occurred early during diagenesis, but appear to postdate the initial stages of silicification and carbonatization.

Carbonatization of diagenetic origin generated magnesian calcite, which replaced feldspars and carbonaceous to tuffaceous mudstones. It also cements arkosic sandstone in the southern part of the area.

Silicification is common in almost all units except the Lower Anderson Mine Member. Some strata, including most carbonaceous beds, are partially to completely silicified. An early phase produced multicolored chalcedony and tends to be associated with disseminated uranium in carbonaceous plant material. A later phase, active after Miocene faulting to probably Recent time, deposited jasper-like chalcedony and opal in voids and fractures. Opaline silica replaced carbonate-clay matrix in sediments and locally includes uranyl silica complexes and colloform coffinite. Carnotite mineralization apparently formed contemporaneously with this silica phase.

Pyritization is reflected by two modes. Fracture-filling pyrite is considered to be of diagenetic origin, whereas an older generation of finely disseminated pyrite crystals is thought to be more likely a syngenetic product.

Mineralization

Uranium mineralization is hosted by lacustrine, locally paludal sediments with tuffaceous components within both the upper and lower carbonaceous units of the Anderson Mine Member. Uranium-hosting strata have a general although variable enrichment in B, Cu, F, Li, Mo, Ni, U, and V. Otton (1977) and Sherborne et al. (1979) recognized two kinds of ores, unoxidized and oxidized.

Unoxidized ore: The principal U mineral is colloform coffinite with highly variable uranium–silica ratios and a content of 4–20% U. It is generally associated with carbonaceous matter with which it shows a linear correlation coefficient. Pitchblende is rare. Most mineralization is in thin-bedded, pyritic, carbonaceous mudstone and siltstone, lignitic mudstone, and bioturbated marlstone that exhibit only minor silicification. Ore minerals occur either as fine disseminations in the matrix of the host rocks or as discontinuous microveinlets or patches. Highest concentrations of up to 2% U are found in individual seams of lignitic coal and as halos around root remains, often associated with frambooidal pyrite. Sherborne et al. (1979) note that uranium and organic carbon show a linear correlation coefficient of 0.55 and that the texture of the uranium–carbon complex is similar to Ambrosia Lake ore, indicating that the organic matter is probably humate. Only very little uranium is associated with organic material that still retains a cell structure. Elements enriched to various degrees in carbonaceous uranium ore include primarily As, Mo, S, V, and in lesser amounts Ag, B, Cu, Ga, Ge, Mn, and Ti. Some of these elements correlate reasonably well with uranium, others more with carbon (Sherborne et al. 1979; Scarborough 1981).

Oxidized ore: Very fine-grained carnotite is present as cement, thin coatings of and coarse-fibrous fillings in fractures, and along bedding planes, or with hematite in jasper pods. Uraniferous silica occurs in the form of massive jasper and in small silica veinlets. Oxidized mineralization is confined to fractured, highly silicified, oxidized, light colored mudstone, tuff, limestone, and marlstone with abundant megascopic plant debris.

Shape and Dimensions of Deposits

Extensive low-grade U accumulations (<100–200 ppm U) occur peneconcordant with bedding within the two carbonaceous units of the Upper Anderson Mine Member. These low-grade zones encompass irregularly shaped higher grade zones of 0.1–0.3% U mainly in the upper unit. The mineralized area covers at least 5 km²; it is limited to the north and east by pinch out of the two carbonaceous units, on the south by a complex of

predominantly sandy delta sediments elongated in an E–W direction, and on the west by an alluvial fan-braided river system intertonguing with the lacustrine sediments (Mueller and Halbach 1983).

The drilled out *Anderson Mine area* covers a minimum of 1,000 by 1,500 m and consists of peneconcordant, blanket-type U mineralization (Fig. 7.7a and b). Mineralized beds average individually 1–3 m in thickness, but the beds may accumulate in highly mineralized zones to a cumulative thickness exceeding 15 m. These beds are hosted by both the upper and the lower carbonaceous units of the Anderson Mine Member, 20–25 m thick each at the Anderson Mine but thicken to about 35 m further south. Drilled reserves amount to about 5,000 t U at grades ranging from 0.03 to 0.12% U averaging about 0.06% U. Less than half of these reserves consists of higher grade material averaging 0.1% U at a cutoff grade of 0.06% U (Sherborne et al. 1979).

Sources of Uranium

Scarborough (1981) and Otton (1977a) note several potential sources for U mineralization in the Date Creek Basin: (a) Miocene alkalic volcanic flows, tuffs, and ashes, specifically high-potassic facies of which contain 10–20 ppm U; (b) Jurassic alkalic volcanics located further south in south-central Arizona, which contain uranium occurrences, e.g., in Santa Cruz County; and (c) Precambrian uraniumiferous granites in the nearby Artillery Peak region, which were presumably exposed and subject to erosion during Miocene time.

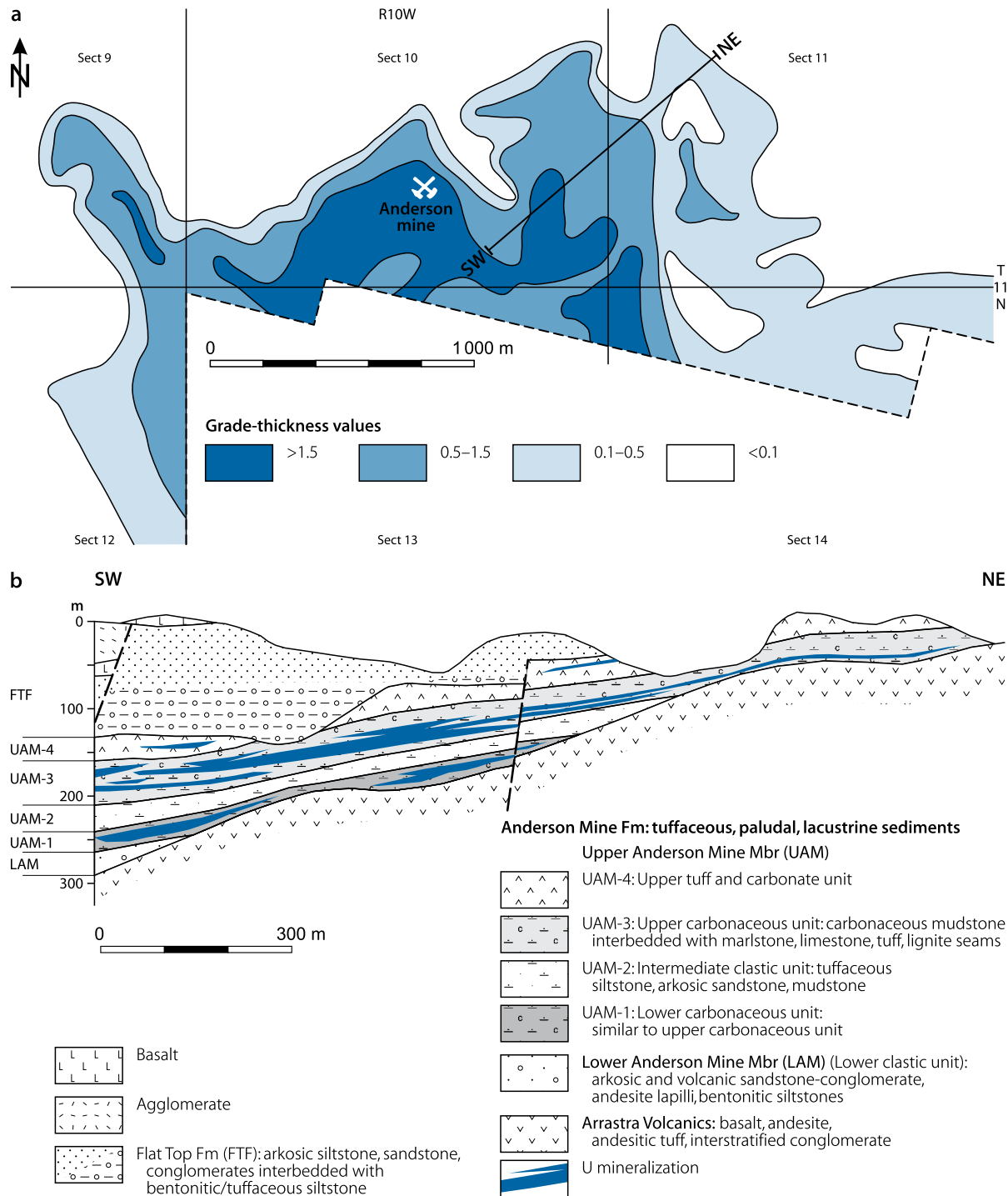
Ore Controls and Recognition Criteria

Sherborne et al. (1979) list the following ore controls or recognition criteria of the mineralization and its geologic setting at the Anderson Mine:

- Emplacement in fine-grained sediments deposited in shallow lacustrine environments
- Close spatial relation between carbonaceous beds and uranium mineralization
- Well-mineralized zones coincide with the greatest thickness of carbonaceous matter accumulation (indicating the importance of a paludal environment in localizing uranium)
- Extensive diagenetic alteration of sediments
- High uranium background (10–50 ppm) of Anderson Mine Member sediments
- Presence of uraniumiferous volcanic and granitic rocks providing potential U sources (felsic volcanic rock fragments comprising a major fraction of the Anderson Mine Member are favored as the principal U source)
- Presence of H₂S as a reductant generated from gastropod-rich marlstones
- Regional geochemical zoning marked by increased values of Li, V, and possibly F, and other elements, and a particular anomalous concentration of Mo and As exclusively associated with zones of uranium mineralization

■ Fig. 7.7.

Anderson mine area, (a) contour map of uranium mineralization subdivided into grade-thickness product (GT) areas based on a cutoff grade of 0.017 % U; (b) SW–NE cross-section of the uranium mineralized interval. (After Sherborne et al. 1979; (AAPG 1979, reprinted by permission of the AAPG whose permission is required for further use))



Mueller and Halbach (1983) note that uranium is preferentially accumulated in thin-bedded carbonaceous siltstone, lignitic mudstone, and bioturbated marlstone of lacustrine provenance, particularly in the upper part of the upper carbonaceous unit of the Anderson Mine Member. Less favored uranium traps include thick-bedded intervals of carbonaceous silt- and sandstone or dense limestone of the intermediate section of the upper unit, the limestone interval, and the lower carboniferous unit.

Metallogenetic Aspects

The genesis of the Anderson deposit may be interpreted as the result of complex groundwater, sorption, and precipitation processes within carbonaceous–humic lacustrine sediments. These processes probably occurred in an early diagenetic low-temperature environment prior to the late Miocene to early Pliocene Basin and Range tectonism.

Sherborne et al. (1979) present the following model: Uranium-bearing tuffaceous sediments were deposited in sheltered backwater areas marginal to an expanding Miocene freshwater lake. Reaction of tuffaceous sediments with lake water caused, in an early diagenetic stage, extensive alteration and development of alkaline carbonatic pore water. Zeolites probably formed at this time.

Compaction and dewatering of uraniferous tuffaceous lake sediments released uranium and silica and led to migration of uranium–carbonate–silica-rich formational waters within the basin. Uranium was most likely transported in groundwater as a uranyl carbonate complex. It precipitated to form coffinite ore in and adjacent to carbonaceous strata and where H_2S acted as a reductant. H_2S was generated to a large extent in intraformational marlstones.

Some remobilization of the original coffinite mineralization and deposition of carnotite ore in fractures has taken place in near-surface oxidation zones in more recent geologic time. But this did not significantly affect uranium mineralization in either carbonaceous unit as indicated by radiometric equilibrium.

Mueller and Halbach (1983) do not explicitly discount the above model but favor some alternative processes particularly with respect to uranium transport and conduit. They propose that the alluvial fan-braided river system, located west of the Miocene Anderson Mine lake, collected uranyl-bearing groundwater from adjacent metamorphic and volcanic highlands. Volcanics of dacitic to rhyolitic composition are believed to have been the principal source of uranium as deduced from the widespread, and most likely volcanic-derived, lithium and fluorine enrichment throughout the lacustrine Anderson Mine Member. Hydrostatic pressure in river beds generated migration of uraniferous water to the delta complex, when northward flowing groundwater introduced it into lacustrine sediments of the Anderson Mine Member along numerous intercalated sandy layers.

Uranium was transported in the form of uranyl carbonate complexes in solutions of slightly alkaline chemistry (pH 7–9) produced by partial dissolution of high magnesian calcite during early diagenesis. This milieu was also favorable for argillization and zeolitization of interbedded rhyolitic glass fragments. Subsequent fixation of uranium began with a preconcentration phase during which considerable amounts of uranium were adsorbed onto humic substance (perhaps similar to processes described from the Grants Uranium Region; see Adams and Saucier 1981, Turner-Peterson et al. 1986, and other authors in chapter 1. Grants Uranium Region), colloidal silica, and zeolite. Most of the adsorption was in the uppermost 10 m of the sediment column where slightly acidic microenvironments developed in response to biochemical humification of plant relics. Local pH values of 6–7 destabilized incoming di- and tricarbonat uranyl complexes. Condensation of the sorbents to organic gels reduced most of the hexavalent U, which then precipitated as submicroscopic coffinite and pitchblende. Formation of coffinite was likewise accomplished by H_2S , which developed as the result of sulfate reduction by bacteria continuously forming H_2S halos around organic fragments. The influence of H_2S as the main reductant is noted by the authors to have been

important in the enrichment of uranium in permeable structures, especially in burrows. Although often associated with and penecontemporaneous with uranium ore, framboidal pyrite spheres started to crystallize earlier than coffinite and resulted from processes at least not directly linked to uranium deposition. This is indicated by the lack of statistical correlation between uranium and total sulfur.

7.8 Sierra Ancha/Apache Proterozoic Basin, Arizona

The Sierra Ancha is located in Gila County in central Arizona, east of the Mazatzal Mountains, approximately 120 km ENE of Phoenix (Fig. 1.1b). After the discovery of uranium in 1950, seventeen small mines produced about 45 t U in the 1950s at an overall ore grade of 0.2% U from vein-type mineralization. The *Hope* mine was the largest producer with 17 t U at grades ranging from 0.15 to 0.32% U. The largest explored deposit is *Workman Creek* with resources of about 3,800 t U (based on a cutoff grade of 0.0085% U).

Sources of Information. Chenoweth and Malan 1969; Elevatorski 1978b; Granger and Raup 1959, 1969a, b; Montgomery et al. 2006; Neuerburg and Granger 1960; Nutt 1981, 1984; Peirce et al. 1970; Scarborough 1981; Schwartz 1957; Walker et al. 1963; Williams 1957. The following description is largely based on Granger and Raup (1959, 1969a, b), amended by data of the other authors mentioned and Adamak P, Free B, and Patterson J Personal Information.

Geology and Mineralization

The Apache Basin is filled with Mesoproterozoic sediments of the Apache Group, which rest unconformably upon Paleo- to Mesoproterozoic metasediments and metavolcanics intruded by granites. Neoproterozoic Troy Quartzite overlies the Apache Group. Sediments are locally folded along two major NE- and NW-trending axes into monoclines. Massive sill-like diabase bodies of gabbroic to syenitic composition cut the Apache Group and Troy Formation. Livingston (1969) reports an age of 1,250–1,050 Ma for these multiple intruded sills. Some diabases exhibit late-stage deuteric alteration and have converted sedimentary wall rock to hornfels.

The ore-hosting **Dripping Spring Quartzite** of the Apache Group is divided into two members that overlie a basal conglomerate. The upper member is 50–120 m and the lower member between 0 and 110 m thick. Lithologies of the upper member are generally finer grained and more thinly stratified than those of the lower member. The upper member includes four units consisting chiefly of arenaceous siltstone and minor shale and coarse-grained orthoquartzite. The about 70 m thick grey unit of the upper member is the principal host for almost all uranium occurrences. It consists of three facies: A lower, thinly stratified, feldspar-rich siltstone, grey in color, 3–42 m thick; a middle, medium- to fine-grained, grey feldspathic sandstone

and orthoquartzite, 1.5–18 m thick; and an upper, 4–37 m thick, dark-grey to black, thinly and irregularly stratified feldspathic siltstone with finely disseminated pyrite and organic particles. Fracturing and jointing is well developed in the Dripping Spring Quartzite, but many of the structures are rehealed and cemented.

Ore mineralogy is described as very fine-grained uraninite and/or pitchblende associated with minor pyrite, marcasite, pyrrhotite, chalcopyrite, galena, and rare molybdenite and sphalerite. Euhedral uraninite is confined to within 30 m of a large diabase body. Uranium also occurs adsorbed on chlorite and less commonly on graphite. Chlorite, which may grade occasionally into nontronite, is the typical gangue or alteration mineral. Thin fracture fillings of quartz, ankerite, siderite, and dark purple fluorite with pyrite were encountered in some deposits. Near-surface mineralization is oxidized and represented by a variety of U^{6+} minerals and secondary Cu and Fe minerals (Neuerburg and Granger 1960). U/Pb isotope datings yield apparent ages for uraninite/pitchblende of 1,300–900 Ma (Granger and Raup 1969a).

Uranium mineralization is predominantly hosted in veins, but also in sediments. Veins strike NNE, or less commonly WNW and dip nearly vertical. They can have a vertical extent of up to 25 m, but average much less. Vein widths are commonly on the order of centimeters to a few tens of centimeters, rarely up to 1 m. In receptacle lithologies, mineralization penetrates from a vein laterally into the wall rock for few meters to, rarely, tens of meters. This sediment-hosted uranium is disseminated and often concentrated along bedding planes.

Uranium is often, but not everywhere, concentrated where the grey unit of the Dripping Spring Quartzite is invaded by diabase dikes or sills. The diabase imposed contact metamorphism locally on wall rocks as reflected by hornfels and related facies in siltstone. The strongest and most consistent U mineralization is spatially associated with the largest and thickest individual diabase sill, called Sierra Ancha sheet, in the central part of the district. This diabase exhibits differentiation and deuteritic alteration. Although the apparent affinity of uranium to the altered diabase and adjacent hornfels may suggest a genetic relationship, this is contradicted by the fact, however, that at other sites uranium accumulations occur without a nearby diabase, or uraniferous veins end abruptly at the contact of a diabase body. Compared with other uranium districts in the world, it appears possible that any diabase body merely acted as a more or less localized energy source for mobilization and perhaps further concentration of uranium into fractures. The grey facies of the Dripping Spring Quartzite is thought to be the probable original source of uranium (Williams 1957).

Nutt (1984) describes the host rocks as diagenetically altered, carbonaceous, potassium-rich volcanogenic siltstones, in which uraninite (pitchblende) and coffinite associated with high concentrations of copper and molybdenum occur in vertical veins and in subhorizontal to horizontal veins along stylolites and bedding planes, and as disseminations in fine-grained, potassium feldspar-rich beds. The author assumes a diagenetic enrichment of uranium that derived from volcanogenic sediments at the time of diagenesis and stylolite formation. Circulation of fluids

associated with the diabase intrusion caused a redistribution of uranium; and post-diabase chloritization led to a further remobilization, but only of limited magnitude.

7.9 Hillside Area, Arizona

This area includes the Hillside uranium prospect near the old Au–Ag–Pb–Zn Hillside mine, 5 km N of the Bagdad porphyry copper deposit, in west-central Arizona, approximately 80 km NW of Wickenburg (Fig. 1.1b). Uranium was found in 1950 on the old dump and was drill-intersected at depth in veinlike ore shoots.

Sources of Information. Anderson 1976; Anderson et al. 1955; Axelrod et al. 1951; Peirce et al. 1970; Scarborough 1981; and Patterson J and Werts L personal communication, unless otherwise stated.

Geology and Mineralization

The Hillside area is part of a NW–SE-trending belt of Lower to Middle Proterozoic metasediments intruded by deuteritic granitic complexes and other intrusions. The belt extends from southeastern Nevada to southwestern New Mexico and follows to some extent the boundary between the Colorado Plateau and the Basin and Range structural provinces. Within this belt, a number of uranium occurrences have been found, among others, the Hillside prospect, Arizona, and the Black Hawk deposit, New Mexico, described later.

The Hillside area is underlain by schists, quartzites, and tightly folded muscovite–chlorite-bearing gneisses of the Yavapai Series. Various leucocratic stocks including two-mica granite and alaskite, and pegmatite dikes have intruded this series. Alaskite locally contains wolframite, beryl, and fluor spar. The basement is in part covered by Tertiary volcanics. Numerous faults, shears, and breccia zones of different fault systems dissect the area. Intense weathering and oxidation have altered crystalline rocks to depths of about 300 m along fractures. Age datings by Anderson (1976) yield ages of 1,820–1,775 Ma for Yavapai metasediments in the Prescott–Jerome area, and about 1,770–1,760 Ma for some of the intrusives. In a subsequent leucocratic plutonic phase, about 1,400 Ma ago (see below), the two-mica granite, alaskite, etc., were intruded.

Vein-type precious and base metal mineralization is present and was formerly mined. Research indicates, however, that much of the base metal mineralization is present as syndimentary Proterozoic exhalative massive sulfide deposits.

Hillside uranium mineralization is structurally controlled and hosted by metasediments adjacent to and at the contact of a two-mica granite. The granite is locally highly argillized. Pitchblende (sooty) is the principal uranium mineral below the water table (100 m or more deep). Hexavalent U species, mainly uranyl carbonates, prevail above the water table. Mineralization occurs as discontinuous veinlets, lenses, and pods in fractures and joints, and disseminated in shear and breccia zones.

Structures range in width from a few millimeters to a few meters and are often filled with hematitic or limonitic gouge. Ore grades reportedly vary between less than 0.1 and 0.35% U and are found intermittently in an area extending more than 1,500 m in a NE–SW direction, more than 100 m in width, and to a depth of at least 250 m.

The local and regional geological setting of uranium mineralization leaves at least three metallogenetic options: (a) A hypogene hydrothermal origin with fluids derived from deuteritic granites, (b) a supergene origin with uranium leached from surrounding uraniferous granites or metasediments by meteoric waters, and (c) an origin by processes involving a combination of hypogene, connate, and meteoric solutions as established by Cuney and his coworkers for vein pitchblende deposits in the Massif Central and Vendée, France (see respective chapters and bibliography in Dahlkamp, Uranium Deposits of the World, Europe, in preparation).

Silver et al. (1980a) investigated 1,450–1,400 Ma old uraniferous granites in southern Arizona including the Lawler Peak Granite in the Bagdad copper porphyry mine area a few kilometers south of the Hillside mine. The Lawler Peak Granite is a two-mica adamellite, which contains 20 ppm U and has an outcrop surface of 25 km². The authors conclude from their findings that the Lawler Peak Granite has lost at least 25% of its uranium endowment, accounting for a release of about 100,000 t uranium into the environment. The loss occurred during or since two geologic events at 230 ± 10 and 75 ± 25 Ma, which can be related to orogenies and volcanism of Permo–Triassic and Laramide age. The 75 Ma event is perhaps related to the emplacement of the nearby Bagdad monzonite porphyry dated 72 Ma.

7.10 Black Hawk District, Burro Mountains, New Mexico

The Black Hawk district, also referred to as *Bullard Peak district*, is situated in the northern Burro Mountains approximately 25 km W of Silver City, in southwestern New Mexico (Fig. 1.1b). Former mining activity dates back to the late 1800s when five underground mines (*Alhambra, Black Hawk, Good Hope, Rose, Silver King-Hobson*) worked the Ag, Co, Ni, Bi, and U-bearing veins with silver as the main metal of interest (estimated production 1–2 mio oz. Ag). Uranium is known since 1919, but there is no record of uranium recovery although the veins have limited intervals with grades of several percent uranium.

Sources of Information. Gillerman 1964, 1968; Gillerman and Whitebread 1956; Granger and Bauer 1952; Hewitt 1959; Leach 1920; Von Bargaen 1979; and Brown N, personal information, unless otherwise cited.

Geological Setting of Mineralization

Two major stratigraphic units separated by a large hiatus dominate the northern Burro Mountains. The first is of Precambrian age and the second is of Cretaceous to Tertiary age.

Precambrian: The oldest unit is an extensive sequence of metasediments, mainly quartzite, gneiss, and schist (Bullard Peak Series) and meta-igneous rocks metamorphosed to the lower amphibolite grade facies. A pyrite-rich gneiss of quartz diorite composition cuts this suite. Metamorphic rocks contain pyrite (up to several percent in the quartz diorite gneiss) and pyrrhotite, along with minor amounts of base metals. These metamorphics were intruded by granite, monzonite, and quartz-monzonite of the Burro Mountain Batholith and by dikes of aplite, granitic pegmatite, and diabase.

Cretaceous-Tertiary: Two Cretaceous sedimentary formations occur in the area, the Beartooth Quartzite and Colorado Shale. In late Cretaceous to early Tertiary time, quartz monzonite and monzonite porphyry stocks (Twin Peaks monzonite porphyry) were intruded. Extrusion and emplacement of volcanics (Datil–Mogollon Volcanics) ranging from rhyolite to andesite and basalt in composition are dated at 35–22 Ma (Elston et al. 1976).

The Twin Peaks monzonite porphyry stock located NW of the Black Hawk area is believed to be the most likely source for mineralization. It has a surface outcrop of about 2.5 by 4 km. Several consanguineous dikes and apophyses, up to 20 m or more wide, extend for some distance away from the stock.

Major structures (lineaments, faults) trend NW and NNE, others strike around WNW, NE, and ENE. Mineralized veins follow primarily N to NNE and NE to E directions. They are brecciated and displaced by younger faulting.

Host Rock Alteration

Ore-hosting rocks are altered by propylitization, sericitization, and argillization. The Twin Peaks monzonite is altered primarily on the eastern side of the stock and its dikes near major deposits are intensely propylitized. Hornblende is altered to chlorite, epidote, and calcite, and finally to clay. Feldspars are altered to clay, and magnetite is replaced by pyrite or goethite. The matrix of completely altered rock has recrystallized to tiny crystals of quartz, illite, and kaolinite, or hydromuscovite/sericite.

Mineralization

Veins of the Black Hawk district characteristically contain Ag, Co, Ni, Bi, and U mineralization. Von Bargaen (1979) identified at least four primary and two secondary ore mineral assemblages.

Primary assemblages and principal minerals

1. Early arsenide assemblage: native silver, argentite, niccolite, rammelsbergite, gersdorffite, and pitchblende
2. Late arsenide assemblage: rammelsbergite, gersdorffite, nickel-skutterudite, native silver, and argentite
3. Sulfide assemblage: chalcocopyrite, galena, tennantite, and sphalerite filling fractures in and replacing pyrite of the country rocks in or near fracture zones
4. Low-temperature native silver and copper sulfide assemblage: fine-grained intergrowth of acanthite, argentite,

jalpaite, native silver, covellite, and chalcopyrite replacing late arsenides

Secondary assemblages and principal minerals

5. Ag-bearing chalcopyrite, bornite, covellite, and digenite formed through alteration of chalcopyrite and tennantite
6. Annabergite, erythrite, millerite, acanthite/argentite, and gypsum formed by weathering of arsenide minerals.

Hematite is abundant in both arsenide stages. Au is reported from the 55 m level of the *Alhambra mine*, where it occurs in the hanging wall of the fracture zone containing the Alhambra vein (Osmer in Von Bargen 1979).

Pitchblende is the principal U mineral. It occurs in at least two stages. Early pitchblende, partly botryoidal, is associated with an arsenide assemblage of Co–Ni and native Ag. An apparent later pitchblende is associated with a sulfide stage composed of a complex assemblage of silver sulfides and sulfoarsenides, and common sulfides. Youngest(?) pitchblende is occasionally accompanied by coffinite.

Gangue minerals are primarily crystalline and cherty quartz and ferroan dolomite. Both are ubiquitous. They began to crystallize in an early stage preceding the deposition of silver. Manganiferous siderite is an early stage mineral. Calcite is the last carbonate gangue mineral to form. Its range of deposition extended beyond the ore distribution. Fe-rich chlorite and kaolinite occur as relatively late minerals filling vugs in veins. Baryte is present in two generations, an early one preceding the carbonate gangue and a late generation deposited after the late calcite but prior to chlorite and kaolinite.

Mineralization occurs in abundant veins predominantly confined to a zone that lies contiguously to the S and E margin of the Twin Peaks monzonite porphyry stock. The most common host rocks are quartz diorite gneiss and less frequently granite. Ore shoots reportedly are almost entirely confined to gneiss. In contrast, veins are rarely mineralized when hosted in the Twin Peaks monzonite porphyry or satellite stocks and apophyses thereof, or in quartzite or schist.

Veins occupy faults and fractures of two intersecting systems, one trending N to NNE, the other NE to E. Ore preferably concentrates in NE veins, except the *Alhambra vein*, which trends NNE. NE veins are generally parallel of foliation of gneiss and appear to be cut by NNE veins.

In most places, the contact between vein filling and host rock is sharp and marked by a smooth fracture plane with a gouge salband. Only occasionally there is a gradational contact with some minor replacement of wall rock. Ore shoots within veins are poddy to lens-like. A crude banding is developed locally, but most commonly vein fillings do not display any distinct textural arrangement or zonation.

The distribution of ore elements within ore bodies is quantitatively rather irregular. Some shoots contain U, Co, Ni, and Ag minerals. Others lack uranium or consist essentially of gangue minerals or gouge. Boundaries between barren zones and rich ore pods are sharp. Uranium preferentially associates with Co and Ni, and occurs as black blebs and small masses disseminated through Co–Ni ore. It also occurs as distinct

veinlets and coatings on fracture surfaces. In the *Alhambra vein*, pitchblende is positioned on the outer margins of ore shoots. Wall rock adjacent to pitchblende ore is stained reddish by hematite and thin hematite veinlets transect wall rock and barren vein fillings. Elsewhere, wall rock is extensively sericitized and argillized.

Some indication of vertical zonation is recorded. Co and Ni were not found between the surface and 30 m below the collar of the Black Hawk shaft, i.e., down to about 80 m below the highest outcrop point of the vein. Both elements increase in abundance downward. Lidstone in Gillerman (1968) reports 8.92% Ni, 0.9% Co, 8.8% Zn, and 2.542 oz Ag per ton in a bulk sample from the lowermost part of the *Black Hawk mine*, 205 m under surface. Argentite also increases in the lower levels. In general, argentite prevails in the lower half and native silver in the upper parts of ore pods.

In the *Alhambra mine*, some correlation appears to exist between the location of ore shoots and changes in dip and strike of the vein. Ore shoots are wider and more persistent where the vein dips steeply. Similar situations are known from the Black Hawk vein.

Oxidation affected the veins to depths of several tens of meters and locally to 100 m.

Shape and Dimensions of Deposits

Ore-bearing veins are confined to a zone 1–1.5 km wide and almost 5 km long in NE–SW direction. The Twin Peaks quartz monzonite complex and the Beartooth Quartzite constitute the NW and NE boundaries, respectively, of the mineralized zone.

The width of many veins is only a few centimeters to a few decimeters. But a vein may open up suddenly into ore shoots up to 3 m or more wide transected by veinlets of ore minerals several millimeters to centimeters wide. Veins are commonly wider in quartz diorite gneiss and granite. They pinch noticeably when entering or passing through dikes of monzonite porphyry or through quartzite. The lengths of individual veins vary between some tens of meters and 300 m or more. The greatest known vertical extent is almost 250 m in the *Black Hawk vein*. Veins dip 60–90° mostly to the N with flexures in their attitudes. Faults displace veins. Subsidiary fractures in the form of stockworks of gouge may dissect veins internally.

The *Black Hawk vein* dips vertically down to about 25 m under the shaft collar, then the inclination changes to about 60° N. The Black Hawk vein cuts a monzonite porphyry dike, which strikes N–S and dips about 45° E. Mineralization occurs on both sides of the dike and ore shoots plunge about 50–60° E.

In the *Alhambra vein*, individual ore accumulations range from scattered ore minerals in gangue, to spherical masses 10 cm or so in diameter, to large shoots as much as 1 m wide, 15 m in vertical and 10 m in horizontal extent. Ore shoots commonly occur in wider veins.

No average uranium grades are recorded, but ore shoots locally contain up to several percent U. Shipments of silver ore assayed as much as 15,000 oz. Ag/sht.

Ore Controls and Recognition Criteria

Gillerman's (1968) and Von Bargaen's (1979) investigations led to the following ore controls or recognition criteria for the Black Hawk mineralization:

Host environment

- Presence of late Cretaceous/early Tertiary monzonite porphyry intrusions (Twin Peaks Batholith)
- Intense alteration of the southern and eastern parts of the Twin Peaks monzonite porphyry stock and related apophyses and dikes
- Presence of relatively sulfide-rich gneisses to the southeast of the stock (mainly pyrite with minor pyrrhotite)
- Restriction of ore-bearing veins to a zone adjacent to the southern and eastern sides of the monzonite stock
- Most favored host for ore-bearing veins is quartz diorite gneiss.

Mineralization

- Polymetallic, multistage mineralization composed of Ag, Bi, Co, Ni, and U minerals associated with mainly quartz and dolomite
- Mineralization occurs in two structure systems. Ore is predominantly in NE to E-trending veins, less often in N to NNE veins, which appear to transect the NE set
- Strong correlation between locations of major ore accumulations in veins and intersections of N-S and NW-SE-trending lineaments, altered Twin Peaks monzonite dikes, or N-S and E-W-oriented fractures
- Pinching and swelling of veins in vertical and horizontal directions, particularly when cutting monzonite dikes in which veins narrow perceptibly, but may widen outside of the dike
- Generally sharp contacts between vein and wall rocks
- Intermittent poddy and lens-like distribution of ore in veins separated by barren or subeconomic intervals
- Some correlation between the location of ore shoots and changes in dip and strike of a vein with wider and more persistent ore shoots in steeply dipping veins
- A probable element zonation is indicated by a relative increase of Ni, Co, and possibly U with depth, whereas Ag prevails on the upper levels.

Metallogenetic Aspects

The Black Hawk Ag-Co-Ni-Bi-U ores are hydrothermal vein-type formations and may be compared with similar deposits in the western Erzgebirge in Czech Republic and Germany, and at Great Bear Lake, Canada.

Von Bargaen (1979) believes hydrothermal lateral secretion has formed the Black Hawk mineralization. He suggests a metallogenetic model, in which Black Hawk mineralization is genetically related to the late Cretaceous or early Tertiary Twin Peaks monzonite porphyry. Emplacement of vein material took

place at the intersection of dikes related to this stock with sets of NW-SE-trending fractures of Precambrian origin. These NW-SE faults were reactivated by intrusion of the Twin Peaks stock. Associated tectonism generated NNE and NE-striking tensional fractures due to differential movements of Precambrian rocks, in particular of quartz diorite gneiss, along NW-SE-trending structures. Furthermore, monzonite intrusion provided heat to generate a circulation of solutions, which were mainly derived from surface waters. These solutions were initially highly oxidizing since their main component was meteoric water. They are considered by the author to have carried such elements as Ag, As, Bi, Cd, Co, Cu, Fe, Hg, Pb, Mn, Mo, Ni, Sb, U, Zn, as well as Al, Ca, K, Si, S, O, and CO₂. These solutions have assumably leached those elements from surrounding country rocks. Pre-existing sulfides in gneisses could possibly have provided all ore elements except for uranium, which could have been derived from Precambrian granites. Sources of Al, Ca, Fe, K, Mg, Mn, and Si are thought to have been the Twin Peaks monzonite and the gneisses.

Solutions established convection cells from which ore minerals were deposited at sites where fluids experienced changes in oxidation potential, or where they started to boil, or in response to a combination of both factors. Preferential sites for ore deposition were at intersections of tensional fractures with both monzonite dikes and around NW-SE-trending reactivated Precambrian structures. Dikes became heavily propylitized near major ore veins.

Von Bargaen (1979) calculated from mineralogical and geological evidences that ore was deposited at depths from about 600 to 900 m below the early Tertiary surface, at fluid pressures between 100 and 200 bars, at temperatures dropping from 350° to 50°C, at a pH between 4.5 and 6, at sulfur fugacities ranging from $\log fS_2$ -20 to -15, and at oxygen fugacities dropping with progressing ore deposition from $\log fO_2$ -42 to -50.

Six ore mineral assemblages have formed (see section Mineralization). Silver minerals are among the earliest and latest minerals to crystallize. Early Ag minerals contain mercury (up to 0.5% Hg). Early silver and its paragenetic minerals of stage 1 were followed by the main arsenic stage (stage 2), in which nickel arsenides are dominant. With progressing mineralization, the Ni content of ore solutions decreased and that of Co, As, and Fe relatively increased. From here on, fluids became richer in sulfide (or less oxidizing) resulting in deposition of predominantly base metal sulfides (stage 3), which were initially limited to chalcopyrite, galena, sphalerite, and tennantite. These minerals are found as fillings in fractures in pyrite of country rocks. The latest sulfide assemblage (stage 4) consists of minerals the components of which were leached from earlier arsenides. For example, silver was derived from earlier native silver and argentite, while copper may have been derived either from continuation of deposition from hydrothermal solutions or from dissolution of chalcopyrite. Deposition temperature is estimated at about 100°C for this stage. Stage 5 minerals may have formed by final hydrothermal or supergene processes at low temperatures deriving their mineral constituents from earlier arsenides. Finally, oxidation produced stage 6 minerals.

7.11 Bingham, Utah

The Bingham copper porphyry deposit is located 55 km SSW of Salt Lake City, Utah (►Fig. 1.1b). The deposit is exploited by an open-pit mine primarily for copper. Uranium was temporarily extracted as a by-product to Cu and other metals from 1978 to 1989 at a maximum rate of about 50 t U per year from Cu-leach liquor containing 8–12 ppm U.

Similarly, uranium was recovered at a rate of up to 100 t U per year from Cu ore of the *Twin Buttes* Cu-porphyry deposit in Pima County, southern Arizona (►Fig. 1.1b) from 1980 to 1985.

Sources of Information. John 1978; Lanier et al. 1978.

Geology and Mineralization

The deposit-hosting Bingham stock is of Eocene age and consists of an epizonal intrusion of six major igneous phases and associated dikes represented by, from oldest to youngest, quartz-poor (<10 vol.% quartz), equigranular to porphyritic monzonite, porphyritic quartz monzonite, and recrystallized monzonite; quartz-rich (>20 vol.% quartz), porphyritic latite, quartz monzonite porphyry, and hybrid quartz monzonite porphyry, as well as latite porphyry dikes and quartz latite porphyry dikes.

Hydrothermal alteration within and peripheral to the ore-hosting quartz monzonite porphyry is reflected by Mg and K metasomatism forming an inner zone of quartz–orthoclase–phlogopite, an outer zone of actinolite–chlorite–epidote, and a late sericitic and argillic (montmorillonite mainly) overprint.

Ore minerals form overlapping sulfide mineral zones composed of, from the interior low-grade core outward, molybdenite, bornite–chalcopyrite, chalcopyrite–pyrite, pyrite, and galena–sphalerite. Gold and silver is present in significant amounts. Bi, Pt, Pd, Re, Se, and U occur in recoverable traces. No uranium mineral is recorded, but U may be present as uraninite or uranothorianite. Molybdenite and Cu sulfides occur as disseminations, and galena–sphalerite with part of the pyrite as veins. Mineralization is concentrated on and drapes around and

through the quartz monzonite porphyry facies. Distribution and zoning of mineralization and alteration is controlled by the location relative to the quartz monzonite porphyry facies within the intrusive complex, rock type, degree of fracturing, and permeability.

Cu and Mo mineralization with which recoverable U is associated extends over an area of about 1,200 m by 2,100 m around and through the quartz monzonite porphyry phase, which measures laterally 420 by 1,000 m. Persistence of mineralization into depths is at least 1,500 m. Uranium content in the Cu–Mo ore is 20–50 ppm.

Selected References and Further Reading for Chapter 7 Basin and Range

For details of literature see Bibliography.

Ahern and Corn 1981; Anderson 1976; Anderson et al. 1955; Arizona Geological Society 1978; Axelrod et al. 1951; Bikun 1980; Birkholz 1978; Bowyer 1963; Bromfield et al. 1982; Brophy and Kerr 1951; Burt and Sheridan 1981, 1985; Callaghan 1939, 1973; Callaghan and Parker 1961; Castor and Berry 1981; Chemillac 2004; Chenoweth and Malan 1969; Cohenour 1960; Cunningham et al. 1980, 1982, 1994, 1998; Cunningham and Steven 1978, 1979; Cupp et al. 1977a, b; Dasch 1967; Dayvault et al. 1985; Dunkhase 1980; Elevatorski 1978b, b; Elston 1978; Elston et al. 1976; Files 1978; Finch 1967; Garside 1973; Gilbert 1957; Gillerman and Whitebread 1956; Gillerman 1964, 1968; Glanzman and Rytuba 1979; Granger and Bauer 1952; Granger and Raup 1959, 1962, 1969a, b; Gruner et al. 1951; Havenstrite and Hardy 2006; Hewitt 1959; John 1978; Kerr 1968; Kerr et al. 1957; Lanier et al. 1978; Leach 1920; Lindsey 1978, 1981, 1982; Livingston 1969; Ludwig et al. 1980; Mahood 1983; McKee 1976; McLemore 1983; Montgomery et al. 2006; Mueller and Halbach 1983; Myers and Underhill 2005; Neuerburg and Granger 1960; Nutt 1981, 1984; Offield 1979; Otton 1977a, b, 1981, 1986; Peirce et al. 1970; Prens and Ronning 2005; Priesemann 1977; Rasmussen et al. 1985; Reyner et al. 1956; Roper and Wallace 1981; Rowley et al. 1988, 1994; Rytuba 1976, 1977 1981; Rytuba and Conrad 1979, 1981; Rytuba and Glanzman 1978; Rytuba et al. 1979; Scarborough 1981; Schwartz 1957; Sharp 1955; Sharp and Hetland 1954; Sharp and Williams 1963; Shawe 1968, 1972; Shea 1982; Shea and Foland 1986; Sherborne et al. 1979; Silver et al. 1980; Staatz and Carr 1964; Steven et al. 1978, 1979, 1981; Steven and Morris 1987; Stewart 1980; Taylor and Powers 1955; Thurlow 1956; US AEC 1959; US DOE 1980; Von Bargen 1979; Walker and Osterwald 1956, 1963; Walker et al. 1963; Wallace and Roper 1981; Waters 1955; Wenrich et al. 1989; Willord and Callaghan 1962; Williams 1957; and Adamak P, Brown N, Chenoweth WL, Otton J, Patterson J, and Pool TC, personal communication.



Chapter 8

Texas Coastal Plain Uranium Region

The Texas Coastal Plain, also referred to as *South Texas Uranium Region* or *South Texas Mineral Belt*, contains uranium deposits in Tertiary sandstones in a 20–45 km wide curvilinear belt, which approximately parallels the coast of the Gulf of Mexico about 130 km inland (▶Figs. 1.1b and ▶8.1). The mineral belt is almost 400 km long in a NE to SSW direction, extending from eastern-central Texas to the Mexican border. It probably continues into Mexico, where uranium mineralization is reported about 50 km SE of Rio Grande City in fluvial channel systems similar to those in south Texas.

Some 100 deposits have been discovered, principally in Karnes, Live Oak, McMullen, and Duval counties, but also in some other counties. The approximate location of major deposits and occurrences is shown in ▶Fig. 8.1. Deposits are generally small, averaging less than 3,000 t U. Most deposits consist of roll-type U mineralization hosted in marginal marine sandstones and are often associated with invaded reducing agents. They are therefore classified as sandstone, rollfront-type U deposits, and attributed to the class of marginal marine deposits containing uranium associated with extrinsic reductants.

Remaining resources (<\$130/kg U category, status end 2002) of the south Texas region are estimated at 88,500 t U at an average grade of 0.053% U (US EIA 2003). Production began in 1960 and amounted through 2007 to about 30,000 t U. Grades commonly averaged 0.08–0.09% U.

Due to the loose or unconsolidated nature of ore-hosting sandstones, which practically prevents underground mining, exploitation is targeted for open-pit mines and in situ leaching operations. In total, 18 properties were exploited between 1975 and 2007 by ISL techniques producing about 14,100 t U.

Sources of Information. See section “References and Further Reading...” at the end of Chap. 8 Texas Coastal Plain and descriptions of individual districts.

Adams and Smith (1981) have published a compilation of the south Texas deposits, which incorporates information from many authors, in particular from Eargle, Fisher, Galloway, Weeks and their coworkers. Adams and Smith (1981) describe the known geology of the south Texas uranium region adequately and present a comprehensive synopsis of the regional setting and local characteristics of uranium deposits, their formation, and their recognition criteria. The following description has drawn extensively from Adams and Smith (1981) amended by information from more recent publications by other authors as cited. In many cases, specific text has been quoted but abbreviated and to some extent modified, and therefore it is not set in quotation marks. RB Smith kindly reviewed this section dealing with south Texas and amended and improved both content and text.

Regional Geological Setting of Mineralization

The Texas Coastal Plain (▶Fig. 8.2a and b) is underlain by Jurassic and Cretaceous sediments, which are covered by more than 15,000 m of flat-lying interbedded marine and nonmarine sediments of Tertiary age. Evolution of the Gulf of Mexico and the Texas Coastal Plain started in Paleozoic times and continued into the Mesozoic. During this time span, periods of regional uplift and basin formation accompanied major episodes of plate subduction and spreading, which created the basic structural features of the south Texas plain. This activity includes uplift of major areas and arches, and subsidence of embayments as well as the general homoclinal inclination to the south of the greater coastal area.

Sedimentation in the Gulf of Mexico began with evaporitic lithologies during the Jurassic. In Cretaceous time, mainly marine and marginal marine sediments were laid down. The end of the Cretaceous was marked by a sharp fall in sea level, which coincided with the major uplift of the Rocky Mountains. With the onset of the Tertiary, major river systems started to transport large volumes of clastic detritus from the Rocky Mountains and to a lesser degree from the Appalachians, into the Gulf Coast, a process that continued for a period exceeding 50 Ma. Deposition of the fluvial clastic sequences was overlapped by marine transgressions, which reflects a complex interaction between climate changes, sediment supply, and regional subsidence (▶Figs. 8.2b and ▶8.3).

The position of the Tertiary paleo-shorelines fluctuated in response to sea level changes (▶Fig. 8.4). At the beginning of clastic deposition in early Tertiary, the Texas coastline was at least as far as 200–240 km inland. Deposition gradually prograded into the subsiding gulf, particularly since the Oligocene.

Constant loading of sediments into the Gulf basin produced instabilities that led to local faulting, particularly to growth faults that become younger toward the coast (▶Fig. 8.5). The principal faults and fault systems form a general arcuate pattern around the basin of sedimentation. Felsic volcanism, synchronous with part of the subsidence, provided pyroclastic-rich sediments to a portion of the Tertiary sedimentary sequence with which all uranium deposits in south Texas are associated.

Occurrences of oil and gas, lignite, geothermal resources, and uranium are associated with the sediments and the contemporaneous growth faults. Oil and gas occurrences are controlled regionally by depositional facies and locally by structures, which in many cases place sands and shales in juxtaposition forming traps for hydrocarbon accumulation. Galloway (1977) has estimated that one third of the South Texas Coastal Plain is underlain by closely spaced hydrocarbon reservoirs that are largely fault-controlled.

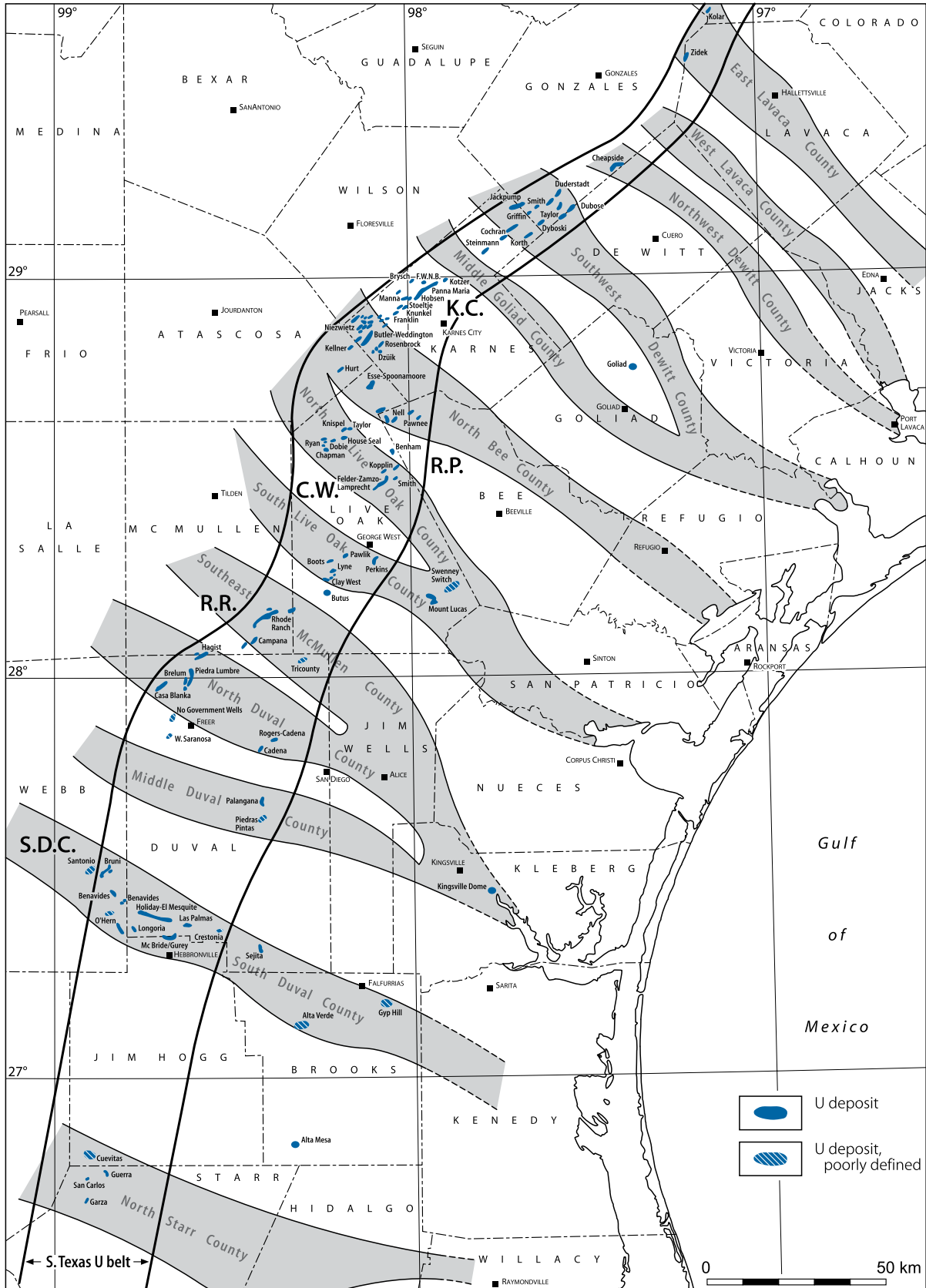
Litho-stratigraphic and Sedimentological Distribution of Uranium Mineralization

Known uranium occurrences are hosted in arenites deposited between middle Eocene and early Pliocene (▶Figs. 8.4 and ▶8.6). *Stratigraphic units* containing major deposits are

Fig. 8.1.

South Texas, location of mega-channels (shown in grey) and related uranium districts and principal deposits in the South Texas Mineral Belt and adjacent areas in the coastal plain. (After Adams & Smith 1981)

(Uranium districts: K.C. Karnes County; R.P. Ray Point; C.W. Clay West-Burns; R.R. Rhodes Ranch area; S.D.C. South Duval County Mineral Trend)



■ Fig. 8.2.

South Texas coastal plain, (a) generalized geological map and (b) NW-SE cross-section of areas with major uranium deposits. Host units for deposits are fluvial-marginal marine sediments of the Eocene Jackson Group, Miocene Oakville and Catahoula formations, and Pliocene Goliad Formation. (After (a) Crawley et al. 1983 based on Eargle et al. 1975; (b) Adams & Smith 1981)

(Uranium districts: K.C. Karnes County; R.P. Ray Point; C.W. Clay West-Burns; R.R. Rhodes Ranch area; S.D.C. South Duval County Mineral Trend. Counties containing U deposits: 1 Washington; 2 Fayette; 3 Gonzales; 4 Karnes; 5 Atascosa; 6 McMullen; 7 Live Oak; 8 Webb; 9 Duval; 10 Zapata; 11 Jim Hogg; 12 Starr)

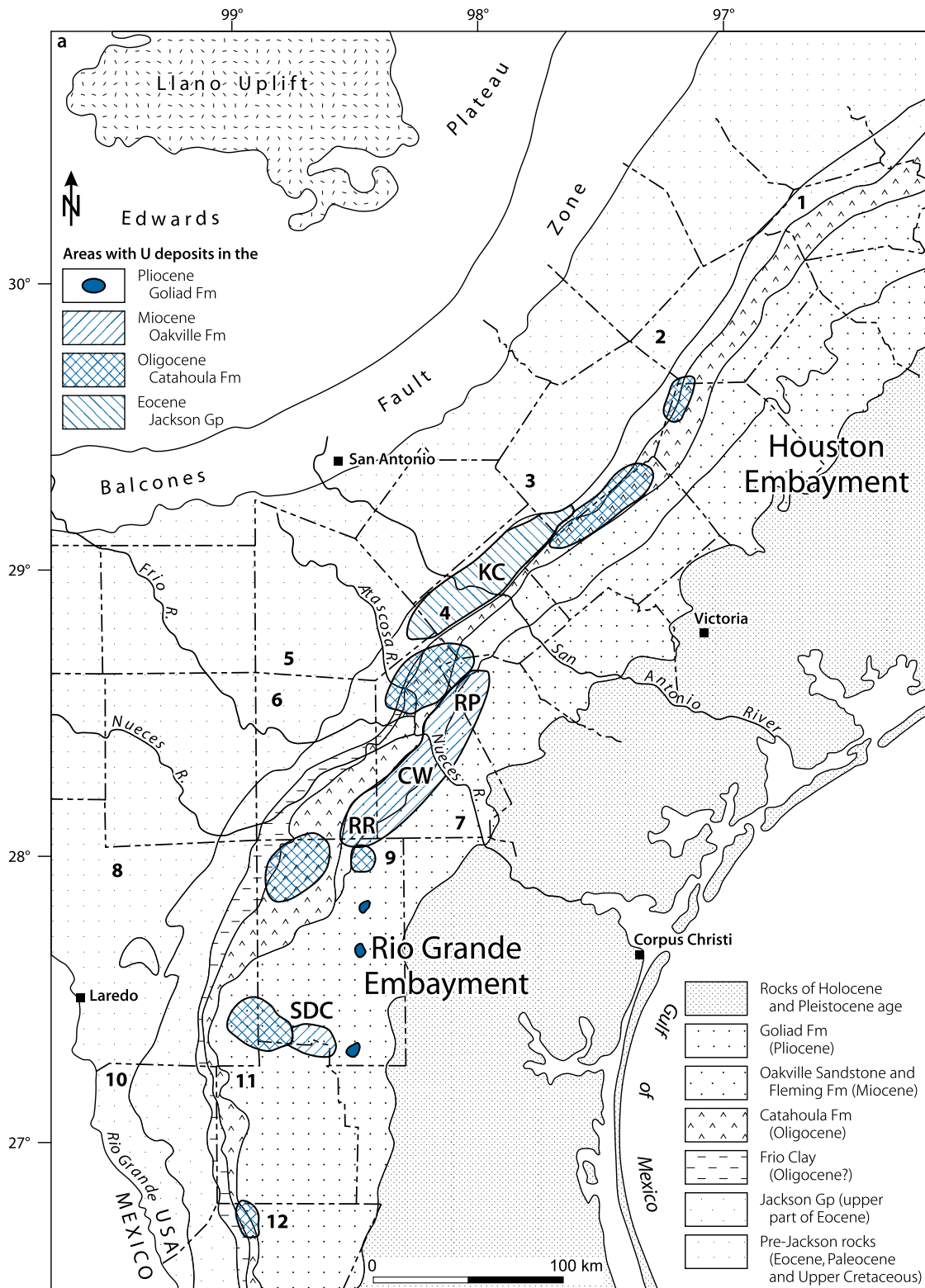
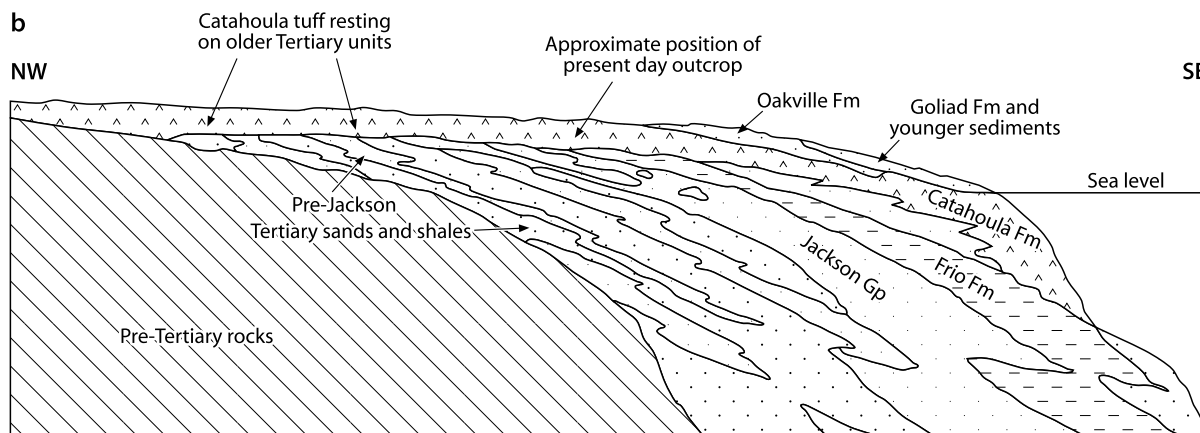


Fig. 8.2. (Continued)



particularly the late Eocene *Jackson Group*, late Oligocene *Catahoula Formation*, early Miocene *Oakville Formation*, and the late Miocene-early Pliocene *Goliad Formation*. Deposits of modest size also occur in the middle Eocene *Carrizo* and *Queen City formations*. Very young uranium was discovered in the Pleistocene *Lissie Formation*. These ore-hosting strata are, in principle, almost flat-lying; they dip about 1° SE and strike around NE-SW, almost parallel to the Gulf coast.

Characteristics of the ore-hosting units are given by Adams and Smith (1981) as follows (in ascending order) in more detail.

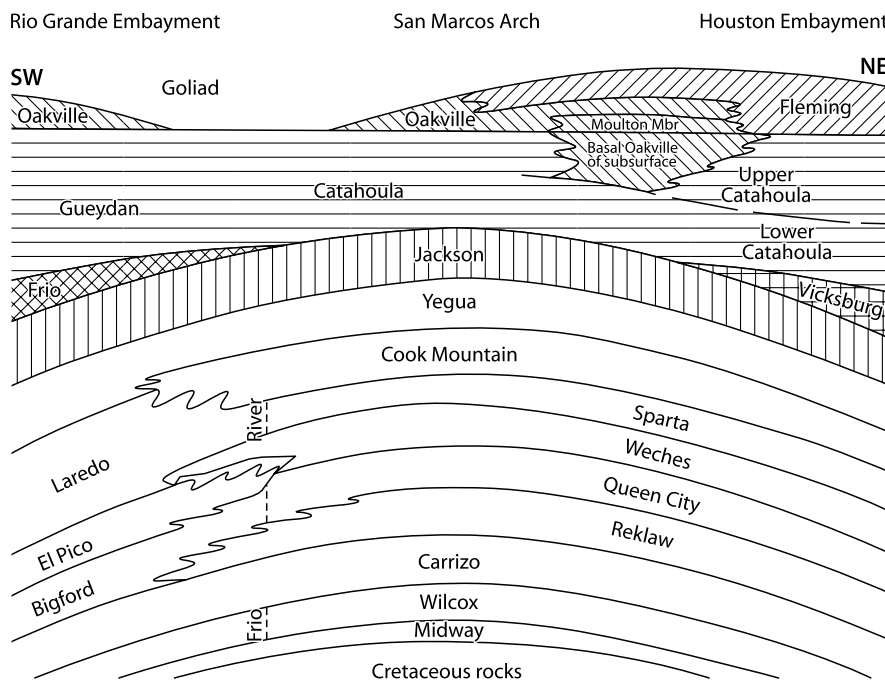
The Jackson Group is of late Eocene age. It overlies the Yegua Formation, which was deposited during a major regressive

episode. The Jackson Group is the oldest unit from which uranium has been mined. This group is characterized by strand-plain/barrier bar sand bodies, associated lagoonal muds and lignites, and minor landward channel sand bodies and gulfward shelf muds (Fig. 8.7a and b). Jackson sediments are important oil and gas reservoirs.

Four formations have been distinguished in the Jackson Group (Fig. 8.4). The *Manning* and the *Caddell formations* largely consist of fossiliferous shelf pelites that flank fluvial deltaic sediments. The *Wellborn Formation* consists generally of delta-front sands, as well as local sand units, such as the *Carlos Sandstone Member*. The *Whitsett Formation* (Fig. 8.6) comprises several local strandplain/barrier bar sand units, such

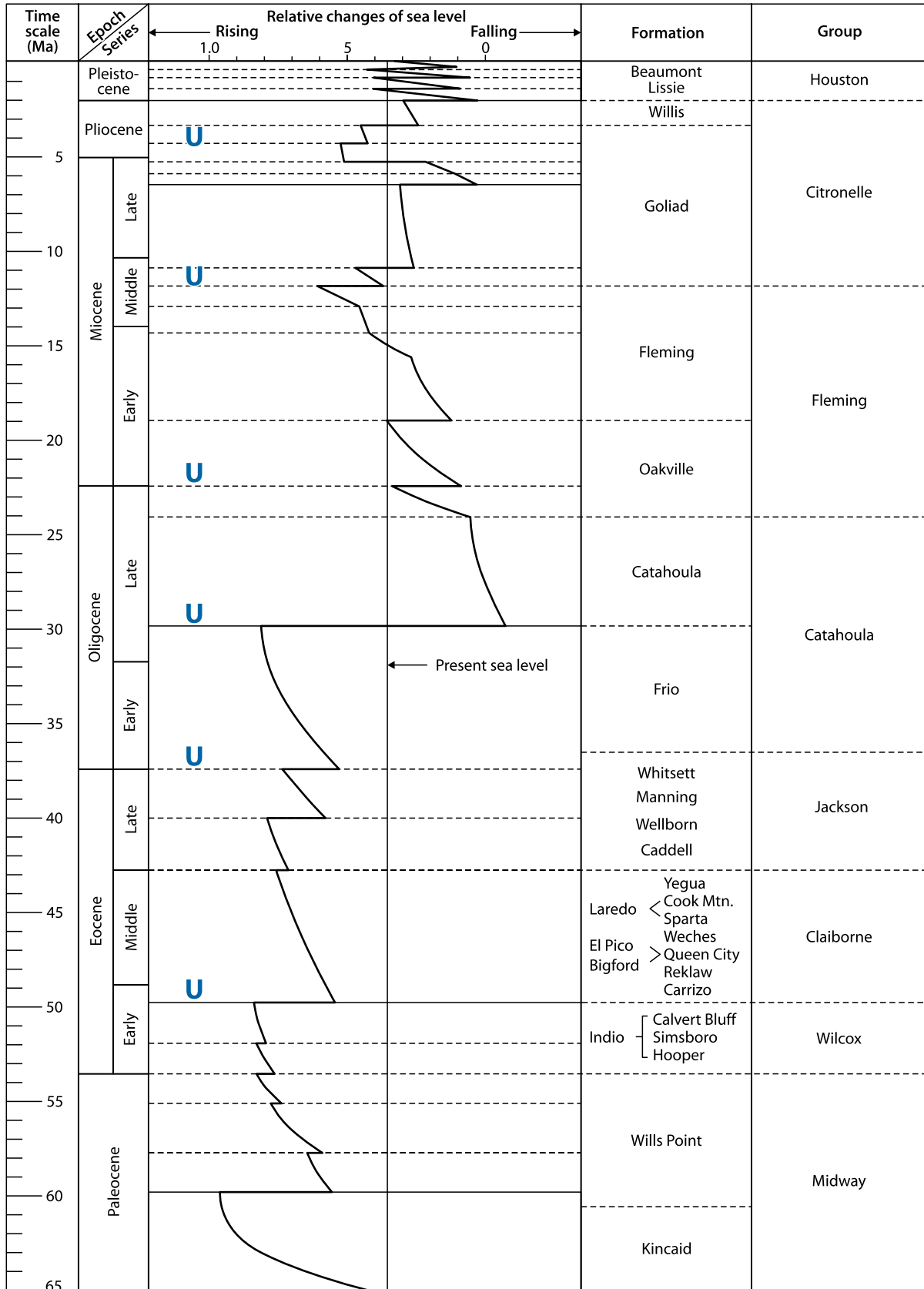
Fig. 8.3.

South Texas, schematic stratigraphic SW-NE longitudinal section along the coastal plain region. (After Adams & Smith 1981 based on Guevara & Garcia 1972, Galloway 1977, Wilbert & Tempain 1978)



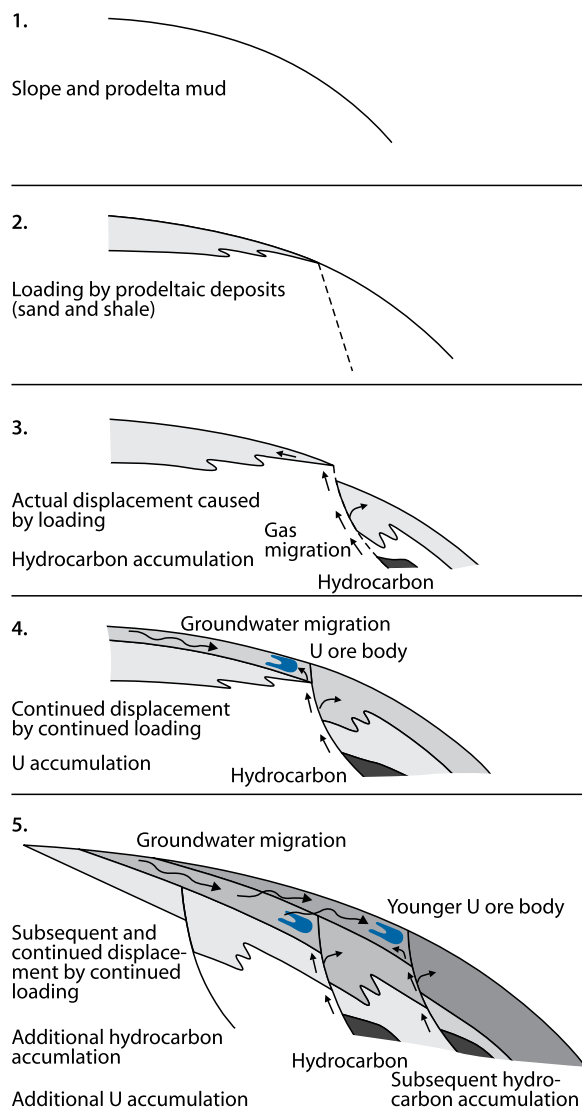
■ Fig. 8.4.

South Texas, section of Cenozoic stratigraphy, global changes of the sea level, and principal uranium-hosting units. (After Adams & Smith 1981 based on Berggren & Van Couvering 1974, Vail et al. 1977)



■ Fig. 8.5.

South Texas, diagrammatic sections illustrating the geologic-metallogenetic sequence of events involved in the genesis of roll-type uranium deposits related to fault-derived H_2S . The ingress of H_2S probably preceded and followed the formation of the rollfront but was not synchronous. (After Adams & Smith 1981)



as the Dilworth, Deweesville (or the Stones Switch), and the Calliham (or the Tordilla) Sandstone members (► Fig. 8.8), and intervening lagoonal or shelf muds (which are locally pyritic) such as the Conquista, Dubose, and the Fashing Clay members.

Lagoonal facies contain minor feeder channels leading to associated downdip strandplain/barrier bar deposits. These channels appear in outcrop in belts 8–15 km in width with thicknesses averaging 12 m. When such channels locally cut strike-oriented lagoonal sediments, such as the Dubose Clay Member, the unit becomes a dip-oriented sand body. Volcanic ash and tuff, or bentonite, commonly occur throughout the Jackson sequence and have long been considered a source for the uranium in the south Texas uranium deposits, but evidence

points more to the overlying Catahoula Formation as the uranium source (Galloway 1977; Galloway and Kaiser 1979).

Lithologies of the Jackson Group reflect lateral facies variation across the Texas Coastal Plain. From the eastern flank of the San Marcos Arch to the axis of the Rio Grande Embayment, the total Jackson Group increases in thickness from 170–205 to 230–260 m and progressively increases from four identified units in the east to nine in the west.

The Catahoula Group of Oligocene age includes the Frio and Catahoula formations. The *Frio Formation*, also named *Frio Clay*, is up to 60 m thick and most likely of lagoonal to marginal marine origin. It conformably overlies the Jackson Group and is unconformably overlain by the tuffaceous Catahoula Formation. The main Frio Clay sequence consists of massive, dark greenish

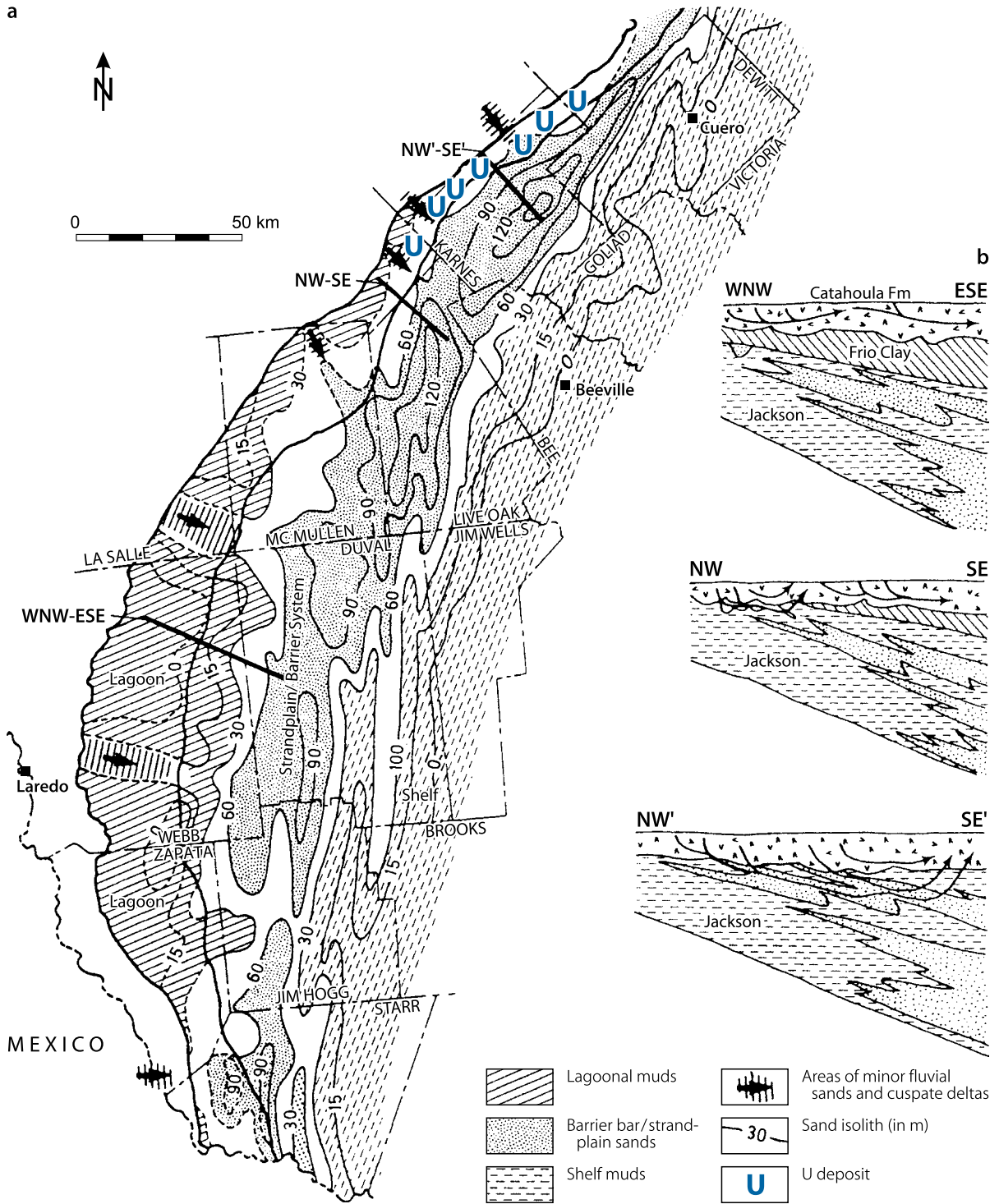
Fig. 8.6.

South Texas, litho-stratigraphic column with principal uranium-bearing units in the Rio Grande Embayment. (After Galloway 1979b)

System	Series	Group	Lithostratigraphic unit	Lithology	
Quaternary	Holocene		Flood-plain alluvium fluvial terrace deposits	Sand, gravel, silt, clay	
			Deweyville Fm, Beaumont Fm, Montgomery Fm, Bentley Fm, Lissie Fm	Sand, gravel, silt, clay	
	Pleistocene	Houston			
			Pliocene (?) Willis Fm		
	Miocene	Citronella		Goliad Fm	Fine to coarse sand and conglomerate; calcareous clay; basal medium to coarse sand- stone. Strongly calichified
				Fleming Fm	Calcareous clay and sand
		Fleming		Oakville Ss	Calcareous, crossbedded, coarse sand. Some clay and silt and reworked sand and clay pebbles near base
	Tertiary	Oligocene	Catahoula	Chusa Tuff	Calcareous tuff; bentonitic clay; some gravel and vari- colored sand near base. Soles- dad in Duval County, grades into sand lenses in northern Duval and adjacent counties
				Soledad Cgl	
(Gueydan Fm of some authors)			Fant Tuff		
			Frio Clay (or Fm)	Light-grey to green clay; local sand-filled channels	
Eocene		Jackson	Whitsett Fm	Fashing Clay	Chiefly clay; some lignite, sand, <i>Corbicula coquina</i> , oysters
				Tordilla Ss, Calliham Ss, West of Karnes Co	Very fine sand
	Dubose			Silt, sand, clay, lignite	
	Deweessville Ss			Mostly fine sand; some carbonaceous silt and clay	
	Conquista Clay			Carbonaceous clay	
	Dilworth Ss			Fine sand, abundant <i>Ophiomorpha</i>	

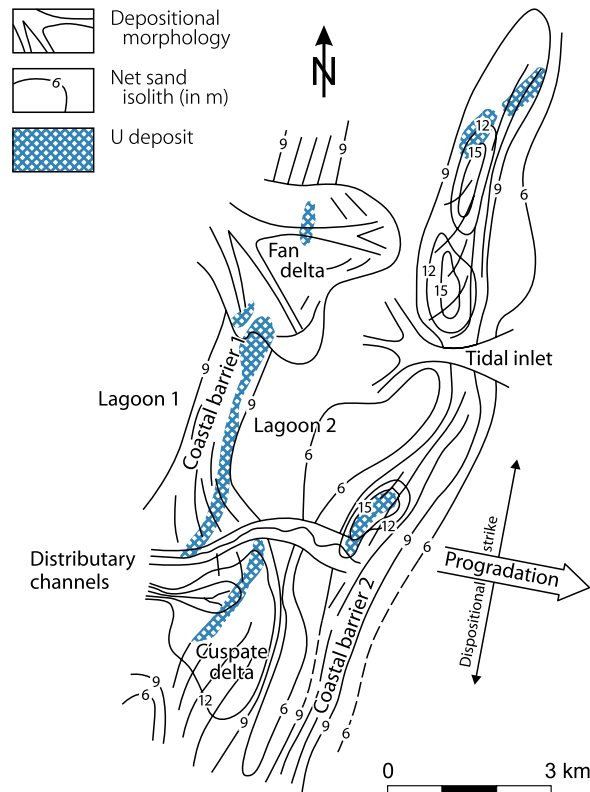
Fig. 8.7.

South Texas, depositional systems and litho-facies, and related position of uranium deposits; (a) facies and net-sand isolith map of the Eocene Jackson Group, and (b) NW-SE cross-sections showing the stratigraphic relationship of the Jackson and Catahoula aquifers, and postulated groundwater flow directions (arrows). (After Galloway 1985 based on a Galloway et al. 1979b)



■ Fig. 8.8.

South Texas, southwestern Karnes County, schematic presentation of relations between uranium deposits, littoral depositional environments, and net-sand isoliths for the Tordilla Sandstone Member of the upper Jackson Group. (After Galloway 1979b)



clay with a very minor amount of sand and sandy silt. The Frio Formation also contains some gypsum and calcareous concretions. In Karnes County, the upper contact with the Catahoula Formation is marked by a sand layer, conglomerate, and coarse detritus. The presence of gypsum as well as green clay suggests restricted, probably brackish, conditions such as found in flat-lying coastal lakes or salt marshes.

The subsurface *Vicksburg Group*, a time-equivalent unit to the Frio Formation, is an important oil- and gas-bearing shale formation representative of a transgressive sea that apparently extended to just south of the Jackson Group outcrop area. In south Texas, sand and clay interbeds indicate deposition in shallower seas as well as the influence of the paleo-Rio Grande River drainage.

The late Oligocene *Catahoula Formation* is a major host for uranium deposits. It ranges in thickness from 35 to 100 m in the area of the San Marcos Arch in the Rio Grande Embayment and increases to 240–270 m in the southern portion of south Texas. The considerable thickening is due, in part, to the greater accumulation of Catahoula tuffs in south Texas.

The Catahoula Formation is a highly tuffaceous fluvial unit that unconformably rests upon the Frio Formation and the overlapped Jackson Group. The marine coastline during deposition of the Catahoula Formation was located about 40–80 km inland from the present shoreline. The Catahoula period of regression was accompanied by major volcanic activity in west Texas and

northern Mexico, which erupted the Catahoula tuffs. Concurrent tectonic activity along the Balcones fault system and erosion of Cretaceous rocks of the Edwards Plateau by Catahoula rivers contributed reworked material including late Cretaceous fossils to the Catahoula and younger units.

As described by Galloway (1977), the Catahoula Formation consists of two distinct depositional systems that occur generally on either side of, or interfingering along the San Marcos Arch. In east Texas, the *Chita-Corrigan fluvial system* occupies the Houston Embayment and comprises three principal mixed-load fluvial drainages, as reflected by lobate constructional deltas. The *Gueydan bed-load fluvial system* occupies the Rio Grande Embayment and consists of one major drainage and several smaller fluvial channels, which lead to cusped destructional deltaic and strandplain systems. Both systems are typified by channel-fill, crevasse splay, floodplain, and lacustrine facies.

The lithology of the Chita-Corrigan fluvial system in east Texas is characterized by a higher percentage of quartzose sands and a lower percentage of volcanic rock fragments than the sands of the Gueydan fluvial system in south Texas. The latter reflects nearby volcanic source areas to the west.

Magnetite and ilmenite constitute up to 4% of Gueydan sands and less than that in Chita-Corrigan sands. Carbonate rock fragments are more abundant in sands in south and central Texas than in east Texas. This probably reflects the closer

proximity and greater exposure of the Edwards Plateau Cretaceous rocks to the Gueydan drainage.

The clay minerals of the Catahoula Formation include a mixed Ca–Na montmorillonite suite in south and central Texas and a mixed montmorillonite–kaolinite suite in east Texas. Both montmorillonite and kaolinite are thought to be alteration products of volcanic ash. Since kaolinite formation is fostered by an acidic environment rich in humic acids, it is inferred that east Texas had a relatively humid environment with more widespread vegetation. Reprecipitated calcium carbonate derived from montmorillonite is common in paleosols in south Texas, which indicates dryer conditions and sparser vegetation. Galloway (1977) points out that Gueydan paleosols commonly contain calcium carbonate concretion and cementation zones. He also notes that red, brown, or bleached oxidized soil zones exist, which attest to repeated wet and dry periods. The dryer climate is indicated by preservation of chemically unstable carbonate rock fragments and plagioclase in the sands.

In the area of Karnes, Live Oak, and McMullen counties, the Catahoula Formation has been subdivided into three members: the basal *Fant Tuff*, the middle *Soledad Conglomerate*, and the upper *Chusa Tuff*.

The Miocene *Fleming Group* is the thickest of the Tertiary litho-stratigraphic units in much of south Texas. The Fleming Group includes the Oakville and Fleming formations. Both have lithologic similarities and their regional boundaries are often gradational and arbitrary. Generally, the Fleming Formation has a larger clay fraction and the Oakville Formation a greater proportion of coarse sandstone.

The *Oakville Formation* is of early Miocene age and ranges from as thick as 60 m just east of the San Marcos Arch up to 150 m in Karnes County. It is a major uranium host and an important aquifer that unconformably overlies the Catahoula Formation. The Oakville Formation is a coarse-clastic fluvial unit characterized by reworked volcanic debris, chert, and Cretaceous rocks and fossils derived from the Edwards Plateau. Galloway et al. (1979b) describe the Oakville Formation as bed-load and mixed-load channel fills and associated sheetflow splay sands, which are bounded by floodplain muds and silts in the lower Oakville Member and the overlying Fleming Formation. Oakville sediments were deposited by several contemporaneous small to large rivers that form the Oakville bedload fluvial system. In the area mapped as the Fleming Formation, Oakville facies are bounded by relatively fine-grained, ferruginous, high-energy, mixed-load fluvial beds. Down-dip, Oakville facies grade into equivalent units of low-coastal plain and strandplain facies of deltaic and barrier bar systems. Poorly defined paleosol occurs laterally in the Oakville Formation. Montmorillonite is the most frequent clay mineral in the Oakville sediments; kaolinite is present in variable amounts, and illite in subordinate quantities. Massive, calcareous floodplain muds also occur; they contain concentrations of pedogenic micrite nodules, which attest to a syn-depositional carbonate precipitation. In outcrop, the latter is often obscured by post-depositional calichification from the Reynosa Caliche.

The Lower to Middle Miocene *Fleming Formation* ranges from 360 to 435 m in thickness from west of the San Marcos Arch to just east of its onlap by the Goliad Formation. The position of the Fleming shoreline was inland about 40 km from that of the Oakville Formation, upon which it conformably rests.

Fleming strata generally have a higher clay content, and sand beds are commonly thinner and less massive than those of the Oakville Formation. Some Fleming sediments, previously referred to as the Lagarto Formation in southwest Texas, consist of 75% calcareous mud, and the remainder being sand and silt, although in some areas the ratio of sand to clay approximates that of the Oakville sediments. Cretaceous calc-lithic fragments and fossils may be found in the sands.

Fleming lithology is described as remarkably uniform from northeast to southwest. The material of these uniform, massive, and thick pelite deposits originated from areas of high vegetation and was deposited by low-energy streams on a low-coastal floodplain or in a paludal environment during a generally more humid and warmer climate. These conditions remained generally constant for a long period as indicated by the thickness of the Fleming Formation.

The *Citronella Group* of Miocene to Pliocene age contains the Goliad Formation and presumably the Willis Formation. The *Goliad Formation* unconformably overlies the Fleming Formation and is considered to be of Miocene to early Pliocene age. The Goliad is a coarse, clastic fluvial unit that was deposited by a series of moderately low-gradient, intermittently torrential streams that crossed a broad, flat coastal plain. It is a host for several uranium ore bodies and is a major aquifer.

The Goliad Formation includes three members: the lower Lapara Sands, composed of a conglomerate largely of quartz and chert cobbles, cross-bedded coarse sand, and limy clay; an unconformable middle unit, the Lagarto Creek Beds (distinct from the Lagarto Formation), a pinkish-brown to reddish mottled limy clay; and the upper La Bahia Beds, composed of fine to coarse, cross-bedded or massive sandstone with conglomerate lenses.

The Goliad drainage consisted of a series of streams that crossed the coastal plain in a southeasterly direction. The source of Goliad rock constituents would have been crystalline rocks of the Llano Uplift and Mesozoic rocks of the surrounding Edwards Plateau in central Texas, as well as the Diablo Plateau in west Texas. Volcanic constituents of Goliad sediments probably originated from still-active volcanic fields in west Texas and northern Mexico. Along the coastal plain, *salt domes* such as Palangana, Piedras Pintas, Kingsville, and Alta Verde were emerging, during which localized areas of pre-Goliad sediments were uplifted, eroded, and redeposited by Goliad streams.

Although short wet periods apparently existed during Goliad time, conditions were generally arid. Discharge of Goliad streams was probably subject to periods of torrential rainfall, during which rivers greatly increased in both velocity and size. Principal drainages in south Texas were the ancestral Rio Grande, as well as the Nueces, Atacosa, San Antonio and Colorado rivers. Since

Goliad strata overlap older Tertiary units extending to the Jackson Group, it is apparent that Miocene and Oligocene sediments were scoured by Goliad streams. This contributed to the massive multi-storied buildup of Goliad sands of as much as 135 m downdip.

The late Pliocene *Willis Formation* is a fluvial unit composed predominantly of quartz and chert gravels, with abundant iron oxide concretions and cement. It overlies Goliad strata in the San Marcos Arch, where it is up to some 10 m thickness. In eastern Texas, Willis beds reach a thickness of 30 m or more and rest unconformably upon the Fleming Formation.

The Lissie and Beaumont formations of the *Pleistocene Houston Group* overlap the Willis Formation. The younger Beaumont Formation consists mainly of clay and silt with lesser amounts of channel and barrier island sands and gravels. It has no known uranium mineralization. During the Pleistocene, the position of the shoreline ranged from several tens to hundreds of meters below the present sea level during glacial periods, and to about 15 m above the present sea level during interglacial intervals.

Ore-hosting sandstones of the various litho-stratigraphic units are of continental fluvial and marginal marine deltaic, lagoonal, and littoral provenance. Permeable, fine-grained, tuffaceous, pyrite-bearing, arkosic sandstones are preferential host rocks. They contain only locally, as in the Jackson Formation, carbonaceous plant material. Sands are interbedded with tuffaceous, zeolitic, and bentonitic mudstones and lignite seams. Volcanics are of rhyolitic, trachytic, and trachy-andesitic composition.

In spite of their wide stratigraphic range, uranium deposits are restricted to a belt (▶ Fig. 8.2a), the boundaries of which do not entirely correspond with regional geologic boundaries. Although the trend does reflect important geologic features, such as strike of formations and positions of favorable lithologic facies in some host sediments, some geologic features cross the trend. Of particular interest are persistent fluvial depositional zones that form mega-channels. These mega-channels tend to provide favorable environments for the location of uranium ore bodies.

Adams and Smith (1981) attribute the various Tertiary fluvial sediments, in particular those of the ore-hosting Jackson Group and the Catahoula, Oakville, and Goliad formations to 13 *mega-channel systems*, which trend in a NW–SE direction across the Tertiary coastal plains of south Texas. The extent of these channel systems varied throughout the Cenozoic Era, at times covering broad areas as during Catahoula and Oakville deposition, and at other times they were restricted to a few trunk channels (e.g., Jackson and Goliad channels). Within mega-channels, positions of fluvial channels in various formations are not independent of one another, but tend to be superimposed and stacked as a succession of younger sand bodies toward the Gulf of Mexico. These sand masses are more or less interconnected and have probably affected growth faulting and groundwater hydrology. There was no major tectonic or volcanic action in the Gulf coast plain during the Tertiary. This is important to the understanding that the stream systems were consistent throughout Tertiary

time. Any changes in stream deposition are related to base line changes relative to changing sea levels.

Most south Texas uranium deposits occur in clusters more or less along fluvial trends in one of the mega-channels, except for deposits in the Jackson Group, which are hosted in littoral environments such as beach sands.

Principal Host Rock Alteration

Prominent alteration modes include repeated oxidation and partial re-reduction of U-hosting sand horizons (▶ Fig. 8.9). Many south Texas U ore bodies, particularly those in the Jackson Group, are of roll-type and are located at the edges of altered sandstone tongues (▶ Fig. 8.10a). Host rocks for these ore bodies exhibit the general mineralogical and geochemical features of the unaltered downdip and altered, oxidized updip sands similar to those of the rollfront deposits in the Wyoming Basins (see Chap. 2 Wyoming Basins for more details on alteration mineralogy and chemistry).

In addition to the normal alteration phenomena of a rollfront, however, some south Texas rolls exhibit peculiarities. Adams and Smith (1981) note, for example, that the mineralogy of a roll-type deposit in the *South Duval County Mineral Trend* indicates that two alteration zones exist within the oxidized tongue: the first is well updip from the rollfront and contains Fe–Ti oxides that are in various states of oxidation. The second extends for a variable distance back updip from the rollfront and contains ilmenite and magnetite. In reduced sands downdip from the rollfront, Fe–Ti oxides have been completely destroyed, in part through replacement by pyrite. Studies indicate that alteration of Fe–Ti oxides to pre-ore-stage pyrite most probably resulted from invading H₂S-bearing solutions. Subsequent introduction of oxygenated solutions into these sulfide-bearing sands oxidized pyrite and produced geometric relations as shown in ▶ Fig. 8.9.

At other places, some roll-type deposits occur entirely within reduced, sulfide-bearing sandstone. H₂S is considered the likely source for re-reduction, supposedly introduced in multiple post-ore stages interspersed with oxidation episodes. The process resulted locally in a complex series of alteration zones and also multiple rollfronts.

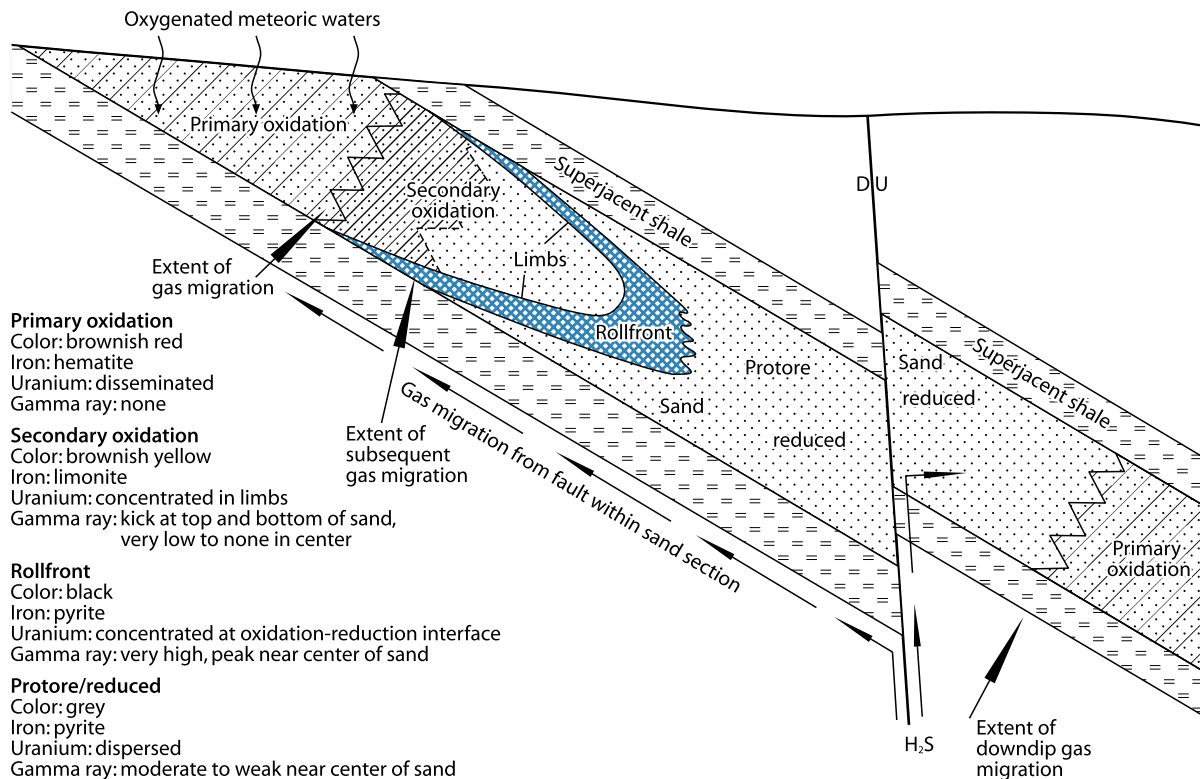
Deposits in the Catahoula and Oakville formations contain marcasite in a broad zone downdip from rollfronts (▶ Fig. 8.10c–g). This marcasite is interpreted to have formed during ore formation by oxidative destruction of pre-ore-stage pyrite in sulfide-rich, carbonaceous-poor sediments.

Principal Characteristics of Mineralization

Unoxidized ore contains pitchblende/sooty pitchblende and coffinite as dominant U minerals. Associated minerals and elements include pyrite, marcasite, calcite, Mo, Se, and locally clinoptilolite, authigenic feldspar, montmorillonite, and opal. Pyrite and marcasite occur in several pre-, syn-, and post-ore stages.

Fig. 8.9.

South Texas, diagrammatic section across a rollfront U ore body illustrating the distribution of alteration zones and their relations to fault-controlled influx of reducing media (H_2S , hydrocarbons) leading to secondary reduction followed by partial re-oxidation of the altered tongue. (After Adams & Smith 1981)



Oxidized ore contains hexavalent U minerals, chiefly uranyl phosphates (autunite), -vanadates (tyuyamunite, more rarely carnotite), and -silicates.

Unoxidized uranium ore is found in two configurations, in *roll-type* and *non-roll-type ore bodies*. Many deposits are of classical rollfront type emplaced at the margins of alteration tongues in sandstone. They display the characteristic uranium disequilibrium pattern, elemental zoning, and mineral distribution of Wyoming roll-type deposits, which indicate that they formed by ingress of oxidizing, uraniferous solutions into reduced sandstones containing pyrite and, in a few cases, carbonaceous plant debris (► Fig. 8.10).

Other deposits do not resemble roll-type mineralization as known from deposits in Wyoming Basins. Important differences include: (1) Mineralization is not situated at the margin of oxidized sandstone tongues, but rather occurs entirely within reduced, pyrite-bearing, practically hematite- and limonite-free sandstone (► Figs. 8.9 and 8.11) and (2) host sands contain essentially no carbonaceous plant material, only abundant disseminated pyrite.

Goldhaber and co-workers have supported early suggestions that the abundance of pyrite within the sands probably reflects introduction of H_2S , which migrated upward along faults from hydrocarbon reservoirs deeper in the sediment sequence. Such introduction prior to ore formation, prepared the sands for

rollfront development, whereas post-ore H_2S ingress caused re-reduction of segments of the altered tongue, leaving the deposit suspended in reduced sandstone. These deposits are, therefore, only a variant of roll-type deposits.

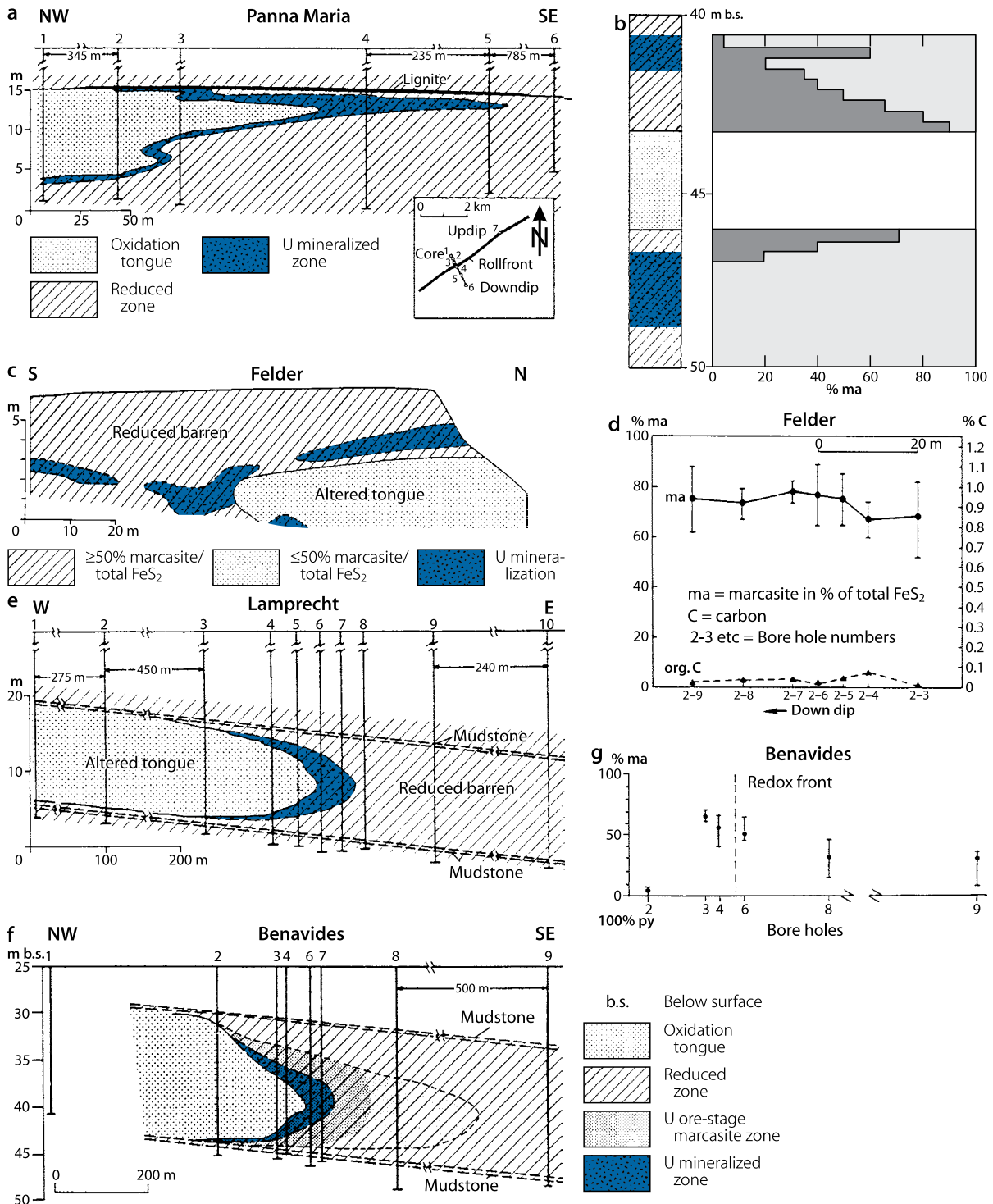
On the other hand, Busche et al. (1981) present evidence from three deposits (Felder, Lamprecht, and Zamzow in the Ray Point district), which suggests that ore formation was not accompanied by introduction of significant amounts of H_2S .

Adams and Smith (1981) point out that, in essence, emplacement of ore in a sequence of mixed fluvial-marginal marine sediments produced rather complex and unpredictable characteristics and distribution of rollfronts and ore bodies. These features of mineralization reflect: (1) alternation of numerous host rock facies typical of a mixed fluvial-shallow marine origin; (2) a complex interrelationship of rapid lateral and vertical changes in lithology; and (3) relations between transmissive sediments and indigenous and extrinsic reductants. All significant uranium concentrations are associated with permeable sandstones. Larger deposits are generally associated with more permeable units, although the actual position of mineralization may now be in close proximity to, or in juxtaposition with finer grained, less permeable sediments.

Uranium deposits are furthermore related to unconformities as documented by their common localization within the lower part of generally porous, regressive sediments and above

Fig. 8.10.

South Texas, comparison of distribution of principal alteration zones, and marcasite (*ma*) abundance relative to total iron disulfide contents in uranium deposits of different districts and hosted by different stratigraphic units. (a) and (b) Karnes County, *Panna Maria deposit*, Eocene Whitsett Formation, Jackson Group [(a) NW-SE cross-section; (b) graph of marcasite/total FeS₂ ratios]; (c), (d), and (e) *Ray Point district*, Miocene Oakville Sandstone, (c) and (d) *Felder deposit/pit 4b* (c) S-N cross-section, (d) graph of marcasite(*ma*)/total FeS₂ ratios and contents of organic carbon(C); (e) *Lamprecht deposit*, (f) and (g) South Duval County Mineral Trend, *Benavides deposit*, Soledad Member of Oligocene Catahoula Formation [(f) NW-SE section, (g) marcasite/total FeS₂ graph]. [After (a-d) and (f) Reynolds, Richard L., Goldhaber, Martin B., 1983, Society of Economic Geologists, Inc., *Economic Geology*, Fig. 3, p. 108; Fig. 4, p. 109; Fig. 5, p. 110; Fig. 6, p. 111; Fig. 7, p. 112; (e) Goldhaber et al. 1979; (g) Goldhaber, Martin B., Reynolds, Richard L., Rye, Robert O., 1978, Society of Economic Geologists, Inc., *Economic Geology*, Fig. 3, p. 1694]



impermeable transgressive units. It seems to make little difference for uranium emplacement whether aquifers of regressive units are of strandplain, barrier bar, deltaic, or fluvial origin. Bounding transgressive aquitards include clays and muds laid down in marine shelf and lacustrine environments.

South Texas U deposits occur in four principal *geological settings*: (1) Beach sandstones and related sediments; (2) sandstones along the margins of major fluvial channel systems; (3) sandstones close to faults along which hydrogen sulfide could have migrated into the aquifer; and (4) sandstones above salt domes. These various deposit settings may overlap or be superimposed upon one another.

Stratigraphically, uranium mineralization has been found at specific intervals throughout two thirds of the Cenozoic stratigraphic column covering a time span from 12 to 8 Ma (Fig. 8.6). The following units contain significant uranium occurrences (from oldest to youngest): Tordilla and Deweesville sandstones of the Whitsett Formation, Jackson Group, Catahoula Formation, Oakville Formation/Sandstone (Moulton Sandstone), Lower Goliad Formation (Lapara Sand), and possibly the Lissie Formation. In all these formations, except for beach sands of the Jackson Group, uranium occurs within permeable regressive sediments that unconformably rest upon impermeable transgressive sediments. The latter include the Upper Wilcox Group, Manning Formation, Frio Clay, Lower Oakville Formation, Fleming Formation, and possibly the Lagarto Creek Member of the Goliad Formation.

Although anomalous uranium concentrations are widespread in the uranium belt of the Texas Coastal Plain, Adams and Smith (1981) suggest that all noteworthy uranium occurrences tend to be grouped in fluvial mega-channel systems as discussed earlier. These channel systems were formed and maintained practically over the entire time span from the early Eocene Wilcox Group to the Pleistocene Lissie Formation. A number of mining districts are known within these systems, the most important of which are shown in Figs. 8.1 and 8.2.

Out of the above listed stratigraphic units, the Catahoula and Oakville formations contain the most productive uranium horizons. They account for more than 60% of the known uranium resources in south Texas.

The *South Duval County Mineral Trend* is by far the largest district and has more established uranium resources than any other district. With Holiday-El Mesquite it hosts one of the largest deposits, as well as several smaller deposits in at least three different stratigraphic formations. The trend represents a mega-channel sand system that extends for about 50 km in WNW–ESE direction. Margins of the trend are believed to be the approximate edges of major channel sands within each of the successive stratigraphic uranium-hosting formations. Sands were deposited in successively younger formations progressively farther down-gradient and are likely interconnected, which granted at least some hydrologic communication.

The base of fresh groundwater crosses formational units and maintains a near-horizontal position. This suggests that the oxygenated groundwater that entered the aquifers throughout geologic time could migrate for considerable distances down the mega-channel system. Uranium in these waters, therefore, could also be transported over great distances until it encountered

reduced sandstone within any of the favorable stratigraphic units where it would precipitate in rollfronts. Reduced environments probably developed where the megachannel system has been cut by faults, through which extrinsic H_2S has invaded into various sands of Tertiary strata.

General Shape and Dimensions of Deposits

The shape of uranium ore bodies in south Texas is commonly cusped or C-shaped when hosted in uniform sands that are bounded by impervious mud- or siltstone beds (Figs. 8.9–8.11, see also figures in the section “Individual U Districts”). Many deposits exhibit a complex configuration, however, due to the often complex interrelationship between sand units of variable permeability and pelitic units of very low permeability. In addition, indigenous and introduced reductants influenced the distribution and habit of uranium rolls. In carbonaceous-rich sediments such as those of the Jackson Group, the shape of a rollfront ore body is governed largely by the shape of the ore-hosting sand bodies, their relations with adjacent and enclosing finer-grained sediments, and the abundance and distribution of carbonaceous material. Large concentrations of carbonaceous material in permeable sands tend to form high-grade uranium concentrations with sharp rollfront boundaries. Dispersed organic trash concentrations appear to form diffuse, lower grade roll-type deposits. Carbonaceous-rich sediments adjacent to permeable sands, such as lignite horizons, commonly have uranium concentrated at the boundary of the sand, but minable grades and thicknesses are rare due to the impervious nature of lignite.

In general, south Texas U ore bodies tend to be smaller and of lower grade than rollfront U deposits in Wyoming Basins. They are generally thin, seldom exceeding 5 m in thickness, and rarely occur as stacked or multiple-front deposits, such as are common in some deposits in Wyoming. Deposits contain only up to about 3,000 t U (e.g., Palangana). The average grade is on the order of 0.08–0.09% U.

Potential Sources of Uranium

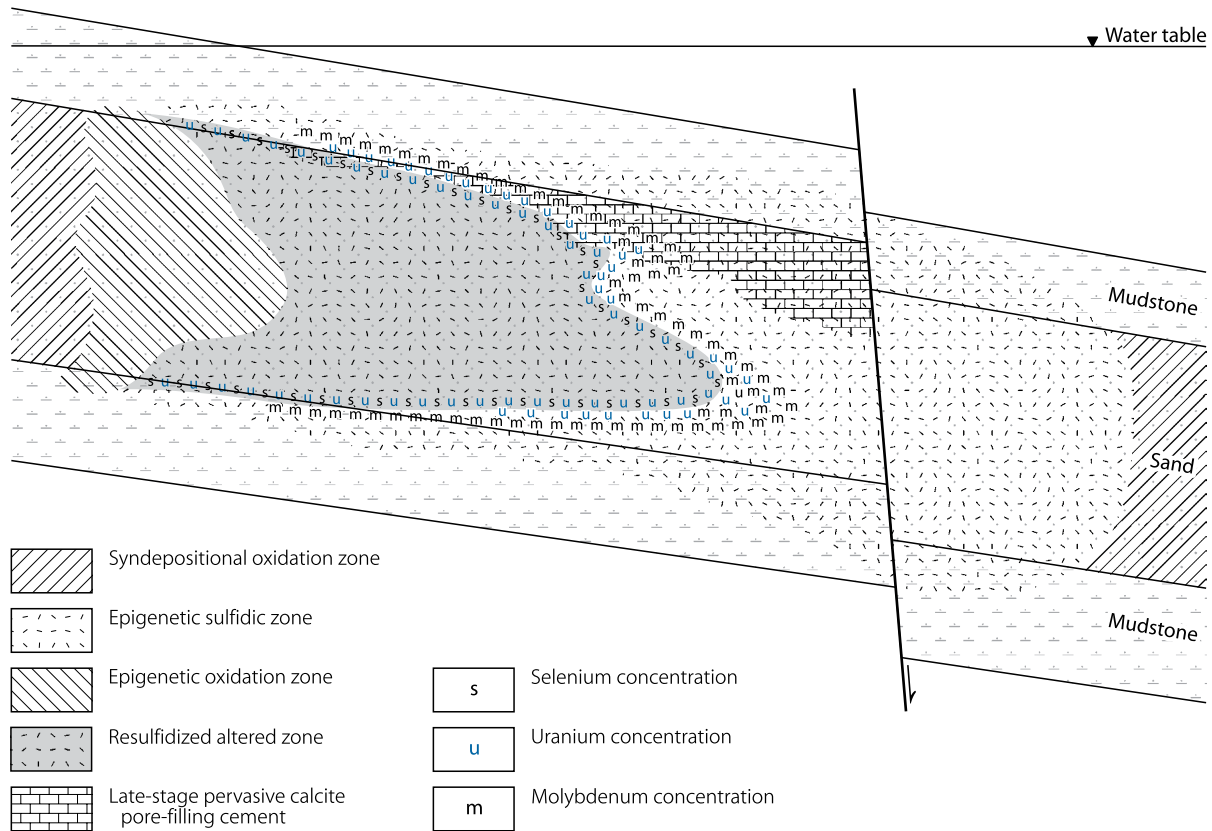
Uraniferous pyroclastics are the most favored source of uranium. This hypothesis is supported by geochemical and geological data provided by Adams and Smith (1981), Dickinson (1976b), Eargle and Weeks (1973), Galloway (1977), and others. The deposits may have derived their uranium either intraformationally from interbedded pyroclastics, as found in the Catahoula, Jackson and Oakville formations, or extraformationally from the (former) superposition of the Catahoula or similar fertile tuffs above an unconformity (for more see subsequently Chap. Metallogenetic concepts/Section Uranium source).

Principal Ore Controls and Recognition Criteria

Following Adams and Smith (1981), significant ore-controlling or recognition criteria of the south Texas uranium deposits include:

■ Fig. 8.11.

South Texas, schematic section across a roll-shaped uranium ore body demonstrating the typical association with a fault zone, and alteration and metal zoning characteristic for uranium-hosting aquifers of the Catahoula and younger formations. Multiple epigenetic alteration stages include pre- and post-ore sulfidization, ore-stage epigenetic oxidation, and modern oxidation. U, Se, and Mo minerals precipitated and are zoned across the front of mineralization. (After Galloway 1985)



Host Environment

- Marginal marine environment of Tertiary age composed of complex heterogeneous sedimentologic systems
- Sediments range from littoral-marine to fluvial-continental facies with intercalated and/or incorporated felsic pyroclastic material
- Fluvial channels in various stratigraphic formations tend to be superimposed and stacked in the form of mega-channels
- Favorable sand facies susceptible for migration of uraniferous groundwater and mineralization include
 - Point bars, lateral bars, and crevasse splays associated with fluvial channel systems (Fig. 8.21) and
 - Barrier bars and off-shore bars deposited in littoral domains (Fig. 8.8)
- Relations between permeable and adjacent non-permeable sediments vary both laterally and vertically
- Original composition and provenance of host arenites at many deposits (e.g., in Oakville Fm.) seem to be of no or only minor importance for the precipitation of uranium except for sands containing carbonaceous debris (e.g., in Jackson Group)

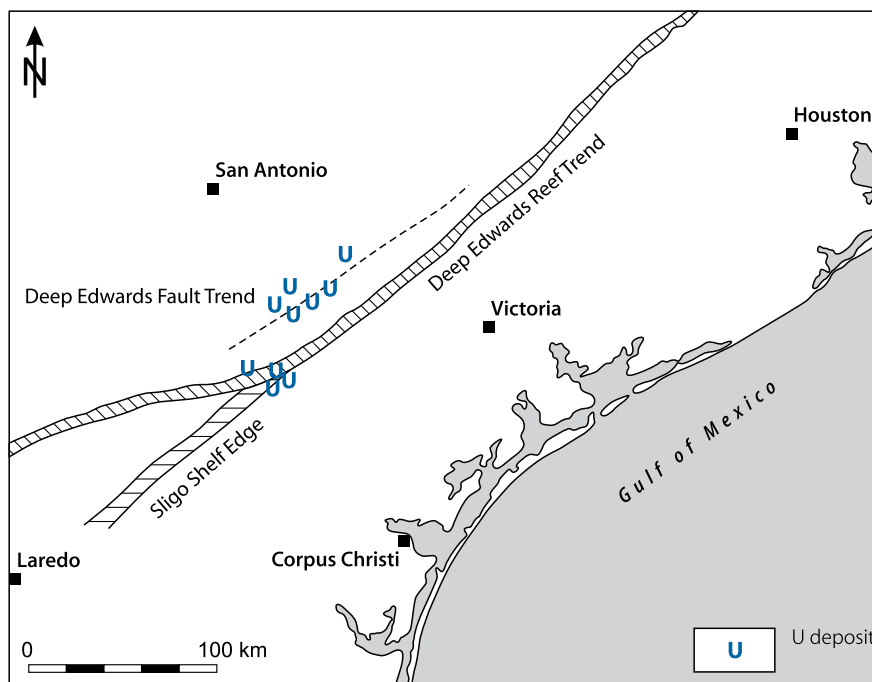
- Growth faults cut the multi-stratigraphic sedimentary sequence, thereby they
 - Interconnect more or less the various permeable sand units
 - Provide interstratigraphic pathways for oxygenated groundwater and migrating reductants, and, consequently
 - Governed the development and spatial distribution of reduced, pyrite-bearing sandstones, and finally uranium emplacement (Figs. 8.9 and 8.5).

Alteration

- Ore-hosting horizons show effects of repeated stages of oxidation and reduction
- Oxidation of mineralized sands is expressed by color changes and the typical mineralogical effects of exposure to oxidizing solutions, in particular oxidation of pyrite
- Reduction phenomena are primarily reflected by sulfidization due to invasion of extrinsic reductants, and by destruction of Fe–Ti oxides
- Sands affected by reduction and subsequent re-oxidation do not contain either Fe–Ti oxides or their oxidation products.

Fig. 8.12.

South Texas, simplified map illustrating the location of uranium deposits with respect to the surface-projected position of the Cretaceous Edwards Carbonate Reef Trend, Deep Edwards Fault Trend, and the Cretaceous Sligo Shelf edge. (After Adams & Smith 1981 based on Goldhaber et al. 1979)



Mineralization

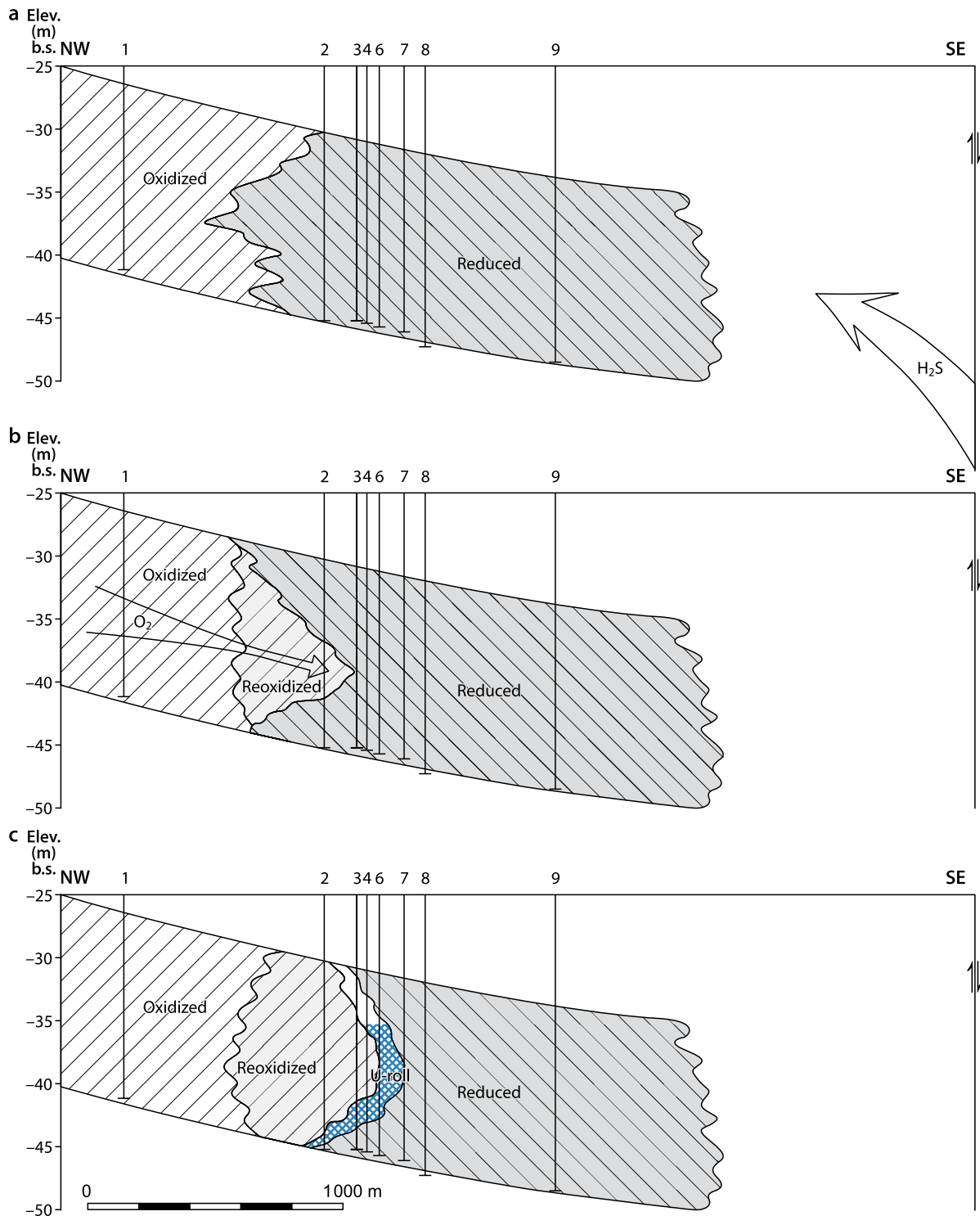
- Most deposits are of low grade (<0.1% U) and low tonnage (<4,000 t U)
- Mineralization essentially consists of pitchblende/sooty pitchblende and coffinite associated with mainly Fe-sulfides and minor Mo, Se, and V minerals
- Mineralization is largely of disseminated texture
- Ore occurs within or in proximity to permeable sandstones ranging in composition from littoral quartz arenites to fluvial arkoses
- Major U deposits are positioned in two different geochemical environments:
 - At the redox boundary on the downdip margin of tongues of oxidized sandstone in the form of classical rollfront deposits (e.g., in the Jackson Group and the Catahoula Formation) and
 - Entirely within reduced, pyrite-bearing sandstone as non-rollfront associated deposits (e.g., in Catahoula, Oakville, and Goliad formations)
- Rollfront-related ore bodies exhibit variable shapes in cross-section ranging from
 - The characteristic C-shaped form and associated element zoning (Fig. 2.6a,b) as typical for a dynamic propagation of the redox front down the hydrologic gradient, to
 - Irregular geometries, where host sands are interbedded with argillaceous material that apparently prevented development of the crescentic roll shape
- Non-rollfront ore bodies can have almost the classic crescentic shape (e.g., Felder, Clay West, Rhode Ranch, etc., deposits in Oakville Fm.) indicating that they are classic rollfronts in shape but are enveloped in later stages of reduction (Figs. 8.9; and 8.11)
- Lenticular deposits (e.g., Holiday-El Mesquite deposit in South Duval County Mineral Trend) are elongate parallel to the axis of groundwater movement and occur at the lateral boundary between oxidized sandstone and H₂S-reduced, pyrite-rich sandstone (Fig. 8.20)
- Broad-scale sedimentary features that control distribution and configuration of major U deposits and ore trends include in particular
 - Mega-channel systems (Fig. 8.1) and
 - Beach environments (Fig. 8.8)
- In mega-channel systems (e.g., South Duval County Mineral Trend), ore trends are dip orientated and deposits are localized in successively younger formations in a downdip direction
- In beach environments (e.g., of the Jackson Group), strike-oriented rollfronts occur in littoral sands instead of continental fluvial channel sands.

Metallogenetic Concepts

Adams and Smith (1981) consider the Texas uranium province to be unique among sandstone-type uranium domains in that

■ Fig. 8.13.

South Texas, stages in the evolution of a roll-type uranium deposit as proposed by Goldhaber et al. (1978) (b.s. elevation below sea level). Stage (a) involves introduction of H_2S from a fault causing progressively updip sulfidization of the host rock. Stage (b) occurs in response to cessation of H_2S influx and ingress of oxygenated uraniumiferous groundwater and by that in the development of an altered tongue and deposition of the uranium at the edge of the redox interface. Ore-stage iron disulfide minerals crystallize via sulfur redistributed from oxidation of pre-ore iron disulfides. Stage (c) finally created the present disposition of the uranium roll within reduced sands adjacent to the oxidized tongue. (After Goldhaber, Martin B., Reynolds, Richard L., Rye, Robert O., 1978, Society of Economic Geologists, Inc., *Economic Geology*, Fig.8, p.1703)



the deposits are developed within a marginal marine environment. The two authors elaborate in depth on the salient criteria that were influential in the genesis of the various modes of uranium mineralization in the South Texas deposits. Adams and Smith (1981) specifically address the following topics as metallogenetically essential as given below in abbreviated form.

Depositional environment

On a regional basis, many U deposits in south Texas are located near major tectonic elements such as the Deep Edwards fault trend (▶ Fig. 8.12). On a sedimentological basis, south Texas U deposits are hosted within a complex heterogeneous sedimentological system ranging from littoral-marine to fluvial-continental environments. The configuration of sand bodies and resulting groundwater regimes are vastly more complicated than those of braided fluvial systems as, e.g., in Wyoming Basins. The distribution and characteristics of uranium deposits depend, therefore, on the local mode of sedimentation and relations between sediments of diverse depositional environments, in addition to the normal geochemical and physico-chemical conditions required for uranium transport and precipitation.

Host environment

1. *Stratigraphic units* containing major uranium deposits are the late Eocene Jackson Group, late Oligocene Catahoula Formation, early Miocene Oakville Formation, and the late Miocene-early Pliocene Goliad Formation (▶ Fig. 8.6)
2. Ore-bearing lithofacies are confined to permeable arenites, which range in composition from quartz sandstone to arkose. Metallogenetically, arenites appear to be of primary importance as aquifers, which permitted migration of uraniferous groundwater, whereas the composition and provenance of sandstones seem to be of no or only minor importance for emplacement of ore provided most clasts are resistant to alteration, i.e., quartz and feldspar. Deposits in the Jackson Group, for example, occur in quartz arenites deposited in a marine beach and bar environment (▶ Fig. 8.7), whereas the balance of deposits in south Texas are largely hosted by arkoses and subarkoses of fluvial origin
3. Depositional environments of sand bodies of sufficient permeability and transmissivity susceptible for mineralization include point bars, lateral bars, and crevasse splays laid down in fluvial environments, and barrier bars and off-shore bars deposited in littoral domains. These favorable sand facies occur in complex relations one to another. Associated unfavorable finer-grained sediments include silt-rich crevasse, floodplain, lagoonal, swamp, and lacustrine sediments. Relations between these permeable and nonpermeable sediments vary both laterally and vertically. The position of fluvial channels in various formations, however, do not appear to be independent of one another but tend to be superimposed and stacked in the form of mega-channels. These masses of sand are cut by growth faults and hence are more or less lithologically interconnected, thus affecting groundwater hydrology.

As a consequence, they have controlled pathways for oxygenated groundwater and mobile reductants and thereby reduction of sandstones through formation of pyrite, and finally uranium emplacement

4. Configuration and continuity of mineralization was strongly governed by the various depositional environments and their interrelationships. The distribution of ore trends, for example, is controlled by broad-scale sedimentary features such as mega-channel systems. They are responsible, for example, for the dip-orientation of ore trends in the South Duval County Mineral Trend as outlined later. A different broad-scale sedimentary feature is reflected by strike-oriented rollfronts in beach sands of the Jackson Group and associated position of U ore bodies (▶ Fig. 8.7a)
5. Mega-channel systems host uranium ore bodies in successively younger formations. For example, the South Duval County Mineral Trend has uranium deposits in successively younger formations along a mega-channel system in a down-dip direction (see later). Similar relations can be seen in the North Bee County Mineral Trend, where mineralization occurs in successive units of the Jackson Group, possibly in Frio sands, in Catahoula sands, and finally in Oakville sands. The North Live Oak County Mineral Trend has ore bodies in the Catahoula, Oakville, and Goliad formations.

Exceptions to this are several deposits in the Jackson Group that do not occur in continental fluvial channel sands, but rather in littoral sands. But even the Jackson deposits appear to be close to a Jackson fluvial channel, which may have supplied oxidizing uraniferous water to basal sands.

Reductants

Two principal reducing agents appear to be critical for south Texas deposits: (a) Hydrocarbons- H_2S in fluvial sands of the Catahoula, Oakville, and Goliad formations, which contain finely dispersed pyrite and (b) detrital vegetal organic matter in littoral sands of the Jackson Group.

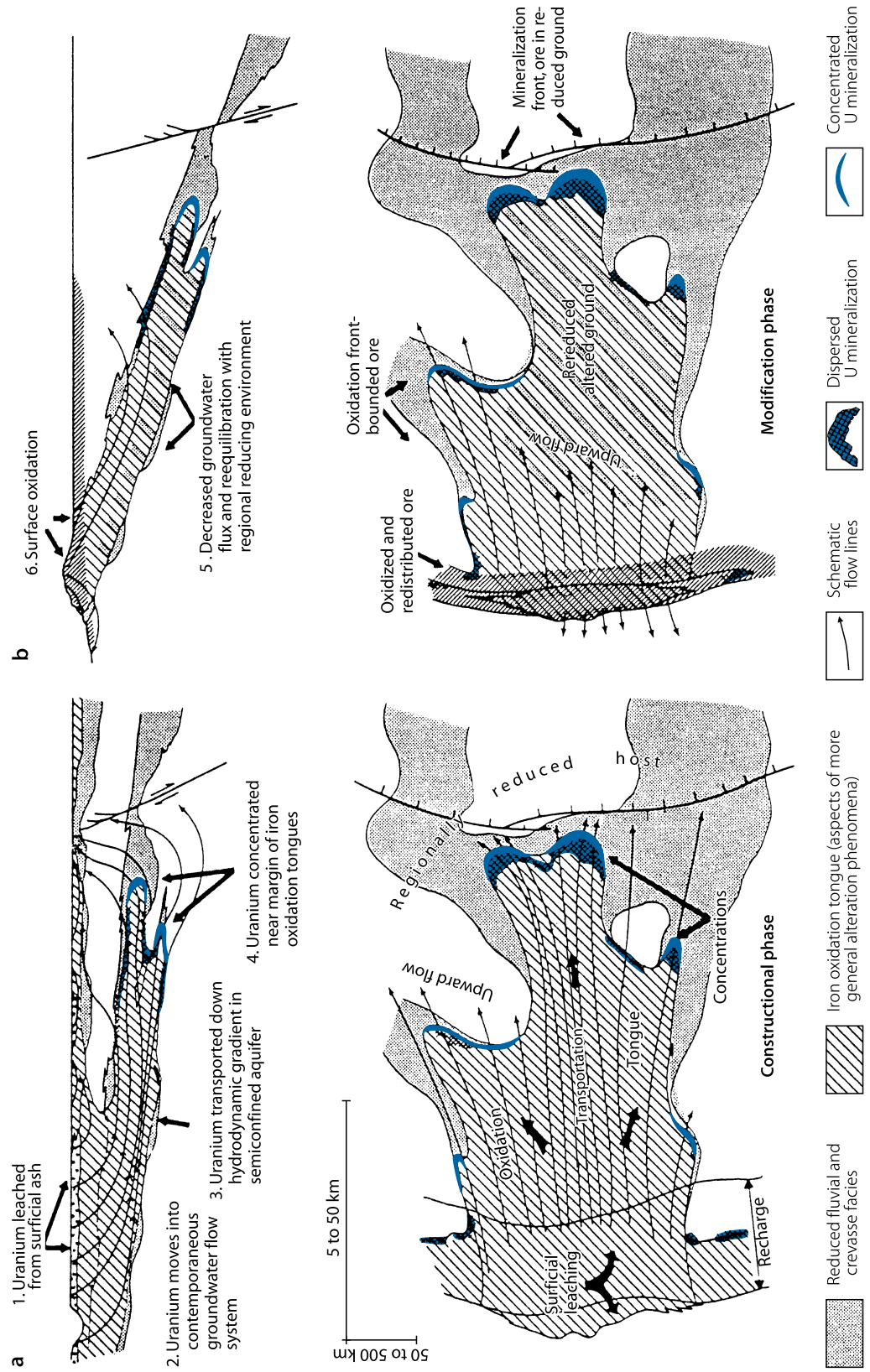
Hydrocarbons- H_2S : The assumption that H_2S invaded the aquifers probably along faults and presumably from hydrocarbon reservoirs at depth is largely based on the following criteria: (a) The spatial association of these pyritiferous sands with respect to faults, (b) sulfur isotope data, (c) the presence of some reduced sandstones entirely within oxidized sandstone, and (d) the virtual absence of carbonaceous material.

The absence of uranium deposits over wide areas of otherwise favorable mega-channel sands may indicate that these sands escaped reduction by H_2S .

Hydrologic and mineralogic data indicate an early formation of uranium ore. Hence, the first introduction of H_2S to form pyrite must have been immediately after burial, but prior to ore formation.

Goldhaber et al. (1979) and Reynolds and Goldhaber (1983) established at least four periods of probable H_2S introduction, and the presence of two different *sulfur isotopes* in sulfides of Oakville host sandstones (▶ Table 8.1): (a) Isotopically heavy sulfur, which may have been derived from deep Edwards

Fig. 8.14. South Texas, diagrammatic illustration of the processes involved in (a) the formation and (b) modification of roll-type uranium deposits proposed by Galloway for the Catahoula fluvial systems. The constructional phase includes mobilization, transport, and concentration of uranium within a semi-confined aquifer system coeval with or soon after deposition of volcanic ash in the groundwater recharge terrane. Development of an extensive oxidation tongue is the most obvious phenomenon in course of the original U concentration stage. Subsequent modification of the original mineralization includes re-reduction of segments of the oxidation tongue where the groundwater becomes stagnant, and reducing solutions entering the ore-hosting sand unit along faults intersect with the oxidation system, and late oxidation with minor remobilization and destruction of shallow ore bodies by meteoric water above the ambient water table. The scale on which this cycle may operate can vary in proportion to the size of the aquifer system. (After Galloway 1979b, 1985)



■ **Table 8.1.**

South Texas, summary of sulfur isotopes and minerals characteristics (Reynolds, Richard L., Goldhaber, Martin B., 1983, Society of Economic Geologists, Inc., *Economic Geology*, Table 1, p. 115)

FeS ₂ generation	Dominant FeS ₂ mineral	δ ³⁴ S (‰) ^a	Origin of and/or sulfur source for FeS ₂
Benavides deposit/Catahoula Formation			
Pre-ore stage	Pyrite	~+12	Fault-leaked aqueous sulfide from sour gas reservoirs
Ore stage	Marcasite	~-35	Sulfur redistributed from pre-ore FeS ₂
Lamprecht and Felder deposits/Oakville Formation			
Pre-ore stage	Pyrite	~-25 to -35	Extrinsic bacterial reduction of sulfate in fault-leaked brine
Ore stage	Marcasite	~-25 to -47	Sulfur redistributed from pre-ore FeS ₂ and mixing of oxidized groundwater with sulfur-enriched brine
Post-ore stage I ^b	Pyrite	~+24 to +10	Fault-leaked aqueous sulfide from sour gas reservoirs
Post-ore stage II ^b	Marcasite	~-45	Mixing of oxidized groundwater with sulfur-enriched brine
Panna Maria deposit/Tordilla Member, Whittsett Formation, Jackson Group			
Pre-ore stage	Pyrite	~-1 to -18	In situ bacterial sulfate reduction
Ore stage	Pyrite	~-20 to -33	Sulfur redistributed from pre-ore FeS ₂

^aSulfur isotopic ratios (<δ³⁴S) represent best estimates only because more than one FeS₂ generation typically was present in each sample. ^bPostore FeS₂ minerals in the Lamprecht and Felder deposits are distinguished by an earlier (I) and later (II) generation.

Limestone oil and gas fields, and isotopically light sulfur, which may have originated by bacterial sulfate reduction in shallow aquifers promoted by seepage of organic matter from Tertiary hydrocarbon deposits.

Detrital carbonaceous matter: Only sediments of the Jackson Group and possibly of the Carrizo Sand contain abundant plant material, which clearly exerted a strong influence on rollfront formation. Compared with host rocks of deposits in other Tertiary units in south Texas, those of the Jackson Group are of beach sand provenance.

Most non-Jackson Group-hosted deposits contain none or negligible quantities of carbonaceous matter. This contrasts with sandstone uranium deposits in other regions such as the Wyoming Basins or the Colorado Plateau. An explanation for the lack of carbonaceous matter in most of the host sands in Texas may be that the sands were apparently oxidized at or shortly after burial, which essentially destroyed any indigenous vegetal debris.

The destruction of carbonaceous matter is not believed important to ore formation in south Texas provided that H₂S was introduced into the sands shortly after deposition and prior to uranium introduction (see previous paragraph). This implies that introduction of H₂S must have been an essential factor in the ore-forming process in case the sands have been widely oxidized previously.

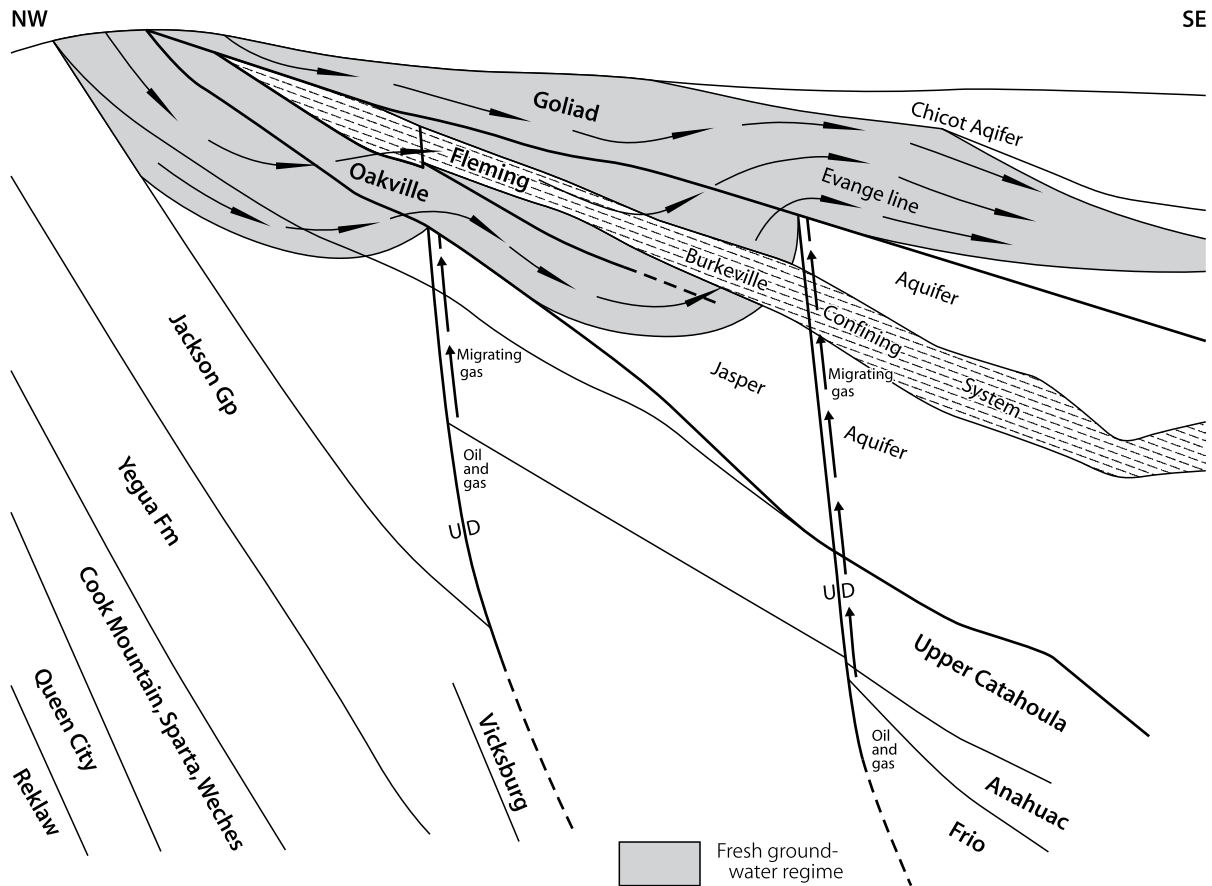
Uranium source

The source of uranium for south Texas deposits is presumed to have been the associated tuffaceous and bentonitic pyroclastic sediments, which are common in the Catahoula Formation, but which also occur in the Jackson Group and the Oakville Formation. Uranium deposits may have derived their uranium either intraformationally from interbedded uraniferous pyroclastics, as in the Catahoula Formation, or extraformationally from (former) superposition of the Catahoula or similar fertile tuffs above an unconformity (► Fig. 8.14). For example, uranium deposits that occur in sediments other than the tuffaceous Catahoula Formation or its immediately overlying or underlying sands, are within hosts that are down the hydrologic gradient from the Catahoula Formation. This suggests that here also the Catahoula tuffs supplied uranium, which groundwater has subsequently transported to the site of ore formation in both younger and older horizons. In another scenario, Catahoula tuffs must have overlain sub-outcrops of older units such as the Carrizo Formation and could have furnished uranium to these hosts.

Pyroclastic components of sediments in the South Texas Coastal Plain area are believed to have originated from volcanic eruptions in the Big Bend region. Volcanic rocks in the Big Bend area contain anomalous concentrations of uranium (see below), hence, they had the potential to provide adequate amounts of

■ Fig. 8.15.

South Texas, schematic section demonstrating the migration paths of fresh groundwater and fault-related H_2S in the Tertiary sediments of the coastal plain. (After Adams & Smith 1981 based on Baker 1979)



uranium to the south Texas region either in volcanic detritus or by groundwater.

Smith RB (personal communication) argues that volcanic centers in the Big Bend region have been the only source for pyroclastics in the South Texas Uranium Region. He has mapped subangular boulders of trachy-andesite in the Soledad Member in Duval County as much as 1 m in diameter. Smith assumes that these boulders derived from a close volcanic source perhaps from along the Balcones Escarpment. Volcanic activity may have occurred here as late as Middle Eocene.

The more pertinent views regarding the source of uranium may be briefly reviewed as follows.

Dickinson (1976b) points to the low uranium content (3 ppm) and the high thorium-uranium ratio (5.6) of the Catahoula Formation as evidence that it has lost considerable uranium. He compares this with the Whitsett Formation of the Jackson Group, which contains an average of 11 ppm U and a thorium to uranium ratio of only 2.4, and concludes that uranium has not been leached and reconcentrated within this formation. The restriction of uranium deposits in the Whitsett Formation to zones where the commonly intervening Frio Formation is absent, and the Whitsett and Catahoula formations

are in direct contact, suggests that uranium in those deposits was supplied from the Catahoula Formation.

Eargle and Weeks (1973) note that uranium deposits in south Texas are restricted to areas where host rocks contain or are proximal to rocks containing about 50% volcanic ash or diagenetically altered ash. They state that Tertiary igneous rocks in the Big Bend region of western Texas, from which the pyroclastics of south Texas were presumably derived, contain as much as 45 ppm uranium. This may suggest that the sediments themselves could have had an adequate uranium content to account for uranium in the deposits.

Galloway (1977) reports that the average uranium content of 60 samples from the Gueydan fluvial system averages between 2 and 3 ppm U. He found that uranium contents increased slightly in finer-grained sediments, but was substantially lower (average less than 1 ppm U) in those sediments, which would have experienced leaching and soil formation. In contrast, sediments in lacustrine environments, which presumably would have been protected from early post-depositional leaching, had the highest uranium contents (nitric acid leachable average U content = 8 ppm). Galloway interprets this to indicate that, as had been suggested earlier by Moxham (1964) and Duex (1971),

uranium has been strongly leached from Catahoula sediments, and that leaching took place very early after sedimentation. In Galloway's (1977) opinion, this is supported by the relation between the uranium contents of sediments and the inferred extent of syndepositional leaching due to soil-forming processes.

Pyroclastic material is also a significant component of both, the Jackson Group and the Oakville Formation (see Sellards et al. 1932, for example). Several authors have suggested that this volcanic material might have provided uranium for the deposits, which occur in the respective sandstones, but there is no compelling evidence that this is the case. As has been pointed out by Dickinson (1976b), however, the Jackson Group is not known to contain uranium deposits except where it is in juxtaposition with the Catahoula Formation, which suggests that ore-forming uranium derived from Catahoula rather than from Jackson sources.

Geochemical environments

Major south Texas uranium deposits occur in two principal geochemical environments:

- (a) At the redox boundary on the downdip margin of tongues of oxidized sandstone in the form of classical rollfront deposits, e.g., in the Jackson Group and the Catahoula Formation (Fig. 8.10) and
- (b) Entirely within reduced sandstone as nonredox front associated deposits, e.g., in the Catahoula, Oakville, and Goliad formations (Figs. 8.9 and 8.11).

Characteristics of redox front associated uranium mineralization

Rollfront U ore bodies exhibit, in many cases, the typical C-shaped configuration in cross-section that reflects the direction of groundwater flow and the propagation of the redox front. Oxidized sands show the typical minero-chemical effects of exposure to oxidizing solutions, in particular decomposition of pyrite. At other places, these ore bodies do not display the crescentic roll shape, obviously due to interbedded argillaceous material, which disrupts solution flow and prevents development of the ideal crescent shape.

Characteristics of nonredox front associated uranium mineralization

Nonredox front (or non-rollfront) associated ore bodies occur entirely within pyrite-bearing sandstone in a distal position from today's boundary of oxidized sandstone. Some of these deposits have nearly the classic crescentic shape such as many deposits in the Oakville Formation, e.g., *Felder*, *Clay West*, *Rhode Ranch*, etc. They are classical rollfronts in shape, but were affected and enveloped by later stages of reduction. This reduction is

attributed to post-ore introduction of H_2S , which entered into the altered interior of ore-hosting sands. As a result, sandstone that had been oxidized during ore formation became re-reduced. For example, *Rhode Ranch* ore zones show at least three stages of reduction and minero-chemical redistribution. They now are in an almost totally reduced host. It seems clear, therefore, that these deposits were also originally generated by the rollfront process.

Element zoning across deposits provides additional evidence in support of an original rollfront nature for these deposits. As established by Harshman (1974), a differential distribution of Se, V, U, and Mo exists across many rollfront deposits. In principle, this zoning is similar to roll-type deposits in the Wyoming Basins (Fig. 2.6a). Harshman explains this zoning as a result of migration of oxidizing groundwater into a reducing sphere as described in Chap. 2 Wyoming Basins. In contrast to Wyoming roll-type deposits, however, many of the south Texas U deposits have a high concentration of ore-stage marcasite.

In addition to the features addressed above, Adams and Smith (1981) note that the combination of intercommunicating sand bodies, growth faults, and their disruption of lithologic units apparently influenced the hydrology of the stack of Tertiary strata, influx and spreading of H_2S , and movement of repetitious reducing and oxidizing water regimes. As a result, these factors, individually or combined, prepared sediments, which were susceptible to ore accumulation in the Catahoula, Oakville, and Goliad formations, e.g., by formation of dispersed pyrite in formerly oxidized ground. They later readjusted the redox regimes, which partly led to destruction of earlier formed ore bodies and to neo-formation of deposits in younger stratigraphic units. These geologic conditions associated with introduced reductants such as H_2S apparently apply to most south Texas deposits except those that formed in the Jackson and possibly in the Carrizo sands and those associated with salt domes.

Adams and Smith (1981) point in particular to the following criteria as distinctive and essential for formation of this non-redox front type of south Texas uranium deposit as follows:

- (a) The position of ore-hosting fluvial channels in subsequent stratigraphic sequences tend to be superimposed. They are more or less interconnected and cut by growth faults, which permitted influx of oxygenated groundwater and emanation of H_2S into aquifers, development of reduced pyrite-bearing sandstones, and evolution of uranium ore. Where these conditions interacted within a mega-channel system, major U deposits or trends of deposits formed
- (b) Hydrologically, any thick sand sequences within major fluvial channels were potential pathways for migrating uraniumiferous groundwater. The uppermost, near-surface section would have contained fresh groundwater, but as aquifers became buried beneath younger sediments they would have become more saline
- (c) Growth faults and inter-communicating sand bodies probably allowed the fresh groundwater system to maintain a near-constant depth below surface. Structural control by the same growth faults led to hydrocarbon accumulation and H_2S migration

- (d) Hydrocarbons and in particular H_2S are thought to have been salient ingredients to formation of non-roll-type uranium deposits. However, two types, heavy and light sulfur isotopes, exist in sulfide minerals, mainly pyrite and marcasite, in host rocks. Only deep Mesozoic reservoirs, presumably the Cretaceous Edwards Formation could have provided the heavy sulfur isotopes found in pyrites of several deposits. If the heavy isotope is considered as indicative for the essential H_2S source, then access to hydrocarbon reservoirs at depth is critical
- (e) Although most non-roll-type deposits obey principal rules and patterns, the position of large deposits in the South Duval County Mineral Trend, for example the *Holiday-El Mesquite* deposit, suggest that particular factors contributed to the genesis of these unusually large deposits. Ore bodies are elongate parallel to the axis of groundwater flow and occur at the boundary between oxidized sandstone and H_2S -reduced sandstone. Orientation of ore bodies parallel to, rather than perpendicular to, the direction of groundwater movement suggests that large volumes of water flowed tangentially past reduced sandstone rather than directly through the redox front. This geometric setting may have permitted the exposure of large volumes of uraniferous water to the rollfront, leading to deposition of considerable amounts of uranium within and along the contact with pyrite-rich sandstone. Reduced and subsequently oxidized sands in proximity to these ore bodies do not contain either Fe-Ti oxides or their alteration products.

Metallogenetic Models

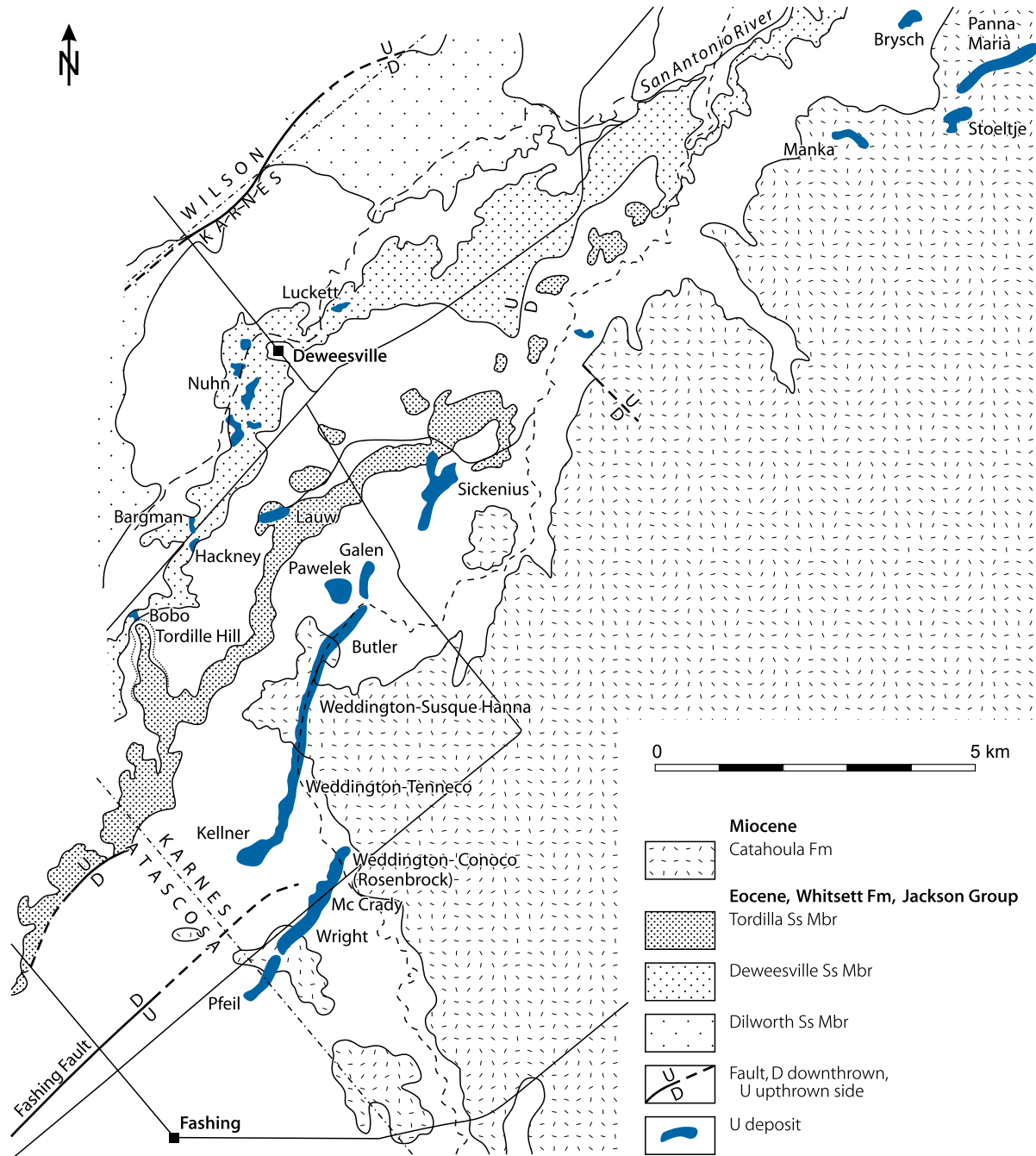
Goldhaber et al. (1978) propose stages in the evolution of roll-type deposits as depicted in [Fig. 8.13](#). The model forwarded by Galloway (1979b, 1985) is presented in [Fig. 8.14](#).

Adams and Smith (1981) summarize the sequence of metallogenetically essential processes, which led to formation of south Texas uranium ore bodies as follows:

- Ore-hosting Tertiary sediments were deposited in highly variable sedimentological environments ranging from continental fluvial to marginal marine. As a result, the stratigraphic-lithologic situation and related hydrologic regimes are rather variable and complex. The transmissivity and hydrology of sediments can range from simple in mega-channels to more contorted and complicated in crevasse splays and barrier bars
- Early oxidation affected mega-channels as reflected by oxidation well beyond the position of many deposits ([Fig. 8.9](#)). It is not known whether this oxidation was produced during deposition, or during early diagenesis as a redox-front phenomenon. This inferred early oxidation episode does not seem to have been related to, and therefore is probably not essential for ore formation
- Uranium was extracted in an early stage from uraniferous tuffaceous components within the Catahoula and adjacent Jackson Group sediments as can be deduced from the findings of Galloway et al. (1979a). These authors suggest that the release of uranium was associated with pedogenic processes, hence, it must have occurred immediately after sedimentation of the respective formations. Sediments escaping these types of soil-forming processes retained much of their uranium
- Uranium was carried by groundwater, for example, from the Catahoula source down into underlying permeable horizons, probably during continued Catahoula sedimentation above a slight angular unconformity with older strata. Where penetrated horizons contained reductants, e.g., in the form of plant debris, oxygenated uranium-bearing water lost its oxidation potential and redox fronts developed along which uranium was precipitated. Roll-type ore bodies in carbonaceous-rich beach sands of the Jackson Group represent this type of deposit. Their uranium was probably infiltrated by solutions flowing along dip-oriented fluvial channels, which extended from the Catahoula unconformity down to the Jackson beach sand environment. These deposits are similar in structural and lithologic settings to U deposits of the Black Hills, Wyoming-South Dakota, and Weld County, Colorado, which formed as roll-type deposits in sandstones below an angular unconformity upon which the tuffaceous White River Formation rests. Except for some minor differences in the nature of the sediments, deposits in the Jackson Group, therefore, are similar in terms of ore-forming processes to deposits in some classical rollfront districts
- With continued sedimentation from the Catahoula into Oakville time, many sands that later became ore hosts were buried. Connate water, which squeezed out by compaction of adjacent and overlying muds, probably moved into these permeable sand systems. This was the period of greatest uranium availability, and it can be assumed that all major deposits in the Catahoula and Oakville formations gained their initial uranium endowment during this early diagenetic period
- In an early stage after deposition of sediments, hydrocarbons and H_2S emanated locally into sands of the Catahoula and Oakville formations and caused crystallization of dispersed pyrite in potential ore hosts. These gases apparently invaded into these sands along growth faults that were contemporaneously active with, and intermittently after sedimentation ([Figs. 8.5](#) and [8.15](#)). Even during sedimentation, reduction of sands may have occurred at sites where the H_2S reached the surface and permeated sands adjacent to faults. Locally preserved carbonaceous trash and highly sulfidic sediments tend to confirm this. Geological relations and sulfur isotope data suggest that the source of some H_2S has been the Cretaceous Edwards Formation (Goldhaber et al. 1979), whereas other sulfur sources are in Tertiary sediments. According to Reynolds and Goldhaber (1983), H_2S introduction was predominantly pre- and post-ore and was apparently limited during ore formation
- As a consequence of the above described lithologic and physico-chemical circumstances, rollfronts within the Catahoula and Oakville formations very probably formed

Fig. 8.16.

Southwestern Karnes County, distribution of uranium deposits in the Eocene Jackson Group. (After Eargle et al. 1975)



by introduction of oxygenated uraniferous waters into sulfidized, pyrite-bearing sandstones. The ore-forming process was similar to the formation of roll-type deposits elsewhere, except that in the virtual absence of carbonaceous matter in ore-bearing sands, H_2S derived pyrite was essentially the only reductant available to establish the redox boundary

8. Subsequent to ore formation, several phases of re-reduction and partial re-oxidation affected some ore-hosting horizons (Figs. 8.9 and 8.13). Renewed introduction, probably of H_2S , resulted in a re-reduction of portions of altered sandstone tongues and arrested ore formation and propagation of the rollfront. Oxidizing groundwater may have moved once more down the sand horizons to generate a second

redox boundary up dip. But the solution may also have proceeded to and joined the original front or may have gone beyond the first front leaving only relict or ghost ore bodies with the main ore formed as a downdip rollfront ore body. The progress of the younger front, however, might also have been disrupted by interference from a renewed introduction of H₂S

9. The formation of uranium mineralization in younger sediments, as in the Goliad Formation, may be the result of continued movement of oxygenated groundwater, particularly in mega-channels. Oxidizing fluids probably destroyed some early mineralization in older formations and moved uranium into younger formations. The apparent presence of both oxidized sandstone and uranium mineralization in younger formations, e.g., in the Goliad sands, well down some mega-channel systems suggests that the two are related.

Description of Uranium Districts and Selected Deposits Based on Stratigraphic Host Units

The following description presents summaries of the principle characteristics of uranium mineralization in the four major ore-hosting stratigraphic formations of Tertiary age in south Texas, amended by more detailed descriptions of selected typical deposits hosted in these formations. The location of uranium districts and deposits is shown in [Fig. 8.1](#).

8.1 Deposits in the Upper Eocene Jackson Group

Major deposits in the Jackson Group occur in the *Karnes County district* in western Karnes County. Principle deposits include *Brysch*, *Butler-Weddington*, *Galen*, *Nietzkiez*, *Nuhn*, *Panna Maria*, and *Sickenius* ([Figs. 8.1](#) and [8.16](#)).

Sources of Information. Adams and Smith 1981; Bowman et al. 1981; Dickinson 1976a, c; Galloway et al. 1979a, b; Galloway and Kaiser 1979; Reynolds et al. 1982.

Geological Setting of Mineralization

Uranium deposits generally occur in carbonaceous and the most coarse-grained sands in the Tordilla Sandstone and the Deweesville (Stones Switch) Sandstone members of the upper Jackson Group. These sandstones are interpreted to be a complex of depositional types that were deposited as part of a strand line, locally interrupted by small bay deltas. They include coastal-barrier, inlet, cusplate-delta, and distributary channel facies. The orientation of the host rock and contained roll systems is parallel to the paleo-coastline.

Fine-grained lagoonal sediments are unproductive except locally, where their basal lignite seams immediately overlie mineralized sands. In these cases, lignite may contain ore-grade uranium concentrations along the contact. Other lignites, such

as in the older Manning Formation usually show anomalously low radioactivity.

Mineralization

Two kinds of U mineralization are present, unoxidized and oxidized. As examples of the two types, the *Panna Maria* and the *Brysch* deposits, respectively, are described later. Unoxidized deposits are generally larger, but of lower grade than oxidized deposits.

Unoxidized mineralization consists of pitchblende/sooty pitchblende and coffinite. Pyrite is the dominant iron-sulfide. It commonly has framboid habits and replaces plant fragments. Marcasite is sparse. Carbonaceous matter is a common constituent. This contrasts with other south Texas deposits, which are devoid of organic carbon. In addition to the customary detrital minerals, clinoptilolite, authigenic feldspar, opal, and montmorillonite are present in ore zones.

Ore is of roll type and occurs commonly at margins of altered sandstone tongues. On the updip, concave side of rolls, sands are oxidized and otherwise altered and have a pale grey to buff color. Unoxidized sands on the downdip side are medium grey.

Several rollfronts in Jackson Group strata show a northerly direction of migration rather than a southeasterly, downdip migration direction (for details see *Panna Maria*).

Oxidized mineralization comprises hexavalent U minerals, chiefly uranyl phosphates and -vanadates. The stratigraphic ore distribution is similar to that of unoxidized Jackson deposits, but ore is generally restricted to the near-surface section (for details see *Brysch*). Radiometric disequilibrium is common in oxidized ore, whereas it is less common in unoxidized ore.

Shape and Dimensions of Deposits

The unoxidized main ore trend in the Jackson Group in Karnes County is a single rollfront approximately 10 km in length. The broader rollfront system, which may be composed of one or more rollfronts, extends for several additional kilometers to the northeast and southwest.

The shape and orientation of rollfronts are irregular and variable depending upon the geometry of host sandstones. In cross-section, rolls commonly exhibit the characteristic crescent shape, convex in the downdip direction.

Ore grades vary between 0.03 and 2% U or more, and average in most ore bodies between 0.07 and 0.17% U. The size of ore bodies ranges from 0.5 to 7.5 m in thickness in sand horizons that are from 6 to 10 m thick. Widths range from 15 to 100 m. Lengths persist for a kilometer or more. The thickness and grade of ore diminish gradually from the rollfront to a cutoff grade at a distance of several tens to a 100 m downdip.

A number of small oxidized deposits cluster along a NE-SW trend a few kilometers updip to the northwest of the unoxidized deposits. This zone is approximately 15 km in length in Karnes and Live Oak counties. Former production has yielded almost 200,000 t ore averaging about 0.17% U.

Metallogenetic Aspects

Jackson Group deposits originated by classical rollfront-style processes. Potential sources for uranium could have been tuffaceous sediments of the overlying Catahoula Formation and perhaps pyroclastic material in Jackson Group sediments.

Galloway et al. (1979a) refuse volcanic material within the Jackson Group as a viable U source, because early mobilization would have occurred in a zone of regional groundwater discharge, and the dissolved uranium would have been transported into surface drainage and further into the Gulf. The optimum recharge for Jackson sands in Karnes County would have occurred later at places where upper Jackson sands were in suboutcrop directly beneath basal Catahoula tuffs. As a consequence, Galloway et al. (1979a) favor Catahoula tuffs as the uranium source.

Reynolds et al. (1982) have investigated the role and relationship of sulfur and carbon on ore formation. Their findings are presented with the description of the Panna Maria deposit.

8.1.0.1 Panna Maria, Karnes County

The Panna Maria deposit is located about 10 km N of Karnes City and 90 km SE of San Antonio. Original resources were estimated at some 3,000 t U at grades of less than 0.08% U. The deposit was mined from 1977 to 1985 by five open-pit operations producing 1,870 t U at a mining grade averaging 0.04% U.

Sources of Information. Bowman et al. 1981; Dickinson 1976a, c; Galloway et al. 1979a; Reynolds et al. 1982.

Geological Setting of Mineralization

Panna Maria ore is hosted in the [Tordilla Sandstone Member](#) of the Whitsett Formation, the uppermost unit of the Jackson Group. The Whitsett Formation consists of alternating very fine- to fine-grained, often tuffaceous sandstone and mudstone, with interbedded lignite. Sediments are of marginal marine origin deposited in beach, distributary-channel, deltaic, and lagoonal environments. Ore-hosting Tordilla Sandstone is light grey, clay-rich, cross-bedded, very fine-grained, and contains organic debris. Grains consist of quartz and volcanic glass. They are loosely cemented with silica. The Tordilla Sandstone is a strike-oriented coastal barrier formation overlain by a lignite bed and underlain by tuffaceous or argillaceous silt and sand of the non-marine Dubose Clay Member.

NE–SW-trending faults dissect outcropping strata and the underlying Cretaceous Edwards Limestone as well. Oil and gas fields occur near the mine area.

Mineralization, Shape and Dimensions of Deposits

Pitchblende, sooty pitchblende, and coffinite are the principal U minerals. They are associated with pyrite and marcasite. U

minerals are uniformly distributed and appear to have formed during or shortly after sedimentation.

The main ore body follows a sinuous ENE–WSW-trending rollfront, which is about 5 km long and lies at a depth between 23 and 61 m. The trend direction is approximately perpendicular to the regional dip of the host formation and is parallel to NE–SW-oriented faults. Sediments on the altered updip side, i.e., to the NW of the rollfront, are light-orange to light-red, whereas those downdip to the SE of the roll are grey. The geometry of the rollfront indicates that the original mineralizing solution flowed in a southeasterly direction following the 1° dip of sediments. At present, however, changes in the groundwater flow pattern resulted in local updip flow from the reduced environment.

According to Reynolds et al. (1982), uranium is concentrated roughly in a crescentic roll in cross-section with the convex side downdip to the SE. The thickest uranium interval, about 3 m, is at the nose of the roll. The mineralized lower limb is as much as 1 m thick and extends at least for 460 m behind the rollfront. A kind of upper limb is in a lignite seam and in subjacent sandstone. It contains anomalously high concentrations of up to 0.38% eq. U. The mineralized lignite bed extends at least 400 m downdip from the rollfront, but does not exist everywhere along the rollfront. The uranium content of the upper and lower limbs averages about 0.18% eq.U. The two limbs are separated by oxidized light-red sandstone, whereas reduced barren sandstone lies above the upper and below the lower limb. In contrast to uranium enriched lignite above the ore roll, any lignite at some distance from the roll generally contains only about 200 ppm eq.U. An additional horizon of mineralization, about 1 m thick, is present, but it is unclear whether it is connected to the main ore roll.

Based on a cutoff factor of 0.3 m of 0.042% U, Bowman et al. (1981) ([Fig. 8.17](#)) report for the Panna Maria deposit a maximum thickness of 7.6 m, a width of 79 m, and a depth to the top of the ore of 55 m. Grades range from an average of <0.11% U over a thickness of 6.3 m and a width of 20–30 m in the higher grade central part of the roll to 0.025% U or less in the limbs. Total length is 5.9 km.

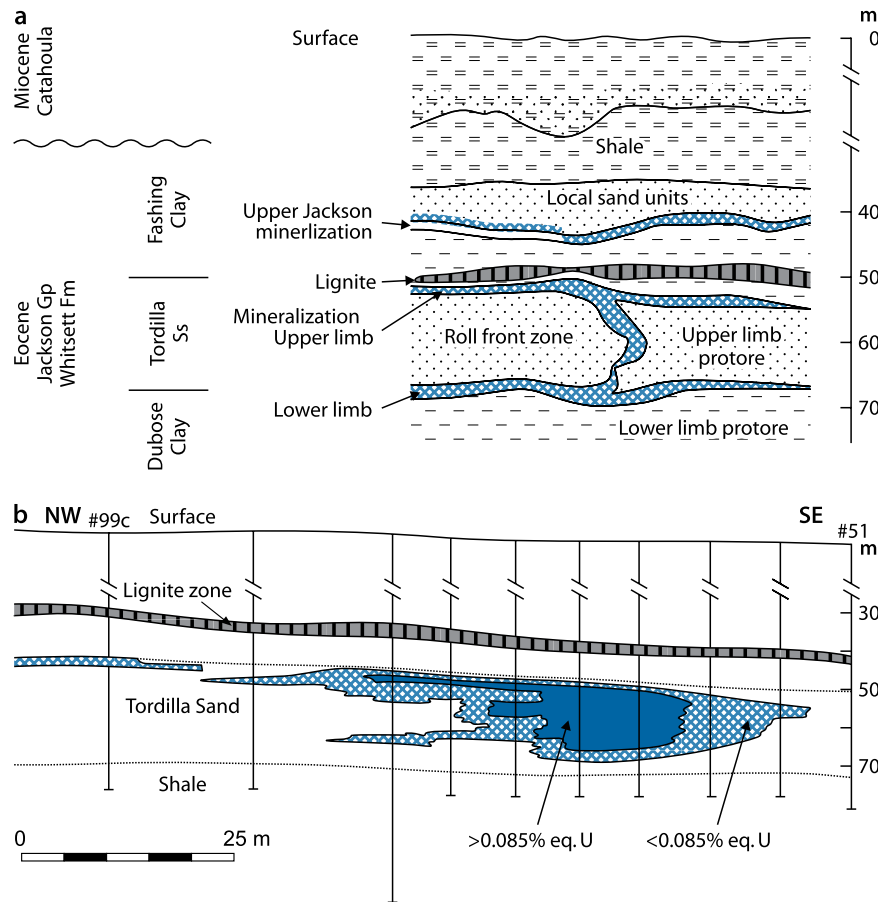
Minerochemistry, Stable Isotopes

Reynolds et al.'s (1982) conclusion from their studies on uranium, sulfur, and carbon geochemistry and mineralogy is, in summary, as follows (modified and abbreviated quotation):

The content of total *sulfur*, which comprises the sum of sulfide sulfur (dominantly in FeS₂ minerals), sulfate sulfur, and organically bound sulfur, is close to zero (0–0.01 wt.%) in the tongue of altered sandstone, and averages 0.37 wt.% in mineralized and reduced barren zones. Except for some samples in and adjacent to mineralized lignite, the sulfur content is similar in the mineralized zone as well as in reduced sandstone elsewhere. Sulfide sulfur commonly constitutes less than half, sulfate sulfur the major proportion, and organically bound sulfur only lesser amounts of the total sulfur. Similar distributions and relative abundances of sulfate and sulfide sulfur are reported by

■ Fig. 8.17.

Karnes County, Panna Maria deposit, (a) diagrammatic lithologic section with distribution of uranium mineralization in Tordilla Sand of the Whitsett Formation, Jackson Group; (b) section of uranium grade distribution. (Note: thickness of ore body is exaggerated). (After Bowman et al. 1981)



Harshman (1974) for two other rollfront uranium deposits (Butler and Pfeil pits) in the Whitsett Formation in Karnes County.

Reynolds et al. (1982) present evidence that sulfate is not an original constituent of the sediments, but an open-air oxidation product formed after recovery of the samples. Consequently, the total sulfur of in situ rocks is bound dominantly in iron mono- and di-sulfides with a lesser amount of sulfur bound organically.

Assuming that all sulfur is bound in FeS_2 minerals, FeS_2 amounts are, with an average of 0.69 wt.%, comparatively low, and only occasionally exceed 1% in reduced barren and mineralized zones. Principally, the FeS_2 content is highest in and adjacent to mineralized lignite but is rather constant throughout reduced sandstone, regardless of proximity to mineralized zones.

Pyrite is the dominant FeS_2 phase. It occurs in a variety of forms and habits. An apparent early generation, which occurs throughout mineralized and reduced barren zones, is present as aggregates of small (2–20 μm) cubes, commonly in a matrix that may be carbonaceous debris, as framboids, as replacement

of structured plant material, as euhedral crystals (approx. 35–100 μm), and rarely as replacement of detrital Fe–Ti oxide grains and biotite flakes. A younger pyrite generation supposedly related to mineralizing processes exists in and adjacent to lignite, in mineralized sandstone of the lower limb, and at the nose of the roll. Younger pyrite forms cement of, and overgrows on framboidal pyrite and on aggregates of small pyrite cubes. Geochemical evidence suggests that there is widespread addition of epigenetic sulfide.

Marcasite is absent or present only in traces except in lignite and in some samples from the NE end of the Panna Maria rollfront. In the NE zone of this deposit, marcasite constitutes 70 and 90% of the FeS_2 content adjacent to the upper and lower redox boundaries, respectively (Fig. 8.10a). Its abundance drops sharply with increasing distance from the altered tongue.

Marcasite distribution may be attributed to low pH values at and near the redox boundary that resulted from oxidation of FeS_2 minerals and organic matter during mineralization and migration of the rollfront (Goldhaber and Reynolds 1979). The lack of a similar pattern along the altered tongue in other parts of the deposit, however, remains an open question.

Marcasite, like pyrite, is present in two generations. The older, probably early diagenetic marcasite is closely associated with structured carbonaceous debris, commonly as a replacement, and as intergrowths with pyrite that replaced plant matter. The second marcasite generation, which may have formed during ore formation, occurs in and adjacent to lignite. It is found as cement of framboids, as euhedral crystals (<80 μm), and as rims on framboidal pyrite and on euhedral pyrite crystals. The sulfur source for marcasite associated with lignite may be aqueous sulfide generated by mineralizing processes.

Sulfur isotopes: Ratios of sulfur isotopes range from -1.4 to -33.7‰. Reynolds et al. (1982) established that light sulfur isotopes are typical of sulfides in lignite and subjacent and superjacent sandstone (about -20 to -30‰), at the nose of the ore roll (-22 to -25‰), and in the lower mineralized limb (-20 to -33.7‰). $\delta^{34}\text{S}$ values are lightest in ore and become systematically heavier with increasing vertical distance away from ore. This relationship – the isotopically lightest values in close proximity to the redox interface – is characteristic of some other roll-type deposits (Warren 1972; Goldhaber et al. 1978). Elsewhere in and adjacent to the deposit, $\delta^{34}\text{S}$ values show strong variations (-1 to -18‰) without any apparent correlation to mineralization. For example, relatively heavy $\delta^{34}\text{S}$ values (-2 to -10‰) exist in mineralized samples of the lower limb, whereas samples from below the lower limb yield lighter $\delta^{34}\text{S}$ values up to -15‰. Reynolds et al. (1982) attribute this distribution of values to the abundance of ore-stage FeS_2 minerals. Relatively light $\delta^{34}\text{S}$ values characterize ore-stage marcasite below the lower redox boundary and ore-stage pyrite at the nose of the roll, whereas the very light $\delta^{34}\text{S}$ ratios (about -20 to -34‰) in sandstone may be partly derived from pre-ore FeS_2 . The latter may have become available by isotopic fractionation of sulfur that originated in pre-ore FeS_2 of the developing altered tongue, and was liberated by oxidation during the mineralizing processes, and was redistributed into the reduced sandstone, where it was incorporated into ore-stage FeS_2 as outlined by Goldhaber et al. (1978).

Warren (1972) explains the heavier, but negative, and variable $\delta^{34}\text{S}$ values as measured in sulfides of reduced barren sandstone as typical of biogenic, early diagenetic FeS_2 formed in the absence of a cyclic process of iron-sulfide oxidation and reprecipitation.

Mineral carbon (carbonate) is practically absent except for local very minor amounts of less than 0.05 wt. %.

Organic carbon appears to be ubiquitous although its distribution and amount is highly variable. In mineralized and reduced barren sandstone, organic carbon averages 0.42% C, whereas in altered sandstone the average content has dropped to 0.04% C. Harshman (1974) attributes this decrease of C values in the altered tongue to decomposition of most of the organic debris by oxidation during rollfront migration.

Although the organic carbon content varies considerably in mineralized segments, there is a positive relationship between vegetal debris and uranium mineralization for the deposit as a whole. Moreover, within the altered tongue, remnants of plant trash stringers and pockets typically retained ore-grade uranium concentrations.

Metallogenetic Aspects

Reynolds et al. (1982) interpret metallogenetically their findings as follows. Panna Maria host sediments contain pre-ore and ore-stage FeS_2 minerals. Textural associations and the relationship of sulfur content to organic carbon content suggest that pre-ore FeS_2 , which is predominantly pyrite, formed under reducing conditions, which were very probably created by organic trash. Hence, it appears that organic carbon exercised a major influence on formation of the first sulfide generation, probably during diagenesis. But the organic carbon content on its own could not have been the only ingredient for sulfur accumulation, since most Panna Maria sediments are relatively enriched in diagenetic sulfur for a given carbon content as compared with other organic carbon/diagenetic sulfur ratios of other recent marine sediments. The apparent sulfur enrichment in sediments at Panna Maria may be the product of an addition of epigenetic, ore-stage sulfide sulfur (which amounts to about 0.3 wt. % sulfur) to diagenetic, pre-ore sulfide sulfur. Such a later sulfide generation can be expected as a result of metallogenetic processes, during which dissolved sulfide was introduced into groundwater on the reduced side of the uranium roll and which, therefore, led to the formation of FeS_2 independent of the local content of organic debris.

Ore-forming processes further enriched U mineralized and reduced barren sediments with FeS_2 , but without a major and systematic FeS_2 concentration at the redox boundary as is characteristic for some roll-type U deposits in Wyoming. Ore-stage sulfur is bound dominantly in pyrite, but locally also in marcasite.

8.1.0.2 Brysch, Karnes County

The Brysch deposit, located approximately 15 km NW of Karnes City, is an example of an oxidized deposit in Jackson Group sediments. The deposit was one of the early discoveries, found in the mid 1950s. The open-pit mine produced 10 t U at an ore grade averaging 0.10% U.

Sources of Information. Dickinson and Sullivan 1976; Eargle et al. 1975; Galloway et al. 1979a.

Geology and Mineralization

The Brysch deposit is in the basal part of the [Deweeseville Sandstone Member](#) of the Whitsett Formation of the Jackson Group. Sandstone at the mine is approximately 20 m thick and is overlain by mud of the Jackson Group.

Ore-hosting sandstone is well sorted, medium grained, and comprised of quartz and feldspar, including plagioclase, orthoclase, sanidine, and microcline, as well as minor amounts of clinoptilolite and alpha-cristobalite. The sand also contains abundant fossil wood, sometimes in log jams and fossil burrows indicating marine influence. It is assumed that the sand was deposited in a beach environment. In general, beach-sandstone

in the Whitsett Formation is fine grained and fluvial sediments are medium grained. The presence of medium-grained sand in the lower unit together with the greater than normal thickness of the Deweesville Member at the mine suggest a nearby fluvial source.

Ore mined consisted mainly of autunite and tyuyamunite contained in a C-shaped ore body with a maximum thickness of almost 3 m. The trailing ends were 0.5–1 m thick and up to 24 m long. The total width perpendicular to strike varied between 7 and 35 m. The length was 170 m in NNE–SSW direction. The shape of the deposit suggests that it originated as a typical ore roll (Fig. 8.18).

The source of uranium in the Brysch deposit is considered to be the Catahoula tuff, but tuffaceous rocks of the Whitsett Formation may also have contributed uranium. Transportation of uranium to the depositional site may have been through fluvial sandstone aquifers that connected the beach-sandstone host rock to updip areas. There is no evidence of introduced H₂S even though faults and oil fields occur in the general vicinity of the deposit. The reductant was apparently plant material and pyrite in the beach sand.

8.2 Deposits in the Late Oligocene Catahoula Formation

Major deposits in the Catahoula Formation are located in the *South Duval County Mineral Trend* in southeastern Webb County and southern Duval County. Minor deposits with considerable amounts of oxidized U mineralization occur near the surface in *northern Live Oak County*, and small, isolated U deposits and occurrences in *southern Jim Hogg and Starr counties*. Some re-reduced deposits are in *northwest Duval County* in the Soledad Member of the Catahoula Formation.

Principle deposits include *Benavides, Bruni, Holiday-El Mesquite, O'Hern, and Santonino*, all in the South Duval County Mineral Trend, and elsewhere *Brelum-Piedra Lumbre, House-Seale, Nell, and Washington-Fayette*.

Sources of Information. Adams and Smith 1981; Galloway et al. 1979a; Galloway and Kaiser 1979; Goldhaber et al. 1978; Goldhaber and Reynolds 1977; Granger and Warren 1974; Harshman 1974; Reynolds and Goldhaber 1978, 1983; Reynolds et al. 1977, 1980a.

Geological Setting of Mineralization

Catahoula sediments are divided into two depositional systems by the San Marcos Arch, the Gueydan fluvial system to the southwest of the arch, and the Chita-Corrigan fluvial system to the northeast. Both systems rest upon and grade into deltaic and barrier-strand plain systems of the Frio Formation.

The Gueydan system hosts all significant uranium deposits. Gueydan sediments consist of a series of complexly interweaving sand belts; the sand-rich portions of which contain from 10 to 50% sand and represent fluvial channel-fill and crevasse-splay

facies. Tuffaceous mudstones and claystones of flood-plain and lacustrine origin constitute the remaining facies.

Fluvial channel-fillings average some 10 m in thickness, but bodies of more than 20 m are common. These bedload channel-fill sediments are composed of coarse- to medium-grained sand with subordinate coarser cobbles and fine-grained sand and silt. Sands were initially well-sorted, but due to diagenetic alteration of their pyroclastic components, they are now poorly sorted matrix-rich sands. Crevasse splay facies consist of medium- to fine-grained sands and mudstone averaging several meters in thickness. They extend for hundreds of meters beyond channel margins into interchannel areas, which are occupied by tuffaceous mudstones, siltstones, and bentonitic claystones of floodplain and locally of lacustrine facies.

Mineralization

Ore mineralogy is similar to other south Texas deposits and more details are given in the description of individual deposits further below. Salient geological features related to major clusters of uranium deposits within the Catahoula Formation have been summarized by Galloway et al. (1979a). In general, mineralization is concentrated along the flanks of principal fluvial channel systems and many, but not all, deposits are related to faults.

The cluster of small ore bodies within *northern Live Oak County* are not related to any known faults. They lie in an inter-fingering zone between tuffaceous crevasse splays and coastal-lake facies at the base of the Catahoula Formation (Galloway 1977), on the flank of a major NE–SW-trending channel belt. Northwestward flowing reducing water in this zone encountered southward migrating oxygenated water (Fig. 8.19).

Host sediments are dominated by mudstone, clay, and ashy, fine-grained sand. Many deposits are completely within reduced pyrite-bearing sandstone at a considerable distance from altered sandstone tongues, which suggests that the sands are re-reduced. Some shallow deposits do contain oxidized U minerals, which probably would have been destroyed but for argillic, relatively impermeable sands.

Deposits in *northern Duval County* occur at the intersection of a subsidiary channel complex and a broad fault zone. The migration direction of fronts is generally downdip in a SE direction. Ore rolls strike nearly parallel to a NE–SW fault system. Mineralization in shallower deposits is out of equilibrium in favor of radiometric assays due to recent leaching of uranium.

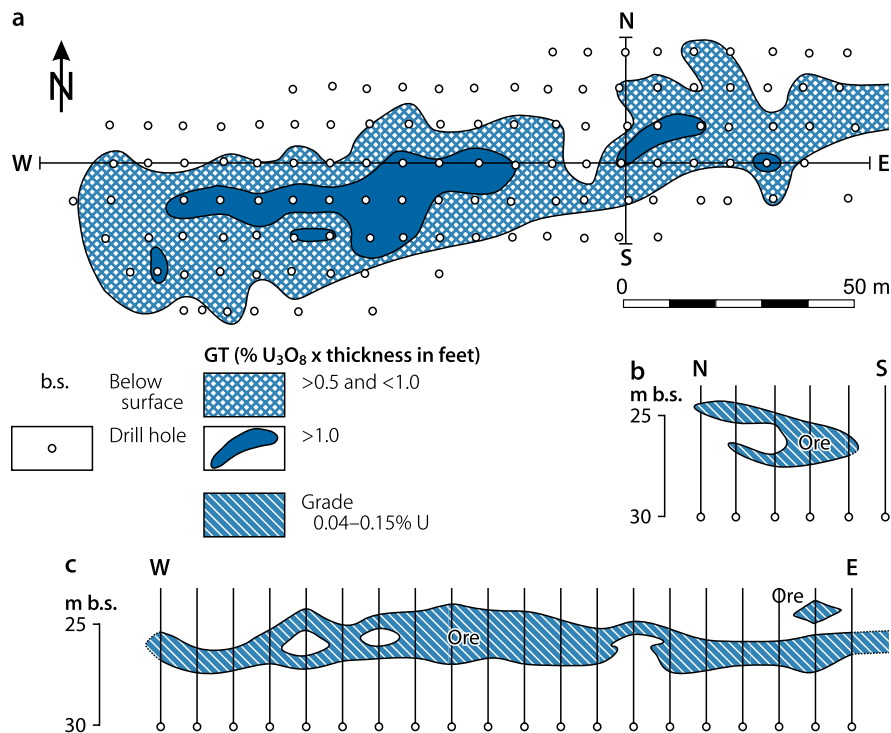
Deposits in *southern Duval County* straddle the margin of a major channel complex and are associated with the more argillaceous parts of the sandstones. These deposits are generally downdip from a belt of growth faults. At least some of these deposits are interpreted to be related to introduced sulfides, e.g., in the South Duval County Trend.

Shape and Dimensions of Deposits

Deposits in *northwestern Duval County* have a classic roll-front configuration except where they are distorted along faults.

Fig. 8.18.

Karnes County, Brysch deposit, (a) map and (b+c) cross-sections showing distribution and grade x thickness values for U mineralization hosted in the Whitsett Formation, Jackson Group. (After Dickinson & Sullivan 1976)



The deposits are small in size, but contain high uranium grades. Deposits are usually 0.3–3 m thick, 50–60 m wide, and have a strike length from several hundred meters to 1.5 km. Average grades of economic deposits are in the range from 0.08 to 0.17% U.

Deposits in northern Live Oak County are erratic in configuration and vary greatly in size, but are never large. Ore of the largest deposit, *Nell*, occurs erratically in several sand zones with little continuity. Grades are usually low, averaging 0.13% U or less. Some deposits are shallow, whereas others extend to a depth of 150 m.

8.2.0.1 House-Seale Deposit, Live Oak County

This small deposit is located about 40 km N of George West and belongs to the re-reduced type of mineralization.

Sources of Information. Adams and Smith 1981; Galloway 1977; Galloway and Kaiser 1979.

Geology and Mineralization

House-Seale is one of several deposits that occur in a zone of interfingering between a major NE–SW-trending fluvial system and a lacustrine sequence. Host sediments are of crevasse splay and lacustrine delta provenance, and include claystone,

tuffaceous mudstone, muddy siltstone, and argillaceous fine sand characterized by partly altered and vitric volcanic debris. Some fresh glass is present within the ore zone.

Mineralization occurs along a series of erratic, local rollfronts that can be traced for several hundred meters. The deposit is entirely enclosed by grey, pyritic sediments that extend updip from the rollfront for at least a 1,000 m; hence, the host rock appears to be re-reduced.

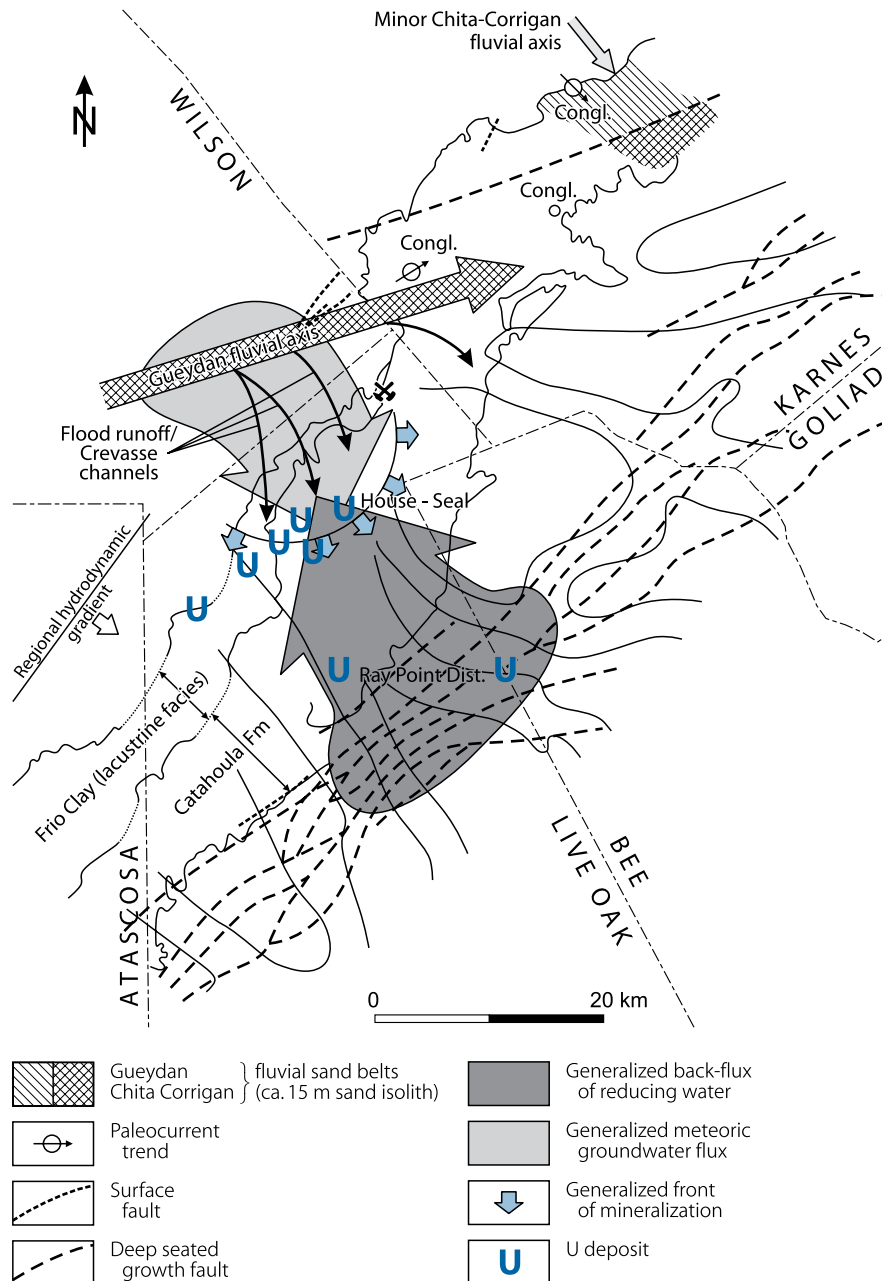
No faults are immediately associated with the deposit, but a zone of growth faults is associated with uranium deposits of the Oakville Formation in the Ray Point district about 15 km to the south (Fig. 8.19). Several sands within the basal Gueydan trend extend northwest from this fault zone toward the House-Seale deposit and could have been pathways for reducing solutions, which obviously have invaded the aquifer.

Uranium appears to be concentrated with matrix Ca-montmorillonite and is accompanied by selenium and molybdenum, which are zoned in a downdip direction across the rolls. The carbon content averages 0.1% in unaltered ground and 0.03% in altered ground. Uranium concentration shows no correlation with organic carbon content.

Although the ratio of Fe₂O₃ to FeS₂ is significantly higher behind the front, the characteristic oxidized tongue has apparently been masked by a post-mineral sulfide formation. As at the Benavides and Bruni deposits, a pre-ore stage of sulfidation is inferred in the House-Seale deposit. Oxidizing solutions, which subsequently migrated down the fluvial channel, formed a rollfront against finer grained sediments of the marginal

■ Fig. 8.19.

Live Oak County, litho-structural map illustrating the interrelationship of invading oxygenated meteoric groundwater flow and back-flux of reducing water, and location of U deposits in the Ray Point district and northerly located U deposits (House-Seale, etc.). Mineralization occurs in crevasse splay facies of the Catahoula Formation that have been reduced by northerly flowing H₂S-bearing waters. (After Adams & Smith 1981 based on Galloway & Kaiser 1979)



crevasse splay and crevasse delta. At a later time, reducing fluids again must have penetrated the aquifer to produce the present re-reduced host sands. An alternate hypothesis may propose that leaching of uranium may precede oxidation of pyrite so that a uranium roll could be formed entirely within pyrite-bearing sands. This would be possible for a rollfront formation by alkaline solutions. Existing data suggest, however, that post-ore H₂S has been introduced in some of the deposits.

8.2.0.2 Unnamed Deposit, Washington–Fayette Counties

This small deposit is located in Washington–Fayette counties at the northeastern extremity of the South Texas uranium belt. It resembles the classic trash-pile accumulations of other sandstone districts, but with uranium accumulations restricted to a well-defined rollfront.

Sources of Information. Adams and Smith 1981; Galloway and Kaiser 1979.

Geology and Mineralization

Uranium mineralization is distributed along an approximately 1,000 m long arcuate alteration front within crevasse splay sand at the downdip margin of a channel-fill sand. Volcanic detritus constitutes a minor portion of the host sands. The rollfront is of complex geometry due to the heterogeneity of host lithologies. Ore occurs as discontinuous pods within a zone of diffuse mineralization along the rollfront. Maximum uranium concentration is found in or close to lenses or pockets of carbonaceous trash and humate-like material dispersed in clay.

Molybdenum is concentrated along the margins of mineralized pods, most commonly on the reduced side. Selenium is locally enriched on the oxidized side. Some copper and lead are present. Iron decreases in concentration from unaltered, reduced sandstone (2.1%) to oxidized sandstone (1.2%). Carbonate exceeds 20% in the vicinity of mineralization, and although it may be related to ore formation, it shows no relation to ore zones.

8.2.0.3 Catahoula Deposits in the South Duval County Mineral Trend

The Catahoula-hosted deposits of the South Duval County Mineral Trend occur over a distance of some 55 km in ESE–WNW direction from southeastern Webb County through southwestern Duval County to northeastern Brooks County. Significant deposits include *Benavides*, *Bruni*, *Holiday-El Mesquite*, *O'Hern*, and *Santonino* (Fig. 8.20).

Sources of Information. Adams and Smith 1981; Galloway and Kaiser 1979; Goldhaber et al. 1978; Goldhaber and Reynolds 1979; Granger and Warren 1974; Harshmann 1974; Reynolds and Goldhaber 1978, 1983; Reynolds et al. 1977, 1980a.

Geological Setting of Mineralization

Uranium is hosted in the *Soledad Member* of the Catahoula Formation. This member is overlain by the Chusa Member of the Catahoula Formation. The Chusa Member is primarily a tuffaceous unit that becomes sandy downdip to the SE.

Coarse sands to gravels, averaging 2–3 mm in grain size, represent the host units. Gravels contain moderate to abundant black chert and volcanic fragments. Some clastic units consist of 70–80% black chert pebbles and cobbles. Organic carbon is practically absent. Gravels occupy higher positions stratigraphically downdip toward the southeast. They grade upward into medium- to fine-grained sand composed of subangular to well-rounded chert, quartz, volcanic fragments, and minor mafic minerals. Montmorillonite and illite constitute much of the interstitial material.

The position of uranium deposits in the *Soledad Member* rises stratigraphically along the mineral trend from west to east. The *Santonino* and *Bruni* deposits to the west occur in the basal sands, whereas the *Benavides*, *O'Hern*, and *Holiday-El Mesquite* deposits further along the trend to the east are positioned higher in the *Soledad Member*.

Mineralization, Alteration, Metallogenetic Aspects

All deposits show essentially classical rollfront configurations at the interface between oxidized and reduced sandstones. No evidence of re-reduction of the ore zones has been observed.

***Bruni* (Prod. by ISL, 1977–1982: ca. 300 t U):** According to Galloway and Kaiser (1979), this deposit occurs at a redox boundary in a plagioclase-rich volcanic litharenite within a proximal crevasse splay sand sequence that is approximately 14 m in thickness. Mineralization along the redox front has been traced for more than 3 km. The deposit has the typical roll shape. Ore-related elements are distributed across the rollfront in the characteristic configuration as established by Harshman (1974) (see Chap. 2 Wyoming Basins), i.e., from selenium adjacent to the altered tongue through vanadium and uranium to molybdenum some distance beyond the rollfront.

***Benavides*, *Holiday-El Mesquite*, *Longoria*, *O'Hern*:** (Prod. by ISL: *El Mesquite*, 1976–1996, 2,070 t U; *Longoria*, 1977–1981, 19 t U): These deposits are associated with a large area of reduced sandstone that is elongate parallel to a sand-filled channel and associated with faults that cross the channel system. The *O'Hern* and *Longoria* deposits are on the southern flank of the area of reduced sands, whereas the *Benavides* and *Holiday-El Mesquite* ore bodies are on the northern flank.

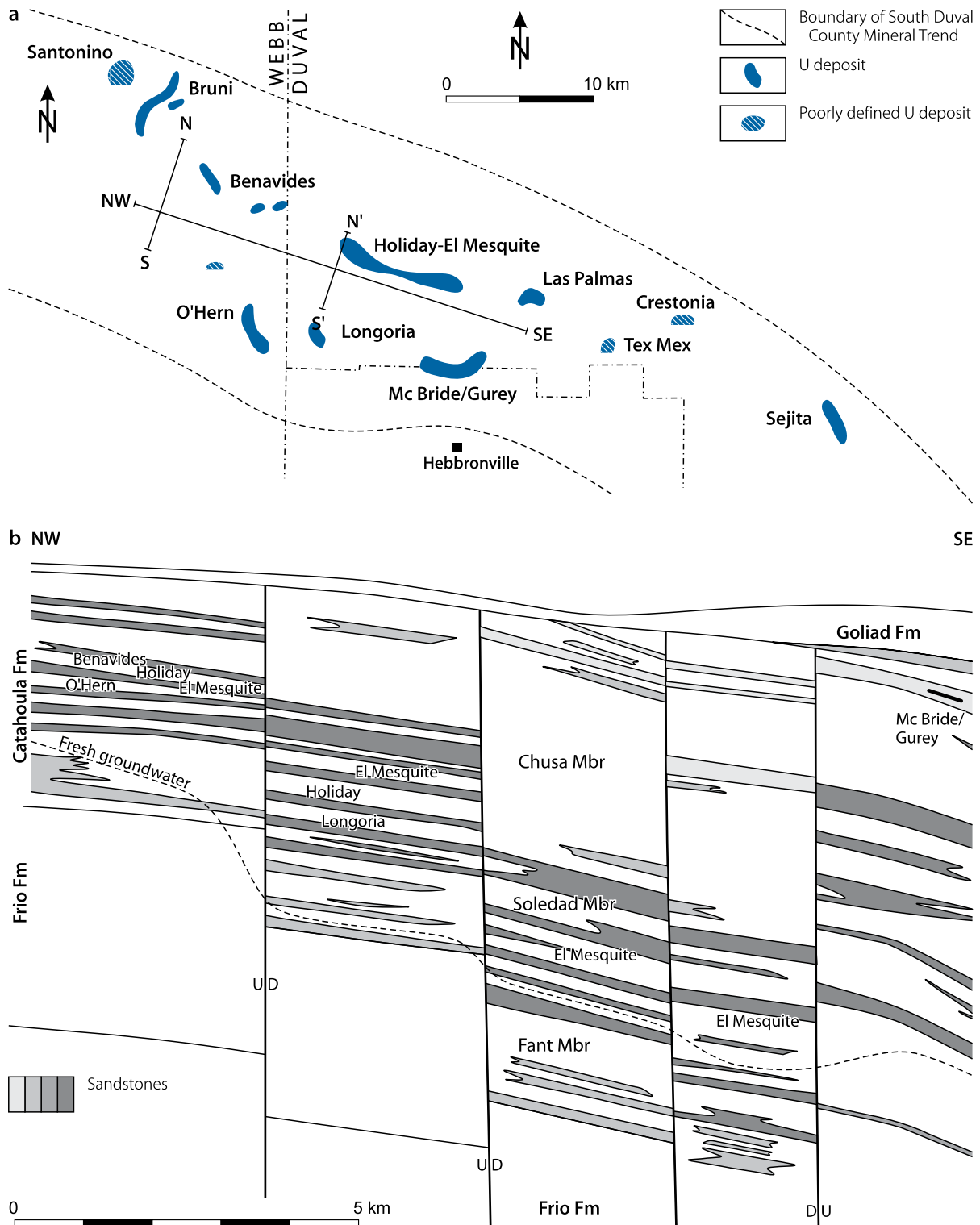
The *O'Hern* and *Holiday-El Mesquite* deposits contain an unusually high accumulation of uranium, probably because the ore bodies extend over several individual sand beds, which are in some manner interconnected within the mega-channel system. The latter deposit has a remarkable length extending 9 km downdip within the same stratigraphic horizons. Over this distance, its depth increases from 150 m to almost 450 m below the surface.

The position of various ore bodies suggests that uraniumiferous oxygenated water percolated down the mega-channel within aquifers of the *Soledad Member*, bifurcated, and flowed around the central mass of reduced sandstone, which strongly resisted oxidation. As a result, rollfronts formed along the boundary of this reduced sand body. Movement of considerable volumes of uraniumiferous oxygenated water tangentially past this interface probably accounts for the size of the deposit.

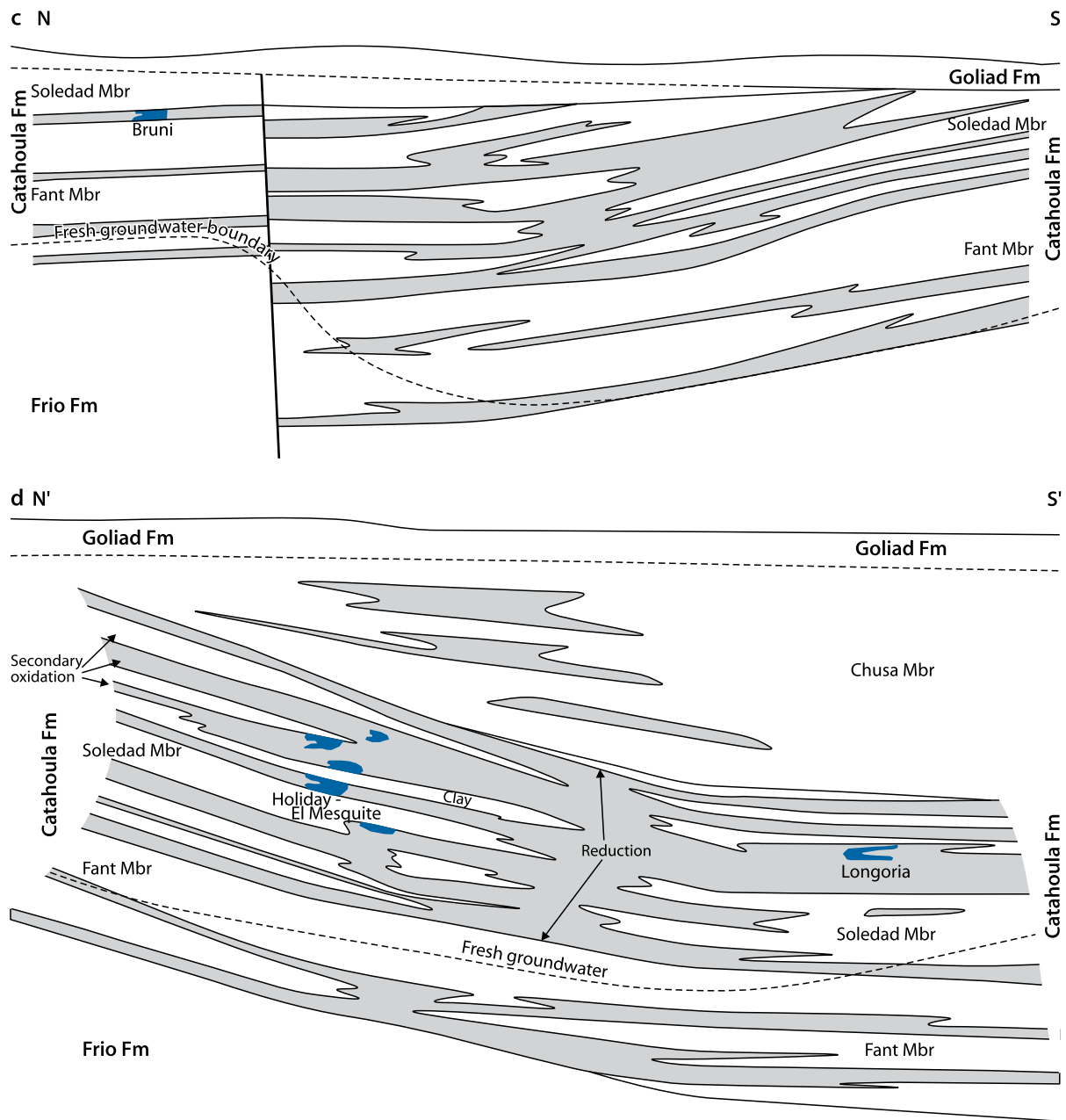
The presence of similar size ore bodies in the *Soledad Member* further downdip from the *Holiday-El Mesquite* and *Longoria* ore bodies is unlikely for the *Soledad Member* changes its coarse sand nature into a brackish-to-salt water facies. Furthermore, the sediments exhibit primary oxidation and lack the reducing constituents in sands required for uranium reduction and precipitation.

Fig. 8.20.

South Duval County Mineral Trend, (a) map with outline of uranium deposits, (b), (c), and (d) schematic sections through the mineral trend showing the stratigraphic position of U deposits hosted in the Soledad Member of the Oligocene Catahoula Formation in the northwestern part, and of minor deposits in the Miocene Oakville Sandstone in the southeastern part of the belt. (Sand horizons are indicated by patterns in sections). (After Adams & Smith 1981)



■ Fig. 8.20. (Continued)



Benavides (Prod. by ISL, 1980–1983: ca. 190 t U): This deposit consists of a typical roll-type ore body positioned at the boundary between downdip-reduced sandstone and updip-oxidized sandstone (▶ Fig. 8.10f). Reynolds and Goldhaber (1978, 1983) and Goldhaber et al. (1978) investigated sulfur isotopes and Fe–Ti oxide minerals and their post-depositional alteration products for a distance of 1.7 km across the redox front. In reduced rock in front of the roll, they found that titanomagnetite and, to a lesser extent titanohematite, had been replaced by pyrite and marcasite. Behind the roll, for a distance of approximately 210 m, the sands contain abundant limonite, but no titanomagnetite or sulfides. By contrast, 1 km updip from the rollfront the sands contain titanomagnetite and martite, with no evidence that they were ever sulfidized. This fact suggests

that heavy minerals were originally sulfidized up to a point between at least 210 m and less than 1 km behind the present rollfront, and that oxygenated solutions subsequently invaded the sandstone and completely destroyed the sulfide replacements of the original titanomagnetite for a distance of at least 210 m during propagation of the rollfront.

Sulfide mineralogy and sulfur isotopes furnished equally significant metallogenetic information. Sands well downdip in front of the rollfront contain predominantly pyrite with isotopically heavy sulfur (greater than zero per mil). Distinct from the pyrite distribution is a later stage of marcasite that is associated with the rollfront. The marcasite forms rims around first-stage sulfides. Sulfur of this ore stage-related sulfide mineralization is isotopically light (–25 to –40‰) and is interpreted

to have formed from pre-ore (first stage) sulfides by a partial oxidation to soluble metastable sulfur oxygen ions. Based on the foregoing observations, the authors propose the following mechanism for formation of the Benavides deposit:

1. Shortly after deposition of the Catahoula sediments, fluids containing dissolved hydrogen sulfide (H_2S and HS) entered the sandstone aquifer along one of the many growth faults in the region. The most likely fault is approximately 1.5 km downdip from the deposit
2. As the fluids migrated updip within the aquifer, Fe–Ti oxide minerals were altered to FeS_2 (dominantly pyrite). Reducing fluids moved only about 2 km updip; at their foremost advance, they produced a boundary within the aquifer between sulfidized (downdip) and unaltered (updip) Fe–Ti oxide-bearing sands
3. Subsequently, oxygenated uraniferous groundwater moved downdip into FeS_2 -bearing sandstone and established a roll-type deposit. Partial oxidation of first stage pyrite was followed by precipitation of marcasite as rims on first stage pyrite in unmineralized sandstones.

Although no comparable mineralogical and geochemical studies have been performed on other Catahoula deposits in the South Duval Trend, it is likely that they formed by similar processes.

8.3 Deposits in the Early Miocene Oakville Formation, Fleming Group

The largest uranium deposits in the Oakville Formation occur in the Ray Point and Clay West-Burns districts, and in the Rhode Ranch area (Fig. 8.1). The *Ray Point district* in northern Live Oak County includes the *Lamprecht-Zamzow-Felder*, *McLean*, and *Kopplin* deposits, and the *Clay West-Burns district* in southwestern Live Oak County the *Clay West*, *Burns*, *Boots*, *Lyne*, *Pawlik*, and *Perkins* deposits. The *Rhode Ranch* and *Campana* deposits are in McMullen County. A few small deposits exist in northern Bee County (e.g., *Pawnee*), and in southern Duval County. The *Mabel* mine exploited oxidized ore.

Sources of Information. Adams and Smith 1981; Galloway et al. 1979a; Goldhaber et al. 1979; Klohn and Pickens 1970; Ludwig et al. 1982; Reynolds et al. 1980a, b; Reynolds and Goldhaber 1983.

Geological Setting of Mineralization

Galloway et al. (1979a) describe the Oakville Formation as derived from a bed-load fluvial system comprised of several coastal-plain rivers. Downdip toward the paleo-coastline, fluvial sediments grade into equivalent strandline facies of deltaic and barrier-bar sedimentary systems. Uranium-hosting sands are part of bed-load and mixed-load channel facies and associated crevasse splay deposits. Less permeable units marginal to the

channel axes include heterogeneous distal crevasse sequences, abandoned channels, channel-margin levees, and calcareous flood-plain muds. Clay minerals of these sequences are dominantly montmorillonite with variable amounts of kaolinite and subordinate illite.

All major Oakville U deposits are closely grouped around a NE–SW-trending fault zone extending the length of the south Texas area. In northern Live Oak County, the Oakville fault, a SE-dipping fault, runs through or close to mines on the north, and a NW-dipping fault trends through deposits on the south, forming a wide graben that extends northeastward through Live Oak County. Two of the northern mines, *McLean 1* and *Kopplin*, are cut by faults and two others, *McLean 2* and *Felder*, are within a kilometer of a fault. The two southern deposits, *Clay West* and *Burns*, are close to a fault (Fig. 8.21).

Mineralization

Pitchblende and coffinite are the principal U minerals. They are accumulated in sinuous rollfronts near the margins of major fluvial sedimentary axes.

Major districts occur in the vicinity of faults as outlined above, but not all deposits are associated with known faults. Several deposits contain post-fault mineralization. At the *McLean* mine, high-grade mineralization occurs within fault gouge for several meters depth.

Larger ore bodies appear to be associated with larger, more transmissive sandstones and occur more commonly within reduced, FeS_2 -bearing sandstone than in other lithologies. Reynolds and Goldhaber (1983) report four distinct generations of iron di-sulfide mineralization in the *Felder* and *Lamprecht* deposits. Some deposits in the *Clay West district* as well as the *Rhode Ranch* deposit also occur entirely within reduced sandstone. The only oxidation associated with mineralization results from surface oxidation of shallow mineralization.

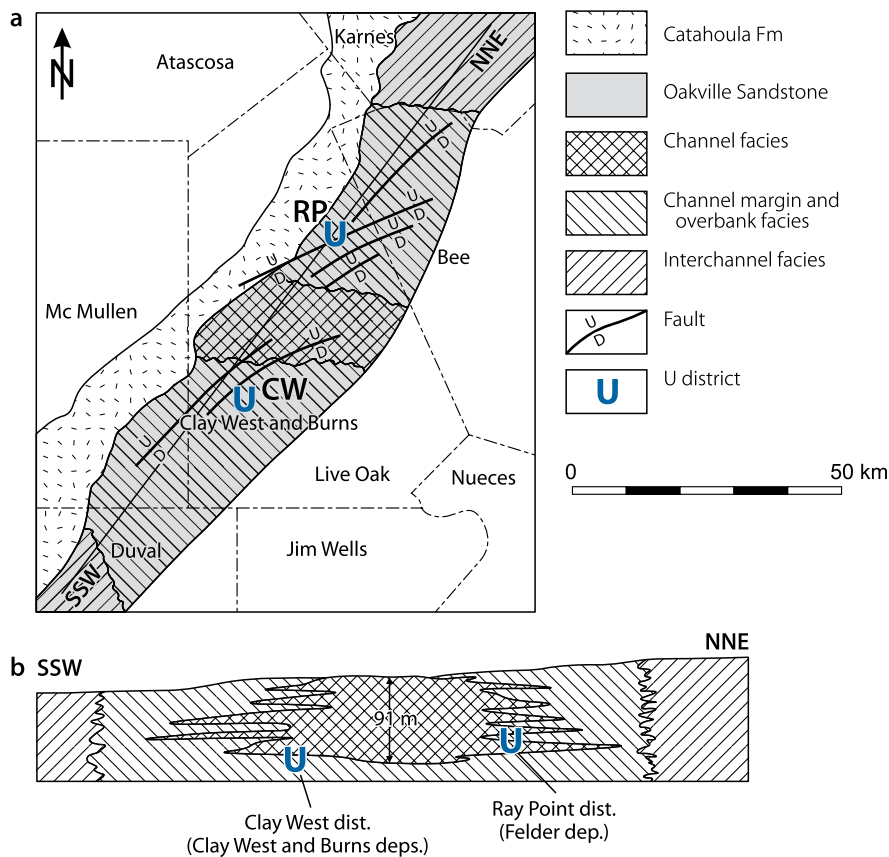
About 20 km to the north of the Ray Point district, some small deposits (50 t U or more) occur in the Lower Oakville sands along a minor fluvial axis and are not associated with any known structure. About 60 km further to the northeast, some ore bodies are in host sands, which lie in a transition zone between Catahoula and Oakville lithologies. Deposits in this zone occur in a thick sand near the margin of an oxidized fluvial axis and are associated with faults.

8.3.0.1 Oakville Deposits in the Ray Point District, Live Oak County

This district includes the *Lamprecht*, *Zamzow*, and *Felder* deposits. Other deposits are *McLean 1* and *2* located about 2 and 1 km SW, respectively, of the *Felder* deposit, and *Kopplin*, ca. 1 km NW of *Lamprecht* (Fig. 8.22a). The original resources of the Ray Point district were reportedly on the order of 4,000–5,000 t U. Production in the Ray Point district began in the early 1970s and amounted cumulatively to about 2,200 t U. The main production period lasted from 1976 through 1988 when uranium was

Fig. 8.21.

Ray Point (RP) and Clay West (CW) districts, (a) generalized geological map and (b) SSW-NNE section showing location of major uranium deposits in, and their relation to depositional facies of the Miocene Oakville Sandstone and faults. [After Eargle et al. 1975 and Klohn & Pickens 1970 (reproduced by permission of AIME)]



recovered by ISL methods at Lamprecht (570 t U) and Zamzow (480 t U), and by open-pit operations at Felder (980 t U, 0.2% U).

Sources of Information. Adams and Smith 1981; Bomber et al. 1980; Goldhaber et al. 1979; Klohn and Pickens 1970; Reynolds et al. 1980a; Reynolds and Goldhaber 1983.

Geology and Mineralization

The *Lamprecht-Zamzow-Felder* deposits (from E to W) form a continuous U zone in excess of 3.2 km long and up to 240 m wide. Klohn and Pickens (1970) describe the *Felder* deposit, which may also be applicable to the two adjacent deposits, as located marginally to a major NW–SE-trending alluvial sand system, the central portion of which is approximately 100 m thick (Figs. 8.22a–d). The axial zone contains coarser sediments. It is flanked on both sides by interbedded sand and clay, which ultimately grade into predominantly clay and silt. Ore is emplaced lithologically in the zone of interbedded sand and clay and structurally between two faults. The major fault is approximately 500 m to the southeast of the deposit. It displaces the Oakville strata by approximately 35 m.

Uranium is concentrated in basal reduced sandstone of the Oakville Formation. The host rock is a fine- to medium-grained, moderately sorted, carbonate-rich arkosic sand. It locally contains large clay galls, as well as clay lenses and stringers. Sand is composed of quartz with lesser amounts of chert, feldspar, detrital carbonate, and fine-grained volcanic fragments. Organic carbonaceous matter is virtually absent.

Molybdenum enrichments occur ca. 300 m downdip from the rollfront in a band of sandstone up to 300 m wide. Anomalous but erratically distributed concentrations of selenium are present in the vicinity of U mineralization. Marcasite is the dominant FeS_2 phase in mineralized and in barren, reduced zones (Fig. 8.10d), whereas pyrite prevails over marcasite in the re-reduced altered tongue.

As mentioned above, the *Felder* deposit occurs within reduced sandstone some distance downdip from a redox boundary. Klohn and Pickens (1979) interpret this situation that, in the virtual absence of carbonaceous debris, pyrite-bearing sandstone probably resulted from introduction of H_2S . Detrital Fe–Ti oxides are still present in updip oxidized sands, but rapidly disappear downdip within reduced sandstone. Some pyrite is still magnetic, which suggests that remnants of magnetite are still present in these sulfidized grains.

■ Fig. 8.22.

Ray Point district, Felder-Zamzow-Lamprecht deposits, (a) map of outline of the Oakville Sandstone-hosted deposits, (b+c) NW-SE sections through the Felder mine with U grade distribution, (d) N-S section through the Zamzow deposit with distribution of primary and secondary ore zones and measured radioactivity. (see Fig. 8.10e for W-E section through the Lamprecht deposit). [After (a) and (d) Galloway et al. 1979b; (b+c) Eargle et al. 1975 (AAPG, 1975, reprinted by permission of the AAPG whose permission is required for further use), and Klohn & Pickens 1970 (reproduced by permission of AIME)]

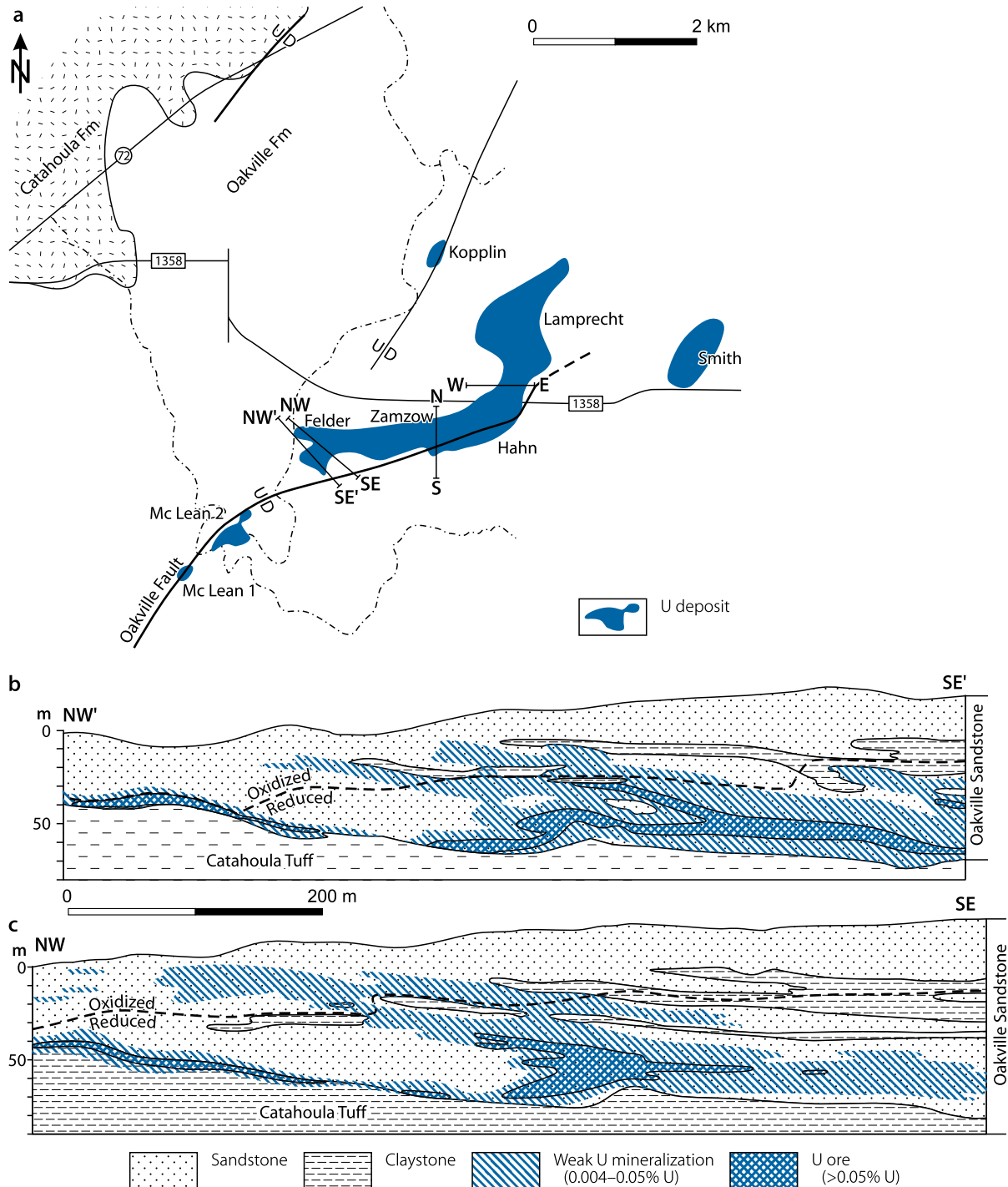
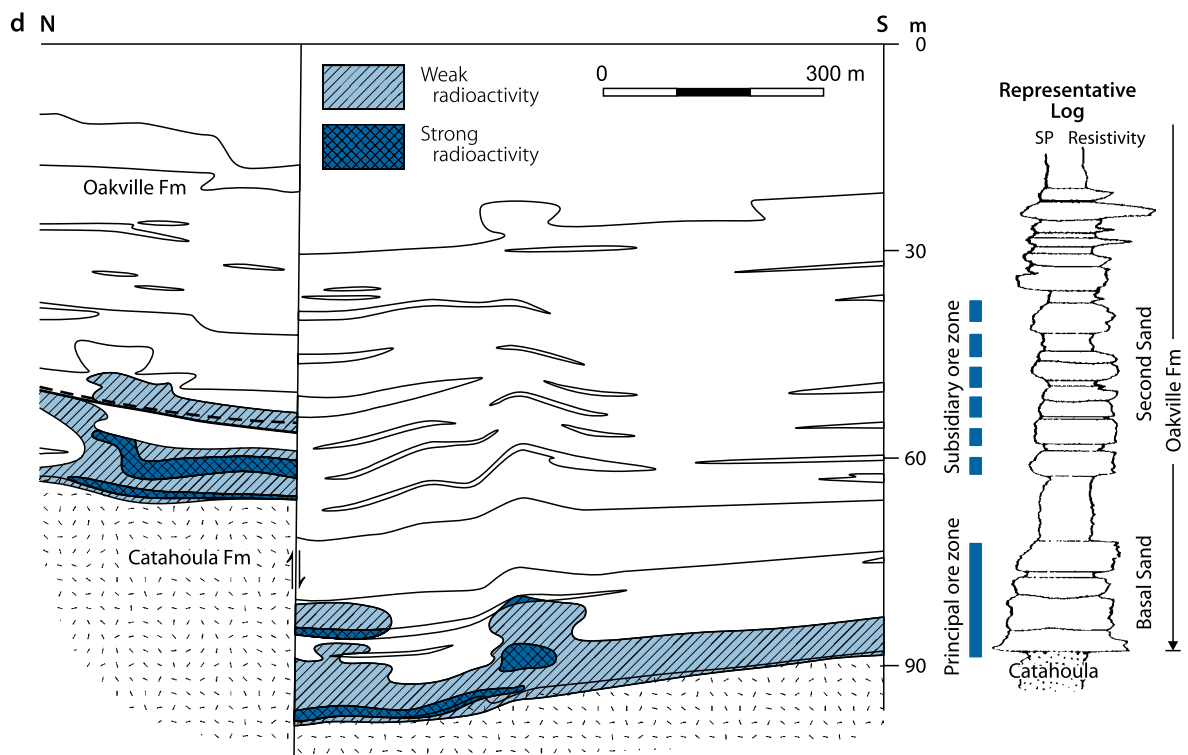


Fig. 8.22. (Continued)



The *McLean No. 5* deposit in the Ray Point district (Bomber et al. 1980) is emplaced in arkosic sands of the Oakville Formation adjacent to a fault. The major detrital constituents of sands are quartz, feldspar, and rock fragments, which are accompanied by authigenic zeolites, micritic calcite, pyrite, marcasite, and clay minerals. In low-grade mineralization, uranium occurs adsorbed on titanium oxides, principally leucoxene, altered rock fragments, and clay galls. In higher grade ore, uranium, principally as pitchblende, coats grains. Molybdenum is enriched in ore, and some uranium occurs within opaline matrix cement.

Shape and Dimensions of Deposits in the Oakville Formation

The *Ray Point district* in northern Live Oak County is essentially one ore body. The individual deposits are only a result of a subdivision by property lines. This ore body is about 3.6–4.5 m thick and 30–90 m wide. The deposit is continuously mineralized for almost 4.5 km, but it is not economic for its entire length. The average ore grades are in the range of 0.13–0.17% U. The greatest concentration of uranium mineralization is always within the basal sands of the Oakville Formation. Isolated, smaller ore pods are known to occur in sands near the middle of the Oakville Formation within the Ray Point district.

Stable Isotopes

Reynolds et al.'s (1980a) comprehensive mineralogical and isotope studies suggest that four distinct generations of FeS_2

minerals exist in the Lamprecht–Felder deposits, including two stages of post-ore sulfidization. The four FeS_2 generations and their respective $\delta^{34}\text{S}$ values are, from oldest to youngest: (1) Pre-ore generation of dominantly pyrite with $\delta^{34}\text{S}$ values of ca. -25 to -35% ; (2) pre- to syn-ore generation of marcasite with $\delta^{34}\text{S}$ values of ca. -25 to -47% ; (3) post-ore generation of pyrite with $\delta^{34}\text{S}$ values of ca. $+10$ to $+24\%$; and (4) late post-ore generation of marcasite with $\delta^{34}\text{S}$ values estimated at ca. -45% . As is apparent from these data, the first post-ore pyrite generation (no. 3), which occurs in re-reduced sands is represented by isotopically heavy sulfur-bearing pyrite, whereas pre- to syn-ore marcasite (no. 2) and late post-ore marcasite (no. 4) generations are represented by isotopically light sulfur-bearing marcasite.

Reynolds and Goldhaber (1983) interpret the above results for the *Felder* and *Lamprecht* deposits as follows. The isotopically light composition of pre-ore FeS_2 (first generation) does not compare with sulfur isotopes of a deep seated source, e.g., with sour gas of the Edwards Formation, which could have fault-leaked into the Oakville Formation. Instead, an origin related to shallow sulfate reduction seems to be more likely. The authors consider a transport of dissolved organic matter in connate brines along the Oakville Fault to shallow depths. Here, bacteria would metabolize organic matter and sulfate in the brine, or within local meteoric groundwater, to form isotopically light pre-ore FeS_2 .

Sulfur isotopes of ore-stage marcasite (second generation) very likely had two sulfur sources. The first source was probably pre-ore sulfide, which was redistributed as the rollfront migrated into barren, reduced and mineralized sands. The second source may have been similar, perhaps identical to that responsible for pre-ore pyrite generation. Mixing of these two sulfur species by

an oxygenated meteoric groundwater and a reduced brine led to formation of ore-stage marcasite along a rather broad zone.

The source of post-ore heavy sulfur (third generation) is thought to have been the Edwards Formation, since sour gas of that formation has an isotopic composition similar to post-ore pyrite. Post-ore light sulfur in marcasite (no. 4 generation), which is still present in solutions in the mining area, may have been derived from the Carrizo or Wilcox formations and may be the result of mixing of connate brines, extrinsic to the Oakville Formation, with meteoric waters (Galloway et al. 1979).

Pb/U isotope analyses of ore from the *Felder* deposit by Ludwig et al. (1982) yielded an apparent age for ore formation of 5.07 ± 0.15 Ma.

Metallogenetic Aspects

Based on their investigations of the *Lamprecht* deposit, Goldhaber et al. (1979) postulate the following metallogenetic evolution, which is supported by the more recent findings by the various scientists mentioned above. The authors demonstrate that the geometric shape of the *Lamprecht* ore body and the suite of elements zoned across it are typical of roll-type deposits that occur at well-developed redox boundaries. This is valid for the unusual occurrence of this deposit, as well as of other deposits in south Texas that are placed within reduced sandstones some distance away from a redox front. This elemental zoning suggests that these deposits originated by the customary rollfront mechanism as known from roll-type deposits elsewhere in the world.

Goldhaber et al. (1979) also provide evidence that, prior to rollfront development, H_2S was introduced into the oxidized host sand forming a pre-ore stage of pyrite (no. 1 generation). Oxidizing water percolating within the host sand impinged upon these reduced, pyritic sediments and formed the redox front. Coeval with and as part of the ore-forming process, marcasite (no. 2 generation) was deposited downdip in sands adjacent to the rollfront. At a later time, additional sulfur was introduced into the aquifer and caused a re-reduction of the altered tongue in oxidized hematitic and limonitic updip sands, leaving the deposit completely within reduced sandstone.

8.3.0.2 Clay West District

Located approximately 30 km SE of Ray Point, deposits in the *Clay West district*, have approximately the same average U grade, but are slightly larger than deposits of the Ray Point district. Individual ore bodies are shorter, but wider than at Ray Point due to faults that have divided the long rollfronts into a series of shorter sections. The Clay West district had original resources on the order of 4,000–5,000 t U, and produced almost 3,100 t U by conventional mining from 1973 through 1987.

8.3.0.3 Rhode Ranch Area

The Rhode Ranch and adjacent area contains the Rhode Ranch and Campana deposits as well as several small deposits

([Fig. 8.1](#)). Original resources in the Rhodes Ranch area were about 3,000 t U; some other properties account for several hundred tonnes U. The Rhode Ranch deposit was exploited by an open-pit mine from 1988 through 1992. Production was reported to be 2,570 t U at an average ore grade of 0.27% U.

As mentioned earlier, the Rhode Ranch deposit is entirely within re-reduced sands, and the multiple rollfronts in this deposit suggest that it may have experienced reduction possibly three and four times.

8.3.0.4 Oakville Deposits in the South Duval County Mineral Trend

This mineral trend contains only a few noteworthy uranium deposits in the Oakville Formation, namely *McBride/Gurey*, *Las Palmas*, and *Trevino*. These deposits are located in Duval and Webb counties, to the north and northeast of the town of Hebronville.

Sources of Information. Adams and Smith 1981.

Geology and Mineralization

The Oakville Formation hosts U deposits to the south and east of the Holiday-El Mesquite area within the mega-channel system of the South Duval County Mineral Trend and near the Crestonia fault system. These deposits may represent nothing more than a uranium emplacement in the next favorable accessible reduced sandstone downdip from the O'Hern-Holiday-El Mesquite area.

Ore bodies are of roll type and commonly small, but locally contain relatively high-uranium grades. They are hosted in the lowest sands of the Oakville Formation, which overlie the Chusa Member of the Catahoula Formation. Sands on the northern side of ore bodies are secondarily oxidized and reduced on the south side.

Mineralization is usually confined to gravel intervals and occurs at depths from 90 to 120 m, i.e., at the same depths as the updip end of the O'Hern and Benavides deposits in the Soledad Member/Catahoula Formation. Host sands are up to 15 m thick and contain mineralization up to 6 m thick.

The source for uranium is thought to be the underlying Chusa Member of the Catahoula Formation, but detritus of trachyandesite reported from the host sand at Las Palmas and other areas indicate a volcanic constituent and a potential uranium source within the Oakville Formation itself. Disequilibrium factors vary between 2.5 and 14 in favor of chemical uranium and indicate in part a very young age of ore. This suggests that the deposits may have experienced continuous formation or may be experiencing some rejuvenation due to recent hydro-dynamic changes. It is also possible that they are forming at the expense of older ore bodies in the underlying Catahoula Formation.

At the *Tex-Mex* and *Crestonia* occurrences, located to the east of the Las Palmas deposit, mineralization occurs at depths from 360 to 420 m in basal sands of the Oakville Formation.

Faulting in this area has evidently permitted introduction of H_2S , which has reduced Oakville sands within this part of the South Duval County Mineral Trend.

8.4 Deposits in the Late Miocene-Early Pliocene Goliad Formation, Citronella Group

Uranium deposits in the Goliad Formation include *Crestonia*, *Palangana Dome*, *Piedras Pintas*, and *Sejita* in Duval County, *Mount Lucas* and *Swinney Switch* in Live Oak County, *Kingsville Dome* in Kleberg County, *Alta Mesa* in Brooks County, *Rosita* in Duval County, and *Goliad* in Goliad County.

Sources of Information. Adams and Smith 1981; Galloway et al. 1979a; Pool 1990, 1993; Weeks and Eargle 1960.

Geology and Mineralization

The Goliad Formation is the youngest of the U-hosting Tertiary units. It stretches along the southeastern side of the older U-bearing sequences and known uranium deposits and occurrences are actually located off the South Texas Mineral Trend (►Fig. 8.1). Some mineralized areas are associated, at least spatially, with salt domes, as at *Kingsville Dome*, *Palangana Dome*, *Piedras Pintas*, *Sejita*, and possibly *Alta Mesa*; but others are not, such as those at *Mount Lucas* and *Swinney Switch*.

Where mineralized, the Goliad Formation contains four to six well-developed channel sands. Generally, up to four of these sand horizons may carry uranium in typical roll-shape fashion. Rollfronts may be arranged in the various sand units en echelon or totally unrelated to each other. It has not been established whether the rollfronts are each separate fronts or whether they are part of a major rollfront system. No obvious source for uranium has been established. The closest source would be pyroclastics of the Catahoula tuffs.

8.4.0.1 Kingsville Dome

Kingsville Dome is located ca. 10 km SE of the town of Kingsville in Kleberg County. In situ resources total 2,700 t U. Grades average 0.12% U. Exploitation by ISL techniques began in 1988 and is ongoing.

Source of information. Pool 1990.

Geology and Mineralization

The Kingsville Dome is one of the largest diapiric structures in southern Texas measuring approximately 25 km². It contains an oil field at depth. Uranium is concentrated around the margin of the dome (►Fig. 8.23) in fluvial-deltaic sediments of the Pliocene Goliad Formation. At the dome, this formation obtains

a thickness of as much as 300 m, with an average thickness of some 200 m. Major faults cut the oil field and U-hosting Goliad strata.

Uranium is hosted in loosely consolidated sands with high porosities and permeabilities. These sands form four sandstone horizons separated by less permeable beds. Sand horizons average about 15 m in thickness each, but where they coalesce thicker sandstone units exist. Uranium may occur in multiple fronts that are commonly less than 30 m wide and can extend for several kilometers in length. The fronts interweave, overlap, and occasionally are stacked on top of each other.

Coffinite and pitchblende tend to be the principal U minerals. They coat and occur interstitial to sand grains. Sites of ore formation tend to be controlled by the above mentioned faults. They permitted migration of methane and H_2S into the shallow host sands to form a favorable reducing environment required for formation of a redox front and associated uranium precipitation.

8.4.0.2 Alta Mesa

Alta Mesa is situated in southern Brooks County. Original in situ resources totalled ca. 1,600 t U at a grade averaging 0.13% U (details see further below). Exploitation by ISL techniques began in 2005 and is ongoing.

Source of information. Pool 1993.

Geology and Mineralization

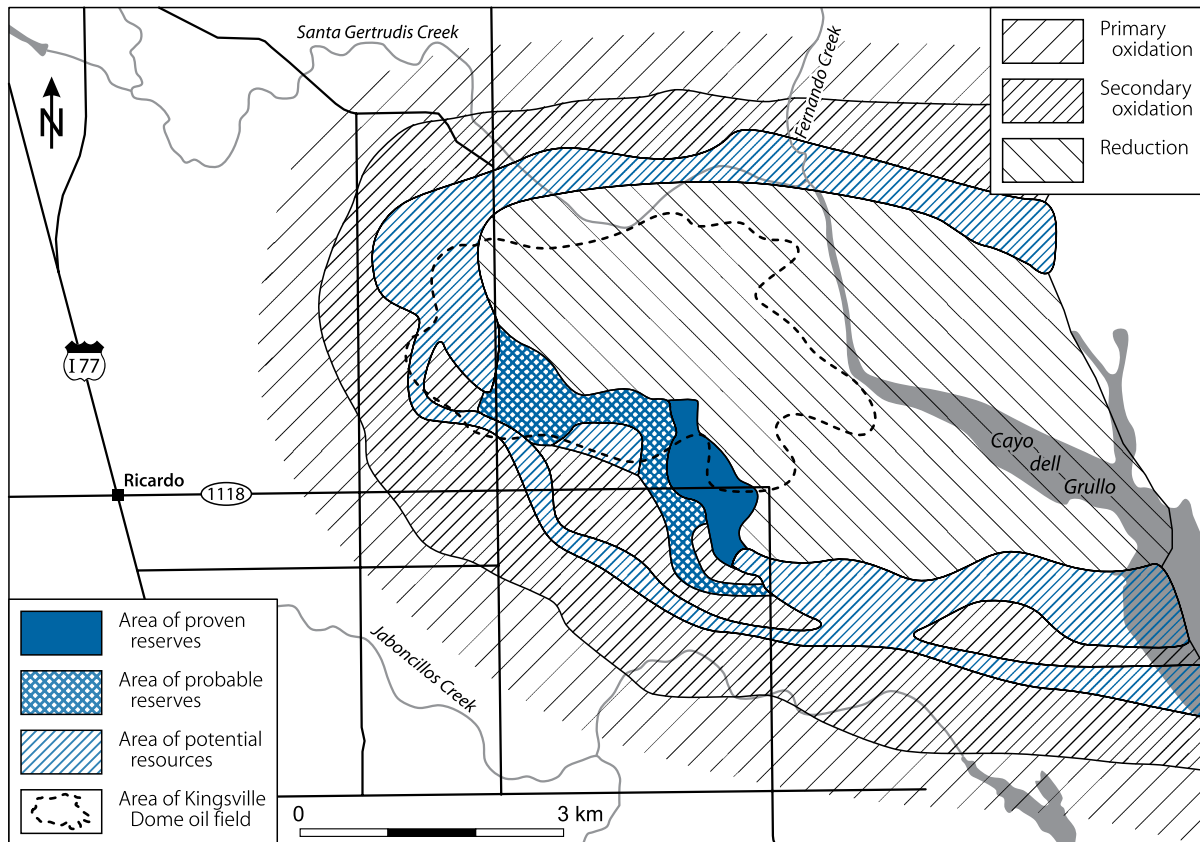
The Alta Mesa area is a closed domal structure (►Fig. 8.24) generated by a deep seated salt diapir associated with the Vicksburg flexure. This structure is bounded on the northwest by the Vicksburg fault zone. The top of the salt is at a depth of approximately 5–6 km. In response to sediment loading, the salt has become reactivated generating extensional fault footwalls. The Vicksburg flexure has created a pattern of normal and antithetic faults against these footwalls. These faults permeate to the near surface and hence provide pathways for hydrocarbons and H_2S .

The uranium-hosting Goliad Formation is 180–210 m thick at Alta Mesa, and comprised of poorly consolidated sands separated by persistent mudstone horizons. These sediments were deposited by low-energy rivers flowing southeasterly toward an oscillating coastline. The Goliad Formation rests unconformably on the Fleming Formation and is unconformably overlain by the Lissie Formation. A thin veneer of Holocene dune sands, clays, and caliche covers the Lissie Formation. Oil and gas accumulations occur in the Goliad and older formations to depths in excess of 2,100 m.

The Goliad Formation is separated into an upper, middle, and lower sequence due to a distinct change in the style of sedimentation approximately 120 m above the base of the formation. The upper sequence includes the A and B sand horizons with intervening clayey to tuffaceous mudstones. No significant uranium concentrations have been identified in these two horizons. The middle and lower sequences include distinct sand horizons with good porosity and permeability,

■ Fig. 8.23.

Kleberg County, Kingsville Dome, map of the domal salt structure documenting the uranium trend peripheral to the reduced facies of the Goliad Formation on the apex of the domal structure and overlying the Kingsville Dome oil field. (After Pool 1990)



from 6 to 24 m thick, designated C to H, separated by thin but relatively continuous mudstone beds. Highest grade and most persistent uranium concentrations tend to be restricted to the C sand horizon.

Host sands are very fine- to medium-grained calcareous arenites, composed of 60–75% quartz, 20–35% calcite, 3–5% lithic fragments, and authigenic minerals including calcite, clay species, zeolite, and pyrite (trace to 3%). U minerals tend to be primarily pitchblende, coffinite, and brannerite(?). They are present in two modes: The first two occur as small globules coated on, and intermixed with clay minerals and other authigenic and detrital minerals, and the latter as large grains composed of U–Ti oxides.

Ore bodies exhibit typical roll shapes with high-grade segments. High-grade ore pods are intermittently localized, interspersed with lower grade mineralization, at the interface between yellow-brown to orange, oxidized sands and grey, pyritic, reduced sands. Grades commonly range from a few 0.0X% U to a few 0.X% U.

Rollfronts are elongate and highly sinuous probably due to the fact that a typical, epigenetic oxidation tongue as known from other regions with rollfront uranium deposits was obviously never developed in the Alta Mesa area. Instead it is postulated that redox fronts developed where migrating uraniferous,

oxygenated groundwater encountered a continually replenished local plume of reducing conditions on the apex of the domal structure. The reducing environment in the Goliad Formation was generated by ingress of oil and gas that migrated upward from deeper reservoirs along fractures of the Vicksburg fault system as outlined earlier.

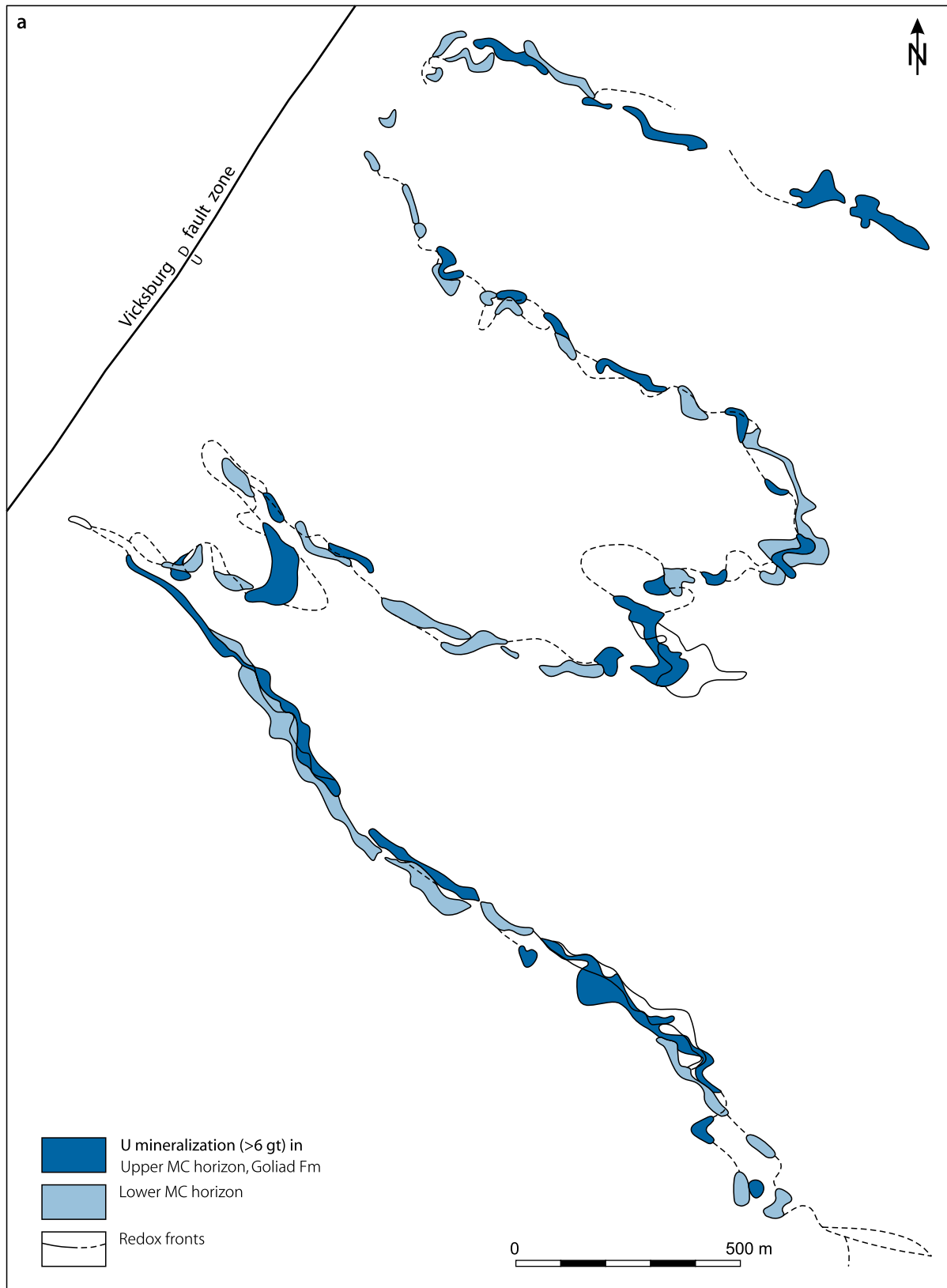
Six ore zones are delineated based on a cutoff factor of 0.025% U and a minimum thickness of 0.3 m. They are spread over a rollfront length of about 6.5 km, range in width from <15 to 30 m, in thickness from several decimeters to few meters, and occur at a depth of 130–140 m. Their in situ resources total 1,600 t U at an average grade of 0.13% U. Individual ore zones range from 45 t U at 0.105% U and a thickness of 2.2 m, to 660 t U at 0.142% U and a thickness of 3.6 m. By using a 0.0085% U cutoff grade, eight ore zones could be defined containing reserves from 200 to 1,060 t U and a total of 3,435 t U.

8.4.0.3 Palangana Dome

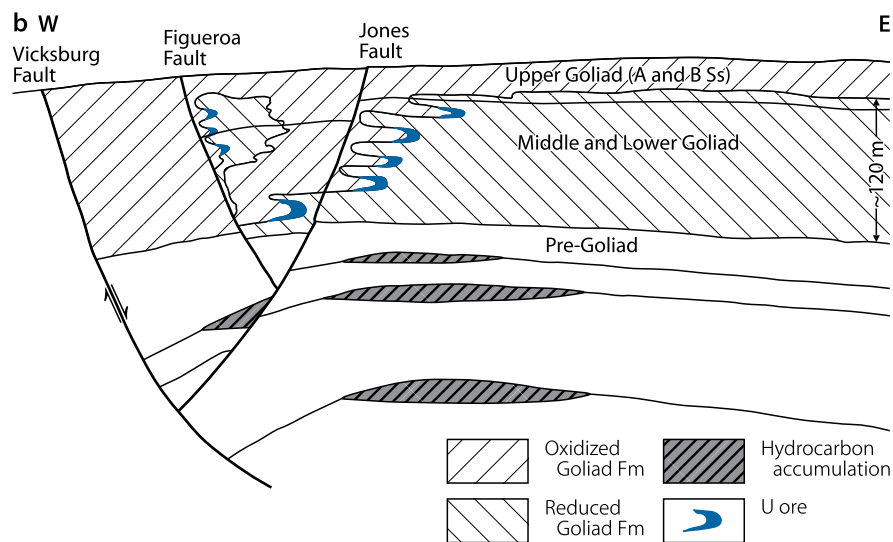
The Palangana Dome deposit (▶ Fig. 8.25), located at a salt dome of the same name in east-central Duval County, is the largest of the Goliad deposits with resources of some 3,000 t U at a grade of 0.07% U.

■ Fig. 8.24.

Brooks County, Alta Mesa, (a) map with redox fronts, in Middle 'C' (MC) sand horizons of the Goliad Formation and associated U-mineralized intervals; (b) schematic W-E cross-section showing the multiply stacked distribution of roll-shaped uranium ore bodies. Ore bodies are hosted in sand horizons separated by thin clayey to tuffaceous mudstones. (After INI 1993 based on Cogema data)



■ Fig. 8.24. (Continued)



Sources of Information. Adams and Smith 1981; Eargle 1960; Smith RB, personal communication.

Geology and Mineralization

The Palangana Dome has been formed by a salt-diapir that pierced all Tertiary sediments except the Goliad and then subsided after Goliad time. The Goliad Formation is draped slightly over this diapir. The dome was apparently a positive feature that bifurcated a major channel system during Goliad (Miocene) time. The relief was so slight, however, that the two channels occur over the diapir. Sulfur occurs in the dome and oil is trapped in the Tertiary formations flanking the dome. Hydrogen sulfide is abundant in the Goliad sands around the dome.

Ore bodies occur as typical rollfronts at the interface between secondary oxidation and reduction within the channel sands on the updip western and southwestern side of the dome. Three successively deeper rollfronts are reportedly arranged en echelon in sands at depths ranging from 60 to 105 m. The sands are up to 15 m thick, but contain numerous, discontinuous clay lenses.

Weeks and Eargle (1960) describe the mineralization as disseminated sooty pitchblende in a highly calcareous, clay-gall conglomerate interbedded with friable sand and locally impregnated with a little oil. The conglomerate contains black chert pebbles, nodular chalcedony, and a few fossilized bones and teeth.

The role of the salt diapir at Palangana, and its association with uranium is not well understood. Probably the relationship is only remote and indirect. It appears that the dome has been important as a site of fracturing that permitted introduction of reductants into aquifers, but that has occurred elsewhere in south Texas without the presence of salt domes. The reductants may have been H_2S derived from deeper formations or H_2S produced from the anhydrite and gypsum of the dome by sulfate-reducing bacteria. There is no report of re-reduction in the Goliad sands.

8.4.0.4 Rosita

Rosita is situated in Duval County, 6 km E of the town of Freer. In situ resources (status 1991) were stated to be approximately 2,300 t U at an average grade of 0.14% U. About 1,000 t U were recovered intermittently from 1990 to 1999 by ISL techniques.

Source of information. Pool 1991.

Geology and Mineralization

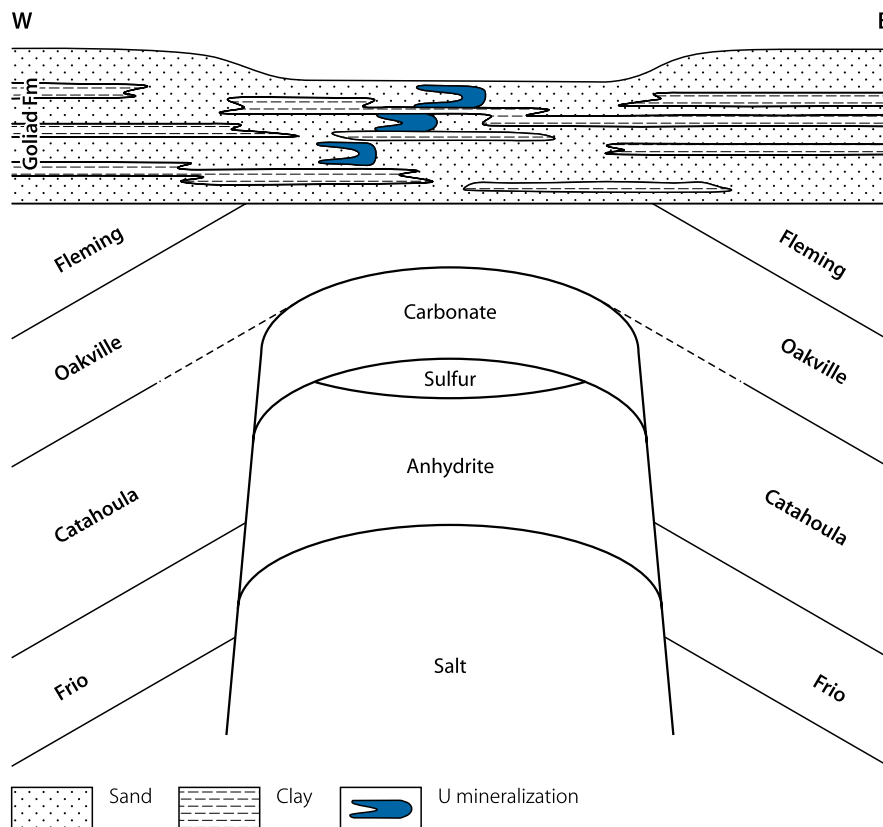
At Rosita, the ore-hosting Pliocene Goliad Formation averages a thickness of about 210 m. Sediments are of fluvial-deltaic origin. Ore bodies are of rollfront type and occur along highly twisted redox fronts in one sandstone unit composed of loosely consolidated sands with high porosities and permeabilities. This unit averages about 9 m in thickness, but may contain several redox fronts. The average depth to the ore is about 60 m. Mineralization is about 3.6 m in thickness and relatively narrow in width, but may extend for many kilometers. Mineralized trends interweave, overlap, and occasionally are stacked one on top of the other. Uranium is in disequilibrium. Reducing conditions required for redox-front development and associated ore formation are considered to be caused by major faulting, allowing migration of methane and hydrogen sulfide into the shallow host sands.

8.4.0.5 Mount Lucas

Mount Lucas is located in southeastern Live Oak County about 30 km SE of the Clay West district. Mineralization at Mt. Lucas is reported to occur as rollfronts in three or four sands at depths between 45 and 135 m. The position of the fronts in the different sands are unrelated to those in overlying or underlying sands, and they apparently cross back and forth above one another.

Fig. 8.25.

Duval County, Palangana Dome, schematic section with position of uranium deposits with respect to the salt diapir. U mineralization is supposedly in basal units of the Miocene-Pliocene Goliad Formation. (After Adams & Smith 1981)



8.4.0.6 Swinney Switch

Located approximately 50 km northwest of Corpus Christi, this deposit extends from eastern Live Oak County into western Bee County. Lattanzi and Pressacco (2005) report in situ resources of about 460 t U present in three sand horizons.

8.4.0.7 Goliad

The Goliad uranium property is located in north-central Goliad County. Uranium mineralization is hosted in four sand horizons of the Goliad Formation at depths from approximately 25–135 m. In situ measured and indicated resources amount to 2,100 t U and inferred resources to 580 t U. Grades average 0.042% U. Average thickness is 4.5 m (Carothers 2007).

8.4.0.8 Goliad Deposits in the South Duval County Mineral Trend

Two small deposits located at the northeastern edge of the trend are known, *Crestonia* and *Sejita* (Fig. 8.20). Subeconomic U

occurrences within the southeastern extension of the South Duval County Mineral Trend have been reported from the *Alta Verde Dome* and *Gyp Hill* in Brooks County.

The *Sejita* deposit occurs on the eastern flank of the *Sejita Dome*, a salt structure similar to the Palangana Dome, located about 40 km to the north. Mineralization occurs as well-defined rolls in four or five sands within the Goliad Formation. Similar to Mount Lucas, the position of various rolls in different sand horizons appears to be unrelated to each other. Host sands are well-sorted and consist of well-rounded, clear and pinkish quartz, black, brown, and red chert, a few limestone and volcanic clasts with moderate amounts of kaolinite. Sands are usually 6–9 m thick. Mineralization occupies nearly the entire thickness and occurs at depths from 75 to 120 m, i.e., at the same depth as deposits in the Soledad Member/Catahoula Formation and the Oakville Formation up the trend. Several high-grade intercepts have been reported.

The area of reduction within the sands is believed to be teardrop shaped and centered over the *Sejita Dome* with a tail extending down-dip to the east. Secondarily oxidized sandstone tongues adjacent to rolls contain limonite that extends west and north along the northern flank of reduced sands.

Selected References and Further Reading for Chapter 8 South Texas

For details of literature see Bibliography.

Adams and Smith 1981; Baker 1979; Boenig 1970; Bomber et al. 1980, 1986; Bonner et al. 1982; Bowman et al. 1981; Brewton 1970; Bunker and MacKallor 1973; Busche et al. 1981; Carothers 2007; Craig 1980; Dickinson and Duval 1977; Dickinson and Sullivan 1976; Dickinson 1976a, b, c; Duex 1971; Eargle and Snider 1957; Eargle and Weeks 1961, 1973; Eargle 1968, 1972; Eargle et al. 1966, 1971, 1975; Fisher et al. 1970; Galloway and Kaiser

1979, 1980; Galloway 1977, 1979a, b, 1982, 1985; Galloway et al. 1979a, b, 1982; Garner et al. 1979; Goldhaber and Reynolds 1977, 1979; Goldhaber et al. 1978, 1979; Granger and Warren 1974; Harshman 1974; Henry et al. 1982; Hoel 1982; Huang 1978; Johnston 1977; Klohn and Pickens 1970; Lattanzi and Pressacco 2005; Ludwig et al. 1982a; McBride et al. 1968; McKnight 1972; Moxham 1964; Pool 1990, 1993; Quick et al. 1977; Renick 1926; Reynolds and Goldhaber 1978, 1983; Reynolds et al. 1977, 1980a, b, 1982; Ricoy and Brown 1977; Sellards et al. 1932; Smith 1977, 1979; Walton et al. 1981; Warren 1972; Weeks and Eargle 1960, 1963; Wilbert and Templain 1978; Adams SS, Pool TC, and Smith RB, personal communication.



Chapter 9

Appalachian Highland and Piedmont Region

This region extends from central Alabama and northern Georgia northeastward to the Canadian border (►Fig. I.1). Although a great number of uranium occurrences are known in the Appalachian, Piedmont, and adjacent territory, only one economic deposit has been found to date, Coles Hill in Virginia, which is described later. Some selected examples of uranium occurrences in the eastern United States are added below to demonstrate the environments in which uranium may be expected. For more information on uranium localities, the reader is referred to authors listed below.

Sources of Information. Ayuso and Ratte 1990; Baillieu and Daddazio 1982; Brimhall and Adams 1969; Bryant and Reed Jr 1966; Butler Jr 1975; Butler Jr and Stansfield 1968; Dribus et al. 1982; Grauch and Zarinski 1976; Klemic 1962; Lesure et al. 1977; Ragland and Rogers 1980; Rogers et al. 1978; Sevon et al. 1978; Smith and Hoff 1984; Turner-Peterson 1980; Turner-Peterson et al. 1985, and other publications as cited.

Conway Granite, New Hampshire: Uraninite occurs within the contact zone of this uraniferous (up to 20 ppm U), post-tectonic pluton of potassic composition and high Th/U ratios. The Conway Granite belongs to intrusives of the White Mountain Magma Series of Mesozoic age, which occur throughout the New England states (Grauch and Zarinski 1976).

Grandfather Mountain Window, western North Carolina: Uraninite/pitchblende fills tiny step-like echelon veinlets cutting through bleached and altered, near vertical phyllonite zones in phyllite, gneiss, and pegmatites of the Precambrian Wilson Creek Gneiss, Elk Park Plutonic Group (Grauch and Zarinski 1976).

Mount Holly Complex, Vermont: This Mesoproterozoic complex in the Green Mountain massif contains stratabound veins, pods, and lenses containing uraninite, quartz, and minor to accessory amounts of epidote, garnet, magnetite, tourmaline, and chlorite near the towns of Ludlow and Jamaica. At Ludlow Mountain and Grant Brook, host rocks consist of sheared and fractured quartzite. Host rocks at College Hill and Pinnacle Hill include micaceous gneiss intercalated with quartzofelspathic gneiss, micaceous schist, and pegmatites. Uranium grades range from <0.2 to 0.5% in veins and pods but can be as high 18%. Thorium content is relatively low and lacks a distinct correlation with uranium (Ayuso and Ratte 1990).

Reading Prong, Pennsylvania–New Jersey–New York: Uranium occurs in Precambrian gneiss, metavolcanics, pyroxenite, pegmatite, locally associated with hematite-stained siliceous granite. Production of less than 1 t U has come from small mines near *Cranberry Lake*, New Jersey, where uraninite, thorite, magnetite, pyrite are accumulated in zones paralleling the

contact between pegmatite and pyroxenite. Selected samples contain up to 2.5% U (Grauch and Zarinski 1976).

Mount Pisgah, near Jim Thorpe, eastern Pennsylvania: Hexavalent uranium minerals, mainly uranyl carbonates and uranyl vanadates are hosted in fractured and folded dark grey, quartz-pebble conglomerate and sandstone in a paleochannel system of the Pennsylvanian Pottsville Formation. Redbed sediments rest upon, and the Mississippian Mauch Chunk Formation underlies the Pottsville Formation. Limited drilling has indicated irregular and discontinuous U–V mineralization in steeply dipping conglomerate beds from the surface to at least a depth of 165 m. Grades range from 0.017 to 0.3% U over thicknesses of 0.6–7 m, and from 0.10 to 1.62% V₂O₅ over thicknesses of 0.3–6 m. Established resources are estimated at about 200 t U (RME 1978).

Penn Haven Junction, eastern Pennsylvania, located in the vicinity of the Jim Thorpe area: Hexavalent uranium minerals associated with copper sulfides/carbonates and pyrite occur in paleochannels filled with grey to green carbonaceous quartzitic sandstone lenses and reddish shales and mudstones of the Upper Devonian Catskill Formation. Uranium is commonly associated with coalified carbonaceous material. Mineralized lenses are small and uranium is erratically distributed (McCauley 1961).

9.1 Piedmont Province, Virginia

The Piedmont Province in the southeastern United States hosts in its western portion the Coles Hill/Swanson deposit in Pittsylvania County, southern Virginia (►Fig. I.1), and a number of yet to be explored uranium occurrences in Virginia and adjacent states to the north and south. Uranium occurrences are mainly hosted in crystalline rocks and most occur at or adjacent to Triassic sandstone basins.

Regional Geology of the Western Piedmont Belt in Virginia

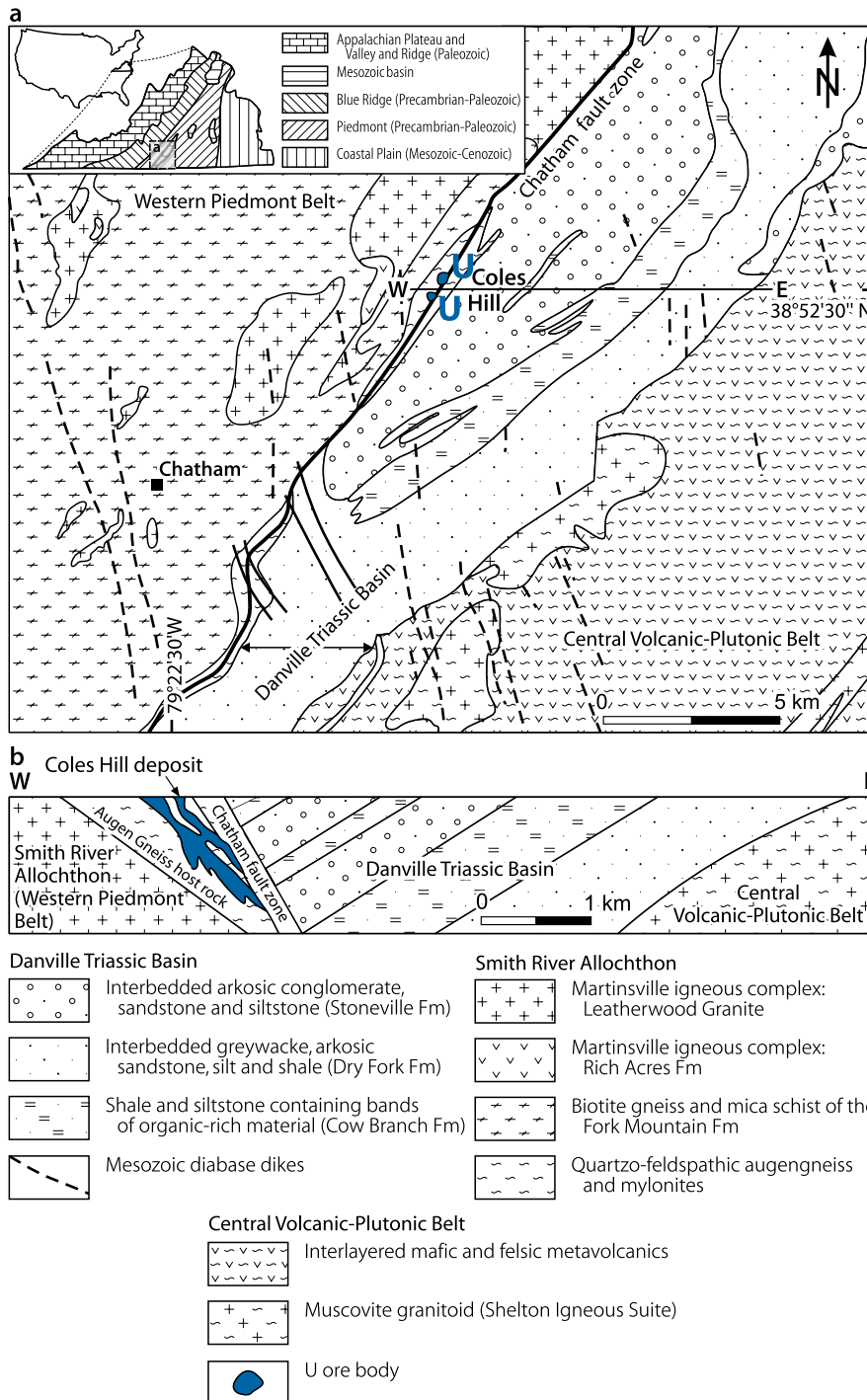
The western Piedmont terrane in Virginia consists mainly of Precambrian and Early to Middle Paleozoic crystalline rocks into which NE–SW-elongate graben-like basins are downfaulted. Triassic continental clastic sediments, as much as several thousand meters thick, fill the basins. Northerly trending diabase dikes of Jurassic age cut these sediments.

Crystalline rocks are constituents of the Smith River Allochthon, a structural nappe that has been thrust westwards upon Neoproterozoic or Early Paleozoic metasediments supposedly in late Carboniferous time (Conley and Henika 1973). This nappe is bounded to the northwest by the Bowen Creek Fault and to the southeast by the Ridgeway Fault (Jerden 2001). Seismic surveys near the Brevard Zone in North Carolina suggest a 3,000 m thick sheet of crystalline rocks overlying about 8,000 m of Lower Paleozoic sediments (Harris et al. 1981). The Smith River Allochthon comprises of two major stratigraphic units, both of which are regionally metamorphosed to amphibolite grade facies. The Basset Formation consists of a lower

biotite gneiss and an upper amphibolite complex. It is overlain by the uranium-hosting Fork Mountain Formation, which is largely composed of mica schist, biotite gneiss, and amphibolite. Adjacent to the east of the Fork Mountain Formation is the Central Volcanic–Plutonic Belt comprising a volcanic-sedimentary sequence with intrusions of muscovite granite and quartz monzonite of the Shelton Formation (Fig. 9.1) dated at 425 Ma (Kish 1977; Kish et al. 1979).

Intrusives of the Martinsville Igneous Complex have invaded the allochthon rock suites. Martinsville intrusions range from early diorite-gabbro of the Rich Acres Formation, followed by alaskitic, leucogranitic to granodioritic rocks of the Leatherwood Granite, to late norite. Age dating of Leatherwood Granite gave 450 Ma (Rankin 1975). Some Leatherwood facies appear to be two-mica granites (5–10% biotite, trace to 15% muscovite).

Fig. 9.1. Western Piedmont region in southern Virginia, (a) regional geological map of the Danville Basin and adjacent terrane, and (b) E–W section with geologic–tectonic setting of the Coles Hill deposit. (After Jerden 2001, based on Henika 1998)



Regional lineaments trending N to NE transect the western Piedmont Belt. Localization of Triassic basins is controlled by such structures. The Brevard Zone in North Carolina is one of these lineaments. It splays northeastward into a number of branches including the Chatham fault in Virginia, which forms the western boundary of the Triassic Danville Basin and represents a prominent structural element in the Coles Hill deposit.

9.1.0.1 Swanson Deposit – Coles Hill, Virginia

The Swanson uranium deposit, also referred to as Coles Hill deposit, was discovered in 1978 at Coles Hill, 30 km N of Danville in south-central Virginia (Fig. 9.1). Two major near-surface ore bodies, North and South, are delineated and are potentially feasible for open-pit and underground mining. They consist of structurally controlled mineralization in the form of vein and disseminated modes.

Ore distribution is heterogeneous with high-grade ore zones enveloped in lower grade material. This is reflected, by using different cutoff grades, in a wide range of resource figures (measured and indicated in situ resources combined, calculated by Maxwell et al. 2008). At extreme cutoff grades of 0.021 and 0.17% U, resources would amount to 45,770 t U grading 0.05% U in average; and to 6,960 t U at 0.235% U, respectively. Using a medium cutoff grade of 0.084% U, resources amount to 11,690 t U at 0.18% U.

Sources of Information. Frishman et al. 1989; Halladay 1989; Halladay et al. 1982; Hauck et al. 1989; Henika 1980, 1981, 1998; Henika and Thayer 1983; Jerden 2001; Jerden and Sinha 1999; Lineberger 1983; Maxwell et al. 2008; Marline Uranium Corporation company internal reports courtesy of Reynolds NN; and Bowdidge C, Glackmeyer K, Halladay CR, Reynolds NN, and Singletary H, personal communication, unless otherwise noted.

Geological Setting of Mineralization

The Coles Hill uranium deposit is hosted in rocks of the Smith River Allochthon on the western side of the Triassic Danville Basin (Figs. 9.1, 9.2a and b). Host rocks are metasediments of the Fork Mountain Formation, striking about NE–SW and dipping about 50° SE. Amphibolite/gabbro of the Rich Acres Formation and Leatherwood Granite occur within this sequence. Granite bodies are not only lenticular parallel to the regional strike of foliation planes but also cut across the Fork Mountain gneiss. Volcanic-sedimentary metamorphics of the Central Volcanic–Plutonic Belt are exposed to the east of the Danville Basin. Metarhyolite, metadacite, and porphyroblastic quartz–feldspar–biotite gneiss with intercalated amphibolite constitute the prevailing lithologies of this sequence.

U-hosting Fork Mountain Formation rocks are regionally metamorphosed to amphibolite grade facies with local retrograde overprints to greenschist rank facies. Metamorphic zonation shows a narrow, NE–SW-trending kyanite zone in which the

Swanson deposit and other uranium occurrences at the exo-contact of the Danville Basin occur. This zone grades to the west and east into sillimanite-bearing metamorphics (Gregory 1980). A similar zoning, reflected by albite and chlorite grading outward into oligoclase, and biotite and garnet, respectively, is mapped by Henika (1980) for at least one of the uranium areas, Dry Fork, to the southwest of Coles Hill.

The NE–SW-elongate *Danville Basin* overlies parts of the deposit area. This half-graben is filled with continental clastic sediments of the Triassic Chatham Group, more specifically, in the Coles Hill area by fluvial deposits of the Stoneville Formation and lacustrine sediments of the Cow Branch Member. Jurassic diabase dikes transect both Triassic sediments and basement (Henika 1998). The basin is bounded to the northwest by the Chatham fault, a major, NE–SW-oriented, medium steep SE-dipping displacement structure.

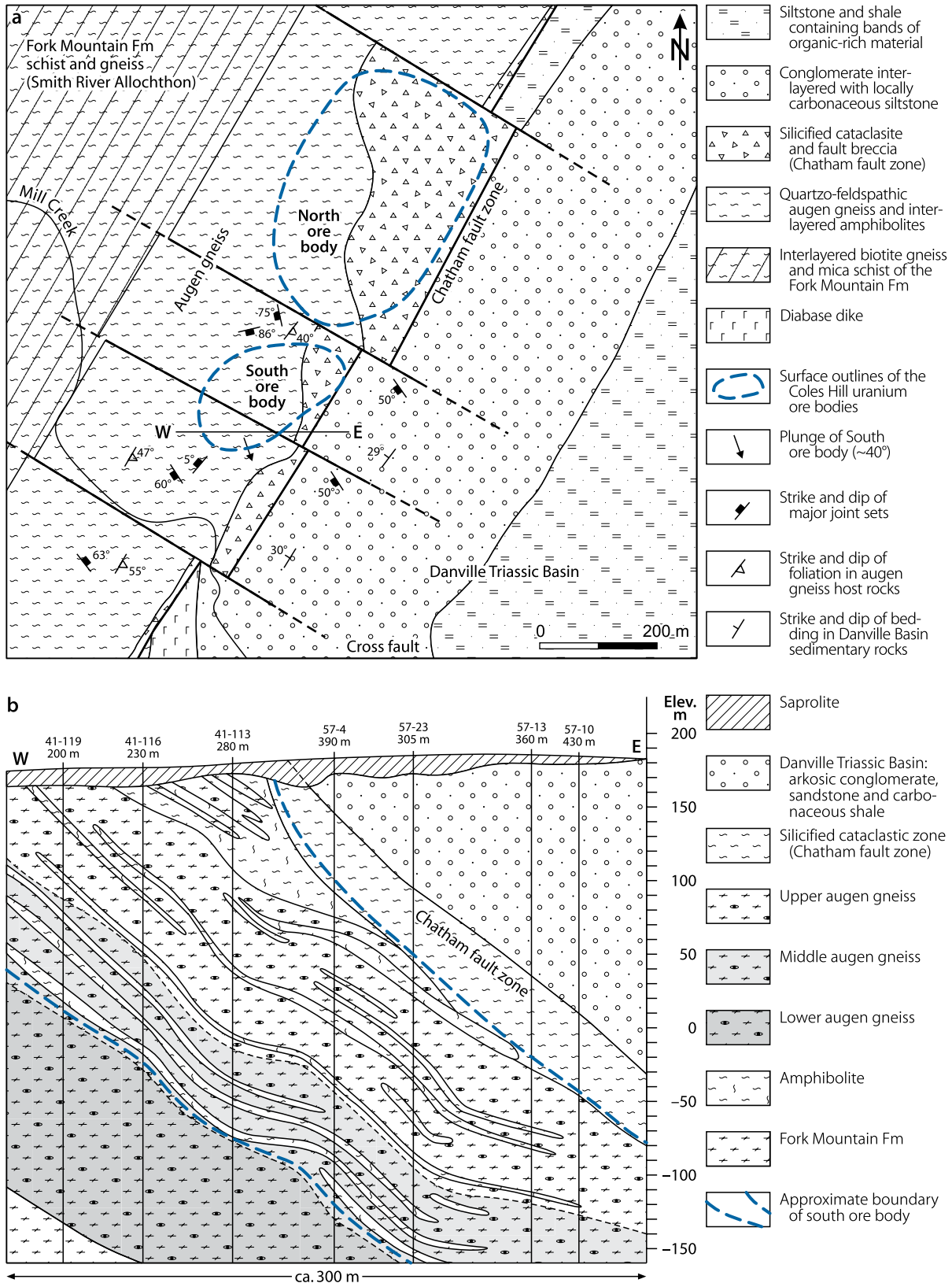
The ore-hosting *Fork Mountain Formation* consists in the vicinity of Coles Hill of an upper, medium- to fine-grained, quartzo-feldspathic biotite gneiss with thin interlayers of muscovite schist and massive interbeds of porphyroblastic biotite gneiss, and some intercalations of amphibolite and hornblende gneiss. The lower part of the formation includes medium- to coarse-grained, garnetiferous muscovite–biotite gneiss, intercalated with garnetiferous mica schist and calc-silicate quartzite, which is locally kyanite bearing (Henika 1981). Biotite gneisses vary greatly in mineralogical composition, particularly near contacts with intrusive bodies of Leatherwood Granite.

At Coles Hill, the litho-stratigraphic interval between more or less undisturbed Fork Mountain rocks to the NW and the Chatham fault to the SE is occupied by a marked wedge, up to 450 m wide, of cataclastic and protomylonitic gneisses related to the Chatham fault zone (Fig. 9.2a and b). This wedge is composed of augen gneiss, about 300–400 m wide, tri-partitioned – from NW or bottom to SE or top – into lower, middle, and upper augengneiss (Jerden 2001). Some amphibolite interlayers, 1–2 m thick, as well as aplite and pegmatite dikes are present in the augen gneiss. The next unit is a zone, ca. 40 m wide, of intense brittle fracturing and silicification as reflected by breccias (protobreccia, microbreccia, fault breccia) and cataclasite that overprints mylonitic fabrics. It is followed by noncohesive fault gouge, 1–5 m thick, which represents the trace of the Chatham fault. These rocks are thought to have developed from porphyroblastic biotite gneiss of the upper Fork Mountain Formation and from porphyritic Leatherwood Granite.

1. Frishman et al. (1989) notes five lithologic facies within the augen gneiss section all of which have been altered:
 1. Lower augen gneiss (formerly named mafic augen gneiss): dark-green to black feldspar–quartz–biotite gneiss containing plagioclase or K-feldspar augens up to 4 mm in diameter
 2. Monzonite or middle augen gneiss (large augen gneiss): distinctive biotite–feldspar gneiss containing feldspar augens <2 cm in diameter
 3. Upper augen gneiss (normal augen gneiss) (main ore-bearing unit): biotite–feldspar±quartz gneiss with a mylonitic fabric containing feldspar augen <1 cm in diameter

Fig. 9.2.

Coles Hill area, (a) generalized geological map with extent of silicified cataclasite and breccia zones as well as that of uranium mineralization in the footwall zone of the Chatham fault, (b) geological W-E section across the footwall zone of the Chatham fault and southern uranium ore body. (After (a) Jerden 2001, based on Henika and Thayer 1983; Lineberger 1983; Marline Uranium Corporation 1983; (b) Jerden 2001)



4. Amphibolite: predominantly fine-grained amphibole–feldspar gneiss
5. Mylonitic granite gneiss: lenses of quartz in a matrix of crushed pink feldspar.

The *Chatham fault*, which separates crystalline rocks from Triassic sediments, is obviously an ancient structure, which has been reactivated repeatedly until post-Triassic time. The Chatham fault zone trends through the Coles Hill area immediately to the SE of the deposit. Several cross-cutting fault and shear systems intersect the Coles Hill area, and displace the Chatham fault. They not only trend mainly NW–SE but also N–S and E–W.

Ore bodies at Coles Hill occur within the above mentioned wedge. This wedge exhibits a tectonic framework that evolved by repeated tectonism, characterized by various fracture systems consisting of numerous small fractures, shears, and joints that form a stockwork pattern with breccia intervals. This structural zone occupies an area roughly coextensive with, but somewhat larger than the zone of uranium mineralization. Foliation also shows a variety of bearings attributable to various tectonic systems. The most prominent foliation cluster trends around NNE–SSW and dips ca. 45° SE.

Host Rock Alteration

Rocks within mineralized zones are Na metasomatized and altered to various degrees, in part pervasively, by carbonatization, chloritization, desilicification, hematitization, sericitization, silicification, and zeolitization. Ubiquitous Na metasomatism is reflected by (a) clear albite rims around feldspar augens, (b) riebeckite formation, in particular in amphibolites, and (c) in the form of small albite veinlets or clusters in augen gneiss and cataclastic rocks. Calcite, epidote, and clinozoisite occur very often in the immediate vicinity of plagioclase indicating a derivation from the latter. Ilmenite and/or sphene are altered partly to idiomorphic rutile, and titanite is altered to anatase.

Hematitization shows a fairly strong correlation with uranium mineralization. In some cases, it forms distinct halos around uranium veinlets. Amphibolite and amphibole–biotite gneiss are consistently stained red by hematite when mineralized, and not hematitic when barren. Mineralized augen gneiss commonly has a hematite hue, but hematite staining is also present in unmineralized augen gneiss. Most hematite is disseminated as minute particles in fine-grained cataclastic matrix. Hematite also reddens feldspar porphyroclasts and is most highly concentrated in those feldspars that are strongly altered by saussuritization or sericitization. Limonitization is typically widespread in the weathering zone. Fractures varying from hairline to a few centimeters in width are filled with a variety of minerals such as apatite, baryte, carbonates, chlorite, gypsum, harmotome and other zeolites, hematite, and quartz. Different mineral assemblages in discrete, cross-cutting fracture sets attest to different hydrothermal events.

Based on chemical whole rock analyses and alteration mineralogy, Halladay et al. (1982) and Jerden (2001) note the

following major trends of chemical changes in host rock composition going from (1) unaltered augen gneiss and amphibolite to (2) altered but unmineralized augen gneiss, amphibolite, and cataclasite, and to (3) altered, mineralized augen gneiss, amphibolite, and cataclasite: An increase of Na₂O by Na metasomatism associated with a decrease of K₂O and SiO₂, an increase of BaO as reflected by growth of Ba zeolite (harmotome) and baryte, and an increase of CaO, P₂O₅, F, and Sr as indicated by introduction of apatite, and depletion of SiO₂ by removal of quartz. SiO₂ was reprecipitated in cataclastic rocks that envelop the deposit.

Iron for hematite formation may have derived by alteration of amphiboles and primary magnetite. The latter is indicated by distinct magnetic lows over the Coles Hill area compared to surrounding fresh rock terrane.

Mineralization

Uranium is present as coffinite, uraninite, pitchblende, sooty pitchblende, U–Ti phases, and bound in fluor-apatite. Hexavalent U minerals occur in weathered, oxidized zones, particularly in the northern ore body. Associated sulfides are rare and are represented mainly by pyrite.

Coffinite is present in subhedral habit and is locally intergrown with uraninite. Uraninite occurs in euhedral to subhedral habit, but is commonly oxidized in various degrees to a stage as typical for pitchblende or sooty pitchblende by maintaining the original habit. Pitchblende with botryoidal habit is also present, however, as outlined further down. Uraninite/pitchblende and coffinite can be intimately intergrown with or replace Ti-minerals. Apatite is present as an accessory rock constituent and as an ore-stage mineral. Both modes are similarly high in fluorine (ca. 2.1–3.6 wt.%), but U contents are different. Accessory rock apatite averages 0.02% U, whereas ore-stage apatite averages 0.4% U with some euhedral, clear apatite crystals containing over 3% U. This ore-stage apatite occurs as felty, prismatic crystals, about 0.2 mm long, and as coating on pre-ore apatite (<1 mm in diameter).

Meta-uranocircite tends to be the prevailing weathering-related U mineral. It occurs together with Ba, Ca, Mn oxides and euhedral quartz, or a Ca-, U-, Pb-bearing lanthanide phosphate mineral (rhabdophane?) in saprolite. (For more information see Jerden 2001 who provides a comprehensive description of processes and related minerals in weathered, oxidized zones of the Coles Hill deposit).

At least three generations of uranium mineralization (not counting weathering-related mineralization) are noted by Halladay and his co-workers, and Jerden (2001): The earliest and strongest mineralization (1) comprises U-rich apatite, coffinite, and minor uraninite/pitchblende associated with albite, chlorite, anatase, and sulfides within breccias and cataclastic rocks. This generation is cut by (2) veinlets of coarse-grained calcite, pitchblende, minor coffinite, Ti oxides (anatase), and traces of sulfides, and (3) younger veinlets of pitchblende, coffinite, harmotome, quartz, Ti oxides, and pyrite. Three uranium-barren sets of veinlets dissect the productive phases. They consist predomi-

nantly of baryte, quartz, calcite, chlorite, and locally some sulfides.

Uranium mineralization occurs in all augen gneisses, but particularly in the upper augen gneiss unit. These host lithologies are characterized by intense granulation and/or brecciation, which have transformed augen gneiss to a rock consisting of rounded feldspar and lithic clasts embedded in fine-grained feldspar-quartz-chlorite±muscovite matrix. Younger authigenic minerals, including disseminated uranium minerals, have partially to totally replaced this matrix of granulated gneiss in zones of mineralization, or occur in crosscutting veinlets.

Uranium mineralization is present in two modes, as (a) disseminated impregnation and (b) in veins/veinlets. As documented by Halladay and his coworkers and Jerden (2001), both modes include a variety of different mineral associations.

Disseminated impregnation-type mineralization consists of coffinite and minor discrete minute crystals (0.03–0.05 mm in diameter) of U oxides often in nearly cubic habit, or as relicts thereof, disseminated in the groundmass of cataclastic/granulated and brecciated gneisses, mainly augen gneiss less commonly amphibolite. The U oxide crystals are interpreted as former uraninite grains, now transformed to an oxidation stage of pitchblende or sooty pitchblende. U minerals occur in two characteristic mineral assemblages:

(a) *Disseminated uraniferous apatite-coffinite-uranium oxide-chlorite association*: This assemblage is predominantly hosted in augen gneiss in which it forms part of the groundmass. Typical constituents are coffinite, minor uranium oxides, feltlike aggregates of small uraniferous fluor-apatite prisms (0.2 mm long) intermixed with chlorite (ripidolite), which occur with or without calcite, anatase/rutile, ilmenite, magnetite, pyrite, and traces of sulfides. Apatite content can be up to 25% (10% P_2O_5). This assemblage also has elevated LREE contents in samples containing in excess of 3 wt.% P_2O_5 (two samples containing >5 wt.% P_2O_5 and >5,000 ppm F also contain >260 ppm La and >340 ppm Ce, Jerden 2001).

Distribution of uranium minerals is erratic. In some zones, they occur throughout the apatite–chlorite matrix, in others they are concentrated in narrow bands or near the border of feldspar or lithic clasts. As mentioned earlier, within the apatite–chlorite mass, coffinite and uraninite/pitchblende crystals are often intergrown with Ti minerals, but are also concentrated near rutile and anatase. In some cases, pitchblende replaces rutile/sphene aggregates.

Although some mineralized breccia zones have sharp boundaries with the enclosing augen gneiss and are conformable with foliation in the gneiss, in most cases this assemblage forms irregularly shaped areas or bands without any obvious correlation to host rock foliation.

(b) *Disseminated pitchblende–calcite association* accompanied by cubic pyrite crystals: This assemblage is mainly hosted in amphibolite in which it is distributed similarly to the apatite–coffinite–U oxide–chlorite assemblage within the matrix of granulated and/or brecciated rock. Pitchblende exhibits botryoidal or cockade textures and commonly rims breccia fragments. Pitchblende is almost always altered to sooty pitchblende, locally

intergrown with coffinite, and in some places associated with goethitic dust. Some relict idiomorphic crystal outlines indicate an origin from uraninite. U–Ti relationships are similar to those described above in minerals assemblage (a).

Vein-type mineralization: Emplaced in fissures ranging in width from hairline to several millimeters, vein mineralization postdates the disseminated type. Mineral assemblages typically consist of pitchblende/sooty pitchblende, occasionally with some U–Ti phases and/or coffinite. Associated gangue minerals are related to host rock lithology and permit a distinction of two different vein mineral assemblages:

(c) *Pitchblende–calcite association* accompanied by pyrite cubes: This assemblage is essentially restricted to amphibolite. Klemm (in Halladay et al. 1982) notes that colloidal pitchblende, together with anatase, preferentially occupies the rims of veinlets. Calcite grains in the interior of veinlets contain uranium inclusions that often exhibit idiomorphic shapes typical for uraninite. Pitchblende has replaced aggregates of sphene and rutile, and has reacted with Ti minerals to form U–Ti phases. Rare inclusions of galena occur in pitchblende. Chalcopyrite and Fe-poor sphalerite are present in trace amounts mostly on calcite. Vein walls contain hematite. Jerden (2001) postulates the following sequence of mineral crystallization for this assemblage:

1. Hematite and traces of pitchblende along vein walls
2. Calcite and pitchblende in vein interior and
3. Pyrite, sphalerite, and galena along grain boundaries of calcite.

(d) *Pitchblende–zeolite association*: Typically hosted in augen gneiss, colloidal pitchblende is commonly concentrated along edges of veinlets up to several millimeters in width. Coarse quartz crystals and large pyrite octahedra pierce inward from portions of the vein walls, while coarse-crystalline harmotome occupies vein centers. Some narrow zeolite veinlets have both wall sides coated with bands of hematite. Zeolite crystals are commonly choked with fine-grained opaque inclusions including Fe–Ti-oxides and pyrite cubes. Pitchblende masses tend to contain traces of coffinite and/or intergrown magnetite, ilmenite, or other titanium minerals. Halladay et al. (1982) propose the following sequence of crystallization for this assemblage:

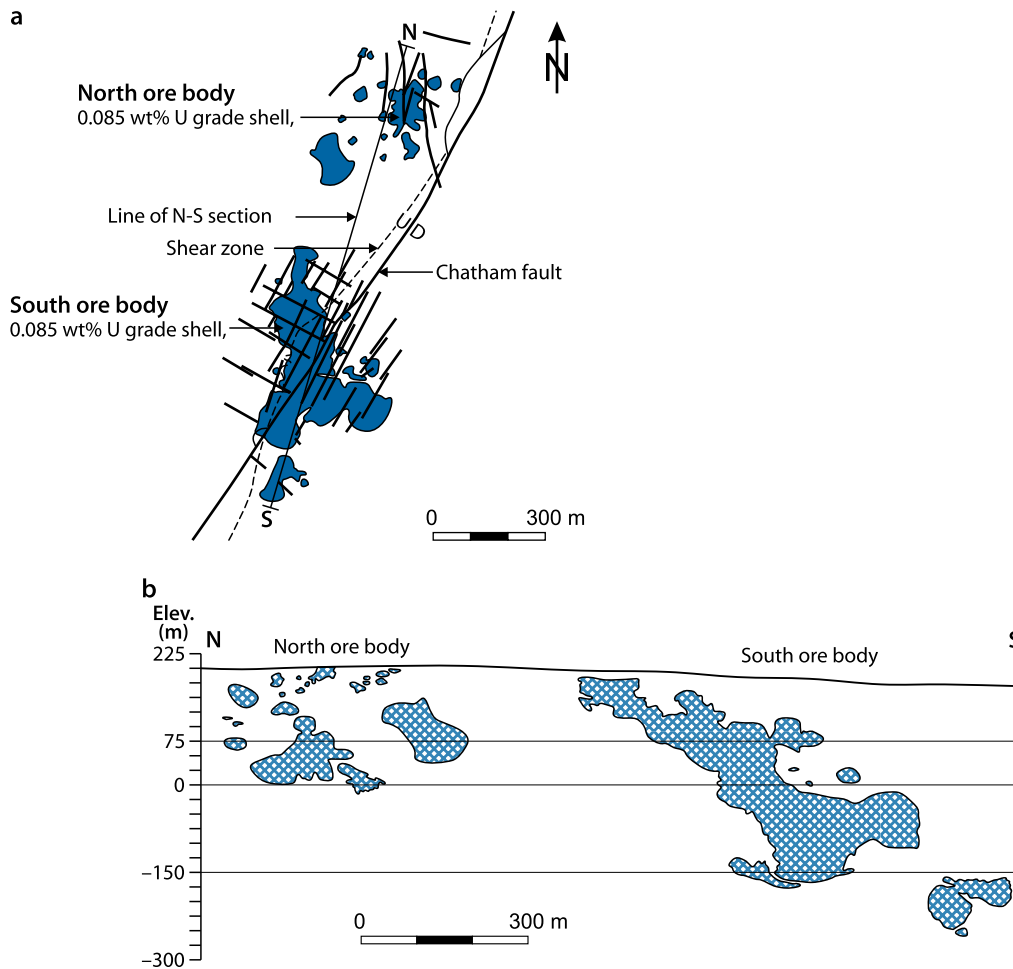
1. Colloidal pitchblende as films and irregular accumulations along vein rims
2. Quartz and pyrite with comb-like textures pointing inward from vein walls and finally
3. Harmotome accompanied by pyrite, magnetite, and/or ilmenite.

Shape and Dimensions of Deposits

The Swanson deposit includes two major ore bodies as shown in [Fig. 9.3a](#) and [b](#). Generally, the internal structure of these ore bodies is essentially a stockwork of U-bearing veinlets with narrow intervals of disseminated mineralization localized within the tectonized footwall zone of the Chatham fault.

■ Fig. 9.3.

Coles Hill/Swanson deposit, (a) plan view of surface projected ore bodies and (b) S–N section outlined by a cutoff grade of 0.084% U. (After Maxwell et al. 2008)



The *South ore body* contains 27,650 t U at a grade averaging 0.06% U (based on a cutoff grade of 0.021% U). Better grade intervals occur within this low-grade shell as indicated by a resource calculation applying a medium cutoff grade of 0.084% U. At this cutoff grade, resources amount to 9,850 t U and average a grade of 0.18% U (Maxwell et al. 2008).

The *South ore body* is roughly an irregularly shaped, flattened cylinder or manto plunging at about 40° S. The horizontal E–W width is up to 300 m, thickness ca. 150 m, and length along the plunge axis at least 700 m. The ore body extends from surface to a depth of about 300 m, but has not been closed off at depth by drilling.

The ore body is transgressive to the host strata, dipping at a slightly lower angle. Its western, stratigraphic lower edge lies at the base of the monzonite or middle augen gneiss unit. The eastern boundary is at the base of the protobreccia/microbreccia zone in the footwall of the Chatham fault, but mineralization does not invade these rocks for more than a meter. Hematitization and granulation of the host rocks are more or less co-extensive with the ore body. Ore is of disseminated and vein-type as well,

with the majority of the uranium present in microfractures. Disseminated U minerals are concentrated in narrow bands rarely more than a quarter of a meter thick. Mineralization occurs in all rock types, but amphibolite contains the richest ore often arranged in narrow zones associated with calcite.

The *North ore body* is larger in volume but lower in uranium tonnage and grade than the *South ore body*. Using a cutoff grade of 0.021% U, it contains 18,115 t U at a grade averaging 0.042% U. This low-grade ore encloses better grade intervals as documented by a resource calculation based on a medium cutoff grade of 0.084% U. At this limit, resources amount to 1,820 t U at a grade of 0.21% U (Maxwell et al. 2008).

The *North ore body* is an irregularly-shaped, more or less flattened spheroid, approximately 350 m in diameter. It extends from surface to a depth of almost 300 m. As at the southern ore body, the stratigraphic upper edge or the eastern side boundary is at the base of microbreccias and cataclasites of the Chatham fault. The lower, western boundary, however, extends substantially into the lower augen gneiss (or mafic augen gneiss) unit. In contrast to the *south ore body*, the northern zone has a

predominance of disseminated-type ore, which tends to form wider and lower grade zones of mineralization.

Weathering has affected the northern ore body to some depth resulting in radioactive disequilibrium and formation of abundant hexavalent U minerals in saprolite, but without noteworthy depletion of uranium (Jerden 2001).

Geochronology

U/Pb isotope analyses by Krishna Sinha (in Halladay et al. 1982) give two principal apparent ages for uranium crystallization: (a) 562 ± 5 Ma for uranium oxide in amphibolite and (b) 417 Ma for uranium oxide in augen gneiss.

U/Pb dating of zircons of the Leatherwood Granite yield likewise two ages: (a) 1,020 Ma for zircons including corroded anhydral crystals (Conley and Henika 1973) and (b) 450 Ma for euhedral zircons (Rankin 1975). It has been inferred from these two zircon ages that the Leatherwood Granite is crystallized at about 450 Ma but retained an inherited component, approximately 1,000 Ma old, that probably had been incorporated into the Leatherwood magma by assimilation of rocks of Grenville age.

Potential Sources of Uranium

The most likely sources of uranium are metasediments of the Fork Mountain Formation or Leatherwood Granite, or perhaps both. Triassic sediments are not considered for various reasons (e.g., age of pitchblende) to be a viable U source. The nature or mode of limited amounts of uranium in Triassic sediments rather suggests an origin and redistribution from basement uranium mineralization.

Ore Controls and Recognition Criteria

The Cole Hill/Swanson deposit is primarily controlled by structure and may be attributed to vein-type uranium deposits. Ore control and/or recognition criteria include:

Host environment

- Regional location is in a terrane of complex geologic history including several cycles of orogeny/regional metamorphism during Precambrian and Paleozoic time, and taphrogenic tectonism in Triassic time
- Local parameters include a position
 - In a metasedimentary sequence (Fork Mountain Formation)
 - Intruded by leucocratic granite (Leatherwood Granite)
 - In the footwall immediately adjacent to a regional lineament with substantial displacement (Chatham fault)
 - At a slight bend in trend of the lineament
 - In a widened cataclastic zone affected by repeated brittle deformation

- Near the edge of a Triassic basin filled with continental clastic sediments (which formerly possibly covered the deposit and protected it against destruction)
- Host rocks are cataclastic, granulated, and heavily fractured facies of originally granitic (Leatherwood Granite) and semimafic and mafic metasedimentary provenance (biotitic gneisses and amphibolites of Fork Mountain Formation) regionally metamorphosed to amphibolite grade with local retrograde metamorphic overprinting
- Presence of syn- to post-Triassic diabase dikes
- Presence of cross-cutting fault/shear zones.

Alteration

- Alteration phenomena of host rocks are reflected by
 - Na metasomatism in the form of albitization and riebeckitization
 - Partly pervasive carbonatization, chloritization, hematitization, desilicification, silicification, and zeolitization
 - Increase of BaO, CaO, F, Na₂O, P₂O₅, and Sr, and decrease of K₂O and SiO₂
- Fissure fillings of apatite, baryte, carbonates, gypsum, harmotome and other zeolites, hematite, quartz, sepiolite
- Destruction of magnetite, ilmenite, and other Ti minerals
- Magnetic and gravity lows at and around ore bodies reflecting destruction of magnetite and other minerals.

Mineralization

- Monometallic mineralization composed of several generations of uranium and associated minerals
- Principal U phases are coffinite, uraninite, pitchblende, sooty pitchblende, uraniferous apatite
- Except for pyrite and Ti minerals, very scarce associated metallic minerals including chalcopyrite, sphalerite, and galena
- Calcite, quartz, and/or zeolites constitute prevailing gangue or associated minerals
- Presence of two modes of mineralization:
 - Disseminated impregnations consisting of coffinite, U oxides (often as subhedral to euhedral cubes of former uraninite), uraniferous apatite associated with chlorite or carbonate
 - Narrow vein and micro-fracture fillings consisting of colloidal pitchblende/sooty pitchblende associated with pyrite and gangue minerals related to host lithologies (carbonate in amphibolite, zeolite and quartz in augen gneiss)
- Correlation of uranium mineralization with hematitization and, to some degree, Na metasomatism/albitization.

Metallogenetic Aspects

Some hypotheses have been proposed for the origin of the U deposit at Coles Hill, partly on comparison with other vein- or veinlike-type uranium deposits. But apparently due to lack of comprehensive research on stable isotopes, fluid inclusions,

geochronology, background uranium geochemistry/potential uranium sources, etc., no convincing metallogenetic model on the origin of the Coles Hill deposit has been established as yet. As far as known, the only comprehensive but subject-specific research was by Jerden (2001) on the formation of mineralization and related processes in the weathering zone of the deposit. As a consequence, origin of uranium, derivation and composition of initial mineralizing fluids, as well as mode of and mechanisms involved in ore emplacement remain enigmatic. In the following, an attempt is made to reflect the status quo of knowledge on metallogenesis relevant criteria and their impact on possible ore formation.

Metallogenesis-related criteria as established to date on mineralogical, geochemical, geochronological, and geological data suggest:

- Structurally controlled uranium was introduced by hydrothermal solutions, but origin (hypogene, connate, meteoric, mixed, etc.), nature, and physico-chemical properties of these solutions forming the first and later uranium generations are largely unknown
- Alteration mineralogy and presence of zeolite in pitchblende veinlets suggest that solutions, at least of late hydrothermal phases, were of moderate to low temperatures
- Apatite and calcite in the gangue minerals suite indicate solutions containing phosphate and carbonate ions
- Coffinite reflects Si-bearing fluids
- Destruction of magnetite, ilmenite, and possibly sphene document reducing activity
- Transformation of uraninite to “pitchblende” and “sooty pitchblende” oxidation stages indicate (probably repeated) oxidation processes.

Several alteration features at Coles Hill are also typical ingredients of other vein U deposits as in the Uranium City region, Canada, and in the European Hercynian chain, and may hint to similar ore-forming processes, in particular:

- Na metasomatism of host rocks resembles that of veinlike- or granite-unrelated vein U deposits (e.g., Beaverlodge, Canada) as well as vein uranium deposits within or adjacent to leucocratic granites (e.g., in Massif Central and Vendée, France, and Erzgebirge, Germany/Czech Republic)
- Desilicification of host rocks (in particular of granite) may perhaps indicate similar processes as known from some French U deposits in which granite was locally transformed to “episyenite” bodies that contain rich uranium ore (e.g., at Bernardan and Pierres Plantées, Massif Central, France), and also from Gunnar, Saskatchewan, Canada
- The pervasive and wide zone of hydrothermal alteration at Coles Hill is more commonly found around veinlike deposits, e.g., at Beaverlodge, Saskatchewan, Canada, than associated with classical vein deposits, e.g., in France, Germany, and Czech Republic. On the other hand, the pervasive distribution of alteration may be due to intense brittle deformation at Coles Hill that provided repeatedly favorable permeability more or less throughout the rocks for fluids independent of their origin and nature.

Localization of the deposit within and adjacent to intrusive granite (Leatherwood Granite) and the approximate coincidence of emplacement time of this granite with an early U concentration phase may suggest some relationship. It remains unknown, however, of what kind.

At least two options are open for discussion, under the precondition, however, that an edifice of adequate pathways for solutions existed. Such an edifice could be hypothesized as a result of brittle deformation related to movements along a precursor structure of the present Chatham fault. (a) Granite intrusion may have generated physico-chemical and hydrodynamic conditions for mobilization and migration of fluids inherent in the intruded metasediments such as connate or meteoric waters. Such lateral-secretory processes by oxygenated hydrotherms are capable of leaching uranium present in anomalous or protore concentrations from country rocks, and of transporting and redepositing it at favorable sites. In the more unlikely case (b), granite could have been the source of late magmatic hypogene fluids and uranium as well.

Case (a) may be valid if anomalous uranium background contents and the presence of leachable uranium (e.g., uraninite) can be documented in Fork Mountain metasediments. The possibility of uraninite existence may be indicated by disseminated (remnant) uraninite crystals in the groundmass of augen gneiss. Uraninite generally forms under higher P–T conditions than those indicated for second and later generation vein mineralization at Coles Hill, but which are typical for metamorphic rocks of amphibolite grade facies as they formerly existed in the now altered Fork Mountain Formation. In case (b), the nature and geochemistry of the granite, particularly its uranium fertility, have to be established to clarify its potential role in Coles Hill uranium mineralization.

Another question is posed by geochronological data. Two apparent U/Pb ages of early uraninite crystallization are established. The 417 Ma age (uraninite in augen gneiss) is close to the 450 Ma emplacement time of Leatherwood Granite and is similar to Acadian ages of shear zones identified throughout the Blue Ridge and Piedmont provinces. The older 562 Ma age (uraninite in amphibolite) is somewhat dubious and can be interpreted as an antecedent uranium generation or a predated value by older lead contamination of the 417 Ma old uranium, inherited perhaps from the same source material as the 1,000 Ma old constituents of the Leatherwood Granite.

Whatever the case, this (these) uraninite(s) probably represents the earliest generation(s) of epigenetic uranium concentration. Whether this (these) initial generation(s) had formed protore or ore-grade mineralization remains speculative, for later overprint by multiple hydrothermal events has eradicated most of the original signature by rejuvenated mineralization. Circumstantial evidence by textural and structural interrelationships of ore-related minerals suggests that mineralization and alteration phenomena, as we know them today, are the result of repetitious hydrothermal systems of variable composition. These solutions circulated in the foot wall of, and in response to reactivations of the Chatham fault including downfaulting of the Danville Basin or other tectonic events, as well as intrusion of diabase dikes.

It is reasonable to assume that these events exposed uranium (and other elements) of earlier generations to redistribution on a variable scale as evidenced by formation of coffinite and uraniferous apatite as well as associated gangue and alteration phases. Whether supplemental uranium was liberated from surrounding rocks by these hydrothermal regimes and introduced or not to the preexisting uranium, endowment remains questionable.

During a final, more or less recent stage as indicated by radioactive disequilibrium, supergene processes affected surficial portions of the Coles Hill deposit and formed hexavalent U mineralization as documented by Jerden (2001).

In order to conceive a comprehensive understanding of the metallogenesis of the Coles Hill ore, it may be worthwhile to consult research work by Cuney and his coworkers. These geoscientists have studied in great depth the geological setting and history of uranium deposits similar to Coles Hill. They have established processes and conditions involved in the formation of vein U deposits in France and elsewhere in the world and their findings may provide examples or clues to ore formation

at Coles Hill (respective bibliography can be found in Dahlkamp, Uranium Deposits of the World, Europe, in preparation).

Selected References and Further Reading for Chapter 9 Appalachian Highland and Piedmont Region

For details of literature see Bibliography.

Ayuso and Ratte 1990; Baillieul and Daddazio 1982; Conley and Henika 1973; Brimhall and Adams 1969; Bryant and Reed Jr 1966; Butler Jr 1975; Butler Jr and Stansfield 1968; Dribus et al. 1982; Frishman et al. 1989; Grauch and Zarinski 1976; Gregory 1980; Halladay 1983, 1989; Halladay et al. 1982; Harris et al. 1981; Hauck et al. 1989; Henika 1980, 1981, 1998; Henika and Thayer 1983; Jerden 2001; Jerden and Sinha 1999; Kish 1977; Kish et al. 1979; Klemic H 1962; Lesure et al. 1977; Lineberger 1983; Marline Uranium Corporation 1983; Maxwell et al. 2008; McCauley 1961; Ragland and Rogers 1980; Rankin 1975; RME 1978; Rogers et al. 1978; Sevon et al. 1978; Smith and Hoff 1984; Turner-Peterson 1980; Turner-Peterson et al. 1985; Marline Uranium Corporation company internal reports courtesy of Reynolds NN, and Bowdidge C, Glackmeyer K, Halladay CR, Reynolds NN, and Singletary H, personal communication, unless otherwise noted.

Chapter 10

Alaska

Alaska accounts for only two small uranium deposits, one is located at the *Bokan Mountain* in southern Alaska as will be discussed below, and another in the *Death Valley area* on *Seward Peninsula* in NW Alaska (Fig. 1.1).

The deposit in *Death Valley* hosts uranium mineralization in Eocene continental sandstone in the southern end of a graben that extends northward into the Death Valley Basin on the eastern flanks of the Darby Mountains. The sandstone contains coal and other carbonaceous matter and is partly covered by basalt. Meta-autunite is the most common U mineral; coffinite was identified in reduced ground. Reported resources amount to some 400 t U at an average grade of 0.23% U (Dickinson et al. 1987).

10.1 Bokan Mountain, Prince of Wales Island, Southeastern Alaska

Bokan Mountain is located near Kendrick Bay at the southeastern end of the Prince of Wales Island, in the southern part of the Alaskan panhandle. Discovered in 1955, the Bokan Mountain deposit was exploited by the Ross-Adams open pit mine and a few underground workings, and produced approximately 720 t U at an ore grade of about 0.8% U. Remaining resources are estimated at about 400–500 t U.

Sources of Information. Collot 1981; de Saint-André et al. 1983, 1984; Mackevett 1963; and Staatz 1978; amended by data of the authors listed in section ‘Selected References and Further Reading...’ at the end of the chapter.

Geological Setting of Mineralization

The oldest rocks of the Bokan Mountain area (Fig. 10.1) are metasediments and metavolcanics (Wales Group) of possibly Precambrian age. They are overlain by Middle Ordovician black slate, phyllite, and impure quartzite. In late Ordovician time, quartz monzonite and quartz diorite were emplaced. They belong to a volcanic–plutonic series found throughout the Alexander Terrane of southeastern Alaska. This Precambrian(?)–Paleozoic complex was intruded by peralkaline Bokan Mountain Granite in Jurassic time. Dacitic, andesitic, aplitic, and pegmatitic dikes occur in the area. Ages of the first two types are not yet established; while the aplite and pegmatite emplacement took place during both Paleozoic and Jurassic intrusive episodes.

The *Bokan Mountain Granite* is, as far as known, a petrographically and chemically unique pluton in the coastal belt of Alaska and British Columbia. It forms a stock, which is roughly circular in planview, with a diameter of about 3,500 m. The granite is peralkaline (ca. 4.8% Na₂O, 4.5% K₂O, Mackevett

1963), and according to Collot (1981), it is hypoaluminous in composition, extremely differentiated in character, and uniform in mineralogy. Principal rock constituents are quartz, microcline, albite, arfvedsonite, and aegirine. Primary accessories are zircon, fluorite, and astrophyllite, secondary accessories are magnetite and hematite. Mackevett (1963) lists riebeckite and acmite as sodic mafic minerals instead of arfvedsonite and aegirine.

Two principal granite facies are identified: (a) a medium to coarse-grained facies constituting the major portion of the pluton, grading from the edge to the center from an albitic aegirine granite into an albitic arfvedsonite granite and (b) a fine-grained facies of albitic arfvedsonite-aegirine granite, located in the center of the complex, which is also topographically the highest part. This fine-grained facies has a relatively higher percentage of albite and a lower percentage of other sodic mafic minerals; and it has the lowest peralkalinity with (Na + K)/Al ratios of 1.06–1.14 as compared with 1.08–1.28 for the coarser facies. Thompson et al. (1980) interpret the compositional zoning as being indicative of several distinct intrusions of a ring-dike type, whereas Collot (1981) suggests that the various facies are magmatically differentiated fractions of the same intrusion.

A peculiar rock type, an albitite, is locally enclosed in albitic aegirine granite, particularly in the southeastern border zone of the pluton. It is characterized by removal of quartz, albitization of microcline, and the presence of a younger authigenic albite. As a result, the albitite consists of up to 80% albite, with the balance of the rock consisting of aegirine. Typically, the intra-granitic U–Th mineralization is at least spatially associated with this albitite.

Jurassic aplite and pegmatite related to, and emplaced inside and outside of the Bokan Mountain Granite are similar in mineralogy to the granite. Feldspars of the pegmatite are identical to first generation albite, which replaces microcline in albitite. In contrast to Paleozoic pegmatites, Jurassic Bokan Mountain pegmatites contain U–Th–REE.

Numerous structures dissect the Bokan Mountain area. Most prominent faults and fractures trend around E to ESE and N to NNW.

Host Rock Alteration

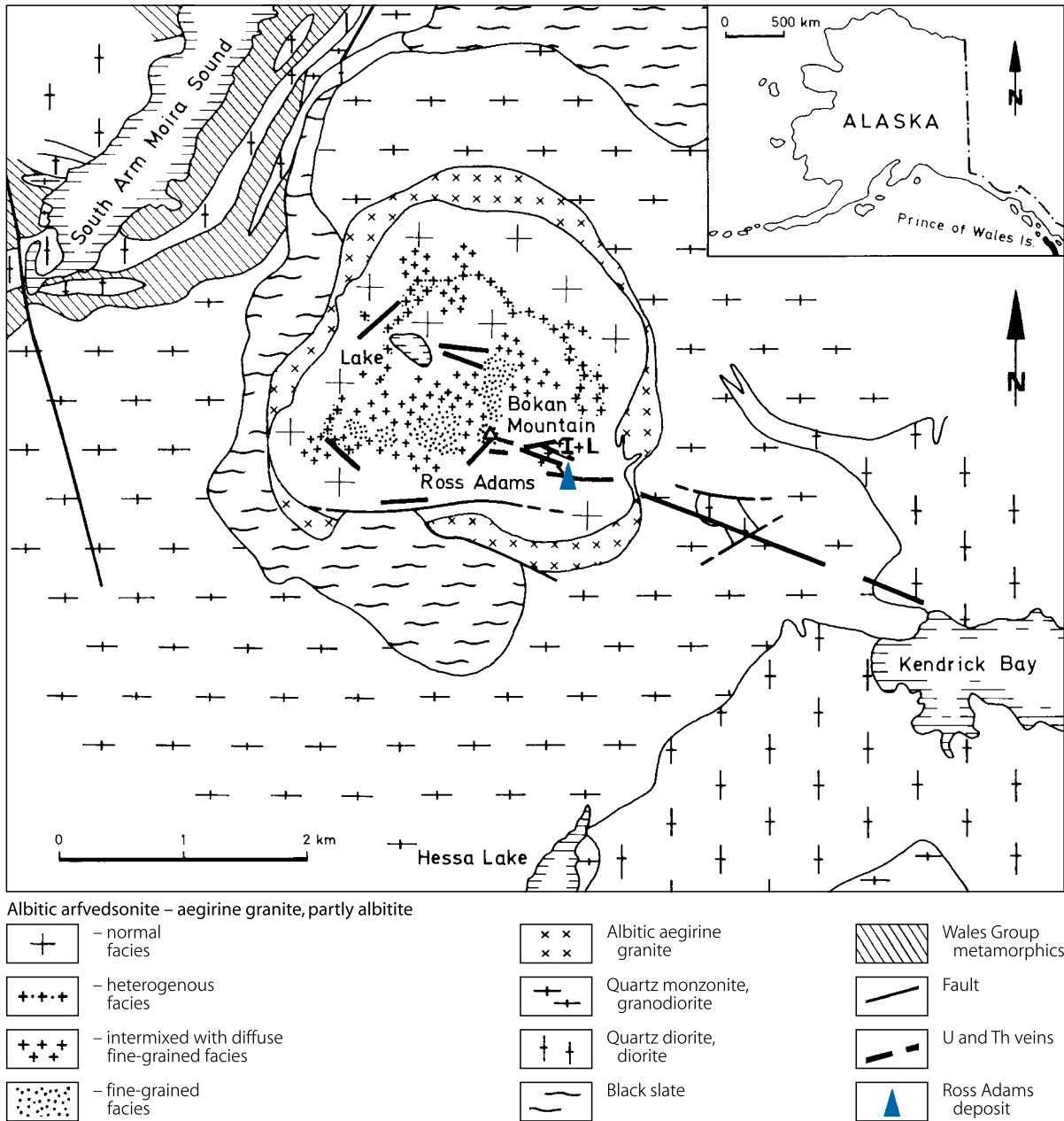
Alteration of host rocks is virtually restricted to desilicification and Na metasomatism, in particular albitization. It affected, to varying degrees, the Bokan Mountain Granite locally forming albitite, as described before, and formed an aureole extending into the surrounding Ordovician quartz monzonite and quartz diorite for more than 2,000 m from the granite contact.

Mineralization

Mackevett (1963) distinguishes four varieties of U–Th mineralization: (1) Primary disseminations and segregations of ore minerals within Bokan Mountain Granite; (2) syngenetic mineralization in pegmatite and aplite dikes related to Bokan

Fig. 10.1.

Bokan Mountain, Alaska, geology and distribution of the peralkaline granite and major U–Th veins. The various facies of the albitic arfvedsonite-aegirine granite are also referred to as Bokan Mountain Granite. (After Collot 1981; de Saint-André et al. 1983, 1984; Mackevett 1963; Staatz 1978) (de Saint-André et al. 1983, U–Pb geochronology of Bokan Mountain peralkaline granite: tectonic implications. *Can J Earth Sci*, v 20, no. 2, pp. 236-245, © 2008 NRC Canada or its licensors. Reproduced with permission)



Mountain Granite; (3) epigenetic hydrothermal mineralization, chiefly open-space fillings with some replacement; and (4) epigenetic hydrothermal mineralization occupying interstices of clastic sediments.

According to Collot (1981), de Saint André et al. (1984), and Staatz (1978), the two major U–Th–REE ore types are (a) intragranitic disseminations associated with fracture fillings and (b) (pegmatitic-)veins.

Intragranitic mineralization consists of uranothorite, uranothorianite, and some coffinite and brannerite. De Saint-André et al. (1984) report contents of 8.2–35.9% U with 9.3–39.6% Th for uranothorite, and 10.1–32.7% U with 13.7–41.8% Th for uranothorianite. U–Th minerals occur as discrete anhedral to rarely euhedral crystals in granite, and as minute grains in microfractures in albite. Intragranitic U and Th contents are not restricted to ore minerals, however; these elements also occur in accessory

minerals such as allanite, apatite, epidote, monazite, sphene, xenotime, and zircon. De Saint-André et al. (1983) document 800–1,800 ppm U in zircons of barren granite and lower values, about 500–700 ppm U, for zircons in low-grade mineralized albite. The same authors report, in a later paper (1984), zircons of a low-grade mineralized albite containing as much as 14,000 ppm U. These zircons have a clear central part surrounded by a metamict rim, are coated by red iron oxides, and have U–Th-rich inclusions. Feldspars are also abnormally rich in U (21–735 ppm U), but unusually low in Pb. Additional ore-associated oxide and sulfide minerals, which are present in variable amounts, include hematite, magnetite, pyrite, and minor galena and sphalerite. Collot (1981) and Thompson et al. (1980) established that intragranitic mineralization is closely associated with zones of intense albitization and impoverishment of quartz.

The *Ross-Adams deposit* is an example of primary intragranitic mineralization. It is located on the SE flank of Bokan Mountain within peralkaline granite and about 300 m from its SE margin (Mackevett 1963) (Fig. 10.1). Mineralization originated in part from primary late stage magmatic segregation of U–Th minerals, and to a larger extent from subsequent hydrothermal readjustments. The deposit is cut by many steeply dipping faults, which predominantly strike about NW–SE and NNE–SSW and which often contain iron-stained gouge.

The deposit consists of a higher grade core (>0.5% U) typically reddish colored due to abundant hematite, surrounded by a light brown zone of lower grade ore, which grades outwardly into white or buff granite. Mineralization in the lower grade halo is limited primarily to parallel structures and related veins. Granite around the ore zone contains more U–Th minerals, fluorite, and xenotime than average granite elsewhere.

Uranothorite and uranothorianite are the dominant ore minerals. They occur as anhedral to euhedral crystals as much as 2 mm across scattered throughout the peralkaline granite host and also occur in numerous veinlets 0.1–0.8 mm wide. Veinlets contain, in addition to U–Th minerals, abundant hematite and calcite, and lesser amounts of fluorite, pyrite, hydrous iron oxides, galena, quartz, and clay minerals.

Ore-hosting granite is texturally similar to nonmineralized granite. It ranges from fine-grained quartz-rich phases to medium-grained granite and porphyritic facies with coarse quartz, or acmite phenocrysts in a medium- to fine-grained groundmass.

Pegmatitic vein-type mineralization occurs in the I and L vein system that transect both the Bokan Mountain Granite and adjacent Ordovician quartz monzonite, quartz diorite, and diorite, in which the veins extend for 2.5 km from the granite contact to the West Arm of Kendrik Bay (Fig. 10.1). The vein system consists of subparallel and interbranching veins emplaced along subsidiary fractures and shears between major faults. Several distinct faults limit this system on the N and S side.

The veins have a texture of pegmatitic tendency and contain a suite of minerals. Staatz (1978) identified 34 minerals, which occur erratically or locally. Th-rich uraninite, thorite, and occasionally brannerite are the principal ore minerals. Most of these minerals are metamict. In addition, there are several REE minerals including allanite, bastnaesite, monazite, and xenotime.

Major gangue minerals are quartz, albite, and rarely microcline. Calcite, epidote, fluorite, Fe–Mn carbonate, zircon, pyrite, magnetite, hematite, and limonite occur locally and in minor amounts. Grain size varies erratically from about 0.05 to >20 mm. Ore minerals average 0.02–0.1 mm and are scattered among larger gangue minerals. Radial cracks extend from U–Th minerals into adjacent grains.

Some veins show locally distinct internal zonation. In these cases, cores consist of coarse-grained, white quartz bounded by selvages of finer grained feldspar, limonite, and various U–Th bearing minerals. Some crude regional zoning of minerals is observed in the I and L and transverse veins. Veins in the NW part of the system principally contain uraninite, thorite, xenotime, and Fe–Mn carbonate. Bastnaesite occurs locally. Veins in the SE part contain abundant allanite, scattered calcite and epidote, which are also in the central part, but are absent in the NW section. Brannerite was identified only in transverse veins, which also locally contain allanite.

The distribution of various REE is somewhat amazing. One section of a vein may have predominantly cerium group elements, e.g., bound in bastnaesite, whereas in another part of the same vein, yttrium-group elements are enriched, e.g., in xenotime. Other elements present in anomalous amounts in the I and L veins include Ba, Be, Cu, Mo, Nb, Pb, Sn, Sr, Zn, and Zr. Zr content is 0.15–2%; Be is locally concentrated up to 0.5%; and Nb appears to be concentrated in the NW section of the vein system where samples yielded 0.1–0.7%.

Shape and Dimensions of Deposits

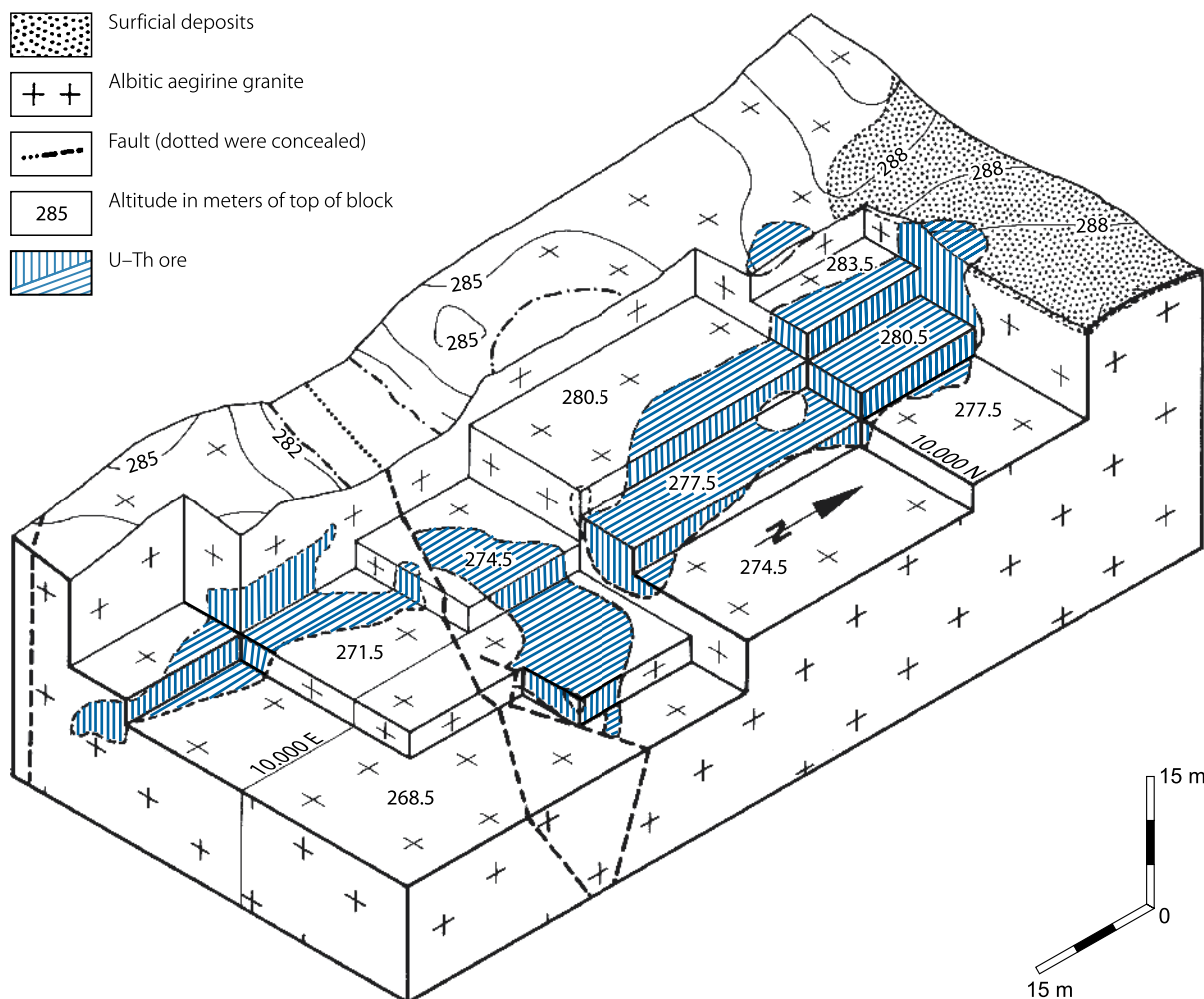
About 40 uranium localities have been noted by Mackevett (1963) within an area extending from the west Arm of Kendrik Bay in the SE for about 7 km in a NW direction to the NW flank of Bokan Mountain. The zone is up to 2 km wide. Individual deposits vary considerably in content and dimensions.

The *Ross Adams deposit*, mined by an open pit operation, is a southward plunging body about 110 m long in a N–S direction, between 7.5 and 22 m wide, and 2–7.5 m thick (Fig. 10.2). Most of the ore body has a gentle southerly plunge increasing to about 35° near faults at its southern end. The higher grade core contains in excess of 0.5% U, a large part of it is about 1% U, and local pods carry up to 3% U. The lower grade halo (<0.5% U) is from 0.5 to 6 m thick. The thorium content generally is slightly higher than uranium. It can locally amount to >5%. A few small irregular zones of barren rock intervene within the ore body.

The *I and L vein system* on the SE side of Bokan Mountain hosts vein-type mineralization for a distance of 2.5 km in a NW–SE direction from the West Arm of Kendrik Bay, at sea level, to about 300 m N of the Ross Adams deposit, at an elevation of 370 m. The system consists of a number of subparallel veins, which interbranch and pinch out. General strike is WNW–ESE, and the dip is mostly steep to the NE, but may change to SW. Nine veins that could be traced vary in length from about 25 to 280 m. Thicknesses of individual veins vary abruptly between a few centimeters and 1.5 m.

Fig. 10.2.

Bokan Mountain, Ross Adams deposit, isometric block-diagram showing the distribution of U–Th mineralization in albitic arfvedsonite–aegirine granite/Bokan Mountain Granite. (After Mackevett 1963)



Several small veins striking almost perpendicular to the main veins occur N of the main vein system. They strike around NE–SW, dip moderately SE, are 5–15 cm wide and are traceable for less than 10 m. Staatz (1978) reports chemical analyses of samples containing 0.005–2.8% U, 0.0033 to >10% Th, and 0.023 to >10% total REE.

Geochronology

Radiometric dating of units in the Bokan Mountain area has established a chronologic framework for events both preceding and following U–Th mineralization:

- ca. 486 Ma or earlier: regional metamorphism of greenschist and amphibolite grade (Churkin and Everlein 1977)
- ca. 446–421 Ma: intrusion of quartz monzonite, quartz diorite, and diorite (Lanphere et al. 1964; Turner et al. 1977)
- ca. 171 Ma: intrusion of peralkaline Bokan Mountain Granite and formation of albitite within the granite (de Saint André et al. 1983) [Armstrong (1986) gives a Rb–Sr age of 151 ± 5 Ma for the Bokan Mountain granite complex, which he considers a minimum value, whereas the published U–Pb date, revised to $167 + 7/-5$ Ma can only be considered as a maximum value]
- ca. 111 Ma: crystallization of uranothorite and uranothorianite (de Saint-André et al. 1984)
- ca. 105–93 Ma: intrusion of granodiorite related to the Coast Range batholith (Turner et al. 1977).

Ore Controls and Recognition Criteria

U–Th(-REE) mineralization at Bokan Mountain occurs in two modes, as an intragranitic, disseminated, and minifracture-filling type and as a (pegmatitic) vein type. Vein mineralization in particular is controlled by both structure and lithology.

Structural control is expressed by emplacement of veins in consistent, northwesterly orientation, which are presumably fracture-controlled, and by microfracturing within these veins. Lithologic control is evident in the restriction of mineralization to the Bokan Mountain pluton and peripheral zones around the pluton, which contain anomalous amounts of U–Th(-REE), and which were affected by Na metasomatism (albitization).

Metallogenic Aspects

Mackevett (1963) suggests a two stage evolution of Bokan Mountain mineralization: (1) Initial U–Th enrichment by partitioning during crystallization of peralkaline magma and (2) remobilization of original U–Th by hydrothermal processes and redeposition of ore-forming elements in fractures, etc., within and adjacent to granite.

Collot (1981) proposes the following genetic link between albitization and mineralization: Albitite is that part of the intrusion that was initially impoverished in quartz by an early desilicification stage, then albitized, and subsequently mineralized with U–Th–Zr–F. This model favors an ore formation during the latest stage of magmatic evolution and implies a contemporaneous intragranitic and perigranitic ore emplacement.

de Saint-André et al. (1984) interpret Bokan Mountain U–Th ore to be the result of a two-stage process. They argue that their U/Pb isotope systematics clearly put the time of U–Th vein mineralization at 111 Ma, i.e., 60 Ma after emplacement of the peralkaline pluton (171 Ma), a time span too long to relate ore formation to deuteritic processes associated with magmatic intrusion. Otherwise, the authors could document that U and Th were initially highly preconcentrated during the end phases of magmatic evolution of Bokan Mountain granite about

171 Ma ago, when these elements were fixed to a large extent in accessory minerals, e.g., in the form of nonsilicate U–Th minerals as inclusions in zircons. High U contents of zircons probably also reflect a high U content of related magmatic phases, from which zircons crystallized.

Contemporaneous with zircon crystallization at 171 Ma, deuteritic fluids caused albitization, which locally resulted in complete replacement of microcline. As a consequence, potassium and lead initially fixed in K-feldspar were released. This kind of Pb loss may explain the abnormally low Pb content of feldspar compared to that commonly found in this mineral.

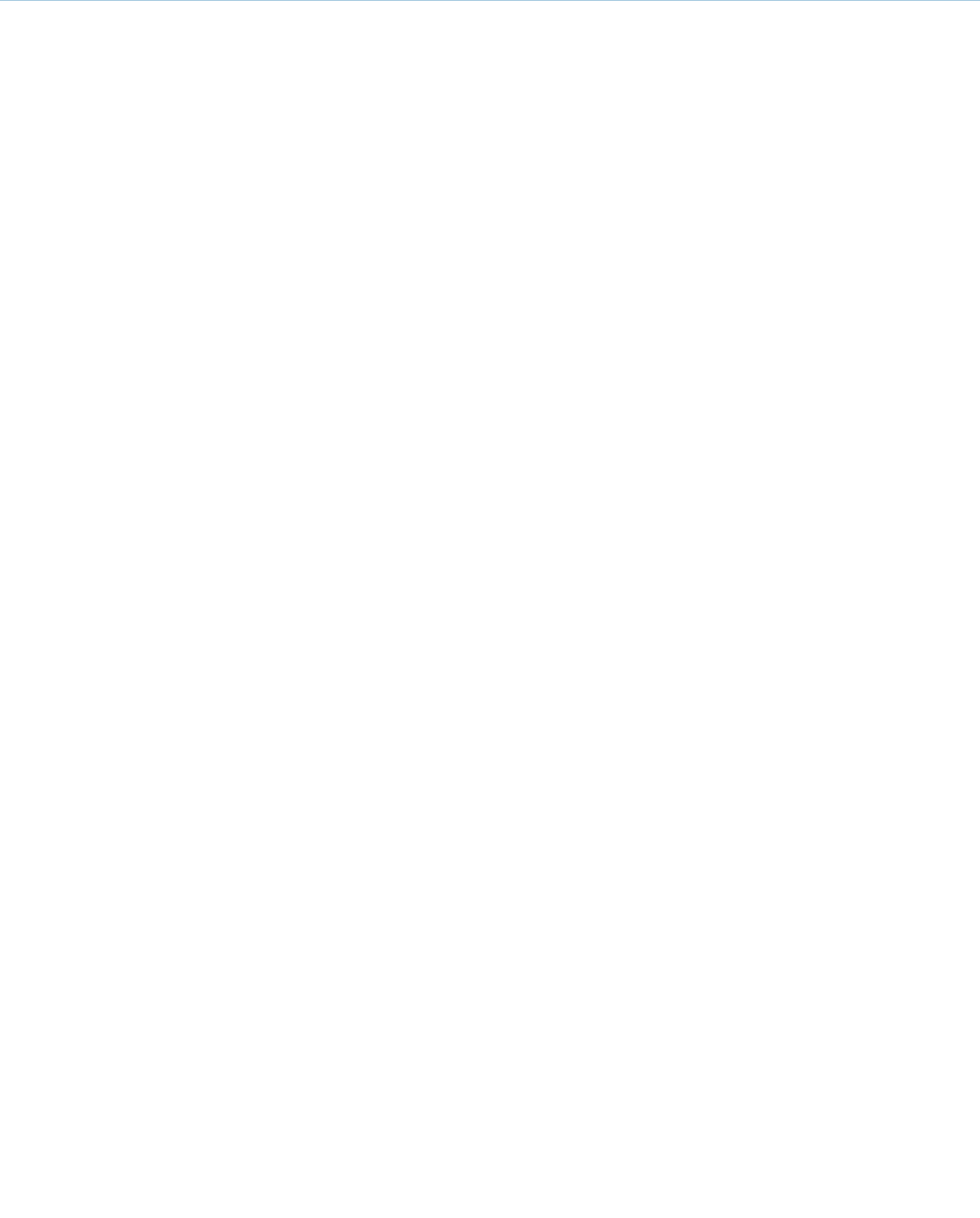
Actual ore formation took place at about 111 Ma, i.e., within the time frame of granodiorite intrusion related to the Coast Range batholith (ca. 105–93 Ma). A possible mechanism of U–Th ore formation may be comparable to that described by Cuney and his co-workers for hydrothermal vein deposits in France (see Dahlkamp, Vol. Uranium Deposits of the World: Europe, in preparation).

As proposed by Thompson et al. (1980) for Bokan Mountain mineralization, meteoric water heated up to 300–350°C may have leached the 171 Ma old uranium from U–Th-rich accessories such as zircon, and redeposited it as uraninite, uranothorianite, and uranothorite in ore-grade accumulations in veins.

Selected References and Further Reading for Chapter 10 Alaska

For details of literature see Bibliography.

Armstrong 1986; Collot 1981; de Saint-André et al. 1983, 1984; Dickinson et al. 1987; Dickson 1982; Johnson et al. 1979; Lancelot and de Saint-André 1982; Lanphere et al. 1964; Mackevett 1958, 1963; Miller and Bunker 1976; Singer and Ovenshine 1979; Stephens 1971; Staatz 1978; Thompson et al. 1980, 1982; Turner et al. 1977.



Chapter 11

Pacific Coast Region

The Pacific Coast region includes most of California and the western portions of Oregon and Washington (Fig. I.1b). Exploration in the 1950s led to the discovery of a number of minor uranium deposits and occurrences mainly of surficial type, but of no major deposit to date. Most discoveries were made from 1954 to 1959 in southeastern and eastern California, namely in the *Mojave Desert* near Big Bear Lake, San Bernardino County, the *McCoy Mountains* in Riverside County, the *Kern River Canyon* area in Kern County, the *Coso Range* in Inyo County, the *Sonora Pass* area in Tuolumne County, and the *Petersen Mountain* area in Lassen County. A total of about 30 t U has been intermittently produced from 1954 to 1968 from a number of small deposits in these areas. About 60% of this total came from the *Juniper Mine* in the Sonora Pass area making it the largest single uranium producer in California.

Sources of Information. Elevatorski 1978b; and US DOE 1980.

Geology and Mineralization

The Pacific Coast region is dominated by the N–S-trending Coast Ranges adjacent to the Pacific Ocean and the Cascade Range and Sierra Nevada to the east. These ranges are partially separated by parallel valleys. The Sierra Nevada consists largely of a batholith that was intruded during the Jurassic and Cretaceous and which was accompanied by widespread metamorphism. The Coast Ranges were uplifted during the Tertiary period, almost coeval with renewed, extensive volcanic activity in the northern part of the region that created the Cascade Range. Intermittent volcanism has continued in the Cascade Range to the present. Sporadic tectonic uplift and subsidence took place throughout the region during late Cenozoic time, particularly along the Pacific coast.

The region contains a wide variety of magmatic, metamorphic, and marine sedimentary lithologies, chiefly of Mesozoic and Tertiary age. Some Paleozoic volcanic and sedimentary rocks occur along the western flank and in xenoliths of the Sierra Nevada. Continental and marginal-marine sediments of Tertiary age cover much of western Oregon and western Washington. Coastal California is composed of folded Tertiary sediments that rest upon Mesozoic metasediments and older basement rocks. Nearly all of the terrane has been tilted, uplifted, and displaced by faulting.

The predominance of hexavalent U minerals indicates that most deposits mined were apparently of surficial type related to a cycle of Tertiary erosion and deposition. These minerals, mainly uranyl phosphates, were present as coatings or fillings of fractures within shear and fault zones (e.g., in the *McCoy*

Mountains, *Kern River Canyon* area, and *Petersen Mountain*) that transect granitic, volcanic, and metamorphic rocks of Mesozoic and Tertiary age. In the Sonora Pass area and the Coso Range, deposits consisted of uranium impregnations in tabular, stratiform ore bodies in Tertiary arkosic and pyroclastic beds. Felsic Tertiary volcanics are thought to have been the principal source of uranium. In more detail, characteristics of individual deposits are as follows:

Petersen Mountain area/Antelope Range, Lassen County: This area straddles the California–Nevada border some 40 km NNW of Reno, Nevada. Intermittent production on nine properties from 1955 through 1968 totaled ca. 2 t U at an ore grade of 0.13% U. Ore consisted mainly of autunite with minor sabugalite and uranophane associated with iron oxides and/or carbonized wood. Ore mined occurred disseminated in ash-flow tuff, and scattered along fractures and bedding planes, locally associated with iron-stained veinlets, within shear zones. Host rocks included silicified rhyolite, tuff, conglomerate, arkose, and mudstone which contained iron oxides, carbonized wood, and minor carbonaceous debris.

Sonora Pass area, Juniper mine, Tuolumne County: Discovered in 1955, the Juniper mine is located near Sonora Pass. Intermittent production from 1955 through 1966 yielded 17.5 t U at an ore grade of 0.25% U. The ore mined consisted of fine-grained sooty pitchblende closely associated with coalified material, hosted in thin-bedded, carbonaceous, tuffaceous sandstone thought to be equivalent to the Relief Peak Formation of Miocene age. Autunite was present in oxidized parts of the deposit. The host rocks fill channels incised into Mesozoic granodiorite and Miocene rhyolitic tuff and are overlain by rhyolitic rocks.

Coso Range, Inyo County: Only the Coso mine situated on Haiwee Ridge on the west flank of the Coso Range, about 15 km SE of Olancho has recorded production of a quarter of a tonne of uranium in 1956. The grade was 0.08% U. Small ore bodies were hosted in paleochannels at the base of the Tertiary Coso Formation, in which they were confined to within 10 m of the contact to a granite cupola. Reddish-brown fanglomerate overlies the channel fill within the contact zone. The rocks are heavily fractured and jointed. Mineralization consisted of uranophane and autunite within an argillaceous matrix in fractures and along bedding planes of iron-stained, yellow-grey conglomeratic arkosic sandstone, cemented by calcite, silica, and clay. Thin veinlets of pitchblende associated with pyrite occur in the granite. Rare haiweeite also occurs. It was first identified on Haiwee Ridge, for which it has been named.

Kern River Canyon area, Kern County: Located ca. 50 km NE of Bakersfield and discovered in 1954, three mines produced 3.5 t U at ore grades averaging 0.34% U during 1954–1959. Autunite, sooty pitchblende, and coffinite associated with jordanite, ilsemanite, and limonite were the predominant ore minerals. Other U⁶⁺ minerals included carnotite, schroekingite,

torbernite, tyuyamunite, uranocircite, uranophane, zeunerite, walpurgite, and/or uraniferous opal. These minerals occurred mostly as thin coatings along intersecting fractures and shear zones within medium to coarse-grained Mesozoic granodiorite or quartz-diorite. Host fractures and shear zones are up to 5 m wide. Fault gouge with interspersed iron and manganese oxides, pyrite, calcite, minor baryte, and fluorite fills the host fractures. Ore shoots dipped steeply, from 0.3 to 1.2 m wide, ranged in grade from 0.1 to 3% U and were commonly separated by wide gaps of barren or very low-grade mineralization. Locally, thin pitchblende veinlets occur in a brecciated and sheared contact zone between quartzite and gneiss.

McCoy Mountains, Riverside County: Intermittent mining from 1958 through 1964 on two properties, located some 20 km W of Blythe, has produced cumulatively ca. 6 t U at an ore grade of 0.17% U. Mineralization consisted of uranophane and autunite coatings along fractures in quartzite and conglomerate.

Selected References and Further Reading for Chapter 11 Pacific Coast Region

For details of literature see Bibliography.
Elevatorski 1978b; US DOE 1980.

Chapter 12

Uraniferous Phosphorite Regions

Major phosphorite resources are known in both the southeastern and northwestern United States; the first covers parts of Florida, Georgia, North Carolina, South Carolina, and Tennessee, and the other spreads through the states of Idaho, Montana, Utah, and Wyoming (Fig. 1.1). Uranium resources contained in phosphorite are estimated to exceed 20 Mio t U (Pool 1995). The uranium content is generally very low (<50–200 ppm), however, and therefore uranium can be produced only as a byproduct to phosphate, and particularly on that quantity of phosphate, which is converted to phosphoric acid. To date, uranium recovery from phosphorite has been restricted to recovery from phosphoric acid. Thus, the recoverable amount relies on the production capacity of phosphoric acid within the phosphate industry. Most uranium production from phosphorite came from the Land Pebble District in Florida and a small amount from Idaho.

12.1 Land Pebble District, Central Florida

Uranium was extracted in eight processing plants, from 1978 to 2000, from wet-process phosphoric acid from phosphorites of the Pliocene Bone Valley Formation that was mined by open pit methods near Bartow, Plant City, and East Tampa in central and southern Florida (Fig. 1.1). Production totaled 17,275 t U (Pool TC, personal communication). Although total resources are estimated at some 500,000 t U or more, uranium resources, estimated economically as a function of phosphate production, may be in the range of 100,000–200,000 t U.

Sources of Information. Altschuler et al. (1956, 1958), Cathcart (1956, 1990), De Voto and Stevens (1979), NUEXCO (1994).

Geology and Mineralization

Phosphorite in Florida and adjacent states is largely of shallow marine near-shore platform provenance. In this environment, relatively low-grade phosphatic and uraniumiferous nodular and sandy phosphorite (average 10–20% P_2O_5 , 20–80 ppm U) and fine- to medium-grained clastics (clay, sand, glauconite), as well as shallow-water limestone and dolomite were deposited. An exception in U and P grades is the land pebble mineralization in the Pliocene Bone Valley Formation.

The *Pliocene Bone Valley Formation*, as much as 15 m thick, consists in its lower two thirds of phosphate pebbles and argillaceous phosphate sands intercalated or interfingering with layers of fine- to medium-grained clastics (clay, sand, glauconite)

and shallow-water limestone and dolomite. It grades upward into sands and clays, 3–4 m thick, and rests upon limy sediments of the Miocene Hawthorn Formation. The nodular phosphorite horizon, locally up to 10 m in thickness, referred to as *land pebble phosphorite*, is flat lying, crudely graded bedded, reworked, and composed of nodules and sand-size grains of fluor-carbonate apatite mixed with clay minerals (smectite, montmorillonite) and quartz grains.

Where affected by weathering, apatite is replaced in the top zone by Al phosphate (wavelite) and in the middle zone by Ca–Al phosphate (crandallite, millisite, referred to as aluminum phosphate zone). Smectite is transformed to kaolinite. Incipiently or incompletely leached residual apatite of the bottom zone is highly porous and enriched in U, whereas secondary Al- and Ca–Al phosphates contain only minor U.

Uranium is concentrated at or near the base of the leached zone in which it occurs in stratiform dissemination bound to Ca phosphate (principally fluor-carbonate apatite) in the form of sand-size particles and nodules in beds mixed with quartz and clay minerals. Although apatite grains and nodules are often enriched up to 500 ppm U and 35% P_2O_5 , and locally up to a few 1,000 ppm U at the bottom of the leached zones, the mineralized lower Bone Valley Formation averages only 100–150 ppm U due to the quartz and clay matrix.

The areal extent of the lower Bone Valley Formation in which deposits of the Land Pebble district occur is about 2,500 km². Mineralized beds range in thickness from less than a meter to 10 m averaging 5–7 m.

Principal Recognition Criteria

Host Environment

- Phosphorite of shallow marine near-shore platform origin
- Nodular phosphorite locally reworked to apatite pebbles interbedded with fine- to medium-grained shallow marine facies (sand, clay) and carbonate beds
- Widespread extension of phosphorite horizons, up to few 1,000 km²
- Bedded phosphorites contain a higher uranium content and are formed distal to shore-line as compared to nodular phosphorites, which are proximal to shore line formation.

Mineralization

- None or only rare discrete primary uranium minerals
- Principal uranium-bearing mineral is cryptocrystalline fluor-Ca carbonate apatite
- Unfavorable minerals for uranium accumulation are Al and Ca–Al phosphates (or other non-Ca phosphates)
- Positive correlation of U and P when concentration of both elements is relatively high
- Negative correlation of U and sedimentary carbonate contents.
- Elevated U grades (av. 100–150 ppm U) in land pebble phosphorite (as a result of reworking and weathering-related secondary U enrichment).

Metallogenetic Aspects

Uranium enrichment in land pebble phosphorite of the Pliocene Bone Valley Formation is attributed to reworking and corresponding re-exposure of the apatite particles to uranium-bearing seawater during repeated marine transgressions. Associated with this evolution is an irregular, up to several meters thick, leached horizon developed within the Bone Valley Formation by weathering. Its upper section is composed of Al phosphates, and its middle section, dominated by Ca–Al phosphates, has released uranium supposedly by acid solution leaching. Altschuler et al. (1958) suggest U reconcentration at or near the base of the leached zone composed of incipiently leached residual apatite took place in response to neutralization of acid fluids by Ca phosphate. Fixing of uranium resulted from adsorption on porous, partially leached, residual apatite leading locally to concentrations of as much as several thousand parts per million U. The distribution of U-bearing Ca phosphates and U-poor Ca–Al and Al phosphates also reflects U-grade zoning within the leached profile.

12.2 Phosphoria Formation, Idaho-Montana-Utah-Wyoming

In the northwestern United States (Fig. I.1), uranium phosphorite mainly occurs in the Phosphoria Formation of Permian age. Uranium grades average <60–200 ppm and resources may be speculated at a few million tonnes of contained uranium, but, as stated in Chapter 11, the recoverable amount is a function of phosphoric acid production.

Some phosphate mined near Montpelier in Idaho was treated for uranium from 1980 to 1987 in a plant at Calgary, Canada. Production amounted reportedly to 184 t U recovered from a concentrate containing 110 ppm U and 24–26% P_2O_5 .

Sources of Information. De Voto and Stevens 1979; Elevatorski 1976; Gulbransen 1966; Love 1964; McKelvey and Carswell 1956; McKelvey et al. 1955, 1956; Sheldon 1959, 1963; Swanson 1970.

Geology and Mineralization

The Permian Phosphoria Formation stretches discontinuously over many thousand square kilometers from Idaho and Montana into Wyoming and Utah. It consists of thick layers of bedded phosphorite within a sequence of very fine-grained miogeosynclinal sediments including black shale, more or less carbonaceous mudstone, chert beds, and minor carbonates, which were laid down at the outer or distal part of a continental shelf.

The Phosphoria Formation includes the uranium-bearing *Meade Peak Member* and *Retort Member*. These members, from 60 to 150 m thick, comprise oolitic, phosphorite pebbles, and massive beds with a phosphoritic matrix. Uranium is bound in carbonate-fluor apatite and occurs in a relatively regular distribution, to some extent as a function of phosphate content,

throughout the host beds. Uranium grades average 40–200 ppm at P_2O_5 contents from 10 to 35% and more.

Idaho Phosphorite deposits located near *Montpelier, Idaho* are composed of bedded apatite as fine-grained oolites, pisolites, pellets, or laminae, and phosphatic fossil fragments (brachiopod shells, fish scales, etc.) mixed with variable amounts of finest-grained detritus, mainly clay particles, carbonaceous matter, and locally carbonate. Associated sediments include over- or underlying, often pyritic cherts, mudstone, black shale, which laterally interfinger with sandy, carbonatic, redbed, and evaporitic shallow water sediments.

Uranium occurs in rather uniform dissemination in phosphatic beds of dominantly bedded cryptocrystalline fluor-carbonate apatite of pelletal, oolitic, etc., texture. Although present in almost all phosphorite beds, U grades vary considerably from 10 to several 1,000 ppm U and to a large extent, but not necessarily, correlate with the phosphate content. Phosphate enrichment is greatest in the top and/or basal segments of phosphatic layers as exemplified by the phosphatic shale of the Meade Peak Member, the main phosphate member of the Phosphoria Formation. This member is from 60 to 150 m thick and averages 11–12% P_2O_5 , whereas the upper and lowermost 1–3 m contain from 25 to 35% P_2O_5 and also contain the highest uranium tenors (locally up to 6,500 ppm, average 50–200 ppm U).

Montana Swanson (1970) lists six phosphate districts located in southwestern Montana containing estimated resources and grades as listed below. The uranium resource calculation is based on rocks containing in excess of 18% P_2O_5 . Uranium resources are contained in two members of the Phosphoria Formation and total over one million tonnes. Two thirds of this estimated total is in the Retort Member (or upper shale) and the remainder in the Meade Peak Member (or lower shale). Grades range from 38 to 73 ppm U and average ca. 50 ppm U.

Centennial Mountains area: Situated on the Idaho border, high-grade phosphorite occurs in both upper and lower shale members. Estimated resources amount to almost 38,500 t U; approximately 70% of which at a grade of 73 ppm U are contained in the Meade Peak Member and the remainder in the Retort Member at 42 ppm U.

Lima area: Located south of the town of Lima and west of the Centennial Mountains district, estimated resources amount to almost 91,000 t U; approximately 70% of which are contained in the Meade Peak Member at a grade of 73 ppm U and the remainder in the Retort Member at 38 ppm U.

Madison Range area: Located west of Yellowstone National Park, the Meade Peak Member is absent and only the Retort Member is present and hosts uranium resources of about 114,000 t at a grade of 51 ppm U.

Melrose area: Situated SW of Butte, only the Retort Member is present and contains uranium resources of almost 91,000 t at a grade of 42 ppm U. P_2O_5 content is 20.1%.

North and South Dillon areas: Located south of Melrose, uranium resources total ca. 152,000 t at a grade of 42 ppm U. Almost all resources are in the Retort Member.

Wyoming In this state, uraniferous phosphates occur in the Permian Phosphoria Formation and in Eocene lake bed deposits. Uranium contents in phosphorite range from 42 to 250 ppm U (Elevatorski 1976) and in lake bed phosphates from 42 to 2,500 ppm U (Love 1964).

Sheldon (1963) has estimated uraniferous *phosphorite resources* in Wyoming at 1,500 mio sh.t containing 0.01% U_3O_8 (1,350 mio t at 0.0084% U). The equivalent number for uranium resources would amount to 113,400t U. The bulk of these resources is hosted in the Phosphoria Formation in the Gros Ventre Range, Hoback Range, Snake Range, and Wyoming Range in western Wyoming.

Uraniferous phosphatic lake bed deposits described by Love (1964) include:

Beaver Divide area: Located in Fremont County, the Eocene Wagon Formation hosts seven or more zones of uraniferous phosphatic shale, as much as 0.6 m thick, with maximum values of 360 ppm U and 5.7% P_2O_5 .

Green River Basin: The Wilkens Peak Member of the Eocene Green River Formation includes extensive phosphatic shale beds, from 0.9 to 1.8 m in thickness, which contain an average of 42 ppm U and 2.2% P_2O_5 , with maximum values of 1,270 ppm U and 18.2% P_2O_5 .

Lysite Mountain area: Located in Fremont and Hot Springs counties, a sequence of phosphatic shale and tuff contains as much as 340 ppm U and 7.25% P_2O_5 .

Pine Mountain area: ca. 15 km ESE of the town of Green River: Uraniferous phosphate beds, up to 1.2 m thick, averaging 51 ppm U and 5.7% P_2O_5 with a maximum of 2,500 ppm U and 19% P_2O_5 , occur within siltstone and sandstone of the Eocene Wasatch Formation.

Principal Recognition Criteria

Host Environment

- Phosphorite of marine origin deposited on a continental shelf
- Bedded phosphorite with oolitic, pisolitic, pelletal, and laminated textures associated with fine-grained miogeosynclinal facies, but with a noticeable absence of carbonates within uraniferous phosphorite
- Widespread extension of phosphorite horizons, up to several 1,000 km²
- Bedded phosphorite is formed distal to shore-line and contains a higher uranium content as compared to nodular phosphorite, which is proximal to shore line formation.

Mineralization

- Either none or only rare discrete primary uranium minerals
- Principal uranium-bearing mineral is cryptocrystalline fluor-carbonate apatite
- Mostly, but not necessarily, positive correlation of U and P
- Ubiquitous, fairly uniform U distribution throughout a given bed, but with variations in grades.

Metallogenetic Aspects

The *Phosphoria Formation* has formed at the outer or distal margin of a continental shelf, where (a) thick layers of bedded phosphorite could develop, (b) the contribution of detrital clay and silt was minimal and the accumulation rate was strongly retarded, and (c) where uranium-bearing deep seawater currents could ascend and flood the phosphorite.

Uranium accumulation is thought to be due to the extraction of U from seawater and synsedimentary incorporation into phosphate minerals, predominantly cryptocrystalline fluor-carbonate apatite, by replacing Ca ions in the apatite lattice.

The relatively high P and more or less proportional high U enrichment (up to 35% P_2O_5 , with a maximum of 6,500 ppm U, average 60–200 ppm U, respectively) in certain phosphorite beds is attributed to the sedimentary environment at the margin of a continental shelf, where (a) upwelling of P-saturated and U-bearing deep marine waters provided a renewable P and U source, (b) a slow rate of sedimentation caused longer exposure of apatite grains, which permitted extraction of U from seawater to replace Ca in apatite, and (c) an absence of carbonate ions in the waters allowed uranium to remain in solution. Variations in U content relative to P are interpreted to have resulted from either one or a combination of items (a) to (c) cited earlier.

Selected References and Further Reading for Chapter 12 Uraniferous Phosphorite Regions

For details of literature see Bibliography.

Altschuler 1980a, b; Altschuler et al. 1956, 1958; Cathcart 1956, 1978, 1990; DeVoto and Stevens 1979; Elevatorski 1976, 1977; Gulbransen 1966; Jasinski 2006, Love 1964; McKelvey and Carswell 1956; McKelvey et al. 1955, 1956; NUEXCO 1994; Pool 1995; Sheldon 1959, 1963; Swanson 1970, U.S. Geological Survey 2007, and Pool TC, personal communication.



Chapter 13

Chattanooga Black Shale Region, Kentucky–Tennessee–Alabama

A potential uranium source is provided by black shales. The most prominent unit is the Paleozoic Chattanooga Shale as described below.

Sources of Information. Conant and Swanson 1961; Mountain States Research and Development (MSR & D) 1978; Mutschler et al. 1976; Swanson 1960, 1961; and US DOE 1980.

Geology and Mineralization

The Chattanooga Shale of Devonian to Mississippian age spreads over an area of some 80,000 km² from southern Kentucky through central Tennessee into northern Alabama (Fig. I.1). It is a flat-lying, massive, siliceous, pyritic marine black shale, on average about 10 m thick and located at a depth from 30 to 600 m. It unconformably rests upon Leipers Limestone and is overlain by the Maury Formation. The Chattanooga Shale includes three members. At the base and only locally developed is the thin *Hardin Sandstone Member*. The middle *Dowelltown Member*, about 5 m thick, has only weak U tenors (av. 23 ppm U).

The *Gassaway Member*, the upper unit of the Chattanooga Shale, ranges from 2 to 12 m and averages 4–5 m in thickness. It consists of an upper and lower black shale horizon, each 1.5–3.5 m thick, separated by an alternating unit of lighter colored grey, silty claystone with black shale. These Gassaway black shales are the main uranium host and contain between 40 and 80 ppm U in addition to other commodities (see below). They consist of massive greyish-black shales with paper-thin partings of siltstone, and films or bands of pyrite and marcasite. About 20 wt.% of the shale is organic material (sapropelite, vitrain, bituminous coal) derived mainly from planktonic marine algae and less from land plant debris. These organics fill interstices and coat minute rock grains of shale. No structures or alteration features are present. Uranium distribution is stratiform, adsorbed mainly on organic material and to a lesser extent on clay particles. At locations where the shales are shattered and fractured, hexavalent U minerals have formed and grades are up to 0.34% U as reported from *Dekalb County, Alabama*.

Mutschler et al. (1976) calculated resources of 4–5 mio t U contained in the Gassaway Member for a restricted area of 12 counties in central Tennessee.

MSR & D (1978) reports from a test area in *Dekalb County, Tennessee*, average contents of 230 ppm Co, 200 ppm Mo, 530 ppm Ni, 55–65 ppm U, 1,360 ppm V₂O₅, 8,600 ppm sulfur, and 9 gal/sht of syncrude oil. Based on an extraction plant with a theoretical processing capacity of 90,000 t/day, and a presumed average content of 55 ppm U, MSR & D (1978) calculated a potential annual recovery of about 1,000 t U, 9,600 t V₂O₅, 710,000 t S, 154,000 t ammonia, and 19.3 million barrels of oil. The deep position of the shale would require underground mining.

An equivalent to the Chattanooga Shale is the *Ohio Shale*. It spreads from Tennessee northwestward into eastern Kentucky and averages 30 ppm U uniformly distributed over a thickness of up to 200 m (Provo 1977).

Principal Recognition Criteria

Host Environment

- Shallow, partially closed epicontinental basin within continental terrane
- Very fine-grained black shales, evenly laminated, dense, with high contents of organic matter, pyrite and/or marcasite, and thin coalified, phosphatic, and/or silty intercalations
- Fairly uniform shale thickness, commonly a few meters and up to some 10 m
- Widespread extension over several 10,000 km²
- No ore-related alteration.

Mineralization

- U is adsorbed on organic and clay particles except for some locally secondary hexavalent U minerals
- U is disseminated uniformly throughout and coextensive with individual beds over large areas
- Very low-grade mineralization ranging from 20 to 100 ppm U
- Presence of small quantities of other *metals* (Co, Cu, Cr, Mo, Mn, Ni, REE, V, and P) as well as oil.

Metallogenetic Aspects

The Chattanooga black shales were deposited in a shallow, partially closed epicontinental basin within continental terrane that was tectonically stable for a long period. The depositional environment is characterized by a low rate of sedimentation, brackish to normal marine salinities, anaerobic, strongly reducing conditions, formation of sapropelic-bituminous, and humic, coaly matter from planktonic marine algae and land plant (wood spores) debris.

Deposition of uranium was synsedimentary from seawater by adsorption dominantly on organic matter with particular concentrations in humic-coaly material. If phosphate nodules are present, they normally collected more uranium than the surrounding shale.

Selected References and Further Reading for Chapter 13 Chattanooga Black Shale Region, Kentucky–Tennessee–Alabama

For details of literature see Bibliography.

Conant and Swanson 1961; Mountain States Research and Development (MSR & D) 1978; Mutschler et al. 1976; Provo 1977; Swanson 1960, 1961; US DOE 1980.

Bibliography-USA

A

- Abrams MJ, Conel JE, Lang HR (1984a) Lisbon Valley, Utah, uranium test site report. *in*: Paley HN, ed., The Joint NASA/Geosat Test Case project, v I, pt 2. AAPG Bookstore, Tulsa, OK, pp 8-1 to 8-158
- Abrams MJ, Conel JE, Lang HR (1984b) Copper Mountain, Wyoming, uranium test site report. *in*: Paley HN, ed., The Joint NASA/Geosat Test Case project, v I, part 2. AAPG Bookstore, Tulsa, OK, pp 9-1 to 9-110
- Adamek P, Behr HJ, von Pechmann E (1990) Gold-bearing collapse-breccia pipe, Copper Mountain, northwestern Arizona. *in*: Short Papers of the US Geol Surv Uran Workshop. US Govt Print Office, pp 51-53
- Adams JW, Gude AJ 3rd, Beroni EP (1953) Uranium occurrences in the Golden Gate Canyon and Ralston ButtCreek areas, Jefferson County, Colorado. US Geol Surv Circ 320, 16 p
- Adams SS, Curtis HS, Hafen PL, Salek-Nejad H (1978) Interpretation of post-depositional processes related to the formation and destruction of the Jackpile-Paguete uranium deposit, northwest New Mexico. *Econ Geol*, v 73, pp 1635-1654
- Adams SS, Curtis HS, Hafen PL (1974) Alteration of detrital magnetite-ilmenite in continental sandstones of the Morrison Formation, New Mexico. *in*: Formation of uranium deposits, IAEA, Vienna pp 219-253
- Adams SS, Saucier AE (1981) Geology and recognition criteria for uraniferous humate deposits, Grants mineral region, New Mexico. US DOE, GJBX-2(81), 225 p
- Adams SS, Smith RB (1981) Geology and recognition criteria for sandstone uranium deposits in mixed fluvial-shallow marine sedimentary sequences, south Texas. Final report, US DOE, GJBX-4(81), 145 p
- Adams JW, Stugard Jr F (1956) Wall-rock control of certain pitchblende deposits in Golden Gate Canyon, Jefferson County, Colorado. US Geol Surv Bull 1030-G, pp 187-209
- Ader HH (1974) Concepts of uranium-ore formation in reducing environments in sandstones and other sediments. *in*: Formation of uranium ore deposits. IAEA, Vienna, pp 141-168
- Ader HH (1977) Geochemical factors contributing to uranium concentration in alkalic igneous rocks. *in*: Recognition and evaluation of uraniferous areas. IAEA, Vienna, pp 35-46
- Ader HH, Sharp BJ (1967) Uranium ore rolls-occurrence, genesis, and physical and chemical characteristics. Utah Geol Soc Guidebook, no. 21, pp 53-77
- Ahern R, Corn RM (1981) Mineralization related to the volcanic center at Beatty, Nevada. *in*: Dickinson WR, Payne WD, eds., Relations of tectonics to ore deposits in the Southern Cordillera. Ariz Geol Soc Dig, v XIV, pp 283-286
- Aiken MJ (1981) Mineralogy and geochemistry of a lacustrine uranium occurrence, Anderson Ranch, Browster County, Texas. MS thesis, Univ Texas, El Paso, 162 p
- Akers JP et al. (1962) Geology of the Cameron Quadrangle Arizona. US Geol Surv map CQ-162
- Albrethsen H Jr, McGinley FE (1982) Summary history of domestic uranium procurement under U.S. Atomic Energy Commission contracts, final report: US DOE, GJBX-220(82), 162 p
- Alief MH, Kern RA (1989) Mt. Taylor mine. *in*: Lorenz IC, Lucas SG, eds., Energy frontiers in the Rockies. Albuquerque Geol Soc, p 28
- Allen RF, Thomas RG (1984) The uranium potential of diagenetically altered sandstones of the Permian Rush Springs Formation, Cement district, southwest Oklahoma. *Econ Geol*, v 79, pp 284-296
- Altschuler ZS (1973) The weathering of phosphate deposits-geochemical and environmental aspects. Environmental Phosphorus Handbook. John Wiley & Sons, New York. pp 33-96.
- Altschuler ZS (1980a) The geochemistry of trace elements in marine phosphorites: I. Characteristic abundances and enrichment. *Soc Econ Paleont Miner Spec Pub* 29, pp 19-30
- Altschuler ZS (1980b) The bearing of geochemistry on the recovery of uranium and rare earths in phosphorites. 2nd Intern Congr Phosphorus Compounds, Boston, Mass., Proc, pp 605-625

- Altschuler ZS, Clarke RS, Jr, Young EJ (1958) Geochemistry of uranium in apatite and phosphorite. US Geol Surv Prof Paper 314-D, pp 45-90
- Altschuler ZS, Jaffe EB, Cuttitta F (1956) Distribution and occurrences of uranium in the calcium phosphate zone of the land-pebble phosphate district of Florida. US Geol Surv Prof Paper 300, pp 495-504
- Anderson CA et al. (1955) Geology and ore deposits of the Bagdad area, Yavapai Co., Arizona. US Geol Surv Prof Paper 278, 103 p
- Anderson DC (1969) Uranium deposits of the Gas Hills. Wyoming Univ Contrib Geol, v 8, pp 93-103
- Anderson WB (1975) Cooling history and uranium mineralization of the Buckshot Ignimbrite, Presidio and Jeff Davis Counties, Texas. MS thesis, Univ Texas. Austin, 135 p.
- Arizona Geological Society (1978) Anderson mine area. Arizona Geol Surv, Spring Field Trip Guide (May 1978)
- Armstrong FC (1970) Geologic factors controlling uranium resources in the Gas Hills district, Wyoming. 22nd Field Conf Guidebook, Wyoming Geol Ass, pp 31-44
- Armstrong RL (1986) Rb-Sr dating of the Boka Mountain granite complex and its country rocks: Reply. *Can. J. Earth Sci.* 23, pp 744-745 (1986)
- Aubrey WM (1986) The nature of the Dakota-Morrison boundary, southeastern San Juan basin. *in*: Turner-Peterson CE, Santos ES, Fishman NS, eds., A basin analysis case study - the Morrison Formation, Grants Uranium Region, New Mexico. Amer Ass Petrol Geol, Studies in Geology, no. 22, pp 93-104
- Ausburn KE (1981) A geochemical and petrographic study of the Hansen sedimentary uranium orebody northwest of Canon City, Colorado. MS thesis, Florida State Univ, Tallahassee, 212 p
- Austin SR (1963) Alteration of Morrison sandstone. *in*: Kelley VC, ed., Geology and technology of the Grants Uranium Region. New Mex Bur Mines Mineral Res Mem 15, pp 38-44
- Austin SR (1964) Mineralogy of the Cameron area, Coconino County, Arizona. US AEC, RME-99, 98 p
- Austin SR (1970) Some patterns of sulfur isotope distribution in uranium deposits. Wyoming Geol Ass, Earth Sci Bull, v 3, no. 2, pp 5-22
- Austin SR (1980) Dissolution and authigenesis of feldspars. *in*: Rautman CA, ed., Geology and mineral technology of the Grants Uranium Region 1979. New Mex Bur Mines Mineral Res Mem 38, pp 107-115
- Austin SR, D'Andrea RF Jr (1978) Sandstone-type uranium deposits. *in*: Mickle DG, Mathews GW, eds., Geologic characteristics of environments favorable for uranium deposits. US DOE, GJBX-67(78), pp 87-120
- Axelrod JM et al. (1951) The uranium minerals from the Hillside Mine, Yavapai County, Arizona. Amer Mineral, v 36, pp 1-22
- Ayuso RA, Ratte CA (1990) Epigenetic uranium mineralization in the Middle Proterozoic Mount Holly Complex near Ludlow and Jamaica, Vermont. US Geol Surv Bull 1887, Chapter P, 18 p

B

- Babcock JW (1980) Tallahassee Creek uranium deposits. *in*: Babcock JW, King JR, eds., Silver Cliff volcanic center and Tallahassee Creek uranium deposits guidebook. *in*: First annual field trip. Denver Reg Explor Geol Soc, pp 15-38
- Bachman GO, Vine JD, Read CB, Moore GW (1959) Uranium-bearing coal and carbonaceous shale in La Ventana Mesa area, Sandoval County, New Mexico. *in*: Uranium in coal in the western United States. US Geol Surv Bull 1055-J, 12 p
- Bailey RV (1965) Applied geology in the Shirley Basin uranium district, Wyoming. Wyoming Univ Contrib Geol, v 4, pp 27-35
- Bailey RV (1969) Uranium deposits in the Great Divide Basin-Crooks Gap area, Fremont and Sweetwater Counties, Wyoming. Wyoming Univ Contr Geol, v 8, pp 105-120
- Bailey RV (1980) Comments on Shirley Basin uranium deposits and on the ages of all Wyoming uranium deposits in Eocene host rocks. *in*: Third annual uranium seminar, New York. Amer Inst Min Met Petrol Eng, pp 41-59
- Bailey RV, Childers MO (1977) Applied mineral exploration with special reference to uranium. Westview Press, Golden, 542 p

- Baillieu TA, Daddazio PL (1982) A vein-type uranium environment in the Precambrian Lovington Formation, central Virginia. *Virginia Div Mineral Res Publ* 38, 12 p
- Baillieu TA, Zollinger RC (1982) National uranium resource evaluation Grand Canyon quadrangle, Arizona. *PGJ-020*, 41 p
- Bain CW (1950) Geology of the fissionable materials. *Econ Geol*, v 45, pp 273-323
- Baird CW, Martin KW, Lowy RM, (1980) Comparison of the braided stream depositional environment and uranium deposits at the Saint Anthony underground mine. *New Mex Bur Mines Mineral Res Mem* 38, pp 292-298
- Baker ET Jr (1979) Stratigraphic and hydrogeologic framework of part of the coastal plain of Texas. *Texas Dpt Water Res Rep* 236, 43 p
- Bargar JR, Bernier-Latman R, Glammar DE, Tebo BM (2008) Biogenic uraninite nanoparticles and their importance for uranium remediation. *Elements*, v 4, no. 6, pp 407-412
- Barrington J, Kerr PF (1961) Uranium mineralization at the Midnite mine, Spokane, Washington. *Econ Geol*, v 56, pp 241-258
- Barrington J, Kerr PF (1963) Collapse features and silica plugs near Cameron, Arizona. *Geol Soc Am Bull*, v 74, pp 1237-1258
- Bastin ES, Hill JM (1917) Economic geology of Gilpin County and adjacent part of Clear Creek and Boulder Counties, Colorado. *US Geol Surv Prof Paper* 94, 379 p
- Beahm D (2006a) Red Rim project, Sweetwater County, Wyoming, USA. Mineral resource report 43-101, prepared for Energy Metals Corporation. BRS Inc. 46 p (June 14, 2006)
- Beahm D (2006b) Moore Ranch uranium project, Campbell County, Wyoming, USA. Mineral resource report 43-101, prepared for Energy Metals Corporation. BRS Inc. 41 p (June 27, 2006)
- Beahm D (2006c) Peterson uranium project, Converse County, Wyoming, USA. Mineral resource report 43-101, prepared for Energy Metals Corporation. BRS Inc. 46 p (June 27, 2006)
- Beahm D (2006d) JAB uranium project, Sweetwater County, Wyoming, USA. Mineral resource report 43-101, prepared for Energy Metals Corporation. BRS Inc. 46 p (July 14, 2006)
- Beahm D (2007) The Antelope uranium project - a comparison of ISR and heap leach extraction. SME Annual Meeting, Denver, Colorado, Feb 2007, 5 p
- Beahm D, Anderson A (2007) Nichols Ranch uranium project, Campbell & Johnson Counties, Wyoming USA. Mineral resource report 43-101, prepared for Uranerz Energy Corp, BRS Inc. 44 p (April 3, 2007, update Sept. 13, 2007)
- Beahm D, Hutson HJ (2007) Velvet Mine uranium project San Juan County, Utah, USA. Mineral resource report 43-101, prepared for Energy Metals Corporation. BRS Inc. 39 p (March 19, 2007)
- Beck RG, Cherrywell CH, Earnest DF, Feirn WC (1980). Jackpile-Paguat deposit - A review. *in: Rautman A, compiler, Geology and mineral technology of the Grants uranium region 1979. New Mex Bur Mines Miner Res Mem* 38, pp 269-275.
- Becraft GE (1956) Uranium deposits of the northern part of the Boulder batholith, Montana. *Econ Geol*, v 51, no 4, pp 362-374
- Becraft GE (1958) Uranium in carbonaceous rocks in the Townshend and Helena Valleys, Montana. *US Geol Surv Bull* 1046-G, pp 149-164
- Becraft GE, Weis PL (1963) Geology and mineral deposits of the Turtle Lake quadrangle, Washington. *US Geol Surv Bull* 1131, 73p
- Bell H, Bales WE (1954) Uranium deposits in Fall River County, South Dakota, Part II. *US Geol Surv, Trace Elements Investigations*, no. 297, 18 p
- Bell H, Bales WE (1955) Uranium deposits in Fall River County, South Dakota. *US Geol Surv, Bull* 1009-G, pp 211-233
- Bell KG (1963) Uranium in carbonate rocks. *US Geol Surv Prof Paper* 474-A, 29 p
- Bell RT (1978) Uranium in black shales: a review. *in: Kimberley MM, ed., Short course in uranium deposits: their mineralogy and origin. Miner Ass Can, Short Course Handbook no. 3*, pp 207-329
- Bell TE (1986) Deposition and diagenesis in the Brushy Basin Member and upper part of the Westwater Canyon Member of the Morrison Formation, San Juan basin, New Mexico. *in: Turner-Peterson CE, Santos, ES, Fishman NS, (eds.), A basin analysis case study the Morrison Formation, Grants Uranium Region, New Mexico. Amer Ass Petrol Geol, Studies in Geology*, no. 22, pp 77-91
- Bergendahl MH, Davis RE, Izett GA (1961) Geology and mineral deposits of the Carlike quadrangle, Crook County, Wyoming: *US Geol Surv Bull* 1082-J, pp 613-706
- Berggren WA, Van Couvering JA (1974) The late Neogene: Biostratigraphy, geochronology and paleoclimatology of the last 15 million years in marine and continental sequences. *Palaeogeography, Palaeoclimatology, Palaeoecology*, v 16, no. 1/2, 216 p
- Bergin MJ (1957) Maybell-Lay area. *in: Geologic investigations of radioactive deposits - semiannual progress report for Dec 1, 1956 to May 31, 1957. US Geol Surv, TEI-690*, pp 280-291
- Bergin MJ (1959) Preliminary geologic map of the Maybell-Lay area, Moffat County, Colorado. *US Geol Surv Open-File Map, scale 1:48,000*
- Berglof WR (1969) Absolute age relationships in selected Colorado Plateau uranium ores. PhD diss, Columbia Univ (unpubl)
- Berglof WR (1992) Isotopic ages of uranium deposits in the Todilto Limestone, Grants district, and their relationship to the ages of other Colorado Plateau deposits. *in: Guidebook 43, New Mex Geol Soc*, pp 351-358
- Berglof WR, McLemore VT (2003) Economic geology of the Todilto Formation. *in: Guidebook XXXX, 54th Field Conf, New Mex Geol Soc*, pp 177-187
- Berglof WR, Wampler JM (1965) Isotopic study of uraninite from the Todilto Limestone; Grants, New Mexico. *Amer Geophys Union Transcript*, v 46, no. 1, p 164
- Beroni EP, Bauer HL Jr (1952) Reconnaissance for uniferous lignites in North Dakota, South Dakota, Montana, and Wyoming. *US AEC, Tech Info Service Ext, TEI-123*, 93 p and *US Geol Surv, Trace Elements Investigations*, no. 123, 93 p
- Berry MR, Castor SB, Robins JW (1982) National uranium resource evaluation, Jordan Valley Quadrangle, Oregon and Idaho. *US DOE, Open-File Rep. PGJ/F-132 (82)*, 33 p
- Berthoud EL (1875) On the occurrence of uranium, silver, iron, etc., in the Tertiary formation of Colorado Territory. *Proc Scad Natur Sci, Philadelphia*, 27
- Bikun JV (1980) Fluorine and lithophile element mineralization at Spor Mountain, Utah. *US DOE, GJBX-225(80)* pp 167-376
- Billingsley GH (1978) A synopsis of stratigraphy in the Western Grand Canyon. *Museum Northern Arizona, Res Paper* 16, 26 p
- Billingsley GH (1978) Mining in the Grand Canyon. *in: Breed WJ, Roat E, eds., Geology of the Grand Canyon (3rd ed.) Museum North Ariz and Grand Canyon Nat Hist Ass*, pp 170-179
- Billingsley GH (1986) Relations of the Surprise Canyon and Watahomigi Formations to breccia pipes in the Grand Canyon, Arizona. *Geol Soc Amer, abstr w progr*, v 18, no. 5, p 342
- Billingsley GH, Wenrich KJ, Huntoon PW (1986) Breccia pipe and geologic map of the southeastern Hualapai Indian Reservation and vicinity, Arizona. *US Geol Surv Open-File Rep* 86-458B, 26 p, 2 plts
- Bird AG (1958) The petrology and ore deposits of the Schwartzwalder uranium mine, Jefferson County, Colorado. *MSc thesis, Univ Colorado, Boulder*, (unpubl)
- Bird AG (1979) An epigenetic model for the formation of the Schwartzwalder uranium deposit - a discussion. *Econ Geol*, v 74, pp 947-948
- Birdseye HS (1957) The relation of the Ambrosia Lake uranium deposits to a pre-existing oil pool. *in: Geology of southwestern San Juan basin. Second Field Conf, Four Corners Geol Soc*, pp 26-29
- Birkholz DO (1978) Uranium deposits in volcanoclastic rocks near Mountain City, Nevada. *in: Ann Conv, Amer Ass Petrol Geol-SEPM*, pp 47-48
- Blake BJ (1988) Geochemistry of the epigenetic uranium-bearing Cretaceous Lakota Formation, southern Black Hill, South Dakota. *MS thesis, South Dakota Sch Mines Tech, Rapid City, South Dakota*
- Boberg B (1979) Applied exploration geology and uranium resources of the Great Divide Basin, Wyoming (abstr.). *Amer Ass Petrol Geol Bull*, v 63, no.5, pp 822-823
- Boberg B (1981) Some speculations on the development of central Wyoming as a uranium province. *in: Energy resources of Wyoming. 32nd Annual Field Conf Guidebook, Wyoming Geol Ass*, pp 161-180
- Boberg B (2005) Uranium geology of the Great Divide Basin, Wyoming. *Ur-Energy USA, Colorado*, 41 p (presentation at SME Central Wyoming Sect, Global Uran Symp; Casper, Wyoming; July 2005)

- Boberg B (2007) The Great Divide Basin, Wyoming and new uranium mine developments. Global Uran Symp, Corpus Christi, Texas (May 2007), 23 p
- Boenig CM (1970) Deltaic and coastal interdeltic environments of the Carrizo Formation (Eocene), Milam County, Texas. MSc thesis, Texas A&M Univ, 104 p
- Bohn RT (1977) A subsurface correlation of Permian-Triassic strata in Lisbon Valley, Utah. Brigham Young Univ Geol Studies, v 24, part 2, pp 103-116
- Bomber BJ, Ledger EB, Tieh TT (1980) Textural study of a sedimentary uranium deposit in south Texas. *in*: Ann Meet, Geol Soc Amer Atlanta, Georgia, abstr w progr, p 389
- Bomber BJ, Ledger EB, Tieh TT (1986) Ore petrography of a sedimentary uranium deposit, Live Oak Count Texas. *Econ Geol*, v 81, pp 131-142
- Bonner JA, Herold CE, Nibbelink KA (1982) Uranium in the marginal marine depositional system. Ann Meet, AIME Dallas, Texas, manuscr, 9 p
- Botinelly T, Weeks AD (1957) Mineralogic classification of uranium-vanadium deposits of the Colorado Plateau. US Geol Surv Bull 1074-A, pp 1-5
- Bourdon B, Henderson GM, Lundstrom CC, Turner SP, eds. (2003) Uranium series geochemistry. Miner Soc Amer, Washington, DC, Reviews Miner Geochem, v 52, 656 p
- Boutwell JM (1905) Vanadium and uranium in southeastern Utah. US Geol Surv Bull 260
- Bowers HE, Shawe DR (1961) Heavy minerals as guides to uranium-vanadium ore deposits in the Slick Rock district, Colorado. US Geol Surv Bull 11, pp 169-218
- Bowles CG (1965) Uranium-bearing pipe formed by solution and collapse of limestone. US Geol Surv Paper 525-A, pp 25-27
- Bowles CG (1977) Economic implications of a hypothesis of origin of uranium- and copper-bearing breccia pipes, Grand Canyon, Arizona. *in*: Campbell J, ed., Short papers of the US Geol Surv uranium and thorium symposium. US Geol Surv Circ 753, pp 25-27
- Bowman A, Livingston Jr (1980) Geology and development of Marquez, New Mexico, uranium deposit. *in*: Rautman CA, ed., Geology and mineral technology of the Grants uranium region 1979. New Mex Bur Mines Miner Res Mem 38, pp 252-261
- Bowman EC, Cygan NE, Alief MH (1981) Exploration of the Panna Maria uranium mine, Karnes County, Texas, USA. *in*: Uranium exploration case histories. IAEA, Vienna, pp 311-327
- Boyden T (1978) Uranium occurrences in breccia pipes. NUEXCO, Rep 123, pp 2.0-2.2
- Boyer WH (1956) Geologic reconnaissance of the northwest White River. US AEC, RME-90, 46 p
- Bramlett LB, Reyher SL, Southard GG (1980) Uranium geology and geochemistry, Copper Mountain, Wyoming. Preprint 80-102, paper presented at Ann Meet, Soc Mining Eng AIME, Las Vegas
- Breckenridge RM, Glass GB, Root FK, Wendell WG (1974) Campbell County, Wyoming: Geologic map atlas and summary of land, water, and mineral resources. County Resource Ser (CRS-) 3, Wyoming State Geol Surv
- Breed WJ, Roat EC, eds. (1976) Geology of the Grand Canyon. Museum Northern Arizona, 186 p
- Breger IA (1974) The role of organic matter in the accumulation of uranium: The organic geochemistry of the coal-uranium association. *in*: Formation of uranium ore deposits. IAEA, Vienna, pp 99-124
- Breger IA, Deul M (1955) The association of uranium with carbonaceous materials on the Colorado Plateau. US Geol Surv Prof Paper 320, pp 139-150.
- Breit GN, Goldhaber M (1983) Relationship of authigenic minerals to the V-U and Cu mineralization of the Salt Wash Member of the Morrison Formation, San Miguel County, Colorado. Geol Soc Amer, Rocky Mtns Cordilleran Sect, abstr w progr, p 399
- Breit GN, Goldhaber MB (1989) Hematite-cemented sandstones and chromium-rich clays - clues to the origin of vanadium-uranium deposits in the Morrison Formation, southwest Colorado and southeast Utah, United States. *in*: Uranium resources and geology of North America. TECDOC-500, IAEA, Vienna, pp 201-225
- Brewton JL (1970) Heavy mineral distribution in the Carrizo Formation (Eocene), east Texas. PhD diss, Univ Texas, Austin, 167 p
- Brimhall WH, Adams JAS (1969) Concentration changes of thorium, uranium and other metals in hydrothermally altered Conway Granite, New Hampshire. *Geochim Cosmochim Acta*, v 33, pp 1308-1311
- Briot P (1983) Géologie et géochimie des gisements d'uranium liés aux milieux pré-évaporitiques intracontinentaux: les calcrètes uranifères. Thèse d'État, Univ Paris, France, 216 p
- Brobst DA (1961) Geology of the Dewey quadrangle, Wyoming-South Dakota. US Geol Surv, Bull 1063-B, pp 13-60
- Bromfield CS, Grauch RI, Otton JK, Osmonson LM (1982) National uranium resource evaluation of the Richfield quadrangle, Utah. US DOE, PGJ/F-044(82), 94 p, 13 plts
- Brookins DG (1975a) Coffinite-uraninite stability relations in Grants Mineral Belt, New Mexico (abstr). *Amer Ass Petrol Geol Bull*, v 59, no. 5, p 905
- Brookins DG (1975b) Uranium deposits of the Grants, New Mexico mineral belt. US DOE, GJBX-16(76), 153 p
- Brookins DG (1976) Position of uraninite and/or coffinite accumulations to the hematite-pyrite interface in sandstone-type deposits. *Econ Geol*, v 71, pp 944-948
- Brookins DG (1979) Uranium deposits of the Grants, New Mexico mineral belt (II). US DOE, GJBX-141(79), 411 p
- Brookins DG (1980a) Geochemical and clay mineralogical studies, Grants mineral belt (abstr), *in*: Rautman CA, ed., Geology and mineral technology of the Grants Uranium Region 1979. New Mex Bur Mines Miner Res Mem 38, p 396
- Brookins DG (1980b) Geochronologic studies in the Grants Mineral Belt. *in*: Rautman CA, ed., Geology and mineral technology of the Grants Uranium Region 1979. New Mex Bur Mines Miner Res Mem. 38, pp 52-58
- Brookins DG (1981a) Primary uranophane from Ambrosia Lake district, Grants mineral belt, USA. *Mineral Deposita*, v 16, pp 3-5
- Brookins DG (1981b) U-Pb Ages for U(VI) hydrosilicates, Grants, New Mexico. *Isotopes West*, no. 32, p 25
- Brookins DG, Lee MJ, Riese WC (1977) Trace elements as possible prospecting tools for uranium in the southern San Juan Basin. *in*: Guidebook, 28th Field Conf, San Juan Basin III, New Mex Geol Soc, pp 263-269
- Brooks RA, Campbell JA (1976) Preliminary investigation of the elemental variation and diagenesis of a tabular uranium deposit, La Sal mine, San Juan County, Utah. US Geol Surv Rep 76-287, 30 p
- Brooks RA, Perry RV, Rackley RI (1978) New model for some Colorado Plateau uranium deposits (abstr). *Amer Ass Petrol Geol Bull*, v 62, no. 6, pp 1091-1092
- Brophy GP, Kerr PF (1951) Hydrous uranium molybdate in Marysville ore. Ann Rep June 30, 1952 to April 1, 1953, US AEC, RME-3046, 45-51
- Brown A (1961) Geologic investigations of radioactive deposits 1942-1960: a bibliography of U.S. Geological Survey Publications on the geology of radioactive deposits. US Geol Surv Rep TEI-777, 69 p
- Brown NA, Mead RH, McMurray JM (1992) Relationship between collapse history and ore distribution in the Sage breccia pipe, northwestern Arizona. *in*: Short Papers US Geol Surv Uran Workshop 1990. US Govt Print Office, pp 54-56
- Bryant B, McGrew LW, Wobus RA (1981) Geologic map of the Denver 1° × 2° quadrangle, north Colorado. US Geol Surv Map I-1163
- Bryant B, Naeser CW (1980) The significance of fission-track ages of apatite in relation to the tectonic history of the Front and Sawatch Ranges, Colorado. *Geol Soc Amer Bull*, v 91, pp 156-164
- Bryant B, Reed JC Jr (1966) Mineral resources of the Grandfather Mountain Window and vicinity, North Carolina. US Geol Surv Circ 521, 13 p
- Bunker CM, MacKallor JA (1973) Geology of the oxidized uranium ore deposits of the Tordilla Hill-Deweeseville area, Karnes County, Texas; a study of a district before mining. US Geol Surv Prof Paper 765, 37 p
- Burgess JW, Alieff MH, Winsor DK, Lewis LE (1987) Mount Taylor uranium project. manuscr, 18 p (unpubl)
- Burns PC, Finch R, eds. (1999) Uranium mineralogy, geochemistry and the environment. *Mineral Soc Amer, Reviews Miner*, v 38, 679 p
- Burt DM, Sheridan MF, eds. (1980) Uranium mineralization in fluorine-enriched volcanic rocks. US DOE, GJBX-225(80), 494 p
- Burt DM, Sheridan MF (1981) A model for the formation of uranium/lithophile element deposits in fluorine-enriched volcanic rocks. *in*: Goodell PC, Waters AC, eds., Uranium in volcanic and volcanoclastic rocks. *Amer Ass Petrol Geol, Studies in Geology*, no. 13, pp 99-109
- Burt DM, Sheridan MF (1985) Relation of topaz rhyolite volcanism to uranium mineralization in the western United States of America. *in*: Uranium deposits in volcanic rocks. IAEA, Vienna, pp 337-344

- Burwell B (1920) Carnotite mining in southwestern Colorado. *Eng Min J*, v 110, no. 16, pp 755-758
- Busche FD, Goldhaber MB, Reynolds RL (1981) Fault leaked H₂S and the origin of south Texas uranium deposits: Implications of sulfur isotopic studies (abstr). *Geol Soc Amer, abstr w progr*, v 13, p 234
- Butler AP Jr (1956) Distribution of uranium in igneous complexes White Mountain plutonic series, New Hampshire. *US Geol Surv Rep TEI-640*, pp 297-300
- Butler AP Jr (compiled by Byers VP) (1975) Uranium and thorium in samples of rocks of the White Mountain plutonic series, New Hampshire, and whole rock chemical and spectrographic analyses of selected samples. *US Geol Surv Open-File Rep 75-59*, 17 p
- Butler AP Jr, Finch WI, Twenhofel WS (1962) Epigenetic uranium deposits in the United States, exclusive of Alaska and Hawaii. *US Geol Surv Min Invest Res Map, MR-21*
- Butler AP Jr, Fischer RP (1978) Uranium and vanadium resources in the Moab 1° × 2° Quadrangle, Utah and Colorado. *US Geol Surv Prof Paper 988-B*, pp B1-B22
- Butler AP Jr, Schnabel RW (1956) Distribution and general features of uranium occurrences in the United States. *US Geol Surv Prof Paper 300*, pp 27-40
- Butler AP Jr, Stansfield RG (1968) Uranium mineral resources of the Appalachian region. *US Geol Surv Prof Paper 580*, pp 443-449
- Butler BS, Loughlin GF, Heikes VC (1920) The ore deposits of Utah. *US Geol Surv Prof Paper 111*, 672 p
- Button A, Adams SS (1981) Geology and recognition criteria for uranium deposits of the quartz-pebble conglomerate type. *US DOE, GJBX-3(81)*, 390 p
- Byers VP (1978) Principal uranium deposits of the world. *US Geol Surv Rep 78-1008*, 308 p
- Byers VP, Finch WI (1979) Preliminary map of the uranium provinces in the conterminous United States. *US Geol Surv Rep 79-756-V*
- belt, Garfield County Utah. MS thesis, Colo Sch Mines, Golden, 156 p (unpubl)
- Carpenter RH, Gallagher JRL, Huber GG (1979) Modes of uranium occurrences in Colorado Front Range. *Colo Sch Mines Quart*, v 74, no. 3, 76 p
- Carter WD, Gualtieri JL (1965) Geology and uranium-vanadium deposits of the La Sal quadrangle, San Juan County, Utah and Montrose County, Colorado. *US Geol Surv Prof Paper 508*, 82 p
- Castor SB, Berry MR (1981) Geology of the Lakeview uranium district, Oregon. *in: Goodell PC, Waters AC, eds., Uranium in volcanic and volcanoclastic rocks. Amer Ass Petrol Geol, Studies in Geology*, no. 13, pp 55-62
- Castor SB, Mitchell TP, Quade JG (1982) National uranium resource evaluation, Vya Quadrangle, Nevada, Oregon, and California. *US DOE, Open-File Rep. PGJ/F-135 (82)*, 25 p
- Catchpole G, Kirchner G (1993) The Crow Butte ISL project - A case history. *in: Uranium in situ leaching. TECDOC-720, IAEA, Vienna*, pp 81-94
- Cathcart JB (1956) Distribution and occurrence of uranium in the calcium phosphate zone of the Land-pebble District of Florida. *US Geol Surv Prof Paper 300*, pp 489-494.
- Cathcart JB (1978) Uranium in phosphate rock. *US Geol Surv Prof Paper 988-A*, 6 pp
- Cathcart JB (1990) Uranium in phosphate rock - with special reference to the Central Florida deposits. *in: Short papers of the US Geol Surv uranium workshop*, pp 32-35
- Cathelineau M, Cuney M, Leroy J, Lhote F, Nguyen Trung C, Pagel M, Poty B (1982) Caractères minéralogiques des pechblendes de la province hercynienne d'Europe - Comparaison avec les oxydes d'uranium du protérozoïque de différents gisements d'Amérique du Nord, d'Afrique et d'Australie. *in: Vein-type and similar uranium deposits in rocks younger than Proterozoic. IAEA, Vienna*, pp 159-177
- Chapin CE (1965) Geologic and petrologic features of the Thirtynine Mile volcanic field, central Colorado. DSc thesis, Colo Sch Mines, Golden, 176 p
- Chapin CE, Cather SM (1981) Eocene tectonics and sedimentation in the Colorado Plateau-Rocky Mountain area. *in: Dickinson WR, Payne WD, eds., Relations of tectonics to ore deposits in the southern Cordillera. Arizona Geol Soc Digest*, v 14, pp 173-198
- Chapin CE, Harlan HM, Bondurant KT, Mignogna CD, Miozzi EJ, Wolfe SW, Colville PA, Stallman GK, Ausburn KE (1982) The Hansen uranium orebody, Tallahassee Creek district, Fremont County, Colorado. *in: The genesis of Rocky Mountain ore deposits: changes with time and tectonics. Denver Region Explor Geol Soc Symp*, pp 117-123
- Chapman, Wood, Griswold, Inc. (1979) Geologic map of the Grants Uranium Region. *New Mex Bur Mines Miner Res, Geol Map 31*, revised, 3 sheets, text on sheet no. 3
- Chemillac R (2004) Géochimie des magmas associés aux gisements d'uranium intravolcaniques. PhD thesis, Nancy Université, 383 p
- Cheney ES, Jensen ML (1966) Stable isotopic geology of the Gas Hills, Wyoming, uranium district. *Econ Geol*, v 61, pp 44-71
- Cheney ES, Trammell JW (1973) Isotopic evidence of inorganic precipitation of uranium roll ore bodies. *Amer Ass Petrol Geol Bull*, v 57, no. 7, pp 1297-1304
- Chenoweth WL (1953) The variegated member of the Morrison Formation in the southeastern part of the San Juan Basin, Valencia County, New Mexico. MS thesis, 86 p
- Chenoweth WL (1967) The uranium deposits of the Lukachukai Mountains, Arizona. *in: 18th Field Conf, Defiance-Zuni-Mt. Taylor region, Arizona and New Mexico, Guidebook. New Mex Geol Soc*, pp 78-85
- Chenoweth WL (1975) Uranium deposits of the Canyonlands area. *in: 8th Field Conf Guidebook, Four Corners Geol Soc*, pp 253-260
- Chenoweth WL (1977) Uranium in the San Juan Basin - an overview. *in: 28th Field Conf, San Juan Basin III, New Mex Geol Soc Guidebook*, pp 257-262
- Chenoweth WL (1978) Uranium in western Colorado. *Mountain Geologist*, v 15, no. 3, pp 89-96
- Chenoweth WL (1980a) Uranium-vanadium deposits of the Henry Mountains, Utah. *in: Henry Mountains Symposium. Utah Geol Ass*, pp 299-304
- Chenoweth WL (1980b) Uranium. *in: Kent HC, Porter KW, eds., Colorado geology. 1980 Symp, Rocky Mtn Ass Geol*, pp 217-224
- Chenoweth WL (1981) The uranium-vanadium deposits of the Uravan Mineral Belt and adjacent areas, Colorado and Utah. *in: Epis RC, Callender JF, eds.,*
- Cadigan RA (1963) Tuffaceous sandstone in the Triassic Chinle Formation, Colorado Plateau. *US Geol Surv Prof Paper 475-B*, B48-B51
- Cadigan RA (1967) Petrology of the Morrison Formation in the Colorado Plateau region. *US Geol Surv Prof Paper 556*, 113 p
- Callaghan E (1939) Volcanic sequence in the Marysvale region in southwest-central Utah. *Trans Amer Geophys Union*, v 20(3), pp 438-452
- Callaghan E (1973) Mineral resource potential of Piute County, Utah and adjoining area. *Utah Geol Min Surv Bull 102*, 135 p
- Callaghan E, Parker RL (1961) Geology of the Monroe Quadrangle, Utah. *US Geol Surv, Geol Quad Map GQ-155*. Scale 1:24,000
- Campbell AR, Banks DA, Phillips BS, Yardley BWD (1995) Geochemistry of Th-U-REE mineralizing magmatic fluids, Capitan Mountain, NM. *Econ Geol*, v 90, pp 1271-1287
- Campbell JA, Steele-Mallory BA (1979) Depositional environments of the uranium-bearing Cutler Formation, Lisbon Valley, Utah. *US Geol Surv Open-File Rep 79-994*, 35 p
- Carlisle D (1980) Possible variations on the calcrete-gypcrete uranium model. *US DOE, GJBX-53(80)*, 38 p
- Carlisle D (1983) Concentration of uranium and vanadium in calcretes and gypcretes. *in: Wilson RCL, ed., Residual deposits: surface related weathering processes and materials. Geol Soc, London*, pp 185-196
- Carlisle D (1984) Surficial uranium occurrences in relation to climate and physical setting. *in: Surficial uranium deposits. TECDOC-322, IAEA, Vienna*, pp 25-35
- Carlisle D, Merifield PM, Orme RR, Kohl MS, Kolker O (1978) The distribution of calcretes and gypcretes in southwestern United States and their uranium favourability based on a study of deposits in Western Australia and South West Africa (Namibia). *US DOE, GJBX-29(78)*, 274 p
- Carlson CA (1957) Operational report on the Maybell-Lay and Baggs areas, Colorado and Wyoming. *US AEC, RMO-1019*, 14 p
- Carothers TA (2007) Technical report for uranium energy corp's Goliad project in situ recovery uranium project, Goliad County, Texas (Oct. 4, 2007)
- Carpenter DJ (1980) Elemental, isotopic and mineralogic distributions within a tabular-type uranium-vanadium deposit, Henry Mountains mineral

C

- 32nd Field Conf, Western Slope Colorado, Guidebook, New Mex Geol Soc, pp 165-170
- Chenoweth WL (1983) Uranium-vanadium deposits on the west flank of the La Sal Mountains, Grand and San Juan Counties, Utah. *in*: 1983 Field Trip, Grand Junction Geol Soc, pp 41-43
- Chenoweth WL (1985a) Historical review of uranium production from the Todilto Limestone, Cibola and McKinley Counties, New Mexico. *New Mex Geol*, v 7, pp 80-83
- Chenoweth WL (1985a) Uranium geology and production history of the Sanostee area, San Juan County, New Mexico. *New Mex Bur Mines Miner Res, Open-File Rep* 223, 37 p
- Chenoweth WL (1985b) Raw materials activities of the Manhattan Project in New Mexico. *New Mex Bur Mines Miner Res, Open-File Rep* OF-241, 12 p
- Chenoweth WL (1986a) The Orphan Lode mine, Grand Canyon, Arizona, a case history of a mineralized, collapse-breccia pipe. *US Geol Surv Rep* 86-510, 126 p
- Chenoweth WL (1986b) Geology and production history of the uranium deposits in the Maybell, Colorado, area. *Rocky Mtn Ass Geol*, pp 289-292
- Chenoweth WL (1988a) Geology and production history of the uranium deposits in the northern Black Hills, Wyoming - South Dakota. *in*: Guidebook, Thirtieth Field Conf, Wyoming Geol Ass, pp 263-270
- Chenoweth WL (1988b) Uranium procurement and geologic investigations of the Manhattan Project in Arizona. *Arizona Bur Geol Miner Tech, Open-File Rep* 88-2, 23 p
- Chenoweth WL (1989a) Geology and production history of uranium deposits in the Dakota Sandstone, McKinley County, New Mexico. *New Mex Geol*, v 11, pp 21-29
- Chenoweth WL (1993) The geology, leasing and production history of the King Tutt Point uranium-vanadium mines, San Juan County, New Mexico. *New Mex Bur Mines Miner Res, Open-File Rep* OF-394, 21 p
- Chenoweth WL (1997) A summary of uranium-vanadium mining in the Carrizo Mountains, Arizona and New Mexico, 1920-1967. *in*: Guidebook 48, *New Mex Geol Soc*, pp 267-268
- Chenoweth WL, Holen HK (1980) Exploration in the Grants Uranium Region since Memoir 15. *in*: Rautman CA, ed., *Geology and mineral technology of the Grants uranium region 1979*. *New Mex Bur Mines Miner Res Mem* 38, pp 17-21
- Chenoweth WL, Learned EA (1984) Historical review of uranium-vanadium production in the eastern Carrizo Mountains, San Juan County, New Mexico, and Apache County, Arizona. *New Mex Bur Mines Miner Res, Open-File Rep* 193, 22 p
- Chenoweth WL, Learned EA (1985) Historical review of uranium-vanadium production in the northern and western Carrizo Mountains, Apache County, Arizona. *Arizona Bur Geol Mineral Tech, Open-File Rep* 85-13, 35 p
- Chenoweth WL, Magleby DN (1971) Mine location map, Cameron uranium area, Coconino County, Arizona. *US AEC, Prelim Map* 20
- Chenoweth WL, Malan RC (1969) Significant geologic types of uranium deposits - United States and Canada. *Remarks at US AEC Uranium Workshop, Grand Junction, Colorado, Paper* 5, 50 p
- Chenoweth WL, Malan RC (1973) Uranium deposits of northeastern Arizona. *in*: James HL, ed., *Guidebook of Monument Valley and vicinity, Arizona and Utah*. 24th Field Conf, *New Mex Geol Soc*, pp 139-149
- Chenoweth WL, Sharp BJ (1970) Uranium deposits of the Hulett Creek area and the TL Creek quadrangle, Crook County, Wyoming. *US AEC, RME-170*, 73 p
- Chenoweth WL, Stehle FT (1957) Reconnaissance for uranium in parts of the San Juan Basin, New Mexico and Colorado, USA. *US AEC, TM-114*, 19 p
- Childers MO (1970) Uranium geology of the Kaycee area, Johnson County, Wyoming. *in*: 22nd Field Conf Guidebook, Wyoming Geol Ass, pp 13-20
- Childers MO (1974) Uranium occurrences in Upper Cretaceous and Tertiary strata of Wyoming and northern Colorado. *Mountain Geologist*, v 11, no. 4, pp 131-147
- Christiansen EH (1980) Uranium mineralization associated with fluorine-rich rhyolites in southwestern Utah. *US DOE, GJBX-225(80)*, pp 415-458
- Clark DS (1980) Uranium ore rolls in the Westwater Canyon sandstone, San Juan Basin, New Mexico. *in*: Rautman, CA, ed., *Geology and mineral technology of the Grants Uranium Region 1979*. *New Mex Bur Mines Miner Res Mem* 38, pp 195-201
- Clark DS, Havenstrite SR (1963) Geology and ore deposits of the Cliffside Mine, Ambrosia Lake area. *in*: Kelley VC, ed., *Geology and technology of the Grants Uranium Region*. *New Mex Bur Mines Miner Res Mem* 15, pp 108-116
- Clark EL, Million I (1956) Uranium deposits in the Morrison Formation of the San Rafael River district. *in*: *Geology and economic deposits of east central Utah*. *in*: 7th Ann Field Conf, IAPG, pp 155-160
- Clary TA, Mobley CM, Moulton GF Jr (1963) Geologic setting of an anomalous ore deposit in the Section 30 Mine, Ambrosia Lake area. *in*: Kelley VC, ed., *Geology and technology of the Grants Uranium Region*. *New Mex Bur Mines Miner Res Mem* 15, pp 72-79
- Cleaveland P (1816) *An elementary treatise on mineralogy and geology*. Boston
- Clement R Jr, Bonner J (2007) The Black Hills uplift - New life for an old district. *Global Uran Symp, Corpus Christi, Texas, May 2007*, 27 p
- Clinton NJ (1956) Uranium reconnaissance of the Black Mountain-Yale Point area, Black Mesa, Navajo Indian Reservation, Arizona. *US AEC, RME-91*, 24 p
- Coffin RC (1921) Radium, uranium, and vanadium deposits of southwestern Colorado. *Colo Geol Surv Bull* 16, 231 p
- Cohenour RE (1960) Geology and uranium occurrences near Lakeview, Oregon. *US AEC, RME-2070*, 33 p
- Cohenour RE (1963) Beryllium and associated mineralization in the Sheepprock Mountains. *in*: Sharp BJ, Williams NC, eds., *Beryllium and uranium mineralization in western Juab County, Utah*. *in*: Guidebook 17, *Utah Geol Soc*, pp 8-13
- Collings SP, Catchpole G, Kirchner G (1996) The Crow Butte ISL project: A case history. *in*: *Innovations in uranium exploration, mining and processing techniques, and new exploration target areas*. *TECDOC-868, IAEA, Vienna*, pp 89-118
- Collings SP, Knode RH (1984) Geology and discovery of the Crow Butte uranium deposit, Dawes County, Nebraska. *in*: *Practical Hydromet '83, 7th Ann Symp Uran and Precious Metals*. *Amer Inst Metall Eng*, pp 5-14
- Collins J, Talbot S (2007) Alta Mesa project: a textbook example of a south Texas uranium deposit. *Global Uran Symp, Corpus Christi, Texas, May 2007* 15 p
- Collot B (1981) Le granite albitique hyperalcalin de Bokan Mountain (SE Alaska) et ses minéralisations U-Th. Sa place dans la Cordillère Canadienne. 3^o cycle thesis, USTL, Montpellier, 238 p
- Conant LC, Swanson VE (1952) Uranium content of Chattanooga Shale in east-central Tennessee and southern Kentucky. *US Geol Surv Rep* TEI-224, 87 p
- Conant LC, Swanson VE (1961) Chattanooga Shale and related rocks of central Tennessee and nearby areas: *US Geol Surv Prof Paper* 357, 91 p
- Condie KC, Leach AP, Baadsgaard H (1969) Potassium-argon ages of Precambrian mafic dikes in Wyoming. *Geol Soc Amer Bull*, v 80, pp 899-906
- Condon SM, Peterson F (1986) Stratigraphy of Middle and Upper Jurassic rocks of the San Juan basin: Historical perspective, current ideas, and remaining problems. *in*: Turner-Peterson CE, Santos ES, Fishman NS, eds., *A basin analysis case study - the Morrison Formation, Grants Uranium Region, New Mexico*. *Amer Ass Petrol Geol, Studies in Geology*, no. 22, pp 7-26
- Conley JF, Henika WS (1973) Field trip across the Blue Ridge anticlinorium, Smith River allochthon and Sauratown Mountains anticlinorium near Martinsville, Virginia. *Virginia Minerals*, v 19, no. 4, 37 p
- Continental Oil Company (1978) Borrego Pass project; mining and reclamation plant. Available from *US Geol Surv Area Mining Supervisor, Albuquerque, New Mex*, 243 p
- Cooper M (1958) Bibliography and index of literature on uranium and thorium and radioactive occurrences in the United States (Pt. 5). *Geol Soc Amer, Spec Paper* 67, 317 p
- Corbett RG (1964) The geology and mineralogy of Section 22 Mine, Ambrosia Lake uranium district, New Mexico. *PhD Diss, Univ Michigan*, 161 p (unpubl)
- Corey AS (1956) Petrographic report on the Martin mine, northwest Carrizo Mountains, Apache County, Arizona. *US AEC, TM-282*, 26 p
- Corey AS (1958) Petrology of the uranium-vanadium ores of the Nelson Point No. I mine, San Juan County, New Mexico. *US AEC, RME-122*, 30 p
- Corey AS (1959) Mineralogy and petrology of the uranium deposits of Cane Springs Canyon, San Juan and Grand counties, Utah. *US AEC, RME-128*
- Cox DP, Singer DA, eds. (1986) *Mineral deposit models*. *US Geol Surv, Bull* 1693, 379 p

- Craig LC, Holmes CN, Cadigan RA, Freeman VL, Mullens TE, Weir GW (1955) Stratigraphy of the Morrison and related formations, Colorado Plateau region - a preliminary report. US Geol Surv Bull 1009-E, pp 125-168
- Craig RM (1980) Geochemical and sedimentologic problems of uranium deposits of Texas Gulf coastal plain: discussion. Amer Ass Petrol Geol Bull, 64, p 583
- Cramer RT, Yellich JA, Kendall RG (1979) Copper Mountain, Wyoming, a uranium district - rediscovered. *in*: 1979 Mining Yearbook. Colo Min Ass, pp 130-137
- Crawley RA (1983) Sandstone uranium deposits in the United States: a review of the history, distribution, genesis, mining areas, and outlook. US DOE, GJBX-15(83), 57 p
- Crawley RA, Holen HK, Chenoweth WL (1985) Geology and application of geologic concepts, Morrison Formation, Grants Uranium Region, New Mexico, USA. *in*: Geological environments of sandstone-type uranium deposits. TECDOC-328, IAEA, Vienna, pp 199-214
- Crew ME (1981) NURE Uranium deposit model studies. *in*: Uranium industry seminar proceedings. US DOE, GJO-108(81)
- Cronk RJ (1963) Geology of the Dysart no. 1 Mine, Ambrosia Lake area. *in*: Kelley VC, ed., Geology and technology of the Grants Uranium Region. New Mex Bur Mines Miner Res Mem 15, pp 60-65
- Cunningham CG, Steven TA (1977) Mount Belknap and Red Hills calderas and associated rocks, Marysvale volcanic field, west-central Utah. US Geol Surv Open-File Rep 77-568, 40 p
- Cunningham CG, Steven TA (1979a) Uranium in the Central Mining Area, Marysvale District, west-central Utah. US Geol Surv Misc Invest Ser Map 1-1177
- Cunningham CG, Steven TA (1979b) Mount Belknap and Red Hills calderas and associated rocks, Marysvale volcanic field, west-central Utah. US Geol Surv Bull 1468, 34 p
- Cunningham CG, Ludwig KR, Naeser CW, Weiland EK, Mehnert HH, Steven TA, Rasmussen JD (1982) Geochronology of hydrothermal uranium deposits and associated igneous rocks in the eastern source area of the Mount Belknap volcanics, Marysvale, Utah. Econ Geol, v 77, 453-463
- Cunningham CG, Rasmussen JD, Steven TA, Rye RO, Rowley PD, Romberger SB, Selverstone J (1998) Hydrothermal uranium deposits containing molybdenum and fluorite in the Marysvale volcanic field, west-central Utah. Mineral Deposita, v 33, pp 477-494
- Cunningham CG, Steven TA, Rasmussen JD (1980) Volcanogenic uranium deposits associated with the Mount Belknap volcanics, Marysvale volcanic field, west-central Utah (abstr). *in*: Energy exploration in the 80's, Annual meeting of the southwest section, Am Assoc Petrol Geol El Paso, Texas, Feb. 25-27, 1980, p 22
- Cunningham CG, Steven TA, Rowley PD, Naeser CW, Mehnert HH, Hedge CE, Ludwig KR (1994) Evolution of volcanic rocks and associated ore deposits in the Marysvale volcanic field, Utah. Econ Geol, v 89, 2003-2005
- Cupp GM, Karp KE (1982) Assessment of intermediate-grade potential uranium resources in part of the McDermitt caldera. US DOE, preliminary rep, 43 p
- Cupp GM, Leedom SH, Mitchell TP, Allen DR (1977) Geology, uranium deposits, and uranium favorability of the Hartford Hill Rhyolite and Truckee Formation, southeastern Washoe County, Nevada, and eastern Lassen County, California. US DOE, GJBX-16(77), 61 p
- Cupp GM, Leedom SH, Mitchell TP, Kiloh KD, Horton RC (1977) Preliminary study of the favorability for uranium in selected areas in the Basin and Range. US DOE, GJBX-74(77), pp 4-13
- Cuppels NP (1963) Geology of the Clifton quadrangle, Wyoming and South Dakota. US Geol Surv, Bull 1063-H, pp 271-321
- Curry DL (1976) Evaluation of uranium resources in the Powder River Basin, Wyoming. *in*: 28th Field Conf, Guidebook, Wyoming Geol Ass, pp 235-242
- Cyprus Mines Corporation (1980) The Hansen project. *in*: Chenoweth WL ed., Colorado uranium field trip guidebook. Amer Ass Petrol Geol, Denver, Colorado
- Dahl AR, Hagmaier JL (1974) Genesis and characteristics of the southern Powder River Basin uranium deposits, Wyoming. *in*: Formation of uranium ore deposits. IAEA, Vienna, pp 201-216
- Dahl AR, Hagmaier JL (1976) Genesis and characteristics of the southern Powder River Basin uranium deposits, Wyoming. *in*: 28th Field Conf, Guidebook, Wyoming Geol Ass, pp 243-252
- Dahlkamp FJ (1993) Uranium ore deposits. Springer-Verlag, Berlin ff, 460 p
- Dahlkamp FJ (2009) Uranium deposits of the world, Asia. Springer-Verlag, Berlin ff, 493 p
- Dahlkamp FJ (2009) Uranium deposits of the world, Europe. Springer-Verlag, Berlin ff, (in preparation)
- Davidson ES (1967) Geology of the Circle Cliffs area, Garfield and Kane Counties, Utah. US Geol Surv Bull 1229, 140 p
- Davis JF (1969) Uranium deposits in the Powder River Basin, Wyoming. Univ Contrib Geol, v 8, pp 131-147
- Davis JF (1979) Uranium in the U.S.A.: genesis and exploration implications. Phil Transact Roy Soc London, ser A, v 291, pp 301-306
- Davis RE, Izett GA (1962) Geology and uranium deposits of the Strawberry Hill quadrangle, Crook County, Wyoming. US Geol Surv Bull 1127, 87 p
- Dayvault RD (1983) Data release on a portion of Eastern Adel Quadrangle, Oregon. US DOE, Open-File Rep. GJBX-38 (83), 21 p
- Dayvault RD, Castor SB, Berry MR (1985) Uranium associated with volcanic rocks of the McDermitt Caldera, Nevada and Oregon. *in*: Uranium deposits in volcanic rocks. IAEA, Vienna, pp 379-410
- de Saint-André B, Lancelot JR, Collot B (1983) U-Pb geochronology of Bokan Mountain peralkaline granite: tectonic implications. Can J Earth Sci, v 20, no. 2, pp 236-245
- de Saint-André B, Lancelot JR, Collot B (1984) U-Pb isotope systematics and the age of uranium-thorium mineralization at Bokan Mountain, S.E. Alaska. (manusc, 33 p, unpubl)
- De Vivo B, Ippolito F, Capaldi G, Simpson PR, eds. (1984) Uranium geochemistry, mineralogy, exploration and resources. IMM, London, 201 p
- De Voto RH (1978) Uranium geology and exploration: lecture notes and references. Colo Sch Mines, Golden, 396 p
- De Voto RH, Paschis JA (1980) Geology of uranium vein deposits (including Schwartzwalder Mine) in Proterozoic metamorphic rocks, Front Range, Colorado. *in*: Ferguson J, Goleby AB, eds., Uranium in the Pine Creek Geosyncline. IAEA, Vienna, pp 683-692
- De Voto RH, Stevens DM, eds. (1979) Uraniferous phosphate resources and technology and economics of uranium recovery from phosphate resources, United States and the free world. US DOE, GJBX-110, v 1, 686 p, v 2, 606 p
- Dean BG (1960) Selected annotated bibliography of the geology of uranium-bearing veins in the United States. US Geol Surv Bull 1059-G
- Deffeyes K, MacGregor I (1978) Uranium distribution in mined deposits and in the earth's crust, US DOE, GJBX-1 (79) p 508 p
- Degraw HM (1969) Subsurface relations of the Cretaceous and Tertiary in western Nebraska. MS thesis, Univ Nebraska, 137 p
- Denson NM et al. (1959) Uranium in coal in the Western United States. US Geol Surv Bull 1055, 315 p
- Denson NM, Bachman GO, Zeller HD (1959) Uranium-bearing lignite in northwestern South Dakota and adjacent states. *in*: Denson NM et al., eds., Uranium in coal in the Western United States. US Geol Surv Bull 1055-B, pp 11-57
- Denson NM, Chisholm WA (1971) Summary of mineralogic and lithologic characteristics of Tertiary sedimentary rocks in the middle Rocky Mountains and the northern Great Plains. US Geol Surv Prof Paper 750-C, pp C117-C126
- Denson NM, Gill JR (1956) Uranium-bearing lignite and its relation to volcanic tuffs in eastern Montana and North and South Dakota. US Geol Surv Prof Paper 300, pp 413-418
- Denson NM, Gill JR, Chisholm WA (1965) Uranium-bearing lignite and carbonaceous shale in the southwestern part of the Williston Basin - a regional study. US Geol Surv Prof Paper 463, 75 p
- Desborough GA, Sharp WN (1979) Uranium and thorium minerals in Precambrian metaconglomerate, Medicine Bow Mountains, south-central Wyoming. *in*: Houston RS, Karlstrom KE, Graff PJ, eds., Progress report on the study of radioactive quartz-pebble conglomerate of the Medicine Bow Mountains and Sierra Madre, southeastern Wyoming. US Geol Surv Open-File Rep 79-1131, pp 38-39
- Dickinson KA (1976a) Sedimentary depositional environments of uranium and petroleum host rocks of the Jackson Group, south Texas. US Geol Surv J Res, v 4, no. 5, pp 615-629

D

- Dickinson KA (1976b) Uranium potential of the Texas coastal plain. US Geol Surv Open-File Rep 76-879, 7 p
- Dickinson KA (1976c) Geologic controls of uranium deposition, Karnes County, Texas. US Geol Surv Open-File Rep 76-331, 16 p
- Dickinson KA (1981) Geologic controls of uranium mineralization in Tallahassee Creek uranium district, Fremont County, Colorado. *Mt Geol*, v 18, no. 4, pp 88-94
- Dickinson KA (1987) Rocks of the Thirtynine Mile volcanic field as possible sources of uranium for epigenetic deposits in central Colorado. *Uranium*, v 4, no.1, pp 43-65
- Dickinson KA, Cunningham KD, Ager TA (1987) Geology and origin of the Death Valley uranium deposit, Seward Peninsula, Alaska. *Econ Geol*, v 82, pp 1558-1574
- Dickinson KA, Duval JS (1977) Trend areas and exploration techniques. *in*: Campbell MD, ed., *Geology of alternate energy resources in the south-central United States*. Houston Geol Soc, pp 45-66
- Dickinson KA, Hills FA (1982) Oligocene volcanic rocks: possible source of uranium in epigenetic deposits in parts of Chaffee, Park, and Fremont counties, Colorado. US Geol Surv Open-File Rep 82-403, 32 p
- Dickinson KA, Sullivan MW (1976) Geology of the Brysch uranium mine, Karnes County, Texas. US Geol Surv J Res, v 4, no. 4, pp 397-404
- Dickson RK (1982) Uranium mineralization in the Nenana coal field, Alaska. Alaska Dep Nat Resources, Div Geol Geophys Surv Rep 73, pp 37-42
- Dix GP Jr, (1953) Reconnaissance of the uranium deposits of the Lockhart Canyon-Indian Creek area, San Juan County, Utah. US AEC, RME-4038
- Dodge HW Jr, Spencer CW (1977) Uranium deposits in the Fox Hills Sandstone, northeastern Wyoming, and their relationship to depositional environments. *in*: Turner-Peterson CE, ed., *Uranium in sedimentary rocks: Application of the facies concept to exploration*. Soc Econ Paleont Miner, Rocky Mtn Sect, pp 3-20
- DOE-EIA (2002) Uranium industry annual 2001. DOE/EIA-0478, 56 p (URL <http://www.eia.doe.gov>.)
- DOE-EIA (2003) Uranium industry annual 2002. US DOE, Washington, DC
- Doelling HH (1969) Mineral resources, San Juan County, Utah, and adjacent areas, Part II: Uranium and other metals in sedimentary host rocks. *Utah Geol Miner Surv Spec Studies 24(II)*, 64 p
- Dooley JR Jr, Harshman EN, Rosholt JN (1974) Uranium-lead ages of the uranium deposits of the Gas Hills and Shirley Basin, Wyoming. *Econ Geol*, v 69, pp 527-531
- Dooley JR, Granger HC, Rosholt JN (1966) Uranium 234 fractionation in the sandstone-type uranium deposits of the Ambrosia Lake district, New Mexico. *Econ Geol*, v 61, pp 1362-1382
- Dooley JR, Tatsumoto M, Rosholt JN (1964) Radioactive disequilibrium studies of roll features, Shirley Basin. *Econ Geol*, v 59, pp 586-595
- Downs GR, Bird AG (1965) The Schwartzwalder uranium mine, Jefferson County, Colorado. *Mountain Geologist*, v 2, pp 183-191
- Drake AA (1957) Geology of the Wood and East Calhoun mines, Central City district, Gilpin County, Colorado. US Geol Surv Bull 1032-C, pp 129-170
- Drever JI, Murphy JW, Surdam RC (1977) The distribution of As, Be, Cd, Cu, Hg, Mo, Pb, and U associated with the Wyodak Coal Seam, Powder River Basin, Wyoming. *Univ Wyoming Contrib Geol*, v 15, pp 93-101
- Dribus JR, Hurlley BW, Lawton DE, Lee EG (1982) National uranium resource evaluation: Greensboro Quadrangle, North Carolina and Virginia. US DOE, PGJ/F-063(82), 30 p
- Drouillard RF, Jones EE (1955) Geology of the Seven Mile Canyon uranium deposits, Grand County, Utah. US AEC, RME-4066
- Dubiel RF (1983) Sedimentology of the lower part of the Upper Triassic, Chinle Formation and its relationship to uranium deposits, White Canyon area, southeastern Utah. US Geol Surv Open File Rep 83-459, 49 p
- Duex TW (1971) K/Ar dates and U, K geochemistry of the Gueydan (Catahoula) Formation. *in*: Adams JAS, ed., *Final report*. US AEC, Res Contract AT (05-1)-935, pt 7, pp 101-145
- Duex TW, Henry CD (1985) Uranium mobility in late magmatic and hydrothermal processes: Evidence from fluorite deposits, Texas and Mexico. *in*: *Uranium deposits in volcanic rocks*. IAEA, Vienna, pp 365-378
- Dunkhase JA (1980) A comparative study of the whole rock geochemistry of the uranium mineralized Central Intrusive at Marysvale, Utah to nonmineralized intrusives in southwest Utah. PhD diss, Colo Sch Mines, Golden, 130 p (unpubl)
- Dupree JA, Maslyn RM (1979) Paleokarst controls on localization of uranium at Pitch Mine, Sawatch Range, Colorado (abstr). *Amer Ass Petrol Geol Bull*, v 63, p 826

E

- Eargle DH (1968) Nomenclature of formations of the Claiborne Group, Middle Eocene coastal plain of Texas. US Geol Surv Bull 1251-D, 25 p
- Eargle DH (1972) Revised classification and nomenclature of the Jackson Group (Eocene), south-central Texas. *Amer Ass Petrol Geol Bull*, v 56, no. 3, pp 561-566
- Eargle DH, Dickinson KA, Davis BO (1975) South Texas uranium deposits. *Amer Ass Petrol Geol Bull*, v 59, no. 5, pp 766-779
- Eargle DH, Hinds GW, Weeks AMD (1971) Uranium geology and mines, south Texas. *Field Trip Guidebook*, Amer Ass Petrol Geol Conv, Houston, Texas, Houston Geol Soc, 59 p
- Eargle DH, Snider JL (1957) A preliminary report on the stratigraphy of the uranium-bearing rocks of the Karnes County area, south central Texas. Univ Texas, Austin, Bur Econ Geol Rep Invest 30, 30 p
- Eargle DH, Stanford JF Jr, Davis BO (1966) Preliminary Geologic Map of the Live Oak County Area, Texas. US Geol Surv Open File Map
- Eargle DH, Weeks AMD (1961) Possible relation between hydrogen sulfide-bearing hydrocarbons in fault-line oil fields and uranium deposits in the southeast Texas coastal plain. US Geol Surv Prof Paper 424-D, pp 7-9
- Eargle DH, Weeks AMD (1973) Geologic relations among uranium deposits, south Texas coastal plain region, USA. *in*: Amstutz GC, *Union Geol Sci Series A*, no. 3, pp 101-113
- Elevatorski EA (1976) Uranium guidebook for Wyoming. *Minobras*, 63 p, plus appendix 24 p
- Elevatorski EA (1977) Uranium deposits of the northern U.S. Region. *Minobras*, 99 p
- Elevatorski EA (1978a) Uranium guidebook for the Paradox Basin, Utah and Colorado. *Minobras*, 95 p
- Elevatorski EA (1978b) Uranium deposits of Arizona, California, and Nevada. *Minobras*, 105 p
- El-Mahady OR (1966) Origin of ore and alteration in the Freedom No. 2 and adjacent mines at Marysvale, Utah. PhD diss, Univ Utah, Salt Lake City, 217 p (unpubl)
- Elston DP, Botinelly T (1959) Geology and mineralogy of the J.J. Mine, Montrose County, Colorado. US Geol Surv Prof Paper 320, 203-211
- Elston WE, Rhodes RC, Erb EE (1976) Control of mineralization by mid-Tertiary volcanic centers, southwestern New Mexico. *New Mex Geol Soc, Spec Publ 5*, pp 125-130
- Elston WE (1978) Mid-Tertiary cauldrons and their relation to mineral resources: a brief review. *New Mex Geol Soc, Spec Publ 7*, pp 107-113
- Energy, Minerals and Natural Resources Department (2002) New Mexico's natural resources 2002. New Mex Energy, Minerals, Natural Res Dpt, Ann Data and Statistics Rep, 72 p
- Epis RC, Chapin CE (1968) Geologic history of the Thirtynine Mile volcanic field, central Colorado. *in*: Epis RC, ed., *Cenozoic volcanism in the southern Rocky Mountains*. Colo Sch Mines Quarterly, v 63, no. 3, pp 51-85
- Epis RC, Chapin CE (1974) Stratigraphic nomenclature of the Thirtynine Mile volcanic field, central Colorado. US Geol Surv Bull 1395-C, 23 p
- Epis RC, Scott GR, Taylor RB, Chapin CE (1976) Cenozoic volcanic, tectonic, and geomorphic features of central Colorado. *in*: *Studies in Colorado field geology*. Epis RC, Weimer RJ, eds., *Prof Contrib Colorado Sch Mines*, no. 8, pp 323-338
- Epis RC, Wobus RA, Scott GR (1979) Geologic map of the Black Mountain quadrangle, Fremont and Park Counties, Colorado. US Geol Surv Map 1-1195
- Ethridge FG, Ortiz NV, Sunada DK, Tyler N (1980) Laboratory, field and computer flow study of the origin of Colorado Plateau-type uranium deposits. US Geol Surv Rep 80-805, 81 p
- Ethridge FG, Tyler N, Thompson TB (1979) The uranium-bearing Fox Hills and Laramie aquifers, Cheyenne Basin, Colorado: Structure, depositional systems

- and groundwater. Dpt Earth Res, interim rep, Colo State Univ, Fort Collins, Colorado, 40 p
- Everhart DL (1950) Reconnaissance examinations of copper-uranium deposits west of the Colorado River. US AEC RMO-659
- Everhart DL (1956) Uranium-bearing vein deposits in the United States. Proc Intern Conf Peaceful Uses Atomic Energy, v 6, Geology of uranium and thorium. UN, Geneva, pp 257-264
- Everhart DL (1985) Tectonic setting of the world's sandstone-type uranium deposits. *in*: Geological environments of sandstone-type uranium deposits. TECDOC-328, IAEA, Vienna, pp 21-46
- Everhart DL, Wright RJ (1953) The geologic character of typical pitchblende veins. *Econ Geol*, v 48, pp 77-96
- ## F
- Falkowski SK (1980) Geology and ore deposits of the Johnny M Mine, Ambrosia Lake district, New Mexico. *in*: Rautman CA, ed., Geology and mineral technology of the Grants Uranium Region 1979. New Mex Bur Mines Miner Res Mem 38, pp 230-239
- Ferguson J (1987) The distribution of uranium in space and time. *Uranium*, v 3, pp 131-144
- Ferguson J (1988) The uranium cycle. *in*: Recognition of uranium provinces. IAEA, Vienna, pp 3-16
- Ferris CS Jr (1968) Tertiary faults with reversed movements near Copper Mountain, central Wyoming. *Wyo Univ, Dpt Geol Contrib Geol*, v 1, pp 117-128
- FGM Consulting Group, Inc. (2007) Technical report on Energy Fuels Resources Corporation's Whirlwind property, Mesa County, Colorado and Grand County, Utah. Prepared for Energy Fuels Incorporated. FGM Consulting Group, Inc. 31 p (Jan 3, 2007)
- Files FG (1970) Geology and alteration associated with Wyoming uranium deposits. Univ California, Berkeley, PhD diss, 113 p
- Files FG (1978) Uranium in volcanic environments in the Great Basin. US DOE, GJBX-98(78) 20 p
- Finch WI (1959) Geology of uranium deposits in Triassic rocks of the Colorado Plateau region. US Geol Surv Bull 1074-D, 164 p
- Finch WI (1967) Geology of epigenetic uranium deposits in sandstone in the United States. US Geol Surv Prof Paper 538, 121 p
- Finch WI (1975) Uranium in west Texas. US Geol Surv Open-File Rep 75-356, 20 p
- Finch WI, ed. (1985a) Geological environments of sandstone-type uranium deposits. TECDOC-328, IAEA, Vienna, 408 p
- Finch WI (1985b) Sandstone-type uranium deposits - summary and conclusions. *in*: Geological environments of sandstone-type uranium deposits. TECDOC-328, IAEA, Vienna, pp 401-408
- Finch WI (1986) Uranium resources. *in*: Bever MB, ed., Encyclopedia of materials science and engineering. Oxford, England, Pergamon Press, v 7, pp 5218-5221
- Finch WI (1987) A synthesis of genetic models for major types of uranium deposits in the United States (abstr). TCM on uranium resources and geology of North America. IAEA Meeting, Saskatoon, 2 p
- Finch WI (1991) Maps showing the distribution of uranium-deposit clusters in the Colorado Plateau uranium province. US Geol Surv, Misc Field Studies Map MF-2080
- Finch WI (1996) Uranium provinces of North America - Their definition, distribution, and models. US Geol Surv Bull 2141, 18 p, 2 pl
- Finch WI (1997) Uranium, its impact on the National and World energy mix - Its history, distribution, production, nuclear fuel-cycle, and relation to the environment. US Geol Surv Circ 1141, 24 p
- Finch WI (2003) Uranium-fuel for nuclear energy 2002. US Geol Surv Bull 2179-A, 18 p (available on-line at <http://pubs.usgs.gov/bul/b2179-a>)
- Finch WI, Davis JF (1985) Sandstone-type uranium deposits - an introduction. *in*: Geological environments of sandstone-type uranium deposits. TECDOC-328, IAEA, Vienna, pp 11-20
- Finch WI, Granger HC, Lupe RD, McCammon RB (1980) Research on interactive genetic geologic models to evaluate favorability for undiscovered uranium resources. *in*: Uranium evaluation and mining techniques. IAEA, Vienna, pp 447-462
- Finch WI, Hoffman AC Jr, Fassett IE, eds. (1989) Coal, uranium, and oil and gas in Mesozoic rocks of the San Juan Basin: Anatomy of a giant energy-rich basin: 28th Intern Geol Congr, Field Trip Guidebook T120
- Finch WI, McLemore VT (1989) Uranium geology and resources of the San Juan Basin. *in*: Finch WI, Hoffman AC Jr, Fassett IE, eds., Coal, uranium, and oil and gas in Mesozoic rocks of the San Juan Basin: Anatomy of a giant energy-rich basin. *in*: 28th Intern Geol Congr, Field Trip Guidebook T120, p. 27-32
- Finch WI, Molina P, Naumov SS, Ruzicka V, Barthel F, Müller-Kahle E, Tauchid M (1995) World distribution of uranium deposits, First Edition. IAEA, Vienna, map
- Finch R, Murakami T (1999) Systematics and paragenesis of uranium minerals. *in*: Burns PC, Finch RJ, eds., Uranium: mineralogy, geochemistry and the environment. Mineral Soc Amer, Reviews in Mineralogy, v 38, pp 89-179
- Finch WI, Smith LL, Chenoweth WL (2000) Characteristics of uranium deposits USA. 31st Intern Geol Congr, Extended Abstr, Rio de Janeiro, Brazil, 4 p
- Finnell TL, Franks PC, Hubbard HA (1963) Geology, ore deposits, and exploration drilling in the Deer Flats area, White Canyon district, San Juan County, Utah. US Geol Surv Bull 1132
- Fischer RP (1947) Deposits of vanadium-bearing sandstone. *in*: Vanderwilt JW, ed., Mineral resources of Colorado. State Colo Miner Res Board, Denver, pp 451-456
- Fischer RP (1950) Uranium-bearing sandstone deposits of the Colorado Plateau. *Econ Geol*, v 45, pp 1-11
- Fischer RP (1957) Localization and origin of the vanadium-uranium deposits on the Colorado Plateau. US AEC, TEI-690, pp 383-389
- Fischer RP (1959) Vanadium and uranium in rocks and ore deposits. *in*: Garrels RM, Larsen ES, III, Compilers, Geochemistry and mineralogy of the Colorado Plateau uranium ores. US Geol Surv Prof Paper 320, pp 219-230
- Fischer RP (1960) Vanadium-uranium deposits of the Rifle Creek area, Garfield County, Colorado. US Geol Surv Bull 1101, 52 p
- Fischer RP (1968) The uranium and vanadium deposits of the Colorado Plateau region. *in*: Ridge JD, ed., Ore deposits of the United States, 1933-1967 (Graton-Sales vol). Amer Inst Min Met Petrol Eng, v 1, pp 735-746
- Fischer RP (1970) Similarities, differences and some genetic problems of the Wyoming and Colorado Plateau types of uranium deposits in sandstone. *Econ Geol*, v 65, pp 778-784
- Fischer RP (1974) Exploration guides to new uranium districts and belts. *Econ Geol*, v 69, pp 362-376
- Fischer RP, Hilpert LS (1952) Geology of the Uravan mineral belt. US Geol Surv Bull 988-A, pp 1-13
- Fischer RP, Stewart JH (1960) Distribution and lithologic characteristics of sandstone beds that contain deposits of copper, vanadium, and uranium. *in*: Geological Survey research 1960. US Geol Surv Prof Paper 400-B, pp 42-44
- Fischer RP, Stewart JH (1961) Copper, vanadium, and uranium deposits in sandstone - their distribution and geochemical cycles. *Econ Geol*, v 56, pp 509-520
- Fisher JC (1976) Remote sensing applied to exploration for vein-type uranium deposits, Front Range, Colorado. Colo Sch Mines, Remote Sensing Rep 76-2, 157 p
- Fisher WI, Proctor CV Jr, Galloway WE, Nagle JS (1970) Depositional systems in the Jackson Group of Texas - their relationship to oil, gas and uranium. Gulf Coast Ass Geol Soc Trans, v 20, pp 234-261
- Fishman NS (1981) Origin of the Mariano Lake uranium deposit, McKinley County New Mexico. MS thesis, Univ Colorado, 97 p (unpubl)
- Fishman NS, Reynolds RL (1986) Origin of the Mariano Lake uranium deposit, McKinley County, New Mexico. *in*: Turner-Peterson CE, Santos ES, Fishman NS, eds., A basin analysis case study - The Morrison Formation, Grants Uranium Region, New Mexico. Amer Ass Petrol Geol, Studies in Geology, no. 22, pp 21-1226
- Fishman NS, Turner-Peterson CE (1986) Cation scavenging: An alternative to a brine for humic acid precipitation in a tabular uranium ore. *in*: Dean WA, ed., Organics and ore deposits. Proc Denver Region Explor Geol Soc Symp, pp 197-204
- Fishman NS, Turner-Peterson CE, Reynolds RL (1984) Alteration of magnetite and ilmenite in Upper Jurassic Morrison Formation, San Juan basin, New Mexico: Relationship to facies and primary uranium mineralization. Amer Ass Petrol Geol Bull, v 68, p 936

- Fitch DC (1980) Exploration for uranium deposits, Grants mineral belt. *in*: Rautman CA, ed., Geology and mineral technology of the Grants Uranium Region 1979. New Mex Bur Mines Miner Res Mem 38, pp 40-51
- Fitch DC (2005) Technical report on the Strathmore Church Rock uranium property, McKinley County, New Mexico. Prepared for Strathmore Minerals Corp. 59 p (Dec 20, 2005)
- Fitch DC (2006) Technical report on the Roca Honda uranium property, McKinley County, New Mexico. Prepared for Strathmore Minerals Corp. 77 p (March 31, 2006)
- Fleck H, Haldane WG (1907) A study of the uranium and vanadium belts of southern Colorado. Col Bur Mines Twelfth Biennial Rep, 47 p
- Fleshman BR (2005) Lisbon Valley uranium project, Lisbon Valley, San Juan County, Utah, USA. Technical report form 43-101F1 prepared for BZU Minerals Ltd. and Fintry Enterprises Inc. 53 p (filed under Mesa Uranium) (Oct 12, 2005)
- Foehl RL (1999) Silver- and uranium-bearing veins in the Sunshine mine, Coeur d'Alene district, Idaho: A genetic relationship? SEG Newsletter Oct '99, no. 39, p 8
- Foord EE, McKee ED, Bowles CG (1978) Status of mineral resource information for the Shivwits Plateau, Parashant, Andrus, and Whitmore Canyons, and Kanab Canyon areas, Grand Canyon, Arizona. US Geol Surv Admin Rep National Park Serv, 30 p
- Forhan R (1977) Grade control in underground mines Grants mineral belt, New Mexico. *in*: Kim YS, ed., Uranium mining technology. Univ Nevada, Reno, 46 p
- Foster JF, Quintanar RJ (1980) An anomalous ore body within the Ambrosia Lake trend at the Sandstone Mine. *in*: Rautman CA, ed., Geology and mineral technology of the Grants Uranium Region 1979. New Mex Bur Mines Mineral Res Mem 38, pp 240-243
- Four Corners Geological Society (1969) Geology and natural history of the Grand Canyon region. Ninth Field Conf, Guidebook, Powell Centennial River Expedition, 212 p
- Frishman D, Halladay CR, Hauck SA, Kendall EW (1989) The Swanson uranium deposit, Pittsylvania County, Virginia, USA: stratigraphy, petrology and ore mineralogy (abstr). *in*: Müller-Kahle E, ed., Uranium resources and geology of North America. TECDOC-500, IAEA, Vienna, pp 521-522
- G**
- Gabelman JW (1956) Uranium deposits in limestone. US Geol Surv Prof Paper 300, pp 387-404
- Gabelman JW (1956) Uranium deposits in limestone. US Geol Surv Prof Paper 300, pp 387-404
- Gabelman JW (1968) Uranium in the Appalachian Mobile Belt. US AEC, RME-4107, 41 p
- Gabelman JW (1970) The Flat Top uranium mine, Grants, New Mexico. US AEC, RME-4112, 81 p
- Gabelman JW (1977) Migration of uranium and thorium - exploration significance. Amer Ass Petrol Geol, Studies in Geology, no. 3, 168 p
- Gabelman JW, Boyer WH (1988) Uranium deposits in Todilto Limestone, New Mexico: The Barbara "J" No. I mine. Ore Geol Rev, v 3, pp 241-276
- Gabelman JW, Krusiewski SV (1964) Zonal distribution of uranium deposits in Wyoming, USA. 22nd Intern Geol Congr, New Delhi, India, pt. 5, pp 661-672
- Gabelman JW, Young RC, Ealy GK (1956) Uranium-Ambrosia Lake-New Mexico's newest bonanza. Mines Mag, v 46, no. 3, pp 58-64
- Gabelman, JW (1970) The Flat Top uranium mine, Grants, New Mexico. US AEC, RME-4112, 81 p.
- Galloway WE (1977) Catahoula Formation of the Texas coastal plain: Depositional systems, composition, structural development, groundwater flow history, and uranium distribution. Univ Texas, Austin, Bur Econ Geol Rep 87, 59 p
- Galloway WE (1979a) Fluvial depositional systems. *in*: Galloway WE, Kreitler CW, McGowen JH, eds., Depositional and groundwater flow systems in the exploration for uranium. Univ Texas, Austin, Bur Econ Geol, pp 13-42
- Galloway WE (1979b) Jackson and Catahoula systems of the Texas Gulf coastal plain. *in*: Galloway WE, Kreitler CW, McGowen JH, eds., Depositional and groundwater flow systems in the exploration for uranium. Univ Texas, Austin, Bur Econ Geol, pp 181-196
- Galloway WE (1979c) Early Tertiary-Wyoming intermontane basins. *in*: Galloway WE, Kreitler CW, McGowen JH, eds., Depositional and groundwater flow systems in the exploration for uranium. Univ Texas, Austin, Bur Econ Geol, pp 197-213
- Galloway WE (1979d) Morrison Formation of the Colorado Plateau. *in*: Galloway WE, Kreitler CW, McGowen JH, Depositional and groundwater flow systems in the exploration for uranium. Univ Texas, Austin, Bur Econ Geol, pp 214-228
- Galloway WE (1980) Deposition and early hydrologic evolution of the Westwater Canyon wet alluvial fan system. *in*: Rautman CA, ed., Geology and mineral technology of the Grants Uranium Region 1979. New Mex Bur Mines Miner Res Mem 38, pp 59-69
- Galloway WE (1982) Epigenetic zonation and fluid flow history of uranium-bearing fluvial aquifer systems, south Texas uranium province, Univ Texas, Austin, Bur Econ Geol Rep Invest no. 119, 31 p
- Galloway WE (1985) The depositional and hydrogeologic environment of Tertiary uranium deposits, south Texas uranium province. *in*: Geological environments of sandstone type uranium deposits. TECDOC-328, IAEA, Vienna, pp 215-228
- Galloway WE, Finley RJ, Henry CD (1979a) South Texas uranium province geologic perspective. Univ Texas, Austin, Bur Econ Geol Guidebook 18, 81 p
- Galloway WE, Henry CD, Smith GE (1982) Depositional framework, hydrostratigraphy, and uranium mineralization of the Oakville Sandstone (Miocene), Texas coastal plain. Univ Texas, Austin, Bur Econ Geol Rep Invest no. 113, 51 p
- Galloway WE, Kaiser WR (1979) Catahoula Formation of the Texas coastal plain: origin, geochemical evolution and characteristics of uranium deposits. US DOE, GJBX-131(79), 139 p
- Galloway WE, Kaiser WR (1980) Catahoula Formation of the Texas coastal plain: origin, geochemical evolution, and characteristics of uranium deposits. Univ Texas, Austin, Bur Econ Geol Rep Invest no. 100, 81 p
- Galloway WE, Kreitler CW, McGowen JH, eds. (1979b) Depositional and groundwater flow systems in the exploration for uranium - a research colloquium. Univ Texas, Austin, Bur Econ Geol, 267 p
- Garner LE, St. Clair AE, Evans TJ (1979) Mineral resources of Texas. Univ Texas, Austin, Bur Econ Geol, map
- Garrels RM (1955) Some thermodynamic relations among the uranium oxides and their relation to the oxidation states of the uranium ores of the Colorado Plateau. Amer Miner, v 40, no. 11-12, pp 1004-1021
- Garrels RM (1957) Geochemistry of "sandstone-type" uranium deposits. *in*: Advances in nuclear engineering. Pergamon Press, New York, v 2, pp 288-293
- Garrels RM (1960) Mineral equilibria. Harper & Brothers, New York, 254 p
- Garrels RM, Christ CL (1959) Behavior of uranium minerals during oxidation. US Geol Surv Prof Paper 320, pp 81-89
- Garrels RM, Christ CL (1965) Solutions, minerals, and equilibria. Harper & Row, New York, 450 p
- Garrels RM, Larsen ES III, eds. (1959) Geochemistry and mineralogy of the Colorado Plateau uranium ores. US Geol Surv Prof Paper 320, 236 p
- Garside LJ (1973) Radioactive mineral occurrences in Nevada. Nevada Bur Mines Geol Bull 81, pp 21-37
- Garside LJ (1982) National uranium resource evaluation, McDermitt quadrangle, Nevada. US DOE, PGJ/F-045(82), 29 p.
- Gashnig J (1980) Development of uranium exploration models for the prospector consultant system: Menlo Park, California. SRI Intern Proj 7856, 603 p
- Genth FA (1868) Contributions to mineralogy VII. Amer J Sci, II, ser 45
- Gilbert RE (1957) Notes on the relationship of uranium mineralization and rhyolite in the Marysvale area, Utah. US AEC, RME-2030, 29 p
- Gill JR, Moore GW (1955) Carnotite-bearing sandstone in Cedar Canyon, Slim Buttes, Harding County, South Dakota. US Geol Surv Bull 1009-L, pp 249-264
- Gill JR, Zeller HD, Schopf JM (1959) Core drilling for uranium-bearing lignite, Mendenhall area, Harding County, South Dakota. US Geol Surv Bull 1055-D, pp 97-145
- Gillerman E (1964) Mineral deposits of western Grant County, New Mexico. New Mex Bur Mines Miner Res, Bull 83, 213 p

- Gillerman E (1968) Uranium mineralization in the Burro Mountains, New Mexico. *Econ Geol*, v 63, pp 239-246
- Gillerman E, Whitebread DH (1956) Uranium-bearing nickel-cobalt-native silver deposits, Black Hawk District, Grants County, New Mexico. *US Geol Surv Bull* 1009, pp 283-313
- Gjelsteen TW, Collings SP (1988) Relationship between groundwater flow and uranium mineralization in the Chadron Formation, Northwest Nebraska. *in: Guidebook*, 39th Field Conf, Wyoming Geol Ass pp 271-283
- Glanzman RK, Rytuba JH (1979) Zeolite-clay mineral zonation of volcanoclastic sediments within the McDermitt caldera complex of Nevada and Oregon. *US Geol Surv Open-File Rep* 79-1668, 25 p
- Glanzman RK, Rytuba JJ, Otton JK (1979) Lithium and boron association with uranium mineralization (abstr). *Geol Soc Amer*, abstr w progr, v 11, p 433
- Glozzi J (1967) Petrology and structure of the Precambrian rocks of the Copper Mountain district, Owl Creek Mountains, Fremont County, Wyoming. PhD diss, Univ Wyoming, 141 p (unpubl)
- GMMV (1995) Jackpot Mine Draft EIS/US Dpt Interior, Rawlins-Wyoming State Office (June 1995)
- Goldhaber MB (1983) Experimental study of metastable sulfur oxy-anion formation during pyrite oxidation at pH 6-9 and 30°C. *Amer J Sci*, v 283, pp 193-217
- Goldhaber MB, Hemingway BS, Mohagheghi A, Reynolds RL (1987) Origin of coffinite in sedimentary rocks by a sequential adsorption-reduction mechanism. *Bull Miner*, v 110, pp 131-144
- Goldhaber MB, Reynolds RL (1979) Origin of marcasite and its implications regarding the genesis of roll-front uranium deposits. *US Geol Surv Rep* 79-1696, 38 p
- Goldhaber MB, Reynolds RL, Campbell JA, Wanty RB, Grauch RI, Northrop HR (1983?) Genesis of the Tony M tabular-type vanadium-uranium deposit, Henry structural basin, Utah: Mechanisms of ore and gangue mineral formation at the interface between brine and meteoric water (manuscr)
- Goldhaber MB, Reynolds RL, Rye RO (1978) Origin of a south Texas roll-type uranium deposit: II. Sulfide petrology and sulfur isotope studies. *Econ Geol*, v 73, pp 1690-1705
- Goldhaber MB, Reynolds RL, Rye RO (1979) Formation and resulfidization of a south Texas roll-type uranium deposit. *US Geol Surv Rep* 79-1651, 41 p
- Goodell PC (1985a) Classification and model of uranium deposits in volcanic environments. *in: Uranium deposits in volcanic rocks*. IAEA, Vienna, pp 1-16
- Goodell PC, Trentham R, Carraway K (1979) Geologic setting of the Peña Blanca uranium deposits, Chihuahua, Mexico: Chap. IX. *in: Henry CD, Walton AW, eds., Formation of uranium ores by diagenesis of volcanic sediments*. US DOE, GJBX-22(79), 38 p
- Goodell PC, Trentham RC (1980) Experimental leaching of uranium from tuffaceous rocks. *US DOE, GJBX-148(80)* 144 p
- Goodell PC, Waters AC, eds. (1981) Uranium in volcanic and volcanoclastic rocks. *Amer Ass Petrol Geol, Studies in Geology*, no. 13, 331 p
- Goodknight CS (1981) Uranium in the Gunnison country, Colorado. *in: Epis RC, Callender JE, eds., New Mex Geol Soc Guidebook*, 32nd Field Conf, Western Slope Colorado, pp 183-189
- Goodknight CS, Ludlam JR (1981) Uranium resource evaluation of the Montrose (1°×2°) quadrangle, central Colorado. *US DOE, GJQ-010*
- Goodknight GS (1983) Intermediate-grade uranium resource assessment project for part of the Maybell district, Sand Wash Basin, Colorado. *US DOE Open-File Rep GJBX-12(83)*, 25 p
- Gorenson P (2005) Alta Mesa project. *Global Uran Symp - 2005, Central Wyoming Sect, Soc Min, Metall, Explor, Casper, Wyoming*, 13 p
- Gorman LA, MacPherson BA (1957) Uranium exploration in the Hulett Creek area, Crook County, Wyoming. *US AEC, TM-D-1-17*, 27 p.
- Gornitz V, Kerr PF (1970) Uranium mineralization and alteration, Orphan mine, Grand Canyon, Arizona. *Econ Geol*, v 65, pp 751-768
- Gornitz V, Wenrich KJ, Sutphin HB, Vidale-Buden R (1988) Origin of the Orphan mine breccia pipe uranium deposit, Grand Canyon, Arizona. *in: Vassiliou AH, Hausen DM, Carson DJ, eds., Process mineralogy VII - As applied to separation technology*. Metall Soc, Warrendale, Penn, pp 281-301
- Gornitz VM (1969) Mineralization, alteration, and mechanism of emplacement, Orphan ore deposit, Grand Canyon, Arizona. PhD diss, Columbia Univ, New York, 186 p
- Gott GB, Schnabel RW (1963) Geology of the Edgemont NE quadrangle, Fall River and Custer Counties, South Dakota. *US Geol Surv, Bull* 1063-E, pp 127-190
- Gott GB, Wolcott DE, Bowles CG (1974) Stratigraphy of the Inyan Kara Group and localization of uranium deposits, southern Black Hills, South Dakota and Wyoming. *US Geol Surv Prof Paper* 763, 57 p
- Gott GB, Wyant DG, Beroni EP (1952) Uranium in black shales, lignites, and limestones in the United States. *in: Selected papers on uranium deposits in the United States*. *US Geol Surv, Circular* 220, pp 31-35
- Gould W, Smith RB, Metzger SP, Melancon PE (1963) Geology of the Homestake-Sapin uranium deposits, Ambrosia Lake area. *in: Kelley VC, ed., Geology and technology of the Grants Uranium Region, New Mex Bur Mines Miner Res Mem* 15, pp 66-71
- Graff PJ, Houston RS (1977) Radioactive conglomerates in Middle Precambrian (Precambrian X) metasedimentary rocks in the Sierra Madre, Wyoming. *US Geol Surv Open-file Rep* 77-830, 7 p
- Granger HC (1960) Pitchblende identified in a sandstone-type uranium deposit in the central part of the Ambrosia Lake District, New Mexico. *US Geol Surv Prof Paper* 400-B, pp 54-55
- Granger HC (1962) Clays in the Morrison Formation and their spatial relation to the uranium deposits at Ambrosia Lake, New Mexico. *US Geol Surv Prof Paper* 450-D, pp 15-20
- Granger HC (1963) Mineralogy. *in: Kelley VC, ed., Geology and technology of the Grants Uranium Region*. *New Mex Bur Mines Miner Res Mem* 15, pp 21-37
- Granger HC (1968) Localization and control of uranium deposits in the southern San Juan Basin Mineral Belt, New Mexico - an hypothesis. *US Geol Surv Prof Paper* 600-B, pp 60-70
- Granger HC (1976) Fluid flow and ionic diffusion and their roles in the genesis of sandstone-type uranium ore bodies. *US Geol Surv Open-File Rep* 76-454, 26 p
- Granger HC, Bauer HL Jr (1952) Uranium occurrences on the Merry Widow claim, White Signal district, Grant County, New Mexico. *US Geol Surv Circ* 189, 16 p
- Granger HC, Finch WI (1988) The Colorado Plateau uranium province, (with contributions by Bromfield CS, Duval JS, Grauch VJS, Green MW, Hills FA, Peterson F, Pierson CT, Sanford RE, Spirakis CS Wahl RR. *in: Recognition of uranium provinces*. IAEA, Vienna, pp 157-193
- Granger HC, Ingram BL (1966) Occurrence and identification of jordsite at Ambrosia Lake, New Mexico. *US Geol Surv Prof Paper* 550-B, pp B120-B124
- Granger HC, Raup RB (1959) Uranium deposits in the Dripping Spring Quartzite, Gila County, Arizona. *US Geol Surv Bull* 1046-P, pp 415-486
- Granger HC, Raup RB (1962) Reconnaissance study of uranium deposits in Arizona. *US Geol Surv Bull* 1147-A, pp 1-54
- Granger HC, Raup RB (1964) Stratigraphy of the Dripping Spring Quartzite, southeastern Arizona. *US Geol Surv Bull* no. 1168, 119 p
- Granger HC, Raup RB Jr (1969a) Geology of the uranium deposits in the Dripping Spring Quartzite, Gila Co., Arizona. *US Geol Surv Prof Paper* 595, 108 p
- Granger HC, Raup RB Jr (1969b) Detailed description of uranium deposits in Dripping Spring Quartzite. *US Geol Surv open file rep*, 69-108, 145 p
- Granger HC, Santos ES (1963) An ore-bearing cylindrical collapse structure in the Ambrosia Lake uranium district, New Mexico. *in: Short papers in geology*. *US Geol Surv, Prof Paper*, 475-C, pp 156-161
- Granger HC, Santos ES (1982) Geology and ore deposits of the Section 23 Mine, Ambrosia Lake district, New Mexico. *US Geol Surv open file rep*, 82-0207, 74 p
- Granger HC, Santos ES (1986) Geology and ore deposits of the Section 23 mine, Ambrosia Lake district, New Mexico. *in: Turner-Peterson CE, Santos ES, Fishman NS, eds., A basin analysis case study - the Morrison Formation, Grants Uranium Region, New Mexico*. *Amer Ass Petrol Geol, Studies in Geology* no. 22, pp 185-210
- Granger HC, Santos ES, Dean BG, Moore FB (1961) Sandstone-type uranium deposits at Ambrosia Lake, New Mexico - an interim report. *Econ Geol*, v 56, pp 1179-1210
- Granger HC, Warren CG (1969) Unstable sulfur compounds and the origin of roll-type uranium deposits. *Econ Geol*, v 64, pp 160-171

- Granger HC, Warren CG (1974) Zoning in the altered tongue associated with roll-type uranium deposits. *in: Formation of uranium ore deposits*. IAEA, Vienna, pp 185-199
- Granger HC, Warren CG (1978) Some speculations on the genetic geochemistry and hydrology of roll-type uranium deposits. *in: 30th Field Conf Guidebook*, Wyoming Geol Ass, pp 349-361
- Granger HC, Warren CG (1979) The importance of dissolved free oxygen during formation of sandstone-type uranium deposits. US Geol Surv open file rep 79-1603, 21 p
- Granger HC, Warren CG (1981) Genetic implications of the geochemistry of vanadium-uranium deposits in the Colorado Plateau region. Amer Ass Petrol Geol, Albuquerque Meeting, New Mexico, abstr w progr
- Grauch RI (1978) Geology of the uranium prospect at Camp Smith, New York, with a model for the formation of uranium deposits in metamorphosed submarine volcanogenic rocks. US Geol Surv Open-File Rep 78-949, 29 p
- Grauch RI (1985) Precambrian submarine volcanogenic uranium deposits: An example from southeastern New York, USA. *in: Uranium deposits in volcanic rocks*. IAEA, Vienna, pp 363-364
- Grauch RI (1985) Precambrian submarine volcanogenic uranium deposits: An example from southeastern New York, United States of America. *in: Uranium deposits in volcanic rocks*. IAEA, Vienna, pp 363-364
- Grauch RI, Kirk AR, Hon K, Ludwig KR, Mehnert HH, Zamudio JA, Bithell LM (1985) Episodic uranium mineralization in the western San Juan Caldera complex, Colorado. *in: Uranium deposits in volcanic rocks*. IAEA, Vienna, pp 315-316
- Grauch RI, Zarinski K (1976) Generalized descriptions of uranium-bearing veins, pegmatites, and disseminations in non-sedimentary rocks, eastern US. US Geol Surv Open-File Rep 76-582, 114 p
- Graves D, Woody DR (2008) The Hank unit property, Campbell County, Wyoming, USA. Technical report 43-101 prepared for Uranerz Energy Corporation. 29 p (May 1, 2008)
- Green MW (1980) Disconformities in the Grants mineral belt and their relationship to uranium deposits. *in: Rautman CA, ed., Geology and mineral technology of the Grants uranium region 1979*. New Mex Bur Mines Miner Res Mem 38, pp 70-74
- Green MW (1982) Origin of intraformational folds in the Jurassic Todilto Limestone, Ambrosia Lake uranium mining district, McKinley and Valencia Counties, New Mexico. US Geol Surv Open-File Rep 82-69, 29 p
- Green MW et al. (1980a) Uranium resource evaluation, Aztec NTMS 1- by 2-degree quadrangle, New Mexico and Colorado US DOE, PGJ/F-012(82), 79 p
- Green MW et al. (1980b) Uranium resource evaluation, Albuquerque NTMS 1- by 2-degree quadrangle, New Mexico. US DOE, PGJ/F-016(82), 79 p
- Green MW, Byers VP, Condon SM, and others (1982) National uranium resource evaluation, Shiprock quadrangle, Arizona, New Mexico, Colorado, and Utah. US DOE, PGJ/F-024(82), 70 p
- Green MW, Jackson TJ (1975a) Geologic map of the Church Rock quadrangle, McKinley County, New Mexico. US Geol Surv Open-File Rep 75-258
- Green MW, Jackson TJ (1975b) Geologic map of the Mariano Lake quadrangle, McKinley County, New Mexico. US Geol Surv Open-File Rep 75-261
- Greenberg JK, Hauck SA, Ragland PC, Rogers JJW (1977) A tectonic atlas of uranium potential in crystal rocks of the eastern U.S. US DOE, GJBX-69(77), 94 p
- Greene RC (1976) Volcanic rocks of the McDermitt caldera, Nevada-Oregon. US Geol Surv Open-File Rep 76-753, 80 p
- Gregg CC, Moore EL (1955) Reconnaissance of the Chinle Formation in the Cameron-St. Johns area, Coconino, Navajo, and Apache Counties, Arizona. US AEC, RME-51, 15 p.
- Gregory JP (1980) Metamorphic gradients in Pittsylvania County, Virginia. *in: Price V Jr, Thayer PA, Ranson WA, eds., Geological Investigations of Piedmont and Triassic Rocks, Central North Carolina and Virginia*. Carolina Geol Soc Field Trip Guidebook, pp 13-17
- Gross EB (1956) Mineralogy and paragenesis of the uranium ore, Mi Vida mine, San Juan County, Utah. Econ Geol, v 51, no. 7, pp 632-648
- Gross EB (1965) A unique occurrence of uranium minerals, Marshall Pass, Saguache County, Colorado. Amer Mineralogist, v 50, pp 909-923
- Gruner JW (1954a) The uranium mineralogy of the Colorado Plateau and adjacent regions. *in: Guidebook 9*, Utah Geol Soc, pp 70-77
- Gruner JW (1954b) The origin of the uranium deposits of the Colorado Plateau and adjacent region. Mines Mag, v 44, no. 3, pp 53-66
- Gruner JW (1956) Concentration of uranium in sediments by multiple migration-accretion. Econ Geol, v 51, no. 6, pp 495-520
- Gruner JW et al. (1954b) The mineralogy of the "Mi Vida" uranium ore deposits of the Utex Exploration Company in the Indian Wash area, Utah. US AEC, RME-3094, pp 15-27
- Gruner JW, Gardiner L, Smith DK Jr (1954a) Mineral associations in the uranium deposits of the Colorado Plateau and adjacent regions, interim report. US AEC, RME-3092, 48 p
- Grutt EW Jr (1957) Environment of some Wyoming uranium deposits: Advances in nuclear engineering. 2nd Nuclear Eng Sci Conf, Philadelphia, Pennsylvania, v 2, pp 313-323
- Grutt EW Jr (1972) Prospecting criteria for sandstone-type uranium deposits. *in: Bowie SHU, Davis M, Ostle D, eds., Uranium prospecting handbook*. IMM, London, pp 47-77
- GSA Rocky Mountain Section, (Wenrich & Billingsley, eds.) (1986) Abstracts with Programs, v 18, 39th Annual Meeting, Geol Soc Amer, Northern Arizona Univ, Flagstaff
- Gueniot B (1983) Distribution et modes de fixation de l'uranium dans les grands types de pédogenèses climatiques et stationnelles sur roches cristallines. Géol Géochim Uranium, Mém Nancy, no. 3, 259 p
- Guevara EH, Garcia R (1972) Depositional systems and oil-gas reservoirs in the Queen City Formation (Eocene), Texas. Gulf Coast Ass Geol Soc Trans, v 22, pp 1-22
- Gulbransen RA (1966) Chemical composition of phosphorites in the Phosphoria Formation. Geochim Cosmochim Acta, v 30, no. 8, pp 760-778

H

- Hafen PL, Adams SS, Secor GB (1976), Application of magnetic susceptibility measurements to uranium exploration in sandstones. *in: Exploration for uranium ore deposits*. IAEA, Vienna, pp 367-378
- Hagmaier JL (1971) Groundwater flow, hydrochemistry, and uranium deposition in the Powder River Basin, Wyoming. Ph.D. thesis, Univ North Dakota, Grand Forks, ND (unpubl)
- Haji-Vassiliou A, Kerr PF (1972) Uranium-organic matter association at La Bajada, New Mexico. Econ Geol, v 67, pp 41-54
- Haji-Vassilou A, Pufler JH, Markewicz FJ (1974) Uranium-rare earth mineralization at Charlotte Mine prospect near Cranberry Lake, New Jersey (abstr). 9th Ann Meet, Geol Soc Amer, Northeastern Sect, Abstr, v 6, no. 1, p 33
- Halladay CR (1983) Report on microprobe analyses. Marline Uranium Corp. report, 19 p (unpubl)
- Halladay CR (1989) The Swanson uranium deposit, Virginia: a structurally controlled U-P albitite deposit (abstr). *in: Müller-Kahle E, ed., Uranium resources and geology of North America*. TECDOC-500, IAEA, Vienna, p 519
- Halladay CR (1989) The Swanson uranium deposit, Virginia: a structurally-controlled, albitite deposit (abstr). *in: Uranium resources and geology of North America*. TECDOC-500, IAEA, Vienna, p 519
- Halladay CR, Bowdidge CR, Singletary HM, Park IG, Lineberger HD, Truckle DM, Lee AJ, Glackmeyer K (1982) Geology, mineralogy and geophysics of the Coles Hill uranium deposits, Pittsylvania County, Virginia. Marline Uranium Corp. report, 117 p (unpubl)
- Hamil MM (1971) Metamorphic and structural environment of Copper Mountain, Wyoming. PhD diss, Univ Missouri (unpubl)
- Hanshaw BB, Dahl HM (1956) Preliminary fracture study, Smith Lake area, McKinley County, New Mexico. US AEC, TM-128, 4 p
- Hansink JD (1976) Equilibrium analysis of a sandstone roll-front uranium deposit. *in: Exploration for uranium ore deposits*. IAEA, Vienna, pp 683-692
- Hansley PL (1984) Feldspar alteration patterns in the Upper Jurassic Morrison Formation, northwestern New Mexico. SEPM, First National Midyear Meeting, Technical Program, p 37
- Hansley PL (1986a) Relationship of detrital, nonopaque heavy minerals to diagenesis and provenance of the Morrison Formation, southwestern San Juan Basin, New Mexico. *in: Turner-Peterson CE et al., eds., A basin analyses case*

- study: the Morrison Formation, Grants Uranium Region, New Mexico. Amer Ass Petrol Geol, Studies in Geology no. 22, pp 257-276
- Hansley PL (1986b) Regional diagenetic trends and uranium mineralization in the Morrison Formation across the Grants Uranium Region. *in*: Turner-Peterson CE et al., eds., A basin analyses case study: the Morrison Formation, Grants Uranium Region, New Mexico. Amer Ass Petrol Geol, Studies in Geology no. 22, pp 277-302
- Hansley PL, Collings SP, Brownfield IK, Skipp GL (1989) Mineralogy of uranium ore from the Crow Butte uranium deposit, Oligocene Chadron Formation, Northwestern Nebraska. US Geol Surv Open-File Rep 89-225, 28 p
- Hansley PL, Dickinson KA (1990) Uranium mineralization and favorability in the Oligocene Chadron Formation, Southeastern Wyoming and Northwestern Nebraska. Short Papers Uranium Workshop 1990, US Geol Surv, pp 27-31
- Hansley PL, Spirakis CS (1992) Organic matter diagenesis as the key to a unifying theory for the genesis of tabular uranium- vanadium deposits in the Morrison Formation, Colorado Plateau. Econ Geol, v 87, no. 2, pp 352-365
- Harmon GF, Taylor PS (1963) Geology and ore deposits of the Sandstone Mine, southeastern Ambrosia Lake area. *in*: Kelley VC ed., Geology and technology of the Grants Uranium Region. New Mex Bur Mines Miner Res Mem 15, pp 102-107
- Harris LD, Harris AG, DeWitt W Jr, Bayer KC (1981) Evaluation of southern eastern overthrust belt beneath Blue Ridge-Piedmont thrust. Amer Ass Petrol Geol Bull, v 65, pp 2497-2505
- Harris RE (1984) Alteration and mineralization associated with sandstone uranium occurrences, Morton Ranch area. Wyoming. Geol Surv Wyoming, Rep Invest no. 25, 29 p
- Harshman EN (1962) Alteration as a guide to uranium ore, Shirley Basin, Wyoming. US Geol Surv Prof Paper 450-D, pp D8-D10
- Harshman EN (1966) Genetic implications of some elements associated with uranium deposits, Shirley Basin, Wyoming. US Geol Surv Prof Paper 550-C, pp C167-C173
- Harshman EN (1968) Uranium deposits of Wyoming and South Dakota. *in*: Ridge JD, ed., Ore deposits of the United States, 1933-1967 (Graton-Sales volume). Amer Inst Min Metal Petrol Eng, v 1, pp 815-831
- Harshman EN (1970) Uranium ore rolls in the United States. *in*: Uranium exploration geology. IAEA, Vienna, pp 219-232
- Harshman EN (1972) Geology and uranium deposits, Shirley Basin area, Wyoming. US Geol Surv Prof Paper 745, 82 p
- Harshman EN (1974) Distribution of elements in some roll-type uranium deposits. *in*: Formation of uranium ore deposits. IAEA, Vienna, pp 169-183
- Harshman EN, Adams SS (1981) Geology and recognition criteria for roll-type uranium deposits in continental sandstones. US DOE, GJBX-1(81), 185 p
- Harshman EN, Bell KG (1970) Uraninite-bearing contact metamorphic deposits, Heaths Peak, Carbon County, Wyoming. Econ geol, v 65, pp 849-855
- Hart OM (1958) Uranium deposits in the Pryor-Big Horn Mountains, Carbon County, Montana, and Big Horn County, Wyoming. 2nd Intern Conf Peaceful Uses of Atomic Energy, UN, Geneva, v 2, pp 523-526
- Hart OM (1968) Uranium in the Black Hills. *in*: Ridge JD, ed., Ore deposits of the United States, 1933-1967. American Inst Mining, Metall, Petrol Engineers, Inc., New York, v 1, pp 832-837
- Hatcher PG, Spiker EC, Orem WH, Romankiw LA, Szeverenyi NM, Maciel GE (1986) Organic geochemical studies of uranium-associated organic matter from the San Juan basin: A new approach using solid state ¹³C nuclear magnetic resonance. *in*: Turner-Peterson CE et al., eds., A basin analysis case study - the Morrison Formation, Grants Uranium Region, New Mexico. Amer Ass Petrol Geol, Studies in Geology no. 22, pp 171-184
- Hauck, SA, Kendall EW, Halladay CR (1989) Detailed mineralogy and alteration of the Swanson uranium deposit, southern Virginia. *in*: Uranium resources and geology of North America. TECDOC-500, IAEA, Vienna, p 523
- Hauptman CM (1956) Uranium in the Pryor Mountains area of southern Montana and northern Wyoming. Uranium and Modern Mining, v 3, no. 11, pp 14-21
- Havenstrite S, Hardy LS (2006) Exploration report, Marysvale uranium project, Sevier and Piute Counties, Utah, USA. Prepared for Trigon Exploration Canada, Ltd. 57 p (June 30, 2006)
- Hawley CC, Robeck RC, Dyer HB (1968) Geology, altered rocks, and ore deposits of the San Rafael Swell, Emery County, Utah. US Geol Surv Bull 1239, 115 p
- Hawley CC, Wyant DG, Brooks DD (1965) Geology and uranium deposits of the Temple Mountain district, Emery County, Utah. US Geol Surv Bull 1192, 154 p
- Hazlett GW (1969) Northeast Churchrock mine-New Mexico's newest uranium deposit (abstr). *in*: Guidebook 20, New Mex Geol Soc, pp 215-216
- Hazlett GW, Kreek J (1963) Geology and ore deposits of the south-eastern part of the Ambrosia Lake area. *in*: Kelley, VC, ed., Geology and technology of the Grants Uranium Region. New Mex Bur Mines Miner Res Mem 15, pp 82-89
- Hedge CE, Houston RS, Tweto OL, Reid RR, Harrison JE, Peterman, Z (1978) The Precambrian of the Rocky Mountains. *in*: Lageson DR, ed., Occurrences of uranium in Precambrian and younger rocks of Wyoming and adjacent states. Wyoming Geol Surv Public Inf Circ 7, p 17
- Heinrich EW (1958) Mineralogy and geology of radioactive raw materials. McGraw Hill, New York-Toronto-London, 654 p
- Henika WS (1980) Metamorphic and structural evidence of an intrusive origin for the Shelton Formation. *in*: Price V et al., eds, Geological investigation of Piedmont and Triassic rocks. *in*: Field Trip Guidebook, Carolina Geol Soc, pp CGS 80-B-V through CGS 80-B-V 17
- Henika WS (1981) Geology of the Spring Garden quadrangle, Virginia. Virginia Div Mineral Res, Open-File Map and Rep
- Henika WS (1997) Geologic map of the Roanoke 30x60 minute quadrangle. Virginia Div Mineral Res, Publ 148
- Henika WS (1998) Digital geologic map of the Virginia portion of the Danville 30x60 minute quadrangle. Virginia Div Mineral Res, Publ DP-43A (unedited draft)
- Henika WS, Thayer PA (1983) Geologic map of the Spring Garden quadrangle, Virginia. Virginia Div Mineral Res, Publ 48, 1 plate with text
- Henry CD, Duex TW (1981) Uranium in diagenesis of the Pruett, Duff and Tascotal formations, Trans Pecos Texas. *in*: Goodell PC, Waters AC, eds., Uranium in volcanic and volcanoclastic rocks. Amer Ass Petrol Geol, Stud Geol 13, pp 167-181
- Henry CD, Galloway WE, Smith GE, Ho CL, Morton JP, Gluck JK (1982) Geochemistry of ground water in the Oakville Sandstone, a major aquifer and uranium host of the Texas coastal plain. Univ Texas, Austin, Bur Econ Rep Invest no. 118, 63 p
- Heron SD Jr, Johnson HS Jr (1969) Radioactive mineral resources of South Carolina. South Carolina Div Geol Misc Rep MR-4, 4 p
- Hess FL (1908) Minerals of the rare-earth metals at Baringer Hill, Llano County, Texas. *in*: Contributions to economic geology, 1907, Part I, Metals and non-metals, except fuels. US Geol Surv Bull 340, pp 286-294
- Hess FL (1914) A hypothesis for the origin of the carnotites of Colorado and Utah. Econ Geol, v 9, pp 675-688
- Hess FL (1933) Uranium, vanadium, radium gold, silver, and molybdenum sedimentary deposits. *in*: Ore deposits of the western states. Amer Inst Min, Metall, Petrol Eng, pp 450-481
- Hess FL, Wells RC (1920), Brannerite, a new uranium mineral. J Frankline Inst, 189, pp 225-237, 779-789
- Hewitt CH (1959) Geology and mineral deposits of the northern Big Burro Mountains - Redrock area, Grant County, New Mexico. New Mex Inst Min Technol, State Bur Mines Miner Res Bull 60
- Heyl AV (1957) Zoning of the Bitter Creek vanadium-uranium deposit near Uravan, Colorado. US Geol Surv Bull 1042-F, pp 187-201
- Heyse JV (1972) Mineralogy and paragenesis of the Schwartzwalder Mine uranium ore, Jefferson County, Colorado. US AEC, GJO-912-1, 87 p
- Hicks RT, Lowy RM, Della Valle RS, Brookings DG (1980) Petrology and geochemistry of Westwater Canyon Member, Morrison Formation, northern San Juan Basin - Similarities and differences with Grants mineral belt. *in*: Rautman CA, ed., Geology and mineral technology of the Grants Uranium Region 1979. New Mex Bur Mines Miner Res Mem 38, pp 208-214
- Hidden WE, McIntosh JB (1889) A description of several yttria and thoria minerals from Llano County (Texas). Amer J Sci, III, ser 38
- Hill C, Forti P (1997) Cave minerals of the world (2nd edition). Nat Speleological Soc, Huntsville, AL, 463 p
- Hillebrand WF (1888) Preliminary remarks on North American uraninites. Bull US Geol Surv 60
- Hillebrand WF, Ransome FL (1900) On carnotite and associated vanadiferous minerals in western Colorado. Amer J Sci, 4th series, v 10, no. 56, pp 120-144

- Hillebrand WF, Ransome FL (1905) On carnotite and associated vanadiferous minerals in western Colorado. *in*: Clarke FW, et al., Contributions to mineralogy from the US Geol Surv. US Geol Surv Bull 262, pp 9-31
- Hills FA (1977) Uranium and thorium in the middle Precambrian Estes Conglomerate, Nemo district, Lawrence County, South Dakota - A preliminary report. US Geol Surv Open-file Rep 77-55, 27 p
- Hills FA (1979) Uranium, thorium and gold in the lower Proterozoic (?) Estes Conglomerate, Nemo district, Lawrence County, South Dakota. Univ Wyoming Contrib Geol, v 17, pp 159-172
- Hills FA, Dickinson KA (1982) Silver Plume Granite-possible source of uranium in sandstone uranium deposits, Tallahassee Creek and High Park areas, Fremont and Teller counties, Colorado. US Geol Surv Open-File Rep 82-404, 23 p
- Hilpert LS (1963) Regional and local stratigraphy of uranium-bearing rocks. New Mex Bur Min Res Mem 15, pp 6-18
- Hilpert LS (1969) Uranium resources of northwestern New Mexico. US Geol Surv Prof Pap 603, 166 p
- Hilpert LS, Moench RH (1960) Uranium deposits of the southern part of the San Juan Basin, New Mexico. Econ Geol, v 55, pp 429-464
- Hintze LF, ed. (1967) Uranium districts of southeastern Utah. Guidebook to the Geology of Utah no. 21, Utah Geol Soc
- Hoel HD (1982) Goliad Formation of the South Texas Gulf Coastal Plain: regional genetic stratigraphy and uranium mineralization. MSc thesis, Univ Texas, Austin, 173 p
- Hoffman ME (1977) Origin and mineralization of breccia pipes Grand Canyon district, Arizona. MS thesis, Univ Laramie, Wyoming, 51 p
- Holen HK (1982) A summary of uranium geology in the Grants mineral belt, New Mexico. US DOE, TM-311, 3 p
- Holen HK, Hatchell WO (1986) Geological characterization of New Mexico uranium deposits for extraction by in situ leach recovery. New Mexico Bur Mines Miner Res Open-File Rep 251, 93 p
- Holen HK, Hatchell WO (1988) Bibliography of uranium in situ leach technology. New Mex Energy, Minerals and Natural Res Dpt, Bur Econ Geol, Rep Invest no. 4, 48 p
- Holmquist RJ (1970) The discovery and development of uranium in the Grants mineral belt, New Mexico. US AEC, Rep RME-172, 122 p
- Hon K (1984) Geology of volcanogenic uranium deposits within the Tallahassee Creek Conglomerate, Tallahassee Creek uranium district, Colorado. US Geol Surv Open-File Rep 84-219, 23 p
- Hoskins WG (1963) Geology of the Black Jack No.2 mine, Smith Lake area. New Mex Bur Miner Res Mem, no.15, pp 49-52
- Hostetler PB, Garrels RM (1962) Transportation and precipitation of uranium and vanadium at low temperatures, with special reference to sandstone-type uranium deposits. Econ Geol, v 57, pp 137-167
- Houston RS (1969) Aspects of the geologic history of Wyoming related to the formation of uranium deposits. Wyoming Univ Contr Geol, v 8, pp 67-79
- Houston RS, Desborough GA, Karlstrom KE, Sharp WN, Graff PJ (1979) Progress report on the study of radioactive quartz-pebble conglomerate of the Medicine Bow Mountains and Sierra Madre, southeastern Wyoming. US Geol Surv open file rep 79-1131, 46 p
- Houston RS, Graff PJ, Karlstrom KE, Root FK (1977) Preliminary report on radioactive conglomerates of Middle Precambrian age in the Sierra Madre and Medicine Bow Mountains of southeastern Wyoming. US Geol Surv Open-File Rep 77-574, 15 p
- Huang Wen H (1978) Geochemical and sedimentologic problems of uranium deposits of Texas Gulf Coastal Plain. Amer Ass Petrol Geol Bull, v 62 pp 1049-1062
- Huber GC (1980) Stratigraphy and uranium deposits, Lisbon Valley district, San Juan County, Utah. Col Sch Mines Quarterly, v 75, no. 2, 44 p
- Huber GC (1981) Geology of the Lisbon Valley uranium district, southeastern Utah. *in*: Epis RC, Callender JF, eds., Guidebook, 32nd Field Conf, Western Slope Colorado, New Mex Geol Soc pp 177-181
- Huff LC, Lesure FG (1962) Diffusion features of uranium-vanadium deposits in Montezuma Canyon, Utah. Econ Geol, v 57, pp 226-237
- Huff LC, Lesure FG (1965) Geology and uranium deposits of Montezuma Canyon area, San Juan County, Utah. US Geol Surv Bull 1190, 102 p
- Huffman CA Jr, Kirk AR, Corken RJ (1980) Depositional environments as ore controls in Salt Wash Member. *in*: Rautman CA, ed., Geology and mineral technology of the Grants Uranium Region 1979. New Mex Bur Mines Miner Res Mem 38, pp 122-129
- Huffman CA Jr, Lupe RD (1977) Influences of structure on Jurassic depositional patterns and uranium occurrences, northwestern New Mexico. *in*: Guidebook, 28th Field Conf, San Juan Basin III, New Mex Geol Soc pp 277-283
- IAEA (1982) Vein-type and similar uranium deposits in rocks younger than Proterozoic. IAEA, Vienna, 391 p
- IAEA (1983) Age, sedimentary environments, and other aspects of sandstone and related host rocks for uranium deposits, Tech Rep Ser no. 231. IAEA, Vienna, 62 p
- IAEA (1984) (Toens D ed.) Surficial uranium deposits. TECDOC-322, IAEA, Vienna, 252 p
- IAEA (1985a) Uranium deposits in volcanic rocks. IAEA, Vienna, 468 p
- IAEA (1985b) (Finch W ed.) Geological environments of sandstone-type uranium deposits. TECDOC-328, IAEA, Vienna, 408 p
- IAEA (1986a) (Fuchs H ed.) Vein-type uranium deposits. TECDOC-361, IAEA, Vienna, 423 p
- IAEA (1986b) (INTURGEO) US DOE National Uranium Resource Evaluation Program (NURE). Uranium occurrence reports: database compiled by the IAEA from Appendix C of the NURE Quadrangle Reports series PGJ/F- and GJQ- published from 1978 through 1982, (available on magnetic media) 5000 p
- IAEA (1987) (Pretorius D ed.) Proterozoic quartz-pebble conglomerates. TECDOC-427, IAEA, Vienna, 459 p
- IAEA (1988a) Recognition of uranium provinces. IAEA, Vienna, 459 p
- IAEA (1988b) Uranium deposits in Asia and the Pacific: geology and exploration. IAEA, Vienna, 341 p
- IAEA (1988c) INTURGEO: The International Uranium Geology Information System, a world atlas of uranium occurrences and deposits. TECDOC-471, IAEA, Vienna, 493 p
- IAEA (1989a) Uranium deposits in magmatic and metamorphic rocks. IAEA, Vienna, 253 p
- IAEA (1989b) Uranium resources and geology of North America. TECDOC-500, IAEA, Vienna, 529 p
- IAEA (1989c) Metallogenesis of uranium deposits. IAEA, Vienna, 489 p
- IAEA (1991) Assessment of uranium resources and supply. TECDOC-597, IAEA, Vienna, 217 p
- IAEA (1992) New developments in uranium exploration, resources, production and demand. TECDOC-650, IAEA, Vienna, 258 p
- IAEA (1993) Uranium in situ leaching. TECDOC-720, IAEA, Vienna, 245 p
- IAEA (1995a) Recent developments in uranium resources and supply. TECDOC-823, IAEA, Vienna, 266 p
- IAEA (1995b) World distribution of uranium deposits. IAEA, Vienna, map, first edition
- IAEA (1995c) Planning and management of uranium mine and mill closures. TECDOC-824, IAEA, Vienna, 157 p
- IAEA (1995d) Application of uranium exploration data and techniques in environmental studies. TECDOC-827, IAEA, Vienna, 352 p
- IAEA (1996) Guidebook to accompany IAEA map - World distribution of uranium deposits. IAEA, Vienna, 224 p
- IAEA (1996) Innovations in uranium exploration, mining and processing techniques, and new exploration target areas. TECDOC-868, IAEA, Vienna, 148 p
- IAEA (1997) Changes and events in uranium deposit development, exploration, resources, production and the world supply-demand relationship. TECDOC-961, IAEA, Vienna, 343 p
- IAEA (2000) International symposium on the uranium production cycle and the environment. Book of extended synopses, SM-362, IAEA, Vienna, 251 p
- IAEA (2001a) Manual of acid in situ leach uranium mining technology. TECDOC-1239, IAEA, Vienna, 283 p
- IAEA (2001b) Impact of new environmental and safety regulations on uranium exploration, mining, milling and management of its waste. TECDOC-1244, IAEA, Vienna, 244 p

- IAEA (2001c) Assessment of uranium deposit types and resources - a worldwide perspective. TECDOC-1258, IAEA, Vienna, 253 p
- IAEA (2001d) Analysis of uranium supply to 2050. IAEA, Vienna, 103 p
- IAEA (2002a) The uranium production cycle and the environment. C&S Papers Series 10/P, IAEA, Vienna, 561 p
- IAEA (2002b) In situ leach uranium mining. TCM Almaty 1996, T1-TC-975, IAEA, Vienna, 179 p
- IAEA (2002c) Technologies for the treatment of effluents from uranium mines, mills and tailings. TECDOC-1296, IAEA, Vienna, 127 p
- IAEA (2003) Guidelines for radioelement mapping using gamma ray spectrometry. TECDOC-1363, IAEA, Vienna, 173 p
- IAEA (2004) Recent developments in uranium resources and production with emphasis on in situ leach mining. TECDOC-1396, IAEA, Vienna, 325 p
- IAEA (2005a) Developments in uranium resources, production, demand and the environment. TECDOC-1425, IAEA, Vienna, 187 p
- IAEA (2005b) Recent developments in uranium exploration, production, and environmental issues. TECDOC-1463, IAEA, Vienna, 80 p
- IAEA (2005c) Uranium production and raw materials for the nuclear fuel cycle - supply and demand, economics, the environment and energy security - Extended Synopses. CN-128, IAEA, Vienna, 343 p
- IAEA (2006) Uranium production and raw materials for the nuclear fuel cycle - supply and demand, economics, the environment and energy security. Proceedings Series, IAEA, Vienna, 352 p
- IAEA (2009) Database on world distribution of uranium deposits (UDEPO). IAEA, Vienna, (in preparation)
- Illsley CT (1957) Hydrogeochemical exploration for uranium in the Mt. Spokane area, Washington (abstr). *Geol Soc Amer Bull*, v 68, no. 12, pt 2, p 1750
- Ingram JA (1974) Uranium deposits. *Austral BMR, Miner Res Rep* 6, 52 p
- INI (2000) Data compilation and analysis of costs relating to environmental restoration of U.S uranium production facilities, Appendix C, Site characterization, data sheets decommissioning of U.S. uranium-related facilities, International Nuclear Inc, Golden, 74 p (unpubl)
- Isachsen YW (1954) Ore deposits of the Big Indian Wash-Lisbon Valley area, uranium deposits and general geology of southeastern Utah. *in: Guidebook* 9, Utah Geol Soc, pp 95-107
- Isachsen YW (1955) Uranium deposits in the Skull Creek and Uranium Peak districts, northwestern Colorado. *in: 6th Annual Field Conf, Salt Lake City, Utah, Intermount Ass Petrol Geol*, pp 124-125
- Isachsen YW, Evensen CG (1956) Geology of uranium deposits of the Shinarump and Chinle Formations on the Colorado Plateau. *US Geol Surv Prof Paper* 302, pp 263-280
- J**
- Jacobs MB, Kerr PF (1965) Hydrothermal alteration along the Lisbon Valley fault zone, San Juan County, Utah. *Geol Soc Amer Bull* 76, pp 423-440
- Jacobsen LC (1980) Sedimentary controls on uranium ore at L-Bar deposits, Laguna district, New Mexico. *in: Rautman CA, ed. Geology and mineral technology of the Grants Uranium Region, 1979. New Mex Bur Mines Miner Res Mem* 38, pp 284-291
- Jasinski SM (2006) Phosphate rock. *in: 2006 Minerals Yearbook. US Geol Surv, Reston*, http://minerals.usgs.gov/minerals/pubs/commodity/phosphate_rock/myb1-2006-phosp.pdf
- Jenkins JT, Jr, Cunningham SB (1980) Depositional environment of the Poison Canyon Sandstone, Morrison Formation, in the Gulf Mariano Lake mine, McKinley County, New Mexico. *in: Rautman CA, ed., Geology and mineral technology of the Grants Uranium Region 1979. New Mex Bur Mines Miner Res Mem* 38, pp 153-161
- Jennings JK (1976) Interaction of uranium with naturally occurring organic substances. *Colorado School Mines, MSc thesis*, 71 p
- Jennings JK, Leventhal JS (1977) A new structural model for humic material which shows sites for attachment of oxidized uranium species. *in: Campbell JA, ed., Short papers of the US Geol Surv uranium-thorium symp 1977. US Geol Surv Circ* 753, pp 10-11
- Jensen ML (1958) Sulphur isotopes and the origin of sandstone-type uranium deposits. *Econ Geol*, v 53, pp 598-616
- Jensen ML (1963) Sulfur isotopos and biogenic origin of uraniferous deposits of the Grants and Laguna districts. *in: Kelley VC, ed., Geology and technology of the Grants Uranium Region. New Mex Bur Mines Miner Res Mem* 15, pp 182-190
- Jensen ML, Field CW, Nakai, Nobuyuki (1960) Sulfur isotopes and the origin of sandstone-type uranium deposits. *Biennial Progress Report for 1959-1960, US AEC AT (30-1)-2261*, 281 p
- Jerden JL Jr (2001) Origin of uranium mineralization at Coles Hill, Virginia (USA) and its natural attenuation within an oxidizing rock-soil-ground water system. *PhD thesis, Virginia Polytech Inst and State Univ, Blacksburg, Virginia*, 145 p
- Jerden JL Jr, Sinha AK (1999) Geology, mineralogy and geochemistry of the Coles Hill uranium deposit, Virginia: an example of a structurally controlled, hydrothermal apatite-coffinite-uraninite orebody. *Geol Soc Amer, abstr w progr*, v 31, no. 7, p A69
- Jobin DA (1962) Relation of the transmissive character of the sedimentary rocks of the Colorado Plateau to the distribution of uranium deposits. *US Geol Surv Bull* 1124, 151 p
- John EC (1978) Mineral zones in the Utah copper orebody. *Econ Geol*, v 73, pp 1250-1259
- Johnson BR, Miller TP, Karl S (1979) Uranium-thorium investigations of the Darby pluton, Seward Peninsula, Alaska. *US Geol Surv Circ* 804-B, pp 68-70
- Johnson CA (1977) Uranium and thorium occurrences in Precambrian rocks, Upper Peninsula of Michigan. *MS thesis, Michigan Tech Univ*, 106 p, 1 map
- Johnson HS Jr (1957) Uranium resources of the San Rafael district, Emery County, Utah - a regional synthesis. *US Geol Surv Bull* 1046-D, pp 37-54
- Johnson HS Jr (1959) Uranium resources of the Green River and Henry Mountains districts, Utah - a regional synthesis. *US Geol Surv Bull* 1087C, 104 p
- Johnson HS, Jr, Thordarson W (1966) Uranium deposits of the Moab, Monticello, White Canyon and Monument Valley districts, Utah and Arizona. *US Geol Surv Bull* 1222-H, pp H1-H53
- Johnson SY, Otton JK, Macke DL (1987) Geology of the Holocene surficial uranium deposit of the north fork of Flodelle Creek, northeastern Washington. *Geol Soc Amer Bull*, v 98, pp 77-85
- Johnson SY, Otton JK, Macke DL (1990) Geology of the Holocene surficial uranium deposit of the north fork of Flodelle Creek, northeastern Washington. *in: Short papers of the US Geol Surv uranium workshop*, pp 21-22
- Johnston JE (1977) Depositional systems in the Wilcox Group and the Carrizo Formation (Eocene) of central and south Texas and their relationship to lignite. *MSc thesis, Univ Texas, Austin*, 113 p
- Jones CA (1978a) A classification of uranium deposits in sedimentary rocks. *in: Mickle DG, ed., A preliminary classification of uranium deposits. US DOE, GJBX-63(78)*, pp 1-16
- Jones CA (1978b) Uranium occurrences in sedimentary rocks exclusive of sandstone. *in: Mickle DG, Mathews GW, eds., Geologic characteristics of environments favorable for uranium deposits. US DOE, GJBX-67(78)*, pp 1-86
- K**
- Kalliokoski J, Johnson CA (1976) Uranium and thorium occurrences in Precambrian rocks, Upper Peninsula of Michigan and northern Wisconsin, with thoughts on other possible settings. *US ERDA, Grand Junction, BJBX-48(76)* 294 p, 3 maps
- Kalliokoski J, Langford FF, Ojakangas RW (1978) Criteria for uranium occurrences in Saskatchewan and Australia as guides to favorability for similar deposits in the United States. *US DOE, GJBX-114(78)*, 480 p
- Karimov et al. (1996) Uranium deposits of the Uchkuduk type in the Republic of Uzbekistan. *Publ House Fan of Acad Sci of Rep Uzbekistan, Tashkent*, 334 p (in Russian)
- Karlson R, Krokosz M (1983) Brecciation and associated mineralization at the Schwartzwalder Mine, Jefferson County, Colorado. *in: Symposium brecciation and mineralization, geologic occurrence and genesis (abstr). Colorado Springs*, 1 p
- Karlstrom TNV, Swann GA, Eastwood RL, eds. (1974). *Geology of northern Arizona, with notes on archeology and paleoclimate; Part I, Regional studies;*

- Part II, Area studies and field guides. Guidebook, Geol Soc Amer, Rocky Mtn Sect Meet, Flagstaff, Arizona, 805 p
- Karsmizki KW (1990) U3O8, Uranium industry context statement. Prepared for UNRAR-West by Western History Research, Bozeman, Montana, 79 p
- Keefer WR (1970) Structural geology of the Wind River Basin, Wyoming. US Geol Surv Prof Paper 495-D, 35 p
- Keller WD (1959) Clay minerals in the mudstones of the ore-bearing formation. *in*: Garrels RM, Larsen ES III, compilers, Geochemistry and mineralogy of the Colorado Plateau uranium ores. US Geol Surv Prof Paper 320, pp 113-119
- Kelley VC (1951) Tectonics of the San Juan Basin. *in*: Guidebook of the south and west sides of the San Juan Basin, New Mexico and Arizona. Second Field Conf, New Mex Geol Soc, pp 124-131
- Kelley VC (1955) Influence of regional structure and tectonic history upon the origin and distribution of uranium on the Colorado Plateau. US Geol Surv Prof Paper 300, pp 171-178
- Kelley VC (1963b) Tectonic setting. *in* Geology and technology of the Grants Uranium Region. New Mex Bur Mines Miner Res Mem 15, pp 19-20
- Kelley VC, ed. (1963a) Geology and technology of the Grants Uranium Region. New Mex Bur Mines Miner Res Mem 15, 277 p
- Kelley VC, Kittel DF, Melancon, PE (1968) Uranium deposits of the Grants region. *in*: Ridge JD, ed., Ore deposits of the United States, 1933-1967 (Graton-Sales Vol), v I. Amer Inst Min, Metall, Petrol Eng, pp 747-769
- Kelly TD, Matos GR, cpls. (2005) Phosphorus statistics. *in*: Historical statistics for mineral and material commodities in the United States. US Geol Surv Data Series, no. 140 (unpaginated, available online only; latest additions 2007)
- Kendall EW (1971) Trend ore bodies of the Section 27 Mine, Ambrosia Lake uranium district, New Mexico. PhD Diss, Univ California, Berkeley, 167 p
- Kerr PF (1958) Uranium emplacement in the Colorado Plateau. Geol Soc Amer Bull, v 69, no. 9, pp 1075-1111
- Kerr PF (1968) The Marysvale, Utah, uranium deposits. *in*: Ridge JD, ed., Ore deposits of the United States, 1933-1967 (Graton-Sales Vol). Amer Inst Min Metall Petrol Eng, New York, v 2, pp 1020-1042
- Kerr PF, Brophy GP, Dahl HM, Green J, Woolard LE (1957) Marysvale, Utah, uranium area. Geol Soc Amer Spec Paper 64, 212 p
- Kerr PF, Kelley DR (1956) Urano-organic ores of the San Rafael Swell, Utah. Econ Geol, v 51, pp 386-390
- Kerr PF, Kulp JL (1952) Precambrian uraninite, Sunshine Mine, Idaho. Science, v 115, pp 86-88
- Kimberley MM (1978a) Short course in uranium deposits: their mineralogy and origin. Miner Ass Can, v 3, Univ Toronto Press, Toronto, 521 p
- Kimberley MM (1978b) Origin of stratiform uranium deposits in sandstone, conglomerate, and pyroclastic rock. *in*: Kimberley MM, ed., Short course in uranium deposits: their mineralogy and origin. Miner Ass Can, v 3, pp 339-381
- King JW, Austin SR (1966) Some characteristics of rolltype uranium deposits at Gas Hills, Wyoming. Min Eng, v 18, no. 5, pp 73-80
- Kirchheimer F (1963) Das Uran und seine Geschichte. E. Schweizerbart'sche Verlagsbuchhandlung, Stuttgart, 372 p
- Kirk AR, Condon M (1986) Structural control of sedimentation patterns and the distribution of uranium deposits in the Westwater Canyon Member of the Morrison Formation, northwestern New Mexico - A subsurface study. *in*: Turner-Peterson CE, Santos ES, Fishman NS, eds., A basin analysis case study - the Morrison Formation, Grants Uranium Region, New Mexico. Amer Ass Petrol Geol, Studies in Geology, no. 22, pp 105-143
- Kirk AR, Huftman Jr, HC, Zech RS (1986) Design and results of the Mariano Lake-Lake Valley drilling project, northwestern New Mexico. *in*: Turner-Peterson CE, Santos ES, Fishman NS, eds., A basin analysis case study - the Morrison Formation, Grants Uranium Region, New Mexico. Amer Ass Petrol Geol, Studies in Geology, no. 22, pp 227-240
- Kirkham RM, O'Leary WJ, Warner JW (1980) Hydrogeologic and stratigraphic data pertinent to uranium mining, Cheyenne Basin, Colorado. Colo Geol Surv, Dpt Natural Res, Info Ser 12, 21 p
- Kish SA (1977) Geochronology of plutonic activity in the Inner Piedmont and Kings Mountain belt in North Carolina. *in*: Burt ER, ed., Field guides for the Geological Society of America Southeastern Section Meeting, Winston-Salem, North Carolina, Raleigh. North Carolina Dpt Natural and Economic Res, Geol Mineral Res Sect, pp 144-149
- Kish SA, Butler JR, Fullager PD (1979) The timing of metamorphism and deformation in the central Piedmont of North Carolina. Geol Soc Amer, abstr w progr, v 11, pp 184-185
- Kittel DF (1963) Geology of the Jackpile Mine area. *in*: Kelley VC, ed., Geology and technology of the Grants Uranium Region. New Mex Bur Mines Miner Res Mem 15, pp 167-176
- Kittel DF, Kelley VC, Melancon PE (1967) Uranium deposits of the Grants region. *in*: 18th Field Conf Guidebook, Defiance-Zuni-Mt Taylor Region, New Mexico Geol Soc, pp 173-183
- Klemic H (1962) Uranium occurrences in sedimentary rocks of Pennsylvania. US Geol Surv Bull 1107-D, pp D243-D288
- Klemic H et al. (1959a) Radioactive rare-earth deposit at Scrub Oaks mine, Morris County, New Jersey. US Geol Surv Bull 1082-B, part IV, pp 29-59
- Klemic H et al. (1959b) Uranium in Phillips mine - Camp Smith area, Putnam and Westchester Counties, New York. US Geol Surv Bull 1074-E, part IV, pp 165-199
- Klemic H, Warman JC, Taylor AR (1963) Geology and uranium occurrences of the northern half of the Leighton, Pennsylvania quadrangle and adjoining areas. US Geol Surv Bull 1138, 97 p
- Klingmuller LML (1989) The Green Mountain uranium district, central Wyoming: type locality of solution front limb deposits. *in*: Uranium resources and geology of North America. TECDOC-500, IAEA, Vienna, pp 173-190
- Klohn ML, Pickens WR (1970) Geology of the Felder uranium deposit, Live Oak County, Texas. Soc Min Eng, Amer Inst Min Metal Petrol Eng, preprint, no. 70-1-38, 19 p
- Knox JW, Gruner JW (1957) Mineralogy of the Ambrosia Lake uranium deposits in McKinley Connty, New Mexico. Annual report for April 1, 1956 to March 31, 1957, US AEC, RME-3148, pp 5-28
- Koch GS, et al. (1964) Statistical interpretation of sample assay data from the Mi Vida uranium mine, Big Indian district, San Juan County, Utah. US Bur Mines Rep Invest 6550, 40 p
- Kochenov AV, Zinevye VV, Lovaleva SA (1965) Some features of the accumulation of uranium in peat bogs. Geochem Intern, v 2, no. 1, pp 65-70
- Koerberlin FR (1938) Sedimentary copper, vanadium-uranium, and silver in southwestern United States. Econ Geol, v 33, pp 458-461
- Kofford ME (1969) The Orphan mine. *in*: Baars DL, ed., Geology and natural history of the Grand Canyon region. *in*: Guidebook, 5th Annual Field Conf Powell Centennial River Expedition, Durango, Four Corners Geol Soc, pp 190-194
- Kovsach AA Jr, Nylund RL (1981) General geology of uranium-vanadium deposits of Salt Wash sandstones, La Sal area, San Juan County, Utah. *in*: Epis RC, Callender JF, eds., Guidebook, 32nd Field Conf, Western Slope Colorado, New Mex Geol Soc, pp 171-176
- Kozusko RG, Saucier AE (1980) The Bernabe Montano uranium deposit, Sandoval County, New Mexico. *in*: Rautman CA, ed., Geology and mineral technology of the Grants Uranium Region 1979. New Mex Bur Mines Miner Res Mem 38, pp 262-268
- Kreitler CW (1979) Ground-water hydrology of depositional systems. *in*: Depositional and ground-water flow systems in exploration for uranium. Univ Texas, Austin, Bur Econ Geol, pp 118-176
- Krewedl D (1979) Stratigraphy and structural analysis of the Gas Hills area, central Wyoming (USA). Z dt geol Ges, v 130, pp 627-640
- Krewedl DA, Carisey JC (1986) Contributions to the geology of uranium mineralized breccia pipes in northern Arizona. Arizona Geol Soc Digest, Tucson, v XVI, pp 179-186
- Kwarteng AY, Chavez, PS Jr, Wenrich KJ, Goodell PC (1988) Application of Landsat Thematic Mapper digital data to the exploration for uranium-mineralized breccia pipes in northwestern Arizona. *in*: 6th Thematic Conf, Houston, Tex, Ann Arbor, Mich, Environ Research Inst Michigan, pp 239-248
- Lageson DR, Hausel DH, eds. (1978) Occurrences of uranium in Precambrian and younger rocks of Wyoming and adjacent areas (abstracts). Geol Surv Wyoming, Publ Inf Circ 7, 37 p

- Lancelot JR, de Saint-André (1982) U-Pb systematics and genesis of U deposits: Bokan Mountain (Alaska) and Lodève (France). 5th Intern Conf Geochron, Cosmochron, Isotope Geol, Nikko National Park, Japan, Abstracts, pp 206-207
- Landais P (1986) Geochemical analyses of the organic matter associated with the breccia pipes in the Grand Canyon area. *Geol Soc Amer, Rocky Mountain Section, abstr w progr* 18(5), p 389
- Landais P, Meyer A, Carisey JC, Krewell DA, Brosse E, Forbes P (1989) Geothermal analyses of the breccia pipes (Arizona) - Organic matter, fluid inclusions, fission tracks and computerized modeling (abstr). *in: Uranium resources and geology of North America*. IAEA, Vienna, p 239
- Landis ER (1962) Uranium and other trace elements in Devonian and Mississippian black shales in the central midcontinent area: *US Geol Surv Bull* 1107-E, pp 289-336
- Landmark/Weston (1988) Navajo AML Project. pp 2-4 to 2-9
- Langen RE, Kidwell AL (1974) Geology and geochemistry of the Highland uranium deposit, Converse County, Wyoming. *Mountain Geologist*, v 11, no. 2, pp 85-93
- Langford FF (1977) Surficial origin of North American pitchblende and related uranium deposits. *Amer Ass Petrol Geol Bull*, v 61, pp 28-42
- Langmuir D (1978) Uranium solution-mineral equilibria at low temperatures with applications to sedimentary ore deposits. *Geochim Cosmochim Acta* 42, pp 547-569
- Langmuir D, Applin K (1977) Refinement of the thermodynamic properties of uranium minerals and dissolved species, with application to the chemistry of ground waters in sandstone-type uranium deposits. *in: Campbell JA, ed., Short papers of the US Geol Surv Uranium-Thorium Symp 1977*. *US Geol Surv Circ* 753, pp 57-60
- Lanier G, John EC, Swensen AJ, Reid J, Bard CE, Caddey SW, Wilson JC (1978) General geology of the Bingham mine, Bingham Canyon, Utah. *Econ Geol* v 73, pp 1228-1241
- Lanphere MA, Mackevett EH Jr, Stern TW (1964) Potassium-argon and lead-alpha ages of plutonic rocks, Bokan Mountain, Alaska. *Sci*, v 145, pp 705-707
- LaPoint DJ, Markos G (1977) Geochemical interpretation of ore zonation at the Rifle vanadium mine, Colorado. *in: Campbell JA, ed., Short papers of the US Geol Surv Uranium-Thorium Symp 1977*. *US Geol Surv Circ* 753, pp 53-55
- Larsen ES Jr, Gottfried D (1961) Distribution of uranium in rocks and minerals of Mesozoic batholiths in Western United States. *US Geol Surv Bull* 1070-C, 63 p
- Larsen ES Jr, Gottfried D, Molloy M (1958) Distribution of uranium in the volcanic rocks of the San Juan Mountains, southwestern Colorado. *Second Intern Conf Peaceful Uses Atomic Energy*, UN, Geneva, 2, pp 509-514
- Lattanzi CR, Pressacco R (2005) Technical report on the Allemand Ross, Wyoming, and Swinney Switch, Texas, uranium projects. (Prepared for) High Plains Uranium, Inc. Micon International Limited. 103 p (Sept 2, 2005)
- Laverty RA, Gross EB (1956) Paragenetic studies of uranium deposits of the Colorado Plateau. *US Geol Surv Prof Paper* 300, pp 195-202
- Leach DL, Hofstra AH, Church SE, Snee LW, Vaughn RB, Zartman, RE (1998) Evidence for Proterozoic and Late Cretaceous-Early Tertiary ore-forming events in the Coeur d'Alene district, Idaho and Montana. *Econ Geol*, v 93, pp 347-359
- Leach FI (1920) Radium ore discovered in White Signal district, N. Mexico. *Eng Min J*, v 109, p 989
- Lease LW (1980) Geologic report on East Chaco drilling project, McKinley and San Juan Counties, New Mexico. *US DOE, GJBX-98(80)*, 62 p
- Lee MJ (1976) Geochemistry of the sedimentary uranium deposits of the Grants mineral belt, southern San Juan Basin, New Mexico. PhD diss, Univ New Mex, Albuquerque, 241 p (unpubl)
- Lee MJ, Brookins DG (1978) Rubidium-strontium minimum ages of sedimentation, uranium mineralization and provenance, Morrison Formation (Upper Jurassic), Grants Mineral Belt, New Mexico. *Amer Ass Petrol Geol*, v 62, no. 9, pp 1673-1683
- Lee MJ, Brookins DG (1980) Rubidium-strontium minimum ages of sedimentation, uranium mineralization, and provenance, Morrison Formation (Upper Jurassic), Grants mineral belt, New Mexico - Reply. *Amer Ass Petrol Geol Bull*, v 64, p 1719
- Lehmann JP (Dec 2007 to Jan 2009) UraNews (monthly press clipping about natural uranium activities around the world), compiled by Jean-Paul Lehmann, Paris, France
- Leicht WC (1971) Minerals of the Grandview mine. *Mineral Record*, Sept/Oct edition, pp 215-221
- Lekas MA, Dahl HM (1956) The geology and uranium deposits of the Lisbon Valley anticline, Utah. *in: Peterson JA, ed., Geology and economic deposits of east-central Utah*. 7th Field Conf, Intermount Ass Petrol Geol, Salt Lake City, pp 161-168
- Lesure FG, Motooka JM, Weis PL (1977) Exploration geochemical studies of some sandstone copper-uranium deposits, Bradford, Columbia, and Lycoming counties, Pennsylvania. *US Geol Surv, J Res*, v 5, pp 609-621
- Leventhal J, Daws T, Frye J (1986) Organic geochemical analysis of sedimentary organic matter associated with uranium. *Appl Geochem*, v 1, pp 241-247
- Leventhal JC, Granger HC (1977) Conceptual-mathematical models of uranium ore formation in sandstone-type deposits. *in: Campbell JA, ed., Short papers of the US Geol Surv Uranium-Thorium Symp 1977*. *US Geol Surv Circ*, p 753
- Leventhal JS (1980) Organic geochemistry and uranium in the Grants mineral belt. *in: Rautman CA, ed., Geology and mineral technology of the Grants Uranium Region 1979*. *New Mex Bur Mines Miner Res Mem* 38, pp 75-84
- Leventhal JS Threlkeld CN (1978) Carbon-13/Carbon-12 fractionation of organic matter associated with uranium ores induced by alpha irradiation. *Sci*, v 202, pp 430-432
- Lewis RQ Sr, Campbell RH (1965) Geology and uranium deposits of Elk Ridge and vicinity, San Juan County, Utah. *US Geol Surv Prof Paper* 474-B
- Lewis RQ Sr, Trimble DE (1959) Geology and uranium deposits of Monument Valley, San Juan County, Utah. *US Geol Surv Bull* 1087-D, pp 105-131
- Lewis WD (1977) Geology of uranium mineralization in the Browns Park Formation, Carbon County, Wyoming, and Moffat County, Colorado. Master's thesis, Colo Sch Mines, Golden, Colorado, 85 p
- Lindgren W (1933) Mineral deposits. McGraw-Hill, New York, London, 930 p
- Lindsey DA (1978) Geology of the Yellow Chief Mine, Thomas Range, Juab County, Utah. *in: Shawe DR, ed., Guidebook to mineral deposits of the central Great Basin*. *Nevada Bur Mines Geol Rep* 32, pp 65-68
- Lindsey DA (1981) Volcanism and uranium mineralization at Spor Mountain, Utah. *in: Goodell PC, Waters AC, eds., Uranium in volcanic and volcanoclastic rocks*. *Amer Assoc Petrol Geol, Studies in Geology* 13, pp 89-98
- Lindsey DA (1982) Tertiary volcanic rocks and uranium in the Thomas Range and northern Drum Mountains, Juab County, Utah. *US Geol Surv Prof Paper* 1221, 71 p
- Lineberger DH Jr (1983) Geology of the Chatham fault zone, Pittsylvania County, Virginia. MS thesis, Univ North Carolina, Chapel Hill, 79 p (unpubl)
- Lisitsyn AK (1969) Conditions of molybdenum and selenium deposition in exogenous epigenetic uranium deposits. *Lithol Mineral Resources*, v 5, p 542 (in Russian)
- Lisitsyn AK, Kuznetsova EC (1967) Role of micro-organisms in development of geochemical reduction barriers where limonitization bedded zones wedge-out. *Intern Geol Review*, v 9, no. 9, pp 1180-1191
- Livingston DE (1969) Geochronology of Older Precambrian rocks in Gila County, Arizona. PhD diss, Univ Arizona, Tucson
- Loring WB (1958) Geology and ore deposits of the northern part of the Big Indian district, San Juan County, Utah. PhD thesis, Univ Arizona, Tucson
- Love JD (1964) Uraniferous phosphatic lake beds of Eocene age in intermontaine basins of Wyoming and Utah. *US Geol Surv Prof Paper* 474-E. 66 p
- Love JD (1970) Cenozoic geology of the Granite Mountains area, central Wyoming. *US Geol Surv Prof Paper* 495-C, pp C1-C154
- Loving JG (1956) Radioactive deposits in New Mexico. *US Geol Surv Bull* 1009-L, pp 315-390
- Loving TS, Goddard EN (1950) Geology and ore deposits of the Front Range, Colorado. *US Geol Surv Prof Paper* 223, 319 p
- Lucas SG, Anderson (1996) The Middle Jurassic Todilto salina basin, American Southwest. *in: Morales M, ed., The continental Jurassic*. *Museum North Arizona Bull* 60, pp 470-482
- Ludwig KR (1978) Uranium-daughter migration and U-Pb isotope apparent ages of uranium ores, Shirley Basin Wyoming. *Econ Geol*, v 73, pp 29-49

- Ludwig KR (1979) Age of uranium mineralization in the Gas Hills and Crooks Gap districts, Wyoming, as indicated by U-Pb isotope apparent ages. *Econ Geol*, v 74, pp 1654-1668
- Ludwig KR (1980) Rubidium-strontium minimum ages of sedimentation, uranium mineralization, and provenance, Morrison Formation (Upper Jurassic), Grants mineral belt, New Mexico: Discussion. *Amer Ass Petrol Geol*, v 64, pp 1718-1719
- Ludwig KR, Goldhaber MB, Reynolds RL, Simmons KR (1982a) Uranium-lead isochron age and preliminary sulfur isotope systematics of the Felder uranium deposit, south Texas. *Econ Geol*, v 77, pp 557-563
- Ludwig KR, Grauch RI (1980) Coexisting coffinite and uraninite in some sandstone-host uranium ores of Wyoming. *Econ Geol*, v 75, pp 296-302
- Ludwig KR, Lindsey DA, Zielinski RA, Simmons KR (1980) U-Pb ages of uraniferous opals and implications for the history of beryllium, fluorine and uranium mineralization at Spor Mountain, Utah. *Earth Planet, Sci Letter*, v 46, pp 221-232
- Ludwig KR, Nash JT, Naeser CW (1981) U-Pb isotope systematics and age of uranium mineralization, Midnite Mine, Washington. *Econ Geol*, v 76, pp 89-110
- Ludwig KR, Rasmussen JD, Simmons KR (1986) Age of uranium ores in collapse-breccia pipes in the Grand Canyon area, northern Arizona. *Geol Soc Amer Bull*, abstr w progr, v 18, no. 5, p 392
- Ludwig KR, Rubin B, Fishman NS, Reynolds RL (1982b) U-Pb ages of uranium ores in the Church Rock uranium district, New Mexico. *Econ Geol*, v 77, pp 1942-1945
- Ludwig KR, Simmons KR (1988) Progress in U/Pb isotope studies of collapse-breccia pipes in the Grand Canyon region, northern Arizona. *Geol Soc Amer*, abstr w progr, v 20, no. 7, p A 139
- Ludwig KR, Simmons KR (1992) U-Pb dating of uranium deposits in collapse breccia pipes of the Grand Canyon region. *Econ Geol*, v 87, pp 1747-1765
- Ludwig KR, Simmons KR, Webster JD (1984) U-Pb isotope systematics and apparent ages of uranium ores, Ambrosia Lake and Smith Lake districts, Grants mineral belt, New Mexico. *Econ Geol*, v 79, pp 322-337
- Ludwig KR, Szabo BN, Granger HC (1977) Pleistocene apparent ages by U-Pb isotope and U-series methods for uranium ore in Dakota Sandstone near Gallup, New Mexico. *US Geol Surv J Res*, v 5, no. 6, pp 669-672
- Ludwig KR, Wallace AR, Simmons KR (1985) The Schwartzwalder uranium deposit, II: Age of mineralization and lead isotope constraints on source areas. *Econ Geol*, v 80, pp 1858-1871
- Ludwig KR, Young EJ (1975) Absolute age of disseminated uraninite in Wheeler Basin, Grand County, Colorado. *US Geol Surv J Res*, v 3, no. 6, pp 747-751
- Lupe R (1976) Deposition environments as a guide to uranium mineralization in the Chinle Formation, San Rafael Swell, Utah. *US Geol Surv Open-File Rep* 76-283, 18 p
- Lyons JB (1961) Uranium and thorium in the older plutonic rocks of New Hampshire. *Art 32, US Geol Surv Prof Paper* 424-B, B 69
- Lyons JB (1964) Distribution of thorium and uranium in three early Paleozoic Plutonic Series of New Hampshire. *US Geol Surv Bull* 1144-F, 43 p
- Magleby DN (1961) Orphan Lode uranium mine, Grand Canyon, Arizona. *US AEC Techn Memo* TM-134, 8 p
- Mahood GA (1983) Review of uranium in volcanic and volcanoclastic rocks. *in: Goodell P, Waters A, eds., (1981) Econ Geol*, v 78, pp 546-551
- Malan RC (1959) Geology and uranium deposits of the Marshall Pass district, Gunnison, Saguache and Chaffee Counties, Colorado. *Natl Western Mining Conf*, Denver, Colorado, *manusc*, 12 p
- Malan RC (1968) The uranium mining industry and geology of the Monument Valley and White Canyon districts, Arizona and Utah. *in: Ridge, J. D., ed., Ore deposits of the United States, 1933-1967*, v 1. *Amer Inst Min Metal Petrol Eng*, pp 790-804
- Malan RC (1972) Summary report - distribution of uranium and thorium in the Precambrian of the western United States. *US AEC, AEC-RD-12*, 59 p
- Malan RC, Ranspot HW (1959) Geology of the uranium deposits in the Cochetopa mining district, Saguache and Gunnison Counties, Colorado. *Econ Geol*, v 54, pp 1-19
- Malan RC, Sterling DA (1969a) A geologic study of uranium resources in Precambrian rocks of the western United States: an introduction to the distribution of uranium and thorium in Precambrian rocks including the results of preliminary studies in the southwestern United States. *US AEC, AEC-RD-9*, 54 p
- Malan RC, Sterling DA (1969b) A geologic study of uranium resources in Precambrian rocks of the western United States: distribution of uranium and thorium in Precambrian rocks of the western Great Lakes Region. *US AEC, AEC-RD-10*, 25 p
- Malan RC, Sterling DA (1970) A geologic study of uranium resources in Precambrian rocks of the western United States: distribution of uranium and thorium in the Precambrian of the west-central and northwest United States. *US AEC, AEC-RD-11*, 64 p
- Mallory WW et al., eds. (1972) *Geologic atlas of the Rocky Mountain region*. Rocky Mountain Ass Geol, Denver, Col, 331 p
- Manheim FT, Gulbransen RA (1979) Marine minerals. *Chap. 6. Burns RG, ed., Reviews in Mineralogy*, v 6, Mineral Soc Amer, pp 151-173
- Marjanemi DK, Basler AL (1972) Geochemical investigations of plutonic rocks in the western United States for the purpose of determining favorability for vein-type uranium deposits. *US AEC, GJO-912-16*, 134 p
- Marjanemi DK, Robins JW (1975a) Uranium favourability of Tertiary sedimentary rocks of the Lower Spokane River Valley and of northern Spokane County, Washington. *US DOE, Grand Junction, GJBX-1(76)*, 64 p
- Marjanemi DK, Robins JW (1975b) Uranium favourability of Tertiary sedimentary rocks of the western Okanogan Highlands and of the upper Columbia River valley, Washington. *US DOE, Grand Junction, GJBX-2(76)*, 388 p
- Marjanemi DK, Robins JW (1975c) Uranium favourability of Tertiary sedimentary rocks of the Pend Oreille River valley, Washington. *US DOE, Grand Junction, GJBX-3(76)* 150 p
- Marline Uranium Corporation (1983) An evaluation of uranium development in Pittsylvania County Virginia: report submitted jointly by Marline Uranium Corporation and Union Carbide Corporation to the Virginia Uranium Administrative Group Pursuant to Section 45.1-285.1 et seq of the Code of Virginia (1983) (Senate Bill 155), (Oct 15, 1983)
- Martinez R (1979) Provenance study of the Westwater Canyon and Brushy Basin Members of the Morrison Formation between Gallup and Laguna, New Mexico. *PhD diss, Univ New Mex, Albuquerque*, 79 p (unpubl)
- Marvin RF, Dobson SW (1979) Radiometric ages, compilation B, *US Geol Surv Isochron West no. 25*
- Maslyn RM (1978) An epigenetic model for the formation of the Schwartzwalder uranium deposit. *Econ Geol*, v 73, pp 552-557
- Masursky H (1962) Uranium-bearing coal in the eastern part of the Red Desert area, Wyoming. *US Geol Surv Bull* 1099-B, pp B1-B152
- Mathews GW (1978a) Uranium occurrences in and related to plutonic igneous rocks. *in: Mickle DG, Mathews GW, eds., Geologic characteristics of environments favorable for uranium deposits*. *US DOE, GJBX67(78)*, pp 121-180
- Mathews GW (1978b) Uranium occurrences of uncertain genesis. *in: Mickle DG, Mathews GW, eds., Geologic characteristics of environments favorable for uranium deposits*. *US DOE, GJBX-67(78)*, pp 221-250
- Mathews GW, Jones CA, Pilcher RC, D'Andrea RF Jr (1979) Preliminary recognition criteria for uranium occurrences: a field guide. *US DOE, GJBX-32(79)*, 41 p

M

- Mathewson DE (1953a) Geology of the Poison Canyon mine, Valencia County, Sec 19, T 13 N, R 9 W, near Grants, New Mexico. US AEC, TM-24, 7 p
- Mathisen IW Jr (1987) Arizona Strip breccia pipe program: Exploration, development, and production [abstr.]. *Amer Ass Petrol Geol Bull*, v 71, p 590
- Maxwell RD (2002) Domestic uranium resources and their availability. *Amer Ass Petrol Geol*, Ann Meet, Houston, Abstr CD-ROM
- Maxwell RD, Gibbs BL, Pool TC, Keim KS, Christopher PA (2008) Technical report on the Coles Hill uranium property, Pittsylvania County, Virginia, United States of America. Report prepared for Virginia Uranium Corp., 30 June 2008, 86 p
- McBride EF, Lindemann WL, Freeman PS (1968) Lithology and petrology of the Gueydan (Catahoula) Formation in south Texas. *Univ Texas, Austin, Bur Econ Geol Rep Invest* 63, 122 p
- McCammon RB, Finch WI, Kork JO, Bridges NJ (1986) Estimation of uranium endowment in the Westwater Canyon Member, Morrison Formation, San Juan Basin, using a data-directed numerical method. *in: Turner-Peterson CE, Santos EC, Fishman NS, eds., A basin analysis case study - The Morrison Formation, Grants Uranium Region, New Mexico. Amer Ass Petrol Geol, Studies in Geology*, no. 22, pp 331-355
- McCammon RB, Finch WI, Kork JO, Bridges NJ (1986) Estimation of uranium endowment in the Westwater Canyon Member, Morrison Formation, San Juan Basin, using a data-directed numerical method. *in: Turner-Peterson CE, Santos EC, Fishman NS, eds., A basin analysis case study - The Morrison Formation, Grants Uranium Region, New Mexico. Amer Ass Petrol Geol, Studies in Geology*, no. 22, pp 331-355
- McCarn DW (2001) The Crownpoint and Churchrock uranium deposits, San Juan Basin, New Mexico: An ISL mining perspective. *in: Assessment of uranium deposit types and resources - a worldwide perspective. TECDOC-1258, IAEA, Vienna*, pp 171-184
- McCauley JF (1961) Uranium in Pennsylvania. *Pennsylvania Geol Surv Bull* M 43, 71 p
- McEldowney RC, Abshier JF, Lootens DJ (1977) Geology of uranium deposits in the Madison Limestone, Little Mountain area, Big Horn County, Wyoming. *in: 1977 Symp, Rocky Mtn Ass Geol*, pp 321-336
- McGinley FE (1980) Potential by-product uranium production in the U.S.A. IAEA Rep-SM-239/15, IAEA, Vienna, pp 293-307
- McKee ED (1978) Paleozoic rocks of the Grand Canyon. *in: Breed WJ, Roat E, eds., Geology of the Grand Canyon (3rd ed.)*. Museum North Arizona and Grand Canyon Natural Hist Ass, pp 42-64
- McKee ED (1982) The Supai Group of Grand Canyon. *US Geol Surv Prof Paper* 1173, 504 p
- McKee ED, Gutschick RC (1969) History of the Redwall Limestone of northern Arizona. *Geol Soc Amer Mem* 114, 726 p
- McKee EH (1976) Origin of the McDermitt caldera in Nevada and Oregon and related mercury deposits. *Trans Soc Min Eng* 260, pp 196-199
- McKee EH, MacLeod NS, Walker GW (1976) Potassium-argon ages of Late Cenozoic silicic volcanic rocks, southeast Oregon. *Isochron West* 15, pp 37ff
- McKee EH, Silberman ML, Marvin RE, Obradovich JD (1971) A summary of radiometric ages of Tertiary volcanic rocks in Nevada and eastern California. Part I. Central Nevada. *Isochron West* 2, pp 21-42
- McKelvey VE (1956) Uranium in phosphate rock. *US Geol Surv Prof Paper* 300, pp 477-481
- McKelvey VE, Carswell LD (1956) Uranium in the Phosphoria Formation. *US Geol Surv Prof Pap* 300, pp 483-487
- McKelvey VE, Everhart DL, Garrels RM (1955) Origin of uranium deposits. 50th Anniversary Vol, *Econ Geol*, pp 474-492
- McKelvey VE, William JS, Sheldon RP, Cressman ER, Cheney TM, Swanson RW (1956) Summary descriptions of Phosphoria, Park City, and Shedhorn Formations in western phosphate field. *Amer Ass Petrol Geol Bull*, v 40, pp 2326-2363
- McKnight WM Jr (1972) A review of South Texas uranium geology. *Gulf Coast Ass Geol Soc Trans*, v 22, pp 97-103
- McLaughlin ED Jr (1963) Uranium deposits in the Todilto Limestone of the Grants District; *in: Kelley VC, compiler, Geology and technology of the Grants uranium region. New Mex Bur Mines Miner Res, Mem* 15, pp 136-149
- McLemore VT (1983) Uranium and thorium occurrences in New Mexico - distribution, geology, production, and resources. *New Mex Bur Mines Miner Res Open-File Rep* 183, 180 p
- McLemore VT (2002) Uranium in New Mexico. *in: Decision-Makers Field Conf 2002. New Mex Bur Geol Miner Res*, pp 30-34
- McLemore VT, Chenoweth WL (1989) Uranium resources in New Mexico. *New Mex Bur Mines Miner Res. Resource Map* 18, 36 p
- McLemore VT, Chenoweth WL (1991) Uranium mines and deposits in the Grants district, Cibola and McKinley Counties, New Mexico. *New Mex Bur Mines Miner Res Open-File Rep* 353, 22 p
- McLemore VT, Chenoweth WL (1997) Geology and uranium-vanadium deposits in the Salt Wash Member, Morrison Formation, King Tut Mesa area, San Juan County, New Mexico. *in: Guidebook* 48, *New Mex Geol Soc*, pp 273-278
- McLemore VT, Chenoweth WL (2003) Uranium resources in the San Juan Basin, New Mexico. *in: Guidebook, 54th Field Conf, New Mex Geol Soc*, pp 163-175
- McLemore VT, Donahue K, Krueger CB, Rowe A, Ulbricht L, Jackson MJ, Breese MR, Jones G, Wilks M (2002) Database of the uranium mines, prospects, occurrences, and mills in New Mexico. *New Mex Bur Geol Miner Res Open-File Rep* 461 (CD-ROM)
- McLennan SM, Taylor SR (1979) Rare earth element mobility associated with uranium mineralization. *Nature*, v 282, pp 247-249
- McMurray JM (2000a) Uranium production in North America. *in: Gavrilin VI et al., eds., Uranium at the turn of the century: resources, production, demand. Abstracts Intern Symp Uran Geol, Moscow, All-Russian Sci-Res Inst Miner Res NM Fedorovsky*, pp 31-32
- McMurray JM (2000b) Geology and uranium resources of the Arizona Strip breccia pipes, U.S.A. *in: Gavrilin VI et al., eds., Uranium at the turn of the century: resources, production, demand. Abstracts Intern Symp Uran Geol, Moscow, All-Russian Sci-Res Inst Miner Res NM Fedorovsky*, pp 85-87
- McRae OM, Grubaugh PL (1957) Geology of uranium deposits in the Inter-River area, Grand and San Juan Counties, Utah. US AEC, RME-112
- Megruie GH, Kerr PF (1965) Alteration of sandstone pipes, Laguna, New Mexico. *Geol Soc Amer Bull*, v 76, no. 12, pp 1347-1360
- Megruie GH, Kerr PF (1968) Alteration of sandstone pipes, Laguna, New Mexico - reply. *Geol Soc Amer Bull*, v 79, pp 791-794
- Melin RE (1964) Description and origin of uranium deposits in Shirley Basin, Wyoming. *Econ Geol*, v 59, pp 835-849
- Melin RE (1969) Uranium deposits in Shirley Basin, Wyoming. *Wyoming Univ Contr Geol*, v 8, pp 143-149
- Melvin JW (1976) Systematic distribution of large uranium deposits in the Grants Uranium Region, New Mexico. *in: Tectonics and mineral resources of southwestern North America. New Mex Geol Ass Spec Publ* 6, pp 144-150
- Meneghel L (1981) A model of the progresses forming sedimentary-hosted uranium deposits. *Econ Geol*, v 76, pp 727-732
- Meunier JD (1984) Les phénomènes d'oxydo-réduction dans un gisement urano-vanadifère de type tabulaire: les grès du Salt-Wash (Jurassique Supérieur), district minier de Cottonwood-Wash (Utah, Etats-Unis). *Géol Géochim Uranium, Nancy, Mém*, no. 4, 214 p
- Meunier JD (1989) Diagenesis and ore deposition in sandstone-hosted uranium-vanadium deposits in the Colorado Plateau: evidence from fluid inclusions. *in: Uranium resources and geology of North America. TECDOC-500, IAEA, Vienna*, pp 227-238
- Meunier JD, Breit GN (1987) Fluid inclusion studies in calcite associated with sandstone-hosted uranium-vanadium deposits of the Colorado Plateau (abstr). IAEA Meeting, Saskatoon, 1 p
- Meunier JD, Landais P, Monthieux M, Pagel M (1987) Oxidation-reduction processes in the genesis of the uranium-vanadium tabular deposits of the Cottonwood Wash mining area (Utah, USA): evidence from petrological study and organic matter analysis. *Bull Minér*, 110, pp 145-156
- Meyertons CT (1963) Triassic formations of the Danville basin. *Virginia Div Mineral Res Rep, Invest* 6, 65 p
- Miall AD (1977) A review of the braided river depositional environment. *Earth Sci Rev*, v 13, pp 1-62
- Mickle DG, ed., (1978) A preliminary classification of uranium deposits. US DOE, GJBX-63(78), 78 p
- Mickle DG, Mathews GW (1978) Geologic characteristics of environments favorable for uranium deposits. US DOE, GJBX-67(78), 250 p

- Miesch AT (1962) Composition of sandstone host rocks of uranium deposits. *Amer Inst Min Metal Petrol Eng Trans*, v 223, pp 178-184
- Miesch AT (1963) Distribution of elements in Colorado Plateau uranium deposits—a preliminary report. *US Geol Surv Bull* 1147-E, pp E1-E57
- Miller DS, Kulp JL (1963) Isotopic evidence on the origin of the Colorado Plateau uranium ores. *Geol Soc Amer Bull*, v 74, pp 609-630
- Miller FK, Engels JC (1975) Distribution and trends of discordant ages of the plutonic rocks of northeastern Washington and northern Idaho. *Geol Soc Amer Bull*, v 86, pp 517-528
- Miller LJ (1955) Uranium ore deposits of the Happy Jack deposit, White Canyon, San Juan Connty, Utah. *Econ Geol*, v 50, pp 156-169
- Miller RD (1954a) Copper-uranium deposit at the Ridenour mine. Hualapai Indian Reservation, Coconino County, Arizona, Part 1. *US AEC, RME-2014*, pp 3-18
- Miller RD (1954b) Reconnaissance for uranium in the Hualapai Indian Reservation area, Mohave and Coconino counties, Arizona. *US AEC, RME-2007*, 15 p
- Miller TS, Bunker CM (1976) A reconnaissance study of the uranium and thorium contents of plutonic rocks of the southeastern Seward Peninsula, Alaska. *US Geol Surv J Research*, v 4, pp 367-77
- Millmine K, Lewis D (2007) ISR production resumption from a historic project at Moore Ranch. *Global Uran Symp*, Corpus Christi, Texas, 24 p
- Milne PC (1979) Uranium in Washington state: proven deposits and exploration targets. *CIM Bull*, v 72, no. 804, pp 95-101
- Mitcham TW, Evensen CG (1955) Uranium ore guides, Monument Valley district, Arizona. *Econ Geol*, v 50, pp 170-176
- Mitchell RJ (1965) Uranium-bearing lignite - North Dakota's newest industry. *Metal Mining Proc*, v 2, no. 3, pp 17-23
- Moench RH (1962) Properties and paragenesis of coffinite from the Woodrow mine, New Mexico. *Amer Miner*, v 47, no. 1, pp 26-33
- Moench RH (1963) Geologic limitations on the age of uranium deposits in the Laguna district. *in: Kelley VC, ed., Geology and technology of the Grants Uranium Region*. *New Mex Bur Mines Miner Res Mem* 15, pp 157-166
- Moench RH, Schlee JS (1959) Laguna district, New Mexico. *in: Geologic investigations of radioactive deposits, Semi-annual progress report for December 1, 1958, to May 31, 1959*. *US AEC, TEI-751*, pp 14-32
- Moench RH, Schlee JS (1967) Geology and uranium deposits of the Laguna district, New Mexico. *US Geol Surv Prof Paper* 519, 117 p
- Montgomery JH, Giroux GH, Barr NR (2006) Report on workman creek uranium project, Gila County, Arizona. (N.I. 43-101 Report) on behalf of Rodinia Minerals Inc, Feb 1, 2006, amended Aug 1, 2006, 115 p
- Moore GW (1954) Extraction of uranium from aqueous solution by coal and some other materials. *Econ Geol*, v 49, pp 652-658
- Moore GW, Melin RE, Kepferle RC (1959) Uranium-bearing lignite in southwestern North Dakota. *US Geol Surv Bull* 1055-E, pp 147-166
- Moore SC, Lavery NG (1980) Magnitude and variability of disequilibrium in San Antonio Valley uranium deposit. *in: Rautman, CA, ed., Geology and mineral technology of the Grants Uranium Region 1979*. *New Mex Bur Mines Miner Res Mem* 38, pp 276-283
- Motica JE (1968) Geology and uranium-vanadium deposits in the Uravan Mineral Belt, southwestern Colorado. *in: Ridge JD, ed., Ore deposits of the United States, 1933- 1967 (Graton-Sales Vol)*. *Amer Inst Min Metal Petrol Eng*, v 1, pp 805-814
- Moxham RM (1964) Radioelement dispersion in a sedimentary environment and its effect on uranium exploration. *Econ Geol*, v 59, pp 309-321
- Mrak VA (1968) Uranium deposits in the Eocene sandstones of the Powder River Basin, Wyoming. *in: Ridge JD, ed., Ore deposits of the United States, 1933-1967 (Graton-Sales Vol)*. *Amer Inst Min Metal Petrol Eng*, v 1, pp 838-848
- MSR&D/Mountain States Research and Development (1978) Engineering assessment and feasibility study of the Chattanooga Shale as a future source of uranium. *US DOE, GJBX-4(79)*, v 1, 257 p, v 2, 365 p, v 3, 216 p
- Mueller A, Halbach P (1983) The Anderson Mine (Arizona): An early diagenetic uranium deposit in Miocene lake sediments. *Econ Geol*, v 78, pp 275-292
- Mullens TE, Freeman VL (1957) Lithofacies of the Salt Wash Member of the Morrison Formation, Colorado Plateau. *Geol Soc Amer Bull*, v 68, no. 4, p 505-526
- Murphy E (2007) Mineral resources of North Dakota: uranium. *North Dakota Geol Surv, Dpt Mineral Res*, <http://www.nd.gov/>, 3 p
- Murphy M et al. (1978) Uranium in alkaline rocks. *US DOE, GJBX-78(78)*, 185 p
- Mutschler PH, Hill JJ, Williams BB (1976) Uranium from the Chattanooga Shale. *US Bur Mines Inf Circ* 8700, 85 p
- Myers G (2006a) Technical report of the Section 24 portion of the Crownpoint Property, McKinley County, New Mexico. Prepared for Quincy Energy Corp. 71 p (March 2, 2006)
- Myers G (2006b) Technical report of the Section 19 and 29 portions of the Crownpoint property, McKinley County, New Mexico. Prepared for Quincy Energy Corp. 79 p (April 7, 2006)
- Myers G (2006c) Technical report of the Hosta Butte property, McKinley County, New Mexico. Prepared for Quincy Energy Corp. 58 p (April 18, 2006)
- Myers G, Underhill D (2005) Technical report of the Aurora uranium project, Malheur County, Oregon. Prepared for Quincy Energy Corp. 82 p (Sept 1, 2005)

N

- Naeser CW (1976) Fission track dating. *US Geol Surv Open-File Rep* 76-190, 58 p
- Nash JT (1967) Geology and uranium deposits of the Jackpile Mine area, Laguna, New Mexico. *PhD Diss*, Columbia Univ, New York, 216 p (unpubl)
- Nash JT (1968) Uranium deposits in the Jaekpile sandstone. *New Mexico. Econ Geol*, v 63, pp 737-750
- Nash JT (1975) Exploration for uranium deposits in metasedimentary rocks in the light of geologic studies of the Midnite mine. *US Geol Surv Open-File Rep* 75-638, 4 p
- Nash JT (1977) Speculation on three possible modes of emplacement of uranium into deposits of the Midnite mine, Stevens County, Washington. *US Geol Surv Circ* 753, pp 33-34
- Nash JT (1980) Supergene uranium deposits in brecciated zones of Laramide upthrust-concepts and applications. *US Geol Surv Open-File Rep* 80-385, 36 p
- Nash JT (1981) Geology of dolomite-hosted uranium deposits at the Pitch Mine, Saguache County, Colorado. *in: Epis RC, Callender JF, eds., Guidebook, 32nd Field Conf, Western Slope Colorado*. *New Mex Geol Soc*, pp 191-198
- Nash JT, Granger HC, Adams SS (1981) Geology and concepts of genesis of important types of uranium deposits. *Econ Geol*, 75th Anniversary Vol, pp 63-116
- Nash JT, Kerr PF (1966) Geologic limitations on the age of uranium deposits in the Jaekpile sandstone, New Mexico. *Econ Geol*, v 61, pp 1283-1287
- Nash JT, Lehrman NJ (1975) Geology of the Midnite Mine area, Stevens County, Washington; A preliminary report. *US Geol Surv Open File Rep* 75-402, 36 p
- Nash JT, Ward FN (1977) Biogeochemical prospecting for uranium with conifers—results from the Midnite mine area, Washington: *US Geol Surv Open-File Rep* 77-354, 20 p
- Nations D, Stump (1981) Geology of Arizona. *Kendall/ Hunt Publ, Dubuque, Iowa*, 221 p
- Nelson CE, Gallagher JRL (1982) Proterozoic origins of uranium mineralization in the Colorado Front Range. *Econ Geol*, v 77, pp 1221-1225
- Nelson-Moore JL, Collins DB, Hornbaker AL (1978) Radioactive mineral occurrences of Colorado and bibliography. *Colorado Geol Surv/Dept Natural Res Bull* 40, 1054 p, 12 plts
- Nestler RK, Chenoweth, WL (1958) Geology of the uranium deposits of the Lukachukai Mountains, Apache County, Arizona. *US AEC, Open-File Rep RME-118*, 64 p
- Neuerburg GJ (1956) Uranium in igneous rocks of the United States. *US Geol Surv Prof Paper* 300, pp 56-64
- Neuerburg GJ, Granger HC (1960) A geochemical test of diabase as an ore source for the uranium deposits of the Dripping Spring district, Arizona. *N J Miner, Abh* 94 (Festband Ramdohr), pp 759-797
- New Mexico State Bureau of Mines and Mineral Resources (1963) Geology and technology of the Grants uranium region. *New Mex State Bur Mines Miner Res Mem* 15, 277 p

- Newman WL (1962) Distribution of elements in sedimentary rocks of the Colorado Plateau - a preliminary report. US Geol Surv Bull 1107-F, pp 337-445
- Newman WL, Elston DP (1959) Distribution of chemical elements in the Salt Wash Member of the Morrison Formation, Jo Dandy area, Montrose County, Colorado. US Geol Surv Bull 1084-E, pp 117-150
- Nininger RD (1977) Recognition of uranium districts. *in*: Recognition and evaluation of uraniumiferous areas. IAEA, Vienna, pp 1-11
- Nishimori RK et al. (1977) Uranium deposits in granitic rocks. US DOE, GJBX-13(77), 298 p
- Nishimori RK, Powell JD (1980) Uranium in carbonatites, USA. US DOE, GJBX-147(80), 180 p
- Nishimori RK, Ragland PC, Rogers JJW, Greenberg JK (1977) Uranium deposits in granitic rocks. US DOE, GJBX-13(77), 298 p
- Nkomo IT, Stuckless JS, Thaden RE, Rosholt JN (1978) Petrology and uranium mobility of a granite of early Precambrian age from the Owl Creek Mountains, Wyoming. *in*: Guidebook, 30th Ann Field Conf, Wyoming Geol Ass pp 335-348
- Noble EA (1960) Genesis of uranium belts of the Colorado Plateau. *in*: Proc Intern Geol Congr, 21st Session, Copenhagen, pt 15, pp 26-39
- Noble EA (1973) Uranium in coal, in mineral and water resources of North Dakota. North Dakota Geol Surv, Bull 63, pp 80-85
- Norman HW (1957) Uranium deposits of northeastern Washington. Mining Eng, v 9, no. 6, pp 662-666
- Norris JD, Drummond P (2000) Uranium recovery by in-situ leaching: The Smith Ranch project. *in*: Uranium 2000. Metall Soc CIM, pp 311-319
- Northrop HR (1982) Origin of the tabular-type vanadium-uranium deposits in the Henry structural basin, Utah. PhD thesis, Col Sch Mines, Golden, 194 p
- Northrop HR, Goldhaber MB, eds. (1990) Genesis of the tabular-type vanadium-uranium deposits of the Henry basin, Utah. Econ Geol, v 85, pp 215-269
- Northrop HR, Goldhaber MB, Landis GP, Rye RO, Whitney CG (1982) Localization of tabular, sediment-hosted uranium-vanadium deposits of Henry structural basin, Utah (abstr). Amer Ass Petrol Geol Bull, v 66, p 613
- Noyes H (1978) Irigaray uranium deposits. *in*: Lageson DR, Hausel DH, eds., Occurrence of uranium in Precambrian and younger rocks of Wyoming and adjacent areas. Geol Surv Wyoming, Publ Inf Circ 7, p 27
- NUEXCO (1979) Chattanooga Shale - an energy resource. NUEXCO, Denver, no. 132, pp 3.0-3.3
- NUEXCO (1982) The Swanson orebody. NUEXCO, Denver, no. 172, pp 24-25
- NUEXCO (1983) Crow Butte deposit uranium deposit. NUEXCO, Denver, no. 178, pp 21-26
- NUEXCO (1994) Uranium from phosphoric acid: IMC's Uncle Sam plant. NUEXCO Review, Denver, pp 15-19
- Nutt CJ (1981) Model of uranium mineralization in the Dripping Spring Quartzite, Gila County, Arizona. US Geol Surv Open-File Rep 81-524, 49 p
- Nutt CJ (1984) Stratabound uranium deposits in the Dripping Spring Quartzite, Gila County, Arizona, USA. *in*: Ferguson J, ed., Proterozoic unconformity and stratabound uranium deposits. IAEA-TECDOC-315, IAEA, Vienna, pp 95-113
- O**
- Obradovich JD, Cobban WA (1975) A time scale for the Late Cretaceous of the western interior of North America. Geol Ass Can Spec Paper 13, 54 p
- OECD-NEA & IAEA (1970 to 2007) Uranium resources, production and demand. Paris (biannual joint reports)
- OECD-NEA & IAEA (1980) World uranium geology and resource potential. IUREP, report on phase I. OECD-NEA, Paris, Miller Freeman Public. Inc., San Francisco, 524 p
- OECD-NEA (1989) Nuclear energy data. OECD-NEA, Paris, 41 p
- Offield TW (1979) U.S. Geological Survey uranium and thorium resource assessment and exploration research program, fiscal year 1980. Uranium Industry Seminar, Grand Junction, 9 p
- Ojakangas RW (1987) The search for Elliot Lake-type uraniumiferous quartz-pebble conglomerates, southern Lake Superior region, USA. *in*: Uranium deposits in Proterozoic quartz-pebble conglomerates. TECDOC-427, IAEA, Vienna, pp 59-74
- O'Loughlin EJ, Kelly SD, Cook RE, Csenesits R, Kemner KM (2003) Reduction of uranium(VI) by mixed iron(II)/iron(III) hydroxide (green rust): Formation of nanoparticles. Environ Sci Technol, v 37, pp 721-727
- Olson JC (1988) Geology and uranium deposits of the Cochetopa and Marshall Pass districts, Saguache and Gunnison Counties, Colorado. US Geol Surv Open-File Rep, 44 p
- Olson JD (1976) Uranium deposits in the Cochetopa district, Colorado, in relation to the Oligocene erosion surface: US Geol Surv Open-File Rep 76-222, 13 p
- Olson JD (1979) Preliminary geologic and structural maps and sections of the Marshall Pass mining district, Saguache, Gunnison, and Chaffee Counties, Colorado. US Geol Surv Open-File Rep 79-1473
- O'Neill AJ, Nystrom RJ, Thiede DS (1981) National uranium resource evaluation, Williams quadrangle, Arizona. US DOE, GJQ-009(81), 56 p
- Orajaka IP (1981) Mineralogy and uranium geochemistry of selected volcanoclastic sediments in the western United States- an exploration model. DGSc diss, Univ Texas, El Paso, 365 p
- Ormond A (1957) Preliminary report on the geology of uranium deposits in the Browns Park Formation in Mottat County, Colorado, and Carbon County, Wyoming. US AEC Open-File Rep TM-D-1-18, 30 p
- Osterwald FW (1965) Structural control of uranium-bearing vein deposits and districts in the conterminous United States. US Geol Surv Prof Pap 455-G, pp 121-146
- Osterwald FW, Osterwald DB, Long JS Jr, Wilson WH (1959) Mineral resources of Wyoming. Geol Surv Wyoming Bull 50, 259 p
- O'Sullivan RB, MacLachlan ME (1975) Triassic rocks of the Moab-White Canyon area, southeastern Utah. *in*: Canyonlands country guidebook. Four Corners Geol Soc, pp 129-142
- Otton JK (1977a) Geology of uraniumiferous Tertiary rocks in the Artillery Peak-Date Creek Basin, west-central Arizona. US Geol Surv Circ 753, pp 35-36
- Otton JK (1977b) Criteria for uranium deposition in the Date Creek Basin and adjacent areas, west-central Arizona. NURE uranium geology symposium. US DOE CJBX-12 (78), pp 101-110
- Otton JK (1981) Geology and genesis of the Anderson mine, a carbonaceous lacustrine uranium deposit, western Arizona: a summary report. US Geol Surv Open-File Rep 81-780, 24 p
- Otton JK (1986) Geological environment of uranium in lacustrine host rocks in the western United States. *in*: Geological environments of sandstone-type uranium deposits. TECDOC-328, IAEA, Vienna, pp 229-241
- Otton JK, Reimer GM (1991) Radiogenic and other gases in shallow ground waters of uraniumiferous Holocene alluvium, Flodelle Creek, Washington. *in*: Gunderson LCS, Wanty RB, eds., Field studies in radon geology. US Geol Surv Bull 1971, 330 p
- Otton JK, Zielinski RA (1985) Movement and concentration of uranium in young, organic-rich sediments, Stevens County, Washington. *in*: Les mécanismes de concentration de l'uranium dans les environnements géologiques. Soc Franç Minér Cristall and CREGU, Nancy, pp 49-52
- Otton JK, Zielinski RA (1986) Movement and fixation of uranium on organic matter in a late Quaternary uranium deposit, Stevens County, Washington. *in*: Carter LMH, ed., V. E. McKelvey Forum on mineral and energy resources-1986. US Geol Surv Circ 974, pp 49-50
- Otton JK, Zielinski RA, Johnson SY (1989) The Flodelle Creek surficial uranium deposit, Stevens County, Washington, USA. *in*: Uranium resources and geology of North America. TECDOC-500, IAEA, Vienna, pp 241-262
- Overstreet WC, Theobald PK Jr, Whitlow JW (1960) Thorium and uranium resources in monazite placers of the western piedmont, North and South Carolina. Amer Inst Metall, Petrol Eng Trans 1959, v 214, pp 709-714
- P**
- Page LR, Redden JA (1952) The carnotite prospects of the Craven Canyon area, Fall River County, South Dakota. US Geol Surv Circ 175, 18 p
- Page LR, Stocking HE, Smith HB, comps. (1956) Contributions to the geology of uranium and thorium by the United States Geological Survey and Atomic

- Energy Commission for the United Nations Inter Conf on the Peaceful Uses of Atomic Energy, Geneva, Switzerland. US Geol Surv Prof Paper 300, 739 p
- Pagel M (1984) Petrology, mineralogy and geochemistry of surficial uranium deposits. *in*: Surficial uranium deposits. TECDOC-322, IAEA, Vienna, pp 37-44
- Pancoast LE, Carden JR (2005) A technical report on the Stanley uranium district project, geology, mineralization, and exploration potential, Basin Creek Area, Custer County, Idaho. Prepared for Magnum Minerals Corp, 77 p (Sept 3, 2005)
- Paschis JA (1979) Mining and geologic developments at Cotter Corporation's Schwartzwalder uranium mine, Jefferson County, Colorado. *in*: 1979 Mining Yearbook, Colo Min Ass, pp 123-129
- Pearson RC, Obradovich JD (1977) Eocene rocks in northeastern Washington—radiometric ages and correlations. US Geol Surv Bull 1433, 41 p
- Peirce HW, Jones N, Rogers R (1977) A survey of uranium favorability of Paleozoic rocks in the Mogollon rim and slope region - east central Arizona. Arizona Bur Geol Miner Technology, Circ 19, 71 p
- Peirce HW, Keith SB, Wilt JC (1970) Coal, oil, natural gas, helium, and uranium in Arizona. Arizona Bur Mines Bull 182, 289 p
- Peirce R (1872) Pitchblende from Russel District, Gilpin County (Colorado). Acad Roy Inst Cornwall (1872); J Roy Inst Cornwall, 4 (1873)
- Pelizza M, McCarn DW (2004) Licensing of in situ leach recovery operations for the Crownpoint and Church Rock uranium deposits, New Mexico: A case study. *in*: Recent developments in uranium resources and production with emphasis on in situ leach mining. TECDOC-1396, IAEA, Vienna, pp 153-173
- Perkins BL (1979) An overview of the New Mexico uranium industry. New Mex Energy Miner Dept Rep, 147 p
- Pernsteiner RK, Ikramuddin M (1979) The relationship between fluorine and uranium in granitic rocks from northeastern Washington (abstr). *in*: Ann Meeting, Geol Soc Amer, abstr w progr, p 494
- Perry BL (1963) Limestone reefs as an ore control in Jurassic Todilto Limestone of the Grants district. *in*: Geology and technology of the Grants uranium region. New Mex State Bur Mines Miner Res Mem 15, pp 150-156
- Peterman ZE, Hedge CE (1968) Chronology of Precambrian events in the Front Range, Colorado. Can J Earth Sci, v 5, pp 749-756
- Peterman ZE, Hedge CE, Braddock WA (1969) Age of Precambrian events in the northeastern Front Range, Colorado. J Geophys Research, v 73, pp 2277-2296
- Peters DC (2007) Technical report on La Jara Mesa uranium property, Cibola County, New Mexico. Prepared for Laramide Resources Ltd. 89 p (Aug 31, 2006; revised July 2, 2007)
- Peterson F (1977) Uranium deposits related to depositional environments in the Morrison Formation (Upper Jurassic), Henry Mountains mineral belt of southern Utah. *in*: Campbell JA, ed., Short papers of the US Geol Surv Uranium-Thorium Symp 1977. US Geol Surv Circ 753, pp 45-47
- Peterson F (1978) Measured sections of the lower member in Salt Wash Member of the Morrison Formation (Upper Jurassic) in the Henry Mountains mineral belt of southern Utah. US Geol Surv Rep 78-1094, 97 p
- Peterson F (1980a) Sedimentology of the uranium-bearing Salt Wash Member and Tidwell Unit of the Morrison Formation in the Henry and Kaiparowits basins, Utah. *in*: Picard MD, ed., Henry Mountains symposium. Utah Geol Ass Publ 8, pp 305-322
- Peterson F (1980b) Sedimentology as a strategy for uranium exploration: concepts gained from analysis of a uranium-bearing depositional sequence in the Morrison Formation of south-central Utah. *in*: Short Course Notes. Turner-Peterson CE, ed., Uranium in sedimentary rocks: application of the facies concept to exploration. Soc Econ Paleont Miner, Rocky Mtn Sect, pp 65-126
- Peterson F, Turner-Peterson CE (1980) Lacustrine-humate model: sedimentologic and geochemical model for tabular sandstone uranium deposits in the Morrison Formation, Utah, and application to uranium exploration. US Geol Surv Open-File Rep 80-319, 43 p
- Peterson F, Turner-Peterson CE (1987) The Morrison Formation of the Colorado Plateau: Recent advances in sedimentology, stratigraphy and paleotectonics. Hunteria, v 2, no. 1, 18 p
- Peterson JA, Loleit AJ, Spencer CW, Ullrich RA (1965) Sedimentary history and economic geology of San Juan basin. Amer Ass Petrol Geol Bull, v 49, pp 2076-2119
- Peterson NV P (1959) Preliminary geology of the Lakeview uranium area, Oregon. The Ore Bin 21, 2, p 11
- Peterson RJ (1980) Geology of a pre-Dakota uranium geochemical cell on Section 13, T 16 N, R 17 W, Churchrock area, McKinley County, New Mexico. *in*: Rautman CA, ed., Geology and mineral technology of the Grants Uranium Region 1979. New Mex Bur Mines Miner Res Mem 38, pp 131-138
- Petrov NN, Yazikov VG, Aubakirov HB, Plekhanov VN, Vershkov AF, Lukhtin VF (1995) Uranium deposits of Kazakhstan (exogenous). Gilym Almaty, 264 p (in Russian)
- Phair G (1952) Radioactive Tertiary porphyries in the Central City district, Colorado, and their bearing upon pitchblende deposition. US Geol Surv TEI-247
- Phair G (1955) Geologic investigations of radioactive deposits. Semiannual Progress Report, Dec 1954 to May 1955, US Geol Surv TEI 540, p 237
- Phair G (1956) Geologic investigations of radioactive deposits. Semiannual Progress Report, Dec 1955 to May 1956, US Geol Surv TEI 620, p 310
- Phair G (1957) Uranium and thorium in the Laramide intrusives of the Colorado Front Range. US Geol Surv TEI-750, pp 103-108
- Phair G (1975) Uranium, thorium, and lead in igneous rocks and veins, Colorado. US Geol Surv Rep 75-595, 34 p
- Phair G (1979) Interpretation of lead-uranium ages of pitchblende deposits in the central Front Range, Colorado. Geol Soc Amer Bull, v 90, pp 858-870
- Phair G, Gottfried D (1964) The Colorado Front Range, Colorado, USA, as a uranium and thorium province. *in*: Adams JAS, Lowder WM, eds., The natural radiation environment. Rice Univ Press, Chicago, pp 7-38
- Phair G, Jenkins LB (1975) Tabulation of uranium and thorium data on the Mesozoic-Cenozoic intrusive rocks of known chemical composition in Colorado. US Geol Surv Open-File Rep 75-501, 57 p
- Phair G, Shimamoto KO (1952) Hydrothermal uranorhite breccias from the Blue Jay mine, Jamestown, Boulder County, Colorado. Amer Miner, v 37, pp 659-666
- Phelps WT, Zech RS, Huffman AC Jr (1986) Seismic studies in the Church Rock uranium district, southwest San Juan Basin, New Mexico. *in*: Turner-Peterson CE, Santos ES, Fishman NS, eds., A basin analysis case study - the Morrison Formation, Grants Uranium Region, New Mexico. Amer Ass Petrol Geol, Studies in Geology, no. 22, pp 145-159
- PhillipsRS (1990) Geochemistry of hydrothermal Th-U-REE quartz/fluorite veins from the Capitan pluton. MS thesis, New Mex Inst Min Techn, 202 p (unpubl)
- Phoenix DA (1958) Uranium deposits under conglomeratic sandstone of the Morrison Formation, Colorado and Utah. Geol Soc Amer Bull, v 69, no. 4, pp 403-417
- Pierson CT, Green MW (1980) Factors that localized uranium deposition in the Dakota Sandstone, Gallup and Ambrosia Lake mining districts, McKinley County, New Mexico. US Geol Surv Bull 1485, 31 p
- Pierson CT, Spirakis CS, Robertson JF (1983) Comparison of abundances of chemical elements in mineralized and unmineralized sandstone of the Brushy Basin Member of the Morrison Formation, Smith Lake district, Grants Uranium Region, New Mexico. US Geol Surv Rep 83-818, 45 p
- Pilcher RC (1978) Volcanogenic uranium occurrences. *in*: Mickle DG, Mathews GW, eds., Geologic characteristics of environments favorable for uranium deposits. US DOE, GJBX-67(78), pp 181-219
- Pillmore CL, Mapel WJ (1963) Geology of the Nefsy Divide quadrangle, Crook County, Wyoming. US Geol Surv Bull 1121-E, pp E1-E52
- Pipiringos GN (1961) Uranium-bearing coal in the central part of the Great Divide Basin, Sweetwater County, Wyoming. US Geol Surv Bull 1099-A pp A1-A104
- Pipiringos GN (1966) Origin of elements associated with uranium in the Cave Hills area, Harding County, South Dakota. US Geol Surv Prof Paper 476-B, 75 p
- Pipiringos GN et al. (1965) Geology and uranium deposits in the Cave Hills area, Harding County, South Dakota. US Geol Surv Prof Paper 476-A, pp A1-A64
- Pipiringos GN, Denson NM (1970) The Battle Spring Formation in south-central Wyoming. 22nd Field Conf, Guidebook, Wyoming Geol Ass, pp 161-168
- Pitman RK (1958) Uranium-vanadium deposits of the Cottonwood Wash mining area, San Juan County, Utah. US AEC, RME-109 (rev)

- Place J, Della Valle RS, Brookins DG (1980) Mineralogy and geochemistry of Mariano Lake uranium deposit, Smith Lake district. *in: Rautman CA, ed., Geology and mineral technology of the Grants uranium region 1979*. New Mex Bur Mines Miner Res Mem 38, pp 172-184
- Plant JA, Simpson PR, Smith B, Windley B (1999) Uranium ore deposits - products of the radioactive Earth. *in: Burns PC, Finch R, eds., Uranium: Mineralogy, geochemistry and the environment. in: Reviews in Mineralogy. Miner Soc Amer v 38*, pp 255-319
- Plateau Resources Ltd (1983) Summary of the Shooting Canyon project, Garfield County, Utah. AIME field trip, (manuscr) 18 p
- Pfliler R (1956) The distribution of thorium and uranium in sedimentary rocks and the oxygen content of the pre-Cambrian atmosphere. MA thesis, Rice Inst
- Pfliler R, Adams JAS (1962a) The distribution of thorium, uranium, and potassium in the Mancos shale. *Geochim Cosmochim Acta*, 26, p 1115
- Pfliler R, Adams JAS (1962b) The distribution of thorium and uranium in a Pennsylvanian weathering profile. *Geochim Cosmochim Acta*, 26, pp 1137-1146
- Pool T, Ross D (2007) Technical report on the Arizona strip project, Arizona, USA. Prepared for Denison Mines Corp by Scott Wilson Roscoe Postle Associates Inc, Feb 2007, 116 p
- Pool TC (1990) Uranium producer profile: Kingsville Dome, Texas, USA. International Nuclear Inc., Golden, Colorado, 7 p (unpubl.)
- Pool TC (1991) Uranium producer profile: Rosita, Texas, USA. International Nuclear Inc., Golden, Colorado, 79 p (unpubl.)
- Pool TC (1993) Uranium producer profile: Alta Mesa, Texas, USA. International Nuclear Inc., Golden, Colorado, 12 p (unpubl.)
- Pool TC (1995) U.S. uranium production capability, how much? and at what price?. Intern Uranium Fuel Seminar, Williamsburg, Virginia, 7 p
- Pool TC (2007a) Technical report on the Shirley Basin uranium properties, Wyoming. Report for NI 43-101, prepared for Target Mining & Exploration Corp. 58 p (July 8, 2007)
- Pool TC (2007a) Technical report on the Shirley Basin uranium properties, Wyoming. Report for NI 43-101, prepared for Target Mining & Exploration Corp. 58 p (July 8, 2007)
- Pool TC (2007b) Technical report on the Henry Mountains Complex uranium project, Utah, U.S.A. Report NI 43-101, prepared for International Uranium Corporation. Scott Wilson Roscoe Postle Ass Inc. 110 p (Sept 9, 2006)
- Pool TC (2007c) Technical report on the Rose breccia pipe uranium deposit, Coconino Plateau, Arizona, U.S.A. Report (draft) NI 43-101, prepared for Monster Uranium Corp. Scott Wilson Roscoe Postle Associates Inc. 61 p (Sept 14, 2007)
- Pool TC (2007c) Technical report on the Rose breccia pipe uranium deposit, Coconino Plateau, Arizona, U.S.A. Report NI 43-101, prepared for Monster Uranium Corp. Scott Wilson Roscoe Postle Ass Inc. 61 p
- Pool TC, Ross DA (2007) Technical report on the Arizona Strip uranium project, Arizona, U.S.A. Report NI 43-101, prepared for Denison Mines Corp. Scott Wilson Roscoe Postle Ass Inc. 116 p (February 26, 2007)
- Pool TC, Ross DA (2007) Technical report on the Arizona Strip uranium project, Arizona, U.S.A. Report NI 43-101, prepared for Denison Mines Corp. Scott Wilson Roscoe Postle Ass Inc. 116 p (Feb 26, 2007)
- Porter DA (1981) Exploration of Bernabe Montano complex of uranium deposits, New Mexico, USA. *in: Uranium exploration case histories*. IAEA, Vienna, pp 279-292
- Porter DA (1981) Exploration of Bernabe Montano complex of uranium deposits, New Mexico. *in: Uranium exploration case histories*. IAEA, Vienna, pp 279-292
- Posey-Dowty J, Axtmann E, Crerer D, Borsik M, Ronk A, Woods W (1987) Dissolution rate of uraninite and uranium roll-front ores. *Econ Geol*, v 82, pp 184-194
- Prenn N, Ronning P (2005) Technical report, Kings Valley uranium, Humboldt County, Nevada. Prepared for Western Energy Development Corporation. Mine Development Ass. 128 p (Dec. 9, 2005) Prepared for Denver Uranium Company. 41 p (Dec 15, 2005)
- Price V, Thayer PA, Ranson WA, eds. (1980) Geological investigations of Piedmont and Triassic rocks, central North Carolina and Virginia. *in: Field Trip Guidebook*. Carolina Geol Soc, pp A1-D35
- Priesemann FD (1977) Sedimentpetrologische Untersuchung einer uranführenden Schichtserie im Tertiär Arizonas (U.S.A.). Diplom thesis, Techn Univ Clausthal, Germany, 145 p (unpubl)
- Provo LJ (1977) Stratigraphy and sedimentology of radioactive Devonian-Mississippian shales of the central Appalachian Basin. US DOE, GJBX-37(77), 54 p
- Purvance D (1978) Geology of the Lisbon mine. San Juan County, Utah. Colo Sch Mines, Prof Contrib, no. 9, pp 53-54

Q

- Quick JV, Thomas NG, Brogdon LD, Jones CA, Martin TS (1977) Uranium favorability of Late Eocene through Pliocene rocks of the south Texas coastal plain. US DOE, GJBX-7(77), 48 p

R

- Rackley RI (1972) Environment of Wyoming Tertiary uranium deposits. *Amer Ass Petrol Geol Bull*, v 56, no. 4, pp 755-774
- Rackley RI (1976) Origin of western-states type uranium mineralization. *in: Wolf KH, ed., Handbook of strata-bound and stratiform ore deposits*. Elsevier Amsterdam, pp 89-156
- Rackley RI (1980) A prospect-scale "western-states" sandstone uranium model. *in: Gaschnig J, ed. Development of uranium exploration models for the prospector consultant system*. Menlo Park, California SRI Intern Proj 7856, pp 15-62
- Ragland PC, Rogers JJW (1980) Favourable tectonic belts for granitic uranium deposits: Pan-Africa and the southern Appalachians. *J Geochem Explor*, 13, pp 181-199
- Ramdohr P (1980) The ore minerals and their intergrowths. Pergamon Press, 1207 p
- Ramdohr P (1986) Die Metamorphose in der Uraninitfamilie. *Bull Geol Soc Finland*, v 58, pt 1, pp 263-269
- Rankin DW (1975) The continental margin of eastern North America in the southern Appalachians: The opening and closing of the proto-Atlantic. *Amer J Sci*, v 275-A, pp 298-336
- Ranspot HW, Spengler RG (1957) Uranium deposits of the of the Marshall Pass area, Gunnison and Saguache Counties, Colorado. US AEC, DAO-3-TM-42, 29 p
- Rapaport I (1952) Interim report on the ore deposits of the Grants district, New Mexico. US AEC, RMO-1031, 19 p
- Rapaport I (1955) General geology of the Grants, New Mexico uranium area. *Uran Info Digest*, v 2, pp 17-18
- Rapaport I (1963) Uranium deposits of the Poison Canyon ore trend, Grants district. *in: Kelley VC, ed., Geology and technology of the Grants Uranium Region*. New Mex Bur Mines Miner Res Mem 15, pp 122-135
- Rapp JS (1978) Juniper uranium mine, Tuolumne, California. *Calif Geol*, v 31, no. 9, pp 199-202
- Rasmussen JD, Cunningham CG, Gautier AM (1986) Primary fluid inclusions in sphalerite from the Hack 1 and 2 mines, Mohave County, Arizona (abstr). *Geol Soc Amer, Rocky Mtn Sect, abstr w progr*, 18(5), p 394
- Rasmussen JD, Cunningham CG, Steven TA, Rye RO, Romberger SB (1985) Origin of hydrothermal uranium vein deposits in the Marysvale volcanic field, Utah. *in: Uranium deposits in volcanic rocks*. IAEA, Vienna, pp 317-318
- Rasor CA (1949) Report on investigation of radioactive minerals at Hack's Canyon Mine, Mohave County, Arizona. US AEC, RMO-24, 7 p
- Rautman CA, ed. (1980) Geology and mineral technology of the Grants Uranium Region 1979. New Mex Bur Mines Miner Res Mem 38, 400 p
- Rawson RR (1980) Uranium in Todilto Limestone (Jurassic) of New Mexico - example of a sabkha-like deposit. *in: Rautmann CA, ed., Geology and mineral technology of the Grants Uranium Region 1979*. New Mex Bur Mines Miner Res Mem 38, pp 304-312
- Reade HJ Jr (1976) Grover uranium deposit: a case history of uranium exploration in the Denver Basin Colorado. *Mountain Geologist*, v 13, no. 1, pp 21-31

- Reade HJ Jr (1978) Uranium deposits: Northern Denver Julesburg Basin, Colorado. *in*: Pruit JD, Coffin PE, eds., Energy resources of the Denver Basin. Rocky Mtn Ass Geol, Denver, Colorado, pp 161-171
- Redden JA (1980) Geology and uranium resources in Precambrian conglomerates of the Nemo area, Black Hills, South Dakota. US DOE Rep 79-311-E, 147 p
- Reimer LR (1969) Stratigraphy, paleohydrology and uranium deposits of Church Rock quadrangle, McKinley County, New Mexico. MS thesis, Colo Sch Mines, Golden, 254 p
- Reineck HE, Singh IB (1973) Depositional sedimentary environments. Springer, New York, 439 p
- Renfro AR (1969) Uranium deposits in the Lower Cretaceous of the Black Hills. Wyoming Univ, Contrib Geol, v 8, no. 2, pt 1, pp 87-92
- Renick BC (1926) The Jackson Group and the Catahoula and Oakville Formations in a part of the Texas Gulf coastal plain. Univ Texas, Austin, Bull 2645, 187 p
- Reyner ML, Ashwill WR, Robison RL (1956) Geology of uranium deposits in Tertiary lake sediments of southwest Yavapai Co., Arizona. US AEC, RME-2057, 43 p
- Reynolds RL, Fishman NS, Scott JH, Hudson MR (1986) Iron-titanium oxide minerals and magnetic susceptibility anomalies in the Mariano Lake-Lake Valley cores - Constraints on conditions of uranium mineralization in the Morrison Formation, San Juan Basin, New Mexico. *in*: Turner-Peterson CE, Santos ES, Fishman NS, eds., A basin analysis case study - the Morrison Formation Grants Uranium Region, New Mexico. Amer Ass Petrol Geol, Studies in Geology, no. 22, pp 303-313
- Reynolds RL, Goldhaber MB (1978) Origin of a south Texas roll-type uranium deposit: I. Alteration of iron-titanium oxide minerals. Econ Geol, v 73, pp 1677-1689
- Reynolds RL, Goldhaber MB (1979) Iron disulfide minerals and the origin of roll-type uranium deposits. Geol Soc Amer, Annual Meeting, San Diego, California, abstr w programs
- Reynolds RL, Goldhaber MB (1983) Iron disulfide minerals and the genesis of roll-type uranium deposits. Econ Geol, v 78, pp 105-120
- Reynolds RL, Goldhaber MB, Rye RO, Fishman NS, Ludwig KR, Grauch RI (1980a) History of sulfidization of the Felder uranium deposit, south Texas. US Geol Surv Open-File Rep 80-1096, 23 p
- Reynolds RL, Goldhaber MB, Blackmon PD, Starkey HC, Fishman NS (1980b) Clay minerals in two south Texas roll-type uranium deposits. US Geol Surv Open-file Rep 80-838, 24 p
- Reynolds RL, Goldhaber MB, Carpenter DJ (1982) Biogenic and nonbiogenic ore-forming processes in the south Texas uranium district: evidence from the Panna Maria deposit. Econ Geol, v 77, pp 541-556
- Reynolds RL, Goldhaber MB, Grauch RI (1977) Uranium associated with iron-titanium oxide minerals and their alteration products in a south Texas roll-type deposits. US Geol Surv Circ 753, pp 37-39
- Reynolds SJ (1980) Geologic framework of west-central Arizona. Arizona Geol Soc Digest, v 12, pp 1-16
- Rhett DW (1980) Heavy mineral criteria for subsurface uranium exploration, San Juan Basin, New Mexico. *in*: Rautman CA, ed., Geology and technology of the Grants Uranium Region 1979. New Mex Bur Mines Miner Res Mem 38, pp 202-207
- Rice CM, Lux DR, Macintyre RM (1982) Timing of mineralization and related intrusive activity near Central City, Colorado. Econ Geol, v 77, pp 1655-1666
- Rich RA, Barabas AH (1982) Genetic implications of preliminary mineralogical, paragenetic, and fluid inclusion data for the Schwartzwalder uranium mine, Colorado, USA. *in*: Vein-type and similar uranium deposits. IAEA, Vienna, pp 181-193
- Rich RA, Holland HD, Petersen U (1977) Hydrothermal uranium deposits. Elsevier Scientific Publ Co, Amsterdam-Oxford-New York, 264 p
- Richardson KA (1964) Thorium, uranium, and potassium in the Conway granite, New Hampshire, USA. *in*: Adams JAS, Lowder WM, eds., The natural radiation environment. Chicago Univ Press, p 47
- Ricoy JU, Brown LF, Jr (1977) Depositional systems in the Sparta Formation (Eocene) Gulf Coast Basin of Texas. Gulf Coast Ass Geol Soc Trans, v 27, pp 139-154
- Ridgley JL (1980) Geology and characteristics of uranium mineralization in the Morrison Formation at the Dennison-Bunn claim, Sandoval County, New Mexico. *in*: Rautman CA, ed., Geology and mineral technology of the Grants Uranium Region 1979. New Mex Bur Mines Miner Res Mem 38, pp 299-303
- Ridgley JL, Goldhaber MB, Green MW, Pierson CT, Finch WI, Lupe RD (1978) Summary of the geology and resources of uranium in the San Juan Basin and adjacent region, New Mexico, Arizona, Utah, and Colorado. US Geol Surv Open-File Rep 78-964, 107 p
- Riese WC (1977) Geology and geochemistry of the Mt. Taylor uranium deposit, Valencia County, New Mexico. MS Thesis, Univ New Mexico, Albuquerque, 146 p (unpubl)
- Riese WC (1979) The Mount Taylor uranium deposit of the Grants Mineral Belt, New Mexico. PhD diss, Univ New Mex, Albuquerque
- Riese WC, Brookins DG (1977) Subsurface stratigraphy of the Morrison Formation in the Mount Taylor area and its relation to uranium ore genesis. *in*: Guidebook, 28th Field Conf, San Juan Basin III. New Mex Geol Soc, pp 271-275
- Riese WC, Brookins DG (1980) Mount Taylor uranium deposit, San Mateo, New Mexico (abstr). *in*: Rautman CA, ed., Geology and mineral technology of the Grants uranium region 1979. New Mex Bur Mines Miner Res Mem 38, p 397
- Riese WC, Brookins DG (1984) The Mount Taylor uranium deposit, San Mateo, New Mexico, USA. Uranium, v 1, pp 189-209
- Riese WC, Brookins DG, Della Valle RS (1980) Scanning electron-microscope investigation of paragenesis of uranium deposits, Mount Taylor and elsewhere, Grants mineral belt. *in*: Rautman CA, ed., Geology and mineral technology of the Grants Uranium Region 1979. New Mex Bur Mines Miner Res Mem 38, pp 244-251
- Ristorcelli SJ (1980) Geology of the eastern Smith Lake ore trend, Grants mineral belt, New Mexico. *in*: Rautman CA, ed., Geology and mineral technology of the Grants Uranium Region 1979. New Mex Bur Mines Miner Res Mem 38, pp 145-152
- RME (1978) Proposed farmout or joint venture properties. Rocky Mountain Energy Co. Denver (May 1978)
- Robbins DA (1976) The Sherwood uranium deposit. AIME meeting, Spokane (manusc)
- Robbins DA (1978) Applied geology in the discovery of the Spokane Mountain uranium deposit, Washington. Econ Geol, v 73, pp 1523-1538
- Robinson CS, Mapel WJ, Bergendahl MH (1964) Stratigraphy and structure of the northern and western flanks of the Black Hills uplift, Wyoming, Montana, and South Dakota: US Geol Surv Prof Paper 404, 134 p
- Roeber MM Jr (1972) Possible mechanics of lateral enrichment and physical positioning of uranium deposits, Ambrosia Lake area, New Mexico. Supplement to New Mex Bur Mines Miner Res Circ 118, 16 p
- Rogers JJW, Adams JAS, Gatlin B (1965) Distribution of thorium, uranium, and potassium concentrations in three cores from the Conway granite, New Hampshire, USA. Amer J Sci, 263, pp 817ff
- Rogers JJW, Ragland PC, Nishimori RK, Greenberg JK, Hauck SA (1978) Varieties of granitic uranium deposits and favourable exploration areas in the eastern United States. Econ Geol, v 73, pp 1539-1555
- Rolker CM (1881) The Silver Sandstone District of Utah. Trans Amer Inst Min Eng, no. 9
- Romberger SB (1984) Transport and deposition of uranium in hydrothermal systems at temperatures up to 300°C: geological implications. *in*: De Vivo B, Ippolito E, Capaldi G, Simpson PR, eds., Uranium geochemistry, mineralogy, geology, exploration and resources. Inst Min Metall, London, England, pp 12-18
- Roper MW, Wallace AB (1981) Geology of the Aurora uranium prospect, Malheur County, Oregon. *in*: Goodell PC, Waters AC, eds., Uranium in volcanic and volcanoclastic rocks. Amer Ass Petrol Geol, Studies in Geology, no. 13, pp 81-89
- Rosenberg PE, Hooper RL (1982) Fission-track dating of sandstone-type uranium deposits. Geology, v 10 pp 481-485
- Rosholt JN (1983) Isotopic composition of uranium and thorium in crystalline rocks. J Geophys Res, 88(B9) pp 7315-7330
- Rosholt JN, Bartel AJ (1969) Uranium, thorium and lead systematics in the Granite Mountains, Wyoming. Earth Planet Sci Lett, 7, pp 141-147
- Rosholt JN, Butler AP, Garner EL, Shields WR (1965a) Isotopic fractionation of uranium in sandstone, Powder River Basin, Wyoming, and Slick Rock district, Colorado. Econ Geol, v 60, pp 199-213

- Rosholt JN, Harshman EN, Shields WR, Garner EL (1964) Isotopic fractionation of uranium related to roll features in sandstone, Shirely Basin, Wyoming. *Econ Geol*, v 59, pp 570-585
- Rosholt JN, Prijana, Noble DC (1971) Mobility of uranium and thorium in glassy and crystallized silicic volcanic rocks. *Econ Geol*, v 66, pp 1061-1069
- Rosholt JN, Tatsumoto M, Dooley JR Jr (1965b) Radioactive disequilibrium studies in sandstone, Powder River Basin, Wyoming, and Slick Rock district, Colorado. *Econ Geol*, v 60, pp 477-484
- Rosholt JN, Zartman RE, Nkomo IT (1973) Lead isotope systematics and uranium depletion in the Granite Mountains, Wyoming. *Geol Soc Amer Bull*, v 84, pp 989-1002
- Roubault M (1958) Géologie de l'uranium. Masson et Cie, Editeurs, Paris, 462 p
- Rouzaud J, Oberlin A, Trichet J (1981) Interaction of uranium and organic matter in uraniferous sediments. *Adv Organic Geochem*, v 1979, pp 505-516
- Rouzaud JN (1979) Étude structurale de matières carbonées associées a de minéralisations uranifères. Doct thesis, Univ Orléans, France
- Rowley PD, Cunningham CG, Steven TA, Mehnert HH, Naeser CW (1988) Geologic map of the Marysvale quadrangle, Piute County, Utah. *Utah Geol Min Surv Map* 105
- Rowley PD, Mehnert HH, Naeser CW, Snee LW, Cunningham CG, Steven TA, Anderson JJ, Sable EG, Anderson RE (1994) Isotopic ages and stratigraphy of Cenozoic rocks of the Marysvale volcanic field and adjacent areas, west-central Utah. *US Geol Surv Bull* 2071, 35 p
- Rowson JW (2002) Cogema's in situ leach uranium mining projects, Wyoming, USA. *in: In situ leach uranium mining*. TCM Almaty, 1996, T1-TC-975, IAEA, Vienna, pp 74-89
- Rozelle JW (2006) Technical report on the Converse uranium project, Converse County, Wyoming. Report NI 43-101, prepared for New Horizon Uranium Corporation on behalf of Crossroads Explorations Inc. Gustavson Associates LLC. 77 p (May 23, 2006, revised Dec 22, 2006)
- Rubin B (1970) Uranium roll-front zonation in the southern Powder River Basin, Wyoming. *Earth Sci Bull*, v 3, no. 4, pp 5-12
- Runnels RT, Schleicher JA, Van Nortwick HS (1953) Composition of some uranium-bearing phosphate nodules from Kansas shales. *State Geol Surv Kansas Bull* 102, pt 3, pp 93-104
- Rurvanec D (1980) Lisbon mine geology. Rio Algom Corp hand-out, 6 p
- Ryan JD (1964) Geology of the Edgemont quadrangle, Fall River County, South Dakota. *US Geol Surv Bull* 1063-J, pp 379-426
- Rytuba JJ (1976) Geology and ore deposits of the McDermitt caldera, Nevada-Oregon. *US Geol Surv Open-File Rep* 76-535, 9 p
- Rytuba JJ (1977) Uranium content of tuffaceous sediments and opalite mercury deposits within the McDermitt caldera, Oregon-Nevada (abstr). *Geol Soc Amer*, abstr w progr, v 9, no. 4, p 492
- Rytuba JJ (1981) Relation of calderas to ore deposits in the western United States, *in: Dickinson WR, Payne WD, eds., Relations of tectonics to ore deposits in the Southern Cordillera*. *Ariz Geol Soc Dig*, v XIV, pp 227-236
- Rytuba JJ, Conrad WK (1979) Structural and petrologic associations of uranium deposits within the McDermitt caldera complex, Nevada-Oregon (abstr). *in: Ann Meet, Geol Soc Amer*, abstr w progr, pp 508-509
- Rytuba JJ, Conrad WK (1981) Petrochemical characteristics of volcanic rocks associated with uranium deposits in the McDermitt caldera complex. *in: Goodell PC, Waters AC, eds., Uranium in volcanic and volcanoclastic rocks*. *Amer Ass Petrol Geol, Studies in Geology*, no. 13, pp 63-72
- Rytuba JJ, Conrad WK, Glanzman RK (1979) Uranium, thorium, and mercury distribution through the evolution of the McDermitt caldera complex. *US Geol Surv Open-File Rep* 79-541, 12 p
- Rytuba JJ, Glanzman RK (1978) Relation of mercury, uranium, and lithium deposits to the McDermitt caldera complex, Nevada-Oregon. *US Geol Surv Open-File Rep* 78-926, 19 p
- Sanford RF (1982) Preliminary model of regional Mesozoic groundwater flow and uranium deposition in the Colorado Plateau. *Geology*, v 10, pp 348-352
- Sanford RF (1992) A new model for tabular-type uranium deposits. *Econ Geol*, v 87, pp 2041-2055
- Sanford RF (1994) Hydrogeology of Jurassic and Triassic wetlands in the Colorado Plateau and the origin of tabular sandstone uranium deposits. *U.S. Geol Surv Prof Paper* 1548
- Santos ES (1963) Relation of ore deposits to the stratigraphy of the Ambrosia Lake area. *in: Kelley VC, ed., Geology and technology of the Grants Uranium Region*. *New Mex Bur Mines Miner Res Mem* 15, pp 53-59
- Santos ES (1968) Reflectivity and microindentation hardness of ferroselite from Colorado and New Mexico. *Amer Miner*, v 53, pp 2075-2077
- Santos ES (1970) Stratigraphy of the Morrison Formation and structure of the Ambrosia Lake District, New Mexico. *US Geol Surv Bull* 1272-E, 30 p
- Santos ES (1975) Lithology and uranium potential of Jurassic formations in the San Ysidro-Cuba and Majors Ranch areas, northwestern New Mexico. *US Geol Surv Bull* 1329, 22 p
- Santos ES (1981) Facies distribution in uranium host rocks of the southern Powder River Basin, Wyoming. *US Geol Surv Open-File Rep* 81-741, 15 p, 2 pls
- Santos ES, Ludwig KR (1983) Age of uranium mineralization at the Highland mine, Powder River Basin, Wyoming, as indicated by U-Pb isotope analyses. *Econ Geol*, v 78, pp 498-501
- Santos ES, Turner-Peterson CE (1986) Tectonic setting of the San Juan Basin in the Jurassic. *in: Turner-Peterson CE, Santos ES, Fishman NS, eds., A basin analysis case study - the Morrison Formation, Grants Uranium Region, New Mexico*. *Amer Ass Petrol Geol, Studies in Geology*, no. 22, pp 27-33
- Santos R (1981) Geology and mining development of the C-09 uranium deposit. *in: Uranium deposits in Latin America: Geology and exploration*. IAEA, Vienna, pp 533-553
- Saucier AE (1967a) The Morrison and related formations in the Gallup region. MS thesis, Univ New Mex, Albuquerque, 106 p (unpubl)
- Saucier AE (1967b) The Morrison Formation in the Gallup Region. *in: Guidebook, 18th Field Conf, Defiance, Zuni, Mt. Taylor Region*. *New Mex Geol Soc* pp 138-144
- Saucier AE (1974) Stratigraphy and uranium potential of the Burro Canyon Formation in the southern Chama Basin, New Mexico. *in: Guidebook, Ghost Ranch, 25th Anniversary Vol*. *New Mex Geol Soc*, pp 211-217
- Saucier AE (1976) Tectonic influence on uraniferous trends in the Late Jurassic Morrison Formation. *in: Tectonics and mineral resources of southwestern North America*. *New Mex Geol Soc Spec Publ* no. 6 pp 151-157
- Saucier AE (1980) Tertiary oxidation in Westwater Canyon Member of the Morrison Formation. *in: Rautman CA, compiler, Geology and mineral technology of the Grants uranium region 1979*. *New Mexico Bur Mines Miner Res, Memoir* 38, pp 116-121
- Sayala D, Ward DL (1983) Multidisciplinary studies of a uranium deposit in the San Juan Basin, New Mexico. *US DOE, GJBX-2(83)*, 220 p
- Scarborough RB (1981) Radioactive occurrences and uranium production in Arizona. *US DOE, GJBX 79-374E*, 297 p
- Scarborough RB, Wilt JC (1979) A study of uranium favorability of Cenozoic sedimentary rocks, Basin and Range province of Arizona, Part I General geology and chronology of pre-late Miocene Cenozoic sedimentary rocks. *US Geol Surv Open-File Report* 79-1429, 106 p
- Schlee J (1957) Petrology of the Jackpile sandstone, New Mexico (abstr). *Geol Soc Amer Bull*, v 68, no. 12, p 1793
- Schlee JS (1959) Sandstone pipes of the Laguna area, New Mexico (abstr). *Geol Soc Amer Bull*, v 70, no. 12, p 1669.
- Schlee JS (1963) Sandstone pipes of the Laguna area, New Mexico. *J Sed Petrol*, v 33, no. 1, pp 112-123
- Schlee JS, Moench RH (1961) Properties and genesis of "Jackpile" sandstone, Laguna, New Mexico. *in: Geometry of sandstone bodies*. *Amer Ass Petrol Geol*, pp 134-150
- Schmidt-Collerus JJ (1969) Part II, Experimental investigations, *in: Investigations of the relationship between organic matter and uranium deposits*. *US AEC, GJO-933-2*, 192 p
- Schmidt-Collerus JJ (1979) Investigation of the relationship between organic matter and uranium deposits. *US DOE, GJBX-130(79)*, 281 p

S

Sachdev SC (1980) Mineralogical variations across Mariano Lake roll-type uranium deposit, McKinley County. *in: Rautman CA, ed., Geology and mineral technology of the Grants Uranium Region 1979*. *New Mex Bur Mines Miner Res Mem* 38, pp 162-171

- Schmitt LJ (1968) Uranium and copper mineralization in the Big Indian Wash-Lisbon Valley mining district, southeast Utah. PhD thesis, Columbia Univ, New York, 173 p
- Schneider B (1981) Kriterien für die Wahl eines sauren oder alkalischen Verfahrensstrombaumes für eine Uranerzaufbereitungsanlage. *Erzmetall*, v 34, no. 6, pp 322-328
- Schreiber HW (1958) The geology and the occurrence of uranium in the Nelson Fond area of the West Point quadrangle, Putnam County, New York. MS thesis, Columbia Univ, New York, NY, 104 p (unpubl)
- Schumm SA (1977) The fluvial system. Wiley-Interscience, New York, 338 p
- Schwartz RJ (1957) Uranium occurrences of Gila County, Arizona. US AEC, RME-2071
- Scott RA (1961) Fossil woods associated with uranium on the Colorado Plateau. *in: Short papers in the geologic and hydrologic sciences*. US Geol Surv Prof Paper 424B, pp B130-B132
- Scott RC, Barker FB (1962) Data on uranium and radium in ground water in the United States, 1954 to 1957. US Geol Surv Prof Paper 426, 115 p
- Sears RS, Marjanieni DK, Blomquist JT (1974) A study of the Morrison Formation in the San Juan Basin, New Mexico and Colorado. US AEC, GJO-912-20, 102 p
- Seeland DA (1976) Relationship between early Tertiary sedimentation patterns and uranium mineralization in the Powder River Basin, Wyoming. *in: Geology and energy resources of the Powder River, Wyoming*. Guidebook, 28th Ann Field Conf. Wyoming Geol Ass, pp 53-64
- Sellards EH, Adkins WS, Plummer RB (1932) The geology of Texas, v 1, Stratigraphy. Univ Texas, Austin, Bull 3232, 1007 p
- Sevon WD, Rose AW, Smith RC II, Hoff DT (1978) Uranium in Carbon, Lycoming, Sullivan, and Columbia Counties, Pennsylvania. Guidebook, 43rd Ann Field Conf Pennsylvania Geologists. Dpt Environ Res, Bur Topogr Geol Surv, Harrisburg, Pennsylvania, 99 p
- Shappirio JR (1963) Geology and petrology of the Tallahassee Creek area, Fremont County, Colorado. PhD thesis, Univ Michigan, Ann Arbor, 282 p
- Sharp BJ (1955) Uranium occurrences at the Moonlight Mine, Humboldt County, Nevada. US AEC, RME-2032, 15 p
- Sharp BJ, Hetland DL (1954) Preliminary report on uranium occurrences in the Austin area, Lander County, Nevada. US AEC RME-2010, 16 p
- Sharp BJ, Williams NC, eds. (1963) Beryllium and uranium mineralization in western Juab County, Utah. Guidebook 17, Utah Geol Soc
- Sharp JWA (1955) Uranium deposits in the Morrison Formation, Church Rock area, McKinley County, New Mexico. US AEC, RME-79, 19 p
- Sharp WN, Gibbons AB (1964) Geology and uranium deposits of the southern part of the Powder River Basin, Wyoming. US Geol Surv Bull 1147-D, pp D1-D60
- Sharp WN, McKeown FA, McKay EJ, White AM (1964) Geology and uranium deposits of the Pumpkin Buttes area of the Powder River Basin, Wyoming. US Geol Surv Bull 1107-H, pp 541-638
- Shaub BM (1938) The occurrence, crystal habit and composition of the uranium from Ruggles Mine, near Grafton Center, New Hampshire. *Amer Miner*, v 23, pp 334-341
- Shawe DR (1956a) Significance of roll ore bodies in genesis of uranium-vanadium deposits on the Colorado Plateau. US Geol Surv Prof Paper 300, pp 239-241
- Shawe DR (1956b) Alteration related to Colorado Plateau ore deposits (abstr). *Geol Soc Amer Bull*, v 67, no. 12, pt 2, pp 1732-1733
- Shawe DR (1962) Localization of the Uranan Mineral Belt by sedimentation. US Geol Surv Prof Paper 450-C, pp C6-C8
- Shawe DR (1966) Zonal distribution of elements in some uranium-vanadium roll and tabular deposits on the Colorado Plateau. *in: Geological Survey Research 1966*, Chap B. US Geol Surv Prof Paper 550-B, pp B169-B175
- Shawe DR (1968) Petrography of sedimentary rocks in the Slick Rock district, San Miguel and Dolores Counties, Colorado. US Geol Surv Prof Paper 576-B, pp B1-B34
- Shawe DR (1972) Reconnaissance geology and mineral potential of the Thomas, Keg, and Desert calderas, central Juab County, Utah. US Geol Surv Prof Paper 800-B, pp B67-B77
- Shawe DR (1976a) Sedimentary rock alteration in the Slick Rock district, San Miguel and Dolores Counties, Colorado. US Geol Surv Prof Paper 576-D, pp D1-D51
- Shawe DR (1976b) Geologic history of the Slick Rock district and vicinity, San Miguel and Dolores Counties, Colorado. US Geol Surv Prof Paper 576-E, 19 p
- Shawe DR, Archbold NL, Simmons GC (1959) Geology and uranium-vanadium deposits of the Slick Rock district, San Miguel and Dolores Counties, Colorado. *Econ Geol*, v 54, pp 395-415
- Shawe DR, Granger HC (1965) Uranium ore rolls - an analysis. *Econ Geol*, v 60, pp 240-250
- Shchetochkin VN & Kislyakov YM (1993) Exogenic-epigenetic uranium deposits of the Kyzylkums and adjacent areas. *Geol Ore Deposits*, v 35, no. 3, pp 199-220
- Shea ME (1982) Uranium migration associated with some hydrothermal veins at Marysvale, Utah: a natural analog for radioactive waste isolation. MS thesis, Univ Calif, Riverside, 123 p (unpubl)
- Shea M, Foland KA (1986) The Marysvale natural analog study: preliminary oxygen isotope relations. *Chem Geol*, v 55, 281-295
- Sheldon RF (1959) Midnite mine - geology and development. *Min Eng*, v 11, no. 5, pp 531-534
- Sheldon RP (1959) Geochemistry of uranium in phosphorites and black shales of the Phosphoria Formation. US Geol Surv Bull 1084-D, pp 83-115
- Sheldon RP (1963) Physical stratigraphy and mineral resources of Permian rocks in Western Wyoming. US Geol Surv Prof Paper 313B, pp 49-273
- Shephard CU (1835) Uranite at Chesterfield (Massachusetts). *Amer J Sci*, no. 28
- Sherborne JE Jr, Buckovic WA, Dewitt DB, Hellinger TS, Pavlak SJ (1979) Major uranium discovery in volcanoclastic sediments, basin and range province, Yavapai County, Arizona. *Amer Ass Petrol Geol Bull*, v 63/4, pp 621-646
- Sherborne JE Jr, Pavlak SJ, Peterson CH, Buckovic WA (1980) Uranium deposits of the Sweetwater Mine area, Great Divide Basin, Wyoming. *in: Third Ann Uran Sem*, New York. Amer Inst Min Metal Petrol Eng, pp 27-37
- Sheridan DM, Maxwell CH, Albee AL (1967) Geology and uranium deposits of the Ralston Buttes district, Jefferson County, Colorado. US Geol Surv Prof Paper 520, 121 p
- Sheridan DM, Maxwell CH, Collier JT (1961) Geology of the Lost Creek schroekingite deposits, Sweetwater County, Wyoming. US Geol Surv Bull 1087-J, pp 391-478
- Shoemaker EM, Miesch AT, Newman WL (1959) Elemental composition of the sandstone-type deposits. *in: Garrels RM, Larsen ES III, comps, Geochemistry and mineralogy of the Colorado Plateau uranium ores*. US Geol Surv Prof Paper 320, pp 25-54
- Shoemaker EM, Roach CH, Byers FM Jr (1962) Diatremes and uranium deposits in the Hopi Buttes, Arizona. *in: Petrologic studies - A volume in honor of A. F. Buddington*. Geol Soc Amer, New York, pp 327-355
- Shrier T, Parry WT (1982) A hydrothermal model for the North Canning uranium deposit, Owl Creek Mountains, Wyoming. *Econ Geol*, v 77, pp 632-645
- Silver LT, Williams IS, Woodhead JA (1980a) Uranium in granites from the southwestern United States: Actinide parent-daughter systems, sites and mobilization - First year report. US DOE, GJBX-45(81), 380 p
- Silver LT, Williams IS, Woodhead JA (1980b) Uranium and thorium endowment, distribution and mobilization in a uraniumiferous Precambrian granite. 1980 Ann Meet, Geol Soc Amer, abstr w progr, p 522
- Silver LT, Woodhead JA, Williams IS (1982) Primary mineral distribution and secondary mobilization of uranium and thorium in radioactive granites. *in: Uranium exploration methods*. OECD-NEA, Paris, pp 355-367
- Silver LT, Woodhead JA, Williams IS, Chappel BW (1984) Uranium in granites from the southwestern United States: Actinide parent-daughter systems, sites, and mobilization. US Geol Surv Open-File Rep GJBX-7 (84), 431 p
- Sims PK (1956) Paragenesis and structure of pitchblende-bearing veins, Central City district, Gilpin County, Colorado. *Econ Geol*, v 51, pp 739-756
- Sims PK (1960) Geology of Central City-Idaho Springs area, Front Range, Colorado. *in: Weimer RJ, Haun JD, eds., Guide to the Geology of Colorado*. Geol Soc Amer, Rocky Mtn Ass Geol, and Colorado Sci Soc, pp 279-285
- Sims PK (1963) Geology of uranium and associated ore deposits, central part of the Front Range mineral belt, Colorado. US Geol Surv Prof Paper 371, 119 p
- Sims PK (1976) Precambrian tectonics and mineral deposits, Lake Superior region. *Econ Geol*, v 71, pp 1092-1127

- Sims PK (1989) Central City and Idaho Springs Districts, Front Range, Colorado. *in: Bryant B, Beaty DW, Mineral deposits and geology of Central Colorado. 28th Intern Geol Congr, Field Trip Guidebook T129, pp 15-19*
- Sims PK, Barton PB (1962) Hypogene zoning and ore genesis, Central City District, Colorado. *in: Engel AE, James HL, Leonard BF, eds., Petrologic studies. Geol Soc Amer, Buddington Vol, pp 373-395*
- Sims PK, Card KD, Lumbers SB (1981) Evolution of early Proterozoic basins of the Great Lakes region. *in: Campbell FHA, ed., Proterozoic basins of Canada. Geol Surv Can Paper 81-10, pp 379-397*
- Sims PK, Card KD, Morey GB, Peterman ZE (1980) The Great Lakes tectonic zone - a major crustal structure in central North America. *Geol Soc Amer, v 91, pp 690-698*
- Sims PK, Drake AA Jr, Tooker EW (1963) Economic geology of the Central City District, Gilpin County, Colorado. *US Geol Surv Prof Paper 359, 231 p*
- Sims PK, Osterwald FW, Tooker EW (1955) Uranium deposits in the Eureka Gulch area, Central City District, Gilpin County, Colorado. *US Geol Surv Bull 1032-A, 29 p*
- Sims PK, Sheridan DM (1964) Geology of uranium deposits in the Front Range, Colorado. *US Geol Surv Bull 1159, 116 p*
- Singer DA, Ovenshine AT (1979) The assessment of metallic mineral resources in Alaska. *US Geol Surv, Open-File Rep 78-1-A, 40 leaves*
- Smith DA, Peterson RJ (1980) Geology and recognition of a relict uranium deposit in Section 28, T 14 N, R 10 W, southwest Ambrosia Lake area, McKinley County, New Mexico. *in: Rautman CA, ed., Geology and mineral technology of the Grants Uranium Region 1979. New Mex Bur Mines Miner Res Mem 38, pp 215-225*
- Smith R, McLemore (2007) Cretaceous age roll front uranium ore deposits in the Grants mineral district. *Global Uran Symp, Corpus Christi, Texas, 45 p*
- Smith RB (1977) The theory of multiple oxidation and reduction of uranium deposits in south Texas. *South Texas Uran Sem, Corpus Christi, Texas*
- Smith RB (1979) Geology of south Texas uranium deposits. *in: South Texas Uran Sem, Denver, Colorado, Amer Inst Min Met Petrol Eng, pp 45-46*
- Smith RB (1991) An evaluation of the Dewey and Burdock Projects uranium resources, Edgemont District. *SD. Consultants report, 40 p*
- Smith RB (2005) Report on the Dewey-Burdock uranium project, Custer and Fall River Counties, South Dakota. Prepared for Denver Uranium Co. 41 p (Dec 15, 2005)
- Smith RC II, Hoff DT (1984) Geology and mineralogy of copper-uranium occurrences in the Picture Rocks and Stonestown quadrangles, Lycoming and Sullivan counties, Pennsylvania: *Pennsylvania Geol Surv, Miner Res Rep 80, 271 p*
- Snow CD (2007a) Technical report on the Sky uranium property, Fremont County, Wyoming. Prepared for Strathmore Minerals Corp, 33 p (Feb 14, 2007)
- Snow CD (2007b) Technical report on the Jeep uranium property, Fremont County, Wyoming. Prepared for Strathmore Minerals Corp. 33 p (June 3, 2007)
- Soister PE (1968) Stratigraphy of the Wind River Formation in south-central Wind River Basin, Wyoming. *US Geol Surv Prof Paper 594-A, 50 p*
- Soister PE, Conklin DR (1959) Bibliography of U.S. Geological Survey reports on uranium and thorium - 1942 through May 1958. *US Geol Surv Bull 1107-A*
- Soliz B (2007) Geologic development of the La Palangana & Hobson projects. *Global Uran Symp, Corpus Christi, Texas, 23 p*
- Southern Interstate Nuclear Board (1969) Uranium in the southern United States. *US AEC, WASH-1128, 230 p*
- Spirakis CS (1977) A theory for the origin of the Rifle-Garfield vanadium-uranium deposit. *in: Campbell JA, ed., Short Papers of the US Geol Surv Uranium-Thorium Symp (1977). US Geol Surv Circ 753, pp 8-10*
- Spirakis CS (1980) A possible relationship between subsidence and uranium mineralization in the Petrified Forest Member of the Chinle Formation in the Cameron - Holbrook - St Johns area of Arizona. *US Geol Surv Open-File Rep 80-808, 9 p*
- Spirakis CS (1981) The possible role of sulfate reduction kinetics in the formation of hydrothermal uranium deposits. *Econ Geol, v 76, pp 2236-2239*
- Spirakis CS (1982) Areas B and C - Chinle Formation (Triassic). *in: Wenrich-Verbeek KJ, Spirakis CS, Billingsley GH, Hereford R, Nealey LD, Ulrich GE, Verbeek ER, Wolfe EW, eds., National uranium resource evaluation, Flagstaff Quadrangle, Arizona. US DOE, PGJ/F-O14(82), pp 32-35*
- Spirakis CS (1991) Genesis of the tabular-type vanadium-uranium deposits of the Henry basin - a discussion. *Econ Geol, v 86, pp 1350-1353*
- Spirakis CS (1996) The roles of organic matter in the formation of uranium deposits in sedimentary rocks. *Ore Geol Reviews 11, pp 53-69*
- Spirakis CS, Pierson CT (1986) Some aspects of the genesis of uranium deposits of the Morrison Formation in the Grants Uranium Region, New Mexico, inferred from chemical characteristics of the deposits. *in: Turner-Peterson CE, Santos ES, Fishman NS, eds., A basin analysis case study - The Morrison Formation, Grants Uranium Region, New Mexico. Amer Ass Petrol Geol, Studies in Geol, no. 22, pp 161-169*
- Spirakis CS, Pierson CT, Granger HC (1981) Comparison of the chemical composition of mineralized and unmineralized (barren) samples of the Morrison Formation in the Ambrosia Lake uranium area, New Mexico. *US Geol Surv Rep 81-508, 43 p*
- Spirakis CS, Pierson CT, Peterson F (1984) Chemical characteristics of the uranium-vanadium deposits of the Henry Mountains mineral belt, Utah. *US Geol Surv Rep 84-367, 11 p*
- Spirakis CS, Pierson CT, Santos ES, Fishman NS (1983) Statistical treatment and preliminary interpretation of chemical data from a uranium deposit in the northeast part of the Church Rock area, Gallup mining district, New Mexico. *US Geol Surv Rep 83-379, 44 p*
- Squyres JB (1963) Geology and ore deposits of the Ann Lee mine, Ambrosia Lake area. *in: Kelley VC, ed., Geology and technology of the Grants Uranium Region. New Mex Bur Mines Miner Res Mem 15, pp 90-101*
- Squyres JB (1970) Origin and depositional environment of uranium deposits of the Grants region, New Mexico. *Stanford Univ, PhD diss, 228 p (unpubl)*
- Squyres JB (1974) Uranium deposits of the south San Juan Basin, New Mexico. Paper presented at Amer Inst Min Eng Ann Meet, Dallas, Texas, preprint no. 74-5-13, 20 p
- Squyres JB (1980) Origin and significance of organic matter in uranium deposits of Morrison Formation, San Juan Basin, New Mexico. *in: Rautman CA, ed., Geology and mineral technology of the Grants Uranium Region 1979. New Mex Bur Mines Miner Res Mem 38, pp 86-97*
- Staatz MH (1978) I and L uranium and thorium vein system, Bokan Mountain, southeastern Alaska. *Econ Geol, v 73, 512-523*
- Staatz MH, Osterwald FW (1956) Uranium in the fluorspar deposits of the Thomas Range, Utah. *US Geol Surv Prof Pap 300, pp 131-136*
- Staatz MH, Carr WJ (1964) Geology and mineral deposits of the Thomas and Dugway Ranges, Juab and Tooele Counties, Utah. *US Geol Surv Prof Paper 415, 188p*
- Stark JH (1979) Geology of the Mena mine area with emphasis on the mineralogy and paragenesis of the Mena mine deposit, Jefferson County, Colorado. *MS thesis, Colo State Univ, Fort Collins, 164 p (unpubl)*
- Steele BA (1984) Preliminary report on the petrography of the Upper Jurassic Morrison Formation, Mariano Lake-Lake Valley drilling project, McKinley County, New Mexico. *US Geol Surv Res 84-170, 43 p*
- Stephens JG, Healy DL (1964) Geology and uranium deposits at Crooks Gap, Fremont County, Wyoming, with a section on gravity and seismic studies. *US Geol Surv Bull 1147-F, pp F1-F82*
- Steven TA, Cunningham CG, Mchette MN (1981) Integrated uranium systems in the Marysvale volcanic field, west-central Utah. *US Geol Surv Rep 80-524, 39 p*
- Steven TA, Cunningham CG, Naeser CW, Mehnert HH (1977) Revised stratigraphy and radiometric ages of volcanic rocks and mineral deposits in the Marysvale area, west-central Utah. *US Geol Surv Open-File Rep 77-569, 45 p*
- Steven TA, Cunningham CG, Naeser CW, Mehnert HH (1979) Revised stratigraphy and radiometric ages of volcanic rocks and mineral deposits in the Marysvale area, west-central Utah. *US Geol Surv Bull 1469, 40 p*
- Steven TA, Morris HT (1987) Summary mineral resource appraisal of the Richfield 1° × 2° quadrangle, west-central Utah. *US Geol Surv Circ 916, 24 p*
- Steven TA, Rowley PD, Cunningham CG (1978) Geology of the Marysvale volcanic field, west-central Utah. *Brigham Young Univ Geol Studies, v 25, pt 1, pp 67-70*
- Stewart CL, Reimann LJ, Swapp SM (2000) Mineralogic considerations for uranium in-situ leach mining - A preliminary study of uranium and associated mineralogy of roll-front uranium deposits in Wyoming and Nebraska. *in:*

- Ozbok E, ed., Process metallurgy of uranium - Uranium 2000. Metall Soc, pp 241-255
- Stewart JH et al. (1959) Stratigraphy of the Triassic and associated formations in part of the Colorado Plateau region. US Geol Surv Bull 1046-Q, pp 487-576
- Stewart JH, Poole FG, Wilson RF (1972) Stratigraphy and origin of the Chinle Formation and related Triassic strata in the Colorado Plateau region. US Geol Surv Prof Paper 690, 336 p
- Stewart JH (1980) Geology of Nevada. Nev Bur Mines Geol Spec Publ 4, 136 p
- Stillwell LW (1885) Uranium minerals in the Black Hills. Amer J Sci, III, ser 30
- Stinnett LA (2007) Technical report on Energy Fuels Resources Corporation's Energy Queen property, San Juan County, Utah. Report NI 43-101, prepared for Energy Fuels Inc. FGM Consulting Group, Inc, 39 p (July 6, 2007)
- Stoick AF, Boltz KL, Buswell MD (1981) Discovery of uranium deposits near Oshoto, East Central Powder River basin, Wyoming, USA. *in*: Uranium exploration case histories. IAEA, Vienna, pp 293-306
- Stokes WL (1953a) Preliminary sedimentary trend indicators as applied to ore findings in the Carrizo Mountains, Arizona and New Mexico. US AEC, RME-3043, pt 1, 48 p
- Stokes WL (1953b) Progress report on relation of sedimentary features of the Salt Wash sandstone to tectonic elements and uranium mineralization (Colorado Plateau). US AEC, RME-3058, 5 p
- Stokes WL (1953c) Sedimentary patterns and uranium mineralization in the Morrison Formation of the Colorado Plateau (abstr). Geol Soc Amer Bull, v 64, no. 12, p 1516
- Stokes WL (1954a) Cyclical deposition of fluvial sediments (Colorado Plateau) (abstr). Geol Soc Amer Bull, v 65, no. 12, pt 2, p 1309
- Stokes WL (1954b) Some stratigraphic, sedimentary, and structural relations in uranium deposits in the Salt Wash sandstone. Final report - April 1, 1952 to June 30, 1954, US AEC, RME-3102
- Stokes WL (1954c) Stratigraphy of the southeastern Utah uranium region. *in*: Stokes WL, ed., Uranium deposits and general geology of southeastern Utah, Guidebook no. 9. Utah Geol Soc, pp 16-47
- Stokes WL (1954d) Relation of sedimentary trends, tectonic features, and ore deposits in the Blanding district, San Juan County, Utah. US AEC, RME-3093 pt 1, 40 p
- Stokes WL (1967a) A survey of southeastern Utah uranium districts. *in*: Uranium districts of southeastern Utah, Guidebook no. 21. Utah Geol Soc, pp 1-11
- Stokes WL, Mobley CM (1954) Geology and uranium deposits of the Thompson area, Grand County, Utah. *in*: Stokes WL, ed., Uranium deposits and general geology of southeastern Utah, Guidebook no. 9. Utah Geol Soc, pp 78-94
- Stout RM, Stover DE (1997) The Smith Ranch uranium project. *in*: Uranium and nuclear energy: 1997. Uran Inst, London, pp 105-118
- Stover DE (2004) Smith Ranch ISL uranium facility: The wellfield management programme. *in*: Recent developments in uranium resources and production with emphasis on in situ leach mining. TECDOC-1396, IAEA, Vienna, pp 189-203
- Stuckless JS (1979) Uranium and thorium concentrations in Precambrian granites as indicators of a uranium province in central Wyoming. Univ Wyoming Contrib Geol, v 17, pp 173-178
- Stuckless JS (1987) A review of applications of U-Th-Pb isotope systematics to investigations of uranium source rocks. Uranium, v 3, no. 2-4, pp 235-244
- Stuckless JS, Bunker CM, Bush CA, Doering WP, Scott JH (1977) Geochemical and petrological studies of a uraniferous granite from the Granite Mountains, Wyoming. J Res US Geol Surv, v 5, no. 1, pp 61-81
- Stuckless JS, Bunker CM, Nkomo IT (1975) Uranium mobility in a uraniferous granite from the Granite Mountains, Wyoming (abstr). Geol Soc Amer, abstr w progr, v 7, pp 1286-1287
- Stuckless JS, Ferreira CC (1976) Labile uranium in granitic rocks. *in*: Exploration of uranium ore deposits. IAEA, Vienna, pp 717-730
- Stuckless JS, Nkomo IT (1978) Uranium-lead isotope systematics in uraniferous alkali-rich granites from the Granite Mountains, Wyoming: Implications for uranium source rocks. Econ Geol, v 73, pp 427-441
- Stuckless JS, Nkomo IT, Doe BR (1981) U-Th-Pb systematics in hydrothermally altered granites from the Granite Mountains, Wyoming. Geochim Cosmochim Acta, v 45, pp 635-645
- Stuckless JS, van Trump G (1982) A compilation of radioelement concentrations in granitic rocks of the contiguous United States. *in*: Uranium exploration methods. OECD-NEA, Paris, pp 191-208
- Stugard F Jr, Wyant DG, Gude AJ (1952) Secondary uranium deposits in the United States. *in*: Selected papers on uranium deposits in the United States. US Geol Surv Circ 220, pp 19-25
- Sutphin HB (1986) Occurrence and structural control of collapse features on the southern Marble Plateau, Coconino County, Arizona. MSc thesis, Northern Ariz Univ, Flagstaff, 139 p
- Sutphin HB, Wenrich KJ (1983) Map showing structural control of breccia pipes on the southern Marble Plateau, Arizona. US Geol Surv Open-File Rep 83-908, 6 p., 2 plates (Superseded by US Geol Surv Misc Invest Ser Map 1-1778, 1988).
- Suzuki Y, Kelly SD, Kemner KM, Banfield JE (2005) Direct microbial reduction and subsequent preservation of uranium in natural near-surface sediment. Applied and Environm Microbiology, v 71, pp 1790-1797
- Swanson RW (1970) Mineral resources in Permian rocks of southwest Montana. US Geol Surv Prof Paper 313-E, pp 661-777
- Swanson VE (1960) Oil yield and uranium content of black shales. US Geol Surv Prof Paper 356A, pp 1-44
- Swanson VE (1961) Geology and geochemistry of uranium in marine black shales, a review. US Geol Surv Prof Paper 356-C, pp 67-112
- Swinehart JB, Souder VL, DeGraw HM, Diffendal RF Jr. (1985) Cenozoic paleogeography of western Nebraska. *in*: Flores RM, Kaplan SS, eds., Cenozoic paleogeography of the west-central United States. Rocky Mtn Sect, Soc Econ Paleont Miner, pp 187-206

T

- Taylor HP Jr, (1979) Oxygen and hydrogen isotope relationships in hydrothermal mineral deposits. *in*: Barnes HL, ed., Geochemistry of hydrothermal ore deposits, (2nd ed). John Wiley & Sons, New York, pp 236-277
- Taylor AO, Anderson TP, O'Toole WL, Waddell GG, Gray AW, Douglas H, Cherry CL, Caywood RM (1951) Geology and uranium deposits of Marysvale, Utah. Interim report on the producing area. US AEC, RMO-896, 30 p
- Taylor AO, Powers JF (1955) Uranium occurrences at the Moonlight Mine and Granite Point claims, Humboldt County, Nevada. US Geol Surv, Trace Element Mem Open-File Rep TEM-874-A, 16 p
- Tessendorf TN (1980) The redistributed orebodies of Poison Canyon, Sections 18 and 19, T13N, R9W, McKinley County, New Mexico. New Mex Bur Mines Miner Res Mem 38, pp 226-229
- Thaden RE (1976a) Preliminary geologic map of the DePass quadrangle, Fremont and Hot Springs Counties, Wyoming. US Geol Surv Open-File Rep 76-207, 1 p
- Thaden RE (1976b) Preliminary geologic map of the Guffy Peak quadrangle, Fremont and Hot Springs Counties, Wyoming: US Geol Surv Open-File Rep 76-229, 1 p
- Thaden RE, Santos ES (1956) Grants area, New Mexico. *in*: Geologic investigations of radioactive deposits. Semi-annual progress report for June 1 to November 30, 1956, pp 73-76
- Thaden RE, Trites AF Jr, Finnell TL (1964) Geology and ore deposits of the White Canyon area, San Juan and Garfield Counties, Utah. US Geol Surv Bull 1125, 166 p
- Thaden RE, Zech RS (1986) Structure contour map of the San Juan Basin and vicinity. *in*: Turner-Peterson CE, Santos ES, Fishman NS, eds., A basin analysis case study - The Morrison Formation, Grants Uranium Region, New Mexico. Amer Ass Petrol Geol, Studies in Geology, no 22, pp 35-45
- Thamm JK, Kovschak AA, Adams SS (1981) Geology and recognition criteria for sandstone uranium deposits of the Salt Wash type, Colorado Plateau province. US DOE, GJBX-6(81), 136 p
- Thayer PA (1970) Stratigraphy and geology of Dan River Triassic basin, North Carolina. Southeast Geol, v 12, pp 1-31
- Thode HG, Kleerekoper H, McElchere D (1951) Isotopic fractionation in the bacterial reduction of sulfate. Research (London), v 4, pp 581-582
- Thompson TB, Lyttle T, Pierson JR (1980) Genesis of the Bokan Mountain, Alaska, uranium-thorium deposit. US DOE, GJBX-38(80), 232 p
- Thompson TB, Pierson JR, Lyttle T (1982) Petrology and petrogenesis of Bokan granite complex, southeastern Alaska. Geol Soc Amer Bull, 93, pp 898-908

- Thomson KC (1967) Structural features of southeast Utah and their relations to uranium deposits. *in*: Uranium districts of southeast Utah. Guidebook 21, Utah Geol Soc, pp 23-31
- Thurlow EE (1952) Preliminary report on uranium-bearing deposits of the northern Boulder batholith region, Jefferson County, Montana. US AEC, RMO-800, 15 p
- Thurlow EE (1956) Uranium deposits at the contacts of metasediments and granitic intrusives in the western United States. US Geol Surv Prof Paper 300, pp 85-89
- Thurlow EE, Wright RJ (1950) Uraninite in the Coeur d'Alene district, Idaho. Econ Geol, v 15, pp 395-404
- Tilsley JE (1980a) Continental weathering and development of paleosurface-related uranium deposits: some genetic considerations. *in*: Ferguson J, Goley AB, eds., Uranium in the Pine Creek Geosyncline. IAEA, Vienna, pp 721-732
- Tooker EW (1983) Correlation of metal occurrence and terrane attributes in the northwestern conterminous United States. Can J Earth Sci, v 20, pp 1030-1039
- Towse D (1957) Uranium deposits in western North Dakota and eastern Montana. Econ Geol, v 52, pp 904-913
- Trentham RC (1981) Leaching of uranium from felsic volcanics and volcanoclastics; model, experimental studies and analysis of sites. DGSc diss, Univ Texas, El Paso, 204 p
- Treuil M (1985) A global geochemical model of uranium distribution and concentration in volcanic rock series. *in*: Uranium deposits in volcanic rocks, IAEA, Vienna, pp 53-68
- Trimble LM, Doelling HH (1978) The geology and uranium-vanadium deposits of the San Rafael River mining area, Emery County, Utah. Utah Geol Miner Surv Bull 113, 122 p
- Trites AF Jr, Chew RT III (1955) Geology of the Happy Jack Mine, White Canyon area, San Juan County, Utah. US Geol Surv Bull 1009-H, pp 235-248
- Trites AF, Chew RT 3rd, Lovering TG (1959) Mineralogy of the uranium deposits of the Happy Jack mine, San Juan County, Utah. *in*: Garrels and Larsen, comp, Geochemistry and mineralogy of the Colorado Plateau uranium ores. US Geol Surv Prof Paper 320, pp 185-195
- Truesdell AH, Weeks AD (1960) Paragenesis of uranium ores in Todilto Limestone near Grants, New Mexico. *in*: Geological Survey Research 1960. US Geol Surv Prof Paper 400-B, pp B52-B54
- Turner CE, Fishman NS, Hatcher PG, Spiker EC (1993) Nature and role of organic matter in sandstone uranium deposits, Grants uranium region, New Mexico, USA. *in*: Parnell J, Kucha H, Landais P, eds., Bitumens in ore deposits. Springer, Berlin ff, pp 239-275
- Turner CL, Herreid G, Bundtzen TK (1977) Geochronology of southern Prince of Wales Island, Alaska. *in*: Short notes on Alaskan geology. US Geol Surv Open-File Rep 77-55, pp 11-16
- Turner Peterson CE, ed. (1980) Uranium in sedimentary rocks-application of the facies concept to exploration. Short course notes. Soc Econ Paleont Miner, Rocky Mtn Sect, Denver, Colorado, 211 p
- Turner-Peterson CE (1980) Sedimentology and uranium mineralization in the Triassic-Jurassic Newark Basin, Pennsylvania and New Jersey. *in*: Turner-Peterson CE, ed., Uranium in sedimentary rocks: application of the facies concept to exploration. Short Course notes. Rocky Mtn Sect, Soc Econ Paleont Miner, Denver, Colorado, p. 149-175
- Turner-Peterson CE (1981) Application of lacustrine-humate model to New Mexico Grants mineral belt and relation between ore types and hydrologic history of San Juan Basin. Amer Ass Petrol Geol Bull, v 65, pp 571-572
- Turner-Peterson CE (1985) Lacustrine-humate model for primary uranium ore deposits, Grants Uranium Region, New Mexico. Amer Ass Petrol Geol Bull, v 69, pp 1999-2020
- Turner-Peterson CE (1986) Fluvial sedimentology of a major uranium host sandstone - a study of the Westwater Canyon Member of the Morrison Formation, San Juan Basin, New Mexico. *in*: Turner-Peterson CE, Santos ES, Fishman NS, eds., A basin analysis case study - the Morrison Formation, Grants Uranium Region, New Mexico. Amer Ass Petrol Geol, Studies in Geology, no. 22, pp 47-75
- Turner-Peterson CE, Fishman NS (1986) Geologic synthesis and genetic models for uranium mineralization in the Morrison Formation, Grants Uranium Region, New Mexico. *in*: Turner-Peterson CE, Santos ES, Fishman NS, eds., A basin analysis case study: the Morrison Formation, Grants Uranium Region, New Mexico. Amer Ass Petrol Geol, Studies in Geology, no. 22, pp 357-388
- Turner-Peterson CE, Gundersen LC, Francis DS, Aubrey WM (1980) Fluvio-lacustrine sequences in the Upper Jurassic Morrison Formation and the relationship of facies to tabular uranium ore deposits in the Poison Canyon area, Grants mineral belt, New Mexico. *in*: Turner-Peterson CE, ed., Uranium in sedimentary rocks-application of the facies concept to exploration. Short Course Notes. Soc Econ Paleont Miner, Rocky Mtn Sect, pp 177-211
- Turner-Peterson CE, Olsen PE, Nuccio VF (1985) Modes of uranium occurrence in black mudstones in the Newark Basin, New Jersey and Pennsylvania. *in*: Robinson GR Jr, Froelich AJ, Proceedings of the Second U.S. Geological Survey Workshop on the Early Mesozoic Basins of the Eastern United States. US Geol Surv Circ 946, 147 p
- Turner-Peterson CE, Peterson F (1978) Uranium in sedimentary rocks, with emphasis on facies control in sandstone-type deposits. US Geol Surv Rep 78-359 15 p
- Turner-Peterson CE, Santos ES, Fishman NS, eds. (1986) A basin analysis case study: the Morrison Formation, Grants Uranium Region, New Mexico. Amer Ass Petrol Geol, Studies in Geology, no. 22, 391 p
- Tweto O (1975) Laramide (Late Cretaceous-Early Tertiary) Orogeny in the southern Rocky Mountains. Geol Soc Amer Mem 144, pp 1-44
- Tweto O (1977) Nomenclature of Precambrian rocks in Colorado. US Geol Surv Bull 1422-D, 22 p
- Tweto O (1979) Geologic map of Colorado. US Geol Surv
- Tweto O, Sims PK (1963) Precambrian ancestry of the Colorado Mineral Belt. Geol Soc Amer Bull, v 74, pp 991-1014
- Tyler N (1981) Jurassic depositional history and vanadium-uranium deposits, Slick Rock district, Colorado Plateau. PhD thesis, Colo State Univ, Fort Collins, 184 p (unpubl)
- Tyler N, Ethridge FG (1983) Depositional setting of the Salt Wash Member of the Morrison Formation, southwest Colorado. J Sediment Res, v 53, no.1, pp 67-82
- Tyler PM (1930) Radium. US Bur Mines Inf Circ 6312, 55 p

U

- US AEC (1959) Guidebook to uranium deposits of the western United States. US AEC, Grand Junction, Colorado, 1-1 to 7-14 p
- US AEC and US Geol Surv (1969) Preliminary reconnaissance for uranium in Connecticut, Maine, Massachusetts, New Jersey, New York and Vermont, 1950 to 1959. US AEC, RME-4106, 129 p
- US Bureau of Mines (1977) Uranium, vanadium, and thorium in Washington. US Bur Mines, Western Field Operations Center, Spokane, Washington, pp 196-267
- US DOE (1968-1983) Statistical data of the uranium industry. US DOE, GJO-100(+ publication year)
- US DOE (1978) Uranium industry seminar. US DOE, Proceed, GJO-108(78), 245 p
- USDOE (1980) An assessment report on uranium in the United States of America. US DOE, GJO-111(80) 150 p
- USDOE (1982) American sources of uranium acquired by the Manhattan Project. US DOE, TM-350, 4 p
- US DOE (ERDA) (1976) National uranium resource evaluation, preliminary report. US DOE, GJO-111(76), 132 p
- US DOE EIA (1989) Uranium industry annual 1988. US DOE, Rep DOE/E-IA-D478(88), 121 p
- US DOE EIA (1994) Decommissioning of U.S. uranium-related facilities. Appendix C site characterization data sheets. web site doeal.gov/oeppm;
- US DOE EIA (2002) Uranium industry annual 2001. DOE/EIA-0478(2001), 60 p (URL <http://www.eia.doe.gov/fuelnuclear.html>)
- US DOE EIA (2003) Uranium industry annual survey, Schedule A, Uranium raw material activities (1984-2002). US DOE, Grand Junction Office of Coal, Nuclear, Electric and Alternate Fuels, Form EIA-858

- US DOE EIA (2003) Domestic uranium production report. US DOE, Grand Junction Office of Coal, Nuclear, Electric and Alternate Fuels, Form EIA-851A
- US DOE EIA (2003) Uranium industry annual 2002. DOE/EIA-0478(2002), 58 p (URL <http://www.eia.doe.gov/fuelnuclear.htm>)
- US DOE EIA (2004) Uranium reserves estimates. (<http://www.eia.doe.gov/cneaf/nuclear/page/reserves/ures.html>)
- US Geological Survey (1963) Geology of uranium-bearing veins in the conterminous United States. US Geol Surv Prof Pap 455-A, B, C, D, E, F, 120 p
- US Geological Survey (1997) Uranium, its impact on the national and global energy mix - and its history, distribution, production, nuclear-fuel-cycle, future, and relation to the environment. US Geol Surv Circular 1141, available on-line: <http://pubs.usgs.gov/circ/>.
- V**
- Vail PR, Mitchum RM Jr, Thompson S III (1977) Global cycles of relative changes of sea level. *Amer Ass Petrol Geol Memoir* 26, pp 83-97
- Van Gosen BS, Hammarstrom J, Eppinger R (2007) Geology and geochemistry of the Stanley uranium district, Custer county, central Idaho. *Global Uran Symp, Corpus Christi, Texas, May 2007*, 25 p
- Van Gosen BS, Wenrich KJ, Sutphin HB, Scott JH, Balcer RA (1989) Drilling of a U-mineralized breccia pipe near Blue Mountain, Hualapai Indian Reservation, northern Arizona. *US Geol Surv Open-File Rep* 89-0100, 80 p
- Van Houten FB (1964) Tertiary geology of the Beaver Rim area, Fremont and Natrona Counties, Wyoming. *US Geol Surv Bull* 1164, 99 p
- Verbeek ER, Grout MA, Van Gosen BS (1988) Structural evolution of a Grand Canyon breccia pipe: The Ridenour copper-vanadium-uranium mine, Hualapai Indian Reservation, Coconino County, Arizona. *US Geol Surv Open-File Rep* 88-006, 75 p
- Vickers RC (1956) Origin and occurrence of uranium in northern Michigan. *US Geol Surv Open-File Rep* 402, 76 p
- Vickers RC (1957) Alteration of sandstone as a guide to uranium deposits and their origin, northern Black Hills, South Dakota. *Econ Geol*, v 52, pp 599-611
- Vine JD (1962) Geology of uranium in coaly carbonaceous rocks. *US Geol Surv Prof Paper* 356-D, pp 113-170
- Vine JD, Bachman GO, Read CB, Moore GW (1953) Uranium-bearing coal and carbonaceous shale in the La Ventana Mesa area, Sandoval County, New Mexico. *US Geol Surv, Trace Element Invest* TEI-24I, 34 p
- Vine JD, Tourtelot EB (1970a) Geochemistry of the black shale deposits - a summary report. *Econ Geol*, v 65, pp 253-272
- Vine JD, Tourtelot EB (1970b) Preliminary geochemical and petrographic analysis of Lower Eocene fluvial sandstones in the Rocky Mountain region. *Guidebook, 22nd Field Conf, Wyoming Geol Ass*, pp 251-263
- Von Barga DJ (1979) The silver-antimony-mercury system and the mineralogy of the Black Hawk district, New Mexico. PhD thesis, Purdue Univ, 228 p
- Voss WC, Gorski DE (2007) Report on the Centennial Project, Weld County, Colorado. Technical report 43-101, prepared for Powertech Uranium Corp., 46 p (March 28, 2007)
- Vredenburg LD, Cheney ES (1971) Sulfur and carbon isotopic investigation of petroleum, Wind River Basin, Wyoming. *Amer Ass Petrol Geol Bull*, v 55, no. 11, pp 1954-1975
- uranium-bearing veins in the conterminous United States. *US Geol Surv Prof Pap* 455-C, pp 36-53
- Walker GW (1963c) Supergene alteration of uranium-bearing veins in the conterminous United States. *in: US Geol Surv, Geology of uranium-bearing veins in the conterminous United States. US Geol Surv Prof Pap* 455-E, pp 91-103
- Walker GW (1981) Uranium, thorium and other metal associations in silicic volcanic complexes of the northern Basin and Range, a preliminary report. *US Geol Surv Open-File Rept* 81-1290, 45 p
- Walker GW (1985) Geology of the Lakeview uranium area, Lake County, Oregon. *in: Uranium deposits in volcanic rocks. IAEA, Vienna*, pp 411-447
- Walker GW, Adams JW (1963) Mineralogy, internal structural and textural characteristics, and paragenesis of uranium-bearing veins in the conterminous United States. *in: US Geol Surv, Geology of uranium-bearing veins in the conterminous United States. US Geol Surv Prof Pap* 455-D, pp 54-90
- Walker GW, Adams JW, Osterwald FW (1963) Geology of uranium-bearing veins in the conterminous United States. *US Geol Surv Prof Pap* 455-A, B, C, D, E, F, 120 p
- Walker GW, Lovering TG, Stephens HG (1956) Radioactive deposits in California. *Calif Div Mines Spec Rep* 49, 38 p
- Walker GW, Osterwald FW (1956a) Relation of secondary uranium minerals to pitchblende-bearing veins at Marysvale, Piute County, Utah. *US Geol Surv Prof Pap* 300, pp 123-129
- Walker GW, Osterwald FW (1956b) Uraniferous magnetite-hematite deposit at the Prince Mine, Lincoln County, New Mexico. *Econ Geol*, v 51, pp 213-222
- Walker GW, Osterwald FW (1963a) Introduction to the geology of uranium-bearing veins in the conterminous United States, including sections on geographic distribution and classification of veins. *in: US Geol Surv, Geology of uranium-bearing veins in the conterminous United States. US Geol Surv Prof Pap* 455-A, pp 1-28
- Walker GW, Osterwald FW (1963b) Concepts of origin of uranium-bearing veins in the conterminous United States. *in: US Geol Surv, Geology of uranium-bearing veins in the conterminous United States. US Geol Surv Prof Pap* 455-F, pp 104-120
- Wall JD, Krumholz LR (2000) Uranium reduction. *Ann Rev Microbiol*, v 60, pp 149-166
- Wallace AB, Drexler JW, Grant NK, Noble DC (1980) Icelandite and aenigmatite-bearing pantellerite from the McDermitt Caldera complex, Nevada-Oregon. *Geology* v 8, no.1, pp 380-384
- Wallace AB, Roper MW (1981) Geology and uranium deposits along the north-eastern margin of the McDermitt caldera complex, Oregon. *in: Goodell PC, Waters AC, eds., Uranium in volcanic and volcanoclastic rocks. Amer Ass Petrol Geol, Studies in Geology*, no. 13, pp 73-79
- Wallace AR (1979) Alteration and vein mineralization, Ladwig uranium mine, Jefferson County, Colorado. *US Geol Surv Open-File Rep* 79-1615, 34 p
- Wallace AR (1982) Structural and mineralogical characteristics and distribution of carbonate-dominated fault breccia associated with uranium deposits, Front Range, Colorado. *Econ Geol*, v 77, pp 1945-1950
- Wallace AR (1983a) Alteration and vein mineralization, Schwartzwalder uranium deposit, Front Range, Colorado. *US Geol Surv Rep* 83-417, 172 p
- Wallace AR (1983b) Analytical data from host rocks and ores, Schwartzwalder uranium deposit, Front Range, Colorado. *US Geol Surv Rep* 83-364, 2 p, 15 tables
- Wallace AR (1986) Geology and origin of the Schwartzwalder uranium deposit, Front Range, Colorado, USA. *in: Vein-type uranium deposits. TECDOC-361, IAEA, Vienna*, pp 159-168
- Wallace AR, Karlson RC (1982) Alteration and vein mineralization, Schwartzwalder uranium mine, Jefferson County, Colorado. *Geol Soc Amer, abstr w programs*, v 14, no. 6, p 353
- Wallace AR, Karlson RC (1985) The Schwartzwalder uranium deposit; I: Geology and structural controls on mineralization. *Econ Geol*, v 80, pp 1842-1857
- Wallace AR, Ludwig KR, Whelan JF (1983) The age and origin of the Schwartzwalder uranium deposit, Front Range, Colorado. *Amer Ass Petrol Geol, Rocky Mtn Cordilleran Sect, abstr w progr*, p 399
- Wallace AR, Whelan JF (1986) The Schwartzwalder uranium deposit, III: Alteration, vein mineralization, light stable isotopes and genesis of the deposit. *Econ Geol*, v 81, pp 872-888
- W**
- Waage KM (1959) Stratigraphy of the Inyan Kara Group in the Black Hills. *US Geol Surv Bull* 1081-B, pp 41-65
- Walker GW (1963a) Age of uranium-bearing veins in the conterminous United States. *in: US Geol Surv, Geology of uranium-bearing veins in the conterminous United States. US Geol Surv Prof Pap* 455-B, pp 29-35
- Walker GW (1963b) Host rocks and their alterations as related to uranium-bearing veins in the conterminous United States. *in: US Geol Surv, Geology of*

- Wallis S (2005) Technical report on the Sahara Mine project, Utah. Report for NI 43-101, prepared for Uranium Power Corp. Roscoe Postle Ass Inc. 38 p (June 22, 2005)
- Wallis S (2006a) Technical report on the Lost Creek project, Wyoming. Report NI 43-101, prepared for Ur-Energy Inc. Roscoe Postle Ass Inc. 52 p (June 15, 2006)
- Wallis S (2006a) Technical report on the Lost Creek project, Wyoming. Report NI 43-101, prepared for Ur-Energy Inc. Roscoe Postle Ass Inc. 52 p (June 15, 2006)
- Wallis S (2006b) Technical report on the Lost Soldier project, Wyoming. Report for NI 43-101, prepared for Ur-Energy Inc. Roscoe Postle Ass Inc. 51 p (July 10, 2006)
- Wallis S (2006b) Technical report on the Lost Soldier project, Wyoming. Report for NI 43-101, prepared for Ur-Energy Inc. Roscoe Postle Ass Inc. 51 p (July 10, 2006)
- Wallis S, Rennie DW (2006) Technical report on the Sheep Mountain uranium project, Wyoming. Report for NI 43-101, prepared for Uranium Power Corp. Scott Wilson Roscoe Postle Ass Inc. 66 p (Oct 10, 2006)
- Walton AW (1978) Release of uranium during alteration of volcanic glass. *in: Formation of uranium ores by diagenesis of volcanic sediments*. US DOE, GJBX-22(79), Sect VI, pp 1-51
- Walton AW, Galloway WE, Henry CD (1981) Release of uranium from volcanic glass in sedimentary sequences: an analysis of two systems. *Econ Geol*, v 76, pp 69-88
- Wanty RB (1986) Geochemistry of vanadium in an epigenetic sandstone-hosted vanadium-uranium deposit, Henry basin, Utah. PhD thesis, Colo Sch Mines, 198 p (unpubl)
- Wanty RB, Chatham JR, Langmuir D (1987a) The solubilities of some major and minor element minerals in ground waters associated with a sandstone-hosted uranium deposit. *Bull Miner*, v 110, pp 209-226
- Wanty RB, Fitzpatrick JJ, Goldhaber MB (1987b) Geochemical and crystallographic constraints on the formation of the vanadium-uranium ores of the Colorado Plateau (abstr). *US Geol Surv Circ* 995, pp 71-72
- Wanty RB, Goldhaber MB, Northrop HR (1990) Geochemistry of vanadium in an epigenetic, sandstone-hosted vanadium-uranium deposit, Henry basin, Utah. *Econ Geol*, v 85, pp 270-284
- Ward JM (1978) History and geology of Homestake's Pitch project, Saguache County, Colorado (abstr). Program 107th ann meet, Amer Inst Mining Metall Petrol Eng, Denver, Colorado
- Warren CG (1971) A method of discriminating between biogenic and chemical origins of the ore-stage pyrite in a roll-type uranium deposit. *Econ Geol*, v 66, pp 919-928
- Warren CG (1972) Sulfur isotopes as a clue to the genetic geochemistry of a roll-type uranium deposit. *Econ Geol*, v 67, pp 759-767
- Waters AC (1955) Some uranium deposits associated with volcanic rocks, western United States. *US AEC*, 13 p
- Waters AC, Granger HC (1953) Volcanic debris in uriferous sandstones, and its possible bearing on the origin and precipitation of uranium. *US Geol Surv Circ* 224, 26 p
- Watkins TA (1975) The geology of the Copper House, Copper Mountain, and Parashant breccia pipes, western Grand Canyon, Mohave County, Arizona. MS thesis, Colo Sch Mines, Golden, 91 p
- Webster JD (1983) Petrography of some Ambrosia Lake, New Mexico, prefault uranium ores, and implications for their genesis. *US Geol Surv Rep* 83-8, 72 p
- Weege RJ (1963) Geology of the Marquez mine, Ambrosia Lake. *in: Kelley VC, ed., Geology and technology of the Grants Uranium Region*. New Mex Bur Mines Miner Res Mem 15, pp 117-121
- Weeks AD (1951) Red and gray clay underlying ore-bearing sandstone of the Morrison Formation in western Colorado. *US AEC, TEM-251*, 19 p
- Weeks AD, Coleman RG, Thompson ME (1959) Summary of the ore mineralogy. *in: Garrels RM, Larsen ES, III, comps, Geochemistry and mineralogy of the Colorado Plateau uranium ores*. *US Geol Surv Prof Paper* 320, pp 65-79
- Weeks AD, Eargle DH (1960) Uranium at Palagana salt dome, Duval County, Texas. *in: Short papers in the geological sciences*. *US Geol Surv Prof Paper* 400-B, pp B48-B52
- Weeks AD, Eargle DH (1963) Relation of diagenetic alterations and soil-forming processes to the uranium deposits of the southeast Texas coastal plain. *in: Clays and clay minerals*, v 10, 10th National Conf on Clays and Clay Minerals, 1961. Macmillan Co, New York, pp 23-41
- Weeks AD, Thompson ME (1954) Identification and occurrence of uranium and vanadium minerals from the Colorado Plateau. *US Geol Surv Bull* 1009-B, pp 13-62
- Weeks AD, Truesdale AH, Haffty J (1957) Nature of the ore boundary and its relation to diagenesis and mineralization, Uravan district, Colorado (abstr). *Geol Soc Amer Bull*, v 68, no. 12, pt 2, pp 1810-1811
- Weir GW, Puffet WP (1960) Similarities of uranium-vanadium and copper deposits in the Lisbon Valley area, Utah-Colorado. *Intern Geol Congr Rep* 21st Sess Norden, Copenhagen, Tl 15, p 133
- Weiss PL, Armstrong FC, Rosenblum S (1958) Reconnaissance for radioactive minerals in Washington, Idaho, and western Montana, 1952-1955. *US Geol Surv Bull* 1074-B, pp 7-48
- Weissenborn AE, Moen WS (1974) Uranium in Washington. *Wash Div Mines Geol Inf Circ* 50, pp 83-97
- Wenrich KJ (1985a) Geochemical characteristics of uranium-enriched volcanic rocks. *in: Uranium deposits in volcanic rocks*. IAEA, Vienna, pp 29-51
- Wenrich KJ (1985b) Mineralization of breccia pipes in northern Arizona. *Econ Geol*, v 80, pp 1722-1735
- Wenrich KJ (1986a) Geochemical exploration for mineralized pipes in northern Arizona, USA. *Applied Geochem*, v 1, pp 469-785
- Wenrich KJ (1986b) Uranium mineralization of collapse breccia pipes in northern Arizona, western United States. *in: Vein-type uranium deposits*. TECDOC-361, IAEA, Vienna, pp 395-414
- Wenrich KJ (2007) Uranium mining in Arizona breccia pipes – high grade and safe. *SME Ann Meet*, Denver, CO, 9 p
- Wenrich KJ, Billingsley GH, Huntoon PW (1986) Breccia pipe and geologic map of the northeastern Hualapai Indian Reservation and vicinity, Arizona. *US Geol Surv Open-File Rep* 86-458A, 29 p, 2 plts
- Wenrich KJ, Chenoweth WL, Finch WI, Scarborough RB (1989) Uranium in Arizona. *in: Jenny JP, Reynolds SJ, eds., Geologic evolution of Arizona*. *Ariz Geol Soc Digest*, Tucson, pp 759-794
- Wenrich KJ, Huntoon PW (1989) Breccia pipes and associated mineralization in the Grand Canyon and vicinity, Arizona. *in: Elston DP, Billingsley GH, Young RA, eds., Geology of Grand Canyon, northern Arizona - Lees Ferry to Pierce Ferry, Arizona*. *Intern Geol Congr, 28th Field Trip Guidebook T115/315*, Washington, D.C., Amer Geophys Union, pp 212-218
- Wenrich KJ, Silberman ML (1984) Potential precious and strategic metals as by-products of uranium mineralized breccia pipes in northern Arizona. *Amer Ass Petrol Geol Bull*, v 68, p 954
- Wenrich KJ, Sutphin HB (1989) Lithotectonic setting necessary for formation of uranium-rich solution collapse breccia-pipe province, Grand Canyon region, Arizona. *in: Metallogenesis of uranium deposits*. IAEA, Vienna, pp 307-344
- Wenrich-Verbeek KJ, Spirakis CS, Billingsley GH, Hereford R, Nealey LD, Ulrich GE, Verbeek ER, Wolfe EW, eds., (1982) National uranium resource evaluation, Flagstaff Quadrangle, Arizona. *US DOE, PGJ/F-014(82)*, 483 p, 17 plts
- Wenrich-Verbeek KJ, Verbeek ER (1982) Collapse breccia pipes. *in: Wenrich-Verbeek et al., eds., National uranium resource evaluation, Flagstaff Quadrangle, Arizona*. *US DOE, PGJ/F-014(82)*, pp 17-31
- Wentworth DW, Porter DA, Jensen HN (1980) Geology of the Crownpoint Section 29 uranium deposit, McKinley County, New Mexico. *in: Rautman CA, ed., Geology and mineral technology of the Grants Uranium Region 1979*. *New Mex Mines Miner Res, Mem* 38, pp 139-144
- Whitney CG (1986) Petrology of clay minerals in the subsurface Morrison Formation near Crownpoint, southern San Juan Basin, New Mexico: An interim report. *in: Turner-Peterson CE, Santos ES, Fishman NS, eds., A basin analysis case study - the Morrison Formation, Grants Uranium Region, New Mexico*. *Amer Ass Petrol Geol, Studies in Geology*, no. 22, pp 315-329
- Whitney CG, Northrop HR (1986) Vanadium chlorite from a sandstone-hosted vanadium-uranium deposit. Henry basin, Utah. *Clays, Clay Minerals*, v 34, pp 488-495

- Whitney G, Northrop HR (1987) Diagenesis and fluid flow in the San Juan basin, New Mexico - regional zonation in the mineralogy and stable isotope composition of clay minerals in sandstone. *Amer J Sci*, v 287, pp 353-382
- Wilbert WP, Templin CJ (1978) Preliminary study of uranium favorability of the Wilcox and Claiborne Groups (Eocene) in Texas. US DOE, GJBX-7(78), 30p
- Williams EJ (1957) Structural control of uranium deposits, Sierra Ancha region, Arizona. US AEC Rep RME-3152, 117 p
- Willard ME, Callaghan E (1962) Geology of the Marysvale Quadrangle, Utah. US Geol Surv, Geol Quad Map GQ-154, Scale 1:24,000
- Witkind IJ (1956) Uranium deposits at the base of the Shinarump Conglomerate, Monument Valley, Arizona. US Geol Surv Bull 1030-C, pp 99-130
- Witkind IJ, Thaden RE (1963) Geology and uranium-vanadium deposits of the Monument Valley area, Apache and Navajo Counties, Arizona. US Geol Surv Bull 1103, 171 p
- Wood CW (1967) The Charlotte Mine, uranium-rare earths deposit, Cranberry Lake, New Jersey. *Books and Minerals*, v 42, no. 6, pp 418-419
- Wood HB (1968) Geology and exploitation of uranium deposits in the Lisbon Valley area, Utah. *in*: Ridge JD, ed., *Ore deposits in the United States, 1933-1967 (Graton-Sales Vol)*. Amer Inst Min Metall Petrol Eng, v 1, pp 770-789
- Woodmansee WC (1976) Uranium. *in*: *Mineral facts and problems, 1975 edition*. US Bur Mines Bull 667, pp 1177-1200
- Wright HD, Bieler BH, Emerson DO, Shulbert WP (1957) Mineralogy of the uranium-bearing deposits in the Boulder batholith, Montana. US AEC, NYO-2074, 229 p
- Wright JH (1980) Economic geology of the Schwartzwalder mine. *in*: *Uranium resource technology*, v III, Golden, Colo Sch Mines Press, pp 73-92
- Wright JH, Wallace AR, Karlson RC (1981) New studies at the Schwartzwalder mine, Jefferson County, Colorado. *in*: *Uran Symp and Field Tours, CIM, Geol Div*, pp 25-26
- Wright RJ (1955) Ore controls in sandstone uranium deposits of the Colorado Plateau. *Econ Geol*, v 50, pp 135-155
- Wrucke CT, Sheridan DM (1968) Precambrian rocks penetrated by the deep disposal well at the Rocky Mountain Arsenal, Adams County, Colorado. US Geol Surv Prof Paper 600-B, pp 852-859
- Wylie ET (1963) Geology of the Woodrow breccia pipe. *in*: Kelley VC, ed., *Geology and technology of the Grants Uranium Region*. New Mex Bur Mines Miner Res Mem 15, pp 177-181
- Young RG (1960) Uranium deposits of the southern San Juan mineral belt, New Mexico. US AEC, TM-170, 48 p
- Young RG (1964) Distribution of uranium deposits in the White Canyon-Monument Valley district, Utah-Arizona. *Econ Geol*, v 59, pp 850-873
- Young RG (1978) Depositional systems and dispersal patterns in uraniumiferous sandstones of the Colorado Plateau, Utah. *Geology*, v 5, pp 85-102
- Young RG, Ealy GK (1956) Uranium occurrences in the Ambrosia Lake area, McKinley County, New Mexico. US AEC, RME-86, 15 p
- Young RG, Million I, Hausen DM (1957) Geology of the San Rafael River Desert mining district, Emery and Grand Counties, Utah. US AEC, RME-98, 100 p
- Young WE, Delicate DT (1965) Mining methods and costs at Section 23 uranium mine, Homestake-Sapin Partners, McKinley County, New Mexico. US Bur Mines Inform Circ 8280, 48 p

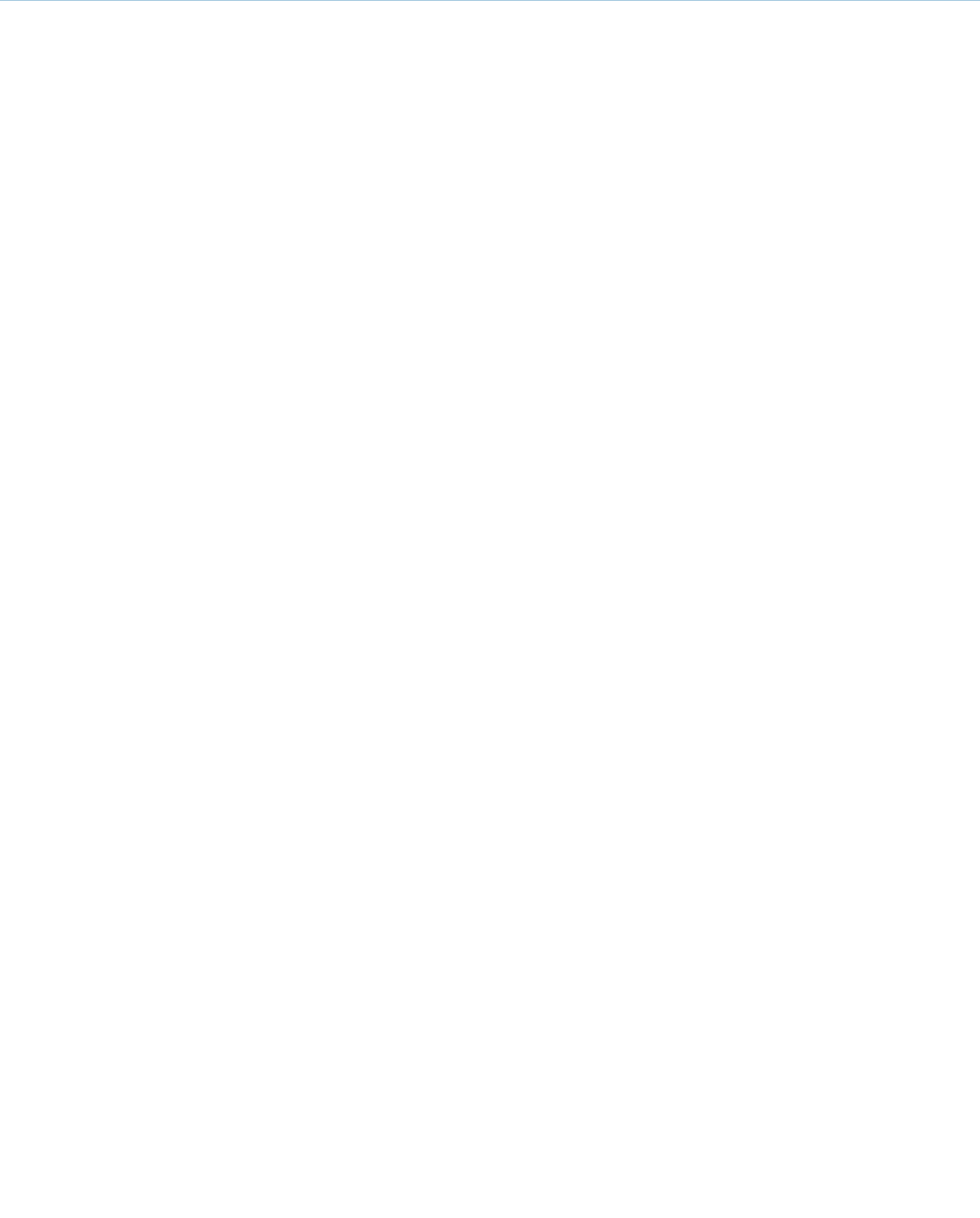
Z

- Zeller HD (1957) The Gas Hills uranium district and some probable controls for ore deposition. *in*: *Guidebook 12th Ann Field Conf Wyoming Geol Ass*, pp 156-160
- Zielinski RA (1978) Uranium abundances and distribution in associated glassy and crystalline rhyolites of the western United States. *Geol Soc Amer Bull*, 89, pp 409-414
- Zielinski RA (1979) Uranium mobility during interaction of rhyolitic obsidian, perlite and feldite with alkaline carbonate solutions. *Chem Geol*, v 27, pp 47-63
- Zielinski RA (1980) Uranium in secondary silica: a possible exploration guide. *Econ Geol*, v 75, pp 592-602
- Zielinski RA (1982a) The mobility of uranium and other elements during alteration of rhyolitic ash to montmorillonite: A case study in the Troublesome Formation, Colorado. USA, *Chem Geol*, v 35, p 185
- Zielinski RA (1982b) Uraniferous opal, Virgin Valley, Nevada: conditions of formation and implications for uranium exploration. *J Geochem Explor*, v 16, pp 197-216
- Zielinski RA (1983) Tuffaceous sediments as source rocks for uranium—a case study of the White River Formation, Wyoming. *J Geochem Explor*, v 18, pp 285-306
- Zielinski RA (1985) Volcanic rocks as sources of uranium: Current perspective and future directions. *in*: *Uranium deposits in volcanic rocks*. IAEA, Vienna, pp 83-97
- Zielinski RA, Bush CA, Rosholt JN (1986) Uranium series disequilibrium in a young surficial uranium deposit, northeastern Washington, U.S.A. *Applied Geochem*, v 1, pp 503-511
- Zielinski RA, Bush CA, Rosholt JN (1990) Uranium series disequilibrium in a young surficial uranium deposit, northeastern Washington. *in*: *Short papers of the US Geol Surv uranium workshop*. pp 18-20
- Zielinski RA, Lindsey DA, Rosholt JN (1980) The distribution and mobility of uranium in glassy and zeolitized tuff, Keg Mountain area, Utah, USA. *Chem Geol*, v 29, pp 139-162
- Zielinski RA, Lipman PW, Millard HT Jr (1977) Minor element abundances in obsidian, perlite and feldite of calc-alkalic rhyolites. *Amer Miner*, v 62, 426-437
- Zielinski RA, Meier AL (1988) The association of uranium with organic matter in Holocene peat: An experimental leaching study. *Appl Geochem*, v 3, pp 631-643
- Zielinski RA, Otton JK (1986) Volcanic ash in organic-rich surficial uranium deposits of northeastern Washington and westernmost Nevada. US Geol Surv Open-File Rep 86-342, 13 p
- Zielinski RA, Otton JK, Wanty RB, Pierson CT (1987) The geochemistry of water near a surficial organic-rich uranium deposit, northeastern Washington State, U.S.A. *Chem Geol*, v 62, pp 263-289
- Zitting RT, Masters JA, Groth FA, Webb MD (1957) Geology of the Ambrosia Lake area uranium deposits, McKinley County, New Mexico. *Mines Mag*, v 47, no. 3, pp 53-58

X

Y

- Yellich JA, Cramer RT, Kendall RG (1978) Copper Mountain, Wyoming, uranium deposit—rediscovered. *in*: *Guidebook, 30th Ann Field Conf, Wyoming Geol Ass*, pp 311-327
- Young EJ (1977) Geologic, radiometric, and mineralogic maps and underground workings of the Schwartzwalder uranium mine and area, Jefferson County, Colorado. US Geol Surv Open-File Rep 77-725, 38 p
- Young EJ (1979a) Analytical data on the Schwartzwalder uranium deposit, Jefferson County, Colorado. US Geol Surv Open-File Rep 79-968, 34 p
- Young EJ (1979b) Genesis of the Schwartzwalder uranium deposit, Jefferson County, Colorado. *Contrib Geol, Univ Wyoming*, v 17, no. 2, pp 179-186
- Young EJ (1985) Summary of the geology, economic aspects, and geochemistry of the Schwartzwalder uranium-bearing area, Ralston Buttes district, Jefferson County, Colorado. US Geol Surv Bull 1555, 32 p
- Young EJ, Hauff PL (1975) An occurrence of disseminated uraninite in Wheeler Basin, Grand County, Colorado. *J Res US Geol Surv*, v 3, no. 3, pp 305-311





Central and South America

Central and South America – Overview

Only few uranium deposits of significant size have been discovered in Latin America, to date. This does not imply, however, that the subcontinent is scarce of uranium.

Mexico is the only country with reported uranium deposits in **Central America**. Deposits are small and largely of volcanic or sandstone type. Well-documented uranium deposits associated with Tertiary volcanic rocks are located in the *Sierra de Peña Blanca*, Chihuahua state. Sandstone-type deposits are known from the Tertiary *La Sierrita-Burgos Basin*, Nuevo Leon state. The latter tends to be in extension of the South Texas Gulf uranium region.

South American countries with uranium deposits include Argentina, Bolivia, Brazil, and Peru (► Fig. II.1). Deposits in these countries are chiefly associated with the following geologic–tectonic units:

- **Andean Orogenic Belt:** Deposits are small and predominantly associated with felsic volcanics of the Cenozoic volcanic belt extending along the western margin of the Cordillera Oriental from southeastern Peru through Bolivia into northwestern Argentina, and Chile. District/deposit examples include *Macusani* in Peru, *Sevaruyo* in Bolivia, *Aquiliri* in Argentina, and *El Laco* in Chile. Chile also reports a few low-grade (ca. 200 ppm U) surficial-type U occurrences such as *Salar Grande* and *Quillagua*, metasomatite U occurrences such as *Estacion Romero* and *Cerro Carmen* (REE) with grades between 0.02 and 0.17% U
- **Austral-Extra Andino Zone:** Deposits are generally small or of low grade and mainly hosted in continental clastic and

pyroclastic sequences of Carboniferous to Tertiary age. Most deposits are located in the Pre-Cordillera Belt of western Argentina including one larger deposit in the *Sierra Pintada*, in Permian sandstone

- **South American Platform–Brazilian–Guyana Precambrian Shield:** So far all significant deposits have been found in *eastern Brazil*. They include a variety of different types but deposits of economic interest appear to be restricted to vein, or impregnation, or metasomatite types, which originated mostly during the Espinhaço and/or Brazilian orogenies of Proterozoic age. They include *Lagoa Real*, Bahia state, where uranium ore bodies occur in albitites associated with Paleoproterozoic orthogneiss; *Itataia*, Ceara state, which is a large uranium–phosphate deposit in marble and gneiss of upper Paleoproterozoic age; and *Espinharas*, Paraiba state, where uranium occurs in albitized gneiss and granite of Proterozoic age.

Subeconomic or by-product uranium deposits or occurrences include Archean Cu–Au–(U–REE) breccia complex-type deposits in the Carajás region, Pará state, as well as Paleoproterozoic oligomictic quartz-pebble conglomerates in the *Quadrilátero Ferrífero* and *Serra de Jacobina* in the Brazilian Shield. In the *Serra de Jacobina*, Bahia state, these paleoconglomerates have been gold producers. Uranium of the *Rio Preto-Campos Belos* district, Goiás state, occurs in Paleoproterozoic crystalline rocks and the occurrences are tentatively attributed to the unconformity type. Intracratonic Paleozoic–Mesozoic basins such as the *Paraná Basin* contain sandstone-type deposits in Paleozoic sediments. Volcanic vein and stratiform uranium–molybdenum deposits are associated with the alkaline *Poços de Caldas* complex of Upper Cretaceous to Lower Tertiary age.

Historical uranium production in Latin America prior to 1995 was of only minor magnitude and came essentially from Argentina (2,513 t U) and Brazil (1,030 t U). Mexico produced 49 t U in the late 1960s. Uranium production was resumed in the *Lagoa Real* district in Brazil in 2000 and is ongoing.

Chapter 1

Mexico

To date, only small and low-grade uranium deposits have been discovered in Mexico. Most occur in the *Sierra de Peña Blanca*, Chihuahua state, and in the *La Sierrita-Burgos Basin*, Nuevo Leon state. The former hosts volcanic-type and the latter sandstone-type uranium deposits. Additional U prospects are reported from areas in the states of Baja California, Chihuahua, Durango, Oaxaca, San Luis Potosi, and Sonora (Fig. 1.1) (OECD-NEA and IAEA 1986). They include uraniferous phosphorite deposits.

Uranium exploration commenced in 1957/1958 and ended in May 1983. Uranium production was restricted to some test mining in the Sierra de Gomez and Sierra de Peña Blanca. Ore from these mines was treated in a plant at Villa Aldama, Chihuahua, which operated from 1969 to 1971 and produced 49 t U as by-product to molybdenum.

OECD-NEA and IAEA (2007) reports remaining recoverable resources of 1,800 t U in the identified resources (RAR + Inferred) <US\$ 130/kg U category (status January 1, 2007). Additional by-product resources of some 150,000 t U are calculated for phosphorite deposits in Baja California (OECD-NEA and IAEA 1999).

1.1 Sierra de Peña Blanca, Chihuahua State

Several of Mexico's larger uranium deposits lie approximately 50 km north of Chihuahua City in the central-eastern part of the Sierra de Peña Blanca (Fig. 1.1), a NNW-SSE-elongated range about 70 km long and 10–15 km wide. Between 1960 and 1982, intensive exploration discovered over 100 uranium occurrences, but only five proved to have resources greater than 100 tonnes uranium each: *Nopal-1*, *Nopal-3*, *Puerto-3*, *Laguna de Cuervos*, and *Las Margaritas* (Fig. 1.2). Four deposits were developed for mining, *Nopal-1*, *Puerto-3*, *Las Margaritas* and *La Domitila*, but only the latter was exploited and is depleted.

Total resources of the Peña Blanca district are estimated at about 4,000 t U. Approximately 90% of which grade about 0.1% U and are contained in the afore mentioned deposits. The remainder is contained in ten small occurrences of low grade (~0.02% U) (OECD-NEA/IAEA 1986).

Sources of Information. Aniel 1983; Cárdenas-Flores 1985; Chemillac 2004; George-Aniel et al. 1985, 1991; Goodell 1981, 1983, 1985b; Goodell et al. 1979; Reyes-Cortés 1985 unless otherwise cited.

Regional Geological Setting of Mineralization

The Sierra de Peña Blanca is within the Basin and Range structural province of western North America, a province characterized by N-S-trending fault-block ranges in northern Mexico.

The Sierra can be litho-stratigraphically divided into a northern and southern section. Flat-lying Cretaceous (Albian) marine sediments, predominantly limestone, crop out in the southern section. They overlie with a distinct unconformity, folded, weakly metamorphosed flysch-like sandstone, and shale of Paleozoic age. The metasediments rest upon Precambrian gneiss and granite, dated at 1,030 and 1,060 Ma (i.e., Grenvillian age), that are cut by amphibolitic mafic and granitic dikes. In the northern half, thinly bedded shaly limestone and shale, and a sequence of pyroclastic rocks of Cenomanian age crop out on the northeastern flank of the Sierra. They are deformed into NW-trending folds overturned to the SW. The Cretaceous sediments exhibit a surface of considerable relief onto which a sequence of volcanic rocks of Tertiary age was deposited. Formerly, the Cretaceous sediments were attributed to the Edwards Formation; now they are divided into three formations: Cuesta del Cura, Tamaulipas, and El Abra.

The Tertiary volcanics consist of six units predominantly of rhyolitic ash-flow tuff, interbedded with epiclastic conglomerate and sandstone. They are part of the vast Sierra Madre Occidental rhyolitic province in northwestern Mexico, which was affected by intense, Basin and Range-type, block-tectonic movement. The movement resulted in N to NNW, E-W, NW-SE, and NE-SW-trending fault systems.

Tertiary rocks in the Peña Blanca uranium district are 200–300 m thick and range in age from Eocene to Oligocene (Fig. 1.3). Characteristics of the Tertiary formations, derived from Cárdenas-Flores (1985) and Reyes-Cortés (1985), are given in the following litho-stratigraphic profile in descending order (former names of formations are given within brackets):

Oligocene (37.3 Ma, sanidine):

- **Mesa Formation**, <75 m thick (most widespread unit in the Sierra de Peña Blanca): trachytic to rhyolitic ignimbrite with subhedral to euhedral quartz and sanidine phenocrysts in a devitrified groundmass of cryptocrystalline cristobalite and feldspars; rests upon dark brown densely welded zone with pumice fragments, and a basal bed of dark red, almost unaltered vitrophyre, 5 m thick.

Disconformity

- **Peña Blanca Formation**, 45–100 m thick: white, compact, rhyolitic ignimbritic layer with strong eutaxitic texture; overlies white rhyolitic vitroclastic tuff with quartz and feldspar phenocrysts in aphanatic vitric matrix, glass is partially devitrified in eutaxitic texture.

Unconformity

- **Chontes Conglomerate**, 0–50 m thick (U in Margaritas and rhyolitic rock fragments): polymictic conglomerate of predominantly volcanic clasts with crossbedded pink sandstone lenses; basal laharic bed of cineritic breccia, 2–3 m thick.

Unconformity

Oligocene (-Eocene) (38.3–44.5 Ma, sanidine)

- **Escuadra Formation**, <100 m thick (rests upon Nopal Fm. or Piloncillos Fm. if present): pinkish crystalline rhyolitic ignimbrite with slightly to densely welded zones, contains quartz and altered sanidine phenocrysts in devitrified

Fig. 1.1. Mexico, location of uranium districts and selected occurrences. (After OECD/NEA-IAEA 1986)

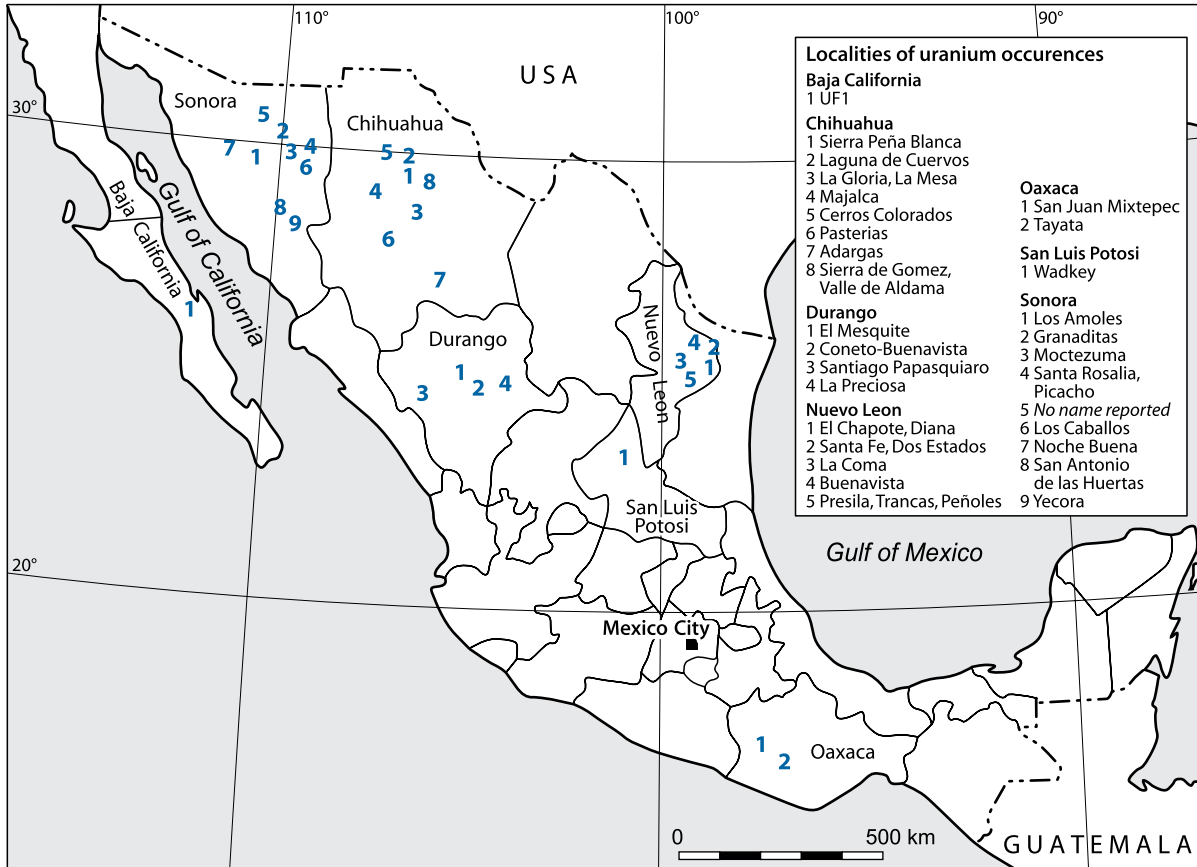
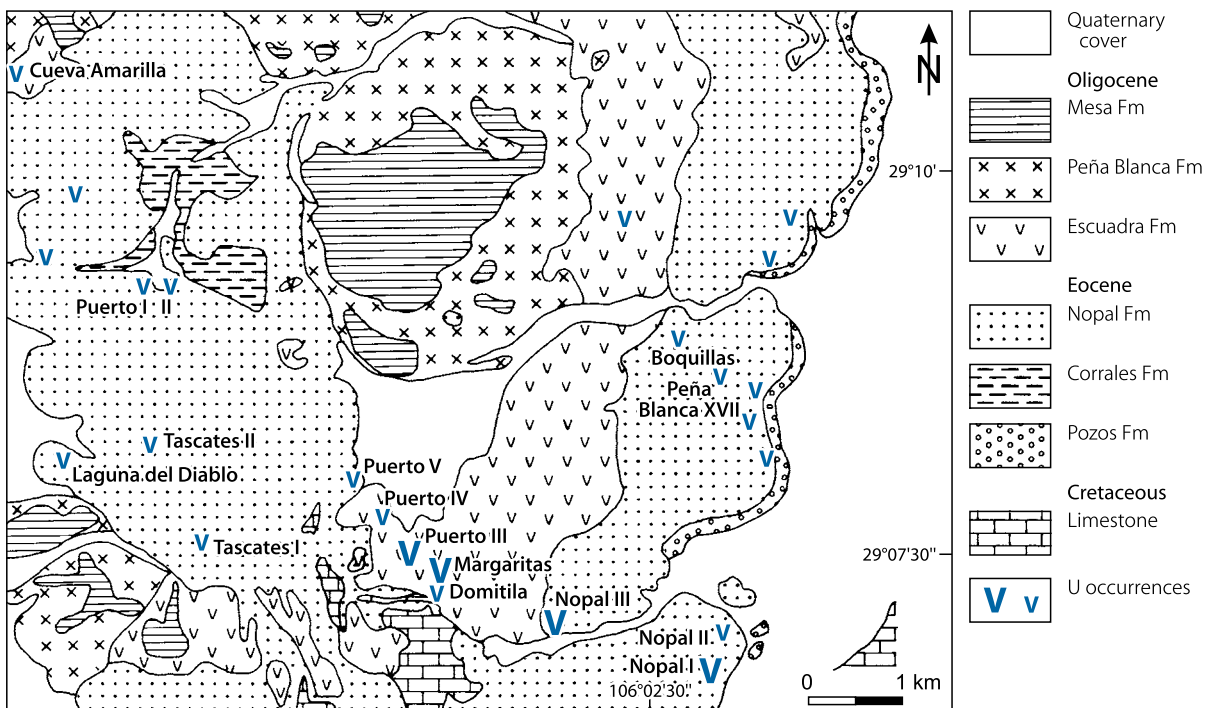
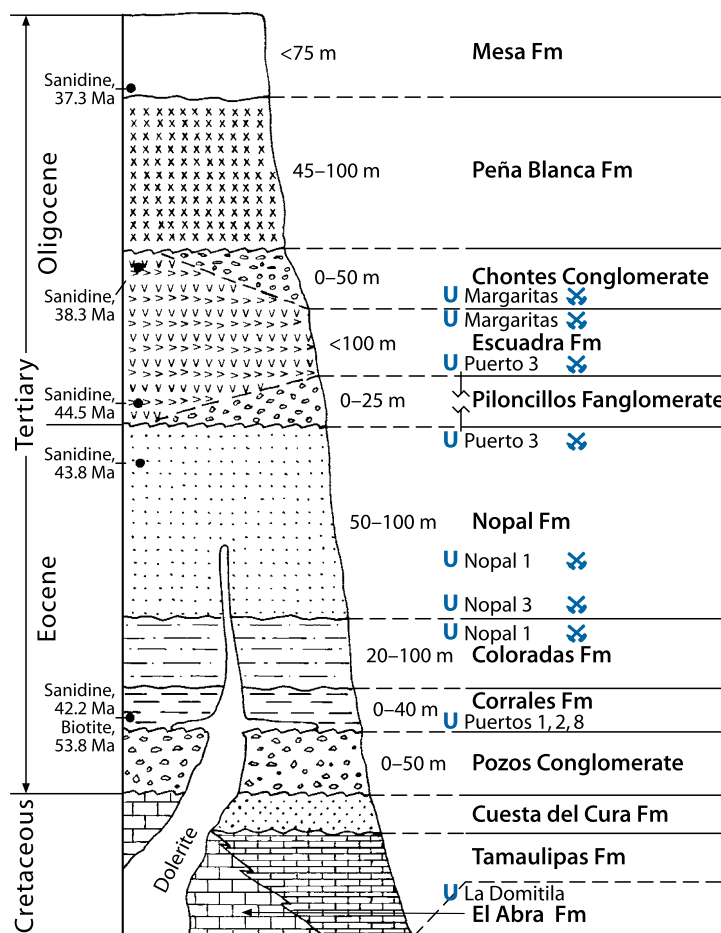


Fig. 1.2. Sierra de Peña Blanca, generalized geological map with location of uranium occurrences. (After URAMEX 1980, unpublished)



■ Fig. 1.3.

Sierra de Peña Blanca, diagrammatic litho-stratigraphic column with position of uranium occurrences. (After Cárdenas-Flores 1985; Reyes-Cortés 1985a; ages from Alba and Chávez 1974)



matrix of cryptocrystalline cristobalite and feldspar, and a pervasive vapor-phase zone in the upper portion (U in Margaritas). It rests upon pinkish crystalline ignimbrite of sillar type with aphanitic texture, only slight argillization of feldspars, and some oxidation (U in Margaritas) that overlies argillized rhyolitic vitrophyre/lapilli tuff, 1–4 m thick, devitrified, altered to montmorillonite and kaolinite (U in Margaritas and Puerto-3).

Unconformity

- **Piloncillos Fanglomerate**, 0–25 m thick (only locally present): interbedded conglomerates and crossbedded sandstones with predominantly volcanic clasts.

Unconformity

Eocene (43.8 Ma, sanidine)

- **Nopal Formation** (Nopal Rhyolite Member), 50–100 m thick (widespread distribution, thickening southward to 225 m in the Sierra de la Gloria, east of Chihuahua City): reddish-brown crystalline rhyolitic ignimbrite with euhedral to subhedral quartz, sanidine, and some biotite phenocrysts, partially to totally altered. The glassy groundmass is devitrified to cryptocrystalline cristobalite and feldspar with some axiolitic texture (U in Puerto-3 and Nopal-1); basal unit of dark rhyolitic vitrophyre, <5 m thick, with variable grades of alteration (U in Nopal-3).

Disconformity

- **Coloradas Formation** (Nopal Tuff Member), 20–100 m thick: reddish lithic-crystal rhyolitic ignimbrite with lithic fragments of andesite(?) up to 10×2 m in size, eutaxitic texture; intense argillization (U in Nopal-1); rests upon dark vitrophyre, unaltered in west-central area, but intensely argillized in Nopal-1 area.

Disconformity

Eocene (42.2 Ma, sanidine; 53.8 Ma, biotite)

- **Corrales Formation**, 0–40 m thick: crystalline rhyolitic ignimbrite with quartz, feldspars, biotite phenocrysts, and angular lithic fragments; matrix is devitrified glass to spherulitic orthoclase; strong kaolinitization around uranium deposits (U in Puerto-1, -2, and -3); basal vitrophyre, few meters thick.

Unconformity

- **Pozos Conglomerate**, 0–50 m thick: epiclastic calcareous conglomerate of continental molasse provenance with some intercalated lenses of sandstone and few hematitic tuffaceous interbeds, pervasive intense silicification, dark brown to pinkish due to thermal alteration in Nopal-1 area.

Unconformity

Cenoman/Albian: Cuesta del Cura, Tamaulipas, and El Abra formations (Edwards Formation).

Dolerite sills and dikes cut the Pozos, Corrales, and Nopal formations in the northwestern Sierra.

Principal Host Rock Alteration

Host rock alteration is reflected by devitrification of the glassy matrix with leaching of certain elements, argillization (kaolinitization, montmorillonitization), hematitization (imprinting a pinkish hue), local neof ormation of potassium feldspar, calcitization, silicification, (particularly along heavily fractured and sheared zones), and minor pyritization.

Kaolinitization generated kaolinite, dickite, and locally alunite, an indication of a more acid and SO_4 -enriched environment. Kaolinite is predominantly derived by supergene alteration of feldspars and rock fragments in the ignimbrites; but, at Nopal-1, kaolinite exhibits a habit typical for hypogene hydrothermal formation (George-Aniel et al. 1991). Most intense kaolinitization is typical for the upper Nopal Formation where many of the uranium concentrations are located. In these areas, the better grades of molybdenum occur beneath the uranium concentration (Reyes Cortés M 1985). *Montmorillonitization* produced nontronite and saponite, in order of abundance, predominantly in vitrophyric horizons. *Silicification* includes quartz and opal development. The opal may contain uranium. *Carbonatization* consists of calcite and is present in all volcanic units. *Pyritization* is rather limited presumably due to an unfavorable environment for pyrite formation as indicated by the frequent replacement of pyrite crystals by hematite and the abundance of jarosite (at least in the Margaritas deposit). *Oxidation* is represented by hematite, limonite/goethite, and jarosite and affected all volcanic lithologies on a wide scale.

Principal Characteristics of Mineralization

Mineralization in the Peña Blanca district is polymetallic composed of uranium and molybdenum. All uranium except at one locality has been found as U^{6+} minerals, predominantly as uranyl silicates (uranophane, weeksite, boltwoodite, soddyite, haiweiite, a.o.), uranyl vanadates (carnotite, tyuyamunite) and uranyl phosphates (autunite, meta-autunite), and uraniferous opal. A cesium-rich carnotite, margaritasite, was identified in the *Margaritas* deposit (Wenrich et al. 1982). Pitchblende has only been found at Nopal-1 where it associates with pyrite. An unidentified U oxide phase has also been noticed in microfissures within accessory ilmenite in the same deposit. Molybdenum occurs as molybdenite and powellite.

Three dominant settings of uranium mineralization are identified (George-Aniel et al. 1991): (a) fault-controlled mineralization, often in step faults, hosted mainly in the Nopal and the immediately underlying formations (e.g., *Nopal-1*, [Fig. 1.4](#); and *La Domitila*); (b) stratiform mineralization in altered vitrophyric horizons (*Puerto-3*, [Fig. 1.5](#)) and more porous units such as altered lapilli-tuffs with abundant pumice fragments; and (c) in combined stratiform-structure-related positions as found within downfaulted blocks (*Las Margaritas*, [Fig. 1.5](#)).

Ore-grade concentrations of uranium are overwhelmingly restricted to the Nopal, Coloradas, and Escuadra formations. The Nopal Formation hosts occurrences at *Nopal-1*, *Nopal-3*, *Peña Blanca 17*, *Tascates 2*, in the Laguna del Diablo area, and

elsewhere. The Escuadra Formation contains uranium at *Las Margaritas*, *Puerto-3*, *-4*, and *-5*, *Tecolotes*, *Cueva Amarilla*, and other prospects. At *Las Margaritas*, some uranium is also found in the basal laharic member of the Chontes Conglomerate that overlies the Escuadra Formation. Some mineralization, always as fissure filling, is in the Corrales Formation at *Puerto-1*, *-2*, and *-8*, and in faults and solution cavities in Cretaceous limestone, for example, in the El Abra Formation at *La Domitila*. All of this mineralization is restricted to zones immediately below the Nopal Formation.

General Shape and Dimensions of Deposits

Ore bodies are variable in shape, ranging from irregular disseminations to stockworks (*Las Margaritas*) to vein and pipe-like bodies (*Nopal-1*). A few occurrences are stratiform (*Puerto-3*). Both the lateral and vertical dimensions are generally small, on the order on a few meters to several tens of meters. Resources of most ore bodies range from a few tonnes to several tens of tonnes uranium, rarely to a few hundred tonnes uranium. The largest deposit (*Las Margaritas*) was estimated to contain some 2,000 t U. Grades are rather variable and average about 0.08–0.2% U, although some small sections may be as high as 10% U or more.

Stable Isotopes and Fluid Inclusions

Studies by George-Aniel et al. (1991) on fluid inclusions in quartz associated with mineralization and/or alteration at the Nopal-1 deposit show that (a) vapor phase samples considered to be related to the uranium oxide-ilmenite complex are not purely aqueous but contain CO_2 and N_2 , and their formation temperatures are calculated at 400°C; (b) quartz associated with the pitchblende-pyrite association has purely aqueous inclusions with low salt contents (0–4.94 wt% equiv. NaCl) that are considered to be stable below 300°C; and (c) fluid inclusions in opal associated with uranophane needles correspond to a temperature of 150°C. The opal-uranophane association occurs together with Fe-oxides and -hydroxides enrichments in a fault at the margin of the Nopal-1 deposit.

Regional Geochronology

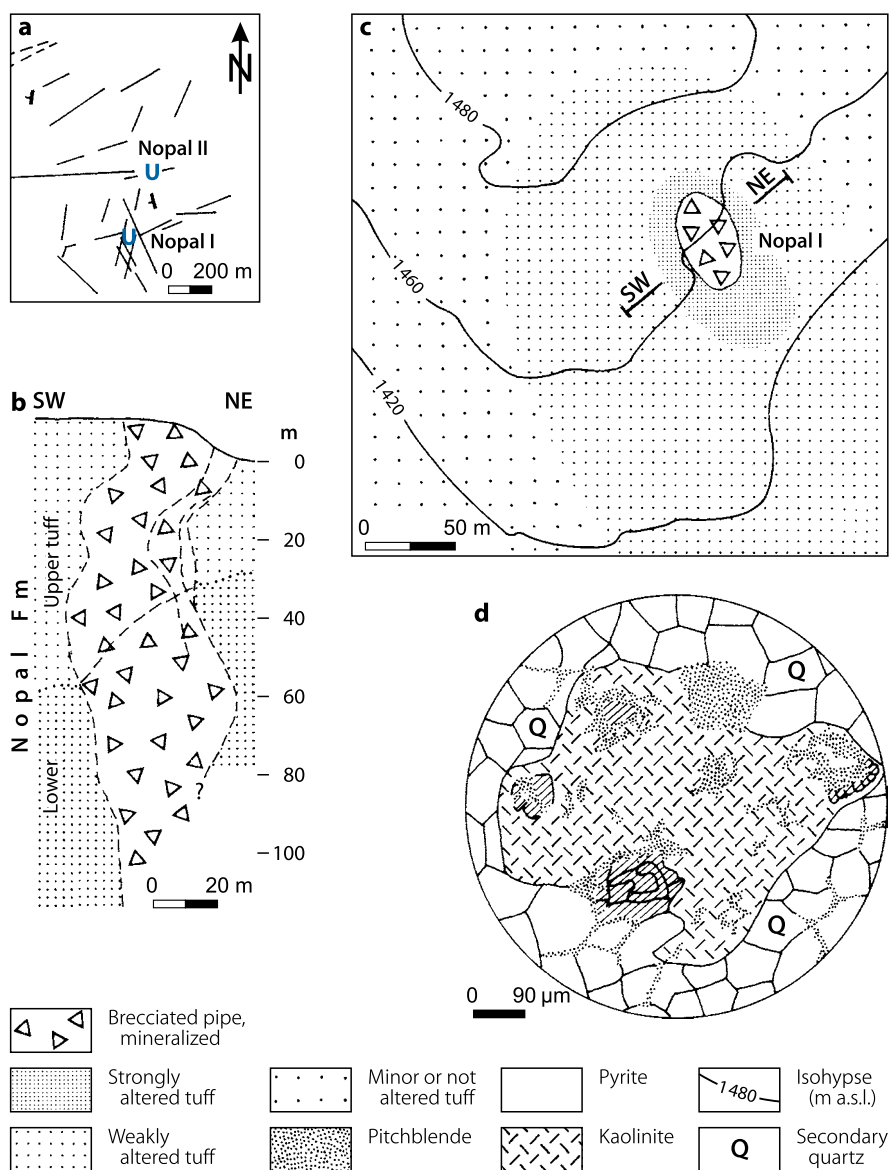
Age datings of the various Tertiary volcanic formations of the Sierra de Peña Blanca district yield ages for sanidines ranging from 37.3 Ma for the youngest volcanic unit, the Mesa Formation to 42.2 and 43.8 Ma for the older units. A biotite sample of the latter formation, however, produced an apparent age of 53.8 Ma (Alba and Chávez 1974) ([Fig. 1.3](#)).

Principal Ore Controls or Recognition Criteria

Uranium mineralization of the Sierra de Peña Blanca district is of volcanic type. Essential ore-controlling parameters appear to be as follows:

■ Fig. 1.4.

Sierra de Peña Blanca, Nopal-1 deposit, (a) structural situation, (b) geological SW–NE section across the mineralized brecciated pipe, (c) map of alteration intensities around the mineralized pipe, (d) polished section of an ore sample showing pitchblende and pyrite distribution in altered upper Nopal tuff. (After (a, b) URAMEX, unpublished; (c, d) George Aniel et al. 1985)



Host Environment

- Vast volcanic province with Eocene-Oligocene volcanics cumulatively 200–300 m thick
- Predominant lithologies include rhyolitic ash-flow tuff, interbedded with conglomerate and sandstone
- Prominent Basin and Range-type block faulting.

Alteration

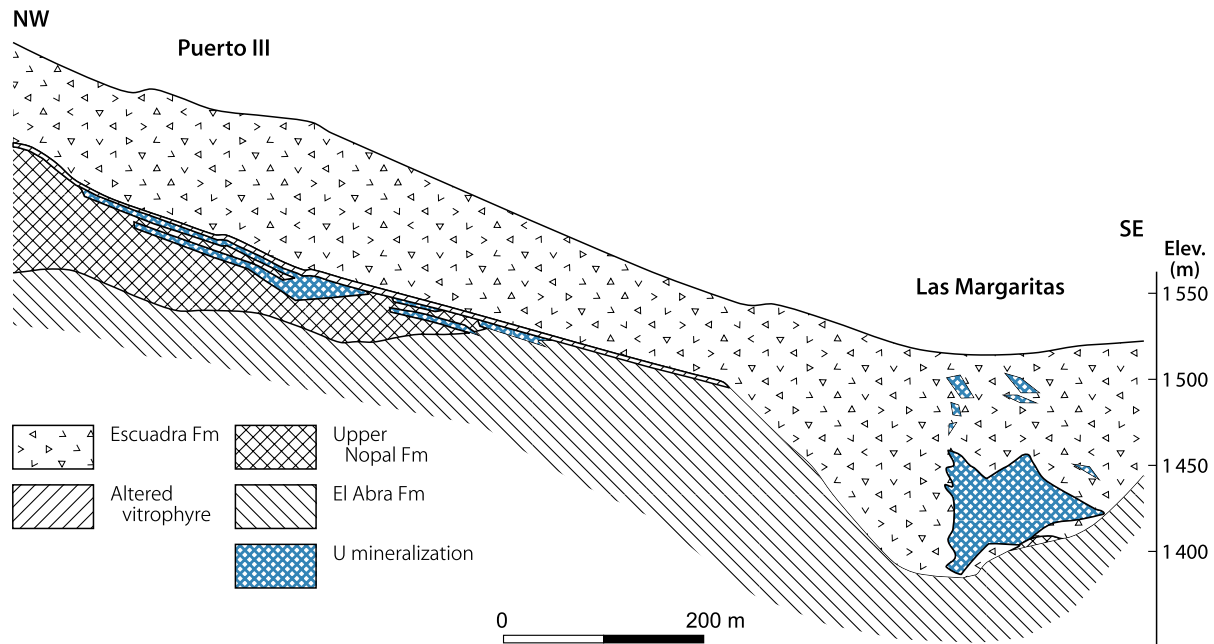
- Intense argillization, oxidation, devitrification of glassy matrix, and carbonatization
- Silicification is mainly restricted to heavily fractured and sheared zones
- Minor pyritization
- Local recrystallization of K feldspar.

Mineralization

- Mineralization consists almost exclusively of U^{6+} minerals, pitchblende is very rare
- Molybdenum is present as molybdenite and powellite
- Mineralization occurs in three main settings
 - Fault controlled, often in step faults, mainly in the Nopal and immediately underlying formations
 - Stratiform in altered vitrophyre horizons and more porous units such as altered lapilli-tuffs with abundant pumice fragments
 - In combined stratiform-structure related positions within downfaulted blocks
- The bulk of uranium is restricted to the Nopal, Coloradas, and Escuadra formations

Fig. 1.5.

Sierra de Peña Blanca, Las Margaritas and Puerto-3 deposits, geological NW–SE section. The depression at Las Margaritas is the result of a number of step faults (not shown) with displacements in excess of 100 m trending approximately N-S and forming a 500 m wide graben. (After URAMEX 1980, unpublished)



- Some mineralization occurs immediately below the Nopal Formation as fissure fillings in the Corrales Formation and in faults and solution cavities in Cretaceous limestone
- Ore bodies are of variable shape, ranging from structurally controlled irregular disseminations to veins, stockworks or pipe-like bodies, and occasionally to stratiform mineralization
- Limited lateral and vertical dimensions of ore bodies
- Small resources of deposits ranging from few tonnes to rarely a few hundred tonnes uranium
- Low uranium grades commonly <0.1% U.

Metallogenetic Concepts

George-Aniel et al. (1985, 1991) distinguish three genetic types of uranium mineralization in the Sierra de Peña Blanca: (a) a hydrothermal, fault-controlled type represented by *Nopal-1*; (b) a supergene type, represented by *Puerto-3*; and (c) a mixed exhalative volcanic hydrothermal-supergene type represented by *Las Margaritas*.

The *hydrothermal type*, exemplified by *Nopal-1* hosted within tuff of the Nopal Formation, apparently derived from volcanic hypogene fluids. The evolution of this type is complex; it apparently took place in three or more stages, beginning shortly after the deposition of the Nopal ignimbrite. Tetravalent uranium precipitated during the first two stages.

Stage 1: Uranium deposition occurred in micro-fissures within ilmenite contemporaneous with hematite exsolution from the ilmenite lattice. Fluid inclusions in quartz associated with the uranium oxide-ilmenite mineralization indicate a temperature

of about 400°C and high CO₂ and N₂ values. Vapor phase and microthermometric studies also indicate temperatures in the 400°C range.

Stage 2: Destabilization of the ilmenite-uranium oxide complexes released uranium. Uranium was reprecipitated as pitchblende-pyrite pseudomorphs after magnetite or disseminated in kaolinized host rock. Kaolinitic alteration associated with the second stage of pitchblende mineralization is evidenced by the replacement of phenocrysts and matrix-bound feldspars in the rhyolite vitroclastic tuff of the upper Nopal Formation. Chemically, the alteration involves the leaching of K, Na, and Rb. This early-formed kaolinite shows well-defined hexagonal plates and tight packets, habits considered typical for a hypogene hydrothermal derivation. Fluid inclusion data indicate temperatures ranging from 250 to 150°C for the pitchblende-pyrite association of the second stage.

Stage 3: (and probably additional stages) was mostly of supergene and oxidizing, but perhaps of hypogene hydrothermal, character. The lower tuff unit became montmorillonitized and the earlier hydrothermal kaolinite was damaged. Earlier pitchblende was remobilized and uranyl silicates were formed instead. A late stage of thermal activity at about 150°C resulted in the formation of uraniferous opal with uranophane.

Sometime during these processes, Sr (288 ppm), Pb (2,000 ppm), and Mo (500 ppm) became enriched in altered and mineralized tuff, whereas Th and REE appear unchanged.

The *supergene type* of mineralization is exemplified by the *Puerto-3* deposit. Only oxidized mineralization in the form of uranyl silicates is present; it is emplaced stratiform in the upper

part of the Nopal Formation under an impermeable, silicified bed assumed to be the lower horizon of a paleosol. A vertical profile of the paleosol, which supposedly derived from a vitrophyric tuff, shows a zoning indicative of weathering processes accompanied by montmorillonitization and leaching of uranium and SiO_2 (from top to bottom):

- An altered zone with montmorillonite development and rare relict quartz and feldspars; the layer is compacted and stressed perhaps due to pressure from the overlying Escuadra volcanics
- A zone with concretions of iron oxides, and kaolinite exhibiting typical low temperature habits
- A zone of non-argillized but silicified Nopal tuff
- A zone of uranium mineralization without molybdenum, but associated with low temperature kaolinite derived from feldspars.

Although the processes are clearly supergene, it is not established whether the ore-forming uranium was locally derived by remobilization during the weathering of the Nopal tuff or whether it was introduced by groundwater over longer distances.

The *intermediate type*, represented by U-Mo mineralization of the Margaritas deposit, is considered to be the result of an interaction between volcanic hydrothermal fluids and groundwater in a downdropped tectonic block. Ore within this deposit comprises only U^{6+} minerals (uranyl-silicates, -vanadates, -phosphates) that occur together with molybdenum sulfide (molybdenite) and molybdate (powellite). The presence of cesium as documented by cesium-rich margaritasite is interpreted by Wenrich et al. (1982) as an indication of a local hydrothermal or pneumatolytic process that was active coeval with the primary emplacement of mineralization.

Alteration of the ore-hosting alkaline vitroclastic rhyolitic tuff of the Escuadra Formation at Margaritas affected only feldspar phenocrysts, which were replaced by kaolinite with a habit typical of a low to medium temperature. Another alteration product is alunite, the presence of which indicates a more acid and sulfate-ion rich environment. A late fumarolic event is considered responsible for the alunite-jarosite-opal formation as found on the eastern side of the Margaritas deposit.

Reyes-Cortés M (1985) also considers a possible low-temperature hydrothermal event together with supergene or geothermal alteration to be responsible for ore formation. His consideration is based on the association of powellite with alunite, jarosite, quartz, and opal as products of argillization, silicification, and oxidation for one part of the process, and the incipient presence of pyrite, fluorite, calcite, and gypsum for the other.

Goodell (1985b) approaches the problem of ore genesis on a more regional basis. In summary, he postulates the peralkaline tuffaceous uraniferous rocks to be the uranium source for the Peña Blanca deposits. These rocks are similar to those in the Campana Peak and Santa Clara Canyon region of the southern Sierra del Nido block located to the northwest of the Peña Blanca block. Here in the Nido block, the 29–30 Ma old Cryptic tuff contains up to 60 ppm U and the overlying Campana tuff

approximately 20 ppm U. The Peña Blanca block was formerly connected with the Nido block until they were rafted from each other by tensional processes post 29 Ma, when the Ojo Laguna Graben was downdropped. Goodell (1985b) proposes a hydrologic regime fed by meteoric water that was subjected to high heat flow conditions present at the margin of the basin and range/rift environment. This paleogeothermal system produced circulating waters, leached the rocks, and collected uranium. Since the regional hydrologic gradient was from west to east, southeast-trending structures within the Peña Blanca block acted as pathways for the hot waters of this epithermal, geothermal system at depth to move the uranium to the sites of the uranium deposits in the Margaritas and Nopal region. Depositional controls may have involved the reducing agents provided by hydrocarbons in the limestone, and/or the siliceous environment provided by the volcanic rocks.

Description of Selected Deposits in the Sierra de Peña Blanca

Five deposits have been explored in some detail, Nopal-1, Nopal-3, Las Margaritas, Puerto-3, and La Domitila (locations see [Fig. 1.2](#)).

Sources of Information. Calas 1977; Cárdenas-Flores 1985; Ferriz 1985; George-Aniel et al. 1985, 1991; Goodell 1981; Rodríguez Torres et al. 1976; amended by data from OECD-NEA/IAEA 1982, 1986.

1.1.0.1 Nopal-1

Nopal-1 is located approximately 30 km NNW of the little village of Villa Aldama. This deposit was investigated by tunnels and crosscuts prior to the development of an open pit. Total in situ reserves are 283 t U. The average grade is about 0.25% U.

Geology and Alteration

Host rocks include vitroclastic tuff of rhyolite composition of the Nopal Formation and lithic rhyolitic ignimbrite of the Coloradas Formation. These rocks are heavily broken at the site of the deposit, a situation caused by the interjunction of an ENE–WSW structure with a set of steeply dipping NNE–SSW faults. A NW–SE-trending and 50–80° W-dipping structure bounds the deposit on the west side and a fault contact along which rocks are uplifted by 15–20 m forms the eastern limit. Rocks of both formations are completely altered within the pipe-like ore body. Outside the pipe, alteration decreases differentially with distance from the pipe in relation to the intensity and density of fractures ([Fig. 1.4](#)). It extends for about 100–150 m to the NNW, 200 m and more to the SSE and 60–100 m to the east and west of the pipe.

Alteration of the Nopal tuff includes kaolinitization corresponding to a K, Na, and Rb removal. Kaolinite progressively replaces the feldspar phenocrysts and the matrix feldspars

outside, and completely within, the ore body. Kaolinite's habit exhibits tight packets of hexagonal plates, which is considered characteristic for a hypogene hydrothermal origin. To the east of the pipe where the rocks are uplifted, the Coloradas tuff is altered to Ca montmorillonite and to some zeolite (heulandite) instead of kaolinite. Montmorillonitization postdates kaolinitization. Silicification is widespread around the ore body and extremely intense in its upper part.

Mineralization/Shape and Dimensions

Uranium minerals include mainly uranyl silicates (uranophane, soddyite, weeksite) and uranyl vanadates (carnotite, tyuyamunite). The latter prevail in the underlying, less consolidated, more permeable Coloradas tuffs. Some disseminated pitchblende occurs in the highly silicified, altered Nopal tuff associated with minor pyrite, fluorite, molybdenite, and magnetite. Mineralized and altered tuffs show some enrichment in Pb (<2,000 ppm), Mo (<500 ppm), and Sr (<288 ppm), but no change in Th and REE.

The Nopal-1 deposit occupies a pipe-like body of tectonic breccia that extends to a depth of over 100 m (Fig. 1.4). At the outcrop, the shape is oval in plan view with a NNW-SSE-trending axis of about 40 m and a cross axis of about 20 m. At depth, in the softer, less-consolidated Coloradas tuff, the diameter increases, but uranium grades decrease. The best grades with locally as much as 10% U occur in the upper 40–50 m, i.e., in the highly silicified and heavily faulted Nopal tuff.

1.1.0.2 Nopal-3

This occurrence is located about 2 km WNW of Nopal-1 (Fig. 1.2) and has reserves of 170 t U at an average grade of 0.08% U.

Uranium lenses, composed of uranophane which often coats feldspar grains and some autunite, occur in an almost flat-lying argillic zone, about 300 by 600 m in size and up to 9 m thick, at the contact of consolidated rhyolite ignimbrite and pyroclastic tuff of the lower Nopal Formation. The argillic zone is mineralized over a thickness of 3 m where it is cut by a breccia zone.

In contrast to Nopal-1, original rock constituents like feldspar, biotite, quartz, and magnetite are not decomposed in mineralized segments of Nopal-3 and only the glassy matrix was transformed into montmorillonite and kaolinite. The original rock constituents have been altered, however, outside the ore zone. There appears to be a direct relationship between the content of residual feldspar and uranium. The uranium content is low where the feldspar is altered, presumably due to leaching.

1.1.0.3 Las Margaritas

Las Margaritas is a uranium-molybdenum deposit located approximately 5 km W of Nopal-1 (Fig. 1.2). An open pit was

developed for mining. Original uranium resources are given as 2,000 t U for Margaritas and Puerto-3 combined by Ferriz (1985), whereas George-Aniel et al. (1991) report 297 t U for Margaritas (and 420 t U for Puerto-3). The average grade is approximately 0.1% U and 0.18% Mo.

Geology and Alteration

The Las Margaritas ore body lies in the center portion of a structural zone composed of a number of step faults with displacements in excess of 100 m trending approximately N-S and forming a 500 m wide graben. The graben is filled with ignimbrites of the Escuadra Formation, predominantly vitroclastic alkaline rhyolitic tuff. Locally, the Escuadra is overlain by the basal laharic member of the Chontes Conglomerate. Mostly, the Escuadra Formation rests directly on Cretaceous limestones of the El Abra Formation, which forms a rudistic mound-reef complex to the west. At some locations, a layer of the Nopal Formation separates the Escuadra Formation from the limestone (Fig. 1.5).

Alteration at Las Margaritas is of lower intensity than at Nopal-1, but affects a much wider volume of tuffs. Vitroclastic tuff is largely devitrified. Feldspar phenocrysts are in part totally dissolved, leaving behind a skeleton of silica, or are altered into kaolinite. Feldspars of the groundmass are not affected. Kaolinite is locally accompanied by alunite indicating a more acid sulfate-ion enriched environment. Some montmorillonite has formed. Intense silicification, apparently post-ore, is present. Hematitization is locally abundant.

Mineralization/Shape and Dimensions

Uranyl-silicates, -vanadates, and -phosphates are the main U minerals at Las Margaritas. A Cs-rich carnotite, margaritasite, was discovered in a sample of the laharic member of the Chontes Conglomerate (Wenrich et al. 1982). Molybdenum is present as molybdenite and powellite. The latter forms phenocrysts up to 2 cm in diameter in the upper part of the ore zone, whereas at depth it occurs in cryptocrystalline to amorphous habit. In general, powellite occurs associated with carnotite, margaritasite, and uranophane. At some places, jarosite, pyrite, calcite, and fluorite occur.

Ore minerals form encrustations and lamina but are also present as disseminations. They occupy fractures, joints, and fill voids of destroyed feldspars or replace kaolinitized feldspars. Better ore grades prevail in intensely oxidized fractures and breccias with jarosite, hematite, and limonite, and where alunite occurs at the contact of ignimbrite with overlying layers of argillized vitrophyres.

The ore body is about 100–150 m wide and 300 m long. The bulk of the mineralization occurs at depths from 55 to 100 m and is between 1 and 7 m thick. Most reserves are present in several higher grade sections with values between 0.1 and 0.4% U and between 0.1 and 3% Mo. Low-grade mineralization inter-venes with these high-grade sections.

1.1.0.4 Puerto-3

This deposit lies about 500 m to the NW of Las Margaritas (► Fig. 1.2 and 1.5). Mining was considered by underground methods through inclines, but was not initiated. Resources are estimated at 420 t U, at grades between 0.1 and 0.2% U.

Mineralization is of stratiform shape emplaced in ignimbrites of the upper Nopal Formation. N–S-trending step faults of the Margaritas Graben separate Puerto-3 from the Margaritas deposit. The top zone of the Nopal ignimbrite is altered to montmorillonite with rare relics of quartz and feldspar and is compacted and stressed, probably by pressure from the overlying Escuadra volcanics. Beneath the montmorillonite zone, a horizon with kaolinite and iron oxide concretions is developed that grades downwards into non-argillized but highly silicified Nopal tuff. This section of altered horizons is considered to be the product of weathering.

Mineralization is positioned below the silicified and impermeable Nopal tuff at depths from 60 to 80 m and consists of U⁶⁺ minerals, predominantly uranyl silicates and some molybdenum in powellite, which occur in several stratiform lenses. Ore lenses have a width of 10–150 m, a length of up to several hundred meters, and are as much as several meters thick.

1.1.0.5 La Domitila

La Domitila is located a few hundred meters to the south of Las Margaritas. It contained some 50 t U and had a grade of about 0.2% U. The deposit was mined in about 1970 and is depleted. Mineralization consists of uranyl-silicates and -vanadates associated with limonite and occurs in fractures and solution cavities in black bituminous, recrystallized portions of limestone of the Cretaceous El Abra Formation, immediately beneath the Nopal and Escuadra formations.

1.2 Burgos Basin, La Sierrita Area, Nuevo León State

The Burgos Basin in northeastern Mexico (► Fig. 1.1) contains sandstone-type uranium occurrences. A number of occurrences are known in the La Sierrita area in eastern Nuevo León state. Cumulative in situ resources of this district are estimated at 4,000 t U. Grades vary between 0.04 and 0.12% U. *Buenavista*, *La Coma*, *El Chapote*, and *Diana* are the largest occurrences.

Sources of Information. OECD-NEA/IAEA 1982, 1986

Regional Geological Setting of Mineralization

The Burgos Basin is a Tertiary depression extending from Nuevo León state into the neighboring state of Tamaulipas and into southern Texas, U.S.A. The La Sierrita area is underlain by Eocene, Oligocene, and Miocene sediments. Uranium occurs in the Oligocene, non-marine, tuffaceous Frio Formation, which rests

upon the Vicksburg and Jackson formations and is covered by a discontinuous conglomerate horizon, the Norma Conglomerate, and the overlying Reynosa Conglomerate, the stratigraphic equivalent to the Pliocene Goliad Formation in south Texas.

Principal Characteristics of Mineralization

Uranium minerals comprise pitchblende, coffinite, and U⁶⁺ minerals. Some Mo and V, but no Se, is reported. Mineralization forms lenses along a redox interface and at the contact of interbedded mudstone. The lenses occur at several intervals within an almost 25 m thick fluvial, carbonaceous sand horizon of the Frio Formation. In contrast to the south Texas deposits, this mineralization does not resemble roll-type ore bodies.

Buenavista contains about 1,200 t U in several lenses over a length of more than 400 m. The lenses are several meters wide, 0.8 m thick on average, and occur at depths of 25–45 m. Some mineralization was also drill intercepted at a depth of 80 m and occasionally of 160 m. The grade is about 0.12% U.

La Coma (Dominguez 1977) is similar to *Buenavista*. The mineralized horizon averages 3 m in thickness and lies at depths of 30–40 m. The host rock is a grey, very fine-grained sand with a moderate content of pyrite and some clayey interbeds. A distinct conglomerate of mud boulders overlies the ore zones. Calcite cements the ore and is present above it. Limonite occurs above and up dip from the mineralization indicating oxidation activities. Resources are estimated at 1,100 t U. The grade is about 0.12% U.

El Chapote and other occurrences are similar to the above described but are smaller. *El Chapote* has resources of 670 t U. The grade is almost 0.07% U.

1.3 Other Uranium Occurrences in Mexico

OECD-NEA/IAEA (1986) reports the following U prospects in Mexico as shown in ► Fig. 1.1.

Chihuahua State: In addition to the Sierra de Peña Blanca, several minor volcanic-related U(-Mo) occurrences are known from the San Marcos caldera (Victorino prospect), the Sierra de Gomez, the Sierra de la Gloria, and San Antonio de Cobre.

Durango State: Four U occurrences with a total of 840 t U are reported. *La Preciosa*, situated near Nazas, is the largest, but is low grade (0.05% U). This occurrence accounts for approximately 400 t U and is situated at a brecciated intrusive contact between Lower Cretaceous sediments and granitic rocks. *El Mesquite* contains a roughly tabular zone of disseminated and fracture-filling mineralization in a tuffaceous bed of probable Middle Tertiary age. The *Coneto-Buenavista* occurrence is hosted in a vein structure in Cretaceous limestone; uranium minerals are associated with fluorite. The *Sierra de*

Coneto contains a number of uranium occurrences in Cenozoic felsic volcanics.

Oaxaca State: *Tayata* and *San Juan Mixtepec* were discovered in the Tlaxiaco Basin in the western part of Oaxaca State in 1980. In situ resources amount to about 400 t U at *Tayata* and 70 t U at *San Juan Mixtepec*. Uranium mineralization is related to a structurally complex area underlain by conglomerate and tuff of Cenozoic age. Both are in fault contact with Cretaceous limestone and silicified sandstone and schist of Jurassic age, which again are in fault contact with pre-Jurassic gneiss.

Sonora State: *Los Amoles* near Rayon includes three ore bodies (Mina Los Amoles, Amoles II, and Martin). The mineralization consists of primary and secondary uranium minerals associated with argentiferous galena and baryte and occurs in fractures in altered trachy-andesite overlying Mesozoic granite. Estimated uranium resources total approximately 1,250 t U in the RAR and EAR-I categories.

Additional uranium occurrences in Sonora with total in situ resources (RAR + EAR-I) of about 1,000 t U include: *Noche Buena*: U⁶⁺ minerals associated with Ag, Pb, and Zn minerals as fracture fillings in altered Mesozoic granite. *San Antonio de las Huertas*: U⁶⁺ minerals associated with Ag, Cu, Pb, and Zn minerals as fracture

fillings in Jurassic sediments intruded by a felsic to intermediate Cenozoic intrusive. *Granaditas-Santa Rosalia-Picacho*: uranium mineralization in felsic to intermediate volcanics of Cenozoic age. *Yecora*: uranium associated with W and Mo in brecciated granite of Mesozoic age. *Huasabas, Moctezuma, Los Caballos*: U⁶⁺ minerals in fractures in Cenozoic felsic to intermediate volcanics and at the contacts of different lava flows.

Baja California: Marine phosphorite with estimated resources of some 150,000 t U (based on an assumed grade of 100 ppm U) is known from *Hilario, San Juan de la Costa, Tembabiche*, and *UF1* (OECD-NEA/IAEA 1986, 1999)

Selected References and Further Reading for Chapter 1 · Mexico

Alba and Chávez 1974; Aniel 1983; Calas 1977; Cárdenas 1983; Cárdenas-Flores 1985; Chemillac 2004; Dominguez 1977; Ferriz 1985; George-Aniel et al. 1985, 1991; Goodell 1981, 1983, 1985b; Goodell et al. 1979; Magonthier 1985; Michel and Schneider 1978; OECD-NEA/IAEA 1982, 1986, 1999, 2007; Reyes-Cortés M 1985; Rodríguez Torres et al. 1976; Stege et al. 1981; Wenrich et al. 1982; maps and figures courtesy of URAMEX 1980.

Chapter 2

Argentina

Numerous uranium occurrences, commonly of small magnitude, have been discovered in western Argentina, particularly in the Sub-Andean zone (Fig. 2.1). Sandstone-type deposits constituted more than 90% of Argentina's recoverable original resources (ca. 30,000 t U, status 1986). The balance was in vein- or veinlike-type deposits within igneous and metamorphic rocks. These vein-type deposits include typical veins of small magnitude (max. 200 t U) but of relative high grades (up to 0.6% U), and stockwork mineralizations with higher reserves but of lower grades (0.03–0.1% U) (Diaz et al. 1984). OECD-NEA & IAEA (2007) reports remaining recoverable resources of 12,000 t U in the identified resources (RAR + Inferred) < US\$ 130/kg U category, and total production of 2,513 t U (status January 1, 2007).

Seven sandstone-type deposits with more than 1,000 t U each have been discovered to date, the largest is Tigre I-La Terraza (12,500 t U) in the Sierra Pintada. All others are on the order of a few ten to some hundred tonnes uranium. These sandstone-type uranium deposits occur preferentially in Permian and Upper Cretaceous and to a lesser degree in Carboniferous and Tertiary sediments.

Antonietti et al. (1984) distinguish four types of strata-bound mineralization based on host rock facies:

- (a) *Host rock*: sandstone, conglomerate
 - Sierra Pintada: Tigre I-La Terraza (Permian)
 - Sierra Pichiñán: Los Adobes (Cretaceous)
 - Guandacol: Urcuschun (Carboniferous)
 - Malargüe: Huemul (Cretaceous)
- (b) *Host rock*: fine-grained marine and continental sediments
 - Tonco-Amblayo: Don Otto (Cretaceous)
 - Tinogasta: Quebrada El León (Permian)
- (c) *Host rock*: calcrete (caliche)
 - Cosquin: Rodolfo (Tertiary)
- (d) *Host rock*: tuffaceous sediment
 - South Chubut province: Tobas Amarillas (Cretaceous).

Seven uranium regions are identified (Fig. 2.1). They encompass, from N to S, the following major uranium districts: principal types of deposits in brackets

Northern Sub-Andean region (Norte Subandino)

- Tonco-Amblayo district, Salta province (sandstone)

Transition Mountain region (Sierras de Transición)

- Tinogasta, Catamarca (sandstone, vein)

Pre-Cordillera region (Precordillera)

- Guandacol, La Rioja-San Juan (sandstone)

Pampas Mountain region (Sierras Pampeanas)

- Los Colorados, La Rioja (sandstone)

- Cosquin, Córdoba (calcrete)
- Los Gigantes, Córdoba (vein)
- Comechingones, San Luis–Córdoba (vein)

Sierra Pintada region (Sierra Pintada)

- San Rafael, Mendoza (sandstone)

Andean Geosyncline region (Geosinclinal Andino)

- Malargüe, Mendoza (sandstone)

Chubut region (Macizo Central de Chubut)

(San Jorge Gulf Basin/Cuenca del Golfo San Jorge)

- Sierra Pichiñán, Chubut (sandstone)
- Sierra Cuadrada, Chubut (sandstone).

Sources of Information. The following descriptions of sandstone-type deposits are largely derived from Antonietti et al. 1984; Belluco et al. 1984; Belluco and Rodrigo 1981; Rodrigo and Belluco 1981a, b; and those of vein- or similar type deposits from Diez et al. (1984) and Stipanovic et al. (1982), whose publications also incorporate earlier investigations by other researchers.

Historical Review

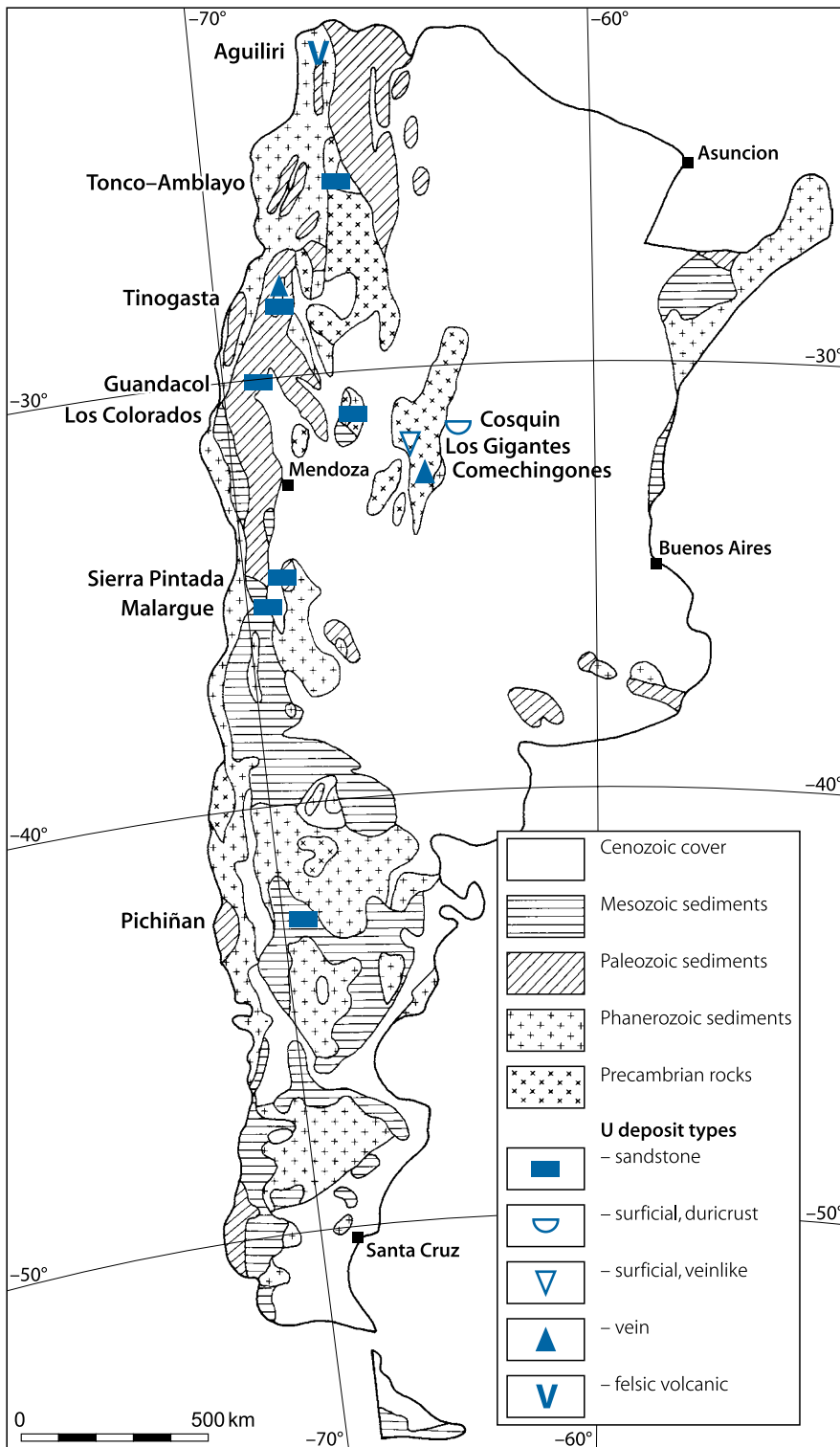
Uranium exploration in Argentina began in 1951–1952. The Huemul sandstone-type deposit was found in 1954 while exploring for redbed-type copper mineralization. The Tonco district, with the Don Otto and Los Berthos sandstone-type deposits, was discovered in 1958. Exploration in the central part of the San Jorge Gulf Basin, Patagonia, began in 1959 and led to the discovery of the Los Adobes sandstone U deposit in the Sierra de los Pichiñanes in the early 1960s. During the 1960s, the vein-type deposits Schlagintweit and La Estela were found, and in 1968, the Dr Baulies deposit was discovered as part of the Sierra Pintada district in Mendoza province.

Follow-up exploration in the Sierra de los Pichiñanes in Patagonia in the 1970s, led to the discovery of the Cerro Condor and Cerro Solo sandstone U deposits, and, in 1978, of the small volcanic-type Laguna Colorada deposit located to the south of the Pichiñanes district.

Several occurrences of vein-type mineralization associated with the Achala batholith were identified during the 1980s, including some in the Schlagintweit and La Estela areas. Subsequently in 1986, uraniumiferous veins were identified at Las Termas. In 1990, an exploration program was initiated at the Cerro Solo deposit in Patagonia and resulted in the delineation of several ore bodies.

Uranium mining began in the mid-1950s, first at the Huemul deposit in Mendoza province. Ore was treated at the Malargüe plant, which started operation in 1954. Subsequently, six more production centers were established; all with a small production capacity. Most of these plants were closed in the 1980s. The San Rafael mill, Mendoza, served open pit mines in the Sierra Pintada since 1979 and remained the only active production center until 1995 when it was put on stand-by.

Fig. 2.1. Argentina, generalized geological map with location of uranium districts. (After OECD-NEA/IAEA 1978)



2.1 Northern Sub-Andean Region (Norte Subandino)

This region is located in northwestern Argentina where uranium occurrences are found in an area 90 km long in N–S direction and 60 km wide. It includes the *Tonco-Amblayo district*, formerly the major uranium producer in Argentina, located in the Salta Subbasin, a southern extension of the Jujuy-Bolivian Basin. Other districts are small and include *Alemania (La Despedida deposit)* and *Pampa Grande*.

Regional Geological Setting of Mineralization

Low-grade metamorphic schists and phyllites of the Upper Precambrian-Lower Paleozoic Puncoviscana Formation intruded by felsic magmatites constitute the basement and crop out to the west of the Salta Basin. Silurian–Devonian marine sediments of flysch and platform facies rest discordantly upon the crystalline complex. They are overlain by diamictic deposits of Carboniferous age.

Subsidence of the Jujuy-Bolivian Basin with the Salta Subbasin started during the Nevada orogenic phase. In Middle Cretaceous time, mainly continental sediments were deposited followed by Upper Cretaceous littoral marginal marine and Paleocene continental molasse sediments.

The Upper Cretaceous includes arenites, pelites, and calcareous sediments of the Salta Group, the Yacorita Formation of which hosts the uranium concentrations in the Tonco-Amblayo and Pampa Grande districts. This uranium-hosting series spreads for about 250 km in a NW–SE direction, and from 10 to 15 km wide. It occupies the western margin of the Tonco Subbasin near the contact with metamorphics and Paleozoic granites which crop out to the west and contain elevated and leachable uranium contents (Belluco and Rodrigo 1981).

2.1.1 Tonco-Amblayo District

The Tonco-Amblayo district is situated approximately 100 km SSW of the town of Salta in southern Salta province. Sandstone-type uranium-vanadium occurrences in Upper Cretaceous sediments extend over a zone about 50 km long in a N–S direction. Several deposits have been mined in the past, the most important were *Don Otto* (ca. 700 t U, 0.1% U) and *Los Berthos* (ca. 350 t U, 0.12% U). *Martin Mighel de Guemes* was also mined. Original reserves of the district were estimated at about 1,700 t U.

Geology and Mineralization

According to Antonietti et al. (1984), Rodrigo and Belluco (1981), the Maastrichtian Yacorita Formation/Balbuena Subgroup, Salta Group, of limnic to littoral provenance is the main host to uranium mineralization (Fig. 2.2). Its upper Don Otto Member (67 m thick) consists of grey-brown to greenish shale, argillaceous and calcareous sandstone, and lutite, whereas

the lower Caliza Amblayo Member (74 m thick) is dominated by limestone with less lutite, sandstone, and shale/mudstone. This sequence rests on the Cretaceous Lecho Formation and is covered by pink to grey psammitic and pelitic sediments of the Paleocene–Eocene Mealla Formation of the Santa Barbara Subgroup. The sediments are folded into a N–S-elongated synclinal structure. Mineralization is found for about 30 km along the western side of this syncline. Inverse faults trending about N–S dissect the area.

At the *Don Otto* deposit, mineralization occurs as peneconcordant lenses over a length of 2,500 m in three horizons within an interval of 16 m in the upper Yacorita Formation. Each horizon is 0.2–1 m thick and is separated by 2–3 m of barren sediments. Mineralized zones have a steep dip of 70° and extend to a depth of 120 m below surface. Carbonaceous lutite and mudstone are the preferential host rocks. Some uranium extends into intercalated sandstone.

Mineralization at depth consists of pitchblende associated with pyrite. U⁶⁺ minerals, particularly uranyl vanadates but also uranyl phosphates and uranyl carbonates, occur closer to the surface. At *Don Otto*, the ratios of uranium–vanadium and uranium–calcium carbonate are 1:1. At *Los Berthos*, the respective ratios are 1:4 and 1:9 (ore grades average 0.11% U, 0.5% V₂O₅), and at *M.M. de Guemes*, 1:2 and 1:3.

The source of uranium is assumed to have been uraniferous granites and pegmatites intruded into metamorphics along the western edge of the basin.

2.2 Transition Mountain Region (Sierras de Transición)/Tinogasta District

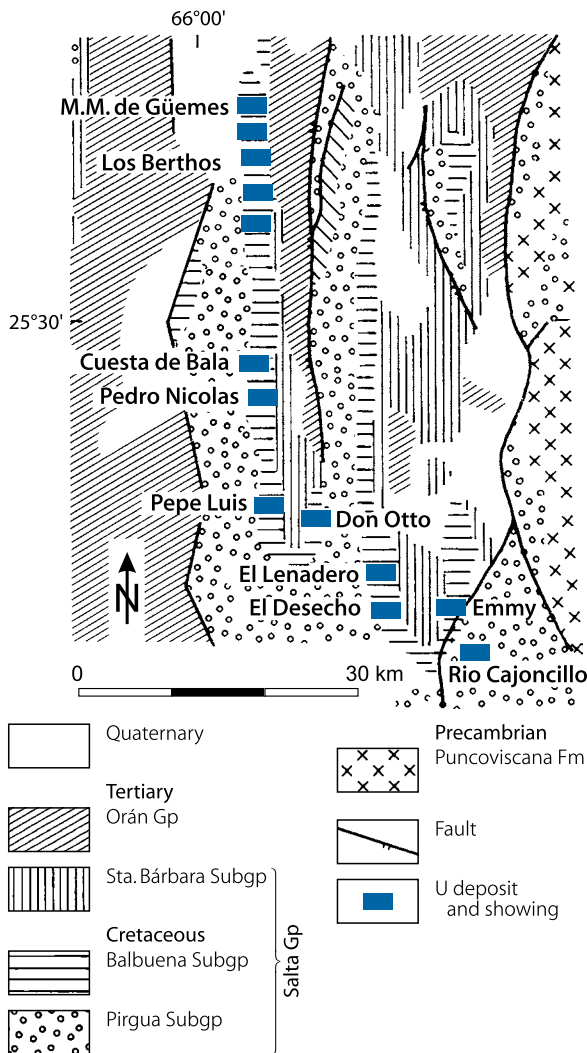
The Sierras de Transición region encompasses the *Tinogasta* uranium district. This district lies near the NW margin of the intracratonic Upper Paleozoic–Triassic Paganzo Basin (for geology s. Guandacol district) in southwestern Catamarca province.

Uranium occurs as peneconcordant mineralization discontinuously spread over several tens of kilometers along strike within Permian sediments. *Quebrada El Leon* is the most prominent occurrence. Some vein-type mineralization, such as that of *Agua de los Pájores*, has been found in Devonian granite. Resources of the district are estimated at approximately 500 t U at an average grade of 0.04% U (OECD-NEA/IAEA 1986).

Geology and Mineralization of Quebrada El Leon

Antonietti et al. (1984) describe the deposit as hosted in grey calcareous mudstone and lutite intercalated with greenish mudstone and sandstone within a 55 m thick unit, which probably represents deposition in a lagoonal environment. This unit is referred to as “Faja Colorada” and is part of the Permian La Cuesta Formation. Uranium-bearing zones are about 0.5 to 2 m thick and extend for approximately 750 m along strike. At depth, pitchblende is the principal uranium mineral and is associated with pyrite, chalcopyrite, chalcocite, and hematite; carnotite, autunite, and copper oxides occur near surface. This mineralization is considered to be comparable with that of Lodève in France.

Fig. 2.2. Tonco-Amblayo district, with location of uranium deposits and occurrences. (After Raskovsky 1970 in Antonietti et al. 1984)



2.3 Precordillera Region

Guandacol, also referred to as *Guandacol-Jáchal*, is the principal uranium district located at the eastern margin of the Pre-Cordillera in northwestern Argentina. Other districts are *Barrel* and *Sañogasta* (*San Sebastian* deposit).

2.3.1 Guandacol District

The Guandacol district lies near the NW edge of and within the Upper Paleozoic–Triassic Paganzo Basin in western La Rio province, at the border with San Juan province. Peneconcordant uranium mineralization is primarily associated with Carboniferous sandstone (e.g. *Urcuschún* deposit), whereas structure-controlled mineralization occurs in Lower Carboniferous and Ordovician calcareous rocks (e.g. *Urcal* mine). The district accounts for original reserves of about 200 t U. Grades are highly variable depending on the type of mineralization.

Regional Geological Setting of Mineralization

The northwestern and western part of the Paganzo Basin is underlain by early Paleozoic biotite gneiss, mica schist, and amphibolite intruded by synorogenic porphyritic biotite granite and granodiorite; these intrusives crop out north, east, and south of the basin.

Ordovician limestone, calcareous sandstone, siltstone, mudstone, and sandstone rest upon the basement. They are disconformably transgressed by a N–S-trending belt of red molasse-type sediments of Carboniferous to Triassic age, which occurs close to the transition zone to the littoral sediments of the westerly adjacent Cuyo Basin. Carboniferous sediments include conglomerate, sandstone, mudstone, and limestone, partly of fluvial origin. Permian sediments are of typical redbed facies. Triassic sediments occur in six formations and include red to grey-greenish conglomerate, sandstone, siltstone, and mudstone. Some of these facies are rich in coaly material and local intercalations of olivine-basalt, tuff, and gypsum beds. Volcanic sills and dikes, presumably of Triassic age (e.g. andesite), intrude the sediments.

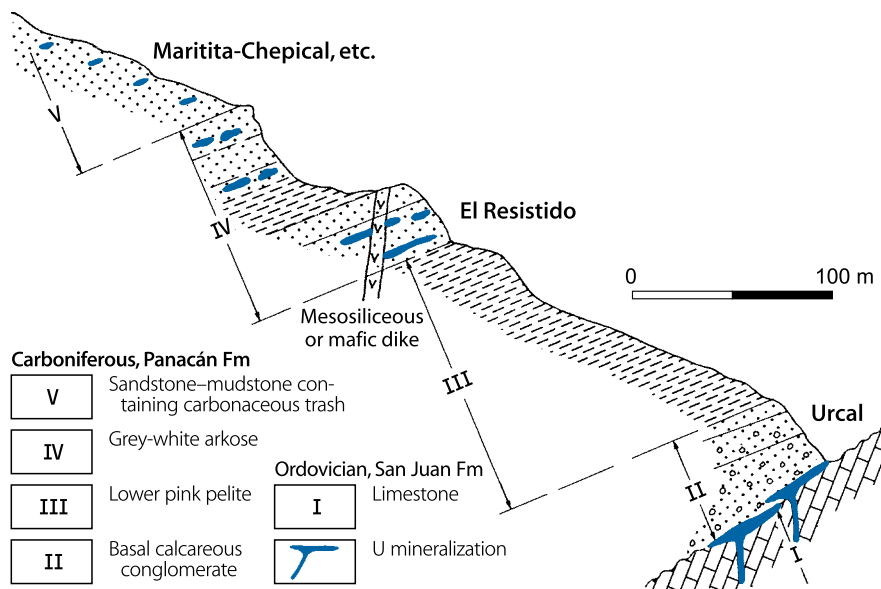
Principal Characteristics of Mineralization

Antonietti et al. (1984) and Rodrigo and Belluco (1981) distinguish three types of settings for the U mineralization (Fig. 2.3):

- Lenticular mineralization** composed of disseminated uranium strongly associated with carbonaceous matter forming small lenses within channels of crossbedded, fine-grained sandstone and mudstone of the Panacán Formation of Upper Carboniferous age. The principal U minerals are pitchblende and uranophane replacing organic matter. Associated minerals are chalcopyrite, bornite, and other sulfides. Mineralized bodies are irregularly distributed and rather small, rarely exceeding some ten tonnes of ore. At places where only tree trunks exist, the mineralization is concentrated at these trunks. Where trunks and abundant finely disseminated organic material are present, the mineralization is more extensive though discontinuous. Grades vary between 0.12 and 1.5% U with local concentrations as high as 30% U. Typical deposits are *La Marthita-Sonia* and *Urcuschún*. The latter has a strike length of about 900 m and averages 0.12% U in beds in excess of 1 m thick.
- Discontinuous mineralization** in grey-white beds of medium-grained arkoses of the Panacán Formation underlying the former strata. Host rocks are heavily altered as reflected by total kaolinitization of feldspar. Mineralization is supergene and consists of hexavalent uranium minerals associated with copper minerals. There is no apparent relationship of uranium to organic material. Instead, mineralization shows some affinity to meso-siliceous and mafic dikes (e.g. andesite) of possibly Triassic age. This appears particularly evident at the *El Resisto* occurrence where mineralization extends for more than 800 m along strike and averages about 0.07% U.
- Fracture-controlled mineralization** related to the unconformity between basal conglomerates of the Panacán Formation and underlying silicified limestone of the

■ Fig. 2.3.

Guadacol-Jáchal district, litho-stratigraphic section documenting the position of U mineralized horizons (dimensions of U lenses not to scale). (After Antonietti et al. 1984)



Ordovician San Juan Formation. The *Urcal* deposit, which has stockwork-type ore bodies up to 50 m wide, is an example of this type of mineralization. The mine yielded 600–700 t of ore grading 0.5% U (~3 t U).

According to de Brodtkorb (1978, 1982), the *Urcal* deposit occurs in a densely fractured zone within calcareous conglomerates of the Cabeza de Montero Member, Volcan Formation (Carboniferous), and extends downward into micrite of the subjacent San Juan Formation. Mineralization fills fractures and forms pockets that range from 20 to 50 cm in diameter. Ore minerals include coffinite, tyuyamunite, metatyuyamunite, and metatorbernite associated with abundant pyrite and minor amounts of marcasite, galena, tetrahedrite, and baryte, plus a number of vanadium oxides (karelianite) and vanadium hydroxo-oxides (montroseite, doloresite, häggite?, pascoite, a.o.). de Brodtkorb (1982) postulates a supergene origin for the V–U mineralization at *Urcal*. The ore-forming elements were derived from groundwater circulating in overlying Carboniferous sandstone beds and were precipitated in the subjacent fractured mineral suite into other oxide and hydro-oxide species of vanadium and uranium.

2.4 Pampas Mountain Region

The Pampas Mountains region, located in central-northern Argentina, includes four uranium districts: *Los Coloradas*, *Cosquin*, *Los Gigantes*, and *Comechingones*.

2.4.1 Los Colorados District

This small district is located in the central part of the Paganzo Basin in southeastern La Rioja province. Peneconcordant sandstone-type uranium mineralization similar to that of the

Guadacol district occurs in the Carboniferous Saladillo Formation, Paganzo Group. Uranium is hosted in lenticular bodies, 0.2–0.4 m thick, of grey sandstone with plant remains, interbedded with red mudstone and tuff. Resources are 110 t U with an average grade of 0.065% U. (OECD-NEA/IAEA 1986).

2.4.2 Cosquin District

The Cosquin district is located in the Valle de Punilla, north-western Córdoba province, and contains calcrete-type uranium mineralization within Tertiary sediments. *Rodolfo*, the principal deposit, accounts for resources of 3,200 t U. Ore averages 0.04% U (Rodrigo et al. 1984).

Geology and Mineralization

A number of uranium occurrences are found over a 50 km long stretch in a narrow, N–S-trending graben structure filled with continental Eocene–Pliocene sediments. Bordering the graben are basement blocks of Precambrian gneiss and schist to the east (Sierra Chica de Córdoba) and uraniumiferous granite of Devonian age to the west (Sierras Grandes and Los Gigantes).

The Tertiary sediments include, from bottom to top, 115 m of calcareous sandstone and siltstone of the Eocene Cosquin Formation and more than 150 m of calcareous, silty sandstone and conglomerate of the Pliocene Casa Grande Formation. Quaternary conglomerates and loess form the cover. Uranium is restricted to the middle member of the Cosquin Formation, 5–12 m thick, of calcite-cemented red siltstone and montmorillonitic clays. Calcite-cemented arkoses with mudstone lenses overlie and underlie the middle member. The Cosquin clastics are composed of white and smoky quartz, potassic feldspar, pistacite, minor fluorite, white mica, garnet, magnetite, ilmenite,

and rare monazite. These minerals were derived from the Sierras Grandes granite and deposited in a lacustrine or low-energy fluvial environment. The lower two members display grey-greenish bleaching along joints and in sandy layers.

Faulting affected the area by tilting the sediments 40–50° E, and caused repetition of beds along N to NW-trending, E-dipping thrusts. A major fault, straddling the eastern side of the graben, thrust Precambrian and Lower Paleozoic metasediments over the Tertiary. On the W edge of the graben, a parallel fault juxtaposed Tertiary sediments onto Quaternary deposits. E–W-trending faults transect the N–S fault system.

At *Rodolfo*, carnotite and tyuyamunite-cemented nodules form ore lenses 1–2 m, locally up to 8 m, thick (average 3.3 m). The lenses occur in a zone 6 km long and 50–300 m wide. Distribution of uranium is irregular, apparently following selected layers in the middle part of the Colquin Formation. The origin of mineralization is thought to be related to paleocalcrete (caliche) processes (Belluco et al. 1985).

2.4.3 Los Gigantes District

This district lies to the west and adjacent to the Cosquin district on the eastern slopes of the Sierra Los Gigantes, about 80 km W of Córdoba City in northwestern Córdoba province. It contains veinlike-type uranium occurrences in granite. *Schlagintweit* is the principal deposit. Original resources were about 1,500 t U. Grades averaged 0.02% U (OECD-NEA/IAEA 1986). Mining took place from 1982 to 1989 and yielded 209 t U. Papers by Diez et al. (1984), Rodrigo et al. (1984), Podda et al. (2003), and Stipanovic et al. (1982) provided the base for the subsequent summary.

Geology and Mineralization

Structure-controlled uranium mineralization occurs in granite of the Achala batholith (see Cuney et al. 1989 for geochemistry of the granitic complex) (Fig. 2.4), which was intruded 329 ± 19 Ma ago into high-grade metamorphics of Upper Precambrian–Lower Paleozoic age. Pegmatite and aplite dikes are abundant. The crystalline complex has been intensely fractured and was exposed to weathering during the late Tertiary. In mineralized zones it is altered.

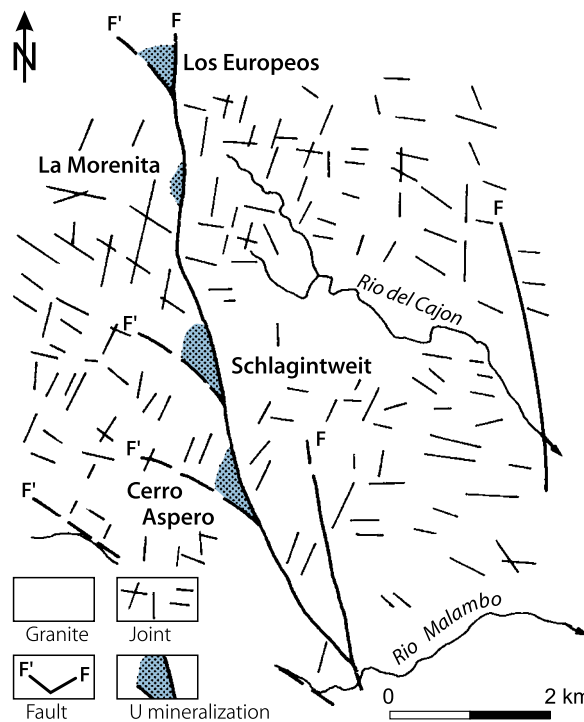
Uranium is hosted by a coarse-grained to porphyritic biotite granite containing large phenocrysts of perthitic microcline. The granite has an elevated background of uranium (6–9 ppm). Part of this uranium is present as uraninite, or bound to biotite. Apatite is a frequent rock constituent and is commonly uraniferous (Lucero et al. 1974).

Principal structures trend NNW–SSE and dip westerly. WNW–ESE-oriented faults branch off from these structures. At the junction of these two sets, wedge-shaped stockworks of intense fracturing developed and were accentuated by flat-lying joints, which provided favorable sites for ore emplacement.

At *Schlagintweit*, this kind of uranium ore-bearing zone measures 600 m in length and up to 300 m in width. Vertically, mineralization is restricted to the upper 40–50 m.

Fig. 2.4.

Los Gigantes district, structural map showing the localization of granite-hosted U deposits controlled by bifurcation of faults. (After Lucero et al. 1974 in Stipanovic et al. 1982)



Ore minerals are principally autunite and meta-autunite and, in lesser quantities, other U⁶⁺ minerals. Some sooty pitchblende occurs at depth. Hexavalent uranium minerals coat joints and fractures and envelop host rock grains. At depth, where the granite is less fractured and altered, mineralization is restricted to narrow veinlets of pitchblende. Mineralization is monometallic and lacks any gangue minerals. It is characterized by a notable disequilibrium.

Structure and lithochemistry are the main controls on mineralization. Structural control is reflected by restriction of uranium enrichment to heavily fractured zones where, in addition, host rock alteration is most intense. Lithochemical control is indicated by the affinity of uranium to zones of high phosphate content.

Lucero et al. (1974) and Nicolli et al. (1974) propose supergene ore-forming processes in Quaternary to recent time. Uranium was leached from surrounding fertile granites by weathering; a hypothesis supported by uranium disequilibrium.

2.4.4 Comechingones District

This district is situated on the western slope of the Sierra de Comechingones, approximately 200 km NNW of San Luis City in northeastern San Luis province. Vein-type uranium occurs in two-mica granite. The most prominent deposit is *La Estela*. It produced, in addition to fluorite, about 15 t U from ore, averaging 0.5% U (Friz et al. 1964). Remaining resources are approximately 300 t U at a grade of 0.08% U (OECD-NEA/IAEA 1986).

Geology and Mineralization

Diez et al. (1984) and Stipanovic et al. (1982) describe the uranium–fluorite *La Estela* deposit as emplaced in Eopaleozoic two-mica granite characteristically containing microcline and orthoclase, with apatite, zircon, and rutile as most frequent accessories. Biotite is commonly chloritized. Locally, epidote has developed by removal of quartz. Wall rocks are commonly strongly altered by kaolinitization and minor sericitization.

Structures are numerous. Those of N–S orientation subdivide the terrane into tectonic blocks. E–W-trending tensional faults crosscut the former causing stockwork-type fracturing and brecciation at the intersections. *La Estela* is emplaced in one of these stockworks. Post-mineral displacements have caused structural complications within the deposit.

Pitchblende is the principal U mineral at depth, whereas uranophane and autunite prevail on upper levels. Associated minerals include chalcopyrite, violet antozonite, calcite, and Cu, Fe, and Mn oxides. On the upper levels, U minerals are distributed in a stockwork, coating fractures and joints and impregnating cataclastic and strongly altered wall rocks. At depth, there is a stronger tendency toward vein development with rich pitchblende veinlets. The mineralized stockwork is about 270 m long in an E–W direction and 7–15 m wide on the upper levels. Depth penetration is 130 m.

Early metallogenetic considerations related *La Estela* mineralization to hypogene epithermal processes due to its uranium–fluorite paragenesis. This hypothesis is supported by an apparent age of about 23 Ma (Stipanovic and Linares 1969), an age corresponding to a magmatic event of the Andean Orogeny.

More recently, studies have shown that the formations of uranium and fluorite are unrelated (Kurat in Diez et al. 1984), hence the hypogene hypothesis has been discarded in favor of a supergene origin. It remains open, however, whether supergene processes overprinted an earlier hypogene mineralization, thereby causing the discrepancy.

2.5 Sierra Pintada Region

The Sierra Pintada region is in the Sub-Andean zone of central-western Argentina. It includes the major *Sierra Pintada district*, also referred to as *San Rafael district*, and the smaller *San Isidro district*. The latter is located north of Sierra Pintada and contains small quartz veins mineralized with pitchblende and hexavalent uranium minerals. Host rocks are Tertiary and Triassic sediments. Several veins were formerly mined selectively and produced a few tonnes of uranium. Selective mining grades ranged from 0.1 to 0.7% U.

2.5.1 Sierra Pintada-San Rafael District

Sierra Pintada was the most important uranium mining district in Argentina during the 1980s and early 1990s. The district is located about 250 km S of Mendoza City, 30 km SW of the town of San Rafael, in north-central Mendoza province. It is within

the Sierra Pintada, a N–S-oriented, some 100 km long and 30–50 km wide mountain range that constitutes the northern part of the San Rafael Block.

A number of peneconcordant sandstone-type uranium deposits were discovered, the first in 1968, in an area about 80 km long in N–S direction and up to 50 km wide. Major deposits are grouped at the western side of the El Tigre brachyanticline. They include the *Dr Baulies-Los Reyunos* deposit, which has as main ore bodies Tigre I-La Terraza and Tigre II–III – Media Luna I–III (Fig. 2.5a). Other ore bodies are La Terraza Norte, Los Gauchos I–II, Los Chañares, La Caverna, and La Ollada. The small deposits of *La Pintada Anticline*, *Los Enriques*, *Pantanito*, and *Carrizalito* occur several kilometers along strike from El Tigre. In addition, some vein-type mineralization is found in Triassic effusives, e.g. *Rincón del Atuel*, and a group around *Las Abejas*, E and S of the Sierra Pintada, respectively.

Original in situ resources of the Sierra Pintada district were estimated at 17,000 t U by Belluco and Rodrigo (1981a) while OECD-NEA/IAEA (1986) reports almost 12,500 t U at a grade of 0.09% U. Low-cost resources amounted reportedly to approximately 4,000 t U.

Exploitation at the Sierra Pintada mine began in 1979 but was terminated in 1995. To this date, about 1,000 t U has been produced from the *Dr Baulies-Reyunos* open pit operation (Tigre I ore body). Uranium was extracted by heap leaching and was processed at the San Rafael plant (120 t U/year nominal capacity).

Sources of Information. Antonietti et al. (1984) and Rodrigo and Belluco (1981a, b) provided much of the basis for this chapter unless otherwise noted. A number of additional papers on the Sierra Pintada deposits have been published by Argentinean geoscientists; they are listed in Selected References... at end of Chap. Argentina).

Regional Geological Setting of Mineralization

The San Rafael Block, the structural unit that dominates the Sierra Pintada region, has an outcropping core of Paleozoic to Triassic rocks. The borders of this block are partially covered by Tertiary continental sediments and more recent deposits. Until Lower Carboniferous time, sedimentation was mainly of marine nature. From Upper Carboniferous onward, only continental sediments formed.

A litho-stratigraphic column of the Sierra Pintada area (Table 2.1) includes (from top to bottom):

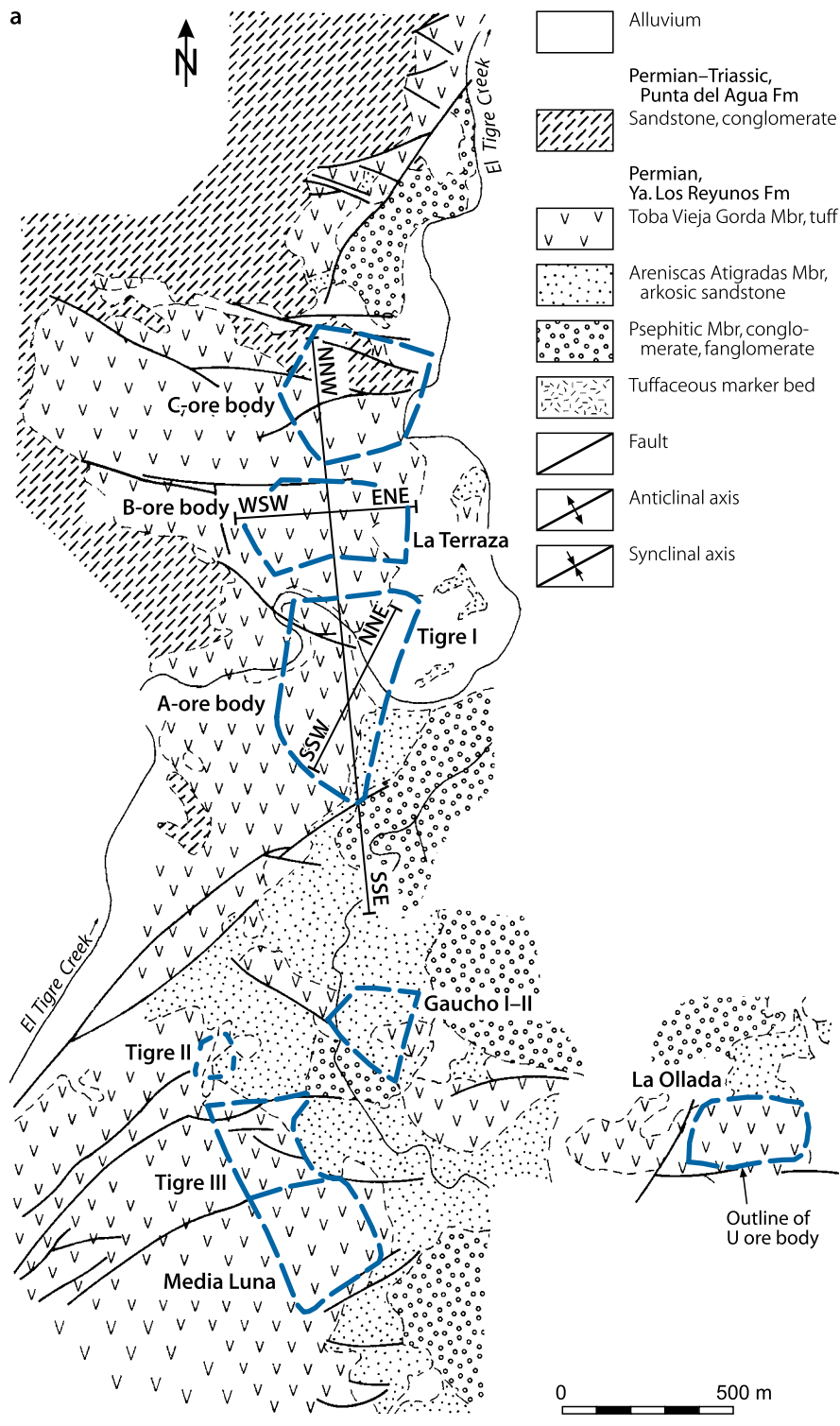
Quaternary: Basaltic and andesitic flows intercalated with continental alluvial and eolian sediments.

Tertiary Rio Seco del Zapallo and Aisol formations: thick continental conglomerates, sandstones intercalated with tuffs and basaltic and andesitic flows deposited after a lengthy hiatus from Jurassic to lower Tertiary time during which the older rocks were subjected to peneplanation.

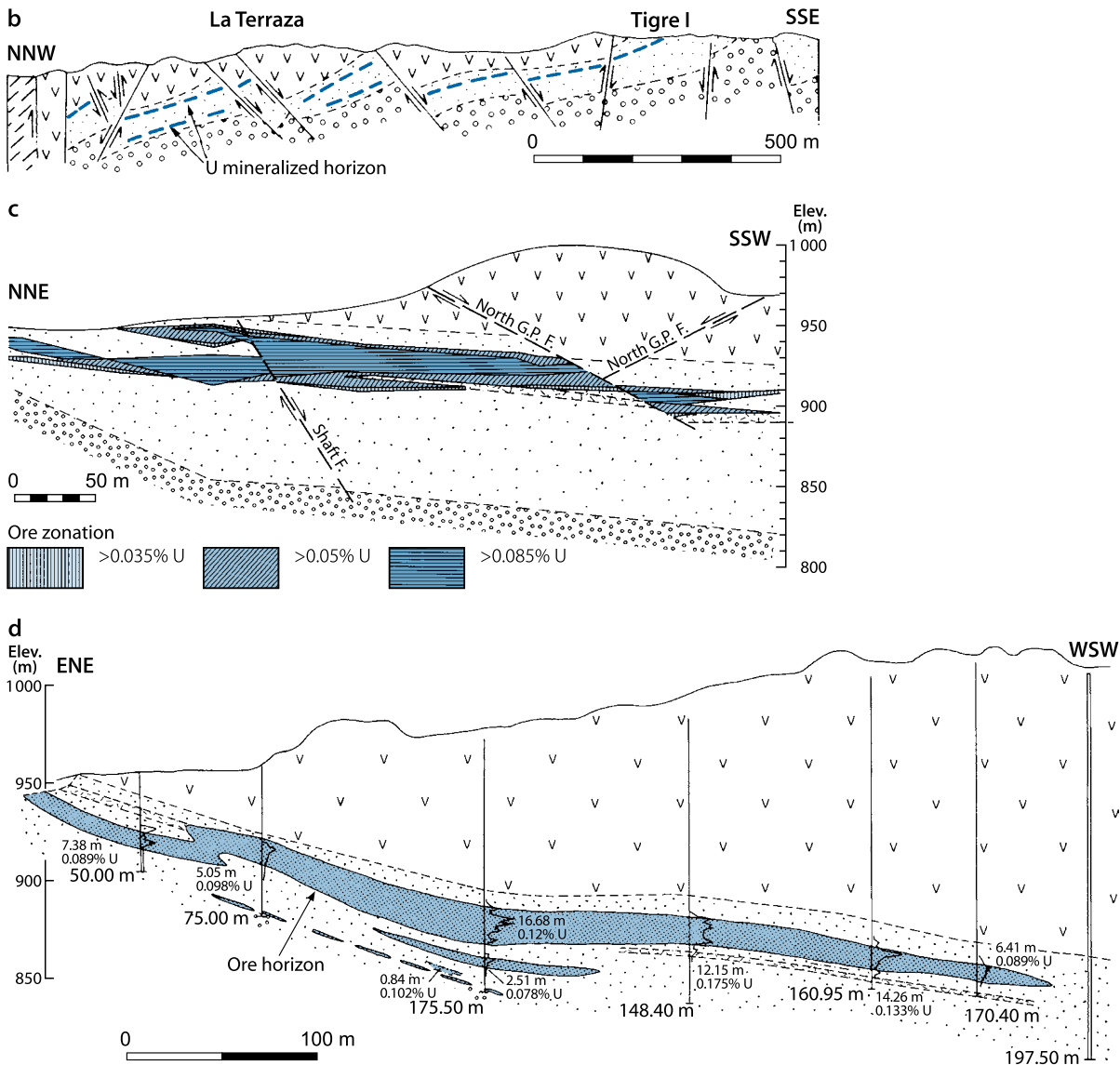
Triassic Puesto Viejo Formation: continental sediments and ignimbrites cut by mafic to andesitic dikes and sills.

Fig. 2.5.

Sierra Pintada, geology and distribution of U deposits in the western El Tigre brachyanticline. (a) Geological map with generalized outline of ore bodies of the principal U deposits. (b) La Terraza and Tigre I deposits, NNW–SSE section displaying lithological and structural settings of ore lenses. (c) Tigre I deposit, NNE–SSW section with uranium grade distribution. (d) La Terraza deposit, geological ENE–WSW section showing drill-intersected grade and thickness of U mineralized intervals. (After (a): Antonietti et al. 1984, Rodrigo and Belluco 1981b; (b): Antonietti et al. 1984; (c): Rodrigo and Belluco 1981b; (d): Rodrigo and Belluco 1981a)



■ Fig. 2.5.
(Continued)



Triassic-Upper Permian Cerro Carrizalito Group: from top to bottom, rhyolite-dacite-basalt interbedded, particularly in the higher levels, with continental sediments.

Permian (-Triassic) Cochico Group (includes the Lower Triassic Punta del Agua and the Permian Los Reyunos formations):

- Punta del Agua Formation: several 100 m thick, pyroclastic and tuffaceous beds plus lavas, interbedded with coarse-grained clastics in the upper section, and alternating beds of pink and yellowish sandstone and conglomerate, deposited after an erosional interlude, in the lower section
- Los Reyunos Formation, separated into three members:
 - Upper Toba Vieja Gorda Member: up to 200 m thick, compact, purplish-grey to violet, lithic crystalline tuff, which includes a few meters of pinkish agglomerate at 80–100 m above the base of the member, and several interstratified marker beds of calcareous sandstone. The sediments rest upon an intraformational unconformity
 - Middle Areniscas Atigradas Member: This member is the most significant uranium host. It is 70–100 m thick and consists of fine- to very coarse-grained, poorly sorted, planar or crossbedded calcareous, argillaceous, arkosic sandstone supposedly of fluvial and eolian origin. A thin tuffitic marker bed occurs interstratified about 50 m above the base. Fresh sandstone is greenish-grey, whereas altered sandstone prevailing in the upper levels is pigmented pinkish to reddish-brown by various Fe oxides. Lateral and vertical facies changes are common. Quartz is the main constituent of the mineralized Atigradas sandstone. Quartz grains are subangular to subrounded and show a habitus similar to that of phenocrysts of porphyritic rhyolites. Feldspars are predominantly plagioclase ranging in composition from albite to oligoclase. Some K feldspar is present. Feldspar is commonly highly altered to kaolinite. Accessories are apatite, rutile, zircon, siderite, and baryte.

Table 2.1. Sierra Pintada district, simplified stratigraphic–lithologic chart. (After Nicolli et al. 1980, Rodrigo and Belluco 1981b; ages from Toubes and Spikermann 1976, 1979)

Era	System	Series	Group	Formation/Member	Lithology	U occur.	Age (Ma)	
Cenozoic	Quaternary	Holocene	Several formations	Río Seco del Zapallo	Alluvial, eolian and piedmont sediments, etc. basaltic and andesitic flows		Basalt 1.5 ± 1	
		Pleistocene					Basalt 3.2 ± 1	
	Tertiary	Miocene	Aisol	Mainly fine-grained sandstones with intercalated basaltic and andesitic sheets		Basalt 13 ± 0		
Mesozoic	Triassic		Cerro Carrizalito	Puesto Viejo	Massive succession of continental sediments		Granodiorite porphyry 192 ± 6	
					Rhyodacitic-rhyolitic facies		Rhyolite porphyry 219 ± 15 Rhyodacite porphyry 223 ± 10 Granite porphyry 238 ± 10 Rhyolite 241/244 ± 10 Granophyre 247 ± 10	
	Permian-Triassic		Cerro Carrizalito	Agua de los Noques	Dacitic facies	Rincón des Atuel U veins		Basalt porphyry 259/260 ± 10 Granophyre 262 ± 10
				Quebrada del Pimiento	Basaltic facies			
	Permian	Lower	Cochico	Arroyo Punta del Agua	Mainly reddish sandstones and conglomerates	Los Enriques U mineral		
				Vieja Gorda Tuff Mbr	Mainly crystallolithic tuffs			Crystalloolithic tuff 272 ± 10
				Atigradas Sandstone Mbr	Fine- to coarse-grained arkoses		Tigre-La Terraza U ore bodies	
				Psephitic Mbr	Mainly conglomerates and fanglomerates			
	Carboniferous	Upper		Cerro Colorado	Mainly conglomerates			Andesite 281 ± 10 Microtonalite 285 ± 10
		Lower		El Imperial	Littoral and continental sediments			
Devonian			La Horqueta	Mainly marine sediments			Schist 353 ± 15	
Cambro-Ordovician			Ponon Trehue	Marine limestone				
				Metasediments intruded by granite and mafic rocks				
Precambrian			C°. La Ventana					

Minor volcanic glass and lithic fragments occur. Matrix, constituting approximately 20% of the rock, consists of clay minerals (10–15%), sericite, chlorite, Fe oxides, finely disseminated organic particles, and interstitial calcite. Calcite replaces feldspar grains. Calcite content is 2–10%

- Lower Psephitic Member: up to 500 m thick, pink polymictic fanglomerates and conglomerates composed of angular boulders in a pink sandy matrix. It is intercalated with thin, crossbedded, yellowish sandstones and two pyroclastic beds and rests unconformably on a pronounced pre-Permian relief and interfingers with the overlying middle member.

Upper Carboniferous: Cerro Colorado (=Brecha Verde) Formation: pink and greenish conglomerates, exposed in the western and southern Sierra Pintada but supposedly eroded over the El Tigre brachyanticline.

Lower Carboniferous El Imperial Formation: 100 m to several hundred meters thick, partially marine and continental clastic sediments of regressive facies resting unconformably upon the Devonian; intrusion of granite, diorite, and tonalite.

Devonian La Horqueta Group: in excess of 1,000 m thick, pelitic-psammitic flysch-facies, metamorphosed to sericitic and chloritic schists with increasing intensity of metamorphism from S to N, intruded by Carboniferous granodiorite and diorite.

Cambro-Ordovician Ponon Trehue Formation: whitish marine limestone.

Precambrian Cerro La Ventana Formation: metamorphosed flysch sediments intruded by granite and mafic rocks (amphibolite), aplite and pegmatite dikes.

Tectonic events, magmatic intrusions and extrusions are associated with the Asturian (Carboniferous) and Saalian (Permo-Triassic) orogenic phases. During these orogenic events, brachyanticlines formed and block faulting commenced. Reactivation of structures took place during the Andean Orogeny (Tertiary-Quaternary).

The structural setting of the Sierra Pintada district is dominated by the El Tigre brachyanticline, 20 km long in a NNW-SSE direction. A great number of around NW-SE, NE-SW, and E-W-trending major and minor faults dissect the brachyanticline. These faults caused vertical displacements of up to several tens of meters and strike-slip movements of as much as 100 m (Fig. 2.5b). Strata inclination is 10–20° W in the principal uranium area (Dr Baulies Tigre I deposit).

Principal Host Rock Alteration

Host rocks are altered by various degrees of oxidation, argillization/kaolinitization, sericitization, chloritization, pyritization, and carbonatization. Labenski et al. (1982) identified four chlorite species based on Fe²⁺ and Fe³⁺ configurations and ratios, and associations with a variety of ferric oxides (lepidocrocite, maghemite/hematite). The various chlorites and Fe oxides characteristically occur in distinct sandstone facies, which may or may not be associated with U mineralization. Recognition criteria for these sandstones are

- Grey sandstone with weak alteration (weathering): predominantly Fe²⁺ and very little Fe³⁺ in chlorite, no influence by U-bearing solutions (low U values)
- Grey to olive-grey sandstone with weak alteration (weathering): Fe³⁺ values in chlorite somewhat greater than in the first group, no influence by U-bearing solutions (low U values)
- Light pink or light reddish-brown sandstone: altered by mineralizing solutions and mineralized, high U values, chlorite contains Fe³⁺, presence of $\gamma\text{Fe}_2\text{O}_3 \times \text{H}_2\text{O}$ (lepidocrocite)
- Pink sandstone: high degree of alteration, high to very high U values, Fe³⁺/Fe²⁺ ratio in chlorite indicates considerable oxidation, presence of maghemite ($\gamma\text{Fe}_2\text{O}_3$) or hematite ($\alpha\text{Fe}_2\text{O}_3$).

The first two sandstone groups were affected by weathering but obviously not by mineralizing solutions. Chlorite with a rather low Fe³⁺/Fe²⁺ ratio is the essential iron-bearing mineral in these sands. The last two groups contain U mineralization and were altered by mineralizing fluids. Their iron content is contained in chlorite and a variety of ferric oxides. Due to oxidation, the Fe³⁺/Fe²⁺ ratio has increased to a value greater than 1. Localized reduction phenomena in these facies are explained by biogenic activity.

Principal Characteristics of Mineralization

Mineralization of the Sierra Pintada deposits is practically monomineralic although some associated metallic minerals occur, but only in very minor quantities. The principal uranium minerals are pitchblende, minor coffinite and brannerite. Oxidized zones contain liebigite and uranophane. U minerals are associated with organic matter and very minor pyrite, arsenopyrite, marcasite, chalcopyrite, bornite, hematite, and goethite, and are accompanied by calcite and dolomite (Arcidiácono and Saulnier 1980).

Pitchblende forms minute grains or fills narrow veinlets, 0.2–1.5 mm thick. Pitchblende grains occur interstitially in the matrix and are intimately associated with maghemite ($\gamma\text{Fe}_2\text{O}_3$), Fe-rich chlorite, and organic matter. Intergranular pitchblende concentrates as bands, streaks, or patches always paralleling bedding. Brannerite commonly coats anatase and leucoxene. Maghemite or hematite, which is more abundant in better grade ore, often imposes a pink pigmentation to these sections.

The Areniscas Atigradas Member of the Permian Los Reyunos Formation is the dominant uranium host. Uranium mineralization occurs in two preferential levels. The main zones of mineralization are above the tuffitic marker bed, whereas smaller, less important, zones occur below the tuff bed. Sericitization, calcitization, and kaolinitization are the principal forms of alteration.

General Shape and Dimensions of Deposits

The main mineralized area has a length of some 15 km in a NNW-SSE direction extending from the Los Reyunos deposit in

the north to Los Chañares in the south, and a width of up to 2 km. Some 10 deposits have been delineated within this zone, which straddles the western side of the El Tigre brachyanticline (dimensions see further below) (Fig. 2.5a).

Deposits consist of peneconcordant lenses within the 70–100 m thick Areniscas Atigradas Member. Lenses spread laterally from a few meters to several hundred meters and have a variable thickness, which may reach as much as 20 m. Within these main lenses, diffuse zones of uranium concentrations exist with better grades related to coarser grained facies. The lenses may occur in an isolated manner or they may be arranged in a loose, ill-defined chain following the N–S-oriented strike direction of the host strata. Lateral boundaries of ore bodies are defined by a lithology-controlled gradual decrease of uranium grades but also by faults displacing one section from the other for up to several tens of meters. Vertically, the uranium tenors vary irregularly, though higher grades tend to accumulate in central parts of the lenses. Uranium grades drop abruptly toward the top of a lens, whereas they decrease gradually toward the bottom.

Rodrigo and Belluco (1981a) note the following dimensions for individual ore bodies of the Dr Baulies-Los Reyunos deposit and other deposits along the El Tigre brachyanticline:

Tigre I-La Terraza: This deposit is structurally divided into three blocks (see below) (Fig. 2.5b–d). Two superjacent ore zones are separated by a tuffitic marker horizon. The *upper or main zone* extends N–S for about 1,800 m, is 600 m wide, and averages 10 m, with a maximum of 30 m, in thickness (ore boundaries at 0.04% U cutoff grade). The uppermost ore commonly occurs 10–20 m below the overlying intraformational unconformity, while the lower boundary plane may extend downward to the tuffitic marker horizon. Ore within the upper zone occurs at depths up to 50 m and crops out in the east where it dips from 10 to 35° NW. The western and southern boundaries are governed by an abrupt decrease in thickness to less than 0.35 m.

The *lower ore zone* is 800 m long, 250 m wide, and averages about 5 m thick, but decreases to less than 0.5 m thickness along the margins. The ore body lies below the tuffitic marker, commonly 10–15 m below the upper ore zone in block C, and 20 m in block A.

Ore grades are highly irregular averaging 0.125% U in the upper ore zone and 0.08% U in the lower ore zone. Original reserves were about 12,500 t U at an ore grade averaging 0.09% U based on a cutoff grade of 0.04% U.

[Castillo (2004) reports an average composition of in situ ore at the Sierra Pintada mine of 0.135% U, 0.02% V₂O₅, <0.001% Mo, 1.72% Fe, 0.017% S, and 3.80% CO₂; and originally used mining parameters for the Dr Baulies-Reyunos open pit operation (*Tigre I ore body*) of 8,500 t U reserves at an average grade of 0.076% U and a cutoff grade of 0.025% U. By increasing the cutoff grade to achieve a mining grade of 0.18% U, remaining reserves would amount to 2,600 t U.]

Two major E–W-striking, moderately steep, south-dipping normal faults with vertical displacements of 50 and 70 m,

respectively, separate the Tigre I-La Terraza ore body into three blocks and produce barren intervals of up to 80 m wide between the blocks. Numerous other steeply dipping, NW–SE, NE–SW, and E–W-trending faults caused additional displacements of as much as 30 m.

Tigre II–III and Media Luna I, II, III: These deposits/ore bodies, located 1.2 km S of Tigre I, constitute cumulatively the second largest deposit in the Sierra Pintada district. Overall dimensions are ca. 1,000 m long in N–S direction, 300 m wide, and 2–20 m thick (average 8 m). Mineralized beds are 25–30 m below the Toba Vieja Gorda Member. They crop out in the east and dip about 20° W. Ore grades average 0.08% U. Resources are about 2,000 t U.

Los Gauchos I–II: Located about 300 m NW of Tigre II–III, this deposit covers an area of 200 m by 250 m. Lens-shaped bodies of mineralization occur in three peneconcordant beds, 1–2 m thick each, separated by thin low-grade interbeds. The beds occur in the uppermost part of the Areniscas Atigradas Member. They are overlain by 15–20 m thick remnants of an eroded tuff horizon. Ore grades are approximately 0.1% U. Resources are estimated at 250 t U.

La Terraza Norte: Located a few hundred meters north of Tigre I-La Terraza, this deposit may be the northern extension of the latter. A barren zone resulting from displacement separates these two deposits. Mineralization occurs in a 7 m thick horizon and grades 0.08% U. Estimated resources are about 700 t U.

Additional small U occurrences at the El Tigre brachyanticline SE of Tigre I include *Gaucha III–IV*, *La Ollada*, *La Caverna*, and *Los Chañares*. They are several tens of meters wide, up to 2 m thick, and grade less than 0.1% U. Reserves are estimated at up to some 100 t U.

Metallogenetic Concepts

Mineralization in the Sierra Pintada district is of peneconcordant sandstone type primarily controlled by lithology and presumably by the presence of uraniumiferous volcanics within the sedimentary sequence. Hypotheses on uranium sources and mineralizing processes are still controversial. Suggested uranium sources are Permo-Triassic felsic volcanics such as the rhyodacitic to andesitic tuffs of the Toba Vieja Gorda Member (2–3 ppm U, in disequilibrium in favor of radium) or rhyolitic effusives of the Cerro Carrizalito Formation (up to 50–100 ppm U). Uranium may have been leached from source rocks during late Mesozoic and early Tertiary periods when intense denudation affected the region as proposed by Rodrigo and Belluco (1981b). Uranium transport may have been as uranyl-carbonate ions as concluded from the presence of abundant authigenic calcite in the host strata. Ferrous iron minerals and/or organic material may have provided reductants to precipitate

uranium as indicated by the intimate association of pitchblende with maghemite and Fe-rich chlorite. Since organic material occurs only sparsely, its role as a reductant may have been only of minor influence.

Ferreyra et al. (1984) assume that the paragenesis of alteration and mineralization (argillization, chloritization, pyritization, uranium mineralization and associated carbonatization) and the distribution of organic matter, sulfides, and chlorite would be in accord with a stable groundwater level during the mineralizing processes. The authors favor an ore formation shortly after the sandstone deposition in Permian time and postulate that the uranium was derived from tuff beds overlying the mineralized sandstone since U and Th contents in these beds suggest uranium leaching.

Labenski et al. (1982) address the phenomenon of higher uranium grades macroscopically corresponding to pinkish-brown beds instead to grey, unoxidized beds. In order to find an answer to this feature, the authors studied chlorite phases by the Mössbauer technique and identified four chlorite species based on Fe^{2+} and Fe^{3+} ratios and associations with a variety of ferric oxides (lepidocrocite, maghemite/hematite). The various chlorites and Fe oxides characteristically occur in distinct rock facies, which may or may not be associated with mineralization as discussed in Chapter "Host Rock Alteration." Two of the chlorite species occur in sandstone sections that were affected only by weathering and not by mineralizing solutions. Locally, reduction phenomena imposed by biogenic activity exist in these facies.

Labenski et al. (1982) conclude from these and other mineralogical data, that uranium leached from overlying, adjacent and intercalated tuffs entered the groundwater system and was redistributed together with other elements such as Ca, Fe, $(\text{CO}_3)^{2-}$ in the Atigradas sandstone. At that time, only incipient diagenesis had affected the sediments hence the sands were practically unconsolidated and highly permeable. The red conglomerate horizon with intercalated pelitic beds underlying the Atigradas sandstone acted as an aquiclude for the groundwater system. This environment provided excellent permeability and facilitated uranium mobility by providing carbonate ions for the formation of uranyl dicarbonate (UDC) and tricarbonatate (UTC). Both complexes are very stable at a pH less than 6.5 for UDC and more than 6.5 for UTC but can be destabilized by noticeable changes in pH, Eh, and CO_2 partial pressure to precipitate uranium. The required conditions supposedly prevailed early in the upper levels of the Atigradas sandstone as indicated by formation of lepidocrocite. Where sufficient oxygen was available, hydrated ferric oxides ($\gamma\text{Fe}_2\text{O}_3 \times n\text{H}_2\text{O}$) precipitated but only at a low CO_2 partial pressure, as may be postulated for upper levels of a free aquifer. On the other hand, lower CO_2 pressure provides a more favorable environment for bacterial development and biogenic action capable of producing locally reducing environments hence providing the required conditions for precipitation of UO_2 . Since lepidocrocite is unstable, it changes into maghemite, which slowly turns into hematite giving the pink to reddish-brown hue to the host sands. In conclusion, the highest uranium concentrations are localized in the upper levels of the Atigradas

sandstone; and these rocks are highly altered by mineralizing fluids, macroscopically reflected by pinkish pigmentation due to Fe oxides and local reduction by biogenic action.

2.6 Andean Geosyncline Region (Geosinclinal Andino)

This region in central-western Argentina contains sandstone-type uranium mineralization. The principal uranium district is *Malargüe*, also referred to as *Pampa Amarilla*. Smaller districts are *Chihuidos* and *Rahueco*.

2.6.1 Malargüe District

The Malargüe district is located in the Pampa Amarilla, 420 km S of Mendoza, the capital of Mendoza province. Peneconcordant, basal-channel-type uranium-copper-vanadium mineralization occurs in Cretaceous sandstone within the Jurassic-Cretaceous Neuquén Basin. The principal deposit was *Huemul*; it produced about 300 t U and 4,000 t Cu and is now exhausted. Ore averaged 0.15% U and 2% Cu (Antonietti et al. 1984, who also provided the basis for the following summary). The conventional Malargüe mill produced 759 t U from 1954 to 1986 when it was closed.

Geology and Mineralization

The Neuquén Basin, part of the Andean Geosyncline, is filled with Permo-Triassic pyroclastic series (Choiyoi Supergroup) followed by continental Triassic and marine Jurassic to Middle Cretaceous sediments. Upper Cretaceous strata consist mainly of continental sediments, including the U-Cu-bearing Diamante Formation. Tertiary sequences are dominantly continental with volcanic intercalations of andesitic and basaltic composition.

Mineralization is confined to the *Huemul Member*, which represents the middle third of the about 250 m thick Diamante Formation. The sediments strike about N-S and dip 35° W. Ore-hosting facies are grey fluvial sandstones and conglomerates filling anastomosing paleochannels incised into pink pelitic beds. The host sands are loosely cemented by abundant bitumen, four types of which have been distinguished, but only one of which acted as a uranium collector.

The principal U minerals are, at depth, pitchblende, often spherulitic, and, on upper levels, hexavalent uranium minerals, particularly uranyl vanadates. Uranium is accompanied by copper mineralization, which predates uranium deposition. Cu minerals include sulfides (chalcopyrite, minor chalcocite, and covellite) and alteration products thereof (malachite, azurite, chrysocolla, chalcantite). Isotope dating of pitchblende yields an Oligocene age (29 Ma).

Mineralized lenses vary in thickness between 0.6 and 2 m and occur in the middle or upper portions of the host channels, which are 3–4 m thick. The main ore body at Huemul has a length of about 100 m and extends for a 125 m downdip.

2.7 San Jorge Gulf Basin/Chubut Region (Cuenca del Golfo San Jorge)

The San Jorge Gulf Basin occupies a large terrane in Chubut and adjacent provinces in Patagonia, southern Argentina. A considerable number of uranium occurrences of sandstone and volcanic type have been discovered in various parts of the basin since the 1950s. Most of them occur in the Cretaceous Chubut Group, some in the Tertiary Rio Chico Formation (► Fig. 2.6 and 2.7).

Established minable deposits are restricted to the *Pichiñán* district, as discussed further below. Other areas with sandstone-type U mineralization are reported from the *Sierra Cuadrada* in the central-eastern, and *El Mirasol* in the northeastern part of the basin. Volcanic-type mineralization associated with pyroclastics occurs in the *Paso de Indios* area (*Laguna Colorada* and *La Potranca* occurrences) located some 50 km south of the *Pichiñán* district, and at the southeastern margin of the basin (*Cerro Tacho*, *Cañadón Gato-Kruger*). Surficial-type uranium occurrences associated with Quaternary calcrete/caliche are known on the eastern and northwestern margins of the basin (► Fig. 2.6).

Sources of Information. Antonietti et al. 1984; Belluco et al. 1985; Benitez et al. 1993; de Brodtkorb and Brodtkorb 1984; Maloberti 1989; Navarra 1992; Navarra and Benitez 1997; Navarra et al. 1993, 2001; Olsen and Berizzo 1980.

Regional Features of Geology and Mineralization of the San Jorge Gulf Basin

The intracratonic San Jorge Gulf Basin covers 170,000 km² and is filled with Tertiary, Cretaceous, and Jurassic continental clastic and pyroclastic sediments, which unconformably rest upon a basement of Permian granite-gneiss intruded into older gneiss and mica schist.

The Mesozoic strata (► Fig. 2.7) include – from bottom to top – *Jurassic* marine platform sediments upon which intermediate pyroclastics of the *Cañadón Puelman* Formation and thereupon fluvial-lagoonal sediments of the *Cañadón Asfalto* Formation were laid down in oxygenated as well as euxinic environments.

After a hiatus, the basin continuously subsided during *Cretaceous* time and the *Chubut Group*, up to 600 m thick, was deposited. Coeval intense volcanic activity in the region of the present Andean orogenic belt, located some hundred kilometers to the west of the central area of the basin, provided pyroclastic material to this group. The basal unit of the *Chubut Group*, the wide-spread *Los Adobes* Formation, consists of high-energy fluvial psammitic-psephitic clastics with interbedded tuffs of variable litho-chemistry that fill paleodepressions scoured into Mesozoic and Paleozoic rocks. This formation is covered by lacustrine-pyroclastic sediments of the *Cerro Barcino* Formation, the constituents of which were derived from the west and make up the bulk of the Cretaceous infill of the basin. These two formations attain an average thickness of several hundred meters in some areas. The *Puesto Manuel Arce* Formation, as much as several tens of meters thick, is the last Cretaceous unit; it comprises a second fluvial system and interbedded tuff and siltstone.

Tertiary strata include marine sediments of the *Salamanca* Formation and fluvial-lagoonal sediments of the *Rio Chico* Formation. Tertiary basalts cover wide areas of the region.

U mineralization of sandstone type occurs on two stratigraphic levels of the *Chubut Group*. Deposits in the *Pichiñán* district, as discussed below, are positioned at the base, within the *Arroyo del Pajarito* Member of the *Los Adobes* Formation, whereas in the eastern part of the San Jorge Gulf Basin, e.g. in the *Sierra Cuadrada* area, occurrences are hosted in the uppermost *Puesto Manuel Arce* Formation. This formation reflects a fluvial system, up to 70 km wide, with channels filled with clastics up to 30 m thick. *Volcanic-type U mineralization* occurs in tuff horizons of the *Chubut Group* at several locations in part associated with pyroclastic dikes (► Fig. 2.8). Uranium showings are also found in fluvial sediments of the Tertiary *Rio Chico* Formation and, at the eastern border of the basin, associated with *calcrete-type* duricrusts in Quaternary soils (► Fig. 2.6). The latter occur spotty within an about 100 km² large area.

Maloberti (1989) suggests that the tuff and tuffite of the *Cerro Barcino* Formation constitute potential uranium sources; they contain significant quantities of uranium, which was partly liberated and transported through permeable pyroclastic units of the *Chubut Group* to sites where conditions were adequate for ore formation in the fluvial systems. In contrast to this classic basal-channel-type metallogenetic model, the origin of volcanic-type uranium mineralization is thought to be related to hydrothermal processes during the Tertiary.

2.7.1 Pichiñán District

This district is situated in the *Sierra de los Pichiñanes*, some 40 km N of the little village of *Paso de Indios* in central Patagonia, Chubut province, approximately 350 km WSW of the town of *Rawson* on the Atlantic coast. The *Chubut River* and the *Arroyo Perdido*, about 40 km apart, are the western and the eastern limits, respectively. Several basal-channel sandstone-type uranium deposits were discovered during the 1960s and 1970s. Two small deposits, *Los Adobes* and, 30 km to the SW thereof, *Cerro Condor*, were mined by open pit methods in the 1970s and produced, in total, about 200 t U. An additional deposit, *Cerro Solo*, located 2 km S of *Los Adobes*, has been under investigation since 1990. Revived exploration in the 2000s discovered additional or satellite ore bodies in vicinity of *Cerro Solo*.

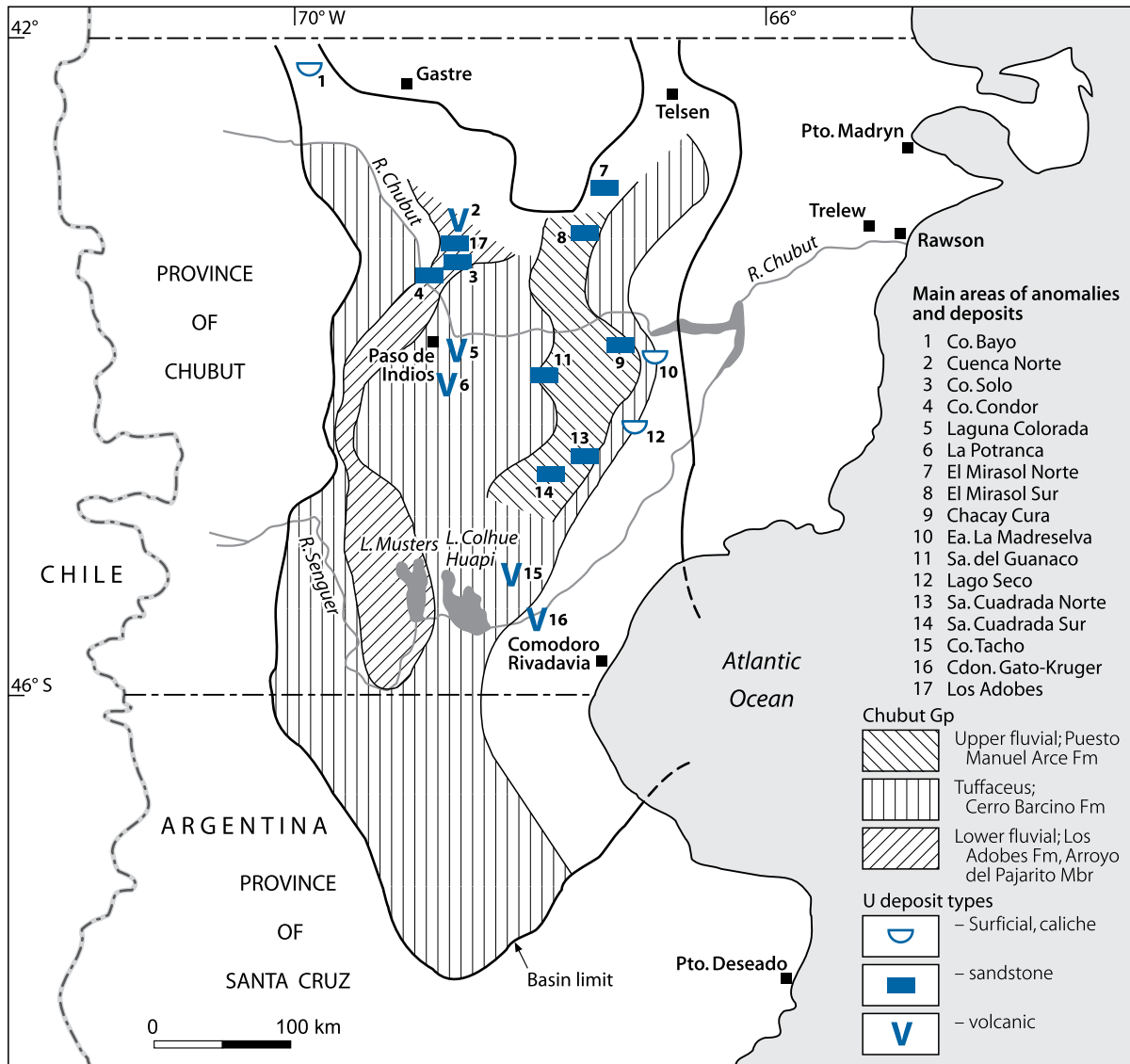
Sources of Information. Antonietti et al. 1984; Belluco et al. 1985; Benitez et al. 1993; de Brodtkorb and Brodtkorb 1984; Maloberti 1989; Navarra 1992; Navarra and Benitez 1997; Navarra et al. 1993, 2001; Olsen and Berizzo 1980.

Regional Geological Setting of Mineralization

The *Pichiñán* district is located in the central-northern part of the San Jorge Gulf Basin. Uranium occurs in the *Arroyo del Pajarito* Member at the base of the Cretaceous *Los Adobes*

■ Fig. 2.6.

San Jorge Gulf Basin, generalized map of the distribution of the two fluvial members of the Chubut Group and location of uranium deposits and occurrences. (After Navarra and Benitez 1997, partially based on Fuente A and Maloberti A, unpublished)



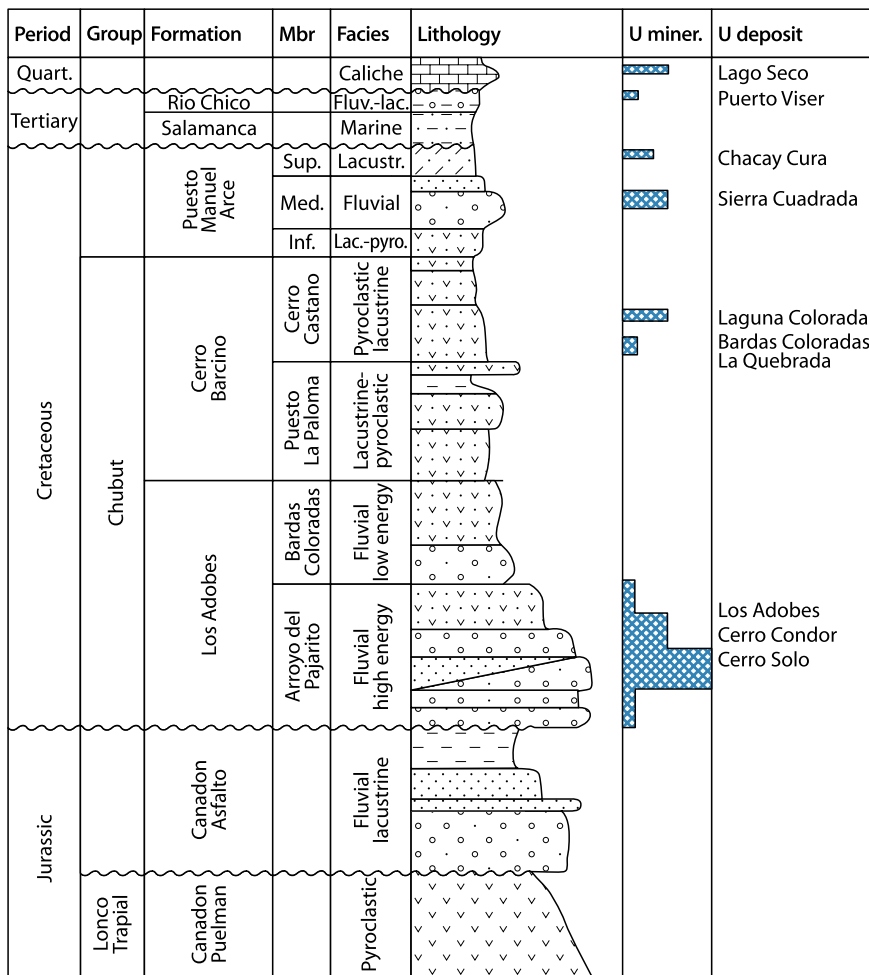
Formation. The member consists in this district of an about E–W-trending, south-turning in the western Pichiñán area, paleodrainage system of anastomosing, high-energy streams. The system is as much as 16 km wide. Individual paleochannels are up to 150 m thick along thalwegs and thin to some ten meters at the margins. Lacustrine-pyroclastic sediments of the Cretaceous Cerro Barcino Formation rest upon the Los Adobes Formation. The volcanic-sedimentary strata form a NNE–SSW-elongated anticline, the Pichiñán Ridge, about 50 km long and 16 km wide. Its outcropping core is a basement complex of Permian granite-gneiss intruded into older gneiss and mica schist. Major structures trend WNW–ESE and ENE–WSW. They originated in pre-Cretaceous time and controlled the position of Cretaceous drainage systems. Tertiary movements reactivated the structures.

Principal Characteristics of Mineralization

Pitchblende, coffinite, uraniferous organic matter, and/or uranyl silicates, -vanadates and -phosphates are the principal U phases. The first three phases often associate with abundant pyrite in grey to greenish reduced zones rich in organic matter.

Uranium occurrences are found discontinuously over a length of more than 50 km and a width of 8 km in a curvilinear E–W-oriented segment of the Arroyo del Pajarito Member on both sides of the Pichiñán Ridge. Mineralization is commonly restricted to fluvial sediments of the upper section of the member that typically contain rhyolitic clasts while volcanic fragments of dacitic and trachitic composition dominate the basal facies. *Cerro Condor* and *Los Adobes* are positioned in the top and *Cerro Solo* in the bottom part of the felsic section.

Fig. 2.7. San Jorge Gulf Basin, litho-stratigraphic column of Mesozoic units and associated uranium occurrences. (After Navarra and Benitez 1997, Gorustovich et al. 1992)



Mineralization occurs preferentially as peneconcordant lenses up to several tens of meters long and a few meters thick, positioned within the basal 20m of the felsic section of the Arroyo del Pajarito Member. Host rocks are almost flat-lying fluvial beds with dips rarely exceeding 5°, composed of crossbedded, carbonaceous sandstone and conglomerate.

Diagenesis tends to have played a significant role in preserving the mineralization, as indicated by the typical presence of abundant carbonatic cement in the mineralized layers, a constituent that gives them a distinctive hard consistency as compared with more friable parts of the sections in the area.

- Host units comprise alternating thin beds/lenses of grey or green sandstone and conglomerate characterized by rhyolitic clasts and clay galls with intervening pelitic lenses
- Abundant organic material and sulfides in reduced facies
- An apparent increasing content of carbonate cement toward mineralized lenses and
- Close association between mineralization, organic material, and sulfides.

Highest ore grades are related to conglomerate-sandstone contacts, tree trunks, and clay galls. The various lithologic properties control on their part the concentrations of organic substance and the permeability.

Principal Ore Controls and Recognition Criteria

Dominant features that control the Pichiñán U deposits are of lithologic-sedimentary nature and include

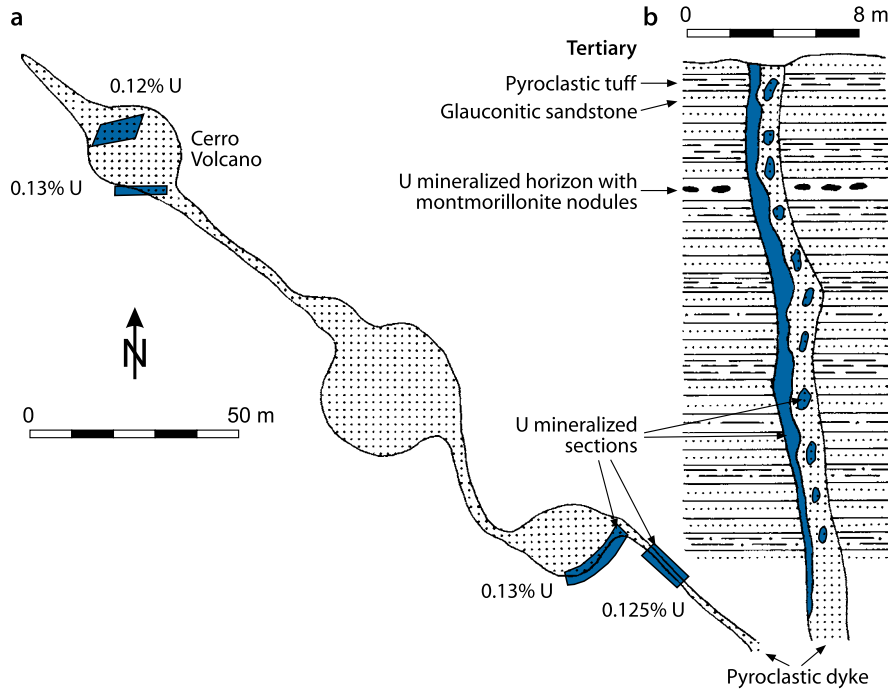
- Position of ore bodies within paleochannels of the same paleodrainage system and the same litho-stratigraphic unit
- Ore-hosting fluvial facies reflect rapid changes in deposition by high-energy streams

2.7.1.1 Cerro Solo Deposit

Discovered in 1979, the *Cerro Solo* U–Mo deposit is situated to the east of the Pichiñán Ridge, 2–3 km to the south of the former Los Adobes mine. It covers 320 ha with several, structurally separated U zones (Fig. 2.9). Recoverable uranium resources in the RAR and EAR-I categories amount to 4,630t U, about

Fig. 2.8.

Chubut region, Patagonia, Cañadón Gato deposit, (a) simplified geological plan and (b) cross-section of pyroclastic dike configuration and dike-related U mineralization. (After Stipanovic et al. 1982)



half of which occur in the main zone that occupies 86 ha (CNEA 1998).

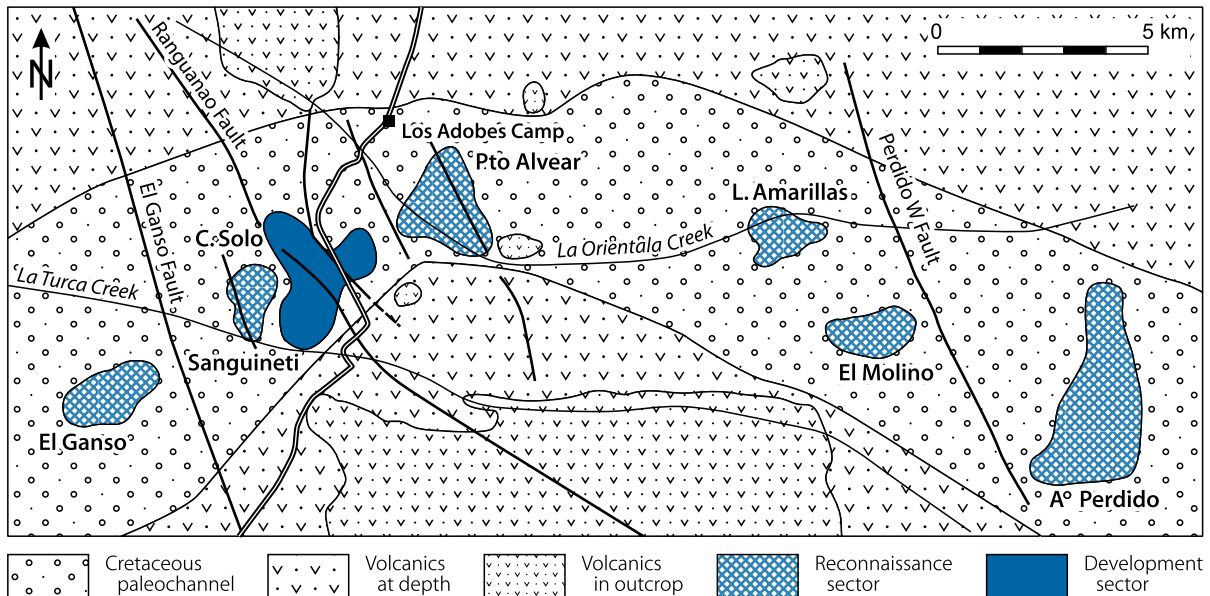
Sources of Information. CNEA 1998; Navarra and Benitez 1997; Navarra et al. 1993, 2001.

Geology and Mineralization

The uranium-hosting *Arroyo del Pajarito Member* fluvial unit of the basal Los Adobes Formation is up to 150 m thick in the Cerro Solo area and consists predominantly of carbonaceous

Fig. 2.9.

Pichián district, Cerro Solo area, outline of the uranium-hosting paleochannel in the Los Adobes Formation with location of Cerro Solo deposit and other uranium occurrences. (After Navarra and Benitez 1997)



conglomerate and sandstone deposited in a high-energy, braided-channel environment (Figs. 2.9, 2.10). Prominent NNW–SSE-trending faults with substantial lateral and vertical displacements separate the deposit into eastward dipping blocks. NE–SW faults further complicate the tectonic setting.

Host rocks comprise reduced, grey or green, alternating lenses of thin, immature sandstone and occasionally conglomerate with a sandy matrix. The clastic fraction consists mainly of lithic fragments (rhyolite, ignimbrite, felsic tuff, and less frequent andesite, silica, and granite-granodiorite), quartz, and feldspars. Matrix constituents include ample clay minerals, predominantly montmorillonite, and calcite. Organic matter is abundant. Ore lenses are notably related to paleochannel sections characterized by rapid facies change, relatively high, original permeability related to gravel and fine-grained sand fractions, minimum clay contents, marked sulfide concentrations, and relatively abundant secondary carbonates contained in matrix and fissures. More homogeneous lithologies overlie and underlie the mineralized beds.

Uranium occurs as coffinite, pitchblende, and uraniferous organic material all of which typically associate with disseminated carbonaceous detritus, notable amounts of jordisite and ilse-mannite, and Fe sulfides. Ore bodies are of lenticular shape, in average 3 m and locally up to 10 m thick, and occur at depths from 50 to 130 m (Fig. 2.10). The grade varies between 0.0x%

and more than 2% U; it averages 0.3% U in the ore bodies of the main zone of the deposit; the higher values are typical for intercalated sandstone beds.

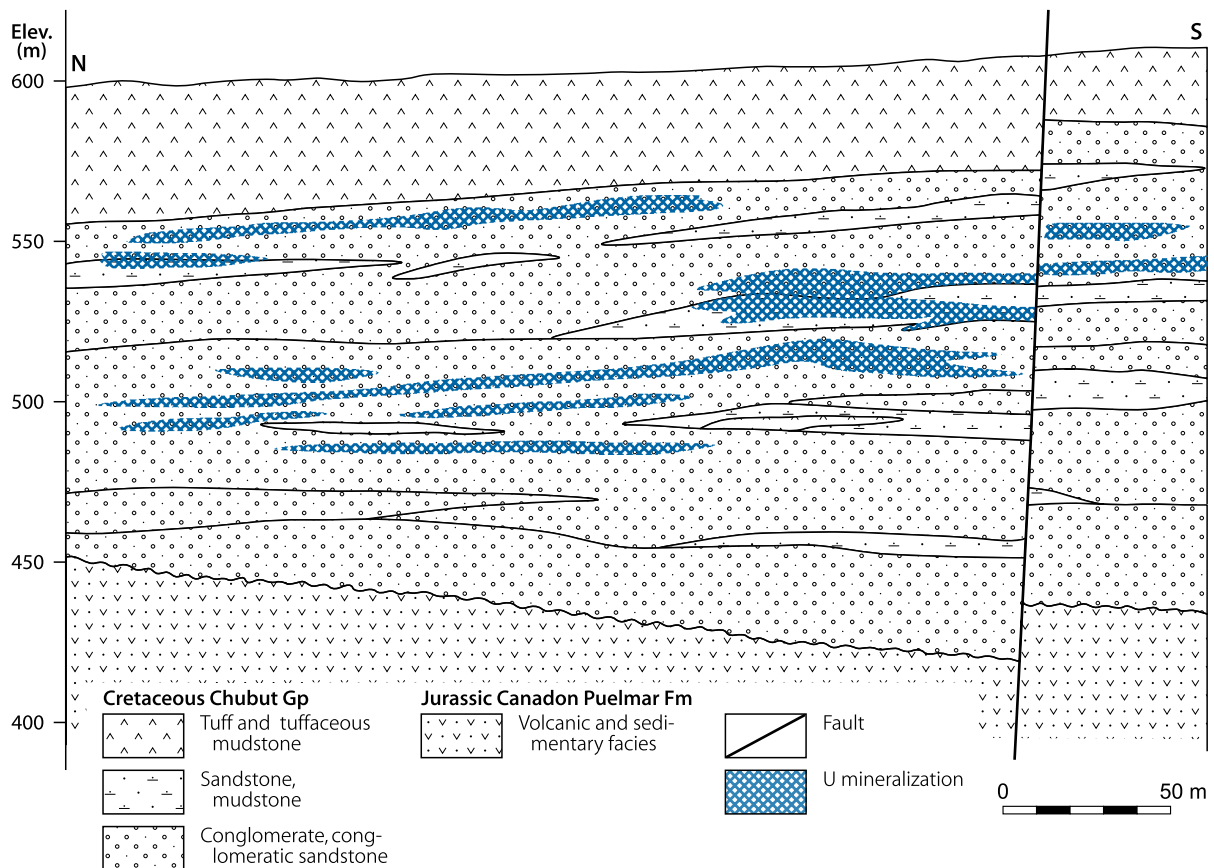
2.7.1.2 Cerro Condor and Los Adobes Deposits

The *Cerro Condor* deposit is located in the SW part of the Pichiñán district, to the west of the Pichiñán Ridge where the U-hosting paleochannel system turns to the south. The open pit mine produced 85 t U at a grade of 0.05% U from oxidized and reduced ore within a 150 m long, 75 m wide, and 5–10 m thick channel interval. Ore mined was predominantly concentrated in a lower conglomerate bed with interspersed sandstone channels. Plant remains are abundant including tree trunks, which may be calcitized, silicified, or replaced by gypsum. Intense jointing is common; joints are coated with calcite and Mn oxides.

The *Los Adobes* deposit is located in the NE part of the district, to the east of the Pichiñán Ridge. The open pit mine produced about 110 t U at an average grade of 0.12% U. The ore consisted solely of oxidized material, contained in a 100 m long, 75 m wide, and, on average, about 5 m thick zone. The channel lithology is separated into two units. The *upper unit* is about 6 m

Fig. 2.10.

Pichiñán district, Cerro Solo deposit, schematic N–S section illustrating the lithographic setting and shape of uranium ore bodies. (After Benitez 1990 in Navarra 1992)



thick, unmineralized, and consists of light colored, laminated, and crossbedded, very fine-grained sandstone with hematite coatings on joints, and greenish mudstone. The *lower unit* is 6–7 m thick and includes two tan, limonitic conglomerate horizons, each 2–3 m thick. Pebbles, up to 20 cm in diameter, dominantly consist of rhyolite, porphyry, and rare siltstone. The matrix is composed of coarse-grained sandstone with kaolinite and contains irregular disseminations of U^{6+} minerals. Sandstone channels are frequent within the conglomerate beds. The two conglomerate horizons are separated by a tan sandstone bed, approximately 1.5 m thick, that contains whitish clay galls with diameters of as much as 1 m. Concentric limonitic halos surround the galls and are commonly highly mineralized. Uranium mineralization occurs in irregular distribution in the conglomerate matrix, in the interbedded sandstone horizon, and in sandstone below the lower conglomerate.

2.7.2 Tobas Amarillas Area

Peneconcordant, tabular uranium mineralization associated with yellow tuffs (=tobas amarillas) occurs near *Laguna Palacios* in central-southern Chubut province. Host rocks are tuffaceous

sandstone and conglomerate cemented by Fe hydroxides within the lower part of the Middle to Upper Cretaceous Tobas Amarillas Series. This series is approximately 40 m thick. Uranium occurs as schröckingerite. Grades vary between 0.03 and 0.14% U and 0.02 and 0.03% V. Similar mineralization is reported from the *Laguna Colorado* area (Antonietti et al. 1984).

Selected References and Further Reading for Chapter 2 Argentina

For details of literature see Bibliography.

Angelelli 1956, 1969; Antonietti et al. 1984; Arcidiácono and Saulnier 1980; Belluco et al. 1974a, b, 1977, 1985; Belluco and Rodrigo 1981; Benitez et al. 1993; Castillo 2004; Cuney et al. 1989; de Brodtkorb 1965, 1966, 1978, 1982; de Brodtkorb and Brodtkorb 1984; CNEA 1998; Diez et al. 1984; Ferreyra et al. 1984; Friz et al. 1964; Kretschmar pers. commun. 1986; Labenski et al. 1982; López and Ford 2002; Lorrai et al. 2003; Lucero et al. 1965, 1974; Maloberti 1989; Moreno and Pujol Ferre 1962; Navarra 1992; Navarra and Benitez 1997; Navarra et al. 1993, 2001; Nicolli 1974; Nicolli et al. 1973, 1974, 1976, 1980; OECD-NEA/IAEA 1977, 1986, 1999, 2007; Olsen and Berizzo 1980; Ortega Furlotti et al. 1974; Podda et al. 2003; Rodrigo and Belluco 1981a, b; Rodrigo et al. 1984; Stipanovic 1970; Stipanovic and Belluco 1984; Stipanovic et al. 1968, 1982.



Chapter 3

Bolivia

Small uranium occurrences of the volcanic type have been found at the western margin of the Cordillera Oriental in southern Bolivia (Fig. 3.1). The *Sevaruyo* district includes several U occurrences that have been investigated in more detail and which will be discussed further below. *Charazani* in northern Bolivia contains structurally controlled pitchblende and coffinite mineralization in Tertiary rhyo-dacitic rocks and Ordovician slate. This setting resembles that of Macusani, Peru. Both Charazani and Macusani appear to be related to felsic volcanic rocks adjacent to granitic batholiths (Limbani-Quillabamba and Coaza batholiths in Peru, Huato in Bolivia).

3.1 Sevaruyo District

The Sevaruyo district is located south of the village of Sevaruyo, on the western edge of the Meseta de los Frailes, approximately 400 km S of La Paz. Several uranium occurrences have been detected in Tertiary volcanics including *Cotaje*, *Huancarani*, *Los Diques*, *Tholapalca*, *Torko*, *San Agustin*, and *Amistad*. All mineralized bodies are small in size and contain only a few tons of uranium; the largest is *Cotaje* (Fig. 3.2), which accounts for resources of about 40 t U, at an average grade of 0.06% U (OECD-NEA/IAEA 1979).

Sources of Information. Aparicio 1981; Leroy et al. 1985; Leroy and Müller-Kahle 1985; Michel and Schneider 1978; Pardo-Leyton 1981, 1985; Pardo-Leyton and Barron 1984; Santivañez 1977; Michel 1980, personal communication.

Regional Geologic Setting of Mineralization

The Meseta de los Frailes covers a large area of Tertiary effusives, which are thought to have poured out along the fault contact between the Cordillera Oriental and the Altiplano. The Los Frailes Formation of Upper Miocene and Pliocene age, in excess of 500 m thick, is the dominant lithologic unit. It consists of rhyolitic and rhyodacitic ignimbrite and tuff layers with intercalated volcanic conglomerates and breccias, and a top layer of vesicular ferruginous andesitic lavas. Pardo-Leyton (1985) subdivides the Los Frailes Formation into two cycles, the first of which was extruded 16–10.5 Ma ago, and the second 9.9–3.6 Ma ago (Santivañez 1977). Michel (1980, personal communication) mapped pronounced erosional features between the various effusive phases including paleochannels filled with highly permeable material.

Pre-Miocene loosely consolidated sandstone and lutite of the Quehua (~100 m thick), Chamarra (60 m), and Coco (80 m) formations, from top to bottom, represent the lower part of the Tertiary. They rest unconformably upon Cretaceous marine and

continental formations in excess of 3,000 m thick. Gypsum-bearing lutite with interbedded lenses of fine sandstone of the Campana Formation was deposited in Permo-Triassic(?) time. Diapirs of the Campana Formation invaded the overlying Cretaceous sediments. The lowermost rocks belong to the Silurian Llalague Formation, which is composed of lutite and quartzite. Subvolcanic dacitic stocks, some 100 m in diameter, intruded the older formations, presumably in post-Pliocene time.

Regional structures trend predominantly NE–SW, E–W, and subordinately N–S. Tectonic stress imposed two systems of intense jointing on the volcanics with maxima around NNE and ENE.

The two basal horizons of the *Los Frailes Formation* are composed of tuffs with abundant phenocrysts (ca. 30%) and are the dominant uranium hosts. Characteristic phenocrysts of the lowermost unit (P1) are quartz, oligoclase-andesine, biotite, minor K feldspar and ilmenite embedded together with some glassy pumice fragments in a crystalline groundmass. Phenocrysts of the next higher unit (P2) are more calcic plagioclase (andesine-labrador), less common K feldspar, quartz, biotite, and ilmenite emplaced in a microcrystalline matrix with some non-compacted shards and disseminated iron oxides. Three subunits (P2a, b, and c) are identified within the P2 unit. P2b has additional phenocrysts of muscovite while P2c contains fewer phenocrysts than the underlying P2b and P2a subunits. Geochemically, the P1 and P2 units show an upwards progressing evolution of K_2O/Na_2O ratios from 1.4 to 3.16, SiO_2/Al_2O_3 ratios from 5.14 to 4.45–4.97, and an increase in Li, Sr, Ba, and REE contents. U and Th tenors of P2a and P2b average 9 ppm and 23 ppm, respectively, with some local enrichment (e.g., 95 ppm U in a 5–20 cm thick, discontinuous P2b tuff bed at Asunción in the southern part of the district as reported by Leroy et al. 1985).

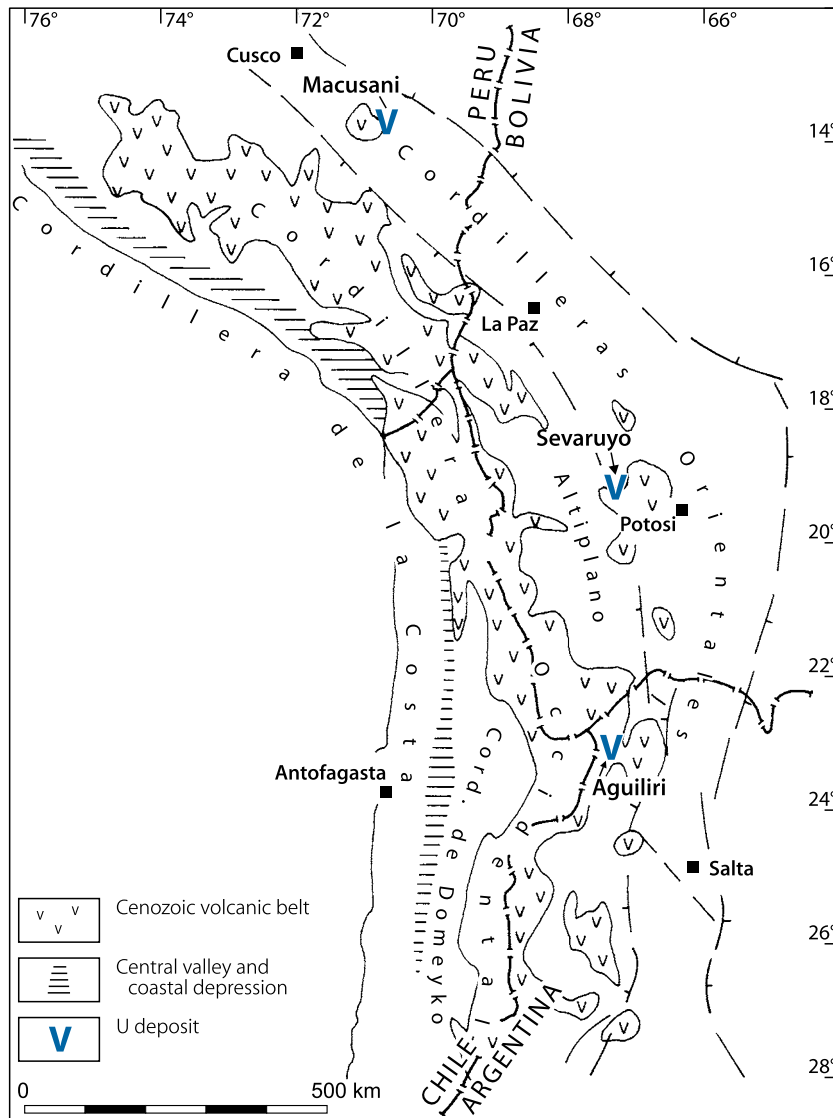
Principal Host Rock Alteration

Each of the three types of uranium occurrences in the Sevaruyo district, described further below, exhibits a characteristic assemblage of host rock alterations (Leroy et al. 1985). (a) Structurally controlled (hydrothermal) mineralization within units P1, P2a, and P2b is associated with kaolinitization of alkaline feldspars, plagioclase, and biotite; and formation of traces of illite, vermiculite, interlayered illite-vermiculite minerals, montmorillonite, and halloysite. Silicification occurs locally. Na, K, Ca, Mg, Li, and Rb were depleted during kaolinitization, whereas V and Mo were enriched. (b) Stratiform mineralization (*Tholapalca III*) is associated with Ca montmorillonite and some chlorite. (c) Mineralization of supposedly hot spring origin within red beds (*Amistad*) is associated with illite, vermiculite, and interlayered illite-vermiculite minerals, whereas kaolinite is absent in the altered tuff. Ba, V, and Li are commonly enriched.

Principal Characteristics of Mineralization

Three types of uranium mineralization occur in the Sevaruyo district:

Fig. 3.1. Central Andes. Distribution of the Cenozoic volcanic belt and location of principal uranium occurrences. (After Stipanovic et al. 1985)



1. **Structurally controlled (hydrothermal) mineralization** represents the most prominent type of uranium concentration. It occurs in heavily fractured and brecciated, kaolinized tuff and ignimbrite of the basal units P1 (at *Cotaje, Huancarani*), P2a (at *Los Diques, Tholapalca II*), and P2b (at *Torko, San Agustin*) of the Los Frailes Formation. Uranium minerals are pitchblende, coffinite, and U^{6+} minerals. Dimensions of mineralization are commonly 10–60 m, rarely some 100 m long, 0.1–10 m wide, and from surface to about 30 m deep. Grades average 0.04–0.06% U, but may exceptionally be as high as 2% U.

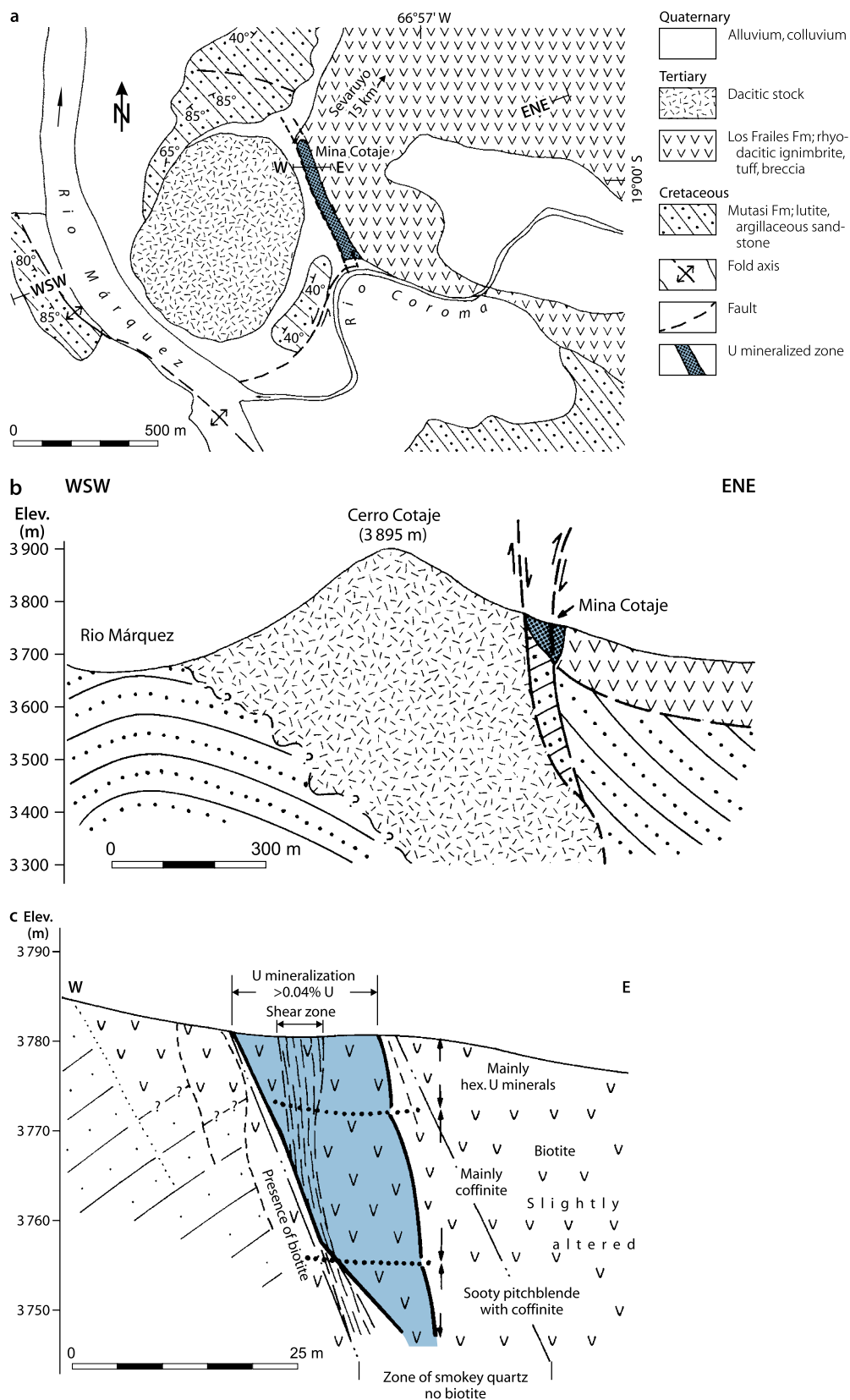
Mina Cotaje. is the best-explored example of structurally controlled (hydrothermal) mineralization (▶ Fig. 3.2). Uranium is emplaced in a subvertical, NW–SE-trending fault zone in which it extends for about 350 m in length, from 1 to 10 m in width, and some 30 m in depth pinching out downwards. Host rocks are heavily fractured and sheared, strongly bleached tuff breccias

and underlying ignimbrite of rhyo-dacitic composition. Biotite disappears in the ore zone, whereas Fe oxides and smoky quartz develop. The mineralized zone occurs in close vicinity to the tectonic contact of the Los Frailes pyroclastics with Cretaceous lutite intruded by a dacitic stock that forms the Cerro Cotaje. Fractures and mineralization cut indiscriminately through both tuff and ignimbrite.

Uranium minerals are pitchblende, coffinite, and uranyl phosphates. The latter prevail from surface to 8 m deep and are associated with siderite and gypsum. From 8 to 30 m deep, coffinite associated with baryte and gypsum is dominant. Below 30 m, pitchblende appears in addition to coffinite associated with baryte and very minor marcasite, pyrite, sphalerite, galena, and melnicovite. Uranium and associated minerals are irregularly distributed in open fractures where they occur in narrow stringers. In zones of intense shearing, uranium minerals are disseminated throughout the commonly oxidized broken rock. The mineralization exhibits a strong radiometric disequilibrium.

Fig. 3.2.

Bolivia, Mina Cotaje, (a) generalized geological map displaying the position of the uranium mineralized zone. (b) WSW–ENE section showing the lithologic-structural setting of the uranium occurrence. (c) W–E section with details of U mineral distribution/zoning and host rock alteration. (After Aparicio 1981)



Gases of arsenic-sulfur mixed with CO and CO₂ occur in appreciable quantities at deeper mine levels (ca. 40 m below surface) (Michel and Schneider 1978).

2. **Sedimentary controlled (stratiform) mineralization** represented by *Tholapalca III* is hosted by unconsolidated, fine-grained detrital material of altered tuff that fills small paleochannels at the base of fresh tuff layers. Disseminated mineralization is discontinuous and occurs in lenses up to a few hundred meters long, 2 m thick, and 26 m deep. Uranium is fixed in sparse uranyl phosphates and apparently in apatite, which is as abundant as smoky quartz in the host rock. Average grade is low (<0.1% U), although local enrichments may be as much as 0.8% U.
3. **Hot springs (?) related mineralization** in redbeds (*Mina Amistad*, a former copper mine) occurs in continental, highly permeable, medium-grained sandstone of the Tertiary Chamarra Formation. The strata strike N-S and dip 30–40° W. Uranium occurs as uranyl phosphates associated with copper carbonates (malachite, azurite), sulfides (bornite, pyrite, pyrrhotite), and abundant Fe and Mn oxides, calcite, and aragonite. Peneconcordant mineralization occurs in three superjacent beds within a vertical interval that ranges from 4 to 6 m and extends for about 100 m laterally. Reported grades are 0.2% U.

Metallogenetic Concepts

Metallogenetic hypotheses on the formation of *Mina Cotaje* as well as on other structurally controlled uranium concentrations

are still controversial. They range from hypogene to supergene and may involve magmatic hydrothermal solutions of medium or low temperature, or meteoric waters to leach uranium from uraniumiferous pyroclastics and redeposit it at favorable sites. For example, redbed-hosted mineralization (e.g., *Mina Amistad*) is thought to have been formed in a near surface environment, possibly by hot springs. Based on the mineral paragenesis, the mixing of two fluids is postulated to have caused the mineral deposition; an ascending sulfuric fluid enriched in Cu, Fe, etc., which encountered solutions enriched in bicarbonate derived from alteration of the Los Frailes volcanics.

Michel (1980, personal communication) undertook an extensive geochemical and mineralogical research program to study the U and Th distribution within the Los Frailes Formation. His findings show practically constant U/Th ratios indicating no differential uranium loss within the Los Frailes volcanics. Based on these data and the common spatial relationship of all notable uranium occurrences with subvolcanic dacitic stocks, Michel favors a hypogene mesothermal origin of the Cotaje deposit with a strong supergene overprint.

Selected References and Further Reading for Chapter 3 Bolivia

For details of literature see Bibliography.

Aparicio 1981; Leroy et al. 1985; Leroy and Müller-Kahle 1985; Michel and Schneider 1978; OECD-NEA/IAEA 1979; Pardo-Leyton 1981, 1985; Pardo-Leyton and Barron 1984; Santivañez 1977; Michel (1980, personal communication).

Chapter 4 Brazil

Prominent uranium deposits are known within five regions in Brazil (principal deposits in brackets): *Lagoa Real*, Bahia state (Cachoeira); *Central Ceará*, Ceará (Itataia); *Poços de Caldas*, Minas Gerais (Agostinho and Cercado); *Serido*, Paraíba (Espinharas); and *Southeastern Paraná Basin*, Paraná (Figueira) (Fig. 4.1).

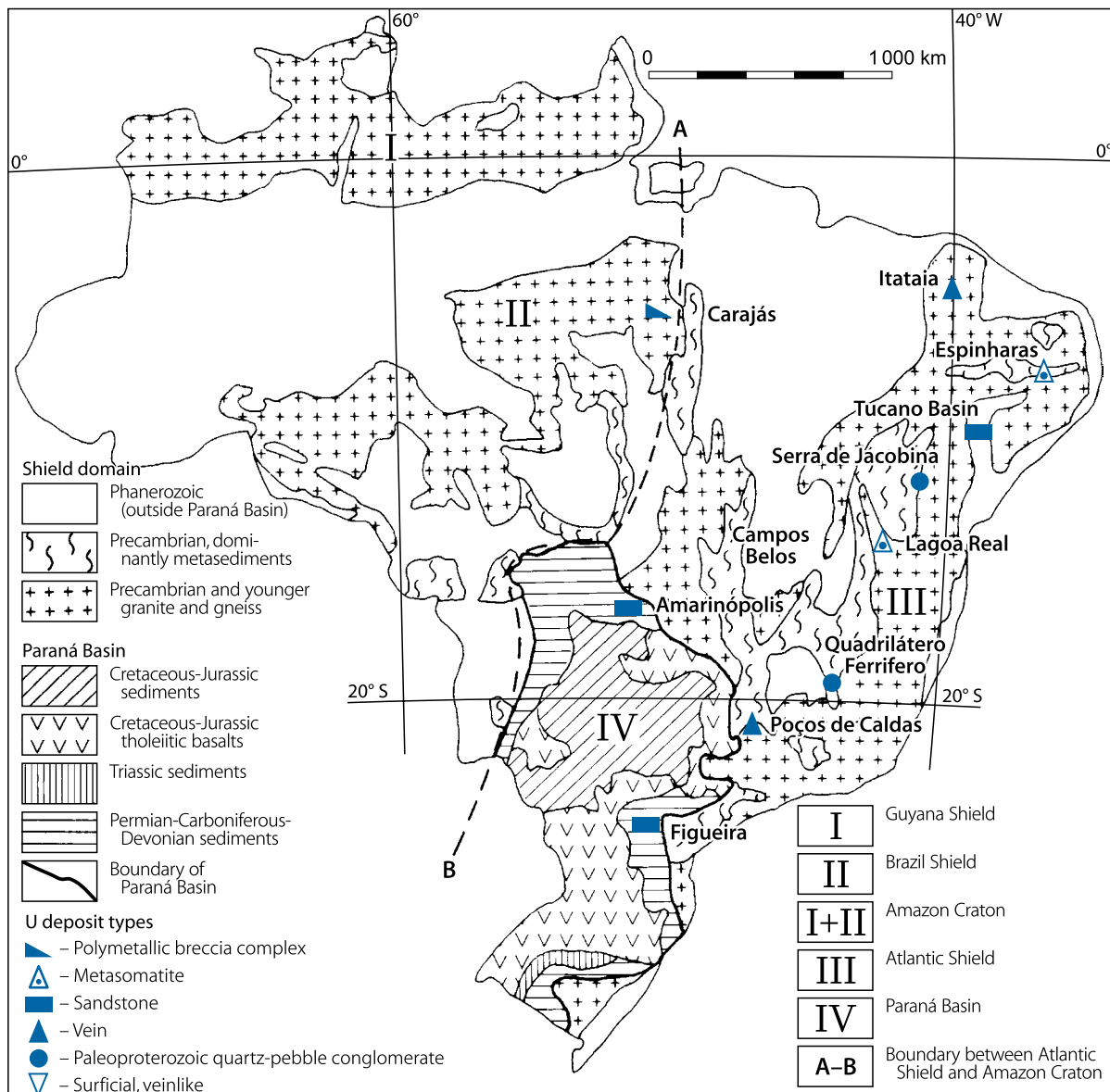
Other regions/districts with small or low-grade uranium occurrences include *Quadrilátero Ferrífero*, Minas Gerais state;

Serra de Jacobina, Bahia; *Rio Preto-Campos Belos*, Goiás; *Northern Paraná Basin* (Amarinópolis area), Goiás; and *Tucano Basin*, Bahia.

The *Cachoeira and Espinharas* deposits are classified as metasomatite (albitite) type with disseminated U mineralization, while *Itataia* is a vein-type deposit with uraniferous phosphate mineralization. These and similar deposits occur within Archean-Paleoproterozoic metamorphic rocks of the São Francisco Craton/Atlantic Shield that were intruded by leucogranites and/or affected by Na metasomatism during the Meso- and/or Neoproterozoic period. Deposits within the *Poços de Caldas* alkaline complex (*Agostinho* and *Cercado*) may be attributed to a (modified) volcanic type. Occurrences in the *Paraná Basin* are largely of sandstone type emplaced in Permian (*Figueira*) and

Fig. 4.1.

Brazil, generalized geological map with location of principal uranium regions/deposits (type attribution of deposits is tentatively). (After d'Elboux 1984; Forman and Waring 1981)



Devonian strata (*Amorinópolis*). Similar mineralization occurs in the Tucano Basin within Cretaceous clastics. Occurrences in the *Rio Preto-Campos Belos* region are hosted in Proterozoic metamorphic rocks and are possibly of unconformity type. Occurrences in the *Quadrilátero Ferrífero* and *Serra de Jacobina* correspond to the oligomictic paleoconglomerate type.

According to Barretto (1988), more than 90% of Brazil's RAR and EAR uranium resources occur in mobile belts within Archean to Mesoproterozoic terrane. These belts are derived by polycyclic metamorphism at the periphery of an older cratonic nucleus and are generally related to deep zones of crustal discontinuity (lineaments, thrusts).

Uranium mineralization associated with sodium metasomatic processes seems to be a more widely distributed phenomenon than originally thought, as regards the Brazilian Platform. Such associations are known to exist not only in the known districts discussed later, but also in central Brazil (*Alecrim*, *Paiol*, and *Bonito* in Goiás state).

Uranium production in Brazil prior to 1999 totals 1,030 t U. It was derived solely from the former production center at Poços de Caldas (OECD-NEA/IAEA 1999). Presently (status 2007), uranium mining is restricted to *Cachoeira* in the Lagoa Real district, which commenced in 2000. *Itataia* was planned to go into production in 2007.

OECD-NEA & IAEA (2007) reports remaining recoverable resources of 278,400 t U in the identified resources (RAR + Inferred) < US\$ 130/kg U category and total production of 2,068 t U (status January 1, 2007).

Sources of Information. See subsequent individual sections.

Historical Review

Systematic exploration for uranium began in 1952. The first discoveries were at Poços de Caldas (Minas Gerais state) and at Serra de Jacobina (Bahia). The Osamu Utsumi deposit in the Poços de Caldas plateau was discovered in 1974/75, Itataia (Ceará) in 1976, and Lagoa Real (Bahia) in 1977. Discoveries in the late 1970s also include Figueira and Amorinópolis in the Paraná Basin, Rio Preto–Campos Belos (Goiás), Espinharas/Serido district (Paraíba), and the Quadrilátero Ferrífero (Minas Gerais). Uranium exploration in Brazil was reduced in 1984 and discontinued in 1991; consequently, the investigation of many of the discoveries was only rudimentary.

Brazil's first uranium mine was the Osami Utsumi open pit operation, which discontinuously worked on the Cercado deposit at Poços de Caldas from 1982 to 1990 and from 1992 to 1995 when it was finally shut down. Uranium exploitation was recently revived in Brazil in the Lagoa Real district in 2000.

4.1 Caetité Massif Region, Lagoa Real District

Uranium was discovered approximately 20 km NE of the town of Caetité in the Polígono das Secas (Polygon of Droughts) area in

1977. This area is located in the Caetité Massif, in central-south Bahia state. Lagoa Real and Lagoa Grande are smaller towns in the region (Figs. 4.1, 4.2).

Ten deposits (with grades > 0.1% U) and more than 20 uranium occurrences of metasomatite type have been identified in the Lagoa Real district to date. Their original in situ resource totals 85,000 t U at grades averaging 0.15% U (INB 2000). These deposits and occurrences, and likewise most of the airborne and airborne uranium anomalies, occur in the eastern part of the Espinhaço belt, parallel to a regional, N-S-trending thrust fault that can be traced for some 600 km. By contrast, the western part of the Espinhaço belt tends to be poor in uranium as reflected by the hitherto negative exploration results.

The uranium deposits considered as economic by NUCLEBRAS S.A. were named “anomalies” and ascendingly numbered (Fig. 4.2). Anomaly 8 corresponds to the *Quebradas* and Anomaly 13 to the *Cachoeira* deposit. *Cachoeira* contains 17,000 t U, about 5,000 t of which can be recovered by open pit and the remainder by underground means. *Engenho* is another deposit considered for mining.

Mining by open pit methods (to depth of 140 m) associated with heap leaching started at *Cachoeira* in 2000, with a nominal capacity of 250 t U/year. Ore is extracted from an ore body averaging 0.26% U (INB 2000). *Indústrias Nucleares do Brasil* (INB) is the operator.

Sources of Information. Amaral 1984; Ayres 1981; Barretto 1988; Brito et al. 1984; Brito Neves et al. 1979; Caby and Arthaud 1987; Cordani et al. 1992; d'Elboux 1984; de Matos CE 2005; de Miranda Filho and Cabaleiro Rodrigues 2003; Departamento Nacional de Produção Mineral/CPRM 1980, 1981; Forman and Waring 1981; Fuzikawa 1980, 1982; Fuzikawa et al. 1990; Geisel et al. 1980; Haddad and Leonardos jr 1980; INB 2000; Inda and Barbosa 1978; Jardim de Sá et al. 1976; Lobato and Fyfe 1990; Lobato et al. 1982; Maruéjol et al. 1987; OECD-NEA/IAEA 1986, 1997, 1999, 2007; Oliveira et al. 1985; Pascholati et al. 2003; Raposo and Matos 1982; Raposo et al. 1984; Rocha 1992; Santos and Brito Neves 1984; Schobbenhaus and Campos 1984; Stein et al. 1980; Surcan Santos 1984; Turpin et al. 1988; Villaça and Hashizume 1982. Barretto (1988) and Lobato et al. (1982) provided the prime source for the subsequent description amended by data from the other authors listed.

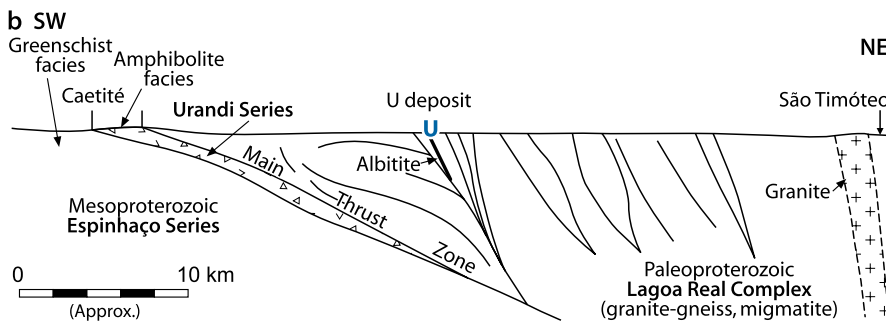
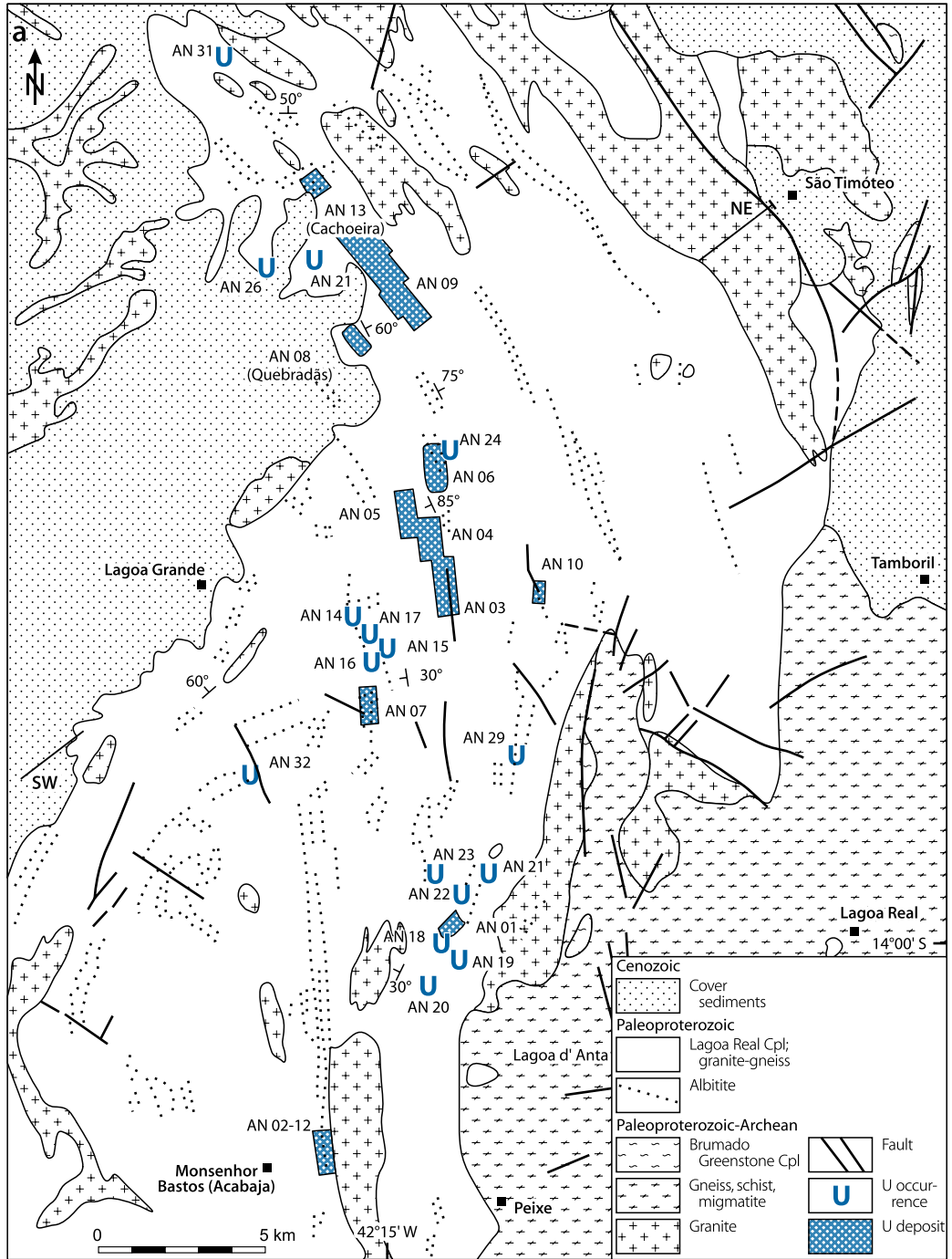
Regional Geological Setting of Mineralization

The uranium-hosting Caetité Massif is in the south-central São Francisco Craton. Superimposed tectonic events by the Gurié-Jequié (~3.0 Ga), Transamazonian (2.2–1.8 Ga), Espinhaço (1.8–1.1 Ga), and Brazilian (650–450 Ma) orogenies imposed a complex structural pattern on this part of the São Francisco Craton (Barretto 1988) (note: other authors, e.g. Turpin et al. 1988, give age frames for these events somewhat different to those listed here).

The Caetité Massif is part of the Espinhaço uranium province corresponding to a NNW-SSE-elongated zone of reactivation, about 80 km in N-S length and 30 to 50 km wide, and

Fig. 4.2.

Lagoa Real district, (a) generalized geological map with location of uranium deposits and major occurrences; (b) schematic geological section across the central part of the São Francisco craton. (After Turpin et al. 1988 based on Costa et al. 1983 and Raposo et al. 1984)



referred to as the Espinhaço Setentrional Belt (Inda and Barbosa 1978). This belt was evolved by Mesoproterozoic orogenic events within a Transamazonian overprinted Archean basement. Basement rocks are predominantly undifferentiated migmatites. The region was subjected to folding, reverse faulting, and low-grade metamorphism during the Espinhaço tectono-metamorphic event.

Submeridional faults limit the fold belt to the east and west. It is bordered to the south by the Ribera (or Araçuaí) fold belt of Brazilian age and submerges under Cenozoic cover in the north. Migmatite, gneiss, schist, amphibolite, itabirite, gondite, and marble of Archean to Paleoproterozoic age border the Espinhaço belt to the east and south. Metasediments and felsic metavolcanics of the Archean to Mesoproterozoic Chapada-Diamantina Supergroup occur to the NE, whereas Archean migmatite and Mesoproterozoic metasediments (phyllite, quartzite, metaconglomerate) and rhyolitic metavolcanics of the Espinhaço Supergroup constitute the western frame (Fig. 4.2a, b).

Lithologies of the Espinhaço fold belt include polymetamorphic microcline-gneiss, amphibolite, granite, granodiorite, and syenite of the Lagoa Real Complex. Younger rocks of Mesoproterozoic platform regimes occur in the eastern part of the Espinhaço belt. Jardim de Sá et al. (1976) have distinguished three lithostratigraphic stages. Oldest is the Rio dos Remédios Group (1,770 Ma) composed of predominantly peralkaline and potassic volcanic and pyroclastic complexes (including aphanitic quartz porphyry, quartz keratophyre). The intermediate stage consists of terrigenous sediments including transgressive shallow marine and fluvio-deltaic sequences represented by fine- to

medium-grained phyllite, quartzite, and sericitic quartzite. The principal period of folding and metamorphism of these rocks took place about 1,250 Ma ago. The last stage derived by anorogenic events such as the effusion of fissure basalts 1.2 to 1.0 Ga ago.

The structural pattern of the Espinhaço belt displays a distinct regional, NNW-SSE-oriented lineation with lineaments that can be traced for hundreds of kilometers along faults and fold axes. The faults have a compressive character on the craton side, whereas normal faults occur toward the center of the belt. Metamorphic grade increases from north to south.

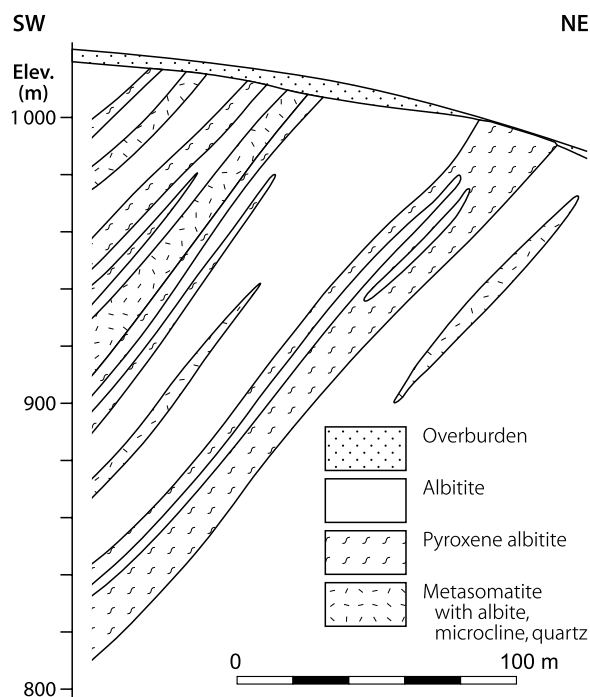
U deposits and occurrences of the Lagoa Real district are confined to a terrane of the litho-stratigraphic Lagoa Real Complex composed of banded gneiss or orthogneiss, and granite such as the Paramirim and São Timóteo plutons, and old, undifferentiated migmatites. Host rocks are believed to be ancient basement material that was successively rejuvenated during: a) the Espinhaço metamorphic phases (1.8–1.1 Ga), and b) tectono-thermal events that affected the entire Espinhaço system at the end of the Precambrian as reflected by a cluster of K-Ar dates around 600–500 Ma (Brito et al. 1984; Raposo et al. 1984).

Turpin et al. (1988) interpret the Lagoa Real granite and related orthogneiss as probable products of calcalkaline magmatism, and that the transformation of this granite to orthogneiss by regional deformation was not accompanied by major geochemical changes except an increase in Rb content resulting from the alteration of amphibole to biotite.

The ore-hosting orthogneiss is an altered, coarse-grained, felsic facies of the Lagoa Real Complex (Fig. 4.3). In unaltered

Fig. 4.3.

Lagoa Real district, Anomaly 3 (AN 03 in Fig. 4.2), generalized geological SW-NE section showing the variably Na-metasomatized facies after felsic orthogneiss of the Lagoa Real Complex. (After Forman and Waring 1981)



state, felsic orthogneiss is of amphibolite-granulite metamorphic facies and is composed of 30 to 40% perthitic microcline, 30 to 40% plagioclase/albite, 30% quartz, hornblende, biotite and accessory magnetite, apatite, zircon, and sphene. Foliation of the felsic orthogneiss essentially parallels the folding. Folds form a N-S-oriented arc. Most faults follow the same regional strike; others trend predominantly NE-SW.

Gravimetric surveys over the São Francisco Craton revealed a NNW-SSE-trending gravimetric anomalous zone that coincides with the Espinhaço reactivated belt and divides the craton into two segments, the Guanambi and the Remanso subcratons (Dept Nac Prod Miner/CPRM 1980). This zone terminates to the north against the Riacho do Pontal and to the south against the Araçuaí mobile belt. The anomalous lineament is interpreted to reflect a structural element of block faulting, with grabens and horsts presumably associated with large vertical crustal movements. A remarkable feature is the position of the Lagoa Real district within the strongest negative Bouguer anomaly of -100 to -120 mgal. This coincidence may suggest a possible relationship between the mineralizing and crustal differentiation processes.

Principal Host Rock Alteration

The principal uranium-hosting felsic orthogneiss of the Lagoa Real Complex has been subjected to metasomatism and alteration. Prominent processes include Na metasomatism and retrograde alteration under epidote-amphibolite facies conditions. Na metasomatism developed along N-S-trending en echelon zones, where it generated elongated, tabular Na-metasomatite bodies that are over 1,000 m long, 100 m wide, and that persist down dip for over 350 m. These bodies consist of coarse-grained, felsic orthogneiss protolith transformed into rocks ranging from albite-bearing, microcline-rich felsic orthogneiss to true albitite (Fig. 4.3). Albitite has an albite component in excess of 70%.

Turpin et al. (1988) have described two albitite types: (type 1) quartz albitite characterized by the replacement of both K feldspar and plagioclase by albite (An 5–1), and (type 2) pyroxene-garnet albitite characterized by quartz depletion and crystallization of albite, clino-pyroxene (salite to hedenbergite), and garnet (andradite).

Orthogneiss and albitite exhibit pronounced shearing and foliation. Biotite and amphibole show mineral stretching lineations. Original textures have survived during metasomatic and metamorphic events as reflected by augen gneiss or albitite after porphyritic granite. The metamorphic fabric dissects the primary lithologic layering of albitite commonly at a low angle, and thus clearly postdates the albitic alteration (Caby and Arthaud pers. commun. in Turpin et al. 1988). Polygonal granular textures as a result of intense recrystallization suggest a high-temperature stage after the deformation event.

Lobato et al. (1982) note the following mineralogical and geochemical changes involved in the metasomatic (albitization), retrograde (epidote-amphibolite facies), and mineralization processes: replacement of potassic feldspar by albite-oligoclase (oligoclase is dominant but some high-grade uranium

facies contain essentially pure albite); ferrohastingsite replaces hornblende; hornblende and biotite alter and give place to acmite; removal of quartz; formation of magnetite and aegirine-augite; oxidation of magnetite to hematite in a late stage; and crystallization of calcite, epidote, and chlorite as the latest phases.

Chemical variations include increase in Na_2O and Al_2O_3 ; decrease in K_2O , SiO_2 , Rb, Ba, and Y (loss of K_2O and gain of Na_2O are almost balanced; SiO_2 loss is about 10%); variable gains or losses of Fe_2O_3 , CaO, TiO_2 , Sr, Zr, and Th; and partial oxidation as indicated by hematitization of magnetite and acmite formation after hornblende and biotite.

According to Turpin et al. (1988), albitite resulted from post-magmatic sodic alteration. Type 1 albitite derived by sodium metasomatism due to a cation exchange between feldspars and a Na-bearing fluid, K and Ba loss, and increasing Na content as Ca leaching progresses while Si remained constant. Type 2 albitite evolved by Si, K, and Rb depletion (quartz and biotite alteration) and Sr, Na, and Ca enrichment (albite, pyroxene, garnet, carbonate crystallization), which led to very low Rb/Sr ratios. These two alteration patterns can be interpreted in terms of metasomatic zoning or successive metasomatic processes. Uranium mineralization is restricted to type 2, whereas Th contents are identical in both types.

Principal Characteristics of Mineralization

Uraninite is the principal uranium mineral. Pitchblende is rare. U^{6+} minerals, predominantly β -uranophane, coat fractures near the surface.

Uranium mineralization is confined to albitite, but not all albitites are mineralized. Turpin et al. (1988) note that uraninite mineralization is predominantly hosted in pyroxene-garnet albitite (type 2) in which uraninite occurs as small patches associated with allanite, sphene, zircon, and mafic minerals, or as small crystals (1 to 5 μm) disseminated in the albitic matrix. Brazilian authors refer to mineralized albitite as “linear albitite” on account of its mineral texture and tabular or lenticular configuration, which equals that of the parent gneiss. Lobato et al. (1982) provide the following mineral composition for albitites of the *Cachoeira* deposit (= anomaly 13): about 70% albite, 0–25% aegirine-augite, 0–25% ferrohastingsite, 0–20% andradite, 0–10% calcite, 0–5% biotite, 0–3% microcline (commonly interstitial to albite and grading into plagioclase), 0–3% epidote, 0–5% magnetite, 0–2% sphene, and 0–2% uraninite. Accessory minerals include quartz, apatite, chlorite, prehnite, zircon, fluorite, hematite, allanite, and minor pyrite and chalcopyrite.

As indicated above, the best host rock is a medium- to coarse-grained, impure pyroxene-albitite that typically contains bands of mafic and opaque minerals such as aegirine-augite, amphibole, biotite, epidote, garnet, and magnetite. Magnetite is partially transformed into hematite. Uraninite occurs as fine grains restricted to and dispersed in bands of mafic and opaque minerals. The highest uranium grades are associated with albitite facies containing 9–11% Na_2O , in excess of 4% Fe_2O_3 , and 55–60% SiO_2 (Raposo et al. 1984). Pure albitite, sheared albitite,

and albitized gneiss with 30 to 90% modal plagioclase are poor to barren in uranium (less than 0.1% U).

General Shape and Dimensions of Deposits

Mineralized albitites occur in a N-S-oriented belt, some 30 km long and 10 km wide. Deposits consist of a variable number of mineralized, foliated, elongated tabular bodies that are arranged in echelon parallel to the regional N-S-trending foliation. Ore lenses dip 30°–40° W in the south part of the district, but steepen vertically in the central section and turn eastward in the north.

Individual ore lenses are 50 m to 1,200 m long and some centimeters to 40 m wide (average 6 m). Ore lenses in any single deposit aggregate to a cumulative thickness of 20 to 100 m. The drill-intercepted depth extension of mineralization is at least 750 m. Barren or low-grade mineralized rock intervenes between ore lenses.

Grades of ore bodies commonly range from 0.1 to 0.3% but can locally be as high as 3% U. The average grade is about 0.15% U at a cutoff grade of 250 ppm U. Thorium tenor is on the order of 0.01% Th.

Stable Isotopes and Fluid Inclusions

Oxygen isotope systematics and fluid inclusion studies evaluating mineral paragenesis and its modifications suggest the following physico-chemical conditions during the alteration and mineralization stages (Lobato et al. 1982):

- Pyroxenes are dominated by acmite and diopside components, which indicate a formation under moderate pressure
- Retrograde formation of oligoclase-albite-epidote-amphibole reflects the conditions of the epidote-amphibolite facies and suggests a low to moderate pressure of 1–4 kbar (3–12 km depth) and a high temperature of 500–600°C
- Oxygen isotope and fluid inclusion data indicate isotopically-light mineralizing fluids undersaturated in salts and a temperature of 500°C
- Volume decreased by about 10% in course of alteration processes.

Regional Geochronology

Barretto (1988) provides the following ages and chronostratigraphic sequence of the Espinhaço belt and its surroundings: Archean migmatites: up to 2,800 Ma; Paleoproterozoic volcano-sedimentary sequences: 2,200 Ma; Mesoproterozoic granitoids: 1,700 Ma, coarse-grained gneisses (which developed into albitites): about 1,400 Ma, quartzites and phyllites: 1,200 Ma; effusion of fissure basalts and other anorogenic events: 1,200 to 1,000 Ma.

An age of ca. 1.3–1.0 Ga is reported by Jardim de Sá et al. (1976) for the thrusting episode of granites over sediments of

the Espinhaço Supergroup, which generated inverse metamorphic isograds.

Turpin et al. (1988) give the ages of 1,725 Ma (U/Pb of zircon) for granitic protolith, $1,366 \pm 31$ Ma for metamorphism, and 1,400 Ma for a hydrothermal event that caused U mineralization in the Lagoa Real district. At 480 Ma the ore-hosting complex was thrust over the Espinhaço belt.

Stein et al. (1980) and Raposo & Matos (1982) report a U/Pb uraninite age of 820 Ma.

Potential Sources of Uranium

No precise uranium source has been identified to date. Regional airborne and carborne surveys have yielded a dense cluster of anomalies within the uranium region, however, which may indicate that the Archean-Proterozoic rocks may constitute a viable uranium source. This contention may be supported by petrochemical analyses by Raposo et al. (1984), which give anomalous uranium tenors of up to 12 ppm U in quartz-feldspar rocks and as much as 90 ppm U in unmineralized albitized rocks. It remains unclear, however, whether these values represent original uranium tenors or introduced uranium. An alternative uranium source may be hypothesized from the fact that gravimetric surveys indicate large vertical crustal movements along the Espinhaço mobile belt that permitted a uranium derivation from crustal differentiation or lateral secretion processes. This concept may be supported by the above mentioned airborne and carborne uranium anomalies since most of which occur parallel to a regional, N-S-trending thrust fault that can be traced for some 600 km.

Principal Ore Controls and Recognition Criteria

Deposits of the Lagoa Real district may be classified as structurally controlled metasomatite-type deposits composed of linear albitite with disseminated uraninite mineralization. Principal ore-controlling or recognition criteria include

Host environment

- A polymetamorphic mobile belt of Archean-Proterozoic origin, last affected by the Brazilian Orogeny
- Intense Na metasomatism along regional structural elements paralleling fold axes and major faults
- Coincidence of the position of the Lagoa Real district with a marked negative gravimetric anomaly.

Mineralization

- Monometallic ore composition
- Principal uranium mineral is fine-grained uraninite
- Preferential host rock is linear, impure albitite containing bands of mafic and opaque minerals
- Restriction of uraninite to and dispersed in mafic mineral bands
- U contents correlate with Na contents
- Highest U grades associate with albitite facies containing ca. 10% Na₂O, < 4% Fe₂O₃, and 55–60% SiO₂

- Deposits consist of elongated tabular bodies of disseminated mineralization partly with relative high grades
- Ore lenses are arranged en echelon parallel to the regional foliation
- Barren or low-grade mineralized rock intervenes between ore lenses
- Mineralization persists to great depth (> 750 m)
- U deposits and anomalies cluster, parallel to a regional thrust fault, in the eastern part of the Espinhaço belt
- Deposits occur near or within large areas of basement enriched in uranium as can be deduced from clusters of airborne radiometric anomalies.

Metallogenic Concepts

Various models have been forwarded to explain the evolution of the Espinhaço fold belt, Na metasomatism, host rock modifications, and associated uranium mineralization.

Gravimetric surveys (Dept Nac Prod Miner/CPRM 1980) registered a NNW-SSE-trending gravimetric anomalous zone that coincides with the Espinhaço reactivated belt, which may reflect block faulting associated with large vertical crustal movements. The location of the Lagoa Real district within the strongest negative Bouguer anomaly of this anomalous zone may indicate a possible relationship between the metasomatic, mineralizing, and crustal differentiation processes.

Brito Neves et al. (1979) and other workers suggest that the Espinhaço fold system developed through a rifting and aulacogenic-type evolution in an intracratonic environment without major accretion of primary material. Barretto (1988) reports that petrographic work by Prates & Fuzikawa indicates moderate pressures of 4 kbar and a relatively low temperature of 500–600°C for the processes involved in Na metasomatism. Lobato et al. (1982) postulate that oxygen isotope systematics and fluid inclusion data suggest a uranium precipitation from fluids characterized by isotopically-light oxygen and undersaturation in salts, at temperatures near 500°C. Pressure, estimated at 1–4 kbar, was low to moderate, as indicated by retrograde metamorphic epidote-amphibolite facies. The processes involved in alteration and mineralization decreased the rock volume and resulted in limited oxidation. A best fitting mechanism, which (1) is compatible with the presented data and (2) explains the metamorphic/metasomatic and ore-forming processes, would include, as suggested by Lobato et al. (1982), thrusting of basement over fluid-loaded Proterozoic sediments from where, in consequence, salty pore fluids were driven up into the overriding complex by processes governed by an inverted thermal gradient.

Although geochronological evidence is scarce, it seems that at least part of the mineralization had occurred 820 Ma ago, which would mean that this uranium generation took place long after albitization that is thought to have provided the favorable textural and geochemical environment for the uranium accumulation (Barretto 1988).

Turpin et al. (1988) exclude any models involving late magmatic or Brazilian thrusting-related U deposition in the Lagoa Real district. Based on their isotope studies and

identification of a uraninite generation distinctly older than the formerly reported (820 Ma), they state that a hydrothermal event caused U mineralization ca. 1,400 Ma ago. The closest magmatic event is reflected by 1,725 Ma old granite that represents the protolith of orthogneiss at Lagoa Real. This 325 Ma gap after granite emplacement excludes a magmatic origin of the U mineralization. On the other hand, the time of mineralization coincides with a calculated age of $1,366 \pm 31$ Ma, which is thought to indicate a stage of metamorphism. It remains unclear, however, whether the metamorphic, metasomatism/alteration, and mineralizing processes were linked or not.

The age of ca. 480 Ma for overthrusting and late reworking can be correlated with the data from southeastern Brazil as well as from the Damara Province in southern Africa, where ca. 450 Ma mineral ages are common. Therefore this correlation may suggest an event of continental collision.

Turpin et al. (1988) apparently consider the 1,725 Ma old granite a potential uranium source. In support of this assumption, they argue that (a) the enclosing granite tends to be the main Nd provider to the albitites, (b) if a closed-system origin can be accepted for Nd and thus for REE, it may be extended to uranium, (c) U-rich accessory minerals of subalkaline granites represent likely sources of mobile uranium when sufficiently metamict as documented by Pagel (1981) for granites in France, and (d) a meteoric water influx may be deduced from oxygen and carbon isotope studies of fluids in altered rocks by Lobato et al. (1983) and Fuzikawa & Alvez (1984).

With respect to the age of 820 Ma reported for uranium mineralization (Stein et al. 1980), Turpin et al. (1988) note that this age is not substantiated by analytical data.

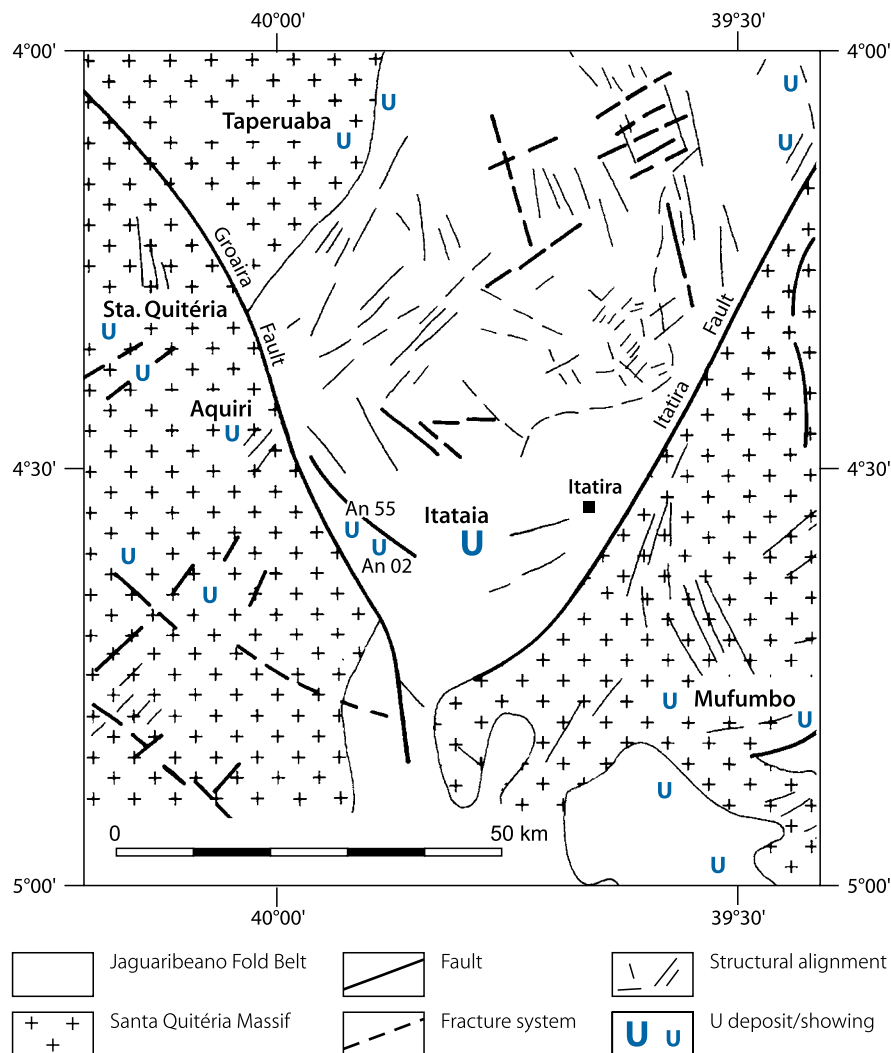
4.2 Central Ceará Region, Itataia/Santa Quitéria Deposit

The Central Ceará region is located in northeastern Brazil in the state of Ceará (Fig. 4.1). More than a dozen uranium-phosphate occurrences have been discovered including *Itataia*, also known as *Santa Quitéria*, the largest uranium deposit known in Brazil. Itataia was discovered in 1976 about 170 km SW of the coast town of Fortalaza and 50 km SE of Santa Quitéria (Fig. 4.4). Smaller satellite deposits, *Alcantil* and *Serrotos Beixos*, occur some 500 m and more to the W and NW of the main deposit. Itataia and the two satellite deposits contain cumulatively 77,000 t U RAR and 43,000 t U EAR-I. Phosphate resources exceed 14.5 mio t P_2O_5 (OECD-NEA/IAEA 1986).

According to OECD-NEA/IAEA (2007), Itataia/Santa Quitéria has reserves of 76,100 t U at an average grade of 0.08% U and is suitable for open pit mining, with a uranium recovery rate from the phosphatic material estimated at 52.5%. Start-up was planned for 2007 with a nominal production capacity of 680 t U/year. Earlier production plans considered a capacity of 964,000 t ore per year with a mining grade of 1,174 ppm U, 17% P_2O_5 , and 140 ppm TbO_2 to yield annually almost 600 t U and 150,000 t phosphoric acid (Saad 2000).

Other uranium occurrences in the area (*Aquiri*, *Mufumbo*, *Taparuaba*) are associated with feldspathic episyenite, and are

Fig. 4.4. Central Ceará region, generalized geological map with location of the Itataia/Santa Quitéria deposit and other uranium occurrences. (After Forman and Angeiras 1981; d'Elboux 1984)



considered comparable with the Espinharas deposit located about 500 km SE of Itataia in a similar geologic environment (see Seridó Region).

Sources of Information. Angeiras et al. 1981; Ayres 1981; d'Elboux 1984; Forman and Angeiras 1981; OECD-NEA/IAEA 1986, 1999, 2007; Netto et al. 1991; Saad et al. 1984, unless otherwise cited.

Regional Geological Setting of Mineralization

Two geotectonic entities of the Precambrian Atlantic Shield dominate the Central Ceará mineral province, the Archean Santa Quitéria-Tamboril Complex, and the Paleoproterozoic Jaguaribeana Fold Belt. At least four orogenic/metamorphic events have affected the region approximately 2,500 Ma, 2,000 Ma, 1,300 Ma, and 600 Ma ago (Wernick et al. 1979).

The *Santa Quitéria-Tamboril Complex* consists of granitic gneiss domes derived from strongly migmatitized and granitized sedimentary, volcanic, and plutonic rocks. The *Jaguaribeana Fold Belt* is composed of metasediments, which originated essentially from transgressive sandstones, arkoses, limestones, and some marls. The metasediments are intensely folded and regionally metamorphosed to amphibolite facies grade, probably first during the Transamazonian Orogeny (~2,000 Ma ago) but definitely during the Brazilian Orogeny (650–470 Ma). Resulting rocks include gneiss, feldspar-quartz rock (metaarkose), quartzite, schist, amphibolite, calc-silicate, marble, and migmatite. Lithologies of these facies found in the Itataia area are attributed to the Caicó Group of the Ceará Series.

Several generations of late- to post-tectonic granite were emplaced during the Neoproterozoic Brazilian Orogeny (Santos and Mello 1979). Autochthonous, synorogenic katazonal granites (650 Ma old) of supposedly anatectic derivation are typically found in the older complexes. Late orogenic granites (550 Ma old)

are rare in the Itataia region. Post-orogenic granites were intruded along dilational lineaments and boundaries between geostructural units such as the Jaguaribeana Fold Belt and the Santa Quitéria Complex between 510 and 450 Ma ago. These granites are represented by stocks and apophyses with associated pegmatite dikes in the Itataia area. Based on analyses published by Angeiras et al. (1981), the post-orogenic granites may be classified as leucocratic, peraluminous in composition, with alkaline tendency and enriched in U and P (average 26 ppm U, range 10–100 ppm U, U/Th ratio > 0.3; av. 0.76% P₂O₅, range 0.65–1.3% P₂O₅).

Gneiss and carbonate rocks of the Precambrian Caicó Group of the Jaguaribeana Fold Belt constitute the principal country rocks at Itataia. The gneissic unit consists of well-foliated biotite-garnet-sillimanite gneiss and amphibolitic gneiss of upper amphibolite grade facies. Rock constituents are microcline, plagioclase, quartz, biotite, sillimanite, garnet porphyroblasts, and accessory titanite, zircon, and apatite. The carbonate unit includes pure and impure marbles, light grey to brown in color, and greenish calc-silicate rocks. These rocks occur as lenses, as much as 10 km or more in length, intercalated in gneiss. Impure marbles have a planar fabric imposed by a subparallel arrangement of phlogopite, graphite, tremolite, and other minerals. Calc-silicate rocks are mostly associated with marble lenses that range from few centimeters to about 10 m in thickness. Their mineral constituents include quartz, diopside, tremolite, feldspars, biotite, scapolite, and titanite.

Numerous post-orogenic granitic and pegmatitic apophyses and stocks, ranging from few centimeters to some tens of meters in thickness, were intruded into the older sequences.

Three phases of folding have been imposed on the metasediments: F-1 folds are E-W-oriented recumbent folds with S vergence; F-2 folds trend N-S and have a holomorphic geometry and vertical axial planes, and they culminate locally in thrusts or overthrusts; and F-3 folds are about NW-SE-trending periclinal folds, which bend F-1 and F-2 folds (OECD- NEA/IAEA 1986).

Regional, about NNW-SSE (Groaira fault) and NNE-SSW (Itatira fault) -trending structures border the tectonic block of Itataia. Minor faults are frequent within the Itataia block. They strike about NE-SW, NW-SE, and E-W. A medium steep, S-dipping reverse fault of the E-W system controls the Itataia deposit. Post-ore, NNW-SSE-oriented faults dissect the deposit.

Principal Host Rock Alteration

Angeiras et al. (1981) note intense late magmatic-deuteric and retrograde greenschist facies alteration, expressed

- *in granite* (Table 4.1) by quartz removal, albitization (replacement of microcline by perthite, albite halos around oligoclase, late post-apatite, albite crystals), complete chloritization and hematitization of biotite, strong apatitization always forming euhedral apatite crystals with as much as 1,430 ppm U, late quartz crystals, and disappearance of muscovite, leading to a more or less vesicular pinkish rock comparable to feldspar

Table 4.1.

Ceará region, Itataia deposit, modal composition of granites and episyenites (in %) indicating the mineralogical changes due to episyenitization. (After Angeiras et al. 1981)

Minerals \ Rocks	Granites		Episyenites		
	1,213	1,204	126	95	120
Perthite	-	-	35	12	42
Microcline	37	37	5	3	5
Oligoclase	26	32	16	43	5
Albite	2	1	9	6	10
Granitic quartz	26	23	-	-	-
Secondary quartz	-	-	3	1	3
Biotite	5	3	-	-	-
Muscovite	2	2	-	-	-
Chlorite	-	-	-	3	2
Apatite	2	2	2	10	5
Collophane	-	-	16	9	20
Vacuoles	-	-	14	13	8
Total	100	100	100	100	100

episyenite as found in France (see documentation in Uranium Deposits of the World: Europe, Chap. Limousin, in preparation);

- *in gneiss* by chloritization of garnet and biotite, sericitization of microcline and plagioclase, strong albitization, analcime formation, and impregnation by collophane; and
- *in marble* by partial scapolitization, superimposed late albitization, and fluor-apatite crystallization.

Principal Characteristics of Mineralization

Collophane, a cryptocrystalline apatite, is the principal uranium-bearing mineral. Collophane contains about 60 to more than 150 ppm U per 1% P₂O₅ in even distribution. No discrete uranium mineral has been detected to date. Collophane forms an almost monomineralic rock referred to as collophanite. Collophanite is stained brownish-red from iron oxide and consists of approximately 80% collophane, the remainder being calcite, graphite, and ankerite when in marble; and albite, microcline, chlorite, zircon (malacon), and calcite when in episyenite. Table 4.2 provides samples of chemical analyses of collophanite and other U-P-bearing rocks.

General Shape and Dimensions of Deposits

Collophanite occurs as (a) massive lenticular lodes filling large cavities, and as veins and veinlets arranged in a stockwork

Table 4.2.

Ceará district, Itataia deposit, chemical composition of U-P-bearing rocks. (After Angeiras et al. 1981)

	Collophanite I	Collophanite II	Collophanized episyenite	Breccia	Episyenite	Granitic rock
Element No. of samples	2	6	5	2	7	4
SiO ₂	25.80	9.20	47.52	47.50	56.39	73.98
Al ₂ O ₃	8.50	2.11	13.98	12.35	16.73	13.70
CaO	25.60	47.10	13.60	16.30	8.06	1.03
Na ₂ O	2.94	0.27	6.99	6.08	6.07	5.30
K ₂ O	0.50	0.1	0.43	0.38	0.76	1.02
MgO	1.73	0.10	0.66	0.13	0.42	0.46
Fe ₂ O ₃	2.27	1.96	1.39	1.09	3.02	1.06
FeO	1.29	0.31	0.40	0.23	0.41	1.39
MnO	0.20	0.04	0.05	0.07	0.07	0.12
TiO ₂	0.55	0.08	0.28	0.44	0.14	0.24
CO ₂	0.24	0.34	0.74	1.62	0.15	0.11
SO ₂	0.19	n.d.	0.11	n.d.	n.d.	n.d.
P ₂ O ₅	29.35	36.60	12.59	11.65	6.54	0.76
RF	1.33	1.55	1.99	3.15	1.18	0.84
TOTAL	100.49	99.81	100.73	100.99	99.92	100.01
U	0.097	0.147	0.096	0.119	0.065	0.0025
ThO ₂	<0.01	0.020	<0.01	<0.01	<0.01	<0.01

pattern in marble, and to a lesser extent in episyenite; (b) veinlets and disseminations in breccias made up of fragments of marble, calc-silicate, and feldspathic (episyenite) rocks; and (c) disseminations in marble and gneiss as well as fillings of voids and intergranular spaces in episyenite.

The main deposit at *Itataia/Santa Quitéria* (Fig. 4.5) occurs along a major reverse fault, along which marble has been thrust upon gneiss. A wide cataclastic zone has developed along this fault. Mineralization transgresses the tectonic partitioning. The surface expression of the main Itataia body is 800 m long in an E-W direction and 300 m wide. Massive ore of the first two collophanite modes mentioned above prevails from the surface to a depth of 150 m and occurs particularly in marble. It includes veins and veinlets of a millimeter to more than 10 m thickness. The third mode and also some stockwork ore extend as discontinuous, lower grade mineralization to a drill-intersected depth exceeding 300 m.

Massive collophanite ore hosted in marble contains about 0.12 to 0.8% U and 30 to 38% P₂O₅, and has a U/Th ratio in excess of 9.7. Respective values for episyenite-hosted ore are 0.05 to 0.12% U, 7.5 to 12.5% P₂O₅, and a U/Th ratio of > 6.5. For stockwork ore in marble, the values are 0.03 to 0.1% U, 5 to 15% P₂O₅, and a U/Th ratio of > 4.5. Other elements include ThO₂ (162 ppm), Y (300 ppm), La (51 ppm), Sr (3,800 ppm), and

locally high values of Mo, Ag, Zn, and Pb in marbles (Forman and Angeiras 1981).

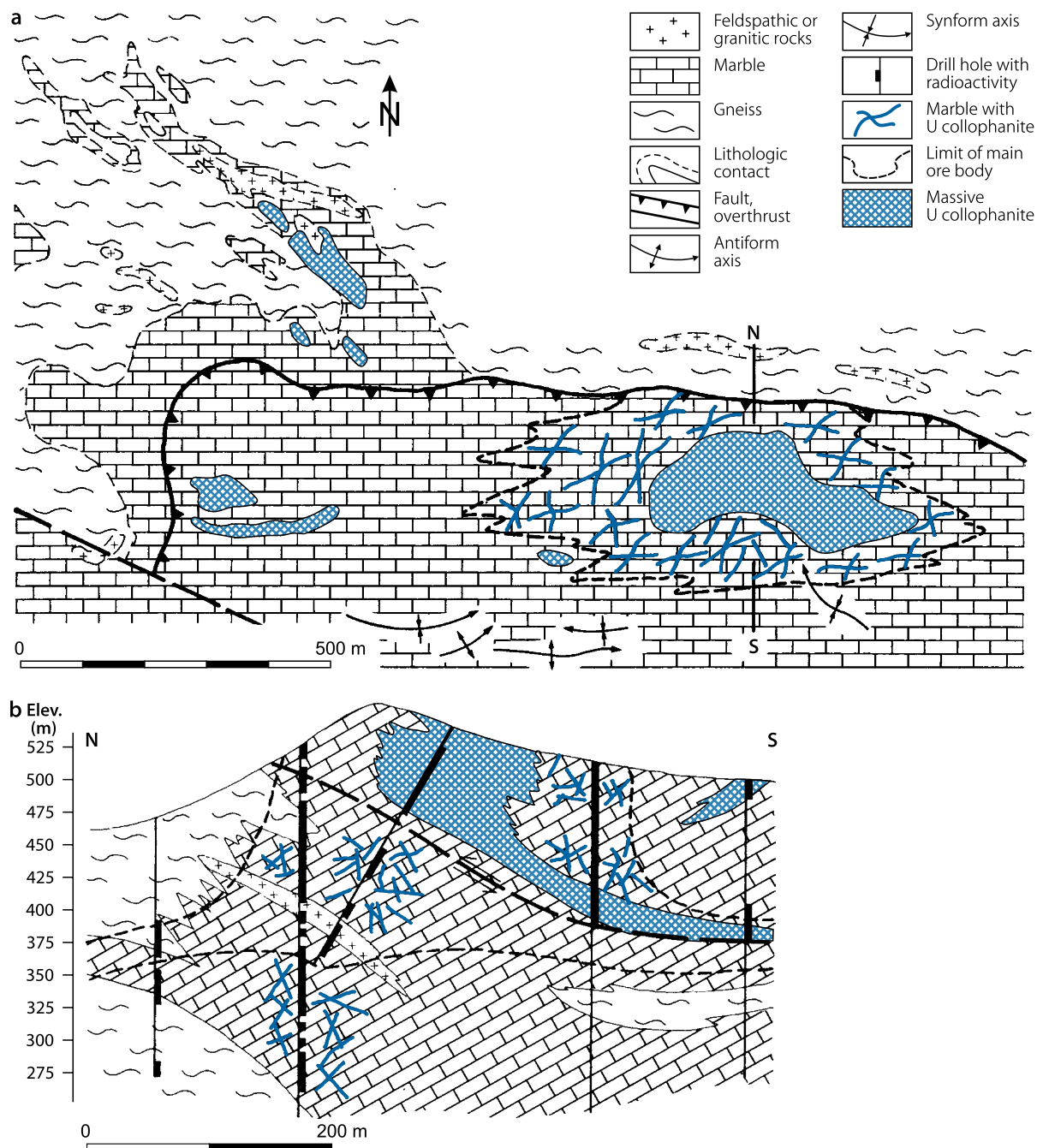
Principal Ore Controls and Recognition Criteria

Itataia is an epigenetic, structurally controlled deposit with a uranium-rich phosphate ore unique in type and metallogenesis. The principal ore-controlling or recognition criteria of the deposit include

- Association with highly uraniferous, peraluminous granite of post-orogenic, final Brazilian origin
- Proximity to lineaments
- Position along a reverse fault with a wide cataclastic aureole
- Principal host rock is cataclastic marble and calc-silicate rock, along with subordinate episyenite and gneiss
- Strong deuteritic and retrograde metamorphic alteration of host rocks including episyenitization of granite
- Ore consists almost exclusively of uraniferous collophane which, together with gangue minerals, forms collophanite
- Collophanite occurs in massive concentrations in veins and veinlets, which aggregate to stockworks

■ Fig. 4.5.

Central Ceará region, Itataia/Santa Quitéria deposit, (a) geological map with distribution of uraniferous collophanite lodes, (b) geological N-S section across the main uranium lode. (After Ayres 1981; Forman and Angeiras 1981)



- Massive collophanite extends from the present-day surface to a depth of 150 m or more
- Disseminated mineralization persists to a depth in excess of 300 m.

Metallogenetic Concepts

Angeiras et al. (1981) and the other authors cited above propose a metallogenetic model, which includes four stages of development.

- (1) Intrusion of post-orogenic peraluminous granite in zones of stress release along lineaments during the waning stage of the Brazilian Orogeny. Characteristically, this granite is highly uraniferous, and its intrusion is thought to have inflicted intense hydraulic fracturing on the country rocks. In the Itataia area, this granite occurs as apophyses and dome-shaped stocks; a larger body is suspected at some depth below the Itataia/Santa Quitéria deposit
- (2) Late magmatic-deuteric processes imposed feldspar episyenitization on granites, and Na metasomatism associated with greenschist facies retrogradation altered all host rocks.

Crystallization of analcime during the ultimate phase of these processes indicates final temperatures of about 200° to 250°C. Chlorite formation, stability of feldspars, and quartz removal are suggestive for fluids of neutral to slightly alkaline pH and of an oxidation potential sufficient to generate hematite development (but with a total iron content to remain essentially constant). Processes involved in this step led to a preconcentration of U and P within episyenite to tenors averaging 0.065% U and 12% P₂O₅. These elements form uraniferous apatite but no discrete uranium minerals

- (3) Local scale deformation of host rocks by cataclasis and brecciation created open spaces for later mineral emplacement. The question arises whether this deformation resulted from normal tectonic dislocations or, alternatively, in response to karst development and subsequent collapse of karst structures as may be speculated from the size and configuration of relatively large ore shoots developed essentially in marble
- (4) Precipitation of uraniferous colophonite associated with calcite, ankerite, and quartz, which partly crystallized in pores within colophonite, and apatite crystals in voids within episyenite. Mineralizing solutions are characterized by initial (?) temperatures of about 130°C and high salinity of about 22% equivalent CaCl₂ as deduced from fluid inclusions in apatite, dropping to 50°C and low salinity of about 5% equivalent CaCl₂ (fluid inclusions in late quartz filling voids in colophonite). Minerals enclosed in fluid inclusions are quartz, apatite, Mg-, Ca-, Ba sulfates, and Mg-, Al chlorides (Forman and Angeiras 1981). Low CO₂ contents suggest low pressures for mineral precipitation.

Uraniferous granite is considered the most likely source of uranium, whereas the origin of phosphorus is still enigmatic. It is assumed that uranium may have been transported as chloride complexes since the mineralizing solutions were rich in chlorine. The provenance of chlorine is unknown. Original pH values of fluids must have been somewhat acidic to permit the transport of the large quantities of calcium and phosphate involved in the formation of colophonite. Infiltration of these fluids into marbles would increase their alkalinity, causing rapid precipitation of colophonite with U⁴⁺ substituting Ca in the apatite structure.

In summary, the mineralization at Itataia is related to a significant metallogenetic event at the end of the Brazilian Orogeny. Mineralization is thought to have derived by post-magmatic fluid circulation triggered by cooling of a deeper-seated granitic pluton. Ore-forming fluids may have been of supergene or hypogene origin or a mixture of both. Mineral deposition took place in cycles of a pulsing regime as inferred from the zoning of apatite and colophonite crystals.

4.3 Poços de Caldas Region

This region, also referred to as Poços de Caldas district, is located approximately 250 km N of São Paulo, in the southern part of Minas Gerais state (Fig. 4.1). Poços de Caldas is an alkaline

intrusive complex with REE, zirconium, molybdenum, uranium, thorium, and bauxite deposits. The principal uranium deposit is *Cercado* in the southeastern sector of the intrusive complex; a smaller deposit, *Agostinho*, is located about 6 km NW of Cercado (Fig. 4.6).

Original resources of the district totaled 27,000 t U (RAR + EAR-I), about 17,000 t U (RAR) of which, at an ore grade averaging 0.072% U, were attributed to Cercado. Additional recoverable elements at Cercado include Mo and Zr with reserves of 25,000 t MoO₃ at an average grade of 0.11% MoO₃, and 172,000 t ZrO₂ at 0.81% ZrO₂. The ore has a high pyrite content.

Cercado was discontinuously exploited by the Osamu Utsumi open pit mine from 1982 to 1990 and from 1992 to 1995. The mine had a nominal production capacity of 750,000 t ore per year from three different blocks. The processing plant (Alamine solvent-type extraction) had a capacity of 2,500 t ore per day, with a recovery rate of approximately 70%. The nominal uranium production capability was 425 t U/year (and 285 t Mo) but the output was only on the order of 100 t U/year and totaled 1,030 t U. (OECD-NEA/IAEA 2000).

Sources of Information. Cathles and Shea 1992; Chapman et al. 1992; de Andrade Ramos and Fraenkel 1974; Forman and Angeiras 1981; Forman and Waring 1981; Holmes et al. 1992; Lichtner and Waber 1992; Miekeley et al. 1992; NAGRA 1993; OECD-NEA/IAEA 1986, 1999; Oliveira 1966, 1968; Read 1992; Romero et al. 1992; Santos 1981; Schorscher and Osmond 1992; Schorscher and Shea 1992; Shea 1992; Ulbrich 1984; Waber 1992; Waber et al. 1992.

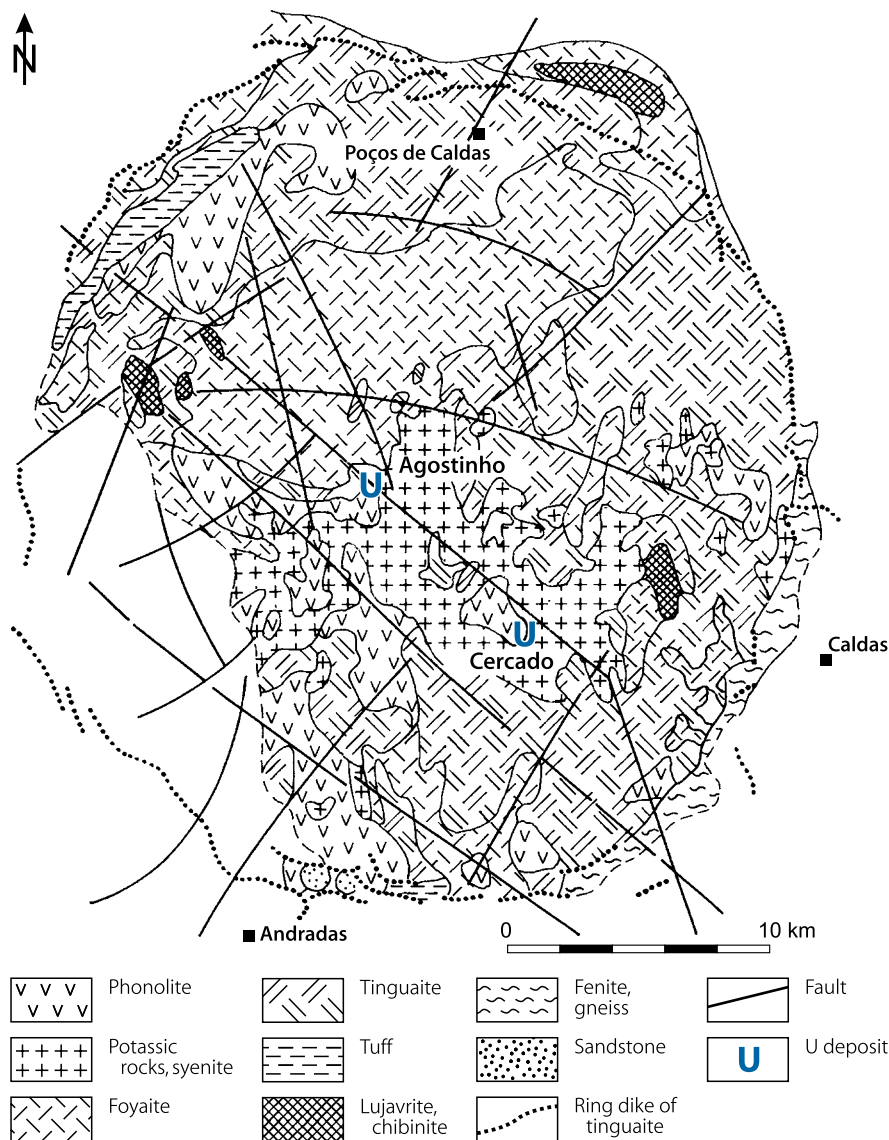
Regional Geological Setting of Mineralization

Poços de Caldas is an alkaline intrusive complex and belongs to a series of alkaline and carbonatite intrusions emplaced in the Atlantic Shield along the eastern edge of the Paraná Basin. The Poços de Caldas complex is a roughly circular caldera structure with a diameter of approximately 30 km emplaced in Precambrian gneiss. The caldera comprises a suite of alkaline volcanic, subvolcanic, and plutonic rocks ranging from miaskitic to strongly agpaitic composition, which evolved through several successive stages during Upper Cretaceous to early Tertiary (80–60 Ma ago). Nepheline syenite facies constitute the bulk of the intrusive material and include in decreasing order of abundance tinguaitite, phonolite, nepheline syenite, foyaite, lujavrite, and chibinitite. These magmatite rocks have normal Clarke tenors of U, Th, and REE, as they are typical for alkaline rocks. A carbonatite stock occurs at Morro do Ferro.

Volcanic extrusives are represented by ash, tuff, welded tuff, and lava. Volcanic breccia pipes, up to 80 m in diameter, transect the older volcanics of the deposit. Discontinuous, narrow, less than 10 cm thick, veins of caldasite, a massive grey rock essentially composed of the zirconium oxide and zirconium silicate minerals baddeleyite and zircon, respectively, occur in association with clay in larger fracture zones. The veins contain 40–75% ZrO₂ and locally as much as 0.3% U. They were the target of early uranium exploration (Ayres 1981). Late stage

■ Fig. 4.6.

Poços de Caldas region, generalized geological map with location of the Cercado and Agostinho deposits in the alkaline caldera complex. (After Forman and Angeiras 1981; d'Elboux 1984)



ultramafic and mafic dikes cut all the former lithologies. An annular ring filled with a series of ring dikes of tinguaitic composition surrounds the caldera markedly separating it from the intruded Precambrian country rocks. Intense weathering, locally penetrating to a depth of 200 m or more along faults, produced a cover of lateritic soil and bauxite.

Two, almost perpendicular fault systems along NW-SE and NE-SW directions dissect the caldera. They correspond to the regional structural pattern found in the Precambrian basement. Local structures associated with intense fracturing trend about NNE-SSW.

The two deposits identified in the Poços de Caldas complex, Cercado and Agostinho, exhibit the following characteristics of mineralization and ore distribution (Fig. 4.7).

4.3.0.1 Cercado/Osamu Utsumi Mine

The Cercado deposit/Osamu Utsumi mine is located about 15 km to the south of the city of Poços de Caldas (Fig. 4.6). The deposit, which is partitioned into three adjacent blocks, A, E, and B (from east to west), is closely related to a circular internal structure within the larger Poços de Caldas caldera (Fig. 4.7a).

Geological Setting of Mineralization

The deposit is hosted by a suite of alkaline volcanic, subvolcanic and plutonic rocks, chiefly phonolites and nepheline syenites.

Volcanic breccia pipes/diatremes, commonly several meters but occasionally up to 80 m in diameter, transect the older volcanics. Late stage lamprophyre dikes, dated at 76 Ma (Ar-Ar in phlogopite, Shea 1992), cut the older lithologies including the altered facies and, as such, put a younger age limit to the hypogene hydrothermal event described below. The rocks are weathered to a thick immature lateritic soil grading downward into a saprolitic zone and then into an oxidized zone (details see next chapter).

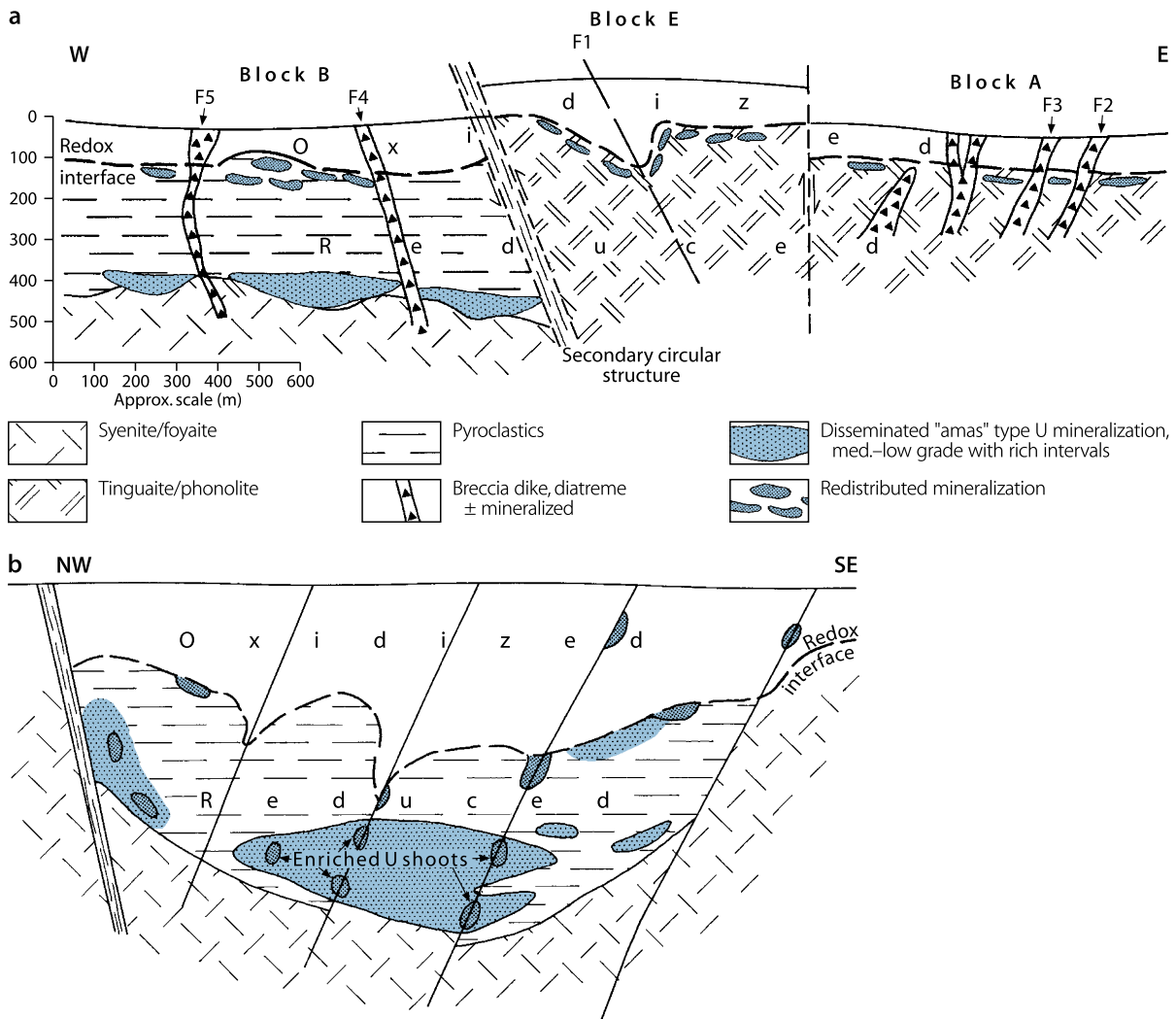
Host Rock Alteration

Waber et al. (1992) provide a comprehensive account of the hypogene and supergene alterations that modified the magmatic rocks of the Poços de Caldas complex on a regional and local scale, and the Cercado area in particular. Regional

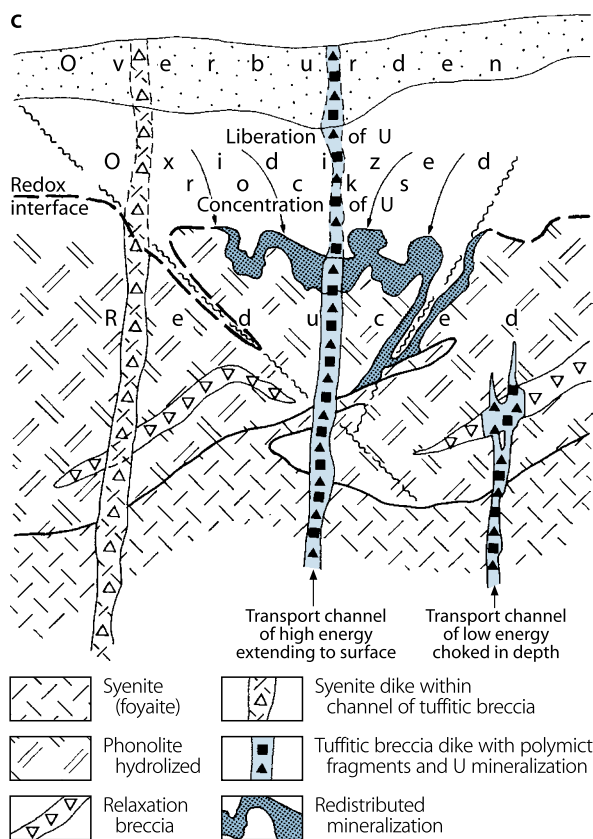
deuteric-hydrothermal alteration of the complex resulted in widespread pervasive argillization and zeolitization. Affected rocks are potassium enriched compared to global phonolites and nepheline syenites (Ulbrich 1984; Schorscher and Shea 1992). The complex was subsequently modified by intense *hydrothermal activity* of local extent, related to the invasion of diatremes, dominated by pyritization and potassic alteration of the phonolites and syenites, and the formation of disseminated, low-grade pitchblende mineralization (primary mineralizing event). All feldspars were transformed into potash feldspars, nepheline into illite and kaolinite, and clinopyroxenes into mixtures of TiO₂-rich phases, clay minerals, and pyrite. The process involved the enrichment of Ba, K, Mo, Pb, Rb, S, Th, and U and a strong diminution of Ca, Mg, Na, and Sr.

Semi-tropical *weathering* has produced an immature lateritic soil, 20 to 40 m thick, grading into a 15 to 60 m thick saprolite zone with original rock texture still preserved. The saprolite-laterite

Fig. 4.7. Poços de Caldas region, Cercado (C-09) deposit/Osamu Utsumi mine, (a) schematic W-E section through the mineralized blocks, (b) NW-SE section through the B-block/Osamu Utsumi ore body, (c) scheme of tuffite dike-related primary and redox interface-related redistributed U mineralization. (After (a) Forman and Angeiras 1981, Santos 1981; (b) Ayres 1981; (c) Tilsley in Forman and Angeiras 1981)



■ Fig. 4.7. (Continued)



contact is marked by gibbsite when potash feldspar has been removed. Further down, to depths varying between 80 and 140 m below surface and to a greater depth along faults, downward migrating oxygenated groundwater has developed an oxidation zone 20 to 60 m thick. This oxidized zone contains 20 ppm U (which is half of the U tenor in hydrothermally affected “reduced” phonolites) in the uppermost 10 to 40 m, and an average of 55 ppm U in the basal 10 to 20 m. The uranium is partly retained by adsorption onto poorly crystalline phases and by incorporation into hydrothermal refractory minerals.

The oxidation zone terminates downward in a spatially, highly irregular *redox front* (▶ Fig. 4.7b, c), which cuts across hydrothermally altered (“reduced”) phonolites, nepheline syenites, and diatremes partly with a very sharp transition from oxidized to reduced rock. It transects individual mineral grains of the parent rocks as well as fragments and matrix components of breccia pipes and dikes. The interface is marked by a contrasting color change from reddish-brown to bluish-grey in oxidized and reduced facies, respectively, in response to the development of hydrous ferric oxides (amorphous Fe hydroxides grading into goethite and hematite with time) and secondary pyrite.

The Fe oxides and hydroxides define the redox front and delineate the oxidized zone. Typical modifications at and on the *oxidized side* of the front include

- Pyrite and other sulfides, fluorite, and carbonates disappear within a few mm of the front

- Jarosite and alunite occur as a product of pyrite oxidation
- Potash feldspar becomes dissolved
- Illite slowly begins to decrease
- Compared to illite, kaolinite decreases slightly adjacent to the front; but locally kaolinite is concentrated in form of up to 5 mm thick white bands separating the redox front from the reduced rock
- Rock porosity almost doubles
- Crandallite group minerals constitute the main REE-bearing minerals in the oxidized part (as compared to clinopyroxenes, which are the primary REE-bearing specimen of unaltered rocks).

The *reduced side* exhibits the following characteristics:

- K feldspar starts to diminish 0.5 to 3 cm into the reduced zone
- Authigenic minerals develop in the rock matrix 1 to 3 cm into the reduced zone; their appearance is directly related to the commencement of K feldspar dissolution
- Secondary pyrite crystallization roughly coincides with the growth of pitchblende nodules (this pyrite has low δS values that indicate involvement of bacterial action)
- Greenockite (CdS) occurs sporadically as a constituent of the pitchblende-secondary pyrite nodules.

REE are hardly mobilized by meteoric fluids as reflected by only a slight difference of REE tenors between oxidized and reduced rocks, with a somewhat greater loss of the light REE.

Mineralization

Waber et al. (1992) distinguish various mineral assemblages of hypogene and supergene origin and provide the following characteristics thereof.

Hypogene hydrothermal U mineralization includes two types, disseminated, low-grade mineralization and relative high-grade mineralization in diatreme breccias and veins. Disseminated, low-grade mineralization consists of a U-Th-Zr-Mo assemblage with pitchblende, fluorite, and monazite. It occurs in potassic-altered and pervasively pyritized phonolites and syenites, in which it is closely related to fine-dispersed small-sized pyrite (50–100 μm). Minute U inclusions also occur in the pyrite and small grains of monazite/cherelite grow on the pyrite. Small veinlets of pyrite and clay minerals transect the disseminated mineralization.

Relatively high-grade U-Th-Zr-REE vein-stockwork mineralization occurs matrix-bound in volcanic breccia pipes or dikes. Uraninite, pitchblende, and uraniferous TiO_2 phases are the principal U minerals; the latter include anatase and brannerite. Monazite is the main REE-bearing mineral. Pitchblende is partly intergrown with pyrite.

The various ore minerals vary considerably in quantity suggesting a polyphase origin. Some mineralization is characterized by a preponderance of certain elements (Zr minerals, Ti minerals, etc.), and other by variable properties of phases (e.g. violet, colorless, or green fluorite). Some stages were

apparently rich in uranium as may be deduced from local enrichments in the order of 0.5% U.

Supergene U mineralization is controlled by redox interfaces. Uranium is present in the form of botryoidal aggregates of pitchblende, a form which is less well crystallized than that of the hydrothermal event and which always contains traces of SiO_2 , K_2O , and Al_2O_3 . The pitchblende accumulates into nodules in which it is finely intergrown with secondary pyrite, kaolinite, illite, K feldspar, and locally with greenockite. REE are largely associated with clay-sized phosphates (including crandallite group minerals). Two generations of pyrite exist. Pyrite with $\delta^{34}\text{S}$ values around 0 ‰ is related to the hydrothermal event, whereas pyrite with very low $\delta^{34}\text{S}$ values (–12 to –14 ‰) is attributed to supergene weathering associated with bacterial activity. Such secondary pyrite mainly occurs in the narrow, secondary pitchblende-bearing zones.

Redox front-controlled narrow bands or lenses of secondary mineralization are a few centimeters to rarely a few decimeters thick, and occur immediately below the redox interface. Pitchblende nodules exist within 20 cm of the redox front into the reduced rock. Nodules are particularly concentrated in faults. Millimeter-sized pitchblende concretions occur along hair fissures, 1–3 cm long, in porous, slightly mineralized phonolite characterized by a 20 cm wide dark-brown zone rich in iron and manganese oxides/hydroxides. When hosted in homogeneous, porous phonolite as in the E block, pitchblende nodules may occur along the whole redox front, whereas in breccia bodies (B block) large nodules in excess of 5 cm in diameter are mainly found along the deeply penetrating tips of oxidation fronts associated with SW-trending faults. (Waber et al. 1992)

Shape and Dimensions of Deposits

Three principal types of ore settings are described by Forman & Angeiras (1981): (a) veins mineralized with U, Mo, F, and minor Zr and Th, emplaced within steeply dipping diatremes/breccia pipes and dikes, up to 5 m wide and at least 250 m deep; (b) clusters or pockets with enriched uranium bands located discontinuously along faults, dikes, and diatremes; and (c) lenticular zones with disseminated uranium mineralization within pyroclastic rocks (Fig. 4.7c). Ore minerals are essentially the same in the first two types, but vary in the third type as shown below.

The **Cercado** deposit contains uranium mineralization in three adjacent blocks, A, E, and B (from east to west), that are separated by faults (Fig. 4.7a).

Block A covers an area about 900 m long and 530 m wide, in which primary mineralization occurs in steeply to vertically dipping pipes and NW-SE-oriented dikes of tuffitic breccia with tinguaita fragments. The dikes cut compact, microgranular lavas of tinguaita and phonolite composition. Uranium minerals are pitchblende and coffinite, which may be associated with zircon, baddeleyite, pyrite, fluorite, jordisite, ilsemannite, galena, and sphalerite. Uranium redistribution resulted in the local formation of neo-pitchblende. The dikes may be mineralized entirely or only partially. Ore penetrates locally into fractured wall rocks. Ore-bearing dikes vary abruptly in thickness both along strike and dip. They may be up to 5 m thick and extend to a known

depth of 250 m. Block A accounts for approximately 20% of the Cercado reserves. Grades average 0.18% U and 0.95% MoO_3 .

Block E is sandwiched between blocks A and B. It occupies a subhorizontal, slightly NE-dipping zone extending 1.1 km in NE-SW length, 500 m in width, and 140 m in depth. Only redistributed mineralization is present. Uranium is concentrated by adsorption to limonite, which prevails in the upper 10 m, and as uraniferous clay nodules up to 10 cm thickness. The nodules have a mixture of clay and black uranium oxides as a core, and a shell of pitchblende with pyrite. Nodules occur preferentially along NE-SW faults and at the intersections of faults. Uranium mineralization forms irregularly shaped bodies of highly variable tenor and size, hosted by strongly fractured and altered tinguaita and phonolite. Block E accounts for about 15% of the Cercado reserves. Grades average 0.1% U, 0.93% ZrO_2 , and 0.09% MoO_3 .

Block B contains mineralization in an area 1,240 m long in NE-SW direction, 440 m wide, and 370 m deep. It is separated from Block E by an arcuate fault. Host rocks are some 300 m thick pyroclastics, which fill a depression and rest upon foyaite. Ultrabasic dikes and diatremes cut the pyroclastics. Ore consists of black uranium oxides associated with fluorite, pyrite, and molybdenum minerals. The ore minerals concentrate to shoots or lenses of disseminated mineralization in the basal part of the pyroclastic unit where they occupy depressions or downfaulted blocks proximal to and somewhat contouring the pyroclastic/foyaite contact. The uranium grade increases toward the basal contact, whereas zirconium values remain stable. Also, ore bodies are thicker in deeper depressions. Both features are considered indicative of some sort of control exerted by the lithological interface on laterally migrating hypogene hydrothermal solutions. Redistributed mineralization occurs in the upper part of Block B. Block B accounts for about 65% of the Cercado reserves. Grades average 0.063% U, 0.072% ZrO_2 , and 0.11% MoO_3 (Forman and Angeiras 1981).

Stable Isotopes and Fluid Inclusions

Fluid inclusions in fluorite indicate temperatures around 250°C and a KCl- H_2O mixture with approximately 7 wt.% KCl for hydrothermal fluids related to the development of diatremes. Solutions that transported additional Zr, Hf, F, and minor REE and circulated almost exclusively within the breccia pipes are portrayed by fluid inclusions, which indicate boiling and provide temperatures of 210°C for a KCl-NaCl- H_2O brine containing 40–45 wt. % KCl, FeSO_4 , and KF.

Secondary pyrite associated with remobilized pitchblende at the redox interface yields δS values of –13 ‰; these low values, as compared to δS values of –3.63 to + 1.24 ‰ for hydrothermal pyrite, are attributed to bacterial action (Waber et al. 1992).

Metallogenetic Concepts

Metallogenetic considerations attribute the magmatic evolution of the Poços de Caldas complex and related polymetallic

mineralization to hypogene processes with late supergene modifications. This concept involves a magma source rich in cogenetic volatiles, which repeatedly affected the area by deuteric, pneumatolytic, and hydrothermal processes (Schorscher and Shea 1992).

Waber et al. (1992) elaborate on the various hypogene and supergene stages and arrive at the following sequence and nature of events. The emplacement of the alkaline volcanic and plutonic rocks, which have normal Clarke tenors of U, Th, and REE as they are typical for alkaline magmatic rocks (Ulbrich 1984), was followed, in a *first regional deuteric stage*, by pervasive pneumatolytic and auto-hydrothermal activity. This activity provoked a partial alkali exchange in alkali-feldspar, rare metals silicate, and fluorite formation, hematite pigmentation, and incipient kaolinitization and zeolitization; the resulting lithofacies are enriched in potassium as compared to global Clarke standards. U, Th, and REE remained stable during this stage.

A *subsequent subvolcanic episode* affected the Poços de Caldas complex locally, including the Cercado area. It includes the explosive development of diatremes, which was preceded and succeeded by several hydrothermal pulses of distinct composition that caused intense alteration of the rocks at Cercado. The polyphase nature of this process is reflected by several generations of minerals (fluorite, pyrite, fluid inclusions of different compositions) and, as compared to unaltered facies, by a differentiated enrichment of Ba, K, Pb, Rb, S, Th, and U in the hydrothermally altered wall rocks and within the diatremes. The breccia pipes and breccia-related veins have markedly higher enrichments of these elements, and they contain, in addition, concentrations of F, Hf, Y, Zr, and occasionally REE.

This *subvolcanic hydrothermal event* commenced with potassium-rich, reducing fluids that caused pervasive potassium metasomatism associated with dispersed pyritization, minor uranium and fluorite mineralization, and argillization of the host rocks. Primary alkali feldspars were transformed into an intermediate microcline, while foidic and mafic minerals decomposed. Sulfur isotope signatures of the disseminated pyrite document a magmatic heritage, and the widespread disseminated precipitation of this pyrite is evidence of a reducing potential for the initial fluid and an increasing sulfur activity during its evolution. Well-crystallized illite that formed in both the altered and virtually unaltered rocks suggests formation under a moderate K activity at an initial temperature of around 350°C.

During the subsequent evolution, K activity augmented progressively and the temperature dropped. Fluid inclusions in fluorite, which formed in all lithologies, testify to a KCl-H₂O-type fluid with 7 wt. % equivalent KCl and a homogenization temperature of about 260°C. Stable isotope ratios indicate an equivalent temperature for the bulk of clay minerals (illite) (Waber 1990). The overall argillic alteration occurred under these conditions, together with the pervasive disseminated-type pyritization and subordinate fluorite, pitchblende, and most probably monazite precipitation.

Subsequent generations of fluorite contain fluid inclusions, which correspond to temperatures of 200–220°C. This temperature drop is thought to be related to a mixing of magmatic fluids with meteoric water, as evidenced by $\delta^{34}\text{S}$ values for pyrite and

$\delta^{18}\text{O}$ and δD signatures of clay minerals. This waning stage of the potassic hydrothermal activity imprinted the present-day host rock chemistry.

A spatially restricted *later stage of hydrothermal activity* revived with the development of several small volcanic breccia pipes. This stage postdates the pervasive potassic alteration process as evidenced by fragments of altered and pyritized phonolite and nepheline syenite in the diatremes. The restricted impact is thought to indicate a rapidly decreasing contribution of magmatic fluids at a coeval increase of the influence of meteoric water. Solutions responsible for this process are reflected by fluid inclusions in fluorite that occur in fissures of diatreme breccias. These inclusions indicate boiling and a composition that corresponds to a KCl-NaCl brine with about 44 wt. % equivalent KCl, and traces of FeSO₄ and KF. This brine existed exclusively in the breccias and mineralized veins. It contained appreciable amounts of F, Hf, Pb, Th, U, Y, Zr, and occasionally REE (especially HREE), and resulted in the precipitation of some microcline. Uranium precipitated mainly as pitchblende of variable composition and as brannerite, while REE were incorporated in monazite and other phases such as cheralite and bastnaesite. Additional minerals formed during this process include zircon and other Zr- and Hf-rich minerals, as well as pyrite, fluorite, and clay minerals.

Two sources for the fluid-contained elements are considered: (a) leaching from phonolite and nepheline syenite in deeper parts of the Poços de Caldas complex and (b) a late-stage differentiate from the same magma that produced the rocks of the complex. The latter source is favored since the chondrite normalized patterns of incompatible elements from the highly mineralized breccias resemble the pattern of late-stage lamprophyre dikes, except for the increased Zr and Hf contents in the breccias. Furthermore, the diatremes are of explosive origin, which involved a rapid rise from their source up through the penetrated rocks and as such limit any long-term residence and efficient leaching process in the lower levels.

Lamprophyre dikes dated at 76 Ma (Shea 1992) represent the latest magmatic event at Cercado. This age put a younger time bracket on the aforementioned hypogene hydrothermal activities since these dikes cut all hydrothermally altered rocks.

Later supergene processes produced an oxidation zone, redistributed uranium and other elements, and generated secondary mineralization along redox fronts. Only part of the U, however, was leached by the supergene processes. The oxidized zone still contains (a) 20 ppm U in the uppermost 10 to 40 m, which is half the concentration of the hydrothermally affected “reduced” phonolites, and (b) a mean value of 55 ppm U in the basal 10 to 20 m. These U tenors imply that finely dispersed U in the rock matrix is much less mobile than that in the previously formed pitchblende nodules. The latter are decomposed when passed by the redox front (Schorscher and Osmond 1992). This retardation may be explained by the incorporation of U into more or less refractory minerals such as brannerite, and by uranium adsorbed onto Fe hydroxides and similar phases. But since the uranium tenor does not correlate either with the Fe or Ti content, an additional unknown scavenging mechanism to retain this U enrichment in the lowest oxidized zone has to be envisioned.

4.3.0.2 Agostinho

The Agostinho deposit contains mineralization similar to that of Block A at Cercado. Two mineralized bodies occur in subvertically dipping breccia dikes, about 2.5 m thick and extending to a depth of 150 m. The dikes occur within strongly hydrothermally altered and potassium-enriched tinguaitite. Mineralization consists of pitchblende and molybdenum minerals (jordanite, molybdenite, ilsemanite) emplaced in a matrix of fluorite, pyrite, sericite, and zircon. Resources are about 4,200 t U and 7,000 t MoO₃ (Forman and Waring 1981).

4.4 Seridó Region

This region extends from southern Rio Grande do Norte state into north-central Paraíba state in northeastern Brazil. A number of uranium showings have been discovered mostly within Upper Proterozoic leucocratic granites, but there are also a few occurrences in Proterozoic metasediments. Those of potential economic significance occur in albitized rocks, and may be classified as metasomatite-type deposits with disseminated mineralization. *Espinharas* is the most prominent of these deposits (► Fig. 4.1).

4.4.0.1 Espinharas Deposit

This deposit was discovered 25 km N of the town of Patos in north-central Paraíba state in 1972. Espinharas contains 4,240 t U RAR and approximately the same amount in the EAR category (OECD-NEA/IAEA 1986). The average grade is about 0.1% U, at a cut off grade of 0.04% U.

Sources of Information. Ballhorn et al. 1981; Forman and Waring 1981; Fuchs et al. 1981; Porto da Silveira et al. 1991, unless otherwise cited.

Geological Setting of Mineralization

Espinharas is situated in the Seridó Basin, one of several paleobasins within the Proterozoic Cariri mobile belt. This belt intervenes between two Archean-Proterozoic cratons, the São Luis Craton to the north and the São Francisco Craton to the south.

The Seridó Basin is filled with Lower Proterozoic metasediments of the Seridó and Caicó groups, which rest unconformably upon crystalline rocks of the São Vicente Group of Archean age. These units have been regionally metamorphosed during the Transamazonian (~ 2000 Ma) and Brazilian (650–450 Ma) orogenies and were intruded by several generations of granite during the Brazilian Orogeny. Wernick (1979) established three intrusive phases of granite of variable composition. Syntectonic granite, dated \pm 650 Ma old, is classified as dry granite. Late tectonic granite (540 \pm 25 Ma) comprises both dry and highly hydrous facies. Post-tectonic, mostly alkaline granites (510–460 Ma) are essentially dry.

The *Seridó Group* consists of a variety of schists with a basal quartzite and metaconglomerate horizon, referred to as the Equador Formation and which rests unconformably upon the older Caicó Group. The *Caicó Group* comprises gneiss intercalated with quartz-feldspar rocks, amphibolite, schist, and large lenses of marble, which enclose scheelite-bearing tactite. The whole sequence has been strongly modified by migmatization.

The structural grain of the metasediments in the northern part of the region shows NNE-SSW-oriented folding, which turns into an E-W direction in the southern section where it parallels the Patos Lineament. Prominent fault systems trend NE-SW and NW-SE. Some faults contain late orogenic alkali granite, pegmatite, or quartz veins.

A facies of coarse-grained alkali granite typified by microclinization of plagioclase contains appreciable amounts of uraninite. Certain metasediments likewise have uraninite concentrations associated with chalcopyrite, galena, magnetite, pyrite, quartz, chlorite, and epidote, and which are distributed either concordantly or discordantly to the foliation.

The predominant rock at Espinharas is amphibole-biotite gneiss with intercalated minor amphibolite and tactite of the Caicó Formation. These metasediments are folded into an anticline, the axis of which plunges NNE. Foliation strikes 10° to 30° and dips 50° to 60° WNW. A basement complex of granodiorite and porphyritic granite crops out west of the deposit. Numerous apophyses and dikes, commonly a few centimeters to 5 m but exceptionally as much as 50 m thick, of alkali granite, pegmatite, and orthopyroxene transect the older rocks. A regional, pre-ore tensional fault trending ENE-WSW parallel to the Patos Lineament and dipping 50° to 70° NW is the prominent structure at the deposit. Many post-ore faults displace the deposit into numerous blocks.

The principal host rock is a pink, porous, albitized feldspathic rock of fine- to coarse-grained texture, essentially composed of oligoclase and albite (77 to 95 vol. %), some biotite, often chloritized, and minor amounts of apatite, carbonate, muscovite, hydromica, sulfides, and hematite, cut by numerous calcite veinlets. Quartz is absent. Clear albite fills voids and fissures. Fuchs et al. (1981) consider the feldspar rock to be a metasomatic derivative of former granite. The metasomatic rock occurs as dikes and lenses ranging in width from a few centimeters to 100 m within amphibole-biotite gneiss mottled by impregnation of pink feldspar. The other main host rock is strongly altered biotite-amphibole gneiss, which is commonly rich in plagioclase, low to barren in quartz, and contains minor quantities of apatite, calcite, epidote, and titanite.

Host Rock Alteration

Ballhorn et al. (1981) note that Na metasomatism is the most characteristic and widespread alteration feature as reflected by albitization (oligoclase is replaced and/or overgrown by albite; clear albite fills fractures and voids) and replacement of green amphibole by arfvedsonite. Other alteration features include hematitization, desilicification by quartz removal, intense argillization of feldspar, chloritization of biotite associated with

decoloration and exsolution of Fe oxides, and carbonatization expressed by replacement of former minerals by calcite or epidote and formation of calcite veinlets. Alteration affecting the biotite-amphibole gneiss and amphibolite has led to the decomposition of feldspar into sericite, calcite, epidote, and hydromica and incipient chloritization of biotite.

Alteration and mineralization related modal changes in the mineral assemblage of biotite-amphibole gneiss are reflected by an increase in feldspar from 58 vol. % in unmineralized to 64 vol. % in mineralized gneiss, and a decrease in quartz from 5 to 1 vol. %, respectively.

Chemical changes related to the alteration of feldspathic rock are documented by a high content of Na (6–10 wt %) and calcium (1–4 wt %), and a low K content (0.1–0.6 wt %). REE of the yttrium group appear to increase. In principle, there is a decrease of SiO_2 , K_2O , Cl, and in the Fe_2/Fe_3 ratio, and an increase of Na_2O , CaO, Y, Yb, and F content in going from unmineralized to mineralized host rocks. d'Elboux (1984) associates these alteration processes with zones of dilational fracturing dated at ± 450 Ma.

Mineralization

Uraninite and betafite are the predominant uranium minerals; they occur as minute grains on grain boundaries and within feldspars. Pitchblende, coffinite, and hexavalent U minerals, mainly β -uranophane, are present in minor amounts. Associated minerals include pyrite, chalcopyrite, and apatite. These uranium minerals are disseminated throughout the albitized host rock and in localized concentrations. In addition to these U minerals, a large part of the contained uranium is present as an unidentified, non-refractory U phase. U/Th ratios of this material range from 1 to 10 at depth, and from 0.3 to 1 at surface, which suggests that this uranium was liberated from some kind of uranium-thorium

mineral. Samples of mineralized gneiss show uniform high U/Th ratios, whereas ratios vary widely in samples of pure feldspathic metasomatite. Fuchs et al. (1981) consider this discrepancy to be the result of Na metasomatism in which Th and U behave differently and U is more mobile. [Similar situations are reported, for example, from the Mortagne Massif, France, by Renard (1974), who explains this phenomenon as being due to a lack of mobility and reconcentration capability of Th during albitization as compared to uranium (see Chap. Vendée, France, in *Uranium Deposits of the World: Europe*, in preparation)].

Shape and Dimensions of Deposits

Uranium mineralization extends over a NNE-SSW length of 2,200 m, a width (at surface) of 20 to 120 m, and a depth of 250 m. Ore occurs in discontinuous and irregular lenses that are a few centimeters to several tens of meters thick. The lenses are stacked in an echelon pattern parallel to the regional foliation (Fig. 4.8). The average grade of most of the ore is approximately 0.08% U with intercalated sections exceeding 0.1% U.

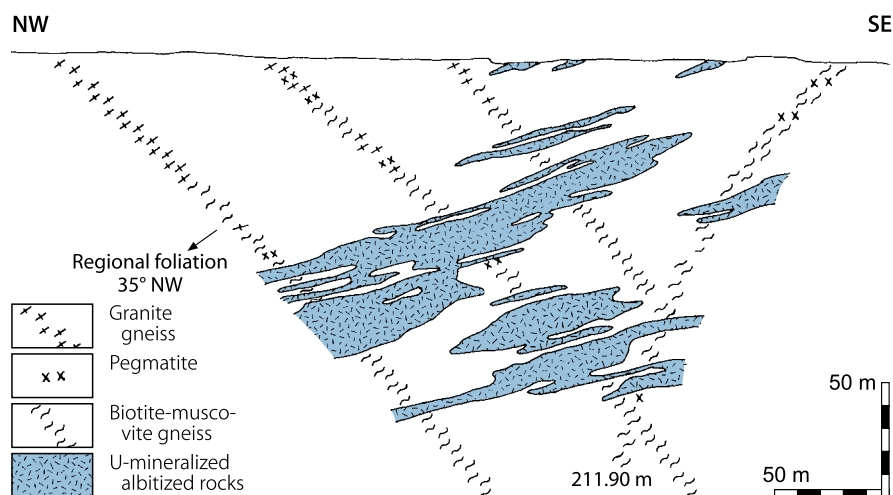
Ore Controls and Metallogenic Aspects

Regional ore controls or recognition criteria of the Espinharas deposit include

- Position of the deposit in a mobile belt (Cariri) composed of rejuvenated older basement lithologies and intrusive granites of variable composition
- Host rocks belong to a polymetamorphic unit (Caicó Group) in the Cariri belt
- Association with post-orogenic alkaline granite intrusions, which elsewhere in the Seridó region contain the majority of radioactive occurrences

Fig. 4.8.

Seridó region, Espinharas deposit, NW-SE section with drill indicated lithology and interpreted distribution of uranium mineralization in albitized gneiss and feldspathic rocks. (211.90 m = length of drill hole). (After Fuchs et al. 1981)



- Position of granite bodies and related pegmatite dikes and quartz veins are controlled by regional compressional zones, which do not exhibit distinct local faults
- Strong Na metasomatism (mainly albitization) imposed on zones of dilational fracturing during the waning phase of the Brazilian Orogeny (it should be noted that Na metasomatism by itself does not appear to be directly related to the mineralizing process but tends to be an apparent prerequisite for later U emplacement)
- Intense hydrothermal host rock alteration including feldspar decomposition, chloritization, hematitization, calcitization, and quartz removal (the latter may indicate episyenitization)
- No obvious structural control by distinct faults, but likely control by more subtle cataclastic deformation as may be deduced from the location of the deposit in a postulated zone of compression.

No convincing hypothesis on the formation of mineralization at Espinharas has been forwarded as yet. Ballhorn et al. (1981) speculate that (volatile-rich) hydrothermal fluids of hypogene origin caused metasomatism, alteration, and mineralization. Forman & Waring (1981) consider Espinharas to be comparable to feldspathic episyenite-hosted mineralization of the uranium-phosphate deposits of the central Ceará district and that both districts evolved by the same metallogenic event.

4.5 Paraná Basin

The Paraná Basin spreads over the southern part of Brazil and into neighboring Argentina, Paraguay, and Uruguay. Two districts with sandstone-type uranium deposits in Paleozoic sediments have been discovered in this basin: *Figueira* in northeastern Paraná state, with approximately 7,000 t U in Permian sediments; and *Amorinópolis* with about 4,000 t U in Devonian sediments, located approximately 800 km north of *Figueira* in Goiás state (► Fig. 4.1). Several other occurrences, most of small size, are located in the Paraná Basin: *Alfredo Wagner*, *Lages*, and *Domo de Lajes* in Santa Catarina state; *Teresa Christina* and *Cândido de Abreu* in Paraná state, *Domo de Araquaiha* in Mato Grosso state; and in the *Melo-Fraile Muerto* area of northeast Uruguay, near the Brazilian border.

Sources of Information. Andrade and Camarço 1982; Ayres 1981; Barretto 1985; d'Elboux 1984; de Figueiredo Filho et al. 1982; Forman and Waring 1981; Hassano and Stein 1979; OECD-NEA/IAEA 1986; Rabelo and Camarço 1982; Saad 1982. Barretto's (1985) paper provided the principal basis for the following synopsis of the Paraná Basin amended by data from the other authors listed.

Regional Geology of the Paraná Basin

The Paraná Basin is a NNE-SSW-elongated intracratonic basin, 1.6 million km² in size, filled with ± 2,500 m thick Paleozoic and less than 750 m thick Mesozoic clastic sediments, intercalated with extensive Early Cretaceous lava flows exceeding 1,500 m in

thickness. Deformation and arches separate the Paraná Basin into five subbasins.

Sedimentation commenced with marine deposits (*Vila Maria Formation*, less than 245 m thick) during the mid-Silurian, and was followed by clastics of the *Furnas Formation*, more than 400 m thick, of marine origin with continental interbeds.

The Devonian *Ponta Grossa Formation* is 600–700 m thick and has three members. The lower member is more than 270 m thick and consists of shallow water conglomerate, siltstone, and shale with intercalated feldspathic sandstone beds, 3 to 8 m thick. Uranium occurs in this unit at *Amorinópolis*. A deltaic, coarse-grained, locally micaceous sandstone of pink color due to ferruginous cement forms the 250 m thick middle member. It contains shale and polymictic pebbles, and exhibits channel structures. The upper member, of about 60–200 m thickness, consists of fine-grained sandstone with calcareous cement and layers of oolitic hematite and chamosite. The sandstone grades upward into dark shales. In outcrop, the ferruginous beds give rise to extensive laterite with localized uranium accumulations, as at *Amorinópolis*.

Permo-Carboniferous sedimentation began after a long erosional interval in the Upper Carboniferous and includes in various parts of the basin (from bottom to top) the

- *Aquidauana Formation*: 1,000 m thick, chiefly pink sandstone and conglomerate
- *Itararé Formation*: ~700 m thick, glacial, fluvial, and marine deposits. This formation unconformably underlies the Rio Bonito Formation
- *Rio Bonito Formation*: 100 to 150 m thick, deltaic, fluvial, paludal, and littoral to marginal marine sediments subdivided into three units. Channel sandstone constitutes the basal unit. The middle unit includes siltstone, shale, limestone, and up to ten seams of interbedded coal, a few centimeters to 2 m thick. The upper unit is composed of dark grey, fine-grained sandstone intercalated with mudstone, carbonaceous shale, and some coal beds. The Rio Bonito Formation is the most prominent host for uranium concentrations in the Paraná Basin, including the *Figueira* deposit
- *Palermo, Irati, and Serra Alta formations* of lacustrine provenance.

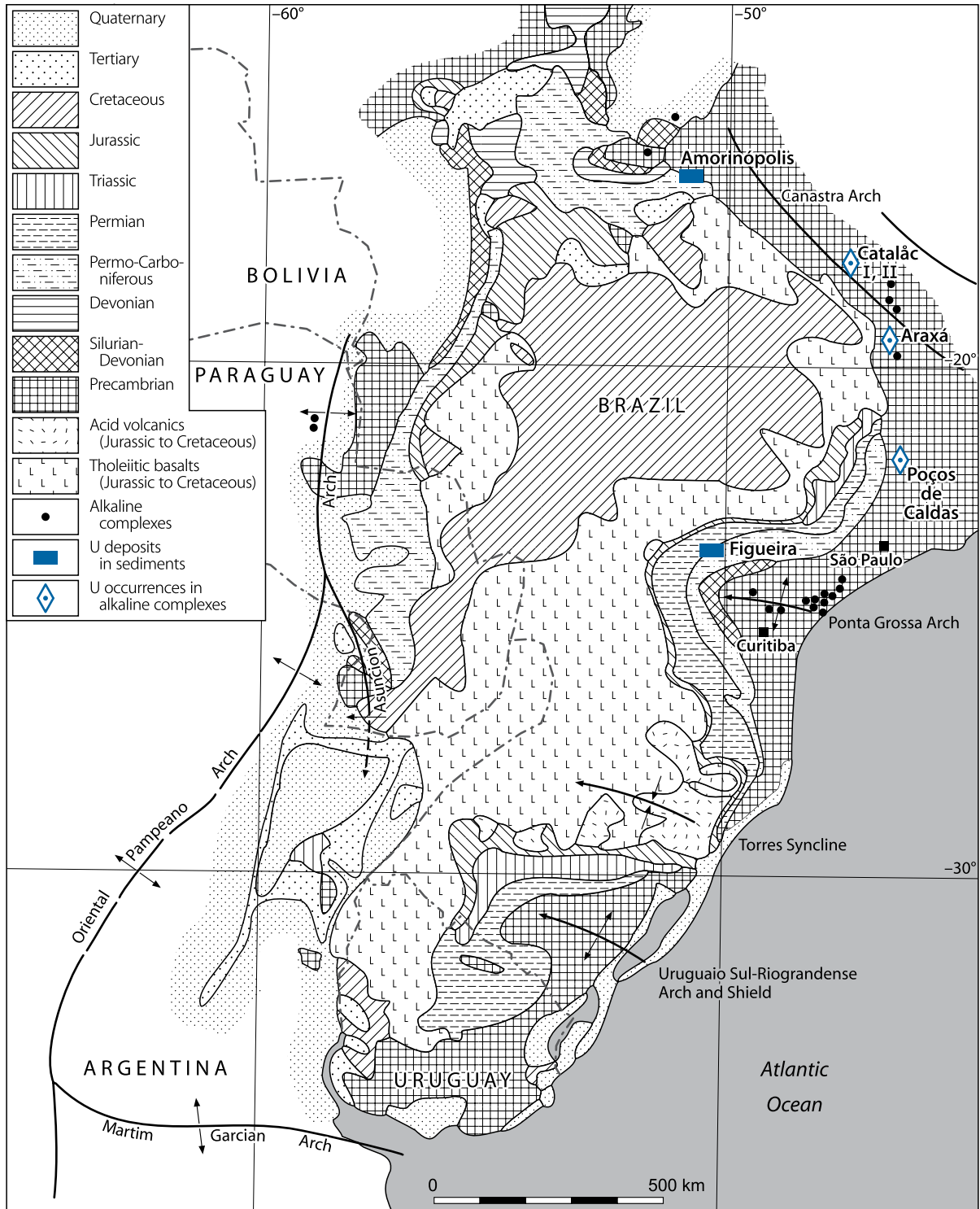
During the Mesozoic era, mainly in Triassic time, redbeds and almost exclusively continental sandstones of eolian and fluvial origin, up to 750 m in thickness, were deposited. In early Cretaceous time (135 to 115 Ma), widespread tholeiitic basalt and felsic volcanics of the *Serra Geral Formation* accumulated to a thickness exceeding 1,500 m.

4.5.1 Figueira District

This district lies near the central-eastern margin of the Paraná Basin, approximately 400 km W of São Paulo. Several sandstone-type uranium occurrences such as *Siqueira Campos*, *Ibaiti*, *Carvaozinho*, *Figueira*, *Sapopema*, and *Telemaco Borba* have been detected in a 100 km-long, N-S-trending belt along the outcropping Permian Rio Bonito Formation (d'Elboux 1984) (► Fig. 4.9).

Fig. 4.9.

Paraná Basin, generalized geological map with uranium occurrences in sediments and alkaline volcanic complexes. (After Ayres 1981; Barretto 1985)



4.5.1.1 Figueira Deposit

The best known deposit in the Figueira district is Figueira, located 5 km NW of the village of Figueira. It contains almost 7,000 t U (OECD-NEA/IAEA 1986); grades average <0.1% U.

Geology and Mineralization

The Figueira deposit is situated in the middle unit of the three-partitioned Permian *Rio Bonito Formation* (Fig. 4.10), which is thought to have been deposited in deltaic and paludal environments. The three lithologic units exhibit the following characteristics at the deposit (Saad (1982):

Upper unit (c): about 20 m thick, fine-grained, laminated sandstone with interbedded siltstone of marginal marine origin locally containing uranium concentrations

Middle unit (b): about 85 m thick, grey-greenish or yellowish siltstone interbedded with variably grey limestone, carbonaceous mudstone, coal seams, and white to red laminated, carbonate cemented sandstone. This unit is the dominant uranium host

Basal unit (a): 15 to 30 m thick, very fine-grained to conglomeratic sandstone, light to dark grey in color, intercalated with arkose, siltstone, dark shale, coal seams, and some grey limestone. Clastic sediments are commonly cemented by carbonate and contain pyrite.

Uranium is present as pitchblende and minor coffinite in the carbonate matrix of sandstone, as urano-organic complexes with phosphate and barium in siltstone and carbonaceous claystone, and as urano-organic complexes in coal. Associated elements are As, Cu, Mo, Pb, Th, and Zn, and traces of Ge, Ni, Se, and V. Mo is present as jordisite and Zn as sphalerite. Pyrite is ubiquitous in uraniumiferous sections.

The main ore body is located in a N-S-trending channel. It is 600 m long and 300 m wide, of lenticular configuration, and consists of mineralized layers ranging from 1.5 to 3.5 m thickness that contain from 0.2 to 0.4% U and 0.12 to 0.42 MoO₃. Uranium grades drop to between 0.02 and 0.07% U outside the channel. U/Mo ratios decrease with increasing U values. The ore is in radiometric disequilibrium in favor (ca. 20%) of chemical uranium. About 30 to 40% of the 7,000 t U resources of Figueira are contained in carbonaceous siltstone and coal.

Metallogenetic Aspects

Baretto (1985), based on the work by Saad (1982), proposes a multistage model for the metallogenesis. Initially, uranium was syngenetically introduced and concentrated in paludal sediments while epigenetic processes concentrated uranium in coarse-grained channel sandstone. This uranium was repeatedly remobilized by diagenetic activity and/or by a renewed influx of oxygenated surface waters. Slightly alkaline intraformational fluids are thought to have transported the uranium to reducing environments where it was deposited and concentrated. With respect to the origin of the ore-forming uranium, Barretto (1985) favors Mesozoic felsic volcanics, which often have high uranium values,

to be the prime uranium source for both the Figueira and Amornópolis deposits, as well as others. During uplift and erosion in Cretaceous time, large quantities of these volcanics were eroded; the contained uranium was released and became available for infiltration into and deposition in the older sediments (Fig. 4.11).

4.5.2 Amornópolis District

A great number of uranium showings have been discovered in the Devonian Ponta Grossa Formation along the northeastern margin of the Paraná Basin. The most explored occurrences are those in the Amornópolis-Iporá area, situated about 375 km SW of Brasilia (Fig. 4.11). They contain low-grade uranium resources estimated at about 5,000 t U.

Geology and Mineralization

The Amornópolis area is underlain by Paleozoic sediments including the Devonian Ponta Grossa Formation, the middle and lower members of which are the prevailing uranium hosts. Characteristics of the Paleozoic suite are shown in the following litho-stratigraphic column (from top to bottom):

Middle Devonian Ponta Grossa Formation

- Laterite capping, locally radioactive
- Purple, ferruginous siltstone and grey, fine-grained sandstone with pink mudstone nodules
- Medium- to coarse-grained, poorly sorted, locally carbonaceous feldspathic sandstone forming continuous horizons, about 3 to 8 m thick, which are interpreted to have originated from meandering and anastomosing streams. This channel sand is the main uranium host
- Yellowish, micaceous, locally pyrite-bearing mudstone locally with low-grade uranium concentrations
- Grey to purple, pyritic siltstone with irregular bedding and interdigitated with mudstone lenses.

Silurian Furnas Formation: grey-yellowish, crossbedded, micaceous sandstone.

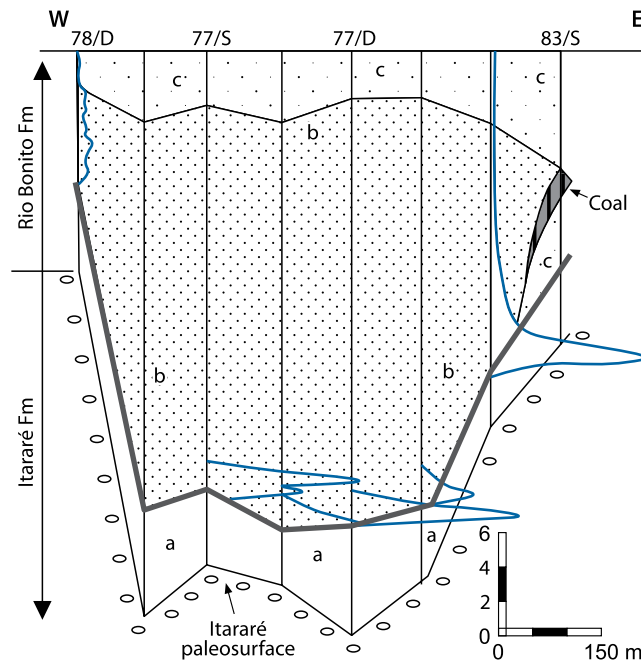
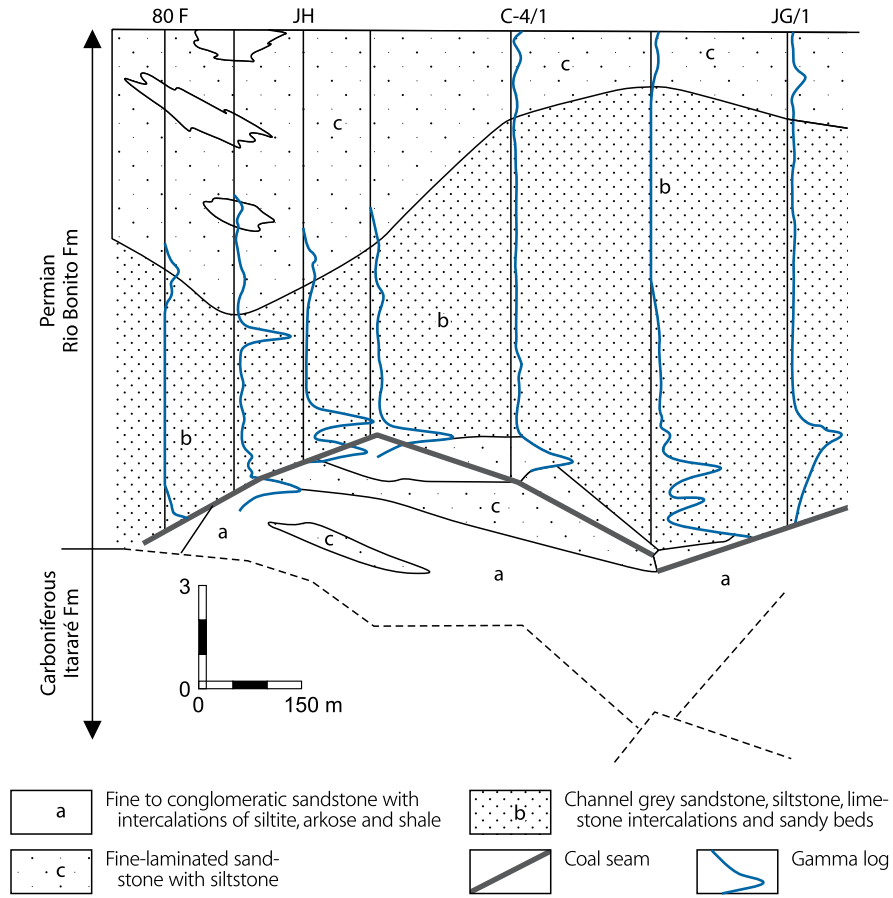
Rocks of the *Precambrian Araxa Group* including gneiss, micaschist, granulite, intrusive granites and ultrabasics form the basement. Some of the granites have high uranium background values. Ultrabasic and alkaline dikes of Late Cretaceous age, dated 70 ± 5 Ma, cut the whole sequence. During Cretaceous time, block faulting with displacements of up to 400 m, mainly along N-S faults, resulted in horst and graben structures.

Baretto (1985) notes three settings of uranium mineralization associated with

- Redox fronts in feldspathic sandstone filling inconspicuous, N to NNW-trending paleochannels
- Faults and fractures, some of them occupied by ultrabasic and alkaline dikes
- Laterite capping large areas.

■ Fig. 4.10.

Paraná Basin, Figuera deposit, cross-sections with drill indicated distribution of uranium mineralization in Permian sediments. (After Barretto 1985 based on Saad 1973)



The first type constitutes the most important U mineralization and includes the *Amorinópolis* deposit. Host rock is a 3 to 8 m thick, yellowish-grey, friable, coarse-grained, poorly sorted, micaceous and carbonaceous feldspathic sandstone, containing clay galls and well-oxidized purple horizons. Uranium occurs in clay galls rich in organic matter and Fe oxides, and in irregular distribution on bedding planes and in fractures. Mineralization, although irregular in grade, is fairly continuous and can be traced along channels about 400 m long, 20 to 40 m wide, and 1 to 10 m thick. It appears to be controlled primarily by coarse-grained sandstone embedded between mudstone or siltstone layers. A degree of structural control has been exerted by faults, dikes, and sills. Uranium minerals include pitchblende and coffinite at depth, and hexavalent uranium minerals in weathered zones. Metallogenetic models of the uranium mineralization at *Amorinópolis* include epigenetic rollfront-type processes as well as syngenetic uranium concentrations.

4.6 Quadrilátero Ferrífero Region

The Quadrilátero Ferrífero (Ferriferous Quadrangle) region is in the southern part of Minas Gerais state (Fig. 4.1). Two areas

with uraniumiferous oligomictic, quartz-pebble conglomerate-type mineralization have been explored in some detail: *Serra das Gaivotas* and *Gandarela*. Cumulative resources are estimated at about 13,000 t U (d'Elboux 1984). Grades are up to 250 ppm U and 0.5 ppm Au (OECD-NEA/IAEA 1978). Similar mineralization also occurs at *Onca do Pitangui*, located about 100 km NW of Belo Horizonte.

Sources of Information. Ayres, 1981; d'Elboux (1984), Forman & Waring (1981), Machado et al. (1989), McNeil (1980), Schorscher (1979), Villaça & Fuzikawa (1973), White (1961, 1964).

Regional Geological Setting of Mineralization

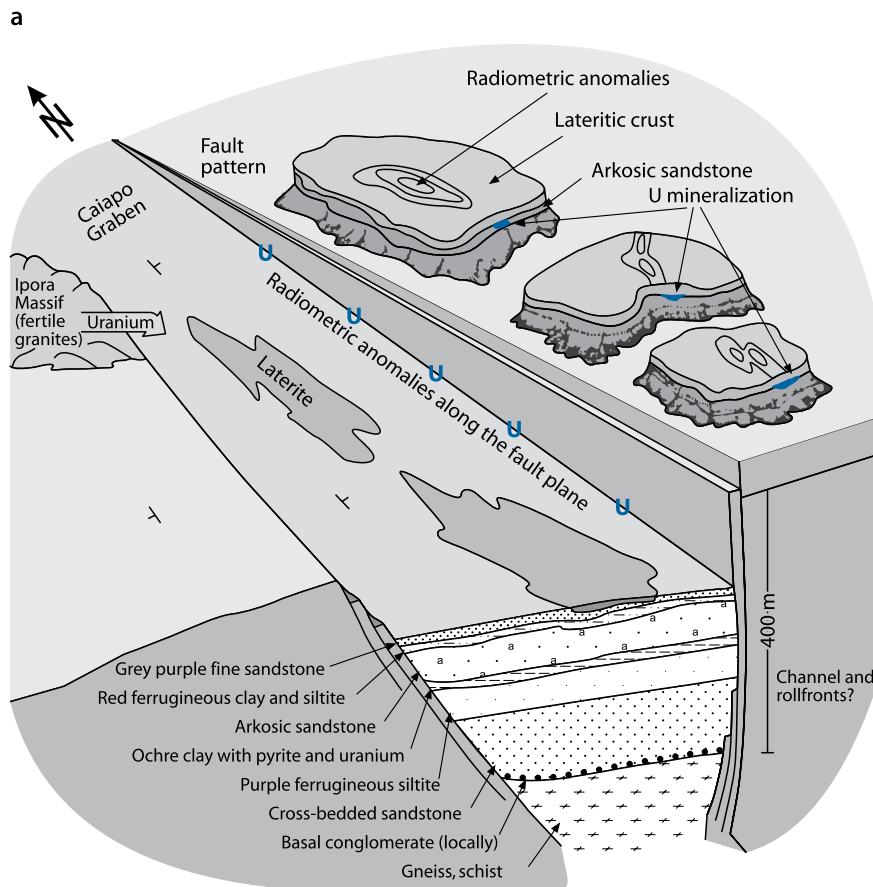
Archean and Paleoproterozoic rocks constitute the Quadrilátero Ferrífero. Following Schorscher (1979), a litho-stratigraphic profile appears as follows (from top to bottom):

Neo- to Mesoproterozoic Itacolomi Series

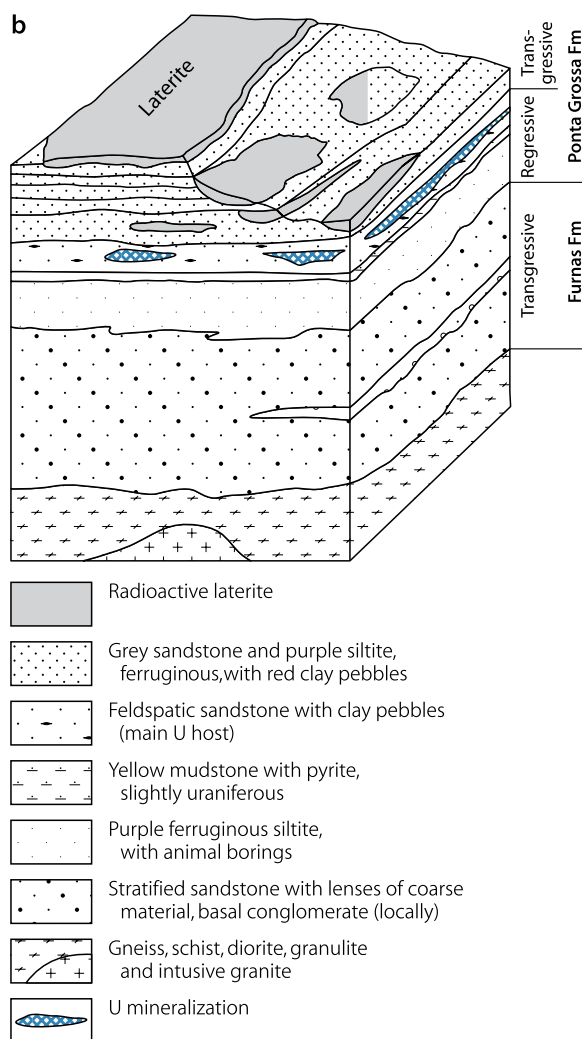
Meso- to Paleoproterozoic Minas Supergroup (or Series): low-grade metamorphosed platform sediments subdivided into three groups (from top to bottom)

Fig. 4.11.

Paraná Basin, Amorinópolis district, (a) blockdiagram of the regional geology, (b) blockdiagram of the litho-stratigraphic sequence, (c) lithologic-sections across U mineralized channels. (After (a) Barretto 1985, (b) and (c) Barretto 1985 based on Saad 1973)



■ Fig. 4.11. (Continued)



- Piracicaba Group: quartzite, phyllite, and dolomitic phyllite
- Itabira Group: carbonates (mainly dolomite) and fine-clastic sediments including large iron and manganese deposits (Superior-type banded iron-formations)
- Caraca Group divided into two formations
 - Batatal Formation: phyllite, shale, and carbonaceous shale
 - Moeda Formation: locally uraniferous oligomictic quartz-pebble conglomerate and quartzite (details see below).

> Unconformity <

Superior Archean Rio das Velhas Supergroup (or Series): divided into three groups of metavolcanics and metasediments contained in a greenstone belt

- Maquiné Group: quartzite, greywacke, and conglomerate
- Nova Lima Group: chiefly heteroclastic biotitic and amphibolitic schists with an Algoma-type banded iron formation (Morro Velho Au deposit)
- Quebra Osso Group: mainly ultramafics.

Inferior Archean basement: granite, granodiorite, and gneiss, polymetamorphosed including retrograde greenschist facies metamorphism.

Isotope dating of the supracrustal and magmatic rocks yields the following ages (Machado et al. 1989): felsic metavolcanics of the Nova Lima Group: $2,776 \pm 23/-10$ Ma; zircon xenocrysts in these metavolcanics: 3,000 to 2,900 Ma; two granite bodies: $2,776 \pm 7/-6$ and $2,730 \pm 10$ Ma; detrital zircon from metagreywacke at top of the Minas Supergroup: $2,125 \pm 4$ Ma; and sphene and monazite from pegmatite: 2,060 to 2,030 Ma. These data suggest an Upper Archean plutonism and a middle Paleoproterozoic magmatic-metamorphic event in the Quadrilátero Ferrífero.

The uraniferous *Moeda Formation* rests unconformably upon Archean granite and gneiss and rocks of the Rio das Velhas Supergroup. A prominent paleorelief exceeding 100 m has locally developed on the basement surface. As a result, the Moeda Formation ranges in thickness from 15 to 320 m. Cyclic sedimentation of conglomerate, quartzite, and minor phyllite is characteristic of this formation with grain sizes decreasing toward the top of each cycle and in the formation as a whole. Conglomeratic horizons of the Moeda Formation, although widespread, are particularly abundant in the northern and central parts of the Quadrilátero Ferrífero. Within these areas, mineralized oligomictic quartz-pebble conglomerates appear to be restricted to the northwestern Serra das Gaivotas and to the central eastern Gandarela areas where they have been deposited along paleochannels in a transitional continental/littoral to marine environment.

Ore Controls and Metallogenetic Aspects

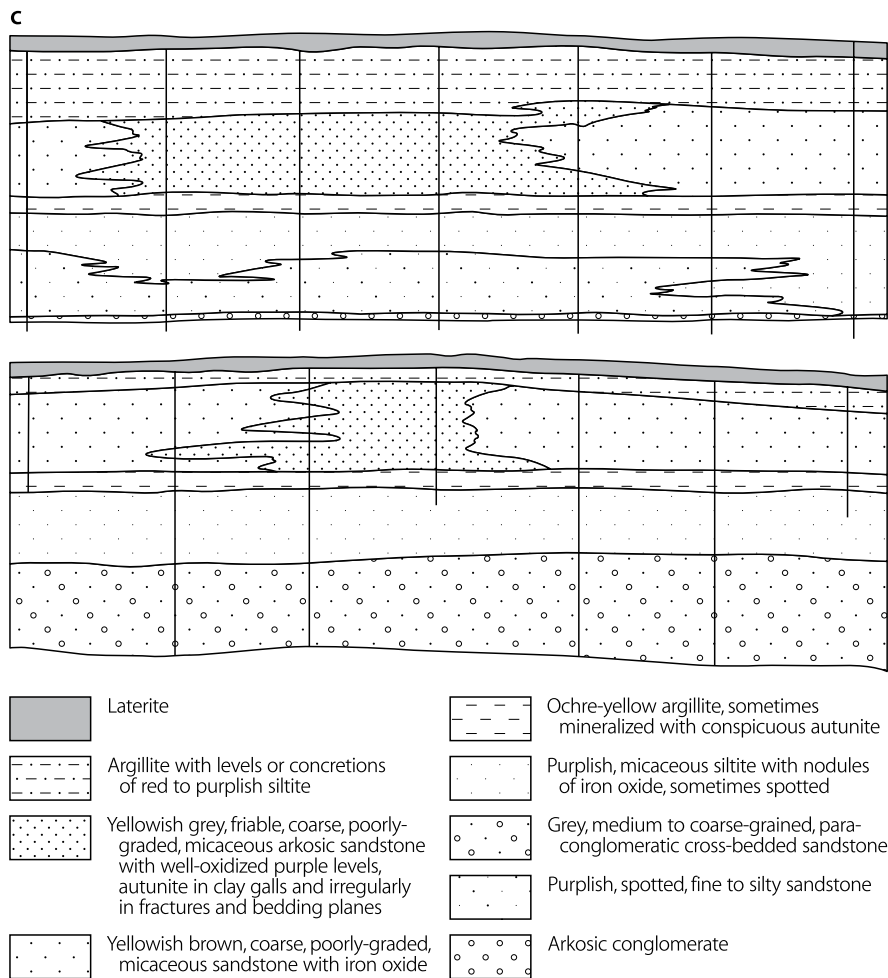
Uranium-gold mineralization in the Paleoproterozoic Moeda Formation is of oligomictic paleoconglomerate type. Host rocks are mature, pyrite-rich, quartz-pebble layers of fluvial provenance. The original introduction of uranium, gold, pyrite, etc., is syngenetic and controlled by lithology. Later processes caused remobilization of the ore constituents and resulted in the formation of pitchblende, coffinite, and new generations of pyrite. These characteristics suggest that a modified placer model would be a best fit for a metallogenetic explanation of the present-day mineralization.

4.6.1 Serra das Gaivotas Area

This area is located 30 km SSW of Belo Horizonte on the western flank of the N-S-oriented Moeda syncline in the northwestern part of the Quadrilátero Ferrífero. Uranium is hosted in the Moeda Formation. Lithologic characteristics of this formation in the Serra das Gaivotas area are as follows (Forman & Waring (1981) (from top to bottom):

- Light grey, fine-grained quartzite, ca. 35 m thick, with abundant sericite in some layers, and occasional intercalations of dark grey phyllite, cut by veins of milky quartz
- Grey phyllite, well laminated by sericite, ca. 5 m thick
- Medium to light grey, medium-grained quartzite, ca. 30 m thick, with interbeds of coarse-grained, moderately to well-sorted quartzite, cut by some veins of milky quartz

Fig. 4.11. (Continued)



- Polymictic conglomerate, ca. 15 m thick, composed of pebbles of quartzite and schists, 1 to 10 cm in diameter, within a matrix of abundant quartz, and frequent intercalations of coarse-grained quartzite
- Oligomictic quartz-pebble conglomerate, ca. 5 m thick (principal mineralized horizon)
- Light grey quartz-sericite schist, 20 to 25 m thick, with some intercalations of conglomerate.

This suite rests unconformably upon a basement of grey to pink schists of the Nova Lima Group/Rio das Velhas Supergroup, and Archean granite and gneiss. Two fault systems dissect the metasediments. Thrust faults trend N-S, and transcurrent faults trend WNW-ESE.

Uranium and low-grade gold mineralization in oligomictic quartz-pebble conglomerate beds, up to 5 m thick, occurs in NE-SW-oriented paleochannels near the base of the Moeda Formation. Quartz and rare quartzite pebbles about 2 to 3 cm in diameter are the principal clasts. They are embedded in a light green matrix of sericite and quartz with abundant pyrite (5 to 20 vol. %) and heavy minerals. The matrix constitutes 60 to 80% by volume of the rock and contains, as principal uranium minerals, uraninite, some pitchblende, coffinite, and thucholite; the latter

associates with amorphous hydrocarbons. Other heavy minerals include chalcopyrite, monazite, pyrite, pyrrhotite, rutile, zircon, and traces of gold. Pyrite is present in at least three varieties: (a) finely disseminated throughout the matrix; (b) as rounded, large aggregates presumably of detrital origin (gold and to a lesser degree uranium minerals are associated with this pyrite); and (c) euhedral pyrite crystals obviously unrelated to uranium minerals. The uranium tenor is about 100 ppm U. Ayres (1981) reports a $\text{ThO}_2/\text{U}_3\text{O}_8$ ratio ranging from 0.11 to 1.15, averaging 0.46.

4.6.2 Gandarela Area

Gandarela is located approximately 65 km SE of Belo Horizonte, at the southern end of the NE-SW-oriented Gandarela syncline in the central-eastern part of the Quadrilátero Ferrífero. Majdalani & Tavares (2001) report resources of 2,000 t U at a grade of 250 ppm U (Forman and Waring, 1981 estimated resources of 6,800 t U). The uraniferous Moeda Formation ranges from 15 to 320 m in thickness. It was deposited by southwesterly flowing paleostreams upon a surface, which exhibits strong relief, locally exceeding 100 m. Subjacent rocks are metamorphics of the Archean Nova Lima Group. The Moeda sequence includes

oligomictic quartz-pebble conglomerates, the pebble size of which decreases from E to W and from N to S. Thrust faults strike E-W and transcurrent faults strike N-S; both caused variable amounts of displacement (Ayres 1981).

Mineralization at Gandarela corresponds to that of Serra das Gaivotas and is hosted by highly matured oligomictic quartz-pebble conglomerates containing pyrite nodules and carbonaceous material. Gold is commonly associated with uranium at the base of the Moeda Formation and occasionally on higher levels.

4.7 Rio Preto-Campos Belos Region

This region is situated north of Brasília, in the central eastern part of Goiás state. A number of small structurally controlled uranium occurrences have been discovered, most of them in the *Rio Preto* area (Figs. 4.1 and 4.12a). Numerous U showings also occur 140 km further to the NE in the *Campos Belos* area. Total resources of the region are estimated at some 1,000 t U.

Sources of Information. d'Elboux 1984; de Figueiredo Filho 1984; Figueiredo & Oesterlen 1981.

Geology and Mineralization

The regional geology (Fig. 4.12a) comprises an Archean to Paleoproterozoic basement complex (granite gneiss with subordinate migmatite and pegmatite), which hosts the uranium occurrences at *Campos Belos*. This basement is overlain by the Paleoproterozoic Ticunzal Formation, host to the uranium occurrences at *Rio Preto*. The Ticunzal Formation is divided into a lower member of biotite paragneiss with intercalated, locally graphitic, biotite-muscovite schist and amphibolite, and an upper member of graphitic muscovite-biotite schist grading upward into garnet- and tourmaline-bearing schist and quartz schist. Partial retrograde metamorphism caused chloritization, sericitization, etc. Dikes of pegmatite, mafic rocks, and quartz are common. Both the basement complex and the Ticunzal Formation have been intruded by a younger generation of granitic-granodioritic plutons. Some of the granite intrusions contain tin greisens, gold, and high uranium tenors.

Metasediments and intercalated metavolcanics of the Mesoproterozoic Arai Group unconformably overlie the older units. The lower metasediments consist dominantly of quartzitic sequences with conglomeratic beds and rhyolitic to andesitic metavolcanics of the Arraias Formation, upon which rest quartz schists with silty, phyllitic, and impure limy intercalations of the Trairas Formation. Locally, marly to limy metasediments of the Bambui Group unconformably repose on the Arai Group or the basement.

Metamorphism affected the region at least three times at about 2,000 Ma, 1,400 to 1,000 Ma, and 650 to 450 Ma ago. The structural grain is reflected by N to NNE-trending fold axes and schistosity.

Uranium concentrations in the *Campos Belos* area are restricted to the basement complex, in which mineralization

(presumably of surficial origin) occurs fault-controlled in early Paleoproterozoic, cataclastic, leucocratic gneiss and schist (Fig. 4.12b). Ore shoots are 2 to 3 m thick and extend to a depth of at least 60 m (d'Elboux 1984).

Uranium occurrences in the *Rio Preto* area are found primarily in two types of host rocks of the late Paleoproterozoic Ticunzal Formation (de Figueiredo Filho 1984):

- Cataclastic, graphitic, biotite-muscovite schist with pegmatite injections and quartz veins contain, on schistosity planes and in fractures, uraninite at depth and hexavalent uranium minerals near the surface.
- Dike-like bodies of biotite schist with locally abundant hornblende and apatite contain uranium, at depth as uraninite, irregularly and discontinuously dispersed in small fractures along the contact with paragneiss. These biotite schist bodies are emplaced with sharp contacts in paragneiss, and both are affected by cataclasis. The biotite is thought to be a recrystallization product of metasomatism.

Uranium is associated with pyrite and chalcopyrite. Host rocks are commonly altered by chloritization, hematitization, and argillization. Schists containing little biotite are usually barren of uranium.

More than ten mineralized zones have been explored in some detail at Rio Preto. They are a few hundred meters (max. 3,000 m) long and about 100 m wide. The larger mineralized structures average 0.85 m in thickness and extend to a depth of at least 80 m. They may contain some hundred tonnes of uranium at grades ranging from 0.05 to 0.2% U and less than 0.01% ThO₂ (de Figueiredo Filho 1984).

Hypotheses on ore formation range from supergene to hypogene hydrothermal related to the granite intrusion, or lateral secretory related to final tectonic phases of the Brazilian Orogeny, with redistribution of uranium from earlier vein deposits along the Proterozoic unconformity.

4.8 Serra de Jacobina Region

This region is located in north-central Bahia state (Fig. 4.1). Mineralization is of oligomictic paleoconglomerate type similar to the Witwatersrand uranium-gold deposits of South Africa.

Sources of Information. Button and Adams 1980; Gross 1968; McNeil 1980; Ramdohr 1958; White 1961.

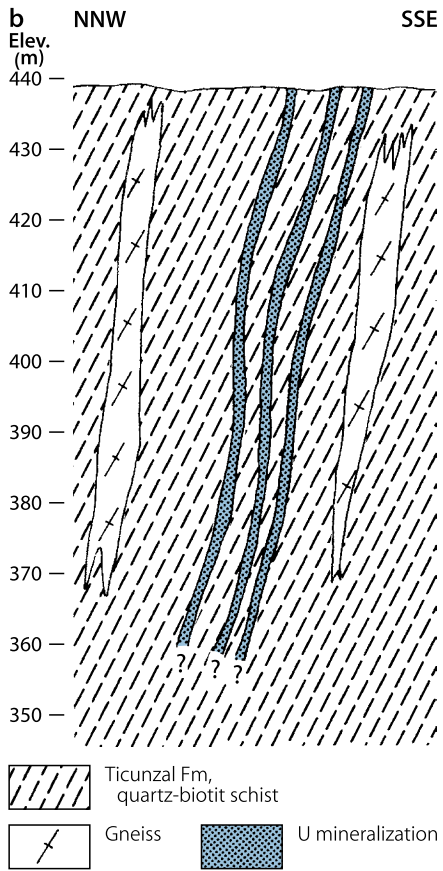
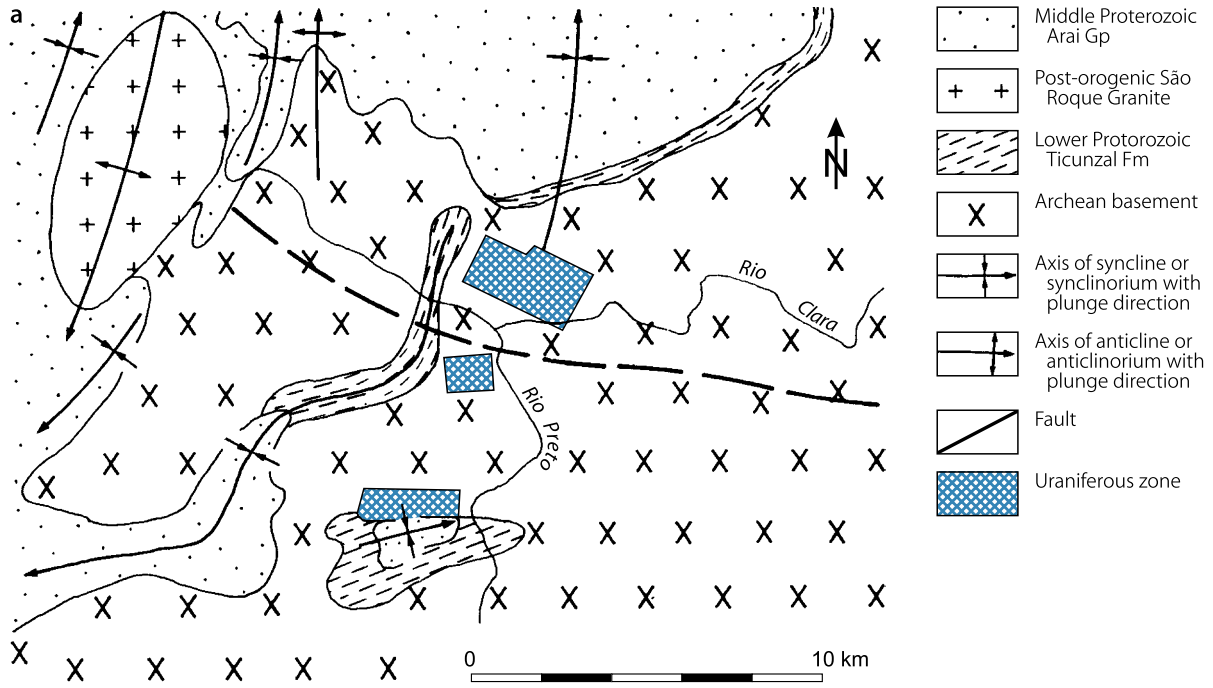
Geology and Mineralization

Uranium and gold mineralization occurs in oligomictic conglomerates of the Serra de Corrego Formation at the base of the Jacobina Series of Paleoproterozoic age, which is correlated with the Minas Series in the Quadrilátero Ferrífero.

The *Jacobina Series* is a folded and metamorphosed sedimentary sequence, several thousand meters thick, which extends for approximately 65 km in a N-S direction and dips about 60°E. Lithologies include thin-bedded to massive quartzite and

Fig. 4.12.

Rio Preto-Campos Belos region, (a) generalized geological map with location of uraniferous zones, (b) schematic NNW-SSE section across a uraniferous zone. Radioactivity ranges from 15 to 4,000 times background in the mineralized zones (bg ~100 cps). (After (a) Forman & Waring 1981, (b) de Figueiredo Filho 1984)



conglomerate beds, overlain by itabirite in the lower section and by phyllite higher up. The metasediments rest unconformably on Archean granite and gneiss of the São Francisco Craton. Faults and basic to ultrabasic dikes dissect the whole complex.

Four conglomeratic horizons are known in the lower section of the Jacobina Series, two of which, the Liberino Reef and the Piritoso Reef, each 1.5 to 2.5 m thick, are uraniferous and lie at least 150 m above the unconformity. The two horizons are composed of well-compacted quartz pebbles, 2–4 cm in diameter, embedded in a highly silicified quartz-sericite matrix containing abundant pyrite and chlorite. The principal uranium minerals are uraninite, some pitchblende, and brannerite. Other heavy minerals include pyrite, rutile, zircon, and chromite, the latter constitutes up to 35% of the heavy mineral fraction in gold operations (Ramdohr 1958). Uranium and gold tenors in the *Canavieiras* gold mine near Jacobina range from 100 to 200 ppm and from 7 to 15 ppm, respectively.

4.9 Serra dos Carajás Region

Located in southeastern Pará state, the Serra dos Carajás hosts large Fe oxide-Cu-Au-(U-REE) deposits that tend to belong to the polymetallic breccia complex type as known from the Olympic Dam deposit in South Australia. Resources of major deposits range from 170 million tonnes (Cento e Dezoito deposit) to almost 1,000 million tonnes ore (Salobo). Copper grades average between 0.94% (Salobo) and 1.4% (Igarapé Bahia) with gold grades between 0.28 g/t (Sossego) and 0.86 g/t (Igarapé Bahia).

Source of Information. Tallarico et al. (2005). In synopsis, these authors provide the following account of the Serra dos Carajás region and, in particular, of the *Igarapé Bahia* deposit.

Regional Geological Setting of Mineralization

The Carajás region lies in the eastern part of the Archean Amazon Craton (Fig. 4.1). Basement rocks comprise gneiss and migmatite of the Xingu Complex and orthogranulite of the Pium Complex, which were metamorphosed 2.8 Ga ago.

Variably metamorphosed volcano-sedimentary rocks of the Late Archean Itacaiúnas Supergroup rest upon the basement in the Carajás Basin. Metamorphic grades range from practically unmetamorphosed to amphibolite or granulite facies. The Grão Pará Group is the most widespread unit in this basin. It comprises low-grade metamorphosed volcanic rocks, dated at ca. 2,750 Ma, and significant accumulations of intercalated banded iron formation (BIF), including very large iron deposits. Shallow marine to fluvial clastic sediments of the Archean Águas Claras Formation/Rio Fresco Group overlie the Grão Pará Group. Archean granitoids and diorites including alkaline monzogranite of A-type geochemistry, and Paleoproterozoic anorogenic granites have been intruded into the older rocks.

A broad, E-W-trending, steeply dipping, ductile shear zone (Itacaiúnas shear zone) that was repeatedly reactivated during the Archean and Paleoproterozoic, transects the basement.

A variety of Cu-Au deposit types are clustered in the Carajás region, of which Fe oxide-Cu-Au-(U-REE) deposits are the most prominent. The latter consist of steeply dipping breccia bodies hosted by variably hydrothermally altered metavolcano-sedimentary rocks. Tallarico et al. (2005) list the characteristic features of these deposits as: (1) intense Fe metasomatism reflected by formation of grunerite, fayalite, and/or magnetite and/or hematite; (2) intense carbonatization (mainly siderite); (3) sulfur-poor ore mineralogy (chalcopyrite, bornite); (4) enrichment in U and Cu; (5) extremely low REE enrichment, and (6) lack of gangue quartz as a result of silica dissolution.

4.9.0.1 Igarapé Bahia Deposit

This deposit consists of four ore bodies with Fe oxide-Cu-Au-(U-REE) mineralization hosted in polymict breccias. Three ore bodies crop out at surface and are planned to be mined by open pit methods. The fourth ore body is down dropped and covered by sandstone 250 m thick. Resources amount to 219 mio. t of ore. Copper and gold grades average 1.4% and 0.86 g/t, respectively.

Geology and Mineralization

Ore-bearing breccia bodies are arranged in a circular structure at surface, on the order of 1,600 m in diameter, and are contained in metavolcano-sedimentary lithologies of the Igarapé Bahia Group, which is presumably a facies of the Grão Pará Group. Arenites of the Águas Claras Formation rest upon this group. These breccia bodies dip ca. 75° outward roughly parallel to the strike of host strata bedding. Mineralized breccias are located at or close to the contact between two lithologic units. The upper unit is dominated by sedimentary and epiclastic facies while the lower unit comprises predominantly volcanic and pyroclastic rocks with intercalated BIF. Breccia fragments, a few millimeters to 20 cm in size, originated from all country rocks and are embedded in variable amounts of hydrothermal matrix minerals. Radial faults as well as quartz diorite and diabase dikes intersect ore bodies and country rocks.

Chloritization with apparently less intense carbonatization is the most pronounced *alteration* phenomenon. Authigenic Fe chlorite prevails in ore-hosting breccias where it associates with siderite, magnetite, and chalcopyrite, while Mg chlorite associated with calcite and dolomite is typical for barren and weakly altered ground outside the breccia bodies.

Weathering has altered the deposit to depths of approximately 200 m, resulting in dissolution of ore minerals and formation of supergene minerals: gold in a gossan to depths of about 150 m and copper in a transition zone from 150 to 200 m.

Primary mineralization occurs at depths below 200 m. Based on matrix mineralogy three principal breccia types are discerned: Fe chlorite, siderite, and magnetite-rich breccias. Except for a highly different ratio of Fe chlorite to siderite, *Fe chlorite breccias* and *siderite breccias* have practically the same matrix mineralogy, which is mainly composed of fine-grained Fe chlorite,

siderite, magnetite, chalcopyrite, and minor tourmaline. *Magnetite breccias* typically contain euhedral magnetite cemented by chalcopyrite intergrown with bornite, and minor actinolite, ankerite, biotite, fluorite, grunerite, K feldspar, minnesotaite, siderite, stilpnomelane, tourmaline, and uraninite. Trace amounts of allanite, altaite, apatite, bastnäsité, cassiterite, cobaltite, ferberite, galena, hessite, monazite, parasite, pyrite, and scheelite may occur in addition in all breccia matrices.

Cu-rich ore contains gold independent of breccia type. Native gold is present as fine-grained (5–20 µm) inclusions in gangue minerals (quartz, siderite, and chlorite), chalcopyrite, and rarely magnetite. Gold grains contain up to 12 wt % Ag and may also have inclusions of hessite, argentite, and/or acanthite. In addition, subeconomic copper occurs disseminated or in veins or nodules in distal, altered rocks. Gold tenors are negligible in these settings.

A variety of veins cut the mineralized breccias and adjacent metavolcanic rocks. Mineral assemblages comprise most commonly (a) calcite + chalcopyrite±fluorite±stilpnomelane; (b) ankerite±chalcopyrite±gold; (c) siderite±calcite±chlorite±chalcopyrite; and (d) chalcopyrite±biotite±Kfeldspar±tourmaline±REE minerals.

As mentioned earlier, ore is confined to four breccia bodies of variable size. As can be deduced from figures in Tallarico et al. (2005), the outcropping Acampanento Sul ore body, located on the NE flank of the circular structure, has surface dimensions on the order of 1,600 m in length and 40–200 m in width, and extends to depths of at least 1,100 m.

Geochemical analyses of drill hole samples from this ore body give, in summary, the following range of elements contents: 25 to 64 wt % FeO_{total}, 0.5 to 11 wt % Cu, 0.5–9 wt % CaO, 0.5–3 wt % MnO, 0.5 to 15 ppm Au, 4 to 52 ppm Ag, 26 to 200 ppm Ba, 450 to 4,400 ppm Ce, 390 to 31,000 ppm F, 260 to 2,300 ppm La, 50–200 ppm Mo, 900 to 6,200 ppm P, 28 to 380 ppm U, and 150–450 ppm Zn.

REE patterns characterized by low REE enrichment (~ 104 chondritic values) are similar in iron chlorite, siderite, and magnetite breccias. But contrasting La/Lu ratios in host metavolcanics (70–250) and ore-bearing breccias (1,000–2,500) indicate a selective concentration of low REE during hydrothermal alteration and mineralization. The positive correlation between La, Ce, P, Cu, and Au supports the assumption that low REE minerals (e.g. monazite) are constituents of ore paragenesis.

SHRIMP dating of zircon from host metavolcanics yields a ²⁰⁷Pb/²⁰⁶Pb age of 2,748 ± 34 Ma, of authigenic monazite from ore-bearing magnetite breccias a ²⁰⁷Pb/²⁰⁶Pb age of 2,575 ± 12 Ma, and of zircon xenocrysts from diabase dikes a maximum ²⁰⁷Pb/²⁰⁶Pb age of ca. 2670 Ma. Based on these data, Tallarico et al. (2005) forward a metallogenetic model in which the time difference of ca. 175 Ma between mineralization and formation of the volcano-sedimentary host together with stable isotope and fluid inclusion, mineralogical, and geochemical data support an epigenetic origin for Fe oxide-Cu-Au-(U-REE) mineralization

from a deep source. The latter is, among other evidence, deduced from carbonates of the Igarapé Bahia deposit, which give a wide range of ⁸⁷Sr/⁸⁶Sr ratios (0.714–0.755), and which is interpreted by the authors to suggest multiple crustal sources, consistent with a magmatic-hydrothermal origin. A possible genetic relationship of mineralizing processes to intrusion of Archean A-type granites in the Carajás belt about 2.57 Ga ago is indicated by the coeval activity of these two events.

4.10 Other Uranium Resources in Brazil

At least eleven U occurrences with uraninite/pitchblende in quartzite and metaarkose are known in the *Rio Cristalino area* in southeastern Pará state. All were discovered prior to 1984 when exploration was interrupted (Majdalani and Tavares 2001). Selected samples contain as much as 5.2% U.

Phosphate deposits in the *Olinda area*, Parabaíba state, contain 120–140 ppm U and resources of 28,000 t U.

The carbonatite of *Araxá*, emplaced in the South Brazilian Shield along the eastern edge of the Paraná Basin in Minas Gerais state, is not only the largest Nb deposit of the world, but also contains 13,000 t U and several hundred thousand tonnes thorium. The uranium tenor is 80 ppm (Majdalani and Tavares 2001).

Selected References and Further Reading for Chapter 4 Brazil

For details of literature see Bibliography.

Amaral 1984; Andrade and Camarço 1982; Andrade Ramos and Fraenkel 1974; Angeiras et al. 1981; Ayres 1981; Ballhorn et al. 1981; Barretto 1985, 1988; Brito et al. 1984; Brito Neves et al. 1979; Button and Adams 1980; Caby and Arthaud 1987; Cathles and Shea 1992; Chapman et al. 1992; Cordani et al. 1992; de Andrade Ramos and Fraenkel 1974; de Figueiredo Filho 1984; de Figueiredo Filho et al. 1982; d'Elboux 1984; de Matos 2005; de Miranda Filho and Cabaleiro Rodrigues 2003; Departamento Nacional de Produção Mineral 1980, 1981; Figueiredo and Oesterlen 1981; Forman and Angeiras 1981; Forman and Waring 1981; Fuchs et al. 1981; Fuzikawa 1980, 1982; Fuzikawa K et al. 1990; Galarza et al. 2008; Geisel et al. 1980; Gross 1968; Haddad and Leonardos jr 1980; Hassano and Stein 1979; Holmes et al. 1992; INB 2000; Inda and Barbosa 1978; Jardim de Sá et al. 1976; Lichtner and Waber 1992; Lobato and Fyfe 1990; Lobato et al. 1982, 1983; Machado et al. 1989; Majdalani and Tavares 2001; Maruéjol et al. 1987; McNeil 1980; Miekeley et al. 1992; NAGRA 1993; Netto et al. 1991; OECD-NEA/IAEA 1986, 1997, 1999, 2007; Oliveira 1966, 1968; Oliveira et al. 1985; Pascholati et al. 2003; Porto da Silveira et al. 1991; Rabelo and Camarço 1982; Ramdohr 1958; Raposo and Matos 1982; Raposo et al. 1984; Read 1992; Rocha 1992; Romero et al. 1992; Saad 1982, 2000; Saad et al. 1984; Santos 1981; Santos and Brito Neves 1984; Santos and Mello 1979; Schobbenhaus and Campos 1984; Schorsch 1979; Schorsch and Osmond 1992; Schorsch and Shea 1992; Shea 1992; Stein et al. 1980; Surcan Santos 1984; Tallarico et al. 2005; Tassinari and Barretto 1992; Turpin et al. 1988; Ulbrich 1984; Villaça & Fuzikawa 1973; Villaça and Hashizume 1982; Waber 1991; Waber et al. 1992; Wernick et al. 1979; White 1961, 1964; Zenker 1982; Zenker and Hohn 1982.

Chapter 5

Peru

Noteworthy uranium occurrences occur in the district of *Macusani*, Department of Puno, in southeastern Peru. OECD-NEA and IAEA (2007) reports recoverable resources of 2,900 t U in the identified resources (RAR + Inferred) <US\$ 130/kg U category (Note: earlier reports state higher amounts as shown below). Additional resources of approximately 173,000 t U are estimated to exist in phosphorite deposits with an average tenor of 100 ppm U (status 1993).

Uranium exploration commenced in Peru in 1953, at first in cooperation with the US-AEC. In 1975, IPEN, the national Nuclear Energy Institute started to search for uranium and proved to be successful with the discovery of the volcanic-type deposits at *Macusani* in 1980 as well as *Colquijirca* (reportedly ca. 500 t U, 0.2% U), *Turmalina* (collapse breccia pipe?, ca. 500 t U, 0.2% U), and *Villacabamba* (vein, ca. 500 t U, 3% U). Exploration was only carried out on a limited scale, however, and ceased in 1992. More recently, exploration has been revived in the *Macusani* and other regions. Reported discoveries include the two volcanic-type deposits *Colibri* and *Corachapi*.

5.1 Macusani District

Macusani is located approximately 150 km NNW of Lake Titicaca (Fig. 3.1). More than 40 uranium occurrences have been discovered in Tertiary felsic volcanics in the NE part of the Meseta Quenamari, mainly in the *Huiquiza-Tantamaco* and *Huacchane areas* with the major occurrences *Esperanza*, *Pinocho*, *Huiquiza*, *Chilcuno*, *Cuychine*, *Kiguitan*, and at *Cerro Calvario*, *Cerro Choncha Rumio*, and *Chapi-Alto* (Fig. 5.1a).

In situ resources of the district (established prior to 1999) amount to 3,650 t U in the RAR and EAR-I category while the potential resources are estimated at 30,000 t U, 10,000 t of which are attributed to *Chapi*, which is considered the most significant occurrence in the *Macusani* district. Uranium grades average about 0.1% U (OECD-NEA/IAEA 1986, 1999).

Sources of Information. Arribas and Figueroa 1985; Cánepa and Rosodo 1981; Chemillac 2004; Herrera and Rosado 1984; Hetland and McMichie 1984; Sosa et al. 1981; Valencia and Arroyo 1985; Locardi 1984, personal communication.

Regional Geological Setting of Mineralization

Uranium mineralization occurs in felsic volcanics forming part of the Tertiary-Quaternary volcanic belt, which stretches along the Altiplano and western flank of the Cordillera Oriental roughly parallel to the coastline of the Pacific Ocean. This belt extends from the Quenamari and Picotani mesetas in southeastern Peru

to Bolivia where it encloses the Sevaruyo and Charazani uranium districts and onward into Chile, and northwestern Argentina (Fig. 3.1).

Tertiary ignimbrites of the Quenamari Formation, ca. 350 m thick in the *Macusani* area, rest unconformably upon a Paleozoic basement that was affected by two Hercynian tectonic events and is composed of schist, slate, quartzite, limestone, dolomite, and pyroclastic rocks of Carboniferous to Permo-Triassic age, and Hercynian granites. Quaternary fluvial and glacial clastics fill valleys, while lacustrine and alluvial formations fill intra-Andean depressions (Fig. 5.1b).

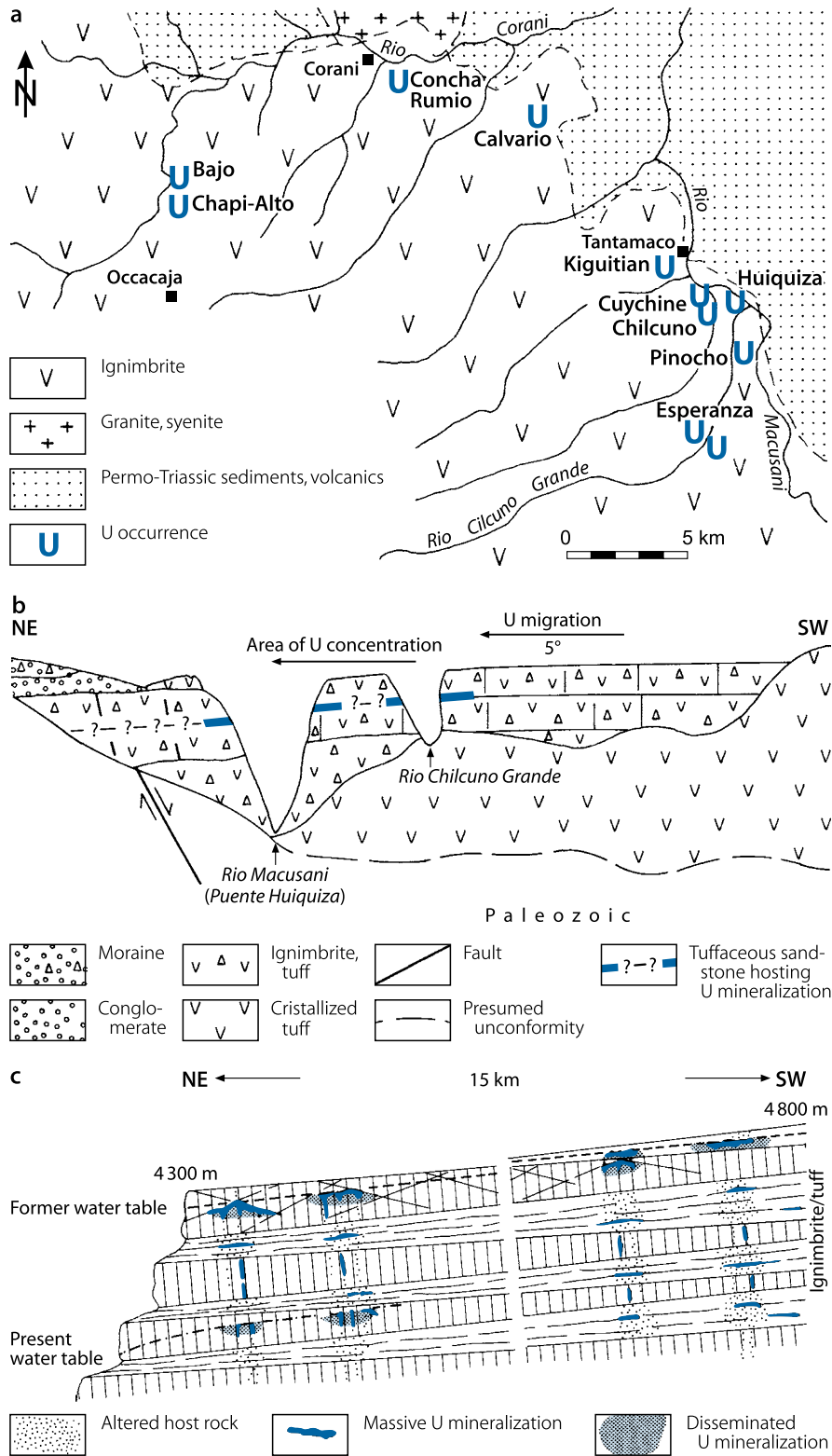
In late Miocene, regional lineaments initiated by the Andean Orogeny displaced the basement into horst and graben structures. Grabens are filled with lacustrine sediments and pyroclastics including the uranium-hosting ignimbrite of the Quenamari Formation, which was emplaced in the *Macusani Graben* and which forms the Quenamari Meseta about 500 km² in size. The *Quenamari Formation* is of Miocene–Pliocene age and exhibits the following stratigraphic-petrologic succession, from top to bottom (Valencia and Arroyo 1985):

- Claystone, diatomite, silicified limestone of lacustrine origin, and redistributed tuff of whitish color; up to roughly 10 m in thickness
- Epiclastic tuff of local distribution derived by in situ disintegration of ignimbrite; up to 10 m thick
- Ignimbrite series of alternating effusions of white to light grey ignimbrite and tuff, separated by erosional surfaces. Ignimbrite units are 30–50 m thick and consist of individual sheets a few meters thick each. Tuffaceous beds average about 10 m in thickness. Total thickness is some 350 m. Dip of the tuff sheets is commonly 5–20°NE except near the eastern edge of the graben where the inclination is opposite. Ignimbrites typically show two systems of partitioning, subvertical, and subhorizontal. The first corresponds to cooling cleavages imprinting columnar jointing on the rocks. It is particularly well developed in the upper units of the volcanic pile. The second system is reflected by conjugating, low-angle (5–15°) divisional planes. These planes result from successive compaction and distention with subsequent gravitational adjustment of the volcanic material. The ruptures, both subvertical and subhorizontal, are abnormally wide, up to a few centimeters, which may be partly due to solution processes. K/Ar dating gives an age of 4.2 ± 1.5 Ma for macusanite, an obsidian-type volcanic glass (see below), and 4.1 ± 1 Ma for biotite in ignimbrite (Pichavant in Valencia and Arroyo 1985)
- Basal flows of vesicular basalt.

Petrographically, the Quenamari Formation corresponds to pyroclastic ignimbrites and tuffs of rhyolitic composition showing vitroclastic to pseudofluidal texture. The rocks are characterized by (a) peraluminous chemistry, (b) an unusual mineralogical association of andalusite, muscovite, sillimanite, and (c) enrichment in volatiles as evidenced by abundant topaz and tourmaline, and in traces of metallic elements. Lithic clasts consist of andesite, granite, ignimbrite, pelite, quartzite, macusanite (with

Fig. 5.1.

Peru, Macusani district, (a) generalized geological map with location of principal uranium occurrences, (b) schematic section across the Huiquiza Deracha No. 1 uranium occurrences at Puente Huiquiza, (c) scheme of uranium distribution and host rock alteration in ignimbrite layers.



inclusions of andalusite crystals), and abundant fragments of devitrified glass. Phenocrysts are composed of authigenic hyaline and smoky quartz crystals, albite, andalusite, apatite, biotite, muscovite, obsidian, sanidine, topaz, zoned plagioclase, and, as relict minerals, ilmenite, sillimanite, tourmaline, zircon, and green spinel. Some apatite, plagioclase, and sanidine appear also to be remnants of anatectic origin. Matrix constituents are biotite, quartz, and feldspar often affected by argillization with kaolinite and montmorillonite formation. The principal petrographic composition is high siliceous and peraluminous with Q + Ab + Or + Co constituting in excess of 95% of the rock.

Though local variations in modal mineral distribution exist, the Quenamari ignimbrites show no overall significant differences in either mineralogical or chemical composition. The ignimbrites include *macusanite*, a local variety of unaltered volcanic glass. Its chemical composition is considered representative for that of the ignimbrite suite as a whole and is taken by Valencia and Arroyo (1985) for the geochemical characterization of the pyroclastics of the Quenamari Formation. Major constituents of macusanite include, on average, 72% SiO₂, 14.3–15.3% Al₂O₃, 4.5–5.7% K₂O, and 3.5–4% Na₂O. Ca, Mg, Fe, Mn, and Ti are very minor amounting cumulatively to less than 2.5%. P₂O₅ is 0.34% and, as such, is higher than in other rhyolites (0.1%) in Peru. The most notable differences in Quenamari ignimbrites are reflected by K₂O/Na₂O ratios showing values of more than 1 in devitrified and less than 1 in unaltered macusanite, which may be attributed to devitrification and argillization of the quartzo-feldspathic matrix. Minor element distribution shows vertical variations with exceptional concentrations of volatile elements as well as of As, Be, Cs, Rb, Sn, and Tl. Mo, Sr, W, and REE are impoverished. U is almost twice as high in macusanite (18 ppm) as in ignimbrite (ca. 10 ppm). Th behaves oppositely with values in excess of 10 ppm in ignimbrite and about 2 ppm in macusanite (Table 5.1). The relative U enrichment versus Th suggests a possible contribution of pelitic rocks to an anatectic magma.

With respect to REE, two groups are distinguished. Rhyolites have a fairly elevated tenor in light REE and an elevated La/Yb ratio of 18.4–26.1. In contrast, macusanite has a lower REE content and a La/Yb ratio of only 2.1. It is low in europium and high in cerium, which is interpreted to indicate a reducing character of the magmatic environment.

Valencia and Arroyo (1985) similar to Arribas and Figueroa (1985) propose, for the Macusani ignimbrite suite, an origin

from an anatectic magma of sialic crustal material with a major pelitic component, as deduced from the presence of aluminous minerals and peraluminous whole rock geochemistry.

Valencia and Arroyo (1985) further support their hypothesis by isotope (¹⁶O/¹⁸O and ⁸⁷Sr/⁸⁶Sr) and paragenetic mineral data. δ¹⁸O is + 12.2‰ and approximates that of oceanic pelitic sediments (15.5–17.5‰) in the NW part of the Pacific Ocean. ⁸⁷Sr/⁸⁶Sr ratios are 0.7216 for ignimbrite and 0.7310 for macusanite, which compare with those of sialic rocks (0.725) and confirm the involvement of crustal material in the magma. Consequently, both pairs of isotopes exclude mantle derivation of the magma. An anatectic, back arch crustal origin of this magmatic episode is also indicated by the Andean geotectonic disposition of the Quenamari Meseta.

Mineralogically, the association of destabilized biotite, prismatic sillimanite, and spinel is indicative of temperatures in excess of 700°C. Under this condition, the composition of opaque minerals (Ilm₉₇Hem₃) suggests very low values of oxygen fugacity (fO₂) and hydrostatic pressure (P-H₂O) compatible with a carbonaceous pelitic origin. Partial fusion must have taken place in equilibrium with sillimanite and must have consisted of a strongly peraluminous liquid from which aluminous minerals such as andalusite, followed by muscovite, could crystallize. Required conditions for this constellation are restricted to shallow magma chambers with low pressure (P < 1 kbar) and temperature (approximately 650°C) that permit the coexistence of andalusite and muscovite. The conjugate effect of volatiles (F, B, Li) at solidus temperature and the ternary minimal composition (Q₂-Ab-O₃) leads to an individualization of residual magmas very rich in normative albite (ab).

Principal Host Rock Alteration

There is only minimal alteration of uranium-hosting ignimbrite. Rocks are normally fresh except for minor argillization and sericitization of the matrix and feldspar phenocrysts, limited chloritization of biotite, and some hematitization associated with quartz and calcite veinlets. Locardi (personal communication) points out, however, that locally, ignimbrites have been altered to kaolinite and quartz along heavily fractured subvertical zones, from 100 to 300 m wide paralleling the San Gabau and Corani faults, which are the major displacements in the area. Locardi considers gases rich in H₂S and CO₂, which are still active at some locations, to be responsible for the alteration. The intensity

Table 5.1.

Macusani district, ranges of selected minor elements in ignimbrite and macusanite of the Quenamari Formation (Valencia and Arroyo 1985)

Lithology/ppm	F	Be ₂ O ₃	Li ₂ O	Rb	Sn	Sr	Th	U
Ignimbrite	1,800–2,900	960	560–1,780	310–560	32–60	90–190	8.6–13.3	5.6–18
Macusanite	13,100	6,200	7,400	990	120	13	2.27	18.44

of the alteration is strongest at the base of the volcanic sequence and also affects the underlying Paleozoic rocks. It gradually decreases in intensity upwards and is less intense but more widespread on upper levels.

Principal Characteristics of Mineralization and Dimensions

Pitchblende, often of botryoidal habit, and coffinite are the principal uranium minerals and associate with minor chalcopyrite, melnicovite, pyrite, and sparse galena. Pitchblende is to a large extent transformed into gummite, autunite, meta-autunite, and other U^{6+} minerals. Locardi identified metahalloysite mantling gummite in a veinlet of the Pinocho ore zone. Metahalloysite only crystallizes at very low pH values and has supposedly formed by the reaction of sulfuric solutions with wall rocks.

Major uranium distribution is confined to a 40–50 m thick unit in the upper Quenamari Formation where grades of mineralization average 0.1–0.4% U (Valencia and Arroyo 1985). Ignimbrite, e.g., at *Pinocho*, and tuff, e.g., at *Chapi Alto*, are the principal host rocks. Some lower grade mineralization also occurs below this unit and in 1–5 m-thick fluvio-lacustrine sediments between two pyroclastic units at grades of 0.02–0.03% U. In both cases, only U^{6+} minerals are present, supposedly of redistributed origin. Ore minerals fill subvertical and subhorizontal joints and fractures in the form of veinlets a few centimeters to several 10 m long and as much as 10 cm wide. Tuff-hosted disseminated mineralization extends from veinlets for several tens of meters into the wall rock (► Fig. 5.1c).

Established mineralization at *Chapi* occurs over a length from 15 to 190 m and a width from 20 to 30 m, in nearly vertical structures, with uranium grades ranging from 0.03 to 0.75% U. The Chapi area is considered to host a potential resource of 10,000 t U (OECD-NEA/IAEA 1999).

Principal Ore Controls and Recognition Criteria

Mineralization appears to be of vein-type character. Although only near surface and not comprehensively investigated, the following parameters may apply tentatively as ore-controlling or recognition criteria:

Host environment

- U mineralization is restricted to a selected unit, 40–50 m thick, in the upper part of an ignimbritic sequence that is about 350 m thick
- U-hosting volcanic sequence consists of highly siliceous and peraluminous pyroclastics characterized by the unusual mineral association of andalusite, muscovite, and sillimanite
- Uranium and other trace metals as well as volatiles are enriched in pyroclastics

- Presence of gases containing H_2S and CO_2 are evidenced by present-day exhalation
- Petrography and chemistry of host rock are indicative of derivation from a sialic crustal anatectic magma, a large component of it being of pelitic origin.

Mineralization

- Practically monometallic U mineralization with pitchblende as the principal primary ore mineral
- Subvertical and subhorizontal shrinkage cracks and fissures created largely by rock contraction serve as principal host to pitchblende veinlets
- Where rocks provide sufficient porosity, disseminated mineralization extends laterally into wall rocks
- Abundance of andalusite, biotite, and smoky quartz in mineralized pyroclastics
- Only limited alteration of wall rocks except along highly fractured zones.

Metallogenetic Concepts

Any metallogenetic modeling faces the problem of having to explain the high-grade pitchblende veinlets unusually rich for volcanic-type U deposits in the given setting. A powerful uranium source has to be established as well as suitable mechanisms for pitchblende precipitation restricted to pyroclastic horizons, which mineralogically and geochemically do not essentially differ from barren ignimbrite that underlies ore zones. Theoretically, it may be assumed that uranium may have been leached by supergene or hypogene fluids from uraniumiferous volcanics, perhaps by matrix devitrification as established elsewhere. This is to some extent contradicted by rather limited rock alteration/devitrification, and a relative uniform geochemical uranium distribution throughout the ignimbrite pile without any noticeable zones of apparent uranium depletion.

Arribas and Figueroa (1985) envisage the uranium mineralization possibly to be of exhalative synvolcanic origin. Transport media would be deuteric hydrothermal solutions enriched in volatiles circulating through the pyroclastics during the ultimate stages of their consolidation. Uranium would have been present in the fluids as uranyl chloride or -bicarbonate. Pitchblende precipitation could have occurred in the presence of H_2S or CO_2 , or perhaps by pH, Eh, and temperature changes in a zone where hydrothermal fluids mixed with meteoric waters. The authors also point out that the nature and disposition of the ignimbrites, which are intruded by granitic porphyry, and the presence of antimony mineralization at some localities reflect a subvolcanic character.

Based on the limited data available, the ignimbrite suite of Macusani compares geochemically and petrologically to some extent with, and hence may represent an effusive equivalent to, peraluminous leucogranites hosting vein-type uranium deposits, for example, in the Hercynian massifs of France. This raises questions as to (a) whether some plutonic or subvolcanic stocks

of similar composition to the effusives in the Macusani area may exist at depth, and (b) whether such stocks may have retained uranium in sufficient quantities in residual fluids for formation of the present-day pitchblende veinlets by deuteritic hydrothermal processes as proposed by Arribas and Figueroa (1985). Other volcanic-type U deposits, which may possibly be compared with Macusani, occur at Streltsovsk in Asian Russia (see volume Uranium Deposits of the World: Asia) and other parts of central Asia.

Selected References and Further Reading for Chapter 5 Peru

For details of literature see Bibliography.

Arribas and Figueroa 1985; Cánepa and Rosado 1981; Chemillac 2004; Herrera and Rosado 1984; Hetland and McMichie 1984; OECD-NEA/IAEA 1986, 1999, 2007; Sosa et al. 1981; Valencia and Arroyo 1985; Locardi 1984 (personal communication).



Bibliography-Latin America

- Alba LA, Chávez R (1974) K-Ar ages from volcanic rocks from the central Peña Blanca, Chihuahua, Mexico. *Isochron West*, v 10, pp 21-23
- Albuquerque-Forman JM, Waring MH (1981) *see* Forman JMA, Waring MH (1981)
- Albuquerque-Forman JM, Angeiras AG (1981) *see* Forman JMA, Angeiras AG (1981)
- Amaral G (1984) Provincias Tapajós e Rio Branco. *in*: Almeida FFM, Hasui Y, coord., O Pré-Cambriano do Brasil, Edgard Blücher Editora, São Paulo, pp 8-35.
- Andrade SM, Camarço PEN (1982) Sequências sedimentares pré-Carboníferas dos flancos nordeste da bacia do Paraná e sudoeste da bacia do Parnaíba e suas possibilidades uraníferas. *Anais do XXXII Congr Brasil Geol* 5, Salvador, BA, pp 2132-2144
- Angeiras AG, Netto AM, de Campos M (1981) Phosphoro-uraniferous mineralization associated with sodium epsyenites in the Ceará Precambrian (Brazil). *in* Uranium deposits in Latin America: geology and exploration, IAEA, Vienna, pp 555-577
- Angelelli V (1956) Distribución y características de los yacimientos y manifestaciones uraníferas de la República Argentina. *in*: Proc Intern Conf Peaceful Uses Atom Energy, UN, Geneva, v 6, pp 63-74
- Angelelli V (1969) Yacimientos uraníferos vetiformes. OIEA/CNEA, Curso Region, Capac. Prospec. Uranio, I, CNEA, Buenos Aires
- Aniel B (1983) Les gisements uraníferes associés au volcanisme acide tertiaire de la Sierra Peña Blanca (Chihuahua, Mexico). *Géol Géochim Uranium*, Nancy, Mém 2, 291 p
- Aniel B, Leroy JL (1985) The reduced uraníferous mineralizations associated with the volcanic rocks of the Sierra Peña Blanca (Chihuahua, Mexico). *Amer Miner*, v.70, pp 1290-1297
- Antonietti C, Gorustovich S, Valdiviezo A, Benítez A, Saucedo P (1984) Geología y metalogénesis de los depósitos uraníferos de Argentina. Parte 1: Acumulaciones con control sedimentario. *in*: Geología metalogénesis de los depósitos y manifestaciones uraníferos de Sudamérica. IAEA, Vienna, pp 49-86
- Aparicio A (1981) Mineralización de uranio en rocas volcánicas terciarias de la formación Los Frailes, Bolivia. *in*: Uranium deposits in Latin America: geology and exploration. IAEA, Vienna, pp 485-520
- Arcidiácono EC, Saulnier ME (1980) Contribución a la interpretación genética de los yacimientos uraníferos del área de Sierra Pintada, San Rafael, Mendoza. *Rev Asoc Arg Miner Petrol Sed*, Buenos Aires, v 11, pp 1-2
- Arribas A, Figueroa E (1985) Geología y metalogénesis de las mineralizaciones uraníferas de Macusani, Puno (Perú). *in*: Uranium deposits in volcanic rocks. IAEA, Vienna, pp 237-243
- Ayres GJ (1981) Uranium in Brazil. *in*: Uranium deposits in Latin America: geology and exploration, IAEA, Vienna, pp 315-356
- Baird JG, Seara JL (1981) Técnicas aéreas de terreno y de sondeo para la exploración de uranio. *in*: Uranium Deposits in Latin America: Geology and Exploration, IAEA, Vienna, pp 105-116
- Ballhorn RK, Thakur VK, da Fonte JEC, Suckau V (1981) Geology of the Espinharas uranium deposit, Brazil. *in*: Uranium deposits in Latin America: geology and exploration. IAEA, Vienna, pp 521-532
- Barretto P (1985) Sedimentary and tectonic environments for uranium mineralization in the Paraná Basin, Brazil. *in*: Geological environments of sandstone-type uranium deposits. TECDOC-328, IAEA, Vienna, pp 173-195
- Barretto P (1988) The identification of uranium provinces in Brazil. *in*: Recognition of uranium provinces. IAEA, Vienna, pp 371-401
- Belluco AE, Diez J, Antonietti C (1974a) Los depósitos uraníferos de las provincias de La Rioja y San Juan. *Actas 5° Congr Geol Arg*, v 2, Buenos Aires, pp 9-33
- Belluco AE, Diez J, Antonietti C, Achen H, Valerdi D (1974b) Los depósitos uraníferos de las provincias de Mendoza y Neuquén. *Actas 5° Congr Geol Arg*, v 2, Buenos Aires, pp 34-53
- Belluco A, Rodriguez E, Gorustovich S, Olsen H, Valdiviezo A (1985) The sedimentary controlled uranium deposits in Argentina and their relation to the geostructural development. *in*: Geological environments of sandstone-type uranium deposits. TECDOC-328, IAEA, Vienna, pp 159-172
- Belluco A, Rodriguez E, Martinez C, Marinkeff K (1977) Bases para la prospección uranífera de la República Argentina. *in*: Recognition and evaluation of uraníferous areas. IAEA, Vienna, pp 183-198
- Belluco AE, Rodrigo F (1981) Favorabilidad geológica y potencial uranífero de la Argentina. *in*: Uranium deposits in Latin America: geology and exploration. IAEA, Vienna, pp 205-252
- Benitez A, Fuente A, Maloberti A, Landi V, Bianchi R, Marveggio N, Gayone M (1993) Evaluación de la mina nuclear Cerro Solo, Prov. del Chubut. Parte 1: Características geológicas del yacimiento y de la cuenca. *Actas TV, XII Congr Geol Arg*, pp 272-278
- Briot P (1983) Géologie et géochimie des gisements d'uranium liés aux milieux pré-évaporitiques intracontinentaux: les calcrètes uraníferes. Thèse d'État, Paris, France, 216 p
- Brito Neves BB, Kawashita K, Cordani UG, Delhal J (1979) A evolução geocronológica da Serra do Espinhaço - dados novos e integração. *Rev Brasil Geoci*, São Paulo (SP), v 9, pp 71-85
- Brito W, Raposo C, Matos EV (1984) Os albitos uraníferos de Lagoa Real. *Anais do XXXIII Congr Bras Geol*, Rio de Janeiro, pp 1475-1488
- Button A, Adams SS (1981) Geology and recognition criteria for uranium deposits of the quartz-pebble conglomerate type. *US-DOE, GJBX-3(81)*, 390 p
- Button A, Adams SS (1981) Geology and recognition criteria for uranium deposits of the quartz-pebble conglomerate type. *US-DOE, GJBX-3(81)*, 390 p
- Caby R, Arthaud M (1987) Petrostructural evolution of the Lagoa Real subalkaline metaplutonic complex (Bahia, Brazil) (abstr). *Rev Brasil Geosci*, v 17
- Calas G (1977) Les phénomènes d'altération hydrothermale et leur relation avec les minéralisations uraníferes en milieu volcanique: le cas de la Sierra Peña Blanca, Chihuahua, Mexico. *Sci Geol Bull*, v 30, pp 3-18
- Cánepa L, Rosodo F (1981) Ambientes favorables para la deposición de uranio en la Faja Subandina y Llano Amazónico del Perú. *in*: Uranium deposits in Latin America: geology and exploration, IAEA, Vienna, pp 269-300
- Cárdenas (1983) Volcanic stratigraphy and uranium deposits of central Sierra Peña Blanca, Chihuahua, Mexico. *in*: Geology and mineral resources of north-central Mexico. *El Paso Geol Soc Guidebook*, pp 325ff
- Cárdenas-Flores D (1985) Volcanic stratigraphy and U-Mo mineralization of the Sierra de Peña Blanca district, Chihuahua, Mexico. *in*: Uranium deposits in volcanic rocks. IAEA, Vienna, pp 125-136
- Castillo A (2004) Leaching method: Changes in Sierra Pintada mine. *in*: Recent developments in uranium resources and production with emphasis on in situ leach mining. TECDOC-1396, IAEA, Vienna, pp 223-229
- Castillo R (1981) Proyecto de investigación de las posibilidades de uranio en Costa Rica. *in*: Uranium deposits in Latin America: geology and exploration. IAEA, Vienna, pp 415-420
- Castuño R, Menicucci S (1984) Geología y mineralización urano-fosfática en el sinclinal de Berlín, Caldas (Colombia). *in*: Geología y metalogénesis de los depósitos y manifestaciones uraníferos de Sudamérica. IAEA, Vienna, pp 239-244
- Cathelineau M, Nieva D (1985a) A chlorite solid solution geothermometer. The Los Azufres (Mexico) geothermal system, *Contrib Mineral Petrol*, 91, pp 235-244
- Cathelineau M, Nieva D (1985b) Behaviour of REE during alteration of a volcanic calcalkaline series (Los Azufres geothermal system, Mexico). *Terra Cognita*, pp 103-104
- Cathelineau M, Oliver R, Nieva D (1987) Geochemistry of volcanic series of the Los Azufres geothermal field (Mexico). *Geol Interp*, v 26, no. 2, pp 273-290
- Cathelineau M, Oliver R, Nieva D, Garfias A (1985) Mineralogy and distribution of hydrothermal mineral zones in Los Azufres (Mexico) geothermal field. *Geothermics*, v 14, no. 1, pp 49-57
- Cathles LM, Shea ME (1992) Near-field high temperature transport: evidence from the genesis of the Osamu Utsumi uranium mine, Poços de Caldas alkaline complex, Brazil. *in*: Chapman et al., eds., The Poços de Caldas project: Natural analogues of processes in a radioactive waste repository, Part 1. *J Geochem Explor*, v 45, no 1-3, pp 565ff
- Chapman NA, McKinley IG, Shea ME, Smellie JAT, eds. (1992) The Poços de Caldas project: Natural analogues of processes in a radioactive waste repository, Part 1. *J Geochem Explor*, v 45, no 1-3

- Chaulot-Talmon JF (1984) Étude géologique et structurale des ignimbrites tertiaires de la Sierra Madre Occidentale, entre Hermosillo et Chihuahua, Mexique. PhD thesis, Orsay Univ, v 35-05, 260 p, unpub
- Chebli G, Nakayama C, Sciutto J, Serraiotto A (1976) Estratigrafía del Grupo Chubut en la región central de la provincia homónima. *Actas VI, Congr Geol Arg*, v I, pp 375-392
- CNEA (1998) Un proyecto para la producción de uranio y molibdeno en la Patagonia / An uranium-molybdenum production project in Patagonia. CNEA, CAE-UAG, Geología económica y regional Patagonia, 17 p
- Cordani UG, Iyer SS, Taylor TN, Kawashita K, Sato K, McReath I (1992) Pb-Pb, Rb-Sr and K-Ar systematics of the Lagoa Real uranium province, South Central Bahia, Brazil and Espinhaço Cycle. *J South Amer Earth Sci*, v 5, pp 33-46
- Costa PE, Vianna I, Andrade A, Lopes G, Souza S (1983) Lagoa Real project, geological map. CBPM Salvador
- Cuney M, Friedrich M (1987) Physicochemical and crystalchemical controls on accessory mineral paragenesis in granitoids: Implications for uranium metallogenesis. *Bull Minéral*, v 110, pp 235-247
- Cuney M, Leroy J, Valdiviezo PA, Daziano C, Gamba M, Zarco AJ, Morello O, Ninci C, Molina P (1989) Geochemistry of the uranium mineralized Achala granitic complex (Argentina): comparison with Hercynian peraluminous leucogranites of western Europe. *in: Metallogenesis of uranium deposits*. IAEA, Vienna, pp 211-232
- da Vinha CA (1981) Métodos indirectos de prospección de uranio aplicados por Nuclebras. *in: Uranium deposits in Latin America: geology and exploration*. IAEA, Vienna, pp 129-152
- de Andrade-Ramos JR, Fraenkel MO (1974) Uranium occurrences in Brazil. *in: Formation of uranium ore deposits*. IAEA, Vienna, pp 637-658
- de Brodtkorb MK (1963) Estudio de la mineralización del yacimiento "La Esperanza", prov. de Salta. *Act. II, J Geol Arg*, v 1, Tucumán, pp 25-33
- de Brodtkorb MK (1966) Mineralogía y consideraciones genéticas del yacimiento Huemul, prov. de Mendoza. *Asoc Geol Arg Rev XXI/3*, pp 165-179
- de Brodtkorb MK (1978) Oxidos de vanadio en calizas: su presencia en el yacimiento Urcal, prov. de La Rioja. *Asoc Geol Arg Rev XXXIII/3*, pp 97-104
- de Brodtkorb MK (1982) Vanadium oxides in the Urcal deposit, Argentina. *in: Amstutz GC et al., eds., Ore genesis, the state of the art*. Springer-Verlag Berlin ff, pp 221-239
- de Brodtkorb MK, Brodtkorb A (1984) Strata-bound deposits of Argentina. *in: Wauschkuhn A et al., eds., Syngensis and epigenesis in the formation of mineral deposits*. Springer-Verlag, Berlin ff, pp 92-101
- de Figueiredo Filho PM (1984) The Rio Preto uranium occurrences, Goiás, Brazil. *in: Ferguson J, ed., Proterozoic unconformity and stratabound uranium deposits*. TECDOC-315, IAEA, Vienna, pp 313-323
- de Figueiredo Filho PM, Andrade SM, Valderano MHW, Saad S (1982) Ocorrências de uranio no Paleozoico das bacias intracratônicas Brasileiras. *Anais do XXXII Congr Bras Geol 5*, Salvador, BA, pp 2124-2131
- d'Elboux CV (1984) Principales modelos brasileños de mineralizaciones uraníferas. *in: Geología metalogénesis de los depósitos y manifestaciones uraníferas de Sudamérica*. IAEA, Vienna, pp 143-176
- de Matos CE (2005) Uranium concentrate production at Caetite, BA, Brazil. *in: Symposium on uranium production and raw materials for the nuclear fuel cycle - supply and demand, economics, the environment and energy security*. Ext synopsis. CN-128, IAEA, Vienna, pp 133-137
- de Miranda Filho CM, Cabaleiro Rodrigues P (2003) The Lagoa Real uranium project- Brazil. *in: Cuney M, ed., Uranium geochemistry 2003*. Nancy, France, pp 107-110
- Departamento Nacional de Produção Mineral (1981) Mapa geológico do Brasil, Escala 1: 2 500 000. Brasília, DNPM
- Departamento Nacional de Produção Mineral/CPRM (1980) Proyecto levantamiento gravimétrico no Estado da Bahia, Relatório Final
- Diez J, Santomero AM, Antonietti C, Gorustovich SA (1981) Favorabilidad uranífera del Paleozoico Superior y Triásico en la Argentina. *Actas 8º Congr Geol Arg*, v 2, Buenos Aires, pp 807-828
- Diez J, Charadia V, Navarra P, Apesteigua J (1984) Geología y metalogénesis de los depósitos uraníferos de Argentina. Parte 2: Depósitos vetiformes y similares. *in: Geología y metalogénesis de los depósitos y manifestaciones uraníferas de Sudamérica*. IAEA, Vienna, pp 87-110
- Dominguez HF (1977) Estudio metalogénico del yacimiento uranífero de La Coma. Tesis prof, Univ Nac Autonomía México, 205 p
- Fernández-Amigut JA, Rodríguez-Triana H (1984) Geología y metalogénesis de las principales anomalías uraníferas descubiertas por ENUSA en Colombia. *in: Geología y metalogénesis de los depósitos y manifestaciones uraníferas de Sudamérica*. IAEA, Vienna, pp 205-218
- Ferreira RE, Saulnier ME, Vullien AR (1984) Genesis of sandstone-type uranium deposits of Sierra Pintada district, Mendoza, Argentina (abstr). *Intern Geol Congr, Moscow, Abstracts*, v IX, pt 1, p 347
- Férriz H (1985) Uranium mineralization in the San Marcos volcanic centre, Chihuahua, Mexico. *in: Uranium deposits in volcanic rocks*. IAEA, Vienna, pp 197-216
- Fiebiger W (1976) Präkambrische Itabirite und Uran-Gold-Konglomerate als geochemische Zeitmarken in der Erdrevolution. *Geol Rundsch*, Bd 65, pp 1035-1055
- Figueiredo AM, Oesterlen M (1981) Prospecção de uranio no Estado de Goiás. *Rev Bras Geosci*, v 11, no 3, pp 147-152
- Figueiredo MCH (1980) Geochemistry of high grade metamorphic terrains in northeastern Bahia (Brazil). PhD thesis, Univ W Ontario, London, Canada
- Finch WI (1985) Map and index list for sandstone-type uranium deposits in South America. *in: Geological environments of sandstone-type uranium deposits*, TECDOC-328, IAEA, Vienna, pp 156-158
- Flükiger MW, Abad E, Martín M (1981) Consideraciones sobre la geología y metalogénesis de algunos indicios chilenos de uranio. *in: Uranium deposits in Latin America: geology and exploration*. IAEA, Vienna, pp 451-484
- Forman JMA, Angeiras AG (1981) Poços de Caldas and Itaitaia, two case histories of uranium exploration in Brazil. *in: Uranium exploration case histories*. IAEA, Vienna, pp 99-139
- Forman JMA, Waring MH (1981) L'uranium en Amérique du Sud et plus spécialement dans la province uranífera brésilienne. *BRGM, Centre d'Etude Geol Min*, v 49, no. 461, pp 5-49
- Friz CT, Rodrigo F, Stipanovic PN (1964) Recursos y posibilidades uraníferos en Argentina. *in: 3rd Intern Conf Peaceful Uses Atom Energy, Session 2.11, UN, Geneva*, pp 42-54
- Fuchs H, da Fonte J, Suckau V, Thakur V (1981) The Espinhaços uranium occurrence, Brazil. *in: Uranium exploration case histories*. IAEA, Vienna, pp 3-13
- Fuzikawa K (1980) Estudos preliminares de inclusões fluidas em albitos do projeto Lagoa Real. Caetité, BA, Brasil. *Anais do XXXI Congr Bras Geol 4*, Camboriú, SC, pp 2038-2049
- Fuzikawa K (1982) Alguns carbonatos do distrito uranífero de Lagoa Real, Bahia: estudos de inclusões fluidas e isótopos estáveis. *Anais do XXXII Congr Bras Geol 5*, Salvador, BA, pp 2072-2085
- Fuzikawa K et al. (1990) Fluid inclusion studies in the Lagoa Real uranium province, Bahia State, Brazil. *Proc Congr Brasil Geol, São Paulo*, pp 248-257
- Gabelman JW, Beard RR (1962) Uranium in Peru. *US AEC, RME-4581*, 162 p
- Galarza MA, Macambira MJB, Villas RN (2008) Dating and isotopic characteristics (Pb and S) of the Fe oxide Cu-Au-U-REE Igarapé Bahia ore deposit, Carajás mineral province, Pará state, Brazil. *J S Amer Earth Sci*, v 25, no. 3, pp 377ff
- Geisel E, Raposo C, Alves JV, de Brito W, Vasconcelos TG (1980) O distrito uranífero de Lagoa Real, Bahia. *Anais do XXXI Congr Soc Bras Geol 3*, Camboriú, SC, pp 1499-1510
- George-Aniel B, Leroy J, Poty B (1985) Uranium deposits of the Sierra Peña Blanca: Three examples of mechanisms of ore deposit formation in a volcanic environment. *in: Uranium deposits in volcanic rocks*. IAEA, Vienna, pp 175-186
- George-Aniel B, Leroy J, Poty B (1991) Volcanogenic uranium mineralizations in the Sierra Peña Blanca district, Chihuahua, Mexico: Three genetic models. *Econ Geol*, v 86, pp 233-248
- Goodell RC (1981) Geology of the Sierra Peña Blanca uranium deposits, Chihuahua, Mexico *in: Goodell PC, Waters AC, eds. (1981) Uranium in volcanic and volcanoclastic rocks*. Amer Ass Petrol Geol, *Studies in Geology*, no. 13, pp 275-291
- Goodell PC (1983) Chemical characteristics of the Peña Blanca uranium district, Chihuahua, Mexico. *in: Geology and mineral resources of north-central Mexico*. El Paso Geol Soc Guidebook, pp 345ff
- Goodell PC (1985b) Chihuahua City uranium province, Chihuahua, Mexico. *in: Uranium deposits in volcanic rocks*. IAEA, Vienna, pp 97-124

- Goodell PC, Trentham RC (1980) Experimental leaching of uranium from tuffaceous rocks. US DOE, GJBX-148(80) 144 p
- Goodell PC, Waters AC, eds. (1981) Uranium in volcanic and volcanoclastic rocks. Amer Ass Petrol Geol Studies in Geology 13, 331 p
- Goodell PC, Trentham R, Carraway K (1979) Geologic setting of the Peña Blanca uranium deposits, Chihuahua, Mexico: Chap. IX. *in*: Henry CD, Walton AW, eds., Formation of uranium ores by diagenesis of volcanic sediments. US-DOE, GJBX-22(79), 38 p
- Gorustovich SA, Brodtkorb MK, Benitez AF, Maloberti AL (1992) Los yacimientos de la paragénesis U-V-Cu del cretácico de la República Argentina. *in*: Brodtkorb MK, Ferreira de Sousa J, eds., Recursos minerales y energéticos del Cretácico de América Latina. Actas IUGS-UNESCO 242, pp 25-90
- Goso HJ (1981) Prospección uranífera y favorabilidad geológica en el Uruguay. *in*: Uranium deposits in Latin America: geology and exploration. IAEA, Vienna, pp 429-450
- Gross WH (1968) Evidence for a modified placer origin for auriferous conglomerates, Canaveiras Mine, Jacobina, Brazil. Econ Geol, v 63, pp 271-276
- Haddad RC, Leonardos OH Jr (1980) Granitos anelares de Taperuaba (Ceará) e processos metalogénéticos associados. Anais do XXXI Congr Bras Geol 21, Camboriú (SC), pp 2626-2633
- Hasbrouck J C (1981) Cost-effective geophysical survey systems for uranium exploration in Bolivia. *in*: Uranium deposits in Latin America: geology and exploration. IAEA, Vienna, pp 123-128
- Hassano S, Stein JH (1978) A mineralização uranífera na Região de Iporá-Amorinópolis, Estado de Goiás (abstr.). XXX Congr Bras Geol, Recife, Bol no. 1, p 341
- Herrera W, Rosado F (1984) Las manifestaciones uraníferas en rocas volcánicas de Macusani, Puno (Perú). *in*: Geología y metalogénesis de los depósitos y manifestaciones uraníferas de Sudamérica, IAEA, Vienna, pp 219-238
- Hetland DL, Michie UMCL (1981) IUREP orientation phase report Peru. IAEA, Vienna, 86 p plus appendices A to E
- Holmes DC, Pitty AE, Noy DJ (1992) Geomorphological and hydrogeological features of the Poços de Caldas caldera analogue study sites. J Geochem Explor, v 45, 215-247
- IAEA (1981) Uranium Deposits in Latin America: Geology and Exploration / Yacimientos de Uranio en América Latina: Geología y Exploración, Vienna, 625 p
- INB (2000) The uraniferous district of Lagoa Real, state of Bahia, Brazil (manusc). Indústrias Nucleares do Brazil, Complexo Industrial de Caetité-CIC; TCM, IAEA Vienna, 24 p
- Inda HAV, Barbosa JF, (1978) Texto explicativo para o mapa geológico da Bahia. Secr Minas Energia, coord., Prod Min, Salvador, p 137
- Ipparea V, Chávez R (1969) Descubrimientos recientes de localidades uraníferas en rocas ígneas extrusivas en la porción central del Estado de Chihuahua. Actas VIII Convenc Nac AIMMG, México, pp 257-260
- Jardim de Sá EF, McReath I, Brito Neves BB, Bartels RL (1976) Novos dados geocronológicos sobre a Craton São Francisco no Estado da Bahia. Anais do XXIX Congr Soc Bras Geol 4, Ouro Preto, MG, pp 185-202
- Labenski F, Nicolli HB, Saragovi-Badler C (1982) (Genesis of sandstone-type uranium deposits in the Sierra Pintada district, Mendoza, Argentina: a Mössbauer study. Uranium, v 1, no.1, pp 1-18
- Leroy J, Müller-Kahle E, comps (1985) IUREP Summary Report, Bolivia. IAEA, Vienna, 29 p
- Leroy J, Aniel B, Poty B (1987) The Sierra Peña Blanca, (Mexico) and the Meseta Los Frailes (Bolivia): The uranium concentration mechanisms in volcanic environment during hydrothermal processes. Uranium, 3, pp 211-234
- Leroy J, George-Aniel B, Pardo-Leyton E (1985) Deposits and radioactive anomalies in the Sevaruyo region (Bolivia). *in*: Uranium deposits in volcanic rocks. IAEA, Vienna, pp 289-300
- Leslie BW, Pearcy EC, Prikryl JD (1993) Oxidative alteration of uraninite at the Nopal I deposit, Mexico. Possible contaminant transport and source term constraints for the proposed repository at Yucca Mountain. *in*: Pablan RT, ed., Scientific basis for nuclear waste management XVI. Interrante CG, Materials research symp proc, v. 294, p. 505-512
- Lichtner PC, Waber N (1992) Redox front geochemistry and weathering: theory with application to the Osamu Utsumi uranium mine, Poços de Caldas, Brazil. *in*: Chapman et al., eds., The Poços de Caldas project: Natural analogues of processes in a radioactive waste repository, Part 1. J Geochem Explor, v 45, no 1-3, pp 521-564
- Lobato LM, Fyfe WS (1990) Metamorphism, metasomatism and mineralization at Lagoa Real, Bahia, Brazil. Econ Geol, v 85, pp 968-989
- Lobato LM, Forman JMA, Fuzikawa K, Fyfe WS, Kerrich R (1982) Uranium enrichment in Archean Basement: Lagoa Real, Brazil. Rev Bras Geol, v 12, pp 484-486
- Lobato LM, Forman JMA, Fyfe WS, Kerrich R, Barnett RL (1983) Uranium enrichment in Archean crustal basement associated with overthrusting. Nature, v 303, pp 235-237
- López LE, Ford KL (2002) Natural radiation at the Cerro Solo U-Mo deposit, Argentina. *in*: The uranium production cycle and the environment. C&S Papers Series 10/P, IAEA, Vienna, pp 513-515
- Lorrai M, Podda F, Lattenzi P (2003) Hydrogeochemistry of the U-mineralised area of Sierra Pintada (San Raphael), Mendoza, Argentina. *in*: Cuney M, ed., Uranium geochemistry 2003. Nancy, France, 227-230
- Lucero HN, Diez JD, Noya JMA (1974) Los depósitos uraníferos de la Sierras Pampeanas (Provincias de Córdoba y San Luis), República Argentina. Actas V Congr Geol Arg, Buenos Aires v 2, pp 153-173
- Lucero HN, Timonieri AJ, Diez JD (1965) Contribución al conocimiento de algunas manifestaciones uraníferas de las provincias de Córdoba, La Rioja y San Luis. Actas de las Segundas Jornadas Geológicas Argentinas (1963), Prov. de Salta, v I, pp 87-114 (publ in Acta Geológica Lilloana, v VII, Tucumán 1965)
- Machado N, Noce CM, Oliveira OAB, Ladeira EA (1989) Evolução geológica do Quadrilátero Ferrífero no Arqueano e Proterozoico Inferior com base geocronologia U-Pb. Soc Bras Geol, Nucleo Minas Gerais, bol no. 10, pp 1-5
- Magonthier MC (1984) Les ignimbrites de la Sierra Madre Occidental et de la province uranífera de la Sierra Peña Blanca, Mexique. Mém Sci Terre, Univ P et M Curie, Paris, v 84-17, 351 p
- Magonthier MC (1985) Características petrográficas y geoquímicas de las unidades ignimbriticas portadoras de mineralización de uranio de la Sierra Peña Blanca, México. *in*: Uranium deposits in volcanic rocks. IAEA, Vienna, pp 137-150
- Magonthier MC (1987) Relations entre les minéralisations d'uranium de la Sierra Peña Blanca (Mexique) et les ignimbrites porteuses. Bull Minéral, v 110, pp 305-317
- Majdalani SA, Tavares AM (2001) Status of uranium in Brazil. *in*: Assessment of uranium deposit types and resources - a worldwide perspective. TECDOC-1258, IAEA, Vienna, pp 119-128
- Maloberti AL (1989) Presencia de uranio en rocas volcanoclasticas cretácicas de la región central de la Prov. del Chubut. *in*: Brodtkorb MK, Schalamuk IA, eds., Contribuciones de los Simposios sobre el Cretácico de América Latina. Depósitos minerales del Cretácico de América Latina. Inst Geol Aplicada, Fac Ciencias Naturales y Museo de La Plata, Prov Buenos Aires, pp 1-14
- Maruéjol P, Cuney M, Fuzikawa K, Netto AM, Poty B (1987) The Lagoa Real subalkaline granitic complex (South Bahia, Brazil), a source for uranium mineralizations associated with Na-Ca metasomatism. Rev Bras Geoci, São Paulo, v 17, no. 4, pp 578-594
- McKinley IG, ed. (1991) Testing models of redox front migration and geochemistry at the Osamu Utsumi mine and Morro do Ferro analogue study sites, Poços de Caldas, Brazil. Nagra Tech Ber NTB 90-30, Nagra, Wettingen (SKB TR 90-21, UK DOE WR 90-052)
- McNeil (1980) Brazil's uranium/thorium deposits. Miller Freeman Publ, San Francisco, 125 p
- Mendonça JGS, de Campos M, Braga APO, Souza EM (1982) Caracteriza estrati-gráfica dos metasedimentos da região de Itaitia-CE (Grupo Itaitia). Ann XXXII Congr Brasil Geologia, v 1, pp 325-338
- Michel H, Schneider HJ (1978) Uranvorkommen im Zusammenhang mit den tertiären Vulkaniten des lateinamerikanischen Koridillerenzuges. Schriftenreihe der GDMB, Clausthal-Zellerfeld, Heft 32, pp 97-104
- Miekeley N, Linsalate P, Osmond JK (1992) Uranium and thorium isotopes in groundwaters from the Osamu Utsumi mine and Morro do Ferro natural analogue sites, Poços de Caldas, Brazil. J Geochem Explor, v 45, 345-363
- Miranda MA (1985) Geología y potencial uranífero de la Sierra los Arados, México. *in*: Uranium deposits in volcanic rocks. IAEA, Vienna, pp 187-196
- Miranda MA, Martínez J, Olvera L (1985) Emanometría de radón en el distrito uranífero de Sierra Peña Blanca y en otras áreas volcánicas de Chihuahua, México. *in*: Uranium deposits in volcanic rocks. IAEA, Vienna, pp 151-160

- Miranda MA, Núñez EP (1985) Exploración de uranio utilizando geoquímica de sedimentos de arroyo y levantamientos de radiaciones gamma en el área Majalca, México. *in: Uranium deposits in volcanic rocks*. IAEA, Vienna, pp 225-236
- Moreno G, Pujol Ferre R (1962) Las manifestaciones uraníferas conocidas en la provincia Neuquén. *Anales 1ª Jornadas Geol Arg, San Juan, v 3*, pp 219-231
- NAGRA (1993) Poços de Caldas: Die Natur experimentiert mit. Nagra informert, Nagra, Wettingen, 53 p
- Navarra PR (1992) The Cerro Solo project. *in: New developments in uranium exploration, resources, production and demand*. TECDOC-650, IAEA, Vienna, pp 147-151
- Navarra PR, Benítez AF (1997) Development of the Cerro Solo deposit and uranium favourability of the San Jorge Gulf Basin, Province of Chubut. *in: Changes and events in uranium deposit development, exploration, resources, production and the world supply-demand relationship*. TECDOC-961, IAEA, Vienna, pp 177-192
- Navarra PR, Sardin P, Urquiza L, Bernal Gy, Guzman Lobos D (1993) Evaluación de la mina nuclear Cerro Solo, Prov. del Chubut, Parte 2: Sobre los parámetros económicos del depósito. *Actas TV, XII Congr Geol Arg*, pp 279-283
- Navarra PR, Tomellini GC, Marveggio NM (2001) Investigation of the characteristics of sandstone type uranium deposits in the Patagonia region. *Recent advances. in: Assessment of uranium deposit types and resources - a worldwide perspective*. TECDOC-1258, IAEA, Vienna, pp 141-148
- Netto AM (1983) Contributions à la minéralogie, à la pétrographie et à la métallogénie du gisement phospho-uranifère d'Itataia-Ceará-Brásil. PhD thesis, Univ Clermont-Fd, France, 203 p
- Netto AM, Cuney M, Mergoil-Daniel J (1991) Paragenèse minérale et distribution de l'uranium dans le "minerai noir" du gisement phospho-uranifère d'Itataia (Ceará, Brésil): Implications génétiques. Submitted to CR Acad Sci, Paris
- Netto AM, Meyer A, Cuney M, Poupeau G (1991) A thermo-geochronological study of the Itataia phospho-uraniferous deposit (Ceara, Brazil) by apatite fission track analyses: genetic implications. *in: Pagel M, Leroy JL, eds., Source transport and deposition of metals*. Proc 25 Years SGA Anniv Meet, Nancy, pp 409-411
- Nicolli HB (1974) Consideraciones sobre la génesis de depositos uraníferos en areniscas: Distrito de Sierra Pintada, Dpto. San Rafael, Prov. de Mendoza, Rep. Argentina. *Actas 5º Congr Geol Arg, v 2, Buenos Aires*, pp 223-242
- Nicolli HB, Chaar E, Latorre CO (1973) Características y genesis de los yacimientos nucleares "Dr. Baulies" y "Los Reyunos", Departamento San Rafael, Provincia de Mendoza. *Bol Acad Nac Cienc, Córdoba*, 50, pp 147-166
- Nicolli HB, Gamba MA, Ferreyra RE (1980) Geochemical characteristics and genesis of sandstone-type uranium deposits, Sierra Pintada district, San Rafael, Mendoza, Argentina. *Proc 26th Intern Geol Congr, Paris, Sect 13, Geoinst Beograd*, pp 163-187
- Nicolli HB, Lucero Michaud HN, Gamba MA (1974) Observaciones geológico-tectónicas y consideraciones sobre la geoquímica del uranio en las plutonitas de las Sierras de Los Gigantes, prov. de Cordoba (Republica Argentina). *Act. V Congr Geol Arg, v 2, Carlos Paz, 2, Buenos Aires*, pp 243-266
- Nicolli HB, Lucero Michaud HN, Gamba MA (1976) Geoquímica del uranio en el faldeo occidental de la Sierra de Comechingones y en el valle del río Conlara, prov. de San Luis. I. Observaciones geológico-tectónicas y distribución del uranio en plutonitas y en aguas de vertientes y de corrientes. *Bol Acad Nac Cienc*, 51, pp 225-242
- Noble EA (1981) Observaciones sobre la relación entre facies lacustrinas y yacimientos de uranio en sedimentos continentales. *in: Uranium Deposits in Latin America: Geology and Exploration*, IAEA, Vienna, pp 421-428
- NUEXCO (1991) Uranium deposits of Brazil. *NUEXCO Monthly Rep*, no. 277, pp 22-32
- OECD(NEA)/IAEA (1970 to 2007) Uranium resources, production and demand. Paris (biannual joint reports) (Red book)
- Oliveira AG, Fuzikawa K, Moura LAM, Raposo C (1985) Provincia uranífera de Lagoa Real - Bahia. *in: Principais Depósitos Minerai do Brasil*. DNPM 1 Cap VI, pp 105-120
- Olsen H, Berizzo J (1980) El potencial uranífero del Cretácico Continental en la Patagónica extrandina de la República Argentina. *in: Uranium evaluation and mining techniques*. IAEA, Vienna, pp 463-480
- Ortega-Furlotti A, Rodriguez-Pujadas EJ, Prieto AD, Valdiviezo A (1974) El nuevo distrito uranífero de Sierra Pintada, prov. de Mendoza, Argentina (abstr). *Actas 5º, Congr Geol Arg, v 2, Buenos Aires*, p 19
- Pagel M (1981) Facteurs de distribution et de concentration de l'uranium et du thorium dans quelques granites de la chaîne hercynienne d'Europe. *INPL, thesis*, 566 p
- Pardo-Leyton E (1981) Determinación de áreas favorables para la prospección de uranio en territorio boliviano. *in: Uranium deposits in Latin America: geology and exploration*. IAEA, Vienna, pp 155-178
- Pardo-Leyton E (1985) Uranio en rocas igneas: Intrusivas sub-efusivas y piroclásticas del Orogeno Andino boliviano. *in: Uranium deposits in volcanic rocks*. IAEA, Vienna, pp 255-274
- Pardo-Leyton E, Barron E (1984) Estudio preliminar sobre la geología y metalogénesis del uranio en Bolivia. *in: Geología y metalogénesis de los depósitos y manifestaciones uraníferos de Sudamérica*. IAEA, Vienna, pp 111-142
- Pascholati EM et al. (2003) Novas ocorrências de urânio na região de Lagoa Real, a partir da superposição de dados geofísicos, geológicos e de sensoriamento remoto. *Rev Brasil Geoci*, v 33, no. 2, pp 91-98
- Pasquali J (1981) Exploración de uranio en Venezuela: Situación a fines de 1978. *in: Uranium deposits in Latin America: geology and exploration*. IAEA, Vienna, pp 191-204
- Pearcy EC, Prikryl JD, Murphy WM, Leslie BW (1994) Alteration of uraninite from the Nopal I deposit, Peña Blanca district, Chihuahua, Mexico, compared to degradation of spent nuclear fuel in the proposed U.S. high-level nuclear waste repository at Yucca Mountain, Nevada. *Applied Geochem*, v 9, pp 713-732
- Pérez LE, Rojo M, Moxham RL (1981) Programa de prospección de uranio en Chile. *in: Uranium Deposits in Latin America: Geology and Exploration*. IAEA, Vienna, pp 357-372
- Pimentel MM, Fuck RA, Cordani UG, Kawashita K (1985) Geocronologia da região de Arenópolis-Piranhas, Goiás. *Rev Bras Geoc, São Paulo*, 16, 2, pp 217-223
- Podda F, Lorrai M, Lattanzi P, Asenjo A, Nievas HO, Tomellini A (2003) Hydrogeochemistry of the U-mineralized area of Los Gigantes, Cordoba, Argentina. *in: Cuney M, ed., Uranium geochemistry 2003*. Nancy, France, pp 301-304
- Porto da Silveira CL, Schorscher HD, Miekely N (1991) The geochemistry of albitization and related uranium mineralization, Espinharas, Paraiba (PB), Brazil. *J Geochem Explor*, v 40, pp 329-347
- Prates SP, Fusikawa K, Aspects petrograficos da jazida uranífera de Lagoa Real da Rabicha, Bahia. *Nota Tecnica EBHO. PM n 6, NUCLEBRAS*, (unpubl)
- Premoli C, Kroonenberg SB (1984) Radioactive mineral potential of carbonatites in western parts of the South American shields. *in: Geología y metalogénesis de los depósitos y manifestaciones uraníferos de Sudamérica*. IAEA, Vienna, pp 245-268
- Premoli C, Lozano H (1984) Some aspects of geology and metallogenesis of uraniferous occurrences in Colombia: Regional context and correlations. *in: Geología y metalogénesis de los depósitos y manifestaciones uraníferos de Sudamérica*. IAEA, Vienna, pp 177-204
- Premoli C, Velazquez J (1981) Preliminary reconnaissance for uranium in Paraguay. *in: Uranium deposits in Latin America: geology and exploration*, IAEA, Vienna, pp 373-394
- Rabelo AMA, Camarço PEN (1982) Estudo comparativo da jazida uranífera de Figueira e dos indícios de Sapopema e Telémaco Borba. *Anais do XXXII Congr Brasil Geol 5, Salvador, BA*, pp 2110-2123
- Ramdohr P (1958) Die Uran- and Goldlagerstätten Witwatersand-Blind River District Dominion Reef-Serra de Jacobina, Abh Deutsch Akad Wiss, Berlin, Klasse Chem Geol Biolog, no. 3, pp 1-35
- Ramos V (1979) El vulcanismo del Cretácico Inferior de la Cordillera Patagónica. *Actas VII, Congr Geol Arg, v 1*, pp 423-435
- Raposo C, Matos EV (1982) Distrito uranífero de Lagoa Real - A história de un exemplo. *Anais do XXXII Congr Bras Geol 22, Salvador, BA*, pp 2035-2047
- Raposo C, Matos EV, Britto W (1984) Zoneamento cálcio-sódico nas rochas da provincia uranífera de Lagoa Real. *Anais do XXXIII Congr Bras Geol 23, Rio de Janeiro*, pp 1489-1502
- Read D (1992) Geochemical modelling of uranium redistribution in the Osamu Utsumi mine, Poços de Caldas. *in: Chapman et al., eds., The Poços de Caldas*

- project: Natural analogues of processes in a radioactive waste repository, Part 1. *J Geochem Explor*, v 45, no 1-3, pp 503-520
- Reyes-Cortés IA (1985b) Ignimbritas uraníferas en la Sierra de Coneto, México. *in: Uranium deposits in volcanic rocks*. IAEA, Vienna, pp 217-224
- Reyes-Cortés M (1985a) Depósito de molibdeno asociado con uranio en Peña Blanca, México. *in: Uranium deposits in volcanic rocks*. IAEA, Vienna, pp 161-174
- Rocha EB (1992) Dispersão e redistribuição de urânio e acompanhadores em mineralizações uraníferas submetidas a alteração lateritizante: exemplo da jazida Laranjeiras, província uranífera de Lagoa Real, Bahia. Doct thesis, IAG-USP (unpubl)
- Rodrigo F (1971) Descubrimiento de importantes yacimientos de uranio en la Sierra Pintada, San Rafael, Mendoza. *Mundo Geol*, Buenos Aires, no. 4
- Rodrigo F, Belluco AE (1981a) Programa nacional de desarrollo de los recursos uraníferos de la Argentina. *in: Uranium deposits in Latin America: geology and exploration*. IAEA, Vienna, pp 395-414
- Rodrigo F, Belluco AE (1981b) Discovery of the Sierra Pintada uranium district, Mendoza province, Argentina. *in: Uranium exploration case histories*. IAEA, Vienna, pp 23-57
- Rodrigo F, Olsen H, Belluco AE (1984) Surficial uranium deposits in Argentina. *in: Surficial uranium deposits*. TECDOC-322, IAEA, Vienna, pp 113-117
- Rodríguez H, Aluja JA, Pfeiffer J, Cortés LA (1981) Manifestaciones uraníferas conocidas en Colombia. *in: Uranium deposits in Latin America: geology and exploration*. IAEA, Vienna, pp 301-314
- Rodriguez Torrez R, Yza-Dominguez R, Chavez Aguirre R, Constantino SE (1976) Rocas volcánicas ácidas y su potencial como objetivos para prospectar uranio. *in: Exploration for uranium deposits*. IAEA, Vienna, pp 601-623
- Romero L, Neretnieks J, Moreno L (1992) Movement of the redox front at the Osamu Utsumi uranium mine, Poços de Caldas, Brazil. *in: Chapman et al., eds., The Poços de Caldas project: Natural analogues of processes in a radioactive waste repository, Part 1*. *J Geochem Explor*, v 45, no. 1-3, pp 471-502
- Saad S (1982) Evidências de paleodrenagem na formação Rio Bonito e sua importância na concentração de urânio. *Anais do XXXII Congr Bras Geol*, Salvador, BA, pp 129-160
- Saad S (2002) Radiological characterization on the industry of phosphate in Brazil with emphasis on the Itateia project. *in: The uranium production cycle and the environment*. Proceed, C&S Papers Ser 10/P, IAEA, Vienna, pp 519-520
- Saad S, Munne AI, Tanaka AY (1984) Proposição de um novo modelo genético para a jazida de Itataia. *Anais do XXXIII Congr Bras Geol* 23, Rio de Janeiro, pp 1410-1423
- Santivañez R (1977) Estudio petrográfico de la region de Sevaruyo (Wichajlupe). Tesis de grado UMSA, La Paz, Bolivia
- Santos E, Mello CBM (1978) Diversidade do plutonismo granítico do Nordeste. *Anais do XXX Congr Bras Geol* 6, Recife, pp 2624-2634
- Santos EJ, Brito Neves BB (1984) Província Borborema. *in: Almeida FFM, Hasui Y, coord., O Pré-Cambriano do Brasil*. Edgard Blücher Editora, São Paulo, pp 123-186
- Santos R (1981) Geology and mining development of the C-09 uranium deposit. *in: Uranium deposits in Latin America: geology and exploration*. IAEA, Vienna, pp 533-554
- Sardin P (1996) Approach to the resource estimation of the Cerro Solo uranium ore deposit using geostatistical methods. *in: Computer application in uranium exploration and production*. NFCM/NENF-96/01, IAEA, Vienna, 17 p
- Schobbenhaus C, Campos DA, (1984) A evolução da Plataforma Sul-Americana no Brasil e suas principais concentrações minerais. *in: Schobbenhaus C, Campos DA, Derze GR, Asmus HE, coord., Geologia do Brasil; texto explicativo do mapa geológico do Brasil*. Dep Nac Prod mineral, Brasília, pp 9-53
- Schorscher HD (1979) Evolução Arqueana e Proterozoica do Quadrilátero Ferrofero e de partes meridionais da Serra do Espinhaço. I Simp Geol do Craton do São Francisco, Bras Geol, Nucleo da Bahia, abstr
- Schorscher HD, Osmond JK (1992) Origin and growth rates of pitchblende nodules at the Osamu Utsumi mine, Poços de Caldas, Brazil. *in: Chapman et al., eds., The Poços de Caldas project: Natural analogues of processes in a radioactive waste repository, Part 1*. *J Geochem Explor*, v 45, no 1-3, pp 159-172
- Schorscher HD, Shea ME (1992) The regional geology of the Poços de Caldas alkaline complex: mineralogy and geochemistry of selected nepheline syenites and phonolites. *in: Chapman et al., eds., The Poços de Caldas project: Natural analogues of processes in a radioactive waste repository, Part 1*. *J Geochem Explor*, v 45, no 1-3, pp 25-52
- Severne B, Peñaherrera PF, Fiallos VS (1981) Uranium exploration in Ecuador. *in: Uranium deposits in Latin America: geology and exploration*. IAEA, Vienna, pp 179-190
- Shea ME (1992) Isotopic geochemical characterization of selected nepheline syenites and phonolites from the Poços de Caldas alkaline complex, Minas Gerais, Brazil. *in: Chapman et al., eds., The Poços de Caldas project: Natural analogues of processes in a radioactive waste repository, Part 1*. *J Geochem Explor*, v 45, no 1-3, pp 173-214
- Sosa JE, Arroyo G, Belluco AE (1981) Antecedentes de la prospección y análisis de la favorabilidad geológico-uranífera del Perú. *in: Uranium deposits in Latin America: geology and exploration*, IAEA, Vienna, pp 253-268
- Stege B, Pintigore N, Goodell PC, Lemone D (1981) Limestone bedrock as a barrier to uranium migration, Sierra Peña Blanca, Chihuahua, Mexico. *Studies in Geol*, v 13, pp 265-274
- Stein IH, Netto AM, Drummond D, Angeiras AG (1980) Nota preliminar sobre os processos de albitização uranífera de Lagoa Real (Bahia) e sua comparação com os da URSS e Suedia. *Anais do XXXI Congr Bras Geol* 3, Camboriú, SC, SBG, pp 1758-1775
- Stipanovic PN (1970) Conceptos geoestructurales generales sobre la distribución de los yacimientos uraníferos con control sedimentario en la Argentina y posible aplicación de los mismos en el resto de Sudamérica. *in: Uranium exploration geology*. IAEA, Vienna, pp 205-216
- Stipanovic PN, Belluco AE (1984) Favorabilidad geológico-uranífera de América del Sur. *in: Geología y metalogénesis de los depósitos y manifestaciones uraníferas de Sudamérica*. IAEA, Vienna, pp 1-48
- Stipanovic PN, Belluco A, Nicolli H, Gorustovich S, Salfity J, Vullien A, Suriano J, Koukharski M, Abril E (1985) Uranium occurrences in the volcanic rocks of northwestern Argentina. *in: Uranium deposits in volcanic rocks*. IAEA, Vienna, pp 301-314
- Stipanovic PN, Olsen H, Antonietti C, Berizzo J, Valdiviezo A (1982) Vein-type and similar uranium deposits of Argentina. *in: Vein-type and similar uranium deposits in rocks younger than Proterozoic*. IAEA, Vienna, pp 211-234
- Stipanovic PN, Rodrigo F, Friz G, Linares E (1968) Provincias uraníferas argentinas. 23th Intern Geol Congr Prague, v 7, pp 57-70
- Surcan dos Santos LC (1984) Ocorrência de urânio em quartzitos da formação Gorotire, Estado do Pará. *Anais do XXXIII Congr Bras Geol* 23, Rio de Janeiro
- Tallarico FHB, Figueiredo BR, Groves DI, Kositcin N, McNaughton N, Fletcher IR, Rego J L (2005) Geology and SHRIMP U-Pb geochronology of the Igarapé Bahia deposit, Carajás copper-gold belt, Brazil: An Archean (2.57 Ga) example of iron-oxide Cu-Au-(U-REE) mineralization. *Econ Geol*, v 100, pp 7-28
- Tassinari CCG, Barretto PMC (1992) Uranium in granitoids: Recognition criteria of uranium provinces in Brazil. *in: New developments in uranium exploration, resources, production and demand*. TECDOC-650, IAEA, Vienna, pp 13-21
- Toens PD, Le Roux, JB, Hartnady CJH, Van Biljon, WJ (1980) The uranium geology and tectonic correlation between the African and Latin American continents. *S Afr Atom Energy Bd Rep PER* 58, 80 p
- Turpin L, Maruejol P, Cuney M (1988) U-Pb, Rb-Sr and Sm-Nd chronology of granitic basement, hydrothermal albitites and uranium mineralization (Lagôa Real, South Bahia, Brazil). *Contrib Mineral Petrol*, 98, pp 139-147
- Ulbrich HH GJ (1984) A petrografia, e estrutura e o quimismo de nefelina sienitos do Maciço Alcalino de Poços de Caldas, MG-SP. Tese de Livre Docência, Univ Sao Paulo, Inst Geosci, 2 vols, 735 pp
- Valencia J, Arroyo G (1985) Consideraciones geoquímicas de los indicios uraníferos de Macusani, Puno (Perú). *in: Uranium deposits in volcanic rocks*. IAEA, Vienna, pp 275-288
- Villaça JN, Fuzikawa K (1973) Urânio no Quadrilátero Ferrofero. *Anais do XXVII Congr Bras Geol*, Nucleo Bahia, Salvador, Bol no. 1, p 34
- Villaça JN, Hashizume BK (1982) Distrito uranífero de Lagoa Real - reservas e potencial. *Anais do XXXII Congr Bras Geol* 22, Salvador, BA, pp 2048-2061
- Virreira V. (1981) Técnicas de exploración de uranio empleadas en Bolivia. *in: Uranium deposits in Latin America: geology and exploration*. IAEA, Vienna, pp 117-122

- Waber N (1991) Mineralogy, petrology and geochemistry of the Poços de Caldas analogue study sites, Minas Gerais, Brazil, II. Morro do Ferro. Nagra Tech Ber NTB 90-21, Nagra, Wettingen (SKB TR 90-12, UK DOE WR 90-043)
- Waber N, Schorscher HD, Peters T (1991) Mineralogy, petrology and geochemistry of the Poços de Caldas analogue study sites, Minas Gerais, Brazil, I. Osamu Utsumi uranium mine. Nagra Tech Ber NTB 90-20, Nagra, Wettingen (SKB TR 90-11, UK DOE WR 90-042)
- Waber N, Schorscher HD, Peters T (1992) Hydrothermal and supergene uranium mineralization at the Osamu Utsumi mine, Poços de Caldas, Minas Gerais, Brazil. *in*: Chapman et al., eds., The Poços de Caldas project: Natural analogues of processes in a radioactive waste repository, Part 1. *J Geochem Explor*, v 45, no 1-3, pp 53-112
- Wenrich KJ, Modreski PJ, Zielinski RA, Seeley JL (1982) Margaritasite, a new mineral of hydrothermal origin from the Peña Blanca uranium district, Mexico. *Amer Miner*, v 67, pp 1273-1289
- Wernick E, Hasuy Y, de Brito Neves BB (1978) As regiões de dobramentos nordeste sudeste. *Anais do XXX Congr Bras Geol* 6, Recife, pp 2943-2506
- White MG (1961) Origin of uranium and gold in the quartzite-conglomerate of the Serra de Jacobina, Brazil. *US Geol Surv Prof Paper* 424-B, p B-9
- White MG (1964) Uranium at Morro do Vento, Serra de Jacobina, Brazil. *US Geol Surv Bull* 1185-A, pp 1-8
- Zarco JJ et al. (1979). Evaluación del indicio uranífero 'Don Vicente' Sector Norte, Pcia. de Córdoba, II Curso Latinoamericano de evaluación de indicios uraníferos. CNEA-Comisión Interamericana de Energía Nuclear
- Zenker AO (1982) Prospecção geoquímica regional para urânio na Amazônia. *Anais do XXXII Congr Bras Geol* 22, Salvador, BA, pp 1854-1868
- Zenker AO, Hohn H (1982) Ambientes geológicos favoráveis para urânio na Amazônia. *Anais do XXXII Congr Bras Geol* 22, Salvador, BA, pp 2086-2098

Subject Index

(Note: *Italics* refer to chapters or sections in the description of uranium districts and deposits, while normal letters refer to other subjects in the index)

A

- Alaskite, alaskitic 234, 305, 358
Albite (see Gangue and alteration minerals)
Albitite 367, 369, 370, 371, 415, 451, 455, 456, 457
 aegirine facies 367, 368;
 pyroxene facies 454–456
Alteration/metasomatism x (see also Gangue and alteration minerals, and Sect. *Alteration*, and Sect. *Metallogenetic Concepts/Aspects*)
 albitization 20, 24, 37, 364, 367, 369, 371, 455, 457, 459, 468, 469, 470
 alunitization 296, 299
 analcimization 21, 282, 459
 argillization 34, 139, 228, 255, 272, 273, 282, 285, 289, 290, 291, 292, 301, 304, 306, 419, 420, 421, 423, 437, 439, 464, 467, 468, 477, 483
 bleaching 37, 55, 57, 97, 99, 105, 125, 126, 132, 133, 139, 141, 143, 146, 158, 241, 248, 255, 260, 279, 307, 357, 432, 448
 calcitization 99, 125, 126, 132, 143, 216, 420, 437, 444, 468, 470
 carbonatization 126, 139, 260, 261, 263, 265, 268, 282, 285, 301, 361, 364, 420, 421, 437, 439, 469, 479
 chloritization 19, 248, 269, 279, 305, 361, 364, 437, 459, 468, 469, 470, 477, 479, 483
 decomposition, destruction, dissolution, corrosion of rock constituents 17, 18, 19, 20, 21, 22, 23, 34, 37, 42, 44, 67, 125, 139, 162, 165, 171, 202, 228, 241, 272, 284, 321, 325, 329, 364, 469, 470, 479
 desilicification 126, 132, 361, 364, 365, 367, 459, 462, 468, 470 (see also episyenitization)
 devitification 52, 284, 287, 419, 421, 483, 484
 dickitization 420
 dolomitization 125, 126, 132, 143, 146
 episyenitization 365, 459, 460, 461, 470
 hematitization 20, 37, 82, 125, 126, 189, 236, 260, 261, 263, 265, 269, 296, 298, 361, 364, 420, 424, 455, 459, 468, 470, 477, 483
 hydromicacization 468, 469
 illitization 126
 kaolinitization 19, 125, 126, 241, 279, 285, 296, 298, 300, 420, 423, 424, 430, 433, 437, 447, 467
 K feldspathization 23, 59, 260, 265, 269, 282, 283, 284, 285, 420, 421, 468
 K metasomatism 265, 284, 292, 309, 464
 limonitization 126, 279, 361
 Mg metasomatism 126, 309, 464
 microclinization 455, 459
 montmorillonitization 19, 236, 237, 238, 285, 420, 423, 424
 muscovitization 261, 459, 484
 Na metasomatism 19, 361, 364, 365, 367, 452, 455, 456, 461, 468, 469, 470 (see also albitization)
 nephelinitization 464, 465, 467
 oxidation 19, 20, 25, 37, 54, 60, 67, 79, 82, 97, 126, 143, 147, 152, 153, 165, 174, 178, 182, 185, 189, 213, 228, 272, 277, 278, 321, 322, 323, 325, 334, 340, 342, 345, 353, 420, 421, 437, 455, 465 (see also –hematitization, and –limonitization)
 phlogopitization 309
 propylitization 269, 306, 308
 pyritization 132, 139, 140, 255, 296, 298, 301, 302, 335, 349, 420, 421, 437, 439, 464, 467
 reduction 19, 34, 60, 61, 78, 82, 83, 97, 110, 125, 126, 133, 134, 135, 143, 145, 165, 229, 267, 273, 287, 321, 322, 325, 327ff, 423, 472 (see also –pyritization, –sulfidization, and Redox)
 sericitization 241, 255, 260, 261, 263, 265, 268, 269, 279, 296, 298, 300, 306, 307, 361, 433, 437, 459, 468, 477, 483
 sideritization 126
 silicification 99, 125, 126, 132, 139, 147, 216, 255, 279, 281, 282, 289, 290, 301, 302, 359, 361, 364, 419, 420, 421, 423, 424, 444, 447
 smectitization 19, 21, 37, 189, 224, 282, 289
 sulfidization 125, 126, 141, 300, 325, 337–338, 340, 345, 348
 tourmalinization 185
 zeolitization 281, 282, 283, 284, 285, 301, 304, 361, 364, 464, 467
Alteration halo (see Halo)
Alunite (see Gangue and alteration minerals)
Anhydrite (see Gangue and alteration minerals)
Anatectic (environment, processes) 458, 483, 484
Ankerite (see Gangue and alteration minerals)
Annular ring (fracture) 125, 127, 129, 132, 133, 134, 135, 137, 138, 139, 140, 141, 144, 463
Apatite 60, 145, 161, 175, 224, 237, 238, 247, 265, 268, 286, 290, 292, 361, 362, 364, 365, 366, 369, 375, 376, 377, 432, 433, 435, 450, 455, 459, 462, 468, 469, 477, 480, 483
Aquiclude/aquitard 153, 186, 196, 197, 198, 223, 274, 324, 439 (see also Impermeable)
Aquifer/solution conduit 35, 40, 80, 137, 177, 189, 219, 223, 226, 318, 320, 324, 325, 328, 329, 330, 331, 332, 339, 340, 341, 345, 349, 353, 439 (see also Permeability)
 oxygenated 35, 37, 40, 45, 52, 57, 61, 68, 81, 92, 100, 109, 110, 166, 168, 169, 172, 173, 186, 191, 196, 212, 215, 216, 219, 321, 324, 325, 327, 328, 332–335, 339, 341, 342, 345, 349, 351, 465, 472
Arenite 34, 46, 79, 99, 101, 105, 135, 165, 174, 176, 183, 185, 189, 193, 206, 216, 226, 311, 325, 326, 328, 342, 351, 429, 479
Arkose 17, 46, 117, 154, 163, 164, 166, 168, 169, 171, 174, 176, 177, 181, 182, 193, 212, 247, 326, 328, 373, 430, 431, 458, 472, 473, 474
Arkosic (see Sand, sandstone)
Ash 15, 17, 20, 21, 39, 41, 52, 67, 82, 83, 100, 101, 110, 136, 163, 173, 219, 221, 223, 224, 226, 241, 242, 270, 272–275, 279, 281, 282, 283, 284, 286, 287, 289, 290, 292, 293, 297, 299, 301, 302, 316, 320, 329, 331, 339, 373, 417, 421, 462
Asphalt, asphaltic 87, 118, 169, 249, 250
Asphaltite 118, 207, 248

B

- Bacteria 42, 127, 167–168, 169, 226, 304, 348, 353
Bacteriogenetic (bacterial, biogenic, biochemical, biological) 167, 168, 169, 173, 304, 307, 330, 439, 465, 466
Banded iron formation 475, 479
Baryte (see Gangue and alteration minerals)
Basins (general)
 Cenozoic 233, 281, 300, 321
 continental, intermontane, intracratonic 3, 12, 42, 56, 149, 164, 181, 218, 227, 233, 253, 281, 328, 364, 415, 429, 439, 440, 470
 Mesozoic 3, 9, 85, 149, 281, 415, 440, 470

- Neoproterozoic 304, 357
 Paleoproterozoic 191, 234
 Paleozoic 99, 149, 281, 415, 429, 430, 440, 470
 paralic 62
 Tertiary (-Cretaceous) 3, 9, 15, 152, 164, 168, 174, 192, 193, 219, 226, 253, 281, 311, 439, 440, 462
- Basins, depressions etc. (geographic locations)
 Andean depressions, Peru 481
 Apache Basin, USA 4, 6, 304–305
 Bighorn Basin, USA 150, 153, 244
 Bison Basin, USA 150, 182, 192–193
 Black Mesa Basin, USA 10, 85, 119
 Burgos Basin, Mexico 415, 417, 425
 Chama Basin, USA 61
 Cheyenne Basin, USA 150, 221, 226, 227, 228, 230–232
 Chu-Sarysu Basin, Kazakhstan 168, 173
 Cuenca del Golfo San Jorge, Argentina 427, 440–445
 Cuyo Basin, Argentina 430
 Danville Basin, USA 358, 359, 360, 366
 Date Creek Basin, USA 4, 6, 7, 281, 300–304
 Death Valley Basin, USA 4, 367
 Denver-Julesburg Basin, USA 4, 5, 6, 7, 226ff
 Echo Park Basin, USA 271
 Great Basin, USA 281
 Great Divide Basin, USA 5, 6, 7, 149, 150, 152, 153, 155, 162, 163, 165, 181ff
 Green River Basin, USA 150, 377
 Henry Basin, USA 65, 66, 81, 88, 89, 93
 Houston Embayment, USA 313, 314
 Jujuy-Bolivian Basin, Bolivia 429
 Kaiparowits Basin, USA 89
 Kyzylkum Basins, Uzbekistan 173
 Neuquén Basin, Argentina 439
 North Fork drainage basin, USA 243
 Paganzo Basin, Argentina 429, 430–431
 Paradox Basin, USA 9, 42, 64, 66, 79, 82, 95, 97, 99, 100
 Paraná Basin, Brazil 415, 451, 452, 462, 470ff, 480
 Pericratonic Andean Basins, 416
 Piceance Basin, USA 10
 Poison Basin, USA 6, 206–207
 Powder River Basin, USA 5, 6, 7, 149, 150, 153, 154, 155, 157, 160, 161, 162, 163, 164, 165, 169, 170, 173, 193ff, 211, 212, 226
 Rio Grande Embayment, USA 313, 314
 Salta Basin, Argentina 429
 Salt Wash basins, USA 12, 64–94
 Sand Wash Basin, USA 149, 150, 206–207
 San Juan Basin, USA 5, 6, 9, 10, 12ff
 Seridó Basin, Brazil 468
 Shirley Basin, USA 5, 6, 7, 8, 149, 150, 152, 153, 154, 157, 159, 160, 161, 162, 163, 164, 165, 173, 174, 175, 176ff, 193, 195
 Tlaxiaco Basin, Mexico 426
 Tucano Basin, Brazil 451, 452
 Uinta Basin, USA 9, 10
 Tucano Basin, Brazil 451, 452
 Washakie Basin, USA 6, 149, 150, 206–207
 Wheeler Basin, USA 255, 268
 Williston Basin, USA 219
 Wind River Basin, USA 5, 6, 7, 149, 150, 152, 153, 154, 173ff, 206, 245
 Wyoming Basins, USA 3, 4, 5, 6, 7, 26, 37, 40, 70, 75, 79, 80, 105, 149ff, 211, 212, 218, 226, 229, 238, 250, 321, 322, 324, 328, 330, 332
- Batholiths (see Intrusive complexes)
 Bedded phosphorite U deposits (see Uranium deposits–types: Type 17)
 Bentonite, bentonitic 12, 34, 46, 53, 55, 58, 60, 87, 95, 100, 101, 113, 119, 132, 149, 174, 206, 209, 219, 223, 247, 249, 270, 272, 273, 274, 292, 300, 301, 303, 316, 317, 321, 330, 339
 Bitumen, bituminous 3, 61, 127, 133, 143, 198, 379, 425, 439
 Bituminous-cataclastic calcareous sediments (see Uranium deposits–types: Type 14)
 Black shale 3, 9, 67, 106, 275, 278, 376, 379–380
 bituminous-sapropelic 379
 deposits (see Uranium deposits–types: Type 19)
 humic, coaly 379
 Bog (see Organic material)
 Bone (see Organic material)
 Brannerite (see Index U Minerals)
 Brazilian (Brazil) Shield 415, 416
 Breccia(s) (see Sect. *Shape and Dimensions of Deposits*, and Uranium deposits–types: Types 8 and 9)
 Breccia pipes (see Geographical Index, U deposits–types: Type 8, and Sandstone-internal breccia pipes)
 Brine 81, 92, 93, 127, 249, 348, 349, 466, 467
- C**
 Calcite (see Gangue and alteration minerals)
 Calcrete (caliche) 427, 431, 432, 440
 Caldasite 462
 Caldera (see Volcanic)
 Carbonaceous (see Organic material)
 Carbonates (see Gangue and alteration minerals)
 Carbonatite/alkaline complex 462, 480 (see also Uranium deposits–types: Type 12)
 Chalcedony (see Gangue and alteration minerals)
 Channel, paleochannel 17, 25ff, 66ff, 95ff, 123, 132, 135, 137, 165, 166, 174, 177, 183, 189, 193, 195, 196, 202, 203, 211, 212, 213, 215, 216, 226, 231, 232, 234, 239, 241, 272, 274, 311, 314, 319, 320, 321, 324, 325, 326, 328, 332, 335, 336, 339, 340, 342, 345, 349, 350, 353, 357, 373, 430, 439, 440–445, 447, 450, 470, 472, 473, 475, 476 (see also Mega-channel)
 Chlorite (see Gangue and alteration minerals)
 Clay (minerals) (see Gangue and alteration minerals)
 Climate, paleoclimate 39, 40, 41, 66, 95, 97, 100, 134, 152, 166, 211, 227, 281, 311, 320
 Coal (see Organic material)
 Coffinite (see Index U Minerals)
 Collapse breccia pipe U deposits (see Uranium deposits–types: Type 8, and Geographical Index)
 Collophane (see Gangue and alteration minerals)
 Collophanite 459–462
 Conglomerate 68, 88, 99, 105, 106, 113, 115, 116, 117, 121, 123, 149, 150, 174, 181, 182, 183, 185, 206, 209, 223, 226, 229, 233, 234, 239, 240, 241, 250, 270, 272, 273, 274, 275, 292, 300, 301, 319, 320, 353, 357, 358, 360, 373, 374, 417, 417, 419, 420, 421, 424, 425, 426, 427, 430, 431, 434, 435, 439, 442, 444, 445, 452, 470, 472, 473, 474, 475, 476, 479
 oligomictic, Paleoproterozoic (see U deposits–types: Type 10)
 Conglomeratic 74, 82, 87, 89, 95, 98, 105, 113, 181, 183, 191, 192, 193, 206, 215, 216, 270, 272, 292, 301, 373, 417, 419, 420, 421, 426, 433, 434, 435, 442, 472, 473, 475, 477, 479, 482
 Contact metamorphism xv, 234, 305
 Contact-metamorphic xv, 238
 Copper porphyry 3, 281, 305, 306, 309
 U deposits (see U deposits–types: Type 12)
- D**
 Deposit (dimensions, grades, resources/reserves) xiv, xvi, 166, 219, 275
 [see Chapters *U districts* and *U deposits* (introductory section), and Sect. *Shape and Dimensions*]
 types (see Uranium deposits–types)
 Deuteric 247, 304, 305, 371, 459, 460, 461, 467, 484, 485
 Diabase/dolerite 245, 247, 249, 255, 304, 305, 306, 357, 359, 364, 419, 479, 480
 Diagenesis, diagenetic 19, 21, 23, 24, 35, 37ff, 52, 56, 60, 61, 68, 69, 76, 80, 81, 82, 84, 93, 126, 136, 152, 153, 154, 165, 166, 168, 171, 177, 178, 211, 224, 282, 284, 286, 301, 302, 303, 304, 305, 333, 337, 338, 339, 439, 442, 472
 Diatreme/volcanic breccia pipe 123, 299, 464, 465, 466, 467
 Dickite (see Gangue and alteration minerals)
 Disequilibrium/equilibrium (radiometric) 240, 242, 277, 304, 364, 366, 432, 448, 472

District (dimensions, grades, resources/reserves) [see Chapters *U districts* (introductory section)]

Dolomite (mineral) (see Gangue and alteration minerals)

Dolomite (rock) 87, 121, 123, 174, 198, 275–279, 291, 292, 375, 475, 481

Duricrust, duricrusted 431, 440

E

Effusive 433, 438, 447, 484, 485

Eh 56, 144, 166, 167, 168, 169, 171, 172, 439, 484

Elements/metals, associated with U mineralization (see Metallic elements, and Sect. *Mineralization*)

Endocaldera (see Intracaldera)

Endogranitic (see U deposits–types: Type 4)

Epigenetic mineralization (see U deposits–types: Type 3, 4, 5, 6, 7, 8, 9, 11, 14, 18)

Episyenite 365, 433, 457, 459, 460, 462, 470

Evaporite, evaporitic, evaporative 9, 42, 63, 79, 80, 81, 88, 92, 93, 97, 100, 123, 125, 126, 132, 134, 256, 281, 311, 376

Extrinsic 39, 44, 311, 322, 325, 330 (see also U deposits–types: Type 3)

Extrusive 238, 281, 287, 292, 298, 299, 462

F

Faults, lineaments, structures (see Lineaments, and Sect. *Geological Setting*)

Fe-Ti oxides (see Gangue and alteration minerals)

Fluid (see Hydrogenic, and Solution)

inclusions (see Sect. *Stable Isotopes and Fluid Inclusions*, and Sect. *Metallogenetic Concepts/Aspects*)

Fluorite (see Gangue and alteration minerals)

Fold belt (see Orogen)

Fossil bone, wood, plant debris (see Organic material)

G

Gangue and alteration minerals (see also Sect. *Mineralization*)

albite 20, 23, 34, 59, 68, 80, 212, 247, 250, 260, 261, 359, 361, 367, 368, 369, 435, 455, 456, 459, 468, 483

alunite 293, 296, 298, 420, 423, 424, 465

ankerite 59, 127, 255, 256, 259, 260, 263, 266, 267, 268, 269, 305, 459, 462, 480

anhydrite 127, 130, 132, 133, 142, 143

apatite 60, 145, 161, 175, 224, 237, 238, 247, 265, 268, 286, 290, 292, 361, 362, 364, 365, 366, 369, 375, 376, 377, 432, 435, 450, 455, 459, 462, 468, 469, 477, 480, 483

baryte 20, 22, 24, 56, 60, 61, 62, 63, 67, 68, 69, 80, 106, 118, 119, 126, 127, 135, 139, 142, 143, 145, 154, 244, 279, 286, 289, 290, 307, 361, 362, 364, 374, 426, 431, 435, 448

calcite 20, 22, 24, 43, 44, 46, 50, 55, 56, 59, 62, 63, 67, 68, 69, 80, 85, 86, 87, 88, 94, 95, 105, 106, 116, 117, 118, 119, 127, 130, 131, 133, 135, 139, 140, 142, 143, 144, 145, 148, 152, 154, 156, 161, 169, 176, 177, 178, 179, 182, 185, 195, 197, 201, 206, 211, 212, 213, 215, 216, 219, 223, 244, 248, 259, 263, 266, 269, 275, 276, 277, 278, 282, 286, 289, 291, 292, 301, 304, 306, 307, 321, 325, 348, 351, 361, 362, 363, 364, 365, 369, 373, 374, 420, 423, 424, 425, 431, 433, 437, 438, 444, 450, 455, 459, 462, 468, 469, 479, 480, 483

carbonate(s) 24, 44, 47, 52, 62, 86, 90, 91, 97, 117, 121, 127, 132, 135, 137, 139, 141, 143, 146, 148, 158, 165, 216, 255, 257, 260, 261, 263, 264, 266, 267, 268, 269, 277, 286, 290, 296, 305, 342, 357, 361, 364, 369, 429, 444, 450, 465, 468, 472, 475, 480 (see also ankerite, calcite, and dolomite)

chalcedony 118, 127, 145, 163, 223, 255, 263, 275, 279, 287, 290, 296, 298, 301, 353

chlorite 20, 21, 24, 32, 33, 34, 35, 36, 37, 42, 51, 52, 56, 59, 60, 61, 63, 68, 69, 80, 81, 92, 93, 97, 185, 224, 248, 249, 250, 260, 263, 266, 282, 288, 290, 305, 306, 307, 309, 357, 359, 361, 362, 364, 437, 439, 447, 455, 459, 462, 468, 479, 480

clay (minerals) 15, 17, 19, 21, 23, 24, 34, 37, 42, 46, 49, 56, 59, 60, 61, 63, 67, 81, 88, 91, 93, 97, 106, 133, 154, 177, 216, 224, 241, 269, 275, 279, 284, 286, 288, 290, 291, 292, 301, 306, 320, 345, 348, 351, 369, 375, 437, 444, 464, 465, 466, 467 (see also chlorite, gibbsite, illite, kaolinite, montmorillonite, and smectite)

collophane 127, 142, 143, 144, 145, 459, 460, 462

dickite 420

dolomite (mineral) 63, 68, 69, 80, 81, 118, 127, 130, 131, 133, 135, 139, 141, 144, 145, 148, 260, 263, 266, 267, 271, 282, 307, 308, 437, 479

Fe-Ti oxides 20, 22, 23, 24, 34, 37, 50, 59, 60, 61, 321, 325, 345, 346, 362

fluorite 62, 63, 127, 244, 255, 263, 266, 269, 277, 286, 288, 290, 291, 292, 296, 297, 298, 299, 300, 305, 367, 369, 374, 423, 424, 425, 431, 432, 433, 455, 465, 466, 467, 468, 480

gibbsite 465

gypsum 24, 42, 62, 68, 80, 82, 88, 118, 119, 122, 126, 127, 130, 132, 133, 134, 142, 143, 145, 161, 168, 182, 219, 244, 288, 296, 298, 300, 307, 319, 353, 361, 364, 423, 444, 447, 448

hydromica 69, 93, 97, 105, 115, 224, 306, 468, 469

hydroxides of Al, Fe 39, 80, 167, 248, 420, 445, 465, 467

illite 19, 20, 21, 24, 34, 55, 56, 59, 63, 67, 81, 119, 139, 145, 224, 273, 301, 306, 320, 342, 345, 447, 464, 465, 466, 467

kaolinite 20, 21, 22, 24, 34, 37, 43, 44, 46, 51, 55, 56, 59, 60, 61, 68, 80, 119, 127, 139, 142, 143, 145, 148, 178, 197, 202, 212, 224, 248, 260, 273, 276, 282, 296, 300, 306, 307, 320, 345, 354, 375, 419, 420, 421, 422, 423, 424, 425, 435, 445, 447, 464, 465, 466, 483

K feldspar (adularia, microcline etc.) 23, 24, 34, 59, 248, 255, 260, 261, 263, 266, 267, 268, 269, 282, 283, 284, 286, 288, 289, 290, 292, 296, 359, 369, 455, 459, 464, 467, 480

montmorillonite 15, 19, 20, 21, 24, 32, 34, 36, 37, 43, 46, 51, 52, 55, 56, 60, 61, 126, 157, 158, 167, 171, 178, 197, 223, 224, 236, 237, 238, 248, 249, 273, 282, 286, 287, 288, 289, 292, 309, 320, 321, 335, 340, 342, 345, 375, 419, 423, 424, 425, 431, 444, 447, 483

opal, opalite 244, 282, 284, 285, 286, 288, 289, 290, 292, 301, 321, 335, 374, 420, 422, 423

quartz 4, 17, 24, 34, 44, 81, 82, 84, 87, 88, 92, 106, 115, 117, 127, 131, 135, 139, 140, 142, 143, 144, 145, 156, 174, 175, 181, 185, 189, 197, 207, 209, 211, 212, 213, 216, 224, 243, 247, 248, 249, 250, 254, 255, 261, 263, 269, 277, 278, 279, 286, 288, 289, 290, 201, 292, 293, 296, 297, 298, 299, 300, 305, 306, 307, 308, 309, 320, 321, 326, 328, 336, 338, 342, 346, 348, 351, 354, 357, 361, 362, 364, 369, 370, 371, 375, 420, 421, 422, 423, 424, 444, 448, 450, 455, 459, 462, 468, 469, 470, 474, 475, 479, 480, 483, 484

radiobaryte 145

sericite 133, 185, 234, 248, 249, 255, 260, 261, 263, 264, 267, 268, 291, 296, 298, 300, 306, 437, 468, 469, 475, 476, 479

siderite 600, 127, 139, 156, 143, 260, 286, 288, 300, 305, 307, 435, 448, 479, 480 (see gangue minerals)

silica 22, 34, 39, 41, 42, 43, 67, 80, 81, 88, 92, 95, 118, 127, 163, 171, 216, 244, 277, 282, 284, 286, 287, 289, 290, 292, 293, 300, 301, 302, 304, 336, 373, 424, 444, 476, 479

smectite 19, 20, 23, 24, 59, 81, 189, 224, 289, 292, 301

zeolites 59, 283, 284, 286, 288, 289, 290, 301, 304, 321, 335, 351, 361, 362, 364, 365, 424

Gas 168, 207, 226, 311, 319, 330, 349, 350, 450, 484 (see also Hydrocarbons, Hydrogen sulfide, and Methane)

Geochemistry, geochemical 21, 24, 26, 27, 35, 38, 39, 45, 57, 60, 61, 76, 80, 98, 99, 100, 101, 109, 110, 136, 156, 159, 160, 162, 163, 167, 169, 171, 213, 243, 268, 274, 290, 296, 302, 316, 321, 322, 324, 326, 328, 330, 331, 332, 336, 337, 345, 351, 365, 432, 447, 450, 454, 455, 457, 479, 480, 483, 484

Geochronological (age) data (see Sect. *Geochronology*)

Gibbsite (see Gangue and alteration minerals)

Glass, glassy 7, 40, 43, 127, 142, 143, 171, 185, 224, 282, 287, 288, 293, 304, 336, 340, 417, 419, 420, 421, 424, 437, 447, 481, 483

volcanic 40, 185, 336, 437, 447, 481, 483

Goethite 60, 118, 126, 146, 154, 156, 165, 167, 171, 175, 189, 195, 211, 306, 420, 437, 465 (see also Alteration–limonitization)

Grade (of uranium deposits and ore bodies) xiv, xvi (see Sect. *Shape and Dimensions*)

Granite xiv, xv, 7, 100, 110, 163, 164, 166, 173, 174, 175, 181, 182, 183, 185, 191, 193, 234, 235, 238, 240, 242, 245ff, 253, 254, 255, 256, 268, 272, 275, 277, 279, 281, 282, 290, 293, 297, 298, 299, 302, 304, 305, 306, 307, 308, 357, 358, 359, 361, 364, 365, 367ff, 373, 415, 417, 426, 429, 430, 431, 432, 433,

- 437, 440, 441, 444, 451, 453, 454ff, 468, 469, 470, 472, 475, 476, 477,
479, 480, 481, 482, 484
alkaline 468, 469, 479
batholiths, plutons (see Intrusive complexes)
leucocratic 364, 365, 468
metasomatized 7, 367, 468
peralkaline 367–371, 459, 461
peraluminous (leucocratic, two-mica) 305, 433
subalkaline 457
two-mica 234, 238, 305, 359, 432, 433
- Granite/felsic plutonic rocks-related U deposits (see Uranium deposits–types:
Type 4)
- Graphite, graphitic 234, 237, 241, 249, 250, 256, 267, 291, 305, 459, 477
- Groundwater 21, 26, 36ff, 44, 45, 52, 56, 57, 68, 80, 83, 94, 95, 100, 109, 110,
119, 124, 136, 163, 164, 165, 166, 167, 169ff, 189, 190, 191, 192, 202, 207,
212, 213, 215, 216, 219, 221, 239, 241, 286, 287, 290, 292, 296, 299, 300,
303, 304, 318, 321, 324, 325, 326ff, 336, 338, 341, 345, 348, 349, 351, 423,
431, 439, 465
table/level 94, 100, 109, 190, 192, 296, 305, 439
- Growth faults 311, 321, 325, 328, 332
- Guyana Precambrian Shield 415, 416
- Gypsum (see Gangue and alteration minerals)
- ## H
- Halo/aureole 32, 45, 60, 91, 105, 119, 135, 140, 145, 146, 179, 191, 213, 234,
249, 250, 255, 260, 265, 272, 274, 296, 298, 302, 304, 361, 367, 369, 445,
459, 460
- Halokinesis, halokinetic 79, 83, 95, 97, 100, 101, 105, 110
- Hematite 17, 37, 38, 40, 44, 56, 57, 60–62, 67, 80, 82, 119, 122, 126, 127, 130,
131, 135, 139, 140, 141, 142, 143, 144, 145, 146, 147, 156, 157, 165, 167, 171,
174, 175, 178, 179, 189, 195, 197, 201, 202, 204, 206, 211, 213, 215, 216, 228,
243, 244, 248, 249, 250, 255, 259, 260, 261, 263, 267, 268, 269, 275, 277, 278,
290, 296, 297, 298, 299, 300, 302, 307, 322, 329, 344, 357, 361, 362, 364, 367,
369, 420, 422, 424, 437, 439, 445, 455, 462, 467, 468, 470, 479 (see also
Alteration -hematitization)
- Host environments, -rocks (see Sect. *Geological Setting*, and Sect. *Ore Controls
and Recognition Criteria*)
- Humate, humic (see Organic material, and Urano-organic complexes)
- Hydrocarbon(s) 110, 123, 126, 127, 133, 134, 135, 248, 249, 311, 322, 328, 330,
332, 333, 350, 423, 476
- Hydrogen sulfide (H₂S) 41, 42, 110, 153, 157, 167, 168, 169, 171, 207, 226, 248,
249, 267, 300, 302, 304, 316, 321, 322, 324, 326, 327, 328, 330, 331, 332, 333,
334, 335, 340, 341, 345, 346, 349, 350, 353, 483, 484
- Hydrologic 38, 40, 41, 72, 74, 80, 100, 109, 110, 119, 133, 136, 137, 165, 173,
179, 211, 212, 230, 237, 238, 324, 326, 328, 329, 330, 333, 423
- Hydromica (see Gangue and alteration minerals)
- Hydrothermal/hydrogenic 80, 81, 136, 238, 239, 241, 242, 245, 248, 249, 250,
254, 266, 268, 269, 281, 282, 284, 286, 288, 290, 292, 297, 299, 300, 306, 308,
309, 361, 365, 366, 368, 369, 371, 422, 423, 424, 440, 447, 448, 450, 456, 457,
464, 465, 466, 467, 470, 477, 479, 480, 484
solutions/systems/water (see also Groundwater, and Solution)
connate 249, 266, 267, 268, 306, 333, 348, 365
hypogene 80, 241, 268, 284, 286, 306, 365, 433, 462, 464, 466, 467, 470,
477, 484
magmatic 136, 248, 297, 369, 450, 480
metamorphic 267, 268, 269
metasomatic 284, 309, 467
supergene, meteoric, phreatic 42, 57, 127, 241, 249, 267, 268, 284, 286,
297, 299, 300, 306, 308, 341, 348, 349, 365, 422, 423, 431, 433, 450,
457, 462, 466, 467, 472, 477, 484
- Hydroxides of Al, Fe (see Gangue and alteration minerals)
- ## I
- Ignimbrite 290, 291, 301, 417, 419, 420, 422, 423, 424, 425, 433, 444, 447, 448,
449, 481, 481, 482, 483, 484
- Illite (see Gangue and alteration minerals)
- Impermeable, impervious 20, 99, 119, 133, 134, 135, 142, 143, 149, 153,
162, 163, 165, 166, 179, 212, 224, 239, 265, 292, 324, 339, 423, 425
(see also Aquiclude)
- Intergranular, interstitial 12, 85, 105, 142, 143, 145, 185, 209, 216, 224, 248,
273, 297, 342, 350, 437, 455, 460 (see also Sect. *Mineralization*)
- Intracaldera 282
- Intrinsic 39, 207 (see also U deposits–types: Type 3)
- Intrusive, igneous, magmatic 136, 137, 234, 237, 238, 248, 253, 254, 255,
265–268, 270, 275, 277, 279, 282, 283, 286, 287, 290, 291, 292, 293, 297, 298,
299, 309, 359, 365, 367, 369, 371, 373, 425, 426, 433, 437, 450, 455, 457, 459,
461, 462, 466, 467, 468, 469, 472, 475, 480, 483, 484 (see also Orogen/
orogenic belt, Volcanic –caldera and -structures)
complexes (batholith, belt, pluton, massif etc.)
Achala batholith, Argentina 427, 432
Andean orogenic belt, Peru 415, 440
Araxá carbonatite, Brazil 471, 480
Bingham quartz monzonite stock, USA 4, 291, 309
Bokan Mountain pluton, USA 3, 4, 6, 7, 367–371
Bolivian-Peruvian Tertiary-Quaternary volcanic belt, S America 481
Boulder Creek Granodiorite, USA 254, 255, 267
Burro Mountain batholith, USA 4, 6, 306–308
Caetité Massif, Brazil 452–457
Carajás belt, Brazil 415, 416, 451, 479, 480
Cariri mobile belt, Brazil 468, 469
Cenozoic volcanic belt, Bolivia-Peru 415, 448
Central Volcanic–Plutonic Belt, Virginia, USA 358, 359
Coast Range batholith, USA 7, 370, 371, 373
Coaza batholith, Bolivia 447
Colorado Mineral Belt, USA 253, 254, 255, 256, 266, 267, 268, 305
Conway Granite, USA 357
Darby Mountain, USA 367
Dells Granite, USA 281
Elk Park Plutonic Group, USA 357
Espinhaço fold/mobile belt, Brazil 452–455, 456, 457
Grandfather Mountain Window, USA 357
Granite Mountains, USA 150, 153, 154, 163, 164, 166, 173, 174, 175,
181, 182, 183, 193, 250–251
Hercynian Massif, France 484
Huato batholith, Peru, 447
Idaho batholith, USA 233, 242, 243
Ipora Massif, Brazil 472
Lagoa Real Complex, Brazil 453–455
Lawler Peak Granite, USA 281, 306
Leatherwood Granite, USA 358, 359, 364, 365
Limbani-Quillabamba batholith, Bolivia 447
Loon Lake batholith, USA 233, 234, 235, 236, 237, 238, 239, 240
Martinsville Igneous Complex, USA 358
Massif Central, France 306, 365
Mortagne Massif, France 469
Mount Spokane quartz monzonite, USA 4, 241
Paramirim pluton, Brazil 454
Phillips Lake Granodiorite, USA 242
Pikes Peak batholith, USA 254
Ruin Granite, USA 281
Santa Quitéria-Tamboril Complex, Brazil 458, 459
São Roque Granite, Brazil 478
São Timóteo pluton, Brazil 451, 454, 455
Sierras Grandes granite, Argentina 432
Silver Plume batholith, USA 254, 268, 266, 268
SE Nevada-Arizona-SW New Mexico alaskite, granite, monzonite
intrusions, USA 305, 306
Sweetwater batholith, USA 249
Tertiary-Quaternary volcanic belt, Bolivia-Peru 481
Trimble Granite, USA, 100
Twin Buttes batholith, USA 4
Twin Peaks batholith, USA 306–308
Western Piedmont belt, USA 357
White Mountain Magma Series, USA 357
Wilson Creek Gneiss, USA 357
type U deposits (see Uranium deposits–types: Type 12)
rocks (see Intrusive complexes, and Uranium deposits–types:
Types 4 and 12)

Isotopes, stable (see Stable isotopes, and Sect. *Stable Isotopes and Fluid Inclusions*)

radiogenic (see Sect. *Geochronology*)

Itabirite 479

K

Kaolinite (see Gangue and alteration minerals)

Karst (cavern) 121, 123, 124, 125, 133, 134, 135, 233, 234, 244–245, 462

(see also Uranium deposits–types: Types 8, 11, and 14)

Kerogen (see Organic material)

L

Lacustrine (see Sediments, and Uranium deposits–types: Type 15)

Lagoon, lagoonal (see Sediments)

Lahar, laharc 417, 425

Lamprophyre 464, 467

Land-pebble phosphate/phosphorite 375–376 (see also Uranium deposits–types: Type 17)

Laterite, lateritic 463, 464, 470, 472, 474

Lignite (see Organic material, and Uranium deposits–types: Type 18)

Limestone 3, 6, 7, 9, 11, 12, 14, 15, 16, 17, 18, 25, 26, 36, 42, 43, 46, 49, 53, 60, 61–63, 88, 95, 97, 116, 117, 121, 122, 123, 124, 125, 126, 127, 129, 131–135, 137, 138, 140, 141, 143, 144, 146, 147, 148, 149, 150, 151, 152, 174, 233, 234, 244, 245, 249, 250, 275, 279, 281, 300, 302, 303, 330, 336, 354, 375, 379, 417, 418, 420, 422, 423, 424, 425, 426, 429, 430, 431, 437, 458, 470, 472, 481 (see also Uranium deposits–types: Type 14)

Limonite 17, 24, 31, 55, 57, 85, 88, 89, 91, 94, 119, 122, 125, 126, 146, 147, 148, 156, 157, 158, 173, 174, 178, 196, 197, 201, 202, 204, 207, 216, 219, 228, 248, 269, 275, 277, 278, 279, 289, 290, 322, 344, 354, 369, 373, 420, 424, 425, 466 (see also Goethite, and Alteration -limonitization)

Lineaments 97, 123, 243, 256, 270, 282, 306, 308, 359, 364, 452, 454, 455, 458, 459, 460, 461, 468, 481

Lutite 300, 429, 447, 448, 449 (see also U deposits–types: Type 15)

M

Macusanite 481, 483

Magmatic (igneous) (see Intrusive, and Volcanic –caldera and -structures)

Marcasite 22, 24, 49, 69, 87, 106, 117, 118, 119, 127, 130, 131, 141, 142, 143, 144, 145, 146, 154, 156, 157, 160, 161, 169, 178, 179, 182, 192, 195, 202, 206, 211, 213, 215, 226, 228, 236, 237, 238, 260, 263, 264, 269, 270, 277, 278, 279, 282, 288, 322, 323, 330, 332, 333, 362, 364, 365, 379, 431, 437, 448

Mega-channel 312, 321, 324, 325, 326, 328, 332, 333, 335, 342

Metallic elements (associated with U)

Ag 7, 69, 97, 98, 117, 120, 127, 128, 132, 137, 138, 139, 140, 146, 234, 243, 249, 255, 256, 262, 264, 281, 286, 290, 297, 298, 302, 305, 306, 307, 308, 426, 460, 480

As 22, 24, 27, 35, 44, 51, 56, 69, 70, 71, 72, 118, 125, 128, 140, 146, 147, 154, 161, 165, 172, 175, 178, 211, 219, 236, 237, 238, 260, 261, 262, 263, 264, 265, 266, 279, 286, 289, 290, 297, 298, 302, 308, 472, 483

Au 3, 7, 120, 127, 128, 132, 136, 138, 139, 140, 146, 209, 234, 249, 255, 292, 297, 298, 305, 307, 309, 415, 475, 476, 477, 479, 480

Be 27, 128, 161, 260, 262, 291, 292, 369, 483

Bi 27, 262, 281, 306, 308, 309

Cd 97, 105, 119, 127, 128, 146, 148, 262, 465

Ce 56, 128, 362, 480

Co 24, 27, 44, 93, 97, 117, 119, 127, 128, 132, 135, 137, 138, 139, 142, 143, 146, 147, 148, 237, 238, 262, 264, 281, 297, 298, 306, 307, 308, 379, 479

Cs 284, 286, 289, 292, 420, 423, 483

Cu 7, 22, 24, 27, 35, 69, 70, 93, 97, 98, 105, 110, 115, 117, 119, 120, 127, 128, 132, 135, 137, 138, 140, 145, 146, 147, 154, 161, 172, 178, 249, 250, 261, 262, 265, 269, 278, 279, 286, 289, 290, 292, 297, 298, 302, 305, 308, 309, 342, 357, 369, 379, 415, 426, 433, 439, 450, 472, 479, 480

Fe 22, 24, 27, 32, 33, 35, 44, 57, 59, 60, 63, 69, 73, 85, 97, 115, 119, 127, 132, 135, 137, 138, 140, 145, 148, 156, 158, 165, 167, 172, 175, 178, 182, 207, 211, 226, 263, 264, 266, 277, 278, 289, 305, 308, 336, 337, 338, 340, 342, 345, 348, 373, 420, 433, 437, 439, 444, 450, 456, 460, 467, 479, 480, 483

Ga 27, 128, 239, 250, 262, 302, 454

Ge 302, 472

Hf 128, 467

Hg 128, 260, 261, 262, 264, 282, 283, 284, 285, 286, 287, 289, 290, 308

La 128, 361, 362, 460, 480, 483

Li 128, 240, 284, 285, 286, 289, 292, 302, 447, 483

Mo 22, 24, 27, 32, 35, 38, 44, 51, 69, 70, 73, 92, 93, 97, 101, 105, 117, 119, 127, 128, 132, 139, 142, 143, 147, 148, 159, 160, 161, 165, 169, 172, 175, 182, 207, 213, 219, 228, 237, 238, 240, 242, 250, 256, 260, 261, 262, 263, 264, 265, 266, 277, 286, 289, 290, 291, 296, 298, 299, 302, 305, 309, 321, 325, 326, 332, 340, 342, 346, 348, 369, 379, 420, 421, 422, 423, 424, 425, 442, 447, 460, 462, 464, 465, 466, 468, 472, 480, 483

Nb 128, 237, 238, 240, 262, 279, 292, 369

Nd 128

Ni 27, 44, 69, 93, 97, 117, 119, 127, 129, 132, 135, 138, 139, 141, 142, 143, 145, 146, 147, 237, 238, 250, 262, 264, 269, 281, 302, 306, 307, 308, 379, 472

Pb 24, 27, 33, 34, 44, 56, 69, 70, 92, 97, 115, 117, 119, 125, 127, 129, 132, 135, 137, 138, 139, 140, 142, 143, 162, 163, 234, 237, 238, 243, 250, 256, 260, 261, 262, 263, 264, 265, 277, 278, 279, 286, 292, 297, 298, 305, 342, 361, 369, 422, 424, 426, 460, 464, 467, 472

Pd 309

Pt 309

Rb 129, 284, 286, 289, 292, 464, 467, 483

Re 309

REE xvi, 7, 24, 37, 38, 117, 362, 367, 368, 369, 370, 371, 379, 415, 422, 424, 447, 457, 462, 465, 466, 467, 469, 479, 480, 483

Sb 24, 127, 129, 132, 260, 261, 262, 263, 264, 265, 286, 289, 290, 297, 298, 484

Sc 129, 262

Se 22, 24, 27, 32, 33, 35, 38, 45, 51, 56, 69, 70, 71, 72, 73, 79, 92, 93, 97, 127, 129, 154, 156, 158, 159, 160, 164, 165, 169, 172, 175, 178, 179, 182, 204, 207, 211, 213, 250, 309, 321, 325, 326, 332, 340, 342, 346, 425, 472

Sm 129

Sn 240, 286, 290, 292, 369, 483

Sr 24, 27, 127, 129, 261, 262, 265, 299, 369, 422, 424, 447, 455, 460, 464, 483

Ta 129, 292

Tb 129

Th 24, 129, 164, 209, 234, 250, 261, 262, 265, 284, 286, 289, 297, 298, 299, 331, 367, 368, 369, 370, 371, 422, 424, 447, 450, 455, 456, 460, 462, 464, 465, 467, 469, 472, 476, 483

Ti 129, 207, 302, 351, 361, 362, 364, 455, 460, 465, 467, 483

Tl 29, 262, 297, 298, 483

V 7, 12, 22, 24, 27, 32, 33, 35, 42, 44, 45, 46, 47, 53, 56, 62, 63, 64ff, 95, 97, 98, 101, 105, 106, 109, 113, 115, 116, 117, 119, 127, 129, 132, 140, 141, 148, 159, 161, 165, 167, 169, 172, 175, 178, 195, 204, 206, 207, 209, 211, 212, 213, 215, 216, 221, 226, 228, 229, 244, 245, 253, 261, 262, 265, 270, 302, 326, 332, 342, 357, 367, 379, 423, 425, 429, 431, 439, 441, 447, 472

W 237, 260, 279, 286, 289, 290, 292, 297, 298, 483

Y 22, 24, 27, 35, 44, 117, 129, 237, 238, 262, 279, 297, 298, 455, 460, 467, 469

Yb 27, 117, 129, 262, 469, 483

Zn 69, 70, 97, 119, 125, 127, 129, 135, 137, 138, 139, 140, 142, 143, 146, 159, 234, 237, 238, 242, 243, 244, 250, 256, 261, 262, 265, 278, 279, 286, 289, 305, 307, 369, 426, 472, 480

Zr 27, 129, 262, 264, 279, 286, 289, 290, 298, 369, 371, 455, 460, 462, 465, 466, 467

Metallic minerals (arsenides, sulfides etc.) associated with U (see Sect.

Mineralization)

Metallogenesis xiii (see Sect. *Metallogenetic Concepts/Aspects*)

Metamorphic environment

amphibolite facies/grade xv, 121, 245, 256, 306, 357, 359, 364, 365, 370, 455, 479

greenschist facies/grade 234, 474

retrograde 364, 455, 457, 460, 461, 475, 477

Metasomatism, metasomatic 3, 6, 19, 124, 126, 239, 247, 265, 268, 269, 282–284, 309, 361, 364, 365, 367, 371, 451, 455–457, 459, 461, 464, 467, 468–470, 477, 479 (see also Alteration)

Metasomatite U deposits (see Uranium deposits–types: Type 6)

Methane 41, 110, 226, 267, 350, 353

Migmatite, migmatitic, migmatization 255, 454, 456, 458, 468, 477, 479

Mineral assemblage/paragenesis (see Sect. *Mineralization*)

- Mineral belt, region, trend
 Big Indian Belt, USA 105
 Central Temple Mountain Belt, USA 96, 97, 117
 Colorado Mineral Belt, USA 253, 254, 255, 256, 266, 267, 268, 305
 Grants Mineral Belt, USA 9, 12, 15
 Grants Uranium Region, USA 6, 8, 10, 12ff
 Henry Mountains Mineral Belt, USA 88, 89
 Lisbon Valley Uranium Belt, USA 109
 Live Oak County Mineral Trend, USA 328
 North Bee County Mineral Trend, USA 328
 South Texas Uranium Region, USA 3, 4, 6, 7, 166, 311ff
 Tidwell Mineral Belt, USA 86
 Uravan Mineral Belt, USA 3, 4, 6, 7, 9, 10, 31, 37, 42, 64ff, 81–83, 84, 94
- Mineralization [see U (deposits) mineralization, Ore –composition, and Sect. *Mineralization*]
- Miogeosynclinal 233, 376, 377
- Moat 282, 283, 284, 286, 287, 289
- Monazite (see Index U Minerals)
- Monometallic [see U (deposits) mineralization]
- Montmorillonite (see Gangue and alteration minerals)
- N**
- Nappe 246, 357
- O**
- Oil 8, 110, 123, 127, 168, 169, 207, 226, 250, 311, 314, 319, 330, 336, 339, 349, 350, 351, 353, 379
- Oligomictic (paleo)conglomerate-hosted U deposits (see U deposits–types: Type 10)
- Opal, opalite (see Gangue and alteration minerals)
- Ore xiii, xiv, xv, xvi
 bodies, shape/configuration, dimension (see Sect. *Shape and Dimensions*)
 composition (see also Gangue minerals, Metallic elements, and Sect. *Mineralization*)
 controls (see Sect. *Ore Controls and Recognition Criteria*)
 districts/fields (see Geographical Index)
- Organic material (see also Asphalt, Asphaltite, Bacteria, Hydrocarbons, Hydrogen sulfide (H₂S), Methane, Oil, Petroleum, and Uranium deposits–types: Types 3, 11, 14, 15, 18, 19)
 algae 379
 bitumen, bituminous 3, 61, 127, 143, 379, 425, 439
 bog, marsh, muskeg, paludal, peat, swamp 7, 39, 57, 61, 106, 110, 181, 187, 196, 233, 242, 243, 281, 300, 302, 320, 328, 470, 472
 bones, fish scales 34, 57, 353, 373
 carbonaceous 4, 20, 38–41, 43, 44, 46, 49, 50, 52, 60, 61, 67, 68, 69, 72, 79, 80, 82, 83, 84, 85, 86, 87, 88, 89, 90, 91, 92, 94, 95, 99–101, 105, 110, 113, 115, 116, 117, 119, 139, 149, 152, 154, 164, 165, 166, 169, 172, 173, 174, 176, 177, 178, 181, 182, 183, 185, 186, 189, 191, 196, 197, 198, 204, 206, 207, 209, 212, 213, 215, 216, 218, 219, 221, 226, 227, 233, 239, 240, 241, 249, 257, 270, 272, 273, 274, 275, 277, 279, 281, 282, 284, 287, 289, 300, 301, 302, 303, 304, 305, 321, 322, 324, 325, 328, 330, 333, 334, 335, 337, 338, 342, 346, 357, 360, 367, 373, 376, 425, 429, 430, 442, 443, 444, 470, 472, 474, 475, 477, 483
 coal, coaly, coalified 4, 35, 49, 57, 101, 149, 168, 181, 187, 193, 195, 197, 198, 199, 201, 209, 239, 270, 277, 278, 302, 367, 373, 379, 430, 470, 472
 humate 12, 15, 17, 19, 20, 21, 22, 24, 25, 29, 32, 34, 35, 37, 38–40, 41, 42, 43, 44, 45, 49, 53, 56, 57, 59, 66, 75, 78, 79, 80, 92, 99, 100, 109, 110, 145, 152, 168, 172, 206, 209, 212, 302, 303, 304, 320, 342, 379 (see also Urano-organic complexes)
 humic 19, 25, 35, 38–40, 41, 42, 49, 66, 79, 80, 92, 110, 118, 152, 172, 303, 304, 320, 379
 kerogen 62, 123, 127
 lignite, lignitic 3, 7, 25, 61, 118, 180, 181, 189, 193, 195, 196, 197, 198, 201, 209, 219–221, 222, 226, 229, 300, 302, 311, 314, 317, 321, 324, 335, 336, 337, 338
 organic (not differentiated) 12, 17, 19, 22, 24, 32, 34, 37, 38, 39, 40, 41, 42, 43, 44, 45, 49, 50, 52, 56, 57, 58, 60, 61, 62, 63, 68, 72, 81, 86, 92, 100, 101, 109, 117, 127, 132, 140, 143, 152, 153, 154, 160, 161, 165, 166, 167, 168, 169, 172, 174, 175, 176, 178, 182, 185, 186, 193, 195, 206, 209, 211, 215, 219, 226, 241, 242, 243, 249, 266, 267, 268, 275, 277, 278, 279, 286, 287, 289, 302, 304, 305, 323, 324, 328, 330, 335, 336, 337, 338, 340, 342, 346, 348, 358, 379, 430, 437, 438, 439, 441, 442, 444, 472, 474
 plant, detrital carbon, vegetal, wood (debris/trash) 17, 19, 35, 38, 39, 40, 41, 43, 61, 68, 69, 80, 83, 85, 86, 87, 88, 89, 92, 93, 94, 95, 97, 152, 157, 165, 166, 179, 192, 211, 213, 215, 218, 219, 229, 301, 315, 317, 321, 322, 324, 330, 333, 337, 338, 346, 379, 430, 431, 442, 444
 tree logs/trunks 17, 82, 83, 85, 154, 152, 430, 442, 444
 uraniferous (see Urano-organic complexes)
- Orogen, orogenic, fold/mobile belt, region, system, zone
 Andean Geosyncline (Geosynclinal Andino), Argentina 427, 439
 Andean orogenic belt, South America 415, 440
 Araçuaí belt, Brazil 454, 455
 Carajás region, Brazil 415, 416, 451, 479–480
 Cariri belt, Brazil 468, 469
 Central Volcanic–Plutonic Belt, Virginia, USA 358, 359
 Espinhaço (Setentrional) belt, Brazil 452–455, 456, 457
 Jaguaribeana belt, Brazil 458, 459
 Precordillera belt, Argentina 415
 Riacho do Pontal belt, Brazil 455
 Ribera belt, Brazil 454
 Western Piedmont belt, USA 357, 358
- Orogeny
 Andean Orogeny 433, 437, 481
 Asturian orogenic phase 437
 Brazilian Orogeny 415, 416, 452, 454, 456, 457, 458, 461, 462, 468, 470, 477
 East Kootenay Orogeny 243
 Espinhaço Orogeny 415, 452, 454
 Hercynian Orogeny 481
 Laramide Orogeny 3, 9, 35, 149, 209, 244, 245, 249, 253, 254, 255, 258, 259, 266, 281
 Nevada orogenic phase 281, 429
 Qurié-Jequié Orogeny 452
 Saalian orogenic phase 437
 Transamazonian Orogeny 452, 454, 458, 468
- Oxidized mineralization (see Sect. *Mineralization*, and Sect. *Metallogenetic Concepts/Aspects*)
- Oxidized environment, zone (see Sect. *Alteration*, and Sect. *Metallogenetic Concepts/Aspects*)
- P**
- Paleosol 224, 320, 423 (see also Saprolite, and Soil)
- Paleoproterozoic quartz-pebble conglomerate U deposits (see Uranium deposits–types: Type 10)
- Paragenesis, paragenetic mineral assemblage, sequence (see Sect. *Mineralization*)
- Peat (see Organic material)
- Pechblende (see Index U Minerals: Pitchblende)
- Pegmatite, pegmatitic xiv, xv, 4, 7, 234, 241, 247, 254, 255, 256, 258, 265, 269, 275, 277, 305, 306, 357, 359, 367, 368, 369, 370, 429, 432, 437, 459, 468, 469, 5470, 475, 477
 U deposits (see Uranium deposits–types: Type 12)
- Peralkaline granite 367–371
 volcanics, nepheline syenite etc. 282, 284, 286, 289, 290, 423, 454 (see also Uranium deposits–types: Type 12)
- Permeability, permeable, transmissivity 20, 37, 39, 42, 51, 52, 57, 59, 63, 70, 72, 78, 99, 133, 134, 141, 144, 146, 156, 162, 163, 165, 176, 179, 196, 197, 199, 211, 212, 219, 228, 268, 272, 274, 309, 324, 325, 328, 350, 353, 365, 439, 442, 444
- Petroleum 63, 169
- pH 37, 39, 41, 42, 80, 144, 167, 168, 169, 171, 172, 267, 268, 269, 287, 300, 304, 308, 462, 484
- Phosphate 8, 24, 132, 144, 161, 172, 182, 213, 243, 249, 296, 335, 361, 365, 373, 375–377, 432, 480 (see also Land-pebble phosphate)
- Phosphatic, phosphorous 172, 279, 375–377, 379, 457–462
- Phosphorite 3, 6, 8, 375–377, 417, 426, 481
 U deposits (minerochemical) (see Uranium deposits–types: Type 17)
- Pitchblende (see Index U Minerals)

Placer, paleoplacer 269, 475 (see also Uranium deposits—types: Type 10)
 Platform, paraplatform 209, 233, 375, 415, 416, 429, 440, 451, 452, 454, 474
 Playa (see Sediments)
 Pluton (see Intrusive complexes)
 Pneumatolytic 423, 467
 Polymetallic [see U (deposits) mineralization]
 iron-oxide (hematite)-breccia-complex U deposits (see Uranium deposits—types: Type 9)
 Potassium/K, potassic 247, 260, 269, 282, 284, 286, 288, 292, 302, 305, 357, 420, 431, 454, 455, 464, 465, 467, 468 (see also Alteration, and Gang minerals –K feldspar)
 Precambrian cratons, shields etc.
 Amazon Craton, South America 416, 451, 479
 Atlantic Craton/Shield, South America 416, 451, 462
 Basin and Range Precambrian terrane, USA 5, 281
 Brazilian/Brazil Shield, South America 415, 416, 451, 480
 Colorado and Southern Rocky Mountains Precambrian terrane, USA 5, 233, 253ff
 Eastern United States Precambrian terrane, USA 357
 Guyana Shield, South America 415, 416, 451, 465
 Northern Rocky Mountains Precambrian terrane, USA 5, 233ff
 São Francisco Craton, Brazil 451, 452, 453, 455, 468, 479
 São Luis Craton, Brazil 468
 Western United States Precambrian terrane, USA 3, 5
 Precipitation (deposition, fixing) of uranium (see Sect. *Metallogenetic Concepts/Aspects*)
 Production of uranium [see Chapters *U districts* and *U deposits* (introductory section)]
 Province, uranium (see Uranium -province)
 Pyrite 22, 34, 35, 44, 45, 49, 52, 57, 59, 60, 62, 67, 85, 86, 87, 88, 94, 105, 106, 117, 118, 119, 125ff, 154ff, 156, 157, 158, 159, 163, 167, 175, 178, 179, 182, 189, 192, 195, 197, 202, 206, 207, 211, 213, 215, 219, 223, 226, 228, 234, 236, 237, 238, 239, 243, 248, 249, 250, 259, 260, 263, 264, 267, 269, 270, 275, 277, 282, 286, 288, 289, 290, 296, 297, 298, 300, 302, 305, 306, 321ff, 362, 364, 369, 374, 379, 420, 421, 422, 423, 424, 425, 429, 431, 437, 441, 448, 455, 466, 468, 469, 472, 474, 475, 476, 477, 479, 480 (see also sect. *Alteration*, and Sect. *Mineralization*)
 Pyroclastic rocks 19, 37, 38, 40, 52, 56, 76, 80, 233, 234, 239, 253, 257, 265, 270, 282, 290, 300, 311, 324, 325, 330–332, 336, 339, 350, 373, 415, 417, 424, 435, 439, 440, 441, 442, 443, 448, 450, 454, 466, 479, 481, 483, 484 (see also Ignimbrite, and Tuff)

Q

Quartz (see Gangue and alteration minerals)
 Quartz-monzonite 233–241, 249, 254, 255, 271, 279, 281, 291, 293, 294–295, 297, 298, 299, 306–308, 309, 358, 359, 363, 367, 370
 deposits (see Uranium deposits—types: Type 12)

R

Radiobaryte (see Gangue and alteration minerals)
 Radium 7, 9, 110, 112, 266, 438
 Radiogenic isotopes (see Sect. *Geochronology*)
 Rare earth elements (REE) (see Metallic elements)
 Recognition criteria (see Sect. *Ore Controls and Recognition Criteria*)
 Redox, reduction-oxidation (conditions, front, interfaces) 19, 26, 40, 55, 57, 61, 70, 73, 78, 149ff, 213, 321ff, 338, 344, 347, 351, 352, 353, 425, 465, 466, 467, 472 (see also Rollfront, Sect. *Alteration*, and Sect. *Metallogenetic Aspects/Concepts*)
 Reducing environments, reduction (see Sect. *Alteration*, Sect. *Mineralization*, and Sect. *Metallogenetic Aspects/Concepts*)
 Reductants, reducing agents (see Asphalt, Asphaltite, Bacteria, Humate, Hydrocarbon, Hydrogen sulfide (H₂S), Methane, Oil, Organic material, Petroleum, and Uranium deposits—types: Types 3, 11, 14, 15, 18, 19)
 Regolith, regolithic (paleosol) xiv, 256, 266, 271, 279
 Reserves/resources (of uranium) [see Chapters *U districts* and *U deposits* (introductory section)]
 cost categories xv
 definitions categories xv, xvi

estimated additional (EAR) (= inferred) xv
 in situ xvi
 inferred xv
 reasonably assured (RAR) xv, xvi
 recoverable xv

Rhyolite, rhyolitic 163, 270, 275, 281–293, 297, 298, 299, 306, 321, 359, 373, 417, 419, 421, 422–424, 435, 438, 441, 442, 444, 445, 447, 477, 481, 483
 Rollfront, roll-shaped, roll-type 25, 26, 30–31, 32, 34, 35, 36, 37, 43, 51, 56, 60, 61, 69, 70, 72, 74, 75, 78, 79, 80, 84, 87, 105, 140, 149ff, 209, 211–212, 213, 216, 221, 224–226, 228–232, 249, 311, 316, 321ff, 335ff, 474 (see also Sect. *Shape and Dimensions*, and Uranium deposits—types: Type 3)

S

Salt domes/diapirs 100, 109, 320, 322, 324, 350, 351, 353, 354 (see also Halokinesis)
 Alta Mesa domal structure, USA 3, 312, 350–353
 Alta Verde Dome, USA 312, 320, 354
 Kingsville Dome, USA 3, 8, 312, 350, 351
 Palangana Dome, USA 312, 320, 350, 351, 353, 354
 Piedras Pintas Dome USA 312, 320, 350
 Sejita Dome, USA 312, 343, 350, 354
 Sand/sandstone (see also Arenite, Sediments, Sect. *Geological Setting*, and Uranium deposits—types: Type 3)
 arkose (see Arkose)
 arkosic 9, 12, 43, 49, 51, 55, 56, 60, 78, 82, 83, 101, 106, 115, 117, 149, 150, 152, 163, 164, 165, 166, 176, 179, 181, 183, 185, 191, 192, 193, 195, 196, 197, 199, 201, 203, 206, 212, 223, 224, 226, 227, 228, 231, 233, 239, 240, 250, 270, 273, 275, 281, 300, 301, 303, 321, 346, 348, 358, 373, 434, 435, 474, 476
 carbonaceous (see Organic material)
 feldspathic 15, 17, 25, 43, 45, 55, 58, 60, 66, 88, 99, 105, 224, 226, 228, 304, 305, 338, 359, 470, 472, 474, 475
 fluvial (see Sediments -fluvial-alluvial)
 marginal marine (littoral) 3, 88, 122, 123, 134, 206, 215, 226, 227, 311ff, 373, 429, 470, 472
 redbed 12, 67, 68, 78–80, 82, 95, 97, 123, 134, 135, 250, 253, 256, 269, 357, 427, 430, 450, 451, 470 (see also Sediments)
 tuffaceous, tuff/felsic volcanic interbeds 84, 99, 164, 219, 270, 300, 419, 425, 435
 Sandstone-hosted U deposits (see Uranium deposits—types: Type 3)
 internal breccia pipes 17, 32, 35, 36, 46–48
 Saprolite, saprolitic 361, 364, 379, 464 (see also Paleosol, and Soil)
 Sediments, sedimentary environment (see also Sect. *Geological Setting*, and Sect. *Ore Controls and Recognition Criteria*)
 alluvial 79, 346
 continental/terrestrial 3, 9, 13ff, 64ff, 95ff, 149ff, 209, 219, 227, 253, 256, 321, 328, 333, 367, 419, 427, 429, 433, 435, 437, 439, 440, 447, 475
 continental shelf 376, 377
 delta, deltaic 229, 300, 302, 314, 319, 320, 321, 324, 335, 336, 339, 341, 345, 350, 454, 470, 472
 epicontinental 379
 fluvial (-alluvial) 12, 13ff, 64ff, 95ff, 121, 122, 123, 135, 149ff, 226, 240, 274, 281, 311ff, 359, 425, 430, 432, 433, 439, 440–445, 470, 479, 481
 lacustrine 7, 9, 15, 17, 25, 39, 40, 42, 67, 88, 89, 91, 97, 101, 110, 149, 181, 187, 193, 196, 206, 253, 270, 281, 282, 284, 287, 289, 290, 292, 300–304, 319, 324, 325, 328, 331, 339, 340, 359, 432, 440, 441, 442, 470, 481, 484 (see also Uranium deposits—types: Type 15)
 lagoon, lagoonal 122, 215, 226, 229, 314, 316, 321, 328, 335, 336, 429, 440
 limnic 429
 littoral/coastal plain 123, 134, 135, 209, 226, 319, 321, 325, 326, 328, 429, 430, 470, 475
 marginal marine 209, 215, 226, 227, 256, 311ff, 373, 429, 470, 472
 marine 42, 121, 135, 253, 256, 281, 311, 322, 338, 373, 375–377, 379, 417, 429, 433, 437, 440, 442, 447, 454, 470, 475, 479
 paludal 281, 300, 301, 302, 320, 470, 472
 playa 17, 42, 281

- redbed 67, 79, 265, 266, 430, 450
 shallow marine (near-shore platform) 253, 322
 terrestrial (see above continental)
 volcanogenic, tuffaceous (see Ignimbrite, Pyroclastic, Tuff)
- Sericite (see Gangue and alteration minerals)
- Shape/configuration (of ore bodies) (see also Sect. *Mineralization*, and Sect. *Shape and Dimensions*)
 lens, lensoid, lenticular (see U deposits–types: Type 3, 10, 15)
 peneconcordant (see U deposits–types: Type 3)
 rollfront, roll-shaped (see U deposits–types: Type 3)
 stack, stacked (see U deposits–types: Type 3 –tectonic-lithologic)
 stockwork (see U deposits–types: Type 4, 5, 6, 7, 9)
 tabular, blanket (see U deposits–types: Type 3, 10, 15, 18)
 vein, veinlike xv (see U deposits–types: Type 4, 5, 6, 7)
- Siderite (see Gangue and alteration minerals)
- Silica (see Gangue and alteration minerals)
- Smectite (see Gangue and alteration minerals)
- Sodium/Na, sodic 20, 37, 38, 92, 247, 249, 452, 455 (see also Albitite, Alteration, and Gang minerals –albite)
- Soil 320, 331, 332, 333, 440, 463, 464 (see also Duricrust, Paleosol, and Saprolite)
- Solution, fluid 37–43, 52, 80–81, 93, 110, 123, 126, 131, 133, 135–138, 141, 142, 144, 156, 166–173, 175, 177, 179, 191, 211, 244, 249, 267–269, 286, 298, 332, 335, 336, 376, 377, 420, 422, 425, 437, 439, 462, 467, 472, 481
 (see also Groundwater, Hydrogenic, and Hydrothermal)
- Source(s) of uranium (see Sect. *Sources of Uranium*)
- Stable isotopes 130, 265, 266, 297, 336, 348–349, 420, 456, 466, 467, 480
 (see also Sect. *Stable Isotopes and Fluid Inclusions*, and Sect. *Metallogenetic Concepts/Aspects*)
- Strata-bound, -controlled U mineralization (see U deposits–types: Type 3, 10, 14, 15, 17, 18, 19)
- Stratigraphy (see Sect. *Geological Setting*)
- Stratigraphic units [U or (U) indicate units with significant or minor U mineralization, respectively]
 Adobes Fm (see Los Adobes Fm)
 Aisol Fm 433, 436
 Amsden Fm 151, 198, 244
 Anderson Mine Mbr U 300–303
 Antero Fm 270
 Apache Gp (U) 6, 7, 85, 86, 279, 304–305
 Arai Gp 477, 478
 Araxa Gp 472
 Areniscas Atigradas Mbr U 434, 435–439
 Arikaree Fm 150, 151, 171, 219, 220, 222, 223, 228
 Arrastra Volcanics 301, 303
 Arroyo del Pajarito Mbr U 440–445
 Ash Fall Mbr U 270–275
 Atigradas Sandstone Mbr (see Areniscas Atigradas Mbr)
 Aurora Lava or Series (U) 282, 286, 287, 288, 289
 Balbuena Sub Gp (U) 429, 430
 Bambui Gp 477
 Bardas Coloradas Mbr 442
 Basset Fm 357
 Battle Spring Fm U 149, 150, 151, 181–187, 189, 191, 250
 Beartooth Quartzite 306, 307
 Beclabito Mbr 15, 16, 17, 18
 Belden Fm (U) 271, 275–279
 Belle Fourche Sh 151
 Belt Super Gp U 233, 234, 242, 243
 Beryllium Tuff Mbr (U) 292
 Bighorn Dol 152, 198
 Bluff Ss 11, 18, 25, 45
 Bone Valley Fm (U) 375, 376
 Bretz Series 282, 287
 Browns Park Fm (U) 151, 206, 207
 Brule Fm 223, 224, 227, 229
 Brushy Basin Mbr U 6, 9, 11, 12, 15ff, 46–47, 49, 53–58, 60, 61, 64, 67, 68, 74, 76, 78, 80, 81, 82, 87, 88, 93
- Bucksprings Fm 250
 Bullard Peak Volcanics or Series (U) 306, 307
 Cabeza de Montero Mbr (U) 431
 Caddell Fm 314
 Caicó Fm or Gp U 458, 459, 468, 469
 Calliham Ss Mbr 316, 317
 Cañadón Puelman Fm 440, 442, 444
 Caraca Gp (U) 475
 Carlisle Sh 151
 Carmel Fm 11, 104
 Carrizo Sand or Fm U 314, 330, 349
 Casa Grande Fm 431
 Catahoula Fm U 313ff, 336, 339–345, 346, 347, 348, 349, 354
 Catskill Fm (U) 357
 Ceará Series 458
 Cerro Barcino Fm 440, 441, 442, 444
 Cerro Castano Mbr 442
 Chadron Ss or Fm U 221, 223, 226–226, 227, 228, 229
 Chamarra Fm (U) 447, 450
 Chapada-Diamantina Super Gp 454
 Chapin Wash Fm U 300
 Chattanooga Sh (U) 3, 379
 Chinle Fm U 9, 11, 12, 16, 18, 87, 92–119, 122, 123, 124, 132, 134, 135, 136
 Choiyoi Super Gp 439
 Chontes Cgl (U) 417, 419, 420, 424
 Chubut Gp U 440ff
 Chugwater Fm 151, 250
 Church Rock Mbr 11, 97, 98, 116
 Chusa Tuff or Mbr 317, 320, 342, 343, 344, 349
 Citronella Gp U 315, 317, 320–321
 Cloverly Fm 151
 Cochita Gp U 435
 Coco Fm 447
 Coconino Ss or Fm 11, 122ff
 Cody Sh or Fm 151, 184, 198, 250
 Colorado Sh 306
 Colorados Fm (U) 419, 420, 421
 Conquista Clay 317
 Corrales Fm (U) 418, 419, 420, 422
 Coso Fm 373
 Cosquin Fm U 431–432
 Cow Branch Mbr 359
 Cow Springs Ss or Mbr 11, 16, 18, 49
 Crooks Gap Cgl 181, 184
 Cuesta del Cura Fm 419
 Cutler Fm (U) 11, 99, 101ff, 113, 114, 116, 117
 Dakota Ss (U) 11, 18, 25, 45, 46, 49, 53, 56, 57, 58, 61, 253, 271
 Datil-Mogollon Volcanics 306
 De Chelly Ss 11, 113
 Deadwood Fm 151
 Dell Tuff 292
 Deweesville (or Stones Switch) Ss or Mbr U 316, 324, 334, 335, 338, 339
 Diamante Fm (U) 439
 Dilworth Ss 316, 317, 334
 Dinwoody Fm 151
 Don Otto Mbr U 429
 Dowelltown Mbr 379
 Dripping Spring Quartzite (U) 281, 304–305
 Dripping Spring Quartzite 305
 Drum Mountain Rhyodacite 292
 Dubose Clay 317, 337
 Dyer Dol 275
 East Gulch Tuff 270, 273
 Echo Park Fm U 270–275
 Edwards Ls or Fm 328, 333, 336, 348, 349, 417, 419
 El Abra Fm 419, 420, 422, 424, 425
 Englewood Fm 151

- Entrada Ss 11, 16, 18, 15, 25, 26, 62, 63, 104, 164, 253, 263
 Escuadra Fm (U) 417 ff
 Espinhaço Series or Super Gp 453, 454
 Esplanade Ss or Fm 121ff
 Estes Cgl 234
 Faja Colorada (U) 429
 Fall River Fm U 151, 209, 212–215, 217
 Fant Tuff or Mbr 317, 320, 343–344
 Fashing Clay 317, 337
 Fiftymile Mbr 11
 Flathead Ss 151, 152, 198, 250
 Fleming Fm or Gp U 314, 315, 317, 320, 321, 324, 339, 343, 345, 350, 354, 425
 Fork Mountain Fm U 357, 358ff
 Fort Union Fm U 7, 149, 150, 151, 181, 184, 193–195, 198, 199, 201–203, 206, 219–221, 222
 Fountain Fm 253, 266
 Fox Hills Ss or Fm U 151, 198, 220, 226, 228–232
 Fremont Dol 271, 275
 Frio Clay or Fm 313, 314, 315, 316–319, 324, 339, 343, 354, 425
 Frontier Fm 151
 Furnas Fm 472, 475
 Gallatin Ls 151, 152
 Gassaway Mbr (U) 379
 Glenn Canyon Gp 11, 16, 103, 104
 Gody Sh 151
 Gold Hill Fm (U) 291
 Golden Valley Fm 219, 220, 222
 Goliad Fm U 313ff, 328, 332, 335, 343, 350–354, 425
 Grão Pará Gp 479
 Gray Hills Rhyolite Mbr 293
 Green River Fm 182, 189, 377
 Greenhorn Fm 151
 Gribbles Park Tuff 270, 273
 Gros Ventre Sh or Fm 151, 198
 Grover Ss (U) 231
 Gypsum Spring Fm 151
 Hansen Andesite 270–272
 Hardin Ss or Mbr 379
 Harding Quartzite (U) 275, 279
 Harding Ss 271
 Hawthorn Fm 375
 Hell Creek Fm 151, 219, 220, 222
 Hermit Sh or Fm 11, 122ff
 Hermosa Fm or Gp 11, 104
 Houston Gp 317, 321
 Huemul Mbr (U) 439
 Idaho Springs Fm 253, 255, 256, 269
 Igarapé Bahia Gp (U) 479
 Inyan Kara Fm or Gp U 7, 151, 171, 198, 209–218
 Itabira Gp 475
 Itacaiúnas Supergroup 479
 Itacolomi 474
 Jackpile Ss U 11, 16, 17, 26, 35, 45, 46–49
 Jackson Gp U 313ff, 335–339, 425
 Jacobina Series (U) 477, 479
 Jelm Fm 151
 Joy Tuff 292
 Junction Creek Fm (U) 279
 Kaibab Fm 11, 12, 123ff
 Kayenta Fm 11, 104, 113, 118, 119
 La Bahia Beds 320
 La Cuest Fm (U) 429
 Lagarto Creek Beds 320, 324
 Lakota Fm U 151, 211–213, 215–218
 Lance Fm (U) 151, 184, 193, 195, 198, 206, 226
 Lapara Sands U 320, 324
 Laramie Fm 226, 229, 231, 232
 Leadville Dol U 275–278
 Leadville Ls 11, 279
 Lewis Sh or Fm 151, 198
 Liberina Reef (U) 479
 Lissie Fm (U) 314, 317, 321, 324, 350
 Los Adobes Fm U 440ff
 Los Frailes Fm (U) 447–450
 Los Reyunos Fm U 435
 Luciano Mesa Mbr 62, 63
 Ludlow Lignite or Mbr (U) 219, 220, 221, 222
 Madison Ls (U) 151, 198, 234, 244–245, 250
 Manakacha Fm 11, 121
 Mancos Sh 15, 18, 25, 33, 45, 46, 67
 Manitou Dol 275
 Manning Fm 314, 324
 Maquiné Gp 475
 Mead Peak Mbr (U) 376
 Mesa Fm 417, 418, 419, 420
 Mesa Verde (Mesaverde) Fm or Gp (U) 25, 151, 184, 198
 Minas Supergroup or Series 474, 477
 Minnekahta Ls 151
 Minnelusa Fm 151
 Moeda Fm (U) 475–477
 Moenkopi Fm (U) 11, 12, 95, 99, 103, 113, 116, 117, 119, 122, 123, 124, 132, 134, 145
 Monitor Butte Mbr (U) 11, 87, 95, 98, 99, 113
 Morrison Fm U 9, 11, 15ff, 64ff, 103, 132, 151, 198, 271, 279
 Moss Back Mbr U 11, 95, 96, 98, 99, 101ff, 113, 116
 Moulton Ss U 314, 324
 Mount Belknap Volcanics 293, 299
 Mount Holy Cplx 357
 Mowry Sh 151, 198
 Mt. Laird Tuff 292
 Mutasi Fm 449
 Navajo Ss 11, 104, 113
 Newcastle Ss 151
 Niobrara Fm 151
 Nopal Fm (U) 418ff
 Norma Cgl 425
 Nova Lima Gp 475, 476
 Nugget Ss 151
 Oakville Ss or Fm U 313ff, 340, 345–350 348, 349, 354
 Ogallala Fm 150, 151
 Ohio Sh (U) 379
 Opeche Fm 151
 Owl Rock Mbr 11, 97, 98, 119
 Paganzo Gp (U) 431
 Pahasapa Ls 151
 Panacán Fm (U) 430, 431
 Paradox Mbr 11, 103, 104
 Park City Fm 151
 Parting Quartzite 275
 Peña Blanca Fm 417, 418, 419
 Petrified Forest Mbr (U) 11, 95, 98, 119, 136
 Phantom Lake Gp 234
 Phosphoria Fm (U) 151, 376, 377
 Pierre Sh or Fm 151, 220, 222, 223, 224–226
 Piloncillos Fonglomerate 419
 Pinta dell Agua Fm (U) 434, 435
 Piracicaba Gp 475
 Piritosa Reef (U) 479
 Pium Cpl 479
 Poison Canyon Ss U 16, 17, 26, 29, 36, 49, 53, 54, 55
 Ponta Grossa Fm 470, 472, 475
 Pottsville Fm (U) 357
 Pozos Cgl 419
 Psephitic Mbr 434, 436
 Puddle Springs Mbr or Fm U 151, 174, 181

- Puesto La Paloma Mbr 442
 Puesto Manuel Arce Fm (U) 440, 441, 442
 Puesto Viejo Fm 433, 436
 Quebra Osso Gp 475
 Queen City Fm (U) 314, 315
 Quehua Fm 447
 Quenamari Fm (U) 481–484
 Recapture Mbr 11, 12, 15, 16, 17, 18, 21, 25, 37, 44, 45, 49, 50, 53, 58, 64
 Red Hills Tuff or Mbr (U) 293, 294, 295, 297, 299
 Redwall Ls 11, 121ff
 Relief Peak Fm 373
 Retort Mbr (U) 376
 Reynosa Cgl 425
 Rich Acres Fm 358, 359
 Rio Bonito Fm (U) 470, 472, 473
 Rio Chico Fm (U) 440, 442
 Rio das Velhas Super Gp or Series 475, 476
 Rio dos Remédios Super Gp 454
 Rio Fresco Gp 479
 Rio Seco del Zapallo Fm 433, 436
 Saladillo Fm (U) 431
 Salt Wash Mbr U 6, 9, 11, 12, 15, 31, 37, 42, 64ff, 101, 103, 218
 Salta Gp U 429, 430
 San Juan Fm 431
 San Rafael Gp 11, 16, 18, 103, 104
 Sand Creek Ss 332
 Sandstone and Siltstone Mbr (U) 118, 119
 Sanpoil Volcanics 238–241
 São Vincente Gp 468
 Sawatch Quartzite 275
 Sentinel Butte Mbr (U) 219, 220, 221, 222
 Seridó Fm or Gp 468
 Shelton Fm 358
 Shinarump Mbr U 11, 95, 96, 98, 99, 100, 110ff, 122, 123, 136
 Skull Creek Sh 151, 209, 215
 Soledad Cgl or Mbr (U) 317, 323, 331, 339, 342–345, 349, 354
 Spearfish Fm 151
 Spor Mountain Fm (U) 292
 Steele Sh 151, 198
 Stones Switch Ss (see Deweesville Mbr)
 Stoneville Fm 359
 Summerville Fm 11, 18, 25, 82, 88, 93, 104
 Sundance Fm 151, 198
 Sunpoil Volcanics 233, 234, 235, 237, 239, 240, 241
 Supai Fm or Gp 11, 12, 122ff
 Tallahassee Creek Cgl U 270–275
 Tamulipas Fm 419
 Teepee Trail Fm 245–249
 Temple Mountain Mbr 98
 Tensleep Ss (U) 151, 198, 234
 Thermopolis Sh or Fm 151, 198
 Thirtynine Mile Andesite 270–275
 Thorn Ranch Tuff 270, 273
 Ticunzal Fm (U) 477, 478
 Tidwell Mbr or Unit 11, 64, 81, 90, 92, 93
 Toba Vieja Gorda Mbr 434, 435, 436, 438
 Tobas Amarillas Series (U) 445
 Todilto Ls or Fm U 11, 14, 16, 18, 25, 46, 53, 61–63
 Todilto Ls or Fm U 61, 62
 Togo Fm U 234–239, 241
 Tongue River Lignite or Mbr (U) 219, 220, 221, 222
 Tonque Arroyo Mbr 62, 63
 Topas Mountain Rhyolite 292
 Tordilla Ss or Mbr U 316, 317, 319, 324, 334, 335, 336–338
 Torowep Fm 123ff, 138, 144, 146, 147
 Troy Fm 304
 Vicksburg Fm 425
 Vieja Gorda Tuff (see Toba Vieja Gorda Mbr)
 Volcan Fm (U) 431
 Wagon Bed Fm U 149, 150, 151, 164, 173
 Wagon Fm 377
 Wales Gp 368
 Wall Mountain Tuff 270–274
 Wanakah Fm 11, 15, 16, 17, 18, 62, 63
 Wasatch Fm U 149, 150, 151, 181, 182, 187ff, 206
 Watahomigi Fm 11, 121
 Wellborn Fm 314
 Wescogame Fm 11, 121
 Westwater Canyon Mbr U 6, 9, 11, 12, 14, 15ff, 87
 White River Fm 150, 151, 163, 166, 169, 171, 172, 173, 177, 193, 215, 219, 222, 223, 226, 227, 333
 Whitewood Ls 151, 152
 Whitsett Fm U 314, 315, 317, 324, 331, 336–339
 Wilcons Peak Mbr (U) 377
 Wilcox Fm 314, 349
 Willis Fm 317, 320, 321
 Wilson Creek Gneiss (U) 357
 Wind River Fm U 151, 168, 169, 174–180, 181, 245, 246
 Wingate Ss 11, 104, 113, 113
 Winnipeg Fm 151
 Xingu Cpl 479
 Ya. Los Reyunos Fm 434, 435
 Yacorite Fm (U) 429
 Yavapai Series (U) 305
 Yegua Fm 314, 315
 Structures, faults, lineaments etc. (see Lineaments, and Sect. *Geological Setting*)
 Supergene 63, 127, 136, 139, 146, 192, 238, 239, 241, 245, 249, 250, 266–269, 279, 284, 286, 296, 298, 300, 306, 308, 366, 420, 422, 423, 430–433, 450, 462, 464–467, 477, 479, 484 (see also Hydrogenic, and Sect. *Metallogenetic Concepts/Aspects*)
 Surficial x, 243
 U deposits (see Uranium deposits–types: Type 11)
 Syenite 462–468, 482
 Syngenetic U mineralization (see Uranium deposits–types: Type 10, 12, 17, 18, 19)
- T**
 Texture (style of mineral distribution) (see Sect. *Mineralization*)
 Thorium (see Metallic elements)
 uranium minerals (see Index U Minerals)
 Tuff, tuffaceous, tuffitic 34, 37, 78, 80, 84, 99, 100, 101, 110, 149, 163, 164, 206, 215, 219, 224, 229, 239, 245, 250, 270ff, 282ff, 292ff, 300ff, 316, 317, 319, 321, 324, 330, 333, 336, 338, 339, 340, 346, 350, 352, 373, 377, 417ff, 427, 430–431, 433ff, 447ff, 462ff, 481ff (see also Sandstone)
 Types of deposits (see Uranium deposits–types)
- U**
 Unconformity, paleounconformity 29, 46, 56, 58, 95, 101, 105, 109, 110, 116, 121, 150, 169, 222, 224, 234, 250, 254, 255, 256, 258, 266, 275, 284, 300, 301, 322, 324, 330, 333, 417, 419, 430, 435, 437, 438, 452, 475, 477, 479
 Undifferentiated (magmatite-unrelated) (meta-)sediment-hosted U-bearing veins, stockworks, and shear-zone fillings, (see Uranium deposits–types: Type 7)
 Uraniferous bituminous-cataclastic calcareous sediments (limestone, dolomite) deposits (see Uranium deposits–types: Type 14)
 Uraniferous carbonaceous lutite (lacustrine) deposits (see Uranium deposits–types: Type 15)
 Uraniferous lignite/coal deposits (see Uranium deposits–types: Type 18)
 Uraniferous minerochemical phosphorite deposits (see Uranium deposits–types: Type 17)
 Uraniferous stratiform black shale deposits (see Uranium deposits–types: Type 19)
 Uraninite (see Index U Minerals)
 Uranium

- ab-, adsorption, ab-, adsorbing agents/material/minerals (see Sect. *Mineralization*, and Sect. *Metallogenetic Concepts/Aspects*)
 contents (background values) (see Sect. *Sources of Uranium*)
 deposition/fixing/precipitation (see Sect. *Metallogenetic Concepts/Aspects*)
 deposits (see Uranium deposits–types)
 districts (see Chapters *U districts* and *U deposits*, and Geographical Index)
 hexavalent (U⁶⁺) ion 69, 267, 357, 430, 432, 433, 439, 474, 477
 metallogenesis ix (see Sect. *Metallogenetic Concepts/Aspects*)
 mineralization (see Uranium (deposits) mineralization, and Sect. *Mineralization*)
 minerals (see Index U Minerals, and Sect. *Mineralization*)
 mobilization, mobility (see Sect. *Metallogenetic Concepts/Aspects*)
 production [see Chapters *U districts* and *U deposits* (introductory section)]
 province 3, 4, 6, 9, 12, 76, 149, 326
 redistribution, remobilization, recrystallization (see Sect. *Metallogenetic Concepts/Aspects*)
 reductants, reducing agents (see Organic, Gas, Oil, and Sect. *Metallogenetic Concepts/Aspects*)
 reduction, reducing 19, 34, 60, 61, 78, 82, 83, 97, 110, 125, 126, 133, 134, 135, 143, 145, 165, 229, 267, 273, 287, 321, 322, 325, 328, 330, 332, 334, 342, 423, 472 (see also Sect. *Mineralization*, and Sect. *Metallogenetic Concepts/Aspects*)
 reserves/resources xiv, xv, xvi [see *U districts* and *U deposits* (introductory section)]
 source (rocks) (see Sect. *Sources of Uranium*)
 transport (see Sect. *Metallogenetic Concepts/Aspects*)
 Uranium (deposits) mineralization (general) (see also Sect. *Mineralization*)
 authigenic/authigenous (see Sect. *Alteration*, Sect. *Mineralization*, and Sect. *Metallogenetic Concepts/Aspects*)
 complex (see below polymetallic)
 composition (see Gangue minerals, Ore composition, Metallic elements, and Sect. *Mineralization*)
 controls (see Sect. *Ore Controls and Recognition Criteria*)
 epigenetic (see Uranium deposits–types: Types 3, 4, 5, 6, 7, 8, 9, 11, 14, 18)
 metals (see Metallic elements, and Sect. *Mineralization*)
 metallogenesis/mode of origin ix (see Sect. *Metallogenetic Concepts/Aspects*)
 mineral assemblages/parageneses (see Sect. *Mineralization*)
 monometallic (or simple) xiv, 233, 304, 364, 432, 456, 484
 oxidized (see Sect. *Mineralization*)
 polymetallic (or complex) xiv, 12, 64ff, 95ff, 119ff, 209ff, 233, 234, 242–245, 250, 255, 269, 282ff, 291–292, 292ff, 305–308, 309, 367–371, 379, 420ff, 432, 439, 441, 442, 462ff, 477, 479–480
 recognition criteria (see Sect. *Ore Controls and Recognition Criteria*)
 redistributed, recrystallized, remobilized, reworked (see Sect. *Metallogenetic Concepts/Aspects*)
 reduced (unoxidized) (see Sect. *Mineralization*)
 shape, configuration (see Shape/configuration, and Sect. *Shape and Dimensions*)
 supergene (see Hydrogenic/hydrothermal, and Sect. *Metallogenetic Concepts/Aspects*)
 surficial (see Uranium deposits–types: Type 11)
 syngenetic (see Uranium deposits–types: Types 10, 12, 17, 18, 19)
 texture (see Sect. *Mineralization*)
 Uranium deposits–types xiv
 [Note: (1) For definitions of U deposit types see Dahlkamp 2009: Uranium Deposits of the World: Asia
 (2) Deposits of ambivalent nature or with characteristics of two or more types are listed under each possibly valid type as indicated]
 collapse breccia pipe, type 8 3, 6, 9, 119ff
 granite/felsic plutonic rocks-related, type 4 233, 234ff, 241 (compare type 11), 242–243, 245ff, 281, 291 (compare type 7), 292ff (compare type 5), 305ff, 367–371 (compare type 6), 425, 429, 432 (compare type 11), 457ff
 contact-granitic vein/stockwork 249–250, 281, 291 (compare type 7), 425, 457–462
 endogranitic (intragranitic) vein/stockwork 233, 241 (compare type 11), 247–249 (compare type 11), 250–251, 367–371 (compare type 6), 429, 432 (compare type 11), 433
 episyenite-hosted 457–462
 perigranitic (exogranitic) vein/stockwork 234–239, 241 (compare type 11), 242–244, 305–306, 306–308, 371, 457–462
 intrusive, type 12 281, 309, 367–371 (compare type 4 and 6), 480
 carbonatite 480
 pegmatite 367, 369–371
 quartz monzonite/copper-porphyry 281, 309
 metasomatite, type 6 367ff, 451, 452ff, 468ff
 vein/stockwork in metasomatized granite 367–371 (compare type 4)
 vein/stockwork in metasomatized metasediments/metavolcanics 452–457, 468–470
 Paleoproterozoic quartz-pebble conglomerate, type 10 233, 451, 452, 474ff
 polymetallic iron-oxide (hematite)-breccia-complex, type 9 451, 479–480
 sandstone, type 3 3, 6, 7, 9, 12ff, 64ff, 94ff, 149ff, 209ff, 219, 221ff, 233, 239–241, 245, 249, 253, 270–275 (compare type 5), 311ff, 357, 416, 425, 427ff, 440ff, 451, 470ff
 basal-channel 94–101, 110–119, 439, 440–445
 tabular/peneconcordant 12–61, 64–95, 101–110, 183–191, 206–207, 214–218, 233, 270–275, 425, 429–431, 433–439, 472–474
 continental, U associated with extrinsic reductant (humate/bitumen) 12–43, 101–110, 207
 continental, U associated with intrinsic reductant (organic debris) 64–95, 101–110, 239–241, 270–275 (compare type 5), 427–431, 433–439, 472–474
 continental, vanadium-uranium 64–95, 214–218, 429, 439, 440–445
 rollfront 149–173, 175–183, 186–207, 209–214, 221–226, 226–232
 continental, U associated with intrinsic reductant 149–173, 175–183, 186–207, 209–214, 221–226
 continental, vanadium-uranium 209–214, 441
 continental to marginal marine, U associated with intrinsic reductant 226–232, 335–339
 marginal marine, U associated with extrinsic reductant 311–335, 339–355
 tectonic-lithologic (stack, redistributed post-fault) 25, 26, 30, 31, 32, 35, 36, 45, 53, 54, 55
 surficial, type 11 233, 241 (compare type 4) 242, 244–245, 247–249 (compare type 4), 427, 431–432, 432–433 (compare type 4), 440, 441, 477
 duricrusted sediments 427, 431–432
 karst cavern 233, 244–245
 peat-bog 233, 242
 fracture filling 241 (compare type 4)
 undifferentiated (magmatite-unrelated) (meta-)sediment-hosted veins, stockworks, and shear-zone fillings, type 7 253–269, 275–279 (compare type 14), 279, 281, 291 (compare type 4), 357, 358–366, 425 (compare type 14), 430–431, 451, 477
 uraniumiferous bituminous-cataclastic calcareous sediments (limestone, dolomite), type 14 61–63, 275–279 (compare type 7), 425 (compare type 5), 430–431, 457–462
 dolomite-hosted 275–279 (compare type 7)
 limestone/marble-hosted 61–63, 279, 425 (compare type 5), 457–462
 uraniumiferous carbonaceous lutite (lacustrine), type 15 281, 300–304
 uraniumiferous lignite/coal, type 18 181, 189, 219–221, 270
 uraniumiferous minerochemical phosphorite, type 17 375ff, 426, 480, 481
 bedded phosphorite 376–377
 land-pebble (reworked) phosphate 375–376
 uraniumiferous stratiform black shale, type 19 379
 volcanic, type 5 3, 6, 270–275 (compare type 3), 281, 282ff (compare type 4), 415, 416, 417ff, 440, 441, 443, 445, 447ff, 462ff, 481ff
 caldera-related 282–290, 291–292, 292–300, 425, 462–468
 diatreme-hosted 464, 465, 466

- strata-bound (tabular-stratiform) 270–275 (compare type 3), 284, 285, 286, 287–290, 420, 424, 425, 445, 450, 464, 466, 484
- structure-bound (fracture filling, vein, stockwork) 284, 285, 286, 290, 291–292, 292–300, 420, 421, 422, 423–424, 425, 426, 448–450, 465, 466, 468, 484
- Uranium deposits—types by type number
- type 3 sandstone 3, 6, 7, 9, 12ff, 64ff, 94ff, 149ff, 209ff, 219, 221ff, 233, 239–241, 245, 249, 253, 270–275 (compare type 5), 311ff, 357, 416, 425, 427ff, 451, 470ff
 - type 4 granite/felsic plutonic rocks-related 233, 234ff, 241 (compare type 11), 242–243, 245ff, 281, 291 (compare type 7), 292ff (compare type 5), 305ff, 367–371 (compare type 6), 425, 429, 432 (compare type 11), 457ff
 - type 5 volcanic 3, 6, 270–275 (compare type 3), 281, 282ff (compare type 4), 415, 416, 417ff, 440, 441, 443, 445, 447ff, 462ff, 481ff
 - type 6 metasomatite 367ff, 451, 452ff, 468ff
 - type 7 undifferentiated (magmatite-unrelated) (meta-)sediment-hosted veins, stockworks, and shear-zone fillings 253–269, 275–279 (compare type 14), 279, 281, 291 (compare type 4), 357, 358–366, 425 (compare type 14), 430–431, 451, 477
 - type 8 collapse breccia pipe 3, 6, 9, 119ff
 - type 9 polymetallic iron-oxide (hematite)-breccia-complex 451, 479–480
 - type 10 Paleoproterozoic quartz-pebble conglomerate 233, 451, 452, 474ff
 - type 11 surficial 233, 241 (compare type 4), 242, 244–245, 247–249 (compare type 4), 431–432, 432–433 (compare type 4), 440, 441, 477
 - type 12 intrusive 281, 309, 367–371 (compare type 4 and 6), 480
 - type 14 uraniferous bituminous-cataclastic calcareous sediments (limestone, dolomite) 61–63, 275–279 (compare type 7), 425 (compare type 5), 430–431, 457–462
 - type 15 uraniferous carbonaceous lutite (lacustrine), 281, 300–304
 - type 17 uraniferous minerochemical phosphorite 375ff, 426, 480, 481
 - type 18 uraniferous lignite/coal 181, 189, 219–221, 270
 - type 19 uraniferous stratiform black shale 379
- Urano-organic complexes 22, 51, 58, 242, 472
- humate 12, 15, 17, 19–22, 24, 29, 34, 35, 38–43, 45, 49, 53, 56, 57, 75, 78, 80, 92, 99, 100, 109, 110, 145, 168, 206, 209, 212, 302, 342
 - humic 19, 35, 38, 39, 41, 42, 49, 79, 80, 92, 110, 152, 172, 303, 304, 320, 379
 - kerogen 62, 123, 127
 - thucholite 476
- Uranyl minerals (see Index U Minerals, and Sect. *Mineralization*)
- U-Ti compounds/phases 207, 351, 361, 362, 422
- V**
- Vanadium (see Metallic elements, and Uranium deposits—types: Type 3)
- Vegetal matter (see Organic material)
- Vein xv, (see Uranium deposits—types: Type 4, 5, 6, 7)
- Volcanic/metavolcanic, volcanite 3, 6, 233, 270–275, 281, 282–290, 291–300, 300–304, 305, 319, 320, 330, 331, 332, 349, 357, 358, 359, 367, 373, 417–425, 426, 440, 443, 444, 447–450, 454, 462–468, 472, 475, 477, 479, 481–485 (see also Uranium deposits—types: Type 5)
- caldera 281, 282–290, 291–293, 298, 425, 462, 463
 - rocks (see Ash, Effusive, Glass, Ignimbrite, Lahar, Moat, Pyroclastic, Tuff, Sand/sandstone, and Uranium deposits—types: Type 5)
 - subvolcanic batholiths, stocks 253, 447, 448, 449, 450, 462, 463, 484–485 (see also Uranium deposits—types: Type 5)
- Volcanic structures—localities (basin, belt, caldera, depression, subvolcanic massif, volcanic-tectonic structure etc.) 3, 6
- Beatty volcanic center, USA 4, 291
 - Cenozoic volcanic belt, Bolivia-Peru 415, 448
 - Central Volcanic–Plutonic Belt, Virginia, USA 358, 359
 - Datil Mogollon Volcanics, USA 306
 - Lakeview, USA 4, 281, 290
 - Long Ridge caldera, USA 286
 - Marysvale volcanic complex, USA 4, 281, 292–300
 - McDermitt caldera, USA 4, 281, 282–290
 - Meseta de los Frailes, Bolivia 442
 - Meseta Picobani, Peru 481
 - Meseta Quenamari, Peru 481–485
 - Monroe Peak caldera, USA 293
 - Mount Belknap, USA 293
 - Poços de Caldas, Brazil 415, 416, 451, 462–468
 - Red Hills caldera, USA 293
 - San Jorge/Gulf Basin, Argentina 440, 441
 - San Juan volcanic field, USA 275
 - San Marcos caldera, Mexico 425
 - Serra dos Carajás, Brazil 479–480
 - Sevaruyo, Bolivia 447
 - Sierra Madre Occidental rhyolitic province, Mexico 417
 - Spor Mountain/Thomas caldera, USA 4, 281, 291–292
 - Sunpoil Volcanics, USA 233ff
 - Tertiary-Quaternary volcanic belt, Bolivia-Peru 481
 - Thirtynine Mile volcanic field, USA 253, 270
 - Thomas caldera, USA 291–292
 - Topaz Mountain, USA 291, 292
- W**
- Wall rock alteration (see Alteration, and Sect. *Alteration*)
- Weathering/paleoweathering 57, 164, 166, 178, 207, 241, 292, 305, 307, 361, 364, 365, 375, 376, 423, 432, 439, 463, 464, 466, 479 (see also Laterite, Paleosol, and Regolith)
- X**
- Xenolith 245, 246, 247, 248, 249, 250, 373
- Z**
- Zeolites (see Gangue and alteration minerals)
- Zircon 60, 145, 158, 185, 189, 224, 234, 237, 238, 247, 289, 290, 292, 293, 364, 367, 369, 371, 433, 435, 455, 456, 459, 462, 466, 467, 468, 475, 476, 479, 480 (see also Index U Minerals)
- Zoning/zonation 21, 24, 37, 45, 51, 56, 69, 70, 78, 80, 105, 109, 115, 127, 133, 140, 165, 263, 299, 302, 307, 309, 322, 325, 326, 332, 349, 359, 367, 369, 376, 423, 449, 455, 462

Geographical Index

(Note: Bold page numbers refer to descriptions of regions, districts, and deposits)

A

A-1 breccia pipe, Arizona Strip, USA, 120
A-20 breccia pipe, Arizona Strip, USA, 120
Abiquin, USA, 61
Achala batholith, Argentina, 427, 432
Ackerman, USA, 215
Adargas, Mexico, 418
Agostinho, Brazil, 451, 462, 463, **468**
Agua de los Pájores, Argentina, 429
Aguiliri, Argentina, 428, 448
A&H mine, USA, 215
Alabama, USA, 357, 379
Aladdin, USA, 210, 215
Alaska, USA, 3, 4, 6, 7, 367ff
Alberta, Canada, 8
Alcantil, Brazil, 457
Alecrim, Brazil, 452
Alemania, Argentina, 429
Alfredo Wagner, Brazil, 470
Alhambra mine, USA, 306, 307
Allemand Ross, USA, **203**
Alma Segin mine, USA, 112
Alta Mesa, USA, 3, 312, **350–353**
Alta Verde, USA, 312, 320, 354
Altiplano, Bolivia, 447, 481
Alunite Ridge, USA, 293
Amazon Craton, South America, 416, 451, 479
Ambrosia Lake district, USA, 7, 13, 14, 15, 17, 20, 21, 24–34, 36, 39, 41, 43, 49, 50, 51, **53–54**, 56, 59, 61, 302
Amistad, Bolivia, 447, 450
Amorinópolis, Brazil, 451, 452, 470, 471, **472–474**
Amorinópolis-Iporá, Brazil, 472
Andean depressions, Peru, 481
Andean Geosyncline (Geosinclinal Andino), Argentina, 427, **439**
Andean orogenic belt, South America, 415, 440
Anderson mine, USA, 4, 281, 300–304
Andrus Canyon, USA, 134, 146
Antelope Range, USA, 4, **373**
Apache Basin, USA, 4, 6, 7, 304–305
Apache County, USA, 85, 86
Apache No. 4 mine, USA, 279
Apex mine, USA, 128, 291
Appalachian Highland and Piedmont, USA, 4, **357–366**
Aquiliri, Argentina, 415
Aquiri, Brazil, 455, 457, 458
Araçuaí mobile belt, Brazil, 454, 455
Araxá, Brazil, 471, 480
Arches National Monument, USA, 88
Argentina, 415, 427ff, 481
Arizona Strip, USA, 3, 5, 6, 9, 10, 12, **119–148**
Arizona, USA, 3, 4, 5, 6, 9, 10, 12, 64, 72, 79, 84, 85, 86, 95, 96, 97, 115, 118, 119ff, 281, 300ff, 309
Arizona 1 breccia pipe, USA, 120, 129, **146**

Arroyo Perdido, Argentina, 440, 443
Arrowhead mine, USA, 245, 249
Ascension mine, USA, 254, 255, 256, 269
Atascosa County, USA, 313
Atacosa River, USA, 320
Atkinson Mesa, USA, 66
Atlantic Craton/Shield, South America, 416, 451, 462
Aubrey Ladwig (or Ladwig) mine, USA, 254, 255, 256, **269**
Aurora-Bretz, USA, 288
Aurora, USA, 282, 283, 284, 286, **287–289**
Austin district, USA, 4, 281, **291**

B

Bagdad mine, USA, 281
Baggs district, USA, 7, 150, 206, **207**
Bahia state, Brazil, 415, 451, 452, 477
Baja California state, Mexico, 417, 418, 426
Bajo, Peru, 482
Balcones Escarpment/zone 313, 331
Baltimore, USA, 3
Bankers Lode, USA, 254
Barbara claims, USA, 271
Bardas Coloradas, Argentina, 442
Bargman, USA, 334
Barlow Canyon, USA, 210, 214, 215
Barrego Pass, USA, 14
Barrel, Argentina, 430
Barringer Hill, USA, 7
Bartow, USA, 375
Basin and Range, USA, 3, 4, 6, 7, **281–309**
Basin Creek, USA, 233
Bear Creek mine, USA, 193, 194, 196, **201–204**
Beatty, USA, 4, **291**
Beaver Divide area, USA, **377**
Beaver Mesa area, USA, 66, 82
Beaver Shaft, USA, 83
Bee County, USA, 328, 345, 354
Belfield, USA, 4, 7
Belle Fourche, USA, 210, 212, 215
Belo Horizonte, Brazil, 474–476
Benavides, USA, 312, 323, 330, 339, 340, **342–345**, 349
Benham, USA, 312
Bernabe-Montano district, USA, 13, 14, 15, 36, **43–46**
Bif Four mine, USA, 112
Big Bend, USA, 281, 330, 331
Big Buck mine, USA, 102, 107, 109
Big Chief mine, USA, 112
Big Eagle, USA, 181, 183, 185
Big Hole mine, USA, 87
Bighorn Basin, USA, 150, 153, 244
Bighorn Mountains, USA, 150, 193
Big Indian Copper mine, USA, 102
Big Indian Mineral Belt, USA, 105
Big Indian prospects, USA, 279
Big Indian Wash, USA, 6, 9, 10, 95, 96, 98, **101–110**
Big Red, USA, 4, 221

- Big Smoke mine, USA, 239, 240
 Billiken, USA, 254
 Bill Smith, USA, 193
 Bingham mine, USA, 4, 281, **309**
 Bison Basin, USA, 150, 182, **192–193**
 Bitlabito, USA, 85
 Bitter Creek mine, USA, 68
 Blackbird Copper, USA, 102
 Black Bonanza-Red Dog, USA, 4, 291
 Black Box breccia pipe, USA, 120
 Black Creek, USA, 89
 Black Hawk district, USA, 4, 6, 281, **306–308**
 Black Hills, USA, 3, 6, 7, 150, 151, 152, 155, 164, 166, 171, 193, 206, **209–218**, 227, 233, 234, 333
 Black Jack No. 1, USA, 14, 36, 54, 55
 Black Jack No. 2, USA, 14, 54, 55
 Black Knight, USA, 254
 Black Mesa Basin, USA, 10, 85, 119
 Black Rock mine, USA, 112
 Blanca XVI, Mexico, 418
 Blanding district, USA, 65
 Blue Eagle mine, USA, 294, 295
 Blue Jay mine, USA, 254, 255
 Blue Mountain breccia pipe, USA, 120, **147**
 Blue Peak mines, USA, 16, 20
 Blue Ridge province, USA, 365
 Bobo Tordille Hill, USA, 334
 Bokan Mountain (pluton), USA, 3, 4, 6, 7, **367–371**
 Bolivia, 415, 447ff, 481
 Bolivian-Peruvian Tertiary-Quaternary volcanic belt, South America, 481
 Bonanza mine, USA, 245, 246, **249**
 Bonita mine, USA, 279
 Bonito, Brazil, 452
 Bonzo, USA, 256
 Boot Jack mine, USA, 112, 115
 Boots, USA, 312, 345
 Boquillas, Mexico, 418
 Borrego Pass district, USA, 7, 13, 14, **61**
 Box Creek district, USA, 150, 193, 195, 199, 202
 Boulder Creek Granodiorite, USA, 254, 255, 267
 Brasilia, Brazil, 468, 472, 477
 Brazil, 415, 451ff
 Brazilian Platform, South America, 452
 Brazilian (or Brazil) Shield, South America, 415, 416, 451, 480
 Brelum, USA, 312, 339
 Bret, USA, 174
 Bretz, USA, 282, 283, 284, 285, 286, **287–290**
 Brevard zone, USA, 357, 359
 Bronze L mine, USA, 148
 Brooks County, USA, 6, 342, 350, 352, 354
 Brown Ranch, USA, 193, 194, **199**
 Bruni, USA, 312, 339, 340, **342–344**
 Brunswick, USA, 3
 Brush-Wellman Spor Mountain, USA, 291
 Brysch-F.W.N.B., USA, 312
 Brysch, USA, 334, 335, **338–339**, 340
 Buckingham, USA, **231**, 232
 Buckmaster Draw, USA, 87
 Buenavista, Mexico, 418, **425**
 Bullard Peak district, USA, 306
 Bull Canyon area, USA, 82, 83
 Bullfrog mine, USA, 88
 Bunker Hill mine, USA, 242
 Burdock, USA, 210, 212, **213–214**
 Burgos Basin, Mexico, 415, 417, **425**
 Burns, USA, 345, 346
 Burro Canyon, USA, 66
 Burro Mountains (batholith), USA, 4, 6, 306–308
 Busfield, USA, 215
 Butler pit, USA, 159, 334
 Butler-Weddington, USA, 312, 335
 Butte County, USA, 210
 Butus, USA, 312
- C**
- Cachoeira, Brazil, 451, 452, 453, 455
 Cadena, USA, 312
 Caetité Massif, Brazil, **452–457**
 California, USA, 3, 4, 373
 Calvario, Peru, 481, 482
 Cameron, USA, 96, 118, 120, 121, 123, 135, 136, 148
 Cameron district, USA, 6, 97, **118–119**
 Campana, USA, 312, 345, 349
 Campos Belos, Brazil, 415, 451, 452, **477**, 478
 Cañadón Gato, Argentina, 443
 Cañadón Gato-Kruger, Argentina, 440
 Cândido de Abreu, Brazil, 470
 Cane Creek-Indian Creek district, USA, 96, 97, **117**
 Cane Springs Canyon, USA, 117
 Canon City, USA, 256, 270
 Canyon breccia pipe, Arizona Strip, USA, 120, 122, 130, 136, **146–147**
 Canyon, Crownpoint, USA, 57
 Caprock, USA, 271
 Carajás, Brazil, 415, 416, 451, **479–480**
 Caribou, USA, 254, 255
 Cariri Mobile Belt, Brazil, 468, 469
 Carlisle/Carlile, USA, 6, 7, 209, 210, 212, 215, **218**
 Caroll, USA, 254
 Carrizalito, Argentina, 433, 435, 438
 Carrizo Mountains, USA, 84, **85–86**
 Carrizo-Luckachuki district, USA, 65, **84–86**
 Carvaozinho, Brazil, 470
 Casa Blanca, USA, 312
 Cascade Range, USA, 373
 Casper Arch, USA, 150, 173, 193, **206**
 Catahoula River, USA, 319
 Catahoula, USA, 313, 314, 316, 318–321, 323–326, 328, 331–333, 336, 339–345, 349, 350, 354
 Catalac, Brazil, 471
 Catamarca province, Argentina, 427, 429
 Cave Hills, USA, 4, 219, 221
 Cdon.Gato-Kruger, Argentina, 441, 443
 Ceará state, Brazil, 415, 451, 452, 457
 Cedar Hills area, USA, 206
 Cenozoic volcanic belt, Bolivia-Peru, 415, 448
 Centennial Mountain, USA, **376**
 Centennial, USA, 7, 226, 227, 228, **230–231**
 Cento e Dezoito, Brazil, 479
 Central America, 415, 417ff
 Central Ceará, Brazil, **457–462**
 Central City district, USA, 3, 7, 253, 254, 255
 Central Temple Mountain Mineral Belt, USA, 96, 97, 117
 Central Volcanic-Plutonic Belt, Virginia, USA, 358, 359
 Cercado, Brazil, 451, 452, 462, **463–467**, 468
 Cerro Aspero, Argentina, 432
 Cerro Bayo, Argentina, 441
 Cerro Calvario, Peru, 481
 Cerro Carmen, Chile, 415
 Cerro Chonche Rumio, Peru, 481, 482
 Cerro Condor, Argentina, 427, 440, 441, 442, **444–445**
 Cerros Colorados, Mexico, 418
 Cerro Solo, Argentina, 427, 440, 441, **442–444**
 Cerro Tacho, Argentina, 440, 441
 Cerro Volcano, Argentina, 443
 Chacay Cura, Argentina, 417, 419, 441, 442
 Chaco Slope, USA, 13

- Chadron Arch, USA, 226, 227
 Chalky Buttes area, USA, 220, 221
 Chama Basin, USA, 61
 Chapel breccia pipe, USA, 120
 Chapi-Alto, Peru, 481, 482
 Chapman, USA, 312
 Charazani, Bolivia, 447, 481
 Charles Huskon 4-Paul Huskie-3 mines, USA, 119
 Charlie, USA, 193, 194
 Chattanooga Shale region, USA, 4, 379
 Cheapside, USA, 312
 Chester fault zone, USA, 276, 277, 278, 279
 Chesterfield, USA, 3
 Cheyenne Basin, USA, 150, 221, 226, 227, 228, **230–232**
 Chicken mine, USA, 128
 Chihuahua state, Mexico, 415, 417–425
 Chihuidos district, Argentina, 439
 Chilchinbito district, USA, **86**
 Chilcuno, Peru, 481, 482
 Chile, 415
 Chinle districts, USA, 12, **94–119**
 Chita-Corrigan fluvial system, USA, 319, 339, 341
 Christensen Ranch, USA, 193, 194, **196–197**, 198
 Chubut province, Argentina, 427, 440, 445
 Chubut River, Argentina, 440
 Church Rock district, USA, 6, 12, 13, 14, 15, 21, 27, 31, 34, 35, 36, 37, **56–57**, 61
 Church Rock No. 1 mine, USA, 56, 57
 Church Rock No. 2 mine, USA, 56, 57
 Chuska Mountains, USA, 61, 86
 Circle Cliffs district, USA, 89, 96, 97, **117–118**
 Clay West-Burns district, USA, 312, 313, 345
 Clay West, USA, 312, 326, 332, 345, 346
 Clay West district, 345, 346, **349**
 Cliffside mine, USA, 29
 Cloys mines, USA, 294, 295
 Cloys-Potts area, USA, 297
 Club Mesa, USA, 66
 Clyde, USA, 174
 Coast Range batholith, USA, 7, 370, 371, 373
 Coaza batholith, Bolivia, 447
 Cochetopa district, USA, 4, 253, **279**
 Cochran, USA, 312
 Cochran Arch, USA, 222, 226
 Coconino Plateau, USA, 120, 146, 147
 Coeur d'Alene district, USA, 4, 233, 234, **242–244**
 Coles Hill, USA, 4, 7, **357–366**
 Colibri, Peru, 481
 College Hill, USA, 357
 Collins Draw, USA, 193, 194, **199**
 Colorado, USA, 3, 4, 5, 6, 7, 85, 94, 150, 206, 207, 221, 226, 233, 253ff
 Colorado City, USA, 121, 135, 136
 Colorado Front Range, USA (see Front Range)
 Colorado Mineral Belt, USA, 253, 254, 255, 256, 266, 267, 268, 305
 Colorado Rocky Mountains, USA, 3, 4, 6, 7, 11, 221, 226, **253–279**
 Colorado Plateau, USA, 3, 4, 6, 7, **9–148**, 218, 293, 305, 330
 Colorado River, USA, 10, 12, 110, 115, 120, 121, 137, 320
 Colquijirca, Peru, 481
 Columbia (Homestake mine), USA, 102, 106
 Columbus-Rim mine, USA, 87
 Comechingones district, Argentina, 427, 428, 431, **432–433**
 Concha Rumio, Peru, 482
 Coneto-Buenavista, Mexico, 418, 425
 Connecticut, USA, 3
 Constanza mine, USA, 102
 Continental mine, USA, 102
 Conway Granite, USA, 357
 Copper House breccia pipe, USA, 120, **148**
 Copper Mountain district, Wyoming, USA, 6, 150, 173, 233, 234, **245–249**, 251
 Copper Mountain breccia pipe, Arizona Strip, USA, 120, 128, 136, **146**
 Copper Prince mine, USA, 7
 Corachapi, Peru, 481
 Cord mine, USA, 102, 106
 Cordillera Oriental, South America, 415, 447, 448, 481
 Córdoba, Argentina, 427, 432
 Córdoba province, Argentina, 427, 431, 432
 Coso Range, USA, 373
 Coso mine, USA, **373**
 Coso Range, USA, 4
 Cosquin district, Argentina, 416, 427, 428, **431–432**
 Costanza, USA, 102
 Cotaje, Bolivia, 447, **448–450**
 Cottonwood Creek, USA, 282, 283, 284, 285, 286, **287–289**
 Cottonwood mine, USA, 86, 87, 94
 Cottonwood Wash district, USA, 79, **87–88**
 Cougar mine, USA, 76
 Cove Mesa, USA, 85
 Crackpot mine, USA, 46
 Cranberry Lake, USA, 357
 Crawford area, USA, 6, **221–226**
 Crestonia, USA, 312, 343, 349, 350, 354
 Critchell area, USA, 254, 269
 Crook County, USA, 210
 Crooks Gap district, USA, 7, 150, 161, 162, 163, 164, 169, 173, **181–183**, 189, 191
 Crooks Mountain, USA, 192
 Crow Butte area, USA, 3, 4, 6, 7, 8, **221–226**, 227
 Crowley Creek zone, USA, 283
 Crownpoint district, USA, 7, 13, 14, 15, 21, 26, 37, **57–59**, 61
 Cuenca del Golfo San Jorge, Argentina, 427, **440–445**
 Cuenca Norte, Argentina, 441
 Cuesta de Bala, Argentina, 430
 Cueva Amarilla, Mexico, 418
 Cuevitas, USA, 312
 Cunningham breccia pipe, USA, 120, **148**
 Custer County, USA, 213
 Cuychine, Peru, 481, 482
 Cuyo Basin, Argentina, 430
 Cyclon Rim syncline; USA, 192
- D**
- Daisy, USA, 4, 291
 Dakota Plains, 4, 6, **219–221**
 Dalton Pass, USA, 14, 57
 Danville, USA, 6, 359
 Danville Triassic Basin, USA, 358, 359, 360, 361, 366
 Darby Mountains, USA, 367
 Date Creek Basin, USA, 4, 6, 7, 281, **300–304**
 Daybreak mine, USA, 4, 233, **241–242**
 Day-Berger prospect, USA, 245, 246, **249**
 Daylight mine, USA, 112
 Day Loma, USA, 174
 DB-1 breccia pipe, USA, 120
 Death Valley Basin/area, USA, 4, 367
 Deep Edwards fault trend, USA, 326, 328
 Deer Flats, USA, 96, 97, 98, 110
 Deer Trail Mountain, USA, 293, 298
 Defiance Uplift, USA, 10, 15, 86
 Dekalh County, USA, 379
 Dell Valley, USA, 291, 292
 Dells Granite, USA, 281
 Del Monte mine, USA, 88, 89, 90, 91
 Dennis, USA, 215
 Denver-Julesburg Basin, USA, 4, 6, 7, **226–232**
 De Pass mine, USA, 245, **249**

Deremo mine, USA, 66, 70, 75, 83
 Deremo-Snyder mine, USA, 83
 Desert View, USA, 183
 Dewey, USA, 210, 212, **213–214**
 Diamond No. 2 mine, USA, 56
 Diana, Mexico, 418, 425
 Dick mine, USA, 174
 Divide mine, USA, 102, 109
 Dobie, USA, 312
 Dolores anticline, USA, 68, 80
 Domitila, Mexico, 418
 Domo de Araguainha, Brazil, 470
 Domo de Lajes, Brazil, 470
 Don Otto, Argentina, 427, 429, 430
 Dos Estados, Mexico, 418
 Doughstick, USA, 194, **199**
 Doris mine, USA, 29
 Dr Baulies, Argentina, 427
 Dr Baulies-Los Reyunos, Argentina, 433, 438
 Dr Baulies Tigre I, Argentina, 437
 Drum Mountain, USA, 292
 Dry Valley district, USA, **87**
 Dubose, USA, 312
 Duderstadt, USA, 312
 Durango mill, USA, 85
 Durango state, Mexico, 417, 418, 425, 426
 Duval County, USA, 6, 7, 312, 313, 318, 331, 339, 342, 345, 350, 351, 353, 354
 Duval County Mineral Trend, USA, (see South Duval County Mineral Trend)
 Dyboski, USA, 312
 Dzuik, USA, 312

E

Ea. La Madreselva, Argentina, 441
 Early Day mine, USA, 291
 East Calhoun mine, USA, 254, 255
 East Canyon district, USA, 65, **87**
 East Coyote-Browns Hole syncline, USA, 83
 Eastern Gulf and Atlantic Coastal Plain, USA, 4
 East Rogers fault, USA, 258
 Eastside mine, USA, 85
 East Tampa, USA, 375
 Echo Park Basin, USA, 271
 Edgemont district, USA, 7, 209, 210, 211, **212–214**
 Edward R. Farley, USA, 88, 90–92
 Edwards Plateau, USA, 319, 320
 Ekalaka Hills, USA, 220, 221
 El Chapote, Mexico, 418, **425**
 El Desecho, Argentina, 430
 El Ganso, Argentina, 443
 Elkhorn Creek, USA, 210, 214, 215
 Elk Park Plutons, USA, 357
 Elk Ridge, USA, 96, 97, 100
 El Laco, Chile, 415
 El Lenadero, Argentina, 430
 El Mesquite, Mexico, 418, 425
 El Mirasol, Argentina, 440
 El Mirasol Norte, Argentina, 441
 El Mirasol Sur, Argentina, 441
 El Molino, Argentina, 443
 El Resistido, Argentina, 430, 431
 El Tigre brachyanticline, Argentina, 433, 434, 437, 438
 Emigrant Trail Thrust, USA, 182, 183
 Emmy, Argentina, 430
 Engenho, Brazil, 452
 ENQ, USA, 182, 186, 187, 189, **190–191**
 Esperanza, Peru, 481, 482

Espinharas, Brazil, 415, 416, 451, 452, 458, **468–470**
 Espinhaço Setentrional belt, Brazil, 452–455, 456, 457
 Esse-Spoonamoore, USA, 312
 Estacion Romero, Chile, 415
 EZ 1 breccia pipe, USA, 120, 129
 EZ 2 breccia pipe, USA, 120, 122, 123, 126, 129, 132, 133, 134, 135

F

Fair Day mine, USA, 254, 255, 256
 Fall River County, USA, 213
 Far West mine, USA, 102, 106
 Fayette County, USA, 313
 Felder pit, USA, 159, 312, 323, 326, 330, **345–349**
 Felder-Zamzow-Lamprecht, USA, 312, 347
 Fern mine, USA, 112
 Feusner mine, USA, 244
 Figueira district, Brazil, 416, 451, 452, 470–472
 First Chance mine, USA, 271
 Flag Mesa mine, USA, 86
 Flat Top mine, USA, 62, 300
 Flodelle Creek, USA, 4, 7, 86, **242, 243**
 Florida, USA, 4, 6, 8, 375
 Foot Hill mine, USA, **269**
 Foothills, USA, 254
 Fortalaza, Brazil, 457
 Fort Collins, USA, 230
 Four-and-a-half (4½) breccia pipe, USA, 120
 Four Corners area, USA, 64, 254
 Frank M, USA, 88, 89, 90, 91, 92, 93
 Frazer mine, USA, 174
 Fredonia City, USA, 121, 136
 Freedom 2 mine, USA, 294, 295, 297
 Fremont County, USA, 181, 182, 183, 192, 377
 Front Range, USA, 3, 4, 5, 6, 150, 226, **253–270**

G

Galen, USA, 334
 Gallup, USA, 15–17, 34, 36, 45, 56, 57
 Gandarela, Brazil, 474, 475, **476–477**
 Garza, USA, 312
 Gas Hills district, 7, 8, 150, 152, 155, 157, 159, 160, 161, 162, 163, 164, 165, 168, 169, **173–176**, 181, 193, 195
 Gate Canyon, USA, 256, 269
 Gateway area, USA, 82
 Gaucho I-II, Argentina, 434
 Georgia, USA, 4, 375
 Geosynclinal Andino, Argentina (see Andean Geosyncline)
 Gila County, USA, 304
 Glenrock, USA, 199, 201
 Glen Williams mine, USA, 271
 Globe-Lake Roosevelt, USA, 281
 Goiás state, Brazil, 415, 451, 452, 470, 477
 Golden Gate Canyon district, USA, 254, 256, 265, 269
 Golden Goose mine, USA, 181, 183, 250
 Goliad County, USA, 312, 318, 350, 354
 Goliad, USA, 312, 350, **354**
 Gonzales County, USA, 312, 313
 Good Hope mine, USA, 306
 Goshen Hole area, USA, 226, 229
 Gould mine, USA, 212, 213
 Granaditas, Mexico, 418, 426
 Grand Canyon, USA, 120, 121, 134, 141, 146, 147
 Grand Canyon village, 136, 137
 Grandfather Mountain Window, USA, **357**
 Grand Gulch breccia pipe, USA, 120
 Grandview breccia pipe, USA, 120, **148**
 Granite Mountains, USA, 150, 153, 154, 163, 164, 166, 173, 174, 175, 181, 182, 183, 193, **250–251**

Granite Point, USA, 282, 283, 290
 Grant Brook, USA, 357
 Grants Mineral Belt, USA, 9, 12, 15
 Grants Uranium Region, USA, 6, 8, 10, **12–63**
 Grapevine mine, USA, 254, 256, **269**
 Greasewood, USA, 193, 194
 Great Basin, USA, 281
 Great Divide Basin, USA, 5, 7, 149, 152, 153, 162, 163, 165, **181–192**
 Great Plains, USA, 3, 6, 7, 12, 150, 219–232
 Greeley Arch, USA, 150, 226, 227
 Green Mountain, USA, 357
 Green Mountain district, USA, 7, 150, 181, 182, **183–186**
 Green Mountains, USA, 150, **181–186**, 250
 Green River Basin, USA, 150, **377**
 Green River district, USA, 6, 64, 65, 75, 79, **86–87**
 Griffin, USA, 312
 Gros Ventre Range, USA, 377
 Grover, USA, 226, 227, **231**, 232
 Guandacol(-Jáchal) district, Argentina, 416, 427, 428, **430–431**
 Guerra, USA, 312
 Gueydan fluvial system, USA, 314, 317, 319, 320, 331, 339, 340, 341
 Gunnison (School Section) mine, USA, 6, 271
 Gurey, USA, 312, 343, 349
 Gyp Hill, USA, 312, 354
 Gypsum Valley anticline, USA, 68, 80, 82
 Guyana Shield, South America, 415, 416, 451, 465

H

Hack Canyon, USA, 123, 127, 134, 141, 142, 145, 146, 148
 Hack (Canyon) 1 breccia pipe, USA, 7, 120, 121, 122, 130, **141–142**
 Hack (Canyon) 2 breccia pipe, USA, 7, 120, 121, 122, 123, 126, 129, 130, 131, 133, 135, **141–142**
 Hack (Canyon) 3 breccia pipe, USA, 120, 121, 122, 123, 129, 130, **141–142**
 Hackney, USA, 334
 Hagist, USA, 312
 Hahn, USA, 347
 Hanksville, USA, 88
 Hank, USA, 194, 197, **199**
 Hansen, USA, 253, **270–274**
 Happy Jack mine, USA, 110, 111, 115
 Harry Creek, USA, 279
 Hartville Uplift, USA, 7, 150, 193, 201, 226
 Harvey Black mine, USA, 112
 Hauber mine, USA, 214, 215, **216–218**
 Heaths Peak, USA, 249
 Hecla mine, USA, 83, 102, 106
 Helmer mine, USA, 215
 Henry Basin, USA, 65, 66, 81, 88, 89, 93
 Henry Mountains district, USA, 6, 10, 64, 65, 74, 75, 79, 80, 81, **88–93**, 117
 Henry Mountains Mineral Belt, USA, 88, 89
 Hermit breccia pipe, USA, 120, 121, 122
 Hesitation prospect, USA, 245, **249**
 Highland Box Creek, USA, 154
 Highland Flats-Box Creek district, USA, 7, 150, 154, 193, 199, 202
 Highland (Flats) mine, USA, 162, 163, 173, 193, 195, **199–201**, 202, 203
 High Plateaus, USA, 10
 Hilario, Mexico, 426
 Hillside mine, USA, 4, **305–306**
 Hoback Range, USA, 377
 Hobsen, USA, 312
 Hogback No. 4 mine, USA, 34, 56, 57
 Holbrook, USA, 96, 97, 119
 Holiday-El Mesquite, USA, 312, 324, 326, 333, 339, **342–344**, 349
 Homestake Nall Lease mine, USA, 177, 180
 Horse Creek, USA, 283
 Horse Creek zone, USA, 282, 283, 284, 285, 286, **290**
 Hot Springs County, USA, 377

House Seale, USA, 312, 339, **340–341**
 Houston Embayment, USA, 313, 314
 Huacchane, Peru, 481
 Huancarani, Bolivia, 447, 448
 Huasabas, Mexico, 426
 Huato batholith, Bolivia, 447
 Huemul, Argentina, 427, 439
 Huiquiza, Peru, 481, 482
 Huiquiza-Tantamaco, Peru, 481
 Hulett Creek area, USA, 209, 210, 214, **215–218**
 Hulett, USA, 6, 215
 Hualapai Plateau, USA, 120
 Hurt, USA, 312
 Huskon No. 10 mine, USA, 119
 Huskon No. 11 mine, USA, 119

I

Ibaiti, Brazil, 470
 Idaho, USA, 4, 6, 8, 233, 234, 242, 243, 244, 253, 255, 256, 269, 375, 376, 377
 Idaho batholith, USA, 233, 242, 243
 Igarapé Bahia, Brazil, **479–480**
 Ike mine, USA, 102, 106
 Indian Creek district, USA, 96, 110, **117**
 Indian Springs, USA, 231
 Inter River district, USA, 6, 96, 97, **115–117**
 Inyo County, USA, 373
 Ipora Massif, Brazil, 472
 Irigaray, USA, 193, 194, 195, 196, **199**
 Itaitia, Brazil, 415, 416, 451, 452, 455, **457–462**
 Itatira, Brazil, 458

J

Jack Daniels, USA, 119
 Jackpile, USA, 6, 14, 27, 47
 Jackpile-Paguete mines, USA, 36, 38, **46**, 49
 Jackpile pipe, USA, 49
 Jackpot/Green Mountain, USA, 7, **183–186**, 191
 Jackpump, USA, 312
 Jaguaribeana fold belt, Brazil, 458, 459
 Jamaica, USA, 357
 Jamestown area, USA, 254
 Jan (or Whiskey Peak), USA, 183
 Jeffrey City, USA, 250
 Jim Hogg County, USA, 312, 313, 318, 339
 Jim Thorpe, USA, 357
 J.J. No.1 mine, USA, **49**
 Joe Rock mine, USA, 112
 John mine, USA, 174
 Johnny M, USA, 53
 Juan Tafoya, USA, 43
 Jujuy-Bolivian Basin, Bolivia, 429
 Juniper mine, USA, **373**
 Juniper Ridge, USA, 206, 207

K

Kaibab Plateau, USA, 10, 120
 Kanab, USA, 135, 141, 142, 144, 145
 Kanab Creek, USA, 120, 121, 122, 134, 141, 144
 Kanab North breccia pipe, USA, 7, 120, 121, 122, 129, **144–145**
 Karnes County, USA, 6, 7, 159, 311, 312, 313, 318, 319, 320, 323, 334, 335, 336, 337, 338, 340
 Kaycee district, USA, 150, 154, 194, **203**, **206**
 Kay, USA, 215
 Kellner, USA, 312, 334
 Kendrick Bay, USA, 367
 Kentucky, USA, 4, 379
 Keota, USA, 226, 227, 228, **231**

- Kern County, USA, 373
 Kern River Canyon, USA, 4, **373**
 Kerr-McGee mine, USA, 177, 180
 Kerr-McGee Section 22 mine, USA, 36
 Kiguitian, Peru, 481, 482
 King mine, USA, 212, 213, 290, 291
 King Solomon mine, USA, 75
 Kingsville Dome, USA, 3, 8, 312, 320, **350**, 351
 King Tutt Mesa, USA, 85
 Kirk, USA, 254
 Kleberg County, USA, 350, 351
 KMc mine, USA, 34
 Knob Hill mine, USA, 271
 Knispel, USA, 312
 Knunkel, USA, 312
 Kolar, USA, 312
 Kopplin mine, USA, 312, 345, 347
 Korth, USA, 312
 Kotzer, USA, 312
- L**
- La Brett, USA, 283
 La Caverna, Argentina, 433
 La Coma, Mexico, 418, **425**
 La Despedida, Argentina, 429
 La Domitila, Mexico, 417, 419, 420, 423, **425**
 Ladwig (or Aubry Ladwig) mine, USA, 254, 255, 256, **269**
 La Estela, Argentina, 427, 432, 433
 Lages, Brazil, 470
 La Gloria, Mexico, 418
 Lagoa Grande, Brazil, 452
 Lagoa Real district, Brazil, 415, 416, **451–457**
 Lago Seco, Argentina, 441, 442
 Laguna Colorada, Argentina, 427, 440, 441, 442, 445
 Laguna de Cuervos, Mexico, 417, 418
 Laguna del Diablo, Mexico, 418, 420
 Laguna district, USA, 6, 13, 15, 17, 20, 21, 26, 29, 36, 39, 43, **46–49**, 61
 Laguna Palacios, Argentina, 445
 Lake Titicaca, Peru, 481
 Lakeview district, USA, 4, 6, 281, **290–291**
 Lamac mine, USA, 174
 La Madreselva, Ea., Argentina, 441
 La Mesa, Mexico, 418
 La Morenita, Argentina, 432
 Lamprecht, USA, 322, 330, 345, 346, **347–349**
 Lamprecht-Zamzow-Felder, USA, 345, 346
 Land Pebble district, USA, 4, 6, **375–376**
 La Ollada, Argentina, 433, 434, 438
 La Paz, Bolivia, 447
 La Pintada Anticline, 433
 La Potranca, Argentina, 440, 441
 La Preciosa, Mexico, 418, 425
 La Quebrada, Argentina, 442
 Laramie Mountains/Range, USA, 150, 163, 166, 176, 177, 193, 201
 La Rioja, Argentina, 427
 La Rioja province, Argentina, 427, 431
 Las Abejas, Argentina, 433
 La Sal Creek, USA, 6, 64, 83, 84
 La Sal–La Sal Creek district, USA, 64, 65, 66, 77, **83–84**
 La Sal mine, USA, 6, 70, 73, 77, 84, 102, 106
 La Sal, USA, 66, 72, 74, 77, 102
 Las Amarillas, Argentina, 443
 La Sierrita, Mexico, 415, 417, **425**
 Las Margaritas, Mexico, 417, 418, 419, 420, 422, 423, **424**
 Las Palmas, USA, 312, 343, 349
 Lassen County, USA, 373
 Last Chance mine, USA, 148, 271
 Last Hope prospect, USA, 245, **249**
 La Terraza, Argentina, 427, 433, 434, 435
 La Terraza Norte, Argentina, 433, **438**
 Lauw, USA, 334
 Lawler Peak Granite, USA, 281, 306
 Laymon, USA, 215
 L-Bar Ranch, USA, 14, 46, **49**
 Leatherwood Granite, USA, 358, 359, 364, 365
 Lee Ranch, USA, 53
 Lee's Ferry, USA, 94, 118
 Leuenberger, USA, 194
 Lima area, USA, **376**
 Limbani-Quillabamba batholith, Bolivia, 447
 Lisa breccia pipe, USA, 120
 Lisbon mine, USA, 105, 106, 109, 116
 Lisbon Valley anticline, USA, 83, 101, 105, 109
 Lisbon Valley (Big Indian Wash) district, USA, 5, 6, 10, 66, 95, 96, 99, 100, **101–110**, 136
 Little Badlands, USA, 220, 222
 Little Beaver mine, USA, 102, 109
 Little Colorado River, USA, 10, 120, 122
 Little Indian mines, USA, **279**
 Little Man mine, USA, 233, **249–250**
 Little Mo-Arrowhead mine, USA, **249**
 Little Mountains, USA, 150, 233, 234, 244
 Little Mountains district, USA, 4, 6, 233, 234, **244–245**
 Little Rockies, USA, 74, 88–90
 Live Oak County, USA, 6, 159, 311, 312, 313, 318, 320, 328, 339, 340, 341, 345–349, 350, 353, 354
 Live Oak County Mineral Trend, USA, 328
 Lizard breccia pipe, USA, 120
 Llano Uplift, USA, 320
 Loco, USA, 174
 Logo Seco, Argentina, 441, 442
 Long Mesa, USA, 66
 Longoria, USA, 312, **342–344**
 Long Park, USA, 66
 Long Pine Hills, USA, 219–221
 Lookout mine, USA, 279
 Loon Lake batholith, USA, 233, 234, 235, 236, 237, 238, 239, 240
 Los Adobes, Argentina, 427, 440, 441, 442, **444–445**
 Los Amoles, Mexico, 418, 426
 Los Berthos, Argentina, 427, 429, 430
 Los Caballos, Mexico, 418, 426
 Los Chañares, Argentina, 433, 438
 Los Colorados district, Argentina, 427, 428, **431**
 Los Diques, Bolivia, 447, 448
 Los Enriques, Argentina, 433
 Los Europeos, Argentina, 432
 Los Gauchos I-II, Argentina, 433, 434, **438**
 Los Gigantes district, Argentina, 416, 427, 428, **431–432**
 Los Ochos fault, USA, 279
 Los Reyunos, Argentina, 433, 435, 437, 438
 Lost Creek, USA, 7, 182, 191, **192**
 Lost Soldier, USA, 182, **191–192**
 Lost Spring mine, USA, 88, 90
 Louise mine, USA, 102, 109
 Louisiana, USA, 4, 8
 Lower Cloys mine, USA, 294
 Lockett, USA, 334
 Lucky Lass mine, USA, 290
 Lucky Mc mine, USA, 7, 159, 174, 175, 177
 Lucky Strike, USA, 91
 Ludlow, USA, 357
 Lukachukai-Carrizo Mountains district, USA, 64, 65, 79, **84–86**
 Lukachukai Mountains, USA, 72, 86
 Lyne, USA, 312, 345
 Lynx breccia pipe, USA, 120, **147**
 Lysite Mountain area, USA, **377**

M

Mabel mine, USA, 345
 Macizo Central de Chubut, Argentina. (see Chubut)
 Mac No. 1, USA, 54
 Mac No. 2, USA, 54
 Macusani district, Peru, 415, 416, 448, **481–485**
 Madison Range area, USA, **376**
 Maine, USA, 3
 Majalca, Mexico, 418
 Malargüe district, Argentina, 427, 428, **439**
 Manka, USA, 334
 Manke, USA, 215
 Manna, USA, 312
 Mann, USA, 254
 Margaritas, Mexico (see Las Margaritas)
 Mariano Lake, USA, 14, 27, 54–56
 Maritita-Chepical, Argentina, 431
 Marquez, USA, 14, 43, 44
 Marquez Canyon, USA, 36, 43, 44
 Marquez district, USA, 7, 14, 15, 36, **43–44**
 Marshall Pass district, USA, 4, 6, **275–279**
 Martin Mighel de Guemes, Argentina, 429, 430
 Martinsville Igneous Complex, USA, 358
 Maryland, USA, 3
 Marysvale district, USA, 4, 6, 7, 281, **292–300**
 Marysvale volcanic field, USA, 292, 293, 298
 Massachusetts, USA, 3
 Mato Grosso state, Brazil, 470
 Maybell district, USA, 150, 206, **207**
 Mazatzal Mountain, USA, 304
 Mc Bride, USA, 312, 343, 349
 McCoy Mountains, USA, 4, 373, **374**
 Mc Crady, USA, 334
 McDermitt caldera/district, USA, 4, 6, 281, **282–290**
 McIntosh pit, USA, 181
 McLean, USA, 345, 348
 Mc Lean 1, USA, 345, 347
 Mc Lean 2, USA, 345, 347
 Mc Lean 5, USA, 348
 McMullen County, USA, 311, 312, 313, 318, 320, 345
 Meadow mine, USA, 242, 243
 Media Luna I, II, III, Argentina, 434, 438
 Medicine Bow Mountains, USA, 4, 150, 233, 234
 Medicine Pole Hills, USA, 220
 Meeker district, USA, 65, 74, **94**
 Melo-Fraile Muerto, Brazil, 470
 Melrose area, USA, **376**
 Mena mine, USA, 254, 256, **269**
 Mendoza, Argentina, 439
 Mendoza province, Argentina, 427, 433, 439
 Mesa II mine, USA, 86
 Mesa I mine, USA, 86
 Mesa IV-1/4 mine, USA, 86
 Meseta de los Frailes, Bolivia, 447
 Meseta Quenamari, Peru, 481, 485
 Mexican Hat, USA, 115
 Mexico, 415, 417ff
 Middletown, USA, 3
 Midnite mine, USA, 4, 7, 233, **234–239**
 Mike, USA, 83
 Mina Amistad, Bolivia, 447, 450
 Mina Cotaje, Bolivia, 448–450
 Minas Gerais state, Brazil, 451, 452, 462, 473, 480
 Mineral Canyon, USA, 96, 97
 Mi Vida mine, USA, 102, 106, 107, 136
 Moab, USA, 96, 99, 115
 Moab district, USA, 6, 65, **93–94**, 96, 99
 Moctezuma, Mexico, 418, 426

Mogollon Highland, USA, 15, 95, 136
 Mohawk Canyon breccia pipe, USA, 120, 128
 Mojave Desert, USA, 4, 373
 Monogram Channel, USA, 66
 Monogram Mesa, USA, 83
 Monroe Peak caldera, USA, 293
 Montana, USA, 4, 5, 6, 7, 221, 233, 244, 375, 376
 Montano Bernabe (see Bernabe-Montano)
 Montezuma Canyon district, USA, 65, **94**
 Monticello, USA, 87, 94
 Monument Hill district, USA, 7, 150, 154, 193, 194, 195, 199, 201, 203–205
 Monument No. 2 mine, USA, 112, 115, 116
 Monument Upwarp, USA, 10, 64, 97, 110, 115
 Monument, Crownpoint, USA, 57
 Monument Valley district, USA, 5, 6, 10, 91, 95, 97, 98, 99, 100, 111, 112, 114, **115**, 116
 Monument Mitten, USA, 112
 Moonlight mine, USA, 111, 112, 115
 Moonlight, USA, 283, 284, 285, 286, **290**
 Moore Ranch, USA, 194
 Morrison, USA, 253, 254, 269
 Mount Belknap, USA, 293
 Mount Holy, USA, **357**
 Mount Lucas, USA, 312, 350, **353**
 Mount Pisgah, USA, 357
 Mount Spokane area, USA, 4, 233, **241–242**
 Mount Taylor district, USA, 7, 14, 15, 36, **49–52**
 Mrak No.2 mine, USA, **203**, 205
 Muddy Gap, USA, 181
 Mufumbo, Brazil, 455, 457

N

Nacimiento Mountains, USA, 61
 Nall Lease, USA, 178
 Narrow Canyon, USA, 14, 57
 Naschey mine, USA, 112
 Natural Bridges district, USA, 110
 Nazas, Mexico, 425
 Near Miss breccia pipe, USA, 120
 Nebraska Plains, USA, 4, **221–226**
 Nebraska, USA, 3, 4, 5, 6, 7, 8, 219, 221, 222, 226
 Nell, USA, 312, 340
 Nemo district, USA, 209, 234
 Neuquén Basin, Argentina, 439
 Nevada, USA, 3, 4, 6, 123, 273, 291
 New Hampshire, USA, 4, 357
 New Haven mine, USA, 215
 New Jersey, USA, 4, 357
 New Mexico, USA, 3, 4, 5, 6, 10, 12ff, 65, 84, 85, 86, 306
 New York state, USA, 357
 New Velvet mine, USA, 102, 109
 Nichols Ranch, USA, 194, **197–199**
 Niezwietz, USA, 312
 Nine Mile Lake, USA, **206**
 Nixon mine, USA, 102, 106
 Noche Buena, Mexico, **418**, 426
 Nopal-1 (I), Mexico, 417, 418, 419, 420, 421, **423–424**
 Nopal-2 (II), Mexico, 418, 421
 Nopal-3 (III), Mexico, 417, 418, 419, 420, **424**
 Norte Subandino, Argentina. (see Northern Sub-Andean)
 North Alice mine, USA, 102, 106
 North Bee County Mineral Trend, USA, 328
 North Belfield, USA, 219, 220, 221
 North Butte, USA, 193, 194, 197, **199**
 North Canning, USA, 245, 246, **247–248**
 North Carolina, USA, 4, 5, 357
 North Cave Hills, USA, 220, 221

North Dakota, USA, 3, 4, 6, 219, 221, 222
 North Dillon area, USA, **376**
 Northeast Church Rock mine, USA, 56, 57
 Northern Black Hills, USA, 6, **214–218**
 Northern Great Plains, USA, 4, 6, **219–232**
 Northern Red Desert, USA, **191–192**
 Northern Rocky Mountains, USA, 4, 6, **233–251**
 Northern Sub-Andean region (Norte Subandino), Argentina, 427, **429**
 North Fork drainage basin, USA, 243
 North Rolling Pin, USA, **199**
 North Star, USA, 254
 North Trend, USA, 57
 North Wash, USA, 89
 Nose Rock district, USA, 7, 14, 15, 37, **59–61**
 Nueces River, USA, 320
 Nuevo León state, Mexico, 415, 417, 418, 425
 Nuhn, USA, 334, 335

O

Oak County, USA, 345
 Oaxaca state, Mexico, 417, 418, 426
 O'Hern, USA, 312, **342**, 343, 349
 Ohman mine, USA, 254, 256, **269**
 Ola, USA, 174
 Old Bonnie breccia pipe, USA, 120
 Old Church Rock mine, USA, 56, 57, 61
 Old Hack Canyon mine, USA, **148**
 Old Leyden (coal) mine, USA, 254, **270**
 Old Man Springs, USA, 283
 Olinda, Brazil, 480
 Oliver Saddle prospect, USA, 271
 Ollie, USA, 220
 Ollie-Carlyle, USA, 219
 Oregon, USA, 3, 4, 6, 281, 290
 Orphan Lode/breccia pipe, USA, 7, 120, 122, 125, 127, 129, 130, 136, **137–141**
 Osamu Utsumi mine, Brazil, 463, 464
 Outlaw Mesa, USA, 66
 Owl Creek Mountains, USA, 150, 173, 234, 245

P

Pacific Coast region, USA, 4, **373–374**
 Paganzo Basin, Argentina, 429–431
 Paguete, USA, 14, 35, 46
 Paiol, Brazil, 452
 Palangana Dome, USA, 312, 320, 350, **351**, **353**, 354
 Pampa Amarilla, Argentina, 439
 Pampa Grande district, Argentina, 429
 Pampas Mountain (Sierras Pampeanas), Argentina, 427, **431–433**
 Pandora mine, USA, 3, 83
 Panna Maria, USA, 8, 312, 330, 335, **336–338**
 Pantanito, Argentina, 433
 Paradox Basin, USA, 9, 42, 64, 66, 79, 82, 95, 97, 99, 100
 Paraíba state, Brazil, 415, 451, 452, 468, 480
 Paramirim pluton, Brazil, 454
 Paraná Basin, Brazil, 415, 451, 452, 462, **470–474**, 480
 Paraná state, Brazil, 451, 470
 Parashant breccia pipe, USA, 120
 Pará state, Brazil, 415, 479, 480
 Paso de Indios, Argentina, 440
 Pasterias, Mexico, 418
 Pat breccia pipe, USA, 120
 Patagonia, Argentina, 427, 440, 443
 Patagonian Platform, Argentina, 416
 Pathfinder mine, USA, 177
 Pathfinder 6900 trend, USA, 183
 Pawelek, USA, 334
 Pawlik, USA, 312, 345
 Pawnee, USA, 228, **231–232**, 312, 345
 Pay Aljob mine, USA, 174
 Peach shaft, USA, 173, 174, 175
 Pedro Mountains, USA, **249–250**
 Pedro Nicolas, Argentina, 430
 Pena, Mexico, 418
 Penn Haven Junction, USA, **357**
 Pennsylvania, USA, 4, 357
 Penoles, Mexico, 418
 Pepe Luis, Argentina, 430
 Pericratonic Andean Basins, South America, 416
 Perkins, USA, 312, 345
 Peru, 415, 481–485
 Petersen Mountain, USA, 4, **373**
 Peters Lease, USA, 239
 Petrotomics Dave, Section 9 and 15 mines, USA, 160, 177, 178
 Pfeil, USA, 159, 334, 337
 Phillips mine, USA, 34, 56, 57
 Phosphoria Formation region, USA, **376–377**
 Phosphorite regions, USA, 4, 6, **375–377**
 Picacho, Mexico, 418, 426
 Piceance Basin, USA, 10
 Pichiñán district, Argentina, 416, 427, 428, **440–445**
 Picnic Tree mine, USA, **270–274**, 275
 Piedmont, USA, 3, 4, 6, 7, **357–366**
 Piedra Lumbre, USA, 312
 Piedras Pintas, USA, 312, 320, 350
 Pigeon breccia pipe, USA, 120, 121, 122, 129, 130, **142–144**
 Pikes Peak batholith, USA, 254
 Pine Mountain area, USA, **377**
 Pinenut breccia pipe, USA, 120, 121, 122, **145–146**
 Pine Ridge anticline, USA, 83
 Pinnacle Hill, USA, 357
 Pinnacle (=Pitch), USA, 275
 Pinocho, Peru, 481, 482, 484
 Pintas, USA, 312
 Pitch mine, USA, **275–279**
 Pittsylvania County, USA, 357
 Plant City, USA, 375
 Plumbic mine, USA, 294
 PNC, Great Divide Basin, USA, 182
 Poços de Caldas, Brazil, 415, 416, 451, 452, **462–468**, 471
 Poison Basin, USA, **206–207**
 Poison Canyon trend/mines, USA, 14, 25, 53, 54
 Polar Mesa, USA, 66
 Poligono das Secas (Polygon of Droughts), Brazil, 452
 Porter Creek, USA, 228, 232
 Potts shaft, USA, 294, 295
 Powder River Basin, USA, 5, 7, 149, 153, 157, 160, 161, 162, 163, 164, 165, 169, 170, 173, **193–206**, 211, 212, 226
 Powell, USA, 244
 Precordillera (belt), Argentina, 415, 427, **430–431**
 Presila, Mexico, 418
 Price, USA, 86
 Prince of Wales Island, USA, 367
 Promontory Butte, USA, 136
 Prospector mine, USA, 294, 295
 Pryor Mountains, USA, 4, 6, 7, 150, 233, 234, 244
 Pryor Mountains-Little Mountains district, USA, 4, **244–245**
 Puerto Alvear, Argentina, 443
 Puerto 1 (I), Mexico, 418, 419
 Puerto 2 (II), Mexico, 418, 419
 Puerto-3 (III), Mexico, 417, 418, 419, 422, 423, **425**
 Puerto 8, Mexico, 419
 Puerto IV, Mexico, 418
 Puerto V, Mexico, 418
 Puerto VI, Mexico, 418
 Puerto Viser, Argentina, 442
 Pumpkin Buttes district, USA, 7, 150, 154, 162, 193, 194, 195, 196–199

Q

Quadrilátero Ferrífero, Brazil, 415, 451, 452, **474–477**
 Quebrada El León, Argentina, 427, **429**
 Quebradas, Brazil, 452, 453
 Quillagua, Chile, 415

R

Radium Hill mine, USA, 112
 Radium King mine, USA, 110
 Radium Mountain, USA, 66
 Radon mine, USA, 102, 106, 108
 Radon Springs, USA, 182
 Rahueco district, Argentina, 439
 Rainbow Moose mine, USA, 271
 Ralston Buttes district, USA, 253, 254, 255, 256, **269**
 Rattlesnake mine, USA, 83
 Rawlins City, USA, 191
 Rawlins Uplift, USA, 181
 Rawson, Argentina, 440
 Ray Point district, USA, 312, 313, 341, **345–349**
 Reading Prong, USA, **357**
 REB, USA, 182, 187, **191**
 Red Butte-Grand Canyon, USA, 121
 Red Canyon, USA, 97, 110
 Red Desert, USA, 181, 182, 186–192
 Red Dog, USA, 4, 291
 Red Hills caldera, USA, 293
 Red Horse Wash breccia pipe, USA, 120
 Reese River, USA, 291
 Reno Creek, USA, 193, 194, **199**
 Reynolds Ranch, USA, 194, **203**
 Rhode Ranch, USA, 8, 312, 313, 332, 345, **349**
 Riacho do Pontal mobile belt, Brazil, 455
 Ribera fold belt, Brazil, 454
 Ridenour breccia pipe, USA, 120, 122, 128, **148**
 Rim breccia pipe, USA, 120
 Rim mines, USA, 174
 Rincón del Artuel, Argentina, 433
 Rio Algom, USA, 102, 105, 109, 116
 Rio Cajoncillo, Argentina, 430
 Rio Cristalino, Brazil, 480
 Rio Grande do Norte state, Brazil, 468
 Rio Grande Embayment, USA, 313, 314
 Rio Grande River, USA, 319
 Rio Grande Trough, USA, 15
 Rio Preto-Campos Belos, Brazil, 451, 452, **477, 478**
 Rio Puerco district, USA, 15, **43–44**
 Riverside County, USA, 373, 374
 Riverton, USA, 245
 Riverview breccia pipe, USA, 119, 120, 122, **148**
 Roc Creek, USA, 7
 Rock Creek zone, USA, 283
 Rock Springs Uplift, USA, 181
 Rocky Mountains, USA, 3, 4, 7, 12, **233–251, 253–280, 311**
 Rocky Mountain Arsenal, USA, 266
 Rodolfo, Argentina, 427, 431, 432
 Rogers-Cadena, USA, 312
 Rolling Pin, USA, 193, 194, 199
 Rosenbrock, USA, 312, 334
 Rose breccia pipe, USA, 7, 120, **147**
 Rose mine, USA, 306
 Rosita, USA, **353**
 Ross Adams, USA, 367, 368, 370
 Round Park, USA, 183
 Ruby No. 1 to No. 4 mines, USA, 27, 54, 55
 Ruby Ranch, USA, 193, 194, **199**
 Ruby Wells, USA, 14
 Ruin Granite, USA, 281

Runge mine, USA, 211, 212
 Ruth, USA, 193, 194, 196, **199**
 Ryan, USA, 312

S

Sage breccia pipe, USA, 120, 122
 Sagebrush mine, USA, 174
 Salar Grande, Chile, 415
 Sally mine, USA, 112
 Salobo, Brazil, 479
 Salta, Argentina, 429
 Salta Basin, Argentina, 429
 Salta province, Argentina, 427, 429
 Salt Lake City, USA, 291, 292, 309
 Salt Wash districts, USA, 12, **64–94**
 San Agustín, Bolivia, 447, 448
 San Antonio de Cobre, Mexico, 425
 San Antonio de las Huertas, Mexico, 418, 426
 San Antonio River, USA, 320
 San Antonio Valley, USA, 43, 44
 San Bernardino County, USA, 373
 San Carlos, USA, 312
 Sand Creek, USA, 228, 232
 Sand Draw, USA, 194, **203**
 Sand Wash Basin, USA, 149, 150, **206–207**
 Sandy mine, USA, 46
 Sanguinetti, Argentina, 443
 San Isidro district, Argentina, 433
 San Jorge Gulf Basin, Argentina, 427, **440–445**
 San Juan Basin, USA, 5, 6, 9, 10, **12ff**
 San Juan County, USA, 85, 102
 San Juan de la Costa, Mexico, 426
 San Juan mine, USA, 102, 106
 San Juan Mixtepec, Mexico, 418, 426
 San Juan Mountains, USA, 100, 253, 279
 San Juan province, Argentina, 427, 430
 San Luis Potosí state, Mexico, 417, 418
 San Luis province, Argentina, 427, 432
 San Marcos Arch, USA, 314, 316, 319, 320, 321, 339
 San Marcos caldera, Mexico, 425
 San Mateo, USA, 29, 36, 49, 51, 54
 Sañogasta, Argentina, 430
 Sanostee, USA, 61
 San Rafael district, Argentina, 427, **433–439**
 San Rafael mill, Argentina, 227
 San Rafael Swell district, USA, 65, 96, 97, 100, **117, 118**
 San Sebastian, Argentina, 430
 Santa Catarina state, Brazil, 470
 Santa Fe, Mexico, 418
 Santa Quitéria, Brazil, 455, **457–462**
 Santa Quitéria-Tamboril Complex, Brazil, 458, 459
 Santa Rosalia, Mexico, 418, 426
 Santiago Papasquiaro, Mexico, 418
 Santonino, USA, 312, 339, 342, 343
 São Francisco Craton, Brazil, 451, 452, 453, 455, 468, 479
 São Luis Craton, Brazil, 468
 São Paulo, Brazil, 462, 470
 São Roque Granite, Brazil, 478
 São Timóteo pluton, Brazil, 451, 454, 455
 Sapopema, Brazil, 470
 Savannic breccia pipe, USA, 120, 148
 Sawatch Range, USA, 253, 275
 SBF breccia pipe, USA, 120, 122, **147**
 Schlagintweit, Argentina, 427, 432
 Schroeckingerite prospect, USA, 245
 Schwartzwalder mine, USA, 7, 253, 254, 255, **256–269**
 Section 23 mine, USA, 30–33
 Sejita, USA, 312, 343, 350, 354

- Sentinel Butte area, USA, 220, 221
 Seridó, Brazil, 451, 452, 468, **469–470**
 Seridó Basin, Brazil, 468
 Serra das Gaivotas, Brazil, 474, **475–476**
 Serra de Jacobina, Brazil, 415, 451, 452, **477–479**
 Serra dos Carajás, Brazil, 415, 416, 451, **479–480**
 Serviceberry, USA, 102, 109
 Sevaruyo district, Bolivia, 415, 416, **447–450**
 Seven Devils mine, USA, 254, **269**
 Seven Mile Canyon district, USA, 96, 97, 115, 116
 Seward Peninsula, USA, 367
 Sheep Creek, USA, 181, **250**
 Sheep Mountain mine, USA, 181
 Sherwood mine, USA, 4, 7, 233, 234, 235, **239–241**
 Ship Rock mill, USA, 85, 86
 Shirley Basin, USA, 5, 6, 7, 8, 149, 150, 152, 153, 154, 157, 159, 160, 161, 162, 163, 164, 165, 173, 174, 175, **176ff**, 193, 195
 Shirley Mountains, USA, 163, 177
 Shitamaring Canyon, USA, 89
 Shivwits Plateau, USA, 146
 Shootering Canyon, USA, 88, 90, 92, 93
 Sickenius, USA, 334
 Sierra Ancha, USA, 4, 6, 7, **304–305**
 Sierra Cuadrada, Argentina, 427, 440, 442
 Sierra Cuadrada Norte, Argentina, 441
 Sierra Cuadrada Sur, Argentina, 441
 Sierra de Comechingones, Argentina, 432
 Sierra de Coneto, Mexico, 425
 Sierra de Gomez, Mexico, 417, 418, 425
 Sierra Del Guanaco, Argentina, 441
 Sierra de la Gloria, Mexico, 419, 425
 Sierra de los Pichiñanes, Argentina, 427, 440
 Sierra de Peña Blanca, Mexico, 415, **417–425**
 Sierra Los Gigantes, Argentina, 432
 Sierra Madre, USA, 234
 Sierra Madre Occidental, Mexico, 417
 Sierra Nevada, USA, 4
 Sierra Pichiñán district (see Pichiñán)
 Sierra Pintada(-San Rafael) district, Argentina, 415, 416, 427, 428, **433–439**
 Sierras de Transición (see Transition Mountain region)
 Sierras Pampeanas (see Pampas Mountain region)
 Silver City, USA, 306
 Silver Cliff mine, USA, 7
 Silver King-Hobson mine, USA, 306
 Siqueira Campos, Brazil, 470
 Slick Rock, USA, 66, 67, 69, 72, 74, 79, 82, 83
 Slim Buttes, USA, 4, 219, 220, 221, 222
 Smaller and Mary L. mines, USA, 271, 275
 Smith Lake district, USA, 13, 14, 15, 21, 26, 27, 33, 34, 36, **54–56**
 Smith Ranch, USA, 3, 193, 194, **201**
 Smith River Allochthon, USA, 357, 358, 359
 Smith, USA, 312, 347
 Snake Range, USA, 377
 Snowball, USA, 83
 Snyder breccia pipe, USA, 120
 Sonora state, Mexico, 417, 418, 426
 Sonora Pass, USA, 4, **373**
 Sossego, Brazil, 479
 South America, 415, 416, 427ff
 South Belfield, USA, 219, 220, 221
 South Brazilian Shield, Brazil, 480
 South Carolina, USA, 4, 375
 South Cave Hills, USA, 220, 221
 South Dakota, USA, 3, 4, 5, 6, 7, 151, 209, 212, 213, 214, 215, 219, 221, 222, 233, 234
 South Dillon area, USA, **376**
 South Duval County Mineral Trend, USA, 312, 313, 321, 323, 324, 326, 328, 333, 339, **342–345**, **349–350**, **354**
 Southern Rocky Mountains, USA, 4, 6, **253–279**
 Southern Appalachians and Piedmont, USA, 4
 Southern Black Hills, USA, 6, **212–214**
 Southern Great Plains, USA, 6
 Southern Granite Mountains, USA, **250**
 South Park, USA, 253
 South Texas Coastal Plains, USA, 7, 173, **311ff**
 South Texas Mineral Belt, USA, 311ff
 South Trend, Crownpoint, USA, 57
 Spokane Mountain area, USA, 4, 6, **234–241**
 Spor Mountain, USA, 4, 6, 281, **291–292**
 Standard mine, USA, 102
 Stanislaus mine, USA, 3
 St. Anthony/M-6 mine, USA, 14, 46, **49**
 Star mine, USA, 174
 Starlight mine, USA, 112
 Starr County, USA, 7, 312, 313, 318, 339
 Steinmann, USA, 312
 Stevens County, USA, 6, 242
 Stoeltje, USA, 312, 334
 Storm, USA, 215
 Strawberry mine, USA, 94
 Suahuarita, USA, 4
 Sugar Daddy mine, USA, 293, 294
 Sunday/St. Jude mine, USA, 3
 Sunlight mine, USA, 112, 115
 Sunny Divide, USA, 210, 215, 218
 Sunnyside shaft, USA, 294, 295
 Sunset mine, USA, 174
 Sunshine mine, USA, 242, 243, 271
 Swanson, USA, **359–366**
 Sweetwater batholith, USA, 249
 Sweetwater County, USA, 182, 191
 Sweetwater Mountain, USA, 177
 Sweetwater Uplift, USA, 163, 174, 176
 Sweetwater district, USA, 150, 181, 182, **186–191**
 Swinney Switch, USA, 312, 350, **354**
- T**
- Table Mountain, USA, 221
 Tallahassee Creek, USA, 3, 253
 Tallahassee Creek district, USA, 3, 4, 5, 6, 7, 253, **270–275**
 Tamaulipos, Mexico, 425
 Taperuaba, Brazil, 455, 457
 Tascates I, Mexico, 418
 Tascates II, Mexico, 418
 Tayata, Mexico, 418, 426
 Taylor, USA, 312
 Telemaco Borba, Brazil, 470
 Tembabiiche, Mexico, 426
 Temple Mountain, USA, 6
 Tennessee, USA, 3, 4, 375, 379
 Teresa Christina, Brazil, 470
 Teton No. 3, USA, 207
 Texas, USA, 3, 4, 7, 8, 149, 159, 168, 169, 311ff
 Texas Coastal Plain Uranium Region, USA, 3, 4, 6, 7, 166, **311ff**
 Tex Mex, USA, 343, 349
 Texwood mine, USA, 102, 106
 Thacker Pass, USA, 283
 Thirtynine Mile volcanic field, USA, 253, 270
 Tholapalca, Bolivia, 447
 Thomas caldera, USA, **291–292**
 Thomas Mountain, USA, 292
 Thomas Range, USA, 291
 Thompson district, USA, 6, 65, 74, **88**
 Thornburg mine, USA, 279
 Thorn Divide area, USA, 210, 215, **218**
 Thorn Ranch mine, USA, 271

Three Point Mesa mine, USA, 86
 Tidwell Mineral Belt, USA, 86
 Tigre I, Argentina, 427, 434, 435
 Tigre II-III, Argentina, 433, 434, **438**
 Tigre I-La Terraza, Argentina, 433, 427, **438**
 Tinogasta district, Argentina, 427–429
 Tlaxiaco Basin, Mexico, 426
 TL Creek, USA, 210, 214, 215
 Tobas Amarillas, Argentina, 427, **445**
 Todilto trend/mines, USA, 6, 14, 25, 53, **61–63**
 Toledale area, USA, **269**
 Tonco-Amblayo district, Argentina, 416, 427, 428, **429**, 430
 Tonco Subbasin, Argentina, 429
 Tony M, USA, 80, 81, 88, 89, 90, 91, 92
 Topaz, USA, 3
 Topaz Mountain, USA, 291, 292
 Torko, Bolivia, 447, 448
 Trachyte, USA, 88, 89
 Tract 2^o, 11, 14 and 17 mines, USA, 112
 Trancas, Mexico, 418
 Transition Mountains (Sierras de Transicion), Argentina, 427, **429**
 Trevino, USA, 349
 Tricounty, USA, 312
 Tsitah Wash, USA, 85
 Tucano Basin, Brazil, 451, 452
 Tuolumne County, USA, 373
 Turmalina, Peru, 481
 Turnercrest district, USA, 150, 154, 193, 194, 195
 Twin Buttes mine, USA, 4, 281, 309
 Twin Peaks batholith, USA, 308

U

UF1, Mexico, 418, 426
 Uinta Basin, USA, 9, 10
 UNC mine, USA, 34
 Uncompahgre Mountains, USA, 15, 95, 100
 Union Carbide mine, USA, 174
 Union Pacific shaft, USA, 254, **269**
 Upper Cloys mine, USA, 294
 Upper Cottonwood district, USA, 96, 97, 110
 Upper Indian Creek district, USA, 96, 97
 Uravan Mineral Belt, USA, 3, 4, 6, 7, 9, 10, 31, 37, 42, 64ff, **81–83**,
 84, 94
 Urcal mine, Argentina, 430, 431
 Urcuschun, Argentina, 427, 430
 Utah, USA, 3, 4, 5, 6, 7, 70, 75, 79, 87, 88, 95, 101, 115, 117, 141, 233,
 242, 309, 375, 376
 Utah mine, USA, 177, 180

V

Valle de Aldama, Mexico, 418
 Valle de Punilla, Argentina, 431
 Vasquez, USA, 3
 VCA shaft, USA, 294
 Vega shaft, USA, 294
 Velvet mine, USA, 102, 109

Vermont, USA, 4, 357
 Villa Aldama mill, Mexico, 417, 423
 Villacabamba, Peru, 481, 482
 Virginia, USA, 3, 4, 357–366
 Virgin No. 3 mine, USA, 71

W

Wadkey, Mexico, 418
 Wamsutter Arch, USA, 181
 Washakie Basin, USA 6, 149, 150, **206–207**
 Washington County, USA, 313, 341
 Washington state, USA, 3, 4, 6, 233, 241, 242, 313
 Wate breccia pipe, USA, 120
 Webb County, USA, 312, 313, 318, 339, 342, 349
 Weddington-Conoco, USA, 334
 Weddington-Susque-Hanna, USA, 334
 Weddington-Tenneco, USA, 334
 Weld County, USA, 4, 6, 155, 221, 226, 228–231, 333
 Western Gulf Coastal Plain, USA, 4
 Western Piedmont belt, **357–358**
 Western United States Precambrian terrane, USA, 3, 5
 West Largo, USA, 14, 53, 61
 West North Butte, USA, 194, **199**
 West Sunday, USA, 3
 Wheeler Basin, USA, 255, 268
 Whiskey Peak (or Jan), USA, 174, 182, 183
 White Canyon district, USA, 6, 10, 95, 96, 97, 98, 100, **110–115**
 White King mine, USA, 290, 291
 White Mesa mill, USA, 3, 8
 White Mountain Magmatites, USA, 357
 Wilhelm incline, USA, 294
 Williston Basin, USA, 219
 Wilson Creek, USA, 357
 Wind River Basin, USA, 5, 7, 149, 150, 152, 153, **173ff**, 206, 245
 Wind River Mountains, USA, 181, 192
 Woodrow pipe, USA, 14, 29, 32, **46–48**
 Wood mine, USA, 3, 7, 253, 254, 255
 Workman Creek, USA, 304
 Wright, USA, 334
 West Saranosa, USA, 312
 Wyoming, USA, 3, 4, 5, 6, 7, 8, 56, 149ff, 209, 215, 218, 219, 221, 226, 233,
 244, 245, 249, 250, 376, 377
 Wyoming Basins, USA, 3, 4, 5, 6, 7, 26, 37, 40, 70, 75, 79, 80, 105, **149ff**, 211,
 212, 218, 226, 229, 238, 250, 321, 322, 324, 328, 330, 332
 Wyoming Range, USA, 377

Y

Yecora, Mexico, 418, 426
 Yellow Chief mine, USA, 4, 291, 292
 Yellow Circle mines, USA, 93

Z

Zamzow, USA, 322, **345–349**
 Zapata County, USA, 313
 Zidek, USA, 312
 Zuni Uplift, USA, 13, 15, 36, 39



Uranium Minerals Index

U oxides, oxide hydrates, molybdates, phosphates, silicates, U-Ti phases etc.

Brannerite/U-Ti phases 141, 207, 243, 351, 368, 369, 437, 465, 467, 479

Broeggerite (see *Uraninite*)

Cleveite (see *Uraninite*)

Coffinite 12, 22, 24, 37, 39, 42, 44, 45, 46, 49, 50, 53, 58, 60, 62, 63, 69, 81, 82, 84, 87, 88, 92, 94, 97, 99, 105, 106, 115, 119, 127, 132, 139, 143, 145, 153, 154, 162, 165, 169, 174, 178, 182, 185, 195, 197, 201, 202, 206, 207, 211, 213, 215, 216, 218, 226, 228, 236, 237, 238, 239, 240, 248, 249, 263, 264, 266, 270, 273, 274, 277, 278, 284, 285, 289, 290, 291, 296, 297, 298, 300, 301, 302, 304, 305, 307, 321, 326, 335, 336, 345, 350, 351, 361, 362, 364, 365, 367, 368, 373, 425, 431, 437, 441, 444, 447, 448, 449, 466, 469, 472, 474, 475, 476, 484

Nivenite 4

Pechblende (see *Pitchblende*)

Pitchblende (nasturan, pechblende, uranpecherz) xv, 3, 4, 12, 22, 24, 44, 45, 49, 50, 53, 57, 62, 63, 69, 81, 82, 84, 85, 86, 87, 88, 93, 94, 97, 99, 105, 106, 109, 113, 115, 117, 118, 119, 127, 129, 130, 131, 132, 135, 136, 139, 140, 141, 142, 143, 144, 145, 148, 153, 154, 156, 157, 162, 165, 169, 174, 178, 179, 182, 185, 195, 197, 201, 202, 206, 207, 211, 213, 215, 216, 218, 219, 226, 228, 233, 234, 236, 237, 238, 239, 240, 241, 242, 243, 248, 249, 253, 255, 256, 259, 260, 261, 263, 264, 265, 266, 267, 268, 269, 270, 273, 274, 275, 277, 278, 279, 284, 285, 289, 290, 291, 296, 297, 298, 300, 302, 304, 305, 306, 307, 321, 326, 335, 336, 345, 348, 350, 351, 353, 357, 361, 362, 364, 365, 373, 374, 420, 421, 422, 424, 425, 429, 430, 432, 433, 437, 439, 441, 444, 447, 448, 455, 464, 465, 466, 467, 468, 469, 472, 474, 475, 476, 479, 480, 484, 485
sooty/earthy 22, 45, 69, 139, 145, 154, 165, 174, 178, 182, 195, 197, 201, 202, 206, 213, 219, 248, 249, 273, 274, 279, 289, 296, 298, 305, 321, 326, 335, 336, 353, 361, 362, 364, 365, 373, 432, 449
unit cell dimensions 296

Ulrichite (see *Uraninite*)

Uraninite (ulrichite, broeggerite, cleveite) xv, 4, 242, 243, 249, 250, 255, 268, 277, 278, 279, 286, 296, 297, 298, 300, 305, 309, 357, 361, 362, 364, 365, 369, 371, 432, 455, 456, 457, 465, 468, 469, 476, 477, 479, 480
lattice constants 139
unit cell dimensions 296

U-Ti compounds/phases 207, 351, 361, 362, 422, 465

Uranium-bearing minerals (niobates, phosphates, tantalates, titanates etc.)

Allanite 369, 455, 480

Apatite 161, 175, 361, 362, 364, 365, 366, 369, 375, 376, 377, 432, 450, 455, 459, 462, 468, 469, 477, 480, 483

Bastnaesite 369, 467, 480

Betafite 469

Cheralite 141, 467

Collophane 127, 142–145, 459–462

Malacon 459

Monazite 145, 369, 432, 465, 467, 475, 476, 480

Navajoite 115

Thorite 357, 369

Thucholite 476

Uranothorianite 309, 368, 369, 370, 371

Uranothorite 255, 368–371

Xenotime 289, 369

Zircon, var. zirtolite 60, 145, 185, 189, 224, 234, 237, 238, 247, 289, 290, 292, 293, 364, 367, 369, 371, 433, 435, 455, 456, 459, 462, 466, 467, 468, 475, 476, 479, 480, 483
var. malacon 459

Uranyl minerals

Abernathyite 118

Autunite 4, 88, 175, 207, 215, 236, 275, 277, 278, 291, 292, 296, 322, 339, 373, 374, 420, 424, 429, 432, 433, 476, 484

Becquerelite 105

Beta-uranophane (old term lambertite) 292, 296, 455, 469

Boltwoodite 119, 420

Carnotite 4, 7, 68, 69, 82, 84, 85, 86, 87, 88, 93, 94, 105, 109, 115, 148, 195, 215, 217, 218, 226, 292, 301, 302, 304, 322, 373, 420, 424, 429, 432

Haiweeite 373, 420

Hewettite 115

Johannite 296

Liebigite 87, 437

Margaritasite 420, 423, 424

Meta-autunite 141, 236, 239, 241, 290, 296, 367, 420, 432, 484

Metahalloysite 484

Metatorbernite 148, 239, 290, 296, 431

Metatyuyamunite 62, 82, 85, 93, 106, 148, 215, 226, 231, 244, 431

Meta-uranocircite 361

Metazeunerite 118

Gummite 4, 484

Phosphuranylite 296

Rauvite 69, 82, 118, 215, 296

Sabugalite 373

Schroëckingerite 87, 119, 192, 245, 296, 373, 445

Soddyite 420, 424

Torbernite 115, 148, 291, 296, 374

Tyuyamunite 62, 69, 82, 84, 85, 86, 87, 88, 91, 93, 94, 115, 127, 195, 215, 218, 226, 231, 244, 296, 322, 339, 374, 420, 424, 431, 432

Uranocircite 119, 374

Uranophane (old term uranotile) 62, 115, 119, 215, 236, 241, 248, 277, 278, 296, 373, 374, 420, 422, 424, 430, 433, 437

Uranopilite 87, 115, 296

Uranotile (see *Uranophane*)

Walpurgite 374

Weeksite 420, 424

Zeunerite 148, 374

Zippeite 119, 148, 226, 296





